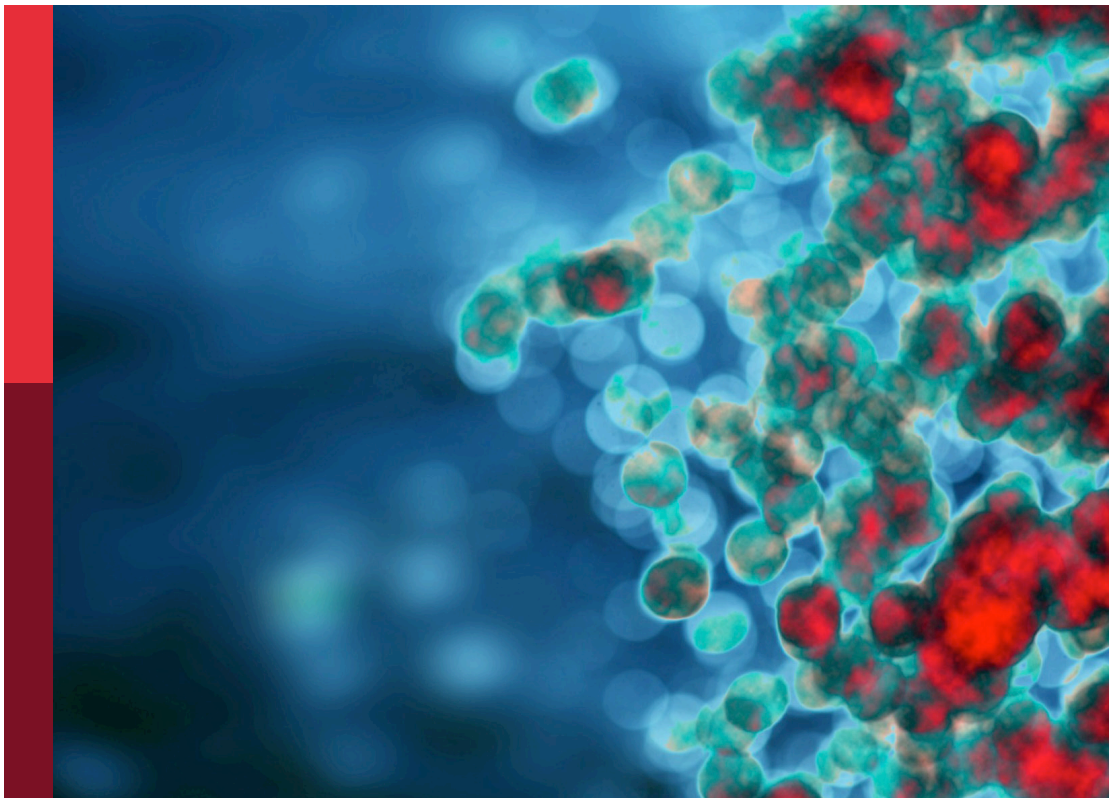
frontiers | Research Topics

Immunotherapy and multimodality therapy for lung cancer

Edited by
Qun Xue, Jie Mei, Zichao Luo, Wenjun Mao, Yuan Wan and Yifei Liu

Published in
Frontiers in Immunology
Frontiers in Oncology
Frontiers in Pharmacology
Frontiers in Medicine



FRONTIERS EBOOK COPYRIGHT STATEMENT

The copyright in the text of individual articles in this ebook is the property of their respective authors or their respective institutions or funders. The copyright in graphics and images within each article may be subject to copyright of other parties. In both cases this is subject to a license granted to Frontiers.

The compilation of articles constituting this ebook is the property of Frontiers.

Each article within this ebook, and the ebook itself, are published under the most recent version of the Creative Commons CC-BY licence. The version current at the date of publication of this ebook is CC-BY 4.0. If the CC-BY licence is updated, the licence granted by Frontiers is automatically updated to the new version.

When exercising any right under the CC-BY licence, Frontiers must be attributed as the original publisher of the article or ebook, as applicable.

Authors have the responsibility of ensuring that any graphics or other materials which are the property of others may be included in the CC-BY licence, but this should be checked before relying on the CC-BY licence to reproduce those materials. Any copyright notices relating to those materials must be complied with.

Copyright and source acknowledgement notices may not be removed and must be displayed in any copy, derivative work or partial copy which includes the elements in question.

All copyright, and all rights therein, are protected by national and international copyright laws. The above represents a summary only. For further information please read Frontiers' Conditions for Website Use and Copyright Statement, and the applicable CC-BY licence.

ISSN 1664-8714
ISBN 978-2-8325-4429-7
DOI 10.3389/978-2-8325-4429-7

About Frontiers

Frontiers is more than just an open access publisher of scholarly articles: it is a pioneering approach to the world of academia, radically improving the way scholarly research is managed. The grand vision of Frontiers is a world where all people have an equal opportunity to seek, share and generate knowledge. Frontiers provides immediate and permanent online open access to all its publications, but this alone is not enough to realize our grand goals.

Frontiers journal series

The Frontiers journal series is a multi-tier and interdisciplinary set of open-access, online journals, promising a paradigm shift from the current review, selection and dissemination processes in academic publishing. All Frontiers journals are driven by researchers for researchers; therefore, they constitute a service to the scholarly community. At the same time, the *Frontiers journal series* operates on a revolutionary invention, the tiered publishing system, initially addressing specific communities of scholars, and gradually climbing up to broader public understanding, thus serving the interests of the lay society, too.

Dedication to quality

Each Frontiers article is a landmark of the highest quality, thanks to genuinely collaborative interactions between authors and review editors, who include some of the world's best academicians. Research must be certified by peers before entering a stream of knowledge that may eventually reach the public - and shape society; therefore, Frontiers only applies the most rigorous and unbiased reviews. Frontiers revolutionizes research publishing by freely delivering the most outstanding research, evaluated with no bias from both the academic and social point of view. By applying the most advanced information technologies, Frontiers is catapulting scholarly publishing into a new generation.

What are Frontiers Research Topics?

Frontiers Research Topics are very popular trademarks of the *Frontiers journals series*: they are collections of at least ten articles, all centered on a particular subject. With their unique mix of varied contributions from Original Research to Review Articles, Frontiers Research Topics unify the most influential researchers, the latest key findings and historical advances in a hot research area.

Find out more on how to host your own Frontiers Research Topic or contribute to one as an author by contacting the Frontiers editorial office: frontiersin.org/about/contact

Immunotherapy and multimodality therapy for lung cancer

Topic editors

Qun Xue — Affiliated Hospital of Nantong University, China
Jie Mei — Wuxi People's Hospital Affiliated to Nanjing Medical University, China
Zichao Luo — National University of Singapore, Singapore
Wenjun Mao — The affiliated Wuxi People's Hospital of Nanjing Medical University, China
Yuan Wan — Binghamton University, United States
Yifei Liu — Affiliated Hospital of Nantong University, China

Citation

Xue, Q., Mei, J., Luo, Z., Mao, W., Wan, Y., Liu, Y., eds. (2024). *Immunotherapy and multimodality therapy for lung cancer*. Lausanne: Frontiers Media SA.
doi: 10.3389/978-2-8325-4429-7

Table of contents

06 Editorial: Immunotherapy and multimodality therapy for lung cancer
Chenghu Song, Weici Liu, Yuan Wan and Wenjun Mao

09 Bevacizumab loaded CalliSpheres® bronchial arterial chemoembolization combined with immunotherapy and targeted therapy for advanced lung adenocarcinoma
Haitao Liu, Yahua Li, Zongming Li, Xinwei Han and Kewei Ren

18 A case report of pulmonary hepatoid adenocarcinoma: promoting standardized diagnosis and treatment of the rare disease
Kun Xu, Jin Gao, Lili Feng, Ying Fang and Xiuliang Tang

30 A novel signature predicts prognosis and immunotherapy in lung adenocarcinoma based on cancer-associated fibroblasts
Qianhe Ren, Pengpeng Zhang, Haoran Lin, Yanlong Feng, Hao Chi, Xiao Zhang, Zhijia Xia, Huabao Cai and Yue Yu

47 Rechallenge with EGFR-TKI after failure of immunotherapy is considered an effective treatment for advanced lung adenocarcinoma patients with EGFR exon 19 deletion: a case report
Shubin Chen, Qitao Yu, Wei Jiang, Yukun Lu, Yun Zhao and Huilin Wang

54 The benefit and risk of PD-1/PD-L1 inhibitors plus anti-angiogenic agents as second or later-line treatment for patients with advanced non-small-cell lung cancer: a systematic review and single-arm meta-analysis of prospective clinical trials
Shubin Chen, Wanying Mo, Wei Jiang, Shaozhang Zhou, Haijie Gan and Qitao Yu

70 Dynamic evaluation of blood immune cells predictive of response to immune checkpoint inhibitors in NSCLC by multicolor spectrum flow cytometry
Weijie Ma, Sixi Wei, Siqi Long, Eddie C. Tian, Bridget McLaughlin, Maria Jaimes, Dennis J. Montoya, Varun R. Viswanath, Jeremy Chien, Qianjun Zhang, Jonathan E. Van Dyke, Shuai Chen and Tianhong Li

83 How single-cell techniques help us look into lung cancer heterogeneity and immunotherapy
Pu Liao, Qi Huang, Jiwei Zhang, Yuan Su, Rui Xiao, Shengquan Luo, Zengbao Wu, Liping Zhu, Jiansha Li and Qinghua Hu

99 Upregulated FADD is associated with poor prognosis, immune exhaustion, tumor malignancy, and immunotherapy resistance in patients with lung adenocarcinoma
Miao He, Yingying He, Jian Xu, Youcai Zhang, Xiaoyu Cao, Li Wang and Feng Luo

110 Mechanisms of exercise in the treatment of lung cancer – a mini-review
Zhiwen Luo, Renwen Wan, Shan Liu, Xinting Feng, Zhen Peng, Qing Wang, Shiyi Chen and Xiliang Shang

120 The influence of anti-cancer therapies on lymphocyte subpopulations of lung cancer patients
Philipp Gessner, Belay Tessema, Markus Scholz, Ulrich Sack, Andreas Boldt, Andreas Kühnapfel and Christian Gessner

132 TAGAP expression influences CD4+ T cell differentiation, immune infiltration, and cytotoxicity in LUAD through the STAT pathway: implications for immunotherapy
Zhanyu Xu, Tiaozhan Zheng, Zhiwen Zheng, Wei Jiang, Liuliu Huang, Kun Deng, Liqiang Yuan, Fanglu Qin, Yu Sun, Junqi Qin and Shikang Li

143 The prognostic biological markers of immunotherapy for non-small cell lung cancer: current landscape and future perspective
Shuai Liang, Hanyu Wang, Haixia Tian, Zhicheng Xu, Min Wu, Dong Hua and Chengming Li

159 Expanding the applications of immune checkpoint inhibitors in advanced lung cancer beyond disease progression
Chao Chen, Xi Xiong, Ying Cheng, Haiyun Gen, Wenqiang Zhu, Fei Zhang, Chuandong Zhu, Siqi Han and Xiufeng Liu

169 Immunotherapy strategies for EGFR-mutated advanced NSCLC after EGFR tyrosine-kinase inhibitors failure
Xingyuan Li, Huayan Huang, Yingjia Sun, Qing Jiang and Yongfeng Yu

180 Survival after radiofrequency ablation and/or chemotherapy for lung cancer and pulmonary metastases: a systematic review and meta-analysis
Ziyi Yang, Xia Lyu, Huilin Yang, Bingbing Wang, Dan Xu, Lingyi Huo, Runzi Zhang, Yingjun Huang and Benshu Diao

194 Single-cell mass cytometric analysis of peripheral immunity and multiplex plasma marker profiling of non-small cell lung cancer patients receiving PD-1 targeting immune checkpoint inhibitors in comparison with platinum-based chemotherapy
Patrícia Neuperger, Klára Szalontai, Nikolett Gémes, József Á. Balog, László Tiszlavicz, József Furák, György Lázár, László G. Puskás and Gábor J. Szebeni

208 Landscape of tumor and immune system cells-derived exosomes in lung cancer: mediators of antitumor immunity regulation
Alejandro Castillo-Peña and Sonia Molina-Pinelo

222 *Plasmodium* immunotherapy combined with gemcitabine has a synergistic inhibitory effect on tumor growth and metastasis in murine Lewis lung cancer models
Xiao Chen, Zhu Tao, Yun Liang, Meng Ma, Dickson Adah, Wenting Ding, Lili Chen, Xiaofen Li, Linglin Dai, Songwe Fanuel, Siting Zhao, Wen Hu, Donghai Wu, Ziyuan Duan, Fang Zhou, Li Qin, Xiaoping Chen and Zhaoqing Yang

233 Case report: Clinical management of recurrent small cell lung cancer transformation complicated with lung cancer-induced acute pancreatitis after lung adenocarcinoma surgery
Suyun Zhang, Ningjing Guo, Qianyuan Zhang, Yao Wang, Sheng Yang and Xiangqi Chen

241 Harnessing the power of traditional Chinese medicine monomers and compound prescriptions to boost cancer immunotherapy
Keyan Miao, Weici Liu, Jingtong Xu, Zhengtao Qian and Qinglin Zhang

260 Efficacy and safety of definitive chemoradiotherapy with or without induction immune checkpoint inhibitors in patients with stage III non-small cell lung cancer
Yin Yang, Jianyang Wang, Tao Zhang, Zongmei Zhou, Yu Wang, Ying Jiang, Wenyang Liu, Zefen Xiao, Lei Deng, Qinfu Feng, Xin Wang, Jima Lv, Wenqing Wang, Qi Xue, Jie Wang, Ye-Xiong Li and Nan Bi

270 Induction chemoimmunotherapy may improve outcomes of chemoradiotherapy in patients with unresectable stage III NSCLC
Song Guan, Shufeng Zhang, Kai Ren, Xingyue Li, Xue Li and Lujun Zhao

281 The role of m6A demethylases in lung cancer: diagnostic and therapeutic implications
Mengjiao Yu, Wenqian Ji, Xu Yang, Kai Tian, Xinyi Ma, Shali Yu, Lin Chen and Xinyuan Zhao

291 Clinical markers predict the efficacy of several immune checkpoint inhibitors in patients with non-small cell lung cancer in China
Yuxin Wang, Jiahui Lu, Chenxi Wu, Fei Fei, Zhuze Chu and Peihua Lu

304 Evaluation of the efficacy and surgical-related safety of neoadjuvant immunochemotherapy in advanced resectable none small cell lung cancer (NSCLC)
Qin Wang, Chen Qi, Jing Luo, Nan Xu, Mao-tian Xu, Yong Qiang, Chi Zhang and Yi Shen

313 Pathological complete response to neoadjuvant therapy with serplulimab and chemotherapy in stage IIIB small cell lung cancer: a case report and literature review
Ting Mei, Ting Wang, Chuanfen Lei, Dan Jiang and Qinghua Zhou

frontiers | Frontiers in Immunology

TYPE Editorial
PUBLISHED 26 January 2024
DOI 10.3389/fimmu.2024.1372513

Check for updates

OPEN ACCESS

EDITED AND REVIEWED BY
Giandomenico Roviello,
University of Firenze, Italy

*CORRESPONDENCE
Wenjun Mao
maowenjun1@njmu.edu.cn
Yuan Wan
ywan@binghamton.edu

†These authors have contributed equally to this work and share first authorship

RECEIVED 18 January 2024
ACCEPTED 22 January 2024
PUBLISHED 26 January 2024

CITATION
Song C, Liu W, Wan Y and Mao W (2024) Editorial: Immunotherapy and multimodality therapy for lung cancer.
Front. Immunol. 15:1372513.
doi: 10.3389/fimmu.2024.1372513

COPYRIGHT
© 2024 Song, Liu, Wan and Mao. This is an open-access article distributed under the terms of the Creative Commons Attribution License (CC BY). The use, distribution or reproduction in other forums is permitted, provided the original author(s) and the copyright owner(s) are credited and that the original publication in this journal is cited, in accordance with accepted academic practice. No use, distribution or reproduction is permitted which does not comply with these terms.

Editorial: Immunotherapy and multimodality therapy for lung cancer

Chenghu Song[1†], Weici Liu[1†], Yuan Wan[2*] and Wenjun Mao[1*]

[1]Department of Thoracic Surgery, The Affiliated Wuxi People's Hospital of Nanjing Medical University, Wuxi People's Hospital, Wuxi Medical Center, Nanjing Medical University, Wuxi, Jiangsu, China, [2]The Pq Laboratory of BiomeDx/Rx, Department of Biomedical Engineering, Binghamton University, Binghamton, NY, United States

KEYWORDS

lung cancer, immunotherapy, immune checkpoint inhibitors, multimodality therapy, predictive biomarker

Editorial on the Research topic
Immunotherapy and multimodality therapy for lung cancer

Lung cancer stands as one of the most prevalent malignant tumor worldwide, with non-small cell lung cancer (NSCLC) accounting for approximately 85% of all lung cancer cases (1). The undesirable prognosis of NSCLC, with a mere 17.8% five-year survival rate due to the advanced-stage diagnosis, greatly poses challenges to modern medicine. Lung cancer treatment incorporates a series of diverse therapeutic approaches, ranging from traditional surgical resection, chemoradiotherapy to emerging targeted therapy and immunotherapy (2). The advances of lung cancer therapeutics have significantly improved patient prognosis.

Since the year of 2013, the therapeutic paradigm for lung cancer has undergone a remarkable shift with the rapid development of immunotherapy. Particularly, immune checkpoint inhibitors (ICIs) occupy a pivotal place in immunotherapy (3). The programmed cell death protein-1/programmed cell death ligand-1 (PD-1/PD-L1) and cytotoxic T lymphocyte antigen-4 (CTLA-4) have displayed desirable performances in terms of safety, efficacy and anti-tumor activity, greatly extending their clinical applicability and playing a crucial role in the treatment of 'immuno-hot' lung tumor (2). The efficacy of immunotherapy is based on the effective activation of immune cells to recognize and kill tumor cells. Gessner et al. revealed a surging in the number of absolute transitional B cells and activated cytotoxic T lymphocytes in NSCLC patients receiving immunotherapy or immunochemotherapy.

As one of the broadly applied monoclonal antibodies, Pembrolizumab nearly doubled the five-year survival rate to 31.9% for lung cancer patients in comparison to the 16.3% in the chemotherapy group (4). For advanced NSCLC patients with over 50% PD-L1 expression, pembrolizumab substantially extended both progression-free survival (PFS) and overall survival (OS) compared with conventional platinum-based chemotherapy (5). As a pivotal member in lung cancer immunotherapy, the approval of pembrolizumab by the Food and Drug Administration (FDA) signifies a new era in treating this challenging disease. Other monoclonal antibodies for lung cancer treatment mainly include cetuximab, bevacizumab and nivolumab, also having favorable clinical efficacy. In this Research Topic,

Chen et al. challenged the established norms and demonstrated the potential of persistent PD-1/PD-L1 immunotherapy even after the progression of advanced lung cancer, which hints at promising survival benefits. This approach could reshape the therapeutic landscape of advanced lung cancer. Wang et al. uncovered that adjuvant immunotherapy had an advantage over conventional neoadjuvant chemotherapy and neoadjuvant targeted therapy for advanced resectable lung adenocarcinoma patients in terms of surgical outcomes, while neoadjuvant immunotherapy showcased superiority over neoadjuvant targeted therapy in lung squamous carcinoma cases. For patients with stage III NSCLC, Yang et al. reported that the induction and consolidation ICIs in combination with chemoradiotherapy showed superior efficacy and manageable toxicity. For unresectable stage III NSCLC, Guan et al. discovered that induction chemoimmunotherapy was safe and could improve chemoradiotherapy-related adverse events, even further enhancing treatment response and survival outcomes.

While immunotherapy holds promising prospects, it is crucial to recognize that nearly 70% of advanced NSCLC and 80% of SCLC patients fail to achieve long-term benefits from it alone. This dilemma underscores the requirement for further investigations into the underlying resistance mechanisms like poor immunogenicity, immunosuppressive tumor microenvironment, and T-cell exhaustion (6). Previous research has indicated the potential for enhancing the survival duration of patients undergoing single-agent immunotherapy treatment (7). Given the limited response rates, high costs and potential side effects of immunotherapy, it is urgently demanded to identify robust predictive biomarkers that can guide immunotherapy selection and to explore novel therapeutic targets or combination approaches that can enhance efficacy and minimize toxicity (8).

The PD-L1 expression remains the most established biomarker for guiding immunotherapy selection in lung cancer patients, yet it still has limitations and some novel biomarkers are needed (9). In this Research Topic, several biomarker studies preliminarily revealed the desirable predictive performances of novel markers, such as cancer-associated fibroblasts (CAFs) by Ren et al., T-cell Activation GTPase Activating Protein (TAGAP) by Xu et al., FAS-associated death structural domain (FADD) proteins by He et al., neutrophil-to-lymphocyte ratio (NLR) by Wang et al. and m6A demethylases by Yu et al. Additionally, Liang et al. delves into the current landscape and future possibilities of both individual and combined biomarkers for lung cancer immunotherapy. Concretely, it summarizes some individual markers like PD-L1, tumor mutation burden (TMB), hematological markers, and even specific gene mutations. Aside from these, it also deals with combined biological markers, including radiological and radiomic markers, as well as prediction models that effectively predict immunotherapy responses in NSCLC patients.

Despite limitations in current ICIs, some novel checkpoints have been uncovered like TIGIT, LAG-3, TIM-3, NKG2A, and CD73. These latent checkpoints, currently undergoing rigorous validation, hold great promise for overcoming resistance to conventional ICIs and potentially revolutionizing lung cancer treatment (10). As for the multimodality therapy, previous studies showed the feasibility of anti-angiogenic drugs to activate the immune system, thereby achieving the combination of lung cancer immunotherapy and synergistic inhibition of tumor activity (11). Li et al. revealed the superiority of combining immunotherapy with chemotherapy and anti-angiogenic drugs in the treatment of advanced NSCLC. This finding was corroborated by a systematic review by Chen et al. incorporating 16 studies and 931 patients, which found that ICIs in combination with anti-angiogenic drugs had good efficacy and safety in the second or later-line treatment of NSCLC. In addition, Chen et al. first revealed the synergistic anti-cancer effects of *Plasmodium* immunotherapy combined with gemcitabine, which were partially attributed to the inhibition of epithelial-mesenchymal transition of tumor cells by blocking the CXCR2/TGF-β-mediated PI3K/Akt/GSK-3β signaling pathway. Similarly, Liu et al. discovered that bevacizumab-loaded CalliSpheres bronchial artery chemoembolization in combination with immunotherapy and targeted therapy was effective and safe in patients with advanced lung adenocarcinoma.

Intriguingly, some external elements can enhance anti-tumor immunity or synergize with cancer immunotherapy beyond our expectation. Miao et al. summarized the potential of single and compound Chinese herbal medicines in regulating cellular pathways, enhancing immunotherapy responses, and inducing tumor cell apoptosis. Notably, it underscored the exciting possibilities of combining traditional Chinese medicine with the burgeoning immunotherapy. Luo et al. summarized the underlying mechanisms by which exercise exerts anti-tumor effects on lung cancer from four aspects—the tumor microenvironment, matrix regulation, apoptosis and angiogenesis, and highlighted the importance of personalized prescription. Moreover, Yang et al. conducted a innovative meta-analysis, discovering that radiofrequency ablation in combination with chemotherapy could improve the OS of NSCLC patients and reduce pulmonary metastases compared with radiofrequency ablation or chemotherapy alone.

This Research Topic delves into the important contributions of clinical scholars in revolutionizing lung cancer treatment through immunotherapy, multimodality approaches, and precision biomarker-driven prognosis. While ICIs have extensive application prospects for advanced NSCLC, their limitations in small cell lung cancer and emerging resistance to ICIs necessitate the therapeutic diversification. Clinical scholars can address these challenges through combining immunotherapy with established therapies such as chemotherapy, radiotherapy and targeted therapy. Moving forward, exploring novel therapeutic targets, combined with DNA repair targeting agents or cellular therapies, could be an exciting and challenging field that will transcend current limitations and hopefully open a new chapter in the treatment of advanced lung cancer in the near future.

Author contributions

CS: Writing – original draft, Writing – review & editing. WL: Writing – original draft, Writing – review & editing. YW: Writing – review & editing, Conceptualization, Methodology, Project administration, Supervision. WM: Writing – review & editing,

Conceptualization, Funding acquisition, Methodology, Project administration, Supervision.

Funding

The author(s) declare financial support was received for the research, authorship, and/or publication of this article. This work was supported by the Natural Science Foundation of Jiangsu Province (BK20210068), the Top Talent Support Program for Young and Middle-aged People of Wuxi Health Commission (BJ2023014, HB2020003), the Mega-project of Wuxi Commission of Health (Z202216), and the General Program of Wuxi Medical Center of Nanjing Medical University (WMCG202305).

Conflict of interest

The authors declare that the research was conducted in the absence of any commercial or financial relationships that could be construed as a potential conflict of interest.

Publisher's note

All claims expressed in this article are solely those of the authors and do not necessarily represent those of their affiliated organizations, or those of the publisher, the editors and the reviewers. Any product that may be evaluated in this article, or claim that may be made by its manufacturer, is not guaranteed or endorsed by the publisher.

References

1. Siegel RL, Miller KD, Wagle NS, Jemal A. Cancer statistics, 2023. *CA: Cancer J Clin* (2023) 73. doi: 10.3322/caac.21763

2. Lahiri A, Maji A, Potdar PD, Singh N, Parikh P, Bisht B, et al. Lung cancer immunotherapy: Progress, pitfalls, and promises. *Mol Cancer* (2023) 22:40. doi: 10.1186/s12943-023-01740-y

3. Couzin-Frankel J. Breakthrough of the year 2013. *Cancer Immunother Sci* (2013) 342:1432–3. doi: 10.1126/science.342.6165.1432

4. Reck M, Rodríguez-Abreu D, Robinson AG, Hui R, Csőszi T, Fülöp A, et al. Five-year outcomes with pembrolizumab versus chemotherapy for metastatic non-small-cell lung cancer with PD-L1 tumor proportion score ≥ 50. *J Clin Oncol* (2021) 39:2339–49. doi: 10.1200/JCO.21.00174

5. Reck M, Rodríguez-Abreu D, Robinson AG, Hui R, Csőszi T, Fülöp A, et al. Pembrolizumab versus chemotherapy for PD-L1-positive non-small-cell lung cancer. *N Engl J Med* (2016) 375:1823–33. doi: 10.1056/NEJMoa1606774

6. Fares CM, Van Allen EM, Drake CG, Allison JP, Hu-Lieskovan S. Mechanisms of resistance to immune checkpoint blockade: Why does checkpoint inhibitor immunotherapy not work for all patients? *Am Soc Clin Oncol Educ Book* (2019) 39:147–64. doi: 10.1200/EDBK_240837

7. Waterhouse D, Lam J, Betts KA, Yin L, Gao S, Yuan Y, et al. Real-world outcomes of immunotherapy–based regimens in first-line advanced non-small cell lung cancer. *Lung Cancer* (2021) 156:41–9. doi: 10.1016/j.lungcan.2021.04.007

8. Wang J, Zou Z-H, Xia H-L, He J-X, Zhong N-S, Tao A-L. Strengths and weaknesses of immunotherapy for advanced non-small-cell lung cancer: A meta-analysis of 12 randomized controlled trials. *PloS One* (2012) 7:e32695. doi: 10.1371/journal.pone.0032695

9. Doroshow DB, Bhalla S, Beasley MB, Sholl LM, Kerr KM, Gnjatic S, et al. PD-L1 as a biomarker of response to immune-checkpoint inhibitors. *Nat Rev Clin Oncol* (2021) 18:345–62. doi: 10.1038/s41571-021-00473-5

10. Mamdani H, Matosevic S, Khalid AB, Durm G, Jalal SI. Immunotherapy in lung cancer: Current landscape and future directions. *Front Immunol* (2022) 13:823618. doi: 10.3389/fimmu.2022.823618

11. De Palma M, Biziato D, Petrova TV. Microenvironmental regulation of tumour angiogenesis. *Nat Rev Cancer* (2017) 17:457–74. doi: 10.1038/nrc.2017.51

frontiers | Frontiers in Pharmacology

TYPE Original Research
PUBLISHED 22 May 2023
DOI 10.3389/fphar.2023.1170344

Check for updates

OPEN ACCESS

EDITED BY
Jie Mei,
Wuxi People's Hospital Affiliated to Nanjing Medical University, China

REVIEWED BY
Zhi Li,
The First Affiliated Hospital of Soochow University, China
Ana Isabel Fraguas,
Complutense University, Spain

*CORRESPONDENCE
Kewei Ren,
renkewei@zzu.edu.cn

RECEIVED 20 February 2023
ACCEPTED 10 May 2023
PUBLISHED 22 May 2023

CITATION
Liu H, Li Y, Li Z, Han X and Ren K (2023), Bevacizumab loaded CalliSpheres® bronchial arterial chemoembolization combined with immunotherapy and targeted therapy for advanced lung adenocarcinoma.
Front. Pharmacol. 14:1170344.
doi: 10.3389/fphar.2023.1170344

COPYRIGHT
© 2023 Liu, Li, Li, Han and Ren. This is an open-access article distributed under the terms of the Creative Commons Attribution License (CC BY). The use, distribution or reproduction in other forums is permitted, provided the original author(s) and the copyright owner(s) are credited and that the original publication in this journal is cited, in accordance with accepted academic practice. No use, distribution or reproduction is permitted which does not comply with these terms.

Bevacizumab loaded CalliSpheres® bronchial arterial chemoembolization combined with immunotherapy and targeted therapy for advanced lung adenocarcinoma

Haitao Liu[1,2], Yahua Li[1], Zongming Li[1], Xinwei Han[1] and Kewei Ren[1]*

[1]Department of Interventional Radiology, The First Affiliated Hospital of Zhengzhou University, Zhengzhou, China, [2]Department of Radiology, Maternal and Child Health Hospital of Hubei Province, Tongji Medical College, Huazhong University of Science and Technology, Wuhan, China

Background: As a new drug delivery and embolization system, drug-eluted bronchial artery chemoembolization (DEB-BACE) can not only embolize the tumor blood supply artery but also load chemotherapy drugs and slowly release them into the local environment. Bevacizumab (BEV) combined with chemotherapy drugs has attained significant achievements in the first-line treatment of advanced non-squamous non-small cell lung cancer (NSCLC). The role of BEV-loaded DEB-BACE combined with immunotherapy and targeted therapy in patients with lung adenocarcinoma (LUAD) is unclear. This study was designed to evaluate the efficacy and safety of bevacizumab-loaded CalliSpheres® bronchial arterial chemoembolization combined with immunotherapy and targeted therapy in patients with lung adenocarcinoma.

Methods: Nine patients with LUAD who received BEV-loaded CalliSpheres® BACE combined with immunotherapy and targeted therapy from 1 Jan 2021 to Dec 2021 were included in this study. The primary endpoint was the disease control rate (DCR) and the objective response rate (ORR). The secondary endpoints were the overall survival rates (OS) at 6 months and 12 months. The tumor response was evaluated according to the mRECIST standard. Safety was assessed by the occurrences of adverse events and the severity of the adverse events.

Results: All patients received CalliSpheres® BACE loaded with BEV (200 mg) in combination with immunotherapy and targeted therapy. A total of nine patients received the BACE procedures 20 times, four of them received a third session of BACE, three underwent a second session of DEB-BACE, and two underwent one cycle of DEB-BACE. Partial response and stable disease were found in seven (77.8%), and two (22.2%) patients, respectively, 1 month after the last multimodal treatment. The ORR at 1, 3, 6, and 12 months was 77.8%, 66.7%, 44.4%, and 33.3%,

Abbreviations: BEV, bevacizumab; BACE, bronchial arterial chemoembolization; CB, CalliSpheres beads; BACE, bronchial arterial chemoembolization; DEB-BACE, Drug-eluting beads bronchial arterial chemoembolization; DCR, the disease control rate; ICIs, immune checkpoint inhibitors; LUAD, lung adenocarcinoma; LC, lung cancer; MWA, microwave ablation; NSCLC, nonsquamousnon-small cell lung cancer; ORR, objective response rate; OS, overall survival; VEGF, vascular endothelial growth factor.

respectively, while the DCR was 100%, 77.8%, 44.4%, and 33.3%, respectively. The OS rates at 6-and 12-month were 77.8% and 66.7%, respectively. There were no serious adverse events.

Conclusion: BEV-loaded CalliSpheres® transcatheter bronchial arterial chemoembolization combined with immunotherapy and targeted therapy is a promising and well-tolerated treatment for patients with lung adenocarcinoma.

KEYWORDS

lung adenocarcinoma, bevacizumab, drug-eluting beads, bronchial arterial chemoembolization, immunotherapy, targeted therapy

Introduction

Lung cancer (LC) is a common lung malignancy, with the highest mortality rate in the world, at 18.4%. The incidence of non-small cell lung cancer (NSCLC) accounts for more than 80% of lung cancer. Lung adenocarcinoma (LUAD), a kind of non-small cell lung cancer, accounts for approximately 50% of lung cancer (Dong et al., 2018). Surgery, chemotherapy, and radiation are the standard treatment for LUAD, but the 5-year overall survival for LUAD patients remains low and the recurrence rate is still unsatisfactory (Martin and Leighl, 2017). For patients with advanced lung cancer or weak physical condition, the above therapy may not be applicable. Immunotherapy and targeted therapy have been well-understood for the past decade. Although clinical development of immunotherapy and targeted therapy has mostly focused on monotherapy as the second line, recent advances have shifted to combination therapy as the first line. Immune checkpoint inhibitors (ICIs) are now first-line therapies for various solid and liquid tumors. Recent studies also show that ICIs can be well combined with conventional chemotherapy, so, currently, this combination is the routine treatment for most patients with metastatic NSCLC. Patients with lung adenocarcinoma might benefit from variegated palliative treatment.

Bronchial arterial chemoembolization (BACE) as an adjuvant therapy has been deemed to be an effective treatment option for NSCLC. Chemotherapy drugs can be injected into tumors by BACE and the local concentration is greatly increased with lower side effects. BACE combined with other local treatments also achieved beneficial results. Pulmonary chemoembolization is a new choice to treat lung tumors, but the best embolization, drug, and technology are still unclear. It is clear that as a new drug delivery and embolization system, DEB-BACE has a better therapeutic effect than BACE. Previous studies have confirmed the efficacy of CalliSpheres drug-eluting beads in hepatocellular carcinoma, and advanced and inoperable lung cancer (Zhou et al., 2018; Bi et al., 2022). Bevacizumab is a recombinant humanized monoclonal antibody that binds to vascular endothelial growth factor (VEGF). The mechanism is that it binds to VEGF-A, preventing its interaction with the VEGF receptor, thus resisting angiogenesis and tumor growth. BEV combined with various chemotherapy drugs can be valuable in the treatment of lung cancer, liver cancer, colorectal cancer, and ovarian cancer. BEV combined with platinum-based chemotherapy is used as the first-line treatment for patients with unresectable advanced, metastatic, or recurrent non-squamous cell NSCLC. Previous studies have shown that the use of drug-loaded microspheres loaded with chemotherapy drugs for bronchial artery infusion chemoembolization can help to improve the tumor control rate and prolong the survival time of patients (Liu et al., 2021b). According to our experiences and basic experiment, the CalliSpheres beads (CB) have a high loading efficiency of BEV; after the CB was loaded for 40 min, the loading efficiency was similar to the maximum loading efficiency. In addition, animal experiments confirmed that BEV-CB-TACE has good safety and effectiveness in the treatment of VX2 tumors. However, as far as we know, the clinical efficacy and safety of

TABLE 1 General information of patients.

Characteristic	Value
Age (years)	61 ± 13.3 (42–79)
Height (cm)	164 ± 7.0 (155–175)
Weight (kg)	62 ± 9.6 (48–75)
Sex	
Male	6
Female	3
Symptom	
Cough and dyspnea	6
Epigastric discomfort	1
Dysphagia	1
No symptoms	1
Preoperative ECOG score	
0	4
1	4
2	1
Treatment history	
Surgical excision	2
Chest drainage	2
None	5
TNM stage	
II	1
III	2
IV	6

ECOG:performance status made by Eastern Cooperative Oncology Group.

TABLE 2 Patient characteristic.

Patient	Age	Sex	Symptom	Combined diseases	Lesion characteristic	Treatment	Embolized artery	Follow-up treatment	Adverse effect
1	72	Male	Cough and dyspnea	Cardiovascular disease	Left upper lobe, maximum diameter 59 mm, with obstructive pneumonia, T3N0M0, stage IIB	DEB-BACE loaded with bevacizumab (200 mg) using CB (300–500 μm), Infusion: carboplatin (300 mg), pemetrexed (500 mg) 3 cycles of BAI/DEB-BACE	Left bronchial artery	Targeted therapy and immunotherapy	Skin itching
2	48	Female	Cough and dyspnea	None	Right lower lobe, maximum diameter 35 mm, with obstructive pneumonia, T2N3M1, stage IVA	DEB-BACE loaded with bevacizumab (200 mg) using CB (300–500 μm), Infusion: carboplatin (300 mg), pemetrexed (500 mg) 2 cycles of BAI/DEB-BACE	Right intercostal artery, left bronchial artery, and right diaphragm artery	Targeted therapy	None
3	77	Male	Dysphagia	Hypertension	Light lower lobe, maximum diameter 53 mm, with obstructive pneumonia, T3N3M0, stage IIIC	DEB-BACE loaded with bevacizumab (200 mg) using CB (300–500 μm) Infusion: carboplatin (60 mg), pemetrexed (500 mg) 2 cycles of BAI/DEB-BACE	Right bronchial artery	Immunotherapy	None
4	53	Male	Cough and dyspnea	None	Right lower lobe, 38 mm × 25 mm, T2N2M0, stage IIIA	DEB-BACE loaded with bevacizumab (200 mg) using CB (300–500 μm) Infusion: carboplatin (300 mg), pemetrexed (500 mg) 1 cycle of BAI/DEB-BACE	Right bronchial artery	Immunotherapy	Ankle edema
5	42	Male	Epigastric discomfort	Cardiovascular disease	Left lung, 42 mm × 34 mm, with obstructive pneumonia, T2N0M1, stage IVA	DEB-BACE loaded with bevacizumab (200 mg) using CB (300–500 μm) Infusion: carboplatin (60 mg), pemetrexed (500 mg) 3 cycles of BAI/DEB-BACE	Left bronchial artery	Immunotherapy	None
6	56	Male	Cough and dyspnea	Diabetes	Right middle lobe and left lower lobe, maximum diameter 38 mm, T3N2M1, stage IVA	DEB-BACE loaded with bevacizumab (200 mg) using CB (300–500 μm) Infusion: carboplatin (300 mg), pemetrexed (500 mg) 2 cycles of BAI/DEB-BACE	Branches of the left bronchial artery and left internal mammary artery	Targeted therapy	None

(Continued on following page)

TABLE 2 (*Continued*) Patient characteristic.

Patient	Age	Sex	Symptom	Combined diseases	Lesion characteristic	Treatment	Embolized artery	Follow-up treatment	Adverse effect
7	79	Male	Cough and dyspnea	Hypertension	Right upper lobe and left lower lobe maximum diameter 38 mm, T2N2M1, stage IVA	DEB-BACE loaded with bevacizumab (200 mg) using CB (300–500 μm) Infusion: carboplatin (300 mg), pemetrexed (500 mg) 1 cycle of BAI/DEB-BACE	Bilateral bronchial arteries	Immunotherapy	None
8	56	Female	Cough and dyspnea	Diabetes	Left upper lobe, 35 mm × 31 mm, T2N2M1, stage IVA	BACE: DEB-BACE loaded with bevacizumab (200 mg) using CB (300–500 μm) Infusion: carboplatin (150 mg), pemetrexed (250 mg) 3 cycles of BAI/DEB-BACE	Bilateral bronchial artery, left internal mammary artery	Targeted therapy and immunotherapy	Skin itching
9	69	Female	No symptoms	Radical resection of lung cancer, Diabetes, Hepatitis	Left lower lobe, 15 mm × 11 mm, postoperative recurrence, with obstructive pneumonia, stage IV	DEB-BACE loaded with bevacizumab (200 mg) using CB (300–500 μm),PVA (350–560 μm) Infusion: carboplatin (300 mg), pemetrexed (500 mg) 2 cycles of BAI/DEB-BACE	Branches of left bronchial artery and left internal mammary artery	Targeted therapy and immunotherapy	Toothache

BEV-loaded DEB-BACE combined with immunotherapy and targeted therapy have not been assessed in patients with LUAD. Therefore, the present study was designed to evaluate the short-term clinical efficacy, survival profile, and safety of BEV-loaded DEB-BACE combined with immunotherapy and targeted therapy for the treatment of LUAD.

Materials and methods

Ethical approval

The study was approved by the Ethical Committee of the first affiliated hospital of Zhengzhou University. The ethical approval number of the study is KY201515. All methods were carried out in accordance with relevant guidelines and regulations. Written informed consent was obtained from all subjects.

Study design and population

This was a retrospective observational study conducted on nine patients with LUAD who underwent DEB-BACE using BEV-loaded beads from 1 January 2021 to December 2021. The indications for DEB-BACE were as follows: 1) pathological diagnosis was confirmed as LUAD, 2) patients with local progression or recurrence after initial treatment or standard treatment; 3) poor candidate for or refused to receive surgical resection, radiotherapy, or chemotherapy because of severe cardiovascular disease or lung diseases; 4) expected survival time ≥3 months and no other acute diseases or active infectious diseases; 5) willingness to receive the combination therapy, etc.; and (6)Eastern Cooperative Oncology Group (ECOG) performance status≤2. The exclusion criteria were as follows: 1) patients with systemic multiple metastases; 2) without other malignancy; 3) severe liver and renal dysfunction; 4) coagulopathy or known bleeding disorders; and 5) allergic to the contrast agent.

CalliSpheres® BACE procedure

All operations were performed by the associate chief physician and chief physician. After the interventional surgery preparation, the right femoral artery was punctured under local anesthesia, and a vascular sheath (5F, Terumo Corp, Japan) was placed. The bronchial artery was selected for angiography under the guidance of preoperative enhanced CT. In addition, it was necessary to perform angiography on the thyroid trunk, internal mammary artery, intercostal artery, and diaphragmatic artery, to find out

TABLE 3 Tumor response according to mRECIST standard (n = 9).

Response 1	1 m (%)	3 m (%)	6 m (%)	12 m (%)
CR	0 (0)	2 (22.2)	4 (44.4)	2 (22.2)
PR	7 (77.8)	4 (44.4)	0 (0)	1 (11.1)
SD	2 (22.2)	1 (11.1)	0 (0)	0 (0)
PD	0 (0)	1 (11.1)	0 (0)	0 (0)
ORR	7 (77.8)	6 (66.7)	4 (44.4)	3 (33.3)
DCR	9 (100)	7 (77.8)	4 (44.4)	3 (33.3)

CR, complete response; PR, partial response; SD, stable disease; PD, progressive disease; ORR, objective response rate; DCR, disease control rate.

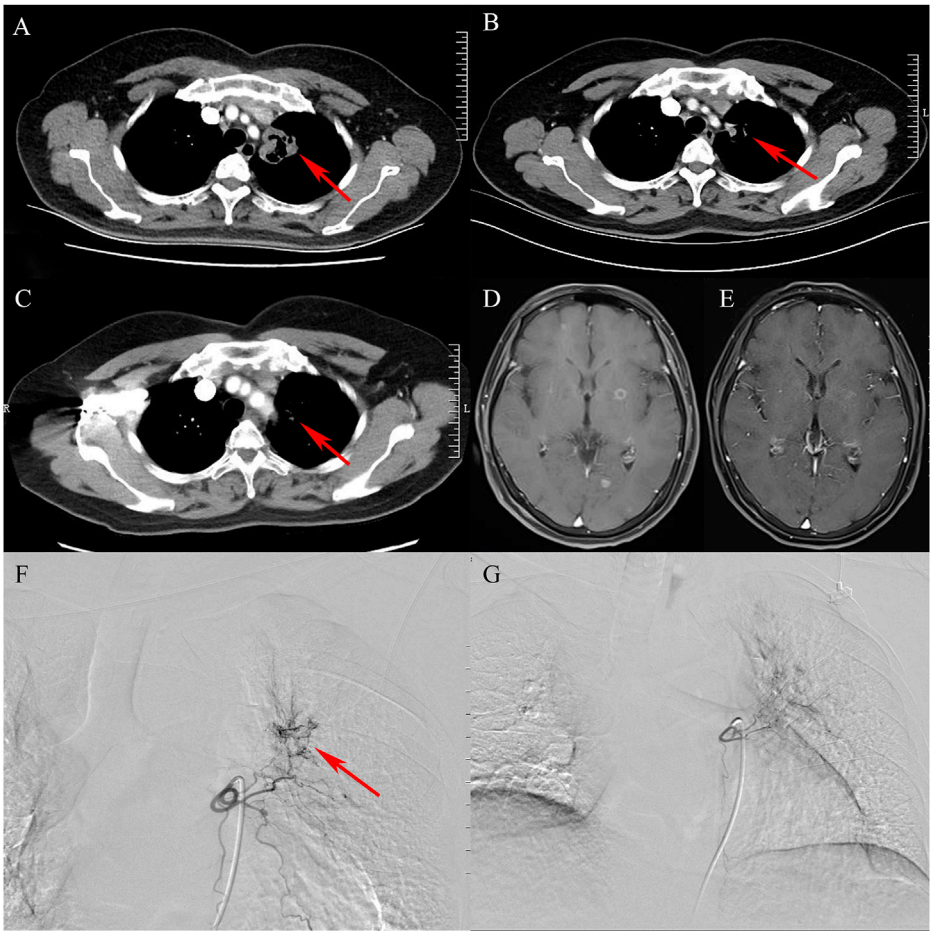


FIGURE 1
A case of lung adenocarcinoma with multiple brain metastases. **(A)**: Contrast-enhanced chest CT shows that cavitary tumor lesions are seen in the upper lobe of the left lung (arrow). **(B)**: After treatment, the tumor entity is smaller than before (arrow). **(C)**: The tumor entity is further reduced and is not enhanced (arrow). **(D)**: Multiple metastatic tumors in bilateral cerebral hemispheres (contrast-enhanced MRI, T1). **(E)**: After comprehensive treatment, the brain metastases became smaller or even disappeared (contrast-enhanced MRI, T1). **(F)**: Bronchial arteriography shows that the upper lobe of the left lung is abnormally stained and the left bronchial artery is the target artery (arrow). **(G)**: In the second cycle of treatment, the staining range of the upper lobe of the left lung is smaller than before.

whether there were abnormal tumor blood supply branches. After defining the tumor-feeding artery, the microcatheter (Terumo Corp, Japan) was super-selected for the responsible vessel by coaxial catheter technology. Carboplatin (60–300 mg) plus pemetrexed (250–500 mg) was used for arterial infusion chemotherapy. After chemotherapy, DEE-BACE was performed. CalliSpheres beads (300–500 μm, Jiangsu Hengrui Medicine Co., Ltd., Jiangsu, China) were used to load bevacizumab (200 mg, Innovent Biologics Co., Ltd., Jiangsu, China). The drug loading method is to mix microspheres with bevacizumab at 23°C–28°C for 30 min and

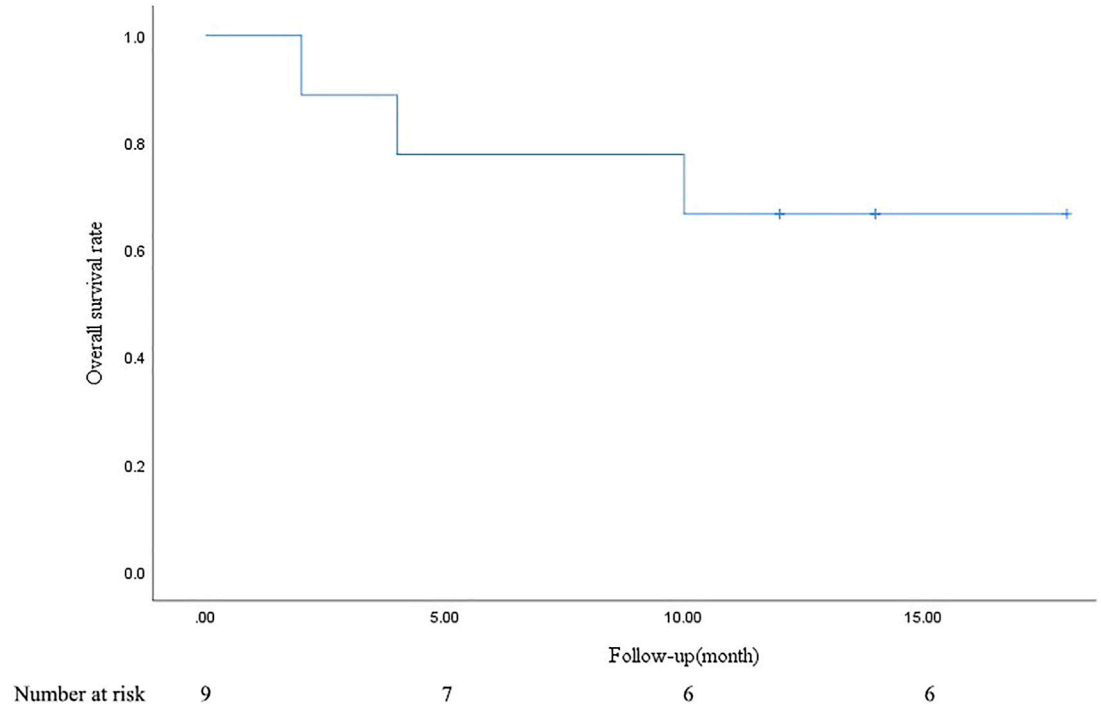


FIGURE 2
Kaplan-Meier survival analysis of overall survival rate.

shake for 30 min every 5 min. Iohexol was added immediately after the loading at the volume ratio 1:1. Then, CB-BEV was slowly and carefully injected into the tumor-feeding artery manually by syringe under fluoroscopic monitoring. After embolization, angiography was performed to evaluate the embolization effect. If the tumor-feeding artery was not completely embolized, PVA particles were used for supplementary embolization. The endpoint of embolization was that the tumor-feeding artery was completely occluded or only a small amount of trunk remains. The interval was 3 weeks between sessions.

After DEB-BACE, nine patients received targeted or immunotherapy. Three patients continued to take targeted drugs and immune drugs after DEB-BACE treatment. Two patients only took targeted drugs orally and four patients took immune preparations. A total of five patients received targeted therapy. Anlotinib (8 mg or 12 mg per day, orally, Chia Tai Tianqing Pharmaceutical Group Co., Ltd., China) was used for targeted therapy. Immunological preparations included bevacizumab (200 mg every 3 weeks, intravenous infusion, Innovent Biologics Co., Ltd., China) and sintilimab (200 mg every 3 weeks, intravenous infusion, Innovent Biologics Co., Ltd., China). Targeted therapy and immunotherapy were maintained until disease progression or prohibitive toxicities.

Evaluation of efficacy and safety

Enhanced CT of the chest was performed after therapy to evaluate its efficacy. CT images were analyzed separately by two attending radiologists with more than 3 years of experience. According to the mRECIST standard, tumor response was evaluated. The primary endpoints were the objective response rate (ORR) and the disease control rate (DCR). Tumor response was classified into four grades: complete response (CR), partial response (PR), stable disease (SD), and progressive disease (PD). The objective response rate (ORR) was defined as CR and PR, while the disease control rate (DCR) was defined as CR, PR, and SD. Local control was defined as the stopping of cancer growth at the origin or the absence of local failure. The secondary endpoints were the overall survival rates (OS) at 6 months and 12 months. Improvements in clinical indices and symptoms, adverse events, and follow-up treatments were also recorded. Adverse events and severe adverse events were graded according to the Common Terminology Criteria for Adverse Events (version 5.0).

Follow-up

All patients received inpatient/outpatient follow-up or telephone follow-up monthly. The endpoint of follow-up was death or the end date of 1 December 2022. Follow-up contents included symptoms, blood routine examination, liver function, renal function, tumor marker, and chest CT examination. Biochemical indicators were used to evaluate the biological toxicity of drugs. CT examination was used to evaluate the efficacy of local tumors. Death was certified through relevant registrations.

Statistical analyses

Data were described as the mean ± standard deviation, median, or count (%). Differences among groups were analyzed by Student's t-test, $\chi 2$ test, or Wilcoxon's rank-sum test. SPSS 26.0 (IBM Cop., Armonk, NY) was used for statistical data analysis. A p-value <0.05 was considered significant. Kaplan-Meier survival analysis was used to evaluate OS.

Results

Patient characteristics

A total of nine patients (six men and three women) were involved in this study. The ages ranged from 42 to 79 years, and the median value was 61 years old. All patients were pathologically diagnosed with adenomatous carcinoma without genetic mutation. One patient had stage II NSCLC, two patients were stage III, and six patients were stage IV. All patients successfully accepted BEV-loaded DEB-BACE. General information on patients is shown in Table 1. The detailed characteristics of each patient are shown in Table 2. All patients were treated with BEV-loaded DEB-BACE (CalliSpheres® beads) combined with immunotherapy and targeted therapy. Nine patients also received transarterial infusion with carboplatin and pemetrexed. Nine patients received 20 BACE, three underwent a second session of DEB-BACE, four underwent a third session of DEB-BACE, and two underwent one cycle of DEB-BACE.

Efficacy

PR and SD were found in seven (77.8%) and two (22.2%) patients 1 month after the combined treatment. No patient achieved CR and PD. The CR, PR, SD, and PD at 1, 3, 6, and 12 months after DEB-BACE are shown in Table 3. The ORR at 1, 3, 6, and 12 months was 77.8%, 66.7%, 44.4%, and 33.3%, respectively, while the DCR was 100%, 77.8%, 44.4%, and 33.3%, respectively. The OS rates at 6- and 12-month were 77.8% and 66.7%, respectively. In a patient with lung adenocarcinoma complicated with multiple brain metastases, after treatment, the lung lesions were significantly reduced and the brain metastases were less than before (Figure 1). Symptoms also improved significantly compared with before. Kaplan-Meier survival analysis of the overall survival rate is shown in Figure 2.

Treatment-related adverse events

Regarding safety, no serious adverse events were observed during the study period. Slight adverse reactions, such as local pain, fever, and cough, were mainly related to chemoembolization and were relieved after symptomatic treatment. This study reported four cases of adverse reactions with targeted drugs and immune agents. Two patients suffered from skin itching, which was tolerable, one patient suffered from ankle edema, which may have been related to abnormal renal function, and one patient suffered from toothache, which was relieved after oral painkillers.

Discussion

This study shows that BEV-loaded DEB-BACE combined with immunotherapy and targeted therapy has a beneficial short-term effect on advanced lung adenocarcinoma with few complications. Transcatheter arterial embolization has achieved a beneficial effect in the treatment of solid tumors such as hepatocellular carcinoma (Galle et al., 2017; Chang et al., 2020). The principle is that chemotherapy drugs are directly injected into the tumor-feeding artery. Because of the 'first-pass effect', a smaller dose of chemotherapy drugs can be used to achieve a higher drug concentration in the tumor (Datta et al., 2019). Meanwhile, the toxic reaction to the whole body is greatly reduced. Previous studies have shown that pulmonary chemoembolization is a safe and effective treatment for lung, mediastinum, and bronchial metastasis (Sieghart et al., 2015). The bronchial artery is considered to be the principal tumor-feeding vessel of lung cancer. Bronchial embolization can have a beneficial effect in the treatment of lung cancers. Cao et al. found that BACE guided by DSA is effective for patients with advanced primary bronchogenic carcinoma. The short-term remission rate of 84 patients was 73.40%, and the short-term disease control rate was 93.62% (Cao et al., 2022). Drug-loaded microspheres have the functions of drug loading and drug slow release, which can keep the local drug concentration at a high level and contribute to the inhibition of tumor cells (Choi et al., 2014; Boas et al., 2021). The safety and efficacy of DEB-BACE in the treatment of advanced lung cancer have been confirmed by some studies. Yu et al. reported a case of lung adenocarcinoma, which was resected after three cycles of DEB-BACE. After the resection of the lung tumor, no tumor cells were discovered by pathology, which suggests PCR (Yu and Hu, 2020). Bie et al. found that after receiving DEB-BACE, the DCRs of NSCLC patients were 100.0%, 83.3%, and 66.7% at 2, 4, and 6 months, respectively (Bie et al., 2019). BEV combined with platinum chemotherapy is the first-line treatment for non-squamous cell carcinoma (Yang et al., 2022).

In the treatment of cancer, the combination of different modes may improve the curative effect. Different immunotherapeutic drugs, targeted therapeutic drugs, and chemotherapy drugs act on different targets and cells, which makes the synergistic or combined treatment of these drugs possible to achieve a greater therapeutic effect. However, it is worth noting that this may bring greater side effects (Yang et al., 2019). PD-1 plus CTLA-4 blockade has achieved a long-term lasting survival result over chemotherapy, but in the first few months of treatment, the survival result may be worse than chemotherapy. This may be related to the more frequent initial response of NSCLC patients to first-line chemotherapy, but it is also shorter. In order to alleviate this pattern, related randomized studies evaluated PD-1 plus CTLA-4 blocking plus chemotherapy, aiming at combining the durability of combined immunotherapy with the initial beneficial effects of chemotherapy (Reck et al., 2022). A randomized controlled study involving 719 patients showed that nivolumab plus ipilimumab plus two cycles of chemotherapy can prolong the overall survival of patients compared with the standard course of four cycles of chemotherapy (median 15.8 months v 11.0 months) (Paz-Ares et al., 2021). Cytotoxicity therapy can be combined with ICBs to kill tumor cells, increase the ratio of T cells to tumors, and restore metabolic restrictions that lead to low T cell reactivity of cancer. (Chang et al., 2015). In this study, the lung lesions in a patient with lung adenocarcinoma and brain metastasis were almost invisible and the brain metastases disappeared after three cycles of BEV-loaded DEB-BACE combined with immunotherapy and targeted therapy, suggesting CR.

DEB-BACE combined with different treatment methods has achieved gratifying results. To some patients with NSCLC, the combined treatment of MWA (microwave ablation) and DEB-BACE has a better local control effect than DEB-BACE, with a higher 6-month PFS rate and a longer PFS (Yang et al., 2016; Xu et al., 2022). Li et al. found that sintilimab plus DEB-BACE in NSCLC was also superior to that with monotherapy of PD-1/PD-L1 blockade as first-line therapy (Li et al., 2021). Liu et al. stated that DEB-BACE combined with anlotinib is effective in the treatment of advanced non-small cell lung cancer, and can effectively improve the OS and PFS of patients (Liu et al., 2021a). In our study, DEB-BACE loaded with BEV resulted in an ORR of 44%, while the DCR was 100% after DEB-BACE. The OS rates at 6- and 12-month were 77.8% and 66.7%, respectively. Therefore, DEB-BACE loaded with BEV is a promising and well-tolerated treatment for patients with lung adenocarcinoma.

However, it is still controversial whether DEB-BACE can prolong the progression-free survival and overall survival of LC. Many short-term studies have shown that DEB-TACE can increase the PFS rate and OS of patients. However, several long-term follow-ups show that there is no difference in survival rate between DBE-TACE and TACE in hepatocellular carcinoma (Cheung et al., 2016). Even so, DEB-BACE can be used as a palliative treatment for advanced lung cancer, effectively relieving symptoms in combination with other therapy (Chen et al., 2017). Consequently, the short-term and long-term efficacy of DEB-BACE in patients with LC needs to be confirmed by larger sample size research.

In terms of safety, DEB-BACE is similar to chemoembolization of solid tumors, mainly with post-embolization syndrome, which can be relieved after appropriate treatment. It should be noted that with DEB-BACE, there is a need to carefully observe the angiographic results to avoid ectopic embolism. The most important aspect to pay attention to is the spinal artery, with the risk of paraplegia if it is embolized by mistake. The main complications of BEV include hypertension, proteinuria, thromboembolism, and hemorrhage. In this study, two patients developed skin pruritus, which is tolerable and may be related to other oral target immune drugs. One patient suffered ankle edema that might have been related to BEV, which leads to abnormal renal function and proteinuria. Another patient developed a toothache, which was relieved after oral painkillers.

In addition, patients with lung cancer often suffer from hemoptysis. Previous reports have shown that BACE/DEB-BACE can effectively stop bleeding. Li et al. stated that BACE for advanced LC with hemoptysis is effective and tolerable, with a clinical success rate of 86.6% (Xiaobing et al., 2022). DEB-BACE combined with BEV is not suitable for lung cancer patients with hemoptysis. BEV may aggravate the bleeding. Patients with pulmonary hemorrhage/hemoptysis within 3 months should not use BEV. According to the patient's condition, conventional chemoembolization or DEB-BACE-loaded chemotherapeutic drugs can be used. In our study, nine patients had chronic diseases of different degrees, and no serious complications occurred. Therefore, it is relatively safe to use DEB-BACE loaded with BEV for LUAD; however, more cases are needed to confirm this conclusion.

Some limitations existed in our study: First, this study is a single-center retrospective study, hence, there may be selection bias and interference factors. Second, in this study, nine LUAD patients were treated by BEV-loaded DEB-BACE combined with immunotherapy and targeted therapy retrospectively. A prospective study with larger sample size is needed to confirm the accuracy of this study. Finally, long-term follow-up is needed to evaluate the long-term efficacy.

In conclusion, BEV-loaded DEB-BACE combined with immunotherapy and targeted therapy is a promising and well-tolerated treatment for patients with lung adenocarcinoma.

Data availability statement

The raw data supporting the conclusion of this article will be made available by the authors, without undue reservation.

Ethics statement

The studies involving human participants were reviewed and approved by The First Affiliated Hospital of Zhengzhou University. The patients/participants provided their written informed consent to participate in this study. Written informed consent was obtained from the individual(s) for the publication of any potentially identifiable images or data included in this article.

Author contributions

HL: Conceptualization, data collection, formal analysis, investigation, methodology, data curation and analysis, manuscript writing original draft, review, editing, and revision. YL: Conceptualization, data collection, formal analysis, investigation, methodology, data curation and analysis, review, editing, and revision. ZL: Data collection, formal analysis, data curation and analysis, supervision, manuscript writing original draft and review. XH: Conceptualization, formal analysis, investigation, methodology, data curation, and analysis, supervision, project administration, manuscript writing original draft, review, editing, and revision. KR: Conceptualization, formal analysis, investigation, methodology, data curation and analysis, supervision, project administration, manuscript writing original draft, review, editing, and revision. All authors listed have made a substantial, direct, and intellectual contribution to the work and approved it for publication.

Funding

The research was funded by the Natural Science Fund of Henan Province (222300420349).

Conflict of interest

The authors declare that the research was conducted in the absence of any commercial or financial relationships that could be construed as a potential conflict of interest.

Publisher's note

All claims expressed in this article are solely those of the authors and do not necessarily represent those of their affiliated organizations, or those of the publisher, the editors and the reviewers. Any product that may be evaluated in this article, or claim that may be made by its manufacturer, is not guaranteed or endorsed by the publisher.

References

Bi, Y., Zhang, B., Ren, J., Han, X., and Wu, W. (2022). Clinical outcomes of gemcitabine-loaded callispheres drug-eluting beads for patients with advanced and inoperable lung cancer: A case series study. *Front. Pharmacol.* 13, 992526. doi:10.3389/fphar.2022.992526

Bie, Z., Li, Y., Li, B., Wang, D., Li, L., and Li, X. (2019). The efficacy of drug-eluting beads bronchial arterial chemoembolization loaded with gemcitabine for treatment of non-small cell lung cancer. *Thorac. Cancer* 10, 1770–1778. doi:10.1111/1759-7714.13139

Boas, F. E., Kemeny, N. E., Sofocleous, C. T., Yeh, R., Thompson, V. R., Hsu, M., et al. (2021). Bronchial or pulmonary artery chemoembolization for unresectable and unablatable lung metastases: A phase I clinical trial. *Radiology* 301, 474–484. doi:10.1148/radiol.2021210213

Cao, H., Jin, S., and Bai, B. (2022). Efficacy analysis of DSA-guided bronchial arterial chemoembolization interventional therapy in patients with middle-advanced primary bronchial lung cancer. *Comput. Math. Methods Med.* 2022, 3722703. doi:10.1155/2022/3722703

Chang, C., Qiu, J., O'Sullivan, D., Buck, M., Noguchi, T., Curtis, J., et al. (2015). Metabolic competition in the tumor microenvironment is a driver of cancer progression. *Cell.* 162, 1229–1241. doi:10.1016/j.cell.2015.08.016

Chang, Y., Jeong, S., Young Jang, J., and Jae Kim, Y. (2020). Recent updates of transarterial chemoembolilzation in hepatocellular carcinoma. *Int. J. Mol. Sci.* 21, 8165. doi:10.3390/ijms21218165

Chen, Y., Li, Y., Jia, Y., Lei, K., Zhang, X., Cao, Y., et al. (2017). Bronchial artery chemoembolization combined with radioactive iodine-125 seed implantation in the treatment of advanced nonsmall cell lung cancer. *J. cancer Res. Ther.* 13, 636–641. doi:10.4103/jcrt.JCRT_93_17

Cheung, A., Lam, C., Tam, H., Cheung, T., Pang, R., and Poon, R. (2016). Nine-year experience of doxorubicin-eluting beads chemoembolization for hepatocellular carcinoma. *Hepatobiliary Pancreat. Dis. Int. HBPD INT* 15, 493–498. doi:10.1016/s1499-3872(16)60133-9

Choi, J., Cho, H., Park, J., Baek, S., Chung, J., Kim, D., et al. (2014). Comparison of drug release and pharmacokinetics after transarterial chemoembolization using diverse lipiodol emulsions and drug-eluting beads. *PloS one* 9, e115898. doi:10.1371/journal.pone.0115898

Datta, J., Narayan, R., Kemeny, N., and D'Angelica, M. (2019). Role of hepatic artery infusion chemotherapy in treatment of initially unresectable colorectal liver metastases: A review. *JAMA Surg.* 154, 768–776. doi:10.1001/jamasurg.2019.1694

Dong, H. X., Wang, R., Jin, X. Y., Zeng, J., and Pan, J. (2018). LncRNA DGCR5 promotes lung adenocarcinoma (LUAD) progression via inhibiting hsa-mir-22-3p. *J. Cell. Physiol.* 233, 4126–4136. doi:10.1002/jcp.26215

Galle, P., Tovoli, F., Foerster, F., WöRNS, M., Cucchetti, A., and Bolondi, L. (2017). The treatment of intermediate stage tumours beyond TACE: From surgery to systemic therapy. *J. hepatology* 67, 173–183. doi:10.1016/j.jhep.2017.03.007

Li, Y. M., Guo, R. Q., Bie, Z. X., Li, B., and Li, X. G. (2021). Sintilimab plus bronchial arterial infusion chemotherapy/drug-eluting embolic chemoembolization for advanced non-small cell lung cancer: A preliminary study of 10 patients. *J. Vasc. Interv. Radiol.* 32, 1679–1687. doi:10.1016/j.jvir.2021.08.019

Liu, J., Zhang, W., Ren, J., Li, Z., Lu, H., Sun, Z., et al. (2021a). Efficacy and safety of drug-eluting bead bronchial arterial chemoembolization plus anlotinib in patients with advanced non-small-cell lung cancer. *Front. Cell. Dev. Biol.* 9, 768943. doi:10.3389/fcell.2021.768943

Liu, X., Lin, H., Wang, Q., Mu, M., Pan, P., Tian, F., et al. (2021b). Drug-eluting bead bronchial arterial chemoembolization vs. chemotherapy in treating advanced non-small cell lung cancer: Comparison of treatment efficacy, safety and quality of life. *Eur. Rev. Med. Pharmacol. Sci.* 25, 2554–2566. doi:10.26355/eurrev_202103_25419

Martin, P., and Leighl, N. B. (2017). Review of the use of pretest probability for molecular testing in non-small cell lung cancer and overview of new mutations that may affect clinical practice. *Ther. Adv. Med. Oncol.* 9, 405–414. doi:10.1177/1758834017704329

Paz-Ares, L., Ciuleanu, T., Cobo, M., Schenker, M., Zurawski, B., Menezes, J., et al. (2021). First-line nivolumab plus ipilimumab combined with two cycles of chemotherapy in patients with non-small-cell lung cancer (CheckMate 9LA): An international, randomised, open-label, phase 3 trial. *Lancet. Oncol.* 22, 198–211. doi:10.1016/s1470-2045(20)30641-0

Reck, M., Remon, J., and Hellmann, M. (2022). First-line immunotherapy for non-small-cell lung cancer. *J. Clin. Oncol. official J. Am. Soc. Clin. Oncol.* 40, 586–597. doi:10.1200/jco.21.01497

Sieghart, W., Hucke, F., and Peck-Radosavljevic, M. (2015). Transarterial chemoembolization: Modalities, indication, and patient selection. *J. Hepatol.* 62, 1187–1195. doi:10.1016/j.jhep.2015.02.010

Xiaobing, L., Meipan, Y., Pengfei, X., Yue, Z., Ying, L., Xiangnan, L., et al. (2022). Bronchial artery chemoembolization for hemoptysis in advanced primary lung cancer. *Clin. lung cancer* 23, e203–e209. doi:10.1016/j.cllc.2021.10.011

Xu, S., Bie, Z. X., Li, Y. M., Li, B., Kong, F. L., Peng, J. Z., et al. (2022). Drug-eluting bead bronchial arterial chemoembolization with and without microwave ablation for the treatment of advanced and standard treatment-refractory/ineligible non-small cell lung cancer: A comparative study. *Front. Oncol.* 12, 851830. doi:10.3389/fonc.2022.851830

Yang, L., Liu, M., Cao, X., Li, N., Zheng, B., Deng, J., et al. (2022). Efficacy and safety of adding bevacizumab biosimilar or original drug to platinum-based chemotherapy as first-line treatment in patients with advanced NSCLC: A systematic review and meta-analysis. *Ther. Adv. Med. Oncol.* 14, 17588359221130501. doi:10.1177/17588359221130501

Yang, S., Zhang, Z., and Wang, Q. (2019). Emerging therapies for small cell lung cancer. *J. Hematol. Oncol.* 12, 47. doi:10.1186/s13045-019-0736-3

Yang, X., Wu, G., Li, Z., Wu, H., Sun, Y., Wen, H., et al. (2016). Efficacy for artery chemoembolization combined with radiofrequency ablation in the treatment of advanced non-small cell lung cancer. *Zhonghua yi xue za zhi* 96, 539–543. doi:10.3760/cma.j.issn.0376-2491.2016.07.010

Yu, G., and Hu, J. (2020). Drug-eluting beads bronchial arterial chemoembolization as a neoadjuvant treatment for squamous non-small cell lung cancer. *Postgrad. Med.* 132, 568–571. doi:10.1080/00325481.2020.1761711

Zhou, G., Han, J., Sun, J., Zhang, Y., Zhou, T., Nie, C., et al. (2018). Efficacy and safety profile of drug-eluting beads transarterial chemoembolization by CalliSpheres® beads in Chinese hepatocellular carcinoma patients. *BMC cancer* 18, 644. doi:10.1186/s12885-018-4566-4

frontiers | Frontiers in Immunology

TYPE Case Report
PUBLISHED 24 May 2023
DOI 10.3389/fimmu.2023.1203876

Check for updates

OPEN ACCESS

EDITED BY
Yuan Wan,
Binghamton University, United States

REVIEWED BY
Yaying Sun,
Fudan University, China
Kewei Wang,
Affiliated Hospital of Jiangnan University, China

*CORRESPONDENCE
Xiuliang Tang
42155894@qq.com
Ying Fang
fangying@njmu.edu.cn

†These authors have contributed equally to this work

RECEIVED 11 April 2023
ACCEPTED 16 May 2023
PUBLISHED 24 May 2023

CITATION
Xu K, Gao J, Feng L, Fang Y and Tang X (2023) A case report of pulmonary hepatoid adenocarcinoma: promoting standardized diagnosis and treatment of the rare disease.
Front. Immunol. 14:1203876.
doi: 10.3389/fimmu.2023.1203876

COPYRIGHT
© 2023 Xu, Gao, Feng, Fang and Tang. This is an open-access article distributed under the terms of the Creative Commons Attribution License (CC BY). The use, distribution or reproduction in other forums is permitted, provided the original author(s) and the copyright owner(s) are credited and that the original publication in this journal is cited, in accordance with accepted academic practice. No use, distribution or reproduction is permitted which does not comply with these terms.

A case report of pulmonary hepatoid adenocarcinoma: promoting standardized diagnosis and treatment of the rare disease

Kun Xu[1†], Jin Gao[1†], Lili Feng[2†], Ying Fang[1*] and Xiuliang Tang[3*]

[1]Department of Medical Oncology, Jiangsu Cancer Hospital and Jiangsu Institute of Cancer Research and The Affiliated Cancer Hospital of Nanjing Medical University, Baiziting, Nanjing, China, [2]Department of Thoracic Surgery, Jiangsu Cancer Hospital and Jiangsu Institute of Cancer Research and The Affiliated Cancer Hospital of Nanjing Medical University, Baiziting, Nanjing, China, [3]Department of Ultrasonography, Jiangsu Cancer Hospital and Jiangsu Institute of Cancer Research and The Affiliated Cancer Hospital of Nanjing Medical University, Baiziting, Nanjing, China

Objective: To investigate the clinical features, pathological characteristics, immunophenotype, differential diagnosis and prognosis of pulmonary hepatoid adenocarcinoma using a clinical case and literature report.

Methods: We analyzed the clinical presentation, histological pattern and immunohistochemistry of a case of primary hepatoid adenocarcinoma of the lung in April 2022. We also reviewed literature on hepatoid adenocarcinoma of the lung from PubMed database.

Results: The patient was a 65-year-old male with smoking history, who was admitted to hospital with an enlarged axillary lymph node. The mass was round, hard, and grayish-white and grayish-yellow in color. Microscopically, it presented hepatocellular carcinoma-like and adenocarcinoma differentiation features, with abundant blood sinuses visible in the interstitium. Immunohistochemistry showed that the tumor cells were positive for hepatocyte markers, including AFP, TTF-1, CK7 and villin, and negative for CK5/6, CD56, GATA3, CEA and vimentin.

Conclusion: Pulmonary hepatoid adenocarcinoma is a rare epithelial malignancy of primary origin in the lung with poor prognosis. Establishing the diagnosis relies mainly on the detection of hepatocellular structural morphology resembling hepatocellular carcinoma, and on clinicopathological and immunohistochemical testing to exclude diseases such as hepatocellular carcinoma. Combination treatment, mainly surgery, can prolong the survival of early-stage cases of the disease, whereas radiotherapy is mostly used for intermediate and advanced

cases. Individualized treatment with molecular-targeted drugs and immunotherapy has shown different therapeutic effects for different patients. Further research is needed to better understand this rare clinical condition for the development and optimization of treatment strategies.

KEYWORDS

lung cancer, pulmonary hepatoid adenocarcinoma, diagnosis and differential diagnosis, immunohistochemistry, genetic testing

1 Introduction

Hepatoid adenocarcinoma (HAC) is a rare clinical condition that occurs outside the liver and has a similar morphology to that of hepatocellular carcinoma. It is highly malignant and aggressive, leading to a poor prognosis for patients. Pulmonary hepatoid adenocarcinoma (PHAC) is a rare epithelial malignancy of primary origin in the lung. The tumor can occur in many organs throughout the body, most frequently the stomach, but can also occur in the lungs. Establishing the diagnosis relies mainly on the detection of hepatocellular structural morphology resembling hepatocellular carcinoma, and on clinicopathological and immunohistochemical testing to exclude diseases such as hepatocellular carcinoma. Combination treatment, mainly surgery, can prolong the survival of early-stage cases of the disease, whereas radiotherapy is mostly used for intermediate and advanced cases. Individualized treatment with molecular-targeted drugs and immunotherapy has shown different therapeutic effects for different patients. Herein, we report a case of PHAC admitted to our hospital, analyze and summarize its clinical and pathological features, multi-omics data, immunophenotype, differential diagnosis, treatment and prognosis in the light of the literature for the first time, with the aim of improving clinical and pathologists' understanding of PHAC for reference in clinical work.

2 Case presentation

2.1 General information

A 65-year-old male was admitted to our hospital in April 2022 for physical examination due to enlarged axillary lymph nodes and a mass in the left upper lung for a month. He had a history of smoking for more than 30 years, no history of hepatitis, and no other specific medical history such as gastric tumor. A chest CT and MRI showed a left upper lung mass indicative of a malignant lesion (Figures 1A, B). A lung puncture biopsy was performed, and metastatic adenocarcinoma was considered (Figure 2). Immunohistochemistry (IHC) of the biopsy suggested that it may have a biliary-pancreatic origin. PET-CT later revealed that: (1) soft tissue nodular hypermetabolic foci in the left upper lung adjacent to the mediastinum, with a high probability of malignancy; (2) multiple nodular hypermetabolic foci in the hilum bilaterally, with a high probability of mediastinal lymph node metastases; (3) nodular hypermetabolic foci in the left axilla. Serum AFP was 5820 ng/ml, and other tumor markers, including CEA, CA125, CA153, CA199 and NSE, were normal. Abdominal CT showed no abnormal masses in the liver, with possible multiple cysts in both kidneys and spleen. There were no abnormalities in the gallbladder, pancreas or abdominal cavity. No masses were palpable in the testes. Clinical diagnosis was left upper lung mass with a high probability of lung cancer.

2.2 Surgical treatment

The patient underwent thoracoscopic lobectomy with intrathoracic lymph node dissection, pulmonary artery trunk repair and radical axillary lymph node dissection in May 2022. 1.3 cm of the seventh intercostal space in the left axillary midline was used as the observation hole and 3.5 cm of the fourth intercostal space in the left anterior axillary line was used as the main operation hole. Intraoperative exploration revealed limited intrathoracic adhesions, no pleural effusion or abnormal nodules, and a 2.5 cm solid mass in the upper lobe of the left lung involving the pleura, with pleural folds. Enlarged lymph nodes of the first branch of the pulmonary artery were observed, surrounded by vessels, and enlarged lymph nodes of groups 5, 6, 7, 10, 11 and 12, were gray-black and hard. This was consistent with the preoperative diagnosis, and the decision was made to perform a left upper lung lobectomy.

The left inferior pulmonary ligament was dissected and released, the posterior mediastinal pleura in front of the pulmonary hilum was dissected, the left superior pulmonary vein was released and skeletonized, and the interlobular fissure

Abbreviations: HAC, Hepatoid Adenocarcinoma; HE, hematoxylin and eosin; TAA, tumor-associated antigen; c-kit, CD117; LUSC: lung squamous cell carcinoma; LUAD, lung adenocarcinoma; TPS, tumor proportion score; AAT, alpha-1 antitrypsin; CT, computerized tomography; PET-CT, Positron Emission Tomography-Computed Tomography; MRI, Magnetic Resonance Imaging; TF, transferrin; M, Male; F,Female; RS, radical surgery; C, chemotherapy; I, Immunotherapy; R, Radiotherapy; LL, left lobe; RL, right lobe; LUL, left upper lobe; RUL, right upper lobe; RLL, right lower lobe; LLL, left lower lobe; RML, Right middle lobe; AFP, Alpha Fetoprotein; N/A, Not applicable.

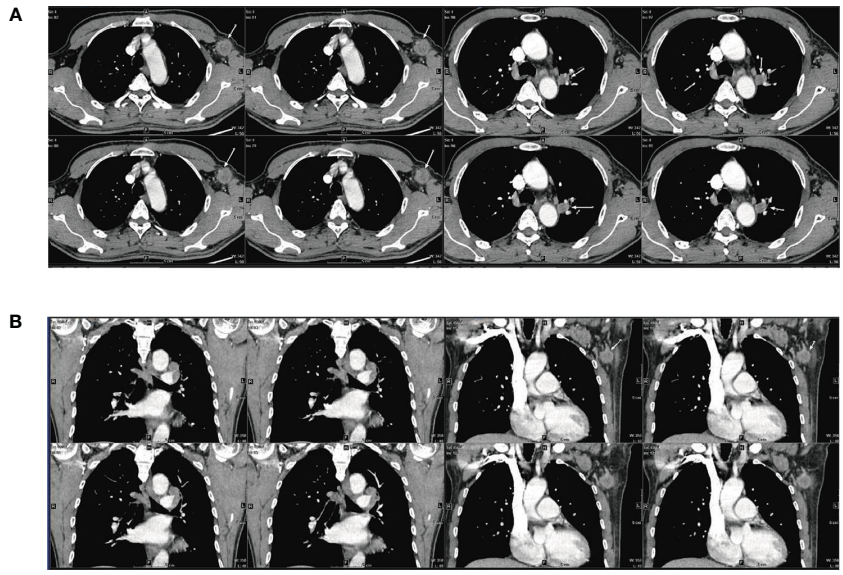


FIGURE 1
CT and MRI scan results for the patient **(A)** CT: Soft tissue nodular mass in the left upper lung adjacent to the mediastinum, measuring approximately 1.31×1.79 cm; multiple masses and enlarged lymph nodes in the aortopulmonary window, above the eminence, and both lung hilums; larger mass at the left lung hilum measuring 1.29×2.06 cm; (3) Mass with slight density visible in the left axilla, unevenly enhanced nodule is visible, measuring approximately 2.32×2.5 cm. **(B)** MRI: Dynamic contrast-enhanced MRI: multiple masses and enlarged lymph nodes in the aortopulmonary window, above the eminence, and both lung hilums; mass in the left lung hilum measuring approximately 1.6×1.6 cm; Enlarged lymph nodes visible in the left axilla, measuring approximately 2.4×1.9 cm.

was dissected. The left pulmonary artery trunk was dissected and skeletonized, the left superior pulmonary hyoid artery was further dissected and severed, and the interlobular fissure between the upper and lower lung lobes was closed and dissected using the endoscopic cutting suture device. The left superior pulmonary vein was closed and severed using the endoscopic cutting suture device. The left superior pulmonary artery was sutured with "4" surgical suture, and the anterior and posterior branches of the left superior pulmonary artery were closed and dissected using the endoscopic cutting suture device. The lymph nodes adjacent to the upper left pulmonary bronchus were cleared, closed and dissected with the endoscopic cutting suture device, and the bronchial stump was interrupted with 3-0 absorbable sutures.

The intraoperative rapid pathology report was "Left upper lung: carcinoma. Resection margin: no obvious malignancy". Lymph nodes were further cleared. Postoperative pathological examination suggested a partial lobectomy specimen measuring 16.0 cm×9.0 cm×3.0 cm, with a round nodule measuring approximately 2.2 cm×1.7 cm×1.5 cm in size along the bronchial incision, with a grayish-white and grayish-yellow, hard surface and some areas of necrosis. Left upper lung: poorly differentiated carcinoma of the central type, pending IHC, no pleura was reached. Bronchial resection margin (-). Metastatic carcinoma was seen in the parabronchial (1/3) lymph node. Left axillary (1/1), group 11 (1/2), group 12 (1/1), 4L (1/1), metastatic carcinoma seen in the lymph nodes of group 11 (1/1), pending immunohistochemistry. No metastatic carcinoma was seen in lymph nodes of groups 5 (0/3), 7 (0/1), or 10 (0/1).

2.3 Specimen processing

Tissue specimens were fixed in 10% neutral formaldehyde, sampled according to standard procedure, dehydrated, paraffin-embedded, sectioned at 4 μm thickness, stained with conventional hematoxylin and eosin (HE) staining and IHC, and imaged by brightfield microscopy. The antibodies used for diagnosis and differential diagnosis were purchased from Beijing Zhong Shan-Golden Bridge Biological Technology Co., Ltd. IHC was performed using the EnVision two-step method and the staining step process was carried out strictly according to the kit instructions with positive and negative controls.

3 Results

3.1 Clinicopathological features

The HAC tissue had a fibrous border (Figure 2A). Tumor cells were glandular in shape, with a nest-like adenoid structure (Figure 2B). Necrosis and phagocytosis were identified in the centers of some glandular lumens (Figure 2C). Some cells were polygonal, with eosinophilic or clear cytoplasm (Figure 2D). Sieve-like structures characterized as neutral mucus in glandular lumens were observed, and intra-cellular features demonstrated abundant cytoplasm, biphasic, with distinct vesicular nuclei, small nucleoli, and apoptotic vesicles (Figures 2E, F). Sub-cellular pathology showed enlarged and highly atypical vesicular nuclei with fine,

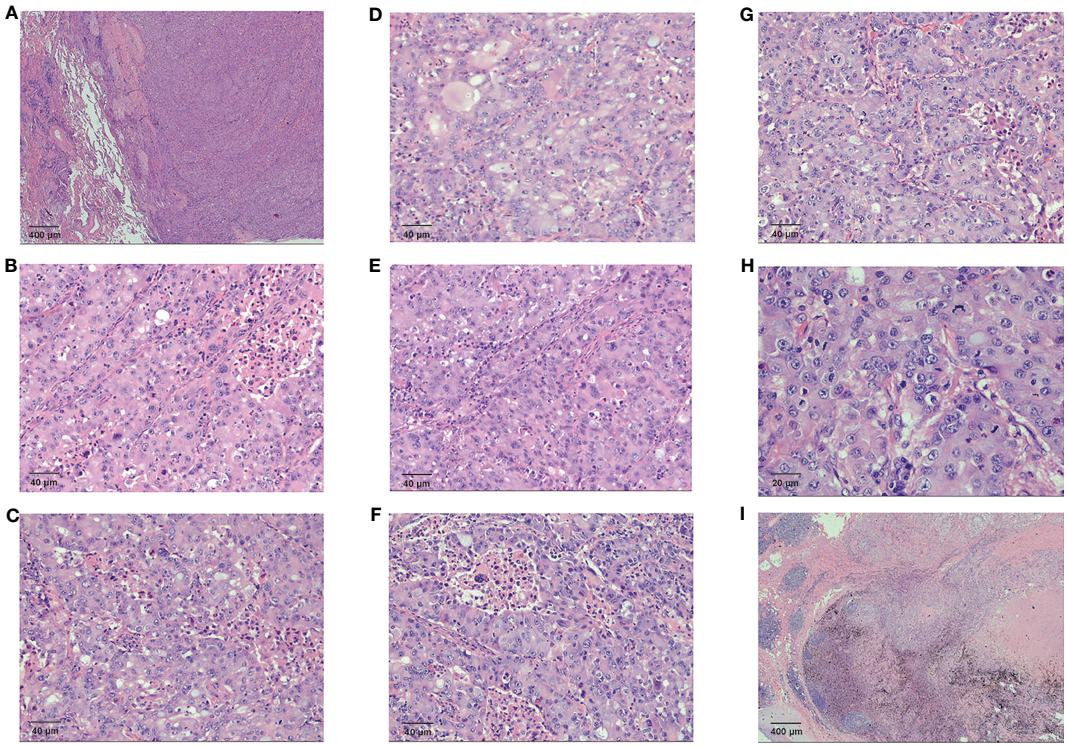


FIGURE 2
Pathological examination results for the patient **(A)** The fibrous border of the tumor (HE 20×) **(B)** Tumor cells were glandular in shape, with a nest-like adenoid structure (HE 200×) **(C)** Necrosis and phagocytosis were seen in the central part of the glandular lumen in some area (HE 200×) **(D)** Some cells were polygonal, with eosinophilic or clear cytoplasm (HE 200×) **(E)** Sieve-like structures were observed. Some of the cytoplasm and the central part of the glandular lumen had neutral mucus (HE 200×) **(F)** Abundant cytoplasm, biphasic, with distinct vesicular nuclei, small nucleoli, and apoptotic vesicles were visible (HE 200×) **(G)** Enlarged nucleoli and high nuclear grade were seen in some of the vesicular nuclei (HE 200×) **(H)** Some of the vesicular nuclei were enlarged and had high nuclear grade, with fine, open chromatin in the nuclei and pathological nuclear divisions (HE 400×) **(I)** The cancerous tissue directly invaded the hilar lymph nodes (HE 20×).

open chromatin and pathological nuclear divisions (Figures 2G, H). Moreover, the cancerous tissue directly invaded the hilar lymph nodes (Figure 2I).

3.2 IHC

Left lung occupancy IHC marker results supported high-grade hepatoid adenocarcinoma. Pathological diagnosis was combined with clinical and other tests (SWI/SNF-deficient tumors were excluded). Results were: CK5/6-, p40-, CK7 3+, TTF1 cytoplasmic 2+, CD56-, S-100, Syn-, GATA3-, KUC43+, CD117 partial 2+, SALL4-, D2-40-, CD30-, D0G1-, Hep-12+, INI-1+, BRG1+, PD-L1 (TPS)+50% <MXR003>, Ki-67 + 70%, ALK(V)-. Left axillary lymph node: GATA3-, villin2+, MUC42+, TTF1 cytoplasmic fraction 2+, SALL4-, CD117 foci+ (Figures 3A–F).

3.3 Genetic testing

Genetic testing covered a total of 111 genes, including the whole exome and specific intronic regions of eight commonly rearranged genes. Eight somatic mutations were detected, among which one had significant clinical significance, three had potential clinical significance, and four had unclear clinical significance. No pathogenic or likely pathogenic germline mutations were detected.

Discussion

Pulmonary hepatoid adenocarcinoma is extremely rare, with only 60 published case reports included on Pubmed to date since its first presentation in the 1990s (Table 1). The tumor differs from common lung cancer subtypes in clinical presentation, pathological features and immunophenotype according to the latest WHO classification. Given the rarity and aggressiveness of the disease, a complete clinical presentation and morphological description, biological behavior and prognosis of any new case may contribute to the study and classification of the disease. Herein, we discuss pulmonary hepatoid adenocarcinoma in detail, in order to improve our understanding of this rare disease.

Hepatoid adenocarcinoma is a rare clinical condition with an aggressive extrahepatic tumor that morphologically resembles hepatocellular carcinoma. It was first named by Ishikura and colleagues in 1985 (56). In 2010, Metzgeroth and colleagues summarized the clinical features and case data of 261 cases of hepatoid adenocarcinoma, with the most frequent site of occurrence being the stomach (63%), with other cases being reported in the

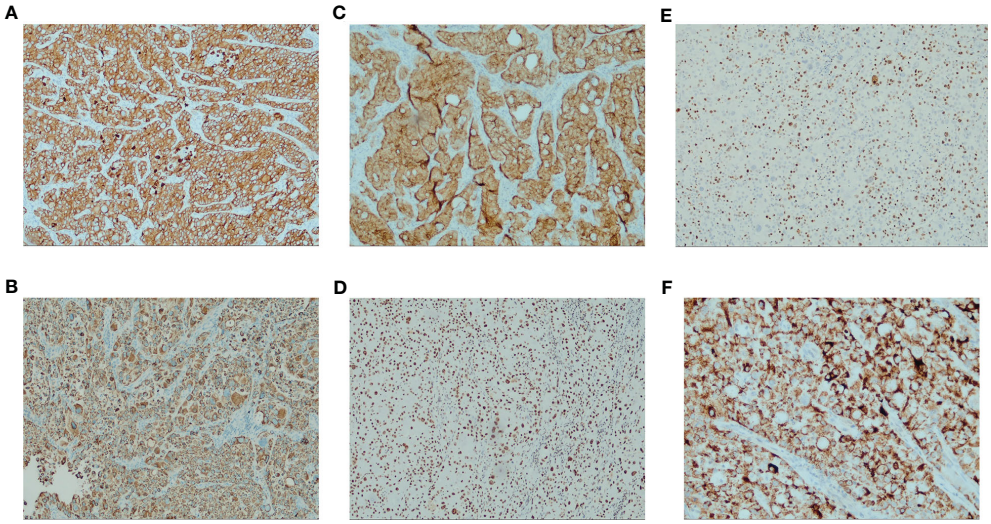


FIGURE 3
Immunohistochemistry results for the patient **(A)** CK7 strong positive (IHC [EnVision] 100×) **(B)** HepPar-1 positive (IHC [EnVision] 100×) **(C)** Villin positive (IHC [EnVision] 100×) **(D)** BRG1 (SMARCA4) Loss not detected (IHC [EnVision] 100×) **(E)** Ki-67 proliferation index > 50% (IHC [EnVision] 100×) **(F)** TTF1 characteristic features: intense cytoplasm staining and no nuclear stain (IHC [EnVision] 400×).

TABLE 1 Summary of publications on pulmonary hepatoid adenocarcinoma cases.

First Author, Year	Country	Sex	Age (Years)	Smoking (pack-year)	Location	Size(cm)	AFP	TNM	Treatment	Survival/ State
(1) Yasunami R, 1981	Japan	M	67	N/A	LUL	8	AFP↑	pT4N0M0 (IIIA)	R, I, C	16 months/ dead
(2) Miyake M, 1986	Japan	M	55	N/A	RUL	5	AFP↑	pT4N2M1c (IVB)	RS	0.13 months/ dead
(3) Tamura T, 1986	Japan	M	80	41	LLL	4.1 × 3.5	AFP↑	cT4N3M1a (IVA)	C	36 months/ alive
(4) Miyake M, 1987	Japan	M	73	N/A	LUL	5 × 6 × 5	AFP↑	pT3N2M0 (IIIB)	RS, R	18 months/ dead
(5) Saka H, 1988	Japan	M	73	N/A	RUL	3.9 × 3 × 3	AFP↑	pT2aN0M0 (IB)	RS	28 months/ alive
(6) Kurimoto I, 1989	Japan	M	75	40	RUL	5	AFP↑	cT3N2M0 (IIIB)	N/A	N/A
(7) Okunaka T, 1992	Japan	M	49	Yes	RUL	6	AFP↑	eT3	RS	11 months/ alive
(8) Yoshino I, 1996	Japan	M	54	N/A	RUL	2	AFP↑	pT1bN0M0 (IA2)	RS	24 months/ alive
(9) Hirota F, 1999	Japan	M	80	45	RLL	5 × 4	AFP↑	pT2bN2M1b (IVA)	C	10 months/ alive
(10) Carlinfante G, 2000	Italy	M	65	Yes	LLL	3.5	N/A	pT2aN0M0 (IB)	RS	84 months/ alive
(11) Genova S, 2001	Plovdiv	M	71	N/A	LUL	7.7 × 6.4	N/A	pT4N0M0 (IIIA)	RS	24 months/ alive
(12) Hayashi Y, 2002	Japan	M	55	87.5	RUL	5 × 4.8 × 6.5	N/A	pT3N0M0 (IIB)	RS	32 months/ alive

(Continued)

10.3389/fimmu.2023.1203876

TABLE 1 Continued

First Author, Year	Country	Sex	Age (Years)	Smoking (pack-year)	Location	Size(cm)	AFP	TNM	Treatment	Survival/ State
(13) Terracciano LM, 2003	Switzerland	M	49	N/A	LLL	5	AFP↑	pT2bN0M0 (IIA)	RS	2 months/ dead
(14) Oshiro Y, 2004	Japan	M	76	N/A	RLL	18 × 17 × 12	N/A	pT4N0M0 (IIIA)	RS	18 months/ dead
(15) Ivan M, 2007	Canada	M	54	40	LUL + RUL	(13 × 11) + (3.3 × 2.6)	AFP↑	pT4N2bM1b (IVA)	C, R	N/A
(16) Kishimoto T, 2008	Japan	M	64	N/A	LLL	7.5 × 7 × 4	AFP↑	cT4N0M0 (IIIA)	RS	N/A
(17) Li CJ, 2008	China	M	65	N/A	RLL	6	AFP↑	cT4N2M1 (IVA)	TACE, TCM	16 months/ dead
(18) Fornasa F, 2010	Italy	F	68	No	LUL	4.5 × 4 × 4	AFP→	pT2bN0M1 (IVA)	C	15 months/ alive
(19) Kitada M, 2011	Japan	M	69	90	RLL	6.5	AFP↑	pT3N2M0 (IIIB)	RS, C	12 months/ alive
(20) Mokrim M, 2012	Morocco	M	52	20	LUL	11.8 × 12 × 8	AFP↑	cT4N1M0 (IIIA)	C	7 months/ alive
(21) Papatsimpas G, 2012	Greece	M	48	N/A	RUL	20 × 11 × 8	AFP↑	cT4N2bM0 (IIIB)	C, R	6 months/ dead
(22) Valentino F, 2012	Italy	M	71	No	RLL	2.8 and 1.9	AFP↑	pT3N3M1b (IVA)	C, R, RS, bevacizumab	14 months/ dead
(23) Cavalcante LB, 2013	Brazil	M	66	40	RLL	5 × 3	N/A	pT2bN0M0 (IIA)	Supportive treatment	0.4 months/ dead
(24) Che YQ, 2014	China	M	66	70	LUL	5.3 × 4.6 and 7.9 × 10.0	AFP↑	pT4N0M0 (IIIA)	C, R	36 months/ dead
(25) Haninger DM, 2014	America	M	51	45	RUL	4.2 × 3.7	N/A	cT2bN3M0 (IIIB)	No	14 months/ dead
(25) Haninger DM, 2014	America	M	52	40	RUL	2.5	N/A	pT1cN0M1c (IVB)	No	37 months/ alive
(25) Haninger DM, 2014	America	M	64	75	LUL	3.2 × 2.2	N/A	pT2aN0M1b (IVA)	No	10 months/ dead
(25) Haninger DM, 2014	America	F	54	35	LUL	1	N/A	pT1aN0M1b (IVA)	C, R	108 months/ alive
(25) Haninger DM, 2014	America	M	60	40	RUL	11.2 × 10.1 × 8.5	AFP↑	cT4N2M1b (IVA)	No	1 months/ alive
(26) Shaib W, 2014	America	F	53	40	RUL	9.5 × 9.0 × 8.0	AFP↑	pT4N0M0 (IIIA)	RS, C	48 months/ alive
(27) Al-Najjar H, 2015	England	M	71	30	RLL	Multiple	AFP↑	cT4N3M1a (IVA)	C	12 months/ dead
(28) Gavrancic T, 2015	America	M	64	N/A	RUL	3.8 × 2.9	AFP↑	cT2aN2M1 (IVA)	C, Sorafenib, R	11 months/ dead
(29) Grossman Kate, 2016	America	M	54	Yes	RUL	5.1 × 4.1	AFP→	cT3N0M1b (IVA)	C, R	3 months/ dead
(30) Qian GQ, 2016	China	M	79	50	RUL	2.7 × 2.6	AFP↑	cT1cN0M0 (IA3)	Erlotinib	0.83 months/ dead
(31) Sun JN, 2016	China	M	59	Yes	RUL	4.5 × 3.5 × 3.5	N/A	pT2bN0M0 (IIA)	RS	23 months/ alive

(Continued)

10.3389/fimmu.2023.1203876

TABLE 1 Continued

First Author, Year	Country	Sex	Age (Years)	Smoking (pack-year)	Location	Size(cm)	AFP	TNM	Treatment	Survival/ State
(32) Wang S, 2016	China	M	56	N/A	RUL	4.0 × 4.1 × 4.8	N/A	cT4N1M0 (IIIA)	N/A	N
(33) Basse V, 2018	France	M	43	8	N/A	N/A	N/A	cTxN3M1c (IVB)	C, durvalumab anti- PD-L1 therapy	dead without following time
(34) Esa NYM, 2018	Malaysia	M	50	40	LUL	6 × 5 × 6	AFP↑	IIIB	R, C	7 months/ dead
(35) Li Q, 2018	China	M	52	60	RUL	N/A	N/A	cT2N2M0 (IIIA)	C, R	2 months/ dead
(36) Nakashima K, 2018	Japan	M	60	40	RUL	6.3 × 4.8	AFP↑	pT3N0M0 (IIB)	RS	8 months/ alive
(37) Ruiz CD, 2018	N/A	F	69	70	LUL	8 × 8 × 5	AFP→	cT4N1M0 (IIIA)	R	1 months/ dead
(38) Ayub A, 2019	America	M	61	40	RUL	2.3	N/A	pT1cN0M0 (IA3)	RS, R	6 months/ dead
(39) Chen HF, 2019	China	M	53	No	RUL	5.3 × 3.5	AFP↑	pT3N0M0 (IIB)	RS, C, R, Icotinib, Osimertinib, Anlotinib	36 months/ alive
(39) Chen Y, 2019	China	M	47	45	RLL	9.7 × 6.1 × 6.9	AFP→	cT4N3M1c (IVB)	C	2 months/ dead
(40) El Khoury A, 2019	England	M	59	>30	RUL	9.3 × 7.2 × 6.8	N/A	cT4N2M1b (IVA)	C	14 months/ alive
(41) Kuan K, 2019	America	M	47	Yes	RUL	14	N/A	cT4N0M0 (IIIA)	RS	4 months/ dead
(42) Li J, 2019	China	M	71	No	RLL	7 × 4.5	AFP↑	cT3N3M1b (IVA)	R	5.5 months/ dead
(43) Malik SA, 2019	N/A	F	56	Yes	RLL	2 × 2	AFP→	N/A	N/A	2 months/ dead
(44) Shi YF, 2019	China	M	60	No	RUL	7 × 7 × 5	AFP↑	pT3N2M0 (IIIB)	RS, C	15 months/ dead
(45) Wang C, 2019	China	M	70	50	RUL	6.0 × 4.6	N/A	cT3N2M0 (IIIB)	C, R, Bevacizumab	9 months/ dead
(46) Yang K, 2019	China	M	70	120	LLL	6 × 6 × 5.5	N/A	pT3N1M0 (IIIA)	RS	18 months/ dead
(47) Chen JX, 2020	China	M	63	N/A	LLL+RUL	N/A	N/A	pT4N3M1c (IVB)	N/A	4 months/ dead
(48) Chen LL, 2020	China	F	65	No	LL+RL	(7 × 5.1) + (9.2 × 4.6)	AFP↑	pT4NxM1b (IVA)	C, Bevacizumab, Anlotinib, Sintilimab	53 months/ dead
(49) Muroyama Y, 2020	America	M	66	30	LUL	8 × 5	AFP↑	T4N3M1b	C+R	19 months/ dead
(50) Tonyali O, 2020	Turkey	F	62	Yes	LUL	8 × 7 × 7 and 3 × 2.5 × 2	AFP↑	T4N1M0	RS +C+I+R	14 months/ dead
(51) Chen Z, 2022	China	M	67	Yes	RML	7.1 × 5.3	AFP→	T4N1M0	C+ RS	13 months/ dead
(52) Xu S, 2022	China	M	55	70	LUL	8.46 × 6.53	AFP↑	cT4N3M1a (IVA)	C+I	13 months/ alive

(Continued)

TABLE 1 Continued

First Author, Year	Country	Sex	Age (Years)	Smoking (pack-year)	Location	Size(cm)	AFP	TNM	Treatment	Survival/ State
(53) Yao Y, 2022	China	M	63	N/A	LUL	7.5 × 5.5	AFP↑	T4N0M0 (IIIA)	RS	6 months/ dead
(54) Galina G, 2022	America	M	54	25	RLL	Multiple (max = 14)	AFP↑	cT4N0M0 (IIIA)	C+I	7 months/ alive
(55) Hou Z, 2021	China	M	66	Yes	RUL	3.3 × 2.5 × 4.0	AFP↑	cT2N2MO (IIIA)	C, R, Sorafenib +Sintilimab	13 months/ dead
This report	China	M	65	Yes	LUL	16.0 × 9.0 × 3.0 (2.2 × 1.7 × 1.5)	AFP↑	cT1cN2aM0 (IIIA)	RS +C +Sintilimab	6 months/ alive

*M, Male; F, Female; RS, radical surgery; C, chemotherapy; I, Immunotherapy; R, Radiotherapy; LL, left lobe; RL, right lobe; LUL, left upper lobe; RUL, right upper lobe; RLL, right lower lobe; LLL, left lower lobe; RML, Right middle lobe; AFP, Alpha Fetoprotein; N/A, Not applicable.

ovaries (10%), lungs (5%), gallbladder (4%), pancreas (4%) and uterus (4%) (57). There were also reports of hepatoid adenocarcinomas in the esophagus, duodenal papilla, jejunum, colon, rectum, peritoneum, thymus, mediastinum, kidney, renal pelvis, ureter and bladder. The prevalence is higher in males (male: female, 2.4:1), and the median age of onset is 65 years (21 to 88 years).

In 1990, Ishikura and colleagues studied seven cases of AFP-producing lung cancer and first proposed the name pulmonary hepatoid adenocarcinoma, five of which were confirmed to be hepatoid adenocarcinoma, and proposed diagnostic criteria for pulmonary hepatoid adenocarcinoma (58). The criteria were: (1) the presence of typical glandular or papillary adenocarcinoma; (2) the composition and expression of AFP are similar to those of hepatocellular carcinoma. However, in clinical practice, AFP expression was heterogenous in hepatoid adenocarcinoma cases. Previously, Haninger and colleagues proposed alternative diagnostic criteria for pulmonary hepatoid adenocarcinoma (25), including: (1) the tumor component can be purely hepatoid adenocarcinoma or hepatoid adenocarcinoma accompanied by typical glandular or papillary adenocarcinomas, imprinted cells, or neuroendocrine carcinoma; (2) positivity for AFP and other markers of hepatocellular differentiation is not essential; (3) adenocarcinoma with morphological features of hepatocellular carcinoma but without AFP production is referred to as AFP-negative hepatocellular lung adenocarcinoma.

Combining this case with the previous publications (Table 1), clinical symptoms of adenocarcinoma of the lung and liver are non-specific and similar to those of common subtypes of lung cancer. It usually starts with a cough and phlegm, chest tightness and shortness of breath, chest pain, and hemoptysis. Intrahepatic lesions are rarely identified, and patients have no history of liver disease, most patients have a smoking history, and the onset age is mostly over 50 years (38, 47). Most adenocarcinomas of the lung and liver are in a clinically progressive stage at the time of detection, and serum AFP is often elevated and correlates with disease activity. AFP levels often decrease after surgical removal of the primary tumors (58). For this patient with pulmonary hepatoid adenocarcinoma, preoperative AFP was 5820 ng/mL, which decreased to 1920 ng/mL five days after lobectomy AFP. Serum AFP was negative at 3 ng/mL on repeat chemotherapy in July, August and September, suggesting that AFP was produced from the tumor tissue.

Regarding pathological features, the tumors are usually large (up to 20 cm in diameter), grayish or gray-brown in color, well-defined, often necrotic, and could be enveloped by fibrous connective tissue. Microscopically, the tumors mainly consist of a hepatic differentiation region and a non-hepatic differentiation region. The tissue in the region of hepatic differentiation has nested masses and beam-like and sieve-like arrangements. Cancer cells appear to be large, polygonal, cytoplasm-rich, eosinophilic or hyaline, with large, PAS-positive nuclei. The interstitium inside the tumor tissue tends to be enriched in blood sinuses and often appears necrotic (20). Regions of non-hepatomatous differentiation are recognized as adenoid and papillary structures, with a few regions of poorly differentiated adenocarcinoma, some cases of steatosis or bile secretion, which may show imprinted cells or neuroendocrine differentiation (25).

Regarding immunohistochemical markers, AFP is a well-established marker for hepatocellular carcinoma, yolk sac tumor, embryonal carcinoma and other tumors of anterior intestinal origin. Elevated serum AFP or immunohistochemical expression of AFP is effective in the diagnosis of pulmonary hepatoid adenocarcinoma, but not all pulmonary hepatoid adenocarcinoma cases have significant AFP expression. Haninger and colleagues used a set of antibodies to compare the IHC features of lung metastases of hepatocellular carcinoma and five cases of pulmonary hepatoid adenocarcinoma. Co-expression of AFP,

Hepar and CK8/18, and negative expression of CK14 were reported (25). In this HAC case, the positive expression of HepPar-1, AFP and CK7 is consistent with the expression of hepatocellular carcinoma. However, CK8, CK18 and CK19 were negative, which helps identify metastatic hepatocellular carcinoma. CK7 and CK19 are markers of bile duct epithelium, and in cases of intrahepatic cholangiocarcinoma, mixed hepatocellular carcinoma and/or hepatocellular carcinoma with bile duct differentiation, CK7 and CK19 are usually positively expressed at the same time. CK8 and CK18 are usually positively expressed at the same time in hepatocellular liver cancer. It suggests that immunohistochemical testing is of some value in identifying metastatic hepatocellular carcinoma. To sum up, our IHC staining showed distinguishing features of digestive system-originated adenocarcinoma, represented by positivity in HepPar-1, AFP, CK7 and MUC4. MUC4 is an immunogenic tumor-associated antigen (TAA) that elicits humoral and cellular immunity, especially in pancreatic cancer (59, 60). Some reports have suggested that MUC4 may be a promising candidate for immunotherapy (61). A peptide vaccine using MUC4 tandem-repeat glycopeptides-conjugated-tetanus toxoid induced an intense antigen-specific immune response in murine models (62). Research on herceptin reported that MUC4 prevented its specific binding to HER2 by steric hinderance (63, 64). Since both HER2 and EGFR are members of the ErbB family, this hepatoid adenocarcinoma case may not respond well to EGFR-targeted therapy. CD117 (c-kit) is expressed by hematological malignancies and mesenchymal neoplasms, and it was investigated as a druggable target for solid tumors as well (65). P40 and TTF1 are diagnostic markers for lung squamous cell carcinoma (LUSC) and lung adenocarcinoma (LUAD). Consistent with previous reports, this HAC case had TTF1 cytoplasmic fraction 2+ for both the primary lesion and axillary metastasis (25, 66). TTF1 expression in lung adenocarcinomas is normally localized within the nuclei, whereas TTF-1 cytoplasmic reactivity is found in hepatocellular carcinoma (67). The TTF1 cytoplasmic reactivity observed in the present and previous HAC cases suggests that TTF1 may play a role in maintaining the hepatic phenotype in HAC, and should be considered as a biomarker for HAC diagnosis (68). Ki-67 70% suggested active cell proliferation of tumor cells and good sensitivity to chemotherapy. Moreover, this tumor was positive for PD-L1 with a 50% tumor proportion score (TPS). Besides the above IHC characteristics, axillary metastasis was positive for villin, another indicator of adenocarcinoma of digestive tract origin.

There is currently no consensus on the origin of pulmonary hepatoid adenocarcinoma. The common view is that during embryonic development, the lung, liver and stomach are derivatives of the primitive foregut, and that certain tumors occurring in tissues and organs such as the lung and foregut may differentiate towards hepatocytes due to derangements in the differentiation process (69). Clinical findings confirm that tumors occurring in the above organs can produce certain products of normal hepatocytes or hepatocellular carcinoma, such as albumin, alpha-1 antitrypsin (AAT), lectins, ferritin, transferrin (TF), and AFP (70). In this case, the pathological pattern was diverse, with typical hepatic differentiation, visible glandular vesicular structures and heterogeneous differentiation. Presumably, the tumor stem cells had the potential for multidirectional differentiation, and the pulmonary hepatoid adenocarcinoma was the result of dysregulated differentiation of primitive multipotent stem cells into hepatocytes.

In clinicopathological practice, we believe that the following criteria, in addition to the diagnostic criteria proposed by Ishikura and Haninger, are also helpful in the diagnosis of pulmonary hepatoid adenocarcinoma: (1) elderly, male, smoker, large lung masses with varying degrees of elevated serum AFP; (2) areas of differentiation similar to that of the liver and/or areas of glandular vesicles or papillary structures are found in lung tumor tissue with a histomorphology similar to that of hepatocellular carcinoma; (3) positive IHC for AFP, hepatocyte, CK7 and/or CK8 and/or CK18 and/or CK19, TTF-1, etc.; (4) no previous history of liver disease and no imaging or clinical evidence of tumors in the liver or elsewhere.

At the same time, pulmonary hepatoid adenocarcinoma needs to be differentiated from the following tumors:

(1) Primary hepatocellular carcinoma with pulmonary metastasis: usually with a history of hepatitis and cirrhosis, and a mass can be found in the liver on imaging. Its morphology is mostly similar to that of pulmonary hepatoid adenocarcinoma. However, hepatocellular carcinoma does not show papillary structures in the histology, nor is it associated with neuroendocrine differentiation or intestinal differentiation. IHC shows expression of AFP and hepatocyte, but not CK5/6, CK20 and CEA (71).

(2) Common types of lung adenocarcinomas: most of the cells are glandular ducts or papillary structures, relatively uniform in size, round or oval, with abundant cytoplasm, often containing mucus, large nuclei, dark staining, often with nucleoli, and relatively clear nuclear membranes. CK7, CK8, CK18, CK19, TTF-1, Napsin-A, etc. can be detected through IHC (72).

(3) Squamous cell carcinoma of the lung: the morphological features are large, polygonal cells, more cytoplasm and darkly stained nuclei. In the more differentiated cases, the cells are arranged in multiple layers, and intercellular bridges and keratinized beads can be seen. In the moderately differentiated cases, the cells are large and polygonal, but there are no keratinized spheres or intercellular bridges. In the less differentiated cases, the cells are small, round or shuttle-shaped, and arranged in a non-hierarchical manner. Adenoid structures are not usually present. Positive expression of IHC CK17, P63, CK5/6, 34BE12, etc (73).

(4) Pulmonary metastasis of hepatoid adenocarcinoma from other sites such as the stomach: the morphology is similar, and the clinical presentation and general imaging are difficult to differentiate. In this case, no mass was seen in the stomach or other regions, and there was no history of relevant surgery, so pulmonary metastasis of hepatoid adenocarcinoma was not considered.

(5) Germ cell tumors: yolk sac tumors and embryonal carcinomas can show increased plasma AFP. There were no yolk cyst-like structures, and no testicular masses in this case. IHC was negative for CD30, ER and PR, so it could be excluded (74).

(6) Neuroendocrine carcinoma: the cells are composed of small to medium-sized cells with indistinct cytoplasmic boundaries, rounded and regular nuclei, arranged in sheets, cords, clusters, adenoid or chrysoidal clusters. IHC is positive for neuroendocrine markers including CD56, CD57, Syn, CgA, etc (75, 76).

In terms of treatment, post-operative genetic testing was performed on the surgical specimen and peripheral blood. We identified co-occurring mutations in KRAS, STK11, CDKN2A, ATM, PTCH1, ARAF, SMO and MAP3K1, among which KRAS G12A is predictive of therapeutic sensitivity to MEK inhibitors and drug resistance to EGFR-TKIs (77). KRAS is an upstream signaling molecule of proliferative pathways such as the PI3K-AKT pathway and the RAF-MEK-MAPK pathway. It is a frequently mutated gene that occurs in 35% of lung adenocarcinomas with heterogeneous isoforms (78). Intriguingly, this hepatoid adenocarcinoma case corresponds with a previous large-scale survey on 3,560 patients that found that STK11 and ATM mutations are enriched in lung cancers with KRAS G12A mutation (77). CDKN2A mutation suggested the promising use of cell cycle inhibitors such as abemaciclib, palbociclib, and ribociclib. Additionally, other small molecules such as everolimus, which targets mTOR signaling pathway, and olaparib, which targets homogenous recombination deficiency, also suggested potential treatment effects based on genetic characteristics of this hepatoid adenocarcinoma case. Based on the results of the genetic test, we formulated a combination regimen of carboplatin 450 mg + pemetrexed 850 mg combined with sintilimab 200 mg on day 1, once every 3 weeks. After 3 months (four courses) of treatment, the efficacy was remarkable: the patient achieved stable disease after one month of treatment according to Response Evaluation Criteria in Solid Tumors v1.1. He was in overall good condition, had no recurrence and a negative serum AFP, and all tumor parameters were within normal range. The assessment on the follow-up visit in March 2023 showed that the patient had achieved a partial response, and he will continue to receive the planned treatment and supportive care (Figure 4).

Pulmonary hepatoid adenocarcinoma is clinically progressive and has a poor prognosis. It is prone to distant metastases to the liver, lung, bone and brain, as well as some uncommon sites such as the intestine, tonsils and gums (38, 47). Clinical staging of the disease is lacking, and no effective treatment has been established. A systematic analysis of pulmonary hepatoid cancer cases reported in the literature suggests that, as with other non-small cell lung cancers, the treatment of options for hepatoid adenocarcinoma of the lung remains surgery combined with chemotherapy and radiotherapy, when the conditions allow. Combination therapy, mainly surgery, can prolong survival in the early phases of the disease, and chemoradiotherapy is mostly used in the intermediate and late phases. Individualized treatment with molecular-targeted drugs and immunotherapy has shown different therapeutic effects in different patients and needs to be further explored. Of the cases with limited follow-up information reported in the literature (Table 1), 35 cases died between 4 days and 53 months after diagnosis, although a longer survival of 108 months was also reported (25). However, these data are still very limited, and further research is needed to elucidate the pathogenesis, diagnosis and comprehensive treatment to improve the prognosis of patients.

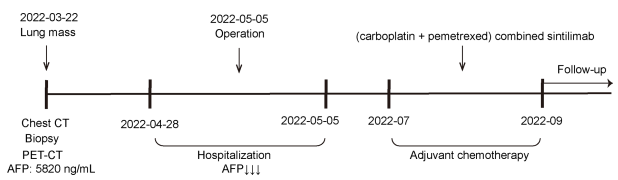


FIGURE 4
The clinical process comprising the patient's treatment.

Conclusion

This case report is the first multi-omic report that combines CT, PET-CT, MRI, pathological examination, IHC and genetic testing in the diagnosis and treatment of pulmonary hepatoid adenocarcinoma. We also discussed the diagnostic criteria and the differential diagnosis of pulmonary hepatoid adenocarcinoma based on the previously published cases, providing a reference for clinical practice. Our findings enriched knowledge about the clinical and pathological characteristics of this rare condition, and highlighted the importance of incorporating mutation status into treatment strategy, which raised critical points for consideration in further studies.

Data availability statement

The original contributions presented in the study are included in the article/supplementary material. Further inquiries can be directed to the corresponding authors.

Ethics statement

The patient provided informed consent to the publication of this article. Written informed consent was obtained from the individual for the publication of any potentially identifiable images or data included in this article.

Author contributions

KX: Conceptualization, Writing — original draft, Investigation. JG, LF: Data curation, Validation. YF: Writing — review and editing. XT: Conceptualization, Supervision, Writing — review and editing, Investigation. All authors contributed to the article and approved the submitted version.

Funding

This work has been funded with support from Jiangsu Cancer Hospital, Nanjing, China. The funders had no role in the study design, data acquisition, data interpretation, or writing of the manuscript.

Conflict of interest

The authors declare that the research was conducted in the absence of any commercial or financial relationships that could be construed as a potential conflict of interest.

Publisher's note

All claims expressed in this article are solely those of the authors and do not necessarily represent those of their affiliated organizations, or those of the publisher, the editors and the reviewers. Any product that may be evaluated in this article, or claim that may be made by its manufacturer, is not guaranteed or endorsed by the publisher.

References

1. Yasunami R, Hashimoto Z, Ogura T, Hirao F, Yamamura Y. Primary lung cancer producing alpha-fetoprotein: a case report. *Cancer* (1981) 47:926–9. doi: 10.1002/1097-0142(19810301)47:5<926::AID-CNCR2820470518>3.0.CO;2-O

2. Miyake M, Ito M, Taki T, Mitsuoka A, Wada H, Hitomi S. [A case report of two patients with primary lung cancer secreting AFP]. *Nihon Kyobu Geka Gakkai Zasshi* (1986) 34:914–9.

3. Tamura T, Saijo N, Shinkai T, Eguchi K, Sasaki Y, Sakurai M, et al. A case report of a three-year survivor with advanced non-small cell lung cancer producing alpha-fetoprotein. *Jpn J Clin Oncol* (1986) 16:175–81. doi: 10.1093/oxfordjournals.jjco.a039135

4. Miyake M, Ito M, Mitsuoka A, Taki T, Wada H, Hitomi S, et al. Alpha-fetoprotein and human chorionic gonadotropin-producing lung cancer. *Cancer* (1987) 59:227–32. doi: 10.1002/1097-0142(19870115)59:2<227::AID-CNCR2820590209>3.0.CO;2-X

5. Saka H, Sakai S, Kondo N, Ito M, Shimokata K. Successful resection of alpha-fetoprotein-producing lung cancer. *Chest* (1988) 94:879–80. doi: 10.1378/chest.94.4.879

6. Kurimoto I, Nakanishi T, Nishikawa M, Kuroda K. [A case of alpha fetoprotein-producing primary lung adenocarcinoma-analysis of lectin binding with AFP]. *Nihon Naika Gakkai Zasshi* (1989) 78:83–4. doi: 10.2169/naika.78.83

7. Okunaka T, Kato H, Konaka C, Yamamoto H, Furukawa K. Primary lung cancer producing alpha-fetoprotein. *Ann Thorac Surg* (1992) 53:151–2. doi: 10.1016/0003-4975(92)90778-3

8. Yoshino I, Hayashi I, Yano T, Takai E, Mizutani K, Ichinose Y. Alpha-fetoprotein-producing adenocarcinoma of the lung. *Lung Cancer* (1996) 15:125–30. doi: 10.1016/0169-5002(96)00577-6

9. Hirota F, Hosaka K, Funahashi K, Oota M, Ikeda A, Oobayashi Y, et al. [Effective treatment of AFP-producing lung cancer with UFT]. *Gan To Kagaku Ryoho* (1999) 26:381–4.

10. Carlinfante G, Foschini MP, Pasquinelli G, Scotti R, Cavazza A. Hepatoid carcinoma of the lung: a case report with immunohistochemical, ultrastructural and in-situ hybridization findings. *Histopathology* (2000) 37:88–9. doi: 10.1046/j.1365-2559.2000.00955-5.x

11. Genova S, Dikov D, Peshev Z, Khekimov K, Vŭzhev Z, Khristova S. [Hepatoid adenocarcinoma of the lung: a case report]. *Khirurgiia (Sofiia)* (2003) 59:45–7.

12. Hayashi Y, Takanashi Y, Ohsawa H, Ishii H, Nakatani Y. Hepatoid adenocarcinoma in the lung. *Lung Cancer* (2002) 38:211–4. doi: 10.1016/S0169-5002(02)00214-3

13. Terracciano LM, Glatz K, Mhawech P, Vasei M, Lehmann FS, Vecchione R, et al. Hepatoid adenocarcinoma with liver metastasis mimicking hepatocellular carcinoma: an immunohistochemical and molecular study of eight cases. *Am J Surg Pathol* (2003) 27:1302–12. doi: 10.1097/00000478-200310000-00002

14. Oshiro Y, Takada Y, Enomoto T, Fukao K, Ishikawa S, Iijima T. A resected case of metachronous liver metastasis from lung cancer producing alpha-fetoprotein (AFP) and protein induced by vitamin K absence or antagonist II (PIVKA-II). *Hepatogastroenterology* (2004) 51:1144–7.

15. Ivan M, Koss MN, Chang C-F. HEPATOID ADENOCARCINOMA OF THE LUNG. *Chest* (2007) 132:690–0. doi: 10.1378/chest.132.4_MeetingAbstracts.690

16. Kishimoto T, Yano T, Hiroshima K, Inayama Y, Kawachi K, Nakatani Y. A case of *-fetoprotein-producing pulmonary carcinoma with restricted expression of hepatocyte nuclear factor-4* in hepatoid foci: a case report with studies of previous cases. *Hum Pathol* (2008) 39:1115–20. doi: 10.1016/j.humpath.2007.12.013

17. Li C, Liu L, Ma H. [A case report of lung adenocarcinoma with high level AFP.]. *Zhongguo Fei Ai Za Zhi* (2008) 11:605–6.

18. Fornasa F. Soft-tissue localization of hepatoid adenocarcinoma: first case report. *Case Rep Oncol* (2010) 3:212–7. doi: 10.1159/000317419

19. Kitada M, Ozawa K, Sato K, Matsuda Y, Hayashi S, Tokusashi Y, et al. Alpha-fetoprotein-producing primary lung carcinoma: a case report. *World J Surg Oncol* (2011) 9:47. doi: 10.1186/1477-7819-9-47

20. Mokrim M, Belbaraka R, Allaoui M, Kairaouani M, Mahassini N, Tahri A, et al. Hepatoid adenocarcinoma of the lung: a case report and literature review. *J Gastrointest Cancer* (2012) 43 Suppl 1:S125–127. doi: 10.1007/s12029-011-9318-5

21. Papatsimpas G, Kamposioras K, Goula K, Papaparaskeva K, Loukides S, Kotoulas C, et al. Hepatoid pancoast tumor. a case report and review of the literature. *Lung Cancer* (2012) 77:239–45. doi: 10.1016/j.lungcan.2012.05.102

22. Valentino F, Torchio M, Morbini P, Danova M. Synchronous presentation of hepatoid alpha-fetoprotein-producing lung cancer and colorectal adenocarcinoma. *Tumori* (2012) 98:130e–4e. doi: 10.1177/030089161209800523

23. Cavalcante LB, Felipe-Silva A, de Campos FPF, Martines J. Hepatoid adenocarcinoma of the lung. *Autops Case Rep* (2013) 3:5–14. doi: 10.4322/acr.2013.002

24. Che YQ, Wang S, Luo Y, Wang JB, Wang LH. Hepatoid adenocarcinoma of the lung: presenting mediastinal metastasis without transfer to the liver. *Oncol Lett* (2014) 8:105–10. doi: 10.3892/ol.2014.2064

25. Haninger DM, Kloecker GH, Bousamra Ii M, Nowacki MR, Slone SP. Hepatoid adenocarcinoma of the lung: report of five cases and review of the literature. *Mod Pathol* (2014) 27:535–42. doi: 10.1038/modpathol.2013.170

26. Shaib W, Sharma R, Mosunjac M, Farris AB3rd, El Rayes B. Hepatoid adenocarcinoma of the lung: a case report and review of the literature. *J Gastrointest Cancer* (2014) 45 Suppl 1:99–102. doi: 10.1007/s12029-013-9558-7

27. Al-Najjar H, Evison M, Doran HM, Booton RC, Taylor PD. Primary pulmonary hepatoid adenocarcinoma: a case report. *Cancer Treat Res* (2015) 4:172–3. doi: 10.1016/j.ctrc.2015.10.001

28. Gavrancic T, Park YH. A novel approach using sorafenib in alpha fetoprotein-producing hepatoid adenocarcinoma of the lung. *J Natl Compr Canc Netw* (2015) 13:387–91. doi: 10.6004/jnccn.2015.0054

29. Grossman K, Beasley MB, Braman SS. Hepatoid adenocarcinoma of the lung: review of a rare form of lung cancer. *Respir Med* (2016) 119:175–9. doi: 10.1016/j.rmed.2016.09.003

30. Qian GQ, Yin FY, Li GX, Chu JG. Hepatoid adenocarcinoma of the lung. *Qjm* (2016) 109:619–20. doi: 10.1093/qjmed/hcw107

31. Sun JN, Zhang BL, Li LK, Yu HY, Wang B. Hepatoid adenocarcinoma of the lung without production of α-fetoprotein: a case report and review of the literature. *Oncol Lett* (2016) 12:189–94. doi: 10.3892/ol.2016.4559

32. Wang S, Li M, Chen H, Li J, Zeng Q. FDG PET/CT in hepatoid adenocarcinoma of the lung. *Clin Nucl Med* (2016) 41:e340–341. doi: 10.1097/RLU.0000000000001231

33. Basse V, Schick U, Guéguen P, Le Maréchal C, Quintin-Roué I, Descourt R, et al. A mismatch repair-deficient hepatoid adenocarcinoma of the lung responding to anti-PD-L1 durvalumab therapy despite no PD-L1 expression. *J Thorac Oncol* (2018) 13:e120–2. doi: 10.1016/j.jtho.2018.03.004

34. Esa NYM, Zamrud R, Bakar NS, Eezamuddeen MAN, Hamdan MF. Is it liver or lung cancer? an intriguing case of lung adenocarcinoma with hepatoid differentiation. *Proc Singapore Healthcare* (2018) 27:55–8. doi: 10.1177/20101058177161185

35. Li Q, Zhou DM. [Hepatoid adenocarcinoma of the lung with negative alpha-fetoprotein: a case report]. *Zhonghua Zhong Liu Za Zhi* (2018) 40:910–1.

36. Nakashima K, Okagawa T. [Hepatoid adenocarcinoma of the lung with high serum AFP and CEA Values;Report of a case]. *Kyobu Geka* (2018) 71:76–9.

37. Memoli JSW, Lee W. "Hepatoid adenocarcinoma of the lung with normal alpha-fetoprotein level". *In B70 Case Rep IN Thorac Oncol II.* (2018) 2018:A4018–8.

38. Ayub A, Nunez Lopez O, Booth A, Okereke I. Pulmonary hepatoid adenocarcinoma. *J Thorac Cardiovasc Surg* (2019) 158:e139–40. doi: 10.1016/j.jtcvs.2019.06.023

39. Chen HF, Wang WX, Li XL, Xu CW, Du KQ, Zhu YC, et al. Hepatoid adenocarcinoma of the lung with EGFR mutation and the response to tyrosine kinase inhibitors. *J Thorac Oncol* (2019) 14:e217–9. doi: 10.1016/j.jtho.2019.04.032

40. El Khoury A, El Khoury M, De Luca R. Immunotherapeutic approach to a case of advanced hepatoid adenocarcinoma of the lung. *memo* (2019) 2019:12, 272–277. doi: 10.1007/s12254-019-0499-0

41. Kuan K, Khader SN, El Hussein S. Hepatoid adenocarcinoma of the lung. *Diagn Cytopathol* (2019) 47:831–3. doi: 10.1002/dc.24195

42. Li J, Qi H, Xu B, Zhao J, Gao H, Ma X, et al. Genomic profiles of a patient of pulmonary hepatoid adenocarcinoma with high AFP level: a case report. *Front Oncol* (2019) 9:1360. doi: 10.3389/fonc.2019.01360

43. Keshava K, Malik SA. A rare case of primary hepatoid adenocarcinoma of the lung in a female patient. *D62 Thorac Oncol Case Rep II.* (2019), A6979–9.

44. Shi YF, Lu JG, Yang QM, Duan J, Lei YM, Zhao W, et al. Primary hepatoid adenocarcinoma of the lung in yungui plateau, China: a case report. *World J Clin cases* (2019) 7:1711–6. doi: 10.12998/wjcc.v7.i13.1711

45. Wang C, Xu G, Wu G, Chen Z, Sun Z, Zheng P, et al. Hepatoid adenocarcinoma of the lung metastasizing to the gingiva. *Onco Targets Ther* (2019) 12:8765–8. doi: 10.2147/OTT.S222974

46. Yang K, Jiang H, Li Q. Primary pulmonary hepatoid adenocarcinoma: a case report and review of the literature. *Med (Baltimore)* (2019) 98:e15053. doi: 10.1097/MD.0000000000015053

47. Chen JX, Lyu LL, Zhu WH, Chen XY, Zheng L. Hepatoid adenocarcinoma of the lung accompanied with multiple systemic metastases. *Chin Med J (Engl)* (2020) 134:237–8. doi: 10.1097/CM9.0000000000000963

48. Chen L, Han X, Gao Y, Zhao Q, Wang Y, Jiang Y, et al. Anti-PD-1 therapy achieved disease control after multiline chemotherapy in unresectable KRAS-positive hepatoid lung adenocarcinoma: a case report and literature review. *Onco Targets Ther* (2020) 13:4359–64. doi: 10.2147/OTT.S248226

49. Muroyama Y, Tamiya H, Tanaka G, Tanaka W, Huang AC, Oldridge DA, et al. Alpha-Fetoprotein-Producing lung hepatoid adenocarcinoma with brain metastasis treated with s-1. *Case Rep Oncol* (2020) 13:1552–9. doi: 10.1159/000511763

50. Tonyali O, Gonullu O, Ozturk MA, Kosif A, Civi OG. Hepatoid adenocarcinoma of the lung and the review of the literature. *J Oncol Pharm Pract* (2020) 26:1505–10. doi: 10.1177/1078155220903360

51. Chen Z, Ding C, Zhang T, He Y, Jiang G. Primary hepatoid adenocarcinoma of the lung: a systematic literature review. *Onco Targets Ther* (2022) 15:609–27. doi: 10.2147/OTT.S364465

52. Xu SZ, Zhang XC, Jiang Q, Chen M, He MY, Shen P. Alpha-fetoprotein-producing hepatoid adenocarcinoma of the lung responsive to sorafenib after multiline treatment: a case report. *World J Clin cases* (2022) 10:10236–43. doi: 10.12998/wjcc.v10.i28.10236

53. Yao Y, Guan X, Bao G, Liang J, Li T, Zhong X. Whole-exome sequencing and bioinformatics analysis of a case of non-alpha-fetoprotein-elevated lung hepatoid adenocarcinoma. *Front Pharmacol* (2022) 13:945038. doi: 10.3389/fphar.2022.945038

54. Lagos GG, Feldman JL, Saqi A, Shu CA. Hepatoid adenocarcinoma of the lung responsive to frontline combination chemotherapy with immunotherapy: case report. *JTO Clin Res Rep* (2021) 2:100130. doi: 10.1016/j.jtocrr.2020.100130

55. Hou Z, Xie J, Zhang L, Dai G, Chen Y, He L. Hepatoid adenocarcinoma of the lung: a systematic review of the literature from 1981 to 2020. *Front Oncol* (2021) 11:702216. doi: 10.3389/fonc.2021.702216

56. Ishikura H, Fukasawa Y, Ogasawara K, Natori T, Tsukada Y, Aizawa M. An AFP-producing gastric carcinoma with features of hepatic differentiation. *A Case Rep Cancer* (1985) 56:840–8.

57. Metzgeroth G, Ströbel P, Baumbusch T, Reiter A, Hastka J. Hepatoid adenocarcinoma - review of the literature illustrated by a rare case originating in the peritoneal cavity. *Onkologie* (2010) 33:263–9. doi: 10.1159/000305717

58. Ishikura H, Kanda M, Ito M, Nosaka K, Mizuno K. Hepatoid adenocarcinoma: a distinctive histological subtype of alpha-fetoprotein-producing lung carcinoma. *Virchows Arch A Pathol Anat Histopathol* (1990) 417:73–80. doi: 10.1007/BF01600112

59. Gautam SK, Kumar S, Dam V, Ghersi D, Jain M, Batra SK. MUCIN-4 (MUC4) is a novel tumor antigen in pancreatic cancer immunotherapy. *Semin Immunol* (2020) 47:101391. doi: 10.1016/j.smim.2020.101391

60. Hanaoka J, Kontani K, Sawai S, Ichinose M, Tezuka N, Inoue S, et al. Analysis of MUC4 mucin expression in lung carcinoma cells and its immunogenicity. *Cancer* (2001) 92:2148–57. doi: 10.1002/1097-0142(20011015)92:8<2148::AID-CNCR1557>3.0.CO;2-6

61. Gautam SK, Kumar S, Cannon A, Hall B, Bhatia R, Nasser MW, et al. MUC4 mucin- a therapeutic target for pancreatic ductal adenocarcinoma. *Expert Opin Ther Targets* (2017) 21:657–69. doi: 10.1080/14728222.2017.1323880

62. Cai H, Palitzsch B, Hartmann S, Stergiou N, Kunz H, Schmitt E, et al. Antibody induction directed against the tumor-associated MUC4 glycoprotein. *Chembiochem* (2015) 16:959–67. doi: 10.1002/cbic.201402689

63. Nagy P, Friedländer E, Tanner M, Kapanen AI, Carraway KL, Isola J, et al. Decreased accessibility and lack of activation of ErbB2 in JIMT-1, a herceptin-resistant, MUC4-expressing breast cancer cell line. *Cancer Res* (2005) 65:473–82. doi: 10.1158/0008-5472.473.65.2

64. Mercogliano MF, De Martino M, Venturutti L, Rivas MA, Proietti CJ, Inurrigarro G, et al. Et al: TNFα-induced mucin 4 expression elicits trastuzumab resistance in HER2-positive breast cancer. *Clin Cancer Res* (2017) 23:636–48. doi: 10.1158/1078-0432.CCR-16-0970

65. Pathania S, Pentikäinen OT, Singh PK. A holistic view on c-kit in cancer: structure, signaling, pathophysiology and its inhibitors. *Biochim Biophys Acta Rev Cancer* (2021) 1876:188631. doi: 10.1016/j.bbcan.2021.188631

66. Laraqui Houssein Y, Derqaoui S, Khouloud R, Jahid A, Zouaidia F, Bernoussi Z, et al. Hepatoid adenocarcinoma of the lung: a rare form of lung cancer. *Clin Pathol* (2022) 15:2632010x221088961.

67. Compérat E, Zhang F, Perrotin C, Molina T, Magdeleinat P, Marmey B, et al. Variable sensitivity and specificity of TTF-1 antibodies in lung metastatic adenocarcinoma of colorectal origin. *Mod Pathol* (2005) 18:1371–6. doi: 10.1038/modpathol.3800422

68. Lei JY, Bourne PA, diSant'Agnese PA, Huang J. Cytoplasmic staining of TTF-1 in the differential diagnosis of hepatocellular carcinoma vs cholangiocarcinoma and metastatic carcinoma of the liver. *Am J Clin Pathol* (2006) 125:519–25. doi: 10.1309/59TNEFALUL5WJ94M

69. deLorimier A, Park F, Aranha GV, Reyes C. Hepatoid carcinoma of the stomach. *Cancer* (1993) 71:293–6. doi: 10.1002/1097-0142(19930115)71:2<293::AID-CNCR2820710204>3.0.CO;2-O

70. Augustin G, Jelincic Z, Tentor D, Majerovic M, Matosevic P. Hepatoid adenocarcinoma of the stomach: case report and short notes on immunohistochemical markers. *Acta Gastroenterol Belg* (2009) 72:253–6.

71. Yatabe Y, Dacic S, Borczuk AC, Warth A, Russell PA, Lantuejoul S, et al. Best practices recommendations for diagnostic immunohistochemistry in lung cancer. *J Thorac Oncol* (2019) 14:377–407. doi: 10.1016/j.jtho.2018.12.005

72. Zhang C, Zhang J, Xu FP, Wang YG, Xie Z, Su J, et al. Genomic landscape and immune microenvironment features of preinvasive and early invasive lung adenocarcinoma. *J Thorac Oncol* (2019) 14:1912–23. doi: 10.1016/j.jtho.2019.07.031

73. Broers JL, Ramaekers FC, Rot MK, Oostendorp T, Huysmans A, van Muijen GN, et al. Cytokeratins in different types of human lung cancer as monitored by chain-specific monoclonal antibodies. *Cancer Res* (1988) 48:3221–9.

74. Rabban JT, Zaloudek CJ. A practical approach to immunohistochemical diagnosis of ovarian germ cell tumours and sex cord-stromal tumours. *Histopathology* (2013) 62:71–88. doi: 10.1111/his.12052

75. Mukhopadhyay S, Dermawan JK, Lanigan CP, Farver CF. Insulinoma-associated protein 1 (INSM1) is a sensitive and highly specific marker of neuroendocrine differentiation in primary lung neoplasms: an immunohistochemical study of 345 cases, including 292 whole-tissue sections. *Mod Pathol* (2019) 32:100–9. doi: 10.1038/s41379-018-0122-7

76. Farinola MA, Weir EG, Ali SZ. CD56 expression of neuroendocrine neoplasms on immunophenotyping by flow cytometry: a novel diagnostic approach to fine-needle aspiration biopsy. *Cancer* (2003) 99:240–6. doi: 10.1002/cncr.11458

77. Ricciuti B, Son J, Okoro JJ, Mira A, Patrucco E, Eum Y, et al. Comparative analysis and isoform-specific therapeutic vulnerabilities of KRAS mutations in non-small cell lung cancer. *Clin Cancer Res* (2022) 28:1640–50. doi: 10.1158/1078-0432.CCR-21-2719

78. Reck M, Carbone DP, Garassino M, Barlesi F. Targeting KRAS in non-small-cell lung cancer: recent progress and new approaches. *Ann Oncol* (2021) 32:1101–10. doi: 10.1016/j.annonc.2021.06.001

frontiers | Frontiers in Immunology

TYPE Original Research
PUBLISHED 31 May 2023
DOI 10.3389/fimmu.2023.1201573

Check for updates

OPEN ACCESS

EDITED BY
Qun Xue,
Affiliated Hospital of Nantong University, China

REVIEWED BY
Guoliang Ye,
The Affiliated Hospital of Medical School of Ningbo University, China
Renjun Gu,
Nanjing University of Chinese Medicine, China

*CORRESPONDENCE
Zhijia Xia
Zhijia.Xia@med.uni-muenchen.de
Huabao Cai
2145011159@stu.ahmu.edu.cn
Yue Yu
yuyue2014@njmu.edu.cn

†These authors have contributed equally to this work and share first authorship

RECEIVED 06 April 2023
ACCEPTED 17 May 2023
PUBLISHED 31 May 2023

CITATION
Ren Q, Zhang P, Lin H, Feng Y, Chi H, Zhang X, Xia Z, Cai H and Yu Y (2023) A novel signature predicts prognosis and immunotherapy in lung adenocarcinoma based on cancer-associated fibroblasts. *Front. Immunol.* 14:1201573. doi: 10.3389/fimmu.2023.1201573

COPYRIGHT
© 2023 Ren, Zhang, Lin, Feng, Chi, Zhang, Xia, Cai and Yu. This is an open-access article distributed under the terms of the Creative Commons Attribution License (CC BY). The use, distribution or reproduction in other forums is permitted, provided the original author(s) and the copyright owner(s) are credited and that the original publication in this journal is cited, in accordance with accepted academic practice. No use, distribution or reproduction is permitted which does not comply with these terms.

A novel signature predicts prognosis and immunotherapy in lung adenocarcinoma based on cancer-associated fibroblasts

Qianhe Ren[1†], Pengpeng Zhang[1†], Haoran Lin[1†], Yanlong Feng[1†], Hao Chi[2], Xiao Zhang[1], Zhijia Xia[3*], Huabao Cai[4*] and Yue Yu[1*]

[1]Department of Thoracic Surgery, The First Affiliated Hospital of Nanjing Medical University, Nanjing, China, [2]Clinical Medical College, Southwest Medical University, Luzhou, China, [3]Department of General, Visceral, and Transplant Surgery, Ludwig-Maximilians-University, Munich, Germany, [4]Department of Neurosurgery, First Affiliated Hospital of Anhui Medical University, Hefei, China

Background: Extensive research has established the significant correlations between cancer-associated fibroblasts (CAFs) and various stages of cancer development, including initiation, angiogenesis, progression, and resistance to therapy. In this study, we aimed to investigate the characteristics of CAFs in lung adenocarcinoma (LUAD) and develop a risk signature to predict the prognosis of patients with LUAD.

Methods: We obtained single-cell RNA sequencing (scRNA-seq) and bulk RNA-seq data from the public database. The Seurat R package was used to process the scRNA-seq data and identify CAF clusters based on several biomarkers. CAF-related prognostic genes were further identified using univariate Cox regression analysis. To reduce the number of genes, Lasso regression was performed, and a risk signature was established. A novel nomogram that incorporated the risk signature and clinicopathological features was developed to predict the clinical applicability of the model. Additionally, we conducted immune landscape and immunotherapy responsiveness analyses. Finally, we performed *in vitro* experiments to verify the functions of EXO1 in LUAD.

Results: We identified 5 CAF clusters in LUAD using scRNA-seq data, of which 3 clusters were significantly associated with prognosis in LUAD. A total of 492 genes were found to be significantly linked to CAF clusters from 1731 DEGs and were used to construct a risk signature. Moreover, our immune landscape exploration revealed that the risk signature was significantly related to immune scores, and its ability to predict responsiveness to immunotherapy was confirmed. Furthermore, a novel nomogram incorporating the risk signature and clinicopathological features showed excellent clinical applicability. Finally, we verified the functions of EXP1 in LUAD through *in vitro* experiments.

Conclusions: The risk signature has proven to be an excellent predictor of LUAD prognosis, stratifying patients more appropriately and precisely predicting immunotherapy responsiveness. The comprehensive characterization of LUAD

based on the CAF signature can predict the response of LUAD to immunotherapy, thus offering fresh perspectives into the management of LUAD patients. Our study ultimately confirms the role of EXP1 in facilitating the invasion and growth of tumor cells in LUAD. Nevertheless, further validation can be achieved by conducting *in vivo* experiments.

KEYWORDS

lung adenocarcinoma, fibroblast, prognosis, tumor immune microenvironment, immunotherapy

1 Introduction

Lung cancer is a highly malignant tumor with a high diagnostic frequency and ranks first in cancer-related deaths worldwide (1). Among the several histologic types of lung cancer, lung adenocarcinoma account for the highest percentage (2, 3). Over the past decades, significant progress has been made in exploring the molecular mechanism of LUAD progression, leading to the development of precision therapeutics such as tyrosine-kinase inhibitors (TKIs) (4). With the advent of molecular profiling, it has become clear that lung adenocarcinoma is a genetically heterogeneous disease, characterized by a range of driver mutations and alterations that are amenable to targeted therapy (5). Besides, mounting evidence has indicated a significant association between m6A regulators and malignant neoplasms (6). For example, the significant correlation between downregulation of METTL14 in liver cancer and tumor metastasis has been observed (7). Several prior studies have identified abnormal expression patterns of m6A regulators in LUAD as well (8). Molecular targeting of lung adenocarcinoma involves the use of drugs or other agents that specifically target the genetic alterations that are present in the cancer cells, with the aim of achieving more effective and less toxic treatments (9). Oncogenic KRAS is a prominent driver of lung adenocarcinoma (LUAD), which has yet to be effectively targeted by therapeutics. One study has presented evidence that the SLC7A11/glutathione axis demonstrates metabolic synthetic lethality with oncogenic KRAS. Research has demonstrated that LUAD cells harboring KRAS mutations are sensitive to SLC7A11 inhibition, suggesting possible therapeutic avenues for this presently untreatable condition (10). This approach has revolutionized the management of lung adenocarcinoma, leading to improved outcomes for patients with specific molecular subtypes of the disease. However, a considerable proportion of LUAD patients still experience poor prognosis due to innate or acquired resistance to targeted therapy (11). For example, Tyrosine kinase inhibitors (TKIs) targeting sensitizing mutations in the epidermal growth factor receptor (EGFR) gene constitute a vital cornerstone of non-small cell lung cancer management. Despite the outstanding disease control obtained through primary EGFR TKI therapy, the development of acquired resistance is pervasive and represents a major obstacle (12). Immunotherapy provides a novel approach to the management of LUAD patients (13). In recent years, immunotherapy has emerged as a promising treatment option for lung adenocarcinoma (14). Immunotherapy works by activating the body's immune system to recognize and attack cancer cells. It does this by targeting specific proteins on the surface of cancer cells, called checkpoint proteins, that can inhibit immune cell activity (15). The two main types of immunotherapies used to treat lung adenocarcinoma are immune checkpoint inhibitors and adoptive cell therapy (16). Immune checkpoint inhibitors block checkpoint proteins on cancer cells, allowing immune cells to attack the cancer. Adoptive cell therapy involves removing immune cells from a patient's body, genetically modifying them to recognize and attack cancer cells, and then infusing them back into the patient (17). Immunotherapy has shown promising results in treating lung adenocarcinoma, particularly in patients whose cancer has spread and is no longer responding to traditional treatments. However, it is not effective for all patients, and there can be significant side effects (18). Further research is needed to determine which patients will benefit most from immunotherapy and how to minimize side effects.

Cancer initiation, progression and immigration incur a range of dynamic alterations in host tissues, bringing about a complex tumor stroma, illustrated as the tumor microenvironment (TME) (19). The evolution and homeostasis of the TME largely depend on an intimate communication within and across several cellular compartments, including malignant, stromal, and immune cells. Among them, cancer-associated fibroblasts (CAFs) are the principal component of stromal cells and release inflammatory, growth factors, and extracellular matrix, accelerating tumor proliferation and contributing to therapy resistance (20). CAFs can promote progression of malignant cells by serving TME crucial nutrients, such as alanine and lipoids (21). Besides, accumulating evidence have confirmed that CAFs are significantly correlated with several cancers, such as breast cancer, gastrointestinal cancer and lung cancer (22–24). In-depth research on the crosstalk between CAFs and other TME cells could provide new insights into subsequent targeted therapy.

Despite significant efforts to study CAFs in LUAD, comprehensive characterization and prediction of immunotherapy response are lacking. Herein, transcriptome and single-cell RNA-sequencing (scRNA-seq) data from public database were collected and further processed. Distinguished CAFs subclusters were obtained and based

on which a risk signature was established for LUAD. The signature's independent prognostic prediction values were validated by several methods. A novel nomogram integrating the risk signature and clinicopathological features was constructed to facilitate the clinical application of CAF in LUAD. The risk signature, along with the novel nomogram, has the potential to enable more accurate patient stratification for LUAD and offer more precise prognostic predictions. Furthermore, the CAF-related signature was evaluated for immune landscape and responsiveness to immunotherapy, providing new insights into the management of LUAD and improving patient outcomes.

2 Methods

2.1 Data collection and processing

We obtained scRNA-seq data from the Gene Expression Omnibus (GEO) database (accession number GSE149655), which comprised four samples: two primary lung adenocarcinoma (LUAD) samples and two normal tissue samples. We filtered out single cells expressing fewer than 250 genes or those with any gene expressed in fewer than three cells. We also evaluated the percentage of mitochondria and rRNA using the PercentageFeatureSet function in the Seurat R package (25, 26). This resulted in a total of 12,554 cells for further analysis.

We collected transcriptome data, copy number variants (CNV), single-nucleotide variants (SNV), and corresponding clinical data of LUAD from The Cancer Genome Atlas (TCGA) database. We excluded samples lacking survival data or outcome status and included 500 tumor samples and 59 normal samples in the analysis. We also utilized two external validation cohorts: GSE72094 cohort with 398 samples and GSE26939 cohort with 115 samples after removing samples without follow-up.

From the literature, we identified ten cancer-associated pathways (HIPPO, Cell Cycle, MYC, NRF1, NOTCH, PI3K, RAS, TP53, TGF-Beta, and WNT) and analyzed their gene expression profiles in our dataset (27).

2.2 CAF definition

The Seurat package was used to re-analyze the scRNA-seq data of LUAD (28), with the aim of systematically characterizing the CAF signature. Firstly, expressed genes were log-normalized after removing cells with below 250 or over 6000 expressed genes. Then, the FindIntegrationAnchors function was employed to remove batch effects for the four samples. Non-linear dimensional reduction was performed using the uniform manifold approximation and projection method, with a resolution of 0.2 and 30 principal components selected. Subsequently, single cells were clustered into different subgroups using the FindNeighbors and FindClusters (dim = 30 and resolution =0.2) functions. UMAP dimensional reduction was performed using the RunUMAP function. Fibroblasts were annotated based on four marker genes, including FAP, PDGFRB, ACTA2, and NOTCH3. The fibroblasts were re-clustered using the same algorithm of FindClusters and FindNeighbors functions. Marker genes for each CAF cluster were defined with the FindAllMarkers function by comparing different clusters with minpct = 0.35, logFC =0.5, and adjust p-value<0.05. We also used the CopyKAT R package (29) to analyze the CNV characteristics of CAFs clusters and distinguish between tumor cells and normal ones. Finally, we performed Kyoto Encyclopedia of Genes and Genomes (KEGG) enrichment analysis on the marker genes using the clusterProfiler package (30).

2.3 Hub genes of CAF identification

Firstly, the limma package (31, 32) was used to identify differentially expressed genes (DEGs) between normal and tumor tissue based on |log2(FoldChange)|>1 and a false discovery rate (FDR)<0.05. Then, correlations between CAF clusters and DEGs were evaluated, followed by the identification of key CAF-related genes with p<0.01 and cor>0.4. To identify prognosis-related genes, univariate Cox regression analysis was conducted using the survival package (33). To reduce the number of genes, the least absolute shrinkage and selection operator (lasso) was performed (34–36). Multivariate Cox regression analysis was conducted using the stepwise regression method to establish a CAF-based risk signature, which was calculated using the formula: 0.123*CLEC3B+0.114*EXO1 + 0.103*CCNB1+-0.177*CD302. Patients were classified into low- and high-risk groups using zero-mean normalization. The predictive value of the risk signature was evaluated using receiver operating characteristic curve (ROC) analysis with the timeROC package (37, 38).

2.4 A novel nomogram constructed based on the risk signature

Following the univariate and multivariate Cox regression analysis based on the risk signature and clinicopathological features (39), we constructed a novel nomogram to predict the prognosis of LUAD using variables with p<0.05 in the multivariate Cox model. We evaluated the predictive accuracy of the model by generating a calibration curve.

2.5 Immune landscape analysis

We comprehensively assessed the correlation between the risk signature and the tumor immune microenvironment (TIME) using several algorithms, including CIBERSORT, EPIC, MCPCOUNTER, and TIMER. The "estimate" R package was used to calculate stromal scores, immune scores, and estimate scores (stromal scores + immune scores) to evaluate differences in the tumor microenvironment of patients. Additionally, we estimated the proportions of 22 immune cell subtypes using the CIBERSORT algorithm based on the TCGA cohort.

2.6 Responsiveness to immunotherapy

Anti-PD-1 or anti-PD-L1 checkpoint inhibition therapy has gained increasing attention as a crucial component of immunotherapy. To evaluate the performance of the risk signature in predicting responsiveness to immunotherapy (immune checkpoint blocks), we collected transcriptomic data as well as corresponding clinical data from patients who received anti-PD-L1 therapy from the IMvigor210 cohort. We also downloaded transcriptomic data from the GSE78220 cohort, which included melanoma patients who received anti-PD-1 checkpoint inhibition therapy before treatment.

2.7 Cell lines culture of lung adenocarcinoma cells and cell transfection

All patients conferred their informed consent before being enrolled in the study. Sample collections were conducted following procedures approved by the Ethics Committee of Jiangsu Province People's Hospital (2019-SR-156). Lung adenocarcinoma cell lines including A549 and H1299 cells was purchased from ATCC. All cells were cultured using Ham's F-12K and RPMI 1640 medium (Gibco, USA), supplemented with 10% FBS (HyClone Sera, USA) and 1% penicillin-streptomycin (Sangon Biotech, China), and maintained in an atmosphere containing 5% CO2 at 37°C. The EXO1 siRNA expression vector and scrambled siRNA nontarget control were obtained from Genewiz (China). Plasmids were transfected using Lipofectamine 3000 (Thermo Scientific, USA), as per the manufacturer's protocols (40).

2.8 RNA extraction and quantitative real-time polymerase chain reaction

Total RNA was extracted from the cell lines using TRIzol in accordance with the manufacturer's instructions (15596018, Thermo). Subsequently, cDNA was synthesized utilizing the PrimeScript TMRT kit (R232-01, Vazyme). Real-time polymerase chain reaction (RT-PCR) was performed using SYBR Green Master Mix (Q111-02, Vazyme). The expression levels of each mRNA were standardized to the level of mRNA GAPDH, and the quantification of expression levels was executed using the $2^{-\Delta\Delta CT}$ method (41).

2.9 Cell counting kit-8 assay and EdU

The suspension of cells was seeded in 96-well plates at a density of 5×10^3 cells per well. After adding 10 µl of CCK-8 labeling agent (A311-01, Vazyme) to each well, the plate was incubated for 2 hours in the dark at 37°C. Cell viability was evaluated by measuring absorbance at 450 nm at 0, 24, 48, 72, and 96 hours using an enzyme-labeled meter (A33978, Thermo). The experiment was performed using a 96-well plate with 2×10^4 treated cells in each well, after the cells had adhered to the wall. The 5-Ethynyl-2'-deoxyuridine (EdU) assay was performed according to the manufacturer's instructions (Ribobio, China), and cell proliferation was quantified using an inverted microscope.

2.10 Wound-healing assay and transwell assay

The transfected cells were seeded in 6-well plates and cultured in a cell incubator until they reached 95% confluence. Each well was gently scraped using a sterile 200 µl plastic pipette tip, and any unattached cells and debris were rinsed twice with PBS. The breadth of the scratch wounds was measured using the Image J program, and photographs were taken at 0 h and 48 h. For the cell invasion and migration experiments, treated A549 and H1299 cells (2×10^4) were incubated in the upper chamber of 24-well plates for 48 hours. The top surface of the plate was either precoated with matrigel solution (BD Biosciences, USA) or left untreated to assess the cells' ability to invade and migrate. After removing the cells from the top surface, the remaining cells on the bottom layer were fixed with 4% paraformaldehyde and stained with 0.1% crystal violet (Solarbio, China).

2.11 Statistical analysis

All statistical analyses were performed using R software (version 4.1.0). Wilcoxon test was used for comparing two groups, while Spearman or Pearson correlation was used for correlation matrices. The Log-rank test was used to assess survival differences through K-M curves, where statistical significance was defined as p-value < 0.05.

3 Results

3.1 CAF clustering and screening in scRNA samples

The flow chart of our study is depicted in Figure 1. Following initial screening, a total of 12,554 cells were obtained from scRNA-seq data. Detailed results of data preprocessing are presented in Figure S1. Firstly, after performing log-normalization and dimensionality reduction, we identified 31 subpopulations (Figure 2A). Using four marker genes (FAP, FDGFRB, ACTA2, and NOTCH3), we further identified five CAF populations, as shown in Figure 2B. Cells collected from the four CAF populations were then separated for clustering and dimensionality reduction in subsequent research. Utilizing the same clustering algorithm, we discovered five clusters, as depicted in Figure 2B. Moreover, after performing the R package 'FindVariableFeatures', we obtained 756 DEGs from the five CAF clusters. The top 5 DEGs, which were characterized as CAF cluster marker genes, are exhibited in Figures 2C, D. Histograms illustrating the proportion of the five clusters in each cohort are shown in Figure 2E. Furthermore, KEGG analysis revealed that these DEGs were enriched in divergent pathways such as ECM-receptor

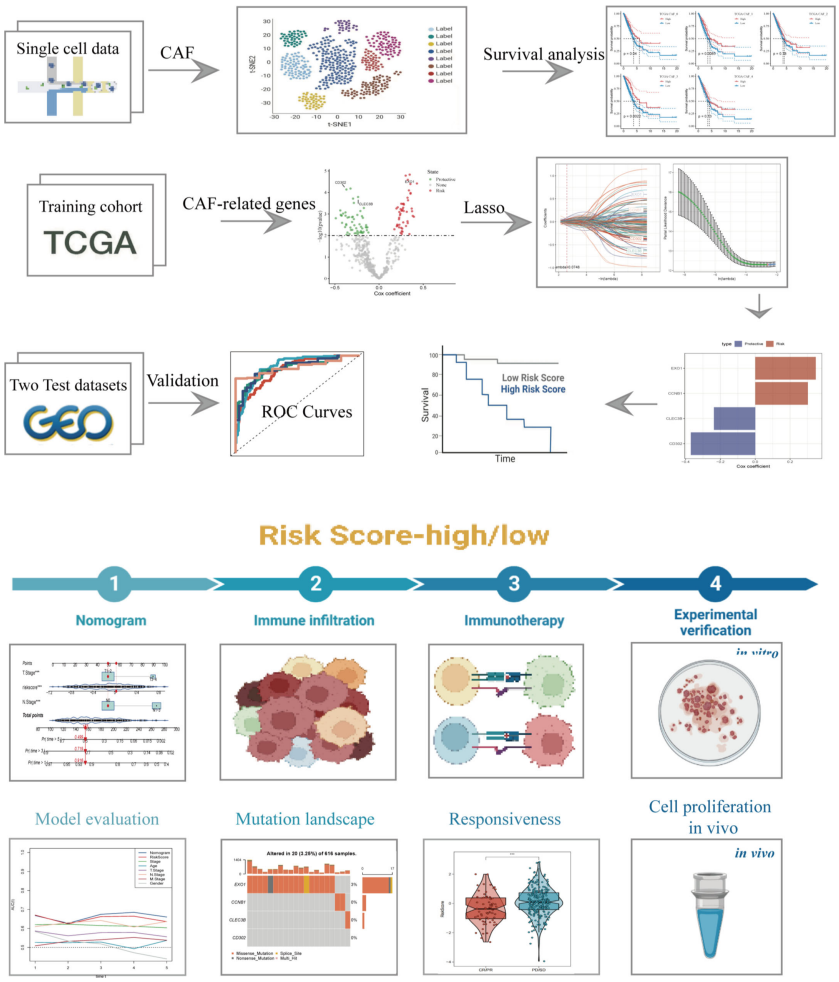


FIGURE 1
The flow chart of this study.

interaction, focal adhesion, proteoglycans in cancer, PI3K-Akt signaling pathway, and others, as presented in Figure 2F. Finally, the distribution of tumor and normal cells based on the five CAF clusters according to the CNV characteristics is shown in Figure 2G.

3.2 The analysis of cancer-related pathways in CAF

We explored the characteristics of ten tumor-related pathways in the five CAF clusters to elucidate the correlations between tumor progression and the CAF clusters. GSVA was employed to investigate the underlying mechanisms involved in the progression and prognostication of LUAD. GSVA scores of those pathways were calculated based on different CAF clusters, and the results are presented in Figure 3A. As shown in Figure 3B, the percentage of normal cells in CAF_0 cluster was the highest, while the ratio of malignant cells from CAF_1 was significantly higher than that in the others. Significant differences were only identified among the CAF_0, CAF_2, and CAF_4. Furthermore, GSVA scores were analyzed based on the ten tumor-related pathways between normal and malignant cells in each CAF cluster, with slight differences observed in CAF_2 and CAF_4 (Figures 3C–F). (The results of GSVA score analysis in CAF_0 is shown in Figure S2).

Moreover, to explore the correlations between the CAF clusters and crucial clinicopathologic features, we analyzed the ssGSEA score of the marker genes (the top 5 DEGs referred to in Figures 2C, D) of each CAF cluster according to the TCGA cohort. The results showed that tumor samples had a significantly higher score compared with normal ones in each cluster (Figure S2B). Using the survminer R package, LUAD samples of TCGA cohort were divided into low-and-high CAF score groups based on the optimal cut-off value. The samples in the low-CAF score group had a significantly worse prognosis in CAF_0, CAF_1, and CAF_3. Although no significant differences were observed in the other two clusters, there was a trend that patients in high-CAF score groups shared a better prognosis (Figure S2C). Furthermore, other clinicopathologic features, including T. stage, N. stage, M. stage, and stage, were included in the analysis. Only slight differences were observed between low-and-high CAF group patients (Figure S3). However, patients in high-CAF groups tended to share favorable clinicopathologic features.

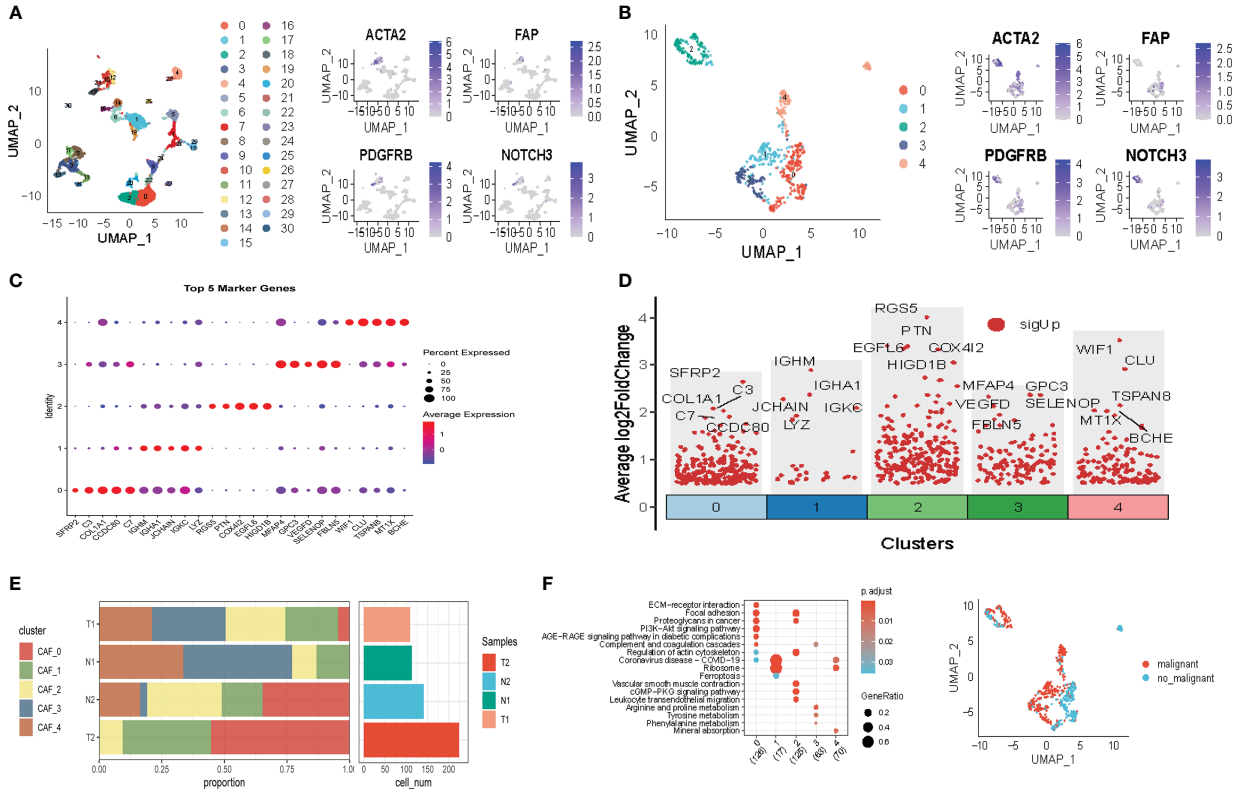


FIGURE 2
The identification of CAF clusters according to scRNA-data of LUAD patients. **(A)** Umap plots of distribution of 31 clusters and fibroblasts-based marker genes expression. **(B)** Umap plots of distributions of five fibroblasts after clustering. **(C)** Bubble diagram of the top5 marker gene expression of subgroups. **(D)** Volcano plot of the top5 marker gene expression of subgroups. **(E)** Subgroups in cancer and adjacent tissue and proportion as well as cell number calculation. **(F)** KEGG analysis of five fibroblasts subgroups. **(G)** Umap distribution of malignant and non-malignant cells predicted by copycat package.

3.3 Hub genes identification and risk signature construction

To construct a risk signature, we first screened for DEGs between normal and tumor tissues. A total of 1731 DEGs were obtained, with 725 up-regulated and 1006 down-regulated (Figure 4A). Out of these, 492 genes were significantly correlated with the prognosis-related CAF clusters. Using univariate Cox regression analysis, we further evaluated the prognosis of each gene, identifying 49 genes related to risk factors and 62 genes exhibiting protective values (Figure 4B). To reduce the number of genes, we conducted Lasso Cox regression analysis, resulting in 4 genes with lambda=0.074 (Figure 4C). Finally, we used the stepwise regression method to construct the risk signature after multivariate Cox regression analysis. The signature consists of 4 genes (Figures 4D, E), namely Exonuclease 1 (EXO1), Cyclin B1 (CCNB1), C-Type Lectin Domain Family 3 Member B (CLEC3B), and Type I C-type lectin receptor CD302. The final signature formula is as follows: RiskScore = -0.123*CLEC3B*+*0.114*EXO1 + 0.103*CCNB1*+-*0.177*CD302. Using z-mean normalization, we calculated the risk score for each sample, dividing patients into high and low-risk groups. Kaplan-Meier survival analysis showed that low-risk patients had significantly better survival outcomes compared to high-risk patients, not only in the TCGA cohort (Figure 4F) but also in the GSE72094 (Figure 4G) and GSE26939 (Figure 4H) cohorts. Additionally, based on the TCGA and GEO cohorts, the AUC values of the signature for 1-3-5-year survival were satisfying, indicating the model's excellent predictive power (Figures 4F-H). We also presented the distribution of risk score, patient survival status, and expression of hub genes in the TCGA cohort in Figure S3A. Similarly, the results of GSE72094 and GSE26939 were shown in Figures S3B-C.

3.4 Recognition of independent risk factors and development of nomogram

To construct a more accurate predictive model, we integrated the risk score with clinicopathological characteristics using both univariate and multivariate Cox regression analyses. The multivariate analysis demonstrated that the risk signature was the most significant independent prognostic factor for lung adenocarcinoma (p-value < 0.001), followed by N-stage (Figures 5A, B). Accordingly, we developed a novel nomogram incorporating T-stage, N-stage, and risk score (Figure 5C), which demonstrated strong predictive power for actual survival outcomes according to calibration plot analysis (Figure 5D). TimeROC analysis in the TCGA cohort confirmed that the AUC of the nomogram and risk score exceeded that of other indicators (Figure 5E).

10.3389/fimmu.2023.1201573

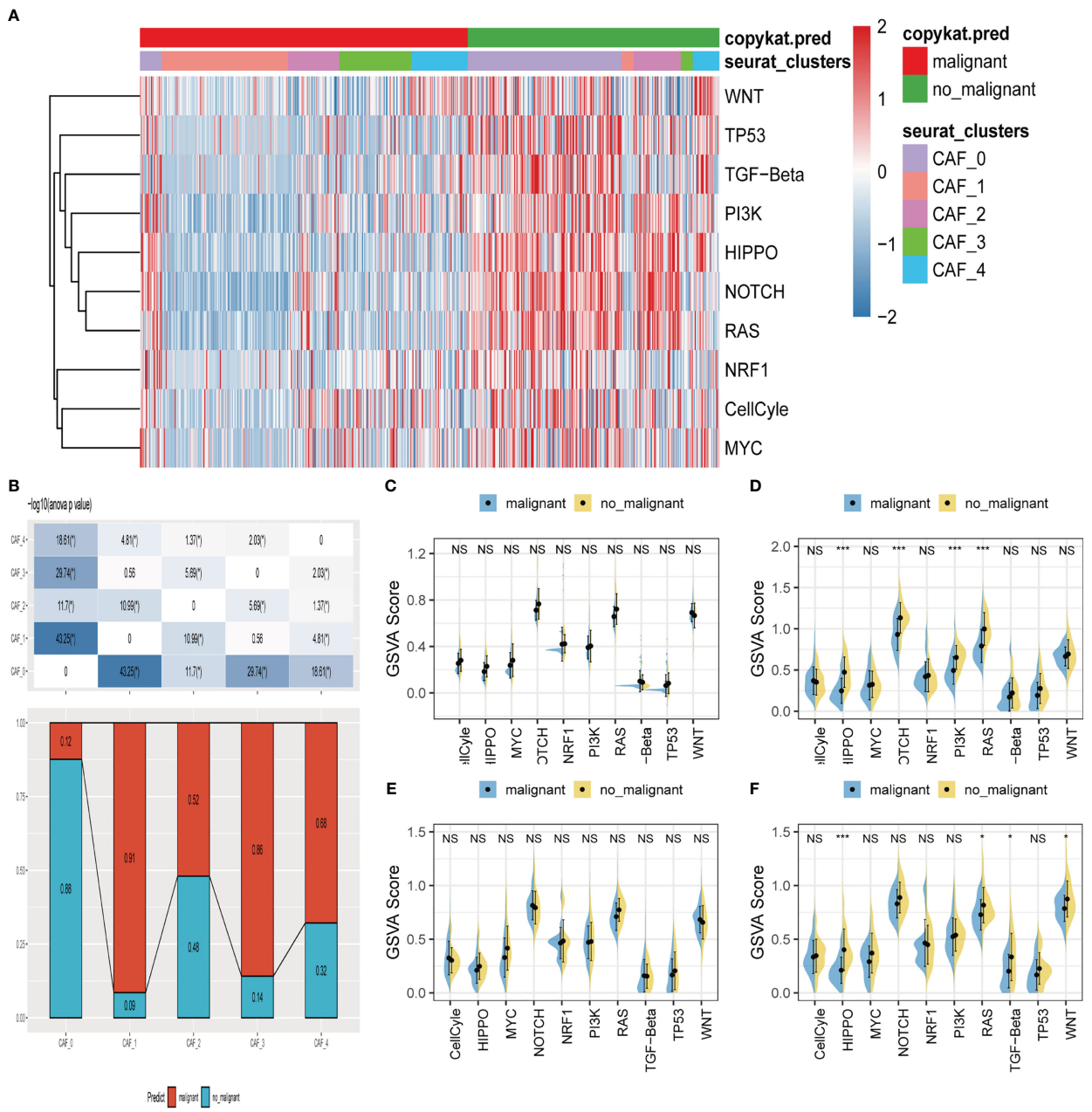


FIGURE 3
The characteristics of tumor-associated pathways in CAF clusters. **(A)** Heatmap of 10 tumor-associated pathways enriched in CAF cells. **(B)** Comparison between each cluster based on proportions of malignant and non-malignant cells. Comparison of each pathway between malignant and non-malignant cells based on GSVA score in CAF_0 (Figure S2A), CAF_1 **(C)**, CAF_2 **(D)** CAF_3 **(E)** CAF_4 **(F)**. (Wilcox. Test, *P < 0.05; ***P < 0.001; ns, not significant.).

3.5 Correlations between the risk signature and clinicopathologic features in LUAD patients

After examining the clinicopathologic features (Age, Gender, Stage, T-stage, N-stage, and M-stage) between high- and low-risk groups, we found that gender, T-stage, N-stage, and stage were significantly associated with the risk signature (Figure S4A). These findings were consistent with previous studies that identified gender as a risk factor for LUAD, with males being more likely to be in the high-risk group (Figure S4B). Moreover, patients in the high-risk group tended to have more advanced clinical stages (Figures S4C-E).

3.6 Tumor mutation analysis

Exploring SNV mutations in lung adenocarcinoma based on the TCGA cohort to investigate the SNV mutations in lung adenocarcinoma, the top 20 genes with the highest mutation

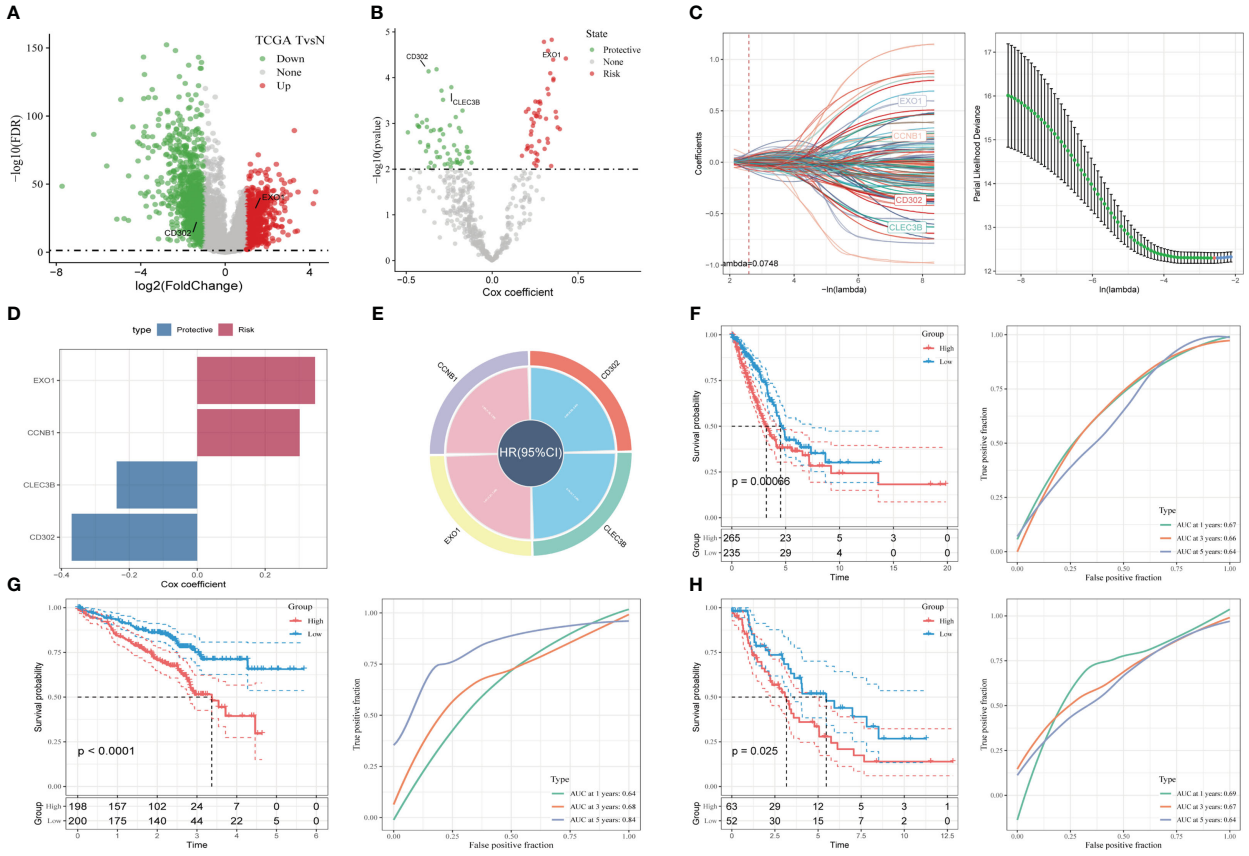


FIGURE 4
A novel risk signature constructed based on several CAF-related genes. **(A)** Volcano plot of differentially expressed genes between tumor and normal samples in TCGA cohort. **(B)** Volcano plot of prognosis-correlated genes obtained by univariate Cox regression analysis. **(C)** Each independent variable's trajectory and distributions for the lambda. **(D-E)** The multivariate Cox coefficients for each gene in the risk signature. **(F)** K-M and ROC curves of the risk signature in TCGA cohort. **(G)** K-M and ROC curves of the risk signature in GSE72094 cohort. **(H)** K-M and ROC curves of the risk signature in GSE26939 cohort.

frequency were analyzed based on the TCGA cohort, as shown in Figure 6A. Subsequently, the SNV mutations of the four genes in the risk signature were examined. As displayed in Figure 6B, EXO1 had the highest mutation frequency, with Missense-Mutation being the most common type of mutation. Conversely, no mutations were observed in CD302. Additionally, the probability of co-occurrence of the 10 most mutated genes and the risk genes (except for CD302) was assessed, and the results indicated a low likelihood of co-occurrence of mutations in these three genes. However, EXO1 was found to significantly co-occur with MUC16, CSMD3, RYR2, ZFHX4, and USH2A (Figure 6C). Further analysis revealed that only a few samples had loss/gain of CNV based on the four genes (Figure 6E). The fraction of the pathway affected by these risk genes was also calculated in the TCGA cohort (Figure 6D). Moreover, the relationships between the risk genes and several molecular signatures of LUAD were explored to demonstrate the links between the risk genes and LUAD. The results indicated that EXO1 and CCNB1 were positively correlated with molecular signatures such as Aneuploidy Score, Homologous Recombination Defects, and Fraction Altered, while CLEC3B and CD302 were negatively correlated with these signatures (Figure 6F).

3.7 Gene set enrichment analysis

Based on these four genes from the risk signature, Gene Set Enrichment Analysis was performed. The results showed that 16 pathways were significantly correlated with these four genes in total (Figures 7A, B), such as the p53 signaling pathway, cell cycle, and DNA replication. Similar to the results obtained previously, EXO1 and CCNB1 were positively correlated with these pathways, while CD302 and CLEC3B were negatively related to them. The GSEA score was estimated based on the high-and-low-risk subgroups (Figures 7C, D). Centromere Complex Assembly, Cell Cycle Checkpoint Signaling, and Cell Cycle G2 Phase Transition were significantly enriched in the high-risk group. In contrast, Positive Regulation of Lipase Activity, Axoneme Assembly, and Cilium Movement were significantly enriched in the low-risk group.

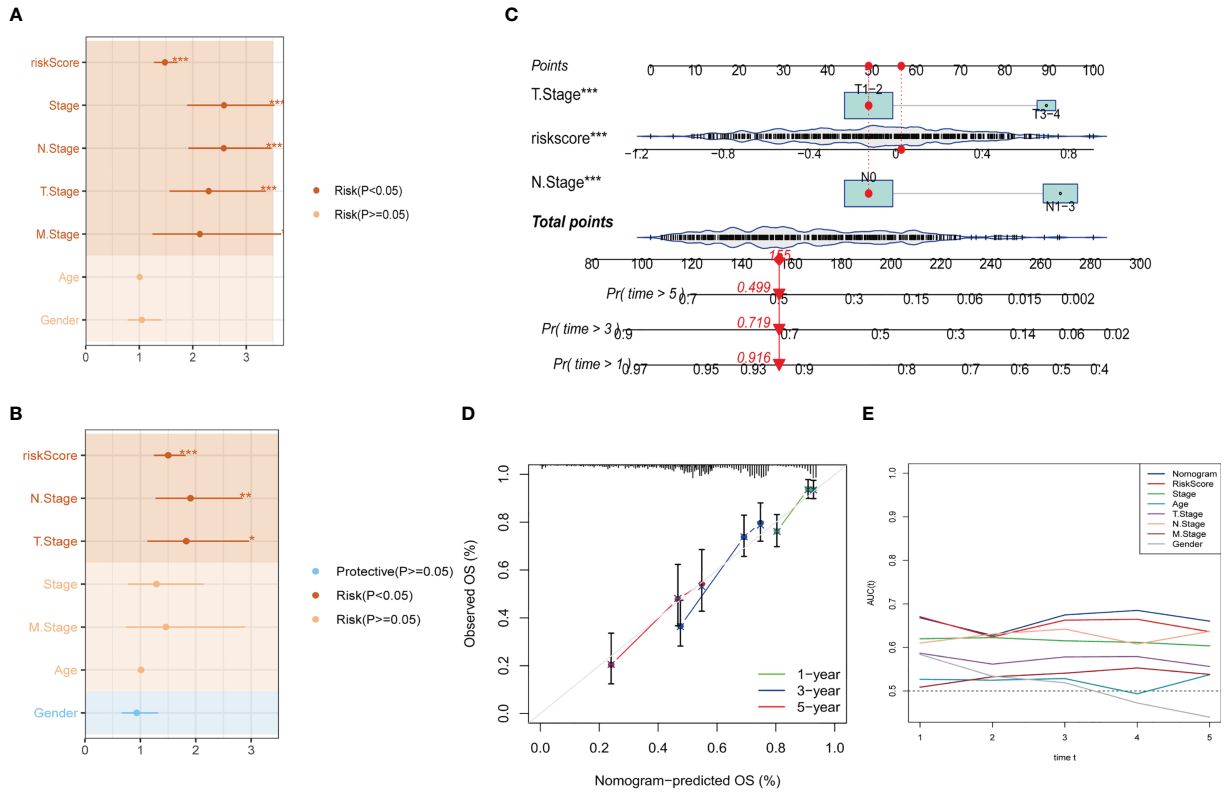


FIGURE 5
Development of a novel nomogram integrating the risk signature and several clinicopathologic features. **(A)** Results of univariate Cox regression analysis based on risk score and clinicopathologic features. **(B)** Results of multivariate Cox regression analysis based on risk score and clinicopathologic features. **(C)** Construction of the nomogram integrating the risk score and clinical stage. **(D)** Calibration curves for 1, 3, and 5 years of nomogram. **(E)** Evaluation of predictive capacity of nomogram and clinicopathologic features by time-ROC analysis. (*P < 0.05; **P < 0.01; ***P < 0.001).

Finally, the results of KEGG and GO analysis are shown in Figure 7E.

3.8 Landscape of immune infiltrations and relationship between risk genes and immunity

After investigating the landscape of immune and stromal cell infiltrations in both low- and high-risk groups, we found that Figure 8A illustrates how patients in the low-risk group have higher proportions of immune and stromal cell infiltrations compared to those in the high-risk group. Moreover, using the CIBERSORT algorithm (42, 43), we calculated the immune cell proportions between the high- and low-risk groups (Figure 8B) and found that patients in the high-risk group significantly shared higher proportions of CD8 T cells, activated memory CD4 T cells, activated NK cells, Macrophages (M0), and Macrophages (M1). On the other hand, B cells, resting memory CD4 T cells, Monocytes, resting dendritic cells, and Activated mast cells were significantly enriched in the low-risk group.

We then explored the relationship between risk genes and immunity. Our results showed that EXO1 and CCNB1 had a significantly negative relationship with the majority of T cells, while CLEC3B and CD302 were remarkably correlated with Macrophages (Figure 8C). Additionally, correlation analysis presented that EXO1 and CCNB1 were negatively linked with Stromal Score, Immune Score, and ESTIMATE Score. In contrast, the other risk genes exhibited the opposite trend (Figures 8D, E, G). Finally, Figure 8F revealed the correlation between the four risk genes and the 75 immune-related genes.

3.9 Response to PD-L1 blockade immunotherapy based on risk signature

We analyzed the response to PD-L1 blockade immunotherapy in the IMvigor210 and GSE78220 cohorts after assessing immune infiltrations. The 348 patients from the IMvigor210 cohort presented different responses to anti-PD-L1 receptor blockers, including stable disease (SD), partial response (PR), complete response (CR), and progressive disease (PD). We found that CR/PR patients had lower risk scores than SD/PD patients (Figure 9B). Additionally, in the low-risk group, the proportion of SD/PD patients was lower than that in the high-risk group (Figure 9C). Our analysis of the IMvigor210 cohort revealed that patients in the low-risk group had significantly better clinical outcomes than those in the high-risk group (Figure 9A). Furthermore, we identified

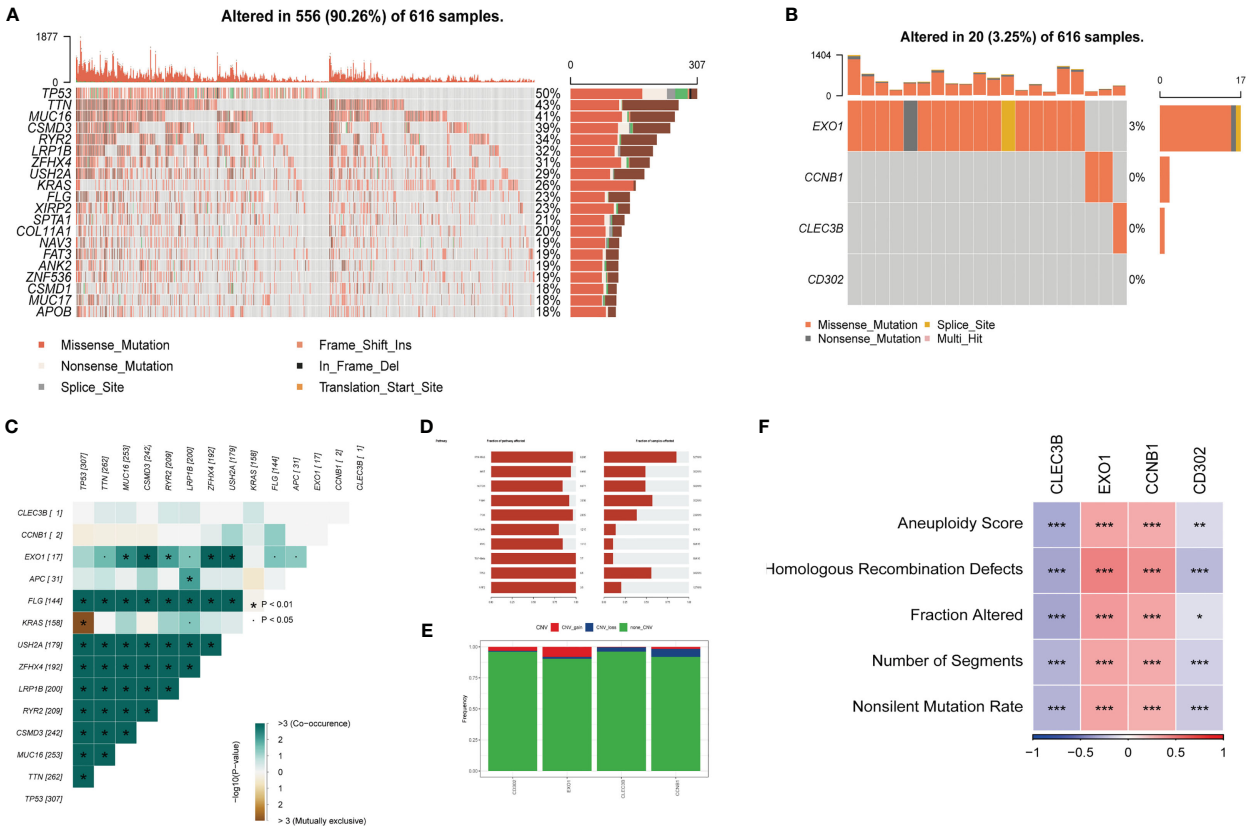


FIGURE 6
Tumor mutations analysis (TMB) **(A)** The landscape of mutations based on the TCGA cohort. **(B)** Waterfall diagram displaying SNV mutations of four key genes. **(C)** Mutual exclusion and collinearity analysis of the four genes and the 10 most mutated genes in tumors. **(D)** The proportions of 10 tumor-related pathways were depicted. **(E)** CNV mutations (gain, loss, none) of four key genes. **(F)** Correlation heatmap of six key genes with Homologous Recombination Defects, Aneuploidy Score, Number of Segments, Fraction Altered, and Nonsilent Mutation Rate. (*P < 0.05; **P < 0.01; ***P < 0.001).

significant survival differences between different risk groups not only in Stage I+II but also in Stage III+IV patients (Figures 9D, E).

To confirm our findings, we enrolled the GSE78220 cohort into further analysis. Corresponding with the results obtained in IMvigor210, PR/CR patients had lower risk scores and shared a lower percentage in the high-risk group (Figures 9F–H).

3.10 Validation of the tumor-related role of EXO1 in NSCLC

In order to further elucidate the function of EXO1 in LUAD, we conducted *in vitro* research to scrutinize the function of EXO1 in LUAD cells. We gauged the degree of EXO1 expression after 24 hours of transfection *via* qRT-PCR to assess the efficacy of siRNA-mediated EXO1 knockdown in A549 and H1299 cell lines. As compared to the NC group, we observed a marked reduction in the expression of EXO1 in A549 and H1299 cells upon treatment with siRNA (Si-1 and Si-2) sequences ($P < 0.001$) (Figures 10). Correspondingly, the CCK-8 assay revealed that suppression of EXO1 significantly curbed the viability of A549 and H1299 cells as compared to control cells (Figure 10A). The findings of the EdU staining assay provided further evidence that inhibition of EXO1 expression impeded the proliferation of A549 and H1299 cells relative to the NC group (Figure 10B). This implies that EXO1 might play an indispensable role in the proliferation of LUAD cells. The transwell experiments confirmed that EXO1 knockdown considerably reduced the migration and invasion of A549 and H1299 cells (Figure 10C). The scratch-wound healing experiment also produced congruent results, wherein decreased EXO1 expression led to a noteworthy deceleration in the rate of wound healing in cells (Figure 10D). To ensure the accuracy and consistency of the results, all tests were performed in two LUAD cell lines (A549 and H1299), and all data were presented as means with standard deviations from three independent experiments. *P < 0.05, **P < 0.01, ***P < 0.001.

4 Discussion

With a growing understanding of the tumor microenvironment (TME), research focus has broadened from immune cells to other cellular components, such as cancer-associated fibroblasts (CAFs) (22). As a crucial component of the TME, CAFs have divergent functions, such as matrix remodeling and deposition, extensive reciprocal signaling interactions with infiltrating leukocytes and crosstalk with cancer cells (44). Cancer-associated fibroblasts (CAFs) present in primary and metastatic neoplasms are

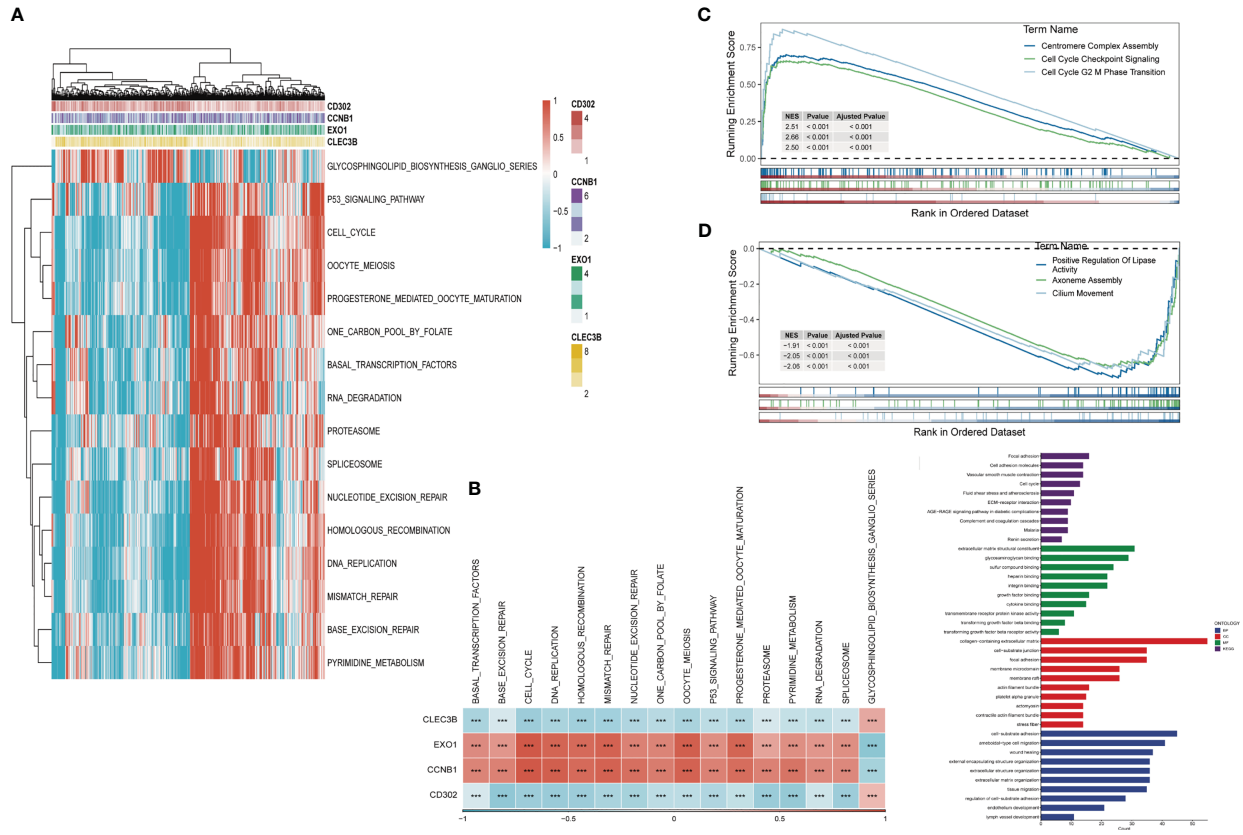


FIGURE 7
Gene Set Enrichment Analysis (GSEA) **(A)** Heatmap exhibiting enrichment score for key pathways based on the hub genes. **(B)** Gene-pathway correlation heatmap, **(C)** Pathways enriched in high-risk group. **(D)** Pathways enriched in low-risk group. **(E)** KEGG and GO analysis. (***P < 0.001).

extremely adaptable, malleable, and robust cells that actively participate in the advancement of cancer by engaging in intricate cross-talk with other cellular entities in the tumor microenvironment (19). Within the microenvironment of cancer, stromal cells play a significant role, and among them, cancer-associated fibroblasts (CAFs) make up the largest portion and are closely linked to cancer progression. Additionally, the cancer stroma can promote tumor recurrence and contribute to therapeutic resistance, explaining why current anti-tumor therapeutic approaches often fail to eliminate malignancy (45). Therefore, investigating the tumor microenvironment (TME) with a focus on cancer-associated fibroblasts (CAFs) could not only enhance our understanding of their phenotypic diversity but also provide new insights into anti-tumor therapies. In this study, we utilized single-cell RNA sequencing (scRNA-seq) data to investigate the heterogeneity of CAFs and systematically identify and classify them in lung adenocarcinoma (LUAD). As a result, we identified five distinct CAF clusters that may play a critical role in regulating the TME's biology. Furthermore, growing evidence suggests that a CAF-related gene signature can accurately predict the prognosis of LUAD patients (46, 47). Consistent with these findings, our results showed that three of the clusters had significant association with LUAD prognosis. By performing the GSVA analysis, a slight correlation was observed between the ten cancer-related pathways and the five clusters. The Hippo signaling was significantly enriched in no-malignant part in our data, and a recent study has revealed that Hippo signaling might work as a crucial tumor suppressor pathway, which may account for the prognostic value of CAF to some extent.

Next, we constructed a CAF-related risk signature using four genes based on the prognostic values of the three identified CAF clusters. The risk signature included two risk genes (EXO1 and CCNB1) and two protective genes (CLEC3B and CD302). To assess the accuracy of this signature, we validated it using external cohorts, including TCGA, GSE72094, and GSE26939, and obtained favorable results. Notably, EXO1, a crucial nuclease associated with the mismatch repair system, was among the genes included in the risk signature. Dysregulation of this gene has been linked to proliferation, migration, and invasion in LUAD (48). Besides, exonuclease 1 (EXO1) constitutes a plausible prognostic biomarker and exhibits significant correlations with immune infiltrates in lung adenocarcinoma (49). Moreover, one research suggested that the high expression of EXO1 was significantly correlated with aneuploidy, promoting tumor invasion in LUAD (50). Cell cycle-promoted factor CCNB1 can be targeted by VPS33B *via* c-Myc/p53/miR-192-3p to modulate the pathogenesis of non-small cell lung cancer (NSCLC) (51). In addition, CCNB1 can be directly targeted by microRNA-718, suppressing tumor immigration NSCLC (52). CLEC3B and CD302 have been verified downregulated in lung cancer and having the diagnostic

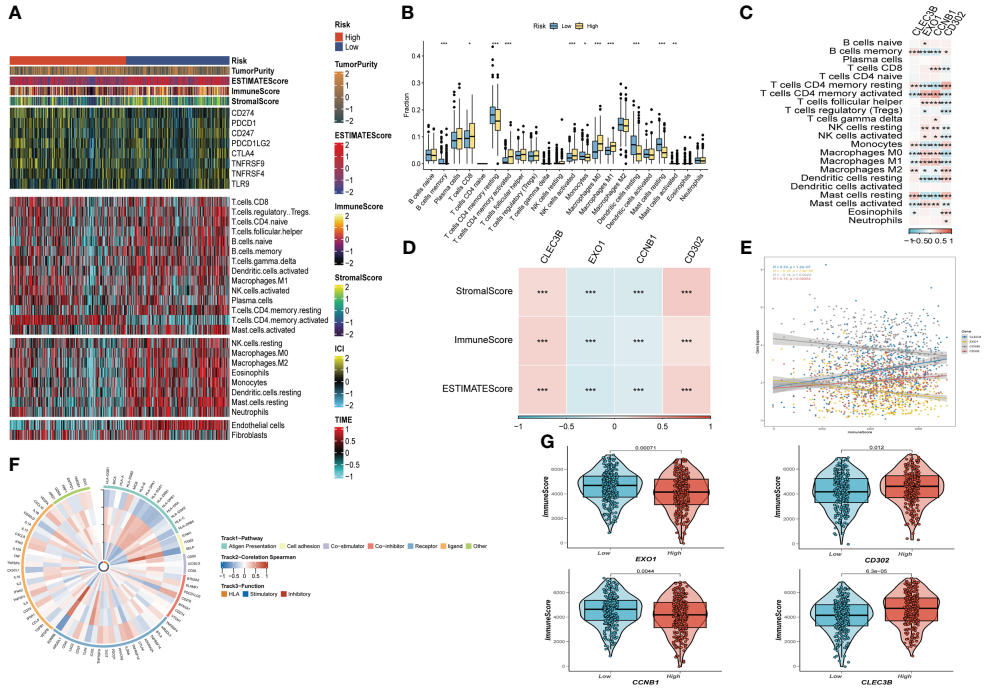


FIGURE 8
The immune infiltrations analysis **(A)** Heatmap of results on immune cells of tumor microenvironment (TME) in LUAD with multialgorithm, including existing data from platform TIMER and MCP-counter. TME-related scores were exhibited in the top bar. **(B)** Comparison of proportions of 22 immune-related cells between high-and-low-risk groups. **(C)** Correlations between four hub genes and 22 immune-related cells. **(D,E,G)** Correlations between the four hub genes and immune score, stromal score, estimate score. **(F)** The correlation analysis between four hub genes and 75 immune-associated genes. (*P < 0.05; **P < 0.01; ***P < 0.001).

and prognostic values in lung cancer (53, 54). The patients were then classified into high- and low-risk groups based on the median risk score, and subsequent analysis demonstrated that the low-risk group had a significantly better prognosis than the high-risk group. Furthermore, univariate and multivariate Cox regression analyses confirmed that the risk score was an independent predictor of overall survival (OS). We developed a nomogram based on the risk signature, which demonstrated a high degree of consistency between predicted and observed results regarding the OS of LUAD patients. In conclusion, our findings indicate that the risk signature we constructed can accurately predict the prognosis of LUAD patients. With the risk signature and novel nomogram, early and accurate diagnosis of LUAD could be achieved and patients will be stratified more appropriately.

Considering the fact that precise therapy for lung cancer rely on comprehensive genomic analyses (55), the mutation profile of LUAD patients based on TCGA cohort were depicted, which reflected the high frequency of mutations of LUAD. The tumor mutation burden was further performed based on our risk signature. Among them, EXO1 was the only gene observed with mutations in our data. Besides, EXO1 was identified co-occurring with several highly mutated genes, including MUC16, CSMD3, RYR2, ZFHX4, and USH2A. Additionally, EXO1 was found positively correlated with several molecular signatures, such as aneuploidy, fraction altered, and so on. One study has indicated that the hyper-excision of DNA triggered by a deficiency in MLH1, *via* exonuclease 1, stimulates the cGAS-STING pathway, thereby facilitating the migration of tumors (56). As reported, high level of aneuploidy is related to lung cancer progression (57). Taken as a whole, we can infer that high expression level of EXO1 might prospect unfavorable clinical outcomes, and further endeavor on EXO1 research might promote the development of precision therapeutics.

To elucidate the divergent pathways that the genes involved in the signature enriched, Gene Set Enrichment Analysis (GSEA) was conducted. The results revealed that risk genes (EXO1 and CCNB1) were positively linked with several pathways, including p53 signaling pathway, cell cycle, DNA replication, etc. The protective genes (CD302 and CLEC3B), however, were positively associated with only one pathway-glycosphingolipid_biosynthesis_ganglio_series. Accumulating evidence has confirmed that several crucial molecules could propel the proliferation, migration, and invasion *via* p53 signaling pathway and DNA replication in LUAD (58–60). Moreover, high expression of EXO1 and CCNB1 was identified significantly correlated with p53 signaling pathway, cell cycle, and DNA replication (61, 62). Then, GSEA was performed according to high-and-low-risk groups. The high-risk group was remarkably enriched in centromere complex assembly, cell cycle checkpoint signaling, and cell cycle G2 M phase transition, which have been confirmed significantly correlated with progression in LUAD (63–65).

Far from only aggregates of malignant cells, tumors are well-organized complex ecosystems (66). Consisting of distinct immune cell populations in tumor islands, the TIME is dramatically correlated with the antitumor immunological state of the TME (67). The TIME

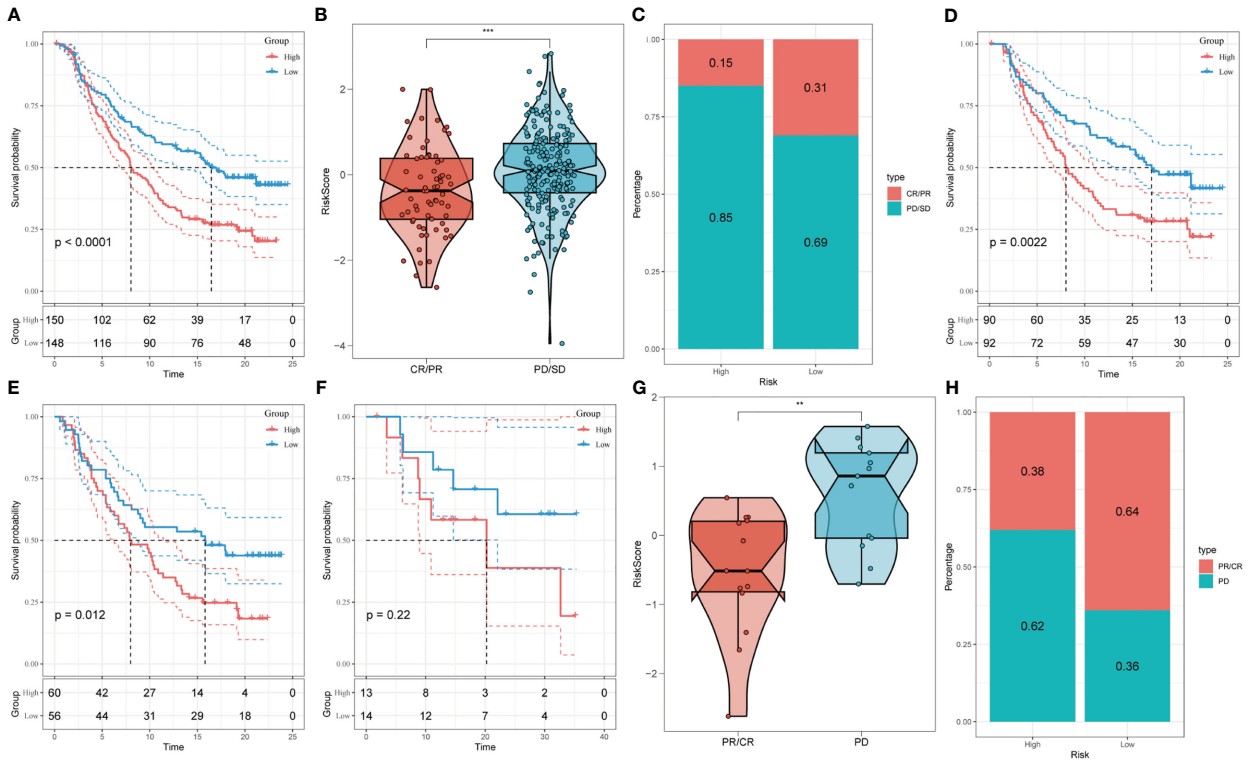


FIGURE 9
Prediction of responsiveness to immunotherapy using our signature based on public database. **(A)** Prognostic differences between risk subgroups in the IMvigor210 cohort. **(B)** Differences among immunotherapy responses based on risk scores in the IMvigor210 cohort. **(C)** Distribution of immunotherapy responses based on risk subgroups in the IMvigor210 cohort. **(D)** Prognostic differences between risk subgroups based on early stage (stage I-II) in the IMvigor210 cohort. **(E)** Prognostic differences between risk subgroups based on advanced patients (stage III-IV) in the IMvigor210 cohort. **(F)** Prognostic differences between risk subgroups in the GSE78220 cohort. **(G)** Differences among immunotherapy responses based on risk scores in the GSE78220 cohort. **(H)** Distribution of immunotherapy responses based on risk subgroups in the GSE78220 cohort. (**P < 0.01; ***P < 0.001).

have long been identified substantially associated with tumor progression, recurrence and metastasis (68). To further understand the implications of our risk signature, we assessed the immune infiltration state using various algorithms. Our results demonstrated that the low-risk group had a higher level of immune cell infiltration, suggesting that this group was more likely to establish a "hot" tumor state that could accelerate the immune system to inhibit tumor progression. In contrast, the high-risk group had higher levels of M0 and M1 macrophages. A recent study has revealed that M0 to M2 polarization is linked to the immune suppression (69). We also investigated the correlations between the four genes included in the risk signature and the 22 immune infiltration cells. Our results showed that EXO1 was positively linked with various types of T cells, suggesting that it could be a potential target for immunotherapy. Moreover, the risk genes (EXO1 and CCNB1) were found to be negatively associated with stromal score, immune score, and estimate score. Despite the emergence of immunotherapy, a significant number of LUAD patients still experience this highly malignant tumor due to innate or acquired resistance to such therapies (70). Therefore, it is crucial to identify patients who are likely to benefit from immunotherapy. Using the IMvigor210 and GSE78220 cohorts, we found that our risk signature could effectively classify patients who were more likely to benefit from immunotherapies. In summary, our risk signature based on CAFs can independently predict the prognosis of LUAD patients and predict their responsiveness to immunotherapy.

Nevertheless, there are some limitations in our study that need to be addressed. Firstly, the risk signature was established using retrospective data from public databases. Therefore, more prospective and multi-center LUAD cohorts are required to eliminate bias. Secondly, we only predicted the responsiveness to anti-PD-L1 immunotherapy using our risk signature. Further research is necessary to evaluate the potential of our risk signature to predict the response to other precision therapies in the future.

5 Conclusion

In our study, we extensively investigated the CAF populations in LUAD and identified five CAF clusters with distinct characteristics. Three of these clusters were found to be significantly associated with LUAD prognosis and were used to establish a prognostic risk signature consisting of 4 genes based on

10.3389/fimmu.2023.1201573

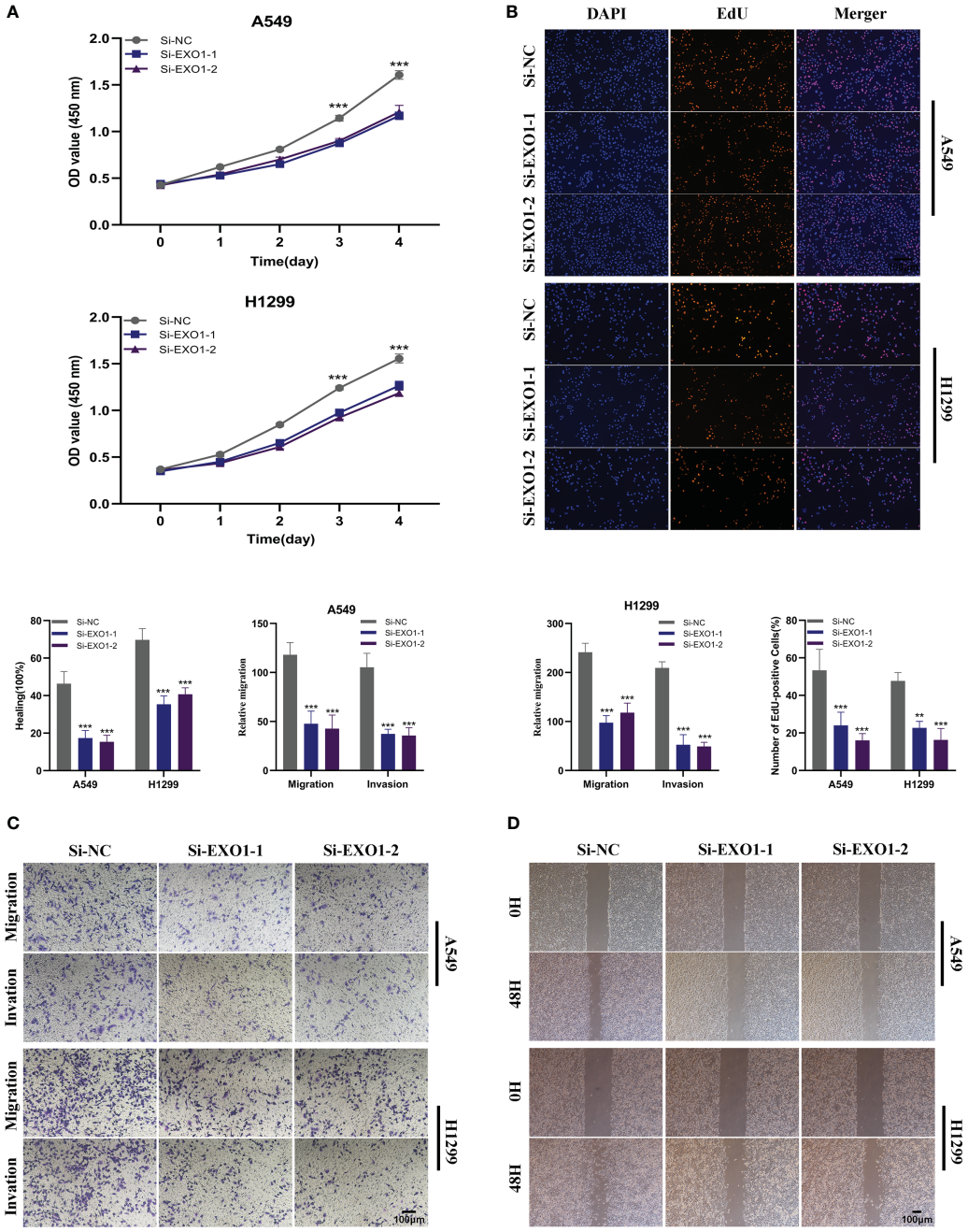


FIGURE 10
The role of EXO1 in LUAD. **(A)** CCK8 assay showed that, after EXO1 knockdown, the cells showed significant reduction in viability. **(B)** EdU staining assay indicated that downregulation of EXO1 expression repressed cell proliferation in LUAD cell lines. **(C)** Transwell assay showed that downregulation of EXO1 expression inhibited the migration and invasion capacity of LUAD cells. **(D)** Scratch-wound healing assay depicted that a significantly slower wound healing rate was observed in cells with a decreased expression of EXO1. To demonstrate the accuracy and reproducibility of the results, all experiments were repeated in two LUAD (A549, H1299) cell lines and all data were presented as the means ± SD of three independent experiments. **P < 0.01, ***P < 0.001.

the CAFs. Furthermore, we developed a novel nomogram that combined the risk signature and clinicopathological characteristics, which performed exceptionally well in predicting the clinical outcome of patients with LUAD. Our risk signature was also observed to be associated with tumor mutations and immune landscape. Additionally, our results indicated that the risk signature is suitable for predicting the responsiveness of LUAD patients to immunotherapy targeting PD-L1 blockade.

6 Ethical approval and consent to participate

All human experiments in this study have been approved by the Ethics Committee of the First Affiliated Hospital of Nanjing Medical University. All subjects gave their informed consent for inclusion before they participated in the study. The study was conducted in accordance with the Declaration of Helsinki, and approved by the

Ethics Committee of the First Affiliated Hospital of Nanjing Medical University (protocol code No.2019-SR-156; 12 June 2019).

Data availability statement

The datasets presented in this study can be found in online repositories. The names of the repository/repositories and accession number(s) can be found within the article/Supplementary Materials.

Ethics statement

This study was approved by the Ethics Committee of Jiangsu Province People's Hospital (2019-SR-156), written informed consent was obtained from the patients/participants.

Author contributions

QR, PZ, HL and YY contributed conception and design of the study. YF, HaC and XZ finished the dada collection. HuC performed the statistical analysis. QR wrote the first draft of the manuscript. HL and YY revised the manuscript. ZX, HuC and YY gave the final approval of the version to be submitted.

Acknowledgments

We are very grateful for data provided by databases such as TCGA, GEO. Thanks to reviewers and editors for their sincere comments.

Conflict of interest

The authors declare that the research was conducted in the absence of any commercial or financial relationships that could be construed as a potential conflict of interest.

Publisher's note

All claims expressed in this article are solely those of the authors and do not necessarily represent those of their affiliated organizations, or those of the publisher, the editors and the reviewers. Any product that may be evaluated in this article, or claim that may be made by its manufacturer, is not guaranteed or endorsed by the publisher.

Supplementary material

The Supplementary Material for this article can be found online at: https://www.frontiersin.org/articles/10.3389/fimmu.2023.1201573/full#supplementary-material

SUPPLEMENTARY FIGURE 1
The details of re-process of scRNA-seq data of LUAD. **(A)** The relationship between the amount of mRNA/UMI and mitochondrial genes, the relationship between the amount of mRNA and UMI. **(B)** The relationship among UMI, mRNA, mitochondrial content, and rRNA of each sample before filtering. **(C)** Violin plots exhibited the expression of CAF-associated marker genes before clustering. **(D)** Violin plots displayed the expression of CAF-associated marker genes after clustering.

SUPPLEMENTARY FIGURE 2
(A) Comparison of each pathway between malignant and non-malignant cells based on GSVA score in CAF_0. **(B)** Comparison of five CAF scores in malignant and non-malignant tissues. **(C)** K-M curves of high-and-low CAF-score groups in the five clusters.

SUPPLEMENTARY FIGURE 3
Validation of the signature's capacity in prognosis prediction **(A)** Distribution of risk scores and survival status in TCGA cohort. **(B)** Distribution of risk scores and survival status in GSE72094 cohort. **(C)** Distribution of risk scores and survival status in GSE26939.

SUPPLEMENTARY FIGURE 4
The relationship between risk score and several clinicopathologic features. **(A)** The landscape of differences between high-and-low-risk subgroups. The differences between high-and-low-risk groups based on Gender **(B)**, Stage **(C)**, T-stage **(D)**, N-stage **(E)**.

References

1. Thai AA, Solomon BJ, Sequist LV, Gainor JF, Heist RS. Lung cancer. *Lancet* (2021) 398:535–54. doi: 10.1016/S0140-6736(21)00312-3

2. Travis WD, Garg K, Franklin WA, Wistuba II, Sabloff B, Noguchi M, et al. Evolving concepts in the pathology and computed tomography imaging of lung adenocarcinoma and bronchioloalveolar carcinoma. *J Clin Oncol* (2005) 23:3279–87. doi: 10.1200/JCO.2005.15.776

3. Devarakonda S, Li Y, Martins Rodrigues F, Sankararaman S, Kadara H, Goparaju C, et al. Genomic profiling of lung adenocarcinoma in never-smokers. *J Clin Oncol* (2021) 39:3747–58. doi: 10.1200/JCO.21.01691

4. Chaft JE, Rimner A, Weder W, Azzoli CG, Kris MG, Cascone T. Evolution of systemic therapy for stages I-III non-metastatic non-small-cell lung cancer. *Nat Rev Clin Oncol* (2021) 18:547–57. doi: 10.1038/s41571-021-00501-4

5. Wang C, Yu Q, Song T, Wang Z, Song L, Yang Y, et al. The heterogeneous immune landscape between lung adenocarcinoma and squamous carcinoma revealed by single-cell RNA sequencing. *Signal Transduct Target Ther* (2022) 7:289. doi: 10.1038/s41392-022-01130-8

6. Chen XY, Zhang J, Zhu JS. The role of m(6)A RNA methylation in human cancer. *Mol Cancer* (2019) 18:103. doi: 10.1186/s12943-019-1033-z

7. Ma JZ, Yang F, Zhou CC, Liu F, Yuan JH, Wang F, et al. METTL14 suppresses the metastatic potential of hepatocellular carcinoma by modulating N(6) -methyladenosine-dependent primary MicroRNA processing. *Hepatology* (2017) 65:529–43. doi: 10.1002/hep.28885

8. Zhuang Z, Chen L, Mao Y, Zheng Q, Li H, Huang Y, et al. Diagnostic, progressive and prognostic performance of m(6)A methylation RNA regulators in lung adenocarcinoma. *Int J Biol Sci* (2020) 16:1785–97. doi: 10.7150/ijbs.39046

9. Xu JY, Zhang C, Wang X, Zhai L, Ma Y, Mao Y, et al. Integrative proteomic characterization of human lung adenocarcinoma. *Cell* (2020) 182:245–261 e17. doi: 10.1016/j.cell.2020.05.043

10. Hu K, Li K, Lv J, Feng J, Chen J, Wu H, et al. Suppression of the SLC7A11/glutathione axis causes synthetic lethality in KRAS-mutant lung adenocarcinoma. *J Clin Invest* (2020) 130:1752–66. doi: 10.1172/JCI124049

11. Wang M, Herbst RS, Boshoff C. Toward personalized treatment approaches for non-small-cell lung cancer. *Nat Med* (2021) 27:1345–56. doi: 10.1038/s41591-021-01450-2

12. Lim SM, Syn NL, Cho BC, Soo RA. Acquired resistance to EGFR targeted therapy in non-small cell lung cancer: mechanisms and therapeutic strategies. *Cancer Treat Rev* (2018) 65:1–10. doi: 10.1016/j.ctrv.2018.02.006

13. Reck M, Remon J, Hellmann MD. First-line immunotherapy for non-Small-Cell lung cancer. *J Clin Oncol* (2022) 40:586–97. doi: 10.1200/JCO.21.01497

14. Rolfo C, Mack P, Scagliotti GV, Aggarwal C, Arcila ME, Barlesi F, et al. Liquid biopsy for advanced NSCLC: a consensus statement from the international association for the study of lung cancer. *J Thorac Oncol* (2021) 16:1647–62. doi: 10.1016/j.jtho.2021.06.017

15. DeNardo DG, Galkin A, Dupont J, Zhou L, Bendell J. GB1275, a first-in-class CD11b modulator: rationale for immunotherapeutic combinations in solid tumors. *J Immunother Cancer* (2021) 9. doi: 10.1136/jitc-2021-003005

16. Hack SP, Zhu AX, Wang Y. Augmenting anticancer immunity through combined targeting of angiogenic and PD-1/PD-L1 pathways: challenges and opportunities. *Front Immunol* (2020) 11:598877. doi: 10.3389/fimmu.2020.598877

17. Xie W, Hu N, Cao L. Immune thrombocytopenia induced by immune checkpoint inhibitrs in lung cancer: case report and literature review. *Front Immunol* (2021) 12:790051. doi: 10.3389/fimmu.2021.790051

18. Dougan M, Luoma AM, Dougan SK, Wucherpfennig KW. Understanding and treating the inflammatory adverse events of cancer immunotherapy. *Cell* (2021) 184:1575–88. doi: 10.1016/j.cell.2021.02.011

19. Chen Y, McAndrews KM, Kalluri R. Clinical and therapeutic relevance of cancer-associated fibroblasts. *Nat Rev Clin Oncol* (2021) 18:792–804. doi: 10.1038/s41571-021-00546-5

20. Biffi G, Tuveson DA. Diversity and biology of cancer-associated fibroblasts. *Physiol Rev* (2021) 101:147–76. doi: 10.1152/physrev.00048.2019

21. Vitale I, Manic G, Coussens LM, Kroemer G, Galluzzi L. Macrophages and metabolism in the tumor microenvironment. *Cell Metab* (2019) 30:36–50. doi: 10.1016/j.cmet.2019.06.001

22. Kobayashi H, Enomoto A, Woods SL, Burt AD, Takahashi M, Worthley DL. Cancer-associated fibroblasts in gastrointestinal cancer. *Nat Rev Gastroenterol Hepatol* (2019) 16:282–95. doi: 10.1038/s41575-019-0115-0

23. Hu H, Piotrowska Z, Hare PJ, Chen H, Mulvey HE, Mayfield A, et al. Three subtypes of lung cancer fibroblasts define distinct therapeutic paradigms. *Cancer Cell* (2021) 39:1531–1547 e10. doi: 10.1016/j.ccell.2021.09.003

24. Risom T, Glass DR, Averbukh I, Liu CC, Baranski A, Kagel A, et al. Transition to invasive breast cancer is associated with progressive changes in the structure and composition of tumor stroma. *Cell* (2022) 185:299–310 e18. doi: 10.1016/j.cell.2021.12.023

25. Cao Y, Fu L, Wu J, Peng Q, Nie Q, Zhang J, et al. Integrated analysis of multimodal single-cell data with structural similarity. *Nucleic Acids Res* (2022) 50:e121. doi: 10.1093/nar/gkac781

26. Pei S, Zhang P, Yang L, Kang Y, Chen H, Zhao S, et al. Exploring the role of sphingolipid-related genes in clinical outcomes of breast cancer. *Front Immunol* (2023) 14:1116839. doi: 10.3389/fimmu.2023.1116839

27. Sanchez-Vega F, Mina M, Armenia J, Chatila WK, Luna A, La KC, et al. Oncogenic signaling pathways in the cancer genome atlas. *Cell* (2018) 173:321–337 e10. doi: 10.1016/j.cell.2018.03.035

28. Zhao Z, Zhang D, Yang F, Xu M, Zhao S, Pan T, et al. Evolutionarily conservative and non-conservative regulatory networks during primate interneuron development revealed by single-cell RNA and ATAC sequencing. *Cell Res* (2022) 32:425–36. doi: 10.1038/s41422-022-00635-9

29. Gao R, Bai S, Henderson Y, Lin Y, Schalck A, Yan Y, et al. Delineating copy number and clonal substructure in human tumors from single-cell transcriptomes. *Nat Biotechnol* (2021) 39:599–608. doi: 10.1038/s41587-020-00795-2

30. Zhao Z, Zheng R, Wang X, Li T, Dong X, Zhao C, et al. Integrating lipidomics and transcriptomics reveals the crosstalk between oxidative stress and neuroinflammation in central nervous system demyelination. *Front Aging Neurosci* (2022) 14:870957. doi: 10.3389/fnagi.2022.870957

31. Chen Y, Chen S, Lei E. DiffChIPL: a differential peak analysis method for high-throughput sequencing data with biological replicates based on limma. *Bioinf (Oxford England)* (2022) 38:4062–9. doi: 10.1093/bioinformatics/btac498

32. Zhang P, Pei S, Gong Z, Feng Y, Zhang X, Yang F, et al. By integrating single-cell RNA-seq and bulk RNA-seq in sphingolipid metabolism, CACYBP was identified as a potential therapeutic target in lung adenocarcinoma. *Front Immunol* (2023) 14:1115272. doi: 10.3389/fimmu.2023.1115272

33. Chi H, Yang J, Peng G, Zhang J, Song G, Xie X, et al. Circadian rhythm-related genes index: a predictor for HNSCC prognosis, immunotherapy efficacy, and chemosensitivity. *Front Immunol* (2023) 14:1091218. doi: 10.3389/fimmu.2023.1091218

34. Pei S, Zhang P, Chen H, Zhao S, Dai Y, Yang L, et al. Integrating single-cell RNA-seq and bulk RNA-seq to construct prognostic signatures to explore the role of glutamine metabolism in breast cancer. *Front Endocrinol* (2023) 14:1135297. doi: 10.3389/fendo.2023.1135297

35. Wang Y, Zhao Z, Kang X, Bian T, Shen Z, Jiang Y, et al. lncRNA DLEU2 acts as a miR-181a sponge to regulate SEPP1 and inhibit skeletal muscle differentiation and regeneration. *Aging* (2020) 12:24033–56. doi: 10.18632/aging.104095

36. Chi H, Zhao S, Yang J, Gao X, Peng G, Zhang J, et al. viaT-cell exhaustion signatures characterize the immune landscape and predict HCC prognosis integrating single-cell RNA-seq and bulk RNA-sequencing. *Front Immunol* (2023) 14:1137025. doi: 10.3389/fimmu.2023.1137025

37. Zhao Z, Li T, Dong X, Wang X, Zhang Z, Zhao C, et al. Untargeted metabolomic profiling of cuprizone-induced demyelination in mouse corpus callosum by UPLC-Orbitrap/MS reveals potential metabolic biomarkers of CNS demyelination disorders. *Oxid Med Cell Longevity* (2021) 2021:7093844. doi: 10.1155/2021/7093844

38. Shen Y, Chi H, Xu K, Li Y, Yin X, Chen S, et al. A novel classification model for lower-grade glioma patients based on pyroptosis-related genes. *Brain Sci* (2022) 12. doi: 10.3390/brainsci12060700

39. Cui Y, Zhang P, Liang X, Xu J, Liu X, Wu Y, et al. KDRAssociation of mutation with better clinical outcomes in pan-cancer for immune checkpoint inhibitors. *Am J Cancer Res* (2022) 12:1766–83.

40. Xu D, Zhi Y, Liu X, Guan L, Yu J, Zhang D, et al. WDR62-deficiency causes autism-like behaviors independent of microcephaly in mice. *Neurosci Bull* (2022). doi: 10.1007/s12264-022-00997-5

41. Peng J, Pei S, Cui Y, Xia Y, Huang Y, Wu X, et al. Comparative analysis of transient receptor potential channel 5 opposite strand-induced gene expression patterns and protein-protein interactions in triple-negative breast cancer. *Oncol Lett* (2022) 24:259. doi: 10.3892/ol.2022.13379

42. Newman A, Liu C, Green M, Gentles A, Feng W, Xu Y, et al. Robust enumeration of cell subsets from tissue expression profiles. *Nat Methods* (2015) 12:453–7. doi: 10.1038/nmeth.3337

43. Zhang P, Pei S, Liu J, Zhang X, Feng Y, Gong Z, et al. Cuproptosis-related lncRNA signatures: predicting prognosis and evaluating the tumor immune microenvironment in lung adenocarcinoma. *Front Oncol* (2022) 12:1088931. doi: 10.3389/fonc.2022.1088931

44. Sahai E, Astsaturov I, Cukierman E, DeNardo DG, Egeblad M, Evans RM, et al. A framework for advancing our understanding of cancer-associated fibroblasts. *Nat Rev Cancer* (2020) 20:174–86. doi: 10.1038/s41568-019-0238-1

45. Chen X, Song E. Turning foes to friends: targeting cancer-associated fibroblasts. *Nat Rev Drug Discovery* (2019) 18:99–115. doi: 10.1038/s41573-018-0004-1

46. Fang T, Lv H, Lv G, Li T, Wang C, Han Q, et al. Tumor-derived exosomal miR-1247-3p induces cancer-associated fibroblast activation to foster lung metastasis of liver cancer. *Nat Commun* (2018) 9:191. doi: 10.1038/s41467-017-02583-0

47. Galbo PMJr., Zang X, Zheng D. Molecular features of cancer-associated fibroblast subtypes and their implication on cancer pathogenesis, prognosis, and immunotherapy resistance. *Clin Cancer Res* (2021) 27:2636–47. doi: 10.1158/1078-0432.CCR-20-4226

48. Jin G, Wang H, Hu Z, Liu H, Sun W, Ma H, et al. Potentially functional polymorphisms of EXO1 and risk of lung cancer in a Chinese population: a case-control analysis. *Lung Cancer* (2008) 60:340–6. doi: 10.1016/j.lungcan.2007.11.003

49. Zhou CS, Feng MT, Chen X, Gao Y, Chen L, Li LD, et al. Exonuclease 1 (EXO1) is a potential prognostic biomarker and correlates with immune infiltrates in lung adenocarcinoma. *Onco Targets Ther* (2021) 14:1033–48. doi: 10.2147/OTT.S286274

50. Ait Saada A, Teixeira-Silva A, Iraqui I, Costes A, Hardy J, Paoletti G, et al. Unprotected replication forks are converted into mitotic sister chromatid bridges. *Mol Cell* (2017) 66:398–410 e4. doi: 10.1016/j.molcel.2017.04.002

51. Liu J, Wen Y, Liu Z, Liu S, Xu P, Xu Y, et al. VPS33B modulates c-Myc/p53/miR-192-3p to target CCNB1 suppressing the growth of non-small cell lung cancer. *Mol Ther Nucleic Acids* (2021) 23:324–35. doi: 10.1016/j.omtn.2020.11.010

52. Wang S, Sun H, Zhan X, Wang Q. [Retracted] MicroRNA−718 serves a tumor −suppressive role in non−small cell lung cancer by directly targeting CCNB1. *Int J Mol Med* (2021) 48. doi: 10.3892/ijmm.2021.5013

53. Sun J, Xie T, Jamal M, Tu Z, Li X, Wu Y, et al. CLEC3B as a potential diagnostic and prognostic biomarker in lung cancer and association with the immune microenvironment. *Cancer Cell Int* (2020) 20:106. doi: 10.1186/s12935-020-01183-1

54. Zhao S, Liu Q, Li J, Hu C, Cao F, Ma W, et al. Construction and validation of prognostic regulation network based on RNA-binding protein genes in lung squamous cell carcinoma. *DNA Cell Biol* (2021) 40:1563–83. doi: 10.1089/dna.2021.0145

55. Chang YS, Tu SJ, Chen YC, Liu TY, Lee YT, Yen JC, et al. Mutation profile of non-small cell lung cancer revealed by next generation sequencing. *Respir Res* (2021) 22:3. doi: 10.1186/s12931-020-01608-5

56. Guan J, Lu C, Jin Q, Lu H, Chen X, Tian L, et al. MLH1 deficiency-triggered DNA hyperexcision by exonuclease 1 activates the cGAS-STING pathway. *Cancer Cell* (2021) 39:109–121 e5. doi: 10.1016/j.ccell.2020.11.004

57. Gao B, Yang F, Han M, Bao H, Shen Y, Cao R, et al. Genomic landscape and evolution of arm aneuploidy in lung adenocarcinoma. *Neoplasia* (2021) 23:870–8. doi: 10.1016/j.neo.2021.06.003

58. Mao C, Wang X, Liu Y, Wang M, Yan B, Jiang Y, et al. A G3BP1-interacting lncRNA promotes ferroptosis and apoptosis in cancer *via* nuclear sequestration of p53. *Cancer Res* (2018) 78:3484–96. doi: 10.1158/0008-5472.CAN-17-3454

59. Zhu J, Ao H, Liu M, Cao K, Ma J. UBE2T promotes autophagy *via* the p53/AMPK/mTOR signaling pathway in lung adenocarcinoma. *J Transl Med* (2021) 19:374. doi: 10.1186/s12967-021-03056-1

60. Venkatesan S, Angelova M, Puttick C, Zhai H, Caswell DR, Lu WT, et al. Induction of APOBEC3 exacerbates DNA replication stress and chromosomal

instability in early breast and lung cancer evolution. *Cancer Discovery* (2021) 11:2456–73. doi: 10.1158/2159-8290.CD-20-0725

61. Kibe T, Zimmermann M, de Lange T. TPP1 blocks an ATR-mediated resection mechanism at telomeres. *Mol Cell* (2016) 61:236–46. doi: 10.1016/j.molcel.2015.12.016

62. Fischer M, Quaas M, Steiner L, Engeland K. The p53-p21-DREAM-CDE/CHR pathway regulates G2/M cell cycle genes. *Nucleic Acids Res* (2016) 44:164–74. doi: 10.1093/nar/gkv927

63. Guan R, Lian T, Zhou BR, He E, Wu C, Singleton M, et al. Structural and dynamic mechanisms of CBF3-guided centromeric nucleosome formation. *Nat Commun* (2021) 12:1763. doi: 10.1038/s41467-021-21985-9

64. Arbour KC, Riely GJ. Systemic therapy for locally advanced and metastatic non-small cell lung cancer: a review. *JAMA* (2019) 322:764–74. doi: 10.1001/jama.2019.11058

65. Lee JH, Sung JY, Choi EK, Yoon HK, Kang BR, Hong EK, et al. C/EBPbeta is a transcriptional regulator of Wee1 at the G(2)/M phase of the cell cycle. *Cells* (2019) 8. doi: 10.20944/preprints201901.0205.v1

66. Fu T, Dai LJ, Wu SY, Xiao Y, Ma D, Jiang YZ, et al. Spatial architecture of the immune microenvironment orchestrates tumor immunity and therapeutic response. *J Hematol Oncol* (2021) 14:98. doi: 10.1186/s13045-021-01103-4

67. Mao X, Xu J, Wang W, Liang C, Hua J, Liu J, et al. Crosstalk between cancer-associated fibroblasts and immune cells in the tumor microenvironment: new findings and future perspectives. *Mol Cancer* (2021) 20:131. doi: 10.1186/s12943-021-01428-1

68. Wang S, Li F, Ye T, Wang J, Lyu C, Qing S, et al. Macrophage-tumor chimeric exosomes accumulate in lymph node and tumor to activate the immune response and the tumor microenvironment. *Sci Transl Med* (2021) 13:eabb6981. doi: 10.1126/scitranslmed.abb6981

69. Noe JT, Rendon BE, Geller AE, Conroy LR, Morrissey SM, Young LEA, et al. Lactate supports a metabolic-epigenetic link in macrophage polarization. *Sci Adv* (2021) 7:eabi8602. doi: 10.1126/sciadv.abi8602

70. Desbois M, Wang Y. Cancer-associated fibroblasts: key players in shaping the tumor immune microenvironment. *Immunol Rev* (2021) 302:241–58. doi: 10.1111/imr.12982

frontiers | Frontiers in Medicine

TYPE Case Report
PUBLISHED 29 June 2023
DOI 10.3389/fmed.2023.1168220

Check for updates

OPEN ACCESS

EDITED BY
Jie Mei,
Wuxi People's Hospital Affiliated to Nanjing Medical University, China

REVIEWED BY
Shenhai Wei,
First Hospital of Tsinghua University, China
Runbo Zhong,
Shanghai Jiao Tong University, China

*CORRESPONDENCE
Huilin Wang
✉ 29605753@qq.com

†These authors have contributed equally to this work and share first authorship

RECEIVED 17 February 2023
ACCEPTED 12 June 2023
PUBLISHED 29 June 2023

CITATION
Chen S, Yu Q, Jiang W, Lu Y, Zhao Y and Wang H (2023) Rechallenge with EGFR-TKI after failure of immunotherapy is considered an effective treatment for advanced lung adenocarcinoma patients with EGFR exon 19 deletion: a case report.
Front. Med. 10:1168220.
doi: 10.3389/fmed.2023.1168220

COPYRIGHT
© 2023 Chen, Yu, Jiang, Lu, Zhao and Wang. This is an open-access article distributed under the terms of the Creative Commons Attribution License (CC BY). The use, distribution or reproduction in other forums is permitted, provided the original author(s) and the copyright owner(s) are credited and that the original publication in this journal is cited, in accordance with accepted academic practice. No use, distribution or reproduction is permitted which does not comply with these terms.

Rechallenge with EGFR-TKI after failure of immunotherapy is considered an effective treatment for advanced lung adenocarcinoma patients with EGFR exon 19 deletion: a case report

Shubin Chen[1†], Qitao Yu[1†], Wei Jiang[1], Yukun Lu[2], Yun Zhao[1] and Huilin Wang[1*]

[1]Medical Oncology of Respiratory, Guangxi Cancer Hospital, Guangxi Medical University Cancer Hospital, Nanning, Guangxi, China, [2]Department of Pathology, Guangxi Cancer Hospital, Guangxi Medical University Cancer Hospital, Nanning, Guangxi, China

In advanced lung adenocarcinoma patients with epidermal growth factor receptor (EGFR) mutation, epidermal growth factor receptor-tyrosine kinase inhibitors (EGFR-TKIs) have an excellent and long-lasting therapeutic response; however, virtually all patients eventually develop drug resistance and experience disease progression. The use of immunotherapy after EGFR-TKIs may be a successful therapeutic option for individuals who are resistant to them. It is still unclear if EGFR-TKIs can be administered again after immunotherapy has failed. We describe a case of a 37-year-old woman who was found to have T4N3M1a stage IVa lung adenocarcinoma. Amplification refractory mutation system PCR (ARMS-PCR) genetic testing suggested EGFR exon 19 deletion. The patient was initially treated with a regimen of icotinib (125 mg tid) combined with anlotinib (8 mg qd d1-d14) with an optimal efficacy rating of partial response (PR) and was granted a PFS of 7 months. In second-line treatment, the patient received three cycles of a KN046 (KN046 is a bispecific antibody inhibitor of PD-L1 and CTLA-4) 295 mg d1, pemetrexed 800mg d1, plus carboplatin 750 mg d1 regimen, with an optimal efficacy rating of stable disease (SD) on CT. The third-line therapy was chosen to be afatinib with docetaxel, and the patient was evaluated for PR on CT. Up to 15 August 2022, the patient had a progression free survival (PFS) of 14months. The successful treatment of this patient is a reminder that EGFR-TKI rechallenge in EGFR exon 19 deletion patients with EGFR-TKI resistance, in which immunotherapy has failed, may be effective.

KEYWORDS

advanced lung adenocarcinoma, EGFR exon 19 deletion, immunotherapy, EGFR-TKI, rechallenge

Introduction

Epidermal growth factor receptor (EGFR) mutations, the most frequent genetic drivers of advanced lung cancer, have a 50% likelihood of occurring in Asian populations, and targeted treatment has rapidly improved over the past 10 years (1). The most prevalent EGFR mutation is the exon 19 deletion (2). EGFR-TKIs block the autophosphorylation of EGFR receptor tyrosine, which further blocks downstream signaling and limits EGFR-dependent cell growth, having an anti-tumor impact. Although advanced lung adenocarcinoma patients with EGFR mutations now have a significantly better prognosis thanks to epidermal growth factor receptor tyrosine kinase inhibitors (EGFR-TKIs), tumors will always acquire medication resistance for a variety of reasons.

The popularity of immune checkpoint inhibitors (ICIs) in the management of advanced non-small cell lung cancer has grown significantly. However, it was unclear from the existing research whether immune checkpoint inhibitors are appropriate for individuals with EGFR mutations. According to certain studies, immune checkpoint inhibitors can cause serious toxic side effects in individuals with EGFR mutations and potential fulminant disease progression (3–5). In contrast, a subgroup analysis of IMPOWER150 revealed that patients with EGFR mutations responded favorably to an atezolizumab, bevacizumab, carboplatin, plus paclitaxel regimen (6).

Several findings regarding the therapeutic effectiveness of EGFR-TKIs rechallenge in EGFR-mutant non-small cell lung cancer (NSCLC) have recently been published (7–9). However, the question of whether patients who have failed EGFR-TKI therapy with an immune checkpoint inhibitor for second-line treatment can be re-challenged with EGFR-TKI following another bout of disease progression lacks a somewhat conclusive response. In this case, we describe the effectiveness of EGFR-TKI rechallenge in a patient with advanced NSCLC with EGFR exon 19 deletion who was treated with an immune checkpoint inhibitor for second-line treatment and recurrence of disease progression.

Case presentation

A 37-year-old woman was hospitalized after an occupying lung lesion and an enlarged right supraclavicular lymph node were discovered. A computed tomography (CT) scan revealed several lymph node metastases in the right supraclavicular area, mediastinum, and lung, in addition to a mass in the upper lobe of the right lung, right pleural metastasis and multiple nodules in both lungs, with a high probability of inflammatory lesions combined with some metastases (Figure 1A). There were no lesions seen on the brain's magnetic resonance imaging (MRI). No bone metastases were detected by bone imaging. A right supraclavicular lymph node biopsy revealed adenocarcinoma and CK7(+), TTF-1(+), and P40(−) immunohistochemistry results were consistent with adenocarcinoma of pulmonary origin (Figure 2). The patient was found to have T4N3M1a stage IVa lung adenocarcinoma. Amplification refractory mutation system PCR (ARMS-PCR) genetic testing suggested EGFR exon 19 deletion, with no detectable aberrant changes in the ALK, ROS1, KRAS, BRAF, RET, NRAS, PIK3CA, and HER2 genes. We advocated that the patient engaged in a clinical trial using both gefitinib and anlotinib, but for a variety of reasons, the patient opted not to do so. However, the patient requested anlotinib therapy; icotinib 125 mg tid and anlotinib 8 mg qd were chosen as the patient's initial treatment regimen. According to the response evaluation criteria for solid tumors (RECIST v1.1), significant lung tumor lesions decreased and developed cavity-like alterations after 5 months of therapy, demonstrating partial response (PR) (Figure 1B). Additionally, there was a decline in the serum tumor biomarkers CA199, CA153, CA125, and CEA. The upper lobe of the right lung had a noticeably larger tumor lesion on 5 January 2021, which was classified as progressing disease (PD) using the RECIST v1.1 assessment criteria (Figure 1C). The patient underwent CT-guided biopsy of lung lesions by puncture on 8 January 2021. Immunohistochemistry showed adenocarcinoma, TTF-1 (+), CK7 (+), P40 (−), and Ki67 (+20%). Further blood and tumor specimens from the patient were subjected to next-generation sequencing (NGS) testing, showing EGFR exon 19 deletion (Figure 3A) with an abundance of 2.4% in tumor specimens and TP53 exon 8 mutation (Figure 3B) with an abundance of 0.9% in tumor specimens. Programmed cell death-Ligand protein 1(PD-L1) expression was also examined, and the result suggested that the PD-L1 tumor cell proportion score (TPS) was <1%. The patient opted to participate in a clinical study as the second line of treatment, receiving three cycles of KN046 (a bispecific antibody inhibitor of PD-L1 and CTLA-4) with pemetrexed 800 mg/d1 and carboplatin 750 mg/d1, with an effectiveness rating of SD on CT scan (Figures 1D,E). Unfortunately, the patient subsequently ceased the treatment because of grade 3 hepatitis brought on by immunotherapy. Forty days after discontinuation of the regimen, the patient was evaluated as PD (Figure 1F), with a significant increase in serum tumor biomarkers. After that, the patient underwent fiberoptic bronchoscopy, and further lung lesions were sampled. Repeated NGS analysis of the patient's blood and tumor samples revealed an EGFR exon 19 deletion with an abundance of 41.9% in tumor specimens, suggesting a potential re-sensitization to EGFR-TKI. Because immune checkpoint inhibitors interact with EGFR-TKI to produce serious adverse effects, we restarted EGFR-TKI therapy after 3 months of discontinuation of immune checkpoint inhibitors based on the elution time of the immune checkpoint inhibitors. Third-line therapy involved the use of afatinib 40 mg every day in conjunction with docetaxel 110 mg every 3 weeks (Figure 1G). On CT, the patient was assessed for a partial response after two cycles of therapy (Figure 1H), with no drug-related adverse events and a decrease in serum tumor biomarkers once again. On 15 August 2022, the patient underwent a CT examination which revealed a significant re-enlargement of the tumour and was considered to be drug resistant again, getting a progression free survival (PFS) of 14 months (Figure 1I). A repeat CT-guided puncture biopsy of the lung lesion and repeat NGS testing of the patient's blood and tumor specimen suggested the presence of a T790M mutation in exon 20 of EGFR (Figure 3C). The patient is currently being treated with osimertinib (Osimertinib, a third-generation EGFR-TKI that targets EGFR mutations and T790M-resistant mutations and inhibits tyrosine kinase phosphorylation by creating a covalent bond with the C797 residue at the ATP binding site of EGFR mutations and T790M mutations, acting as a tumor suppressor). On 11 March 2023, the patient underwent a CT examination that revealed a significant shrinking of the tumor, considered to be a partial response. The timeline of the treatment of the patient is presented in Figure 4.

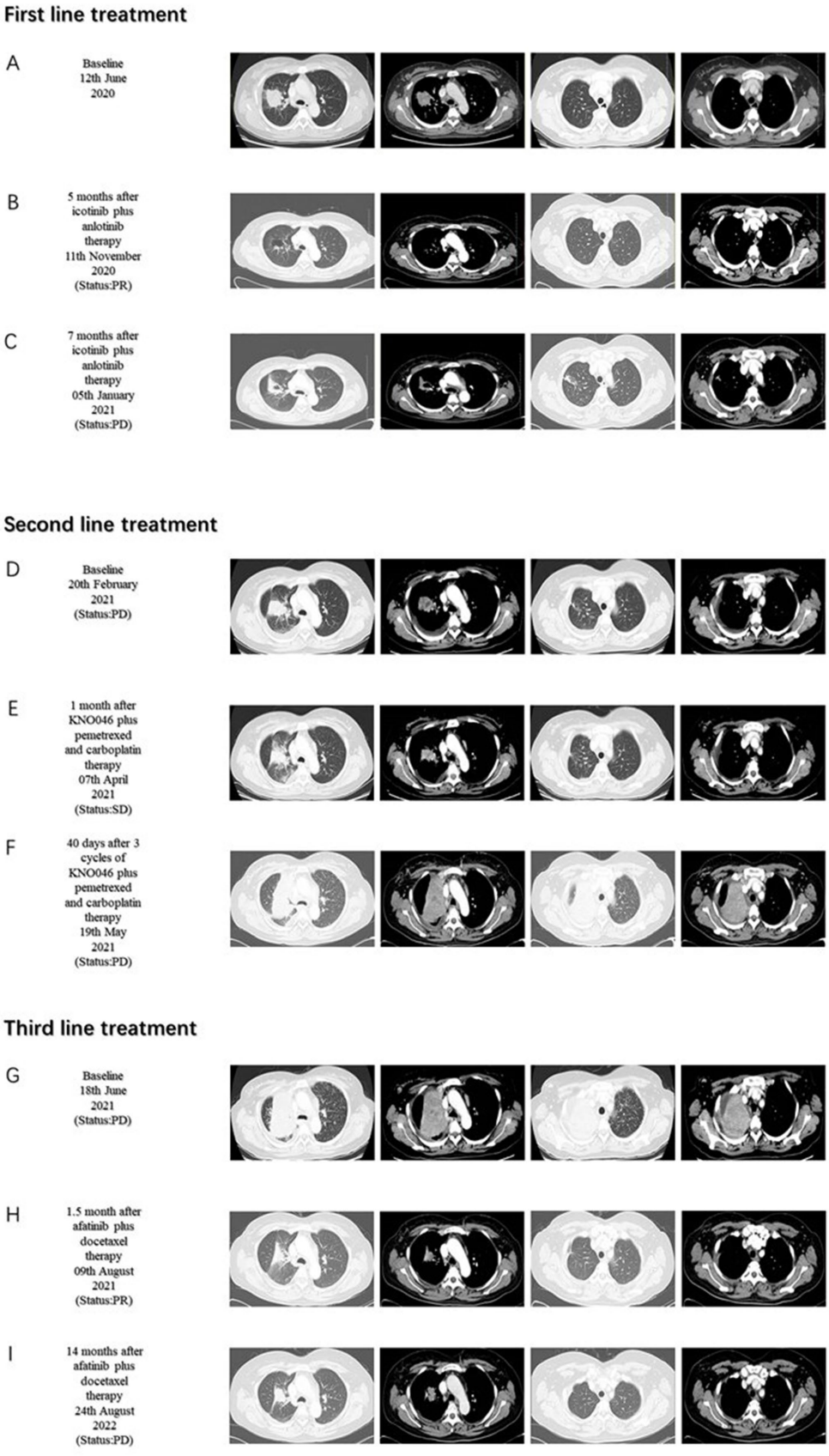


FIGURE 1
Chest computed tomography (CT) scans before and after treatment. First-line treatment baseline **(A)**. Five months after icotinib plus anlotinib therapy **(B)**. Seven months after icotinib plus anlotinib therapy **(C)**. Second-line treatment baseline **(D)**. One month after KNO046 plus pemetrexed and

(Continued)

FIGURE 1 (Continued)
carboplatin therapy **(E)**. Forty days after three cycles of KNO046 plus pemetrexed and carboplatin therapy **(F)**. Third-line treatment baseline **(G)**. 1.5month after afatinib plus docetaxel therapy **(H)**. Fourteen months after afatinib plus docetaxel therapy **(I)**.

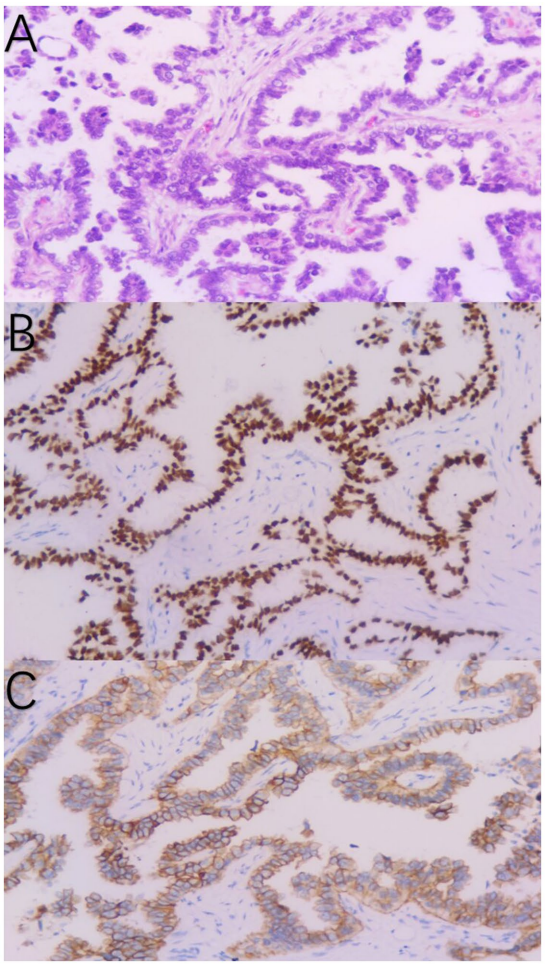


FIGURE 2
Pathological diagnosis of the right supraclavicular lymph node biopsy **(A)**. Immunohistochemistry staining: TTF-1 **(B)** and CK7 **(C)** were positive, consistent with adenocarcinoma of pulmonary origin.

Discussion

With the publication of the IPASS study results (10), EGFR-TKIs have officially become the treatment of choice for patients with EGFR mutations. EGFR-TKIs have startlingly high effectiveness; however, tumors will inevitably acquire therapeutic resistance. The results of several clinical trials (11–13) show that immunotherapy may also be an effective therapeutic option for individuals with EGFR mutations, even though the effectiveness of immunotherapy for patients with EGFR mutations is currently unclear. The feasibility of resuming EGFR-TKIs therapy for these patients after immunotherapy has failed is still a hotly contested issue.

In our case report, we described the treatment of a patient with advanced lung adenocarcinoma who had an EGFR exon 19 deletion mutation. The above patient received first-line treatment with a first-generation EGFR-TKI in conjunction with anti-angiogenic medications and was granted a PFS of 7 months as a result. Immunotherapy was discontinued after a short course due to immunotherapy-related adverse effects. Subsequently, the patient received second-generation EGFR-TKI in combination with chemotherapy. The rationale for the program was based on the good efficacy reported by NEJ009 (14), demonstrating 14 months PFS with a partial response, showing that TKI combination chemotherapy had good anti-tumor activity against EGFR mutation combined with TP53 mutation. This example serves as proof that treating these patients sequentially with immune checkpoint inhibitors after EGFR-TKI treatment has failed, followed by an EGFR-TKI rechallenge, may improve their therapeutic effectiveness.

We searched for EGFR-TKI rechallenge following immunotherapy failure in the literature. In a study byKaira et al. (15), a retrospective analysis of 75 patients with advanced NSCLC and sensitive EGFR mutations revealed that approximately half of the patients had a good response to EGFR-TKI rechallenge, while approximately 25% of all patients had no response to EGFR-TKI rechallenge following the failure of immunotherapy. In the study, two cases were reported in which a dramatic response upon EGFR-TKI rechallenge was achieved. Nivolumab was started in Case 1 in a 64-year-old woman with advanced lung cancer since EGFR-TKI and systemic chemotherapy were ineffective. One month after its administration, PD was observed; therefore, the patient was treated with afatinib rechallenge. Two weeks after afatinib treatment, a drastic response of tumor shrinkage in multiple pulmonary metastases was identified, with an eventual PFS of 10 months. In Case 2, a 39-year-old woman with lung adenocarcinoma underwent multiple treatments with platinum-based or second or third generation EGFR-TKIs regimens; however, the patient developed therapeutic resistance. Nivolumab was started as a result, but a month after it was administered, indication of considerable growth of many brain metastases was evident. The brain metastases nearly completely vanished after 1 month of treatment with erlotinib and bevacizumab, leading to a PFS of 9 months. For NSCLC patients who have developed resistance to EGFR-TKIs, EGFR-TKI rechallenge after immunotherapy treatment may be an effective therapeutic option.

The underlying mechanisms through which EGFR-TKIs rechallenge immediately after the preceding immunotherapy is effective in patients with EGFR-TKIs resistance is unknown. Previous research has demonstrated that the expression of PD-L1 changes throughout the use of EGFR-TKIs, with certain patients showing a tendency to upregulate its expression after developing resistance to EGFR-TKIs (16–18). Peng et al. proposed that EGFR-TKI resistance promotes immune escape in lung cancer via increased PD-L1 expression; increased PD-L1 expression after EGFR-TKI resistance impairs lymphocyte activation and cytotoxicity *in vitro* and *in vivo*, whereas PD-L1 downregulation partially restores lymphocyte cytotoxicity (19). The idea is that PD-1/PD-L1 blocking therapy may restore EGFR-TKI sensitivity in patients with malignancies that are resistant to treatment. According to Sugiyama et al. (20), the use of EGFR-TKI in conjunction with PD-1 inhibitor may be preferable since it affects the function of regulatory T cells in the tumor

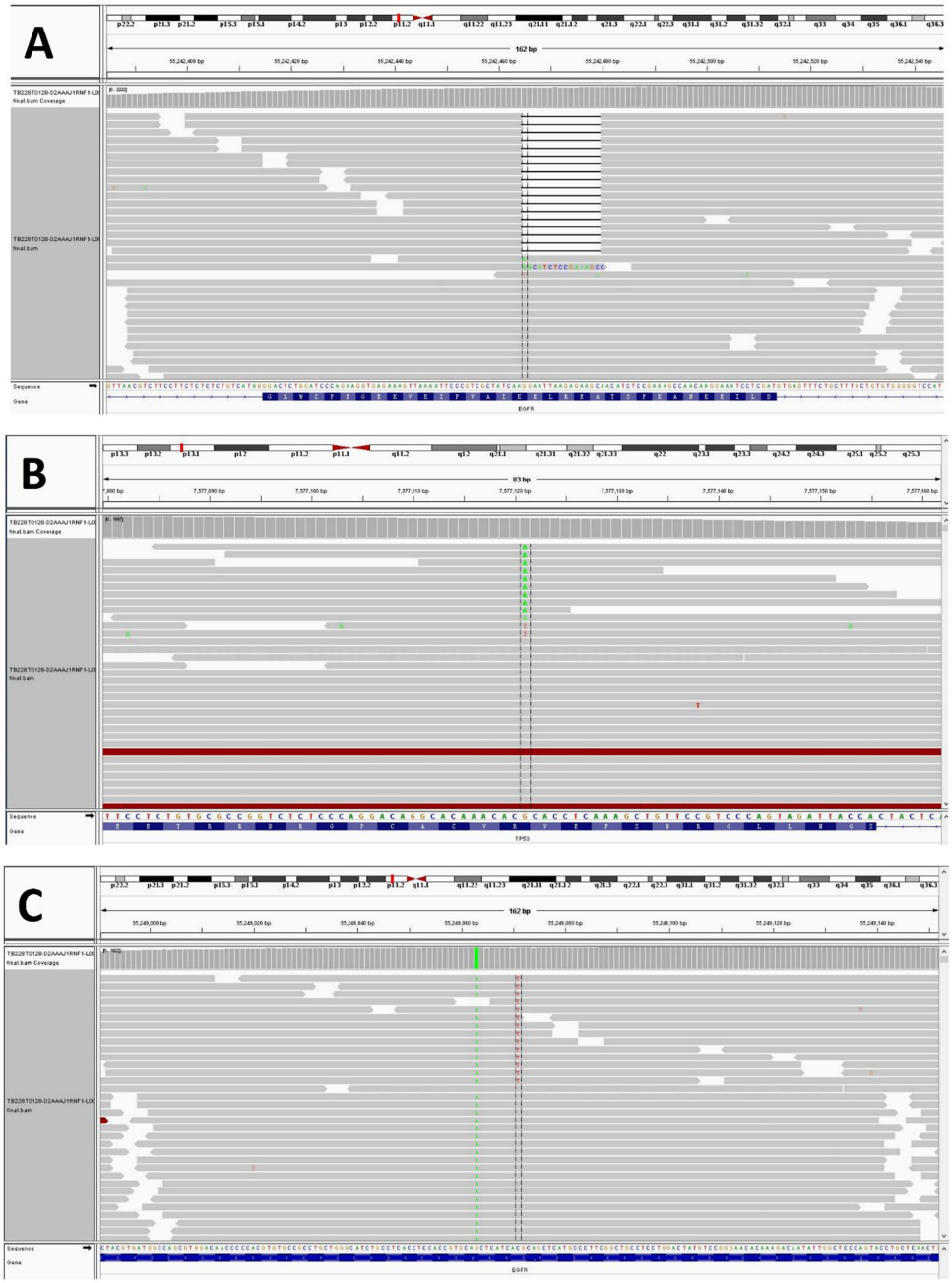


FIGURE 3
NGS test result showing the EGFR exon 19 p.E746_A750del **(A)**, TP53 exon 8 p.R273C **(B)**, and EGFR exon 20 p.T790M **(C)**.

microenvironment. The synergistic impact of EGFR-TKI and PD-1 inhibitor in the setting of long-term EGFR-TKI treatment may restore the anti-tumor activity. According to studies (21, 22), patients' tumor mutation burden (TMB) increases after receiving EGFR-TKI treatment. This increased TMB has a negative correlation with the response to EGFR TKIs (21). Patient's TMB declines after a certain period of immune checkpoint blockade therapy, and the EGFR-TKI may be reverted to show sensitivity to the tumor. Jia et al. investigated the immunological environment of lung cancer tumor cells that showed a strong early reaction to EGFR-TKI. The authors discovered a short-term increase in CD8+ T cells during the initiation of EGFR-TKI treatment, indicating that CD8+ T cell activity may impact EGFR-TKI effectiveness (23). We have reason to assume that PD-1/PD-L1 inhibition, which restores the initial activity of CD8+ T cells, will also restore the activity of EGFR-TKI. Further research on this potential follow-up therapy should be pursued, even if it is complicated to pinpoint the precise mechanism by which sensitivity to EGFR-TKIs is immediately restored following immune checkpoint blockade treatment.

As a whole, the following aspects standout in our case: in order to determine the patient's potential medication resistance mechanisms, a second biopsy was taken after the disease progressed in the patient.

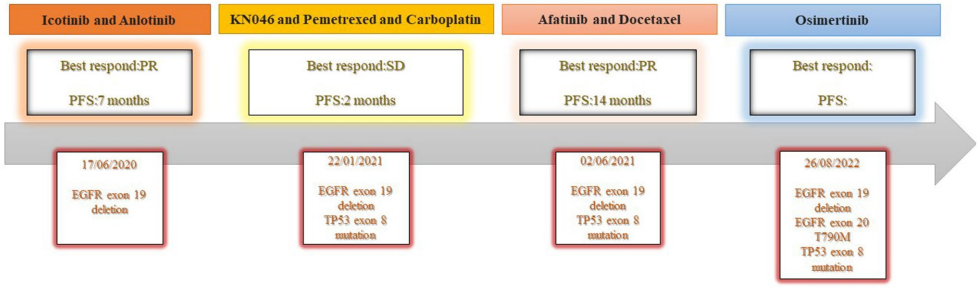


FIGURE 4
Timeline of the treatment of the patient.

Secondly, the patient developed immune-related hepatitis after using immunotherapy, which persisted after stopping immunotherapy. Aafatinib is not hepatically metabolized, and it has the potential to exacerbate liver damage if other EGFR-TKIs were used. Finally, investigations on the EGFR mutation in conjunction with TP53 mutation are ongoing, and our novel application of TKI in combination with chemotherapy has resulted in a longer PFS for the patient. Despite the significance of the case's findings, there is one drawback: osimertinib was not selected as the first-line therapy in this instance.

The successful treatment of this patient serves as a reminder that EGFR-TKI rechallenge in EGFR exon 19 deletion patients with EGFR resistance, in which immunotherapy has failed, may be effective. A sizable prospective clinical study may be required to further corroborate the case's conclusion.

Data availability statement

The original contributions presented in the study are included in the article/supplementary material, further inquiries can be directed to the corresponding author.

Ethics statement

The studies involving human participants were reviewed and approved by Guangxi Medical University Affiliated Cancer Hospital's Ethical Committee. The patients/participants provided their written informed consent to participate in this study. Written informed consent was obtained from the individual(s) for the publication of any potentially identifiable images or data included in this article.

Author contributions

SC and QY wrote the manuscript. WJ provided constructive discussion and revised the paper. YL and YZ provided the pathology and CT images. HW obtained informed consent from the patient, administered treatment to the patient, and provided the clinical data of the patient. All authors contributed to the article and approved the submitted version.

Conflict of interest

The authors declare that the research was conducted in the absence of any commercial or financial relationships that could be construed as a potential conflict of interest.

Publisher's note

All claims expressed in this article are solely those of the authors and do not necessarily represent those of their affiliated organizations, or those of the publisher, the editors and the reviewers. Any product that may be evaluated in this article, or claim that may be made by its manufacturer, is not guaranteed or endorsed by the publisher.

References

1. Shi Y, Au JS, Thongprasert S, Srinivasan S, Tsai CM, Khoa MT, et al. A prospective, molecular epidemiology study of EGFR mutations in Asian patients with advanced non-small-cell lung cancer of adenocarcinoma histology (PIONEER). *J Thorac Oncol.* (2014) 9:154–62. doi: 10.1097/JTO.0000000000000033

2. Wang W, Tang Y, Li J, Zhang Y, Zou Y, Su X. Identification of EGFR mutations in cytological specimens of non-small cell lung carcinoma from a single institute. *Int J Clin Exp Pathol.* (2018) 11:929–35.

3. Schoenfeld AJ, Arbour KC, Rizvi H, Iqbal AN, Gadgeel SM, Girshman J, et al. Severe immune-related adverse events are common with sequential PD-(L)1 blockade and osimertinib. *Ann Oncol.* (2019) 30:839–44. doi: 10.1093/annonc/mdz077

4. Oxnard GR, Yang JC, Yu H, Kim SW, Saka H, Horn L, et al. TATTON: a multi-arm, phase Ib trial of osimertinib combined with selumetinib, savolitinib, or durvalumab in EGFR-mutant lung cancer. *Ann Oncol.* (2020) 31:507–16. doi: 10.1016/j.annonc.2020.01.013

5. Oshima Y, Tanimoto T, Yuji K, Tojo A. EGFR-TKI-associated interstitial pneumonitis in nivolumab-treated patients with non-small cell lung cancer. *JAMA Oncol.* (2018) 4:1112–5. doi: 10.1001/jamaoncol.2017.4526

6. Socinski MA, Jotte RM, Cappuzzo F, Orlandi F, Stroyakovskiy D, Nogami N, et al. Atezolizumab for first-line treatment of metastatic nonsquamous NSCLC. *N Engl J Med.* (2018) 378:2288–301. doi: 10.1056/NEJMoa1716948

7. Han ZJ, Luo N, Li L, Liu ZL. Successful osimertinib rechallenge following subsequent chemotherapy regimen in a patient with metastatic non-small cell lung carcinoma: a case report. *Ann Palliat Med.* (2021) 10:8413–9. doi: 10.21037/apm-20-2369

8. Yamaguchi O, Kaira K, Mouri A, Shiono A, Hashimoto K, Miura Y, et al. Re-challenge of afatinib after 1st generation EGFR-TKI failure in patients with previously treated non-small cell lung cancer harboring EGFR mutation. *Cancer Chemother Pharmacol.* (2019) 83:817–25. doi: 10.1007/s00280-019-03790-w

9. Tanaka H, Sakamoto H, Akita T, Ohyanagi F, Kawashima Y, Tambo Y, et al. Clinical efficacy of dacomitinib in rechallenge setting for patients with epidermal growth factor receptor mutant non-small cell lung cancer: a multicenter retrospective analysis (TOPGAN2020-02). *Thorac Cancer*. (2022) 13:1471–8. doi: 10.1111/1759-7714.14415

10. Mok TS, Wu YL, Thongprasert S, Yang CH, Chu DT, Saijo N, et al. Gefitinib or carboplatin-paclitaxel in pulmonary adenocarcinoma. *N Engl J Med*. (2009) 361:947–57. doi: 10.1056/NEJMoa0810699

11. Masuda K, Horinouchi H, Tanaka M, Higashiyama R, Shinno Y, Sato J, et al. Efficacy of anti-PD-1 antibodies in NSCLC patients with an EGFR mutation and high PD-L1 expression. *J Cancer Res Clin Oncol*. (2021) 147:245–51. doi: 10.1007/s00432-020-03329-0

12. Chen K, Cheng G, Zhang F, Zhu G, Xu Y, Yu X, et al. PD-L1 expression and T cells infiltration in patients with uncommon EGFR-mutant non-small cell lung cancer and the response to immunotherapy. *Lung Cancer*. (2020) 142:98–105. doi: 10.1016/j.lungcan.2020.02.010

13. Yamada T, Hirai S, Katayama Y, Yoshimura A, Shiotsu S, Watanabe S, et al. Retrospective efficacy analysis of immune checkpoint inhibitors in patients with EGFR-mutated non-small cell lung cancer. *Cancer Med*. (2019) 8:1521–9. doi: 10.1002/cam4.2037

14. Miyauchi E, Morita S, Nakamura A, Hosomi Y, Watanabe K, Ikeda S, et al. Updated analysis of NEJ009: gefitinib-alone versus gefitinib plus chemotherapy for non-small-cell lung cancer with mutated EGFR. *J Clin Oncol*. (2022) 40:3587–92. doi: 10.1200/JCO.21.02911

15. Kaira K, Kobayashi K, Shiono A, Yamaguchi O, Hashimoto K, Mouri A, et al. Effectiveness of EGFR-TKI rechallenge immediately after PD-1 blockade failure. *Thorac Cancer*. (2021) 12:864–73. doi: 10.1111/1759-7714.13864

16. Han JJ, Kim DW, Koh J, Keam B, Kim TM, Jeon YK, et al. Change in PD-L1 expression after acquiring resistance to gefitinib in EGFR-Mutant Non-Small-Cell lung cancer. *Clin Lung Cancer*. (2016) 17:263–270.e2. doi: 10.1016/j.cllc.2015.11.006

17. Gainor JF, Shaw AT, Sequist LV, Fu X, Azzoli CG, Piotrowska Z, et al. EGFR mutations and ALK rearrangements are associated with low response rates to PD-1 pathway blockade in non-small cell lung cancer: a retrospective analysis. *Clin Cancer Res*. (2016) 22:4585–93. doi: 10.1158/1078-0432.CCR-15-3101

18. Hata A, Katakami N, Nanjo S, Okuda C, Kaji R, Masago K, et al. Programmed death-ligand 1 expression and T790M status in EGFR-mutant non-small cell lung cancer. *Lung Cancer*. (2017) 111:182–9. doi: 10.1016/j.lungcan.2017.07.022

19. Peng S, Wang R, Zhang X, Ma Y, Zhong L, Li K, et al. EGFR-TKI resistance promotes immune escape in lung cancer via increased PD-L1 expression. *Mol Cancer*. (2019) 18:165. doi: 10.1186/s12943-019-1073-4

20. Sugiyama E, Togashi Y, Takeuchi Y, Shinya S, Tada Y, Kataoka K, et al. Blockade of EGFR improves responsiveness to PD-1 blockade in EGFR-mutated non-small cell lung cancer. *Sci Immunol*. (2020) 5:5. doi: 10.1126/sciimmunol.aav3937

21. Offin M, Rizvi H, Tenet M, Ni A, Sanchez-Vega F, Li BT, et al. Tumor mutation burden and efficacy of EGFR-tyrosine kinase inhibitors in patients with EGFR-mutant lung cancers. *Clin Cancer Res*. (2019) 25:1063–9. doi: 10.1158/1078-0432.CCR-18-1102

22. Isomoto K, Haratani K, Hayashi H, Shimizu S, Tomida S, Niwa T, et al. Impact of EGFR-TKI treatment on the tumor immune microenvironment in EGFR mutation-positive non-small cell lung cancer. *Clin Cancer Res*. (2020) 26:2037–46. doi: 10.1158/1078-0432.CCR-19-2027

23. Jia Y, Li X, Jiang T, Zhao S, Zhao C, Zhang L, et al. EGFR-targeted therapy alters the tumor microenvironment in EGFR-driven lung tumors: implications for combination therapies. *Int J Cancer*. (2019) 145:1432–44. doi: 10.1002/ijc.32191

frontiers | Frontiers in Immunology

TYPE Systematic Review
PUBLISHED 08 August 2023
DOI 10.3389/fimmu.2023.1218258

Check for updates

OPEN ACCESS

EDITED BY
Jie Mei,
Wuxi People's Hospital Affiliated to Nanjing Medical University, China

REVIEWED BY
Mattia Falchetto Osti,
Sapienza University of Rome, Italy
Raheleh Roudi,
Stanford University, United States
Raffaele Addeo,
ASLNAPOLI2NORD ONCOLOGIA, Italy

*CORRESPONDENCE
Haijie Gan
516318173@qq.com
Qitao Yu
yqt178@163.com

†These authors have contributed equally to this work and share first authorship

RECEIVED 06 May 2023
ACCEPTED 24 July 2023
PUBLISHED 08 August 2023

CITATION
Chen S, Mo W, Jiang W, Zhou S, Gan H and Yu Q (2023) The benefit and risk of PD-1/PD-L1 inhibitors plus anti-angiogenic agents as second or later-line treatment for patients with advanced non-small-cell lung cancer: a systematic review and single-arm meta-analysis of prospective clinical trials.
Front. Immunol. 14:1218258.
doi: 10.3389/fimmu.2023.1218258

COPYRIGHT
© 2023 Chen, Mo, Jiang, Zhou, Gan and Yu. This is an open-access article distributed under the terms of the Creative Commons Attribution License (CC BY). The use, distribution or reproduction in other forums is permitted, provided the original author(s) and the copyright owner(s) are credited and that the original publication in this journal is cited, in accordance with accepted academic practice. No use, distribution or reproduction is permitted which does not comply with these terms.

The benefit and risk of PD-1/PD-L1 inhibitors plus anti-angiogenic agents as second or later-line treatment for patients with advanced non-small-cell lung cancer: a systematic review and single-arm meta-analysis of prospective clinical trials

Shubin Chen†, Wanying Mo†, Wei Jiang, Shaozhang Zhou, Haijie Gan* and Qitao Yu*

Medical Oncology Of Respiratory, Guangxi Medical University Cancer Hospital, Nanning, Guangxi, China

Background: Previous studies revealed that Programmed cell death protein 1 (PD-1)/Programmed cell death-Ligand protein 1 (PD-L1) inhibitors plus anti-angiogenic agents had extensive anti-tumor activities. However, almost all studies on the efficacy and safety of PD-1/PD-L1 inhibitors plus anti-angiogenic agents as second or later-line treatment for patients with advanced non-small cell lung cancer are non-randomized controlled trials with small sample sizes, which might lead to a lack of effective metrics to assess the effectiveness and safety of the therapeutic regimen. Here, this meta-analysis aimed to evaluate the efficacy and safety of PD-1/PD-L1 inhibitors plus anti-angiogenic agents as second or later-line treatment for patients with advanced non-small cell lung cancer

Methods: A single-arm meta-analysis was performed, and published literature from PubMed, Web of Science and Embase databases as of January 13, 2023, was systematically retrieved. We used the Cochrane risk of bias tool and methodological index for non-randomized studies (MINORS) Methodological items to evaluate the quality of eligible clinical trials. Outcomes including overall response rate (ORR), disease control rate (DCR), progression-free survival (PFS), overall survival (OS), and adverse events (AEs) were extracted for further analysis. The random effect model is used to calculate the pooled parameters.

Results: 19 studies (16 were non-comparative single-arm clinical trials and 3 were randomized controlled trials) were enrolled in this meta-analysis. In terms of tumor response, the pooled ORR and DCR were 22.4% (95% CI, 16.6-28.1%) and 76.8% (95% CI, 72.6-81.1%), respectively. With regard to survival analysis, the pooled PFS and OS were 5.20 (95% CI, 4.46-5.93) months and 14.09 (95% CI, 13.20-14.97) months, respectively. The pooled grade ≥3 adverse effect (AE) rate was 47.6% (95% CI, 33.1-62.0%)

Conclusion: PD-1/PD-L1 inhibitors plus anti-angiogenic agents has promising efficacy and safety as second or later-line treatment in patients with advanced non-small cell lung cancer.

Systematic review registration: https://www.crd.york.ac.uk/prospero/, identifier CRD42023407559.

KEYWORDS

advanced non-small cell lung cancer, second or later-line therapy, PD-1/PD-L1 inhibitors, anti-angiogenic agents, meta-analysis

Introduction

Non-small-cell lung cancer (NSCLC), which makes up around 80–85% of each diagnosis, is the most common kind of lung cancer and the leading cause of cancer-related death globally. The most recent "Global Cancer Statistics 2020" data from the World Health Organization show that its incidence rate is more than 1/10 of the world's malignant tumors (1). Approximately 70% of patients with stage I to stage III non-small cell lung cancer are surgically curable (2). Only 5% of patients with advanced non-small cell lung cancer survived 5 years (3). About 62 percent of non-small cell lung cancer patients are given a stage IV diagnosis at their initial diagnosis because they don't exhibit the typical signs of lung cancer (4). Chemotherapy, targeted therapy, and immunotherapy are the three most widely used therapies for persons with advanced non-small cell lung cancer (5).

Since the introduction of immunotherapy, the area of therapeutic approaches for NSCLC has taken on a whole new perspective and demonstrated considerable promise. Jianwei Zhu presented a review (6) of immunotherapy, which found that immunotherapies other than immune checkpoint inhibitor therapy, the current literature does not provide evidence that suggests a survival benefit from adding immunotherapy (excluding checkpoint inhibitors) to conventional curative surgery or radiotherapy, for people with localized NSCLC (stages I to III). However, patients with metastatic NSCLC who receive treatment with checkpoint inhibitors that target programmed cell death protein 1 (PD-1) and programmed death ligand-1 (PD-L1) have shown improved disease response rates and longer lifetime (7–9). The benefit of PD-1/PD-L1 inhibitor monotherapy is limited, a systematic review (10) was conducted by Fausto Petrelli et al. The study showed that the addition of immune checkpoint inhibitors to chemotherapy may improve both OS compared with chemotherapy alone, it is critically necessary to investigate the efficacy of combination treatment modalities to help doctors optimize their treatment regimens.

Anti-angiogenic agents, including monoclonal antibodies like bevacizumab and small molecule inhibitors like anlotinib, apatinib, and lenvatinib, inhibit the VEGF signaling pathway, exhibiting anti-tumor effects. Clinical studies have demonstrated the efficacy of this family of drugs in the treatment of advanced non-small cell lung cancer, including BEYOND (11) and ALTER0303 (12). Results from several clinical trials have been reported on the potential efficacy of PD-1/PD-L1 inhibitors in combination with anti-angiogenic drugs. Atezolizumab was shown to be beneficial in prolonging progression-free survival and overall survival in patients with advanced non-small cell lung cancer in IMpower150 (13) when used in conjunction with chemotherapy and bevacizumab. Pembrolizumab with lenvatinib was shown to have an objective response rate (ORR) of 33.3% when used as the first-line therapy for advanced non-small cell lung cancer in KEYNOTE-524 (14). These findings offer a scientific rationale for the PD-1/PD-L1 inhibitor plus anti-angiogenic drug therapy regimen.

Although various effective compounds for the second or later-line treatment of advanced non-small cell lung cancer improved the overall survival, the optimal regimen remains controversial. Due to the paucity of scientific evidence supporting the use of PD-1/PD-L1 inhibitors in combination with other drugs in the second or later-line treatment of patients with advanced non-small cell lung cancer, a number of clinical studies are being conducted worldwide to further examine the viability of combination regimens. However, almost all studies on the efficacy and safety of PD-1/PD-L1 inhibitors plus anti-angiogenic agents as second or later-line treatment for patients with advanced non-small cell lung cancer are non-randomized controlled trials with small sample sizes, which might lead to a lack of effective metrics to assess the effectiveness and safety of the therapeutic regimen. Here, this meta-analysis aimed to evaluate the efficacy and safety of PD-1/PD-L1 inhibitors plus anti-angiogenic agents as second or later-line treatment for patients with advanced non-small cell lung cancer

Materials and methods

Single-arm meta-analysis is in accordance with PRISMA (Preferred Reporting Items for Systematic Review and Meta-Analysis) guidelines (15) and has been registered with PROSPERO (ID: CRD42023407559, https://www.crd.york.ac.uk/prospero/).

Search strategy

We systematically searched PubMed, Embase and Web of Science databases as of January 13, 2023, for non-comparative clinical trials and randomized controlled trials (RCTs). The complete search we used for PubMed was supplied in Table S1. We also manually searched the abstract of European Society for Medical Oncology (ESMO) and American Society of Clinical Oncology (ASCO) for further eligible articles.

Selection criteria

Studies that satisfied the following inclusion criteria were taken into consideration: (1) Patients in prospective clinical trials having an advanced NSCLC diagnosis confirmed by histology; (2) taking PD-1/PD-L1 inhibitors plus anti-angiogenic drugs as a second or later-line therapy; (3) Clinical tumor outcomes, such as the objective response rate (ORR), disease control rate (DCR), progression-free survival (PFS), overall survival (OS), and adverse events (AEs), were reported for patients. To reduce the possibility of bias, the following studies were disregarded: (1) Studies that did not cover NSCLC; (2) No prospective clinical trials; (3) Lack of essential data or overlapping studies; (4) animal experiments, cell research, reviews, meta-analyses, duplicates, case reports, or letters were not taken into consideration; Through inclusion and exclusion criteria, two scientists independently selected possible suitable articles. Any disagreements about the inclusion of the study were settled by these two or a third investigator.

Data extraction and quality assessment

Two investigators independently retrieved the necessary data from each included studies after which the studies' quality was evaluated. First author, publication year, registration number, country, patient count, histology, median age, proportion of men, trial phase, and trial design are a brief summary of the retrieved characteristics. Grade 3 AE, ORR, DCR, median PFS, and OS were among the outcomes that were also retrieved. We used the MINORS Methodological items (16) to assess the quality of non-comparative single-arm clinical trials, and the Cochrane risk of bias instrument (17) to assess the quality of eligible RCTs.

Statistical analysis

Utilizing Stata statistical software, evidence synthesis was carried out. With Stata (Stata Corp, USA), we entered the overall clinical setting percentage for the primary outcome and the total number of research participants, and then computed the relevant standard errors of these quasinormal distribution "rates" using Stata. The lower interval (LI) and upper interval (UI), which have a 95% confidence level, may be justified using the "rates" and standard errors. Finally, the output included the pooled effect sizes (ES), which represented median "rates" and 95% confidence intervals (95% CI). The I2 statistic was used to analyze heterogeneity between studies. Studies were categorized as having low, moderate, or high heterogeneity based on their I2 statistics, which ranged from 25 to 50%, 50 to 75%, and >75%. For the I2 test, substantial heterogeneity was defined as P 0.05. We used random-effects models for all pooled ES because there was great subjectivity given the lack of related control groups in the noncomparative studies, and a tendency toward high heterogeneity. The large amount of data that was provided allowed for the meta-regression and subgroup analyses to be carried out. Additionally, sensitivity analysis was done to assess the consistency and dependability of the information that was merged. Finally, Egger's tests looked for a possible publication bias.

Results

Study identification

A total of 1439 records were found after searching the aforementioned databases Pubmed (n=259), Web of Science (n=646) and Embase (n=534), we also found 3 more records in the abstracts of the ESMO and ASCO conferences. We excluded 532 articles for duplication. 634 records were excluded with no relation to the topic. 257 of records excluded with reasons:(1) Case reports, Replies and comments;(2)Reviews and meta-analyses;(3)First-line treatment articles;(4)No clinical trials;(5)No available outcome data. For the remaining 19 publications, a quantitative synthesis was possible. The selection procedure was depicted in Figure 1.

Study characteristics

The present single-arm meta-analysis included a total of 19 studies (18–36) involving 931 participants; Table 1 describes the main study characteristics, and Table 2 presents the outcome results. The studies were all published between 2019 and 2022. Three studies (25, 28, 30) were randomized clinical trials, and 16 studies (18–24, 26, 27, 29, 31–36) were non-comparative clinical trials. Nine studies (19, 22, 23, 25–27, 30, 34, 35) were published abstracts, and 10 studies (18, 20, 21, 24, 28, 29, 31–33, 36) were original studies.

Quality assessment

Utilizing the Cochrane risk of bias tool, the three RCTs (25, 28, 30) were evaluated and did not demonstrate allocation concealment, but generated random sequences, provided complete outcome data, reported no selective outcome, and were free of other bias (Figure S1). To evaluate the non-comparative single-arm clinical trials' quality, we utilized the MINORS Methodological items; the quality evaluation specifics are included in Table 3.

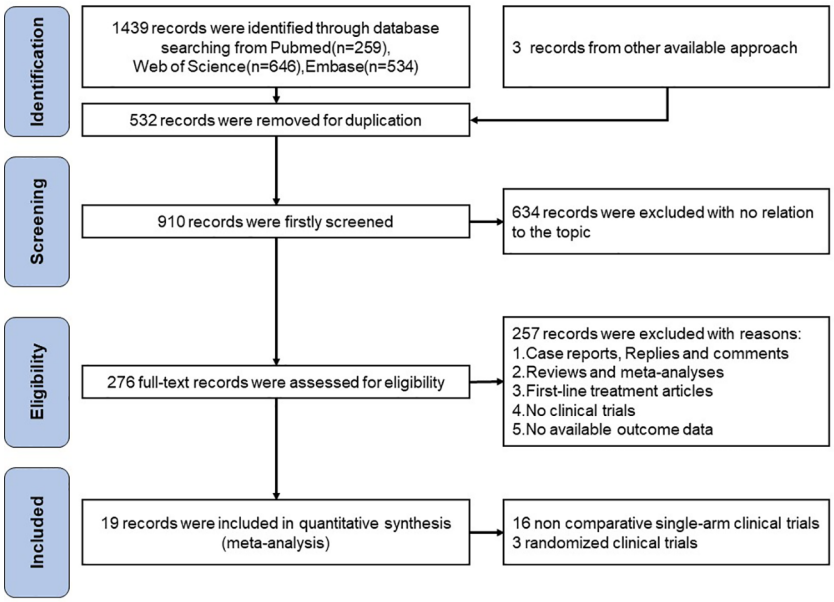


FIGURE 1
Flow chart of the single-arm meta-analysis.

TABLE 1 Characteristics of clinical trials included in the single-arm meta-analysis.

Study	Year	Register number	Country	Patients	Histology	Age (years)	Male (%)	Phase	Design
Herbst et al. (18)	2019	NCT02443324	5-countries*	27	NSCLC	65.0	78.0%	Ia/Ib	Single-arm
Galffy et al. (19)	2020	NCT03472560	Hungary	41	NSCLC	NR	NR	II	Single-arm
Bang et al. (20)	2020	NCT02572687	8-countries^	28	NSCLC	64.5	68.0%	Ia/Ib	Single-arm
Zhou et al. (21)	2021	NCT04670107	China	45	NSCLC	62.0	72.5%	Ib	Single-arm
Puri et al. (22)	2021	NCT03377023	USA	18	NSCLC	NR	66.7%	Ib/II	Single-arm
Pan et al. (23)	2021	ChiCTR2000034597	China	10	NSCLC	NR	33.3%	II	Single-arm
Zhou et al. (24)	2021	NCT04203485	China	105	N-Sq NSCLC	58.0	75.2%	Ib/II	Single-arm
Han et al. (25)	2021	NCT03910127	China	68	NSCLC	NR	NR	II	RCT
Leal et al. (26)	2022	NCT02954991	USA	68	N-Sq NSCLC	66.0	43.0%	II	Single-arm
Fang et al. (27)	2022	NCT04426825	China	19	EGFR+NSCLC	63.0	42.0%	II	Single-arm
Reckmap et al. (28)	2022	NCT03971474	USA	69	NSCLC	66.4	59.0%	II	RCT
Lv et al. (29)	2022	ChiCTR1900023664	China	34	NSCLC	60.0	67.6%	II	Single-arm
Lu et al. (30)	2022	NCT03802240	China	158	EGFR+ NSCLC	58.5	41.1%	III	RCT
Lee et al. (31)	2022	NCT03616691	Korea	24	NSCLC	63.0	54.2%	II	Single-arm
Herzog et al. (32)	2022	NCT03689855	USA	21	NSCLC	67.0	19.0%	II	Single-arm
Gao et al. (33)	2022	NCT03083041	China	25	Sq NSCLC	63.0	92.0%	II	Single-arm
Neal et al. (34)	2022	NCT03170960	9-countries#	81	N-Sq NSCLC	67.0	57.0%	Ib	Single-arm
Gao et al. (35)	2022	NCT03666143	China	47	NSCLC	60.0	NR	Ib	Single-arm
Gao et al. (36)	2022	NCT03083041	China	43	EGFR/ALK+ NSCLC	55.0	58.1%	II	Single-arm

5-countries*: USA, France, Germany, Spain and the UK; 8-countries^: France, Germany, Israel, Italy, Republic of Korea, Spain, Taiwan, and the USA; 9-countries#: Australia, Belgium, France, Germany, Italy, Netherlands, Spain, United Kingdom and the USA.

TABLE 2 Original data extracted from included clinical trials.

Study	Year	Patients	Intervention	DCR (%)	ORR (%)	mPFS (months)	mOS (months)	Grade 3-4 AE (%)
Herbst et al. (18)	2019	27	Pembrolizumab Ramucirumab	85.0%	30.0%	9.7(4.6-27.6)	26.2(11.8-NR)	NR
Galffy et al. (19)	2020	41	Avelumab Axitinib	70.7%	31.7%	5.5(2.5-7.0)	NR	58.5%
Bang et al. (20)	2020	28	Durvalumab Ramucirumab	57.0%	11.0%	2.7(1.6-5.8)	11.0(6.2-15.2)	32.1%
Zhou et al. (21)	2021	45	Camrelizumab Anlotinib	82.2%	13.3%	8.2(4.3-12.1)	12.7(10.2-15.1)	03.7%
Puri et al. (22)	2021	18	Nvolumab Ipilimumab Nintedanib	61.0%	22.0%	2.7(1.4-NR)	7.7(5.0-NR)	NR
Pan et al. (23)	2021	10	Camrelizumab Chemotherapy Apatinib	80.0%	20.0%	NR	NR	NR
Zhou et al. (24)	2021	105	Camrelizumab Apatinib	73.3%	27.6%	5.7(4.5-8.8)	15.5(10.9-24.5)	69.5%
Han et al. (25)	2021	68	TQB-2450(PD-L1) Anlotinib	73.5%	30.9%	6.9(5.3-12.4)	NR	67.7%
Leal et al. (26)	2021	68	Nivolumab Sitravatinib	NR	16.0%	6.0	15(9.3-21.1)	60.0%
Fang et al. (27)	2022	19	Atezolizumab Bevacizumab	68.4%	15.8%	2.8	NR	40.0%
Reckmap et al. (28)	2022	69	Pembrolizumab Ramucirumab	75.0%	22.0%	4.5(4.2-6.1)	14.5(13.9-16.1)	42.0%
Lv et al. (29)	2022	34	Nivolumab Recombinant human endostatin	64.7%	41.2%	6.8(1.1-12.1)	17.1(6.6-27.6)	11.8%
Lu et al. (30)	2022	158	Sintilimab Bevacizumab biosimilar IBI305 Chemotherapy	86.1%	48.1%	7.2(6.6-9.3)	NR	59.5%
Lee et al. (31)	2022	24	Atezolizumab Bevacizumab	87.5%	12.5%	5.6(4.1-7.1)	14.0(10.7-17.4)	4.2%
Herzog et al. (32)	2022	21	Atezolizumab Ramucirumab	81.0%	4.80%	3.4	16.5	43.0%
Gao et al. (33)	2022	25	Camrelizumab Apatinib	84.0%	32.0%	6.0(3.5-8.1)	13.3(6.4-18.8)	84.0%
Neal et al. (34)	2022	81	Atezolizumab Cabozantinib	80%	19.0%	4.5(3.5-5.6)	13.8(7.2-15.7)	52.0%
Gao et al. (35)	2021	47	Tislelizumab Sitravatinib	86.0%	14.0%	5.2(4.1-5.9)	NR	68.0%
Gao et al. (36)	2022	43	Camrelizumab Apatinib	58.1%	18.6%	2.8(1.9-5.5)	NR	65.1%

Therapeutic efficacy assessments of ORR

The effectiveness response was recorded in every study analyzed. The ORRs ranged from 11 to 48% among the investigations. The analysis revealed considerable heterogeneity (I^2 = 78.5%, P<0.0001) and a pooled ORR of 22.4% (95% CI: 16.6%-28.1%, Figure 2A). We further evaluated possible sources of heterogeneity by using meta-regression because there was high ORR heterogeneity across trials. For the meta-regression analysis, we selected 9 variables (year, region, phase, immunotherapy inhibitor, anti-angiogenic drug, tumor histology, study design, EGFR mutation and whether or not to combine chemotherapy). According to the meta-regression findings, there is no statistically significant difference between the p-values for each variable

TABLE 3 Quality assessment of the non-comparative single-arm clinical trials included in the meta-analysis.

Study	Q1	Q2	Q3	Q4	Q5	Q6	Q7	Q8	Score†
Herbst et al. (18)	2	2	2	2	0	2	2	2	14
Galffy et al. (19)	2	2	2	2	0	2	0	2	12
Bang et al. (20)	2	2	2	2	0	2	2	2	14
Zhou et al. (21)	2	2	2	2	0	2	2	2	14
Puri et al. (22)	2	2	2	2	0	2	2	1	13
Pan et al. (23)	2	2	2	2	0	2	1	0	11
Zhou et al. (24)	2	2	2	2	0	2	1	2	13
Leal et al. (26)	2	2	2	2	0	2	2	1	13
Fang et al. (27)	2	2	2	2	0	2	2	0	12
Lv et al. (29)	2	2	2	2	0	2	1	2	13
Lee et al. (31)	2	2	2	2	0	2	2	2	14
Herzog et al. (32)	2	2	2	2	0	2	2	1	13
Gao et al. (33)	2	2	2	2	0	2	2	2	14
Neal et al. (34)	2	2	2	2	0	2	2	2	14
Gao et al. (35)	2	2	2	2	0	2	2	2	14
Gao et al. (36)	2	2	2	2	0	2	2	2	14

Numbers Q1-Q8 in heading signified:
Q1: A clearly stated aim: the question addressed should be precise and relevant in the light of available literature.
Q2: Inclusion of consecutive patients: all patients potentially fit for inclusion (satisfying the criteria for inclusion) have been included in the study during the study period (no exclusion or details about the reasons for exclusion).
Q3: Prospective collection of data: data were collected according to a protocol established before the beginning of the study.
Q4: Endpoints appropriate to the aim of the study: unambiguous explanation of the criteria used to evaluate the main outcome which should be in accordance with the question addressed by the study. Also, the endpoints should be assessed on an intention-to-treat basis.
Q5: Unbiased assessment of the study endpoint: blind evaluation of objective endpoints and double-blind evaluation of subjective endpoints. Otherwise the reasons for not blinding should be stated.
Q6: Follow-up period appropriate to the aim of the study: the follow-up should be sufficiently long to allow the assessment of the main endpoint and possible adverse events.
Q7: Loss to follow up less than 5%: all patients should be included in the follow up. Otherwise, the proportion lost to follow up should not exceed the proportion experiencing the major endpoint.
Q8: Prospective calculation of the study size: information of the size of detectable difference of interest with a calculation of 95% confidence interval, according to the expected incidence of the outcome event, and information about the level for statistical significance and estimates of power when comparing the outcomes.
†The items are scored 0 (not reported), 1 (reported but inadequate) or 2 (reported and adequate).

(Figure 3A). The results failed to clearly identify significant influences on heterogeneity. We selected four variables (immunotherapy inhibitor, anti-angiogenic agent, EGFR mutation and whether or not to combine chemotherapy) for further subgroup analysis. Subgroup analysis revealed that the pooled ORR in patients who received PD-1 as immunotherapy was 25.8% (95% CI: 18.9%–32.7%), which was higher than that of patients receiving PD-L1 for treatment, with a statistical difference. The pooled ORR of patients receiving TKI as treatment was 19.8% (95% CI: 15.5%–24.1%). The pooled ORR of patients without EGFR mutation was 20.6% (95% CI: 15.6%–25.2%). The pooled ORR of patients receiving chemotherapy was 45.6% (95% CI: 38.1%–53.0%), which was higher than that of patients who did not receive chemotherapy, with a statistical difference (Figure 4).

Therapeutic efficacy assessments of DCR

18 studies included available data on DCR, and the DCR across the studies varied from 58 to 87%. The analysis showed a pooled DCR of 76.8% (95% CI: 72.6%–81.1%) and revealed considerable heterogeneity (I^2 = 52.1%, P=0.005, Figure 2B). As the significant heterogeneity of DCR across the studies existed, we also further investigated potential sources of heterogeneity by meta-regression and subgroup analysis. For the meta-regression analysis, we also selected the same 9 variables (year, region, phase, immunotherapy inhibitor, anti-angiogenic drug, tumor histology, study design, EGFR mutation and whether or not to combine chemotherapy). The results showed the phase of study contributed to the heterogeneity of DCR (Figure 3B), thus we carried out further subgroup analysis of the phase of the study, the results show a high DCR for Phase III studies, but with only one Phase III study, more studies need to be included in the analysis before certain conclusions can be drawn (Figure S2). We also chose four factors (immunotherapy inhibitor, anti-angiogenic agent, EGFR mutation, whether or not to combine chemotherapy) for further subgroup analysis. Subgroup analysis revealed that the pooled DCR in patients who received PD-1 as immunotherapy was 77.1% (95% CI: 72.0%–82.3%).The pooled DCR of patients receiving TKI as treatment was 76.1% (95% CI: 71.7%–80.4%). The pooled DCR of patients without EGFR mutation was 77.3% (95% CI: 73.5%–81.2%). The pooled DCR of patients receiving chemotherapy was

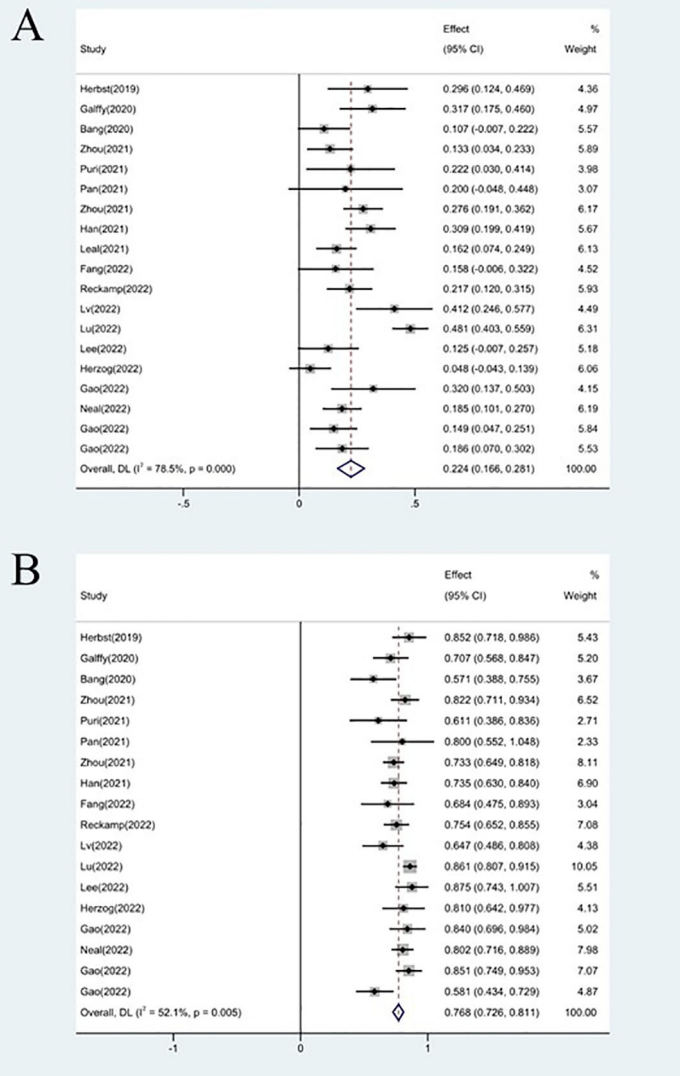


FIGURE 2
Forest plot about the pooled results of ORR **(A)** and DCR **(B)**.

85.8% (95% CI: 80.5%–91.1%), which was higher than that of patients who did not receive chemotherapy, with a statistical difference (Figure 5).

Efficacy evaluation of OS and PFS

Studies that did not provide specified 95% confidence intervals were eliminated, 9 studies included in the analysis reported OS and 14 studies reported PFS. In the random-effects model, the pooled median OS was 14.09 months (95% CI 13.20–14.97 months), as shown in Figure 6A. With regard to PFS, the results showed that the pooled median PFS was 5.20 months (95% CI: 4.46–5.93 months, Figure 6B). We further analyzed potential sources of heterogeneity by using meta-regression and subgroup analysis because there was a heterogeneity of PFS between different trials(I^2 = 55.5%, P=0.006). For the meta-regression analysis, we also selected the same 9 variables (year, region, phase, immunotherapy inhibitor, anti-angiogenic drug, tumor histology, study design, EGFR mutation, whether or not to combine chemotherapy). According to the meta-regression results, there is no statistically significant difference between the p-values for each variable (Figure 7A). We also chose four factors (immunotherapy inhibitor, anti-angiogenic agent, EGFR mutation and whether or not to combine chemotherapy) for further subgroup analysis. Subgroup analysis revealed that the pooled median PFS in patients who received PD-1 as immunotherapy was 5.54 months (95% CI: 4.55–6.52).The pooled median PFS of patients receiving TKI as treatment was 4.80 months (95% CI:4.09–5.51), which was shorter than that of patients who received recombinant human endostatin and bevacizumab as treatment, with a statistical difference. The pooled median PFS of patients without EGFR mutation was 5.03 months (95% CI: 4.47–5.59). The pooled median PFS of patients receiving chemotherapy was 7.20 months (95% CI: 5.85–8.85), which was higher than that of patients who did not receive chemotherapy, with a statistical difference (Figure 8).

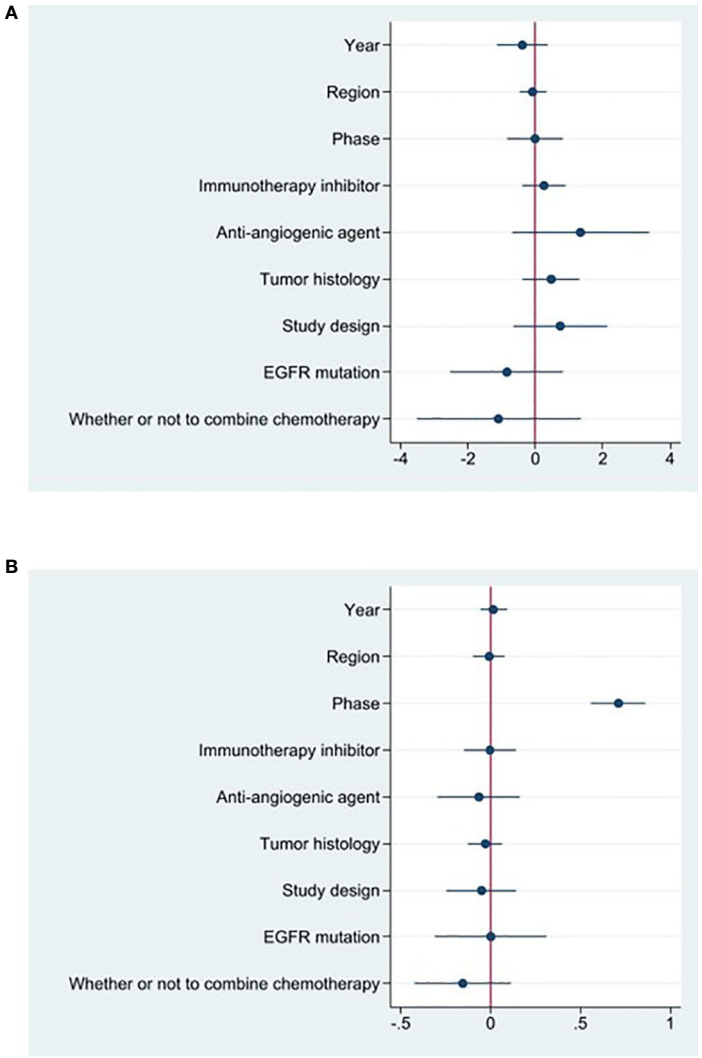


FIGURE 3
Coefplot of the results of meta-regression of ORR **(A)** and DCR **(B)**.

Toxicities

16 studies included in the meta-analysis provided the available incidence of AE (≥ grade 3). The most commonly reported adverse event was hypertension, the pooled AE≥ grade 3 was 47.6% (95% CI 33.1%–62.0%), as shown in Figure 9. As the significant heterogeneity of AE≥ grade 3 across the studies existed, we also further investigated potential sources of heterogeneity by meta-regression and subgroup analysis. For the meta-regression analysis, we selected the same 4 variables (immunotherapy inhibitor, anti-angiogenic drug, EGFR mutation, whether or not to combine chemotherapy), there is no statistically significant difference between the p-values for each variable (Figure 7B). We also chose the same four factors (immunotherapy inhibitor, anti-angiogenic agent, EGFR mutation and whether or not to combine chemotherapy) for further subgroup analysis. Subgroup analysis revealed that the pooled AE≥ grade 3 in patients who received PD-1 as immunotherapy was 52.9% (95% CI: 33.8%–71.9%). The pooled AE≥ grade 3 of patients receiving TKI as treatment was 53.7% (95% CI: 36.9%–70.5%). The pooled AE≥ grade 3 of patients without EGFR mutation was 45.7% (95% CI: 28.9%–62.4%). The pooled AE≥ grade 3 of patients receiving chemotherapy was 59.5% (95% CI: 51.4%–67.2%, Figure 10).

Sensitivity analysis

One study was left out at a time throughout the sensitivity analysis to determine how it might affect the combined results. According to the analysis's findings, no one research significantly affected any of the pooled results with 95% CIs. This proved the overall reliability of the meta-analysis's findings. Figure S3 displays the sensitivity analysis's findings.

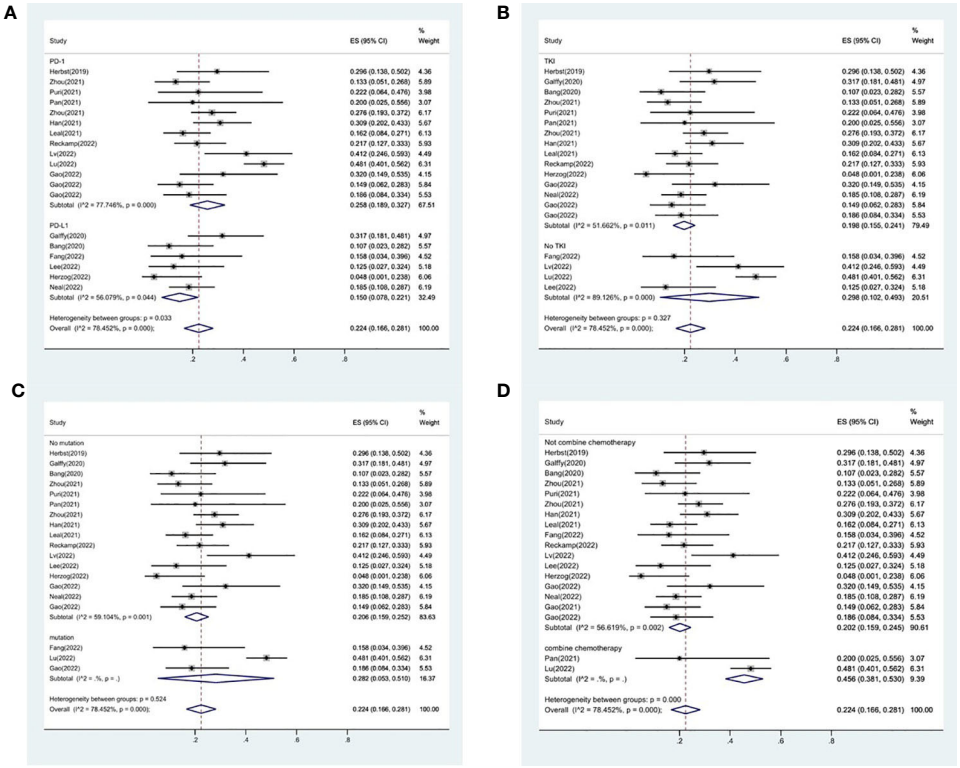


FIGURE 4
Subgroup analysis of ORR in immunotherapy inhibitor **(A)**, anti-angiogenic agent **(B)**, EGFR mutation **(C)** and whether or not to combine chemotherapy **(D)**.

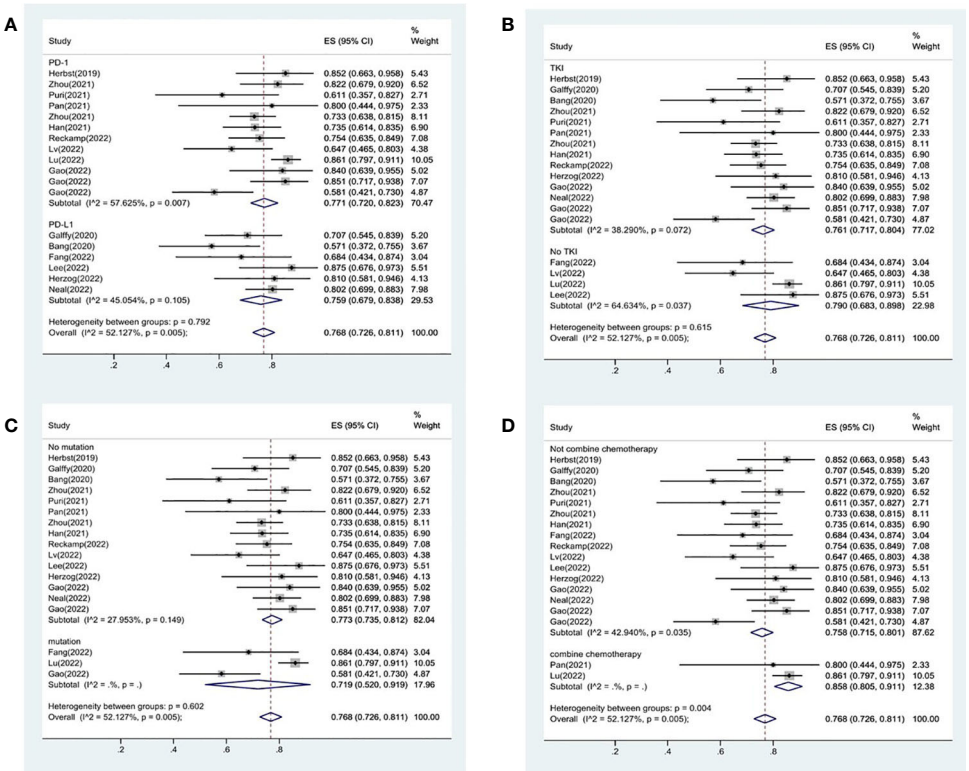


FIGURE 5
Subgroup analysis of DCR in immunotherapy inhibitor **(A)**, anti-angiogenic agent **(B)**, EGFR mutation **(C)** and whether or not to combine chemotherapy **(D)**.

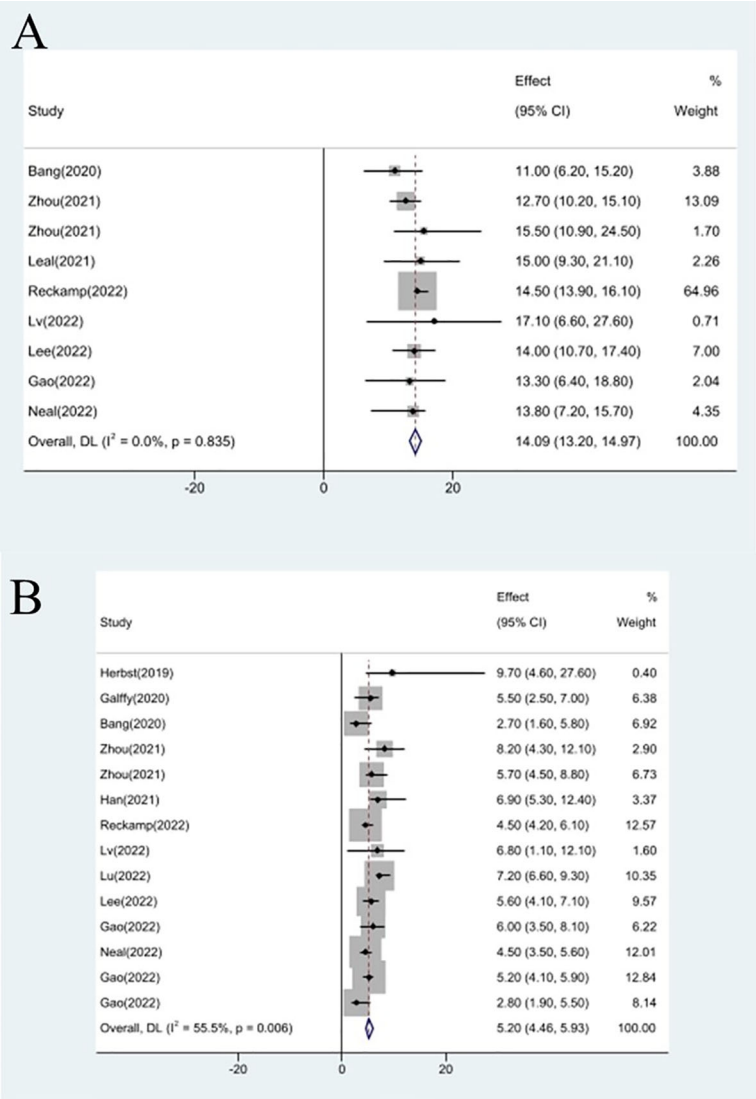


FIGURE 6
Forest plot about the pooled results of OS **(A)** and PFS **(B)**.

Publication bias

Using Egger's tests, the publication bias was estimated. We assumed that no publication bias existed for the ORR (Egger's test: 0.929), the PFS (Egger's test: 0.321), the OS (Egger's test: 0.559), and the AE grade 3 (Egger's test: 0.067). The test findings were consistent with most of the results, except for the DCR (Egger's test: 0.016). The Funnel graphs of publication bias were showed in Figure S4.

Discussion

In this era of numerous drugs, the treatment of lung cancer has evolved fast. The availability of second or later-line treatment for advanced non-small cell lung cancer is still constrained. Docetaxel was established as the standard chemotherapy regimen for second-line treatment of NSCLC in the TAX317/TAX320 studies (37, 38) and the results of the TAX317 study demonstrated that it significantly increased overall survival when used in the treatment of driver-negative advanced NSCLC compared to best supportive care (7 months vs. 4.6 months). The advent of immunotherapeutic medications has further changed the paradigm of second or later-line therapy for patients with advanced NSCLC. Based on the results of KEYNOTE-010, CheckMate 078 and OAK (9, 39, 40). PD-1/PD-L1 inhibitors monotherapy have been approved by the Food and Drug Administration (FDA) and the National Medical Products Administration (NMPA) of China for the second or later-line treatment of patients with driver-negative advanced non-small cell lung cancer. Alfredo Tartarone also conducted a Meta-analysis (41), this meta-analysis confirms the superiority of ICIs over docetaxel in pretreated non-small-cell lung cancer patients and would indicate a slight benefit from anti-PD-1 than from anti-PD-L1 inhibitors. The ALTER0303 study (12) demonstrated a median

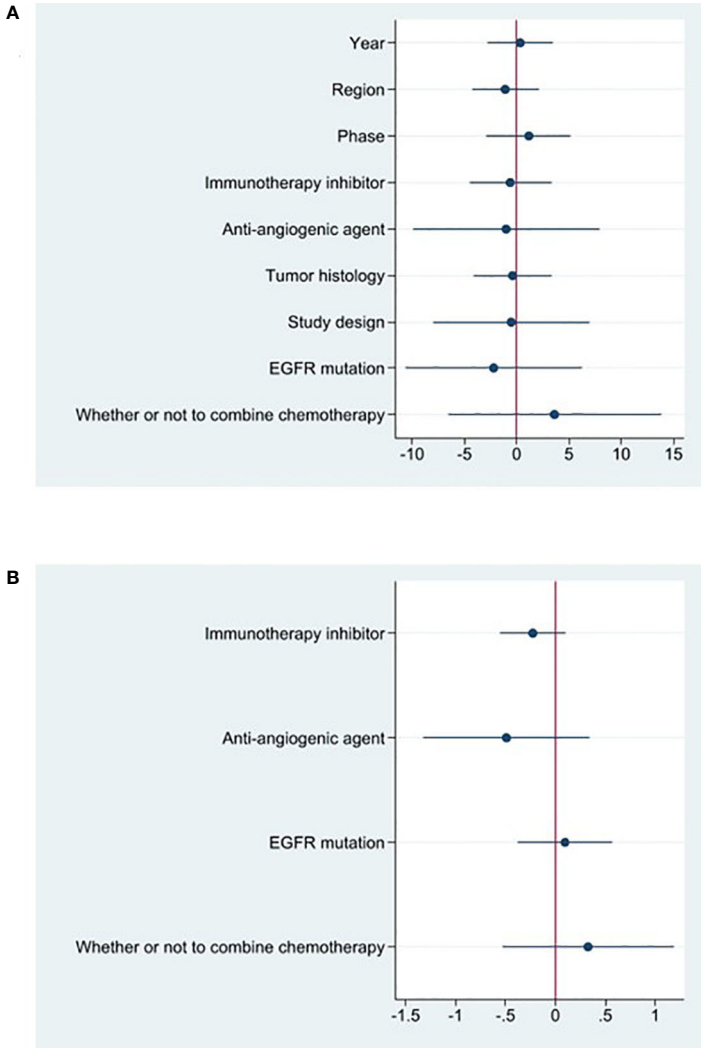


FIGURE 7
Coefplot of the results of meta-regression of PFS **(A)** and AE **(B)**.

OS extension of 3.3 months for patients in the anlotinib arm compared to the placebo arm (9.6 months vs. 6.3 months); and a median PFS extension of 4.0 months (5.4 months vs. 1.4 months). Based on the results of this study, anlotinib was approved for third-line treatment of patients with driver-negative advanced non-small cell lung cancer. There is a dearth of scientific data to support the use of combination regimens in the second or later-line therapy of patients with advanced non-small cell lung cancer, hence several clinical trials are being carried out globally to further investigate the viability of combination regimens.

Combination regimen based on small molecule VEGF signaling pathway inhibitors like anlotinib, apatinib, and lenvatinib is a popular issue in current research. Many academics have provided compelling justifications for the mechanisms at work when small molecule VEGF signaling pathway inhibitors are taken with additional medications, of these, the treatment options with the most established grounded theory were PD-1/PD-L1 inhibitors plus anti-angiogenic agents. A blockade of the VEGF signaling pathway with anti-angiogenic agents can have an enhanced anti-tumor immune effect because prior research has demonstrated that the Vascular Endothelial Growth Factors (VEGF)/VEGFR signaling pathway inhibits anti-tumor immune responses not only by producing a hypoxic microenvironment but also through other complex mechanisms to produce immunosuppressive effects (42–45). Activated immune cells can inhibit tumor angiogenesis both directly and indirectly, according to studies (46–48), resulting in a positive feedback loop between immunotherapy and anti-angiogenic treatment. A growing number of clinical studies focus on PD-1/PD-L1 inhibitors plus anti-angiogenic agents.

In our meta-analysis, nineteen clinical trials with 931 patients were included to evaluate the efficacy and safety of PD-1/PD-L1 inhibitors plus anti-angiogenic agents as second or later-line treatment for patients with advanced non-small cell lung cancer. The pooled analyses presented that PD-1/PD-L1 inhibitors plus anti-angiogenic agents exhibited efficacy and manageable safety with promising ORR, DCR, OS, and PFS. The pooled results showed that the ORR and DCR were 22.4% and 76.8%, respectively, and the median OS and PFS were 14.09 months and

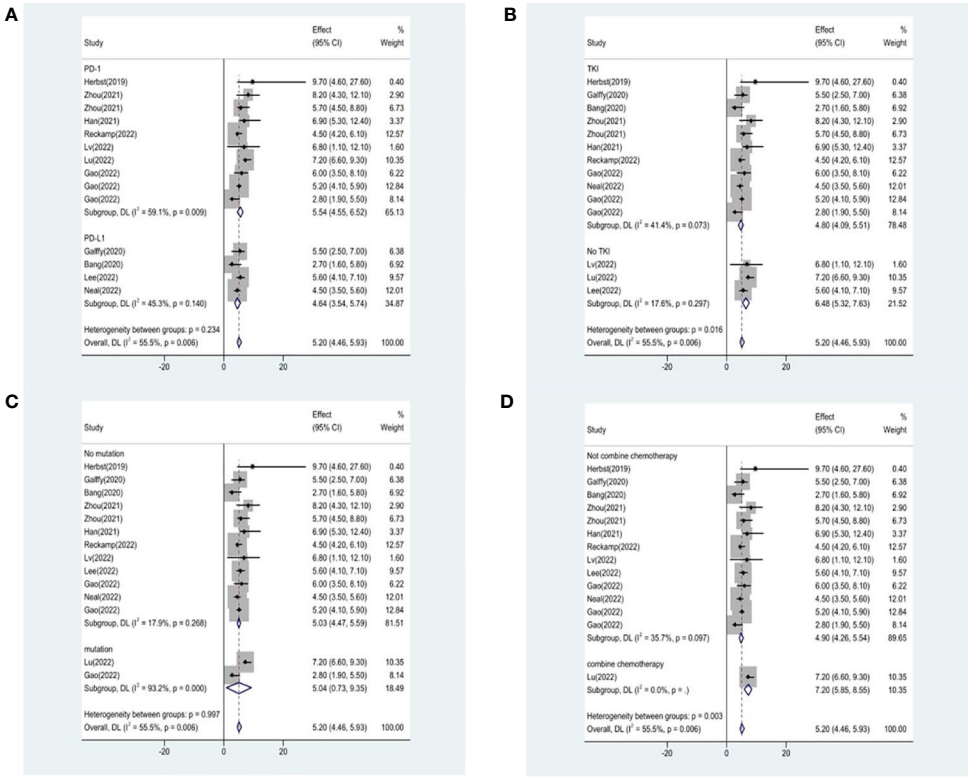


FIGURE 8
Subgroup analysis of PFS in immunotherapy inhibitor **(A)**, anti-angiogenic agent **(B)**, EGFR mutation **(C)** and whether or not to combine chemotherapy **(D)**.

5.20 months, respectively. The subgroup analysis indicated that it was likely that combination of chemotherapy resulted in an increased ORR and DCR. The pooled median PFS of patients receiving small molecule VEGF signaling pathway inhibitors as treatment was lower than that of patients who received recombinant human endostatin and bevacizumab as treatment. In the meantime, our research shows that the pooled AE≥ grade 3 was 47.6%, and the most commonly reported adverse event was hypertension. Xiaoying Sun et al. conducted a meta-analysis (49) to assess the immune-related adverse events associated with programmed cell death protein-1 and programmed cell death ligand 1 inhibitors for non-small cell lung cancer, study showed only a 4% probability of serious

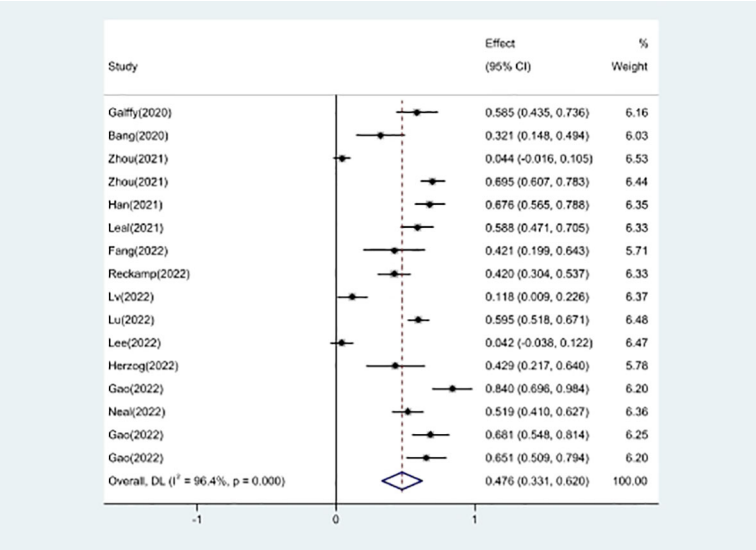


FIGURE 9
Forest plot about the pooled results of AE.

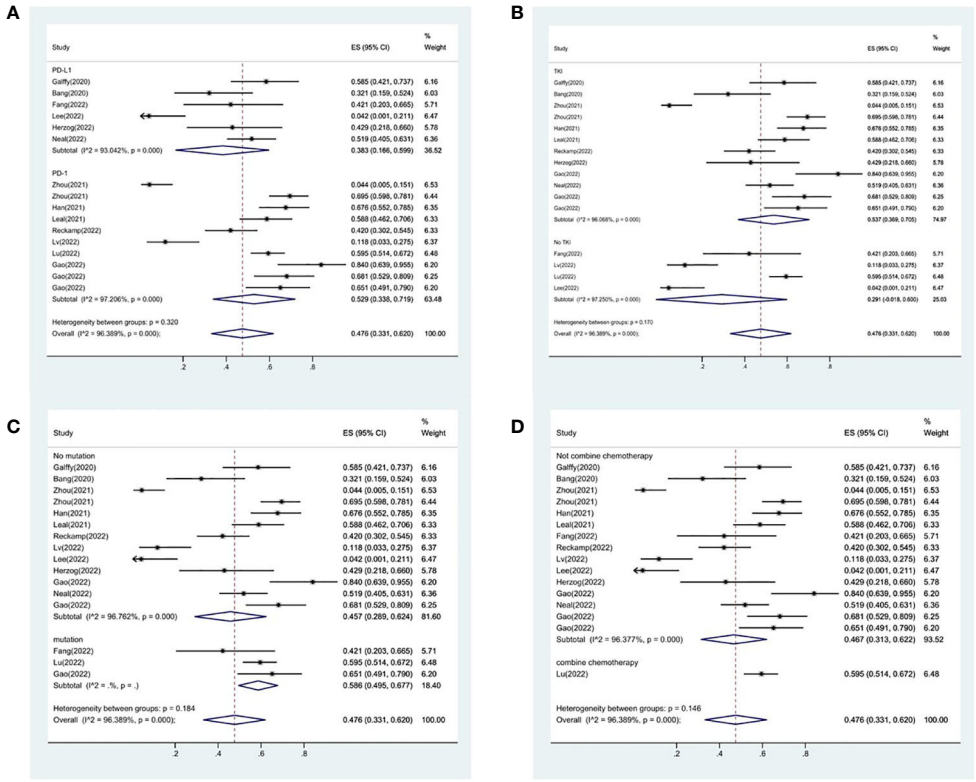


FIGURE 10
Subgroup analysis of AE in immunotherapy inhibitor **(A)**, anti-angiogenic agent **(B)**, EGFR mutation **(C)** and whether or not to combine chemotherapy **(D)**.

adverse events. However, that study included data from a large number of patients and addressed adverse reactions associated with PD-1 and PD-L1 drugs, whereas our study addressed a smaller number of patients in the study and addressed data from a combination anti-vascular drug regimen. And a large number of in our meta-analysis have shown that serious adverse events are hypertensive, and associated with anti-vascular drugs, the adverse events are relatively safe and manageable.

In monotherapy, nivolumab's effectiveness and safety in treating advanced non-small-cell lung cancer after prior treatment were evaluated by a meta-analysis (50). According to the research, the pooled ORR of the 817 patients who received nivolumab was 20%, and the pooled DCR of the 657 patients who received nivolumab was 36%. According to OAK (9) data, the ORR of 425 patients in the atezolizumab group was 14%, while the DCR was 49%. According to ALTER 0303's results (12), the ORR of 437 patients in the anlotinib group was 9.2%, and the DCR was 81%. The ORR of 353 patients in the nintedanib group was 9.1%, and the DCR was 60.9%, according to the results of LUME-Lung 2 (51). And the data from our study suggest that PD-1/PD-L1 inhibitors plus anti-angiogenic agents have more promising efficacy as second or later-line treatment in patients with advanced non-small cell lung cancer.

Another hot topic in current research is the use of chemotherapy plus PD-1/PD-L1 inhibitors combination regimens as second or later-line treatment for patients with advanced non-small cell lung cancer. The effectiveness of nivolumab with docetaxel in the second or later-line therapy of patients with advanced non-small cell lung cancer was examined in a clinical study (52). According to the results of the trial, the ORR was 41.8% and the DCR was 80% in the nivolumab plus docetaxel group. As second-line treatment for advanced non-small cell lung cancer without targetable mutations, sintilimab with docetaxel showed promising outcomes, according to Zhang et al. (53). The ORR was 36.7%, the DCR was 76.6%, the median PFS was 5.0 months, and the median OS was 13.4 months. The effectiveness of these two trials' findings was comparable to that of PD-1/PD-L1 inhibitors combined with anti-angiogenic medicines in this meta-analysis. Real-world data from our hospitals were analyzed by our team, and the findings of the study demonstrated that PD-1/PD-L1 inhibitors plus anti-angiogenic medicines were superior than PD-1/PD-L1 inhibitors plus chemotherapy (54). According to the data indicated above, PD-1/PD-L1 inhibitors combined with anti-angiogenic drugs had a satisfactory impact when used as a second or later-line treatment for patients with advanced non-small cell lung cancer. Our study is based on data from second and later line therapy, a population for which most existing clinical studies have not focused on PD-L1 expression in a timely manner, and which is therefore not mentioned in the extensive literature. Even the available studies agree that different countries and different

populations will have different PD-L1 expressions, but it is unknown whether this difference causes differences in therapeutic efficacy. This also suggests that studying the relationship between PD-L1 expression and drug efficacy after treatment with various drugs is a key research direction for the future.

In conclusion, our study has a number of advantages: First and foremost, our meta-analysis was conducted on better quality clinical trials, and a sufficient number of clinical trials were included. Second, we carry out rigorous statistical analysis of the data to ensure the stability and reliability of the results. The last but not least, we compared the results of previous studies to confirm the effectiveness of the treatment options. The meta-analysis's findings are valuable for physicians in that they may be used to create more effective treatment strategies for various individuals in a clinical environment.

The present meta-analysis had some shortcomings. First, the included studies showed significant heterogeneity. Despite our best efforts, we were unable to accurately identify the source of heterogeneity using meta-regression and subgroup analysis. Second, because all of the included studies had small sample sizes and were noncontrolled trials, we were only able to assess the effectiveness and risk without drawing any firm conclusions. Third, we haven't been able to thoroughly analyze the AE in further depth. In order to validate the clinical function of PD-1/PD-L1 inhibitors in combination with anti-angiogenic medicines in contrast to other medications and the general population, further large-scale RCTs need be developed.

Conclusion

PD-1/PD-L1 inhibitors plus anti-angiogenic agents has promising efficacy and safety as second or later-line treatment in patients with advanced non-small cell lung cancer.

Data availability statement

The original contributions presented in the study are included in the article/Supplementary Material. Further inquiries can be directed to the corresponding authors.

Author contributions

Material preparation, data collection, analysis and writing were performed by SC and WM. WJ and SZ given some constructive discussions make revisions to the paper. QY and HG conceptualized the research process and guided its conduct. All authors contributed to the article and approved the submitted version.

Conflict of interest

The authors declare that the research was conducted in the absence of any commercial or financial relationships that could be construed as a potential conflict of interest.

Publisher's note

All claims expressed in this article are solely those of the authors and do not necessarily represent those of their affiliated organizations, or those of the publisher, the editors and the reviewers. Any product that may be evaluated in this article, or claim that may be made by its manufacturer, is not guaranteed or endorsed by the publisher.

Supplementary material

The Supplementary Material for this article can be found online at: https://www.frontiersin.org/articles/10.3389/fimmu.2023.1218258/full#supplementary-material

SUPPLEMENTARY FIGURE 1
Risk of bias assessments for three randomized studies.

SUPPLEMENTARY FIGURE 2
Subgroup analysis of the phase of DCR.

SUPPLEMENTARY FIGURE 3
Sensitivity analysis. Sensitivity analysis for ORR **(A)**; Sensitivity analysis for DCR **(B)**; Sensitivity analysis for OS **(C)**; Sensitivity analysis for PFS **(D)**; Sensitivity analysis for AE **(E)**.

SUPPLEMENTARY FIGURE 4
The Funnel graphs of publication bias of ORR **(A)**, DCR **(B)**, OS **(C)**, PFS **(D)** and AE **(E)**.

References

1. Sung H, Ferlay J, Siegel RL, Laversanne M, Soerjomataram I, Jemal J, et al. Global Cancer Statistics 2020: GLOBOCAN Estimates of Incidence and Mortality Worldwide for 36 Cancers in 185 Countries. *CA Cancer J Clin* (2021) 71:209–49. doi: 10.3322/caac.21660

2. Hoy H, Lynch T, Beck M. Surgical treatment of lung cancer. *Crit Care Nurs Clin North Am* (2019) 31:303–13. doi: 10.1016/j.cnc.2019.05.002

3. Arbour KC, Riely GJ. Systemic therapy for locally advanced and metastatic Non-Small cell lung cancer: A review. *JAMA* (2019) 322:764–74. doi: 10.1001/jama.2019.11058

4. Jones GS, Baldwin DR. Recent advances in the management of lung cancer. *Clin Med (Lond)* (2018) 18:s41–6. doi: 10.7861/clinmedicine.18-2-s41

5. Yang CY, Yang JC, Yang PC. Precision management of advanced Non-Small cell lung cancer. *Annu Rev Med* (2020) 71:117–36. doi: 10.1146/annurev-med-051718-013524

6. Zhu J, Yuan Y, Wan X, Yin D, Li R, Chen W, et al. Immunotherapy (excluding checkpoint inhibitors) for stage I to III non-small cell lung cancer treated with surgery or radiotherapy with curative intent. *Cochrane Database Syst Rev* (2021) 12:D11300. doi: 10.1002/14651858.CD011300.pub3

7. Gandhi L, Rodríguez-Abreu D, Gadgeel S, Esteban E, Felip E, De Angelis F, et al. Pembrolizumab plus chemotherapy in metastatic non-small-cell lung cancer. *N Engl J Med* (2018) 378:2078–92. doi: 10.1056/NEJMoa1801005

8. Paz-Ares L, Luft A, Vicente D, Tafreshi A, Gümüş M, Mazières J, et al. Pembrolizumab plus chemotherapy for squamous non-small-cell lung cancer. *N Engl J Med* (2018) 379:2040–51. doi: 10.1056/NEJMoa1810865

9. Rittmeyer A, Barlesi F, Waterkamp D, Park K, Ciardiello F, von Pawel J, et al. Atezolizumab versus docetaxel in patients with previously treated non-small-cell lung

cancer (OAK): A phase 3, open-label, multicentre randomised controlled trial. *Lancet* (2017) 389:255–65. doi: 10.1016/S0140-6736(16)32517-X

10. Petrelli F, Ferrara R, Signorelli D, Ghidini A, Proto C, Roudi R, et al. Immune checkpoint inhibitors and chemotherapy in first-line NSCLC: A meta-analysis. *Immunotherapy-Uk* (2021) 13:621–31. doi: 10.2217/imt-2020-0224

11. Zhou C, Wu YL, Chen G, Liu X, Zhu Y, Lu S, et al. BEYOND: A randomized, Double-Blind, Placebo-Controlled, multicenter, phase III study of First-Line Carboplatin/Paclitaxel plus bevacizumab or placebo in chinese patients with advanced or recurrent nonsquamous Non-Small-Cell lung cancer. *J Clin Oncol* (2015) 33:2197–204. doi: 10.1200/JCO.2014.59.4424

12. Cheng Y, Han B, Li K, Wang Q, Zhang L, Shi J, et al. Effect of anlotinib as a third- or further-line therapy in advanced non-small cell lung cancer patients with different histologic types: Subgroup analysis in the ALTER0303 trial. *Cancer Med* (2020) 9:2621–30. doi: 10.1002/cam4.2913

13. Socinski MA, Jotte RM, Cappuzzo F, Orlandi F, Stroyakovskiy D, Nogami N, et al. Atezolizumab for First-Line treatment of metastatic nonsquamous NSCLC. *N Engl J Med* (2018) 378:2288–301. doi: 10.1056/NEJMoa1716948

14. Taylor MH, Lee CH, Makker V, Rasco D, Dutcus CE, Wu J, et al. Phase IB/II trial of lenvatinib plus pembrolizumab in patients with advanced renal cell carcinoma, endometrial cancer, and other selected advanced solid tumors. *J Clin Oncol* (2020) 38:1154–63. doi: 10.1200/JCO.19.01598

15. Page MJ, McKenzie JE, Bossuyt PM, Boutron I, Hoffmann TC, Mulrow CD, et al. The PRISMA 2020 statement: An updated guideline for reporting systematic reviews. *BMJ* (2021) 372:n71. doi: 10.1136/bmj.n71

16. Slim K, Nini E, Forestier D, Kwiatkowski F, Panis Y, Chipponi J. Methodological index for non-randomized studies (minors): Development and validation of a new instrument. *Anz J Surg* (2003) 73:712–6. doi: 10.1046/j.1445-2197.2003.02748.x

17. Higgins JP, Altman DG, Gøtzsche PC, Jüni P, Moher D, Oxman AD, et al. The Cochrane Collaboration's tool for assessing risk of bias in randomised trials. *BMJ* (2011) 343:d5928. doi: 10.1136/bmj.d5928

18. Herbst RS, Arkenau HT, Santana-Davila R, Calvo E, Paz-Ares L, Cassier PA, et al. Ramucirumab plus pembrolizumab in patients with previously treated advanced non-small-cell lung cancer, gastro-oesophageal cancer, or urothelial carcinomas (JVDF): A multicohort, non-randomised, open-label, phase 1a/b trial. *Lancet Oncol* (2019) 20:1109–23. doi: 10.1016/S1470-2045(19)30458-9

19. Galffy G, Lugowska I, Poddubskaya E, Cho BC, Ahn MJ, Han JY, et al. A phase II open-label trial of avelumab plus axitinib in previously treated non-small-cell lung cancer or treatment-naïve, cisplatin-ineligible urothelial cancer. *ESMO Open* (2020) 8: 101173. doi: 10.1016/j.esmoop.2023.101173

20. Bang YJ, Golan T, Dahan L, Fu S, Moreno V, Park K, et al. Ramucirumab and durvalumab for previously treated, advanced non-small-cell lung cancer, gastric/gastro-oesophageal junction adenocarcinoma, or hepatocellular carcinoma: An open-label, phase Ia/b study (JVDJ). *Eur J Cancer* (2020) 137:272–84. doi: 10.1016/j.ejca.2020.06.007

21. Zhou N, Jiang M, Li T, Zhu J, Liu K, Hou H, et al. Anlotinib combined with anti-PD-1 antibody, camrelizumab for advanced NSCLCs after multiple lines treatment: An open-label, dose escalation and expansion study. *Lung Cancer* (2021) 160:111–7. doi: 10.1016/j.lungcan.2021.08.006

22. Puri S, Tanvetyanon T, Creelan B, Shafique M, Saltos A, Chiappori A, et al. MA13.02 phase II study of nivolumab and ipilimumab combined with nintedanib in recurrent Non-Small cell lung cancer. *J Thorac Oncol* (2021) 16:S924–5. doi: 10.1016/j.jtho.2021.08.176

23. Pan Y, Jiang F, Du Y, Wang Y, Liu H, Wang Z, et al. A clinical study of camrelizumab combined with chemotherapy and sequential apatinib in the second-line treatment of patients with advanced non-small cell lung cancer. *J Clin Oncol* (2021) 39: e21051. doi: 10.1200/JCO.2021.39.15_suppl.e21051

24. Zhou C, Wang Y, Zhao J, Chen G, Liu Z, Gu K, et al. Efficacy and biomarker analysis of camrelizumab in combination with apatinib in patients with advanced nonsquamous NSCLC previously treated with chemotherapy. *Clin Cancer Res* (2021) 27:1296–304. doi: 10.1158/1078-0432.CCR-20-3136

25. Han B, Zhang W, Shi C, Chu T, Yang Z. P15.07 safety and efficacy profile of TQB-2450 alone/with anlotinib in Previously-Treated advanced NSCLC: A phase IB Single-Arm trial. *J Thorac oncology: Off Publ Int Assoc Study Lung Cancer.* (2021) 16: S346. doi: 10.1016/j.jtho.2021.01.544

26. Leal TA, Berz D, Rybkin I, Iams WT, Bruno D, Blakely C, et al. 43P MRTX-500: Phase II trial of sitravatinib (sitra) + nivolumab (nivo) in patients (pts) with non-squamous (NSQ) non-small cell lung cancer (NSCLC) progressing on or after prior checkpoint inhibitor (CPI) therapy. *Ann Oncol* (2022) 33:S19–20. doi: 10.1016/j.annonc.2022.01.052

27. Fang WF, Fang J, Tian P, Fan Y, Yu Q, Zhang X, et al. 1032P ML41256: Phase II study of atezolizumab (atezo) in combination with bevacizumab (beva) in advanced non-squamous non-small cell lung cancer (nsqNSCLC) patients (pts) pretreated with epidermal growth factor receptor (EGFR) tyrosine-kinase inhibitors (TKIs). *Ann OncologyAbstract Book ESMO Congress* (2022) 9. doi: 10.1016/j.annonc.2022.07.1158

28. Reckamp KL, Redman MW, Dragnev KH, Minichiello K, Villaruz LC, Faller B, et al. Phase II randomized study of ramucirumab and pembrolizumab versus standard of care in advanced Non-Small-Cell lung cancer previously treated with Immunotherapy-Lung-MAP S1800A. *J Clin Oncol* (2022) 40:2295–306. doi: 10.1200/JCO.22.00912

29. Lv W, Pei X, Zhao W, Cong Y, Wei Y, Li T, et al. Safety and efficacy of nivolumab plus recombinant human endostatin in previously treated advanced non-small-cell lung cancer. *Transl Lung Cancer Res* (2022) 11:201–12. doi: 10.21037/tlcr-22-49

30. Lu S, Wu L, Jian H, Cheng Y, Wang Q, Fang J, et al. LBA58 Sintilimab with or without IBI305 plus chemotherapy in patients with EGFR mutated non-squamous non-small cell lung cancer (EGFRm nsqNSCLC) who progressed on EGFR tyrosine-kinase inhibitors (TKIs) therapy: Second interim analysis of phase III ORIENT-31 study. *Ann OncologyAbstract Book ESMO Congress* (2022) 9. doi: 10.1016/j.annonc.2022.08.060

31. Lee J, Koh J, Kim HK, Hong S, Kim K, Park S, et al. Bevacizumab plus atezolizumab after progression on atezolizumab monotherapy in pretreated patients with NSCLC: an open-label, two-stage, phase 2 trial. *J Thorac Oncol* (2022) 17:900–8. doi: 10.1016/j.jtho.2022.04.001

32. Herzog BH, Waqar SN, Devarakonda S, Ward JP, Gao F, Govindan R, et al. Ramucirumab plus atezolizumab in patients with stage IV non-small cell lung cancer previously treated with immune checkpoint inhibitors. *Lung Cancer* (2022) 173:101–6. doi: 10.1016/j.lungcan.2022.09.011

33. Gao G, Zhao J, Ren S, Wang Y, Chen G, Chen J, et al. Efficacy and safety of camrelizumab plus apatinib as second-line treatment for advanced squamous non-small cell lung cancer. *Ann Transl Med* (2022) 10:441. doi: 10.21037/atm-21-4792

34. Neal J, Lim F, Felip E, Gentzler R, Aix SP. FP14.08 cabozantinib plus atezolizumab in NSCLC patients previously treated with a checkpoint inhibitor: results from COSMIC 021. *J Thorac Oncol* (2021) 16:S230–1. doi: 10.1016/j.jtho.2021.01.151

35. Gao B, Ma Z, Yu X, Huang D, Zhao J, Day D, et al. 1P Sitravatinib + tislelizumab in patients with anti-PD-(L)1 refractory/resistant metastatic non-small cell lung cancer (NSCLC). *Ann Oncol* (2022) 33:S1. doi: 10.1016/j.annonc.2022.01.063

36. Gao G, Ni J, Wang Y, Ren S, Liu Z, Chen G, et al. Efficacy and safety of camrelizumab plus apatinib in previously treated patients with advanced non-small cell lung cancer harboring EGFR or ALK genetic aberration. *Transl Lung Cancer Res* (2022) 11:964–74. doi: 10.21037/tlcr-22-22

37. Shepherd FA, Dancey J, Ramlau R, Mattson K, Gralla R, O'Rourke M, et al. Prospective randomized trial of docetaxel versus best supportive care in patients with non-small-cell lung cancer previously treated with platinum-based chemotherapy. *J Clin Oncol* (2000) 18:2095–103. doi: 10.1200/JCO.2000.18.10.2095

38. Fossella FV, DeVore R, Kerr RN, Crawford J, Natale RR, Dunphy F, et al. Randomized phase III trial of docetaxel versus vinorelbine or ifosfamide in patients with advanced non-small-cell lung cancer previously treated with platinum-containing chemotherapy regimens. *TAX 320 Non-Small Cell Lung Cancer Study Group J Clin Oncol* (2000) 18:2354–62. doi: 10.1200/JCO.2000.18.12.2354

39. Herbst RS, Baas P, Kim DW, Felip E, Pérez-Gracia JL, Han JY, et al. Pembrolizumab versus docetaxel for previously treated, PD-L1-positive, advanced non-small-cell lung cancer (KEYNOTE-010): A randomised controlled trial. *Lancet* (2016) 387:1540–50. doi: 10.1016/S0140-6736(15)01281-7

40. Wu YL, Lu S, Cheng Y, Zhou C, Wang J, Mok T, et al. Nivolumab versus docetaxel in a predominantly chinese patient population with previously treated advanced NSCLC: CheckMate 078 randomized phase III clinical trial. *J Thorac Oncol* (2019) 14:867–75. doi: 10.1016/j.jtho.2019.01.006

41. Tartarone A, Roviello G, Lerose R, Roudi R, Aieta M, Zoppoli P. Anti-PD-1 versus anti-PD-L1 therapy in patients with pretreated advanced non-small-cell lung cancer: A meta-analysis. *Future Oncol* (2019) 15:2423–33. doi: 10.2217/fon-2018-0868

42. Oyama T, Ran S, Ishida T, Nadaf S, Kerr L, Carbone DP, et al. Vascular endothelial growth factor affects dendritic cell maturation through the inhibition of nuclear factor-kappa B activation in hemopoietic progenitor cells. *J Immunol* (1998) 160:1224–32. doi: 10.4049/jimmunol.160.3.1224

43. Nefedova Y, Huang M, Kusmartsev S, Bhattacharya R, Cheng P, Salup R, et al. Hyperactivation of STAT3 is involved in abnormal differentiation of dendritic cells in cancer. *J Immunol* (2004) 172:464–74. doi: 10.4049/jimmunol.172.1.464

44. Curiel TJ. Tregs and rethinking cancer immunotherapy. *J Clin Invest* (2007) 117:1167–74. doi: 10.1172/JCI31202

45. Wada J, Suzuki H, Fuchino R, Yamasaki A, Nagai S, Yanai K, et al. The contribution of vascular endothelial growth factor to the induction of regulatory T-cells in Malignant effusions. *Anticancer Res* (2009) 29:881–8.

46. Tian L, Goldstein A, Wang H, Ching LH, Sun KI, Welte T, et al. Mutual regulation of tumour vessel norMalization and immunostimulatory reprogramming. *Nature* (2017) 544:250–4. doi: 10.1038/nature21724

47. De Palma M, Biziato D, Petrova TV. Microenvironmental regulation of tumour angiogenesis. *Nat Rev Cancer.* (2017) 17:457–74. doi: 10.1038/nrc.2017.51

48. Bruno A, Pagani A, Pulze L, Albini A, Dallaglio K, Noonan DM, et al. Orchestration of angiogenesis by immune cells. *Front Oncol* (2014) 4:131. doi: 10.3389/fonc.2014.00131

49. Sun X, Roudi R, Dai T, Chen S, Fan B, Li H, et al. Immune-related adverse events associated with programmed cell death protein-1 and programmed cell death ligand 1 inhibitors for non-small cell lung cancer: A PRISMA systematic review and meta-analysis. *BMC Cancer.* (2019) 19:558. doi: 10.1186/s12885-019-5701-6

50. Huang J, Zhang Y, Sheng J, Zhang H, Fang W, Zhan J, et al. The efficacy and safety of nivolumab in previously treated advanced non-small-cell lung cancer: A meta-analysis of prospective clinical trials. *Onco Targets Ther* (2016) 9:5867–74. doi: 10.2147/OTT.S115262

51. Hanna NH, Kaiser R, Sullivan RN, Aren OR, Ahn MJ, Tiangco B, et al. Nintedanib plus pemetrexed versus placebo plus pemetrexed in patients with relapsed or refractory, advanced non-small cell lung cancer (LUME-Lung 2): A randomized, double-blind, phase III trial. *Lung Cancer* (2016) 102:65–73. doi: 10.1016/j.lungcan.2016.10.011

52. Taniguchi Y, Shimokawa T, Takiguchi Y, Misumi T, Nakamura Y, Kawashima Y, et al. A randomized comparison of nivolumab versus nivolumab + docetaxel for previously treated advanced or recurrent ICI-Naïve Non-Small cell lung cancer: TORG1630. *Clin Cancer Res* (2022) 28:4402–9. doi: 10.1158/1078-0432.CCR-22-1687

53. Zhang Y, Song L, Zeng L, Xiong Y, Liu L, Zhou C, et al. Sintilimab plus docetaxel as second-line therapy of advanced non-small cell lung cancer without targetable mutations: A phase II efficacy and biomarker study. *BMC Cancer* (2022) 22:952. doi: 10.1186/s12885-022-10045-0

54. Chen S, Wei H, Zhao W, Jiang W, Ning R, Zhou S, et al. PD-1/PD-L1 inhibitors plus anti-angiogenic agents with or without chemotherapy versus PD-1/PD-L1 inhibitors plus chemotherapy as second or later-line treatment for patients with advanced non-small cell lung cancer: A real-world retrospective cohort study. *Front Immunol* (2022) 13:1059995. doi: 10.3389/fimmu.2022.1059995

frontiers | Frontiers in Immunology

TYPE Original Research
PUBLISHED 10 August 2023
DOI 10.3389/fimmu.2023.1206631

Check for updates

OPEN ACCESS

EDITED BY
Wenjun Mao,
The Affiliated Wuxi People's Hospital of Nanjing Medical University, China

REVIEWED BY
Julien Faget,
INSERM U1194 Institut de Recherche en Cancérologie de Montpellier (IRCM), France
Sara Trabanelli,
University of Geneva, Switzerland

*CORRESPONDENCE
Tianhong Li
thli@ucdavis.edu

†PRESENT ADDRESSES
Weijie Ma,
Department of Pathology and Laboratory Medicine, Dartmouth Hitchcock Medical Center, Geisel School of Medicine at Dartmouth, Lebanon, NH, United States
Sixi Wei,
Center for Clinical Laboratories, The Affiliated Hospital of Guizhou Medical University, Guiyang, Guizhou, China

RECEIVED 16 April 2023
ACCEPTED 20 July 2023
PUBLISHED 10 August 2023

CITATION
Ma W, Wei S, Long S, Tian EC, McLaughlin B, Jaimes M, Montoya DJ, Viswanath VR, Chien J, Zhang Q, Van Dyke JE, Chen S and Li T (2023) Dynamic evaluation of blood immune cells predictive of response to immune checkpoint inhibitors in NSCLC by multicolor spectrum flow cytometry. *Front. Immunol.* 14:1206631. doi: 10.3389/fimmu.2023.1206631

COPYRIGHT
© 2023 Ma, Wei, Long, Tian, McLaughlin, Jaimes, Montoya, Viswanath, Chien, Zhang, Van Dyke, Chen and Li. This is an open-access article distributed under the terms of the Creative Commons Attribution License (CC BY). The use, distribution or reproduction in other forums is permitted, provided the original author(s) and the copyright owner(s) are credited and that the original publication in this journal is cited, in accordance with accepted academic practice. No use, distribution or reproduction is permitted which does not comply with these terms.

Dynamic evaluation of blood immune cells predictive of response to immune checkpoint inhibitors in NSCLC by multicolor spectrum flow cytometry

Weijie Ma[1,2†], Sixi Wei[1†], Siqi Long[1], Eddie C. Tian[1], Bridget McLaughlin[3], Maria Jaimes[4], Dennis J. Montoya[5], Varun R. Viswanath[1], Jeremy Chien[5], Qianjun Zhang[6], Jonathan E. Van Dyke[3], Shuai Chen[7] and Tianhong Li[1,8*]

[1]Division of Hematology/Oncology, Department of Internal Medicine, University of California Davis Comprehensive Cancer Center, University of California Davis School of Medicine, Sacramento, CA, United States, [2]Department of Pathology and Laboratory Medicine, Dartmouth-Hitchcock Medical Center, Geisel School of Medicine, Dartmouth, NH, United States, [3]University of California Davis, Flow cytometry Shared Resource, Davis, CA, United States, [4]Cytek Biosciences, Fremont, CA, United States, [5]Department of Biochemistry and Molecular Medicine, University of California Davis, Sacramento, CA, United States, [6]Beckman Coulter Life Sciences, San Jose, CA, United States, [7]Division of Biostatistics, Department of Public Health Sciences, University of California, Davis, Davis, CA, United States, [8]Medical Service, Hematology and Oncology, Veterans Affairs Northern California Health Care System, Mather, CA, United States

Introduction: Immune checkpoint inhibitors (ICIs) only benefit a subset of cancer patients, underlining the need for predictive biomarkers for patient selection. Given the limitations of tumor tissue availability, flow cytometry of peripheral blood mononuclear cells (PBMCs) is considered a noninvasive method for immune monitoring. This study explores the use of spectrum flow cytometry, which allows a more comprehensive analysis of a greater number of markers using fewer immune cells, to identify potential blood immune biomarkers and monitor ICI treatment in non-small-cell lung cancer (NSCLC) patients.

Methods: PBMCs were collected from 14 non-small-cell lung cancer (NSCLC) patients before and after ICI treatment and 4 healthy human donors. Using spectrum flow cytometry, 24 immune cell markers were simultaneously monitored using only 1 million PBMCs. The results were also compared with those from clinical flow cytometry and bulk RNA sequencing analysis.

Results: Our findings showed that the measurement of CD4+ and CD8+ T cells by spectrum flow cytometry matched well with those by clinical flow cytometry (Pearson R ranging from 0.75 to 0.95) and bulk RNA sequencing analysis (R=0.80, P=1.3 x 10-4). A lower frequency of CD4+ central memory cells before treatment was associated with a longer median progression-free survival (PFS) [Not reached (NR) vs. 5 months; hazard ratio (HR)=8.1, 95% confidence interval (CI) 1.5–42, P=0.01]. A higher frequency of CD4-CD8- double-negative (DN) T cells was associated with a longer PFS (NR vs. 4.45 months; HR=11.1, 95% CI 2.2–55.0, P=0.003). ICIs significantly changed the frequency of cytotoxic CD8+PD1+ T

cells, DN T cells, CD16+CD56dim and CD16+CD56- natural killer (NK) cells, and CD14+HLDRhigh and CD11c+HLADR + monocytes. Of these immune cell subtypes, an increase in the frequency of CD16+CD56dim NK cells and CD14 +HLADRhigh monocytes after treatment compared to before treatment were associated with a longer PFS (NR vs. 5 months, HR=5.4, 95% CI 1.1-25.7, P=0.03; 7.8 vs. 3.8 months, HR=5.7, 95% CI 169 1.0-31.7, P=0.04), respectively.

Conclusion: Our preliminary findings suggest that the use of multicolor spectrum flow cytometry helps identify potential blood immune biomarkers for ICI treatment, which warrants further validation.

KEYWORDS

immune biomarker, blood, predictive, multiplex, peripheral blood mononuclear cells, immune checkpoint inhibitors, spectrum flow cytometry, non-small cell lung cancer

1 Introduction

The field of cancer immunotherapy has undergone a renaissance due to a greater understanding of the complex pathways that regulate tumor-induced immunosuppression. Immune checkpoint inhibitors (ICIs) targeting programmed cell death protein 1 (PD-1), its ligand PD-L1, and cytotoxic T-lymphocyte-associated protein 4 (CTLA-4) pathways have become the most potent and durable cancer immunotherapy, which has been shown to increase tumor control and extend life in many cancer types (1, 2). As ICIs have become an essential treatment modality in non-small cell lung cancer (NSCLC) treatment for those patients without EGFR or ALK mutations (3, 4), it becomes necessary to develop reliable methods of predicting and monitoring immune responses to these drugs (5, 6). Currently, the only validated biomarkers for ICI treatment are derived from tumor tissue: PD-L1 protein expression or tumor mutational burden (7). However, obtaining tumor biopsies may not be feasible in patients who are critically ill or whose tumors are in inaccessible locations.

Alternatively, peripheral blood offers a minimally invasive approach for examining tumor biology and tracking the evolution of molecular and immune biomarkers throughout cancer therapy (8, 9). We and others have shown that early changes in blood immune cells can correlate with clinical response to ICIs (10–12). However, the assessment for the phenotype changes of immune responses in lung cancer patients following ICI therapy has been hampered by limitations in the multiplexing capability of traditional flow cytometry, the high skill requirement for multiplexing a higher number of fluorochromes, and cost of equipment and filters for advanced multiplexing. Other options, such as mass cytometry (13) (e.g., CyToF), allow for significantly greater multiplexing of antigens, but are accompanied by higher costs and decreased sensitivity compared to conventional flow cytometry (14).

Traditional flow cytometry relies on matched filter and detector sets to measure the fluorescence emission peak for each fluorochrome marker. However, this method has limited resolution and multiplexing capabilities, which has driven the development of more sophisticated and sensitive instruments, often at increased costs when advanced multiplexing is required. In contrast, spectrum flow cytometry employs prisms to capture the complete emission spectrum across the entire visible light wavelength range for each fluorophore using an array of detectors.

Instead of using compensation to correct for fluorescence spillover like conventional flow cytometry, spectrum flow cytometry employs a technique known as spectrum unmixing. This process involves a mathematical algorithm that leverages the distinct spectrum signature of each fluorophore to differentiate multiple fluorophore signatures within a sample. Consequently, fluorophores with nearly identical peak emissions but differing off-peak emissions can be distinguished and utilized simultaneously in a panel (15, 16). As a result, spectrum flow cytometry can differentiate fluorophore combinations that conventional systems are unable to discern. This increased differentiation capability allows for enhanced flexibility when designing highly complex multicolor panels for comprehensive immunophenotypic analysis. Additionally, since more markers can be evaluated concurrently, spectrum flow cytometry effectively addresses the issue of limited sample availability by expanding the range of immune cell subtypes that can be assessed from a single sample. The aim of this study was to showcase the application of a 24-color spectrum flow cytometry panel in monitoring immune cell alterations in peripheral blood mononuclear cells (PBMCs) obtained from freshly collected or cryopreserved samples from lung cancer patients undergoing treatment with ICIs.

2 Materials and methods

2.1 Study patients and biospecimen collection

Whole blood samples (30 mL) were collected in sodium-EDTA Vacutainer tubes (BD) from patients (N=19) and healthy

human donors (N=4) *via* an Institutional Review Board (IRB) approved protocol (University of California, Davis Protocol No. 226210) (Figure 1). Demographics, immune and molecular biomarkers, blood collection, and treatment information of 19 study patients were abstracted from electronic medical records (Table 1). Of these 19 patients, 14 had blood samples before and after ICI treatment, and 5 only had post-treatment blood samples. Of the 14 patients with paired blood samples, 11 (78.5%) had good tumor response (cohort A), and 3 (22.5%) had poor tumor response (cohort B). PBMCs were isolated within 4 hours of collection at room temperature using the Ficoll-Paque Plus (GE Healthcare, Chicago, IL, USA) density gradient. A total of 2-5 x 10^7 cells were cryopreserved in RPMI-1640 medium (Biowest, Nuaillé, France) with 10% dimethyl sulfoxide (DMSO, Sigma-Aldrich, St. Louis, MO, USA) and 10% heat-inactivated fetal bovine serum (FBS, Gibco™, ThermoFisher Scientific, Waltham, MA, USA) (17–19). The cell suspensions were aliquoted into 1 mL portions in freezing tubes and stored overnight at -80°C using a Cryo-Safe™ Cooler before being transferred to liquid nitrogen for long-term storage. To thaw, PBMCs were immersed in a 37°C water bath without agitation. Thawed PBMCs were then gradually added to 19 mL of pre-warmed complete RPMI1640 medium, supplemented with 10% FBS and 1% penicillin/streptomycin (Gibco), and gently mixed by inverting the tube. Following two washes with PBS, viable PBMCs were counted using trypan blue dye.

Multiple samples from the same patients were collected at various time points throughout their disease progression. Strict operating procedures were employed for sample collection, processing, and storage to reduce any potential variation in sample handling.

2.2 Flow cytometry staining

Fresh and thawed PBMCs were assessed for immunophenotypic alterations in key innate and adaptive immune cell populations using a 24-color antibody panel on the Aurora spectrum flow cytometer (Cytek Biosciences, Inc, California). The immune cell subtypes examined included various T cell subsets (such as effector, activated, memory, exhausted, and regulatory subsets), B cells, and natural killer (NK) cells. Specifically, $1x10^6$ PBMCs were stained with well-established antibodies targeting markers of interest, including CD3, CD45, CD4, CD8, PD-1, CD25, CCR7, CD127, CD11b, HLA-DR, CD11c, CD56, CD16, and others, following standard protocols. Central Memory (CM) T cells are defined as CCR7+ and CD45RA- subsets of CD4+ or CD8+ T cells. Supplemental Table S2 summarizes the antibodies and dyes used for multicolor flow cytometry in this study. The immune cell subtypes analyzed by this multicolor flow cytometry panel are illustrated in Supplemental Figure S1. Supplemental Figure S2 illustrates the gating strategy for a 24-marker panel and immune cell subtypes of the multicolor spectrum flow cytometry. Immuno-labeling of cells was performed by adding 150 µL Zombie Near IR fixable viability cell dye (Biolegend, San Diego, CA, USA) at a dilution of 1:2500 in PBS and left on ice to incubate for 20 minutes in the dark. One million PBMCs in 100 µL of PBS + 2% FBS were added to each DURAClone tube (Beckman Coulter Inc, CA). Cells were stained in 100 µL predetermined antibody volumes. Tubes were vortexed for 10 seconds and incubated for 15 minutes in the dark. To remove unbound antibodies prior to fixing, 300 µL of PBS with 2% FBS was added to each tube, cells were spun down at 800 x *g* for 5 minutes, and the supernatant was discarded. Cells were resuspended in staining buffer [PBS with 1% bovine serum albumin and 0.1% sodium azide (Sigma-

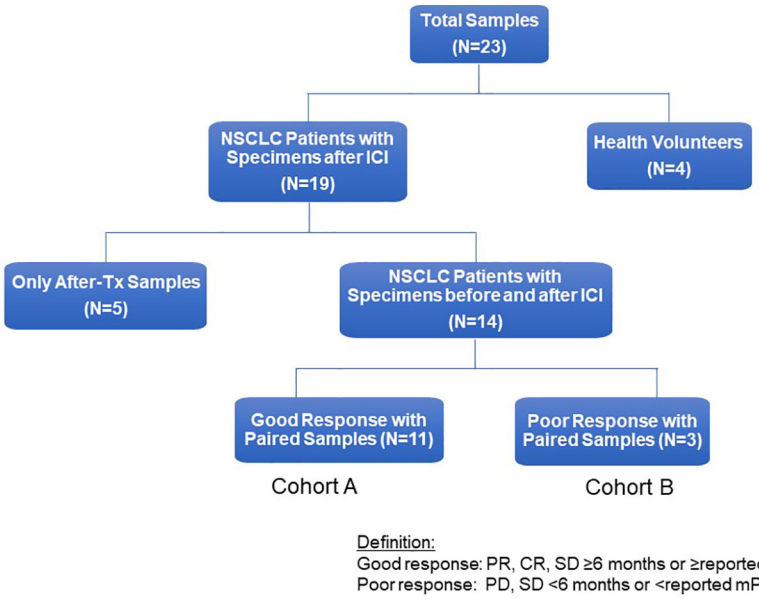


FIGURE 1
Flow chart of study patients. Flow chart for study patients. ICI, immune checkpoint inhibitor; NSCLC, non-small cell lung cancer; Tx, treatment, PD, progressive disease; PR, partial response; mPFS, median Progression-Free Survival.

TABLE 1 Patient demographics, histology, biomarkers, blood collection, and treatment information of study patients.

Category	All Patients: N (%)	Paired Patients: N (%)
Blood collection timepoints	Post-treatment	Pre-treatment
No. Patient	19	14
Age: median (SD)	68.0. (8.9)	67.0 (9.3)
Gender: Female	8 (42%)	8 (57.1%)
Race/ethnicity:		
Non-Hispanic White	17 (89.5%)	14 (100%)
Other	2 (10.5%)	0 (0%)
Smoking history		
Yes	16 (84.2%)	13 (92.9%)
Stage		
II	2 (10.5%)	2 (14.3%)
III	1 (5.2%)	1 (7.1%)
IV	16 (84.3%)	11 (78.6%)
Histology		
LUAD	11 (57.9%)	8 (57.1%)
LUSC	7 (36.8%)	6 (42.9%)
Other	1 (5.3%)	0
PD-L1 expression		
Negative (0%)	5 (26.3%)	7 (50.0%)
Positive (≥1%)	12 (63.2%)	7 (50.0%)
NA	2 (10.5%)	NA
Drug choice		
ICI Mono	8 (42.1%)	4 (28.6%)
Pembrolizumab	7 (87.5%)	4 (100%)
Durvalumab	1 (12.5%)	0
ICI Combo	11 (57.9%)	10 (71.4%)
PD-1/PD-L1 + CTLA4 inhibitors or ant-LAG3 antibody	6 (54.5%)	5 (50.0%)
ICI +Chemotherapy	5 (45.5%)	5 (50.0%)

Aldrich)] and acquired in the flow cytometer. We compared the expression of CD4+ and CD8+ cells by the spectrum flow cytometry with those of clinical flow cytometry at our institution.

2.3 Data acquisition, collection and statistical analysis

One-peak Rainbow Beads (Biolegend) informed voltage settings, and compensation controls were established using auto-compensation with single-color control ultra-comp beads (ThermoFisher Scientific). Voltages for each parameter minimized spillover between fluorophores. Data acquisition was performed on the Aurora spectrum flow cytometer (Cytek Biosciences, CA), and the SpectroFlo™ software was used for analysis. The resulting FCS files were examined using the Cytobank platform (Beckman Coulter Inc, CA) (20). Qualitative variables were summarized by frequency and percentage, while quantitative variables were reported as mean ± standard deviation (SD), unless stated otherwise. The 95% confidence interval for survival was calculated using the exact binomial distribution. Cell proportions or frequencies were presented as mean and SD for before and after ICI treatment cohorts and response subgroups. To compare two groups, Wilcoxon rank-sum tests were used (or Kruskal-Wallis tests for three cohorts). A two-sided $P<0.05$ indicated statistical significance. Due to the study's exploratory nature, no statistical adjustment for multiple hypothesis testing was performed for multiple blood cell types (21). Statistical analyses were conducted using SAS version 9.4 (SAS Institute, Cary, NC). The best

responses to systemic therapies, including complete or partial response (CR or PR), stable disease (SD), or progressive disease (PD), were evaluated using Response Evaluation Criteria in Solid Tumors (RECIST) version 1.1 (22). Progression-free survival (PFS) was calculated from the first cancer therapy administration to progression as defined by RECIST1.1 or death from any cause. Patients without progression at the time of analysis were censored at the initiation of new therapy or last follow-up. Good clinical response was determined in patients who achieved CR, PR, SD ≥6 months, or PFS exceeding the reported median PFS for each ICI therapy. Poor clinical response was defined in patients who had PD, SD <6 months, or PFS shorter than the reported median PFS for each ICI therapy. Overall survival (OS) was measured from the first administration of cancer therapy to death from any cause. Patients who were alive at the time of analysis were censored at the initiation of new therapy or last follow-up. Survival data were estimated using the Kaplan-Meier method and compared using the log-rank test in each cohort and response subgroups.

2.4 RNA sequencing analysis and estimation of T cell frequency

RNA was isolated from 1 million PBMCs using the RNeasy mini kit (Qiagen). RNA-sequencing was implemented at Novogene Corporation Inc. (https://en.novogene.com), which performed the quality control analysis and constructed the library using TruSeq Stranded Total RNA Sample Prep Kit (Illumina). Sequencing was performed using the NovaSeq 6000 system (NovaSeq PE150, Novogene UC Davis Sequencing Center). The sequencing data were accessible at the Gene Expression Omnibus (GEO) repository (accession number GSE235048) for analysis. Reads were aligned to human hg38 genome using Salmon with standard settings (23). Transcripts per million (TPM) counts for all genes were then inputted into CIBERSORTx (https://cibersortx.stanford.edu) for imputing cell fractions using the LM22 signature matrix, disabling quantile normalization. CD4+ T cell frequency was calculated by summing all the CD4+ subtypes (CD4+ naïve cells, CD4+ memory resting cells, CD4+ memory activated cells, follicular helper T cells, regulatory T cells). CD8+ T cell frequency was calculated by CIBERSORTx as pan-CD8+ T cell value.

3 Results

3.1 Validation of multi-color spectrum flow cytometry data by clinical flow cytometry and RNA sequencing

CD3+CD4+ and CD3+CD8+ cell frequencies are two commonly used parameters in the clinical flow cytometry analysis. Next, we compared the expression of CD3+CD4+ and CD3+CD8+ cell frequenciesby 24-color spectrum flow cytometry with those cell frequencies by clinical reports of classical flow cytometry at our institution. According to Pearson's correlation analysis, there is a strong positive correlation between 24-color spectrum flow panels and clinical flow cytometry in detecting CD4+ and CD8+ populations in patient samples before and after treatment, ranging from 0.75 to 0.95 (Supplemental Figures S3A–D). As an orthogonal validation, RNA was isolated from the same PBMC samples, sequenced, and cell composition estimated by CIBERSORTx (23). Given that the standard CIBERSORTx cell types are different from the specific cell subtypes profiled by 24-color spectrum flow cytometry, we focused only on comparing the pan-CD4+ and pan-CD8+ T cell (CD3+) populations. We found a strong and significant correlation between the CIBERSORTx estimates and 24-color spectrum flow measurements for CD4+ T cells ($r = 0.80$, $p = 1.3 \times 10^{-4}$) and CD8+ T cells ($r = 0.80$, $p = 1.3 \times 10^{-4}$) (Supplemental Figures S3E, F).

3.2 Baseline level of immune cell subtypes in NSCLC patients

We compared the immune cell subtypes in PBMCs from NSCLC patients with those from healthy donors as the control group (Table S2). At baseline, CD8+ naive T cells, double-negative (DN) CD3+CD4-CD8- T cells, and B cells were significantly lower in the patient's samples, whereas the CD14+CD16- monocytes, CD8+ CM cells, and lineage-negative cells were higher in patient's samples than the control group (Table 2). Representative dot plots and histograms illustrate significantly different levels of CD14+CD16- monocytes (Figure 2A), lineage negative and B cells (Figure 2B), CD8+ naïve and CD8+ CM T cells (Figure 2C), and DN (CD4-CD8-CD3+) T cells (Figure 2D) in NSCLC patients compared to healthy volunteers at baseline. Of these immune cell subtypes, patients with a baseline CD4+ CM (CCR7+CD45RA-CD4+) T cell proportion of <31% exhibited longer median PFS compared to those with a proportion of ≥31% [not reached (NR) vs. 5 months; hazard ratio (HR) 8.1, 95% confidence interval (CI) 1.5–42, P = 0.01] (Figure 2E). Additionally, patients with a baseline double-negative (DN) (CD4-CD8-CD3+) T cell proportion of ≥3% demonstrated significantly improved PFS compared to those with a DN proportion of <3% (NR vs. 4.45 months; HR=11.1, 95% CI 2.2–55, P < 0.01) (Figure 2F). An optimal cut-off value for predicting PFS based on a receiver operating characteristic (ROC) curve was also examined for CD4+ CM T cells and DN T cells (Supplementary Figures S4A, B), respectively.

3.3 Blood immune cell changes after ICI treatment in NSCLC patients

To assess the impact of ICI therapy on immune cells, we analyzed T cells, B cells, NK cells, and monocytes, along with their subtypes, in the peripheral blood of patients with advanced NSCLC, before and after ICI treatment (Table S3). Individual NSCLC patients had unique patterns of immune cell expression and changes to ICI treatment (Figure 3). Compared to poor

TABLE 2 Significantly changed immune cell subtypes before treatment.

Cell Marker	Patients (N=14)		Normal control (N=4)		P value
	Percent (%)	SD (%)	Percent (%)	SD (%)	
CD14+CD16-	62.7	25.6	24.0	10.5	0.02
CD8 naive	9.5	8.3	56.2	23.2	0.001
CD8 CM	31.7	14.4	16.3	6.1	0.03
LINEAGE NEGATIVE	48.0	26.8	20.6	3.2	0.03
DN	6.5	7.8	13.3	1.6	0.048
B cells	21.9	14.1	40.6	10.1	0.03

responders, ICI treatment led to significant alterations in the frequencies of CD8+PD-1+ T cells (P=0.02, Figures 4A, B), CD16+CD56dim NK cells (P=0.006, Figures 4C, D), CD14+HLADRhigh monocytes (P=0.04, Figures 4E, F), CD4-CD8- DN T cells (P=0.04, Figures 4G, H), CD16+CD56- NK cells (P=0.03, Figures 4I, J), and CD11c+ HLADR+ monocytes (P=0.02, Figures 4K, L) in overall good responders. Although all 3 poor responders had decreased CD8+PD1+ T cells, 6 out of 11 (54.5%) good responders also had decreased CD8+PD1+ T cells (Figure 4A). In addition, we observed a significant increase in both CD16+CD56dim NK cell frequency and CD14+HLADRhigh monocyte frequency among good responders after ICI therapy, which was not seen in poor responders (Figures 4B, E, respectively). Nonetheless, there were no significant disparities in the frequencies of CD4+ T cells, CD8+ T cells, CD19+ B cells, CD38+ T cells, and CD27+ T cells (Table S3; Figure 3).

3.4 Dynamic changes of CD16+CD56dim NK cells and CD14+HLADRhigh monocytes were associated with clinical benefits in NSCLC patients

Next, we explored whether the expression of these T cell, NK cell, and monocyte subtypes before and after ICI treatment correlated with clinical outcomes. There was no significant prognostic correlation in the expression of PD1+CD8+ T cells (PFS NR vs. 5 months, HR=2.4, 95% CI 0.57-10.29, P=0.23) (Figure 5A) nor DN T cells (*data not shown*). However, a post-treatment increase in CD16+CD56dim (but not CD16+CD56- NK cell) frequency of ≥3% following ICI treatment was associated with superior PFS (NR vs. 5 months, HR=5.4, 95% CI 1.1-25.7, P=0.033) (Figure 5B). Of the monocytes, an increase in CD14+HLADRhigh monocyte frequency by ≥0.1% following ICI treatment was

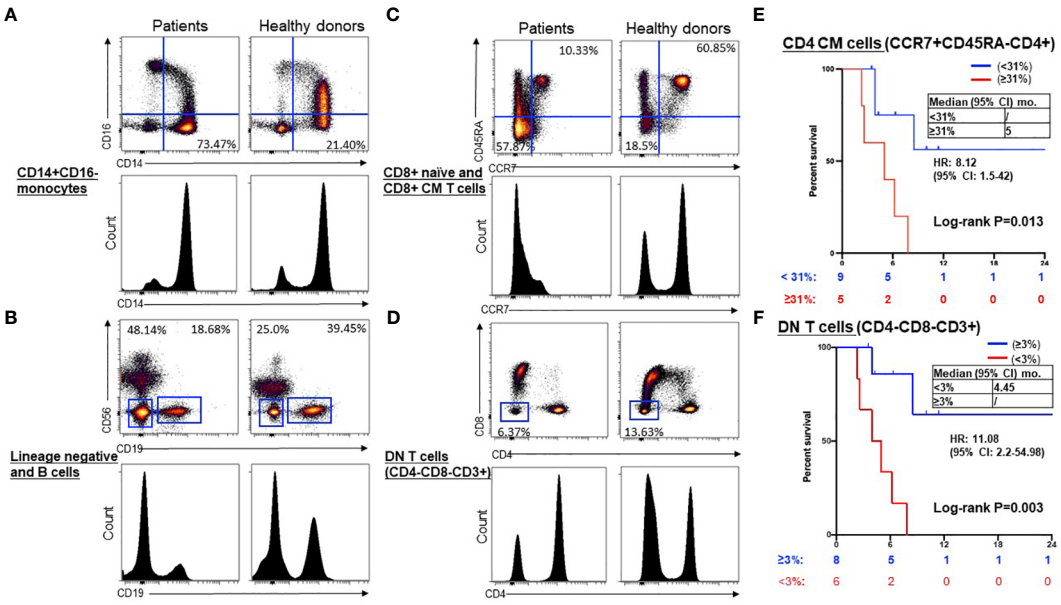


FIGURE 2
Representative dot plots and histograms of significantly different levels and prognostic significance in NSCLC patients compared to healthy volunteers at baseline. Representative dot plots and histograms illustrate significantly different levels of CD14+CD16- monocytes **(A)**, lineage negative and B cells **(B)**, CD8+ naïve and CD8+ CM T cells **(C)**, and DN (CD4-CD8-CD3+) T cells **(D)** in NSCLC patients compared to healthy volunteers at baseline. Kaplan-Meier curves showed low CD4+ CM (CCR7+ CD45RA-) T cells (< 31%, blue) were associated with longer PFS compared to high (≥31%, red) **(E)**, and higher DN (CD4-CD8-CD3+) T cells (≥3%, blue) were associated with longer PFS compared to low (< 3%, red) **(F)**. Groups were compared by the paired t-test. *$P < 0.05$ for statistical significance. CM, central memory; ICI, immune checkpoint inhibitors.

10.3389/fimmu.2023.1206631

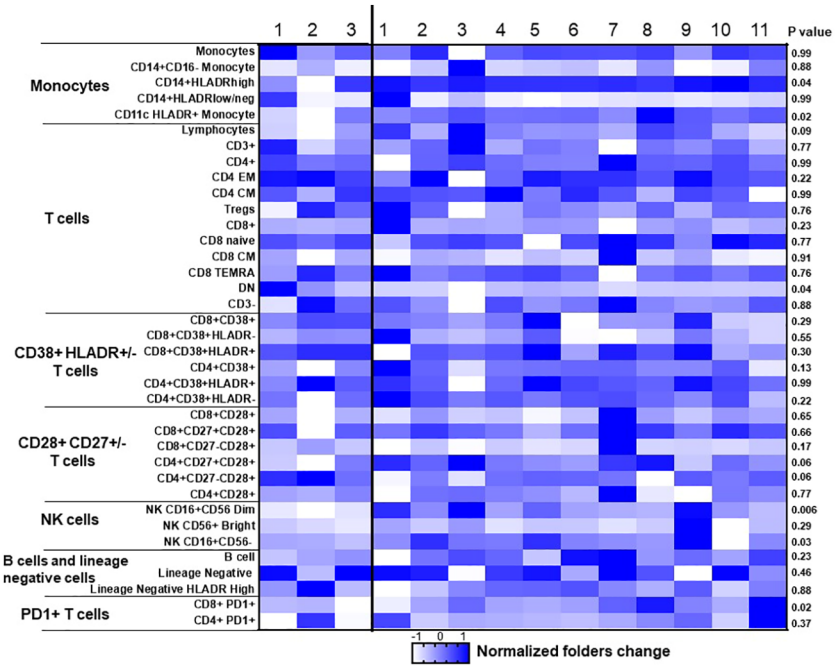


FIGURE 3
Dynamic changes of immune cells before and after ICI treatment in NSCLC patient samples. Heat map of 37 cell populations defined from flow cytometric analysis of a subset of NSCLC samples from responders (n = 11) and nonresponders (progressive disease; n = 3). For each population, two-tailed P values were calculated using the Wilcoxon rank-sum test. Data for each row were logged and mean-centered; each column shows data from one sample. *$P < 0.05$ for statistical significance. EM, effector memory; CM, Central memory; NK, Natural killer; DN, double negative.

associated with improved PFS (7.8 vs. 3.8 months, HR=5.7, 95% CI 1.0-31.7, P =0.04) (Figure 5C).

3.5 Serial assessments of immunophenotypic changes of PBMCs in patients who received ICI combination by 24-color spectrum flow cytometry

Quantitative assessment of immune biomarkers on PBMCs during disease course was assessed using this multicolor panel by spectrum flow cytometry. Figure 6 summarizes the clinical course of two patients who received ICIs or ICI and chemotherapy combination at diagnosis. Case 1 (Figures 6A, B) was a 93-year-old female, former smoker who was diagnosed with stage 4 NSCLC adenocarcinoma in August 2020. The tumor had high PD-L1 IHC expression (tumor proportion score was 60%) (DAKO, clone 22C3). Tumor genomic profiling did not identify any actionable oncogene alterations. The patient received pembrolizumab for four cycles with significant clinical and radiographic improvements. As shown in viSNE land (Figure 6A) and heatmap (Figure 6B), the ICI treatment increased CD3+ T cells, CD16+CD56dim NK cells, CD16+CD56- NK cells, CD4+ Effector Memory (EM), CD8+ CM T cells, CD14+HLADRhigh monocyte and decreased CD4+ CM, Double Negative (DN), CD8+ T cells, lineage negative cells, CD14+HLADRlow/neg monocytes, PD1+ CD4+ cells, and PD1+ CD8+ cells. The patient continued to have pembrolizumab for 35 cycles with clinical remission. The second case (Figures 6C, D) was a 66-year-old male with controlled AIDS (CD4 >200 cells per cubic millimeter on antiviral treatment) for over ten years. The patient was diagnosed with stage 4 NSCLC adenocarcinoma in June 2020. The tumor was negative for PD-L1 IHC stain with a tumor mutation burden of 7.4 m/MB. He received PD-1 and CTLA-4 inhibitors and chemotherapy for two cycles with a partial response. The patient subsequently received IO combination therapy for three cycles before tumor progression. As shown in viSNE analysis (Figure 6C) and heatmap (Figures 6D), the ICI treatment increased CD3+, NK cells, CD4+ EM, and decreased CD4+ CM, DN CD3+ cells, naive cells, lineage negative cells, CD14+HLADRhigh monocytes, PD1+CD4+ T cells, and PD1+CD8+ T cells when the tumor responded to the therapy. However, CD3+, CD16+CD56dim NK cells, CD14+HLADRhigh monocytes, and CD8+ cells were found to decrease when the patient experienced the tumor progression.

4 Discussion

Although the tumor-specific cytotoxic T cells are the prime targets of ICIs, they can modulate the expression of additional immune cells and molecules in the tumor microenvironment (TME) and lymphoid organ frequencies (24, 25). These immune cell subtypes include macrophages, T cells, NK cells, monocytes, B cells, dendritic cells, myeloid-derived suppressor cells (MDSCs), and neutrophils. These components can collectively contribute to

10.3389/fimmu.2023.1206631

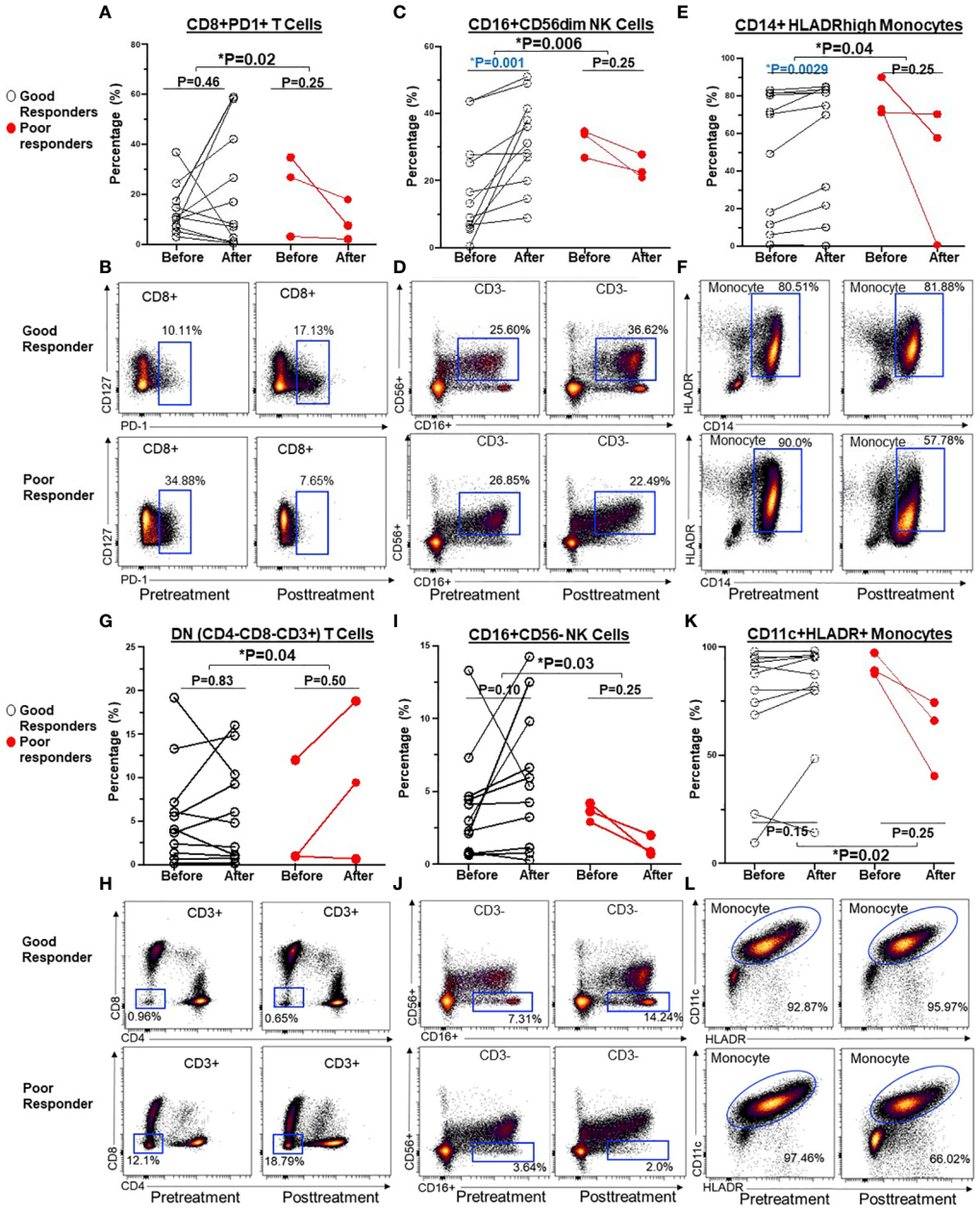


FIGURE 4
Before and after graphs for dynamic changes of immune cells after ICI treatment were associated with clinical benefits in NSCLC patients. Compared to poor responders, ICI treatment led to significant alterations in the frequencies of CD8+ PD-1+T cells **(A, B)**, CD16+CD56dim NK cell **(C, D)**, CD14+HLADRhigh monocyte **(E, F)**, CD4-CD8- DN T cells **(G, H)**, CD16+CD56- NK cells **(I, J)**, and CD11c+ HLADR+ monocytes **(K, L)** in overall good responders. Groups were compared by the paired t-test. *P < 0.05 for statistical significance. Blue highlights statistically significant difference before and after ICI treatment.

the regulation of tumor cell immune evasion. Moreover, imbalances in the levels of specific immunoregulatory cells and cytokines within the TME may influence tumor responsiveness (26). Cancer cells may employ several immune escape mechanisms, including inadequate presentation of tumor neoantigens, secretion of inhibitory chemokines or cytokines (e.g., TGF-β, IL-10), mutations that make molecules unrecognizable by the immune system, and recruitment of suppressive cells (e.g., Treg, MDSC) (27). A growing body of evidence suggests circulating immune cells in peripheral blood of patients may reflect the dynamic immune cell changes in the tumor tissue (28).

Our study presents several important clinical implications through the immunophenotypic analysis of immune subtypes in patient PBMCs before and after ICI treatment by the multicolor spectrum flow cytometry. Firstly, we found that at baseline monocytes, CD8+ naive T cells, double-negative CD3+CD4-CD8- T cells, and B cells were significantly lower in the patient's samples, whereas the CD14+CD16- monocytes, CD8+ CM cells, and lineage-negative cells were higher in patient's samples compared to healthy donors. Of these markers, NSCLC patients with a lower baseline proportion of CD4+ CM cells (<31%) or a higher baseline proportion of DN (CD4-CD8-CD3+) T cells (≥3%) experienced

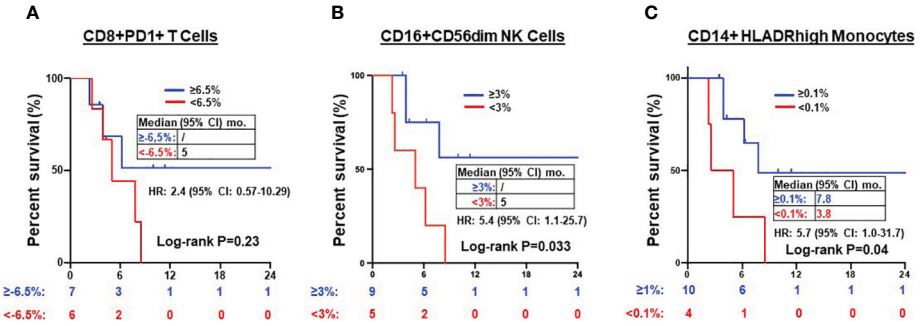


FIGURE 5
Prognosis of after treatment immune cells in NSCLC patients. Kaplan-Meier PFS estimates according to post-treatment changes (post-treatment minus baseline) in CD8+PD1+ T cells **(A)**, CD16+CD56dim NK cells **(B)** and CD14+HLADRhigh monocytes **(C)**. Tick marks indicate censored data. Groups were compared using the log-rank test. $P < 0.05$ for statistical significance.

longer median PFS to ICI treatment. The function of CD4+ helper T cells has been shown to be crucial for effective CD8+ T cell responses to ICI therapy. CD4+ T cells can promote tumor regression through various mechanisms, including cytokine secretion (IL-2), enhancing tumor-specific CD8+ T-cell function, or directly eliminating cancer cells (29). Several preclinical studies have demonstrated that tumor-specific CD4+ T cells might recognize immunogenic mutations (30, 31). Consistent with our result, Tada et al. showed that a decrease in baseline CD4+ CM T cells in 7 out of 10 patients with head and neck squamous cell carcinoma exhibiting PR or SD to PD-1 inhibitor nivolumab (32). However, due to the small sample size, the result did not achieve statistical significance. Furthermore, the expansion of CD4+ naïve T cells to CD4+ CM T cells after ICI therapy predicted long-term survival benefits in patients with malignant melanoma (33). CD4+ CM T cells, characterized by CCR7 or CD62L expression and lacking CD45RA, can circulate within secondary lymphoid organs. While the functional interplay of CD4+ memory cells directly shapes the effects of PD-L1/PD-1 inhibitors on CD8+ anti-tumor responses, the exact mechanisms mediating this response remain elusive (29). Additionally, various studies have shown other T cell subtypes involved in response to ICI therapy. For instance, a significant decrease of CD4+ FOXP3- PD-1 high T cells during the initial stages of therapy correlated with an improvement in OS (30). There was a trend suggesting that a lower proportion of circulating CD4+ T cells, including CD38+CD4+ T cells in peripheral blood, could indicate a favorable prognosis (31). Further studies are needed to characterize the role of different T cell subtypes in mediating response to ICIs.

Secondly, we observed that individual NSCLC patients had unique patterns of blood immune cell expression and changes to ICI treatment (Figure 3). Although all 3 poor responders had decreased frequencies of CD8+PD1+ T cells, 6 out of 11 (54.5%) good responders also had decreased frequencies of CD8+PD1+ T cells (Figure 4A). Overall, there was a correlation between increased frequencies of cytotoxic CD8+PD1+ T cells in PBMCs and good clinical responses to ICIs. This finding aligns with previous reports that PD-1 expression in CD8+ tumor infiltrating lymphocytes (TILs) within tumor samples had clonally expanded tumor-reactive lymphocytes (34, 35). A majority of patients experiencing clinical benefits demonstrated CD8+ PD-1+ T-cell responses within four weeks of therapy (36). We further showed that ICI treatment modulated the expression of subtypes of NK cells and monocytes. Although there was no statistically significant difference in the expression of NK cell subtypes in NSCLC patients before ICI treatment compared to healthy donors (Table S2), we observed ICI treatment led to significant increase in the frequencies of CD16+CD56dim NK cell (P=0.006) (Figures 4C, D) and CD16+CD56- NK cells (P=0.03) (Figures 4I, J) compared to poor responders. Furthermore, an increase in the CD16+CD56dim NK cell frequency of ≥3% after ICI treatment compared to before treatment was associated with a longer PFS (NR vs. 5 months, HR=5.4, 95% CI 1.1-25.7, P=0.03) (Figure 5B). Our findings are consistent with several reports showing that NK cells, either alone or in combination with cytotoxic T cells, play an essential role in mediating tumor response to ICI treatment in multiple cancer types (32, 33, 37). In mouse models, NK cells promote the function of cytotoxic T cells in response to anti-PD-L1 treatment (38, 39). NK cells also acted as the primary cytotoxic cells in tumors with low MHC expression, even in PD-L1 negative tumors (40). A single dose of tumor vaccine targeting resistant tumors by dual T and NK cells was able to increase CD8+ and CD4+ T cell frequencies by 17.9 and 29.3 fold, and NK cell counts by about 40 fold, respectively, compared to the control in murine models (41). Recently, the expression of NK cell frequency in the peripheral blood was independently associated with longer survival of gastric cancer patients and colorectal patients (33, 37). The frequency of NK cells was positively correlated to the frequencies of T and B lymphocytes (33). However, these reports did not analyze the CD16 and CD56 subtypes of NK cells. In this study, we found that CD16+CD56dim NK cells played a more significant role in mediating response to ICI compared to CD16+CD56- NK cells. CD16+CD56dim NK cells comprise the majority of circulating human NK cells, which are the most cytotoxic NK cells. Upon target recognition, CD16+CD56dim NK cells release perforin and granzyme granules and mediate antibody-dependent cellular cytotoxicity through CD16 (FcγRIII) to clear cancer cells. In contrast, increased CD16+CD56- NK cells were associated with

10.3389/fimmu.2023.1206631

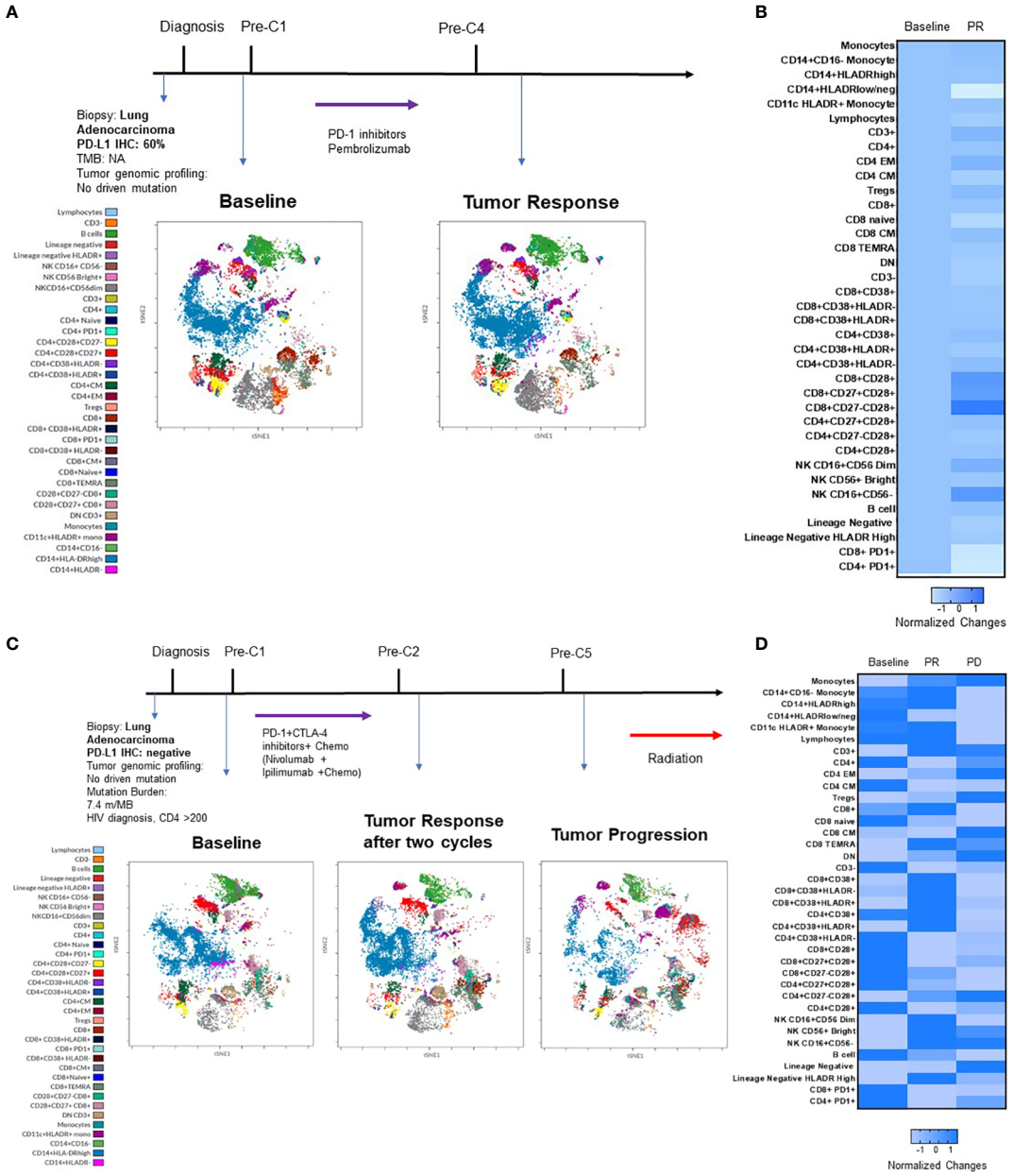


FIGURE 6
Immunophenotypic changes of PBMCs in two patients who received ICI alone or in combination. **(A)** summarizes the key events in the clinical course of a patient with good response to pembrolizumab. Cell amounts before and after ICI treatment are represented by a t-distributed stochastic neighbor embedding (t-SNE) plot displayed as a 2D plot using the resultant t-SNE 1 and t-SNE 2 dimensions according to the per cell expression of the 24 proteins assayed. Colors represented each defined cellular subtype as indicated. **(B)** Heatmap representing the fold-change in percentage of each cellular subtype before and after treatment. **(C)** summarizes the clinical course of a patient with good response to pembrolizumab and then progression in a similar t-SNE plot and heatmap **(D)**.

immune escape from innate immunity during AML progression (42).

Previous studies suggested that CD14+HLADRhigh, low or neg monocytes play distinct roles in the regulation of inflammatory and immune-suppressive conditions (43, 44). Patients who responded to ipilimumab had significantly lower levels of pre-treatment CD14+HLA-DRlo/neg monocytes compared to their non-responsive counterparts (45). Another independent study linked lower pre-treatment frequencies of CD14+HLA-DRlo/neg monocytes to improved OS of patients (46). In this study, we did not observe any significant difference in the pre-treatment frequency of CD14+HLADRhigh and low/neg monocytes in NSCLC patients compared to healthy donors (Table S2). Instead, we found that there were significant increases in the frequency of CD14+HLADRhigh monocyte (P=0.04) (Figures 4E, F), and CD11c+HLADR+ monocytes (P=0.02) (Figures 4K, L) in good responders compared to poor responders after ICI treatment. Of these two monocyte subtypes, only an increase in CD14+HLADRhigh monocyte frequency by ≥0.1% following ICI treatment was associated with improved PFS (7.8 vs. 3.8 months,

HR=5.7, 95% CI 1.0-31.7, P=0.04) (Figure 5C). Consistent with our results, single cell analysis revealed that high levels of CD14+CD16-HLADRhigh monocytes before ICI correlated with significantly increased PFS in melanoma patients (47) and NSCLC patients (48). Further study is warranted to validate these findings in NSCLC patients and delineate underlying mechanisms.

Individual NSCLC patients had unique patterns of immune cell expression and changes to ICI treatment and other cancer therapy (Figure 6). The 24-color spectrum flow cytometry assay may be used to monitor treatment response during the disease course with the optimal goal of improving the prediction of patient responses to cancer therapy and identify those who may benefit most from a specific treatment. However, this study has several limitations, including a small sample size, a retrospective design, and no adjustment for multiplicity due to its exploratory nature. Additionally, we did not analyze the changes in T cell receptor repertoire and various immunoregulatory cytokines in the blood. Potential selection bias and imbalances in patients' baseline characteristics and treatment history could have influenced the outcomes. Compared to the liquid biopsy for tumor genomic profiling of plasma circulating tumor DNA, flow cytometry of blood immune cells requires special skills and the cost of appropriately collecting and processing blood immune cells in a timely manner. Before this method can be used in routine practice, the sensitivity, turnaround time, and cost need to be evaluated. Further study is warranted to use the established multicolor flow cytometry and RNA sequencing tools to monitor the dynamic changes of blood immune cells during cancer immunotherapy treatment.

5 Conclusions

Multicolor spectrum flow cytometry can simultaneously evaluate 1 million blood immune cells for changes in major immune cell subpopulations in NSCLC patients receiving ICIs. Our data support the critical role of subsets of T cells, NK cells and monocytes in mediating response to ICI. Further studies are needed to validate the predictive biomarkers and assays to select the appropriate patients for ICI therapy.

Data availability statement

The RNA sequencing data presented in the study are deposited in the Gene Expression Omnibus (GEO) repository, accession number GSE235048. Other original contributions presented in the study are included in the article/Supplementary Material. Further inquiries can be directed to the corresponding author.

Ethics statement

The studies involving human participants were reviewed and approved by University of California, Davis Institutional review board (IRB)-approved protocol (Protocol No. 226210). The patients/participants provided their written informed consent to participate in this study.

Author contributions

TL contributed to the conception and design of the study. WM, SW, and TL contributed to the patient sample and data collection. WM, SW, SL, ET, BM, MJ, DM, VV, JC, QZ, JVD, SC, and TL contributed to the acquisition, analysis, or interpretation of data. WM, SW, SL, DM, SC, and TL drafted and revised the manuscript. All authors contributed to the article and approved the submitted version.

Funding

This work was supported by the UC Davis Research Core Facilities Program (RCFP) Pilot and Feasibility Award, VA Merit Award (I01BX003895), VA-Lung Precision Oncology Program (1I50CU000157), and Personalized Cancer Therapy Gift Fund (TL). The Biostatistics Shared Resource (SC) and Flow cytometry shared Resource (BML) are supported by the UC Davis Comprehensive Cancer Center Support Grant (CCSG) awarded by the National Cancer Institute (NCI P30CA093373).

Conflict of interest

Author MJ was employed by the company Cytek Biosciences. Author QZ was employed by the company Beckman Coulter Life Sciences.

The remaining authors declare that the research was conducted in the absence of any commercial or financial relationships that could be construed as a potential conflict of interest.

Publisher's note

All claims expressed in this article are solely those of the authors and do not necessarily represent those of their affiliated organizations, or those of the publisher, the editors and the reviewers. Any product that may be evaluated in this article, or claim that may be made by its manufacturer, is not guaranteed or endorsed by the publisher.

Supplementary material

The Supplementary Material for this article can be found online at: https://www.frontiersin.org/articles/10.3389/fimmu.2023.1206631/full#supplementary-material

References

1. Marin-Acevedo JA, Kimbrough EO, Lou Y. Next generation of immune checkpoint inhibitors and beyond. *J Hematol Oncol* (2021) 14:45. doi: 10.1186/s13045-021-01056-8

2. Bagchi S, Yuan R, Engleman EG. Immune checkpoint inhibitors for the treatment of cancer: Clinical impact and mechanisms of response and resistance. *Annu Rev Pathol* (2021) 16:223–49. doi: 10.1146/annurev-pathol-042020-042741

3. Ettinger DS, Wood DE, Aisner DL, Akerley W, Bauman JR, Bharat A, et al. NCCN guidelines insights: Non-small cell lung cancer, version 2.2021. *J Natl Compr Canc Netw* (2021) 19:254–66. doi: 10.6004/jnccn.2021.0013

4. Hanna NH, Robinson AG, Temin S, Baker SJr., Brahmer JR, Ellis PM, et al. Therapy for stage IV non-Small-Cell lung cancer with driver alterations: ASCO and OH (CCO) joint guideline update. *J Clin Oncol* (2021) 39:1040–91. doi: 10.1200/JCO.20.03570

5. Chen JA, Ma W, Yuan J, Li T. Translational biomarkers and rationale strategies to overcome resistance to immune checkpoint inhibitors in solid tumors. *Cancer Treat Res* (2020) 180:251–79. doi: 10.1007/978-3-030-38862-1_9

6. Nakamura Y. Biomarkers for immune checkpoint inhibitor-mediated tumor response and adverse events. *Front Med (Lausanne)* (2019) 6:119. doi: 10.3389/fmed.2019.00119

7. Ready N, Hellmann MD, Awad MM, Otterson GA, Gutierrez M, Gainor JF, et al. First-Line nivolumab plus ipilimumab in advanced non-Small-Cell lung cancer (CheckMate 568): outcomes by programmed death ligand 1 and tumor mutational burden as biomarkers. *J Clin Oncol* (2019) 37:992–1000. doi: 10.1200/JCO.18.01042

8. Rolfo C, Mack PC, Scagliotti GV, Baas P, Barlesi F, Bivona TG, et al. Liquid biopsy for advanced non-Small cell lung cancer (NSCLC): A statement paper from the IASLC. *J Thorac Oncol* (2018) 13:1248–68. doi: 10.1016/j.jtho.2018.05.030

9. Malapelle U, Pisapia P, Addeo A, Arrieta O, Bellosillo B, Cardona AF, et al. Liquid biopsy from research to clinical practice: focus on non-small cell lung cancer. *Expert Rev Mol Diagn* (2021) 21:1165–78. doi: 10.1080/14737159.2021.1985468

10. Naidus E, Bouquet J, Oh DY, Looney TJ, Yang H, Fong L, et al. Early changes in the circulating T cells are associated with clinical outcomes after PD-L1 blockade by durvalumab in advanced NSCLC patients. *Cancer Immunol Immunother* (2021) 70:2095–102. doi: 10.1007/s00262-020-02833-z

11. Ma W, Zeng J, Chen S, Lyu Y, Toomey KA, Phan CT, et al. Small molecule tyrosine kinase inhibitors modulated blood immune cell counts in patients with oncogene-driven NSCLC. *biomark Res* (2021) 9:69. doi: 10.1186/s40364-021-00324-6

12. Rogado J, Pozo F, Troule K, Sanchez-Torres JM, Romero-Laorden N, Mondejar R, et al. Peripheral blood mononuclear cells predict therapeutic efficacy of immunotherapy in NSCLC. *Cancers (Basel)* (2022) 14:2898. doi: 10.3390/cancers14122898

13. Spitzer MH, Nolan GP. Mass cytometry: Single cells, many features. *Cell* (2016) 165:780–91. doi: 10.1016/j.cell.2016.04.019

14. Iyer A, Hamers AAJ, Pillai AB. CyTOF((R)) for the masses. *Front Immunol* (2022) 13:815828. doi: 10.3389/fimmu.2022.815828

15. Park LM, Lannigan J, Jaimes MC. OMIP-069: Forty-color full spectrum flow cytometry panel for deep immunophenotyping of major cell subsets in human peripheral blood. *Cytometry A* (2020) 97:1044–51. doi: 10.1002/cyto.a.24213

16. Bonilla DL, Reinin G, Chua E. Full spectrum flow cytometry as a powerful technology for cancer immunotherapy research. *Front Mol Biosci* (2020) 7:612801. doi: 10.3389/fmolb.2020.612801

17. Li B, Yang C, Jia G, Liu Y, Wang N, Yang F, et al. Comprehensive evaluation of the effects of long-term cryopreservation on peripheral blood mononuclear cells using flow cytometry. *BMC Immunol* (2022) 23:30. doi: 10.1186/s12865-022-00505-4

18. Johnson RK, Overlee BL, Sagen JA, Howe CL. Peripheral blood mononuclear cell phenotype and function are maintained after overnight shipping of whole blood. *Sci Rep* (2022) 12:19920. doi: 10.1038/s41598-022-24550-6

19. Turner RJ, Geraghty NJ, Williams JG, Ly D, Brungs D, Carolan MG, et al. Comparison of peripheral blood mononuclear cell isolation techniques and the impact of cryopreservation on human lymphocytes expressing CD39 and CD73. *Purinergic Signal* (2020) 16:389–401. doi: 10.1007/s11302-020-09714-1

20. Kotecha N, Krutzik PO, Irish JM. Web-based analysis and publication of flow cytometry experiments. *Curr Protoc Cytom* (2010) 10:Unit10 17. doi: 10.1002/0471142956.cy1017s53

21. Li G, Taljaard M, Van den Heuvel ER, Levine MA, Cook DJ, Wells GA, et al. An introduction to multiplicity issues in clinical trials: the what, why, when and how. *Int J Epidemiol* (2017) 46:746–55. doi: 10.1093/ije/dyw320

22. Eisenhauer EA, Therasse P, Bogaerts J, Schwartz LH, Sargent D, Ford R, et al. New response evaluation criteria in solid tumours: revised RECIST guideline (version 1.1). *Eur J Cancer* (2009) 45:228–47. doi: 10.1016/j.ejca.2008.10.026

23. Newman AM, Liu CL, Green MR, Gentles AJ, Feng W, Xu Y, et al. Robust enumeration of cell subsets from tissue expression profiles. *Nat Methods* (2015) 12:453–7. doi: 10.1038/nmeth.3337

24. Ma W, Gilligan BM, Yuan J, Li T. Current status and perspectives in translational biomarker research for PD-1/PD-L1 immune checkpoint blockade therapy. *J Hematol Oncol* (2016) 9:47. doi: 10.1186/s13045-016-0277-y

25. Morad G, Helmink BA, Sharma P, Wargo JA. Hallmarks of response, resistance, and toxicity to immune checkpoint blockade. *Cell* (2022) 185:576. doi: 10.1016/j.cell.2022.01.008

26. Anderson NM, Simon MC. The tumor microenvironment. *Curr Biol* (2020) 30:R921–5. doi: 10.1016/j.cub.2020.06.081

27. Kerkar SP, Restifo NP. Cellular constituents of immune escape within the tumor microenvironment. *Cancer Res* (2012) 72:3125–30. doi: 10.1158/0008-5472.CAN-11-4094

28. Gascon M, Isla D, Cruellas M, Galvez EM, Lastra R, Ocariz M, et al. Intratumoral versus circulating lymphoid cells as predictive biomarkers in lung cancer patients treated with immune checkpoint inhibitors: Is the easiest path the best one? *Cells* (2020) 9:1525. doi: 10.3390/cells9061525

29. Zuazo M, Arasanz H, Bocanegra A, Fernandez G, Chocarro L, Vera R, et al. Systemic CD4 immunity as a key contributor to PD-L1/PD-1 blockade immunotherapy efficacy. *Front Immunol* (2020) 11:586907. doi: 10.3389/fimmu.2020.586907

30. Zappasodi R, Budhu S, Hellmann MD, Postow MA, Senbabaoglu Y, Manne S, et al. Non-conventional inhibitory CD4(+)Foxp3(-)PD-1(hi) T cells as a biomarker of immune checkpoint blockade activity. *Cancer Cell* (2018) 34:691. doi: 10.1016/j.ccell.2018.09.007

31. Takahashi H, Sakakura K, Ida S, Kawabata-Iwakawa R, Matsuyama T, Tada H, et al. Circulating naive and effector memory T cells correlate with prognosis in head and neck squamous cell carcinoma. *Cancer Sci* (2022) 113:53–64. doi: 10.1111/cas.15195

32. Youn JI, Park SM, Park S, Kim G, Lee HJ, Son J, et al. Peripheral natural killer cells and myeloid-derived suppressor cells correlate with anti-PD-1 responses in non-small cell lung cancer. *Sci Rep* (2020) 10:9050. doi: 10.1038/s41598-020-65666-x

33. Tang YP, Xie MZ, Li KZ, Li JL, Cai ZM, Hu BL. Prognostic value of peripheral blood natural killer cells in colorectal cancer. *BMC Gastroenterol* (2020) 20:31. doi: 10.1186/s12876-020-1177-8

34. Gros A, Robbins PF, Yao X, Li YF, Turcotte S, Tran E, et al. PD-1 identifies the patient-specific CD8(+) tumor-reactive repertoire infiltrating human tumors. *J Clin Invest* (2014) 124:2246–59. doi: 10.1172/JCI73639

35. Odorizzi PM, Pauken KE, Paley MA, Sharpe A, Wherry EJ. Genetic absence of PD-1 promotes accumulation of terminally differentiated exhausted CD8+ T cells. *J Exp Med* (2015) 212:1125–37. doi: 10.1084/jem.20142237

36. Kamphorst AO, Pillai RN, Yang S, Nasti TH, Akondy RS, Wieland A, et al. Proliferation of PD-1+ CD8 T cells in peripheral blood after PD-1-targeted therapy in lung cancer patients. *Proc Natl Acad Sci USA* (2017) 114:4993–8. doi: 10.1073/pnas.1705327114

37. Xie MZ, Tang YP, Hu BL, Li KZ, Li JL, Liang XQ. Percentage of natural killer (NK) cells in peripheral blood is associated with prognosis in patients with gastric cancer: A retrospective study from a single center. *Med Sci Monit* (2021) 27:e927464. doi: 10.12659/MSM.927464

38. Fabian KP, Padget MR, Donahue RN, Solocinski K, Robbins Y, Allen CT, et al. PD-L1 targeting high-affinity NK (t-haNK) cells induce direct antitumor effects and target suppressive MDSC populations. *J Immunother Cancer* (2020) 8:e000450. doi: 10.1136/jitc-2019-000450

39. Le DT, Huynh TR, Burt B, Van Buren G, Abeynaike SA, Zalfa C, et al. Natural killer cells and cytotoxic T lymphocytes are required to clear solid tumor in a patient-derived xenograft. *JCI Insight* (2021) 6:e140116. doi: 10.1172/jci.insight.140116

40. Quatrini L, Mariotti FR, Munari E, Tumino N, Vacca P, Moretta L. The immune checkpoint PD-1 in natural killer cells: Expression, function and targeting in tumour immunotherapy. *Cancers (Basel)* (2020) 12:3285. doi: 10.3390/cancers12113285

41. Badrinath S, Dellacherie MO, Li A, Zheng S, Zhang X, Sobral M, et al. A vaccine targeting resistant tumours by dual T cell plus NK cell attack. *Nature* (2022) 606:992–8. doi: 10.1038/s41586-022-04772-4

42. Chretien AS, Devillier R, Granjeaud S, Cordier C, Demerle C, Salem N, et al. High-dimensional mass cytometry analysis of NK cell alterations in AML identifies a subgroup with adverse clinical outcome. *Proc Natl Acad Sci USA* (2021) 118:e2020459118. doi: 10.1073/pnas.2020459118

43. Mengos AE, Gastineau DA, Gustafson MP. The CD14(+)HLA-DR(lo/neg) monocyte: An immunosuppressive phenotype that restrains responses to cancer immunotherapy. *Front Immunol* (2019) 10:1147. doi: 10.3389/fimmu.2019.01147

44. Ugel S, Cane S, De Sanctis F, Bronte V. Monocytes in the tumor microenvironment. *Annu Rev Pathol* (2021) 16:93–122. doi: 10.1146/annurev-pathmechdis-012418-013058

45. Meyer C, Cagnon L, Costa-Nunes CM, Baumgaertner P, Montandon N, Leyvraz L, et al. Frequencies of circulating MDSC correlate with clinical outcome of melanoma patients treated with ipilimumab. *Cancer Immunol Immunother* (2014) 63:247–57. doi: 10.1007/s00262-013-1508-5

46. Kitano S, Postow MA, Ziegler CG, Kuk D, Panageas KS, Cortez C, et al. Computational algorithm-driven evaluation of monocytic myeloid-derived suppressor cell frequency for prediction of clinical outcomes. *Cancer Immunol Res* (2014) 2:812–21. doi: 10.1158/2326-6066.CIR-14-0013

47. Krieg C, Nowicka M, Guglietta S, Schindler S, Hartmann FJ, Weber LM, et al. High-dimensional single-cell analysis predicts response to anti-PD-1 immunotherapy. *Nat Med* (2018) 24:144–53. doi: 10.1038/nm.4466

48. Escors D, Bocanegra A, Chocarro L, Blanco E, Pineiro-Hermida S, Garnica M, et al. Systemic CD4 immunity and PD-L1/PD-1 blockade immunotherapy. *Int J Mol Sci* (2022) 23:13241. doi: 10.3390/ijms232113241

frontiers | Frontiers in Immunology

TYPE Review
PUBLISHED 21 August 2023
DOI 10.3389/fimmu.2023.1238454

Check for updates

OPEN ACCESS

EDITED BY
Qun Xue,
Affiliated Hospital of Nantong University, China

REVIEWED BY
Marco Greppi,
School of Medical and Pharmaceutical Sciences, University of Genoa, Italy
Jia-Ren Lin,
Harvard Medical School, United States

*CORRESPONDENCE
Qinghua Hu
qinghuaa@mails.tjmu.edu.cn
Jiansha Li
lijiansha@163.com
Liping Zhu
zhulp626@hust.edu.cn

†These authors have contributed equally to this work and share first authorship

RECEIVED 11 June 2023
ACCEPTED 03 August 2023
PUBLISHED 21 August 2023

CITATION
Liao P, Huang Q, Zhang J, Su Y, Xiao R, Luo S, Wu Z, Zhu L, Li J and Hu Q (2023) How single-cell techniques help us look into lung cancer heterogeneity and immunotherapy.
Front. Immunol. 14:1238454.
doi: 10.3389/fimmu.2023.1238454

COPYRIGHT
© 2023 Liao, Huang, Zhang, Su, Xiao, Luo, Wu, Zhu, Li and Hu. This is an open-access article distributed under the terms of the Creative Commons Attribution License (CC BY). The use, distribution or reproduction in other forums is permitted, provided the original author(s) and the copyright owner(s) are credited and that the original publication in this journal is cited, in accordance with accepted academic practice. No use, distribution or reproduction is permitted which does not comply with these terms.

How single-cell techniques help us look into lung cancer heterogeneity and immunotherapy

Pu Liao[1,2†], Qi Huang[3†], Jiwei Zhang[1,2†], Yuan Su[2,3], Rui Xiao[2,4], Shengquan Luo[2,4], Zengbao Wu[5], Liping Zhu[2,4*], Jiansha Li[2,6*] and Qinghua Hu[2,4*]

[1]Department of Pathology, Union Hospital, Tongji Medical College, Huazhong University of Science and Technology, Wuhan, Hubei, China, [2]Key Laboratory of Pulmonary Diseases of Ministry of Health, Tongji Medical College, Huazhong University of Science and Technology, Wuhan, China, [3]Department of Respiratory and Critical Care Medicine, Hubei Province Clinical Research Center for Major Respiratory Diseases, National Health Commission (NHC) Key Laboratory of Pulmonary Diseases, Union Hospital, Tongji Medical College, Huazhong University of Science and Technology, Wuhan, Hubei, China, [4]Department of Pathophysiology, School of Basic Medicine; Tongji Medical College, Huazhong University of Science and Technology, Wuhan, China, [5]Department of Neurosurgery, Tongji Hospital, Tongji Medical College, Huazhong University of Science and Technology, Wuhan, Hubei, China, [6]Institute of Pathology, Tongji Hospital, Tongji Medical College, Huazhong University of Science and Technology, Wuhan, Hubei, China

Lung cancer patients tend to have strong intratumoral and intertumoral heterogeneity and complex tumor microenvironment, which are major contributors to the efficacy of and drug resistance to immunotherapy. From a new perspective, single-cell techniques offer an innovative way to look at the intricate cellular interactions between tumors and the immune system and help us gain insights into lung cancer and its response to immunotherapy. This article reviews the application of single-cell techniques in lung cancer, with focuses directed on the heterogeneity of lung cancer and the efficacy of immunotherapy. This review provides both theoretical and experimental information for the future development of immunotherapy and personalized treatment for the management of lung cancer.

KEYWORDS

single-cell analysis, lung cancer, immunotherapy, heterogeneity, tumor microenvironment

1 Introduction

1.1 Tumor heterogeneity is an unmet challenge in the immunotherapy of lung cancer

The advent of immune checkpoint inhibitors (ICIs) over the past decade has ushered in an rapid-growth era of immunotherapy. At present, ICIs used in clinical practice mainly include monoclonal antibodies against programmed death ligand 1 (PD-L1), programmed death receptor 1 (PD-1) and cytotoxic T lymphocyte-associated protein 4 (CTLA 4). With its unique mechanism of action and excellent clinical efficacy, it represents a revolution in tumor treatment following surgery, radiotherapy, chemotherapy and targeted treatment for a variety of malignancies (1). Lung cancer is currently the deadliest malignancy across the globe (2). Thanks to the antibodies targeting PD-1 or PD-L1, the overall survival in patients with advanced non-small cell lung cancer (NSCLC) has been significantly improved, and the five-year survival in PD-L1-positive patients has been raised from no more than 5% to virtually 30% (3, 4). Integration of PD-L1 inhibitors into the first-line platinum-based chemotherapy could enhance survival rate in patients with widespread small cell lung cancer (SCLC) (5). Nonetheless, lung cancer is a highly heterogeneous tumor and studies showed that the heterogeneity of tumor microenvironment (TME) mediates cancer progression and response to immune checkpoint inhibitors (ICI) (6, 7). The current development of immunotherapies for lung cancer has been hampered by the lack of biomarkers predictive of efficacy, and the lack of more immunotherapeutic targets, and lower remission rate (8). Hence, a comprehensive look at the lung cancer ecosystem is warranted in order to improve personalized immunotherapies.

The ecosystem of lung cancer consists of cancer cells, immune cells, stromal cells, non- cellular tissue components, among others. Their interactions dictate the disease progression and the response to treatment (9, 10). Heterogeneity of tumor ecosystem is an important factor that renders tumor therapy difficult, and the genes and morphology related to tumor heterogeneity depend on the intricate interaction between genetic factors and environment (11, 12). Extensive phenotypic and genetic variations exist not only among tumor patients (heterogeneity between tumors), but also within a single tumor (heterogeneity within tumors), including spatial heterogeneity (different genotypes and phenotypes are found in different regions of the same tumor) and temporal heterogeneity (genes and phenotypes differ in primary and secondary tumors). Tumor heterogeneity leads to diversity in cancer signaling pathways and variation in cancer phenotypes, presenting a major challenge for personalized cancer treatment (12).

The molecular heterogeneity of lung cancer (including the differences among and within tumors) has become a subject of active investigations of lung cancer immunotherapy. The heterogeneity includes but is not limited to the molecular expression heterogeneity of tumor and immune cells, especially the heterogeneity of genetic phenotypes and antigen presentation molecule expression etc. (13, 14). The rapid development of single-cell techniques has allowed for the determination of the heterogeneity and immune microenvironment of lung cancer cells and other cell types (15–17). These techniques can help us gain insights into the development and progression of lung cancer, and the complicated mechanism of immunotherapy, thereby improving immunotherapeutic strategies.

1.2 Technical advantages of the single-cell technology over traditional bulk sequencing

Conventional bulk transcriptome and genome analyses have substantially contributed to our understanding of tumor evolution and growth. Whereas, signals displayed by some particular group or state of cells will be masked in the process of bulk sequencing, and such specific cell populations or states are sometimes very critical, such as tumor stem cells and infiltrating immune cells that are related to the tumor response to treatment. Therefore, examining individual cells at the genomic, transcriptomic, epigenomic and proteomic levels can help us better understand tumor heterogeneity at molecular levels and overcome the limitations of the traditional bulk sequencing and allows for high-granularity analyses at cellular and molecular levels (18, 19). This feature has a good prospect of application in the field of tumor immunotherapy, since single-cell analysis can identify cell pathways and types involved in tumor response and immune escape.

The current single-cell technology involves a series of rapidly developing methodologies. The most commonly used single-cell technologies for tumor immunotherapy include single-cell RNA sequencing for transcriptomic analysis, mass spectrometry flow cytometry for proteomic analysis, and spatial molecular analysis (20–22). Each of these techniques delineates a high-dimensional molecular contour for a single cell, which can be classified, by calculation, into different cell groups. For instance, the results of these techniques are more representative than typical cell type markers. Meanwhile, the high-dimensional characteristics of these methods can more accurately describe cell types and infer the relationship among molecular pathways and transition of cell status (21). These characterizations identify the pathways underlying the behavior of each different cell type through complementary computational techniques, and infer the intercellular and intracellular interactions associated with cell state transitions. Therefore, the inference of those pathways mirrors the ongoing clinical research effort in anti-tumor immunotherapy, and the exact medical strategies being developed to reconnect TME using combination therapies to achieve immunotherapy sensitization.

1.3 How to combine single-cell analysis with immunotherapy for lung cancer?

(Figure 1) First of all, single-cell omics analysis is performed on tumor tissues from lung cancer patients, and appropriate single-cell

analysis strategies are selected according to the purpose of the study. It is desirable if peripheral blood samples of corresponding patients are used to monitor immune indicators. Secondly, components of TME are analyzed based on single-cell omics data, with focus being directed at tumor cell heterogeneity, the subtype and status of immune cells, then tumor immunity-related indicators or signatures are established. Finally, appropriate data sets regarding immunotherapeutic strategies are used for further clinical verification of treatment mode selection and monitoring of response, prognosis and other aspects of lung cancer patients.

(Table 1) Here, we first investigated, in general, how single-cell analysis has been used for the study of the interaction between lung cancer cells and TME, and, in particular, how it is related to the response to anti-tumor immunotherapy. Then, we examined the role of single-cell TCR analysis in immune oncology. After this, we looked at the emerging technologies for single-cell spatial analysis, especially their utility to immune oncology. Finally, we discussed the future trend of single-cell technology and its potential role in promoting the application of immune oncology in lung cancer.

2 Single-cell omics in lung cancer

2.1 Transcriptome

Single-cell RNA sequencing (scRNA-seq) is a non-targeted technology for the quantification of transcripts in a single cell, and is often used to identify new cell types, find rare cell populations, and construct maps of cell status and phylogeny (50–52). scRNA-seq can help us gain insights into the distribution, status, action process and cooperation mechanism of different subpopulations of similar cells, and, from a new perspective, look at the heterogeneity of lung cancer, and the interaction between lung cancer cells and TME, especially their relationship with anti-tumor immunotherapy response (15–17). Due to the rapid technical development of scRNA-seq and cell separation, the number of cells sequenced has grown from hundreds to thousands, and the technique is becoming increasingly cost-effective. The analytical methods are also improving constantly, covering determination of cell types, dimensionality reduction of high-dimensional data, unsupervised clustering, phylogenetic modeling, trajectory inference, RNA velocity analysis, and collaborative analysis of multiple data sets (53–57).

2.1.1 Tumor cells and immunotherapy responses

The main feature of lung cancer revealed by scRNA-seq is intratumoral and intertumoral heterogeneity. The scRNA-seq can make more precise diagnosis and prognostic predictions, and facilitate the development of new anti-lung cancer agents. For example, Wu F et al. (35) utilized scRNA-seq and analyzed 42 samples from patients with advanced NSCLC at various stages. They found that the intertumoral and intratumoral heterogeneity of lung adenocarcinoma (LUAD) was lower than that of lung squamous cell carcinoma (LUSC). In addition, cancer cells from different patients exhibited higher heterogeneity. Next, the researchers used scRNA-seq data to infer copy number changes (CNAs) in the cancer cell population and to reveal heterogeneity between and within patients. Most patients, especially LUAD patients, had dominant clones, while in a few LUSCs, malignant cells were distributed in multiple clusters. To quantify intratumoral heterogeneity, they obtained expression-based and CNA-based intratumoral heterogeneity scores (ITH), which were designated ITH_{GEX} and ITH_{CNA}, respectively. The patients were further divided into three categories in terms of lung cancer types and mutations: LUAD patients with driving mutations (LUADm), LUAD patients without driving mutations (LUADn) and LUSC patients without driving mutations (LUSCn). Their results showed

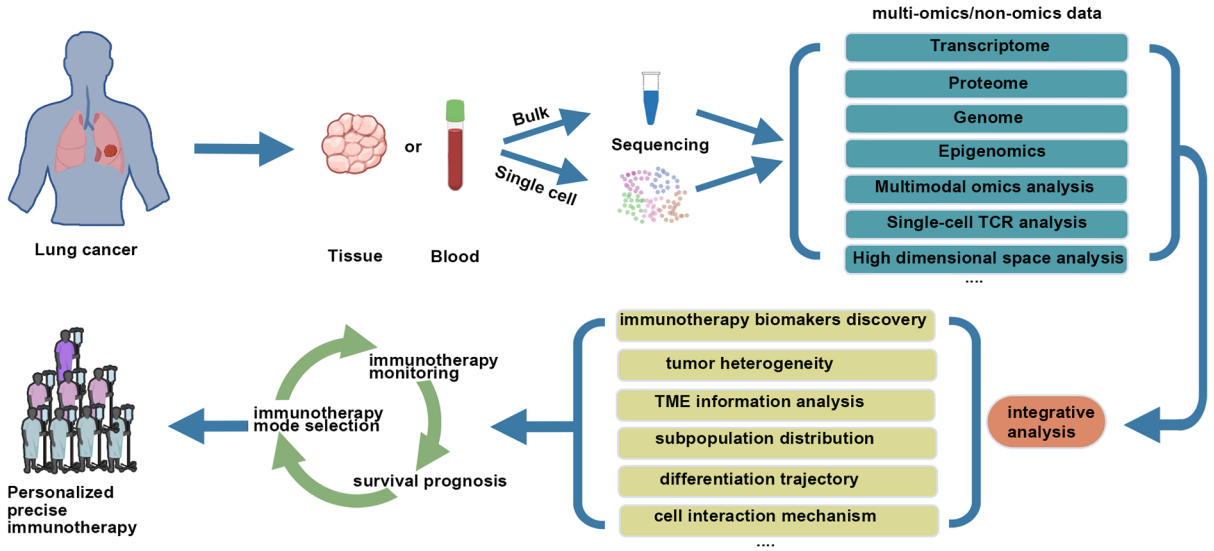


FIGURE 1
Combining single cell analysis with immunotherapy for lung cancer.

TABLE 1 Applications of single-cell analyses in lung cancer immuno-oncology.

PMID/ Refs.	Author	Single-cell technologies used	lung cancer type	Cell types characterized	Clinical/ cellular/ animal level	Key findings
33144684 (23)	He D et al.	scRNA-seq	EGFR mutant LUAD	tumor cells	clinical	ELF3 is upregulated in tumor cells under the secretion of immunoinfiltrating inflammatory cytokines, which activates the PI3K/Akt/NF-κB pathway and up-regulates the expression of proliferative and anti-apoptotic genes.
30821712 (24)	Ma KY et al.	scRNA-seq	LUAD	tumor cells	cellular	Miscoordinated expression of IFN-γ signaling pathway and lower expression of MHC II gene, MHC II and IFN-γ signaling pathway jointly determine the formation of immunotherapy resistance.
36195615 (25)	Tian Y et al.	scRNA-seq	SCLC	tumor cells, T cells, macrophages	clinical	1.Patients with weak immune characteristics SCLC are more likely to benefit from immune checkpoint block (ICB) than those with strong immune characteristics SCLC.
						2. Established a detailed immune map of SCLC.
						3. The detailed classification of T cells in SCLC also revealed the expression pattern of dysfunction and exhaustion markers (such as PDCD1, CTLA4, HAVCR2, LAG3, TIGIT and LAYN), which may be used as immunotherapeutic targets.
						4. Non neuroendocrine SCLC subtype cells tend to have more interactions with other cells and immune and stromal cells, and may be related to the clinical results of immunotherapy.
34653364 (26)	Chan JM et al.	scRNA-seq	SCLC	tumor cells	clinical	PLCG2 overexpression subsets were associated with metastasis, immunosuppression and poor prognosis.
29942094 (27)	Guo X et al.	scRNA-seq, scTCR-seq	NSCLC	T cells	clinical	1. Mapped the immune map of lung cancer T cells at the single cell level.
						2. Higher rates of "pre-exhausted" and exhausted CD8 T cells are associated with a better prognosis for lung adenocarcinoma, the proportion of activated Treg cells is negatively correlated with the prognosis of lung adenocarcinoma patients.
						3. The state transition of CD8+T cell cluster in NSCLC was deduced by scTCR-Seq.
34099454 (28)	Zhang Y et al.	scRNA-seq	NSCLC	T cells	clinical	In immunotherapy resistant patients with MET gene amplification, the proportion of XTIST/CD96/KLRG1 triple positive NK cell subpopulation increased and the proportion of CD8+T cells and NK cell subpopulations decreased.
33506299 (29)	Zhong R et al.	scRNA-seq	NSCLC	T cells	clinical	The change in the percentage of NK cells and T cells may be related to the effective treatment of pabolizumab.
33777802 (30)	Liu S et al.	scRNA-seq	NSCLC	T cells, macrophages	clinical	CD8+T cells, INF-γ+CD8+T cells and the ratio of M2/M1 like macrophages was related to the subsequent better immunotherapy results in patients receiving EGFR-TKI treatment.
35140113 (31)	Yang L et al.	scRNA-seq	EGFR mutant LUAD	T cells	clinical	EGFR mutated tumor cells secrete cytokines to recruit various immunosuppressive cells, while activated immune cells (CD8 +TRM and CXCL9+TAM) are seriously insufficient.
30979687 (32)	Zilionis et al	scRNA-seq	NSCLC	TIMs	clinical	Found 25 TIMs states, which may become a new target for immunotherapy.
28475900 (33)	Lavin et al.	scRNA-seq, CyTOF	LUAD	macrophages, T cells	clinical	1. Obtained the characteristic genes of tumor infiltrating macrophages such as TREM2, CD81, MARCO, APOE, etc.
						2. The immune cells in the microenvironment of early lung adenocarcinoma were mapped in detail, and T cells were divided into 21 subgroups with different Marker expression patterns.
						3. The content of Treg cells in early tumor stage patients was significantly increased, and it grew rapidly in early tumor stage, and PD-1 was significantly expressed in CD4+and CD8+cells in tumor tissue.

(Continued)

TABLE 1 Continued

PMID/ Refs.	Author	Single-cell technologies used	lung cancer type	Cell types characterized	Clinical/ cellular/ animal level	Key findings
32385277 (34)	Kim N et al.	scRNA-seq	LUAD	vascular endothelial cells	clinical	Vascular endothelial cells in LUAD reduced their antigen presentation and homing activity of immune cells through remodeling, thereby promoting tumor immune tolerance.
33953163 (35)	Wu F et al.	scRNA-seq	NSCLC	macrophages	clinical	Macrophages play a major role in inhibiting T cell function through checkpoint pathway.
31811131 (36)	Karacosta LG et al.	CyTOF	NSCLC	tumor cells	cellular	The increased expression of PD-L1 during EMT confirms that EMT is associated with tumor immune escape.
31957112 (37)	Shaul ME et al.	CyTOF	NSCLC and SCLC	neutrophils	clinical	Three main subtypes of LDN/HDN have immune characteristics and inherent plasticity.
336725934 (38)	Sorin M et al.	IMC	LUAD	Neutrophils, monocyte, T cells, macrophage	clinical	1. Tissue relationship of cells in the immune microenvironment is of uniquely prognostic value. 2. The increased proportion of HIF1α+ neutrophils subgroup was significantly correlated with poor overall survival.
36725085 (39)	Sorin M et al.	IMC	NSCLC	tumor cells, T cells,monocyte	clinical	The expression of CXCL13 was related to the ICI efficacy, and the recombinant CXCL13 enhanced the response to anti-PD-1 *in vivo*, which could be ascribed to increased T-cell subpopulations subjected to antigen stimulation and decreased CCR2+ monocytes.
34767762 (40)	Leader AM et al.	scRNA-seq, CITE-seq, TCR-seq	NSCLC	tumor cells, T cells, plasma cells, macrophages	clinical	Constructed the immunoreactive cell atlas of early lung cancer, and established the LCAM module, which can be used as a more direct indicator of antigen-specific anti-tumor immune activation.
35452604 (41)	Hanada KI et al.	CITE-seq, TCR-seq	NSCLC	TILs	clinical	A molecular label of neoantigen reactive T cells based on CD39 protein and CXCL13 mRNA expression was defined to rapidly and efficiently identify CD4+ and CD8+T cells with neoantigen reactive TCRs.
35331733 (42)	Ma Y et al.	scTCR-Seq	NSCLC	TILs	clinical	Tumor specific TCRS were identified, and the corresponding TCR-T cells can specifically recognize and kill autologous tumor cells, which can be used for personalized immunotherapy in advanced cancer patients.
33064988 (43)	Ott PA et al.	scTCR-Seq	NSCLC	T cells	clinical	Revealed the dynamic changes of the clonal type of tumor neoantigen vaccine-specific T cells, and proved that the T cell immune response induced by tumor new antigen vaccine was highly specific and effective.
35831283 (44)	Hui Z et al.	scRNA-seq, scTCR-Seq	NSCLC	T cells	clinical	TNFRSF4 can be used as a potential target to reduce the function of Treg and improve the anti-tumor immunity to NSCLC.
32591861 (45)	Zhang F et al.	scRNA-seq, scTCR-Seq	NSCLC	T cells	clinical	1. Tumor-related CD4+T cell clones had higher cytotoxicity than CD8+T cell clones. 2. After lung cancer progression, the abundance of tumor-related CD4+T cell clones decreased significantly, and the percentage of PD-1+T cells decreased. 3. The pseudo-time track of CD8+T cell clone corresponds to the immunotherapy time point, indicating that the activity of the "cytokine and cytokine receptor interaction" pathway decreased.
33514641 (46)	Gueguen P et al.	scRNA-seq, scTCR-Seq	NSCLC	TILs	clinical	The differentiation of these two CD8+TIL subpopulations from precursor to late stage is related to TCR amplification and T-cell cycle in tumor.
36434043 (47)	Zhu J et al.	scRNA-seq, spatial transcriptome	LUAD	tumor cells, Treg	clinical	The spatial changes of TGF-β signaling pathway in the interaction between cancer cells and TME and in the regulation of immune escape in the invasion of LUAD.

(Continued)

TABLE 1 Continued

PMID/ Refs.	Author	Single-cell technologies used	lung cancer type	Cell types characterized	Clinical/ cellular/ animal level	Key findings
33972311 (47)	Sinjab et al.	scRNA-seq, spatial transcriptome	LUAD	tumor cells, dendritic cells, macrophages	clinical	1. The overlap of immune checkpoint-receptor and cytokine receptor (L-R) interactions between LUAD tumor-distal regions was reduced compared with L-R interactions between LUAD tumor-proximal regions.
						2.The interaction between the immune checkpoint proteins CD24 and LGALS9 in tumor epithelial cells, SIGLEC10 in dendritic cells, SIGLEC10 and HAVCR2 in macrophages increased.
32253229 (48)	Zugazagoutia J et al.	DSP, mIF	NSCLC	tumor cells, T cells	clinical	The high level of CD56 expression in the immune cell region (CD45+) was associated with longer PFS and OS in NSCLC patients receiving PD-1 checkpoint inhibitor monotherapy.
32253229 (49)	Moutafi MK et al.	DSP	NSCLC	tumor cells	clinical	The expression of CD44 in tumor cells is closely related to the prolonged PFS and OS, which can be used as an independent evaluation factor to predict the clinical benefits of patients receiving PD-1 inhibitor treatment.

scRNA-seq, single-cell RNA sequencing; scTCR-seq, single-cell T cell receptor sequencing; CyTOF, mass spectrometry flow cytometry; IMC, imaging mass cytometry; CITE-seq, cellular indexing of transcriptomes and epitopes by sequencing; DSP, digital spatial profiling; mIF, multiplexed immunofluorescence; EGFR, epidermal growth factor receptor; LUAD, lung adenocarcinoma; SCLC, small cell lung cancer; NSCLC, non small cell lung cancer; TIMs, tumor infiltrating myeloid cells; TILs, tumor infiltrating lymphocytes; Treg, regulatory T cells.

that, compared with LUADm patients, LUSCn patients had significantly higher ITH_{CNA}, but no significant difference was found in ITHGEX. ScRNA-seq demonstrated a transcriptional heterogeneity within the malignant cell population, which was associated with driving mutations. Identification of alterations in more diverse subpopulations may have implications for immunotherapy.

It is also feasible to use scRNA-seq to identify ubiquitous tumor cells with specific transcriptomic status in lung cancer patients, which helps us better understand the tumor type and cell hierarchy of lung cancer, and single out transcriptome signature related to the response and resistance to treatment (23, 58). Mounting evidence shows that EGFR mutation is an important factor affecting the therapeutic efficacy of PD-1 inhibitors in NSCLC patients, and patients with EGFR mutation responded to the treatment less well than their counterparts without EGFR mutation (59–62). He D et al. (23), by employing scRNA-seq, revealed a significant heterogeneity in EGFR mutation in patient with early-stage LUAD, and found that ELF3 was one of the most up-regulated genes in advanced tumor cells. Under the effect of immune infiltrating inflammatory cytokines (such as IL1B), ELF3 in tumor cells was up-regulated, thereby activating PI3K/Akt/NF- κB pathway, and up-regulating the expression of proliferation and anti-apoptosis genes, such as BCL2L1 and CCND1. These findings suggested that there existed an involved interaction among tumor cells, stromal cells and immune infiltration cells in TME. These results may pave the way to immunotherapy targeting EGFR mutant LUAD.

Meanwhile, scRNA-seq analysis has multiple advantages in that it not only can reveal the molecular diversity of different samples and show the impact of clinical treatment on different cell subsets. Ke-Yue Ma, et al. (24) utilized scRNA-seq to examine the heterogeneity of genes associated with response of LUAD to immunotherapy. They compared LC2/ad (Vandetanib sensitive) and LC2/ad-R (Vandetanib tolerant) cell lines, and found that LC2/ad had a higher level of MHC II gene and IFN-γ signal pathway coexpression gene. However, the IFN-γ signaling pathway in LC2/ad-R was down-regulated and the expression of MHCII gene was low. They revealed a possible mechanism of Vandetanib resistance: that is, MHC II and IFN-γ signaling pathways jointly determined the development of immunotherapy resistance.

Tian Y, et al. (25), by using scRNA-seq, examined about 5000 matched normal adjacent tissues (NAT) and primary tumors (PT) cells from 11 SCLC patients (including a patient with both primary tumor (PT) and recurrent tumor (RT)). They found that human SCLC had a significant inter-tumor and intra-tumor heterogeneity, and many tumors contained separate subpopulations, indicating there is a remarkable intra-tumor heterogeneity at the transcriptomic level. In addition, most SCLCs with neuroendocrine (NE) characteristics, such as SCLC-N and SCLC-A, tended to have strong immunological features, while non-NE SCLCs, such as SCLC-P and SCSC-Y, tended to possess weak immune traits. Patients with SCLC having weak immune features were more likely to benefit from immune checkpoint blockade (ICB) than their counterparts with strong immune characteristics. The scRNA-seq data revealed that multiple SCLC subtypes showed different proportions in practically all SCLC patients, highlighting the importance of scRNA-seq and the need for functional research on tumor progression and immunotherapy of ITH. Moreover, Chan JM et al. (26) applied scRNA-seq to analyze the transcriptome of 21 fresh SCLC samples from 19 patients and 155098 cells from 24 LUAD samples and 4 normal lung tissue samples from the area adjacent to cancer. They found that the level of copy number variation (CNV) was higher in SCLC than in LUAD and had significant heterogeneity. They exhibited that PLCG2 overexpression subsets were associated with metastasis, immunosuppression and poor prognosis. Therefore, it is potentially of great significance for the design of novel strategies of the targeted therapy and immunotherapy. These observations

collectively demonstrated that ScRNA-seq can help researchers better understand tumor heterogeneity and the intricate interactions between tumor cells and their microenvironment, thereby facilitating the identification of lung cancer cell subpopulations amenable to immunotherapy.

2.1.2 Immune, stromal cells, and immunotherapeutic responses

Infiltrating immune cells, cancer-associated fibroblasts and vascular endothelial cells are important components of TME (63). By means of scRNA-seq, we can identify the features of various types of immune, stromal cells, heterogeneous expression profiles, and look into mechanisms involved in immunosuppression, thus better understanding the heterogeneity and diversity of cancer immune responses.

In view of the intricacies of the TME, in recent years, single-cell transcriptome sequencing has been incrementally used in the study of infiltrating immune cells in lung cancer (25, 27–31, 45). It has an important implication for the research of the mechanism underlying the lung cancer tumor immunity, especially for the study of the functional status of T cells in the tumor, which play a pivotal part in killing tumor cells, for the development of efficacious immunotherapy and the identification of sensitive targets and markers. Guo X et al. (27) conducted scRNA-seq on 12346 T cells from the peripheral blood, cancer-adjacent tissues and cancer tissues of 14 NSCLC patients prior to drug treatment, worked out the immune map of lung cancer T cells at the single-cell level, revealed the heterogeneity of lung cancer T cells, and provided a new notion for immunotherapy to specifically target T cell subsets. This study identified 16 major clusters of T cells (7 CD8 and 9 CD4 types). In addition to exhausted CD8 T cells, the infiltrating CD8 T cell population of lung cancer was also found to include two groups of "pre-exhausted" CD8 T cells that may bear a state transition relationship with exhausted CD8 T cells. Moreover, higher ratios of "pre-exhausted" and exhausted CD8 T cells were associated with a more favorable prognosis for lung adenocarcinoma. Apart from that, in terms of the expression of TNFRSF9 (4-1BB), a group of activated Tregs could be distinguished from lung cancer-infiltrating regulatory T cells (Tregs). The expression of inhibition-related genes in this group of Tregs was higher, suggesting that they were the Treg cells that actually serve the inhibition function in tumors. At the same time, the proportion of activated Treg cells was negatively correlated with the prognosis of lung adenocarcinoma.

In NSCLC patients receiving ICI, Zhang Y et al. (28) found that patients with MET gene amplification were refractory to the treatment. After analysis of more than 20000 immune cells with scRNA-seq, the researchers identified a new XTIST/CD96/KLRG1 triple positive NK cell subpopulation in patients with MET amplification. In immunotherapy-resistant patients, the proportion of this subpopulation was elevated and the proportion of NK cells and CD8+T cell subpopulations dropped. Moreover, some researchers used scRNA-seq to study the dynamic change of peripheral blood T cell clones in NSCLC patients receiving PD-1 inhibitors (45), and found that the number of a CD4+T cell clone related to tumor significantly dropped upon tumor progression, and the proportion of PD-1+T cells also decreased significantly. What's more, an NSCLC patient with negative PD-L1 expression benefited from the treatment of pabolizumab (PD-1 inhibitor) (29). An scRNA-seq analysis of the patient's peripheral blood revealed that the NKG7+NK cells and NKG7+T (NKT) cells of the patient were significantly lowered, while the CD8+T cells and Naive T cells were prominently increased, suggesting that the change in the percentage of NK cells and T cells might be related to the efficacy of pabolizumab treatment.

Liu S et al. (30) examined whether the patient's previous response to EGFR-TKI was related to the subsequent immunotherapy results. They found that, in patients receiving TKI (Tyrosine Kinase Inhibitor) treatment, the objective response rate (ORR) of immunotherapy was significantly higher in patients with short progression free survival (PFS) than in those with long PFS. By comparing the TME of the two groups using scRNA-seq, the researchers found that the infiltration rate of INF-γ+CD8+T cells and CD8+T cells in the immune microenvironment was higher in patients with short PFS, and the ratio between M2- and M1-like macrophages was significantly lower in short-PFS patients than in their counterparts with long PFS. Therefore, this study provided a marker reference from the angle of a single cell for the ensuing treatment in patients who had received EGFR-TKI targeted therapy. scRNA-seq analysis by Yang L et al. (31) revealed that the TME of EGFR mutant LUAD and wild type LUAD had different heterogeneity in cell composition, function and their interaction. The loss of proinflammatory cells, enrichment of inhibitory cell types and the low expression of immune checkpoint proteins may lead to an immune silence environment for EGFR-mutated LUAD, i.e., EGFR-mutated tumor cells secrete cytokines to recruit various immunosuppressive cells, while activated immune cells (CXCL9 +TAM and CD8+TRM) were seriously insufficient. Therefore, in future, effective immunotherapy can be accomplished in EGFR mutant LUAD patients by improving the inhibitory tumor immune microenvironment (TIME).

Tian Y, et al. (25) employed scRNA-seq to develop a detailed immunity map of SCLC. Compared with normal adjacent tissues, the proportion of lymphocytes in primary SCLC was higher and the proportion of myeloid cells lower, indicating that adaptive immunity in TME played a more important role. Then, the researchers re-classified T cells and myeloid cells and categorized macrophage into four groups: a tumor-associated macrophage groups and three groups of resident alveolar macrophages. T cells from normal adjacent tissues and TME were predominantly CD8+ T cells and highly expressed cytotoxic markers, suggesting that immunological assessment of SCLC is of great significance. Moreover, reclassification of T cells in SCLC patients can better mirror the expression pattern of T cells dysfunction and exhaustion markers (such as HAVCR2, CTLA4, LAYN, PDCD1, LAG3, TIGIT), which may be used as immunotherapeutic targets. scRNA-seq of T cell subsets of TME in SCLC revealed that HAVCR2 had the highest expression level in exhausted T cell subsets, while LAYN was sporadically expressed in exhausted CD8 + T cells, and CTLA4 was preferentially expressed on other T cells. T cell heterogeneity and co-inhibitory receptor expression preference in SCLC patients provide potential immunotherapeutic targets.

Tumor-infiltrating myeloid cells (TIMs), such as monocytes, macrophages, dendritic cells and neutrophils, have been identified

as a key regulator of cancer growth (64, 65). Zilionis et al. (32) used scRNA-seq to locate TIMs in NSCLC patients and identified 25 TIMs states, most of which could be found repeatedly in patients. This study provides a new theoretical basis for future elucidation of the role of myeloid cells in cancer, and TIMs may serve as a new target for immunotherapy. Lavin et al. (33) conducted scRNA-seq to analyze the TME of 18 LUAD patients, and identified the characteristic genes of tumor infiltrating macrophages, such as TREM2, CD81, MARCO, APOE, etc. In addition, analysis with scRNA-seq found that vascular endothelial cells from NSCLC patients reduced their antigen presentation and the homing activity of immune cells through remodeling, thereby promoting tumor immune tolerance (34, 66). A subgroup of cancer-associated fibroblasts (CAFs) that highly expressed extracellular matrix protein genes were found to induce immunotherapy resistance by increasing the levels of PD-L1 and CTLA-4 proteins in Treg cells through cell cross talk (67).

Overall, a comprehensive understanding of the composition and state of immune cells is crucial to the elucidation of the responsiveness and resistance to current immunotherapies, and to the design of new immunomodulatory therapies. Use of the single-cell transcriptomic analysis in lung cancer patients receiving immunotherapy also revealed the heterogeneity and diversity of lung cancer immune responses. Clusters based on non-targeted transcriptional assessment of cell state often cannot be completely separated into traditional immune cell subpopulations in terms of cell surface protein expression. For immunotherapy, application of these methods to immune cells and stromal cells in TME can help elucidate the response to immunotherapy (such as ICIs) and the transcriptional state of drug-resistant cells. Importantly, the analysis aimed at mapping the immune picture of multiple lung cancer types has identified multiple new transcriptional states, which are related to the responsiveness of lymphocytes, DC cells, monocytes, macrophages and fibroblast compartment of TME to immunotherapy. Researchers can now look into how lung cancer and the immune system co-evolve during treatment and recurrence at the single-cell level.

2.1.3 Cell interaction analysis

Very complex interactions take place between tumor or immune cells and/or stromal cells, which together dictate the tumor progression and response to treatment. This cell-cell interaction can be studied by calculating the expression level of receptor and ligand from scRNA-seq data. At the same time, for the exploration of the complex interaction between tumor cells and TME, new technologies, including single-cell space transcriptome methods, are also developing rapidly, making it possible to look into the cell-cell physical interaction. At present, the extensively used cell interaction analysis algorithms include CellPhoneDB, CellChat, iTALK, NicheNet, among others (68–71), which is out of the scope of the review.

To look into the interaction between different cell types in TME, Wu F et al. (35) examined the cell-cell interaction by using scRNA-seq to get a full picture of TME in NSCLC patients, including angiogenesis, T cell activation, CAF activation, immunosuppressive cell recruitment, and activation of checkpoint routes. Obvious interactions were found between cancer cells and fibroblasts, endothelial cells and macrophages. An analysis of the cross cell interaction molecules revealed a complex network involving multiple carcinogenic and inflammatory signaling pathways. The researchers found that, in patients' immune environment, macrophages played a key role in the inhibition of T cells *via* checkpoint pathway. Furthermore, predominant pathways vary with different subgroups of NSCLC. For instance, LUAD driving gene mutation had a high level of TIGIT pathway activation, but a low level of TIM3 (HAVCR2) pathway activation. Except in few LUSC patients, the authors did not detect any significant activation of PD1/PD-L1 axis, which might be ascribed to the low expression of PD1/PD-L1 at the transcriptomic level. Even in the same subtype of lung cancer, the interactions related to immunotherapy were different, highlighting the need for more precise biomarkers to improve the efficacy of immunotherapy. In addition, Tian Y, et al. (25) used CellPhoneDB to study the interaction between ligand-receptor pairs, and confirmed that the non-neuroendocrine small cell lung cancer subtypes (SCLC-non-NE) interacted more with other cells, including immune and stromal cells than other subtypes of SCLC, and may be related to the clinical outcomes of immunotherapy. By correlating the expression of ligand receptor pairs between different cell types, important information on cell-to-cell interactions related to lung cancer immunotherapy can be inferred from scRNA seq data, which may help us better understand the complicated arrangement and interaction between tumor cells and TME, as well as to find new indicators or signatures related to lung cancer immunotherapy.

2.1.4 Limitations of scRNA-seq

ScRNA-seq is the most widely used single-cell sequencing technique. With its extensive application in scientific research, scRNA-seq gradually some methodologically inherent problems began to emerge. First, efficiency of mRNA capture in the single-cell transcriptome method is low, standing at somewhere between 5% and 15%, leading to data sparsity, sampling deviation, and loss of low-level transcript gene expressions (72). Second, it is only applicable to fresh tissue samples. For frozen samples, since cells have lost their activity, scRNA-seq cannot be performed. This substantially restricts its application, increases the difficulty of operation and reduces the sample flux. For example, in order to ensure the stability of RNA, many clinical samples need to be frozen. Such archived frozen samples are no longer amenable to scRNA-seq and their value could not be fully tapped by the latest technology (73). Third, the dissociation process induces the expression of stress genes, resulting in "artificial transcriptional stress responses" of cell transcription and eventually to transcription bias. The data so obtained cannot truly reflect the cell transcription status of the sample, and the reliability of the results is greatly impaired. This has been demonstrated by a great many experiments. For example, Brink et al. found that the process of protease dissociation at 37°C would induce the expression of stress genes, thereby introducing human errors, and leading to inaccurate results of cell type identification (74). The latest

comparative experiment further confirmed this limitation: Dissociation at 37°C induced an increased expression of multiple stress genes, which yielded seriously distorted results, and the low-temperature dissociation could effectively avoid this phenomenon (75). Fourth, for many solid tissues, such as cerebral, cardiac and renal tissues, protease tends to dissociate the cell types that are subject to dissociation, thus losing the cells that are not easy to dissociate. At the same time, some sensitive cells may be damaged due to excessive dissociation. Therefore, the dissociation process cannot effectively obtain all cell types in the tissue, and the accuracy of the results is substantially affected (76–79). It is believed that, with the continuous improvement and breakthroughs of the technology, single-cell sequencing technology has a good prospect of being widely used in the research and treatment of lung cancer.

2.2 Proteome

2.2.1 single-cell proteomic analysis

Single-cell proteomics allows for analysis of protein expression at the single-cell level, thus revealing fine differences between individual cells. It provides a powerful tool for the analysis of cell and tumor heterogeneity, specific cell types, circulating tumor cells (CTC), immunological research, the genetic study of cell cycle, and the examination of trace/rare samples. Working on different principles and depending on various scenarios, many methods for the quantitative detection of single-cell proteins have emerged in recent years, including microfluidic techniques, microporous methods, optical fiber nano biosensoring, fluorescent probing and mass spectrometry-based single-cell protein detection (80, 81). Especially in recent years, with the rapid development of mass spectrometry technology, the bottleneck of proteomic research based on mass spectrometry has been removed, and the scanning speed and detection sensitivity have been greatly improved, which makes it possible to detect extremely trace protein samples.

2.2.2 Mass spectrometry flow cytometry

CyTOF is a flow cytometry technique based on mass spectrometry principles and is used for multi-parameter detection of individual cells. By integrating mass spectrometry and traditional flow cytometry, CyTOF not only keeps the high-speed of traditional flow cytometry, but also attains the high-resolution of mass spectrometry, overcomes the problem of overlapping light spectra of traditional flow cytometry fluorescence emission groups, and is able to simultaneously detect more than 30 protein markers in tumor cells. This high-dimensional single-cell technique is described as the “single-cell atlas” of the tumor ecosystem. As a single-cell high-dimensional immune analysis, it can better link the tumor immunity map with its clinicopathological characteristics (82, 83).

Lavin Y et al. (33) separated immune cells from tumor tissue, normal lung tissue and peripheral blood from lung cancer patients, detected specific transcripts of cells and more than 30 protein markers on the surface using CyTOF and other technologies, and drew a detailed map of immune cells in the TME of early-stage lung adenocarcinoma, to provide an experimental basis for the design of immunotherapeutic regimen for early lung cancer. The unsupervised cluster analysis of the three tissues divided T cells into 21 subgroups in terms of different surface marker expression patterns, including new subgroups (IX, XX, etc.) that had not been previously identified by traditional methods. In addition, the analysis of the proportion of subpopulations in different samples showed that the content of Treg cells in early-stage tumor patients was significantly increased, and it grew rapidly at the early stage of tumor, and PD-1 expression was significantly elevated in CD4+ and CD8+ T cells in tumor tissue.

Karacosta LG et al. (36) used CyTOF to identify and characterize the epithelial mesenchymal transformation (EMT) state of clinical lung cancer specimens according to the immune state map obtained in lung cancer cell lines. The researchers used HCC827 cell line for study of EMT, and examined 28 protein expression markers to characterize the EMT status and proliferation-, signal transduction- and apoptosis-related status by employing qualitative CyTOF. Their study observed an increased expression of PD-L1 during EMT, confirming that EMT was related to tumor immune escape. Notably, the researchers found that, among the EMT transcription factors, Oct3/4 and Nanog expression was significantly up-regulated during the entire EMT process, indicating that the co-expression of Oct3/4 and Nanog was crucial to the EMT of lung cancer cell lines. Shaul ME et al. (37) clinically assessed the level of circulating high-density neutrophils (HDN) and low-density neutrophils (LDN) in patients with advanced lung cancer by using CyToF, and found that the three main subtypes of LDN/HDN possessed immune characteristics and inherent plasticity. These findings laid foundation to the development of new tumor immunotherapies.

2.2.3 Imaging mass cytometry

Imaging mass spectrometry (IMC) combines high-resolution imaging technology and CyTOF technology to generate tissue structure images involving multiple factors such as cell markers, transcripts, and transduction signals, so as to achieve single-cell proteome spatial analysis (84). In the field of immune oncology, IMC can classify infiltrating immune cells in a high parameter space while maintaining its spatial coordinates, which may provide useful information about host responses and inform the selection of appropriate immunotherapies (85).

Sorin M et al. (38) used IMC to describe histopathological patterns of pulmonary adenocarcinoma and the immune cell landscape in 416 patients, and analyzed more than 1.6 million cells, and conducted spatial analyses on immune cell lineages and activation status with different clinical relevance (including survival). Their analyses on the category of cellular neighborhood and survival time confirmed the association between specific cell interactions and survival rate, indicating that the tissue relationship of cells in the immune microenvironment is of uniquely prognostic value. They also studied the relationship between cell phenotype and survival in the TME. The results showed that the total number of neutrophils exerted no significant impact on survival, but the increased proportion of HIF1α+ subgroup was significantly correlated with poor overall survival.

Sorin M and their colleagues (39) also performed IMC on 114,524 single cells from 27 NSCLC patients receiving ICI, and achieved spatial resolution of immune spectrum and activation state with different clinical results. These studies proved that the expression of CXCL13 was related to the ICI efficacy, and the recombinant CXCL13 enhanced the response to anti-PD-1 *in vivo*, which could be ascribed to increased T-cell subpopulations subjected to antigen stimulation and decreased CCR2+ monocytes. These findings highlighted the importance of major immune cell lineages and their functional states in the response to ICIs and help us better understand the role of the tumor immune microenvironment in such response.

These observations highlighted the importance of evaluating immune cell phenotypes at the single-cell level. In fact, both CyTOF and IMC are particularly useful methods for characterizing the specific phenotypes of cells involved in responses to immunotherapy at the single-cell level. With immunotherapy, single-cell proteomic analysis can provide insights into the signaling pathways related to the effectiveness of immunotherapies and drug resistance. At the entrance into the era of single-cell proteomics, we are still faced with great challenges in proteome coverage depth and flux. We believe that these challenges can be addressed by integrating mass spectrometry flow cytometry, measurement strategies, and algorithms.

2.3 Genome

Single-cell genome sequencing is a new technique that sequences and amplifies the entire genome within a single cell (86). A complete genome with high coverage can be obtained by efficient amplification of a small amount of whole-genome DNA from isolated single cells, followed by high-throughput sequencing. In fact, single-cell genome sequencing has become a powerful tool for study of the heterogeneity between cells in biological samples and identification of genomic changes (such as copy number variation and point mutation). This technology presents unique advantages in the research of cell lineage differentiation, especially cell evolution during tumorigenesis, and cell heterogeneity in complex biological samples (87, 88).

In recent years, many single-cell genome amplification technologies have been developed, such as DOP-PCR, multiple annealing, multiple displacement amplification (MDA) and loop-based amplification cycle (MALBAC), transposon insertion-mediated linear amplification (LIANTI), etc. (89). Single-cell whole exome and whole genome sequencing techniques have been developed (90). Although they have not been used for the study of lung cancer immunotherapies, single-cell genome sequencing has been employed for the analysis of a large number of single cells. In the entire process of lung cancer management, we can track the specific gene variation of lung cancer patients and the heterogeneity of tumor cell population clonal evolution (91–93), which suggests that this technology has a good prospect of being applied in the research of lung cancer immunotherapies.

The single-cell genome sequencing of single circulating tumor cells (CTC) shows some unique advantages in the diagnosis, differential diagnosis, monitoring and prognosis of lung cancer. For example, Su Z et al. (91) conducted single-cell whole genome sequencing on CTC from 48 SCLC patients, and compared the sequence data with the mutations in tumor tissue of the same patient. They found that most gene mutations in tumor tissue could be accurately detected in CTC, and DNA had conspicuous heterogeneity, suggesting that single-cell genome detection of CTC is an effective way to monitor the genetic variation and disease progression of SCLC. Ni X et al. (92) used MALBAC technology to sequence the whole exome and genome of a single cell in CTC of lung cancer patients, and found a new copy number variation profile. By detecting the copy number change (CNV) of CTC, tumor metastasis could be monitored. The research team further analyzed the CNV profile of individual CTC from 11 patients with different subtypes of lung cancer, and identified the different lung cancer subtypes, indicating that it is feasible to use the CNV analysis of CTC to classify tumors in the future. Chen J et al. (93) found, by using the dimensional analysis of the single-cell genome, that different driver changes and the initial EGFR mutation co-existed in the same cancer cell in the patients with Osimertinib-resistant NSCLC. The heterogeneity of clonal evolution of tumor cell populations led to the development of Osimertinib resistance. However, at present, no literature reported single-cell genome sequencing for the prognostic prediction of immunotherapy for lung cancer. Further studies are needed in this field.

2.4 Epigenomics

Single-cell epigenomics allows for the analysis of information about chromatin modifications and their potential regulatory effects at single-cell resolution, and can complement data beyond RNA expression and DNA variation obtained by single-cell DNA sequencing and RNA sequencing (94, 95). Combination of single-cell epigenomics with single-cell transcriptomics can help us better understand the cell type-specific gene regulation program and how the tumor cells change in response to environmental stimuli (96–98). These subjects are the important directions of future studies on single-cell analysis in lung cancer immunotherapy. Epigenomic analysis has been used for single-cell study, such as ATAC-seq, ChIP-seq, bisulfite-based DNA methylation sequencing, and chromosome conformation capture techniques (3C and Hi-C) (99–101). Among these techniques, single-cell ATAC-seq (scATAC-seq) is currently the only widely used method with sufficiently high throughput, being capable of detecting the openness of chromatin in different cells at the single-cell level and showing the sites of different transcription factors and regulatory factors. Although it has not been used in the study of lung cancer immunotherapy, it has found widespread application in the research of lung cancer heterogeneity, tumor microenvironment and other fields.

In order to gain insights into the intratumoral heterogeneity of lung squamous cell carcinoma, Wang et al. (102) performed single-cell ATAC seq on an LUSC patient, and detected a total of 50486 peaks. The open chromatin map was highly consistent with the bulk NSCLC sample. On the level of single-cell analysis, high heterogeneity was observed in some open chromatin regions.

LaFave LM et al. (103) used single-cell epigenomics to analyze the chromatin state transition in the mouse model of LUAD, and identified a pre-metastasis transition in lung adenocarcinoma, characterized by the activation of the RUNX transcription factor, which mediates the remodeling of extracellular matrix to facilitate metastasis, and is indicative of the survival rate of LUAD patients. Their findings proved that the single-cell epigenomics plays an important role in the identification of regulatory programs and can help reveal the mechanism of tumor progression and key biomarkers.

Compared with scRNA-seq, one of the main advantages of scATAC-seq lies in that it can provide more in-depth understanding of gene regulation and transcription or other processes, and more information about cell lineages and characteristics. However, the scATAC-seq is still restricted by some technological limitations, including limited data and high sensitivity to tissue separation. In addition, no literature covered the application of single-cell epigenome in lung cancer immunotherapy, and further studies are warranted in the future.

2.5 multimodal omics analysis

Single-cell multiomics refers to the cutting-edge technology of measuring multiple omics data simultaneously in the same cell (18, 104). For example, the recently developed CITE-seq (105) technology is designed to couple specific oligonucleotides to different antibodies, so that it can convert the measurement of proteins into the measurement of DNA tags (ADTs) connected to antibodies. Therefore, CITE-seq can determine the abundance of RNA and cell surface protein in the same cell by sequencing. In addition, with the progress of new technologies, transcriptome has been able to be used simultaneously with other genomics at the level of single-cell analysis, including ATAC (97, 106), DNA methylation (107), nucleosome distribution (108), spatial location (109, 110), among others, which overcomes the inherent limitations of scRNA-seq and helps researchers further understand how other genomics affect the state and function of cells (18). The utilization of single-cell multiomics technology in immune oncology can identify the heterogeneity of immune cells in tumors and reveal the interaction and mode among multiple cell groups in the process of differentiation, so that researchers can look into the role of immune cells in the growth of tumor, so it has significant application prospects in immunotherapy research (111).

In order to study the molecular state and composition of immune cells in NSCLC, Leader AM et al. (40) carried out single-cell analysis of NSCLC by using scRNA-seq, CITE-seq and TCR-seq (T cell receptor sequencing), and constructed the immunoreactive cell atlas of early lung cancer, and established the LCAM module for detailed classification of NSCLC tumors by analyzing immune cell types. The high score of LCAM indicates that the patient was undergoing a stronger antigen-specific anti-tumor adaptive immune response. Therefore, LCAM can serve as a more direct indicator of the activation of antigen-specific anti-tumor immunity, providing important reference data for the selection of targets for immunotherapy. Hanada KI et al. (41) used CITE-seq and TCR-seq to analyze tumor-infiltrating lymphocytes (TILs) in NSCLC, and defined a new antigen-reactive T cell molecular tag in terms of the expression of CD39 protein and CXCL13 mRNA to efficiently identify CD4+and CD8+T cells with new antigen-reactive TCRs. Zhang L et al. (112) showed the unique cell composition and gene expression profile of LUAD and LUSC through the multi-group analysis on the basis of single-cell transcriptome, which provided insights into the pathogenesis and heterogeneity formation of various types of lung cancer. At the same time, several highly-expressed genes identified in early lung cancer samples can provide clues to potential targets for early treatment of lung cancer.

Single-cell multimodal omics aims to integrate multiple molecular information from the same single cell (such as at DNA and RNA, RNA and ATAC levels) or at all three levels. These methods can provide more insights into genotype phenotype relationship and epigenomic regulation of gene expression. Although the initial result has proven the feasibility of sequencing DNA and RNA in the same cell, currently, their throughput remains low and the cost is high. The future development of these methods using nanopore systems, droplet platforms, and combinatorial indexing is expected to overcome many of these technical barriers, thereby expanding their application in lung cancer research.

2.6 Single-cell TCR analysis

In our immune system, T cells play an important part in the acquired immune response. T cell receptor (TCR) is a protein on the surface of T cells responsible for specific recognition and binding with major histocompatibility complex (MHC) antigen peptides (113). In tumor tissue, when TCR on tumor-infiltrating T cells recognizes and binds to tumor antigen-MHC complex, T lymphocytes are activated *via* signal transduction and enter the subsequent immune response process, which enables immunotherapy to effectively elicit antigen-specific anti-tumor immune response (114). TCR sequencing targeting tissue or population cells can reflect the expression status of cell groups to a certain extent, but cannot determine the state of specific cells in a certain cell group. With the rapid development of single-cell sequencing techniques, TCR sequencing has also advanced from bulk TCR sequencing to single-cell TCR sequencing (scTCR-seq). ScTCR-seq is a high-throughput sequencing technique for detecting TCR molecular sequences at the level of single-cell analysis, and can provide information on the role of TCR sequences in T cells-specific selection, activation, and phenotypic identification, as well as T cell differentiation pathways. ScTCR-seq can achieve higher cell-processing throughput and accuracy, so immunophenotypic analysis at the level of single-cell analysis is increasingly used in immunological research (115–117).

In a study on lung cancer immunotherapy, Ma Yd et al. (42) developed a scTCR-seq technology based on RNA pre-amplification, and used this technology to identify tumor-specific TCR from lung cancer-specific TILs at high efficiency and low cost. Further functional verification showed that its corresponding TCR-T cells could specifically recognize and kill autotumor cells, which can be potentially used for individualized immunotherapy for

advanced lung cancer. Ott PA et al. (43), in their clinical trials, used personalized tumor neoantigen vaccine (NEO-PV-01) and PD-1 inhibitor in the treatment of three kinds of high TMB, metastatic tumors (NSCLC, advanced bladder and melanoma cancer) for the first time, and the scTCR-seq analysis revealed the dynamic changes in the clonal type of tumor neoantigen vaccine-specific T cells, and accurately detailed characterized the T cell response. From the cellular level, they proved that the T cell immune response induced by tumor new antigen vaccine was highly specific and effective. Hui Z et al. (44) conducted scRNA-seq and scTCR-seq analyses on the immune cells from NSCLC patients who had received neoadjuvant immunotherapy but not immunotherapy. They found that the enrichment of B cells and CD4+T cells was related to the more favorable prognosis in NSCLC patients. IL-21 was essential for tumor control and the transformation of the B-cells to anti-tumor IgG1 and IgG3 subtypes. In addition, TNFRSF4 can potentially be used as a molecular target to reduce the function of Treg and improve the anti-tumor immunity against NSCLC, which help us better understand the mechanism of cell synergy in the clinical response to neoadjuvant immunotherapy.

It is of importance to have an in-depth understanding of the clonal dynamics and functional status of T cells in NSCLC to improve the efficacy of immunotherapy. Zhang F et al. (45) conducted scRNA-seq and scTCR-seq on T cells from the peripheral blood of NSCLC patients before and after PD-1 blockade, identified single peripheral T cell clones, and dynamically monitored their changes during immunotherapy. They found that tumor-related CD4+T cell clones had higher cytotoxicity than their CD8+T counterparts. When lung cancer progresses, the number of tumor-related CD4+T cell clones decreased significantly, and the proportion of PD-1+T cells dropped. In addition, the pseudo-time track of CD8+T cell clone corresponded to the treatment time point, indicating that the "cytokine receptor-cytokine interaction" pathway was down-regulated. These analyses help us better understand the dynamics of T cell clones from the peripheral blood of NSCLC patients during PD-1 blockade. To study cloning relationship between NSCLC single T cells, Guo X et al. (27), again, used scTCR-seq and obtained, in 16 cell clusters, 8038 full-length TCRs containing both α-chain and β-chain. Of them, 5015 cells had unique TCRs, and 3023 cells repeatedly used TCRs, indicating that the clones were expanding. The state transition of CD8+T cell clusters in NSCLC was deduced by detecting TCRs, including the inherent T cell development and tumor-induced T cell exhaustion. By using single-cell RNA sequencing and TCR sequencing, Gueguen P et al. (46) found two CD8+TIL sub-populations in NSCLC that expressed memory-like gene modules. The differentiation of these two sub-populations from precursor to late stage was found to be related to TCR amplification and T-cell cycle in tumor. These findings provided important evidence regarding the origin, ontogenesis and functional organization of TIL in NSCLC.

In summary, scTCR-seq adds key information about the antigenic specificity of T cells to immune cell analysis, enabling a more refined dissection of the role of antigenic specific T cells in the response to immunotherapy. What is more, non-invasive identification of amplified TCR clones in vertically collected blood samples during lung cancer immunotherapy can accurately characterize the immune activity of T cell subpopulations related to treatment response, making immunotherapy monitoring more accurate.

3 High dimensional space analysis

The spatial cell composition of tumors is inconsistent. The spatial distribution of tumor subclones and the spatial variability of immune microenvironment are believed to be responsible for the heterogeneity of most cancer types and the variability of immunotherapy response (118–120). Single-cell space technology includes image-based spatial proteomics technology in combination with analyses of single-cell resolution, and variation information at DNA level and changes in RNA level expression, and multi-dimensionally analyzes research objectives (121). By quantitatively determining tens to hundreds of genes, transcripts or proteins, single-cell space technology can garner valuable molecular, cellular and micro-environmental information under the background of cell structure, and help researchers to look into the interaction between cells, the relationship between tumor cells and TME, and patients' response to immunotherapy from the perspective of cell spatial configuration (122, 123).

Because obtaining single-cell suspension entails enzymatic hydrolysis of tissues, the single-cell transcriptomic sequencing leads to loss of the spatial location information of cells during tissue lysis, and the spatial information is crucial for the understanding of the cell microenvironment and the interaction between cells (124). Single-cell space transcriptome technology (121) overcomes the limitations of scRNA-seq, and can combine gene expression with the immunohistochemical image of tissue samples, thereby locating the gene expression information of various cells in the tissue in terms of the original spatial location of the tissue, identify genes that are active in the tissue, and can visually detect the gene expression difference in various parts of the tissue. Single-cell space transcriptome technology has been widely used in the study of spatial distribution of cancer cells and TME, which are important to the understanding of the relationship between tumor heterogeneity and TME (125, 126).

Zhu J et al. (47) used single-cell transcriptome and spatial transcriptomic technology to map the changes of cell heterogeneity and spatial distribution in the progression from adenocarcinoma *in situ* to microinvasive adenocarcinoma and further to invasive adenocarcinoma, and found that, with LUAD progressing from adenocarcinoma *in situ* to invasive adenocarcinoma, the spatial distribution of cancer cells became increasingly evident, and the malignant features of the tumor margin became more conspicuous, while UBE2C+cancer cell subgroup played a crucial role in promoting this process. The results of single-cell space transcriptome showed that, in adenocarcinoma in situ, there was no Treg in the cancer area, while in invasive adenocarcinoma, cancer cells recruited Treg to the cancerous regions, suggesting that Treg accumulation in the cancer area initiated the invasion process of LUAD and that TGF-β signaling pathways are involved in cancer cell interaction with the TME and spatial changes in regulating immune escape in the invasion of LUAD. The crosstalk between the components of

TME impacts the tumor progression largely by mediating the immunosuppressive phenotype. Sinjab et al. (127) found that the overlap of immune checkpoint-receptor and cytokine receptor (L-R) interactions between LUAD tumor-distal regions was reduced compared with L-R interactions between LUAD tumor-proximal regions (including adjacent tissues and moderately distant tissues). It is noteworthy that, in the samples of multiple patients, the interaction between the immune checkpoint proteins CD24 and LGALS9 in tumor epithelial cells, SIGLEC10 in dendritic cells, SIGLEC10 and HAVCR2 in macrophages increased. These intercellular interactions exhibited differential enrichment in LUAD tumor tissues and LUAD normal tissues. These findings suggested that the LUAD ecosystem had intercellular communication that promotes tumor inflammation and enhances immunosuppressive states.

Visual imaging of proteins is usually achieved by the fusion expression of antibodies or fluorescent proteins. Currently, image-based single-cell spatial proteomics improves the multiple capabilities of proteomic spatial analysis of up to nearly 100 markers, thereby expanding the number of representable cell states and cell types, and providing an opportunity to visualize and study proteins in the cellular environment (128, 129). Growing studies have shown that cell populations with the same genetic background also present differences in protein expression and protein location. The image-based spatial proteomic technology is helpful to the study of this variability since it captures the protein spatial distribution at single-cell resolution, so as to obtain the protein characteristic expression spectrum of tissues of different regions, and it is widely used in the studies of tumor cell heterogeneity, which is of great value for the analysis of TME, diagnosis and prognosis (130, 131).

Zugazagoutia J et al. (48) performed DSP spatial proteomic analysis and multiplexed immunofluorescence (mIF) detection on FFPE samples in the form of tissue microarray (TMA) in 53 patients with advanced NSCLC who had received PD-1 checkpoint inhibitor monotherapy. They demonstrated that the high-level CD56 expression in the immune cell region (CD45+) was associated with longer PFS and OS in NSCLC patients receiving PD-1 checkpoint inhibitor monotherapy. Moutafi MK et al. (49) analyzed the spatial *in situ* expression data of 71 proteins in NSCLC samples by using DSP technology, and found that the expression of CD44 in tumor cells was closely related to the prolonged OS and PFS, which can be used as an independent factor for the prediction of the clinical efficacy in patients receiving PD-1 inhibitor treatment. However, for patients without receiving immunotherapy, the high expression of CD44 in tumor cells had no prognostic effect. In addition, researchers also found that a unique immune microenvironment developed in the tumor region whose tumor cells had high expression of CD44, suggesting that the expression of an array of immunoregulatory molecules, such as PD-L1, TIM-3, ICOS and CD40, was significantly up-regulated. It showed that the expression of CD44 in lung cancer cells can function as a new independent biomarker that supplements the existing biomarkers for optimal patient stratification, and may open up a new and better immunotherapeutic strategy for lung cancer.

Although single-cell space technology remains at its early stages, spatially resolved multiplex analyses are reshaping our way to look at cellular interactions and structural relationships between tumor cells and TME cells, which affect tumor immunity and dictate patients' response to immunotherapy. Moreover, spatial localization multiple techniques can add genotypic and phenotypic dimensions to our understanding of cell interactions in the tumor immune microenvironment, and represents the next frontier in the elucidation of the mechanism underlying the resistance of lung cancer to immunotherapy. Therefore, clinical application of single-cell space technology can help us better understand the tumor response and resistance to immunotherapy.

4 Conclusion

Single-cell techniques have revolutionized our way to look at complex diseases, such as lung cancer, providing unprecedented insights into the heterogeneity of tumor cells and the tumor microenvironment. In fact, these techniques help us better understand lung cancer and its response to immunotherapy, and thereby develop more efficacious therapeutic strategies.

1. **In-depth Understanding of Tumor Heterogeneity:** By studying tumor heterogeneity at a single-cell level, researchers can identify subpopulations of cells that drive resistance to treatment, leading to the development of more personalized therapies.
2. **Characterizing Tumor-Immune Interactions:** Single-cell techniques enable the profiling of both tumor and immune cells simultaneously, shedding light on the communications and signaling pathways involved in the immune evasion and tumor progression.
3. **Discovery of Novel Biomarkers:** Single-cell analyses can identify rare cell populations or immune cell subsets that are specifically implicated in the modulation of the tumor immune response. These new biomarkers can be validated and used for patient selection.
4. **Uncovering Mechanisms Underlying Resistance:** Single-cell techniques help researchers look into the cellular and molecular mechanisms that underlie drug resistance, help us understand how tumors evolve and escape immune surveillance. This knowledge can inform the development of combination therapies that overcome resistance.
5. **Targeting Tumor-Resident Immune Cells:** Single-cell techniques aid in the identification of tumor-resident immune cells and their functional features. By targeting these cells, researchers can work out therapies to reprogram the immune response and thereby enhance anti-tumor immunity.
6. **Treatment Monitoring and Precision Medicine:** Single-cell techniques can be applied to the analysis of liquid biopsies (e.g., circulating tumor cells or cell-free DNA) from patients. This allows for non-invasive monitoring of treatment response and disease progression, informing

treatment decisions and the adjustment of therapies in real-time manner to achieve precision medicine.

Author contributions

PL, QH, JZ are equal contribution and first authorship. QHH, JL, LZ are correspondence. The authors declare that they have no competing interests.

Funding

This work was supported by the National Natural Science Foundation of China (81900095).

Conflict of interest

The authors declare that the research was conducted in the absence of any commercial or financial relationships that could be construed as a potential conflict of interest.

Publisher's note

All claims expressed in this article are solely those of the authors and do not necessarily represent those of their affiliated organizations, or those of the publisher, the editors and the reviewers. Any product that may be evaluated in this article, or claim that may be made by its manufacturer, is not guaranteed or endorsed by the publisher.

References

1. Glode AE, May MB. Immune checkpoint inhibitors: Significant advancements in non-small cell lung cancer treatment. *Am J Health Syst Pharm* (2021) 78(9):769–80. doi: 10.1093/ajhp/zxab041

2. Siegel RL, Miller KD, Fuchs HE, Jemal A. Cancer statistics, 2022. *CA Cancer J Clin* (2022) 72(1):7–33. doi: 10.3322/caac.21708

3. Gandhi L, Rodriguez-Abreu D, Gadgeel S, Esteban E, Felip E, De Angelis F, et al. Pembrolizumab plus chemotherapy in metastatic non-small-cell lung cancer. *N Engl J Med* (2018) 378(22):2078–92. doi: 10.1056/NEJMoa1801005

4. Nadal E, Massuti B, Domine M, Garcia-Campelo R, Cobo M, Felip E. Immunotherapy with checkpoint inhibitors in non-small cell lung cancer: insights from long-term survivors. *Cancer Immunol Immunother* (2019) 68(3):341–52. doi: 10.1007/s00262-019-02310-2

5. Melosky B, Cheema PK, Brade A, McLeod D, Liu G, Price PW, et al. Prolonging survival: the role of immune checkpoint inhibitors in the treatment of extensive-stage small cell lung cancer. *Oncologist* (2020) 25(11):981–92. doi: 10.1634/theoncologist.2020-0193

6. Passaro A, Brahmer J, Antonia S, Mok T, Peters S. Managing resistance to immune checkpoint inhibitors in lung cancer: treatment and novel strategies. *J Clin Oncol* (2022) 40(6):598–610. doi: 10.1200/JCO.21.01845

7. Genova C, Dellepiane C, Carrega P, Sommariva S, Ferlazzo G, Pronzato P, et al. Therapeutic implications of tumor microenvironment in lung cancer: focus on immune checkpoint blockade. *Front Immunol* (2021) 12:799455. doi: 10.3389/fimmu.2021.799455

8. Mamdani H, Matosevic S, Khalid AB, Durm G, Jalal SI. Immunotherapy in lung cancer: current landscape and future directions. *Front Immunol* (2022) 13:823618. doi: 10.3389/fimmu.2022.823618

9. Binnewies M, Roberts EW, Kersten K, Chan V, Fearon DF, Merad M, et al. Understanding the tumor immune microenvironment (TIME) for effective therapy. *Nat Med* (2018) 24(5):541–50. doi: 10.1038/s41591-018-0014-x

10. Ostman A. The tumor microenvironment controls drug sensitivity. *Nat Med* (2012) 18(9):1332–4. doi: 10.1038/nm.2938

11. Turajlic S, Sottoriva A, Graham T, Swanton C. Resolving genetic heterogeneity in cancer. *Nat Rev Genet* (2019) 20(7):404–16. doi: 10.1038/s41576-019-0114-6

12. Pe'er D, Ogawa S, Elhanani O, Keren L, Oliver TG, Wedge D. Tumor heterogeneity. *Cancer Cell* (2021) 39(8):1015–7. doi: 10.1016/j.ccell.2021.07.009

13. Vitale I, Shema E, Loi S, Galluzzi L. Intratumoral heterogeneity in cancer progression and response to immunotherapy. *Nat Med* (2021) 27(2):212–24. doi: 10.1038/s41591-021-01233-9

14. Zhang Y, Zhang Z. The history and advances in cancer immunotherapy: understanding the characteristics of tumor-infiltrating immune cells and their therapeutic implications. *Cell Mol Immunol* (2020) 17(8):807–21. doi: 10.1038/s41423-020-0488-6

15. Fan XX, Wu Q. Decoding lung cancer at single-cell level. *Front Immunol* (2022) 13:883758. doi: 10.3389/fimmu.2022.883758

16. Zhang J, Song C, Tian Y, Yang X. Single-cell RNA sequencing in lung cancer: revealing phenotype shaping of stromal cells in the microenvironment. *Front Immunol* (2021) 12:802080. doi: 10.3389/fimmu.2021.802080

17. Chong ZX, Ho WY, Yeap SK, Wang ML, Chien Y, Verusingam ND, et al. Single-cell RNA sequencing in human lung cancer: Applications, challenges, and pathway towards personalized therapy. *J Chin Med Assoc* (2021) 84(6):563–76. doi: 10.1097/JCMA.0000000000000535

18. Zhu C, Preissl S, Ren B. Single-cell multimodal omics: the power of many. *Nat Methods* (2020) 17(1):11–4. doi: 10.1038/s41592-019-0691-5

19. Stuart T, Satija R. Integrative single-cell analysis. *Nat Rev Genet* (2019) 20(5):257–72. doi: 10.1038/s41576-019-0093-7

20. Gohil SH, Iorgulescu JB, Braun DA, Keskin DB, Livak KJ. Applying high-dimensional single-cell technologies to the analysis of cancer immunotherapy. *Nat Rev Clin Oncol* (2021) 18(4):244–56. doi: 10.1038/s41571-020-00449-x

21. Davis-Marcisak EF, Deshpande A, Stein-O'Brien GL, Ho WJ, Laheru D, Jaffee EM, et al. From bench to bedside: Single-cell analysis for cancer immunotherapy. *Cancer Cell* (2021) 39(8):1062–80. doi: 10.1016/j.ccell.2021.07.004

22. Liu J, Qu S, Zhang T, Gao Y, Shi H, Song K, et al. Applications of single-cell omics in tumor immunology. *Front Immunol* (2021) 12. doi: 10.3389/fimmu.2021.697412

23. He D, Wang D, Lu P, Yang N, Xue Z, Zhu X, et al. Single-cell RNA sequencing reveals heterogeneous tumor and immune cell populations in early-stage lung adenocarcinomas harboring EGFR mutations. *Oncogene* (2021) 40(2):355–68. doi: 10.1038/s41388-020-01528-0

24. Ma KY, Schonnesen AA, Brock A, Van Den Berg C, Eckhardt SG, Liu Z, et al. Single-cell RNA sequencing of lung adenocarcinoma reveals heterogeneity of immune response-related genes. *JCI Insight* (2019) 4(4):e121387. doi: 10.1172/jci.insight.121387

25. Tian Y, Li Q, Yang Z, Zhang S, Xu J, Wang Z, et al. Single-cell transcriptomic profiling reveals the tumor heterogeneity of small-cell lung cancer. *Signal Transduct Target Ther* (2022) 7(1):346. doi: 10.1038/s41392-022-01150-4

26. Chan JM, Quintanal-Villalonga A, Gao VR, Xie Y, Allaj V, Chaudhary O, et al. Signatures of plasticity, metastasis, and immunosuppression in an atlas of human small cell lung cancer. *Cancer Cell* (2021) 39(11):1479–96 e18. doi: 10.1016/j.ccell.2021.09.008

27. Guo X, Zhang Y, Zheng L, Zheng C, Song J, Zhang Q, et al. Global characterization of T cells in non-small-cell lung cancer by single-cell sequencing. *Nat Med* (2018) 24(7):978–85. doi: 10.1038/s41591-018-0045-3

28. Zhang Y, Yang Q, Zeng X, Wang M, Dong S, Yang B, et al. MET amplification attenuates lung tumor response to immunotherapy by inhibiting STING. *Cancer Discovery* (2021) 11(11):2726–37. doi: 10.1158/2159-8290.CD-20-1500

29. Zhong R, Zhang Y, Chen D, Cao S, Han B, Zhong H. Single-cell RNA sequencing reveals cellular and molecular immune profile in a Pembrolizumab-responsive PD-L1-negative lung cancer patient. *Cancer Immunol Immunother* (2021) 70(8):2261–74. doi: 10.1007/s00262-021-02848-0

30. Liu S, Wu F, Li X, Zhao C, Jia Y, Jia K, et al. Patients with short PFS to EGFR-TKIs predicted better response to subsequent anti-PD-1/PD-L1 based immunotherapy in EGFR common mutation NSCLC. *Front Oncol* (2021) 11:639947. doi: 10.3389/fonc.2021.639947

31. Yang L, He YT, Dong S, Wei XW, Chen ZH, Zhang B, et al. Single-cell transcriptome analysis revealed a suppressive tumor immune microenvironment in EGFR mutant lung adenocarcinoma. *J Immunother Cancer* (2022) 10(2):e003534. doi: 10.1136/jitc-2021-003534

32. Zilionis R, Engblom C, Pfirschke C, Savova V, Zemmour D, Saatcioglu HD, et al. Single-cell transcriptomics of human and mouse lung cancers reveals conserved myeloid populations across individuals and species. *Immunity* (2019) 50(5):1317–34 e10. doi: 10.1016/j.immuni.2019.03.009

33. Lavin Y, Kobayashi S, Leader A, Amir ED, Elefant N, Bigenwald C, et al. Innate immune landscape in early lung adenocarcinoma by paired single-cell analyses. *Cell* (2017) 169(4):750–65 e17. doi: 10.1016/j.cell.2017.04.014

34. Kim N, Kim HK, Lee K, Hong Y, Cho JH, Choi JW, et al. Single-cell RNA sequencing demonstrates the molecular and cellular reprogramming of metastatic lung adenocarcinoma. *Nat Commun* (2020) 11(1):2285. doi: 10.1038/s41467-020-16164-1

35. Wu F, Fan J, He Y, Xiong A, Yu J, Li Y, et al. Single-cell profiling of tumor heterogeneity and the microenvironment in advanced non-small cell lung cancer. *Nat Commun* (2021) 12(1):2540. doi: 10.1038/s41467-021-22801-0

36. Karacosta LG, Anchang B, Ignatiadis N, Kimmey SC, Benson JA, Shrager JB, et al. Mapping lung cancer epithelial-mesenchymal transition states and trajectories with single-cell resolution. *Nat Commun* (2019) 10(1):5587. doi: 10.1038/s41467-019-13441-6

37. Shaul ME, Eyal O, Guglietta S, Aloni P, Zlotnik A, Forkosh E, et al. Circulating neutrophil subsets in advanced lung cancer patients exhibit unique immune signature and relate to prognosis. *FASEB J* (2020) 34(3):4204–18. doi: 10.1096/fj.201902467R

38. Sorin M, Rezanejad M, Karimi E, Fiset B, Desharnais L, Perus LJM, et al. Single-cell spatial landscapes of the lung tumour immune microenvironment. *Nature* (2023) 614(7948):548–54. doi: 10.1038/s41586-022-05672-3

39. Sorin M, Karimi E, Rezanejad M, Yu MW, Desharnais L, McDowell SAC, et al. Single-cell spatial landscape of immunotherapy response reveals mechanisms of CXCL13 enhanced antitumor immunity. *J Immunother Cancer* (2023) 11(2): e005545. doi: 10.1136/jitc-2022-005545

40. Leader AM, Grout JA, Maier BB, Nabet BY, Park MD, Tabachnikova A, et al. Single-cell analysis of human non-small cell lung cancer lesions refines tumor classification and patient stratification. *Cancer Cell* (2021) 39(12):1594–609 e12. doi: 10.1016/j.ccell.2021.10.009

41. Hanada KI, Zhao C, Gil-Hoyos R, Gartner JJ, Chow-Parmer C, Lowery FJ, et al. A phenotypic signature that identifies neoantigen-reactive T cells in fresh human lung cancers. *Cancer Cell* (2022) 40(5):479–93 e6. doi: 10.1016/j.ccell.2022.03.012

42. Ma Y, Liu F, Li B, Zhou H, Qiao D, Deng L, et al. Rapid identification of tumor-reactive T-cell receptors by RNA preamplification-based single-cell sequencing. *J Immunol Methods* (2022) 504:113260. doi: 10.1016/j.jim.2022.113260

43. Ott PA, Hu-Lieskovan S, Chmielowski B, Govindan R, Naing A, Bhardwaj N, et al. A phase ib trial of personalized neoantigen therapy plus anti-PD-1 in patients with advanced melanoma, non-small cell lung cancer, or bladder cancer. *Cell* (2020) 183 (2):347–62 e24. doi: 10.1016/j.cell.2020.08.053

44. Hui Z, Zhang J, Ren Y, Li X, Yan C, Yu W, et al. Single-cell profiling of immune cells after neoadjuvant pembrolizumab and chemotherapy in IIIA non-small cell lung cancer (NSCLC). *Cell Death Dis* (2022) 13(7):607. doi: 10.1038/s41419-022-05057-4

45. Zhang F, Bai H, Gao R, Fei K, Duan J, Zhang Z, et al. Dynamics of peripheral T cell clones during PD-1 blockade in non-small cell lung cancer. *Cancer Immunol Immunother* (2020) 69(12):2599–611. doi: 10.1007/s00262-020-02642-4

46. Gueguen P, Metoikidou C, Dupic T, Lawand M, Goudot C, Baulande S, et al. Contribution of resident and circulating precursors to tumor-infiltrating CD8(+) T cell populations in lung cancer. *Sci Immunol* (2021) 6(55):eabd5778. doi: 10.1126/sciimmunol.abd5778

47. Zhu J, Fan Y, Xiong Y, Wang W, Chen J, Xia Y, et al. Delineating the dynamic evolution from preneoplasia to invasive lung adenocarcinoma by integrating single-cell RNA sequencing and spatial transcriptomics. *Exp Mol Med* (2022) 54(11):2060–76. doi: 10.1038/s12276-022-00896-9

48. Zugazagoitia J, Gupta S, Liu Y, Fuhrman K, Gettinger S, Herbst RS, et al. Biomarkers associated with beneficial PD-1 checkpoint blockade in non-small cell lung cancer (NSCLC) identified using high-plex digital spatial profiling. *Clin Cancer Res* (2020) 26(16):4360–8. doi: 10.1158/1078-0432.CCR-20-0175

49. Moutafi MK, Molero M, Martinez Morilla S, Baena J, Vathiotis IA, Gavrielatou N, et al. Spatially resolved proteomic profiling identifies tumor cell CD44 as a biomarker associated with sensitivity to PD-1 axis blockade in advanced non-small-cell lung cancer. *J Immunother Cancer* (2022) 10(8):e004757. doi: 10.1136/jitc-2022-004757

50. Elmentaite R, Dominguez Conde C, Yang L, Teichmann SA. Single-cell atlases: shared and tissue-specific cell types across human organs. *Nat Rev Genet* (2022) 23 (7):395–410. doi: 10.1038/s41576-022-00449-w

51. Travaglini KJ, Nabhan AN, Penland L, Sinha R, Gillich A, Sit RV, et al. A molecular cell atlas of the human lung from single-cell RNA sequencing. *Nature* (2020) 587(7835):619–25. doi: 10.1038/s41586-020-2922-4

52. Jovic D, Liang X, Zeng H, Lin L, Xu F, Luo Y. Single-cell RNA sequencing technologies and applications: A brief overview. *Clin Transl Med* (2022) 12(3):e694. doi: 10.1002/ctm2.694

53. Chen G, Ning B, Shi T. Single-cell RNA-seq technologies and related computational data analysis. *Front Genet* (2019) 10:317. doi: 10.3389/fgene.2019.00317

54. Qi R, Ma A, Ma Q, Zou Q. Clustering and classification methods for single-cell RNA-sequencing data. *Brief Bioinform* (2020) 21(4):1196–208. doi: 10.1093/bib/bbz062

55. Luecken MD, Theis FJ. Current best practices in single-cell RNA-seq analysis: a tutorial. *Mol Syst Biol* (2019) 15(6):e8746. doi: 10.15252/msb.20188746

56. Saelens W, Cannoodt R, Todorov H, Saeys Y. A comparison of single-cell trajectory inference methods. *Nat Biotechnol* (2019) 37(5):547–54. doi: 10.1038/s41587-019-0071-9

57. Lahnemann D, Koster J, Szczurek E, McCarthy DJ, Hicks SC, Robinson MD, et al. Eleven grand challenges in single-cell data science. *Genome Biol* (2020) 21(1):31. doi: 10.1186/s13059-020-1926-6

58. Maynard A, McCoach CE, Rotow JK, Harris L, Haderk F, Kerr DL, et al. Therapy-induced evolution of human lung cancer revealed by single-cell RNA sequencing. *Cell* (2020) 182(5):1232–51 e22. doi: 10.1016/j.cell.2020.07.017

59. Lee CK, Man J, Lord S, Cooper W, Links M, Gebski V, et al. Clinical and molecular characteristics associated with survival among patients treated with checkpoint inhibitors for advanced non-small cell lung carcinoma: A systematic review and meta-analysis. *JAMA Oncol* (2018) 4(2):210–6. doi: 10.1001/jamaoncol.2017.4427

60. Herbst RS, Heymach JV, Lippman SM. Lung cancer. *N Engl J Med* (2008) 359 (13):1367–80. doi: 10.1056/NEJMra0802714

61. Yamada T, Hirai S, Katayama Y, Yoshimura A, Shiotsu S, Watanabe S, et al. Retrospective efficacy analysis of immune checkpoint inhibitors in patients with EGFR-mutated non-small cell lung cancer. *Cancer Med* (2019) 8(4):1521–9. doi: 10.1002/cam4.2037

62. Yoshida H, Kim YH, Ozasa H, Nagai H, Sakamori Y, Tsuji T, et al. Nivolumab in non-small-cell lung cancer with EGFR mutation. *Ann Oncol* (2018) 29(3):777–8. doi: 10.1093/annonc/mdx745

63. Belli C, Trapani D, Viale G, D'Amico P, Duso BA, Della Vigna P, et al. Targeting the microenvironment in solid tumors. *Cancer Treat Rev* (2018) 65:22–32. doi: 10.1016/j.ctrv.2018.02.004

64. Domagala M, Laplagne C, Leveque E, Laurent C, Fournie JJ, Espinosa E, et al. Cancer cells resistance shaping by tumor infiltrating myeloid cells. *Cancers (Basel)* (2021) 13(2):165. doi: 10.3390/cancers13020165

65. Awad RM, De Vlaeminck Y, Maebe J, Goyvaerts C, Breckpot K. Turn back the TIMe: targeting tumor infiltrating myeloid cells to revert cancer progression. *Front Immunol* (2018) 9:1977. doi: 10.3389/fimmu.2018.01977

66. Lambrechts D, Wauters E, Boeckx B, Aibar S, Nittner D, Burton O, et al. Phenotype molding of stromal cells in the lung tumor microenvironment. *Nat Med* (2018) 24(8):1277–89. doi: 10.1038/s41591-018-0096-5

67. Kieffer Y, Hocine HR, Gentric G, Pelon F, Bernard C, Bourachot B, et al. Single-cell analysis reveals fibroblast clusters linked to immunotherapy resistance in cancer. *Cancer Discovery* (2020) 10(9):1330–51. doi: 10.1158/2159-8290.CD-19-1384

68. Efremova M, Vento-Tormo M, Teichmann SA, Vento-Tormo R. CellPhoneDB: inferring cell-cell communication from combined expression of multi-subunit ligand-receptor complexes. *Nat Protoc* (2020) 15(4):1484–506. doi: 10.1038/s41596-020-0292-x

69. Jin S, Guerrero-Juarez CF, Zhang L, Chang I, Ramos R, Kuan CH, et al. Inference and analysis of cell-cell communication using CellChat. *Nat Commun* (2021) 12(1):1088. doi: 10.1038/s41467-021-21246-9

70. Zeng Z, Li W, Zhang D, Zhang C, Jiang X, Guo R, et al. Development of a chemoresistant risk scoring model for prechemotherapy osteosarcoma using single-cell sequencing. *Front Oncol* (2022) 12:893282. doi: 10.3389/fonc.2022.893282

71. Browaeys R, Saelens W, Saeys Y. NicheNet: modeling intercellular communication by linking ligands to target genes. *Nat Methods* (2020) 17(2):159–62. doi: 10.1038/s41592-019-0667-5

72. Baslan T, Hicks J. Unravelling biology and shifting paradigms in cancer with single-cell sequencing. *Nat Rev Cancer* (2017) 17(9):557–69. doi: 10.1038/nrc.2017.58

73. Kharchenko PV. The triumphs and limitations of computational methods for scRNA-seq. *Nat Methods* (2021) 18(7):723–32. doi: 10.1038/s41592-021-01171-x

74. van den Brink SC, Sage F, Vertesy A, Spanjaard B, Peterson-Maduro J, Baron CS, et al. Single-cell sequencing reveals dissociation-induced gene expression in tissue subpopulations. *Nat Methods* (2017) 14(10):935–6. doi: 10.1038/nmeth.4437

75. Denisenko E, Guo BB, Jones M, Hou R, de Kock L, Lassmann T, et al. Systematic assessment of tissue dissociation and storage biases in single-cell and single-nucleus RNA-seq workflows. *Genome Biol* (2020) 21(1):130. doi: 10.1186/s13059-020-02048-6

76. Grindberg RV, Yee-Greenbaum JL, McConnell MJ, Novotny M, O'Shaughnessy AL, Lambert GM, et al. RNA-sequencing from single nuclei. *Proc Natl Acad Sci U S A* (2013) 110(49):19802–7. doi: 10.1073/pnas.1319700110

77. Habib N, Li Y, Heidenreich M, Swiech L, Avraham-Davidi I, Trombetta JJ, et al. Div-Seq: Single-nucleus RNA-Seq reveals dynamics of rare adult newborn neurons. *Science* (2016) 353(6302):925–8. doi: 10.1126/science.aad7038

78. Wu H, Kirita Y, Donnelly EL, Humphreys BD. Advantages of single-nucleus over single-cell RNA sequencing of adult kidney: rare cell types and novel cell states revealed in fibrosis. *J Am Soc Nephrol* (2019) 30(1):23–32. doi: 10.1681/ASN.2018090912

79. Koenitzer JR, Wu H, Atkinson JJ, Brody SL, Humphreys BD. Single-nucleus RNA-sequencing profiling of mouse lung. Reduced dissociation bias and improved rare cell-type detection compared with single-cell RNA sequencing. *Am J Respir Cell Mol Biol* (2020) 63(6):739–47.

80. Perkel JM. Single-cell proteomics takes centre stage. *Nature* (2021) 597 (7877):580–2. doi: 10.1038/d41586-021-02530-6

81. Vistain LF, Tay S. Single-cell proteomics. *Trends Biochem Sci* (2021) 46(8):661–72. doi: 10.1016/j.tibs.2021.01.013

82. Kelly RT. Single-cell proteomics: progress and prospects. *Mol Cell Proteomics* (2020) 19(11):1739–48. doi: 10.1074/mcp.R120.002234

83. Iyer A, Hamers AAJ, Pillai AB. CyTOF((R)) for the masses. *Front Immunol* (2022) 13:815828. doi: 10.3389/fimmu.2022.815828

84. Chang Q, Ornatsky OI, Siddiqui I, Loboda A, Baranov VI, Hedley DW. Imaging mass cytometry. *Cytometry A* (2017) 91(2):160–9. doi: 10.1002/cyto.a.23053

85. Le Rochais M, Hemon P, Pers JO, Uguen A. Application of high-throughput imaging mass cytometry hyperion in cancer research. *Front Immunol* (2022) 13:859414. doi: 10.3389/fimmu.2022.859414

86. Lee TL. Single cell genomics. *Int J Biochem Cell Biol* (2019) 116:105596. doi: 10.1016/j.biocel.2019.105596

87. Bohrson CL, Barton AR, Lodato MA, Rodin RE, Luquette LJ, Viswanadham VV, et al. Linked-read analysis identifies mutations in single-cell DNA-sequencing data. *Nat Genet* (2019) 51(4):749–54. doi: 10.1038/s41588-019-0366-2

88. Lim B, Lin Y, Navin N. Advancing cancer research and medicine with single-cell genomics. *Cancer Cell* (2020) 37(4):456–70. doi: 10.1016/j.ccell.2020.03.008

89. Huang L, Ma F, Chapman A, Lu S, Xie XS. Single-cell whole-genome amplification and sequencing: methodology and applications. *Annu Rev Genomics Hum Genet* (2015) 16:79–102. doi: 10.1146/annurev-genom-090413-025352

90. Gawad C, Koh W, Quake SR. Single-cell genome sequencing: current state of the science. *Nat Rev Genet* (2016) 17(3):175–88. doi: 10.1038/nrg.2015.16

91. Su Z, Wang Z, Ni X, Duan J, Gao Y, Zhuo M, et al. Inferring the evolution and progression of small-cell lung cancer by single-cell sequencing of circulating tumor cells. *Clin Cancer Res* (2019) 25(16):5049–60. doi: 10.1158/1078-0432.CCR-18-3571

92. Ni X, Zhuo M, Su Z, Duan J, Gao Y, Wang Z, et al. Reproducible copy number variation patterns among single circulating tumor cells of lung cancer patients. *Proc Natl Acad Sci U S A* (2013) 110(52):21083–8. doi: 10.1073/pnas.1320659110

93. Chen J, Facchinetti F, Braye F, Yurchenko AA, Bigot L, Ponce S, et al. Single-cell DNA-seq depicts clonal evolution of multiple driver alterations in osimertinib-resistant patients. *Ann Oncol* (2022) 33(4):434–44. doi: 10.1016/j.annonc.2022.01.004

94. Preissl S, Gaulton KJ, Ren B. Characterizing cis-regulatory elements using single-cell epigenomics. *Nat Rev Genet* (2023) 24(1):21–43. doi: 10.1038/s41576-022-00509-1

95. Harada A, Kimura H, Ohkawa Y. Recent advances in single-cell epigenomics. *Curr Opin Struct Biol* (2021) 71:116–22. doi: 10.1016/j.sbi.2021.06.010

96. Mimitou EP, Lareau CA, Chen KY, Zorzetto-Fernandes AL, Hao Y, Takeshima Y, et al. Scalable, multimodal profiling of chromatin accessibility, gene expression and protein levels in single cells. *Nat Biotechnol* (2021) 39(10):1246–58. doi: 10.1038/s41587-021-00927-2

97. Cao J, Cusanovich DA, Ramani V, Aghamirzaie D, Pliner HA, Hill AJ, et al. Joint profiling of chromatin accessibility and gene expression in thousands of single cells. *Science* (2018) 361(6409):1380–5. doi: 10.1126/science.aau0730

98. Reyes M, Billman K, Hacohen N, Blainey PC. Simultaneous profiling of gene expression and chromatin accessibility in single cells. *Adv Biosyst* (2019) 3(11):1900065. doi: 10.1002/adbi.201900065

99. Kelsey G, Stegle O, Reik W. Single-cell epigenomics: Recording the past and predicting the future. *Science* (2017) 358(6359):69–75. doi: 10.1126/science.aan6826

100. Shema E, Bernstein BE, Buenrostro JD. Single-cell and single-molecule epigenomics to uncover genome regulation at unprecedented resolution. *Nat Genet* (2019) 51(1):19–25. doi: 10.1038/s41588-018-0290-x

101. Ludwig CH, Bintu L. Mapping chromatin modifications at the single cell level. *Development* (2019) 146(12):dev170217. doi: 10.1242/dev.170217

102. Wang Z, Tu K, Xia L, Luo K, Luo W, Tang J, et al. The open chromatin landscape of non-small cell lung carcinoma. *Cancer Res* (2019) 79(19):4840–54. doi: 10.1158/0008-5472.CAN-18-3663

103. LaFave LM, Kartha VK, Ma S, Meli K, Del Priore I, Lareau C, et al. Epigenomic state transitions characterize tumor progression in mouse lung adenocarcinoma. *Cancer Cell* (2020) 38(2):212–28 e13. doi: 10.1016/j.ccell.2020.06.006

104. Hao Y, Hao S, Andersen-Nissen E, Mauck WM 3rd, Zheng S, Butler A, et al. Integrated analysis of multimodal single-cell data. *Cell* (2021) 184(13):3573–87 e29. doi: 10.1016/j.cell.2021.04.048

105. Stoeckius M, Hafemeister C, Stephenson W, Houck-Loomis B, Chattopadhyay PK, Swerdlow H, et al. Simultaneous epitope and transcriptome measurement in single cells. *Nat Methods* (2017) 14(9):865–8. doi: 10.1038/nmeth.4380

106. Chen S, Lake BB, Zhang K. High-throughput sequencing of the transcriptome and chromatin accessibility in the same cell. *Nat Biotechnol* (2019) 37(12):1452–7. doi: 10.1038/s41587-019-0290-0

107. Gaiti F, Chaligne R, Gu H, Brand RM, Kothen-Hill S, Schulman RC, et al. Epigenetic evolution and lineage histories of chronic lymphocytic leukaemia. *Nature* (2019) 569(7757):576–80. doi: 10.1038/s41586-019-1198-z

108. Clark SJ, Argelaguet R, Kapourani CA, Stubbs TM, Lee HJ, Alda-Catalinas C, et al. scNMT-seq enables joint profiling of chromatin accessibility DNA methylation and transcription in single cells. *Nat Commun* (2018) 9(1):781. doi: 10.1038/s41467-018-03149-4

109. Rodriques SG, Stickels RR, Goeva A, Martin CA, Murray E, Vanderburg CR, et al. Slide-seq: A scalable technology for measuring genome-wide expression at high spatial resolution. *Science* (2019) 363(6434):1463–7. doi: 10.1126/science.aaw1219

110. Vickovic S, Eraslan G, Salmen F, Klughammer J, Stenbeck L, Schapiro D, et al. High-definition spatial transcriptomics for in *situ* tissue profiling. *Nat Methods* (2019) 16(10):987–90. doi: 10.1038/s41592-019-0548-y

111. Ma A, Xin G, Ma Q. The use of single-cell multi-omics in immuno-oncology. *Nat Commun* (2022) 13(1):2728. doi: 10.1038/s41467-022-30549-4

112. Zhang L, Zhang Y, Wang C, Yang Y, Ni Y, Wang Z, et al. Integrated single-cell RNA sequencing analysis reveals distinct cellular and transcriptional modules associated with survival in lung cancer. *Signal Transduct Target Ther* (2022) 7(1):9. doi: 10.1038/s41392-021-00824-9

113. Davis MM. T cell receptor gene diversity and selection. *Annu Rev Biochem* (1990) 59:475–96. doi: 10.1146/annurev.bi.59.070190.002355

114. Yang JC, Rosenberg SA. Adoptive T-cell therapy for cancer. *Adv Immunol* (2016) 130:279–94. doi: 10.1016/bs.ai.2015.12.006

115. Pai JA, Satpathy AT. High-throughput and single-cell T cell receptor sequencing technologies. *Nat Methods* (2021) 18(8):881–92. doi: 10.1038/s41592-021-01201-8

116. Zhang SQ, Ma KY, Schonnesen AA, Zhang M, He C, Sun E, et al. High-throughput determination of the antigen specificities of T cell receptors in single cells. *Nat Biotechnol* (2018) 10.1038/nbt.4282. doi: 10.1101/457069

117. Segaliny AI, Li G, Kong L, Ren C, Chen X, Wang JK, et al. Functional TCR T cell screening using single-cell droplet microfluidics. *Lab Chip* (2018) 18(24):3733–49. doi: 10.1039/C8LC00818C

118. Sun R, Hu Z, Sottoriva A, Graham TA, Harpak A, Ma Z, et al. Between-region genetic divergence reflects the mode and tempo of tumor evolution. *Nat Genet* (2017) 49(7):1015–24. doi: 10.1038/ng.3891

119. Waclaw B, Bozic I, Pittman ME, Hruban RH, Vogelstein B, Nowak MA. A spatial model predicts that dispersal and cell turnover limit intratumour heterogeneity. *Nature* (2015) 525(7568):261–4. doi: 10.1038/nature14971

120. Jamal-Hanjani M, Wilson GA, McGranahan N, Birkbak NJ, Watkins TBK, Veeriah S, et al. Tracking the evolution of non-small-cell lung cancer. *N Engl J Med* (2017) 376(22):2109–21. doi: 10.1056/NEJMoa1616288

121. Park J, Kim J, Lewy T, Rice CM, Elemento O, Rendeiro AF, et al. Spatial omics technologies at multimodal and single cell/subcellular level. *Genome Biol* (2022) 23 (1):256. doi: 10.1186/s13059-022-02824-6

122. Gerdes MJ, Sevinsky CJ, Sood A, Adak S, Bello MO, Bordwell A, et al. Highly multiplexed single-cell analysis of forMalin-fixed, paraffin-embedded cancer tissue. *Proc Natl Acad Sci U S A* (2013) 110(29):11982–7. doi: 10.1073/pnas.1300136110

123. Longo SK, Guo MG, Ji AL, Khavari PA. Integrating single-cell and spatial transcriptomics to elucidate intercellular tissue dynamics. *Nat Rev Genet* (2021) 22 (10):627–44. doi: 10.1038/s41576-021-00370-8

124. Shen X, Zhao Y, Wang Z, Shi Q. Recent advances in high-throughput single-cell transcriptomics and spatial transcriptomics. *Lab Chip* (2022) 22(24):4774–91. doi: 10.1039/D2LC00633B

125. Ahmed R, Zaman T, Chowdhury F, Mraiche F, Tariq M, Ahmad IS, et al. Single-cell RNA sequencing with spatial transcriptomics of cancer tissues. *Int J Mol Sci* (2022) 23(6):3042. doi: 10.3390/ijms23063042

126. Saltz J, Gupta R, Hou L, Kurc T, Singh P, Nguyen V, et al. Spatial organization and molecular correlation of tumor-infiltrating lymphocytes using deep learning on pathology images. *Cell Rep* (2018) 23(1):181–93 e7.

127. Sinjab A, Han G, Treekitkarnmongkol W, Hara K, Brennan PM, Dang M, et al. Resolving the spatial and cellular architecture of lung adenocarcinoma by multiregion single-cell sequencing. *Cancer Discovery* (2021) 11(10):2506–23. doi: 10.1158/2159-8290.CD-20-1285

128. Mund A, Brunner AD, Mann M. Unbiased spatial proteomics with single-cell resolution in tissues. *Mol Cell* (2022) 82(12):2335–49. doi: 10.1016/j.molcel.2022.05.022

129. Liu X, Mao D, Song Y, Zhu L, Isak AN, Lu C, et al. Computer-aided design of reversible hybridization chain reaction (CAD-HCR) enables multiplexed single-cell spatial proteomics imaging. *Sci Adv* (2022) 8(2):eabk0133. doi: 10.1126/sciadv.abk0133

130. Mund A, Coscia F, Kriston A, Hollandi R, Kovacs F, Brunner AD, et al. Deep Visual Proteomics defines single-cell identity and heterogeneity. *Nat Biotechnol* (2022) 40(8):1231–40. doi: 10.1038/s41587-022-01302-5

131. van Ineveld RL, Kleinnijenhuis M, Alieva M, de Blank S, Barrera ROman M, van Vliet EJ, et al. Revealing the spatio-phenotypic patterning of cells in healthy and tumor tissues with mLSR-3D and STAPL-3D. *Nat Biotechnol* (2021) 39(10):1239–45. doi: 10.1038/s41587-021-00926-3

frontiers | Frontiers in Oncology

TYPE Original Research
PUBLISHED 21 August 2023
DOI 10.3389/fonc.2023.1228889

Check for updates

OPEN ACCESS

EDITED BY
Jie Mei,
Wuxi People's Hospital Affiliated to Nanjing Medical University, China

REVIEWED BY
Qiang Lu,
Tangdu Hospital, China
Cailian Wang,
Southeast University, China

*CORRESPONDENCE
Li Wang
wangli37029192@sina.com
Feng Luo
luofeng66666@sina.com

RECEIVED 25 May 2023
ACCEPTED 24 July 2023
PUBLISHED 21 August 2023

CITATION
He M, He Y, Xu J, Zhang Y, Cao X, Wang L and Luo F (2023) Upregulated FADD is associated with poor prognosis, immune exhaustion, tumor malignancy, and immunotherapy resistance in patients with lung adenocarcinoma.
Front. Oncol. 13:1228889.
doi: 10.3389/fonc.2023.1228889

COPYRIGHT
© 2023 He, He, Xu, Zhang, Cao, Wang and Luo. This is an open-access article distributed under the terms of the Creative Commons Attribution License (CC BY). The use, distribution or reproduction in other forums is permitted, provided the original author(s) and the copyright owner(s) are credited and that the original publication in this journal is cited, in accordance with accepted academic practice. No use, distribution or reproduction is permitted which does not comply with these terms.

Upregulated FADD is associated with poor prognosis, immune exhaustion, tumor malignancy, and immunotherapy resistance in patients with lung adenocarcinoma

Miao He[1,2], Yingying He[1,2], Jian Xu[1,2], Youcai Zhang[2], Xiaoyu Cao[2], Li Wang[1*] and Feng Luo[1*]

[1]Lung Cancer Center, West China Hospital, Sichuan University, Chengdu, China, [2]Department of Oncology, Deyang People's Hospital, Chengdu, China

Background: FAS-associated death structural domain (FADD) proteins are important proteins that regulate apoptosis and are also involved in many nonapoptotic pathways in tumors. However, how dysregulated FADD affects the development of lung adenocarcinoma (LUAD) remains unknown.

Method: Transcriptome profiles and corresponding clinical information of LUAD patients were convened from different databases, and the results were validated by qRT–PCR and cell counting kit-8 using LUAD cell lines. Potential associations between FADD and tumor malignancy, the immune microenvironment, genomic stability, and treatment sensitivity in LUAD patients were revealed by systematic bioinformatics analysis.

Results: FADD was significantly overexpressed in LUAD, and patients with higher expression levels of FADD had a worse prognosis and more advanced tumor stage. Functional analysis revealed that elevated expression of FADD was associated with cell cycle dysregulation, angiogenesis, and metabolic disturbances. In addition, overexpression of FADD was associated with a higher infiltration of suppressive immune cells. From a single-cell perspective, cells with lower FADD expression are more active in immune-related pathways. FADD was associated with more genomic mutations, especially TP53. Patients with high FADD expression are more likely to benefit from conventional chemotherapy, while those with low FADD expression are more suitable for immunotherapy.

Conclusions: Upregulated FADD is associated with worse prognosis, immune exhaustion, and tumor malignancy in LUAD patients. In addition, FADD can be an efficient indicator for assessing sensitivity to chemotherapy and immunotherapy. Therefore, FADD has the potential to serve as a new target for precision medicine and targeted therapy for LUAD.

KEYWORDS

lung adenocarcinoma (LUAD), Fas-associated death domain protein (FADD), prognosis, immune microenvironment, Immunotherapy

Introduction

Lung cancer is currently one of the most common malignancies worldwide and is the leading cause of death due to cancer (1). In particular, lung adenocarcinoma (LUAD) is the most common histopathological type of lung cancer, accounting for approximately more than half of all diagnosed lung cancer cases (2). In recent years, the incidence and mortality rates of LUAD have remained elevated, although advances in medical technology and clinical protocols have driven advances in diagnostic and therapeutic approaches (2). One of the biggest existing challenges is that the symptoms of early-stage LUAD are not obvious, resulting in many patients being diagnosed at an advanced stage and unfortunately missing the best opportunity for treatment. Fortunately, the development of molecularly targeted drugs and immunotherapies has led to more possibilities for the treatment of advanced LUAD (3). In addition, big data approaches and technologies of whole genome precision sequencing have provided breakthrough tools for the study of the pathogenesis and progression of LUAD, offering the possibility of individualized precision medicine (4). However, despite some advances, prevention, early diagnosis and treatment of LUAD still face great challenges due to its complexity and heterogeneity.

FADD (Fas-associated death domain protein) is an intracellular protein that plays a key role in the process of programmed cell death or apoptosis (5). FADD interacts with various proteins through its death domain (DD) and death effector domain (DED), leading to the activation of the caspase protein family and ultimately inducing apoptosis (6). In many cases, excessive activity or inhibition of FADD can have an effect on cell survival, especially in cases of cancer, immune diseases, and viral infections (7). For example, FADD expression may be increased in certain types of solid tumors (such as LUAD, glioma, and hepatocellular carcinoma), which may lead to enhanced cell death signaling and prevent the growth of cancer cells (8). Conversely, deletion or decreased expression of FADD may lead to cellular resistance to apoptotic signaling, which can lead to tumor development and growth (8). For example, FADD expression levels may be decreased in certain types of cancer, which may lead to resistance of tumor cells to apoptotic signaling (5). In these cases, restoring or increasing the expression of FADD may help restore sensitivity to apoptotic signals and stop further tumor development (5).

Immunotherapy is a revolutionary approach to cancer treatment designed to attack cancer cells by enhancing or altering the patient's own immune system (9). FADD may influence the immune system's response to cancer by regulating T-cell activity and viability (10). For example, the absence or loss of function of FADD may lead to reduced T-cell activity, which in turn may affect the effectiveness of immunotherapy (10, 11). In other studies, FADD activity has also been found to be associated with the immune escape mechanism of cancer cells. For example, certain types of cancer may resist apoptosis mediated by cytotoxic T cells or natural killer cells by reducing FADD activity (12). In recent years, studies targeting FADD have provided many important insights into its function and regulatory mechanisms, as well as the possibility of designing potential therapeutic strategies for cancer and other diseases (8). However, further studies are still needed to fully understand the specific role of FADD in cellular physiological and pathological processes.

Based on multiple LUAD datasets and a pancancer database, this study systematically explored the potential of FADD as an oncogene and prognostic marker. The correlation of FADD expression with the prognosis of LUAD patients, potential pathogenic mechanisms, dysregulated biological pathways, immune exhaustion, genomic instability, and therapeutic sensitivity was further evaluated. Our study aims to provide potential evidence to support novel precision medicine and targeted therapies for LUAD.

Material and methods

Data access and processing

We collected compliant LUAD sequencing datasets from two different databases. First, the count matrix of the TCGA-LUAD dataset, the maf format files of genomic mutant sites, and the corresponding clinical information were collected from the UCSC-Xena database (https://xena.ucsc.edu/). We included only patients without missing clinical information, containing a total of 492 LUAD patients, and used the count matrix as a development cohort after normalizing it to a transcripts per kilobase million (TPM) matrix. In addition, we collected the pancancer dataset from UCSC Xena. Three compliant LUAD datasets were retrieved from the GEO database (http://www.ncbi.nlm.nih.gov/geo/) and convened: GSE30219 (GPL570 Platform), GSE42127 (GPL6884 Platform), and GSE72094 (GPL15048 Platform). After including

patients diagnosed with LUAD among them, the "sva" package was used to integrate the three datasets to remove batch effects between platforms (13), resulting in a meta-GEO dataset of 615 patients with LUAD for external validation. Finally, the single-cell dataset GSE131907 of LUAD was collected without additional processing and analyzed according to the original parameters (14). We used the "seurat" package to preprocess and analyze the single-cell data. In short, we log-normalized the data by "NormalizeData". Subsequently, 1500 feature variables in the dataset were identified by "FindVariableFeatures". PCA analysis was performed on the data set based on the 1500 feature variables. Finally, neighbors and cell clusters were identified by the first 40 principal components.

Cell culture and transfection

We obtained two lung cancer cell lines (HCC827 and A849) and a normal lung epithelial cell line (16HBE) from GAINING-Bioscience (China). These cells were cultured in DMEM (Biological, Israel) supplemented with 10% heat-inactivated FBS, 1% penicillin, and 1% streptomycin. The cells were grown at a constant temperature of 37°C and with 5% CO2. We used Lipofectamine 8000 reagent (Invitrogen, USA) for transient transfection of siRNA according to the manufacturer's instructions, aiming to suppress the expression of specific genes. The siRNAs used and their corresponding blank controls were as follows: si-FADD: GGAAGAAGACCTGTGTGCAGCATTT; siNC: GGAAGAAGTCCGTGTCGACAGATTT.

qRT–PCR

Whole RNA was extracted using TRIzol reagent (Invitrogen, CA, USA) according to the instructions. cDNA of FADD was amplified according to the following primers: Forward: CATCTACCTCCGAAGCGTCC; Reverse: GGGCTACCTTCCT GGAGAGA. The 7500 Fast Real-time PCR system (Thermo Fisher, USA) was used for gene quantification according to the instructions, and the internal reference was GAPDH.

Cell counting Kit-8 assay

Following the operating manual of the kit, we applied the Cell Counting Kit-8 (CCK-8, Bioss, China) to detect the growth activity of various LUAD cell lines. An enzyme-linked immuno-absorbance assay (BioTek, USA) was used to reflect the cell numbers by measuring the absorbance at 450 nm during cell growth.

FADD-related functional enrichment

To assess the significant biological pathways of subgroups with different levels of FADD, we first identified significantly differentially expressed genes (DEGs) among FADD subgroups based on a threshold of fold change>2 and adjusted p value<0.05 utilizing the "limma" package. Functional annotation and enrichment analysis of DEGs were achieved through the Metascape online database (https://metascape.or). The differentially enriched pathways among different FADD subgroups were subsequently analyzed and identified by GSEA software (version 4.0.1) based on the KEGG background database.

Dissecting the immune microenvironment associated with FADD

We systematically analyzed the heterogeneity of the immune microenvironment in different FADD subgroups from different perspectives. First, we evaluated the differences in cell types among different FADD subgroups from a single-cell perspective and assessed the cellular interaction pathways between cells with different FADD levels using the "CellChat" R package (15). The immune scores between different FADD subgroups were generated by the "ESTIMATE" algorithm (16). Subsequently, ssGSEA was executed by the "gsva" package to assess the relative activity of tumor immune-related pathways among different FADD subgroups (17). Finally, the abundance of immune cell infiltration among FADD subgroups was assessed by the "Cibersort" algorithm containing the reference expression profiles of 22 immune cells (18).

Dissecting FADD-associated gene mutations

We collected homologous recombination defect (HRD) scores and MSI scores of different LUAD patients in the TCGA cohort from previous studies and assessed the differences between different FADD subgroups by "ggpubr" (19). We processed the raw maf files using "maftools" and calculated the tumor mutation burden (TMB) of individual patients after excluding nonsense mutated fragments (20). We classified significantly mutated genes according to a threshold of mutation number >45 and evaluated their differences and mutational cooccurrence among different FADD subgroups.

Assessment of treatment sensitivity among FADD subgroups

Based on the ridge regression algorithm in the R package "pRRhetic", we evaluated the differences in sensitivity of five first-line lung adenocarcinoma chemotherapeutic agents among different FADD subgroups (21). The results were generated as the patient's half-maximal inhibitory concentration (IC50) values for a given drug, with lower IC50 values being more sensitive to treatment. We then assessed the sensitivity of patients to immunotherapy based on the level of immune cell exhaustion using the TIDE algorithm (22). Finally, we assessed the similarity of the expression profiles of the TCGA and Meta-GEO cohorts to the immunotherapy cohort by the subclass mapping algorithm and generated the sensitivity to anti-PD-1 and anti-CTLA-4 treatments.

Statistical analysis

We used R software (Version 4.1.0) and GraphPad Prism 9.0 to analyze the data and draw figures. Appropriate t tests or Wilcoxon tests were applied to compare differences between the two subgroups according to the data structure. $\chi 2$ tests were used to compare differences in percentages. The significance of survival prediction was assessed by the log-rank test and univariate and multivariate Cox regression. The correlation of continuous variables was examined by Pearson's coefficient. The threshold of significance was set at P<0.05.

Results

The pancancer perspective of FADD

In the TCGA database, the mRNA levels of FADD were significantly overexpressed in 27 solid malignancy tissues, including LUAD (P < 0.05, Figure 1A). Survival analysis from a pancancer perspective showed that FADD was a significant risk indicator for seven malignancies, including LUAD (Figure 1B). We further confirmed by qRT–PCR that the mRNA levels of FADD were significantly higher in two LUAD cell lines (A549 and HCC827) than in the normal lung tissue cell line 16HBE (Figure 1C). By CCK8 assay, we confirmed that FADD played a role in promoting tumor cell proliferation in LUAD cell lines (Figure 1D). At the protein level, we found significantly higher FADD levels in LUAD tumor tissues than in normal alveolar epithelium by two FADD antibody staining results (CAB010209 and HPA001464) in the HPA database (https://www.proteinatlas.org/) (Figure 1E).

Prognostic potential of FADD in LUAD

Survival analysis showed significantly worse survival in both TCGA-LUAD and GEO-LUAD datasets in patients with high FADD than in patients with low FADD (P<0.001, P=0.034, respectively; Figures 2A, B). Both univariate and multifactorial Cox regression analyses corrected for clinical characteristics showed that FADD could be an independent risk factor for OS in patients with LUAD (P<0.05, Figures 2C, D). Furthermore, by analyzing clinical characteristics, we found a significant positive correlation between FADD and stage in the TCGA dataset (P<0.001, Figure 2E) and a positive trend in the GEO dataset (P=0.087, Figure 2F). Comprehensive meta-analysis in the small cell lung cancer database (https://lce.biohpc.swmed.edu/lungcancer) showed that FADD was

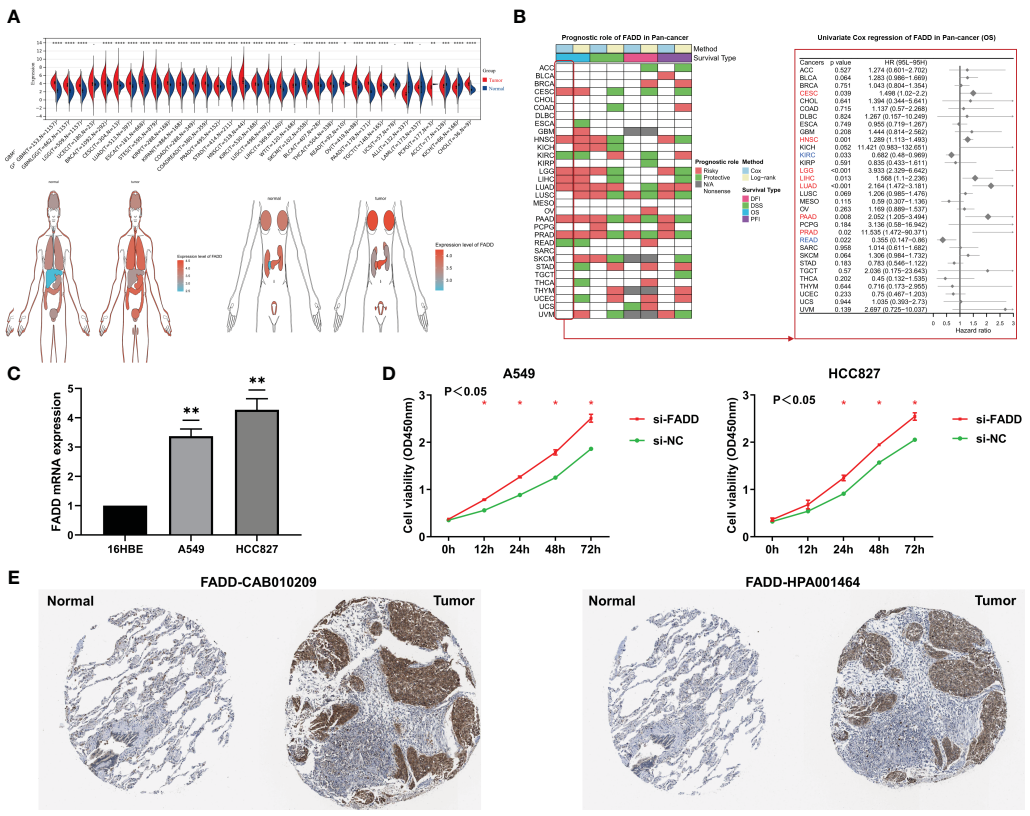


FIGURE 1
Analysis of FADD from a pan-cancer perspective **(A)** Differential expression of FADD in normal and tumor organs or tissues. **(B)** Log-rank and univariate Cox regression analysis of FADD in 32 solid tumors for survival. **(C)** FADD mRNA expression in LUAD cell lines (A549, and HCC827) compared with the normal lung cell line 16HBE by qRT–PCR. **(D)** The proliferation levels of lung cancer cell lines (A549, and HCC827) with knockdown of FADD by CCK-8. **(E)** Immunohistochemical staining analysis of FADD in normal lung and LUAD tissues from HPA database, left: CAB010209 antibody; right: HPA001464 antibody. *: P<0.05, **: P<0.01, ***: P<0.001, ****: P<0.0001, -: not significant.

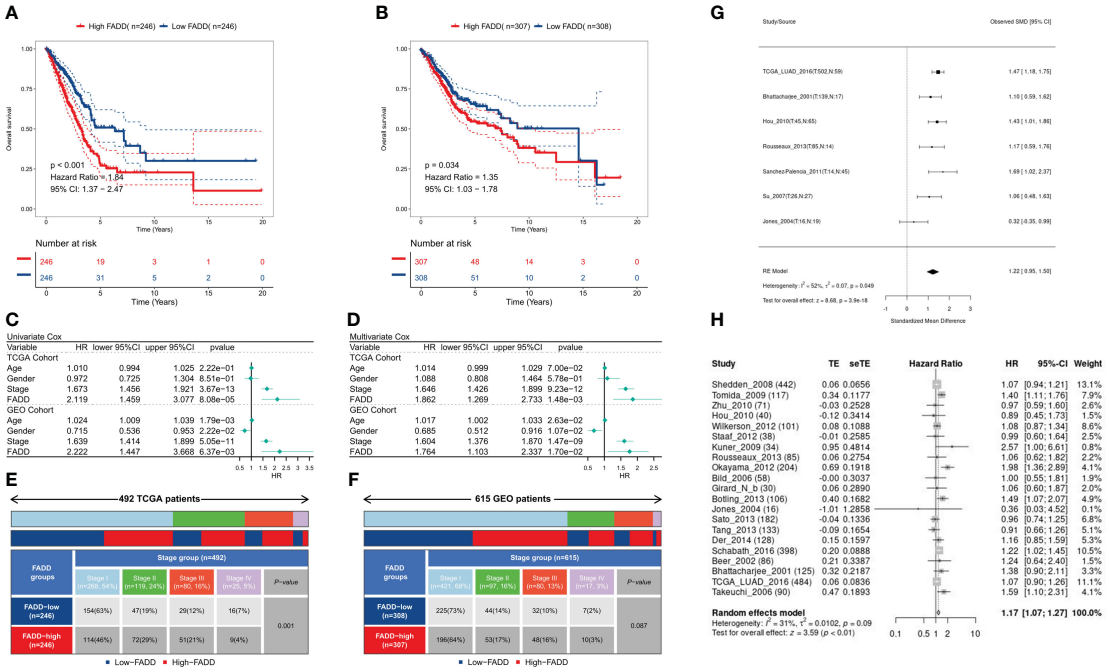


FIGURE 2
Prognostic potential of FADD in LUAD **(A)** KM survival curves for the high-FADD and low-FADD groups in the TCGA cohort. **(B)** KM survival curves for the high-FADD and low-FADD groups in the Meta-GEO cohort. **(C)** Univariate Cox regression analysis of FADD and OS in TCGA and meta-GEO cohorts. **(D)** Multivariate Cox regression analysis of FADD and OS in TCGA and meta-GEO cohorts. **(E)** Correlation analysis of FADD expression with stage in TCGA cohort. **(F)** Correlation analysis of FADD expression with stage in Meta-GEO cohort. **(G)** Meta-analysis of differential expression of FADD in LUAD normal and tumor tissues. **(H)** Meta-analysis of FADD in LUAD for predicting overall survival.

significantly elevated in tumor tissues (Figure 2G) and was an unfavorable prognostic indicator for OS in lung adenocarcinoma patients (Figure 2H). In addition, subgroup survival analysis showed excellent prognostic efficacy of FADD in patients with early-stage LUAD in the TCGA cohort, especially in patients with stage II LUAD and age >= 70 years (Figure S1A), whereas FADD in the GEO cohort showed good prognostic performance in patients younger than 70 years and in male patients (Figure S1B).

Dissecting the functional differences at different FADD levels

We identified a total of 201 DEGs, of which 91 DEGs were upregulated in the high FADD subtype and 110 DEGs were upregulated in the low FADD subtype. Functional enrichment analysis showed that the upregulated genes in the high FADD subtype mainly modulated cell growth, cell junctions, and epidermal development (Figure 3A), while the upregulated genes in the low FADD subtype mainly modulated biological oxidation and cellular morphogenesis (Figure 3B). GSEA revealed that the pathways enriched in the high FADD subtype were cell cycle, pyrimidine metabolism, P53 signaling pathway, and apoptosis (Figure 3C). In contrast, the pathways enriched in the low FADD subtype were primary immune defense, ABC transport, and asthma (Figure 3D). In conclusion, these results suggest that patients with low FADD subtypes have a stronger oxidative stress response and immune activity, whereas tumor cells with high FADD subtypes have a dysregulated cell cycle with hyperactive cell division and cell proliferation.

Single-cell heterogeneity at different FADD levels

We first assessed the microenvironmental heterogeneity of different levels of FADD from a single-cell perspective. We identified eight cell subtypes according to the original parameters (Figure 4A). We then found that FADD was highly expressed in most malignant and myeloid cells (Figure 4B). Specifically, low FADD cells were more predominant in B cells, NK cells, and T cells, while high FADD cells were more predominant in malignant cells and endothelial cells (Figure 4C). We identified significant cellular communication pairs based on a threshold of P<0.05, and the results showed that cells with low FADD expression had more cellular communication activity overall, especially myeloid and malignant cells (Figure 4D). Figure 4E shows the detailed communication pathways between different FADD cell subgroups, with fewer active pathways in high FADD cells and more active pathways in low FADD cells. Most of the communication pathways are associated with antitumor immunity (e.g., CXCL, CCL, TNF, etc.) (Figure 4E). In addition, malignant cells significantly received VEGF signaling (Figure 4E).

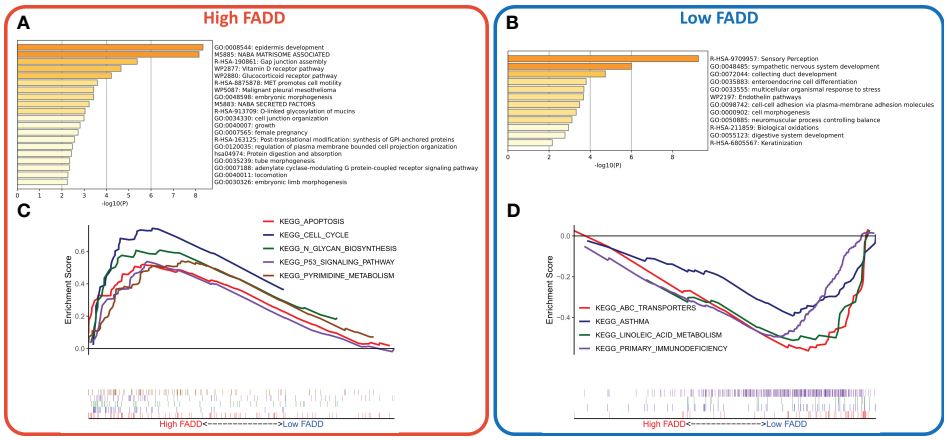


FIGURE 3
Construction and evaluation of a CDSig-based nomogram **(A)** Bar plot showed the biological pathways of upregulated gene enrichment in the high FADD group. **(B)** The barplot showed the biological pathways of upregulated gene enrichment in the low FADD group. **(C)** GSEA analysis revealed the top five enriched KEGG pathways in the high FADD group. **(D)** GSEA analysis revealed the top five enriched KEGG pathways in the low FADD group.

Dissecting immune infiltration heterogeneity at different FADD levels

We then assessed the heterogeneity of immune infiltration due to different FADD levels from a Bulk-seq perspective. As assessed by the ESTIMATE algorithm, low FADD subtypes had higher immune scores, while high FADD subtypes had higher tumor purity (Figure 5A). We then examined the expression differences of seven classical immune checkpoints and therapeutic targets (CD8A, CTLA-4, LAG-3, PD-1, PD-L1, TIM-2, TNF) and found that TIM-2 and PD-L1 were significantly upregulated in the low FADD subtype (Figure 5B). Subsequently, by the ssGSEA algorithm, we found that the type II interferon response pathway was upregulated in the low FADD subgroup. While angiogenesis, EMT, hypoxia, paracrine immunity, and APC-coinhibitory pathways were upregulated in the high FADD subgroup (Figure 5C), the corresponding correlation analysis is shown in Figure 5D. Finally, Cibersort results showed that CD8 T cells, plasma cells, and memory B cells were upregulated in the low FADD subtype, whereas Tregs and M0 macrophages were upregulated in the high FADD subtype (Figure 5E), and the corresponding correlation analysis is shown in Figure 5F. Notably, M2 macrophages and FADD expression were significantly positively correlated (Figure 5F). In conclusion, these results suggest that low FADD levels may indicate “hot” tumors with active antitumor immunity. In contrast, high FADD levels were positively correlated with Tregs and M2 macrophages, which may represent immunosuppressed “cold” tumors.

Assessment of FADD-associated genetic mutations

We first assessed overall the differences in two indicators of genomic mutations at different FADD levels. The results showed that patients with high FADD had significantly higher HRD scores (Figure 6A), but there was no significant difference in MSI scores between the two FADD subtypes (Figure 6B). We calculated the TMB for each patient and showed that the high FADD subtype had a higher TMB, but the difference in TMB between the two subtypes was not significant (Figure 6C). We processed the raw mutation data with the maftools package, and the oncoplot showed the difference in mutation profiles between the two FADD subtypes for a total of 26 high-frequency mutated genes (Figure 6D). The chi-square test showed an increased frequency of TP53 mutations in the high FADD subtype but no significant differences in the other 25 high-frequency mutated genes (Figure 6E). The co-occurrence analysis showed that all high-frequency mutated genes were highly co-occurring and showed significant concordance (Figure 6F).

FADD can guide clinical decision-making in patients with LUAD

We then evaluated the efficacy of FADD in predicting sensitivity to chemotherapy and immunotherapy. Using ridge regression calculations, we found that patients with high FADD expression had lower IC50 values for the five first-line agents for LUAD (cisplatin, docetaxel, gemcitabine, paclitaxel, and vincristine), indicating that patients with high FADD are more sensitive to conventional chemotherapy (Figure 7A). The same results were observed in the externally validated Meta-GEO cohort (Figure 7B). The heterogeneity of the immune microenvironment due to different FADD levels suggested the existence of differences in immunotherapy sensitivity; therefore, we first evaluated the response rate of patients with different FADD levels to immunotherapy using the TIDE algorithm. The results showed that patients in the low FADD group in the TCGA-LUAD cohort had a higher response rate to immunotherapy (P=<0.001, Figure 7C). In the GEO-LUAD cohort, patients in the low FADD group also responded more to immunotherapy (P<0.001, Figure 7D). Finally, after subclass mapping assessment of the

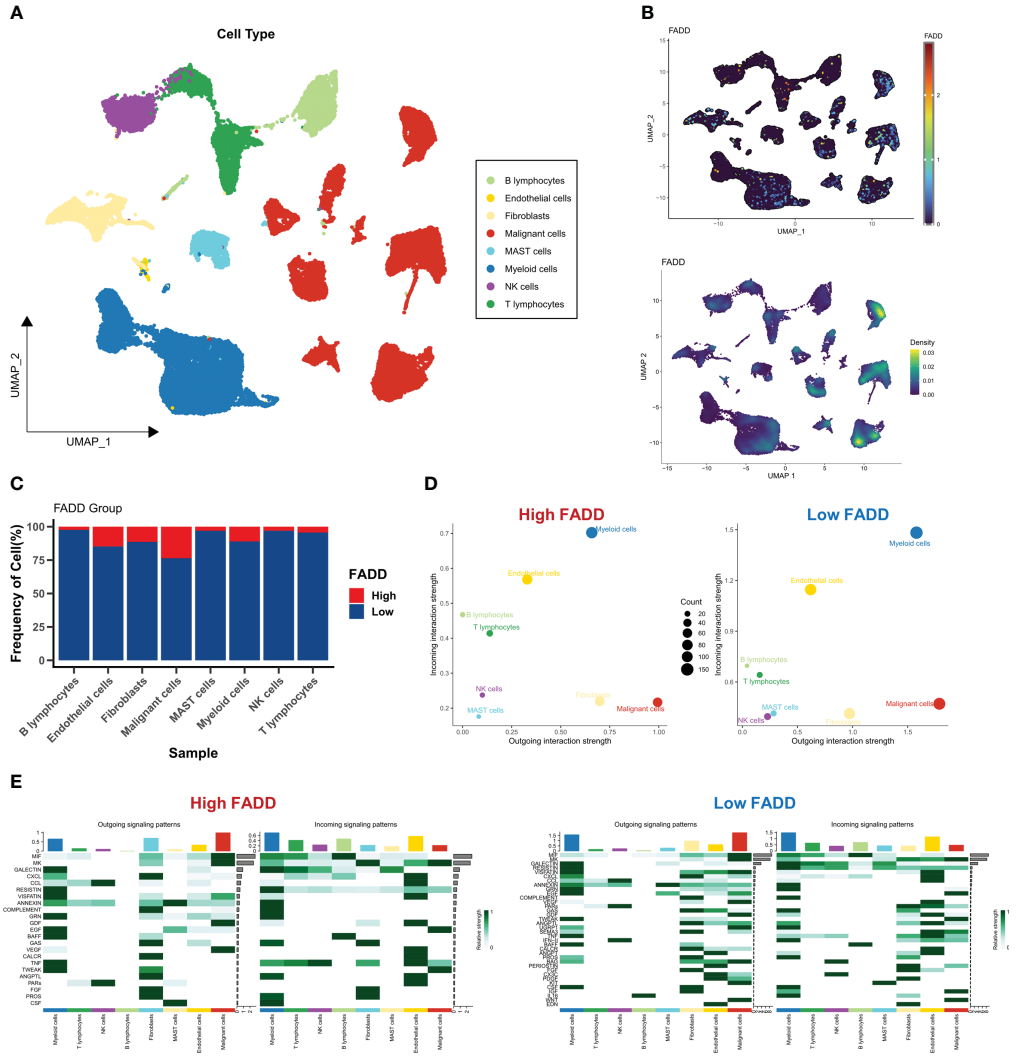


FIGURE 4
Single-cell perspective analysis of CDSig **(A)** Umap demonstrates 8 cell subgroups in LUAD patients. **(B)** The expression levels of CDSig in different cells. **(C)** The proportion of cells in different FADD subgroups. **(D)** Overall cellular communication pairs in cells with high FADD (left) and low FADD (right). **(E)** Specific communication pathways between different cells with high FADD (left) and low FADD (right).

transcriptome, patients in the low FADD group in the TCGA and GEO cohorts were predicted to be more sensitive to anti-PD1 therapy (TCGA: FDR=0.008; GEO: FDR=0.042) (Figures 7E, F).

Discussion

Lung cancer remains a major healthcare challenge worldwide today, and LUAD is the most common histopathological subtype of lung cancer (1). Although advances in medical technology and clinical protocols have driven advances in diagnostic and therapeutic approaches, the morbidity and mortality rates of LUAD remain high (23). FADD is a widely studied regulator of apoptosis, and recent novel findings propose a close relationship between FADD and cancer immunity (24). FADD not only enhances the activity of effector immune cells (especially T cells) (10, 11) but also reduces immune escape (12). Therefore, FADD has emerged as a promising new target for tumor immunotherapy. Our study defined two heterogeneous subtypes in LUAD based on FADD expression, one of which has more FADD expression and is defined as a high FADD subtype. The other subtype with low FADD expression was defined as the low FADD subtype. The subtype with high FADD expression has a dysregulated cell cycle that may lead to active tumor cell replication and proliferation. The subtype with low FADD expression is associated with stronger antitumor immunity. In addition, both subtypes showed heterogeneity in genomic mutation sites, clinical outcomes and immunotherapeutic response, revealing the potential of FADD as a novel target for precision and targeted medicine in LUAD.

These two subtypes exhibit different clinical features, and we observed that patients with a low FADD phenotype had significantly better overall survival than those with a high FADD phenotype and that more patients with advanced LUAD had the high FADD phenotype. Functional enrichment suggests that the high FADD phenotype is enriched in purine pyrimidine metabolism-related pathways and cell cycle-related pathways,

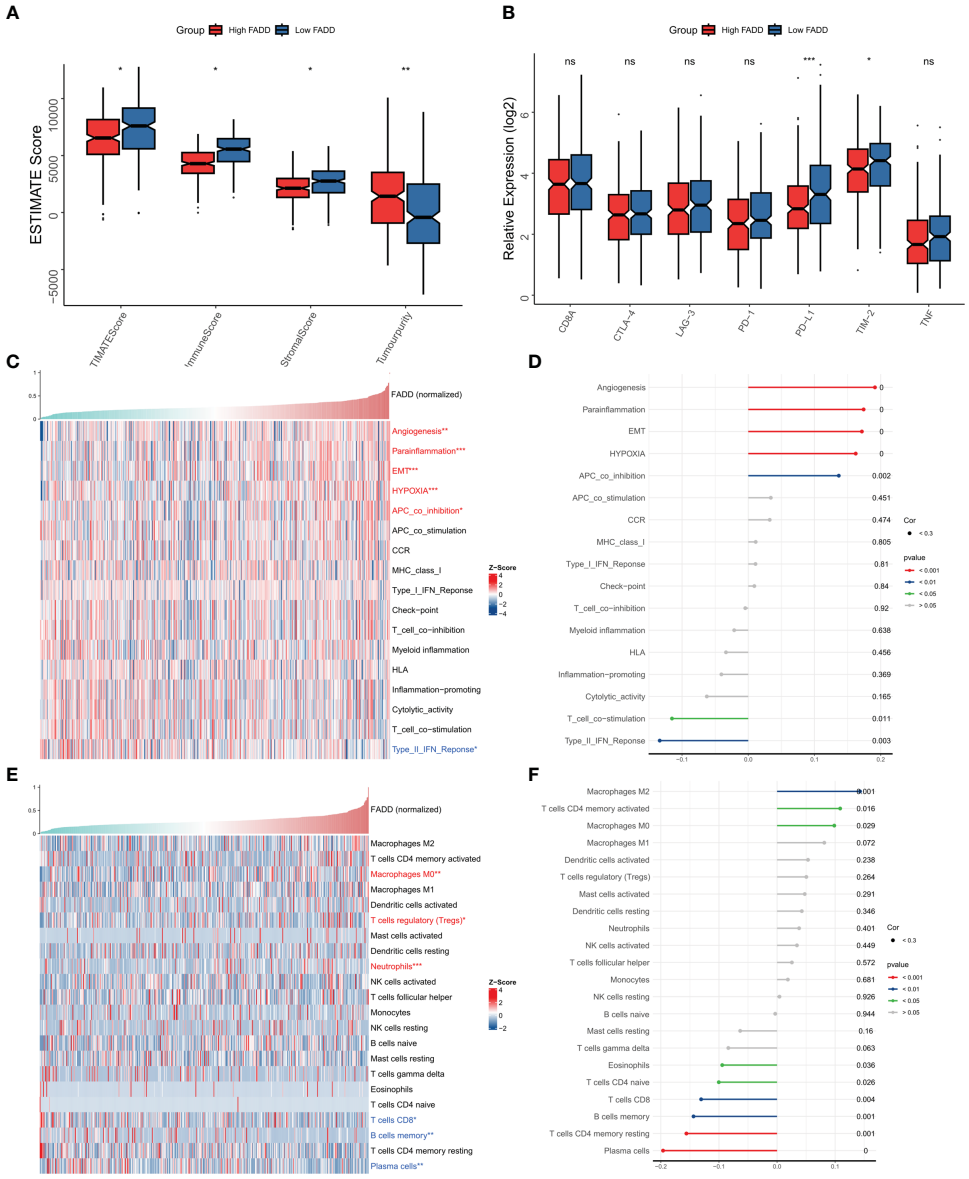


FIGURE 5
Immune microenvironment of different FADD subgroups **(A)** Box plots showing ESTIMATE results between different FADD subgroups. **(B)** Box plot showing immune checkpoint expression between different FADD subgroups **(C)** The landscape of immune-related pathways in different FADD subgroups. **(D)** Correlation between the immune-related pathways and expression level of FADD. **(E)** The landscape of immune cell infiltration in different FADD subgroups. **(F)** Correlation between the immune cell infiltration and expression level of FADD. *: P<0.05, **: P<0.01, ***: P<0.001; ns, not significant.

which are hallmarks and one of the fundamental mechanisms of cancer, suggesting that high FADD is a dysregulated, hyperproliferative LUAD subtype (25, 26). Further analysis revealed a significant increase in angiogenic, EMT, and hypoxic pathway activity in patients with high FADD, which represents a positive correlation between high FADD and the malignant features of the tumor. Moreover, high FADD could indicate patients with higher malignancy of LUAD (27–29). In addition to the enrichment of immune-related pathways in patients with low FADD expression, immune infiltration analysis also suggested a higher infiltration of effector immune cells (CD8+ T cells) and B cells in the low FADD phenotype (30). As important components of the antitumor immune system, the enrichment of CD8+ T cells and B cells provides an additional source of power for patients with low FADD to exert stronger antitumor immunity and may ultimately lead to a better prognosis for patients with low FADD (31, 32). Notably, higher FADD expression is positively associated with increased infiltration of suppressive immune cells (Tregs and M2 macrophages), which may lead to suppressed antitumor activity and immune escape of active tumor cells in patients with high FADD (33, 34). The high FADD subtype exhibits features of immune exhaustion and ultimately leads to a poor prognosis.

One of the features of tumorigenesis is the abnormal accumulation of genetic mutations, and therefore, mutational differences among different FADD subtypes may contribute to the eventual phenotypic differences (35). We found that high FADD

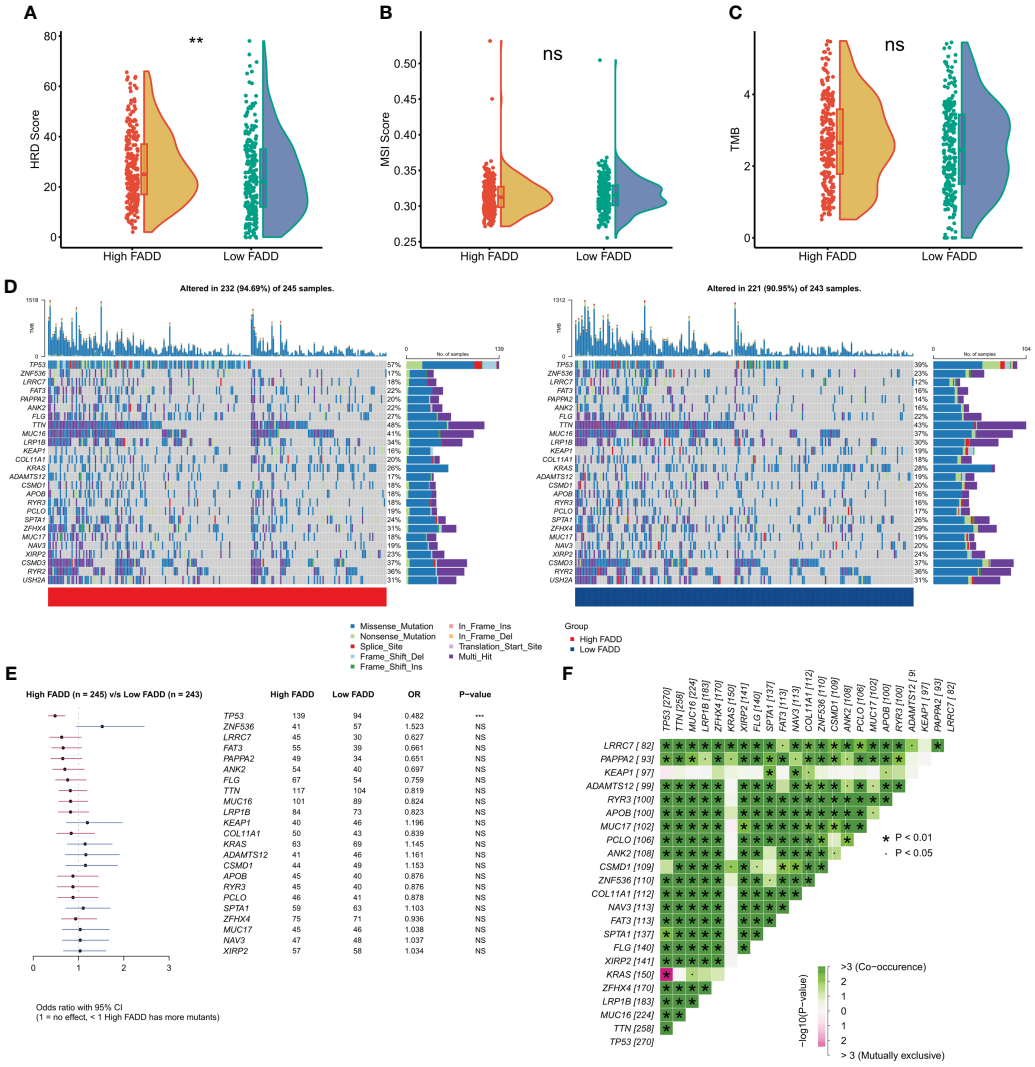


FIGURE 6
Genomic mutations in different FADD subgroups **(A)** Violin plot displayed the difference in **(A)** HRD score, **(B)** MSI score, and **(C)** TMB between different FADD subgroups. **(D)** Oncoplot showed the mutation landscape of high-frequency mutant genes between different cells with high FADD (left) and low FADD (right). **(E)** Forestplot showed statistically significant differences in high-frequency mutated genes between the high- and low-FADD subgroups. **(F)** Analysis of co-occurrence between high-frequency mutated genes **: P<0.01, ***: P<0.001; ns, not significant.

was associated with a significantly higher HRD score, and existing reports suggest that an increased HRD score can identify immunophenotypically "cold" tumors, which is consistent with our findings (36). In addition, higher HRD scores were also associated with increased sensitivity to platinum-based chemotherapy (37). Although we failed to find significant differences in TMB among patients with different FADD levels, we found that patients with high FADD had more TP53 mutations. TP53 is a reported classical cancer suppressor gene that is highly mutated in most patients with LUAD (38). Therefore, we infer that more cumulative TP53 mutations are also a factor contributing to the worse prognosis of patients with high FADD.

Taken together, our results suggest that FADD represents different states of the "cold" and "hot" tumor microenvironment and may contribute to the heterogeneity of tumor treatment sensitivity. Accordingly, our subsequent analysis focused on the differences in sensitivity to conventional chemotherapy and immunotherapy among patients with different FADD levels. We first found that patients with high FADD had a lower IC50 for first-line chemotherapeutic agents for LUAD, and therefore, patients with high FADD were more amenable to conventional chemotherapy. Our GSEA suggests that tumor cell cycle pathways are enriched and cell proliferation is active in high FADD, and the active cell cycle provides more targets for conventional chemotherapeutic agents, thus leading to greater sensitivity to chemotherapy (39). After evaluation by the TIDE algorithm and the subclass mapping algorithm, we were able to determine that patients with low FADD have a higher response rate to anti-PD-1 inhibitors. Notably, our results suggest that low FADD is associated with greater PD-1 and PD-L1 expression and that patients with low FADD have immune-active tumor microenvironments. Therefore, our prediction for the applicability of immunotherapy in patients

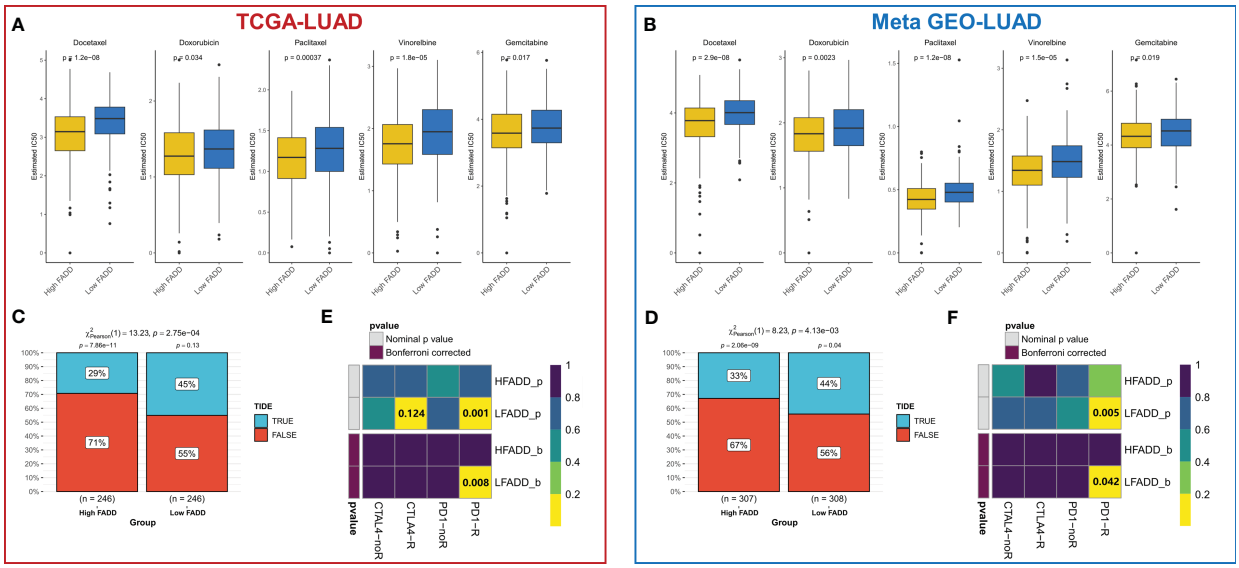


FIGURE 7
Treatment sensitivity among different FADD subgroups **(A)** Box plots displayed the predicted IC50 values for five first-line drugs of LUAD in high- and low-FADD groups in the TCGA cohort. **(B)** Box plots displayed the predicted IC50 values for five first-line drugs of LUAD in high- and low-FADD groups in the Meta-GEO cohort. **(C)** Response rates to immunotherapy in different FADD subgroups based on TIDE predictions in the TCGA cohort. **(D)** Response rates to immunotherapy in different FADD subgroups based on TIDE predictions in the Meta-GEO cohort. **(E)** Predicting the sensitivity of patients in high and low FADD groups to PD1 and CTLA4 treatment regimens by subclass mapping in the TCGA cohort. **(F)** Predicting the sensitivity of patients in high and low FADD groups to PD1 and CTLA4 treatment regimens by subclass mapping in the Meta-GEO cohort.

with low FADD is reliable. In conclusion, FADD can be applied to specify individualized treatment regimens for LUAD patients in the clinic, with high FADD more applicable to conventional chemotherapy and low FADD more applicable to novel immunotherapy represented by anti-PD-1 inhibitors.

Conclusion

In conclusion, this study suggests that upregulated FADD is associated with worse prognosis, immune exhaustion, and tumor malignancy in patients with LUAD. Furthermore, FADD could be a useful indicator for assessing sensitivity to chemotherapy and immunotherapy. Therefore, FADD has the potential to become a new target for precision medicine and targeted therapy for LUAD.

Data availability statement

The original contributions presented in the study are included in the article/Supplementary Material. Further inquiries can be directed to the corresponding authors.

Author contributions

LW and FL designed and supported this study, MH analyzed the data and drafted the manuscript, YH and JX drew figures and improved the manuscript, YZ and XC collected the data and completed the experiment. All authors contributed to the article and approved the submitted version.

Acknowledgments

We thank previous researchers for generously providing the raw data.

Conflict of interest

The authors declare that the research was conducted in the absence of any commercial or financial relationships that could be construed as a potential conflict of interest.

Publisher's note

All claims expressed in this article are solely those of the authors and do not necessarily represent those of their affiliated organizations, or those of the publisher, the editors and the reviewers. Any product that may be evaluated in this article, or claim that may be made by its manufacturer, is not guaranteed or endorsed by the publisher.

Supplementary material

The Supplementary Material for this article can be found online at: https://www.frontiersin.org/articles/10.3389/fonc.2023.1228889/full#supplementary-material

SUPPLEMENTARY FIGURE 1
Subgroup survival analysis of FADD Subgroup KM survival curves of FADD in TCGA **(A)** and Meta-GEO **(B)** cohorts.

References

1. Siegel RL, Miller KD, Fuchs HE, Jemal A. Cancer statistics, 2022. *CA: Cancer J Clin* (2022) 72(1):7–33. doi: 10.3322/caac.21708

2. Hirsch FR, Scagliotti GV, Mulshine JL, Kwon R, Curran WJJr., Wu YL, et al. Lung cancer: current therapies and new targeted treatments. *Lancet (London England)* (2017) 389(10066):299–311. doi: 10.1016/s0140-6736(16)30958-8

3. Nooreldeen R, Bach H. Current and future development in lung cancer diagnosis. *Int J Mol Sci* (2021) 22(16). doi: 10.3390/ijms22168661

4. Tan AC, Tan DSW. Targeted therapies for lung cancer patients with oncogenic driver molecular alterations. *J Clin Oncol* (2022) 40(6):611–25. doi: 10.1200/jco.21.01626

5. Marín-Rubio JL, Vela-Martín L, Fernández-Piqueras J, Villa-Morales M. FADD in cancer: mechanisms of altered expression and function, and clinical implications. *Cancers* (2019) 11(10). doi: 10.3390/cancers11101462

6. Zhang X, Vallabhaneni R, Loughran PA, Shapiro R, Yin XM, Yuan Y, et al. Changes in FADD levels, distribution, and phosphorylation in TNFalpha-induced apoptosis in hepatocytes is caspase-3, caspase-8 and BID dependent. *Apoptosis* (2008) 13(8):983–92. doi: 10.1007/s10495-008-0228-3

7. Mouasni S, Tourneur L. FADD at the Crossroads between Cancer and Inflammation. *Trends Immunol* (2018) 39(12):1036–53. doi: 10.1016/j.it.2018.10.005

8. Liu Y, Li X, Zhou X, Wang J, Ao X. FADD as a key molecular player in cancer progression. *Mol Med (Cambridge Mass)* (2022) 28(1):132. doi: 10.1186/s10020-022-00560-y

9. Zhang Y, Zhang Z. The history and advances in cancer immunotherapy: understanding the characteristics of tumor-infiltrating immune cells and their therapeutic implications. *Cell Mol Immunol* (2020) 17(8):807–21. doi: 10.1038/s41423-020-0488-6

10. Kabra NH, Kang C, Hsing LC, Zhang J, Winoto A. T cell-specific FADD-deficient mice: FADD is required for early T cell development. *Proc Natl Acad Sci USA* (2001) 98(11):6307–12. doi: 10.1073/pnas.111158698

11. Walsh CM, Wen BG, Chinnaiyan AM, O'Rourke K, Dixit VM, Hedrick SM. A role for FADD in T cell activation and development. *Immunity* (1998) 8(4):439–49. doi: 10.1016/s1074-7613(00)80549-x

12. Osborn SL, Diehl G, Han SJ, Xue L, Kurd N, Hsieh K, et al. Fas-associated death domain (FADD) is a negative regulator of T-cell receptor-mediated necroptosis. *Proc Natl Acad Sci USA* (2010) 107(29):13034–9. doi: 10.1073/pnas.1005997107

13. Leek JT, Johnson WE, Parker HS, Jaffe AE, Storey JD. The sva package for removing batch effects and other unwanted variation in high-throughput experiments. *Bioinf (Oxford England)* (2012) 28(6):882–3. doi: 10.1093/bioinformatics/bts034

14. Kim N, Kim HK, Lee K, Hong Y, Cho JH, Choi JW, et al. Single-cell RNA sequencing demonstrates the molecular and cellular reprogramming of metastatic lung adenocarcinoma. *Nat Commun* (2020) 11(1):2285. doi: 10.1038/s41467-020-16164-1

15. Jin S, Guerrero-Juarez CF, Zhang L, Chang I, Ramos R, Kuan CH, et al. Inference and analysis of cell-cell communication using CellChat. *Nat Commun* (2021) 12(1):1088. doi: 10.1038/s41467-021-21246-9

16. Yoshihara K, Shahmoradgoli M, Martínez E, Vegesna R, Kim H, Torres-Garcia W, et al. Inferring tumour purity and stromal and immune cell admixture from expression data. *Nat Commun* (2013) 4:2612. doi: 10.1038/ncomms3612

17. Chen DS, Mellman I. Oncology meets immunology: the cancer-immunity cycle. *Immunity* (2013) 39(1):1–10. doi: 10.1016/j.immuni.2013.07.012

18. Newman AM, Liu CL, Green MR, Gentles AJ, Feng W, Xu Y, et al. Robust enumeration of cell subsets from tissue expression profiles. *Nat Methods* (2015) 12(5):453–7. doi: 10.1038/nmeth.3337

19. Thorsson V, Gibbs DL, Brown SD, Wolf D, Bortone DS, Ou Yang TH, et al. The immune landscape of cancer. *Immunity* (2018) 48(4):812–30.e14. doi: 10.1016/j.immuni.2018.03.023

20. Mayakonda A, Lin DC, Assenov Y, Plass C, Koeffler HP. Maftools: efficient and comprehensive analysis of somatic variants in cancer. *Genome Res* (2018) 28(11):1747–56. doi: 10.1101/gr.239244.118

21. Geeleher P, Cox N, Huang RS. pRRophetic: an R package for prediction of clinical chemotherapeutic response from tumor gene expression levels. *PloS One* (2014) 9(9):e107468. doi: 10.1371/journal.pone.0107468

22. Jiang P, Gu S, Pan D, Fu J, Sahu A, Hu X, et al. Signatures of T cell dysfunction and exclusion predict cancer immunotherapy response. *Nat Med* (2018) 24(10):1550–8. doi: 10.1038/s41591-018-0136-1

23. Thai AA, Solomon BJ, Sequist LV, Gainor JF, Heist RS. Lung cancer. *Lancet (London England)* (2021) 398(10299):535–54. doi: 10.1016/s0140-6736(21)00312-3

24. Tourneur L, Chiocchia G. FADD: a regulator of life and death. *Trends Immunol* (2010) 31(7):260–9. doi: 10.1016/j.it.2010.05.005

25. Liu J, Peng Y, Wei W. Cell cycle on the crossroad of tumorigenesis and cancer therapy. *Trends Cell Biol* (2022) 32(1):30–44. doi: 10.1016/j.tcb.2021.07.001

26. Evan GI, Vousden KH. Proliferation, cell cycle and apoptosis in cancer. *Nature* (2001) 411(6835):342–8. doi: 10.1038/35077213

27. Ramjiawan RR, Griffioen AW, Duda DG. Anti-angiogenesis for cancer revisited: Is there a role for combinations with immunotherapy? *Angiogenesis* (2017) 20(2):185–204. doi: 10.1007/s10456-017-9552-y

28. Babaei G, Aziz SG, Jaghi NZZ. EMT, cancer stem cells and autophagy; The three main axes of metastasis. *Biomedicine pharmacotherapy = Biomedecine pharmacotherapie* (2021) 133:110909. doi: 10.1016/j.biopha.2020.110909

29. Jing X, Yang F, Shao C, Wei K, Xie M, Shen H, et al. Role of hypoxia in cancer therapy by regulating the tumor microenvironment. *Mol Cancer* (2019) 18(1):157. doi: 10.1186/s12943-019-1089-9

30. van der Leun AM, Thommen DS, Schumacher TN. CD8(+) T cell states in human cancer: insights from single-cell analysis. *Nat Rev Cancer* (2020) 20(4):218–32. doi: 10.1038/s41568-019-0235-4

31. St Paul M, Ohashi PS. The roles of CD8(+) T cell subsets in antitumor immunity. *Trends Cell Biol* (2020) 30(9):695–704. doi: 10.1016/j.tcb.2020.06.003

32. Sarvaria A, Madrigal JA, Saudemont A. B cell regulation in cancer and anti-tumor immunity. *Cell Mol Immunol* (2017) 14(8):662–74. doi: 10.1038/cmi.2017.35

33. Shan F, Somasundaram A, Bruno TC, Workman CJ, Vignali DAA. Therapeutic targeting of regulatory T cells in cancer. *Trends Cancer* (2022) 8(11):944–61. doi: 10.1016/j.trecan.2022.06.008

34. Wu K, Lin K, Li X, Yuan X, Xu P, Ni P, et al. Redefining tumor-associated macrophage subpopulations and functions in the tumor microenvironment. *Front Immunol* (2020) 11:1731. doi: 10.3389/fimmu.2020.01731

35. Martínez-Jiménez F, Muiños F, Sentís I, Deu-Pons J, Reyes-Salazar I, Arnedo-Pac C, et al. A compendium of mutational cancer driver genes. *Nat Rev Cancer* (2020) 20(10):555–72. doi: 10.1038/s41568-020-0290-x

36. Budczies J, Kluck K, Beck S, Ourailidis I, Allgäuer M, Menzel M, et al. Homologous recombination deficiency is inversely correlated with microsatellite instability and identifies immunologically cold tumors in most cancer types. *J Pathol Clin Res* (2022) 8(4):371–82. doi: 10.1002/cjp2.271

37. Telli ML, Timms KM, Reid J, Hennessy B, Mills GB, Jensen KC, et al. Homologous recombination deficiency (HRD) score predicts response to platinum-containing neoadjuvant chemotherapy in patients with triple-negative breast cancer. *Clin Cancer Res* (2016) 22(15):3764–73. doi: 10.1158/1078-0432.Ccr-15-2477

38. Skoulidis F, Heymach JV. Co-occurring genomic alterations in non-small-cell lung cancer biology and therapy. *Nat Rev Cancer* (2019) 19(9):495–509. doi: 10.1038/s41568-019-0179-8

39. Sun Y, Liu Y, Ma X, Hu H. The influence of cell cycle regulation on chemotherapy. *Int J Mol Sci* (2021) 22(13). doi: 10.3390/ijms22136923

frontiers | Frontiers in Immunology

TYPE Mini Review
PUBLISHED 24 August 2023
DOI 10.3389/fimmu.2023.1244764

Check for updates

OPEN ACCESS

EDITED BY
Qun Xue,
Affiliated Hospital of Nantong University, China

REVIEWED BY
Yiheng Ye,
Wenzhou Medical University, China
Yan Zhang,
Wuxi Maternity and Child Health Care Hospital, China

*CORRESPONDENCE
Shiyi Chen
shiyichen_huashan@163.com
Xiliang Shang
sxl00720@163.com
Qing Wang
Doctorwq1983@163.com

†These authors contributed equally to this work and share the first authorship

RECEIVED 23 June 2023
ACCEPTED 07 August 2023
PUBLISHED 24 August 2023

CITATION
Luo Z, Wan R, Liu S, Feng X, Peng Z, Wang Q, Chen S and Shang X (2023) Mechanisms of exercise in the treatment of lung cancer – a mini-review. *Front. Immunol.* 14:1244764. doi: 10.3389/fimmu.2023.1244764

COPYRIGHT
© 2023 Luo, Wan, Liu, Feng, Peng, Wang, Chen and Shang. This is an open-access article distributed under the terms of the Creative Commons Attribution License (CC BY). The use, distribution or reproduction in other forums is permitted, provided the original author(s) and the copyright owner(s) are credited and that the original publication in this journal is cited, in accordance with accepted academic practice. No use, distribution or reproduction is permitted which does not comply with these terms.

Mechanisms of exercise in the treatment of lung cancer – a mini-review

Zhiwen Luo[1†], Renwen Wan[1†], Shan Liu[2†], Xinting Feng[1], Zhen Peng[3], Qing Wang[4*], Shiyi Chen[1*] and Xiliang Shang[1*]

[1]Department of Sports Medicine, Huashan Hospital, Fudan University, Shanghai, China, [2]Department of Endocrinology, Huashan Hospital, Fudan University, Shanghai, China, [3]Department of Sports Medicine, Shanghai General Hospital, Shanghai, China, [4]Department of Orthopaedics, Kunshan Hospital of Traditional Chinese Medicine, Kunshan, Jiangsu, China

Lung cancer constitutes a formidable menace to global health and well-being, as its incidence and mortality rate escalate at an alarming pace. In recent years, research has indicated that exercise has potential roles in both the prevention and treatment of lung cancer. However, the exact mechanism of the coordinating effect of exercise on lung cancer treatment is unclear, limiting the use of exercise in clinical practice. The purpose of this review is to explore the mechanisms through which exercise exerts its anticancer effects against lung cancer. This review will analyze the biological basis of exercise's anticancer effects on lung cancer, with a focus on aspects such as the tumor microenvironment, matrix regulation, apoptosis and angiogenesis. Finally, we will discuss future research directions and potential clinical applications.

KEYWORDS

lung cancer, exercise, prevention, treatment, anticancer mechanisms, tumor microenvironment

Introduction

Lung cancer constitutes a formidable menace to global health and well-being, as its incidence and mortality rates escalate at an alarming pace (1). According to the worldwide cancer data of 2020, lung cancer ranks among the most prevalent malignancies and exhibits the highest mortality rate among all major cancers (2, 3). Annually, more than 2.1 million new cases of lung cancer and approximately 1.8 million deaths are recorded (2). Non-small cell lung cancer (NSCLC) is the most prevalent subtype of lung cancer, accounting for approximately 80% of newly diagnosed cases (4). The 5-year survival rate for this malignancy is a mere 15%, attributable in part to the inadequacy of early detection techniques and the absence of effective treatments for advanced disease (1, 4). Approximately fifty percent of non-small cell lung malignancies contain mutations in the tumor suppressor gene p53, which plays a key role in numerous biological pathways, including DNA repair, cell cycle arrest, apoptosis, senescence, autophagy, and metabolism (5). Currently, treatment modalities entail surgical resection, chemotherapy, radiotherapy,

targeted therapy, and immunotherapy (6). Therapeutic options for lung cancer patients hinge upon the cancer type, disease stage, and patient functional status. These interventions may also induce adverse effects, which, in conjunction with the cancer symptoms, impose a considerable burden on patients and exacerbate numerous patient-related outcomes, including exercise capacity and physical function (1). Consequently, it is of utmost importance to seek treatment strategies for lung cancer that are less harmful.

Physical activity serves a vital role in the prevention and management of lung cancer (7). Regular physical activity yields substantial health advantages, mitigating the risk of various chronic health disorders, such as obesity, brain disorders, cardiovascular diseases, and diabetes (8–12). The World Health Organization advises adults to partake in a minimum of 150 minutes of moderate-intensity aerobic exercise weekly, fostering cardiorespiratory, muscular, and skeletal health while diminishing the risk of depression. Exercise correlates with a lower risk of diverse cancers, encompassing colorectal, breast, esophageal, pancreatic, endometrial, and ovarian malignancies (10). Moreover, habitual exercise markedly curtails cancer-related mortality rates following breast and colorectal cancer diagnoses (13, 14). However, the molecular mechanisms underlying exercise's function in lung cancer prevention and treatment remain obscure.

In the realm of lung cancer therapy, exercise has unequivocally exhibited its efficacy in bolstering the quality of life for patients subjected to arduous treatment modalities (6). A salubrious lifestyle characterised by regular exercise and physical activity is associated with a lower incidence of cancer (including lung cancer) and cancer mortality (10, 15, 16). Exercise also improves the overall physical condition of cancer patients undergoing chemotherapy or surgery, thereby reducing treatment-related adverse effects and complications (6, 7, 17). Accumulating evidence underscores the safety and effectiveness of exercise interventions, with pre-operative exercise considerably decreasing the prevalence of post-operative complications (7). In recent scrutinies concerning individuals afflicted with non-small cell lung cancer, a compelling revelation has surfaced, elucidating the transformative potential of physical exercise. This enlightening research has unveiled significant advancements in terms of ambulatory stamina, maximal exercise capability, breathlessness alleviation, reduction in hospitalization risk, and amelioration of postoperative pulmonary complications (2, 3, 18).

Exercise constitutes an essential component in both the prevention and management of lung cancer, with potential underlying biological mechanisms comprising p53-mediated apoptosis, inhibition of lung cancer cell proliferation and survival, augmentation of host immunity, facilitation of immune cell infiltration, refinement of the tumor microenvironment, attenuation of chronic inflammation, activation of DNA repair enzymes, and fortification against oxidative stress (3, 5, 7, 18–24). Furthermore, research has indicated that aerobic exercise and high-intensity interval training exert therapeutic effects on tumors (18, 22, 25). By modulating the microenvironment of tumors and boosting the activity of immune cells such as T lymphocytes and NK cells, exercise can boost immune function and aid in the fight against tumors (3, 17–20).

Although further investigation of the potential anti-tumor effects of combining exercise with immunotherapy is warranted, the implementation of exercise in lung cancer treatment has already shown promise (3, 18). This study chiefly synthesizes all recent fundamental research on exercise's anti-tumor effects, offering an exhaustive overview of established mechanisms, with the intent of aiding scholars in their investigation of exercise's anti-cancer properties and furnishing a theoretical foundation for clinical trials.

The influence of exercise on the tumor immune microenvironment (TIME) of lung cancer

Within the Tumor Microenvironment (TME), three distinct classifications have been identified, namely "Immune inflamed," "Immune desert," and "Immune excluded," based on the infiltration and distribution patterns of immune cells (26–30). In an 'Immune inflamed' TME, immune cells are widely infiltrated within the tumor tissues, while in an 'Immune desert' TME, immune cells are virtually absent within and around the tumor. An 'Immune excluded' TME sees immune cells primarily concentrated at the tumor margins (26, 27, 30).

An increasing body of research suggests that exercise may facilitate the shift in the tumor microenvironment class (13, 31). Although the precise mechanisms are still under investigation, one possible explanation is that exercise may modulate both systemic and local immune responses (19, 22). For instance, exercise may enhance systemic immune responses by augmenting the number of immune cells in circulation; simultaneously, it may influence the activities of immune cells within the tumor by adjusting the local environmental conditions surrounding the tumor, such as oxygen and nutrient supply, as well as the extent of inflammatory and stress responses (31, 32). This could lead to the transformation of the TME from an 'Immune desert' or 'Immune excluded' type to an 'Immune inflamed' type, thereby making it more conducive for the immune system's assault on the tumor (18, 33). Nonetheless, the precise impact of exercise on TME alterations requires further exploration. A deeper understanding of this not only sheds light on the role of exercise in cancer treatment but also may provide novel insights for the development of new immunotherapeutic strategies.

Various bioactive substances, such as myokines, endorphins, glucocorticoids, growth hormones, insulin-like growth factor-1, and nitric oxide, can be affected by exercise (34–38). These substances play a regulatory role in the immune system by modulating inflammatory responses, promoting immune cell activity, and enhancing resistance against pathogens (35, 36). Moderate and regular exercise helps maintain a balance in the levels of these substances, thereby positively regulating the immune system (10, 17, 36).

Research has shown that exercise can reduce the levels of inflammatory factors (such as TNF-α, IL-6, IL-1β) and reactive oxygen species (ROS) within tumor tissue, thus inhibiting the inflammatory immune microenvironment in tumors (22, 38). Animal studies demonstrated that aerobic exercise could reduce lung cancer inflammation, increase the levels of the anti-

inflammatory cytokine IL-10, and decrease the levels of pro-inflammatory cytokines (such as TNF-α, IL-6, and IL-1) (18, 20). A systematic review and meta-analysis on lung cancer patients indicated that exercise could improve immune function, reduce inflammation, and enhance the quality of life (1). These studies suggest that exercise's anti-lung cancer mechanism involves the regulation of tumor inflammation.

Animal and human studies indicate that exercise can affect innate immune components by elevating the levels of myeloid cells, including macrophages, monocytes, and neutrophils, in peripheral blood and tissue exudates (17, 39–41). Exercise modulates the tumor microenvironment by acting on both the innate and adaptive immune systems, increasing peripheral blood T lymphocyte and NK cell levels, enhancing their mobilization to the tumor stroma, or tumor cell cytotoxicity (18, 19, 22, 42). Furthermore, exercise can regulate the tumor microenvironment's reprogramming by promoting myeloid cell polarization towards a more anti-tumor phenotype (15, 18, 22). However, research on exercise and the regulation of the immune microenvironment in lung cancer is limited, and the mechanism is not yet clear.

Tumor-associated macrophages (TAMs) serve a crucial role in tumor promotion (43–45). Studies have found that TAMs can constitute 30-50% of the total tumor tissue volume. Tumor cells can recruit and induce macrophages to differentiate into TAMs, which then promote tumor growth (46–48). Research has confirmed that long-term swimming training can reduce TAMs infiltration in tumor tissue and delay tumor growth (18). However, 8 weeks of voluntary wheel running does not change the number of TAMs in subcutaneously implanted leukemia tumors, suggesting that exercise's impact on TAM accumulation in tumor tissue depends on the tumor types (18).

Endurance exercise and high-intensity interval training (HIIT) have been found not to prevent TAM accumulation in lung cancer tissue (18). Although TAMs accumulate abundantly in tumor tissue, they primarily exhibit an M2 phenotype, promoting tumor growth and immune suppression (43, 48, 49). Numerous studies are investigating how to target TAMs and polarize them from M2 to M1 phenotype to eliminate tumors (43, 47, 49, 50). Some research suggests that exercise can enhance anti-tumor activity by increasing the M1/M2 TAM ratio (18, 22). However, research indicates that endurance exercise reduces the quantity of M1-type TAMs in lung cancer tissue significantly (18). Additionally, endurance exercise downregulates TNF-α and iNOS expression in lung cancer tissue but upregulates IL-6 and IL-10 expression (18). This indicates that endurance exercise reduces the proportion of M1-type TAMs and pro-inflammatory cytokines while enhancing anti-inflammatory cytokines. HIIT also downregulates TNF-α and iNOS expression in lung cancer tissue but increases IL-12 expression and plasma IFN-γ levels. IL-12 promotes IFN-γ production, which can induce monocyte differentiation into M1-type macrophages (18). Therefore, HIIT may promote M1 polarization and immune tumor control by increasing IL-12 and IFN-γ levels. Moreover, HIIT upregulates CD47 and CD24 expression, which is associated with inhibiting macrophage phagocytic activity and enhancing tumor immunogenicity (18). In summary, HIIT may bidirectionally regulate TAM polarization and improve the immune microenvironment of lung cancer by modulating IL-10, IL-12, CD47, and CD24. In comparison, endurance exercise upregulates PD-L1 and Sirpα expression, potentially enhancing tumor immunogenicity and inhibiting macrophage phagocytic activity (18). Overall, endurance exercise and HIIT improve the immune microenvironment of lung cancer by regulating TAM polarization and immune checkpoint expression. These findings provide new therapeutic strategies for lung cancer immunotherapy.

Pedersen et al. found that exercise can mediate epinephrine-dependent and IL-6-dependent NK cell mobilization and redistribution, thus limiting tumor growth (20). In their study, gene chip analysis revealed that exercise training induced upregulation of immune function-related pathways. In tumor-bearing mice subjected to running, NK cell infiltration increased significantly, and lung tumor burden decreased (20). In addition, Asunción et al. found that aerobic and resistance training can promote myeloid tumor infiltrates (mostly neutrophils) and reduce tumor growth rate (3). These results suggest that exercise can enhance immune surveillance, increase NK cell and neutrophils infiltration into lung tumor tissue, and inhibit tumor growth.

In conclusion, exercise can influence the immune microenvironment of lung cancer tumors by modulating the production and release of bioactive substances, inflammatory factors, and immune cell activity. Exercise may regulate tumor inflammation, inhibit tumor growth, and improve the immune response by affecting the innate and adaptive immune systems, TAM polarization, and immune checkpoint expression (Table 1) (Figure 1). However, the specific mechanisms underlying these effects remain to be further elucidated.

The impact of exercise on the tumor microenvironment matrix in lung cancer

The effect of exercise on the matrix of the tumor microenvironment is a multifaceted process involving the extracellular matrix (ECM), matrix rigidity, matrix metalloproteinase (MMP) regulation, and modulation of extracellular signaling pathways (32, 53–55). The tumor microenvironment matrix, which includes the extracellular matrix (ECM), matrix rigidity, MMP regulation, and cell signaling modulation, plays a crucial role in tumor growth, invasion, metastasis, and treatment response (56, 57).

Exercise can affect ECM components, such as collagen and fibronectin. Some studies suggest that exercise can reduce collagen density and stiffness within the tumor microenvironment matrix, thereby slowing tumor growth and metastasis (53). However, these effects may vary depending on the tumor type and exercise modality. Tumor microenvironment matrix stiffness is closely related to tumor invasiveness and metastatic potential (58, 59). Exercise may influence ECM components and extracellular signaling pathways, altering the stiffness of the tumor microenvironment matrix. Some studies reported exercise can also affect the expression or activity of MMPs, further regulating ECM degradation and remodeling, thereby influencing tumor invasion and metastasis (22, 23). Ge et al. found that exercise can decrease MMP expression, suppressing tumor growth and

10.3389/fimmu.2023.1244764

TABLE 1 Benefits and mechanisms of exercise for lung cancer.

Species	Type	Results	Underlying mechanism	Ref
Mouse	Aerobic exercise	Slowing the progression of lung cancer	Ki67↓ MMP9↓	(23)
Mouse	HIIT	Slowing the progression of lung cancer	Ki67↓ MMP2↓	(23)
Mouse	HIIT	Diminishing the incidence of lung tumors	Unknown	(51)
Mouse	Aerobic exercise	Slowing the progression of lung cancer	p53↑; Bax↑; Ac-caspase 3↑; Apoptosis in lung cancer↑	(5)
Mouse	Voluntary Running	Showing over 60% reduction in tumor incidence and growth	NK Cell Mobilization and Redistribution	(20)
Mouse	Endurance exercise	Avoiding the resumption of tumor growth.	Protein degradation levels↓; Muscle atrophy↓	(52)
Mouse	Aerobic and resistance training	Promoting cancer immunotherapy treatment. Reducing tumor growth rate	Myeloid tumor infiltrates↑ (mostly neutrophils)	(3)
Mouse	Voluntary Running	Reducing the incidence of lung cancer	Reducing lung nodule numbers	(21)
Mouse	Aerobic exercise	Modulating the expression of some immune checkpoints in lung cancer. Reducing the proportion of M1-type TAMs in lung cancer tissues	M1 TAMs↓; SIRPα↓; PD-L1↑; Plasma IFN-γ↑	(18)
Mouse	HIIT	Modulating the expression of some immune checkpoints in lung cancer. Antagonistically regulating M1 and M2 polarization of TAMs;	IL-10, IL-12, CD47, CD24↑; Plasma IFN-γ↑	(18)

↑ means gene expression is upregulated, ↓ means gene expression is downregulated.

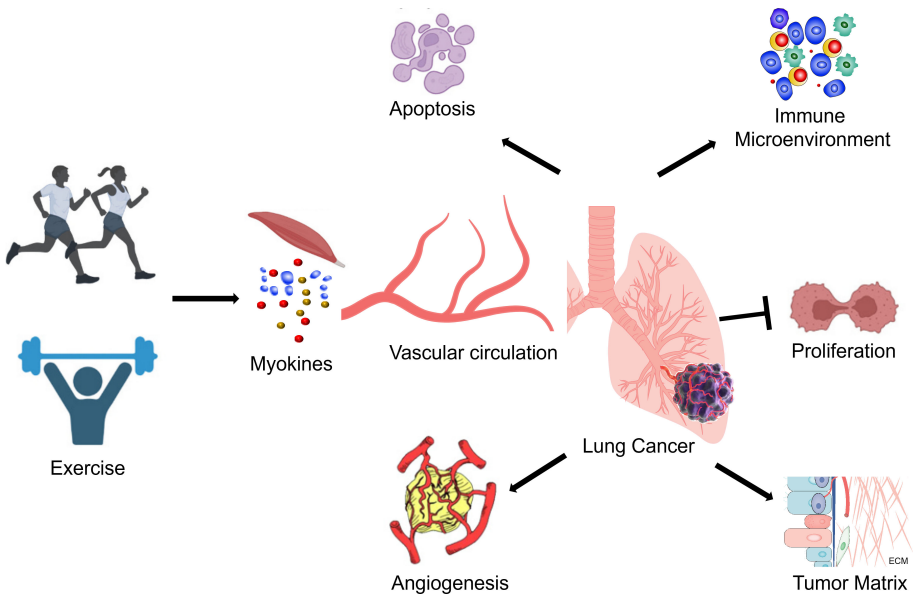


FIGURE 1
Mechanism of exercise's anticancer influence on lung cancer.

metastasis (23). The study indicated that exercise can modulate the tumor microenvironment matrix composition and function by regulating extracellular signaling pathways, such as transforming growth factor-β (TGF-β), inflammatory factors, and growth factors (23). In details, high-intensity interval exercise (HIIE) can significantly increase the expression of transforming growth factor-β1 (TGF-β1) in lung cancer tissue, suggesting that HIIE may stimulate lung cancer cell epithelial-mesenchymal transition (EMT) via TGF-β1 (23). However, although TGF-β1 can activate the Smad3/4 complex and upregulate the expression of N-cadherin in non-small cell lung cancer, the impact of HIIE on N-cadherin is not well-defined, and the specific mechanism requires further investigation. Regrettably, They have shown that exercise cannot reduce the elevated expression of type I collagen in lung cancer tissue, meaning that neither mice nor HIIE can modulate lung cancer cell EMT through type I collagen regulation (23) (Table 1) (Figure 1). These findings provide new insights into the mechanisms underlying exercise's effects on the matrix of lung cancer cells, but further research is needed to reveal more details, such as the impact of different exercise modalities on the tumor microenvironment matrix and the changes in different collagen subtypes within the matrix due to exercise.

The extracellular matrix composition is diverse and includes a range of components such as collagen, elastin, and fibronectin (54). But rare studies have reported the effects of exercise on those components. Future studies would certainly benefit from further investigation into how elastin, fibronectin, and other matrix components respond to exercise. Additionally, the influence of exercise on Cancer-Associated Fibroblasts (CAFs) within the tumor matrix warrants further exploration. CAFs are key players in tumor progression, as they contribute to matrix production, modulate immune responses, and facilitate angiogenesis (59). Thus, a deeper understanding of how exercise influences TGF-β and consequently, the behavior of CAFs, could provide key insights into the mechanism underlying the benefits of physical activity in cancer treatment. Further studies in this field could potentially pave the way for synergistic approaches combining exercise and targeted therapies.

The impact of exercise on apoptosis in lung cancer

The influence of exercise on tumor cell apoptosis has been confirmed in numerous studies, which involve intricate mechanisms, including endocrine alterations, activation of signaling pathways, improvement of the tumor microenvironment, and regulation of apoptosis-related genes (60, 61). These findings suggest that exercise could serve as a beneficial adjuvant therapy, aiding in the suppression of tumor growth and promotion of tumor cell apoptosis.

The effect of exercise on apoptosis in lung cancer cells has been corroborated in murine models. Moderate-intensity aerobic exercise training can induce tumor cell apoptosis, activating caspases and diminishing the expression of Bcl-2 (3, 22). However, in certain models, apoptosis may not be the primary reason for tumor regression; instead, it might be associated with the response to the drug nivolumab, exercise, or their combination (62–64). Exercise can inhibit cell proliferation via multiple mechanisms, including the reduction of circulating growth factors such as insulin-like growth factor-1 (IGF-1), activation of AMP-activated protein kinase (AMPK), and inhibition of protein kinase B and mammalian target of rapamycin (mTOR) activity (5, 6).

Conversely, lung cancer tumors in exercised mice exhibit elevated levels of P53 and Bax, suggesting that exercise might enhance P53-driven apoptosis (5, 6, 18). This discovery, which involves the observation of increased functional P53 protein levels in lung cancer of exercised mice, holds significant implications for a broad range of malignant tumors. Moreover, exercise might stabilize wild-type P53 protein, rendering it more effective in tumor suppression (6). However, the current understanding of the impact of exercise on tumors carrying p53 mutations remains unclear (Table 1) (Figure 1).

Future research directions encompass the investigation of endocrine pathways, such as exercise-induced IGF-1 reduction, systemic metabolic changes, the relationship between exercise-derived exosomes and the promotion of apoptosis, and an array of related pathways (65–67).

In summary, the impact of exercise on lung cancer cell apoptosis potentially involves multiple complex mechanisms, including the activation of P53 and the modulation of endocrine pathways, thereby contributing to the deceleration of tumor growth and the promotion of tumor cell apoptosis. Further research on this topic can support that exercise can synergize with other treatment modalities (such as chemotherapy, molecular-targeting agents, immunotherapy, etc.).

The influence of exercise on tumor angiogenesis

The impact of exercise on vascular endothelial growth factor-A (VEGF-A) remains contentious. Studies have reported decreased expression of VEGF-A in the peritumoral region or breast tumor tissue, while others have documented increased expression (68–70). Recent research indicates that after exercise intervention in mice with Lewis lung carcinoma, serum VEGF-A levels increased relative to baseline, but there were no significant disparities in survival rate or tumor growth compared to the control group (3). Alternatively, other studies have shown that high-intensity interval training (HIIT) can significantly reduce tumor VEGF-A mRNA levels, decrease tumor volume, and improve survival rates (23). But Pedersen et al. showed that voluntary running did not change expression of markers of angiogenesis (i.e., CD31 and VEGF-A) (20). In addition, exercise may lead to increased tumor blood flow (by upregulating VEGF-A), which can enhance drug delivery but may also promote tumor progression (6, 22).

Tumor growth is closely associated with the expression of Ki67 and angiogenic factors, VEGF and CD31, in tumor tissues (71, 72). CD105 is an endothelial cell marker that is highly expressed in actively proliferating endothelial cells and tumor blood vessels (73, 74). High expression of Ki67 and CD105 in tumor tissues also signifies increased tumor cell proliferation and poor prognosis (23). Ge et al. reported that both murine exercise and HIIT can reduce

the expression of Ki67 and angiogenic factors in tumor tissues, suggesting that exercise may influence tumor cell proliferation by inhibiting tumor angiogenesis (23). Meanwhile, Asunción et al. has shown that moderate-intensity training can reduce the percentage of Ki67-positive cells in lung cancer tissue, suggesting that exercise can inhibit lung cancer cell proliferation (3). However, neither murine exercise nor HIIT were able to reduce the percentage of CD105-positive cells in lung cancer tissue, indicating that exercise may have a weak inhibitory effect on tumor angiogenesis (23). In addition, high expression of VEGF-C is also favorable for tumor cell metastasis. Lung cancer tissue expresses VEGF-C at substantially higher levels than normal lung tissue. However, neither murine exercise nor HIIT decreased the expression of VEGF-C in lung cancer tissue, indicating that both exercise modalities may have a modest effect on inhibiting lung cancer cell proliferation and metastasis (23) (Table 1) (Figure 1).

In summary, regular exercise can significantly inhibit local tumor growth, but its effect on suppressing distant metastasis remains uncertain and controversial. Current evidence supported that exercise may inhibit tumor proliferation by reducing the expression of Ki67 and angiogenesis-related factors in tumor tissues; however, the impact on VEGF-A/C and CD105 expression is inconsistent, indicating that exercise may have a weaker effect on inhibiting tumor angiogenesis.

Additional mechanisms

Apart from the aforementioned mechanisms, the anticancer effects of exercise may also involve several biological processes, including autophagy, ferroptosis, anti-muscle atrophy effects and oxidative stress (52, 75–78). For example, exercise can induce cellular autophagy, a process of intracellular degradation and recycling of damaged or outdated organelles (79, 80). Exercise promotes autophagy by activating the AMPK/mTOR signaling pathway, which helps eliminate aberrant proteins and damaged cellular structures, reducing the likelihood of tumor development (81). Exercise can rescue TBI-induced ferroptosis via STING pathway (82). Exercise can also enhance the functionality of the antioxidant system, decrease reactive oxygen species (ROS) levels, and alleviate oxidative stress (83, 84). Oxidative stress is closely associated with tumor initiation and progression (85, 86). Exercise contributes to maintaining the balance between oxidative and antioxidative processes, lowering the risk of tumor development (60, 87). These mechanisms have been experimentally validated in other types of cancer, but their role in exercise as an anticancer intervention for lung cancer has not yet been confirmed. Further research is needed to explore these potential mechanisms in the context of lung cancer prevention and treatment (Figure 1).

Conclusion

Exercise holds significant importance in the prevention and treatment of lung cancer. Firstly, in terms of prevention, exercise can reduce the risk of lung cancer development. By suppressing inflammatory responses, enhancing immune function, regulating cellular autophagy, and alleviating oxidative stress, exercise helps maintain a healthy physiological environment to resist cancer onset.

Secondly, in the context of treatment, exercise acts as a supplemental therapy that patients with lung cancer can benefit from in order to enhance their quality of life. Exercise helps reduce side effects during lung cancer treatment by improving cardiorespiratory function, alleviating fatigue, enhancing muscular strength, and boosting psychological well-being. Additionally, exercise can strengthen patients' physical fitness, increasing their tolerance to other treatment modalities (such as surgery, radiotherapy, and chemotherapy), thereby enhancing treatment outcomes. Hence, we zealously promote the inclusion of exercise as a vital component in holistic lung cancer treatment plans, creating a powerhouse of support for patients. To safeguard the well-being and efficacy of exercise interventions, we propose tailoring personalized workout regimens under the expert guidance of medical professionals.

In summary, the biological basis of exercise as an anticancer intervention for lung cancer primarily includes modulation of the tumor immune microenvironment, inhibition of tumor angiogenesis, promotion of tumor cell apoptosis, and regulation of the tumor extracellular matrix. Through these mechanisms, exercise can reduce the risk of developing lung cancer, slow its progression, and enhance lung cancer patients' quality of life. To provide a robust and comprehensive theoretical framework for clinical exercise interventions, it is imperative to engage in further investigation and unravel the intricate and nuanced anticancer mechanisms elicited by exercise within the intricate realm of lung cancer.

Perspectives

The fundamental research on exercise as an anticancer intervention for lung cancer will continue to delve deeper into its underlying biological mechanisms, providing more precise theoretical guidance for clinical practice (Figure 2). We hope that the following directions can offer insights for researchers:

1. Molecular pathways: Researchers will investigate the molecular pathways involved in the anticancer effects of exercise. This includes studying how exercise regulates the expression of genes and proteins associated with inflammation, immune responses, cell growth, and cell death in both healthy and cancerous cells (88–90).
2. Different exercise modalities: Research can also explore the optimal type, intensity, frequency, and duration of exercise interventions in animal models, providing more targeted recommendations for preventive strategies (91–93).
3. Precision therapy: Research may focus on the role of exercise interventions in combination with different therapeutic approaches, as well as the impact of exercise on specific lung cancer subtypes, disease stages, and individual patient differences, offering more personalized and precise guidance for clinical practice (92, 94–96).
4. Interactions with other lifestyle factors: Studies may investigate the interactions between exercise and other

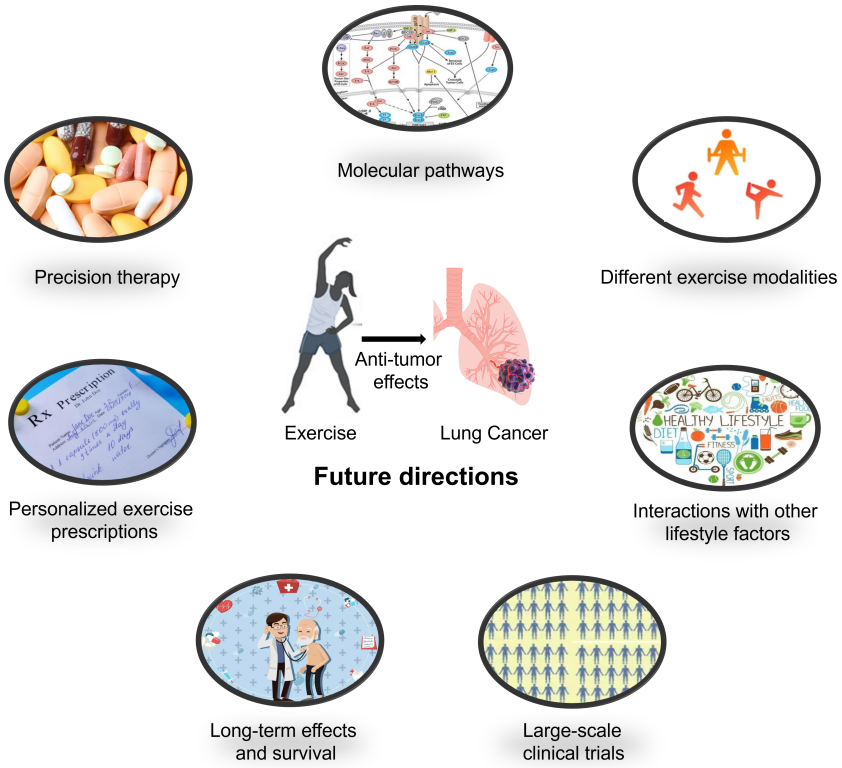


FIGURE 2
Future research directions for the treatment of lung cancer using exercise anti-tumor effects.

lifestyle factors (such as diet, smoking, and alcohol consumption) in terms of lung cancer risk and prognosis (87, 97). This will help develop more comprehensive lifestyle intervention strategies for more effective prevention and treatment of lung cancer.

5. Personalized exercise prescriptions: With the advancement of research, personalized exercise prescriptions may be formulated for lung cancer patients based on factors such as age, sex, physical fitness, cancer stage, and treatment plan (98, 99). These individualized prescriptions will help maximize the benefits of exercise while minimizing the risk of injuries or adverse reactions.
6. Long-term effects and survival: Future research should also focus on the long-term impact of exercise interventions on lung cancer survival, including outcomes such as overall survival, disease-free survival, and quality of life (92, 100). This will help determine the optimal duration and intensity of exercise programs for lung cancer patients and survivors.
7. Large-scale clinical trials: To further validate the benefits of exercise in lung cancer prevention and treatment, large-scale clinical trials are needed. These trials should be designed to compare the effects of different exercise modalities, frequencies, and intensities on lung cancer outcomes (94, 101).

By deepening our understanding of the mechanisms and potential applications of exercise in the context of lung cancer, we can strive to develop more targeted, effective, and evidence-based preventive and therapeutic interventions. Ultimately, this will contribute to an improvement in the general standard of life for lung cancer patients as well as a reduction in the total burden caused by this disease.

Author contributions

SC, WQ and XS contributed to the conception and design of the study. ZL, SL and RW designed and wrote the whole manuscript. TF and ZP completed subsequent revisions of the manuscript. ZL, RW, TF and ZP collected the references and prepared figures of the manuscript. All authors contributed to the article and approved the submitted version.

Funding

This work was supported by the National Natural Science Foundation of China (Grant No. 82172511,81972125, and 82172510).

Conflict of interest

The authors declare that the research was conducted in the absence of any commercial or financial relationships that could be construed as a potential conflict of interest.

Publisher's note

All claims expressed in this article are solely those of the authors and do not necessarily represent those of their affiliated organizations, or those of the publisher, the editors and the reviewers. Any product that may be evaluated in this article, or claim that may be made by its manufacturer, is not guaranteed or endorsed by the publisher.

References

1. Voorn MJJ, Driessen EJM, Reinders RJEF, van Kampen-van den Boogaart VEM, Bongers BC, Janssen-Heijnen MLG. Effects of exercise prehabilitation and/or rehabilitation on health-related quality of life and fatigue in patients with non-small cell lung cancer undergoing surgery: A systematic review. *Eur J Surg Oncol* (2023). doi: 10.1016/j.ejso.2023.04.008

2. Cavalheri V, Granger CL. Exercise training as part of lung cancer therapy. *Respirology* (2020) 25:80–7. doi: 10.1111/resp.13869

3. Martín-Ruiz A, Fiuza-Luces C, Rincón-Castanedo C, Fernández-Moreno D, Gálvez BG, Martínez-Martínez E, et al. Benefits of exercise and immunotherapy in a murine model of human non-small-cell lung carcinoma. *Exerc Immunol Rev* (2020) 26:100–15.

4. Li X, Li S, Yan S, Wang Y, Wang X, Sihoe ADL, et al. Impact of preoperative exercise therapy on surgical outcomes in lung cancer patients with or without COPD: A systematic review and meta-analysis. *Cancer Manage Res* (2019) 11:1765–77. doi: 10.2147/CMAR.S186432

5. Higgins KA, Park D, Lee GY, Curran WJ, Deng X. Exercise-induced lung cancer regression: Mechanistic findings from a mouse model. *Cancer* (2014) 120:3302–10. doi: 10.1002/cncr.28878

6. Avancini A, Sartori G, Gkountakos A, Casali M, Trestini I, Tregnago D, et al. Physical activity and exercise in lung cancer care: will promises be fulfilled? *Oncologist* (2020) 25:e555–69. doi: 10.1634/theoncologist.2019-0463

7. Bade BC, Thomas DD, Scott JAB, Silvestri GA. Increasing physical activity and exercise in lung cancer: Reviewing safety, benefits, and application. *J Thorac Oncol* (2015) 10:861–71. doi: 10.1097/JTO.0000000000000536

8. Yisheng C, Sun Y, Luo Z, Lin J, Qi B, Kang X, et al. Potential mechanism Q4 underlying exercise upregulated circulating blood exosome miR-215-5p to prevent necroptosis of neuronal cells and a model for early diagnosis of alzheimer's disease. *Front Aging Neurosci* (2022) 14:860364. doi: 10.3389/fnagi.2022.860364

9. Chen Y, Luo Z, Sun Y, Li F, Han Z, Qi B, et al. Exercise improves choroid plexus epithelial cells metabolism to prevent glial cell-associated neurodegeneration. *Front Pharmacol* (2022) 13:1010785. doi: 10.3389/fphar.2022.1010785

10. Luo Z, He Z, Qin H, Chen Y, Qi B, Lin J, et al. Exercise-induced IL-15 acted as a positive prognostic implication and tumor-suppressed role in pan-cancer. *Front Pharmacol* (2022) 13:1053137. doi: 10.3389/fphar.2022.1053137

11. Chen Y, Sun Y, Luo Z, Chen X, Wang Y, Qi B, et al. Exercise modifies the transcriptional regulatory features of monocytes in alzheimer's patients: A multi-omics integration analysis based on single cell technology. *Front Aging Neurosci* (2022) 14:881488. doi: 10.3389/fnagi.2022.881488

12. Chen Y, Sun Y, Luo Z, Lin J, Qi B, Kang X, et al. Potential mechanism underlying exercise upregulated circulating blood exosome miR-215-5p to prevent necroptosis of neuronal cells and a model for early diagnosis of alzheimer's disease. *Front Aging Neurosci* (2022) 14:860364. doi: 10.3389/fnagi.2022.860364

13. Jones LW, Alfano CM. Exercise-oncology research: Past, present, and future. *Acta Oncol (Madr)* (2013) 52:195–215. doi: 10.3109/0284186X.2012.742564

14. Bohlen J, McLaughlin SL, Hazard-Jenkins H, Infante AM, Montgomery C, Davis M, et al. Dysregulation of metabolic-associated pathways in muscle of breast cancer patients: preclinical evaluation of interleukin-15 targeting fatigue. *J Cachexia. Sarcopenia Muscle* (2018) 9:701–14. doi: 10.1002/jcsm.12294

15. Ligibel JA, Dillon D, Giobbie-Hurder A, McTiernan A, Frank E, Cornwell M, et al. Impact of a pre-operative exercise intervention on breast cancer proliferation and gene expression: Results from the pre-operative health and body (PreHAB) study. *Clin Cancer Res* (2019) 25:5398–406. doi: 10.1158/1078-0432.CCR-18-3143

16. Pereira MG, Voltarelli VA, Tobias GC, de Souza L, Borges GS, Paixão AO, et al. Aerobic exercise training and in *vivo* akt activation counteract cancer cachexia by inducing a hypertrophic profile through eif-2α modulation. *Cancers (Basel)* (2022) 14 (1). doi: 10.3390/cancers14010028

17. Morrisson MJ, Bi F, Yang K, Cady SL, Hartwich TM, Cerchia AP, et al. Effect of exercise on peritoneal microenvironment and progression of ovarian cancer. *Am J Cancer Res* (2021) 11:5045–62.

18. Ge Z, Wu S, Qi Z, Ding S. Exercise modulates polarization of TAMs and expression of related immune checkpoints in mice with lung cancer. *J Cancer* (2022) 13:3297–307. doi: 10.7150/jca.76136

19. Murphy EA, Davis JM, Brown AS, Carmichael MD, Mayer EP, Ghaffar A. Effects of moderate exercise and oat β-glucan on lung tumor metastases and macrophage antitumor cytotoxicity. *J Appl Physiol* (2004) 97:955–9. doi: 10.1152/japplphysiol.00252.2004

20. Pedersen L, Idorn M, Olofsson GH, Lauenborg B, Nookaew I, Hansen RH, et al. Voluntary running suppresses tumor growth through epinephrine- and IL-6-dependent NK cell mobilization and redistribution. *Cell Metab* (2016) 23:554–62. doi: 10.1016/j.cmet.2016.01.011

21. Elisia I, Cho B, Hay M, Li MY, Hofs E, Lam V, et al. The effect of diet and exercise on tobacco carcinogen-induced lung cancer. *Carcinogenesis* (2019) 40:448–60. doi: 10.1093/carcin/bgz060

22. Huang Q, Wu M, Wu X, Zhang Y, Xia Y. Muscle-to-tumor crosstalk: The effect of exercise-induced myokine on cancer progression. *Biochim Biophys Acta - Rev Cancer* (2022) 1877:188761. doi: 10.1016/j.bbcan.2022.188761

23. Ge Z, Wu S, Qi Z, Ding S. Compared with High-intensity Interval Exercise, Moderate Intensity Constant Load Exercise is more effective in curbing the Growth and Metastasis of Lung Cancer. *J Cancer* (2022) 13:1468–79. doi: 10.7150/jca.66245

24. Washington TA, Schrems ER, Haynie WS, Rosa-Caldwell ME, Brown JL, Saling L, et al. Development of skeletal muscle fibrosis in a rodent model of cancer cachexia. *Cell Biochem Funct* (2023) 41(4):478–89. doi: 10.1002/cbf.3797

25. Bartlett JD, Close GL, Drust B, Morton JP. The emerging role of p53 in exercise metabolism. *Sport Med* (2014) 44:303–9. doi: 10.1007/s40279-013-0127-9

26. Fu M, Han X, Chen B, Guo L, Zhong L, Hu P, et al. Cancer treatment: from traditional Chinese herbal medicine to the liposome delivery system. *Acta Mater Med* (2022) 1:486–506. doi: 10.15212/AMM-2022-0035

27. Xu X, Li R, Dong R, Yang Y, Wang H, Cheng J, et al. *In vitro* characterization and cellular uptake profiles of TAMs-targeted lipid calcium carbonate nanoparticles for cancer immunotherapy. *Acta Mater Med* (2022) 1:400–10. doi: 10.15212/AMM-2022-0030

28. Chang M, Gao F, Chen J, Gnawali G, Wang W. MDM2-BCL-XL PROTACs enable degradation of BCL-XL and stabilization of p53. *Acta Mater Med* (2022) 1:333–42. doi: 10.15212/AMM-2022-0022

29. Chang M, Gao F, Chen J, Gnawali G, Wang W. MDM2-BCL-XL PROTACs enable degradation of BCL-XL and stabilization of p53. *Acta Mater Med* (2022) 1:172–90. doi: 10.15212/AMM-2022-0022

30. Tan J, Peeraphong L, Ruchawapol C, Zhang J, Zhao J, Fu W, et al. Emerging role of HJURP as a therapeutic target in cancers. *Acta Mater Med* (2023) 2:157–71. doi: 10.15212/AMM-2023-0008

31. Jia N, Zhou Y, Dong X, Ding M. The antitumor mechanisms of aerobic exercise: A review of recent preclinical studies. *Cancer Med* (2021) 10:6365–73. doi: 10.1002/cam4.4169

32. Esteves M, Monteiro MP, Duarte JA. Role of regular physical exercise in tumor vasculature: favorable modulator of tumor milieu. *Int J Sports Med* (2021) 42:389–406. doi: 10.1055/a-1308-3476

33. Brett Whalen L, Zachary Wright W, Kundur P, Angadi S, Modesitt SC. Beneficial effects of exercise on chemotherapy-induced peripheral neuropathy and sleep disturbance: A review of literature and proposed mechanisms. *Gynecol Oncol Rep* (2022) 39:100927. doi: 10.1016/j.gore.2022.100927

34. Dethlefsen C, Hansen LS, Lillelund C, Andersen C, Gehl J, Christensen JF, et al. Exercise-induced catecholamines activate the Hippo tumor suppressor pathway to reduce risks of breast cancer development. *Cancer Res* (2017) 77:4894–904. doi: 10.1158/0008-5472.CAN-16-3125

35. Schwappacher R, Dieterich W, Reljic D, Pilarsky C, Mukhopadhyay D, Chang DK, et al. Muscle-derived cytokines reduce growth, viability and migratory activity of pancreatic cancer cells. *Cancers (Basel)* (2021) 13(15):3820. doi: 10.3390/cancers13153820

36. Kim JS, Galvão DA, Newton RU, Gray E, Taaffe DR. Exercise-induced myokines and their effect on prostate cancer. *Nat Rev Urol* (2021) 18:519–42. doi: 10.1038/s41585-021-00476-y

37. Chung KH, Park SB, Streckmann F, Wiskemann J, Mohile N, Kleckner AS, et al. Mechanisms, mediators, and moderators of the effects of exercise on chemotherapy-induced peripheral neuropathy. *Cancers (Basel)* (2022) 14:1–27. doi: 10.3390/cancers14051224

38. Mader T, Chaillou T, Alves ES, Jude B, Cheng AJ, Kenne E, et al. Exercise reduces intramuscular stress and counteracts muscle weakness in mice with breast cancer. *J Cachexia. Sarcopenia Muscle* (2022) 13:1151–63. doi: 10.1002/jcsm.12944

39. Tidball JG. Regulation of muscle growth and regeneration by the immune system. *Nat Rev Immunol* (2017) 17:165–78. doi: 10.1038/nri.2016.150

40. Perandini LA, Chimin P, Lutkemeyer D, Câmara NOS. Chronic inflammation in skeletal muscle impairs satellite cells function during regeneration: can physical exercise restore the satellite cell niche? *FEBS J* (2018) 285:1973–84. doi: 10.1111/febs.14417

41. Saito Y, Chikenji TS. Diverse roles of cellular senescence in skeletal muscle inflammation, regeneration, and therapeutics. *Front Pharmacol* (2021) 12:739510. doi: 10.3389/fphar.2021.739510

42. Dort J, Fabre P, Molina T, Dumont NA. Macrophages are key regulators of stem cells during skeletal muscle regeneration and diseases. *Stem Cells Int* (2019) 2019:4761427. doi: 10.1155/2019/4761427

43. Shapouri-Moghaddam A, Mohammadian S, Vazini H, Taghadosi M, Esmaeili SA, Mardani F, et al. Macrophage plasticity, polarization, and function in health and disease. *J Cell Physiol* (2018) 233(9):6425–40. doi: 10.1002/jcp.26429

44. Tian X, Wu Y, Yang Y, Wang J, Niu M, Gao S, et al. Long noncoding RNA LINC00662 promotes M2 macrophage polarization and hepatocellular carcinoma progression via activating Wnt/β-catenin signaling. *Mol Oncol* (2020) 14:462–83. doi: 10.1002/1878-0261.12606

45. Mohapatra S, Pioppini C, Ozpolat B, Calin GA. Non-coding RNAs regulation of macrophage polarization in cancer. *Mol Cancer* (2021) 20:1–15. doi: 10.1186/s12943-021-01313-x

46. Stout RD, Jiang C, Matta B, Tietzel I, Watkins SK, Suttles J. Macrophages sequentially change their functional phenotype in response to changes in microenvironmental influences. *J Immunol* (2005) 175(1):342–9. doi: 10.4049/jimmunol.175.1.342

47. Cooks T, Pateras IS, Jenkins LM, Patel KM, Robles AI, Morris J, et al. Mutant p53 cancers reprogram macrophages to tumor supporting macrophages via exosomal miR-1246. *Nat Commun* (2018) 9(1):771. doi: 10.1038/s41467-018-03224-w

48. Pritchard A, Tousif S, Wang Y, Hough K, Khan S, Strenkowski J, et al. Lung tumor cell-derived exosomes promote M2 macrophage polarization. *Cells* (2020) 9:1303. doi: 10.3390/cells9051303

49. Davis MJ, Tsang TM, Qiu Y, Dayrit JK, Freij JB, Huffnagle GB, et al. Macrophage M1/M2 polarization dynamically adapts to changes in cytokine microenvironments in cryptococcus neoformans infection. *MBio* (2013) 4(3):e00264–13. doi: 10.1128/mBio.00264-13

50. Nahrendorf M, Swirski FK. Abandoning M1/M2 for a network model of macrophage function. *Circ Res* (2016) 119:414–7. doi: 10.1161/CIRCRESAHA.116.309194

51. Paceli RB, Cal RN, dos Santos CH, Cordeiro JA, Neiva CM, Nagamine KK, et al. The influence of physical activity in the progression of experimental lung cancer in mice. *Pathol Res Pract* (2012) 208(7):377–81. doi: 10.1016/j.prp.2012.04.006

52. de Lima EA, Teixeira AA, de S, Biondo LA, Diniz TA, Silveira LS, et al. Exercise reduces the resumption of tumor growth and proteolytic pathways in the skeletal muscle of mice following chemotherapy. *Cancers (Basel)* (2020) 12:1–17. doi: 10.3390/cancers12113466

53. Verma VK, Singh V, Singh MP, Singh SM. Effect of physical exercise on tumor growth regulating factors of tumor microenvironment: Implications in exercise-dependent tumor growth retardation. *Immunopharmacol Immunotoxicol* (2009) 31:274–82. doi: 10.1080/08923970802562042

54. Leight JL, Drain AP, Weaver VM. Extracellular matrix remodeling and stiffening modulate tumor phenotype and treatment response. *Annu Rev Cancer Biol* (2017) 1:313–34. doi: 10.1146/annurev-cancerbio-050216-034431

55. Zhang X, Ashcraft KA, Betof Warner A, Nair SK, Dewhirst MW. Can exercise-induced modulation of the tumor physiologic microenvironment improve antitumor immunity? *Cancer Res* (2019) 79:2447–56. doi: 10.1158/0008-5472.CAN-18-2468

56. Kessenbrock K, Plaks V, Werb Z. Matrix metalloproteinases: regulators of the tumor microenvironment. *Cell* (2010) 141:52–67. doi: 10.1016/j.cell.2010.03.015

57. Pedersen L, Christensen JF, Hojman P. Effects of exercise on tumor physiology and metabolism. *Cancer J* (2015) 21:111–6. doi: 10.1097/PPO.0000000000000096

58. Schedin P, Keely PJ. Mammary gland ECM remodeling, stiffness, and mechanosignaling in normal development and tumor progression. *Cold Spring Harb. Perspect Biol* (2011) 3:a003228–a003228. doi: 10.1101/cshperspect.a003228

59. Najafi M, Farhood B, Mortezaee K. Extracellular matrix (ECM) stiffness and degradation as cancer drivers. *J Cell Biochem* (2019) 120:2782–90. doi: 10.1002/jcb.27681

60. Hojman P, Gehl J, Christensen JF, Pedersen BK. Molecular mechanisms linking exercise to cancer prevention and treatment. *Cell Metab* (2018) 27:10–21. doi: 10.1016/j.cmet.2017.09.015

61. Zhong D, Li Y, Huang Y, Hong X, Li J, Jin R. Molecular mechanisms of exercise on cancer: A bibliometrics study and visualization analysis via citespace. *Front Mol Biosci* (2022) 8:797902. doi: 10.3389/fmolb.2021.797902

62. Oya Y, Yoshida T, Kuroda H, Mikubo M, Kondo C, Shimizu J, et al. Predictive clinical parameters for the response of nivolumab in pretreated advanced non-small-cell lung cancer. *Oncotarget* (2017) 8:103117–28. doi: 10.18632/oncotarget.21602

63. Eshghi N, Lundeen TF, Kuo PH. Dynamic adaptation of tumor immune response with nivolumab demonstrated by 18F-FDG PET/CT. *Clin Nucl Med* (2018) 43:114–6. doi: 10.1097/RLU.0000000000001934

64. Taha T, Meiri D, Talhamy S, Wollner M, Peer A, Bar-Sela G. Cannabis impacts tumor response rate to nivolumab in patients with advanced Malignancies. *Oncologist* (2019) 24:549–54. doi: 10.1634/theoncologist.2018-0383

65. Suzuki K, Tominaga T, Ruhee RT, Ma S. Characterization and modulation of systemic inflammatory response to exhaustive exercise in relation to oxidative stress. *Antioxidants* (2020) 9:401. doi: 10.3390/antiox9050401

66. Estébanez B, Jiménez-Pavón D, Huang C, Cuevas MJ, González-Gallego J. Effects of exercise on exosome release and cargo in *in vivo* and ex vivo models: A systematic review. *J Cell Physiol* (2021) 236:3336–53. doi: 10.1002/jcp.30094

67. Guo B, Yuan L-Q. Editorial: the role of exosomes in metabolic and endocrine disease. *Front Endocrinol (Lausanne)* (2022) 13:859650. doi: 10.3389/fendo.2022.859650

68. Greb RR, Maier I, Wallwiener D, Kiesel L. Vascular endothelial growth factor A (VEGF-A) mRNA expression levels decrease after menopause in normal breast tissue but not in breast cancer lesions. *Br J Cancer* (1999) 81:225–31. doi: 10.1038/sj.bjc.6690681

69. Parr C, Gan CH, Watkins G, Jiang WG. Reduced vascular endothelial growth inhibitor (VEGI) expression is associated with poor prognosis in breast cancer patients. *Angiogenesis* (2006) 9:73–81. doi: 10.1007/s10456-006-9033-1

70. Zhao Y-C, Ni X-J, Li Y, Dai M, Yuan Z-X, Zhu Y-Y, et al. Peritumoral lymphangiogenesis induced by vascular endothelial growth factor C and D promotes lymph node metastasis in breast cancer patients. *World J Surg Oncol* (2012) 10:165. doi: 10.1186/1477-7819-10-165

71. Fuckar D, Dekanic A, Stifter S, Mustac E, Krstulja M, Dobrila F, et al. VEGF expression is associated with negative estrogen receptor status in patients with breast cancer. *Int J Surg Pathol* (2006) 14:49–55. doi: 10.1177/106689690601400109

72. Syed BM, Green AR, Morgan DAL, Ellis IO, Cheung K-L. Liver kinase B1—A potential therapeutic target in hormone-sensitive breast cancer in older women. *Cancers (Basel)* (2019) 11:149. doi: 10.3390/cancers11020149

73. Gurung S, Williams S, Deane JA, Werkmeister JA, Gargett CE. The transcriptome of human endometrial mesenchymal stem cells under TGFβR inhibition reveals improved potential for cell-based therapies. *Front Cell Dev Biol* (2018) 6:164. doi: 10.3389/fcell.2018.00164

74. Jiang S, Tian G, Yang Z, Gao X, Wang F, Li J, et al. Enhancement of acellular cartilage matrix scaffold by Wharton's jelly mesenchymal stem cell-derived exosomes to promote osteochondral regeneration. *Bioact Mater* (2021) 6:2711–28. doi: 10.1016/j.bioactmat.2021.01.031

75. White E. The role for autophagy in cancer. *J Clin Invest* (2015) 125:42–6. doi: 10.1172/jci73941

76. Bebber CM, Müller F, Prieto Clemente L, Weber J, von Karstedt S. Ferroptosis in cancer cell biology. *Cancers (Basel)* (2020) 12:164. doi: 10.3390/cancers12010164

77. Gunadi JW, Welliangan AS, Soetadji RS, Jasaputra DK, Lesmana R. The role of autophagy modulated by exercise in cancer cachexia. *Life* (2021) 11:781. doi: 10.3390/life11080781

78. Kim MJ, Yun GJ, Kim SE. Metabolic regulation of ferroptosis in cancer. *Biol (Basel)* (2021) 10:83. doi: 10.3390/biology10020083

79. Mooren FC, Krüger K. Exercise, autophagy, and apoptosis. *Prog Mol Biol Transl Sci* (2015) 135:407–22. doi: 10.1016/bs.pmbts.2015.07.023

80. Halling JF, Pilegaard H. Autophagy-dependent beneficial effects of exercise. *Cold Spring Harb Perspect Med* (2017) 7:a029777. doi: 10.1101/cshperspect.a029777

81. Singletary K, Milner J. Diet, autophagy, and cancer: A review. *Cancer Epidemiol. Biomarkers Prev* (2008) 17:1596–610. doi: 10.1158/1055-9965.EPI-07-2917

82. Chen J, Zhu T, Yu D, Yan B, Zhang Y, Jin J, et al. Moderate intensity of treadmill exercise rescues TBI-induced ferroptosis, neurodegeneration, and cognitive impairments via suppressing STING pathway. *Mol Neurobiol* (2023) 60(9):4872–96. doi: 10.1007/s12035-023-03379-8

83. Gomez-Cabrera M-C, Domenech E, Viña J. Moderate exercise is an antioxidant: Upregulation of antioxidant genes by training. *Free Radic Biol Med* (2008) 44:126–31. doi: 10.1016/j.freeradbiomed.2007.02.001

84. Ristow M, Zarse K, Oberbach A, Klöting N, Birringer M, Kiehntopf M, et al. Antioxidants prevent health-promoting effects of physical exercise in humans. *Proc Natl Acad Sci* (2009) 106:8665–70. doi: 10.1073/pnas.0903485106

85. Gorrini C, Harris IS, Mak TW. Modulation of oxidative stress as an anticancer strategy. *Nat Rev Drug Discovery* (2013) 12:931–47. doi: 10.1038/nrd4002

86. Saha SK, Lee SB, Won J, Choi HY, Kim K, Yang G-M, et al. Correlation between oxidative stress, nutrition, and cancer initiation. *Int J Mol Sci* (2017) 18:1544. doi: 10.3390/ijms18071544

87. Thomas RJ, Kenfield SA, Jimenez A. Exercise-induced biochemical changes and their potential influence on cancer: a scientific review. *Br J Sports Med* (2016) 51:640–4. doi: 10.1136/bjsports-2016-096343

88. Gould DW, Lahart I, Carmichael AR, Koutedakis Y, Metsios GS. Cancer cachexia prevention via physical exercise: molecular mechanisms. *J Cachexia. Sarcopenia Muscle* (2012) 4:111–24. doi: 10.1007/s13539-012-0096-0

89. Betof AS, Dewhirst MW, Jones LW. Effects and potential mechanisms of exercise training on cancer progression: A translational perspective. *Brain. Behav Immun* (2013) 30:S75–87. doi: 10.1016/j.bbi.2012.05.001

90. Luo Z, Qi B, Sun Y, Chen Y, Lin J, Qin H, et al. Engineering bioactive M2 macrophage-polarized, anti-inflammatory, miRNA-based liposomes for functional muscle repair: from exosomal mechanisms to biomaterials. *Small* (2022) 18:2201957. doi: 10.1002/smll.202201957

91. Hayes SC, Spence RR, Galvão DA, Newton RU. Australian Association for Exercise and Sport Science position stand: Optimising cancer outcomes through exercise. *J Sci Med Sport* (2009) 12:428–34. doi: 10.1016/j.jsams.2009.03.002

92. Spence RR, Heesch KC, Brown WJ. Exercise and cancer rehabilitation: A systematic review. *Cancer Treat Rev* (2010) 36:185–94. doi: 10.1016/j.ctrv.2009.11.003

93. Cataldi S, Greco G, Mauro M, Fischetti F. Effect of exercise on cancer-related fatigue: A systematic review. *J Hum Sport Exerc* (2020) 16. doi: 10.14198/jhse.2021.163.01

94. Bland KA, Zadravec K, Landry T, Weller S, Meyers L, Campbell KL. Impact of exercise on chemotherapy completion rate: A systematic review of the evidence and recommendations for future exercise oncology research. *Crit Rev Oncol Hematol* (2019) 136:79–85. doi: 10.1016/j.critrevonc.2019.02.005

95. Luo Z, Sun Y, Qi B, Lin J, Chen Y, Xu Y, et al. Human bone marrow mesenchymal stem cell-derived extracellular vesicles inhibit shoulder stiffness via let-7a/Tgfbr1 axis. *Bioact Mater* (2022) 17:344–59. doi: 10.1016/j.bioactmat.2022.01.016

96. Cai J, Xu J, Ye Z, Wang L, Zheng T, Zhang T, et al. Exosomes derived from kartogenin-preconditioned mesenchymal stem cells promote cartilage formation and collagen maturation for enthesis regeneration in a rat model of chronic rotator cuff tear. *Am J Sports Med* (2023) 51:1267–76. doi: 10.1177/03635465231155927

97. Kerr J, Anderson C, Lippman SM. Physical activity, sedentary behaviour, diet, and cancer: an update and emerging new evidence. *Lancet Oncol* (2017) 18:e457–71. doi: 10.1016/s1470-2045(17)30411-4

98. Zubin Maslov P, Schulman A, Lavie CJ, Narula J. Personalized exercise dose prescription. *Eur Heart J* (2017) 39:2346–55. doi: 10.1093/eurheartj/ehx686

99. Galiuto L, Fedele E, Vitale E, Lucini D. Personalized exercise prescription for heart patients. *Curr Sports Med Rep* (2019) 18:380–1. doi: 10.1249/JSR.0000000000000646

100. Campbell KL, Winters-Stone KM, Wiskemann J, May AM, Schwartz AL, Courneya KS, et al. Exercise guidelines for cancer survivors: consensus statement from international multidisciplinary roundtable. *Med Sci Sport Exerc* (2019) 51:2375–90. doi: 10.1249/MSS.0000000000002116

101. Yang L, Morielli AR, Heer E, Kirkham AA, Cheung WY, Usmani N, et al. Effects of exercise on cancer treatment efficacy: A systematic review of preclinical and clinical studies. *Cancer Res* (2021) 81:4889–95. doi: 10.1158/0008-5472.CAN-21-1258

frontiers | Frontiers in Immunology

TYPE Original Research
PUBLISHED 28 August 2023
DOI 10.3389/fimmu.2023.1239097

Check for updates

OPEN ACCESS

EDITED BY
Yuan Wan,
Binghamton University, United States

REVIEWED BY
Guosheng Wang,
Tongji University, China
Zhu Chuandong,
Nanjing Second Hospital, China

*CORRESPONDENCE
Christian Gessner
ch.gessner@pneumologe-leipzig.de

†These authors share first authorship

‡These authors share senior authorship

RECEIVED 12 June 2023
ACCEPTED 07 August 2023
PUBLISHED 28 August 2023

CITATION
Gessner P, Tessema B, Scholz M, Sack U, Boldt A, Kühnapfel A and Gessner C (2023) The influence of anti-cancer therapies on lymphocyte subpopulations of lung cancer patients.
Front. Immunol. 14:1239097.
doi: 10.3389/fimmu.2023.1239097

COPYRIGHT
© 2023 Gessner, Tessema, Scholz, Sack, Boldt, Kühnapfel and Gessner. This is an open-access article distributed under the terms of the Creative Commons Attribution License (CC BY). The use, distribution or reproduction in other forums is permitted, provided the original author(s) and the copyright owner(s) are credited and that the original publication in this journal is cited, in accordance with accepted academic practice. No use, distribution or reproduction is permitted which does not comply with these terms.

The influence of anti-cancer therapies on lymphocyte subpopulations of lung cancer patients

Philipp Gessner[1,2†], Belay Tessema[1,3†], Markus Scholz[4], Ulrich Sack[1], Andreas Boldt[1], Andreas Kühnapfel[4‡] and Christian Gessner[1,5*‡]

[1]Institute of Clinical Immunology, Faculty of Medicine, University of Leipzig, Leipzig, Germany, [2]Department of Respiratory Medicine, University Hospital Leipzig, Leipzig, Germany, [3]Department of Medical Microbiology, College of Medicine and Health Sciences, University of Gondar, Gondar, Ethiopia, [4]Institute for Medical Informatics, Statistics and Epidemiology (IMISE), University of Leipzig, Leipzig, Germany, [5]Pulmonary Practice, Leipzig, Germany

Introduction: There are limited data on the influence of different anti-cancer therapies on lymphocyte subpopulations and their relationships to survival of non-small cell lung cancer (NSCLC) patients. This study aimed to assess the effect of immunotherapy, chemotherapy, immunochemotherapy, adjuvant chemotherapy after surgery, and antibodies against Vascular Endothelial Growth Factors (VEGF) on B cell, T cell, and NK cell subpopulations, and the survival time of NSCLC patients.

Methods: A total of 32 consecutive NSCLC patients were recruited at Pulmonology Clinic, Leipzig from January 2018 to March 2020 and enrolled in this study. Immunophenotyping was done using a FACS Canto II flow cytometer (BD Biosciences) before the administration of the planned therapy and during therapy with up to 7 observational windows for each patient targeting 130 immunologic parameters.

Results: Absolute transitional B cells was significantly increased after immunotherapy ($p = 0.032$), immunochemotherapy ($p = 0.030$), and antibodies against VEGF ($p = 0.024$). Similarly, absolute counts and percentage of B cells were significantly increased after adjuvant chemotherapy ($p = 0.023$). However, absolute counts and percentage of transitional B cells are significantly decreased after chemotherapy ($p = 0.001$). Activated cytotoxic T cells were significantly increased after immunotherapy ($p = 0.031$) and immunochemotherapy ($p = 0.030$). The overall survival rate of NSCLC patients was 31%.

Conclusions: In conclusion, this study suggests that different types of anti-cancer therapies affect lymphocyte subpopulations of NSCLC patients. Further large-scale and multicentre studies are required to confirm our results and to evaluate the prognostic value of lymphocyte subpopulations.

KEYWORDS

non-small cell lung cancer, B cells, T cells, NK cells, anti-cancer therapies

Introduction

Lung cancer is one of the most frequent malignancies with 2.2 million new cases a year and the most common cause of cancer death in the world (1). Non-small cell lung cancer (NSCLC) is about 80–85% of all lung cancer cases (2). Majority (> 55%) of NSCLC patients are diagnosed late at the advanced stages of the disease (3). Currently, the treatment options for NSCLC are systemic therapies such as chemotherapies, drugs targeting commonly mutated pathways in lung cancer, and immune checkpoint inhibitors, surgical resection of the primary tumor or metastatic lesion and radiation therapy (4). The management and therapy of patients with advanced NSCLC have changed markedly in the last few years. Early detection methods and therapeutic options have been improved tremendously. However, the overall survival rate of patients with advanced NSCLC did not improve much and is still dismal (5). The reported 5-year survival rate of NSCLC patients was 17.8%, which is one of the highest fatality rates in non-communicable diseases (6). Reliable markers of treatment response and survival outcomes are urgently needed to enable early adaptation of treatment strategies in advanced NSCLC patients. Tumorigenesis and programmed cell death ligand 1 (PD-L1) status became standard markers influencing therapy regimes (7). Expression of PD-L1 has shown a significant predictive role (8). Other biomarkers such as lung immune prognostic index (LIPI) and tumor mutation burden (TMB) have revealed inconsistent results (9). Several studies have also demonstrated that lung cancer patients have lower levels of CD4+/CD8+ ratio, CD4+T cells, NK cell levels, and higher regulatory T cells (Tregs) than healthy subjects (10, 11). Patient-related factors such as age and comorbidities also affect peripheral blood lymphocyte subpopulations and treatment outcomes of NSCLC patients (12). Anti-cancer therapies, tumor surgery and wound healing may also have an impact on the immunophenotyping of lymphocyte subpopulations. So far, there are limited data concerning changes or developmental shifts in the most relevant B cell, T cell, and NK cell subpopulations caused by different anti-cancer therapies. Understanding the potential changes in lymphocyte subpopulations during different therapies is crucial to understand the effect of different therapies on the immune system and to adapt effective therapy regimens for better management of NSCLC patients. Therefore, in this study, we investigated the influence of immunotherapy, chemotherapy, immunochemotherapy, adjuvant chemotherapy after surgery, and antibodies against Vascular Endothelial Growth Factors (VEGF) on B cell, T cell, and NK cell subpopulations. Additionally, the relationship between therapy regimens and survival was assessed.

Materials and methods

Study design, population, and period

A longitudinal cohort study was performed on 32 consecutive NSCLC patients who visited the Pulmonology Clinic, Leipzig from January 10, 2018 to March 3, 2020. Socio-demographic information such as age, sex, smoking status, and clinical information such as type of cancer and the stage of cancer were collected from patients using a standardized questionnaire. Active smokers were defined as patients actively smoking at the time of data collection or up to 6 months before the data collection. To be qualified as former smoker, it was required that the patient quit smoking more than 6 months prior to data collection. Immunophenotyping was done before the administration of the planned therapy and during therapy with up to 7 observational windows (3 to 4 weeks each window) in the laboratory of the Institute of Clinical Immunology, University Hospital Leipzig resulting in a total of 135 observations with 130 immunologic parameters assessed. The median follow-up period for the study participants included in this study was 1,220 days.

Ethical considerations

Ethical approval was made by the Medical Faculty of the University of Leipzig ethics committee (Ref. No: 201/18-ek). The socio-demographic information, clinical data, and venous blood were collected from NSCLC patients following the ethical considerations recommended by the Declaration of Helsinki of 1975, revised in 2013. Data identifying study participants were removed prior to analyses. Safeguards for appropriate and ethical use of data were in place. Informed consent was acquired from all NSCLC patients included in the study.

Treatment options used

Patients were treated with one of the following five different treatment options: Immunotherapy (Nivolumab, Pembrolizumab, or Atezolizumab), Cytotoxic chemotherapy (Carboplatin + Nab-Paclitaxel, Carboplatin + Pemetrexed + Bevacizumab or Cisplatin + Pemetrexed + Bevacizumab), Immunochemotherapy (Carboplatin + Pemetrexed + Pembrolizumab, Carboplatin + Nab-Paclitaxel + Atezolizumab, Carboplatin + Nab-Paclitaxel + Pembrolizumab or Carboplatin + Nab-Paclitaxel + Bevacizumab + Atezolizumab), Adjuvant chemotherapy after tumor surgery (Cisplatin + Vinorelbin or Carboplatin + Vinorelbin) and Antibodies against VEGF (Bevacizumab).

Blood collection

Ethylenediaminetetraacetic acid (EDTA) venous blood was collected from each patient in the pulmonology clinic before the administration of the planned therapy at the time of treatment start and during observational windows. EDTA blood specimen was immediately brought to the laboratory of the Institute of Clinical Immunology for analysis of the cellular immune status. Blood samples were processed and analyzed within 3 hours of collection.

Cell surface markers staining

The staining and flow cytometry analysis of B cell, T cell, and NK cell subpopulations were performed according to previously

published protocols (13, 14). In brief, whole blood sample was divided into 8 different panel tests to analyze the following specific cell populations: (i) general lymphocytes, (ii) B cell subsets, (iii) CD4 T cell subsets, (iv) CD8 T cell subsets, (v) regulatory T cells, (vi) recent thymic emigrants (RTEs), (vii) NK cell subsets, and (viii) NK cell activation markers. To each panel test, a 100 µl whole blood specimen was added and incubated with specific antibodies to the chosen cell subsets. The antibody mixes, cell markers, fluorochromes, IgG subtypes, antibody concentration, and clones used for every panel test are explained in Supplementary Table S1.

To decide the optimum dilution for each staining, each antibody for eight-color analysis panels was titrated separately and compared with isotype controls. Cell surface markers were stained for 15 minutes in the dark at room temperature and then erythrocytes were lysed by lysis buffer (BD Biosciences, Heidelberg, Germany) after incubation or 10 minutes. After centrifugation and washing with phosphate-buffered saline (PBS) (Biochrom, Berlin, Germany), cells were fixed with 200 µl PBS that contains 1% formaldehyde and ready for flow cytometry analysis.

Flow cytometry analysis

The flowcytometry data acquisition was made using FACS Canto II (BD Biosciences) machine. The FACS Canto II is has three lasers: a 647 nm red laser, a 488 nm blue laser, and a 405 nm violet laser. During the analysis of all panel tests, automatic standard compensation was done, except for the B cell subsets panel, where the spectral overlap of the allophycocyanin (APC) toward peridinin-chlorophyll-protein (PerCP) was set to 12.66, to achieve optimal separation of memory and naive B cells. A total of 50,000 cell events were collected in the lymphocyte collection gate (CD45+ versus SSClow) for eight-color analysis, and the FACS DIVA (BD Biosciences) software version was used for data analysis 8. The absolute cell counts were determined using the relative flow cytometric cell counts measured by BD FACS Canto II Flow Cytometer set in relation to absolute cell counts analyzed by Sysmex XP-300 automated hematology analyzer (Sysmex Germany GmbH, Bornbarch, Germany) based on the standard protocol.

General lymphocytes gating strategy

The general lymphocyte gating strategy gives an overview of changes in the lymphocyte subpopulations. B cells (CD19+), T cells (CD3+), and NK cells (CD16+/56+) as well as HLA-DR+CD38+ activated T cells were gated from the lymphocyte gate using specific markers. Moreover, NK-T cells (T cells co-expressing CD16 molecule) were separated by gating CD3 versus CD16/56. The CD8 versus CD4 plot was used to separate 4 different T cell subsets: CD4+ and CD8+ T cells, CD4-/CD8- double-negative and CD4+/CD8+ double-positive T cells (Figure 1).

B cell subsets gating strategy

B cells (CD19+) subsets were idetnified from the lymphocyte gate. The CD21 vs. CD27combination was used for the separation of immature, CD21low, and memory B cells. Double-negative immature B cells were used as a baseline for CD21+ or CD27+ B cells. Non-switched and switched memory B cells were separated

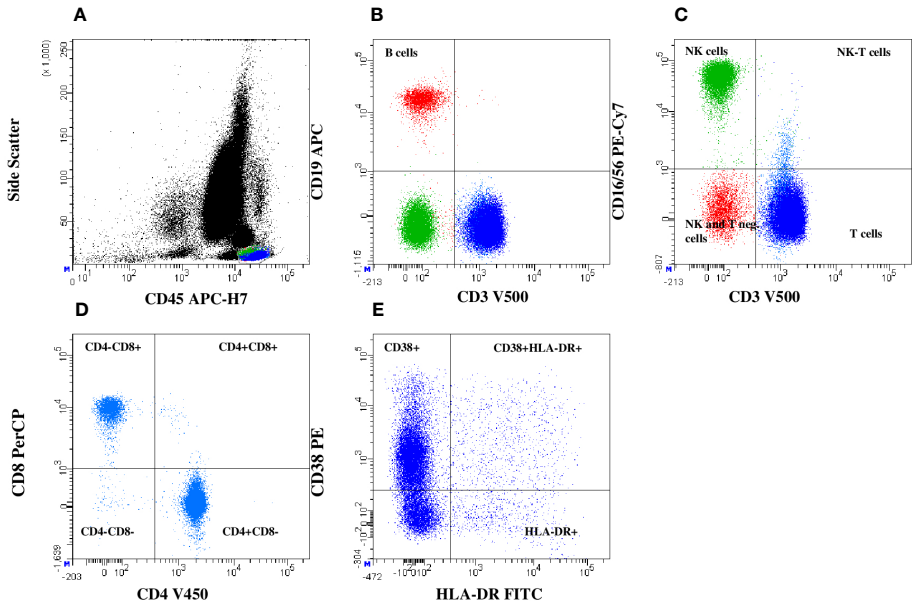


FIGURE 1
General lymphocytes gating strategy. Based on lymphocyte separation (SSC vs. CD45) **(A)**, T cells, B cells **(B)**, NK cells, and NK-T cells **(C)** were detected. From CD3+T cells gating, T helper (CD4+) cells, cytotoxic T cells (CD8+), CD4 and CD8 double positive and double negative T cells **(D)** and T cells activation status by HLA-DR+CD38+ expression were determined **(E)**.

from the CD27 gate by IgD versus IgM demarcation. The CD38low versus CD21low plot creates the gates for the activated CD21lowCD38low B cells and immature transitional B cells, which are specified to be CD21lowCD38+ B cells. IgM+ and CD38+ co-expressions were used for gating Transitional B cells. From this plot, plasma-blasts were separated using CD38+ expression and the absence of surface IgM. Additionally, CD27 +CD138+ peripheral plasma cells were identified (Supplementary Figure S1(I)).

T cell subpopulations gating strategy

T cells were separated from other lymphocytes using CD3 staining. To analyze T cell subpoulations, a combination of CD45RO, CD45RA, and CCR7 markers was used to separate effector cells (CD45RA +CD45RO-CCR7-), naive (CD45RA+CD45RO-CCR7+), central memory (CD45RA-CD45RO+CCR7+) and effector memory (CD45RA-CD45RO+CCR7-) cells. Additionally, from the CD3+CD4 + T helper cell population, regulatory T cells were detected as CD25 +CD127 low cells (Supplementary Figure S1(II)).

NK cells subsets gating strategy

For NK cells subsets analysis, T cells were excluded by gating the CD3 negative cells. From the CD3 negative cells, CD16 and CD56 markers were used to separate mature NK cells (CD16+CD56dim) and CD56 bright NK cells. In the next step, the expression of NK cells activation markers such as Nkp30, Nkp44, Nkp46, and CD57 was analyzed on mature NK cells (Supplementary Table S1(III)).

Statistical analysis

Descriptive statistics were used to analyze demographic and clinical characteristics of patients before and after anti-cancer treatment. Treatment effects on the immunologic parameters compared to their baseline values were determined by applying linear mixed models (random intercept and random slope) with the statistical software suite R (version 4.2.0, R packages “lme4” and “lmerTest”) to consider multiple measurements per subject. Time points were assumed to be equidistant for this purpose. We further adjusted for age. Parameters were initially log- or logit-transformed if they were on an absolute or percentage scale, respectively. We corrected for multiple significance testing of changes in lymphocyte subpopulations after anti-cancer treatment by controlling the False Discovery Rate (FDR, Benjamini–Hochberg) for the 130 tests performed, so that FDR is less than or equal to 5%. In the following we denote the corrected p-values (according to FDR) as “q-values”. For survival analysis, the ratios of survivors to all included patients within each treatment option were calculated.

Results

Demographic and clinical characteristics of study participants

A total of 32 patients with NSCLC were enrolled in this study. Median age of patients included in this study was 68 years (range, 50–83 years), and 22 (68.7%) patients were ≥ 65 years old. The majority of study participants were male (N=24, 75%). The most frequent type of NSCLC, was squamous cell carcinoma in 16 (50%) of patients. Moreover, 20 (62.5%) patients had stage IV advanced NSCLC. Almost all patients 30 (96.9%) were current or former smokers. Immunochemotherapy was the most commonly administered therapy (N=12, 37.5%) followed by cytotoxic chemotherapy (N=8, 25%), adjuvant chemotherapy after surgery (N=7, 21.9%), and immunotherapy (N=4, 12.5%) (Table 1).

Effects of anti-cancer therapies on B cell subpopulations

Absolute number of transitional B cells was significantly increased after therapy with immunotherapy (q=0.032), immunochemotherapy (q=0.030), and antibodies against VEGF (q=0.024). The transitional B cells percentage was significantly increased after immunotherapy (q=0.033). The percentage of B cells and absolute number of B cells were significantly increased after adjuvant chemotherapy (q=0.023). However, the percentage and absolute number of transition cells were significantly decreased after chemotherapy (q=0.001). Likewise, the absolute number of memory B cells and non-switched B cells were decreased significantly after adjuvant chemotherapy (q=0.023, and q=0.018, respectively) (Table 2, Figure 2).

Effects of anti-cancer therapies on T cell subpopulations

After immunotherapy, a significant increase was observed in activated cytotoxic T cells (CD8/CD38) (q=0.050), activated cytotoxic T cells (HLA-DR+) (q=0.031), and activated cytotoxic (HLA-DR +CD38+) T cells (q=0.031). Similarly, after immunochemotherapy, a significant increase was revealed in activated cytotoxic T cells (CD8/CD38) (q<0.0001), activated cytotoxic T cells (HLA-DR+) (q=0.030), and activated cytotoxic (HLA-DR+CD38+) T cells (q=0.002). There was a trend that the percentage of cytotoxic T cells (CD8+) and T cells (CD3+) were increased after immunotherapy (q=0.057) and immunochemotherapy (q=0.080), respectively. Chemotherapy, adjuvant chemotherapy, and antibodies against VEGF therapies did not induce significant changes in numbers of T cell subpopulation and activation (Table 3, Supplementary Table S2, Figure 2).

10.3389/fimmu.2023.1239097

TABLE 1 Socio-demographic and clinical characteristics of study participants by treatment group (N = 32).

Characteristics		Treatment groups						Total (N=32) N (%)
		Immuno-therapy (N=7)	Chemo-therapy (N=7)	Immuno-chemo-therapy (N=9)	Adjuvant chemo-therapy (N=5)	Antibodies against VEGF (N=1)	Baseline (N=3)	
Age group (years)	< 65	3	2	2	2	1	0	10 (31)
	> 65	4	5	7	3	0	3	22 (69)
	Median	67	69	68	65	59	79	68.5
Sex	Male	6	4	6	4	1	3	24 (75)
	Female	1	3	3	1	0	0	8 (25)
Smoking status	Active smoker	3	3	4	4	0	1	15 (47)
	Former smoker	4	4	4	1	1	2	16 (50)
	Non-smoker	0	0	1	0	0	0	1 (3)
NSCLC type	Squameus cell carcinoma	5	3	2	4	0	2	16 (50)
	Adenocarcinoma	1	4	7	1	1	1	15 (47)
	Non specific carcinoma	1	0	0	0	0	0	1 (3)
Cancer stage	IA3	0	0	0	1	0	0	1 (3)
	IIB	0	1	0	2	0	1	4 (13)
	IIIA	0	0	2	1	0	0	3 (9)
	IIIB	0	0	0	1	0	1	2 (6)
	IIIC	1	1	0	0	0	0	2 (6)
	IVA	4	2	2	0	0	0	8 (25)
	IVB	2	3	5	0	1	1	12 (38)

NSCLC, Non-small cell lung cancer; VEGF, Vascular endothelial growth factors; N, number. Baseline = Measurement before therapy initiation.

Effects of anti-cancer therapies on NK cells subsets

In our study, none of the treatment options used had a statistically significant effect on NK cell subsets. However, an increased trend in the percentage of immature NK cells II (CD56+CD16-) after immunotherapy (q=0.057) and a decreased trend in the percentage of CD16+CD56 NK cells (cytolytic activity) after immunochemotherapy (q=0.059) was observed (Table 4; Figure 2).

Effects of anti-cancer therapies on monocytes and granulocytes

In addition to lymphocytes, we assessed possible changes in monocytes and granulocytes after our therapy options. Percentages of monocytes significantly increased from 3.7% to 11.7% (q=0.033) after immunotherapy. Moreover, in the chemotaxis of granulocytes, the number of migrated granulocytes was significantly increased (q=0.023), while chemotaxis of granulocytes and percentages of active granulocytes (L-selectin) significantly decreased (q=0.018) after adjuvant chemotherapy. Other therapy options did not show significant changes in monocyte and granulocyte parameters (Supplementary Table S2).

Effect of age on T cell, B cell, and NK cell subpopulations

Age showed significant association with CD4+ T-lymphocytes, naive (CD45RA+CCR7+) CD8+T cells, and CD4- recent thymus migrations cells (q<0.05). However, age was not significantly associated with lymphocyte subpopulations showing significant changes after anti-cancer therapies. These findings suggest that the observed changes in lymphocyte subpopulations after anti-cancer therapies are not confounded by age (Figure 2, Supplementary Figure S2).

Survival of NSCLC patients

Overall, 9/29 (31%) of the patients survived. For adjuvant chemotherapy we observed that 4/5 (80%) of patients survived.

TABLE 2 Changes in B cell subpopulations in NSCLC patients during different anti-cancer therapies.

B cell subpopulations	Immunotherapy			Chemotherapy			Immuno-chemotherapy			Adjuvant chemotherapy			Antibodies against VEGF		
	before	after	q-value	before	after	q-value	before	after	q-value	before	after	q-value	before	after	q-value
B cells (cells/µL)	111.4	75.3	0.064	101.6	165.1	0.775	132.7	73.0	0.088	273.0	373.6	0.023	99	162	0.732
B cells % of lymphocytes	9.1	7.0	0.057	11.7	9.7	0.839	10.3	6.6	0.159	14.6	20.2	0.023	9	9	0.856
Immature % of B cells	9.8	8.1	0.896	5.7	7.0	0.892	8.6	10.7	0.815	7.0	7.3	0.566	4.1	2.6	0.856
Immature B cells (cells/µL)	10.1	5.9	0.525	5.9	11.3	0.754	12.3	6.5	0.336	6.9	16.3	0.524	4.1	4.2	0.856
Transitional B cells % of B cells	1.1	7.8	0.033	2.2	0.4	0.001	1.2	1.1	0.209	0.7	0.0	0.450	1.3	9.9	0.175
Transitional B cells (cells/µL)	1.1	7.4	0.032	1.9	1.1	0.001	1.3	1.5	0.030	1.2	0.0	0.681	1.3	16	0.024
Immature transitional B cells % of B cells	6.7	1.4	0.848	15.5	2.2	0.775	NA	NA	NA	58.0	82.5	0.524	NA	NA	NA
Immature transitional B cells (cells/µL)	2.5	0.2	0.800	11.3	4.5	0.897	NA	NA	NA	30.2	280.5	0.450	NA	NA	NA
Naive % of B cells	64.6	65.1	0.951	67.9	69.8	0.775	55.9	56.8	0.674	39.0	28.4	0.566	86.2	90	0.732
Naive B cells (cells/µL)	66.8	52.4	0.885	70.5	103.9	0.986	60.4	41.2	0.548	100.4	58.0	0.422	85.3	145.8	0.732
Memory % of B cells	15.3	17.3	0.896	7.8	14.0	0.893	22.3	18.7	0.629	32.3	30.0	0.493	4.8	3.3	0.732
Memory B cells (cells/µL)	23.3	10.7	0.743	9.5	33.8	0.839	37.5	14.9	0.318	148.7	57.4	0.023	4.8	5.3	0.988
Non-class-switched % of B cells	3.7	3.8	0.896	1.3	2.2	0.897	6.6	4.7	0.974	24.4	16.5	0.334	2	1.2	0.732
Non-class-switched B cells (cells/µL)	7.3	2.5	0.987	1.4	5.4	0.775	12.8	3.7	0.606	135.9	35.6	0.018	2	1.9	0.936
Class-switched % of B cells	8.9	11.1	0.903	6.7	10.3	0.893	172.2	10.4	0.499	6.0	10.3	0.875	2.5	1.9	0.856
Class-switched B cells (cells/µL)	13.5	6.7	0.896	8.5	24.5	0.839	11.5	8.2	0.345	6.4	15.1	0.334	2.5	3.1	0.907
CD21low % of B cells	3.2	5.5	0.477	2.5	3.4	0.865	NA	NA	NA	NA	NA	NA	NA	NA	NA
CD21low B cells (cells/µL)	1.3	0.9	0.743	3.2	8.4	0.897	NA	NA	NA	NA	NA	NA	NA	NA	NA
Activated CD21low CD38low % of B cells	2.2	3.5	0.650	1.7	2.1	0.893	NA	NA	NA	NA	NA	NA	NA	NA	NA
Activated CD21low CD38low B cells (cells/µL)	0.9	0.6	0.885	2.4	5.1	0.775	NA	NA	NA	NA	NA	NA	NA	NA	NA
Plasmablasts (CD38) % of B cells	1.4	1.2	0.987	0.8	4.5	0.588	2.0	2.2	0.590	0.9	1.4	0.831	0.2	0.2	0.856
Plasma cells (CD38) (cells/µL)	2.7	1.0	0.553	0.7	8.3	0.754	3.3	1.8	0.559	0.9	2.4	0.546	0.2	0.3	0.856
Plasma cells (CD138) % of B cells	1.5	1.0	0.903	0.7	2.1	0.955	1.7	2.2	0.227	1.5	1.2	0.833	1.5	0.4	0.880
Plasma cells (CD138) (cells/µL)	1.0	0.7	0.743	0.6	3.5	0.839	2.9	1.7	0.987	1.8	2.3	0.488	1.5	0.6	0.732

Values "before" and "after" correspond to the measured values before the initial treatment and the measured value after the last treatment, respectively, after an average observation time of 718/459/473/1,060/1,462 days of immunotherapy/chemotherapy/immunochemotherapy/adjuvant chemotherapy/antibodies against VEGF. Q-values correspond to the significance of the estimated change over time from linear mixed modelling. VEGF, Vascular endothelial growth factors; NA, Not available.

10.3389/fimmu.2023.1239097

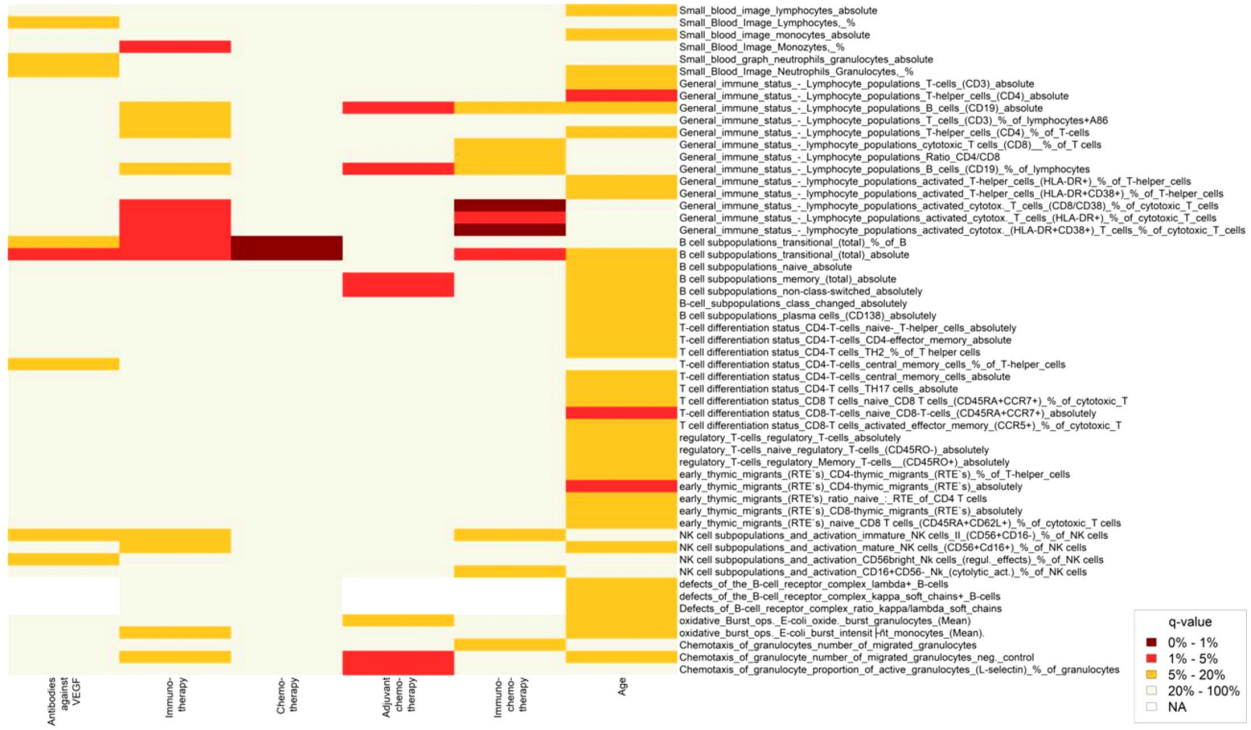


FIGURE 2
Heatmap showing changes in lymphocyte subpopulations after treatment with different anti-cancer therapies and aging. Statistically significant changes in lymphocyte subpopulations are indicated by dark red and red color boxes (FDR = 0 - 1% and 1 - 5%, respectively).

Patients with immunotherapy and immunochemotherapy achieved comparable survival with 2/7 (29%) and 2/9 (22%), respectively. Within chemotherapy 0/7 (0%) of patients survived in contrast to the patient who received therapy with antibodies against VEGF (1/1 (100%)).

Discussion

This study was aimed to analyse the impact of different therapeutic regimens on the immune system of NSCLC patients investigating changes in B-, T-, and NK cell subsets during therapy.

The absolute numbers of transitional B cells were significantly increased after therapy with immunotherapy, immunochemotherapy, and antibodies against VEGF. Percentages of transitional B cells also significantly increased after immunotherapy. Similarly, absolute numbers and percentages of B cells were significantly increased after adjuvant chemotherapy. The observed upregulation of B cells and transitional B cells during these therapies suggest activation of immune defense. These effects of therapies on B cells also imply the potential use of these cells as a target for vaccination against lung cancer. In line with this, targeted strategies to enhance B cells by using stimulated B cell ligands have been applied to inhibit lung metastasis and tumor growth (15, 16).

B cells are important immune cells that support an effective antitumor immune response by their capability to present tumor antigens, activate cytotoxic T cell and T-lymphocytes, response, as well as their ability to generate cytokines and anti-tumor antibodies (17–19). In line with the findings of this study, previous studies suggest that B cell counts increase in tumors of patients responding to immunotherapy, and tumor-infiltrating B cells were associated with, tumor stage and longer survival in NSCLC (20, 21). Even though the importance of B cells in making anti-cancer immune responses was progressively unraveled in the last years, a better understanding about the role of different B cell subsets, particularly transitional B cells is still required in cancer patients (17).

Interestingly, absolute numbers and percentages of transitional B cells significantly decreased after chemotherapy. Similarly, the absolute number of memory B cells and non-class switched B cells significantly decreased after adjuvant chemotherapy. Down-regulation of B cells during chemotherapy suggests a potential suppression of immune defense due to cytotoxic side-effects on the bone marrow. A previous study also reported that chemotherapy reduced the absolute counts of B cells (22). Another study showed that chemotherapy reduced absolute counts of B cells followed by a slow increase but not reaching baseline levels. This suggests that the chemotherapy has a long-term effect on lymphocyte subsets (23).

In this study, we noticed a significant increase in activated cytotoxic T cells in patients treated with immunotherapy and immunochemotherapy. The immune system activation by immunotherapy and immunochemotherapy is a desired therapeutic effect. T lymphocytes are the most important inflammatory cells that infiltrate the tumor, exert a direct cytotoxic effect, or cause lysis of tumor by cytokine release (24–26). CD8+ T cells can also increase and differentiate into CD8+ T

TABLE 3 Changes in T cell subpopulations in NSCLC patients after different anti-cancer therapies.

T cell subpopulations	Immunotherapy			Chemotherapy			Immuno-chemotherapy			Adjuvant chemotherapy			Antibodies against VEGF		
	before	after	q-value	before	after	q-value	before	after	q-value	before	after	q-value	before	after	q-value
T cells (cells/µL)	575.7	952.6	0.896	631.7	1099.1	0.839	946.1	811.1	0.548	983.2	1131.4	0.673	869	1530	0.841
T helper cells (cells/µL)	336.3	546.0	0.985	429.0	758.7	0.981	652.7	577.8	0.503	628.6	706.0	0.646	583	954	0.749
Cytotoxic T cells (cells/µL)	173.3	334.9	0.743	158.1	266.7	0.882	219.7	194.4	0.618	268.8	352.4	0.566	242	504	0.789
T cells % of lymphocytes+A86	63.9	72.9	0.057	67.9	69.4	0.588	73.4	72.8	0.994	71.0	66.8	0.605	79	85	0.934
T helper cells % of T cells	37.1	43.7	0.111	45.3	40.3	0.814	51.1	51.4	0.590	45.0	41.8	0.708	53	53	0.907
Cytotoxic T cells % of T cells	21.7	24.0	0.848	17.9	23.3	0.588	16.9	17.8	0.080	19.8	20.6	0.781	22	28	0.732
CD4/CD8 ratio	2.4	2.6	0.487	3.6	2.5	0.897	3.8	3.3	0.159	2.3	2.1	0.877	2.4	1.9	0.749
Double negative T cells (CD4-CD8-) % of T cells	6.2	4.9	0.920	2.1	4.0	0.986	5.3	4.2	0.318	5.5	4.6	0.697	4.7	3.6	0.907
Double positive T cells (CD4+CD8+) % of T cells	0.7	1.6	0.729	4.0	3.7	0.839	1.1	1.2	0.953	2.2	1.7	0.781	0.9	1.2	0.856
Activated T-helper cells (CD38+) % of T-helper cells	53.7	50.4	0.987	41.6	44.9	0.839	66.1	68.4	0.326	44.0	47.0	0.784	46	46	0.732
Activated T-helper cells (HLA-DR+) % of T-helper cells	15.9	15.4	0.431	10.7	16.1	0.893	8.6	9.9	0.807	15.8	10.6	0.566	11	7	0.856
Activated T helper cells (HLA-DR+CD38+) % of T helper cells	9.3	7.4	0.525	4.1	9.9	0.588	4.0	6.5	0.330	6.6	5.8	0.903	4	3	0.907
Activated cytotoxic T cells (CD8/CD38) % of cytotoxic T cells	44.4	57.4	0.050	32.4	38.0	0.588	34.9	51.3	0.000	31.8	40.2	0.546	36	49	0.856
Activated cytotoxic T cells (HLA-DR+) % of cytotoxic T cells	26.9	38.1	0.031	19.1	35.4	0.588	14.7	19.5	0.030	37.6	42.2	0.566	40	52	0.732
Activated cytotoxic (HLA-DR+CD38+) T cells % of cytotoxic T cells	17.7	29.7	0.031	10.1	23.7	0.588	7.6	14.4	0.002	18.8	26.8	0.334	13	32	0.732

Values "before" and "after" correspond to the measured values before the initial treatment and the measured value after the last treatment, respectively, after an average observation time of 718/459/473/1,060/1,462 days of immunotherapy/chemotherapy/immunochemotherapy/adjuvant chemotherapy/antibodies against VEGF. Q-values correspond to the significance of the estimated change over time from linear mixed modelling. VEGF, Vascular endothelial growth factors; HLA-DR, Human Leukocyte Antigen-DR isotype.

10.3389/fimmu.2023.1239097

TABLE 4 Changes in the NK cell subpopulations in NSCLC patients after different anti-cancer therapies.

NK cell subpopulations	Immunotherapy			Chemotherapy			Immuno-chemotherapy			Adjuvant chemotherapy			Antibodies against VEGF		
	before	after	q-value	before	after	q-value	before	after	q-value	before	after	q-value	before	after	q-value
NK cells (CD16/56) (cells/μL)	238.1	180.7	0.219	174.4	205.9	0.588	198.6	193.6	0.659	199.0	210.0	0.697	123	104	0.841
NK cells (CD16/56) % of lymphocytes	26.5	19.6	0.232	19.6	20.4	0.588	15.7	19.5	0.583	14.2	12.7	0.334	11.2	5.8	0.732
NK T cells (CD3/56) % of lymphocytes	6.4	5.2	0.801	6.3	5.1	0.865	6.1	5.6	0.499	5.7	3.7	0.508	4.3	3.1	0.856
Immature NK cells I (CD56-CD16-) % of NK cells	0.1	0.2	0.243	0.3	0.5	0.882	0.4	0.4	0.953	0.4	0.2	0.857	1.7	0.9	0.732
Immature NK cells II (CD56+CD16-) % of NK cells	3.3	4.4	0.057	3.6	4.2	0.588	4.5	5.4	0.159	3.2	4.3	0.508	14.7	13.9	0.122
Mature NK cells (CD56+Cd16+) % of NK cells	90.8	81.8	0.158	83.5	85.5	0.991	84.6	84.5	0.949	77.9	76.3	0.392	69.8	57.2	0.732
CD56bright Nk cells (regulatory effects) % of NK cells	2.8	4.4	0.729	2.9	3.7	0.588	2.9	3.5	0.548	3.1	6.0	0.546	1.3	7.6	0.130
CD16+CD56- Nk cells (cytolytic activity) % of NK cells	4.2	11.2	0.920	10.5	7.7	0.775	8.3	7.6	0.059	15.9	15.3	0.718	7.1	21.3	0.856
Activated CD94/NKG2D complex % of NK cells	36.0	39.4	0.985	31.7	27.9	0.853	42.0	41.2	0.629	32.4	41.4	0.833	8.9	28.8	0.856
Nkp30% of NK cells	81.1	73.7	0.800	76.8	76.3	0.897	61.6	79.4	0.930	62.8	57.1	0.566	77.8	63.1	0.732
Nkp46% of NK cells	62.7	57.9	0.985	46.5	53.2	0.865	57.1	64.0	0.618	44.5	42.3	0.711	44.6	46.2	0.856
Nkp44 (cytolytic activity) % of NK cells	0.5	0.6	0.920	5.1	1.2	0.588	0.6	0.8	0.953	2.1	0.6	0.780	0.1	0.7	0.907
CD57% of NK cells	47.7	43.2	0.650	44.1	44.0	0.977	55.0	55.6	0.604	42.9	39.4	0.646	56.6	43.3	0.732

VEGF, Vascular endothelial growth factors.

10.3389/fimmu.2023.1239097

cells that can infiltrate tumors by peripheral blood migration and play an essential role in the direct killing of tumor cells (27). Our finding is in line with the reported increase of CD8+ T cells after immunotherapy in lung cancer patients (28). Another study also suggested that as part of a successful immunotherapy response, effector memory tumor antigen-specific cytotoxic T cells are increased (29). However, in contrast to our findings, other studies reported decreased proportion of CD8+ T cells after immunotherapy as compared to baseline values (30, 31).

The observed differences in cytotoxic T cell response after immunotherapy could be explained as follows. First, lung cancer patients treated with PD-1 inhibitors are characterized by expressing effector-like phenotypes (HLA-DR+, CD38+, Bcl-2lo), co-stimulatory molecules (CD28, CD27, ICOS), a highly specific subset of proliferating CD8+ T cells in the peripheral blood, and high levels of PD-1 (32). Second, different timings of blood sampling could contribute to the observed contradictory findings across studies. CD8+ T cell response induction by blocking the PD-1 pathway in the peripheral blood is transient and detected during the first four weeks after treatment start. Then these specific CD8+ T cells migrate to the tumor sites (32).

Although none of the therapies investigated in this study showed a significant effect on NK cells, a trend increase in the percentage of immature NK cells was observed after immunotherapy. A decrease in the percentage of CD16+CD56 NK cells was also observed after immunochemotherapy. A previous study demonstrated that the PD-L1 leads blockage of causes activation of NK cells and increases the direct antitumor effect of NK cells (33). Another study showed that in NSCLC patients, NK cell activity is a marker to predict the immunotherapy response (34). Drugs modulating the function and proliferative activity of NK cells have been developed to produce synergistic effect in combination with immunotherapy (35, 36).

In addition to lymphocyte subpopulations, we assessed the possible effects of anti-cancer therapies on monocytes and granulocytes. Percentage of monocytes showed a significant increase after immunotherapy. This could be interpreted as the effect of a T cell interaction and activation by immunotherapy as described in a previous study (37). In several tumor types, an increase in HLA-DR low monocytes has been reported (38). As already described for HLA-DR low monocytes in sepsis, these monocytic cells might decrease T cell function in patients with cancer (39). Moreover, the number of migrated granulocytes in this chemotaxis study was significantly increased, while the percentage of active granulocytes (L-selectin) decreased after adjuvant chemotherapy. This is possibly due to the consequence of high baseline activity, postoperative inflammation, and wound healing processes. Previous studies also reported that the number of neutrophils in tumor tissues and blood is correlated with poor patient outcomes and disease progression (40). Neutrophil count was associated with the percentage of HLA-DR low monocytes in patients with lung cancer managed by surgery of the primary tumor as an important subpopulation of the myeloid-derived suppressor cells (MDSC). Nevertheless, in the late tumor stages, this observation was not confirmed (41).

In the present study, NSCLC patients treated with adjuvant chemotherapy showed the highest survival of 80%. In contrast, patients treated with chemotherapy alone showed the lowest survival with 0%. This could be explained by the fact that adjuvant chemotherapy is usually applied for early-stage NSCLC; stage IIA, IIB, and IIIA NSCLC to kill remaining cancer cells after surgery (42). Adding immunotherapy to chemotherapy in a palliative setting increased observed survival to 22% compared to chemotherapy alone.

This is consistent with previous reports showing a significant increase in overall response rates, overall survival and progression-free survival in NSCLC patients treated with immunotherapy compared to chemotherapy (43). Five-year follow-up study showed a significantly increased median time of overall survival, which doubled from 13.4 months in chemotherapy to 26.3 months in immunotherapy; and a higher overall survival rate, 31.9% in the immunotherapy group compared to 16.3% in the chemotherapy group (44). Immunotherapy enhances the immune system that targets cancer cells and slows or stops the cancer cells metastasis and growth (45). Previous studies also showed that improved survival is correlated with a strong immune response to tumers. Moreover, higher numbers of CD8+ T cells and natural killer cells are linked with better patient survival (46, 47).

We repeated all the analyses twice, with further adjustment for tumor stage, and with further adjustment for tumor stage and exclusion of patients with adjuvant therapy to check that stage of tumor did not bias our initial analysis with adjustment for age only. Indeed, the results were comparable yielding no significant additional information.

This study has some limitations to be mentioned. Firstly, despite multiple measurements, due to the limited sample size our study might be underpowered to identify smaller changes in the lymphocyte subpopulations before and after treatment with different anti-cancer therapies. Likewise, survival analysis is limited by the small sample size. Secondly, this study was conducted at a single health care facility, therefore, selection bias cannot be fully excluded.

Since this study was the first one investigating such a large spectrum of parameters in cytomics, further research is needed to determine prognostic significance, further potential confounding factors and long-term survival.

Data availability statement

The original contributions presented in the study are included in the article/Supplementary Material, further inquiries can be directed to the corresponding author/s.

Ethics statement

The studies involving humans were approved by ethics committee of the University of Leipzig. The studies were conducted in accordance with the local legislation and institutional requirements. The participants provided their written informed consent to participate in this study.

Author contributions

Conceptualization, PG, CG, MS, US. Methodology, PG, CG, US. Formal analysis, AK, BT. Investigation, PG, AB. Data curation, PG, CG, AK, BT. Original draft preparation, BT. Review and editing, PG, CG, US, AK, BT, AB, MS. Project administration, PG, CG. All authors contributed to the article and approved the submitted version.

Funding

Funded by the Open Access Publishing Fund of Leipzig University supported by the German Research Foundation within the program Open Access Publication Funding. Markus Scholz was supported by "ChemoTox-AI", a project financed by the German Federal Ministry of Education and Research (BMBF) within the Computational Life Science line of funding (grant number 031L0261).

Acknowledgments

The authors would like to acknowledge Katrin Bauer, Bettina Glatte, and Sabine Seiffert for their contribution to flow cytometry analysis in the institute of Clinical Immunology laboratory. We also would like to thank the staff members of the Pulmonology Clinic for their assistance in blood sample collection and timely delivery of blood samples to the institute of Clinical Immunology laboratory.

Conflict of interest

CG declare to have received honoraria for lectures and advisory boards from BMS, MSD, Roche, and Regeneron. MS received funding from Pfizer Inc. for a project not related to this research.

The remaining authors declare that the research was conducted in the absence of any commercial or financial relationships that could be construed as a potential conflict of interest.

Publisher's note

All claims expressed in this article are solely those of the authors and do not necessarily represent those of their affiliated organizations, or those of the publisher, the editors and the reviewers. Any product that may be evaluated in this article, or claim that may be made by its manufacturer, is not guaranteed or endorsed by the publisher.

Supplementary material

The Supplementary Material for this article can be found online at: https://www.frontiersin.org/articles/10.3389/fimmu.2023.1239097/full#supplementary-material

References

1. Ferlay J, Colombet M, Soerjomataram I, Parkin DM, Piñeros M, Znaor A, et al. Cancer statistics for the year 2020: An overview. *Int J Cancer* (2021) 149:778–89. doi: 10.1002/ijc.33588

2. Inamura K. Lung cancer: understanding its molecular pathology and the 2015 WHO classification. *Front Oncol* (2017) 7:193/full. doi: 10.3389/fonc.2017.00193/full

3. Siegel RL, Miller KD, Jemal A. Cancer statistics, 2019. *CA Cancer J Clin* (2019) 69:7–34. doi: 10.3322/caac.21551

4. Zappa C, Mousa SA. Non-small cell lung cancer: current treatment and future advances. *Transl Lung Cancer Res* (2016) 5:288–300. doi: 10.21037/tlcr.2016.06.07

5. Wang T, Nelson RA, Bogardus A, Grannis FW. Five-year lung cancer survival. *Cancer* (2010) 116:1518–25. doi: 10.1002/cncr.24871

6. Wong MCS, Lao XQ, Ho KF, Goggins WB, Tse SLA. Incidence and mortality of lung cancer: global trends and association with socioeconomic status. *Sci Rep* (2017) 7:14300. doi: 10.1038/s41598-017-14513-7

7. Ettinger DS, Wood DE, Aisner DL, Akerley W, Bauman JR, Bharat A, et al. Non–small cell lung cancer, version 3.2022, NCCN clinical practice guidelines in oncology. *J Natl Compr Cancer Netw* (2022) 20:497–530. doi: 10.6004/jnccn.2022.0025

8. Aguiar PN, De Mello RA, Hall P, Tadokoro H, Lima Lopes G. PD-L1 expression as a predictive biomarker in advanced non-small-cell lung cancer: updated survival data. *Immunotherapy* (2017) 9:499–506. doi: 10.2217/imt-2016-0150

9. Proto C, Ferrara R, Signorelli D, Lo Russo G, Galli G, Imbimbo M, et al. Choosing wisely first line immunotherapy in non-small cell lung cancer (NSCLC): what to add and what to leave out. *Cancer Treat Rev* (2019) 75:39–51. doi: 10.1016/j.ctrv.2019.03.004

10. Wei Z, Zhang W, Gao F, Wu Y, Zhang G, Liu Z, et al. Impact of lymphocyte subsets on chemotherapy efficacy and long-term survival of patients with advanced non-small-cell lung cancer. *Zhongguo Yi Xue Ke Xue Yuan Xue Bao* (2017) 39:371–6. doi: 10.3881/j.issn.1000-503X.2017.03.012

11. Qiu J, Che G, Liu F, Sha X, Ju S, Ma H, et al. The detection and clinical significance of peripheral regulatory CD4+CD25hiCD127low T cells in patients with non-small cell lung cancer. *Clin Transl Oncol* (2019) 21:1343–7. doi: 10.1007/s12094-019-02063-5

12. Wang S, Wong ML, Hamilton N, Ben DJ, TM J, Walter LC. Impact of age and comorbidity on non–small-cell lung cancer treatment in older veterans. *J Clin Oncol* (2012) 30:1447–55. doi: 10.1200/JCO.2011.39.5269

13. Boldt A, Borte S, Fricke S, Kentouche K, Emmrich F, Borte M, et al. Eight-color immunophenotyping of T-, B-, and NK cell subpopulations for characterization of chronic immunodeficiencies. *Cytom Part B Clin Cytom* (2014) 86:191–206. doi: 10.1002/cyto.b.21162

14. Maecker HT, McCoy JP, Nussenblatt R. Standardizing immunophenotyping for the human immunology project. *Nat Rev Immunol* (2012) 12:191–200. doi: 10.1038/nri3158

15. Gonzalez NK, Wennhold K, Balkow S, Kondo E, Bölck B, Weber T, et al. In vitro and in vivo imaging of initial B-T cell interactions in the setting of B cell based cancer immunotherapy. *Oncoimmunology* (2015) 4:e1038684. doi: 10.1080/2162402X.2015.1038684

16. Sorrentino R, Morello S, Forte G, Montinaro A, De VG, Luciano A, et al. B cells contribute to the antitumor activity of cpG-oligodeoxynucleotide in a mouse model of metastatic lung carcinoma. *Am J Respir Crit Care Med* (2011) 183:1369–79. doi: 10.1164/rccm.201010-1738OC

17. Largeot A, Pagano G, Gonder S, Moussay E, Paggetti J. The B-side of cancer immunity: the underrated tune. *Cells* (2019) 8. doi: 10.3390/cells8050449

18. Sharonov GV, Serebrovskaya EO, Yuzhakova DV, Britanova OV, Chudakov DM. B cells, plasma cells and antibody repertoires in the tumour microenvironment. *Nat Rev Immunol* (2020) 20:294–307. doi: 10.1038/s41577-019-0257-x

19. Kinker GS, Vitiello GAF, Ferreira WAS, Chaves AS, Cordeiro de Lima VC, Medina TDS. B cell orchestration of anti-tumor immune responses: A matter of cell localization and communication. *Front Cell Dev Biol* (2021) 9:678127/full. doi: 10.3389/fcell.2021.678127/full

20. Germain C, Gnjatic S, Tamzalit F, Knockaert S, Remark R, Goc J, et al. Presence of B cells in tertiary lymphoid structures is associated with a protective immunity in patients with lung cancer. *Am J Respir Crit Care Med* (2014) 189:832–44. doi: 10.1164/rccm.201309-1611OC

21. Wang SS, Liu W, Ly D, Xu H, Qu L, Zhang L. Tumor-infiltrating B cells: their role and application in anti-tumor immunity in lung cancer. *Cell Mol Immunol* (2019) 16:6–18. doi: 10.1038/s41423-018-0027-x

22. Spitzer MH, Carmi Y, Reticker-Flynn NE, Kwek SS, Madhireddy D, Martins MM, et al. Systemic immunity is required for effective cancer immunotherapy. *Cell* (2017) 168:487–502.e15. doi: 10.1016/j.cell.2016.12.022

23. Xia Y, Li W, Li Y, Liu Y, Ye S, Liu A, et al. The clinical value of the changes of peripheral lymphocyte subsets absolute counts in patients with non-small cell lung cancer. *Transl Oncol* (2020) 13:100849. doi: 10.1016/j.tranon.2020.100849

24. Aerts JG, Hegmans JP. Tumor-specific cytotoxic T cells are crucial for efficacy of immunomodulatory antibodies in patients with lung cancer. *Cancer Res* (2013) 73:2381–8. doi: 10.1158/0008-5472.CAN-12-3932

25. Kataki A, Scheid P, Piet M, Marie B, Martinet N, Martinet Y, et al. Tumor infiltrating lymphocytes and macrophages have a potential dual role in lung cancer by supporting both host-defense and tumor progression. *J Lab Clin Med* (2002) 140:320–8. doi: 10.1067/mlc.2002.128317

26. Martínez-Lostao L, Anel A, Pardo J. How do cytotoxic lymphocytes kill cancer cells? *Clin Cancer Res* (2015) 21:5047–56. doi: 10.1158/1078-0432.CCR-15-0685

27. Zhang N, Bevan MJ. CD8(+) T cells: foot soldiers of the immune system. *Immunity* (2011) 35:161–8. doi: 10.1016/j.immuni.2011.07.010

28. Saravia J, Chapman NM, Chi H. Helper T cell differentiation. *Cell Mol Immunol* (2019) 16:634–43. doi: 10.1038/s41423-019-0220-6

29. Principe N, Kidman J, Goh S, Tilsed CM, Fisher SA, Fear VS, et al. Tumor infiltrating effector memory antigen-specific CD8+ T cells predict response to immune checkpoint therapy. *Front Immunol* (2020) 11:584423/full. doi: 10.3389/fimmu.2020.584423/full

30. Yan Y, Wang X, Liu C, Jia J. Association of lymphocyte subsets with efficacy and prognosis of immune checkpoint inhibitor therapy in advanced non-small cell lung carcinoma: a retrospective study. *BMC Pulm Med* (2022) 22:166. doi: 10.1186/s12890-022-01951-x

31. Zhuo M, Chen H, Zhang T, Yang X, Zhong J, Wang Y, et al. The potential predictive value of circulating immune cell ratio and tumor marker in atezolizumab treated advanced non-small cell lung cancer patients. *Cancer Biomarkers* (2018) 22:467–76. doi: 10.3233/CBM-171089

32. Kamphorst AO, Pillai RN, Yang S, Nasti TH, Akondy RS, Wieland A, et al. Proliferation of PD-1+ CD8 T cells in peripheral blood after PD-1–targeted therapy in lung cancer patients. *Proc Natl Acad Sci* (2017) 114:4993–8. doi: 10.1073/pnas.1705327114

33. Kamata T, Suzuki A, Mise N, Ihara F, Takami M, Makita Y, et al. Blockade of programmed death-1/programmed death ligand pathway enhances the antitumor immunity of human invariant natural killer T cells. *Cancer Immunol Immunother* (2016) 65:1477–89. doi: 10.1007/s00262-016-1901-y

34. Choi MG, Kim YJ, Lee JC, Rho JK, Choi C. Efficacy of natural killer cell activity as a biomarker for predicting immunotherapy response in non-small cell lung cancer. *Thorac Cancer* (2020) 11:3337–45. doi: 10.1111/1759-7714.13677

35. Zingoni A, Fionda C, Borrelli C, Cippitelli M, Santoni A, Soriani A. Natural killer cell response to chemotherapy-stressed cancer cells: role in tumor immunosurveillance. *Front Immunol* (2017) 8:1194. doi: 10.3389/fimmu.2017.01194

36. Yang Y, Li L, Jiang Z, Wang B, Pan Z. Anlotinib optimizes anti-tumor innate immunity to potentiate the therapeutic effect of PD-1 blockade in lung cancer. *Cancer Immunol Immunother* (2020) 69:2523–32. doi: 10.1007/s00262-020-02641-5

37. Vermare A, Guérin MV, Peranzoni E, Bercovici N. Dynamic CD8+ T cell cooperation with macrophages and monocytes for successful cancer immunotherapy. *Cancers (Basel)* (2022) 14:3546. doi: 10.3390/cancers14143546

38. Greten TF, Manns MP, Korangy F. Myeloid derived suppressor cells in human diseases. *Int Immunopharmacol* (2011) 11:802–7. doi: 10.1016/j.intimp.2011.01.003

39. Döcke WD, Randow F, Syrbe U, Krausch D, Asadullah K, Reinke P, et al. Monocyte deactivation in septic patients: Restoration by IFN-γ treatment. *Nat Med* (1997) 3:678–81. doi: 10.1038/nm0697-678

40. Kasuga I, Makino S, Kiyokawa H, Katoh H, Ebihara Y, Ohyashiki K. Tumor-related leukocytosis is linked with poor prognosis in patients with lung carcinoma. *Cancer* (2001) 92:2399–405. doi: 10.1002/1097-0142(20011101)92:9<2399::AID-CNCR1588>3.0.CO;2-W

41. Riemann D, Cwikowski M, Turzer S, Giese T, Grallert M, Schütte W, et al. Blood immune cell biomarkers in lung cancer. *Clin Exp Immunol* (2019) 195:179–89. doi: 10.1111/cei.13219

42. Arriagada R, Cartmell-Davies J, Girling DJ, Le Chevalier T, Marsoni S, Parmar MKB, et al. Chemotherapy in non-small cell lung cancer: a meta-analysis using updated data on individual patients from 52 randomised clinical trials. Non-small Cell Lung Cancer Collaborative Group. *BMJ* (1995) 311:899–909. doi: 10.1136/bmj.311.7010.899

43. Reck M, Rodríguez-Abreu D, Robinson AG, Hui R, Csőszi T, Fülöp A, et al. Pembrolizumab versus chemotherapy for PD-L1–positive non–small-cell lung cancer. *N Engl J Med* (2016) 375:1823–33. doi: 10.1056/NEJMoa1606774

44. Reck M, Rodríguez-Abreu D, Robinson AG, Hui R, Csőszi T, Fülöp A, et al. Five-year outcomes with pembrolizumab versus chemotherapy for metastatic non–small-cell lung cancer with PD-L1 tumor proportion score ≥ 50%. *J Clin Oncol* (2021) 39:2339–49. doi: 10.1200/JCO.21.00174

45. Banchereau J, Steinman RM. Dendritic cells and the control of immunity. *Nature* (1998) 392:245–52. doi: 10.1038/32588

46. Zhuang X, Xia X, Wang C, Gao F, Shan N, Zhang L, et al. A high number of CD8 + T cells infiltrated in NSCLC tissues is associated with a favorable prognosis. *Appl Immunohistochem Mol Morphol* (2010) 18:24–8. doi: 10.1097/PAI.0b013e3181b6a741

47. Villegas FR, Coca S, Villarrubia VG, Jiménez R, Chillón MJ, Jareño J, et al. Prognostic significance of tumor infiltrating natural killer cells subset CD57 in patients with squamous cell lung cancer. *Lung Cancer* (2002) 35:23–8. doi: 10.1016/s0169-5002(01)00292-6

frontiers | Frontiers in Immunology

TYPE Original Research
PUBLISHED 06 September 2023
DOI 10.3389/fimmu.2023.1224340

Check for updates

OPEN ACCESS

EDITED BY
Jie Mei,
Wuxi People's Hospital Affiliated to Nanjing Medical University, China

REVIEWED BY
Anastasios D. Giannou,
University Medical Center Hamburg-Eppendorf, Germany
Sohini Chakraborty,
New York University, United States

*CORRESPONDENCE
Shikang Li
shikangli@hotmail.com

†These authors have contributed equally to this work

RECEIVED 17 May 2023
ACCEPTED 22 August 2023
PUBLISHED 06 September 2023

CITATION
Xu Z, Zheng T, Zheng Z, Jiang W, Huang L, Deng K, Yuan L, Qin F, Sun Y, Qin J and Li S (2023) TAGAP expression influences CD4+ T cell differentiation, immune infiltration, and cytotoxicity in LUAD through the STAT pathway: implications for immunotherapy.
Front. Immunol. 14:1224340.
doi: 10.3389/fimmu.2023.1224340

COPYRIGHT
© 2023 Xu, Zheng, Zheng, Jiang, Huang, Deng, Yuan, Qin, Sun, Qin and Li. This is an open-access article distributed under the terms of the Creative Commons Attribution License (CC BY). The use, distribution or reproduction in other forums is permitted, provided the original author(s) and the copyright owner(s) are credited and that the original publication in this journal is cited, in accordance with accepted academic practice. No use, distribution or reproduction is permitted which does not comply with these terms.

TAGAP expression influences CD4+ T cell differentiation, immune infiltration, and cytotoxicity in LUAD through the STAT pathway: implications for immunotherapy

Zhanyu Xu[1†], Tiaozhan Zheng[1†], Zhiwen Zheng[1†], Wei Jiang[1], Liuliu Huang[1], Kun Deng[1], Liqiang Yuan[1], Fanglu Qin[2], Yu Sun[1], Junqi Qin[1] and Shikang Li[1*]

[1]Department of Thoracic and Cardiovascular Surgery, The First Affiliated Hospital of Guangxi Medical University, Nanning, Guangxi Zhuang Autonomous Region, China, [2]School of Information and Management, Guangxi Medical University, Nanning, Guangxi Zhuang Autonomous Region, China

Background: T-cell Activation GTPase Activating Protein (TAGAP) plays a role in immune cell regulation. This study aimed to investigate TAGAP's expression and its potential impact on CD4+ T cell function and prognosis in lung adenocarcinoma (LUAD).

Methods: We analyzed TAGAP expression and its correlation with immune infiltration and clinical data in LUAD patients using multiple datasets, including The Cancer Genome Atlas (TCGA-LUAD), Gene Expression Omnibus (GEO), and scRNA-seq datasets. *In vitro* and *in vivo* experiments were conducted to explore the role of TAGAP in CD4+ T cell function, chemotaxis, and cytotoxicity.

Results: TAGAP expression was significantly lower in LUAD tissues compared to normal tissues, and high TAGAP expression correlated with better prognosis in LUAD patients. TAGAP was positively correlated with immune/stromal/ESTIMATE scores and immune cell infiltration in LUAD. Single-cell RNA sequencing revealed that TAGAP was primarily distributed in CD4+/CD8+ T cells. *In vitro* experiments showed that TAGAP overexpression enhanced CD4+ T cell cytotoxicity, proliferation, and chemotaxis. Gene Set Enrichment Analysis (GSEA) indicated that TAGAP was enriched in the JAK-STAT signaling pathway. *In vivo* experiments in a xenograft tumor model demonstrated that TAGAP overexpression suppressed tumor growth and promoted CD4+ T cell cytotoxicity.

Conclusions: TAGAP influences CD4+ T cell differentiation and function in LUAD through the STAT pathway, promoting immune infiltration and cytotoxicity. This study provides a scientific basis for developing novel LUAD immunotherapy strategies and exploring new therapeutic targets.

KEYWORDS

TAGAP, CD4+ T cells, lung adenocarcinoma (LUAD), JAK-STAT signaling pathway, immunotherapy

1 Introduction

Lung cancer is the leading cause of cancer-related deaths worldwide, with lung adenocarcinoma (LUAD) accounting for nearly 50% of all cases and a 5-year overall survival (OS) rate still below 20% (1, 2). In recent years, immunotherapy has become an established strategy in cancer treatment, including LUAD (3). The main difference between immunotherapy and traditional radio-chemotherapy or molecular targeted therapy is that immunotherapy can provide long-term and stable therapeutic effects for some patients, greatly improving their prognosis and quality of life (4). However, tumor heterogeneity and individual differences limit its practical application, as immune therapy benefits only a small group of patients due to the suppression of immune effects in some tumor microenvironments and the occurrence of drug resistance and adverse reactions (5).

Most antitumor immunotherapies focus on stimulating cytotoxic T lymphocytes (CTLs), the main T cell group that kills tumors. Current research suggests that activating CD8+ T cells is the primary way of antitumor immunity, while CD4+ T cells are also essential (6). In the context of cancer, multiple lines of evidence highlight the importance of CD4+ T cell recognition of tumor antigens for cancer immunotherapy responses. CD4+ T cells have complex immunoregulatory functions, with different subtypes exerting opposing effects on cancer progression (7, 8). However, research on CD4+ T cell differentiation and tumor regulation in LUAD tumor microenvironment is still insufficient.

Rho GTPases act as molecular switches in various cellular processes by transitioning between GTP-bound "on state" and GDP-bound "off state" (9). Rho GTPases reportedly coordinate the biochemical or cytoskeletal pathways that cause T cells to polarize towards antigen-presenting cells (APCs), and disruption of these pathways interferes with T cell responses to stimulation and affects effector T cell differentiation (10). The functions of most Rho GTPase-activating proteins (RhoGAPs) in T cells remain largely unexplored. The T cell-activated Rho GTPase activating protein (TAGAP) encodes a member of the RhoGAP superfamily, which participates in the Rho GTPase cycle.

TAGAP is highly expressed in the immune system, including T and B lymphocytes, dendritic cells, and natural killer cells, but mainly transiently expressed in activated T lymphocytes (11). As a GTPase-activating protein, TAGAP may be involved in T cell activation through its interaction with IL2, affecting the development of autoimmune diseases (12). TAGAP has been shown to be associated with immune cell infiltration in various cancers. In LUAD-related research, TAGAP was found to be a key gene affecting the tumor microenvironment and closely related to LUAD prognosis (13). However, the role of TAGAP in the progression of malignant tumors remains unclear.

In this study, we first analyzed the expression of TAGAP in LUAD patient tumor tissue samples using bioinformatics and collected corresponding tissue samples. We further investigated the essential role of TAGAP in CD4+ T cell immunoregulation through functional cellular experiments and validated that TAGAP overexpression promotes CD4+ T cell immune infiltration and cytotoxicity, slowing LUAD growth in animal models. Mechanistically, we preliminarily examined the JAK-STAT pathway-related proteins in CD4+ T cells with TAGAP overexpression and found that TAGAP overexpression activates the STAT pathway. In summary, our research provides initial insights into how TAGAP affects CD4+ T cell differentiation and function within the tumor microenvironment through the STAT pathway, thereby inhibiting LUAD malignancy progression. This study offers a scientific basis for developing novel LUAD immunotherapy strategies and exploring new therapeutic targets.

2 Materials and methods

2.1 Datasets and bioinformatics analyses

The RNA-seq expression, somatic mutation data, and clinical data of lung cancer patients were retrieved from The Cancer Genome Atlas (TCGA) (http://cancergenome.nih.gov/) (14). 535 LUAD samples were divided into high and low expression groups based on the median TAGAP expression. The "Limma" R package was used for differential expression analysis of RNA-seq data (15). The relationship between mRNA expression levels and overall survival (OS) of LUAD patients were analyzed using the "survival" R package. Gene expression profiling interaction analysis (GEPIA) was used for TAGAP survival and immune cell signature correlation analyses (16).

2.2 Immune infiltrates analysis

The high and low immune groups with median cutoff were studied with the "CIBERSORT" and "ESTIMATE" algorithms in TCGA samples to assess TAGAP expression levels in immune cells. CIBERSORT is based on a deconvolution algorithm that can be used to quantify 22 immune cell types.

The single cell RNA sequencing data (GSE99254) was downloaded from Gene Expression Omnibus (GEO; https://www.ncbi.nlm.nih.gov/). LUAD case samples were selected from the matrix for further analyses. A total of 9553 single-cell RNA sequencing samples (1,894 normal, 4274 tumor, and 3,385 peripheral blood samples) were collected from 11 LUAD cases. We used the "Seurat V4.0.4" R package to process the single-cell data expression matrix. First, "CreateSeuratObject" was used to screen gene expression data, "NormalizeData" to normalize gene expression data, and "FindVariableGenes" to confirm 2000 highly variable genes. Then, the principal component analysis (PCA) was performed using "RunPCA". The PCs that could be used were screened by the "FJackStraw" function and grouped with "Find Clusters" at the highest resolution. Finally, "tSNA" was used for visualization. Moreover, we used the "Single R" and "celldex" R packages through "HumanPrimaryCellAtlasData" for the cell to perform the annotation. "Feature Plot" and "Vln Plot" were used to visualize TAGAP expression.

Tumor Immune Dysfunction and Exclusion (TIDE, http://tide.dfci.harvard.edu/) was utilized to investigate the relationship between TAGAP expression and immune cells, as well as to calculate immunotherapy response prediction (17). GEO datasets were included if the following criteria were met: the source of the dataset samples was

non-small cell lung cancer or lung adenocarcinoma tissue specimens, each of which had a clear pathological diagnosis; and the dataset type was microarray or high-throughput sequencing data. Exclusion criteria: data analysis required the removal of all data in each dataset except for lung adenocarcinoma.

2.3 Gene set enrichment analysis

GSEA is a reliable molecular spectrum data analysis tool. It links previous knowledge with newly generated data and uses overlapping statistics to reveal gene behavior in health and disease states (18). In the present study, we used the GSEA 4.1.0 software to perform analyses based on the TAGAP expression matrix. The median of TAGAP expression was the cut-off value, divided into high- and low-expression groups. A thousand genome permutations were analyzed. We used *p*-value and normalized enrichment score (NES) to classify enriched pathways of each phenotype, and evaluate the correlation between TAGAP expression and immune expression-related factors.

2.4 Sample collection

From July 2020 to January 2021, 26 LUAD tissue samples were acquired from the Guangxi Medical University's First Affiliated Hospital by surgical excision and preserved at -80°C. Two independent pathologists verified the LUAD diagnosis. The ethics committee of the Guangxi Medical University's First Affiliated Hospital gave approved this investigation (2020-KY-NSFC-074).

2.5 Quantitative real-time polymerase chain reaction

We used qRT-PCR to predict the correlation between TAGAP and CD4 and CD8 expressions. After total RNA extraction, cDNA synthesis was performed using random hmers and SuperScript III reverse transcriptase for qRT-PCR. The results were estimated by the 2-Δ method. A $p < 0.05$ was considered statistically significant. The primer sequences were as follows: TAGAP Forward Sequence 5'-3': GACAGACTTGAAAGCATCGC and Reverse Sequence 5'-3': CTCCTGAATATCCCTTCCGTTG; CD8 Forward Sequence 5'-3': GGACTTCGCCTGTGATATCTAC and Reverse Sequence 5'-3': TTGTCTCCCGATTTGACCAC; CD4 Forward Sequence 5'-3': GCCCTTGAAGCGAAAACAG and Reverse Sequence 5'-3': CTCCTTGTTCTCCAGTTTCAAAC; GAPDH Forward Sequence 5'-3': ACATCGCTCAGACACCATG and Reverse Sequence 5'-3': TGTAGTTGAGGTCAATGAAGGG. GAPDH was used as an internal control.

2.6 Plasmid construction, cell transfection, and efficiency verification

The coding sequence (CDS) region of TAGAP was obtained by querying the NCBI website (https://www.ncbi.nlm.nih.gov/nuccore/NM_152133.3). Based on the sequence, the CDS region of TAGAP was inserted into the cloning vector LV5 (EF-1a/GFP&Puro), with the restriction enzyme sites NotI and BamHI used for digestion. The overexpression plasmid of TAGAP was successfully constructed, and sequencing and comparative analysis of the vector confirmed that the gene sequence matched the intended sequence, verifying the successful construction of the vector.

CD4 T cells were seeded in a 24-well plate and transfected with lentivirus carrying the expression vectors LV-TAGAP and LV-NC. After transfection, cells were collected, and RNA was extracted using the Trizol method. The RNA was dissolved in 30 μL of DEPC-treated water, and its quality was assessed using Nanodrop. Qualified RNA samples were stored at -80°C. The $2^{-}\Delta\Delta Ct$ method was employed to calculate the relative gene expression normalized to GAPDH.

2.7 Cell culture

Peripheral blood mononuclear cells (hPBMC) from healthy individuals were purchased from ATCC (PCS-800-011). The Dynabeads® CD4 Positive Isolation Kit (cat. 11331D, Invitrogen™) was used for cell sorting, and Dynabeads™ Human T-Activator CD3/CD28/CD137 (cat. 11163D, Gibco™) were used to activate CD4 T cells.

2.8 Cell proliferation

CD4 T cells transfected with LV-NC and LV-TAGAP were collected and resuspended. The cell suspension was seeded in a 96-well plate at a density of 2000 cells per well in 90 μL of culture medium. The plate was incubated at 37°C with 5% CO2. On days 0, 1, 3, 5, and 7, the absorbance of each well was measured at 490 nm using an MTT assay kit.

2.9 Cell cytotoxicity assay

A549 cells are a human lung adenocarcinoma cell line, commonly used in non-small cell lung cancer research for its pathological relevance and chemoresistance traits. A549 cells (5000 cells per well) were seeded in a 96-well plate and incubated at 37°C with 5% CO2. After 24 hours, LV-NC and LV-TAGAP CD4 T cells were added to the wells at ratios of 1:2, 1:3, and 1:5. The co-cultures were incubated for 24 hours, and the absorbance of each well was measured at 490 nm using an LDH cytotoxicity assay kit.

2.10 Chemotaxis assay

A 5.0-μm pore size Transwell chamber was used for the experiment. 1×10^5 A549 cells in 600 μL of medium were added to the lower chamber, while 5×10^5 CD4 T cells in 100 μL of medium were added to the upper chamber. The chambers were incubated at

37°C for 24 hours. After incubation, the CD4 T cell suspension in the upper chamber was aspirated, and the remaining cells in the upper chamber were counted using a cell counting plate. The migrated cell number was determined, and the migration rate was analyzed.

2.11 Western blot analysis

In brief, protein extraction, quantification, and isolation were performed using 10% SDS-PAGE. Subsequently, the protein bands were transferred onto PVDF membranes (Bio-Rad, CA, USA). After blocking with 4% skim milk powder, the membranes were incubated overnight at 4°C with primary antibodies, followed by incubation with secondary antibodies (diluted 1:5000, Cell Signaling Technology, Beverly, MA, USA) for 2 hours. Finally, chemiluminescence was used for band detection. The antibody information used in the Western blot is provided in the Table 1 below.

2.12 *In vivo* experiment

A total of 12 female NSG mice aged 4-5 weeks (Shanghai Southern Model Biological Technology Co., Ltd., China) were used to establish a subcutaneous tumor model of lung adenocarcinoma A549. Tumor volumes were determined using caliper measurements and calculated using the formula: V = 0.5 × L × W^2, where V represents the tumor volume, L indicates the longest diameter, and W stands for the width at the widest point perpendicular to the length. When the tumor volume reached 100 mm^3, the mice were randomly divided into two groups. Stable TAGAP-expressing CD4+ T cells were intravenously injected into the mice, with each mouse receiving 1×10^7 CD4+ T cells. A control group was also included. Tumor volume was measured every three days, and the changes in volume were recorded to plot the tumor growth curve. After 30 days, the mice were euthanized, and the tumors were excised, photographed, and preserved in formalin for subsequent pathological experiments.

2.13 Immunohistochemistry

The anti-TAGAP (1:100) and anti-CD8/CD4 (1:100) were purchased from Solarbio-Beijing and ABclonal.The goat anti-rabbit secondary antibody was purchased from Beyotime Institute of Biotechnology.

Fixed tumor tissues were dehydrated, embedded in paraffin, and sliced into 4 μm sections. The sections were deparaffinized in two xylene baths for 20 minutes each, followed by hydration in a series of graded ethanol baths for 5 minutes each. Antigen retrieval was performed using EDTA antigen retrieval solution for 20 minutes. After PBS washing, the sections were incubated with a peroxidase-blocking reagent at room temperature for 10 minutes to block endogenous peroxidase activity. The sections were then blocked with normal goat serum for 30 minutes. CD4 antibody (ABCAM, USA) was added to the tissue sections and incubated overnight at 4°C. Afterward, the sections were incubated with HRP-conjugated goat anti-rabbit secondary antibody (Beyotime, China) at 37°C for 30 minutes, followed by 5-minute DAB staining. After PBS washing, the sections were counterstained with hematoxylin, dehydrated in graded ethanol and xylene, and mounted. Photographic documentation and analysis of the staining results were performed using an upright light microscope (Leica DM 4000B, Germany).

2.14 ELISA

The harvested tumor tissues were ground, and the expression levels of CD4+ T cell-related cytokines were measured using an ELISA kit according to the manufacturer's instructions (Elabscience, China). The optical density (OD) values were measured at a wavelength of 450 nm using an ELISA reader.

2.15 Statistical analysis

Pearson or Spearman correlation coefficients were used to assess the correlation between TAGAP mRNA expression and the various categories of scores in the LUAD dataset. Differences in expression between normal and malignant samples were calculated for each tumor using the Wilcoxon test. $p<0.05$ was considered to be statistically significant.

3 Results

3.1 Expression level and prognostic significance of TAGAP in LUAD

We analyzed the TCGA-LUAD dataset (59 normal and 535 LUAD samples). A significantly low expression was observed in LUAD tissues compared to normal ones, similar to LUAD and paired paracancerous tissues (Figures 1A, B). The GEPIA survival analysis indicated that a higher TAGAP expression was related to a more favorable prognosis in LUAD patients (Figure 1C). Additionally, after excluding incomplete data, we analyzed the correlation between TCGAP and clinical data in 474 TCGA-LUAD samples. Univariate Cox regression analysis and multivariate Cox regression analysis showed that TAGAP expression and tumor stage were risk factors for overall survival in LUAD and were independent prognostic factors (Figure 1D). Furthermore, TAGAP mRNA expression levels in LUAD were significantly correlated with gender ($p<0.001$), pathological stage ($p=0.015$), and T stage($p=0.001$), but not with N stage($p=0.132$), M stage($p=0.216$), or pathological subtype($p=0.54$) (Figure 1E).

3.2 Correlation of TAGAP expression levels with immune cell infiltration in LUAD

According to previous immune-related research, TAGAP is primarily engaged in the activation of antifungal signaling

10.3389/fimmu.2023.1224340

TABLE 1 Antibodies Used in the Study, Dilution Ratios, Manufacturers, and Species.

Antibody	Dilution Ratio	Manufacturer	Species
GAPDH (primary)	1:5000	Huabio	Rabbit
JAK1 (primary)	1:1000	ABclonal	Rabbit
pJAK1 (primary)	1:1000	ABclonal	Rabbit
JAK2 (primary)	1:1000	ABclonal	Rabbit
pJAK2 (primary)	1:1000	ABclonal	Rabbit
STAT1 (primary)	1:1000	ABclonal	Rabbit
pSTAT1 (primary)	1:1000	ABclonal	Rabbit
STAT3 (primary)	1:1000	ABclonal	Rabbit
pSTAT3 (primary)	1:1000	ABclonal	Rabbit
IgG (secondary)	1:2000	Beyotime	Goat anti-rabbit

pathways in macrophages and DC, as well as directing T-helper cell differentiation and regulating thymocyte formation (11, 19). Given the known immune functions of TAGAP, it could be hypothesized that its expression might be associated with the immune landscape of LUAD. Using ESTIMATE, we first determined the stromal, immune, and ESTIMATE scores for each TCGA-LUAD tumor sample. These scores were then aggregated by median to depict the K-M survival analysis. According to these findings, high immune and ESTIMATE scores were linked to a positive LUAD prognosis, whereas the stromal score did not affect prognosis (Figure 2A). Then, we calculated the relationship between TAGAP expression and the abovementioned results. The TAGAP expression had a strong positive connection with stromal, immune, and ESTIMATE scores (Figure 2B).

To further explore the correlation between TAGAP and different immune cells, we used the CIBERSORT algorithm to infer the content of 22 immune cells in each LUAD sample. Results showed clear differences in the distribution of immune cell subpopulations in the TAGAP high and low expression groups. In the TAGAP high expression group, the expression of T cell CD8, T cell CD4 memory resting, T-cell CD4 memory activation, macrophage M1, and dendritic cells resting were significantly higher (Figure 2C).

Then, GEPIA was used to evaluate the association between TAGAP expression and immune cell signature genes of different tumor invasion types. The GEPIA correlation analysis results confirmed that, in LUAD, TAGAP expression was correlated with marker gene sets of different immune cells in different degrees. The gene markers affected by TAGAP expression included Naive T cells, Effector T cells, Memory T cells, Treg T cells, Neutrophils, Mast cells, NK cells, DCs, and Macrophages gene sets. TAGAP showed a significant positive correlation with all of the above gene sets (Figure 2D).

To validate the association between TAGAP and tumor-infiltrating lymphocytes, we analyzed publicly available single-cell RNA sequencing datasets of lung adenocarcinoma. After quality control and normalization, t-distributed stochastic neighbor

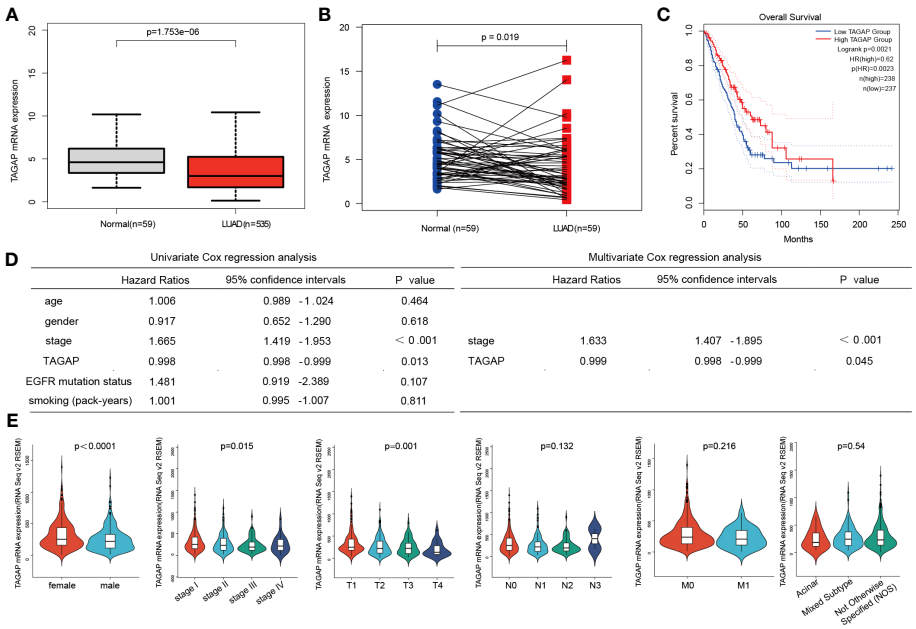


FIGURE 1
Expression and prognostic role of TAGAP in LUAD. **(A, B)** Paired and unpaired differential expressions of TAGAP in LUAD and normal tissues. **(C)** TAGAP's KM survival analysis curve in LUAD. **(D)** Univariate and multivariate regression analyses of TAGAP and LUAD's clinicopathological characteristics. **(E)** Association between TAGAP expression and clinicopathologic characteristics.

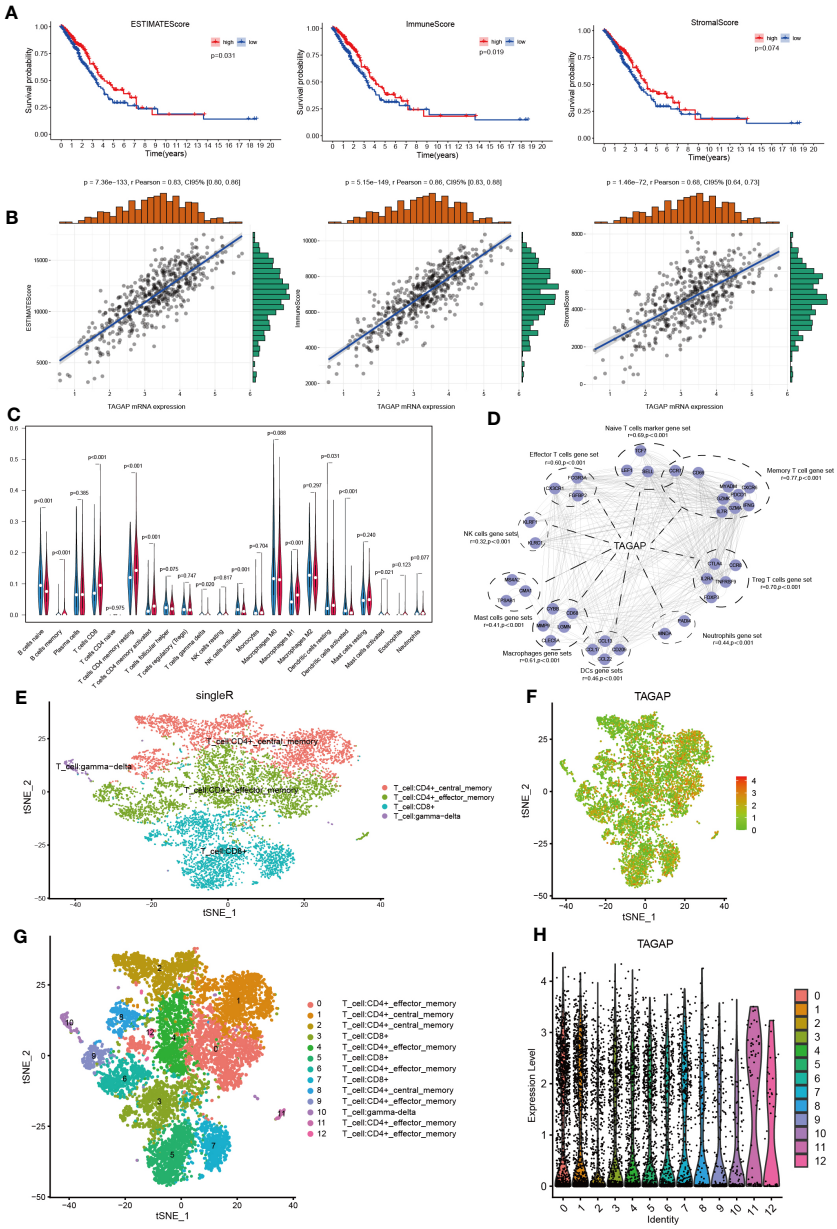


FIGURE 2
Correlation analysis of TAGAP and immune cell infiltration in LUAD. **(A)** Survival analyses of high- and low- ESTIMATE, immune, and stromal scores groups in LUAD. **(B)** Correlation analyses between TAGAP and ESTIMATE, immune, and stromal scores in LUAD. **(C)** Analyses of the difference in immune cell infiltration between the high and low TAGAP expression groups in LUAD by CIBERSORT. **(D)** Correlation analyses between TAGAP expression and different types of immune cell signatures in LUAD by GEPIA. **(E, G)** Cells were annotated in 4 and 12 clusters. **(F, H)** Expression and distribution of TAGAP in 4 and 12 clusters of immune cells.

embedding (tSNE) was performed on peripheral cells (PCs) to cluster cell populations. Subsequent immunophenotyping revealed an enriched expression of TAGAP in specific clusters. It's important to note that similar names across different clusters were used to denote cells of similar type or state. For example, the same names in Figures 2E, G represent similar cellular populations, albeit the different number of clusters resulted from the level of granularity in the analysis. Immunophenotyping revealed enriched expression of TAGAP in CD4+ and CD8+ T cell clusters (Figures 2E-H).

3.3 TAGAP expression levels can predict immunotherapy responsiveness

We used the Tumor Immune Dysfunction and Exclusion (TIDE) framework to confirm TAGAP's relevance to immune cells and determine whether it has predictive value for immunotherapy. Pearson correlation analysis was used to quantify the expression of TAGAP and the level of cytotoxic T lymphocytes (CTL) in GSE11969, GSE13213, and GSE31210. TAGAP expression levels and CTL were shown to be

significantly correlated in above three GEO-LUAD datasets (Figure 3A). We compared the area under the ROC curve (AUC) for TAGAP expression to other biomarker signatures, such as CD8, CD274 (PD-L1), interferon gamma (IFNG), TIDE, and microsatellite instability (MSI) score, as a tool for predicting immunotherapy response. TAGAP had the greatest predictive performance in a NSCLC (20) cohort (Ruppin_PD1_NSCLC, positive=7, negative =15), comparable to CD8. TAGAP, CD8, and CD274 all had an AUC greater than 0.7, indicating a significant probability of a positive immunotherapy response (Figure 3B).

3.4 IHC and RT-qPCR experimental validation of TAGAP expression increases

The expression of TAGAP, CD8, and CD4 was detected in 26 LUAD tissues (Figures 4A, B). Results showed a significant positive correlation between TAGAP and the expression of CD8 (R^2 = 0.6951, $p < 0.0001$) and CD4 (R^2 = 0.6464, $p < 0.0001$). Additionally, we collected tumor tissues from 26 LUAD patients and performed immunohistochemical experiments to detect the proportion of positive cells for CD8 and CD4 surface antigen, and TAGAP in immune infiltrating cells. Results showed that the expression of TAGAP in immune cells was significantly and positively correlated with the expression of CD8 (R^2 = 0.2027, p = 0.021) and CD4 (R^2 = 0.1572, p = 0.0449). Altogether, these results suggested that TAGAP expression was also higher in tissues with more infiltration of CD8+ and CD4+ T cells.

3.5 Enhancement of CD4+ T cell chemotaxis and cytotoxicity by TAGAP

Although TAGAP expression showed a stronger correlation with CD8+ T cell infiltration, we focused on the impact of TAGAP on CD4+ T cell function in this study. CD4+ T cells play a central role in regulating anti-tumor immune responses by secreting cytokines to activate other immune cells such as CD8+ T cells and macrophages. Additionally, subsets of CD4+ T cells also combat tumors through various mechanisms including direct killing of tumor cells and regulation of inflammation within the microenvironment. Therefore, we sought to investigate whether TAGAP could modulate CD4+ T cell activity, which would imply an important role of TAGAP in orchestrating anti-tumor immunity. To investigate the impact of TAGAP on CD4+ T cell function, we first transfected CD4+ T cells with a lentiviral vector overexpressing TAGAP. The expression of TAGAP in CD4+ T cells was examined using qRT-PCR. The results showed a significant upregulation of TAGAP expression in CD4+ T cells of the LV-TAGAP group compared to the control group (Figure 4C). Subsequently, to assess the effect of TAGAP on CD4+ T cell cytotoxicity, we co-cultured tumor cells with activated CD4+ T cells at different target-to-effector cell (T:E) ratios of 1:2, 1:3, and 1:5. The cytotoxicity of CD4+ T cells was determined using an LDH assay. The results demonstrated that overexpression of TAGAP significantly enhanced the cytotoxicity of CD4+ T cells against lung adenocarcinoma cells compared to the control group, with the highest cytotoxicity observed at the T:E ratio of 1:5 (Figure 4D). Additionally, the effect of TAGAP on the proliferation of CD4+ T cells was evaluated using the MTT assay. The results revealed that overexpression of TAGAP significantly promoted the proliferation capacity of CD4+ T cells compared to the control group (Figure 4E). Lastly, a chemotaxis assay was performed to examine the impact of TAGAP on the chemotaxis of CD4+ T cells. The results showed that overexpression of TAGAP significantly enhanced the chemotaxis ability of CD4+ T cells compared to the control group (Figure 4F).

3.6 Activation of the STAT pathway by TAGAP overexpression

To further elucidate the specific molecular mechanisms through which TAGAP regulates CD4+ T cell function, we performed Gene Set Enrichment Analysis (GSEA) on TAGAP. The results revealed a significant enrichment of TAGAP in the JAK-STAT signaling pathway (Figure 4G). Subsequently, we examined the expression of JAK-STAT pathway-related proteins (JAK1, JAK2, STAT1, STAT3, p-JAK1, p-JAK2, p-STAT1, p-STAT3) in CD4+ T cells overexpressing TAGAP. The results demonstrated that TAGAP overexpression activated the STAT pathway signaling (Figure 4H).

3.7 *In vivo* validation of the impact of TAGAP on CD4+ T cell cytotoxicity

To validate the findings from the *in vitro* cell experiments, we utilized B-NSG severely immunodeficient mice and established a xenograft tumor model by subcutaneously injecting A549 cells.

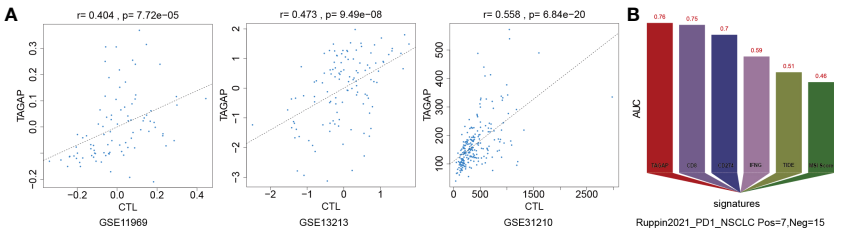


FIGURE 3
TAGAP expression correlates with CTLs and immunotherapy response in NSCLC. **(A)** Correlation analysis of TAGAP expression and cytotoxic T lymphocytes (CTL) in GSE11969, GSE13213 and GSE31210 by TIDE **(B)** TIDE biomarker evaluation of TAGAP response to immunotherapy in NSCLC.

10.3389/fimmu.2023.1224340

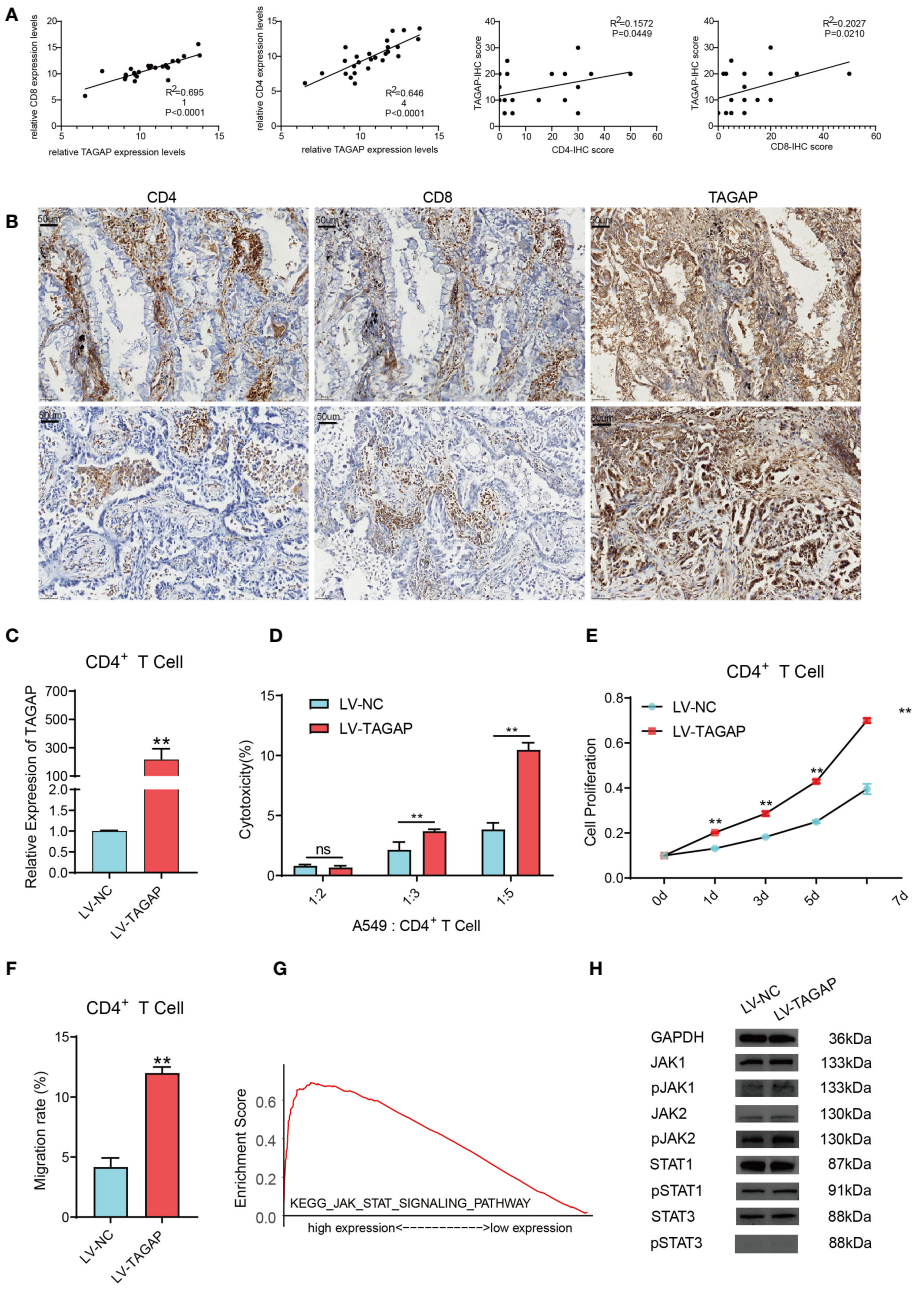


FIGURE 4
TAGAP enhances the cytotoxicity and chemotaxis of CD4+ T cells and activates the STAT pathway. **(A)** RT-qPCR and immunohistochemical correlation analyses of TAGAP with CD8 and CD4 in 26 pairs of LUAD tissues. **(B)** Representative images of CD8, CD4, and TAGAP immunohistochemistry in 26 pairs of LUAD tissues. **(C)** TAGAP expression in CD4+ T cells was detected; **(D)** LDH assay was used to determine the cytotoxicity of CD4+ T cells; **(E)** MTT assay was performed to assess the proliferation capacity of CD4+ T cells; **(F)** Transwell assay was conducted to measure the chemotaxis of CD4+ T cells. **(G)** GSEA pathway enrichment analysis was performed; **(H)** Expression of JAK/STAT pathway-related proteins was detected; ** p<0.01; ns, not significant.

Subsequently, LV-NC and LV-TAGAP CD4+ T cells were intravenously injected via the tail vein. Tumor growth was monitored, and it was observed that LV-TAGAP significantly suppressed tumor growth (Figures 5A-C). Immunohistochemistry (IHC) results demonstrated that LV-TAGAP significantly enhanced the expression of CD4 (Figure 5D). Additionally, LV-TAGAP increased the levels of the cytokines IFN-γ, IL-4, and IL-17A secreted by CD4+ T cells (Figure 5E). Collectively, these findings suggest that TAGAP overexpression can promote the cytotoxicity of CD4+ T cells (Figure 5E).

4 Discussion

With the recent advancements in immunotherapy, there has been increasing interest in the activation, differentiation, and function of

immune cells and their relationship to the efficacy of immunotherapy (21). However, the majority of research has focused on CD8+ T cells, NK cells, and macrophages, while CD4+ T cells have received less attention due to their complex immunoregulatory roles (22–24). Our study presents novel insights into the critical role of TAGAP in Lung Adenocarcinoma (LUAD), emphasizing its prognostic potential, relationship with immune cell infiltration, influence on CD4+ T cell activity, and predictive value for immunotherapy responsiveness.

TAGAP is a T cell Rho-GTPase activating protein that is expressed when T cells are activated. In granulocytes, TAGAP induction in response to Mycobacterium tuberculosis infection involves enrichment of differential acetylation (DA) peaks (25). Moreover, dectin-induced signaling was linked to the activation of an effective T helper cell immune response during antifungal host defense and autoimmunity, with TAGAP participation (11). On the other hand, the function of TAGAP in cancer is currently unknown.

In the present study, we confirmed that TAGAP can be considered as a gene associated with the tumor microenvironment and LUAD's overall survival. TAGAP is a novel biomarker associated with immune scoring in LUAD, and its low expression independently predicts poor outcomes in LUAD patients. Additionally, we found that different immunomarker groups and immune infiltration levels were positively correlated with TAGAP expression in LUAD. Previous studies have demonstrated that the tumor microenvironment can promote tumor progression and immune response through inflammation, angiogenesis, immunomodulatory, and therapeutic responses (26). Understanding the molecular composition and function of the tumor microenvironment is

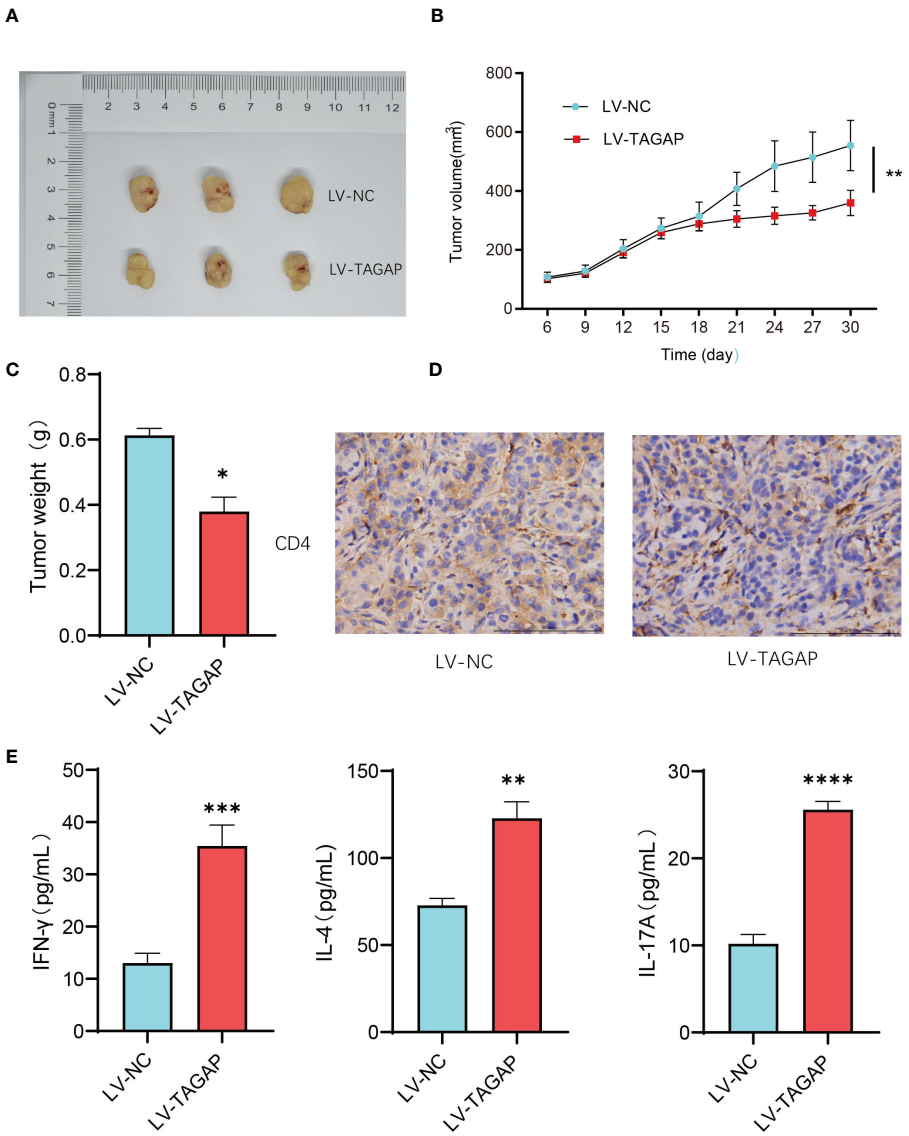


FIGURE 5
The effect of TAGAP on CD4+ T cell cytotoxicity was validated in a mouse xenograft tumor model. **(A)** Tumor size after different treatments; **(B, C)** Tumor volume and weight were measured in different treatment groups; **(D)** Immunohistochemistry staining was used to detect the expression of CD4; **(E)** Expression of cytokines IFN-γ, IL-4, and IL-17A secreted by CD4+ T cells was assessed. * $p < 0.05$, ** $p < 0.01$, *** $p < 0.001$, **** $p < 0.0001$.

critical for the development of LUAD therapies targeting angiogenesis and recent immune checkpoints.

We extended our investigations to explore the influence of TAGAP on CD4+ T cell function, which is pivotal in orchestrating anti-tumor immune responses. The results revealed that TAGAP overexpression enhanced CD4+ T cell cytotoxicity and chemotaxis, bolstering the proliferation capacity of these cells. The activation of the JAK-STAT signaling pathway by TAGAP overexpression offers a plausible molecular mechanism underlying TAGAP's impact on CD4+ T cell function, warranting further investigations. The JAK/STAT pathway is the main signal transduction mechanism of various cytokines and growth factors (27, 28). Its role in lung cancer has been confirmed by several previous studies. These results further supported the hypothesis that TAGAP plays a reliable role in the occurrence and development of LUAD.

Although studies have shown the relationship between TAGAP and the prognosis of LUAD patients, the detailed mechanism and immunoclustering distribution of TAGAP in NSCLC is still unclear. In the current study, the results of analysis of lung cancer samples from the GEO single-cell dataset, RT-qPCR, and immunohistochemical analysis showed that T CD4+/CD8+ cell expression was correlated to TAGAP. A previous study showed that cytokines released by T cells can influence the activation of STATs (29). We speculated that the regulation of TAGAP on the immune microenvironment, especially on T cells, can affect the release of cytokines, and ultimately promote the occurrence and development of tumor cells through the JAK-STAT pathway.

TAGAP has been discovered to have crucial effects through additional pathways and systems, in addition to studies in the tumor immune microenvironment. TAGAP-deficient macrophages had enhanced viral replication of herpes simplex virus type 1, lower expression of pro-inflammatory chemokines and cytokines, and lower production of IFN-β, according to Juan Liao et al., implying that TAGAP plays a significant role in antiviral cytokine production (30). TAGAP governs the cytoskeletal architecture of actin fibers via RhoA, which is required for cell contractility and the cycle of integrin attachment and separation required for directional migration of thymocytes, according to Jonathan S. Duke-Cohan et al (19). Given the widespread link of TAGAP with a variety of disorders, further research is needed to figure out how TAGAP works.

In terms of immunotherapy responsiveness, our study suggests that TAGAP expression levels can predict immunotherapy efficacy, with TAGAP outperforming established biomarkers such as PD-L1 in certain contexts. Finally, our *in vivo* and *in vitro* validation further strengthened the hypothesis of TAGAP's role in enhancing CD4+ T cell cytotoxicity. These results suggest that TAGAP could be an effective therapeutic target to improve the antitumor immune response in LUAD, providing a novel angle for future research.

Altogether, our findings shed light on the multifaceted role of TAGAP in LUAD, emphasizing its prognostic and therapeutic potential. Further studies are warranted to fully elucidate the underlying mechanisms of TAGAP's interaction with the tumor microenvironment and its potential clinical applications.

Data availability statement

The original contributions presented in the study are included in the article/supplementary material. Further inquiries can be directed to the corresponding author.

Ethics statement

Ethical approval was not required for the studies on humans in accordance with the local legislation and institutional requirements because only commercially available established cell lines were used. The animal study was approved by Animal Ethics Committee of the First Affiliated Hospital of Guangxi Medical University. The study was conducted in accordance with the local legislation and institutional requirements.

Author contributions

ZX and ZZ devised and developed the experiments, carried out the RT-qPCR and IHC tests, created figures and/or tables, and approved the final document. ZZ, WJ, and LH evaluated bioinformatics data, prepared or reviewed drafts of the publication, and approved the final draft. Figures and/or tables were developed by YS, TZ, FQ, and JQ, who also approved the final draft. The experiments were devised and designed by SL, who also authorized the final draft. All authors contributed to the article and approved the submitted version.

Funding

The Guangxi Natural Science Foundation (2022GXNSFAA035513), the National Key Clinical Specialty Construction Project and the Guangxi Key Clinical Specialty Construction Project funded this research.

Acknowledgments

The authors express their gratitude to the personnel of the Department of Thoracic Surgery at Guangxi Medical University's First Affiliated Hospital, as well as all participants and contributions to this study.

Conflict of interest

The authors declare that the research was conducted in the absence of any commercial or financial relationships that could be construed as a potential conflict of interest.

Publisher's note

All claims expressed in this article are solely those of the authors and do not necessarily represent those of their affiliated organizations, or those of the publisher, the editors and the reviewers. Any product that may be evaluated in this article, or claim that may be made by its manufacturer, is not guaranteed or endorsed by the publisher.

References

1. Sung H, Ferlay J, Siegel RL, Laversanne M, Soerjomataram I, Jemal A, et al. Global cancer statistics 2020: GLOBOCAN estimates of incidence and mortality worldwide for 36 cancers in 185 countries. *CA Cancer J Clin* (2021) 71(3):209–49. doi: 10.3322/caac.21660

2. Dalwadi SM, Lewis GD, Bernicker EH, Butler EB, Teh BS, Farach AM. Disparities in the treatment and outcome of stage I non-small-cell lung cancer in the 21st century. *Clin Lung Cancer* (2019) 20(3):194–200. doi: 10.1016/j.cllc.2018.11.004

3. Kita T, Araya T, Sakai T, Uchida Y, Matsuoka H, Kasahara K. Nivolumab-induced polymyalgia rheumatica in a patient with lung adenocarcinoma. *Am J Med Sci* (2021) 362(3):321–3. doi: 10.1016/j.amjms.2021.04.010

4. Reck M, Remon J, Hellmann MD. First-line immunotherapy for non-small-cell lung cancer. *J Clin Oncol* (2022) 40(6):586–97. doi: 10.1200/JCO.21.01497

5. Niknafs N, Balan A, Cherry C, Hummelink K, Monkhorst K, Shao XM, et al. Persistent mutation burden drives sustained anti-tumor immune responses. *Nat Med* (2023) 29(2):440–9. doi: 10.1038/s41591-022-02163-w

6. Liu S, Meng Y, Liu L, Lv Y, Yu W, Liu T, et al. CD4(+) T cells are required to improve the efficacy of CIK therapy in non-small cell lung cancer. *Cell Death Dis* (2022) 13(5):441. doi: 10.1038/s41419-022-04882-x

7. Wang L, Wu W, Zhu X, Ng W, Gong C, Yao C, et al. The ancient chinese decoction Yu-Ping-Feng suppresses orthotopic lewis lung cancer tumor growth through increasing M1 macrophage polarization and CD4(+) T cell cytotoxicity. *Front Pharmacol* (2019) 10:1333. doi: 10.3389/fphar.2019.01333

8. Chao JL, Savage PA. Unlocking the complexities of tumor-associated regulatory T cells. *J Immunol* (2018) 200(2):415–21. doi: 10.4049/jimmunol.1701188

9. Tamehiro N, Nishida K, Yanobu-Takanashi R, Goto M, Okamura T, Suzuki H. T-cell activation RhoGTPase-activating protein plays an important role in T(H)17-cell differentiation. *Immunol Cell Biol* (2017) 95(8):729–35. doi: 10.1038/icb.2017.27

10. Saoudi A, Kassem S, Dejean A, Gaud G. Rho-GTPases as key regulators of T lymphocyte biology. *Small GTPases* (2014) 5:e28208. doi: 10.4161/sgtp.28208

11. Chen J, He R, Sun W, Gao R, Peng Q, Zhu L, et al. TAGAP instructs Th17 differentiation by bridging Dectin activation to EPHB2 signaling in innate antifungal response. *Nat Commun* (2020) 11(1):1913. doi: 10.1038/s41467-020-15564-7

12. Arshad M, Bhatti A, John P, Jalil F, Borghese F, Kawalkowska JZ, et al. T cell activation Rho GTPase activating protein (TAGAP) is upregulated in clinical and experimental arthritis. *Cytokine* (2018) 104:130–5. doi: 10.1016/j.cyto.2017.10.002

13. Wang Z, Xu H, Zhu L, He T, Lv W, Wu Z. Establishment and evaluation of a 6-gene survival risk assessment model related to lung adenocarcinoma microenvironment. *BioMed Res Int* (2020) 2020:6472153. doi: 10.1155/2020/6472153

14. Chang JT, Lee YM, Huang RS. The impact of the Cancer Genome Atlas on lung cancer. *Transl Res* (2015) 166(6):568–85. doi: 10.1016/j.trsl.2015.08.001

15. Ritchie ME, Phipson B, Wu D, Hu Y, Law CW, Shi W, et al. limma powers differential expression analyses for RNA-sequencing and microarray studies. *Nucleic Acids Res* (2015) 43(7):e47. doi: 10.1093/nar/gkv007

16. Tang Z, Li C, Kang B, Gao G, Li C, Zhang Z. GEPIA: a web server for cancer and normal gene expression profiling and interactive analyses. *Nucleic Acids Res* (2017) 45 (W1):W98–98W102. doi: 10.1093/nar/gkx247

17. Fu J, Li K, Zhang W, Wan C, Zhang J, Jiang P, et al. Large-scale public data reuse to model immunotherapy response and resistance. *Genome Med* (2020) 12(1):21. doi: 10.1186/s13073-020-0721-z

18. Subramanian A, Tamayo P, Mootha VK, Mukherjee S, Ebert BL, Gillette MA, et al. Gene set enrichment analysis: a knowledge-based approach for interpreting genome-wide expression profiles. *Proc Natl Acad Sci U.S.A.* (2005) 102(43):15545–50. doi: 10.1073/pnas.0506580102

19. Duke-Cohan JS, Ishikawa Y, Yoshizawa A, Choi YI, Lee CN, Acuto O, et al. Regulation of thymocyte trafficking by Tagap, a GAP domain protein linked to human autoimmunity. *Sci Signal* (2018) 11(534):eaan8799. doi: 10.1126/scisignal.aan8799

20. Lee JS, Ruppin E. Multiomics prediction of response rates to therapies to inhibit programmed cell death 1 and programmed cell death 1 ligand 1. *JAMA Oncol* (2019) 5 (11):1614–8. doi: 10.1001/jamaoncol.2019.2311

21. Sharma P, Allison JP. Immune checkpoint targeting in cancer therapy: toward combination strategies with curative potential. *Cell* (2015) 161(2):205–14. doi: 10.1016/j.cell.2015.03.030

22. Geginat J, Paroni M, Facciotti F, Gruarin P, Kastirr I, Caprioli F, et al. The CD4-centered universe of human T cell subsets. *Semin Immunol* (2013) 25(4):252–62. doi: 10.1016/j.smim.2013.10.012

23. Zhu J, Yamane H, Paul WE. Differentiation of effector CD4 T cell populations (*). *Annu Rev Immunol* (2010) 28:445–89. doi: 10.1146/annurev-immunol-030409-101212

24. Kather JN, Suarez-Carmona M, Charoentong P, Weis CA, Hirsch D, Bankhead P, et al. Topography of cancer-associated immune cells in human solid tumors. *Elife* (2018) 7:e36967. doi: 10.7554/eLife.36967

25. Sivakumaran D, Blatner G, Bakken R, Hokey D, Ritz C, Jenum S, et al. A 2-dose AERAS-402 regimen boosts CD8(+) polyfunctionality in HIV-negative, BCG-vaccinated recipients. *Front Immunol* (2021) 12:673532. doi: 10.3389/fimmu.2021.673532

26. Altorki NK, Markowitz GJ, Gao D, Port JL, Saxena A, Stiles B, et al. The lung microenvironment: an important regulator of tumour growth and metastasis. *Nat Rev Cancer* (2019) 19(1):9–31. doi: 10.1038/s41568-018-0081-9

27. Pastuszak-Lewandoska D, Domańska-Senderowska D, Kordiak J, Antczak A, Czarnecka KH, Migdalska-Sęk M, et al. Immunoexpression analysis of selected JAK/STAT pathway molecules in patients with non- small-cell lung cancer. *Pol Arch Intern Med* (2017) 127(11):758–64. doi: 10.20452/pamw.4115

28. Sánchez-Ceja SG, Reyes-Maldonado E, Vázquez-Manríquez ME, López-Luna JJ, Belmont A, Gutiérrez-Castellanos S. Differential expression of STAT5 and Bcl-xL, and high expression of Neu and STAT3 in non-small-cell lung carcinoma. *Lung Cancer* (2006) 54(2):163–8. doi: 10.1016/j.lungcan.2006.07.012

29. Kryczek I, Lin Y, Nagarsheth N, Peng D, Zhao L, Zhao E, et al. IL-22(+)CD4(+) T cells promote colorectal cancer stemness via STAT3 transcription factor activation and induction of the methyltransferase DOT1L. *Immunity* (2014) 40(5):772–84. doi: 10.1016/j.immuni.2014.03.010

30. Liao J, Jijon HB, Kim IR, Goel G, Doan A, Sokol H, et al. An image-based genetic assay identifies genes in T1D susceptibility loci controlling cellular antiviral immunity in mouse. *PloS One* (2014) 9(9):e108777. doi: 10.1371/journal.pone.0108777

frontiers | Frontiers in Immunology

TYPE Review
PUBLISHED 11 September 2023
DOI 10.3389/fimmu.2023.1249980

Check for updates

OPEN ACCESS

EDITED BY
Qun Xue,
Affiliated Hospital of Nantong University, China

REVIEWED BY
Chuan Lan,
the Affiliated Hospital of North Sichuan Medical College, China
Haiyan Zeng,
West China Hospital, Sichuan University, China

*CORRESPONDENCE
Dong Hua
wx89211@163.com
Chengming Li
chengming0401@163.com

†These authors have contributed equally to this work

RECEIVED 29 June 2023
ACCEPTED 24 August 2023
PUBLISHED 11 September 2023

CITATION
Liang S, Wang H, Tian H, Xu Z, Wu M, Hua D and Li C (2023) The prognostic biological markers of immunotherapy for non-small cell lung cancer: current landscape and future perspective. *Front. Immunol.* 14:1249980. doi: 10.3389/fimmu.2023.1249980

COPYRIGHT
© 2023 Liang, Wang, Tian, Xu, Wu, Hua and Li. This is an open-access article distributed under the terms of the Creative Commons Attribution License (CC BY). The use, distribution or reproduction in other forums is permitted, provided the original author(s) and the copyright owner(s) are credited and that the original publication in this journal is cited, in accordance with accepted academic practice. No use, distribution or reproduction is permitted which does not comply with these terms.

The prognostic biological markers of immunotherapy for non-small cell lung cancer: current landscape and future perspective

Shuai Liang[1†], Hanyu Wang[2†], Haixia Tian[1†], Zhicheng Xu[1], Min Wu[3], Dong Hua[1,2*] and Chengming Li[4*]

[1]Department of Oncology, The Affiliated Wuxi People's Hospital of Nanjing Medical University, Wuxi, China, [2]Wuxi School of Medicine, Jiangnan University, Wuxi, China, [3]Suzhou Cancer Center Core Laboratory, The Affiliated Suzhou Hospital of Nanjing Medical University, Suzhou, China, [4]Department of Radiation Oncology, Shandong Cancer Hospital and Institute, Shandong First Medical University and Shandong Academy of Medical Sciences, Jinan, China

The emergence of immunotherapy, particularly programmed cell death 1 (PD-1) and programmed cell death ligand-1 (PD-L1) produced profound transformations for treating non-small cell lung cancer (NSCLC). Nevertheless, not all NSCLC patients can benefit from immunotherapy in clinical practice. In addition to limited response rates, exorbitant treatment costs, and the substantial threats involved with immune-related adverse events, the intricate interplay between long-term survival outcomes and early disease progression, including early immune hyperprogression, remains unclear. Consequently, there is an urgent imperative to identify robust predictive and prognostic biological markers, which not only possess the potential to accurately forecast the therapeutic efficacy of immunotherapy in NSCLC but also facilitate the identification of patient subgroups amenable to personalized treatment approaches. Furthermore, this advancement in patient stratification based on certain biological markers can also provide invaluable support for the management of immunotherapy in NSCLC patients. Hence, in this review, we comprehensively examine the current landscape of individual biological markers, including PD-L1 expression, tumor mutational burden, hematological biological markers, and gene mutations, while also exploring the potential of combined biological markers encompassing radiological and radiomic markers, as well as prediction models that have the potential to better predict responders to immunotherapy in NSCLC with an emphasis on some directions that warrant further investigation which can also deepen the understanding of clinicians and provide a reference for clinical practice.

KEYWORDS

non-small cell lung cancer (NSCLC), immunotherapy, prognostic biological markers, anti-PD-(L)1, review

1 Introduction

Lung carcinoma is widely acknowledged as being the foremost reason for mortality connected to neoplasms in both the U.S. and China, which is with around 85% of pulmonary neoplasms classified as non-small cell lung carcinomas (NSCLCs) (1, 2). And the advent of immunotherapeutic agents targeting programmed cell death 1 (PD-1) and programmed cell death ligand-1 (PD-L1), also known as one of immunoregulatory checkpoint inhibitors (ICIs), altered thoroughly the management of patients with progressive or metastatic NSCLC. Furthermore, the utilization of PD-1 inhibitors (Nivolumab, Pembrolizumab) and PD-L1 inhibitors (Atezolizumab) has been endorsed by the U.S. Food and Drug Administration (FDA) in terms of patients' treatments with advanced NSCLC experiencing disease progression in or post initial-line therapy due to their superior disease progression-free survival (PFS) and overall survival (OS) outcomes in comparison to the conventional chemotherapy comparator (3–6). Nevertheless, the favorable response to PD-1/PD-L1 inhibitors is not universal, as merely 20 - 40% of patients exhibit a response, fewer achieve long-term disease remission, and even some patients could experience immune hyperprogression at the early stage of immunotherapy (7–9). Given the exorbitant costs and potential for severe adverse effects associated with ICIs, it becomes imperative to find patients with the most likely to derive therapeutic advantage from such treatments and enhance the efficacy of ICIs for precise therapeutic interventions. Consequently, the pursuit of reliable and effective biological markers for assessing the reaction to anti-PD-1/PD-L1 immunotherapy has become the focal point of oncoimmunology investigations in NSCLC patients. Although biological markers including PD-L1 expression levels, tumor mutational burden (TMB), hematological biological markers, and composite biological markers are presently under scrutiny as potential indicators for assessing the reaction to ICIs in NSCLC patients, none have gained widespread and accurate clinical utilization. Thus, in this review, we comprehensively examine the current landscape of biological markers for anti-PD-1/PD-L1 immunotherapy in NSCLC with an emphasis on some directions that warrant further investigation which can also deepen the understanding of clinicians and provide a reference for clinical practice.

Abbreviations: AUC, area under curve; bTMB, blood TMB; CA19-9, carbohydrate antigen; CEA, carcinoembryonic antigen; CT, computed tomography; ctDNA, circulating tumor DNA; Cyfra21-1, cytokeratin fragment 21-1; FDA, food and drug administration; DCB, disease clinical benefit; DCR, durable clinical rate; dNLR, derived NLR; HR, hazard ratio; ICIs, immune checkpoint inhibitors; LDA, linear discriminant analysis; LDH, lactate dehydrogenase; LIPI, lung immune prognostic index; MHC, major histocompatibility complexes; mOS, median OS; mPFS, median PFS; mpRS, multiparametric radiomics signature; MTVwb, tumor metabolic volume; NCCN, national comprehensive cancer network; NLR, neutrophil/lymphocyte ratio; NSCLC, non-small cell lung cancer; NSE, neuron specific enolase; ORR, overall response rate; OS, overall survival; PD-1, programmed cell death protein 1; PD-L1, programmed cell death ligand 1; PFS, progression-free survival; ROC, receiver operating characteristic curve; SUVmax, maximum standardized uptake value; TCR, T cell receptors; TLGwb, total lesion glycolysis; TMB, tumor mutation burden; TMB-H, high TMB; TMB-L, low TMB; TMTV, total metabolic tumor volume; TTP, time to progression; ULN, upper limit of normal.

2 Single biological marker

2.1 PD-L1 expression

Currently, PD-L1 expression serves as one of the highest extensively utilized biological markers to predict the ICIs efficiency in NSCLC. As per the guidelines by the National Comprehensive Cancer Network (NCCN), anti-PD-L1 immunotherapy (Atezolizumab) is suggested as first-line treatment for NSCLC patients exhibiting PD-L1 expression ≥ 50% or as second-line treatment for those with PD-L1 expression ≥ 1% (3). PD-1, an immunoregulatory checkpoint receptor expressed on activated T cells, including tumor-infiltrating lymphocytes, plays a pivotal role in immune evasion when it interacts with its ligands, PD-L1 and PD-L2, resulting in the suppression of cytotoxic T cell responses (10–13). Upregulation of PD-L1 is frequently observed on tumor cell surfaces, with PD-L1 expression reported in approximately 20% to 40% of NSCLC cases (14). Extensive investigations have delved into the connection between PD-L1 expression levels and immunotherapy efficacy, although the predictive value of PD-L1 remains controversial (Table 1) (15–20, 22–30, 34, 35). The KEYNOTE-024 trial showed that Pembrolizumab exhibited better OS in comparison to chemotherapy in patients displaying high PD-L1 expression (≥ 50%) (21). For PACIFIC trials, unresectable stage III NSCLC patients who completed radiotherapy and chemotherapy were administered Durvalumab for up to one year (36). It was observed that Durvalumab improved survival in patients with PD-L1 expression ≥ 25%. However, patients with low PD-L1 expression (< 1%) did not derive significant benefits from immune consolidation therapy. A meta-analysis involving 12 randomized clinical trials encompassing 6,932 patients with locally advanced NSCLC who received PD-1/PD-L1 inhibitors indicated that individuals with high PD-L1 expression levels exhibited longer PFS, OS, and overall response rate (ORR) in comparison to those with low PD-L1 levels (37). Of note, patients with PD-L1 expression ≥ 1% demonstrated a significant improvement in ORR, whilst little statistically significant disparity had been noted among patients with PD-L1 expression < 1% ($P = 0.12$).

Even though individuals exhibiting elevated PD-L1 expression exhibited a higher likelihood of responding ICIs, around 10% of PD-L1-negative patients also displayed a reaction to ICIs. Conversely, there were instances where patients with substantial PD-L1 expression exhibited an unresponsive state (4, 5, 31, 32). Within the framework of the KEYNOTE-024 trial, the ORR for PD-L1 ≥ 50% NSCLC patients receiving Pembrolizumab was a mere 44.8%, thereby indicating a considerable proportion of individuals with heightened PD-L1 expression did not manifest a response to this treatment (28). Moreover, the CheckMate-026 trial revealed that a PD-L1 expression level of ≥ 50% failed to serve as a reliable predictor of the effectiveness

10.3389/fimmu.2023.1249980

TABLE 1 Clinical outcomes of NSCLC patients treated with anti-PD-1/anti-PD-L1 agents according to the expression of PD-L1.

Study	Patients (N)	Drug	Assay	Cut-off value	(m)PFS (months)	(m)OS (months)	ORR (%)	Ref.
POPLAR	287	Atezolizumab **vs.** Docetaxel	SP142	50% (TC) or 10% (IC)	7.8 vs. 3.9	19.9 vs. 11.1	38 vs. 13	(3, 15)
KEYNOTE 010	442	Pembrolizumab (2 or 4 mg/kg) **vs.** Docetaxel	22C3	50% (TPS)	5.0 or 5.2 vs. 4.1	14.9 or 17.3 vs. 8.2	30 or 29 vs. 8	(4)
Based on KEYNOTE 010	1033	Pembrolizumab **vs.** Docetaxel	22C3	50% (TPS) 1% (TPS) 1-49% (TPS)	5.3 vs. 4.1 3.9 vs. 4.1 2.6 vs. 4.1	17.1 vs. 8.2 11.9 vs. 8.6 10.2 vs. 8.7	32.4 vs. 8.6 20.9 vs. 9.3 NA	(4, 16)
Checkmate 017	272	Nivolumab **vs.** Docetaxel	28-8	NA	3.5 vs. 2.8	9.2 vs. 6.0	20 vs. 9	(5)
OAK	850	Atezolizumab **vs.** Docetaxel	SP142	1% (TC or IC) 50% (TC or IC)	Similar	12.6 vs. 8.9 20.5 vs. 8.9	8 vs. 11 31 vs.11	(6)
Based on Checkmate 017	272	Nivolumab **vs.** Docetaxel	28-8	1% (TPS) 50% (TPS)	NA	NA	17 vs. 11 29 vs. 10	(5, 17)
Based on OAK	850	Atezolizumab **vs.** Docetaxel	SP142	1% (TC or IC) 50% (TC or IC)	NA	20.5 vs. 9.7 11.8 vs. 8.9	NA NA	(6, 15)
Checkmate 057	457	Nivolumab **vs.** Docetaxel	28-8	1% (TPS) 5% (TPS) 10% (TPS)	4.2 vs. 4.5 5.0 vs. 3.8 5.0 vs. 3.7	17.7 vs. 9.0 19.4 vs. 8.1 19.0 vs. 8.0	38 vs. 15 34 vs. 11 32 vs. 10	(18)
Based on Checkmate 057	582	Nivolumab **vs.** Docetaxel	28-8	1% (TPS) 50% (TPS)	NA	NA	31 vs. 12 41 vs. 7	(17, 18)
CheckMate 078	252 205	Nivolumab **vs.** Docetaxel	28-8	≥1% (TPS) <1% (TPS)	NA	12.3 vs. 7.9 11.4 vs. 10.2	NA	(19)
KEYNOTE 042	1274	Pembrolizumab **vs.** Chemotherapy	22C3	1% (TPS) 20% (TPS) 50% (TPS)	5.4 vs. 6.5 6.2 vs 6.6 7.1 vs. 6.4	16.7 vs. 12.1 NA NA	27 vs. 27 33 vs. 29 39 vs. 32	(20)
KEYNOTE 024	305	Pembrolizumab **vs.** Chemotherapy	22C3	50% (TC)	10.3 vs. 6.7	NA	44.8 vs. 27.8	(21)
Based on KEYNOTE 010 KEYNOTE 024 KEYNOTE 042	264 (elderly) 2348 (younger)	Pembrolizumab **vs.** Chemotherapy	22C3	1% (TPS) 50% (TPS) 1% (TPS) 50% (TPS)	NA	15.7 vs. 11.7 23.1 vs. 8.3 14.6 vs. 11.1 19.2 vs.11.9	NA	(4, 20–22)
MYSTIC	488	Durvalumab **vs.** Durvalumab + Tremelimumab **vs.** Chemotherapy	SP263	25% (TC)	NA	11.1 vs 10.5 vs. 13.3 (25-49%)	35.6 vs. 34.4	(23)

(Continued)

10.3389/fimmu.2023.1249980

TABLE 1 Continued

Study	Patients (N)	Drug	Assay	Cut-off value	(m)PFS (months)	(m)OS (months)	ORR (%)	Ref.
						18.3 vs. 15.2 vs. 12.7 (50%)	vs. 37.7	
CheckMate 568	252	Nivolumab + Ipilimumab	28-8	1% (TC)	6.8 vs. 2.8	NA	41 vs. 15	(24)
Checkmate 012	44	Nivolumab + Ipilimumab (12 weeks **vs.** 6 weeks)	28-8	1% (TC)	8.1 vs. 10.6	NA	57 vs 57	(25)
EMPOWER-Lung 1	563	Cemiplimab **vs.** Chemotherapy	22C3	50% (TC)	8.2 vs. 5.7	NR vs. 14.2	36.5 vs. 20.6	(26)
Impower 110	554	Atezolizumab **vs.** Chemotherapy	NA	50% (TC) or 10% (IC) 5% (TC or IC) 1% (TC or IC)	NA NA NA	20.2 vs. 13.1 18.2 vs. 14.9 17.5 vs. 14.1	NA NA NA	(27)
CameL	255	Camrelizumab + Chemotherapy **vs.** Chemotherapy	22C3	1% (TPC)	15.4 vs. 9.9	NA	NA	(28)
CheckMate 227	1189 550	Nivolumab + Ipilimumab **vs.** Nivolumab **vs.** Chemotherapy	28-8	≥ 1% (TC) < 1% (TC)	5.1 **vs.** 4.2 **vs.** 5.6 5.1 **vs.** 5.6 **vs.** 4.7	17.1 **vs.** 15.7 **vs.** 14.9 17.4 **vs.** 15.2 **vs.** 12.2	36 **vs.** 28 **vs.** 30 27 **vs.** 38 **vs.** 23	(29, 30)
KEYNOTE 407	207	Pembrolizumab combination **vs.** Placebo combination	22C3	1% (TPS)	7.2 vs. 5.2	14.0 vs. 11.6	49.5 vs. 41.3	(31)
	146			50% (TPS)	8.0 vs. 4.2	NR vs. NR	60.3 vs. 32.9	
GP28328	76	Atezolizumab + Chemotherapy	SP142	1% (TC or IC)	6.0 vs. 5.6	15.0 vs. 12.9	45.2 vs.41.2	(32)
CheckMate 026	423 214	Nivolumab **vs.** Chemotherapy	28-8	5% (TPS) 50% (TPS)	4.2 vs. 5.9 NA	14.4 vs. 13.2 NA	26 vs. 33 34 vs. 39	(33)

NA, not available; NR, not reached.

of Nivolumab in first-line NSCLC treatment (ORR, 34% vs. 39%) (33). And CheckMate 227 also found that Nivolumab plus Ipilimumab increased 5-year survivorship verse chemotherapy regardless of PD-L1 expression (29). One of the most obstacles impeding the clinical implementation of PD-L1 as a biological marker for predicting response to anti-PD-1/PD-L1 could be the absence of standardization in PD-L1 testing. Presently, the FDA has sanctioned the utilization of three PD-L1 immunohistochemistry (IHC) assays as companion diagnostics: Dako 22C3 (22C3) for Pembrolizumab in patients with diverse solid tumors, including NSCLC; Ventana SP142 (SP142) for Atezolizumab in NSCLC patients; and Dako 28-8 (28-8) for the combination of Ipilimumab and Nivolumab in NSCLC patients (38). Then, discrepancies in the findings of various studies could potentially arise from disparities in antibodies, detection methodologies, environmental conditions at the time of analysis, and the threshold values employed to determine PD-L1 expression (39, 40). For instance, the KEYNOTE-028 phase Ib study necessitated PD-L1 expression exceeding 1% on tumor or stromal cells, per measurement by the 22C3 assay, for advanced-stage solid tumors patients who received Pembrolizumab (41). Furthermore, variations in previous treatments administered to patients across different studies could have also contributed to inconsistencies in the research outcomes (42, 43). Last, the expression of PD-L1 is dynamic, influenced by treatments such as chemotherapy, radiotherapy, or chemoradiotherapy, which can influence PD-L1 expression within the tumor (44–46). Consequently, studies encompassing larger cohorts are imperative to validate the significance of PD-L1 as a predictive biological marker for ICI response in NSCLC patients.

10.3389/fimmu.2023.1249980

TABLE 2 Clinical outcomes of NSCLC patients treated with anti-PD-1/anti-PD-L1 agents according to the expression of TMB.

Study	Patients (N)	Therapy	TMB cut-off (mut/Mb)	(m)PFS (months)	(m)OS (months)	ORR (%)	Ref.
MYSTIC	809 460	Durvalumab **vs.** Durvalumab + Tremelimumab **vs.** Chemotherapy	20 (bTMB) 10 (tTMB)	2.7 vs.4.2 vs. 4.4 3.1 vs. 3.1 vs. 5.1	12.6 vs. 21.9 vs. 10.0 18.6 vs. 16.6 vs. 11.9	NA	(23)
CheckMate 568	98	Nivolumab + Ipilimumab	10 (tTMB)	7.1 vs.2.6	NA	44 vs. 12	(24)
CheckMate 026	312	Nivolumab **vs.** Chemotherapy	243 (tTMB and bTMB)	9.7 vs. 5.8	Similar	47 vs. 28	(33)
CheckMate 227	299	Nivolumab + Ipilimumab **vs.** Chemotherapy	10 (tTMB and bTMB)	7.2 vs. 5.5	NA	45.3 vs. 26.9	(29, 35)
Based on POPLAR	273	Atezolizumab **vs.** Docetaxel	16 (bTMB)	4.2 vs. 2.9	13.0 vs. 7.4	NA	(3, 50)
Based on OAK	797	Atezolizumab **vs.** Docetaxel	16 (bTMB)	NA	13.5 vs. 6.8	NA	(6, 50)
B-F1RST	119	Atezolizumab	16 (bTMB)	4.6 vs. 3.7	NR vs. 13.1	28.6 vs. 4.4	(51)
Based on CheckMate 012	75	Nivolumab + Ipilimumab	158	NR	NA	51 vs. 13	(25, 52)

NA, not available; NR, not reached.

2.2 TMB

Apart from PD-L1 expression, TMB stands as another extensively studied biological marker for predicting the efficacy of immunotherapy in NSCLC (10, 47). Somatic mutations can induce substantial modifications in protein sequences, resulting in the generation of abnormal proteins. These anomalous proteins can act as novel antigenic peptides, exhibiting a strong affinity for major histocompatibility complexes (MHC) I or MHC II. Thereafter, these neoepitopes are presented on the cell surface, where they are identified as non-self by the immune system, thereby instigating the activation of T lymphocytes that are specific to these neoantigens. Consequently, the immunogenicity of a tumor is intimately associated with the accumulation of somatic mutations within tumor cells (48). Elevated tumor mutational burden (referred to as TMB-H) leads to an augmented production and release of neoantigens, thereby enhancing the recognition and elimination of tumor cells by activated cytotoxic T cells after treatment with ICIs (48). Notably, NSCLC demonstrates a comparatively higher TMB-H than other solid tumor types (49). Consequently, the potential value of TMB as a biological marker for predicting the efficacy of immunotherapy has been extensively investigated in NSCLC patients (Table 2) (50–52).

During the phase III clinical trial also known as CheckMate-026, researchers conducted a retrospective assessment of the TMB in 312 patients diagnosed with NSCLC who received either Nivolumab or chemotherapy through whole-exome sequencing (33). Among the patients with high TMB (≥ 243 mut/Mb), Nivolumab exhibited a superior ORR of 47% in comparison to 28% in the chemotherapy group, along with a longer PFS of 9.7 vs. 5.8 months. *Gandara* et al. conducted a retrospective analysis of blood-based tumor mutational burden (bTMB) in patients participating in the OAK and POPLAR studies. They confirmed that a bTMB of ≥ 16 mut/Mb could serve as a predictive factor for OS and PFS in NSCLC patients treated with second-line Atezolizumab (3, 6, 50). Subsequently, a prospective study called B-F1RST categorized NSCLC patients receiving Atezolizumab into two groups based on their bTMB levels: a high bTMB group (bTMB-H) with ≥ 16 mut/Mb, and a low bTMB group (bTMB-L) with < 16 mut/Mb (51). The bTMB-H group exhibited a significantly higher ORR of 28.6% in comparison to 4.4% in the bTMB-L group ($P = 0.0002$). Additionally, patients in the bTMB-H group experienced a longer PFS of 4.6 months in comparison to 3.7 months in the bTMB-L group ($P = 0.12$). Similarly, a positive correlation was observed between bTMB-H and improved OS ($P = 0.48$), despite that the correlations between OS and PFS yielded little statistical significance. Furthermore, the MYSTIC study, a phase III clinical trial involving NSCLC patients, demonstrated that Durvalumab, when in comparison to chemotherapy, did not provide a substantial overall survival benefit in patients with high bTMB (23). Another trial, CheckMate-227, compared the effectiveness of Nivolumab plus Ipilimumab to that of dual-drug chemotherapy containing platinum in patients with TMB ≥ 10 mut/Mb (29). In the TMB-H group, patients treated with the combination of Ipilimumab and Nivolumab showed higher ORR (45.3% vs. 26.9%) and a lower hazard ratio for PFS (0.58, $P < 0.001$) in comparison to those treated with chemotherapy. Descriptive analyses of overall survival in the CheckMate-227 trial revealed an improvement in patients with high TMB and low TMB (< 10 mut/Mb) who were treated with Nivolumab plus Ipilimumab. A meta-analysis encompassing 14,395 NSCLC patients demonstrated that the combination of programmed cell death ligand 1 (PD-L1) expression levels and TMB served as a reliable biological marker for predicting response to immunotherapy. The area under the curve (AUC) for 1-year and 3-year PFS exceeded 0.8 (53). Notably, the findings from CheckMate-026 indicated a lack of significant

association between TMB and PD-L1 expression level (r = 0.059) (33).

However, it is important to note that TMB testing is a costly endeavor. At present, TMB determination primarily relies on two methods: tissue-based next-generation sequencing (FoundationOne) and whole exome sequencing (WES). WES necessitates samples with high DNA quality and a substantial tumor cell fraction, making high-quality samples a prerequisite for TMB testing. In the CheckMate-227 study, only 57.7% of the samples were available for TMB analysis, and a mere 10.3% of those patients tested positive for TMB (30, 35). Additionally, the variability in gene sequences and cutoff values employed by different studies to detect TMB using various panels contributes to inconsistencies in the results (54, 55). For instance, in the CheckMate-568 study, the ability of TMB = 10 mut/Mb to predict the effectiveness of Nivolumab plus Ipilimumab in NSCLC patients was ascertained via receiver operating characteristic (ROC) curve assessment (24). It is worth highlighting that the sample used for TMB analysis is obtained from a specific part of the tumor. Consequently, the molecular detection method based on biopsy is inevitably influenced by sampling deviation owing to intratumoral heterogeneity (56). In light of these factors, the combination of PD-L1 expression and TMB appears to hold more promise in clinical practice. Nonetheless, further prospective, randomized, controlled trials are warranted to ascertain the reliability of TMB as a biological marker for predicting the response to ICIs.

2.3 Hematological biological markers

2.3.1 $CD8^+$ T cells

The key to eliciting the host's immune response against malignant cells lies in the recognition of novel antigens by T cell receptors (TCR) (57). Consequently, biological markers founded on TCR may hold the potential to forecast the response to immunotherapy (Table 3). The sequencing of TCR lineages can be readily performed utilizing peripheral blood samples, thereby affording a non-intrusive approach for prognosticating the response to ICIs. *Han* and colleagues performed a sequencing analysis of PD-1^+CD8^+ TCRs in the peripheral blood of 25 patients diagnosed with NSCLC undergoing ICI treatment. The study revealed that patients exhibiting heightened diversity of PD-1^+CD8^+ TCRs before immunotherapy demonstrated superior treatment response and PFS in comparison to those with diminished TCR diversity (6.4 vs. 2.5 months, $P = 0.021$) (58). These findings were subsequently validated in a cohort comprising 15 patients. Importantly, the sensitivity and specificity of pre-immunotherapy PD-1^+CD8^+ TCR diversity in predicting PFS were determined to be 0.87 and 0.94, respectively. Patients with elevated clonality of PD-1^+CD8^+ TCRs following immunotherapy displayed prolonged PFS in contrast to those with diminished clonality (7.3 vs. 2.6 months, $P = 0.002$). Similarly, the proliferative response of peripheral blood PD-1^+CD8^+ T cells (quantified as the fold change in the percentage of Ki-67+ cells seven days post-treatment) proved to be a valuable surrogate biological marker for predicting the response to ICIs in NSCLC patients (59). Additionally, *Kamphorst et al.* ascertained that within the cohort of patients with advanced NSCLC, PD-1^+CD8^+ T cell responses were either delayed or absent in 70% of those experiencing disease progression, while 80% of the patients who positively responded to immunotherapy exhibited PD-1^+CD8^+ T cell responses within four weeks of treatment initiation (78). Given the paucity of clinical evidence, the amalgamation of TCR diversity and clonality in PD-1^+CD8^+ T cells derived from peripheral blood might serve as a non-invasive biological marker in conjunction with PD-L1 levels and TMB for predicting the response to immunotherapy and prognosticating outcomes in NSCLC patients.

2.3.2 Circulating tumor DNA

Circulating tumor DNA (ctDNA) is a potent prognostic biological marker due to its resemblance to DNA obtained from solid tumor biopsies, often referred to as a "liquid tissue biopsy" (79–81). Many studies have demonstrated that alterations in ctDNA levels during chemotherapy are correlated with treatment response across various tumor types, including NSCLC (Table 3) (60–62, 82–86). In a study encompassing a cohort of five patients afflicted with metastatic melanoma who underwent treatment with Ipilimumab, alterations in ctDNA levels during therapy exhibited concurrence with the outcomes derived from imaging-based evaluation of treatment response (86). Hence, modifications in ctDNA levels during immunotherapy hold the potential to serve as a biological marker for monitoring immunotherapy response and prognosticating patient outcomes. Moreover, there exists evidence supporting the utility of ctDNA levels as a biological marker in foretelling the response to immunotherapy among NSCLC patients. *Cabel et al.* executed a study involving 15 patients diagnosed with advanced cancer, ten of whom had NSCLC (60). Pre-treatment blood specimens were procured and subsequently, eight weeks following the initiation of immunotherapy, ctDNA levels were evaluated. The findings demonstrated a positive correlation between tumor regression 8 weeks post-treatment and a decline in ctDNA levels (r = 0.86, $P = 0.002$). Furthermore, ctDNA levels assessed eight weeks after treatment exhibited a significant association with both PFS ($P < 0.001$) and OS ($P = 0.004$). In another study involving 45 NSCLC patients who underwent Nivolumab immunotherapy, *Passiglia et al.* demonstrated that a 20% increase in ctDNA levels observed 6 weeks after treatment was indicative of inferior OS (median OS, 5.7 vs. 14.2 months, $P < 0.001$) and time to progression (TTP) (3.3 vs. 10.2 months, $P < 0.001$) (61). Subsequent investigations further validated the capacity of ctDNA level alterations in predicting response to immunotherapy, emphasizing that changes in ctDNA levels could predict response earlier than assessments based on imaging (24.5 vs. 72.5 days) (62). Nevertheless, it is noteworthy that the sample sizes of the aforementioned studies were relatively small, and there exists a lack of uniformity in the threshold for ctDNA change and the timing of evaluating molecular response across each study. Consequently, it is imperative to establish a standardized framework for monitoring dynamic changes in ctDNA. The potential to proactively modify patients' survival outcomes based on dynamic changes in ctDNA before observable imaging progression, as well as the prospect of employing liquid biopsy as a replacement for traditional imaging in the evaluation of early

10.3389/fimmu.2023.1249980

TABLE 3 Clinical outcomes of NSCLC patients treated with anti-PD-1/anti-PD-L1 agents according to hematological biological markers.

Characteristics	Patients (N)	Category	(m)PFS (months)	(m)OS (months)	Ref
PD-1^{+}CD8^{+} T cells	25	High **vs.** Low	6.4 vs. 2.5	NR vs. 6.9	(58)
	19	Increased **vs.** Decreased	7.3 vs. 2.6	NR vs. 7.5	
Ki-67$^{+}_{D7/D0}$	33	≥ 2.8 **vs.** < 2.8	6.0 vs. 1.4	13.8 vs. 2.0	(59)
	46	≥ 2.8 **vs.** < 2.8	10.9 vs. 2.1	NR vs. 7.0	
ctDNA	15	at w8 **vs.** persistently detectable	11 vs. 2	NA	(60)
ctDNA and NLR	45	increased >20% at w6 **vs.** decreased	NA	5.7 vs. 14.2	(61)
		increased >20% at w6 **vs.** decreased	NA	8.7 vs. 14.6	
		combined increased >20% of both ctDNA and NLR at w6 **vs.** others	NA	5.8 vs. 15.5	
ctDNA	28	Responders **vs.** non-responders A ctDNA response was associated with superior PFS and OS			(62)
ANC, ALC, AEC	134	Low **vs.** High Low ANC, high ALC, and high AEC were significantly and independently associated with better PFS and OS			(63)
ANC : ALC ratio, M:L ratio	157	Increased baseline **vs.** decreased	Increased baseline ANC : ALC ratio and M:L ratio before initiation of anti-PD1 antibodies were associated with poor PFS and OS		(64)
NLR PLR	187	Low levels (<5) **vs.** others	7.0 vs. 4.0	15.0 vs. 6.0	(65)
		levels below 200 **vs.** others	7.0 vs. 4.0	15.0 vs. 11.0	
NLR PLR SII	44	≤ 3.07 **vs.** > 3.07	6.7 vs. 3.9	19.8 vs. 8.9	(66)
		≤ 144 **vs.** > 144	28.5 vs. 10.5	6.9 vs. 3.9	
		≤ 603.5 **vs.** > 603.5	6.9 vs. 2.4	19.8 vs. 8.9	
NLR ALI	201	< 4 **vs.** ≥ 4	3.5 vs. 1.5	NA	(67)
		< 18 **vs.** ≥ 18	3.7 vs. 1.4	NA	
NLR	52	Higher **vs.** Lower Elevated pre-treatment NLR was associated with worse OS and response rates			(68)
NLR	175	< 5 **vs.** ≥ 5	2.8 vs. 1.9	8.4 vs. 5.5	(81)
NLR	52	< 5 **vs.** ≥ 5	3.3 vs. 1.7	NR vs. 4.2	(69)
NLR baseline NLR at w8 ANC at w8	88	≤ 4 **vs.** > 4 Baseline NLR ≤ 4 and lower NLR and ANC ≤ 4 **vs.** > 4 during treatment might correlate with disease Lower **vs.** Higher control and treatment response			(70)
NLR at w6	54	< 5 **vs.** ≥ 5	6.1 vs. 1.3	14.0 vs. 2.1	(71)
NLR PLR	119	≤ 5 **vs.** NLR > 5	18.82 vs. 6.86 (mean)	40.59 vs. 19.42 (mean)	(72)
		High **vs.** Low	11.01 vs. 15.96 (mean)	22.05 vs. 38.47 (mean)	
dNLR	466	≤ 3 **vs.** > 3 A dNLR greater than 3 was independently associated with OS			(73)
dNLR	63	≤ 3 **vs.** > 3 High dNLR was the independent statistically significant parameter associated with PFS and OS			(74)
CEA	189	≥13.8 **vs.** < 13.8 Higher CEA was associated with inferior PFS			(75)
CYFRA 21-1	50	≥2.2 **vs.** < 2.2	155 vs. 51.5 (days)	NA	(76)
CEA	84	≥5 **vs.** < 5	1.7 vs. 2.7	5.6 vs. 12.1	(77)
		Reduction≥20% after 4 cycles of nivolumab **vs.** others	7.1 vs. 1.9	15 vs. 9.9	
CYFRA 21-1		≥3.3 vs. < 3,3	NA	5.6 vs. 13.2	
		Reduction≥20% after 4 cycles of nivolumab **vs.** others	7.9 vs. 1.9	14.6 vs. 10	

Ki-67$^{+}_{D7/D0}$, Ki-67^{+} cells among PD-1^{+}CD8^{+} T cells 7days after the first dose; NLR, neutrophil-to-lymphocyte radio; ANC, absolute neutrophil count; ALC, absolute lymphocyte count; AEC, absolute eosinophil count; ANC : ALC radio, ANC to ALC radio; M:L radio, myeloid to lymphoid radio; SII = platelet count × neutrophil count/lymphocyte count; ALI, inflammation index (which was calculated as BMI×ALB/NLR); dNLR, derived neutrophils/(leukocytes minus neutrophils) ratio; CEA, carcinoembryonic antigen; W6, week 6; W8, week 8.

treatment response to immunotherapy, necessitate further deliberation.

2.3.3 Blood cell count

The changes of lymphocytes and neutrophils in peripheral blood can reflect the immune state of the body and can predict the curative effect to some certain extent. And tumor microenvironment with high neutrophils and low lymphocyte infiltration can promote blood tube formation, inhibit fine cell apoptosis, and promote tumor occurrence, resulting in poor prognosis. *Tanizaki et al.* substantiated that among individuals afflicted with locally advanced NSCLC subjected to Nivolumab treatment, PFS and OS experienced substantial elongation among those possessing elevated absolute neutrophil count and lymphocyte count before immunotherapy (63). Multiple investigations and meta-analyses have elucidated that a heightened neutrophil/lymphocyte ratio (NLR) correlates with an unfavorable prognosis in lung cancer patients (Table 3) (64–67, 87–89). Consequently, the association between NLR and immunotherapy response has been explored within the NSCLC patient cohort. In a study comprising 52 NSCLC patients, an elevated NLR exhibited an association with diminished OS ($P < 0.001$) and objective response rate ($P = 0.013$), albeit lacking correlation with PFS ($P = 0.114$). NLR demonstrated an AUC value of 0.738 for prognosticating the 10-month survival rate and 0.776 for predicting the efficacy of Nivolumab (66). Furthermore, the integration of NLR, among other variables, into a multivariate model substantially enhanced the prognostic capability of the model for predicting OS (68). *Bagley et al.* and *Fukui et al.* have corroborated the predictive worth of NLR in patients subjected to ICIs (69, 90). However, the optimal NLR threshold necessitates further establishment (70).

In addition to studies examining the potential utility of baseline NLR as a biological marker for immunotherapy response, various investigations have assessed the predictive and prognostic value of NLR during or post-treatment. *Suh et al.* made noteworthy observations regarding the median PFS and OS among patients with elevated NLR (≥ 5) six weeks after PD-1 blockade, demonstrating significantly shorter durations in comparison to patients with low NLR (median PFS: 1.3 vs. 6.1 months, $P < 0.001$; median OS: 2.1 vs. 14.0 months, $P < 0.001$) (71). Multivariate analysis confirmed that heightened NLR following treatment served as an independent prognostic indicator for OS ($P = 0.003$), indicating the potential of NLR six weeks after initiation of anti-PD-1 immunotherapy as a promising prognostic factor for patients with advanced NSCLC. Similarly, *Passiglia et al.* observed that a 20% or greater increase in NLR six weeks after Nivolumab treatment was associated with inferior OS (median OS: 8.7 vs. 14.6 months, $P = 0.035$) and TTP (5.2 vs. 10.3 months, $P = 0.039$) (61). The derived NLR (dNLR) may possess greater relevance than NLR, as it incorporates monocytes and other granulocyte subpopulations. Elevated dNLR has been linked to reduced survival in patients with multiple tumor types, including melanoma, pancreas, bladder, and renal cancer (72, 91–94). *Mezquita et al.* determined that a dNLR exceeding 3 represents the most suitable cutoff value for PFS and OS (73). Intriguingly, an inflammatory state (dNLR > 3) exhibited associations with shorter OS and durable clinical benefit among patients with advanced NSCLC receiving ICIs (95). Similarly, elevated dNLR (>3) demonstrated significant correlations with inferior PFS and OS (both $P < 0.05$) in patients with advanced NSCLC expressing at least 50% PD-L1 on tumor cells and treated with first-line Pembrolizumab (74). Although numerous studies have proposed the potential of peripheral blood cell count and its derivative indices as informative predictors of immunotherapy efficacy and prognosis, their clinical application remains limited due to considerations of peripheral blood cell count volatility and the absence of standardized research criteria.

2.3.4 Serum neoplasm biological markers

Serum neoplasm biological markers assume a pivotal function in monitoring the efficacy of interventions in individuals afflicted with NSCLC, specifically those undergoing chemotherapeutic or targeted interventions. Several frequently evaluated serum neoplasm biological markers encompass carcinoembryonic antigen (CEA), neuron-specific enolase (NSE), cytokeratin fragment 21-1 (Cyfra21-1), and carbohydrate antigen (CA19-9) (96, 97). Under the simplicity associated with acquiring serum samples, extensive scrutiny has been devoted to these markers as prognosticators of the response to immunotherapy (Table 3). In a multicenter investigation encompassing 189 subjects with advanced NSCLC subjected to Nivolumab as a second- or later-line treatment, *Kataoka et al.* uncovered an association linking pre-immunotherapy CEA concentrations to PFS; a crucial threshold of 13.8 ng/ml for CEA was established (75). The cohort surpassing 13.8 ng/ml of CEA exhibited a significantly abbreviated PFS ($P = 0.002$). Conversely, no such correlation manifested between Cyfra21-1 serum levels and the aforementioned outcome. In contrast, *Shirasu et al.* identified Cyfra21-1 as a prognostic indicator for individuals with lung adenocarcinoma undergoing Nivolumab (76). Discrepancies in the outcomes can be ascribed to the limited sample sizes and variations in subgroup categorizations based on pathological classifications. Intriguingly, an additional study demonstrated that a minimal 20% reduction in CEA and Cyfra21-1 concentrations after immunotherapy correlated with enhanced durable clinical rate (DCR; $P = 0.021$ for CEA; $P < 0.001$ for Cyfra21-1), PFS ($P = 0.028$ for CEA; $P < 0.001$ for Cyfra21-1), and OS ($P = 0.026$ for CEA; $P = 0.019$ for Cyfra21-1) (98). Moreover, *Lang et al.* substantiated that individuals experiencing diminished levels of serum neoplasm markers (CEA, Cyfra21-1, CA19-9, and NSE) after immunotherapy demonstrated significantly protracted PFS and OS (77).

2.4 Gene mutations

Multiple investigations have documented the correlation between the expression of programmed death-ligand 1 (PD-L1) and driver mutations in NSCLC; nevertheless, the findings exhibit contradictoriness (10, 99–102). The recent meta-analysis hath manifested a considerable level of heterogeneity amidst the

expression of PD-L1 and driver mutations (10, 103). In accordance with the NCCN guidelines, immunotherapy is recommended for patients with NSCLC who test negative for *EGFR* mutations and *ALK* rearrangements (3). Ergo, data about the clinical efficacy of immunotherapy in patients with NSCLC harboring driver mutations art constrained. Another meta-analysis hath disclosed that, in comparison to patients with *EGFR* mutations, those afflicted with *EGFR* wild-type NSCLC evince significantly protracted progression-free survival ($P < 0.00001$) and OS ($P < 0.05$) after immunotherapy with programmed cell death protein 1 (PD-1)/PD-L1 inhibitors (37). Through the employment of second-generation sequencing and exon sequencing methodologies, it hath also been ascertained that the median progression-free survival of patients with *EGFR* mutations is significantly briefer than that of patients sans *EGFR* mutations (51.0 versus 70.5 days, $P = 0.0037$) (104). *Cinausero et al.* hath assessed the impact of *KRAS* mutations on the effectiveness of anti-PD-1 immunotherapy (105). The neoplastic deoxyribonucleic acid (DNA) of 47 patients was sequenced, and 43% of these individuals did present with *KRAS* mutations. An observable disparity in the frequency of *KRAS* mutations hath been observed betwixt responders and non-responders. The PFS and OS of patients with *KRAS* mutations hath been superior to that of patients with wild-type *KRAS* ($P = 0.032$, 0.010 separately). Notwithstanding, a comprehensive retrospective study hath debunked any association between *KRAS* mutations and the effectiveness of immunotherapy in a cohort of 328 patients with advanced NSCLC (106).

The effectiveness of immunotherapy in NSCLC has been examined concerning *TP53* mutations. Non-synonymous *TP53* mutations were observed in 57% (41 out of 65) of NSCLC individuals. Following a median follow-up period of 15.2 mos, individuals with *TP53* mutations demonstrated a median OS of 18.1 months (95% CI, 6.6 – not reached), as opposed to 8.1 months for individuals with wild-type *TP53* (95% CI: 2.2 – 14.5; $P = 0.04$). Patients with *TP53* mutations also exhibited significantly longer median PFS (4.5 vs. 1.4 months, $P = 0.03$) and a higher ORR (51.2% vs. 20.7%; $P = 0.01$) in comparison to patients without *TP53* mutations. Multivariate analysis disclosed an independent correlation between *TP53* mutations and extended OS ($P = 0.009$) (107). Interestingly, *Shi et al.* have also found that patients with *TP53/KMT2C* co-mutation would get longer PFS and greater DCB ($P = 0.033$) when undergoing ICIs (108). A study involving 78 Chinese NSCLC individuals revealed that those with *FAT1* mutations exhibited higher rates of clinical benefit and objective response rates in comparison to individuals without *FAT1* mutations (71.4% vs. 22.7%, $P = 0.01$; 57.1% vs. 15.2%, $P = 0.02$) after undergoing ICIs. Furthermore, the loss of copy numbers in specific chromosome 3p fragments containing the tumor suppressor gene *TIGA9* and several chemokine receptor genes were strongly associated with unfavorable clinical outcomes (6-month survival rate: 0% vs. 31%; $P = 0.012$) (104). Elevated PD-L1 expression has been linked to deficiencies in DNA repair through homologous recombination (109). Consequently, a study explored the methylation status of the *Rad51B* promoter (*RAD51B*^{me}), a crucial mediator of homologous recombination, PD-L1 expression, and the effectiveness of immunotherapy. *RAD51B*^{me} levels were markedly higher in PD-L1-expressing individuals in comparison to PD-L1-negative individuals ($P < 0.05$). Furthermore, *RAD51B*^{me} levels were significantly associated with the response to ICIs, suggesting its potential as a predictive indicator for the efficacy of immunotherapy in NSCLC (110). Although ICIs have demonstrated efficacy in NSCLC, the benefits of ICIs for individuals with positive driver gene mutations remain inconclusive. Targeted therapy is expected to continue playing a role in the treatment of NSCLC individuals with positive driver gene mutations in the future.

3 Combined biological markers

3.1 Radiology and radiomics

Radiomics encompasses the systematic assessment of tumor phenotype through the utilization of radiological images and bioinformatics tools. Its primary objective is to construct clinical models that enable the evaluation of tumor heterogeneity and the microenvironment in a high-throughput manner. Notably, multiple investigations have provided evidence that the radiological attributes of the peritumoral region hold potential as indicators of survival outcomes in individuals afflicted with lung cancer (111–113).

Artificial intelligence (AI)-assisted enhanced computed tomography (CT) was employed for the analysis of 1055 primary and metastatic lesions derived from patients diagnosed with advanced melanoma and NSCLC who underwent anti-PD-1 therapy. The objective of this study was to ascertain non-invasive biomarkers that could predict the response to treatment (114). In the case of NSCLC, the field of imageology revealed a highly significant marker (the highest AUC value was 0.83, $P < 0.001$), and a similar trend was observed in melanoma lymph nodes (AUC value = 0.64; $P = 0.001$). The pooled analysis yielded a maximum AUC value of 0.76 ($P < 0.001$) for the prediction of immunotherapy response, and it also highlighted a 24% disparity in the 1-year survival rate ($P = 0.02$). These findings suggest that radiological characteristics observed in CT imaging have the potential to serve as non-invasive biomarkers for the prediction of immunotherapy response. In a separate investigation conducted by Khorrami et al., machine learning techniques were employed to examine alterations in radiation texture parameters obtained from internal and external CT scans of tumor lesions, both before and after 2-3 cycles of ICIs therapy (DelRADx) (115). The retrospective analysis encompassed 139 NSCLC patients recruited from two research centers, with a division into a discovery group (D1 = 50) and two independent verification cohorts (D2 = 62 and D3 = 27). Through the implementation of machine learning methodologies, texture parameters within and surrounding the tumor were extracted, facilitating the computation of relative differences between pre-ICIs and post-ICIs treatment conditions. DelRADx proved capable of predicting both ICI response and overall survival (OS) among NSCLC patients. The linear discriminant analysis (LDA) classifier achieved AUC values of 0.88 ± 0.08 (D1), 0.85 (D2), and 0.81 (D3), effectively discriminating responders from non-responders.

Moreover, the delta-radiomic risk score (DRS) demonstrated a significant correlation with OS (P = 0.0011; C-index = 0.72), thereby suggesting the potential utility of DelRADx as a tool for identifying NSCLC patients likely to exhibit a positive response to immunotherapy.

An analysis was undertaken encompassing 32 patients who had been diagnosed with NSCLC before undergoing treatment with Nivolumab. The utilization of 18F-FDG PET/CT scans facilitated this examination. The findings reveal a substantial disparity in the maximum standardized uptake value (SUVmax) between individuals who responded positively (N = 21) and those who did not (N = 11) (48.97 vs. 20.85, P = 0.002) (116). Furthermore, non-responders exhibited a tendency towards elevated tumor metabolic volume (MTVwb) and total lesion glycolysis (TLGwb) in comparison to responders. Likewise, a study involving one hundred and ninety-four patients with histologically confirmed stage IIIB-IV NSCLC investigated the potential of 18F-FDG PET/CT images acquired before treatment to identify a radiomics signature capable of predicting the response to immunotherapy (117). The resulting multiparametric radiomics signature (mpRS) demonstrated promising prognostic capabilities for durable clinical benefit (DCB), with respective AUC values of 0.86, 0.83, and 0.81 in the training, retrospective, and prospective test cohorts. Moreover, the nomogram models attained C-indexes of 0.74, 0.74, and 0.77 for prognosticating PFS, along with C-indexes of 0.83, 0.83, and 0.80 for predicting OS across the three cohorts. Furthermore, *Seban et al.* discovered through the analysis of FDG PET/CT that a total metabolic tumor volume (TMTV) surpassing 75 cm^3 was linked to diminished overall survival and the absence of DCB in patients with advanced NSCLC who received treatment with ICIs (95). The study also established a significant correlation between high TMTV and unfavorable PFS and OS (both $P < 0.05$) in patients with advanced NSCLC who underwent first-line Pembrolizumab treatment (74). These findings suggest the potential usefulness of 18F-FDG PET/CT imaging parameters as predictive indicators for the efficacy of immunotherapy in patients with NSCLC. However, the clinical implementation of these parameters has been impeded by the redundancy and lack of replicability of several image features (118). Several ongoing prospective studies (NCT03304639, NCT03387761, and NCT03237780) are presently assessing the value of radiology and radiomics in predicting the response to ICIs.

3.2 Prediction models

3.2.1 Metabolic score

A composite prognostic biological marker employing dNLR and TMTV exhibits promising prospects in the domain of NSCLC. The metabolic scoring system classifies patients into three distinct categories: favorable prognosis (TMTV ≤ 75 cm3, dNLR ≤ 3), intermediate prognosis (TMTV > 75 cm^3 or dNLR > 3), and unfavorable prognosis (TMTV > 75 cm^3 and dNLR > 3). In a retrospective analysis encompassing 109 patients with advanced NSCLC who underwent ICIs, the metabolic score showcased noteworthy variances in terms of median OS and median PFS across the aforementioned categories ($P < 0.001$) (92). The favorable prognosis group exhibited the lengthiest median OS of 35.0 months, followed by the intermediate prognosis group (12.5 months), and finally, the unfavorable prognosis group (2.4 months). Median PFS values were recorded as 9.8, 2.7, and 1.4 months, respectively ($P < 0.001$). Notably, the metabolic score exhibited a correlation with ICI response, particularly in terms of durable clinical (P = 0.003)

TABLE 4 Clinical outcomes of NSCLC patients received anti-PD-1/anti-PD-L1 agents according to different prediction models.

Model	Patients (n)	Groups	(median)PFS (month)	(median)OS (month)	Ref
LIPI	126 (Test)	Good **vs.** Intermediate **vs.** Poor	6 vs. 3 vs. 1	34 vs. 10 vs. 3	(73)
	305 (Validation)	Good **vs.** Intermediate **vs.** Poor	6.7 vs. 4.2 vs. 3.6	14.2 vs. 10.0 vs. 6.2	
	431 (Pool)	Good **vs.** Intermediate **vs.** Poor	6.3 vs. 3.7 vs. 2.0	16.5 vs. 10.0 vs. 4.8	
Metabolic Score	80	Good **vs.** Intermediate **vs.** Poor	9.8 vs. 2.7 vs. 1.4	35 vs. 12.5 vs. 2.4	(95)
Metabolic Score	63	Good **vs.** Intermediate **vs.** Poor	15.1 vs. 5.2 vs. 1.9	17.9 vs. 13.8 vs. 6.6	(74)
iSEND Model	159	Good **vs.** Intermediate **vs.** Poor	17.4 vs. 5.3 vs. 2.8	NR vs. 23.4 vs. 7.1	(119)
iSEND Model	439	Good **vs.** Intermediate **vs.** Poor	6.5 vs. 4.0 vs. 1.9	23 vs. 13.4 vs. 4.5	(120)
EPSILoN Score	154	Good **vs.** Moderate **vs.** Poor	10.2 vs. 4.9 vs. 1.7	NA	(121)
EPSILoN Score	193	Good **vs.** Intermediate **vs.** Poor	6.0 vs. 3.8 vs. 1.9	24.5 vs. 8.9 vs. 3.4	(122)
LIPI	216	Good **vs.** Intermediate **vs.** Poor	6.1 vs. 2.3 vs. 2.1	24.2 vs. 14.5 vs. 9.3	(123)
Dynamic LIPI	179	Good vs. Intermediate vs. poor	8.4 vs. 2.1 vs. 1.4	NA	
LIPI	153	Good **vs.** Intermediate **vs.** Poor	6.6 vs. 5.1 vs. 2.8	20.8 vs. 7.3 vs. 3.4	(124)
LIPI	1489	Good **vs.** Intermediate **vs.** Poor	4.2 vs. 2.7 vs. 1.4	18.4 vs. 11.3 vs. 4.5	(125)
LIPI	1368	Good **vs.** Intermediate **vs.** Poor	5.7 vs. 3.5 vs. 2.1	15.6 vs. 8.9 vs. 4.5	(126)

NA, not available; NR, not reached; iSEND Model, the NLR and Delta NLR model; EPSILoN Score, ECOG PS, smoking, liver metastasis, LDH, and NLR score; LIPI, lung immune prognostic index.

(Table 4). Within a multicenter study comprising 63 NSCLC patients possessing a PD-L1 tumor proportion score (TPS) ≥ 50, who were administered first-line Pembrolizumab and fluorodeoxyglucose positron emission tomography/computed tomography (FDG PET/CT), the favorable prognosis group exhibited a median OS of 17.9 months, in contrast to 13.8 and 6.6 months for the intermediate and unfavorable prognosis groups, respectively (74). Median PFS values were reported as 15.1, 5.2, and 1.9 months. The unfavorable prognosis group demonstrated associations with the DCR and ORR ($P < 0.05$). These findings lend support to the potential utilization of the metabolic score as a prognostic factor for NSCLC patients undergoing ICI treatment. Nonetheless, it is imperative to conduct prospective studies to validate the prognostic worthiness of this scoring system, given the retrospective nature of the existing evidence.

3.2.2 iSEND model

The NLR and Delta NLR (iSEND) model was initially introduced within the context of predicting the clinical efficacy of Nivolumab among patients diagnosed with NSCLC (119). An analysis conducted retrospectively on a cohort of 139 patients with locally advanced NSCLC, who had received second-line Nivolumab treatment, yielded correlations between sex, ECOG score, NLR, as well as pre-treatment and post-treatment changes in NLR, and PFS. The aforementioned variables were subsequently integrated into the iSEND model. By the iSEND model, patients were stratified into low-, medium-, and high-risk groups. The median follow-up period extended to 11.5 months. Within the low-risk group, the rates of 3, 6, 9, and 12-month PFS were observed at 78.4%, 63.7%, 55.3%, and 52.2%, respectively. Correspondingly, the medium-risk group experienced rates of 79.4%, 44.3%, 25.9%, and 19.2%, while the high-risk group exhibited rates of 65%, 25.9%, 22.8%, and 17.8%. As for the iSEND model's ability to predict 3, 6, 9, and 12-month PFS, the respective AUC values amounted to 0.718, 0.74, 0.746, and 0.774. Significantly, disease progression within the high-risk group at 12 ± 2 weeks exhibited a strong correlation ($P < 0.0001$). These findings convey that the iSEND model can serve as a valuable tool in forecasting the prognosis of locally advanced NSCLC patients post Nivolumab treatment. In a subsequent investigation featuring a median follow-up duration of 18.2 months, patients classified as low-risk demonstrated notably superior OS rates in comparison to those deemed high-risk ($P < 0.0001$) (120). Furthermore, the prognostic capability of the iSEND model was assessed relative to PD-L1 expression levels. The time-dependent mortality rates in the iSEND low-risk group (N = 119) and the PD-L1 TPS = 0% group (N = 47) were found to be 0.75 vs. 0.53 at 12 months ($P = 0.01$) and 0.85 vs. 0.46 at 18 months ($P = 0.03$), respectively. Nevertheless, no significant distinction was observed in terms of the prognostic value between the iSEND model and PD-L1 TPS ≥ 50%. As such, the iSEND model holds potential as a prognostic factor applicable to patients with locally advanced NSCLC following Nivolumab therapy (Table 4).

3.2.3 EPSILoN score

The EPSILoN scoring system, which encompasses the ECOG PS, smoking history, liver metastasis, lactate dehydrogenase (LDH), and NLR, has been proposed as a prognostic tool for predicting the response to immunotherapy in individuals diagnosed with NSCLC (Table 4). Within a cohort comprising 154 patients with locally advanced NSCLC, who were administered second-line or later-line anti-PD-1 therapy, the ECOG score, smoking history, liver metastasis, LDH, and NLR demonstrated significant associations with both PFS and OS. Consequently, these aforementioned factors were incorporated into the EPSILoN scoring system. The patients were subsequently stratified into categories denoting favorable, moderate, and unfavorable prognoses based on their EPSILoN scores. The resulting median PFS values for each category were observed to be 10.2, 4.9, and 1.7 months, respectively ($P < 0.001$) (121). During the validation study of the EPSILoN scoring system among patients with locally advanced NSCLC who underwent anti-PD-1 immunotherapy, participants were divided into high, moderate, and low-risk groups (122). The corresponding PFS durations were 6.0, 3.8, and 1.9 months, respectively ($P < 0.001$), while the OS values were 24.5, 8.9, and 3.4 months ($P < 0.001$). These results affirm the prognostic significance of the EPSILoN scoring system for individuals with NSCLC who are receiving ICIs.

3.2.4 LIPI score

The lung immune prognostic index (LIPI) has been postulated as a novel categorical hematological biological marker to select individuals diagnosed with NSCLC who are suitable candidates for PD-1/PD-L1 therapy. LIPI integrates the dNLR and LDH to categorize patients into three distinct prognostic subsets. These subsets are demarcated by the subsequent thresholds: dNLR ≤ 3 and LDH ≤ upper limit of normal (ULN) to identify the low-risk cohort, dNLR ≥ 3 or LDH ≥ ULN to classify the moderate-risk group, and dNLR ≥ 3 and LDH ≥ ULN to allocate patients to the high-risk category (Table 4) (123–126). The work carried out by *Mezquita et al.* entailed a seminal investigation that established a noteworthy association between LIPI and treatment outcomes in patients with advanced NSCLC undergoing ICIs, namely Nivolumab, Pembrolizumab, Atezolizumab, Durvalumab, or Durvalumab plus Ipilimumab (73). The study demonstrated that dNLR values exceeding 3 and LDH levels surpassing the ULN were independently linked to OS. The high-risk, intermediate-risk, and low-risk groups exhibited median OS durations of 3, 10, and 34 months, respectively ($P < 0.001$). Median PFS values were measured at 2.0, 3.7, and 6.3 mos ($P = 0.001$), respectively. Moreover, the disease control rate displayed a positive correlation with dNLR values surpassing 3 and LDH levels exceeding the ULN ($P = 0.004$). Nevertheless, the prognostic value of the LIPI score failed to attain statistical significance within the chemotherapy cohort. The investigators concluded that pretreatment LIPI, encompassing dNLR values greater than 3 and LDH levels surpassing the ULN, was indicative of unfavorable outcomes in patients receiving ICIs, thereby suggesting its

TABLE 5 Some advantages and disadvantages of single biological markers for predicting immunotherapy in NSCLC.

Characteristics	Advantages	Disadvantages
PD-L1 expression	● NCCN guidelines recommend testing, commonly use in clinic due to strong forecasting efficiency. ● The detection in convenient and moderate cost.	● Part of the tumor is difficult to reflect the whole. ● Easily to be affected by sampling time and location, and is not completely related to the curative effect of treatment.
TMB	● Commonly used in clinic and easy to detect. ● The performance of prediction is better.	● The amount of samples needed for detection is larger. ● Long testing period, high cost and lack of unified testing standards.
CD8+ T Cells	● It has a broad prospect and may become a method of tumor treatment.	● Fewer clinical applications and lack of large-scale clinical trials.
ctDNA	● The change is prior to the imaging change, which is helpful to judge the immune effect in advance. ● Sampling is simple.	● Not all NSCLC patients can be detected. ● The cost of testing is higher.
Blood cell count	● Can be used as a dynamic monitoring index due to the sampling is convenient and the testing cost is low.	● Easily disturbed by other factors such as inflammation of the body.
Gene mutation	● The detection is convenient and the cost is moderate.	● Lack of large clinical trials on the relationship between rare driving gene mutations and immune efficacy.

potential utility in identifying individuals unlikely to derive benefit from ICIs.

In a subsequent investigation conducted across multiple centers, the prognostic and predictive value of the LIPI score was examined among patients diagnosed with advanced NSCLC who were undergoing Nivolumab monotherapy (124). An insufficient LIPI score demonstrated a significant correlation with unfavorable OS according to both univariate analysis ($P < 0.0001$) and multivariate analysis ($P < 0.0001$). Although a noticeable association with diminished PFS was observed in the univariate analysis ($P = 0.03$), this correlation failed to reach statistical significance in the multivariate analysis ($P = 0.09$). Moreover, a low LIPI score displayed a statistically significant relationship with a reduced DCR based on both univariate analysis ($P = 0.001$) and multivariate analysis ($P = 0.005$). *Sorich et al.* conducted an extensive aggregated examination, assimilating data from the BIRCH, FIR, OAK, and POPLAR clinical trials, encompassing a total of 1489 patients who received Atezolizumab. The analysis unveiled a noteworthy correlation between the Lymphocyte Monocyte Ratio (LMR) score and the OS, PFS, and response rates, all possessing a level of significance below $P < 0.001$. Within the low-risk, intermediate-risk, and high-risk cohorts, the durations of median OS were found to be 18.4, 11.3, and 4.5 months, respectively (125). Importantly, the LMR score also exhibited correlations with survival ($P < 0.001$) and response rates ($P = 0.005$) in patients subjected to docetaxel treatment. In an additional pooled analysis comprising 11 clinical trials involving patients with metastatic NSCLC, a high LMR score displayed a favorable association with overall survival. Specifically, patients with a high LMR score demonstrated an estimated median survival of 15.6 months, whereas those with a low score had a median survival of 4.5 months ($P < 0.001$) (12). Analogous associations between elevated LMR scores and enhanced survival outcomes were observed among patients who underwent chemotherapy. In this context, patients with a high LMR score experienced a protracted period of survival in comparison to those with a low score, with an estimated median survival of 10.4 mos versus 5.3 mos ($P < 0.001$). Thus, the pretreatment LMR score exhibits promise as a valuable instrument for identifying patients who are likely to derive benefits from ICIs and chemotherapy.

4 Conclusion and future perspectives

The clinical application of PD-1/PD-L1 inhibitors in patients diagnosed with NSCLC has achieved unprecedented success in terms of enhancing long-term outcomes. However, the relatively low response rates, elevated treatment costs, and notable likelihood of immune-related adverse reactions necessitate an urgent quest for effective predictive and prognostic biological markers. At present, PD-L1 expression and TMB appear to hold the most promising potential as biological markers for predicting the response to immunotherapy. Nonetheless, these single biological markers require comprehensive exploration and optimization in various aspects due to certain limitations identified in specific cases (Table 5). Furthermore, emerging and promising biological markers encompass hematological biological markers, driver mutations, radiology, and radiomics. Going forward, it is imperative to standardize the diverse range of biological markers, leverage omics technologies to expedite the identification of robust biological markers, examine the feasibility of employing combination biological markers, and harness the capabilities of computer algorithms and AI technologies to establish innovative prognostic models. In the context of this review, it appears that prediction models incorporating multiple factors hold greater promise as tools for prognosticating the effectiveness of

immunotherapy in NSCLC. During clinical trials, stratified analyses can be conducted based on the factors included in these models to identify subgroups that are more likely to benefit from immunotherapy.

Author contributions

DH and CL conceived of the review and edited the manuscript. SL, HW, and HT analyzed the data and drafted the manuscript. ZX, and MW contributed to the data collection. All authors read and approved the final manuscript. All authors contributed to the article and approved the submitted version.

Funding

This work was supported by the Major Science and Technology Demonstration of Wuxi Science and Technology Bureau (No. WX18IVJN017), Top Medical Expert Team of 2021 Taihu Talent Plan Project, Medical Innovation Team of Wuxi (CXTD2021001).

Acknowledgments

The authors wish to thank editors as well as reviewers for reading the manuscript.

Conflict of interest

The authors declare that the research was conducted in the absence of any commercial or financial relationships that could be construed as a potential conflict of interest.

Publisher's note

All claims expressed in this article are solely those of the authors and do not necessarily represent those of their affiliated organizations, or those of the publisher, the editors and the reviewers. Any product that may be evaluated in this article, or claim that may be made by its manufacturer, is not guaranteed or endorsed by the publisher.

References

1. Siegel RL, Miller KD, Wagle NS, Jemal A. Cancer statistics, 2023. *CA Cancer J Clin* (2023) 73(1):17–48. doi: 10.3322/caac.21763

2. Xia C, Dong X, Li H, Cao M, Sun D, He S, et al. Cancer statistics in China and United States, 2022: profiles, trends, and determinants. *Chin Med J (Engl).* (2022) 135 (5):584–90. doi: 10.1097/CM9.0000000000002108

3. Fehrenbacher L, Spira A, Ballinger M, Kowanetz M, Vansteenkiste J, Mazieres J, et al. Atezolizumab versus docetaxel for patients with previously treated non-small-cell lung cancer (POPLAR): a multicentre, open-label, phase 2 randomised controlled trial. *Lancet* (2016) 387(10030):1837–46. doi: 10.1016/S0140-6736(16)00587-0

4. Herbst RS, Baas P, Kim DW, Felip E, Pérez-Gracia JL, Han JY, et al. Pembrolizumab versus docetaxel for previously treated, PD-L1-positive, advanced non-small-cell lung cancer (KEYNOTE-010): a randomised controlled trial. *Lancet* (2016) 387(10027):1540–50. doi: 10.1016/S0140-6736(15)01281-7

5. Brahmer J, Reckamp KL, Baas P, Crinò L, Eberhardt WE, Poddubskaya E, et al. Nivolumab versus docetaxel in advanced squamous-cell non-small-cell lung cancer. *N Engl J Med* (2015) 373(2):123–35. doi: 10.1056/NEJMoa1504627

6. Rittmeyer A, Barlesi F, Waterkamp D, Park K, Ciardiello F, von Pawel J, et al. Atezolizumab versus docetaxel in patients with previously treated non-small-cell lung cancer (OAK): a phase 3, open-label, multicentre randomised controlled trial. *Lancet* (2017) 389(10066):255–65. doi: 10.1016/S0140-6736(16)32517-X

7. Garon EB, Hellmann MD, Rizvi NA, Carcereny E, Leighl NB, Ahn MJ, et al. Five-year overall survival for patients with advanced non–small-cell lung cancer treated with pembrolizumab: results from the phase I KEYNOTE-001 study. *J Clin Oncol* (2019) 37:2518–27. doi: 10.1200/JCO.19.00934

8. Brahmer JR, Govindan R, Anders RA, Antonia SJ, Sagorsky S, Davies MJ, et al. The society for immunotherapy of cancer consensus statement on immunotherapy for the treatment of non-small cell lung cancer (NSCLC). *J Immunother. Cancer* (2018) 6:75. doi: 10.1186/s40425-018-0382-2

9. Hamid O, Robert C, Daud A, Hodi FS, Hwu WJ, Kefford R, et al. Five-year survival outcomes for patients with advanced melanoma treated with pembrolizumab in KEYNOTE-001. *Ann Oncol* (2019) 30:582–8. doi: 10.1093/annonc/mdz011

10. Tumeh PC, Harview CL, Yearley JH, Shintaku IP, Taylor EJ, Robert L, et al. PD-1 blockade induces responses by inhibiting adaptive immune resistance. *Nature* (2014) 515(7528):568–71. doi: 10.1038/nature13954

11. Hanahan D, Weinberg RA. Hallmarks of cancer: the next generation. *Cell* (2011) 144(5):646–74. doi: 10.1016/j.cell.2011.02.013

12. Petrelli F, Maltese M, Tomasello G, Conti B, Borgonovo K, Cabiddu M, et al. Clinical and molecular predictors of PD-L1 expression in non-small-cell lung cancer: systematic review and meta-analysis. *Clin Lung Cancer.* (2018) 19(4):315–22. doi: 10.1016/j.cllc.2018.02.006

13. Syn NL, Teng MWL, Mok TSK, Soo RA. *De-novo* and acquired resistance to immune checkpoint targeting. *Lancet Oncol* (2017) 18(12):e731–41. doi: 10.1016/S1470-2045(17)30607-1

14. Shi Y. Regulatory mechanisms of PD-L1 expression in cancer cells. *Cancer Immunol Immunother.* (2018) 67(10):1481–9. doi: 10.1007/s00262-018-2226-9

15. Mazieres J, Rittmeyer A, Gadgeel S, Hida T, Gandara DR, Cortinovis DL, et al. Atezolizumab versus docetaxel in pretreated patients with NSCLC: final results from the randomized phase 2 POPLAR and phase 3 OAK clinical trials. *J Thorac Oncol* (2021) 16(1):140–50. doi: 10.1016/j.jtho.2020.09.022

16. Herbst RS, Baas P, Perez-gracia JL, Felip E, Kim DW, Han J, et al. Use of archival versus newly collected tumor samples for assessing PD-L1 expression and overall survival: an updated analysis of KEYNOTE-010 trial. *Ann Oncol* (2019) 30(2):281–9. doi: 10.1093/annonc/mdy545

17. Horn L, Spigel DR, Vokes EE, Holgado E, Ready N, Steins M, et al. Nivolumab versus docetaxel in previously treated patients with advanced non-small-cell lung cancer: two-year outcomes from two randomized, open-label, phase III trials (CheckMate 017 and CheckMate 057). *J Clin Oncol* (2017) 35(35):3924–33. doi: 10.1200/JCO.2017.74.3062

18. Borghaei H, Paz-Ares L, Horn L, Spigel DR, Steins M, Ready NE, et al. Nivolumab versus docetaxel in advanced nonsquamous non-small-cell lung cancer. *N Engl J Med* (2015) 373(17):1627–39. doi: 10.1056/NEJMoa1507643

19. Wu YL, Lu S, Cheng Y, Zhou C, Wang J, Mok T, et al. Nivolumab versus docetaxel in a predominantly Chinese patient population with previously treated advanced NSCLC: CheckMate 078 randomized phase III clinical trial. *J Thorac Oncol* (2019) 14(5):867–75. doi: 10.1016/j.jtho.2019.01.006

20. Mok TSK, Wu YL, Kudaba I, Kowalski DM, Cho BC, Turna HZ, et al. Pembrolizumab versus chemotherapy for previously untreated, PD-L1-expressing, locally advanced or metastatic non-small-cell lung cancer (KEYNOTE-042): a randomised, open-label, controlled, phase 3 trial. *Lancet* (2019) 393(10183):1819–30. doi: 10.1016/S0140-6736(18)32409-7

21. Reck M, Rodriguez-Abreu D, Robinson AG, Hui R, Csőszi T, Fülöp A, et al. Pembrolizumab versus chemotherapy for PD-L1-positive non–small-cell lung cancer. *N Engl J Med* (2016) 375(19):1823–33. doi: 10.1056/NEJMoa1606774

22. Nosaki K, Saka H, Hosomi Y, Baas P, de Castro G Jr, Reck M, et al. Safety and efficacy of pembrolizumab monotherapy in elderly patients with PD-L1–positive advanced non–small-cell lung cancer: pooled analysis from the KEYNOTE-010, KEYNOTE-024, and KEYNOTE-042 studies. *Lung Cancer.* (2019) 135:188–95. doi: 10.1016/j.lungcan.2019.07.004

23. Peters S, Cho BC, Reinmuth N, Lee KH, Luft A, Ahn Mj , et al. Tumor mutational burden (TMB) as a biomarker of survival in metastatic non-small cell lung cancer (mNSCLC): Blood and tissue TMB analysis from MYSTIC, a Phase III study of first-line durvalumab ± tremelimumab vs chemotherapy. *Cancer Res* (2019). doi: 10.1158/1538-7445.AM2019-CT074

24. Ready N, Hellmann MD, Awad MM, Otterson GA, Gutierrez M, Gainor JF, et al. First-line nivolumab plus ipilimumab in advanced non-small-cell lung cancer (CheckMate 568): outcomes by programmed death ligand 1 and tumor mutational burden as biomarkers. *J Clin Oncol* (2019) 37(12):992–1000. doi: 10.1200/JCO.18.01042

25. Hellmann MD, Rizvi NA, Goldman JW, Gettinger SN, Borghaei H, Brahmer JR, et al. Nivolumab plus ipilimumab as first-line treatment for advanced non-small-cell lung cancer (CheckMate 012): results of an open-label, phase 1, multicohort study. *Lancet Oncol* (2017) 18(1):31–41. doi: 10.1016/S1470-2045(16)30624-6

26. Sezer A, Kilickap S, Gümüs M, Bondarenko I, Ozguroglu M, Gogishvili M, et al. EMPOWER-Lung 1: Phase III first-line (1L) cemiplimab monotherapy vs platinum-doublet chemotherapy (chemo) in advanced non-small cell lung cancer (NSCLC) with programmed cell death-ligand 1 (PD-L1) ≥50%. *Ann Oncol* (2020). doi: 10.1016/j.annonc.2020.10.372

27. Spigel D, Marinis FD, Giaccone G, Reinmuth N, Vergnenegre A, Barrios CH, et al. IMpower110: Interim overall survival (OS) analysis of a phase III study of atezolizumab (atezo) vs platinum-based chemotherapy (chemo) as first-line (1L) treatment (tx) in PD-L1–selected NSCLC. *Ann Oncol* (2019). doi: 10.1093/annonc/mdz394

28. Zhou CC, Chen GY, Huang YC, Zhou J, Lin L, Feng J, et al. Camrelizumab plus carboplatin and pemetrexed versus chemotherapy alone in chemotherapy-naive patients with advanced non-squamous non-small-cell lung cancer (CameL): a randomised, open-label, multicentre, phase 3 trial. *Lancet Respir Med* (2020) 9 (3):305–14. doi: 10.1016/S2213-2600(20)30365-9

29. Brahmer JR, Lee JS, Ciuleanu TE, Bernabe Caro R, Nishio M, Urban L, et al. Five-year survival outcomes with nivolumab plus ipilimumab versus chemotherapy as first-line treatment for metastatic non-small-cell lung cancer in CheckMate 227. *J Clin Oncol* (2023) 41(6):1200–12. doi: 10.1200/JCO.22.01503.

30. Reck M, Ciuleanu TE, Lee JS, Schenker M, Audigier-Valette C, Zurawski , et al. First-line nivolumab plus ipilimumab vs chemotherapy in advanced non-small cell lung cancer with tumor PD-L1 ≥ 1%: patient-reported outcomes from CheckMate 227 part 1. *J Thorac Oncol* (2021) 16(4):665–76. doi: 10.1016/j.jtho.2020.12.019

31. Paz-Ares L, Luft A, Vicente D, Tafreshi A, Gümüş M, Mazières J, et al. Pembrolizumab plus chemotherapy for squamous non–small-cell lung cancer. *N Engl J Med* (2018) 379(21):2040–51. doi: 10.1056/NEJMoa1810865

32. Zinner RG, Obasaju CK, Spigel DR, Giaccone G, Heist RS, Hodi FS, et al. Long-term survival follow-up of atezolizumab in combination with platinum-based doublet chemotherapy in patients with advanced non-small-cell lung cancer. *Eur J Cancer*. (2018) 101:114–22. doi:10.1016/j.ejca.2018.06.033

33. Carbone DP, Reck M, Paz-Ares L, Creelan B, Horn L, Steins M, et al. First-line Nivolumab in stage IV or recurrent non-small-cell lung cancer. *N Engl J Med* (2017) 376(25):2415–26. doi: 10.1056/NEJMoa1613493

34. Gray JE, Villegas A, Daniel D, Vicente D, Murakami S, Hui R, et al. Three-year overall survival with durvalumab after chemoradiotherapy in stage III NSCLC-update from PACIFIC. *J Thorac Oncol* (2020) 15(2):288–93. doi: 10.1016/j.jtho.2019.10.002

35. Hellmann MD, Ciuleanu TE, Pluzanski A, Lee JS, Otterson GA, Audigier-Valette C, et al. Nivolumab plus ipilimumab in lung cancer with a high tumor mutational burden. *N Engl J Med* (2018) 378(22):2093–104. doi: 10.1056/NEJMoa1801946

36. Antonia SJ, Villegas A, Daniel D, Murakami S, Hui R, Kurata T, et al. Overall survival with durvalumab after chemoradiotherapy in stage III NSCLC. *N Engl J Med* (2018) 379(24):2342–50. doi: 10.1056/NEJMoa1809697

37. Li J, Gu J. PD-L1 expression and EGFR status in advanced non-small-cell lung cancer patients receiving PD-1/PD-L1 inhibitors: a meta-analysis. *Future Oncol* (2019) 15(14):1667–78. doi: 10.2217/fon-2018-0639

38. US Food and Drug Administration. *List of cleared or approved companion diagnostic devices (in vitro and imaging tools)*. FDA (2020). Available at: https://www.fda.gov/medical-devices/vitro-diagnostics/list-cleared-or-approved-companion-diagnostic-devices-vitro-and-imaging-tools.

39. Fusi A, Festino L, Botti G, Masucci G, Melero I, Lorigan P, et al. PD-L1 expression as a potential predictive biomarker. *Lancet Oncol* (2015) 16(13):1285–7. doi: 10.1016/S1470-2045(15)00307-1

40. Meng X, Huang Z, Teng F, Xing L, Yu J. Predictive biomarkers in PD-1/PD-L1 checkpoint blockade immunotherapy. *Cancer Treat Rev* (2015) 41(10):868–76. doi: 10.1016/j.ctrv.2015.11.001

41. Ott PA, Bang YJ, Berton-Rigaud D, Elez E, Pishvaian MJ, Rugo HS, et al. Safety and antitumor activity of pembrolizumab in advanced programmed death ligand 1-positive endometrial cancer: results from the KEYNOTE-028 study. *J Clin Oncol* (2017) 35(22):2535–41. doi: 10.1200/JCO.2017.72.5952

42. Mclaughlin J, Han G, Schalper KA, Carvajal-Hausdorf D, Pelekanou V, Rehman J, et al. Quantitative assessment of the heterogeneity of PD-L1 expression in non-small-cell lung cancer. *JAMA Oncol* (2016) 2(1):46–54. doi: 10.1001/jamaoncol.2015.3638

43. Herbst RS, Soria JC, Kowanetz M, Fine GD, Hamid O, Gordon MS, et al. Predictive correlates of response to the anti-PD-L1 antibody MPDL3280A in cancer patients. *Nature* (2014) 515(7528):563–7. doi: 10.1038/nature14011

44. Formenti SC, Demaria S. Combining radiotherapy and cancer immunotherapy: a paradigm shift. *J Natl Cancer Inst* (2013) 105(4):256–65. doi: 10.1093/jnci/djs629

45. Ramakrishnan R, AsSudani D, Nagaraj S, Hunter T, Cho HI, Antonia S, et al. Chemotherapy enhances tumor cell susceptibility to CTL-mediated killing during cancer immunotherapy in mice. *J Clin Invest.* (2010) 120(4):1111–24. doi: 10.1172/JCI40269

46. Twymansaint VC, Rech AJ, Maity A, Rengan R, Pauken KE, Stelekati E, et al. Radiation and dual checkpoint blockade activate non-redundant immune mechanisms in cancer. *Nature* (2015) 520(7547):373–7. doi: 10.1038/nature14292

47. Rizvi NA, Hellmann MD, Snyder A, Kvistborg P, Makarov V, Havel JJ, et al. Cancer immunology. Mutational landscape determines sensitivity to PD-1 blockade in non-small cell lung cancer. *Science* (2015) 348:124–8. doi: 10.1126/science.aaa1348

48. Schumacher TN, Schreiber RD. Neoantigens in cancer immunotherapy. *Science* (2015) 348(6230):69–74. doi: 10.1126/science.aaa4971

49. Alexandrov LB, Nik-Zainal S, Wedge DC, Aparicio SA, Behjati S, Biankin AV, et al. Signatures of mutational processes in human cancer. *Nature* (2013) 500 (7463):415–21. doi: 10.1038/nature12477

50. Gandara DR, Paul SM, Kowanetz M, Schleifman E, Zou W, Li Y, et al. Blood-based tumor mutational burden as a predictor of clinical benefit in non-small-cell lung cancer patients treated with atezolizumab. *Nat Med* (2018) 24(9):1441–8. doi: 10.1038/s41591-018-0134-3

51. Kim ES, Velcheti V, Mekhail T, et al. LBA55: Primary efficacy results from B-FIRST, a prospective phase II trial evaluating blood-based tumour mutational burden (bTMB) as a predictive biomarker for atezolizumab (atezo) in 1L non-small cell lung cancer (NSCLC). *Annal Oncol* (2018). doi: 10.1093/annonc/mdy424.067

52. Hellmann MD, Nathanson T, Rizvi H, Creelan BC, Sanchez-Vega F, Ahuja A, et al. Genomic features of response to combination immunotherapy in patients with advanced non-small-cell lung cancer. *Cancer Cell* (2018) 33(5):843–52.e4. doi: 10.1016/j.ccell.2018.03.018

53. Yu Y, Zeng D, Ou Q, Liu S, Li A, Chen Y, et al. Association of survival and immune-related biomarkers with immunotherapy in patients with non-small cell lung cancer: A meta-analysis and individual patient-level analysis. *JAMA Netw Open* (2019) 2(7):e196879. doi: 10.1001/jamanetworkopen.2019.6879

54. Camidge DR, Doebele RC, Kerr KM. Comparing and contrasting predictive biomarkers for immunotherapy and targeted therapy of NSCLC. *Nat Rev Clin Oncol* (2019) 16(6):341–55. doi: 10.1038/s41571-019-0173-9

55. Costantini A, Kamga PT, Dumenil C, Chinet T, Emile JF, Leprieur EG. Plasma biomarkers and immune checkpoint inhibitors in non-small cell lung cancer: new tools for better patient selection? *Cancers (Basel)* (2019) 11(9):1269. doi: 10.3390/cancers11091269

56. Ilie M, Long-Mira E, Bence C, Butori C, Lassalle S, Bouhlel L, et al. Comparative study of the PD-L1 status between surgically resected specimens and matched biopsies of NSCLC patients reveal major discordances: a potential issue for anti-PD-L1 therapeutic strategies. *Ann Oncol* (2016) 27(1):147–53. doi: 10.1093/annonc/mdv489

57. Riaz N, Havel JJ, Makarov V, Desrichard A, Urba WJ, Sims JS, et al. Tumor and microenvironment evolution during immunotherapy with nivolumab. *Cell* (2017) 171 (4):934–49.e16. doi: 10.1016/j.cell.2017.09.028

58. Han J, Duan J, Bai H, Wang Y, Wan R, Wang X, et al. TCR repertoire diversity of peripheral PD-1+CD8+ T cells predicts clinical outcomes after immunotherapy in patients with non-small cell lung cancer. *Cancer Immunol Res* (2020) 8(1):146–54. doi: 10.1158/2326-6066.CIR-19-0398

59. Kim KH, Cho J, Ku BM, Koh J, Sun JM, Lee SH, et al. The first-week proliferative response of peripheral blood PD-1 + CD8 + T cells predicts the response to anti-PD-1 therapy in solid tumors. *Clin Cancer Res* (2019) 25(7):2144–54. doi: 10.1158/1078-0432.CCR-18-1449

60. Cabel L, Riva F, Servois V, Livartowski A, Daniel C, Rampanou A, et al. Circulating tumor DNA changes for early monitoring of anti-PD1 immunotherapy: a proof-of-concept study. *Ann Oncol* (2017) 28(8):1996–2001. doi: 10.1093/annonc/mdx212

61. Passiglia F, Galvano A, Castiglia M, Incorvaia L, Calò V, Listì A, et al. Monitoring blood biomarkers to predict nivolumab effectiveness in NSCLC patients. *Ther Adv Med Oncol* (2019) 11:1758835919839928. doi: 10.1177/1758835919839928

62. Goldberg SB, Narayan A, Kole AJ, Decker RH, Teysir J, Carriero NJ, et al. Early assessment of lung cancer immunotherapy response via circulating tumor DNA. *Clin Cancer Res* (2018) 24(8):1872–80. doi: 10.1158/1078-0432.CCR-17-1341

63. Tanizaki J, Haratani K, Hayashi H, Chiba Y, Nakamura Y, Yonesaka K, et al. Peripheral blood biomarkers associated with clinical outcome in non-small cell lung cancer patients treated with nivolumab. *J Thorac Oncol* (2018) 13(1):97–105. doi: 10.1016/j.jtho.2017.10.030

64. Soyano AE, Dholaria B, Marin-Acevedo JA, Diehl N, Hodge D, Luo Y, et al. Peripheral blood biomarkers correlate with outcomes in advanced non-small cell lung Cancer patients treated with anti-PD-1 antibodies. *J Immunother Cancer.* (2018) 6 (1):129. doi: 10.1186/s40425-018-0447-2

65. Diem S, Schmid S, Krapf M, Migliorino MR, Aprile G, Mansueto G, et al. Neutrophil-to-lymphocyte ratio (NLR), platelet-to-lymphocyte ratio (PLR), and outcomes with nivolumab in pretreated non-small cell lung cancer (NSCLC): A large retrospective multicenter study. *Adv Ther* (2020) 37(3):1145–55. doi: 10.1007/s12325-020-01229-w

66. Liu J, Li S, Zhang S, Liu Y, Ma L, Zhu J, et al. Systemic immune-inflammation index, neutrophil-to-lymphocyte ratio, platelet-to-lymphocyte ratio can predict clinical outcomes in patients with metastatic non-small-cell lung cancer treated with nivolumab. *J Clin Lab Anal* (2019) 33(8):e22964. doi: 10.1002/jcla.22964

67. Bagley SJ, Kotharis S, Aggarwal C, Tamiya A, Tanaka A, Okamoto N, et al. Pretreatment advanced lung cancer inflammation index (ALI) for predicting early

progression in nivolumab-treated patients with advanced non-small cell lung cancer. *Cancer Med* (2018) 7(1):13–20. doi: 10.1002/cam4.1234

68. Diem S, Schmid S, Krapf M, Flatz L, Born D, Jochum W, et al. Neutrophil- to-Lymphocyte Ratio (NLR) and Platelet-to- Lymphocyte ratio (PLR) as prognostic markers in patients with non-small cell lung cancer (NSCLC) treated with nivolumab. *Lung Cancer.* (2017) 111:176–81. doi: 10.1016/j.lungcan.2017.07.024

69. Fukui T, Okuma Y, Nakahara Y, Otani S, Igawa S, Katagiri M, et al. Activity of nivolumab and utility of neutrophil-to-lymphocyte ratio as a predictive biomarker for advanced non-small-cell lung cancer: a prospective observational study. *Clin Lung Cancer.* (2019) 20(3):208–14. doi: 10.1016/j.cllc.2018.04.021

70. Zer A, Sung MR, Walia P, Khoja L, Maganti M, Labbe C, et al. Correlation of Neutrophil to lymphocyte ratio and absolute neutrophil count with outcomes with PD-1 axis inhibitors in patients with advanced non-small- cell lung cancer. *Clin Lung Cancer.* (2018) 19(5):426–34. doi: 10.1016/j.cllc.2018.04.008

71. Suh KJ, Kim SH, Kim YJ, Kim M, Keam B, Kim TM, et al. Post-treatment neutrophil-to-lymphocyte ratio at week 6 is prognostic in patients with advanced non-small cell lung cancers treated with anti-PD-1 antibody. *Cancer Immunol Immunother.* (2018) 67(3):459–70. doi: 10.1007/s00262-017-2092-x

72. Petrova MP, Eneva MI, Arabadjiev JI, Conev NV, Dimitrova EG, Koynov KD, et al. Neutrophil to lymphocyte ratio as a potential predictive marker for treatment with pembrolizumab as a second line treatment in patients with non-small cell lung cancer. *Biosci Trends.* (2020) 14(1):48–55. doi: 10.5582/bst.2019.01279

73. Mezquita L, Auclin E, Ferrara R, Charrier M, Remon J, Planchard D, et al. Association of the lung immune prognostic index with immune checkpoint inhibitor outcomes in patients with advanced non-small cell lung cancer. *JAMA Oncol* (2018) 4 (3):351–7. doi: 10.1001/jamaoncol.2017.4771

74. Seban RD, Assié JB, Giroux-Leprieur E, Massiani MA, Soussan M, Bonardel G, et al. Association of the metabolic score using baseline FDG-PET/CT and dNLR with immunotherapy outcomes in advanced NSCLC patients treated with first-line pembrolizumab. *Cancers (Basel).* (2020) 12(8):2234. doi: 10.3390/cancers12082234

75. Kataoka Y, HIrano K, Narabayashi T, Hara S, Fujimoto D, Tanaka T, et al. Carcinoembryonic antigen as a predictive biomarker of response to nivolumab in non-small cell lung cancer. *Anticancer Res* (2018) 38(1):559–63. doi: 10.21873/anticanres.12259

76. Shirasu H, Ono A, Omae K, Nakashima K, Omori S, Wakuda K, et al. CYFRA 21-1 predicts the efficacy of nivolumab in patients with advanced lung adenocarcinoma. *Tumour Biol* (2018) 40(2):1010428318760420. doi: 10.1177/1010428318760420

77. Lang D, Horner A, Brehm E, Akbari K, Hergan B, Langer K, et al. Early serum tumor marker dynamics predict progression-free and overall survival in single PD-1/PD-L1 inhibitor treated advanced NSCLC - A retrospective cohort study. *Lung Cancer.* (2019) 134:59–65. doi: 10.1016/j.lungcan.2019.05.033

78. Kamphorst AO, Pillai RN, Yang S, Nasti TH, Akondy RS, Wieland A, et al. Proliferation of PD-1+ CD8 T cells in peripheral blood after PD-1-targeted therapy in lung cancer patients. *Proc Natl Acad Sci USA* (2017) 114(19):4993–8. doi: 10.1073/pnas.1705327114

79. Bidard F-C, Weigelt B, Reis-Filho JS. Going with the flow: from circulating tumor cells to DNA. *Sci Transl Med* (2013). doi: 10.1126/scitranslmed.3006305

80. Diaz LA, Bardelli A. Liquid biopsies: genotyping circulating tumor DNA. *J Clin Oncol* (2014) 32(6):579–86. doi: 10.1200/JCO.2012.45.2011

81. Alix-Panabières C, Pantel K. Clinical applications of circulating tumor cells and circulating tumor DNA as liquid biopsy. *Cancer Discovery* (2016) 6(5):479–91. doi: 10.1158/2159-8290.CD-15-1483

82. Diehl F, Schmidt K, Choti MA, Romans K, Goodman S, Li M, et al. Circulating mutant DNA to assess tumor dynamics. *Nat Med* (2008) 14(9):985–90. doi: 10.1038/nm.1789

83. Siravegna G, Mussolin B, Buscarino M, Corti G, Cassingena A, Crisafulli G, et al (2015). Clonal evolution and resistance to EGFR blockade in the blood of colorectal cancer patients. *Nat Med* 21(7):795–801. doi: 10.1038/nm.3870

84. Riva F, Bidard F-C, Houy A, Saliou A, Madic J, Rampanou A, et al. Patient-specific circulating tumor DNA detection during neoadjuvant chemotherapy in triple-negative breast cancer. *Clin Chem* (2017) 63(3):691–9. doi: 10.1373/clinchem.2016.262337

85. Olsson E, Winter C, George A, Chen Y, Howlin J, Tang MH, et al. Serial monitoring of circulating tumor DNA in patients with primary breast cancer for detection of occult metastatic disease. *EMBO Mol Med* (2015) 7(8):1034–47. doi: 10.15252/emmm.201404913

86. Lipson EJ, Velculescu VE, Pritchard TS, Sausen M, Pardoll DM, Topalian SL, et al. Circulating tumor DNA analysis as a real-time method for monitoring tumor burden in melanoma patients undergoing treatment with immune checkpoint blockade. *J Immunother Cancer.* (2014) 2(1):42. doi: 10.1186/s40425-014-0042-0

87. Mei Z, Shi L, Wang B, Yang J, Xiao Z, Du P, et al. Prognostic role of pretreatment blood neutrophil-to-lymphocyte ratio in advanced cancer survivors: a systematic review and meta-analysis of 66 cohort studies. *Cancer Treat Rev* (2017) 58:1–13. doi: 10.1016/j.ctrv.2017.05.005

88. Yu Y, Qian L, Cui J. Value of neutrophil- to-lymphocyte ratio for predicting lung cancer prognosis: a meta-analysis of 7219 patients. *Mol Clin Oncol* (2017) 7(3):498–506. doi: 10.3892/mco.2017.1342

89. Derman BA, Macklis JN, Azeem MS, Sayidine S, Basu S, Batus M, et al. Relationships between longitudinal neutrophil to lymphocyte ratios, body weight changes, and overall survival in patients with non-small cell lung cancer. *BMC Cancer.* (2017) 17(1):141. doi: 10.1186/s12885-017-3122-y

90. Bagley SJ, Kothari S, Aggarwal C, Bauml JM, Alley EW, Evans TL, et al. Pretreatment neutrophil-to-lymphocyte ratio as a marker of outcomes in nivolumab-treated patients with advanced non-small-cell lung cancer. *Lung Cancer.* (2017) 106:1–7. doi: 10.1016/j.lungcan.2017.01.013

91. Ferrucci PF, Ascierto PA, Pigozzo J, Del Vecchio M, Maio M, Antonini Cappellini GC, et al. Baseline neutrophils and derived neutrophil-to-lymphocyte ratio: prognostic relevance in metastatic melanoma patients receiving ipilimumab. *Ann Oncol* (2016) 27(4):732–8. doi: 10.1093/annonc/mdw016

92. Suzuki R, Takagi T, Hikichi T, Konno N, Sugimoto M, Watanabe KO, et al. Derived neutrophil/lymphocyte ratio predicts gemcitabine therapy outcome in unresectable pancreatic cancer. *Oncol Lett* (2016) 11(5):3441–5. doi: 10.3892/ol.2016.4381

93. van Kessel KEM, de Haan LM, Fransen van de Putte EE, van Rhijn BW, de Wit R, van der Heijden MS, et al. Elevated derived neutrophil-to- lymphocyte ratio corresponds with poor outcome in patients undergoing pre-operative chemotherapy in muscle-invasive bladder cancer. *Bladder Cancer.* (2016) 2(3):351–60. doi: 10.3233/BLC-160055

94. Amato RJ, Flaherty A, Zhang Y, Ouyang F, Mohlere V. Clinical prognostic factors associated with outcome in patients with renal cell cancer with prior tyrosine kinase inhibitors or immunotherapy treated with everolimus. *Urol Oncol* (2014) 32 (3):345–54. doi: 10.1016/j.urolonc.2013.09.008

95. Seban RD, Mezquita L, Berenbaum A, Dercle L, Botticella A, Le Pechoux C, et al. Baseline metabolic tumor burden on FDG PET/CT scans predicts outcome in advanced NSCLC patients treated with immune checkpoint inhibitors. *Eur J Nucl Med Mol Imaging.* (2020) 47(5):1147–57. doi: 10.1007/s00259-019-04615-x

96. Noonan SA, Patil T, Gao D, King GG, Thibault JR, Lu X, et al. Baseline and on-treatment characteristics of serum tumor markers in stage IV oncogene-addicted adenocarcinoma of the lung. *J Thorac Oncol* (2018) 13(1):134–8. doi: 10.1016/j.jtho.2017.08.005

97. Holdenrieder S, Wehnl B, Hettwer K, Simon K, Uhlig S, Dayyani F, et al. Carcinoembryonic antigen and cytokeratin-19 fragments for assessment of therapy response in non-small cell lung cancer: a systematic review and meta-analysis. *Br J Cancer.* (2017) 116(8):1037–45. doi: 10.1038/bjc.2017.45

98. Dal Bello MG, Filiberti RA, Alama A, Orengo AM, Mussap M, Coco S, et al. The role of CEA, CYFRA21-1 and NSE in monitoring tumor response to Nivolumab in advanced non-small cell lung cancer (NSCLC) patients. *J Transl Med* (2019) 17(1):74. doi: 10.1186/s12967-019-1828-0

99. Koh J, Go H, Keam B, Kim MY, Nam SJ, Kim TM, et al. Clinicopathologic analysis of programmed cell death-1 and programmed cell death-ligand 1 and 2 expressions in pulmonary adenocarcinoma: comparison with histology and driver oncogenic alteration status. *Mod Pathol* (2015) 28(9):1154–66. doi: 10.1038/modpathol.2015.63

100. Ota K, Azuma K, Kawahara A, Hattori S, Iwama E, Tanizaki J, et al. Induction of PD-L1 expression by the EML4-ALK oncoprotein and downstream signaling pathways in non-small cell lung cancer. *Clin Cancer Res* (2015) 21(17):4014–21. doi: 10.1158/1078-0432.CCR-15-0016

101. Rangachari D, VanderLaan PA, Shea M, Le X, Huberman MS, Kobayashi SS, et al. Correlation between classic driver oncogene mutations in EGFR, ALK, or ROS1 and 22C3-PD-L1 ≥50% Expression in lung adenocarcinoma. *J Thorac Oncol* (2017) 12 (5):878–83. doi: 10.1016/j.jtho.2016.12.026

102. Song Z, Yu X, Cheng G, Zhang Y. Programmed death-ligand 1 expression associated with molecular characteristics in surgically resected lung adenocarcinoma. *J Transl Med* (2016) 14(1):188. doi: 10.1186/s12967-016-0943-4

103. Lan B, Ma C, Zhang C, Chai S, Wang P, Ding L, et al. Association between PD-L1 expression and driver gene status in non-small-cell lung cancer: a meta-analysis. *Oncotarget* (2018) 9(7):7684–99. doi: 10.18632/oncotarget.23969

104. Fang W, Ma Y, Yin JC, Hong S, Zhou H, Wang A, et al. Comprehensive genomic profiling identifies novel genetic predictors of response to anti-PD-(L)1 therapies in non-small cell lung cancer. *Clin Cancer Res* (2019) 25(16):5015–26. doi: 10.1158/1078-0432.CCR-19-0585

105. Cinausero M, Laprovitera N, De Maglio G, Gerratana L, Riefolo M, Macerelli M, et al. KRAS and ERBB-family genetic alterations affect response to PD-1 inhibitors in metastatic nonsquamous NSCLC. *Ther Adv Med Oncol* (2019) 11:1758835919885540. doi: 10.1177/1758835919885540

106. Gianoncelli L, Spitaleri G, Passaro A, Radice D, Fumagalli C, Del Signore E, et al. Efficacy of anti-PD1/PD-L1 therapy (IO) in KRAS mutant non-small cell lung cancer patients: A retrospective analysis. *Anticancer Res* (2020) 40(1):427–33. doi: 10.21873/anticanres.13970

107. Assoun S, Theou-Anton N, Nguenang M, Cazes A, Danel C, Abbar B, et al. Association of TP53 mutations with response and longer survival under immune checkpoint inhibitors in advanced non-small-cell lung cancer. *Lung Cancer.* (2019) 132:65–71. doi: 10.1016/j.lungcan.2019.04.005

108. Shi Y, Lei Y, Liu L, Zhang S, Wang W, Zhao J, et al. Integration of comprehensive genomic profiling, tumor mutational burden, and PD-L1 expression to identify novel biomarkers of immunotherapy in non-small cell lung cancer. *Cancer Med* (2021) 10(7):2216–31. doi: 10.1002/cam4.3649

109. Rodrigue A, LaFrance M, Gauthier MC, McDonald D, Hendzel M, West S, et al. Interplay between human DNA repair proteins at a unique double-strand break in vivo. *EMBO J* (2006) 25(1):222–31. doi: 10.1038/sj.emboj.7600914

110. Guerreiro IM, Barros-Silva D, Lopes P, Cantante M, Cunha AL, Lobo J, et al. RAD51B^{me} levels as a potential predictive biomarker for PD-1 blockade response in non-small cell lung cancer. *J Clin Med* (2020) 9(4):1000. doi: 10.3390/jcm9041000

111. Zeng H, Tohidinezhad F, De Ruysscher DKM, Willems YCP, Degens JHRJ, van Kampen-van den Boogaart VEM, et al. The association of gross tumor volume and its radiomics features with brain metastases development in patients with radically treated stage III non-small cell lung cancer. *Cancers (Basel).* (2023) 15(11):3010. doi: 10.3390/cancers15113010

112. Khorrami M, Khunger M, Zagouras A, Patil P, Thawani R, Bera K, et al. Combination of peri- and intratumoral radiomic features on baseline CT scans predicts response to chemotherapy in lung adenocarcinoma. *Radiol Artif Intell* (2019) 1(2): e180012. doi: 10.1148/ryai.2019180012

113. Khorrami M, Jain P, Bera K, Alilou M, Thawani R, Patil P, et al. Predicting pathologic response to neoadjuvant chemoradiation in resectable stage III non-small cell lung cancer patients using computed tomography radiomic features. *Lung Cancer.* (2019) 135:1–9. doi: 10.1016/j.lungcan.2019.06.020

114. Trebeschi S, Drago SG, Birkbak NJ, Călin AM, Delli Pizzi A, et al. Predicting response to cancer immunotherapy using noninvasive radiomic biomarkers. *Ann Oncol* (2019) 30(6):998–1004. doi: 10.1093/annonc/mdz108

115. Khorrami M, Prasanna P, Gupta A, Patil P, Velu PD, Thawani R, et al. Changes in CT radiomic features associated with lymphocyte distribution predict overall survival and response to immunotherapy in non-small cell lung cancer. *Cancer Immunol Res* (2020) 8(1):108–19. doi: 10.1158/2326-6066.CIR-19-0476

116. Evangelista L, Cuppari L, Menis J, Bonanno L, Reccia P, Frega S, et al. 18F-FDG PET/CT in non-small-cell lung cancer patients: a potential predictive biomarker of response to immunotherapy. *Nucl Med Commun* (2019) 40(8):802–7. doi: 10.1097/MNM.0000000000001025

117. Mu W, Tunali I, Gray JE, Qi J, Schabath MB, Gillies RJ, et al. Radiomics of 18F-FDG PET/CT images predicts clinical benefit of advanced NSCLC patients to checkpoint blockade immunotherapy. *Eur J Nucl Med Mol Imaging.* (2020) 47 (5):1168–82. doi: 10.1007/s00259-019-04625-9

118. Berengure R, Pastor-Juan MDR, Canals-Vazquez J, Castro-García M, Villas MV, Mansilla Legorburo F, et al. Radiomics of CT features may be nonreproducible and redundant: influence of CT acquisition parameters. *Radiology* (2018) 288(2):407–15. doi: 10.1148/radiol.2018172361

119. Park W, Kwon D, Saravia D, Desai A, Vargas F, El Dinali M, et al. Developing a predictive model for clinical outcomes of advanced non-small cell lung cancer patients treated with nivolumab. *Clin Lung Cancer.* (2018) 19(3):280–288.e4. doi: 10.1016/j.cllc.2017.12.007

120. Park W, Mezquita L, Okabe N, Chae YK, Kwon D, Saravia D, et al. Association of the prognostic model iSEND with PD-1/L1 monotherapy outcome in non-small-cell lung cancer. *Br J Cancer.* (2020) 122(3):340–7. doi: 10.1038/s41416-019-0643-y

121. Prelaj A, Rebuzzi SE, Pizzutilo P, Bilancia M, Montrone M, Pesola F, et al. EPSILoN: A prognostic score using clinical and blood biomarkers in advanced non-small-cell lung cancer treated with immunotherapy. *Clin Lung Cancer.* (2020) 21 (4):365–77. doi: 10.1016/j.cllc.2019.11.017

122. Prelaj A, Ferrara R, Rebuzzi SE, Proto C, Signorelli D, Galli G, et al. EPSILoN: A prognostic score for immunotherapy in advanced non-small-cell lung cancer: A validation cohort. *Cancers (Basel).* (2019) 11(12):1954. doi: 10.3390/cancers11121954

123. Wang W, Huang Z, Yu Z, Zhuang W, Zheng W, Cai Z, et al. Prognostic value of the lung immune prognostic index may differ in patients treated with immune checkpoint inhibitor monotherapy or combined with chemotherapy for non-small cell lung cancer. *Front Oncol* (2020) 10:572853. doi: 10.3389/fonc.2020.572853

124. Ruiz-Bañobre J, Areses-Manrique MC, Mosquera-Martínez J, Cortegoso A, Afonso-Afonso FJ, de Dios-Álvarez N, et al. Evaluation of the lung immune prognostic index in advanced non-small cell lung cancer patients under nivolumab monotherapy. *Transl Lung Cancer Res* (2019) 8(6):1078–85. doi: 10.21037/tlcr.2019.11.07

125. Sorich MJ, Rowland A, Karapetis CS, Hopkins AM. Evaluation of the Lung Immune Prognostic Index for prediction of survival and response in patients treated with Atezolizumab for Non-Small Cell Lung Cancer: Pooled analysis of clinical trials. *J Thorac Oncol* (2019) 14(8):1440–6. doi: 10.1016/j.jtho.2019.04.006

126. Kazandjian D, Gong Y, Keegan P, Pazdur R, Blumenthal GM. Prognostic value of the Lung Immune Prognostic Index for patients treated for metastatic Non–Small Cell Lung Cancer. *JAMA Oncol* (2019) 5(10):1481–5. doi: 10.1001/jamaoncol.2019.1747

frontiers | Frontiers in Immunology

TYPE Original Research
PUBLISHED 15 September 2023
DOI 10.3389/fimmu.2023.1266992

Check for updates

OPEN ACCESS

EDITED BY
Yuan Wan,
Binghamton University, United States

REVIEWED BY
Guosheng Wang,
School of Medicine, Tongji University, China
Bo Kong,
Technical University of Munich, Germany

*CORRESPONDENCE
Chuandong Zhu
zhucd@njucm.edu.cn
Siqi Han
hansiqi1228@126.com
Xiufeng Liu
superchenym@163.com

†These authors have contributed equally to this work

RECEIVED 25 July 2023
ACCEPTED 30 August 2023
PUBLISHED 15 September 2023

CITATION
Chen C, Xiong X, Cheng Y, Gen H, Zhu W, Zhang F, Zhu C, Han S and Liu X (2023) Expanding the applications of immune checkpoint inhibitors in advanced lung cancer beyond disease progression. *Front. Immunol.* 14:1266992. doi: 10.3389/fimmu.2023.1266992

COPYRIGHT
© 2023 Chen, Xiong, Cheng, Gen, Zhu, Zhang, Zhu, Han and Liu. This is an open-access article distributed under the terms of the Creative Commons Attribution License (CC BY). The use, distribution or reproduction in other forums is permitted, provided the original author(s) and the copyright owner(s) are credited and that the original publication in this journal is cited, in accordance with accepted academic practice. No use, distribution or reproduction is permitted which does not comply with these terms.

Expanding the applications of immune checkpoint inhibitors in advanced lung cancer beyond disease progression

Chao Chen[1†], Xi Xiong[2†], Ying Cheng[3], Haiyun Gen[1], Wenqiang Zhu[4], Fei Zhang[5], Chuandong Zhu[6*], Siqi Han[1*] and Xiufeng Liu[1*]

[1]Department of Oncology, Jinling Hospital, Nanjing Medical University, Nanjing, China, [2]Department of Hepatology, Jinling Hospital, Nanjing Medical University, Nanjing, China, [3]Department of Oncology, Jiangsu Province Hospital of Chinese Medicine, The Affiliated Hospital of Nanjing University of Chinese Medicine, Nanjing, China, [4]Department of Surgical Oncology, Jiangsu Province Hospital of Chinese Medicine, The Affiliated Hospital of Nanjing University of Chinese Medicine, Nanjing, China, [5]Department of Clinical Laboratory, Jinling Hospital, Nanjing Medical University, Nanjing, China, [6]Department of Oncology, the Second Hospital of Nanjing, Nanjing University of Chinese Medicine, Nanjing, China

Background: Immunotherapy, particularly the utilization of immune checkpoint inhibitors (ICIs), assumes a pivotal role in the comprehensive management of advanced lung cancer. There has been substantial deliberation regarding the appropriateness of extending ICIs treatment beyond the point of disease progression. This study delves into the potential benefits of sustained utilization of ICIs subsequent to disease progression in patients.

Methods: A retrospective analysis was conducted on a cohort of 248 patients diagnosed with advanced lung cancer who received treatment with ICIs. The study population comprised 99 patients in the treatment beyond progression (TBP) group and 42 patients in the non-treatment beyond progression (NTBP) group. Parameters including progression-free survival (PFS), overall survival (OS), objective response rate (ORR), and disease control rate (DCR) were assessed. The Cox proportional hazard regression model was employed to analyze prognostic factors related to immunotherapy.

Results: Patients undergoing primary treatment with PD-1/PD-L1 inhibitors exhibited a median progression-free survival (mPFS) of 5.3 months. In the context of disease progression, a comparison between the TBP and NTBP groups was performed with respect to mPFS. The results demonstrated that the TBP group manifested an mPFS of 8.6 months, contrasting with the NTBP group's mPFS of 4.0 months (p=0.028). The mean overall survival (mOS) in the TBP group exhibited a statistically significant increase in comparison to the NTBP group (14.1 months vs. 6.0 months, p=0.028). Evaluation of the objective response rate (ORR) between the TBP and NTBP groups revealed a substantial distinction. The TBP group displayed an ORR of 12.1%, while the NTBP group exhibited a lower ORR of 2.4%. The statistical analysis yielded a p-value of 0.068, signifying a notable trend towards significance. The disease control rate (DCR)

was also assessed and exhibited a noteworthy variance between the two groups, with a higher DCR of 92.9% in contrast to 71.4% in the control group (p = 0.001).

Conclusion: Subsequent to ICIs treatment, a subset of patients may derive continued benefits from anticancer therapy, notwithstanding the progression of their advanced lung cancer.

KEYWORDS

advanced lung cancer, PD-1, treatment beyond progression, immunotherapy, retrospective study

Introduction

Lung cancer stands as the leading cause of tumor-related mortality on a global scale. The notable decrease in lung cancer mortality observed in recent years can be largely attributed to substantial advancements in early detection, molecular targeted therapy, and immunotherapy. Nevertheless, the 5-year survival rate for patients with non-small cell lung cancer (NSCLC) remains modest, hovering below 20% (1). Among the remarkable breakthroughs in lung cancer treatment, immunotherapy has emerged as a pivotal development. PD-1, a type I transmembrane protein comprising 268 amino acids from the immunoglobulin B7CD28 family, plays a crucial role. PD-1, with its primary ligand PDL1 expressed widely in antigen-presenting and non-blood cells, operates as a negative regulator in human immune responses. Its distinct therapeutic mechanism sets it apart from conventional chemotherapy and radiotherapy, activating the immune system to combat cancer cells. Notably, immune checkpoint inhibitors, including PD-1 and PD-L1 inhibitors, exemplify immunotherapy's forefront, stimulating the immune system through T cell activation against tumors (2, 3).

The PD-1/PD-L1 signaling pathway exerts significant influence on T cell activation and exerts control over the generation of growth factors and cellular proliferation (4). Pathological stimulation of this pathway impedes T lymphocyte activation and replication, fosters regulatory T lymphocyte development, and facilitates evasive tactics by neoplastic cells against immune recognition and elimination (5). The utilization of immune checkpoint inhibitors (ICIs) has ushered in a new era of immunotherapy for advanced NSCLC in clinical settings (6).

Distinguished from conventional chemotherapy and targeted therapy, the anti-neoplastic mechanism of immune checkpoint inhibitors (ICIs) necessitates distinct approaches to evaluating treatment effectiveness. Due to the potential for atypical delayed responses and pseudo-progression in tumor patients undergoing ICIs treatment, assessment of progression-free survival (PFS) and objective response rate (ORR) for solid tumors relies on the Response Evaluation Criteria in Solid Tumors (RECIST) v1.1. Nevertheless, the assessment of immunotherapy presents challenges, as immune-related Response Evaluation Criteria in Solid Tumors (irRECIST) and modified immune-related Response Evaluation Criteria in Solid Tumors (iRECIST) remain infrequently employed in clinical practice (7, 8).

Traditionally, disease progression in the context of immunotherapy signifies treatment failure and often leads to its discontinuation. However, reports from the literature suggest that even in metastatic renal cell carcinoma cases, patients may continue receiving PD-1 monoclonal antibodies post-disease progression, potentially yielding survival benefits (9).

Amidst the backdrop of ongoing debates within various studies, a pertinent discussion surrounds the potential advantages of maintaining immunotherapy with immune checkpoint inhibitors (ICIs) for patients with advanced lung cancer following disease progression. The relevance of continuing immunotherapy after disease progression diminishes in patients with advanced lung carcinoma who have previously undergone immunotherapy or a combination of immunotherapy and chemotherapy, and reports vary in their findings (9–13). Our study endeavors to validate the clinical efficacy of ICIs in lung cancer patients facing disease progression subsequent to ICIs therapy.

Patients and methods

Patients

A retrospective analysis was conducted on a cohort of 248 patients with advanced lung cancer who underwent treatment with immune checkpoint inhibitors (ICIs) at Nanjing Jinling Hospital between January 1, 2018, and October 31, 2022. Inclusion criteria were as follows: a) age ranging from 18 to 80 years; b) confirmed pathological diagnosis of small cell lung cancer or non-small cell lung cancer, including adenocarcinoma, squamous cell carcinoma, adenosquamous cell carcinoma, etc.; c) accordance with the eighth edition of the cancer TNM classification, with patients at stage IIIB or IV or those with recurrent disease; d) receipt of at least 2 cycles of ICIs treatment with a minimum interval; e) absence of intolerable toxic reactions from prior immunotherapy; f) Eastern Cooperative Oncology Group (ECOG) score less than 3; g) receipt of PD-1 monoclonal antibodies at least twice following disease progression. The final follow-up date was April

01, 2023. All participants provided informed consent, adhered to the ethical principles outlined in the Helsinki Declaration, and received approval from the hospital's ethics committee.

Study design

Oncologists and radiologists collaborated to perform imaging evaluations, classifying efficacy into complete remission (CR), partial remission (PR), disease stability (SD), and disease progression (PD) based on RECISTv1.1 criteria. The objective response rate (ORR) was calculated by combining complete remission (CR) and partial remission (PR), while the disease control rate (DCR) was computed using the sum of complete remission, partial remission, and standard deviation (CR+PR+SD).

The initial assessment of disease response occurred after the completion of two treatment cycles or earlier if clinically indicated. ORR analysis was based on the best overall response (BOR), encompassing both partial and complete response rates. Disease control rate (DCR) was determined by evaluating the rates of partial remission, complete remission, and disease stability.

The PFS was defined as the time between commencement of immune checkpoint inhibitor treatment and disease progression. PFS2 represented the interval between the first occurrence of immunotherapy-induced progression and the subsequent progression or mortality from any cause. Overall survival (OS) was calculated from the first progression after ICIs treatment to mortality from any cause. Baseline characteristics evaluated included age, gender, smoking history, surgery, radiotherapy, ECOG status, histology, brain metastasis, bone metastasis, and liver metastasis.

Safety evaluations encompassed all eligible patients, with adverse events (AEs) graded according to the National Cancer Institute Common Terminology Criteria for Adverse Events, version 5.0.

Statistical analysis

The statistical analysis of the data in this research was carried out utilizing SPSS 22.0 (Chicago, IL, USA) or GraphPad Prism 8.0 (San Diego, California, USA). To assess differences in continuous variables between the treatment and control groups, the Mann-Whitney U test was employed. For discrete data group comparisons, the Pearson χ^2 test or Fisher's exact test was applied. PFS and OS rates were calculated using the Kaplan-Meier method, with disparities between groups evaluated using the log-rank test. The Cox proportional hazard regression model was used for both univariate and multivariate analyses of prognostic factors associated with overall survival post-immunotherapy. Relative risk between groups was evaluated through the hazard ratio (HR) and a 95% confidence interval (CI). A statistical significance level of $\alpha = 0.05$ was set for all conducted tests.

Results

Patient clinical characteristics

The patient selection process is depicted in Figure 1. Between January 1st, 2018, and October 31st, 2022, a total of 248 patients with advanced lung cancer received ICIs treatment at Nanjing Jinling Hospital. Following RECIST 1.1 criteria, disease progression was observed in 156 patients, while 10 patients were lost to follow-up, and 5 patients had incomplete data. Ultimately, the analysis encompassed 141 patients, comprising 99 patients in the Treatment beyond Progression (TBP) group, which is refers to the practice of continuing a treatment regimen without any interruption or cessation, even after disease progression has been observed. This approach involves maintaining the therapy without a predefined stop time,

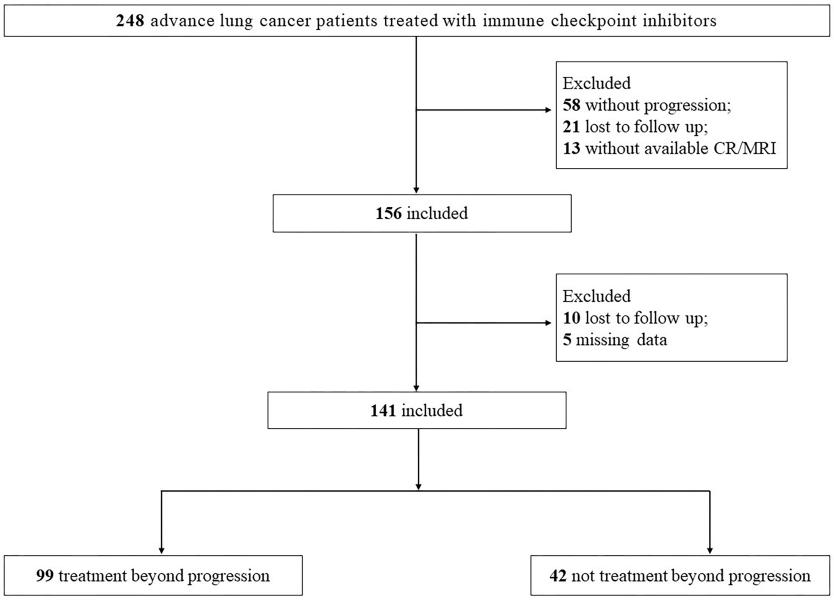


FIGURE 1
Flow chart of the study.

allowing for ongoing management and potential benefits for the patient and 42 patients in the Non-Treatment beyond Progression (NTBP) group.

The characteristics of the patients are summarized in Table 1. The TBP group exhibited an average age of 62.9 ± 9.5 years, with 16 female patients (16.2%), 35 patients (35.4%) having undergone surgical treatment, and 47 patients (47.5%) receiving radiotherapy. In contrast, the NTBP group had an average age of 63.0 ± 9.7 years, comprising 11 female patients (26.2%), 11 patients (26.2%) with a history of surgical treatment, and 21 patients (50.0%) who had received radiotherapy.

Clinical outcomes

Among the 141 patients included in this clinical trial, the mPFS after initial treatment with PD-1/PD-L1 therapy was 5.3 months (95% CI: 4.4-6.2). Subsequent to disease progression, the TBP group

TABLE 1 Clinical information of included patients.

Factors	NTBP,n=42(%)	TBP,n=99(%)	P value
Age			0.929
	63.0 ± 9.7	62.9 ± 9.5	
Gender			0.166
Female	11(26.2)	16(16.2)	
Male	31(73.8)	83(83.8)	
Smoking history			0.722
Current/Former	14(33.3)	30(30.3)	
Never	28(66.7)	69(69.7)	
ECOG PS			0.011
0	11(26.2)	38(38.4)	
1	23(54.8)	57(57.6)	
2	8(19.0)	4(4.0)	
Surgery			0.179
No	32(76.2)	64(64.6)	
Yes	10(23.8)	35(35.4)	
Radiotherapy			0.784
No	21(50.0)	52(52.5)	
Yes	21(50.0)	47(47.5)	
Pathology			0.084
Small Cell	6(14.3)	16(16.2)	
Squamous	13(31.0)	28(28.3)	
Adenocarcinoma	19(45.2)	54(54.5)	
Other	4(9.5)	1(1.0)	
PD-1 inhibitors			0.914
Atezolizumab	1(2.4)	3(3.0)	
Durvalumab	4(9.5)	4(4.0)	
Camrelizumab	19(45.2)	49(49.5)	
Nivolumab	2(4.8)	6(6.1)	
Pembrolizumab	3(7.1)	4(4.0)	
Toripalimab	3(7.1)	10(10.1)	
Tislelizumab	6(14.3)	14(14.1)	
Sintilimab	4(9.5)	9(9.1)	

exhibited notably extended mPFS in comparison to the NTBP group (8.6 vs. 4.0 months, HR=0.620, 95% CI: 0.405-0.950, P=0.028). Furthermore, the TBP group demonstrated a significantly higher mOS in contrast to the NTBP group (14.1 vs. 6.0 months, HR=0.484, 95% CI: 0.405-0.950, P=0.028), as depicted in Figure 2. Notably, no significant correlation emerged between PFS2 and PFS1 in the NTBP group (Y = 0.03108*X + 6.399, R^2=0.002, P=0.797). Similarly, no significant correlation was observed between mOS and PFS1 (Y=0.04328*X+8.068, R^2=0.002, P=0.756). While no statistically significant correlation emerged between PFS2 (Y = 0.03229*X + 9.225, R^2=0.001, P=0.749) and OS (Y = 0.01212*X+13.43, R^2=0.001, P=0.914) with PFS1 in the TBP group, a consistent trend was evident (Figure 3).

Based on pathological classification, small cell lung cancer patients in the TBP group (16 cases) displayed a lengthier mOS trend compared to the NTBP group (6 cases) (7.9 vs. 3.5 months, HR=0.522, 95% CI: 0.180-1.511, P=0.230). In the cohort diagnosed with squamous cell carcinoma and treated with TBP (28 cases), a prolonged mOS was evident relative to NTBP (13 cases) (14.3 vs. 6.0 months, HR=0.280, 95% CI: 0.121-0.647, P=0.003). Similarly, patients diagnosed with adenocarcinoma and treated with TBP (54 cases) exhibited a higher mOS than the NTBP group (19 cases) (16.3 vs. 7.5 months, HR=0.602, 95% CI: 0.320-1.132, P=0.115), though statistical significance was not reached (Figure 4). The TBP group displayed an ORR of 12.1% compared to 2.4% in the NTBP group, yielding a p-value of 0.068. Furthermore, the disease control rate (DCR) was 92.9% versus 71.4% (p-value = 0.001), as outlined in Table 2. Analysis of the forest plot involving patient age, gender, smoking status, ECOG performance status, therapy line, radiotherapy, presence of lung metastasis, bone metastasis, and lymph node metastasis indicated the TBP group's enhanced efficacy (Figure 5).

Safety

A comprehensive safety assessment was conducted on all patients (Figure 6). The incidence of immune-related adverse events in the TBP group paralleled that of the PRE-PD group. Primary severe adverse effects encompassed immune-mediated pneumonia, dermatitis, and asthenia. The TBP group did not manifest an elevation in severe adverse events, and treatment-related fatalities were absent. Additionally, no additional severe adverse events were reported in the TBP group.

Discussion

Immunotherapy, characterized by the use of immune checkpoint inhibitors (ICIs), has the potential to eradicate tumor

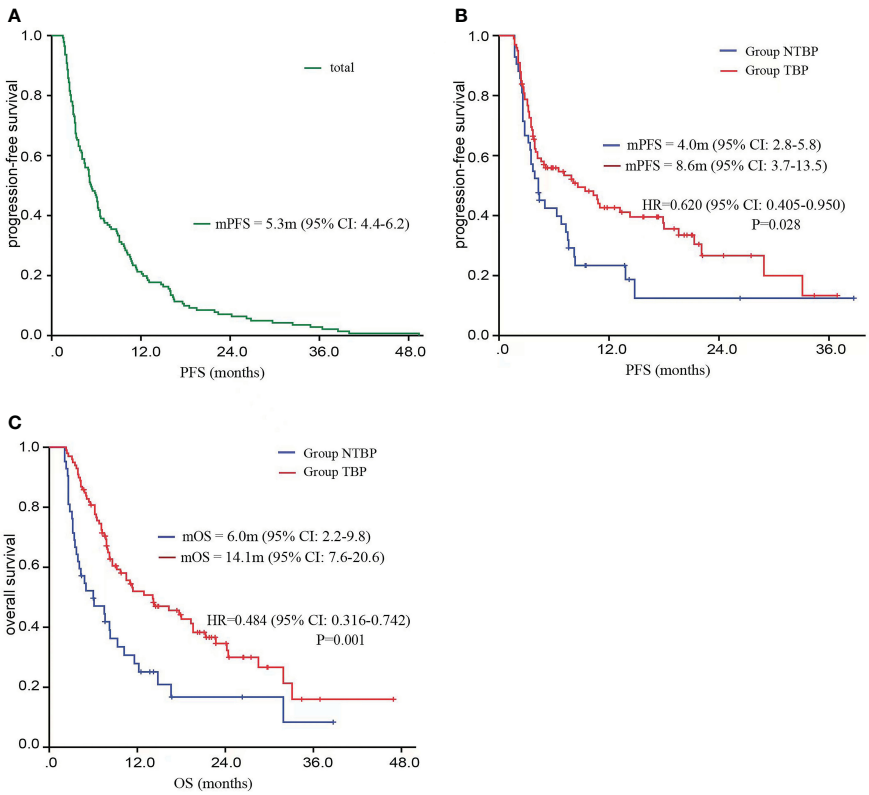


FIGURE 2
Kaplan–Meier curves of PFS and OS in advance lung cancer patients according to response to ICIs. **(A)** the PFS of advance lung cancer patients received ICIs treatment at first time. **(B)** the PFS of advance lung cancer patients in TBP and NTBP. **(C)** the OS of advance lung cancer patients in TBP and NTBP.

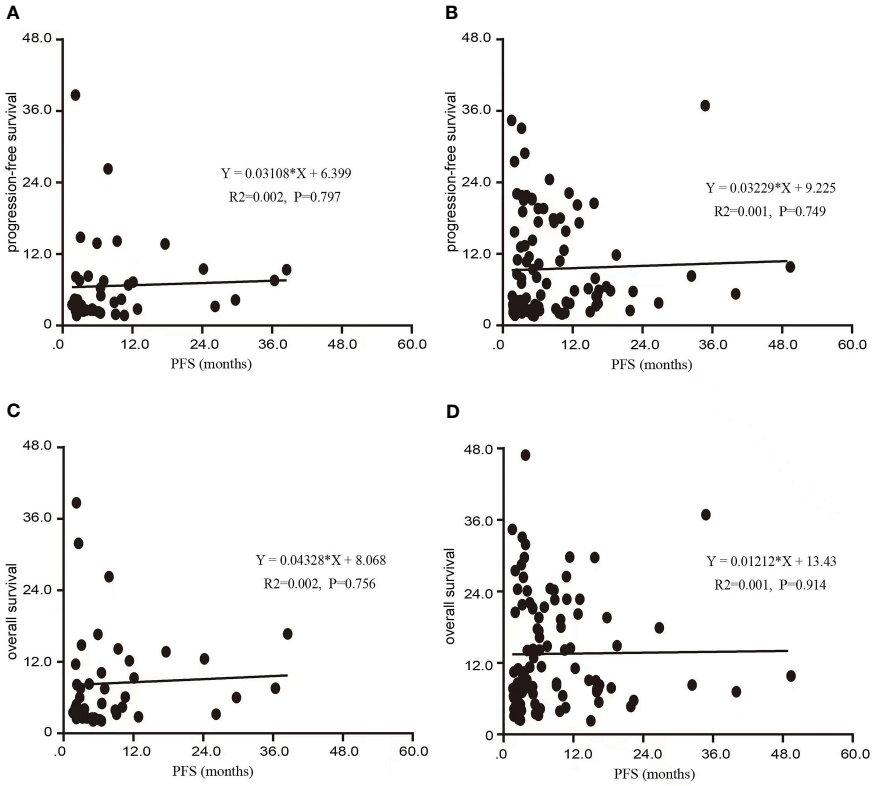


FIGURE 3
Scatter diagram of the association between PFS1 and PFS 2, OS in this study. **(A)** Scatter diagram of the association between PFS1 and PFS in NTBP. **(B)** Scatter diagram of the association between PFS1 and PFS in TBP. **(C)** Scatter diagram of the association between PFS1 and OS in NTBP. **(D)** Scatter diagram of the association between PFS1 and OS in TBP.

cells by activating the anti-tumor immune function of patients' own T lymphocytes. This therapeutic approach has gained widespread adoption within clinical settings (14). In cases of tumor progression among NSCLC patients undergoing PD-1 inhibitor immunotherapy, the optimal anti-tumor regimen and the feasibility of continuing PD-1 inhibitor maintenance therapy lack clear guidelines.

The concept of cross-line therapy, involving the replacement of chemotherapy drugs after first-line treatment progression, while retaining drugs that could provide ongoing benefit for second-line treatment, has been explored. These potentially beneficial drugs often complement cytotoxic agents, addressing aspects such as improved tumor vascularization or modulation of the immune microenvironment. Cross-line therapy has been investigated in diverse tumor types, including the combination of human epidermal growth factor receptor-2 monoclonal antibodies with chemotherapy in breast cancer treatment (15), and the application of anti-angiogenesis therapy alongside chemotherapy for colon and non-small cell lung cancer (16). These studies have imparted certain impacts on clinical practice.

Within the realm of lung cancer immunotherapy, a retrospective analysis of the OAK trial revealed that among 322 patients diagnosed with non-small cell lung cancer who received atezolizumab, disease progression occurred (9). Among these patients, those who persisted with atezolizumab treatment exhibited prolonged overall survival (OS) compared to those who received alternative treatments or no additional therapy. Similarly, the clinical investigation of nivolumab demonstrated that the TBP (treatment beyond progression) and NTBP (no treatment beyond progression) groups exhibited comparable overall survival (OS: 15.6 vs. 13.4 months; P=0.40). An analysis of real-world data from 134 instances indicated that the continuation of immunotherapy after progression can lead to extended survival, with a statistically significant benefit (OS: 17.2 vs. 7.5 months; p<0.01) (17).

The KEYNOTE-407 trial, evaluating the efficacy of PD-1 monoclonal antibody combined with chemotherapy versus placebo in the management of advanced lung squamous cell carcinoma, revealed that the group receiving immune combined chemotherapy had a mOS of 17.2 months, compared to a mOS of 11.6 months in the group receiving placebo combined chemotherapy (HR=0.71, 95%CI: 0.59-0.85) (18, 19). Our study included 41 patients diagnosed with advanced lung squamous cell carcinoma, among whom 28 received PD-1 monoclonal antibody treatment, resulting in a significantly longer median overall survival of 14.3 months compared to 6.0 months (p=0.003). This study underscores the potential benefits of continuous PD-1 monoclonal antibody administration for patients with lung squamous cell carcinoma.

While the IMPower133 (20) and KEYNOTE604 (21) studies have established the importance of immunotherapy in managing small cell lung cancer, limited literature exists on the effectiveness of PD-1 monoclonal antibody treatment for advanced small cell lung cancer following PD-1 therapy progression. Our study included 22 patients diagnosed with small cell lung cancer, of whom 16 were administered

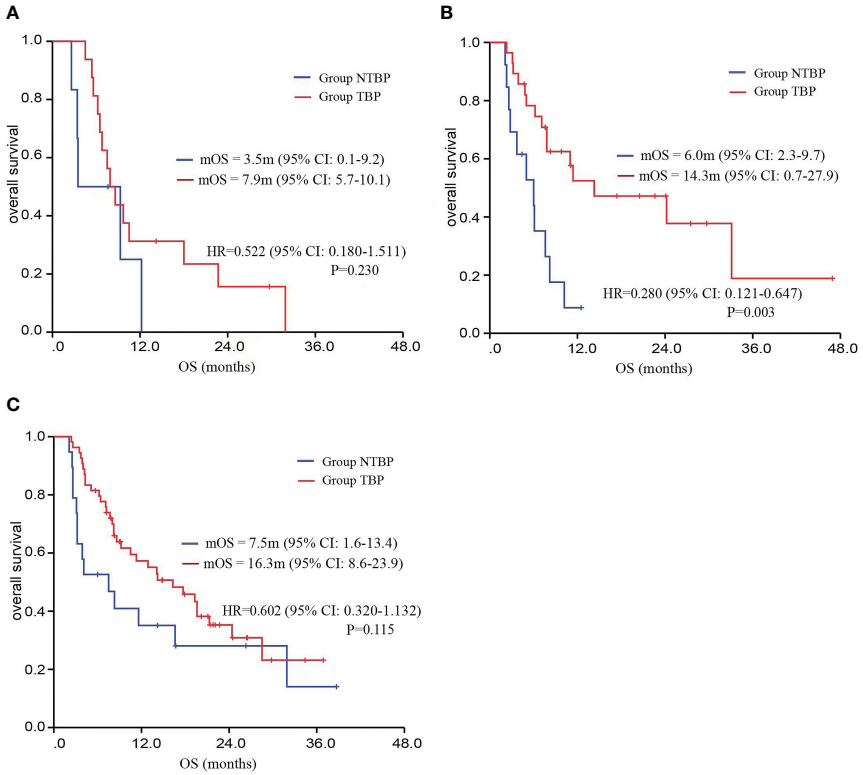


FIGURE 4
Kaplan–Meier curves for OS comparing TBP and NTBP in different pathological types of lung cancer patients. **(A)** Kaplan–Meier curves of OS comparing TBP and NTBP in small cell lung cancer. **(B)** Kaplan–Meier curves of OS comparing TBP and NTBP in squamous cell lung carcinoma. **(C)** Kaplan–Meier curves of OS comparing TBP and NTBP in lung adenocarcinoma.

PD-1 monoclonal antibody immunotherapy. Although a positive trend of efficacy was observed, the lack of statistical significance could be attributed to the constrained sample size. Subgroup analysis focusing on pathological characteristics of the total lung cancer population demonstrated advantages in terms of mPFS and mOS for the TBP group compared to the NTBP group, with significant findings in patients diagnosed with squamous cell carcinoma.

Concurrently, a forest plot analysis revealed that age, gender, smoking status, ECOG performance status, surgical intervention, radiotherapy, metastasis location, and therapy line variables all favored the TBP group. Notably, the overall TBP group exhibited a lower ECOG score compared to the NTBP group, indicating that patients with superior overall health status are more likely to persist with PD-1 monoclonal antibody treatment after progression.

Furthermore, among the 141 patients who experienced disease progression when undergoing immunotherapy in this study, the TBP group (99) was compared to the NTBP group (42). This comparison was made in relation to prior literature from 2018 (7 vs. 87) (9), 2019 (60 vs. 116) (10), and 2020 (67 vs. 67) (11). The growing preference for TBP treatment options appears to stem from an enhanced understanding among clinicians of the effectiveness and safety of PD-1 monoclonal antibody therapy. Concurrently, the progressive reduction in pharmaceutical costs contributes to the increased utilization of extended treatment by individuals.

TABLE 2 Summary of efficacy of PD-1Treat beyond progression.

	NTBP,n=42	TBP,n=99	P value
Objective response rate, N (%)	1(2.4)	12(12.1)	0.068
Disease control rate, N (%)	30(71.4)	92(92.9)	0.001
Best overall response, N (%)			0.003
Progressive disease	12(28.6)	7(7.1)	
Stable disease	29(69.0)	80(80.8)	
Partial response	1(2.4)	12(12.1)	
Complete response	0	0	

TBP, treatment beyond progression; NTBP, not treatment beyond progression.

10.3389/fimmu.2023.1266992

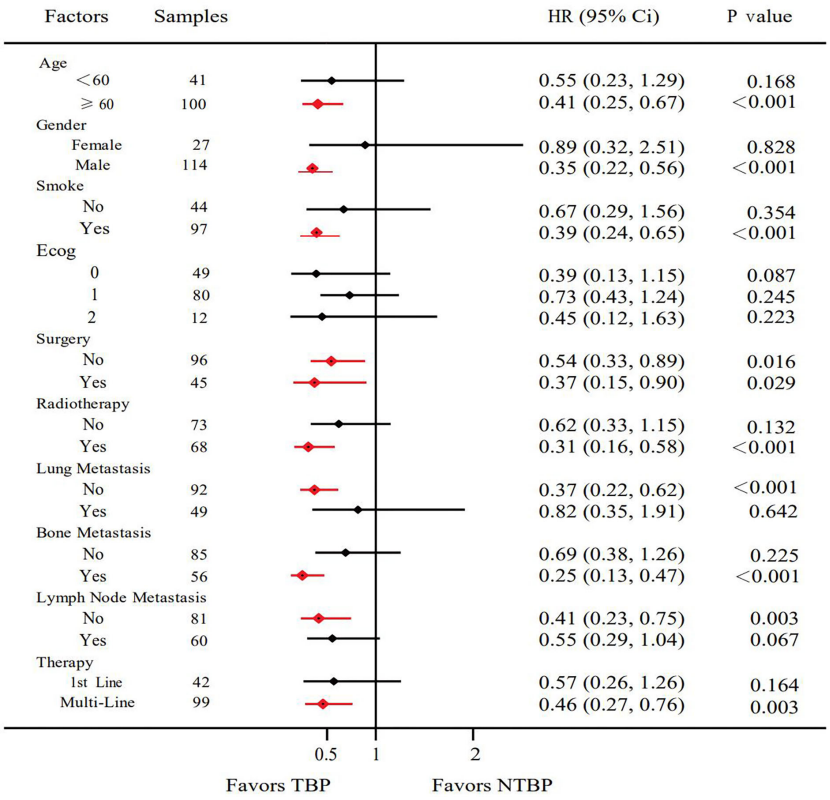


FIGURE 5
Forest plots for the clinical characteristics in TBP and NTBP.

Nevertheless, this study bears certain limitations, including its nature as a single-center retrospective investigation with a limited sample size. Variability in the utilization of different PD-1/PD-L1 monoclonal antibodies and potential confounding factors must also be acknowledged. The assessment criterion adopted, RECIST1.1, while straightforward and expedient, may not fully capture the complexities of real-world clinical settings, impeding its widespread implementation.

A

Adverse Events, n (%)	NTBP，n=42	TBP，n=99	P value
Grade 1-2	20(47.6)	35(35.4)	0.172
Grade 3-4	7(16.7)	6(6.1)	0.047

B

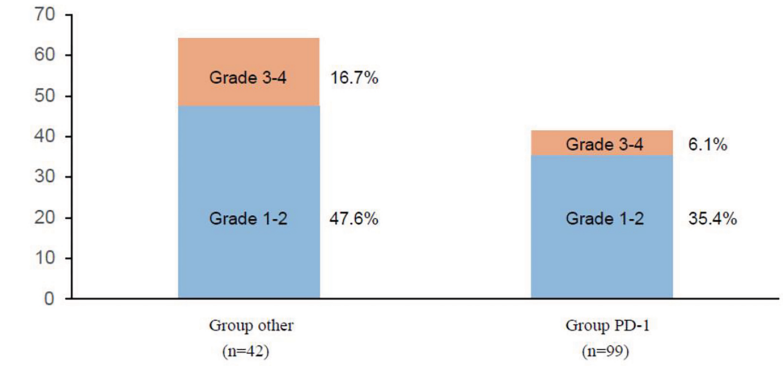


FIGURE 6
Adverse events in the study before and after PD. **(A)** Adverse events of special interest. **(B)** Treatment-related adverse events.

The findings of this study suggest that the administration of PD-1 monoclonal antibodies to patients with advanced lung cancer experiencing progression, as determined by RECIST1.1 criteria, could lead to improved survival outcomes upon continued usage. The interval between the initiation of PD-1 monoclonal antibody therapy and the initial progression of the disease does not impact the correlation between PFS and OS subsequent to cross-line treatment. While prolonged immunotherapy administration is often linked to an increased incidence of adverse effects, our study demonstrated that the persistence of PD-1 monoclonal antibody therapy post-progression did not result in a higher occurrence of grade 3-4 adverse outcomes, indicating its tolerability. Therefore, the application of PD-1 monoclonal antibodies after disease progression could offer enhanced survival benefits with minimal unfavorable events. Larger-scale medical investigations are warranted to further elucidate the insights gained from this study.

Data availability statement

The raw data supporting the conclusions of this article will be made available by the authors, without undue reservation.

Ethics statement

The studies involving humans were approved by Ethics Committee of Jinling Hospital. The studies were conducted in accordance with the local legislation and institutional requirements. The participants provided their written informed consent to participate in this study.

Author contributions

CC: Conceptualization, Investigation, Writing – original draft. XX: Data curation, Methodology, Software, Writing – original draft. YC: Formal Analysis, Project administration, Validation, Writing – review & editing. HG: Methodology, Software, Writing – original draft. WZ: Project administration, Resources, Validation, Writing – review & editing. FZ: Data curation, Software, Writing – original draft. CZ: Conceptualization, Investigation, Writing – original draft. SH: Funding acquisition, Software, Validation, Visualization, Writing – original draft. XL: Supervision, Writing – original draft.

Conflict of interest

The authors declare that the research was conducted in the absence of any commercial or financial relationships that could be construed as a potential conflict of interest.

Publisher's note

All claims expressed in this article are solely those of the authors and do not necessarily represent those of their affiliated organizations, or those of the publisher, the editors and the reviewers. Any product that may be evaluated in this article, or claim that may be made by its manufacturer, is not guaranteed or endorsed by the publisher.

References

1. Siegel RL, Miller KD, Fuchs HE, Jemal A. Cancer statistics, 2022. *CA Cancer J Clin* (2022) 72(1):7–33. doi: 10.3322/caac.21708

2. Berger KN, Pu JJ. PD-1 pathway and its clinical application: A 20year journey after discovery of the complete human PD-1 gene. *Gene* (2018) 638:20–5. doi: 10.1016/j.gene.2017.09.050

3. Woo SR, Turnis ME, Goldberg MV, Bankoti J, Selby M, Nirschl CJ, et al. Immune inhibitory molecules LAG-3 and PD-1 synergistically regulate T-cell function to promote tumoral immune escape. *Cancer Res* (2012) 72(4):917–27. doi: 10.1158/0008-5472.CAN-11-1620

4. Saresella M, Rainone V, Al-Daghri NM, Clerici M, Trabattoni D. The PD-1/PD-L1 pathway in human pathology. *Curr Mol Med* (2012) 12(3):259–67. doi: 10.2174/156652412799218903

5. Ma W, Gilligan BM, Yuan J, Li T. Current status and perspectives in translational biomarker research for PD-1/PD-L1 immune checkpoint blockade therapy. *J Hematol Oncol* (2016) 9(1):47. doi: 10.1186/s13045-016-0277-y

6. Waterhouse D, Lam J, Betts KA, Yin L, Gao S, Yuan Y, et al. Real-world outcomes of immunotherapy-based regimens in first-line advanced non-small cell lung cancer. *Lung Cancer* (2021) 156:41–9. doi: 10.1016/j.lungcan.2021.04.007

7. Blumenthal GM, Theoret MR, Pazdur R. Treatment beyond progression with immune checkpoint inhibitors-known unknowns. *JAMA Oncol* (2017) 3(11):1473–4. doi: 10.1001/jamaoncol.2017.1819

8. Eisenhauer EA, Therasse P, Bogaerts J, Schwartz LH, Sargent D, Ford R, et al. New response evaluation criteria in solid tumours: revised RECIST guideline (version 1.1). *Eur J Cancer* (2009) 45(2):228–47. doi: 10.1016/j.ejca.2008.10.026

9. Gandara DR, von Pawel J, Mazieres J, Sullivan R, Helland Å, Han JY, et al. Atezolizumab treatment beyond progression in advanced NSCLC: results from the randomized, phase III OAK study. *J Thorac Oncol* (2018) 13(12):1906–18. doi: 10.1016/j.jtho.2018.08.2027

10. Ricciuti B, Genova C, Bassanelli M, De Giglio A, Brambilla M, Metro G, et al. Safety and efficacy of nivolumab in patients with advanced non-small-cell lung cancer treated beyond progression. *Clin Lung Cancer* (2019) 20(3):178–185.e2. doi: 10.1016/j.cllc.2019.02.001

11. Won SE, Park HJ, Byun S, Pyo J, Kim JH, Choi CM, et al. Impact of pseudoprogression and treatment beyond progression on outcome in patients with non-small cell lung cancer treated with immune checkpoint inhibitors. *Oncoimmunology* (2020) 9(1):1776058. doi: 10.1080/2162402X.2020.1776058

12. Reinhorn D, Jacobi O, Icht O, Dudnik E, Rotem O, Zer A, et al. Treatment beyond progression with immune checkpoint inhibitors in non-small-cell lung cancer. *Immunotherapy* (2020) 12(4):235–43. doi: 10.2217/imt-2019-0131

13. Stinchcombe TE, Miksad RA, Gossai A, Griffith SD, Torres AZ. Real-world outcomes for advanced non-small cell lung cancer patients treated with a PD-L1 inhibitor beyond progression. *Clin Lung Cancer* (2020) 21(5):389–394.e3. doi: 10.1016/j.cllc.2020.04.008

14. Arbour KC, Mezquita L, Long N, Rizvi H, Auclin E, Ni A, et al. Impact of baseline steroids on efficacy of programmed cell death-1 and programmed death-ligand 1 blockade in patients with non-small-cell lung cancer. *J Clin Oncol* (2018) 36 (28):2872–8. doi: 10.1200/JCO.2018.79.0006

15. Hammerman A, Greenberg-Dotan S, Feldhamer I, Bitterman H, Yerushalmi R. Second-line treatment of her2-positive metastatic breast cancer: trastuzumab beyond progression or lapatinib? A population based cohort study. *PloS One* (2015) 10(9): e0138229. doi: 10.1371/journal.pone.0138229

16. Takeda M, Yamanaka T, Seto T, Hayashi H, Azuma K, Okada M, et al. Bevacizumab beyond disease progression after first-line treatment with bevacizumab plus chemotherapy in advanced nonsquamous non-small cell lung cancer (West Japan Oncology Group 5910L): An open-label, randomized, phase 2 trial. *Cancer* (2016) 122 (7):1050–9. doi: 10.1002/cncr.29893

17. Enomoto T, Tamiya A, Matsumoto K, Adachi Y, Azuma K, Inagaki Y, et al. Nivolumab treatment beyond progressive disease in advanced non-small cell lung cancer. *Clin Transl Oncol* (2021) 23(3):582–90. doi: 10.1007/s12094-020-02452-1

18. Paz-Ares L, Luft A, Vicente D, Tafreshi A, Gümüş M, Mazières J, et al. Pembrolizumab plus chemotherapy for squamous non-small-cell lung cancer. *N Engl J Med* (2018) 379(21):2040–51. doi: 10.1056/NEJMoa1810865

19. Novello S, Kowalski DM, Luft A, Gümüş M, Vicente D, Mazières J, et al. Pembrolizumab plus chemotherapy in squamous non-small-cell lung cancer: 5-year update of the phase III KEYNOTE-407 study. *J Clin Oncol* (2023) 41(11):1999–2006. doi: 10.1200/JCO.22.01990

20. Mansfield AS, Każarnowicz A, Karaseva N, Sánchez A, De Boer R, Andric Z, et al. Safety and patient-reported outcomes of atezolizumab, carboplatin, and etoposide in extensive-stage small-cell lung cancer (IMpower133): a randomized phase I/III trial. *Ann Oncol* (2020) 31(2):310–7. doi: 10.1016/j.annonc.2019.10.021

21. Rudin CM, Awad MM, Navarro A, Gottfried M, Peters S, Csőszi T, et al. Pembrolizumab or placebo plus etoposide and platinum as first-line therapy for extensive-stage small-cell lung cancer: randomized, double-blind, phase III KEYNOTE-604 study. *J Clin Oncol* (2020) 38(21):2369–79. doi: 10.1200/JCO.20.00793

frontiers | Frontiers in Oncology

TYPE Original Research
PUBLISHED 05 October 2023
DOI 10.3389/fonc.2023.1265236

Check for updates

OPEN ACCESS

EDITED BY
Jie Mei,
Wuxi People's Hospital Affiliated to Nanjing Medical University, China

REVIEWED BY
Wenying Peng,
Yunnan Cancer Hospital, China
Alberto Pavan,
Azienda ULSS 3 Serenissima, Italy

*CORRESPONDENCE
Yongfeng Yu
yuyongfeng212@126.com

†These authors share first authorship

RECEIVED 22 July 2023
ACCEPTED 11 September 2023
PUBLISHED 05 October 2023

CITATION
Li X, Huang H, Sun Y, Jiang Q and Yu Y (2023) Immunotherapy strategies for EGFR-mutated advanced NSCLC after EGFR tyrosine-kinase inhibitors failure. *Front. Oncol.* 13:1265236. doi: 10.3389/fonc.2023.1265236

COPYRIGHT
© 2023 Li, Huang, Sun, Jiang and Yu. This is an open-access article distributed under the terms of the Creative Commons Attribution License (CC BY). The use, distribution or reproduction in other forums is permitted, provided the original author(s) and the copyright owner(s) are credited and that the original publication in this journal is cited, in accordance with accepted academic practice. No use, distribution or reproduction is permitted which does not comply with these terms.

Immunotherapy strategies for EGFR-mutated advanced NSCLC after EGFR tyrosine-kinase inhibitors failure

Xingyuan Li[1†], Huayan Huang[1†], Yingjia Sun[1], Qing Jiang[2] and Yongfeng Yu[1*]

[1]Department of Medical Oncology, Shanghai Chest Hospital, Shanghai Jiao Tong University School of Medicine, Shanghai, China, [2]Department of Respiratory and Critical Care Medicine, Fuyang People's Hospital, Fuyang, China

Background: This study aimed to investigate the efficacy of immunotherapy, as monotherapy or in combination, comparing to chemotherapy with or without anti-angiogenesis for advanced non-small cell lung cancer (NSCLC) patients progressing to epidermal growth factor receptor (EGFR)-tyrosine kinase inhibitors (TKIs).

Methods: We retrospectively analyzed patients with advanced NSCLC harboring EGFR mutations who received immune checkpoint inhibitors (ICI) and/or chemotherapy after EGFR-TKIs failure at Shanghai Chest Hospital between Aug 2016 and Oct 2022. According to the subsequent immunotherapy regimen, the patients were assigned to ICI monotherapy (IM), IO plus anti-angiogenesis (IA), ICI plus chemotherapy (IC), ICI plus chemotherapy plus anti-angiogenesis (ICA). Eligible patients undergoing standard chemotherapy were assigned to chemotherapy plus anti-angiogenesis (CA) and chemotherapy alone (CM). Efficacy was evaluated according to the RECIST 1.1version, and calculated the objective response rate (ORR) and disease control rate (DCR). Survival curves were plotted using the Kaplan-Meier method, and the median progression-free survival (PFS) was calculated. Differences among survival curves of the six groups were assessed using the log-rank test.

Results: A total of 237 advanced NSCLC patients with EGFR mutations were included in this study. Of the 160 patients who received immunotherapy, 57 received ICI monotherapy, 27 received ICI plus anti-angiogenesis therapy, 43 received ICI plus chemotherapy, and 33 received ICI plus anti-angiogenesis plus chemotherapy. 77 patients received standard chemotherapy, of which 30 received chemotherapy plus anti-angiogenesis and 47 received chemotherapy alone. Patients in ICA group showed significant longer PFS than IM (7.2 vs 1.9 months, P=0.011), IA (7.2 vs 4.8 months, P=0.009) and CM group (7.2 vs 4.4 months, P=0.005). There was no significant difference in PFS between the ICA and IC (7.2 vs 5.6 months, P=0.104) or CA (7.2 vs 6.7 months, P=0.959) group. Meanwhile, the ICA group showed the highest ORR and DCR (36.4% and 90.9%) compared to the other five groups. The IC group had a higher ORR than the IA and CA group (32.6% vs 7.4% vs 10.0%, respectively), but the DCR was comparable (79.1% vs 74.1% vs 76.7%, respectively). The ORR of the CM group

was 6.4% and the DCR was 66.0%. IM group showed the lowest ORR and DCR (1.8% and 36.8%). Treatment-related adverse events (TRAEs) of grade 3 or worse occurred in 9 (27.3%) patients in the ICA group, 6 (20.0%) in the CA group, 7 (14.9%) in the CM group, 5 (11.6%) in the IC group, 5 (8.8%) in the IM group, and 2 (7.4%) in the IA group.

Conclusion: NSCLC patients with positive EGFR mutations after EGFR-TKIs failure received subsequent immunotherapy plus anti-angiogenesis and chemotherapy are likely to have more benefits in ORR, DCR and mPFS.

KEYWORDS

non-small cell lung cancer, immunotherapy, EGFR mutation, progression, EGFR-TKIs

Highlights

Key findings

- Immunotherapy plus anti-angiogenesis and chemotherapy may have survival benefits than other regimens in NSCLC patients after EGFR-TKIs failure.

What is known and what is new?

- Patients with advanced NSCLC harboring EGFR mutations have limited benefit from chemotherapy or ICI monotherapy after TKIs failure, and combination therapy is the trend. But the optimal treatment strategy is currently controversial.
- Our study compared the efficacy of four immunotherapy-based therapies with chemotherapy alone or chemotherapy plus anti-angiogenesis to find the optimal treatment regimen for NSCLC patients after EGFR-TKIs failure.

What is the implication, and what should change now?

- Our results can provide references for clinicians' treatment choice. Immunotherapy plus anti-angiogenesis and chemotherapy may be the optimal immunotherapy-based combination therapy, but more prospective studies are needed.

Introduction

The most common driver gene mutation of non-small cell lung cancer (NSCLC) in East Asians is epidermal growth factor receptor (*EGFR*) mutation (1). EGFR receptor tyrosine kinase inhibitors (TKIs) are preferred for *EGFR*-sensitive mutations in clinical setting; however, most patients experience problems with acquired resistance and disease progression after receiving EGFR-TKIs for approximately 10 to 18 months (2, 3). The use of standard platinum-based dual-drug chemotherapy as subsequent therapy had a limited effect; therefore, more effective treatment strategies should be investigated for patients who progress on EGFR-TKIs therapy.

Immune checkpoint inhibitors (ICI), including cytotoxic T lymphocyte-associated antigens-4 (CTLA-4) inhibitors, programmed cell death 1 (PD-1) inhibitors and programmed cell death ligand 1 (PD-L1) inhibitors, counteract the immunosuppressive effect of tumors and reactivate the immune response of T cells to inhibit tumor cell growth (4). Several studies have demonstrated the efficacy of ICI therapy in advanced NSCLC (5). Immune checkpoint inhibitors such as the PD-1 inhibitor Nivolumab, Pembrolizumab, and the PD-L1 inhibitor Atezolizumab, and the CTLA-4 inhibitor Ipilimumab have been approved for the treatment of advanced NSCLC. However, first-line immunotherapy has poor efficacy for NSCLC with *EGFR* mutations (6). Clinical studies have found that the tumor immune microenvironment is altered after receiving EGFR-TKIs targeted therapy, including an increase in $CD8^+$ tumor-infiltrating lymphocytes (TILs) density, TMB, and PD-L1 expression in tumor cells (7, 8). This finding suggests the possibility of ICI monotherapy or ICI-based combination therapy for this population. Results from the IMpower150 and ORIENT31 studies further support the administration of ICI-based combination therapy in this setting (9, 10). However, the phase 3 clinical trials CheckMate-722 and KEYNOTE-789 comparing immunotherapy combined with chemotherapy with chemotherapy alone did not show significant results (11, 12). There remains controversy regarding subsequent therapeutic strategies for NSCLC patients harboring *EGFR* mutations previously treated with EGFR-TKIs. Therefore, our study retrospectively reviewed patients with advanced NSCLC after EGFR-TKIs failure in Shanghai Chest Hospital and analyzed clinical outcomes, safety and relevant influential factors of different treatment options.

Materials and methods

Clinical data

This single-center retrospective study was conducted to compare the efficacy of immunotherapy-based regimens with chemotherapy after EGFR-TKIs resistance in *EGFR*-mutant advanced NSCLC patients. Patients with advanced NSCLC after EGFR-TKIs failure at Shanghai Chest Hospital between September 2016 and May 2020 were identified. Patients who interrupted the treatment or did not have imaging data for efficacy assessment were excluded. Due to the small size of the dual immunotherapy patients, they were ultimately not included in the analysis. The baseline clinical characteristics including age, sex, smoking history, tumor pathology type, EGFR mutation subtype, TNM stage, PD-L1 expression status, Eastern Cooperative Oncology Group (ECOG) performance status (PS) score, and lines of therapy were calculated. This study was conducted in accordance with the tenets of the Declaration of Helsinki and the principles of good clinical practice. The protocol and its amendments were approved by the institutional ethical review board of Shanghai Chest Hospital. The ethical review committee waived the requirement for individual informed consent from the patients in this study because of the use of anonymous medical records.

The inclusion and exclusion criteria

The inclusion criteria were as follows: 1. histologically or cytologically confirmed non-small cell lung cancer; 2. diagnosis of stage IIIB-IV based on the 8th edition of TNM staging system; 3. harboring *EGFR*-activating mutations confirmed by tumor histology, cytology, or circulating tumor DNA; 4. previously received at least one EGFR-TKI and had evidence of radiological disease progression; 5. the participants had an ECOG PS of 0-1; 6. at least one measurable lesion according to the Response Evaluation Criteria in Solid Tumors (RECIST) v1.1.

The exclusion criteria were as follows: 1. Prior systemic immunotherapy before EGFR-TKIs; 2. The clinical data were incomplete; 3. Simultaneous diagnosis of any active autoimmune disease or history of autoimmune diseases; 4. no available imaging data to assess the response to immunotherapy or chemotherapy; 5. discontinuation of treatment for any reason.

Pathology, biomarkers and molecular diagnostics

Tumor samples collected from biopsy or surgical resection were used for immunohistochemical detection and confirmed pathological diagnosis of NSCLC. The PD-L1 status was determined by immunohistochemistry (IHC) staining. PD-L1 tumor proportion score (TPS) was defined as the proportion of tumor cells with partial or complete cell membrane staining. PD-L1 expression <1% was classified as a negative result; PD-L1 expression ≥1% and <50% was classified as a positive result; PD-L1 expression ≥50% was classified as a strong positive result. EGFR gene subtype mutations were evaluated by detecting blood or tumor tissue samples using next-generation sequencing (NGS) or polymerase chain reaction (PCR).

Efficacy and safety assessment

Tumor response was assessed using RECIST v1.1. Complete response (CR), complete disappearance of the target lesion, and the short diameter of the pathological lymph nodes decreased to less than 10 mm; partial response (PR), the sum of the target lesion diameter decreased by at least 30%; progressive disease (PD), the sum of the target lesion diameter increased by at least 20% or the appearance of new lesions; stable disease (SD), the increase in diameter of the target lesion did not achieve PD, and the degree of decrease did not achieve PR. Efficacy evaluation includes the overall response rate (ORR) and disease control rate (DCR), where ORR was defined as the proportion of patients who had a CR or PR, and DCR was defined as the proportion of patients who had CR, PR, or SD. Imaging was performed for at least once per cycle during the treatment phase. Interruption of treatment occurred at the time of radiographically identified disease progression. Long term outcomes were evaluated using progression-free survival (PFS), which was measured from the initiation of treatment to radiographic progression. The cut-off date was March 2023, and patients who remained unprogressive at this time were recorded as censored. Adverse events were reported during study treatment and for 30 days after treatment ended and graded as per the National Cancer Institute Common Terminology Criteria for Adverse Events (version 5.0).

Statistical analysis

Data were analyzed by the software SPSS version 25.0 and GraphPad Prism version 8.0. Continuous variables (e.g age) were presented as medians and ranges. Categorical variables were presented as numbers and percentiles. Survival curves were plotted and median PFS (mPFS) was calculated using the Kaplan-Meier (KM) method. The Log-Rank test was used to compare survival differences between groups. PFS relevant influential factors were explored by evaluating hazard ratios (HR) and associated 95% CIs using the Cox proportional hazard model. Differences in ORR, DCR or the other categorical variables were evaluated using Chi-square ($\chi 2$) test or Fisher exact test, as appropriate. Statistical significance was defined as two-sided *P* values of less than 0.05.

Results

Patient characteristics

In total, 855 patients were assessed for eligibility. Based on the inclusion and exclusion criteria, 237 patients were finally included in the analysis. According to the subsequent regimen, the patients

who received immunotherapy were further subdivided into four groups: 57 received ICI monotherapy (IM), 27 received ICI plus anti-angiogenesis (IA), 43 received ICI plus chemotherapy (IC), and 33 received ICI plus chemotherapy plus anti-angiogenesis (ICA). Patients who received standard chemotherapy were separated into two groups: 30 received chemotherapy plus anti-angiogenesis (CA) and 47 received chemotherapy alone (CM) (Figure 1). The median age of all patients was 61 years (range 35-77 years), and 56.5% of the patients were female (n=134). 98.7% of patients were diagnosed with lung adenocarcinoma (n=234). Two patients who received immunotherapy were diagnosed with poorly differentiated non-small cell lung cancer. One patient who received chemotherapy was diagnosed with lung squamous cell carcinoma. Of the patients, 89% (n=211) harbored common *EGFR* mutations, with *EGFR* exon 19 deletion (19del) in 54.8% (n=130), *EGFR* exon 21 L858R mutation (21L858R) in 34.2% (n=81), and the remaining 11.0% (n=26) harbored EGFR rare mutations. 66.2% (n=157) of patients were diagnosed with stage IVB, 25.3% (n=60) with stage IVA, and 8.4% (n=20) with stage IIIB or IIIC. All patients had good performance status (ECOG=0-1). 30.8% (n=73) of the patients acquired the T790M mutation after receiving the first or second generation of EGFR-TKIs. PD-L1 expression was detected in 45.6% (n=108) of all patients, and 41.4% (n=98) of those patients had received immunotherapy. In total, 61.6% (n=146) of the patients received PD-1 inhibitors, 5.9% (n=14) received PD-L1 inhibitors, and 32.5% (n=77) received chemotherapy. Detailed treatments of immunotherapy populations are showed in Table S1. 36.3% (n=86) of the patients received fourth line or later line of therapy, 29.5% (=70) received third line of therapy, and 34.2% (n=81) received second line of therapy. Except lines of therapy and PD-L1 status, demographic and clinical characteristics were well balanced among the groups at baseline, and the data are listed in Table 1.

Efficacy evaluation

For the entire study population, the ORR was 14.8% and the DCR was 67.1% (Table 2). Comparative analysis of six groups, the highest ORR was observed in the ICA group, followed by the IC, CA, IA, CM group, and the lowest ORR was observed in the IM group (36.4% vs 32.6% vs 10.0% vs 7.4% vs 6.4% vs 1.8%, Table 2). Similarly, the highest DCR was observed in the ICA group, followed by the IC, CA, IA, CM group, and the lowest DCR was observed in the IM group (90.9% vs 79.1% vs 76.7% vs 74.1% vs 66.0% vs 36.8%, Table 2). The ICA group and IC group showed similar ORR (36.4% and 32.6%, respectively, Table 2), which were higher than those of the other four groups. Meanwhile, the ICA group showed a higher DCR (90.9%) than the other five groups (Table 2). There was no significant difference between the DCR of the IC, IA, and CA group (79.1% vs 74.1% vs 76.7%, respectively) (Table 2). ICI monotherapy resulted in a significant lower DCR (36.8%) than those of other five groups (Table 2).

Long term outcomes

The median PFS of all eligible patients was 4.9 months (Table 2). The mPFS was longest in the ICA group, followed by CA, IC, IA and CM group, and shortest in IM group (7.2 [95%CI:

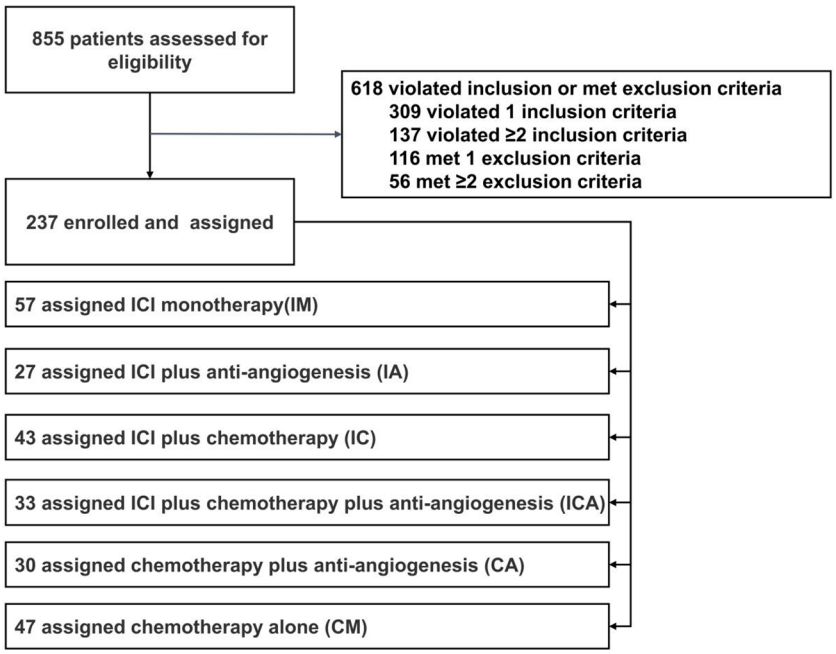


FIGURE 1
Study flow chart. Between September 2016 and May 2020,855 patients were assessed for eligibility, and 237 patients were finally brought into the analysis, include 57 received ICI monotherapy (IM), 27 received ICI plus anti-angiogenesis (IA), 43 received ICI plus chemotherapy (IC), 33 received ICI plus chemotherapy plus anti-angiogenesis (ICA),30 received chemotherapy plus anti-angiogenesis (CA) and 47 received chemotherapy alone (CM).

TABLE 1 Baseline demographic and clinical characteristics of patients stratified by treatment strategies after TKIs failure (n=237).

Characteristics	Total (n=237)	IM (n=57)	IA (n=27)	IC (n=43)	ICA (n=33)	CA (n=30)	CM (n=47)	P value
Age, years, median (range)	61 (35-77)	63 (39-77)	62 (35-73)	58 (35-75)	64 (39-76)	58 (37-74)	61(39-76)	0.157
Gender, n (%)								0.426
Male	103(43.5)	26(45.6)	7(25.9)	20(46.5)	14(42.4)	12(40.0)	24(51.1)	
Female	134(56.5)	31(54.4)	20(74.1)	23(53.5)	19(57.6)	18(60.0)	23(48.9)	
Smoking history, n (%)								0.538
Current or former	53(22.4)	13(22.8)	3(11.1)	12(27.9)	7(21.2)	5(16.7)	13(27.7)	
Never	184(77.6)	44(77.2)	24(88.9)	31(72.1)	26(78.8)	25(83.3)	34(72.3)	
TNM Stage, n (%)								0.713
III Stage	20(8.4)	5(8.8)	3(11.1)	3(7.0)	2(6.1)	2(6.7)	5(10.6)	
IVA Stage	60(25.3)	14(24.6)	3(11.1)	14(32.6)	11(33.3)	9(30.0)	9(19.1)	
IVB Stage	157(66.2)	38(66.7)	21(77.8)	26(60.5)	20(60.6)	19(63.3)	33(70.2)	
PD-L1 percentage expression, n (%)								<0.001
<1%	45(19.0)	6(10.5)	8(29.6)	15(34.9)	13(39.4)	1(3.3)	2(4.3)	
1-49%	33(13.9)	10(17.5)	8(29.6)	4(9.3)	6(18.2)	1(3.3)	4(8.5)	
≥50%	30(12.7)	8(14.0)	3(11.1)	8(18.6)	9(27.3)	0	2(4.3)	
Not examined	129(54.4)	33(57.9)	8(29.6)	16(37.2)	5(15.2)	28(93.3)	39(83.0)	
EGFR subtypes, n (%)								*0.810*
19Del	130(54.9)	32(56.1)	18(66.7)	24(55.8)	14(42.4)	18(60.0)	24(51.1)	
L858R	81(34.2)	19(33.3)	7(25.9)	12(27.9)	15(45.5)	10(33.3)	18(38.3)	
Rare mutations[a]	26(11.0)	6(10.5)	2(7.4)	7(16.3)	4(12.1)	2(6.7%)	5(10.6)	
Lines of therapy, n (%)								<0.001
2	81(34.2)	3(5.3)	6(22.2)	15(34.9)	17(51.5)	13(43.3)	27(57.4)	
3	70(29.5)	17(29.8)	3(11.1)	11(25.6)	9(27.3)	14(46.7)	16(34.0)	
≥4	86(36.3)	37(64.9)	18(66.7)	17(39.5)	7(21.2)	3(10.0)	4(8.5)	

[a]Rare mutations included one 18G719X and 18E709K co-mutations, one 18G719X and 20R776C co-mutations, one 19del and 21L861Q co-mutations, one 19del and 4S177L co-mutations, two 20ins, one 20S768I, one 20S768I and 18G719X co-mutations, two 21L858R and 20S768I co-mutations, one 21L858R and 21A871G co-mutations, one 21L858R and 7A289D co-mutations, one 21L858R and 21T854A co-mutations, one 21L858R and 21V834L co-mutations, one 21L858R and 4del and 8S315R co-mutations, two 21L861Q, one 21L861Q and 20V769L co-mutations, one EGFR amplification and 20ins co-mutations in immunotherapy population. One 18G719X and 20S768Ico-mutations, one 18G719X and 241L861Q co-mutations, one 20ins, one 20S768I, one 21L858R and 20S768I co-mutations, one 21L858R and 21L838V co-mutations, one 21L861Q in chemotherapy population. IM, ICI monotherapy; IA, ICI plus anti-angiogenesis; IC, ICI plus chemotherapy; ICA, ICI plus chemotherapy plus anti-angiogenesis; CA, chemotherapy plus anti-angiogenesis; CM, chemotherapy alone; ICI, immune checkpoint inhibitors; TNM, tumor node metastasis classification; PD-L1, programmed cell death ligand 1; EGFR, epidermal growth factor receptor.

4.4-10.0 months] vs 6.7 [95%CI: 4.6-8.8 months] vs 5.6 [95%CI: 4.8-6.4 months] vs 4.8 [95%CI: 2.8-6.8 months] vs 4.4 [95%CI: 3.6-5.5 months] vs 1.9 [95%CI: 1.0-2.8 months]) (Figure 2A). Patients in ICA group showed significant longer PFS than IM (7.2 vs 1.9 months, *P*=0.011), IA (7.2 vs 4.8 months, *P*=0.009) and CM (7.2 vs 4.4 months, *P*=0.005) group (Figure 2B). Similarly, patients in CA group showed significant longer PFS than IM (6.7 vs 1.9 months, *P*=0.012), IA (6.7 vs 4.8 months, *P*=0.018) and CM (6.7 vs 4.4 months, *P*=0.008) group (Figure 2B). There was no significant difference in PFS between the ICA and CA (7.2 vs 6.7 months, *P*=0.959) group (Figure 2B). The mPFS of IC group was longer than IM (5.6 vs 1.9 months, *P*=0.183), IA (5.6 vs 4.8 months, *P*=0.083) and CM (5.6 vs 4.4 months, P=0.145) group, but without statistical difference (Figure 2B). In these analyses, both ICA and CA therapy showed superior mPFS than other therapeutic strategies.

Safety

TRAEs had the highest incidence rate in the ICA group(26 [78.8%]) followed by the CA group(21 [70.0%]).TRAEs of any grade occurred in a similar proportion of patients in IA, IC, CM group (16 [59.3%] vs 25 [58.1%] vs 30 [63.8%]).While the IM group had the lowest incidence of TRAEs(22 [38.6%]).TRAEs of grade 3

10.3389/fonc.2023.1265236

TABLE 2 Efficacy of subsequent therapy of patients.

Efficacy	Total (n=237)	IM (n=57)	IA (n=27)	IC (n=43)	ICA (n=33)	CA (n=30)	CM (n=47)	P value
CR, n (%)	0	0	0	0	0	0	0	<0.001
PR, n (%)	35(14.8)	1(1.8)	2(7.4)	14(32.6)	12(36.4)	3(10.0)	3(6.4)	
SD, n (%)	125(52.7)	20(35.1)	18(66.7)	20(46.5)	18(54.5)	21(70.0)	28(59.6)	
PD, n (%)	77(32.5)	36(63.2)	7(25.9)	9(20.9)	3(9.1)	6(20.0)	16(34.0)	
ORR (%)	14.8	1.8_a	$7.4_{a,b}$	32.6_b	36.4_b	$10.0_{a,b}$	6.4_a	<0.001
DCR (%)	67.1	36.8_a	74.1_b	79.1_b	90.9_b	76.7_b	66.0_b	<0.001
mPFS (months)	4.9	1.9	4.8	5.6	7.2	6.7	4.4	0.0107

ORR and DCR for each group with the same letter (a or b) are not significantly different. CR, Complete response; PR, partial response; PD, progressive disease; SD, stable disease; ORR, overall response rate; DCR, disease control rate; mPFS, median progression-free survival.

or worse occurred in 9 (27.3%) patients in the ICA group, 6 (20.0%) in the CA group, 7 (14.9%) in the CM group, 5 (11.6%) in the IC group, 5 (8.8%) in the IM group, and 2 (7.4%) in the IA group. The most common TRAEs were leukopenia (4 [7.0%] in the IM group vs 0 in the IA group vs 18 [41.9%] in the IC group vs 19 [57.6%] in the ICA group vs 14 [46.7%] in the CA group vs 21 [44.7%] in the CM group). Details of TRAEs were provided in Table S2.

Clinical factors associated with PFS

A total of 160 patients who received immunotherapy were included in the univariate and multivariate analyses. Age, gender, smoking history, TNM stage, and line of therapy were included as independent variables. Age was taken as a continuous numerical variable, and its measured value was taken. All of the categorical

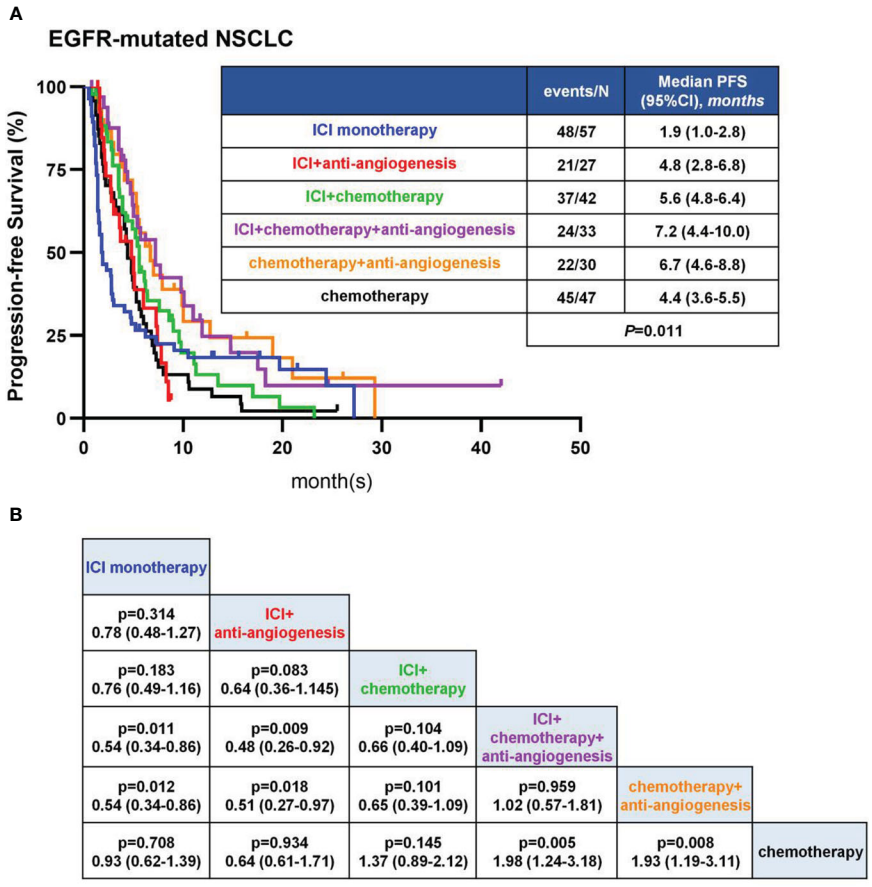


FIGURE 2
PFS in EGFR-mutant patients. **(A)** Kaplan-Meier analyses in different therapies. **(B)** Pairwise comparisons among therapies in log-rank test.

TABLE 3 Clinical parameters associated with PFS in univariate and multivariate analyses.

Univariate	Age	Gender	Smoking history	TNM stage	Lines of therapy
HR (95%CI)	0.988 (0.971-1.004)	0.971 (0.685-1.378)	1.154 (0.758-1.758)	1.432 (1.066-1.922)	1.382 (1.118-1.710)
p	0.149	0.870	0.505	0.017	0.003
Multivariate					
HR (95%CI)	0.993 (0.976-1.010)	0.826 (0.540-1.263)	1.323 (0.792-2.207)	1.304 (0.957-1.777)	1.309 (1.047-1.635)
p	0.397	0.377	0.285	0.092	0.018

TNM, tumor node metastasis classification; HR, hazard ratios; CI, confidence interval.

variables were summarized with frequencies and percentages and were analyzed using the χ^2 or Fisher exact test, as appropriate. Univariate COX regression analysis showed that age, sex, and smoking history were not risk factors for disease progression in the patients receiving immunotherapy (Table 3). A more advanced disease stage seems to be related with a shorter PFS (Table 3). Patients receiving an earlier line of immunotherapy showed enhanced survival benefits compared with those who received immunotherapy as a later line (Table 3). Multivariate COX regression analysis showed that gender, age, smoking history, and TNM stage were not risk factors of disease progression in the immunotherapy group (Table 3). Similarly, the earlier immunotherapy was applied, the more it delayed disease progression (Table 3). It should be noted that, owing to the limited case size, the univariate and multivariate analyses did not include the *EGFR* mutant subtype and PD-L1 expression status as independent variables.

Subgroup analysis of patients with common *EGFR* mutations

Among 211 patients with common *EGFR* mutations, 141 patients received immunotherapy, including 88 patients with 19del and 53 patients with 21L858R mutation. There was no significant difference in ORR and DCR between 19del and 21L858R mutations subgroups (P=0.066, P=0.870, respectively) (Table S3). The mPFS was 3.7 months (95%CI: 2.6-4.8 months) in 19del group, and 4.9 months (95%CI: 3.5-6.3 months) in 21L8585R mutations group, with a tendency for longer PFS in 21L858R subgroup, but the difference was not significant (P=0.767) (Figure 3).

Subgroup analysis of patients with PD-L1 expression

Among 160 patients receiving immunotherapy, PD-L1 expression was detected in 98 patients, of which 42 patients were PD-L1 negative (<1%), 28 patients were PD-L1 positive (1% -49%), and 28 patients were PD-L1 strongly positive (≥50%). All patients with PD-L1 expression who received immunotherapy had an ORR of 24.5%, DCR of 72.5%, and median PFS of 5.6 months (95%CI, 4.7-6.5 months) (Table S4). ORR of PD-L1 negative patients was 21.4%, DCR was 71.4%, median PFS was 5.1 months (95%CI, 3.2-7.0 months); for patients with PD-L1 positive, ORR was 14.3%, DCR was 64.3%, and median PFS was 5.6 months (95%CI, 3.6-7.6

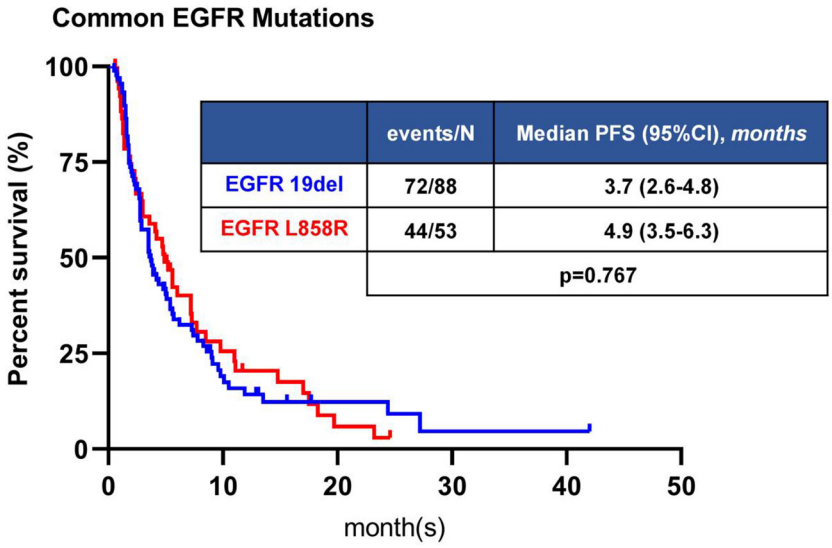


FIGURE 3
Kaplan-Meier analyses of PFS of patients with common *EGFR* mutation. The difference in PFS was not statistically significant between 19del and L858R.

months); for patients with PD-L1 strongly positive, ORR was 39.3%, DCR was 82.1%, and median PFS was 5.7 months (95%CI, 4.6-6.8 months) (Table S4). There was no significant difference in the ORR and DCR (P=0.078, P=0.312, respectively) among these three groups for pairwise comparisons (Table S4). The PD-L1 positive and strongly positive groups tended to have a longer PFS than the PD-L1 negative group, but the difference was not significant (P=0.211) (Figure 4).

Discussion

The standard first-line treatment for patients with advanced EGFR-mutated NSCLC are EGFR-TKIs. There are limited treatment options for patients who are refractory to third-generation EGFR-TKIs and for T790M-negative patients who have received first- or second-generation EGFR-TKIs. The most commonly recommended treatment is platinum-containing doublet chemotherapy with or without bevacizumab. *In vitro* experiments confirmed that the co-culture system of *EGFR*-mutant tumor cells with immune cells was able to reduce the viability of tumor cells after treatment with PD-1 inhibitors (13). The anti-tumor effect of PD-1 inhibitors has also been demonstrated in preclinical models with *EGFR* mutations (14). These preclinical studies suggested the possibility of treating *EGFR*-mutant NSCLC with ICI. However, the initial clinical findings did not support this. Several prospective studies have shown no survival benefit from the use of immunosuppressive agents versus chemotherapy in NSCLC patients with *EGFR* mutations (15–18). Moreover, most clinical trials of immune checkpoint suppression have also excluded NSCLC patients with driver gene mutations. Therefore, there is an urgent need to develop immune-based combination therapies for NSCLC patients with *EGFR* mutations.

Our study basically included a variety of mainstream and non-mainstream treatment regimens after TKIs resistance. Analysis of these regimens revealed that the mPFS was longest in the ICA group, followed by the CA, IC, IA, and CM group, and the shortest in the IM group. The ICA group had the highest ORR and DCR, followed by the IC, CA, IA, and CM group, and the lowest was in the IM group. Further differential analysis showed that in terms of mPFS, there was no significant difference between the ICA, CA, and IC group for pairwise comparisons. The same results were obtained from the IC, IA, CM, and IM group for pairwise comparisons. There were many interesting conclusions to draw from these analyses.

Combination regimens were superior to monotherapy. In terms of PFS, the ICA group was longer than the CM or IM group in our study. In terms of the ORR and DCR, the ICA group was better than the IM group. The prospective study ORIENT31 included 444 patients with *EGFR* mutations after EGFR-TKIs failure, randomly assigned to sintilimab plus IBI305 plus pemetrexed and cisplatin (ICA), sintilimab plus pemetrexed and cisplatin (IC), or pemetrexed and cisplatin groups (CM). The mPFS of the ICA group was 6.9 months and the mPFS for the CM group was 4.3 months in ORIENT31. The difference in PFS between the two groups was statistically significant (P<0.0001) (9). The mPFS in both groups was consistent with the results of our study. Otherwise, our study analysis showed a longer mPFS in the CA group than in the CM or IM group. According to a prospective study, the mPFS of patients with advanced NSCLC received bevacizumab plus chemotherapy was 6.2 months and chemotherapy alone was 4.5 months, and the difference was statistically significant (19). The results were also consistent with the results of our analysis. However, one study showed that chemotherapy combined with anti-angiogenesis was not superior to chemotherapy alone in patients with advanced non-small cell lung cancer (20). Many studies have confirmed the poor efficacy of ICI monotherapy in patients with EGFR-mutant NSCLC. A Japanese randomized controlled study included 102 patients with EGFR-mutant NSCLC after TKIs resistance, with a mPFS of 1.7 months in the nivolumab group and 5.6 months in the carboplatin-pemetrexed group and

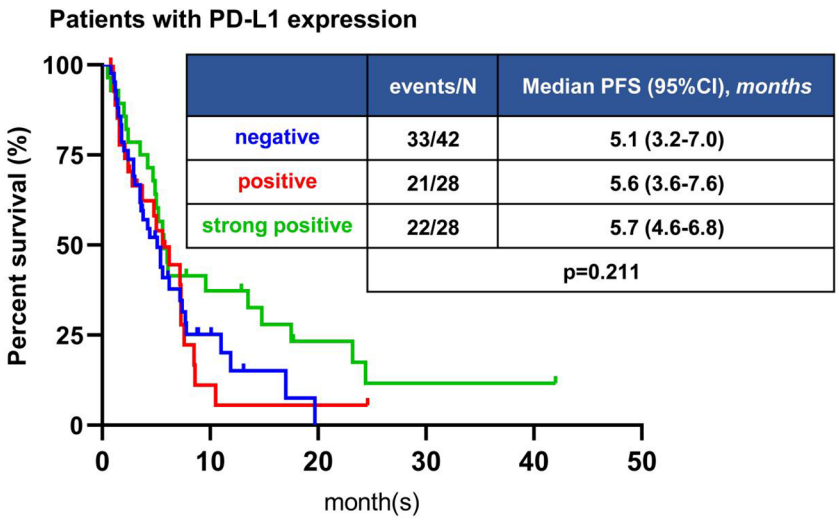


FIGURE 4
Kaplan-Meier analyses of PFS of patients with different PD-L1 expression. The difference in PFS was not statistically significant among different PD-L1 status.

differences were significant (21). Therefore, CA efficacy was better than IM, which was in line with our expectations.

A subsequent question has to be raised: which regimen has better efficacy comparing ICA with CA? The prospective study Impower150 included 124 chemotherapy-naive NSCLC patients with *EGFR* mutations, of which 91 patients with EGFR sensitive mutations were assigned to three different regimens: atezolizumab plus bevacizumab plus carboplatin plus paclitaxel (ABCP), bevacizumab plus carboplatin plus paclitaxel (BCP), and atezolizumab plus carboplatin plus paclitaxel (ACP). The results showed that in the 124 EGFR mutation subgroup, the HR for ABCP versus BCP was 0.61 (95% CI 0.36-1.03). The mPFS was 10.2 months for the ABCP group, 6.9 months for the BCP group. With respect to the mOS, the ABCP group also improved compared to the BCP group (10). In conclusion, ICA tended to be better than CA, which was consistent with our results. Given that IMpower150 is a small-scale subgroup analysis, it cannot be concluded that ICA was superior to the CA regimen, and the results need to be confirmed by more prospective studies. The mPFS from each treatment group obtained from the IMpower150 study had a gap to compare with our results, and it needed to be considered that we were based on real-world research; most patients received overline therapy, immunotherapy for these patients was a very posterior treatment, and our study showed that the line of therapy on the efficacy of immunotherapy is very obvious. In addition, IMpower150 enrolled patients before osimertinib was approved as first-line treatment.

In addition, pairwise combination regimens of anti-angiogenesis, immunotherapy, and chemotherapy included the CA, IC, and IA group. For the CA or IA group, anti-angiogenesis combination chemotherapy or immunotherapy was feasible. According to previous studies, there was a synergistic effect between chemotherapeutic agents and antiangiogenic agents. Elevated VEGF levels could lead to tumor vascular disorders, increased permeability and interstitial pressure, and affect the delivery of chemotherapeutic agents into the tumor (22). Bevacizumab could promote the delivery of chemotherapeutic agents into the tumor (23). On the other hand, there was also synergy between antiangiogenic agents and immune checkpoint inhibitors, and antiangiogenic agents showed immunomodulatory effects (24), could improve the tumor microenvironment for immunosuppression in patients with EGFR mutations. Our results indicate that the CA group had a significant longer mPFS than the IA group. However, the ORR and DCR were similar between the two groups. For the CA and IC group, combining immunotherapy or anti-angiogenesis based on chemotherapy, the former mPFS was longer than the latter, but there was no significant difference. In the IMpower150 study, in the EGFR mutation subgroup, the HR for PFS with ACP versus BCP was 1.14 (95% CI 0.73-1.18), mPFS 6.9 months in the ACP group, and mPFS 6.9 months in the BCP group. However, in the 56 patients who had previously received EGFR-TKIs, the mPFS of the BCP group was 6.1 months, which was slightly longer than that of the ACP group (mPFS=5.7 months) (10). The results of the subgroup analysis of IMpower150 were similar to our conclusions. Another real-world retrospective study from Shanghai Pulmonary Hospital achieved similar conclusions: the mPFS was 6.90 months in the CA group and 7.59 months in the IC group, and there was no significant difference in PFS (25). However, another retrospective study showed that OS was worse in the IC group comparing with the CA group (HR 2.37, 95%CI 1.09-5.65, *P*=0.030) (26). Similarly, comparing IC with IA regimens, based on immunotherapy combined with chemotherapy or anti-angiogenesis, the former mPFS was longer than the latter, no significant difference was observed in PFS.

Although combination therapy was superior to monotherapy, some exceptions existed. For example, the IC group had a longer mPFS than the CM and IM group, but there was no significant difference in PFS. CheckMate-722 and KEYNOTE-789 study also showed no survival benefit between the IC and CM group (11, 12). However, the results of the latest ORIENT31 second interim analysis showed that mPFS was 5.5 months in the IC group and 4.3 months in the CM group, which was similar with our results. But the difference between these two groups in ORIENT31 trail was statistically significant (*P*=0.016) (27). In addition, the mPFS of the IA group was longer than the CM and IM group, and no significant difference was observed. For IA and CM regimen, the prospective study of Runbo Zhong's team showed that anlotinib combined with PD-1 inhibitors exhibited better mPFS than chemotherapy group (4.33 vs 3.6 months), a significant increase of nearly 1 month (*P*=0.005). The mOS was 14.17 months in the combination therapy group and 9.00 months in the chemotherapy group, with a significant extension of 5.17 months (*P*=0.029). The DCR of anlotinib combined with PD-1 inhibitor group was 92.1% (28). Compared with our analysis results, we found that the study IA regimen mPFS was longer, the DCR was higher, and the CM regimen mPFS was shorter.

In terms of safety, despite higher rates of grade ≥3 TRAEs, our results show that the ICA group was generally well tolerated with no new safety signals. This is similar to previous studies of such regimens in other patient populations (9, 10).

Multivariate analysis showed that for NSCLC patients with *EGFR* mutations who failed EGFR-TKIs treatment, the earlier they received immunotherapy, the superior benefit in PFS. A clinical study reported that patients who received EGFR-TKIs had alteration in their tumor microenvironment that contributed to immunotherapy. If other treatments were performed during this period, it might lead to the interference of the favorable tumor microenvironment, which could affect the subsequent treatment of ICI (29). Therefore, the timing of immunotherapy administration was equally important.

Subgroups with common *EGFR* mutations receiving immunotherapy were analyzed in our study. The results indicated that patients with the 21L858R mutation tended to have longer mPFS compared with the 19del-mutant population, but the difference was not statistically significant. However, a clinical study showed that patients with the L858R mutation receiving immunotherapy had a better response and an OS benefit compared with 19del population (30).

Analysis of the population detecting PD-L1 status showed that there was no significant difference in the median PFS, ORR and DCR in the PD-L1 high expression group compared with the low expression and negative groups. However, clinically relevant studies were controversial. A single-arm study of toripalimab combined with chemotherapy at the Shanghai Pulmonary Hospital confirmed that the PD-L1 expression levels were not associated with ICI efficacy (31).

The study by Shunli Peng et al. found that the ORR in the high PD-L1 expression group was higher than that in the low PD-L1 expression group in *EGFR* mutant patients receiving ICI (32). Another study showed that TMB might be a more suitable biomarker for predicting ICI efficacy than PD-L1 (33). Although high PD-L1 expression suggested a better response to PD-1/PD-L1 inhibitors, it was not absolute, and some patients with high PD-L1 expression still could not benefit from ICI. The reasons included a range of factors, such as tumor mutation burden (TMB), coexisting other gene mutations, microsatellite instability (MSI), "cold" or "hot" tumor microenvironment can affect the efficacy of ICI (34–37).

Our study had several limitations. It was retrospective in nature, leading to the possibility of bias in clinical data. No additional patients receiving dual immunotherapy were included because only eight patients were identified when we reviewed the medical records. However, our study is the first to compare most treatment regimens after EGFR-TKIs failure. Moreover, because driver gene-positive patients did not respond to ICI, most of the current studies did not set an IM group for patients after receiving EGFR-TKIs, and our study precisely included these population. In contrast, our study might able to draw more comprehensive conclusions. To some extent, our analytical results provided a reference for subsequent immunotherapy strategies for similar patients. ICI-based combination therapy, especially immunotherapy combination chemotherapy and anti-angiogenesis might be the preferred treatment regimen for advanced NSCLC patients with *EGFR* mutations after EGFR- TKIs failure.

Conclusions

In conclusion, our results suggest that immunotherapy combination chemotherapy and anti-angiogenesis are more likely to prolong PFS and improve ORR and DCR than other strategies. However, more prospective clinical studies are still needed to further confirm the efficacy of this strategy.

Data availability statement

The original contributions presented in the study are included in the article/Supplementary Material. Further inquiries can be directed to the corresponding author.

Ethics statement

The studies involving humans were approved by institutional ethical review board of Shanghai Chest Hospital (ethical approval number:KS22021). The studies were conducted in accordance with the local legislation and institutional requirements. The ethics committee/institutional review board waived the requirement of written informed consent for participation from the participants or the participants' legal guardians/next of kin because individual consent for this retrospective analysis was waived.

Author contributions

YY: Conceptualization, Formal Analysis, Methodology, Validation, Writing – review & editing. XL: Conceptualization, Data curation, Formal Analysis, Investigation, Methodology, Software, Validation, Visualization, Writing – original draft, Writing – review & editing. HH: Conceptualization, Data curation, Formal Analysis, Investigation, Methodology, Software, Validation, Visualization, Writing – original draft, Writing – review & editing. YS: Conceptualization, Validation, Writing – review & editing. QJ: Conceptualization, Data curation, Validation, Writing – review & editing.

Funding

The authors declare financial support was received for the research, authorship, and/or publication of this article. This study was supported by the Beijing Xisike Clinical Oncology Research Foundation (grant number: Y-HR2020MS-0982) and the National Natural Science Foundation of China (grant numbers: 82172633).

Acknowledgments

We thank all investigators in our center for supporting this study.

Conflict of interest

YY reported that he received fundings of the Beijing Xisike Clinical Oncology Research Foundation grant number: Y-HR2020MS-0982, the National Natural Science Foundation of China 82172633.

The remaining authors declare that the research was conducted in the absence of any commercial or financial relationships that could be constructed as a potential conflict of interest.

Publisher's note

All claims expressed in this article are solely those of the authors and do not necessarily represent those of their affiliated organizations, or those of the publisher, the editors and the reviewers. Any product that may be evaluated in this article, or claim that may be made by its manufacturer, is not guaranteed or endorsed by the publisher.

Supplementary material

The Supplementary Material for this article can be found online at: https://www.frontiersin.org/articles/10.3389/fonc.2023.1265236/full#supplementary-material

References

1. Sharma SV, Bell DW, Settleman J, Haber DA. Epidermal growth factor receptor mutations in lung cancer. *Nat Rev Cancer* (2007) 7(3):169–81. doi: 10.1038/nrc2088

2. Thai AA, Solomon BJ, Sequist LV, Gainor JF, Heist RS. Lung cancer. *Lancet* (2021) 398(10299):535–54. doi: 10.1016/S0140-6736(21)00312-3

3. Soria JC, Ohe Y, Vansteenkiste J, Reungwetwattana T, Chewaskulyong B, Lee KH, et al. Osimertinib in untreated EGFR-mutated advanced non-small-cell lung cancer. *N Engl J Med* (2018) 378(2):113–25. doi: 10.1056/NEJMoa1713137

4. Zarour HM. Reversing T-cell dysfunction and exhaustion in cancer. *Clin Cancer Res* (2016) 22(8):1856–64. doi: 10.1158/1078-0432.CCR-15-1849

5. Dafni U, Tsourti Z, Vervita K, Peters S. Immune checkpoint inhibitors, alone or in combination with chemotherapy, as first-line treatment for advanced non-small cell lung cancer. *A Systematic Rev Netw Meta-Analysis Lung Cancer* (2019) 134:127–40. doi: 10.1016/j.lungcan.2019.05.029

6. Lisberg A, Cummings A, Goldman JW, Bornazyan K, Reese N, Wang T, et al. A phase II study of pembrolizumab in EGFR-mutant, PD-L1+, tyrosine kinase inhibitor naïve patients with advanced NSCLC. *J Thorac Oncol* (2018) 13(8):1138–45. doi: 10.1016/j.jtho.2018.03.035

7. Sugiyama E, Togashi Y, Takeuchi Y, Shinya S, Tada Y, Kataoka K, et al. Blockade of EGFR improves responsiveness to PD-1 blockade in EGFR-mutated non-small cell lung cancer. *Sci Immunol* (2020) 5(43):eaav3937. doi: 10.1126/sciimmunol.aav3937

8. Isomoto K, Haratani K, Hayashi H, Shimizu S, Tomida S, Niwa T, et al. Impact of EGFR-TKI treatment on the tumor immune microenvironment in EGFR mutation-positive non-small cell lung cancer. *Clin Cancer Res* (2020) 26(8):2037–46. doi: 10.1158/1078-0432.CCR-19-2027

9. Lu S, Wu L, Jian H, Chen Y, Wang Q, Fang J, et al. Sintilimab plus bevacizumab biosimilar IBI305 and chemotherapy for patients with EGFR-mutated non-squamous non-small-cell lung cancer who progressed on EGFR tyrosine-kinase inhibitor therapy (ORIENT-31): first interim results from a randomised, double-blind, multicentre, phase 3 trial. *Lancet Oncol* (2022) 23(9):1167–79. doi: 10.1016/S1470-2045(22)00382-5

10. Reck M, Mok TSK, Nishio M, Jotte RM, Cappuzzo F, Orlandi F, et al. Atezolizumab plus bevacizumab and chemotherapy in non-small-cell lung cancer (IMpower150): key subgroup analyses of patients with EGFR mutations or baseline liver metastases in a randomised, open-label phase 3 trial. *Lancet Respir Med* (2019) 7 (5):387–401. doi: 10.1016/S2213-2600(19)30084-0

11. Mok TSK, Nakagawa K, Park K, Ohe Y, Girard N, Kim HR, et al. LBA8 Nivolumab (NIVO) + chemotherapy (chemo) vs chemo in patients (pts) with EGFR-mutated metastatic non-small cell lung cancer (mNSCLC) with disease progression after EGFR tyrosine kinase inhibitors (TKIs) in CheckMate 722. *Ann Oncol* (2022) 33: S1561–S2. doi: 10.1016/j.annonc.2022.10.350

12. Yang JC-H, Lee DH, Lee J-S, Fan Y, de Marinis F, Okamoto I, et al. Pemetrexed and platinum with or without pembrolizumab for tyrosine kinase inhibitor (TKI)-resistant, EGFR-mutant, metastatic nonsquamous NSCLC: Phase 3 KEYNOTE-789 study. *Am Soc Clin Oncol* (2023) 41(17_suppl):LBA9000-LBA9000. doi: 10.1200/JCO.2023.41.17_suppl.LBA9000

13. Chen N, Fang W, Zhan J, Hong S, Tang Y, Kang S, et al. Upregulation of PD-L1 by EGFR activation mediates the immune escape in EGFR-driven NSCLC: implication for optional immune targeted therapy for NSCLC patients with EGFR mutation. *J Thorac Oncol* (2015) 10(6):910–23. doi: 10.1097/JTO.0000000000000500

14. Akbay EA, Koyama S, Carretero J, Altabef A, Tchaicha JH, Christensen CL, et al. Activation of the PD-1 pathway contributes to immune escape in EGFR-driven lung tumors. *Cancer Discovery* (2013) 3(12):1355–63. doi: 10.1158/2159-8290.CD-13-0310

15. Borghaei H, Paz-Ares L, Horn L, Spigel DR, Steins M, Ready NE, et al. Nivolumab versus docetaxel in advanced nonsquamous non-small-cell lung cancer. *N Engl J Med* (2015) 373(17):1627–39. doi: 10.1056/NEJMoa1507643

16. Herbst RS, Baas P, Kim DW, Felip E, Perez-Gracia JL, Han JY, et al. Pembrolizumab versus docetaxel for previously treated, PD-L1-positive, advanced non-small-cell lung cancer (KEYNOTE-010): a randomised controlled trial. *Lancet* (2016) 387(10027):1540–50. doi: 10.1016/S0140-6736(15)01281-7

17. Fehrenbacher L, Spira A, Ballinger M, Kowanetz M, Vansteenkiste J, Mazieres J, et al. Atezolizumab versus docetaxel for patients with previously treated non-small-cell lung cancer (POPLAR): a multicentre, open-label, phase 2 randomised controlled trial. *Lancet* (2016) 387(10030):1837–46. doi: 10.1016/S0140-6736(16)00587-0

18. Rittmeyer A, Barlesi F, Waterkamp D, Park K, Ciardiello F, von Pawel J, et al. Atezolizumab versus docetaxel in patients with previously treated non-small-cell lung cancer (OAK): a phase 3, open-label, multicentre randomised controlled trial. *Lancet* (2017) 389(10066):255–65. doi: 10.1016/S0140-6736(16)32517-X

19. Sandler A, Gray R, Perry MC, Brahmer J, Schiller JH, Dowlati A, et al. Paclitaxel-carboplatin alone or with bevacizumab for non-small-cell lung cancer. *N Engl J Med* (2006) 355(24):2542–50. doi: 10.1056/NEJMoa061884

20. Zinner RG, Obasaju CK, Spigel DR, Weaver RW, Beck JT, Waterhouse DM, et al. PRONOUNCE: randomized, open-label, phase III study of first-line pemetrexed + carboplatin followed by maintenance pemetrexed versus paclitaxel + carboplatin + bevacizumab followed by maintenance bevacizumab in patients ith advanced nonsquamous non-small-cell lung cancer. *J Thorac Oncol* (2015) 10(1):134–42. doi: 10.1097/JTO.0000000000000366

21. Hayashi H, Sugawara S, Fukuda Y, Fujimoto D, Miura S, Ota K, et al. A randomized phase II study comparing nivolumab with carboplatin-pemetrexed for EGFR-mutated NSCLC with resistance to EGFR tyrosine kinase inhibitors (WJOG8515L). *Clin Cancer Res* (2022) 28(5):893–902. doi: 10.1158/1078-0432.CCR-21-3194

22. Jain RK. Normalizing tumor vasculature with anti-angiogenic therapy: a new paradigm for combination therapy. *Nat Med* (2001) 7(9):987–9. doi: 10.1038/nm0901-987

23. Willett CG, Boucher Y, di Tomaso E, Duda DG, Munn LL, Tong RT, et al. Direct evidence that the VEGF-specific antibody bevacizumab has antivascular effects in human rectal cancer. *Nat Med* (2004) 10(2):145–7. doi: 10.1038/nm988

24. Manegold C, Dingemans AC, Gray JE, Nakagawa K, Nicolson M, Peters S, et al. The potential of combined immunotherapy and antiangiogenesis for the synergistic treatment of advanced NSCLC. *J Thorac Oncol* (2017) 12(2):194–207. doi: 10.1016/j.jtho.2016.10.003

25. Yu X, Li J, Ye L, Zhao J, Xie M, Zhou J, et al. Real-world outcomes of chemo-antiangiogenesis versus chemo-immunotherapy combinations in EGFR-mutant advanced non-small cell lung cancer patients after failure of EGFR-TKI therapy. *Transl Lung Cancer Res* (2021) 10(9):3782–92. doi: 10.21037/tlcr-21-681

26. White MN, Piper-Vallillo AJ, Gardner RM, Cunanan K, Neal JW, Das M, et al. Chemotherapy plus immunotherapy versus chemotherapy plus bevacizumab versus chemotherapy alone in EGFR-mutant NSCLC after progression on osimertinib. *Clin Lung Cancer* (2022) 23(3):e210–e21. doi: 10.1016/j.cllc.2021.11.001

27. Lu S, Wu L, Jian H, Cheng Y, Wang Q, Fang J, et al. Sintilimab plus chemotherapy for patients with EGFR-mutated non-squamous non-small-cell lung cancer with disease progression after EGFR tyrosine-kinase inhibitor therapy (ORIENT-31): second interim analysis from a double-blind, randomised, placebo-controlled, phase 3 trial. *Lancet Respir Med* (2023) 11(7):624–36. doi: 10.1016/S2213-2600(23)00135-2

28. Yu L, Hu Y, Xu J, Qiao R, Zhong H, Han B, et al. Multi-target angiogenesis inhibitor combined with PD-1 inhibitors may benefit advanced non-small cell lung cancer patients in late line after failure of EGFR-TKI therapy. *Int J Cancer* (2023) 153 (3):635–43. doi: 10.1002/ijc.34536

29. Tian T, Yu M, Li J, Jiang M, Ma D, Tang S, et al. Front-line ICI-based combination therapy post-TKI resistance may improve survival in NSCLC patients with EGFR mutation. *Front Oncol* (2021) 11:739090. doi: 10.3389/fonc.2021.739090

30. Hastings K, Yu HA, Wei W, Sanchez-Vega F, DeVeaux M, Choi J, et al. EGFR mutation subtypes and response to immune checkpoint blockade treatment in non-small-cell lung cancer. *Ann Oncol* (2019) 30(8):1311–20. doi: 10.1093/annonc/mdz141

31. Jiang T, Wang P, Zhang J, Zhao Y, Zhou J, Fan Y, et al. Toripalimab plus chemotherapy as second-line treatment in previously EGFR-TKI treated patients with EGFR-mutant-advanced NSCLC: a multicenter phase-II trial. *Signal Transduct Target Ther* (2021) 6(1):355. doi: 10.1038/s41392-021-00751-9

32. Peng S, Wang R, Zhang X, Ma Y, Zhong L, Li K, et al. EGFR-TKI resistance promotes immune escape in lung cancer via increased PD-L1 expression. *Mol Cancer* (2019) 18(1):165. doi: 10.1186/s12943-019-1073-4

33. Dong ZY, Zhang JT, Liu SY, Su J, Zhang C, Xie Z, et al. EGFR mutation correlates with uninflamed phenotype and weak immunogenicity, causing impaired response to PD-1 blockade in non-small cell lung cancer. *Oncoimmunology* (2017) 6 (11):e1356145. doi: 10.1080/2162402X.2017.1356145

34. Ribas A, Hu-Lieskovan S. What does PD-L1 positive or negative mean? *J Exp Med* (2016) 213(13):2835–40. doi: 10.1084/jem.20161462

35. Rooney MS, Shukla SA, Wu CJ, Getz G, Hacohen N. Molecular and genetic properties of tumors associated with local immune cytolytic activity. *Cell* (2015) 160(1-2):48–61. doi: 10.1016/j.cell.2014.12.033

36. Brahmer JR, Tykodi SS, Chow LQ, Hwu WJ, Topalian SL, Hwu P, et al. Safety and activity of anti-PD-L1 antibody in patients with advanced cancer. *N Engl J Med* (2012) 366(26):2455–65. doi: 10.1056/NEJMoa1200694

37. Topalian SL, Hodi FS, Brahmer JR, Gettinger SN, Smith DC, McDermott DF, et al. Safety, activity, and immune correlates of anti-PD-1 antibody in cancer. *N Engl J Med* (2012) 366(26):2443–54. doi: 10.1056/NEJMoa1200690

frontiers | Frontiers in Immunology

TYPE Systematic Review
PUBLISHED 06 October 2023
DOI 10.3389/fimmu.2023.1240149

Check for updates

OPEN ACCESS

EDITED BY
Jie Mei,
Wuxi People's Hospital Affiliated to Nanjing Medical University, China

REVIEWED BY
Hashem Obaid Alsaab,
Taif University, Saudi Arabia
Gaia Piperno,
European Institute of Oncology (IEO), Italy

*CORRESPONDENCE
Ziyi Yang
18508323310@163.com

RECEIVED 14 June 2023
ACCEPTED 20 September 2023
PUBLISHED 06 October 2023

CITATION
Yang Z, Lyu X, Yang H, Wang B, Xu D, Huo L, Zhang R, Huang Y and Diao B (2023) Survival after radiofrequency ablation and/or chemotherapy for lung cancer and pulmonary metastases: a systematic review and meta-analysis. *Front. Immunol.* 14:1240149. doi: 10.3389/fimmu.2023.1240149

COPYRIGHT
© 2023 Yang, Lyu, Yang, Wang, Xu, Huo, Zhang, Huang and Diao. This is an open-access article distributed under the terms of the Creative Commons Attribution License (CC BY). The use, distribution or reproduction in other forums is permitted, provided the original author(s) and the copyright owner(s) are credited and that the original publication in this journal is cited, in accordance with accepted academic practice. No use, distribution or reproduction is permitted which does not comply with these terms.

Survival after radiofrequency ablation and/or chemotherapy for lung cancer and pulmonary metastases: a systematic review and meta-analysis

Ziyi Yang*, Xia Lyu, Huilin Yang, Bingbing Wang, Dan Xu, Lingyi Huo, Runzi Zhang, Yingjun Huang and Benshu Diao

Chengdu Seventh People's Hospital & Chengdu Tumor Hospital, Chengdu, Sichuan, China

Background: Radiofrequency ablation (RFA) and chemotherapy are used to treat lung cancer or pulmonary metastases, but no direct comparison of overall survival (OS) has been published. The present study aimed to assess the OS of RFA and/or chemotherapy in patients with lung cancer or pulmonary metastases who were not candidates for surgical resection.

Methods: To identify relevant studies, the following databases were electronically searched from their inception to 31 March 2023: PubMed, Embase, Web of Science, Cochrane Library, Scopus, Ovid, ScienceDirect, SinoMed, China National Knowledge Infrastructure Database, Chongqing VIP Chinese Science and Technology Periodical Database, Wanfang Database, LILACS, ClinicalTrials.gov, and Chictr.org. Manual retrieval was also conducted. We used published hazard ratios (HRs) if available or estimates from other survival data.

Results: A total of 1,387 participants from 14 trials were included in the final analysis. Patients treated with RFA combined with chemotherapy significantly improved OS compared with those treated with chemotherapy alone [HR 0.50, 95% confidence interval (CI) 0.41–0.61; $p < 0.00001$], with an absolute difference at 12 months of 29.6% (95% CI 23.7–35.5), at 24 months of 19.2% (95% CI 10.1–28.2), and at 36 months of 22.9% (95% CI 12.0–33.7). No statistically significant difference was observed in the subgroups of case type, cancer type, chemotherapy drugs, and tumor size. The HR for OS with RFA plus chemotherapy vs. RFA alone was 0.53 (95% CI 0.41–0.70; $p < 0.00001$), corresponding to a 27.1% (95% CI 18.3–35.8), 31.0% (95% CI 19.9–41.9), and 24.9% (95% CI 15.0–34.7) absolute difference in survival at 12 months, 24 months, and 36 months, respectively. Subgroup analysis by geographic region and TNM stage showed that RFA combined with chemotherapy still significantly improved OS compared to RFA. The HR of RFA vs. chemotherapy was 0.98 (95% CI 0.60–1.60; $p = 0.94$), with an absolute difference at 12 months of 1.4% (95% CI -19.2 to 22.1), at 24 months of 7.8% (95% CI -11.3 to 26.8), and at 36 months of 0.3% (95% CI -13.2 to 13.8). The overall indirect comparison of OS for RFA vs. chemotherapy was 0.95 (95% CI 0.72–1.26; $p = 0.74$). Data on progression-free survival were not sufficiently reported.

Conclusion: RFA combined with chemotherapy might be a better treatment option for patients with lung cancer or pulmonary metastases than chemotherapy alone or RFA alone. The comparison between RFA and/or chemotherapy remains to be specifically tested.

Systematic review registration: https://www.crd.york.ac.uk/PROSPERO/display_record.php?RecordID=335032, identifier CRD42022335032.

KEYWORDS

lung cancer, pulmonary metastases, radiofrequency ablation, chemotherapy, systematic review, meta-analysis, RFA

Introduction

In 2020, the estimated number of new cases of lung cancer diagnosed worldwide was 2,206,771 (11.4%) and lung cancer-related deaths were 1,796,144 (18.0%) (1). Lung cancer is the second most commonly diagnosed cancer and the top cause of cancer deaths globally (1, 2). Because the prophase of clinical symptoms is not obvious, over 70% of patients already have advanced disease at the time of presentation (3–5). The survival of lung cancer in advanced stages is still very poor, with an overall 5-year survival rate of 9.5%–18% (5, 6). Above 54%, patients with cancer may develop pulmonary metastases, for many tumors involve the lung for distant spread (5). In colorectal cancer, patients who present with lung metastasis have a 5-year survival rate of less than 10% compared with 91% of those without metastasis (7).

Surgical resection is preferred in the treatment of lung tumors and pulmonary metastases. However, a significant number of patients who are not candidates for surgical resection receive multidisciplinary synthetic treatment (8). Chemotherapy, as the main adjuvant method in the treatment of cancer, has been widely applied in advanced lung cancer treatment. Platinum-based chemotherapy is an essential part of the treatment of locally advanced lung cancer. Their effects on the survival of patients are still far from satisfactory because the median overall survival (OS) was only 9 months and the over 1-year survival rate was 30% (9). Radiofrequency ablation (RFA), a minimally invasive technique, has been gradually introduced for pulmonary tumor treatment in recent years. In a large prospective trial of RFA for lung cancer (10), there was no difference in response between primary and metastasized lung tumors. The OS of 1 year is 70% in patients with non-small cell lung cancer (NSCLC) and 89% at 1 year in patients with colorectal metastases. Combining systemic therapy with local therapy is always the focus of clinical inquiry. The combination of RFA with chemotherapy improves survival, offers higher treatment efficacy, and delays disease progression (11–13).

Three reviews and meta-analyses have been published on this subject (14–16). They focused on lung tumors in nonsurgical patients, short-term clinical effects, survival rate, local tumor progression, quality of life, recrudescence, and drug toxicity (14–16). However, all of the trials that were included in these meta-analyses were conducted before 2014. Furthermore, they did not evaluate survival by hazard ratio (HR). The limited scope of previous reviews and the recent publication of a number of studies assessing OS for patients treated with RFA and/or chemotherapy require a new comprehensive meta-analysis.

Our objective was to conduct a systematic review and meta-analysis to compare the survival of RFA and/or chemotherapy on lung cancer and pulmonary metastases in patients who are nonsurgical candidates and try to provide evidence in support of clinical work in choosing appropriate treatment options.

Methods

We conducted and reported this systematic review and meta-analysis according to the Preferred Reporting Items for Systematic reviews and Meta-Analyses (PRISMA) guidelines (17). The protocol was registered with PROSPERO (registration number: CRD42022335032) at the start of our investigation.

Research question

We aimed to evaluate the survival of RFA, chemotherapy, and RFA plus chemotherapy for patients with lung cancer and pulmonary metastases.

Types of studies

We included randomized controlled trials (RCTs), cohort studies, and case-control studies. Case series lacking comparator groups or follow-up less than 12 months were excluded. Published and unpublished studies, full articles, and abstracts satisfying the criteria listed below were included without any language restriction. For publications and unpublished works not subject to peer review (such as theses or reports), we would contract the authors to get the

key data. We also hand-searched the reference lists of the included studies and topical reviews for potentially relevant articles.

Type of participant

We reviewed studies reporting on patients with lung cancer and/or pulmonary metastases who were not eligible for surgical resection and were receiving the treatment of RFA, chemotherapy, and RFA plus chemotherapy.

Type of intervention

The arms of the studies were only chemotherapy, RFA, and RFA plus chemotherapy. Other adjunctive therapies (e.g., microwave ablation and radiotherapy) and targeted treatments were excluded.

Type of outcome measure

The primary outcome was OS, defined as the time from randomization to death from any cause. The secondary outcome was progression-free survival (PFS), defined as the time from randomization to disease progression or death.

Search strategy

We systematically searched the following databases from their date of inception to 31 March 2023: PubMed, Embase, Web of Science, Cochrane Library, Scopus, Ovid, ScienceDirect, SinoMed, China National Knowledge Infrastructure Database (CNKI), Chongqing VIP Chinese Science and Technology Periodical Database (VIP), Wanfang Database, LILACS, ClinicalTrials.gov, and Chictr.org. There were no language restrictions, and they carried out translations if necessary. The search strategy included four core components: 1) lung cancer; 2) pulmonary metastases; 3) chemotherapy; and 4) RFA. The retrieval model was ((a) OR (b)) AND (c) AND (d). Medical Subject Headings (MeSH) terms, free-text terms, keywords, and subject words were identified for each of the above core components. MeSH terms were retrieved from PubMed. The search was based on PubMed and then adapted for other English databases. For other databases, the subject-word retrieval method was used. The searching strategy is presented in Supplementary Table S1. References from previous reviews and key articles retrieved were also reviewed and cross-referenced for relevant studies.

Selection of studies

We downloaded all titles and abstracts obtained by electronic searches to a reference management database (Microsoft Excel) and removed duplicate articles. The remaining titles and abstracts were independently reviewed by two authors. They excluded studies that clearly did not meet the inclusion criteria. We obtained full-text articles of the remaining articles, and two independent reviewers determined the eligibility of the retrieved papers. We resolved disagreements by consensus or by consulting the senior author if necessary. We documented reasons for exclusion during this process.

Data extraction and management

Two review authors independently extracted the data using the extraction template, which include study characteristics (authors, journal, year of publication, location, and funding), study questions (participants, comparison, aims, design, follow-up time, type of study, and size), results (outcomes, key findings), and conclusions. When a consensus on the data extraction cannot be obtained through consultations, the senior author will make a decision.

Assessment of risk of bias and reporting of study quality

Two reviewers independently evaluated the methodological quality of the included studies. For RCTs, we assessed the risk of bias and created applicability concerns graph using the Cochrane Risk of Bias Tool, which is structured into seven domains: random sequence generation, allocation concealment, blinding of participants and personnel, blinding of outcome assessment, incomplete outcome data, selective outcome reporting, and other sources of bias. The outcomes include low risk of bias, unclear risk of bias, and high risk of bias (18, 19).

For cohort and case-control studies, the Newcastle–Ottawa Scale (NOS) was used to assess the risk of bias (19). It assigns up to a maximum of nine points for the least risk of bias in three domains: 1) selection of the study groups (4 points); 2) comparability of groups (2 points); and 3) ascertainment of exposure and outcomes (3 points) (20). The maximum score of each study was 9. Studies with scores of 7 were considered to have a low risk of bias, scores of 4–6 were considered to have a moderate risk of bias, and scores <4 were considered to have a high risk of bias. We assessed that follow-up was adequate if the follow-up was in excess of 12 months. Any disputes will be settled via consensus or with the involvement of the senior author.

Measures of treatment effect

We used the HR for the comparison in each trial to assess the treatment effects.

Management of missing data

If there are missing data for the primary results, we will contact the corresponding authors to request the missing data. If the missing data cannot be obtained, the analysis will rely on the

available data. HRs and 95% confidence intervals (CIs) not reported or supported were calculated by the survival curves (21).

Statistical synthesis

The meta-analysis was performed using Review Manager (RevMan V.5.4.1 for Windows; the Nordic Cochrane Centre, The Cochrane Collaboration, 2020) and R version 4.2.1. The chi-square heterogeneity test and I^2 statistic were used to investigate the overall heterogeneity between trials. $p < 0.10$ or $I^2 > 50\%$ indicated significant heterogeneity. If considerable heterogeneity was observed, a random-effects model was used to analyze the pooled effect estimate; otherwise, the fixed-effects model was used. If more than 10 trials were included, funnel plots and the Egger test were used to assess publication biases. To estimate the 12-month, 24-month, and 36-month absolute differences, survival rates were computed on all patients and the HR at the corresponding time period was used to compute survival in each group (22). We used indirect comparison to obtain estimates of the benefit of RFA compared with chemotherapy.

Subgroup analysis

When significant heterogeneity was found, subgroup and sensitivity analyses were performed to explore possible reasons for the heterogeneity. However, given that the main purpose of subgroup analyses was to assess differences between subgroups rather than to explore reasons for heterogeneity, we performed subgroup analyses regardless of the presence or absence of statistically significant heterogeneity. Subgroup analyses were conducted assessing the impact of case type, geographic region, cancer type, TNM stage, age, tumor size, chemotherapy drugs, and time of RFA and follow-up.

Results

Results of the search

Figure 1 is a flowchart of the literature retrieval. Our literature identified 3,804 records from the database search results, and 11 additional articles were identified from manual searches. After removing the duplicate publications, 1,965 unique references were screened for eligibility by titles and abstracts. The remaining 185 publications were retrieved as full text or abstracts for detailed evaluation. Another 171 articles were excluded for the following reasons: interventions not assessed (n = 86), outcomes not assessed (n = 59), and not sharing more information about HR, OS, and PFS (n = 26). Finally, 14 trials representing 1,387 patients were included in this meta-analysis (11, 12, 23–34).

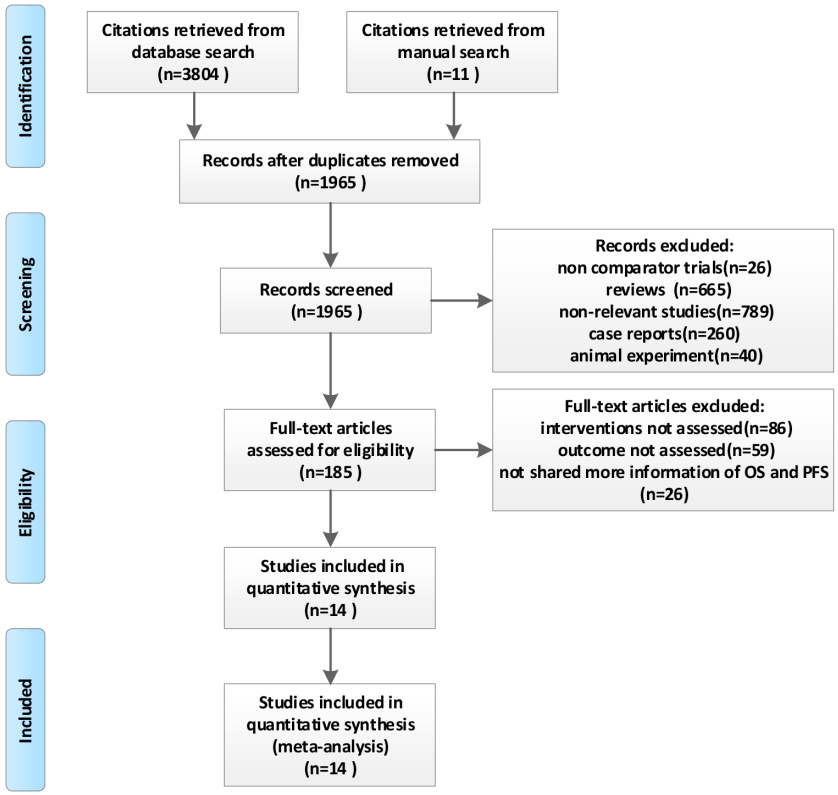


FIGURE 1
Flow diagram of study selection in the meta-analysis.

Study description

The characteristics of the studies in the evidence synthesis were summarized in Tables 1, 2. All of the studies were non-randomized comparisons. Nine studies were published from 2014 to 2022, and five were published before 2014. Most studies (11/14, 78.6%) were based in China. The sample size ranged from 29 to 256 patients. For NSCLC, the main lung cancer type, nine (n = 768) trials were only focused on NSCLC (23, 26–32, 34), and only one (n = 100) included patients with pulmonary metastases (11). Most patients in the trials were diagnosed with stage III or IV. Eleven studies were included in the comparison of RFA plus chemotherapy vs. chemotherapy alone

TABLE 1 Characteristics of the trials.

Reference	Inclusion period	RFA schedule	Chemotherapy schedule	Sample size	Follow-up (months)
RFA plus chemotherapy vs. chemotherapy					
Xu et al., 2022 (12)	2017-2019	CT-guided RFA, given before chemotherapy; 60–100 W, 10.5 min, 85.0°C ± 15.0°C	Four cycles: paclitaxel 135 mg/m^2 days 1 and 8; cisplatin 60 mg/m^2 day 1, every 21 days	256	Median: 16.5 Range: 2–24
Yu, 2020 (23)	2013-2014	CT-guided RFA; 15 KJ, 10 min, approximately 85.0°C	Gemcitabine 1,250 mg/m^2 days 1 and 8; cisplatin 60 mg/m^2 days 2–4	80	Range: 6–36*
Sun et al., 2019 (24)	2012-2016	Color Doppler ultrasonography-guided RFA	Etoposide 100 mg/m^2 days 1–3; cisplatin 75 mg/m^2 day 1 or carboplatin ACU 5–6 day 1, every 21 days	54	Range: 1–18.5*
Chen et al., 2018 (25)	2014-2017	CT-guided RFA, given before chemotherapy; 10–15 min, 90°C	Six cycles: gemcitabine 1,000 mg/m^2 days 1 and 8; cisplatin 30 mg/m^2 days 1–3, every 21 days	80	Median: 21 Range: 6–32
Du et al., 2017 (34)	2012-2015	CT-guided RFA; 25.32 ± 8.16 min, 90.1°C ± 1.71°C	Vinorelbine-cisplatin or paclitaxel-cisplatin/carboplatin or gemcitabine-cisplatin/carboplatin or docetaxel-cisplatin/carboplatin or pemetrexed-cisplatin/carboplatin	133	Median: 31 Range: 1–43*
Yang et al., 2016 (26)	2011-2014	2–3 cycles: CT-guided RFA, after artery chemoembolization 3–7 days, 15 KJ; every 30 days	Two to three cycles: artery chemoembolization, gemcitabine (1.2–2.0 g) and cisplatin (60–80 mg) day 1, every 21–28 days	104	Range: 1–36*
Zhou et al., 2015 (27)	2011-2013	1 cycle: CT-guided RFA, in the middle of chemotherapy	Two to six cycles: docetaxel-cisplatin or gemcitabine-carboplatin, every 21 days	122	Median 22.8 Range: 6–36
Zhu et al., 2014 (28)	2010-2012	CT-guided RFA, given before chemotherapy 7 days; 15 min, 90°C	Four cycles: gemcitabine 1,000 mg/m^2 days 1 and 8; cisplatin 30 mg/m^2 days 1–3, every 21 days	55	Range: 1–24*
Pu et al., 2013 (29)	2009-2012	CT-guided RFA, given before chemotherapy 7 days; 10–15 min, 90°C	Gemcitabine 1,000 mg/m^2 day 1 and 8, cisplatin 30 mg/m^2 days 1–3, every 21 days	32	Range: 6–24*
Lee et al., 2012 (30)	2000-2004	CT-guided RFA, given before chemotherapy; 60–70 W, 6–12 min	Three to nine cycles: gemcitabine-cisplatin or Taxol-carboplatin	30	Range: 6–48*
Wang et al., 2005 (31)	1999-2004	CT-guided RFA, given before chemotherapy 7–15 days	Three to six cycles: gemcitabine 1,250 mg/m^2 days 1 and 8, cisplatin 75 mg/m^2 day 1, every 21 days	64	Range: 3–36*
RFA plus chemotherapy vs. RFA					
Wang et al., 2020 (32)	2013-2015	2–3 cycles; CT-guided RFA day 1, every 30 days	Two to three cycles: artery chemoembolization, gemcitabine (1.2–2.0 g) and cisplatin (60–80 mg) day 1, every 21–28 days	114	Range: 1–36*
Yang et al., 2016 (26)	2011-2014	1–3 cycles: CT-guided RFA, 15 KJ, every 30 days	Two to three cycles: artery chemoembolization, before RFA 3–7 days, gemcitabine (1.2–2.0 g) and cisplatin (60–80 mg) day 1, every 21–28 days	77	Range: 1–36*
Chua et al., 2010 (11)	2000-2009	CT-guided RFA; 35–150 W, 90°C, 15–37 min	5-fluorouracil–based chemotherapy or capecitabine	100	Median: 23 Range: 1–96
Sun et al., 2010 (33)	2007-2009	CT-guided RFA; 5–15 min	Artery chemoembolization, before or after RFA 7 days, cisplatin 100 mg, epirubicin 40 mg, vincristine 2 mg	29	Range: 1–20*
RFA vs. chemotherapy					
Yang et al., 2016 (26)	2011-2014	1–3 cycles: CT-guided RFA, 15 KJ, every 30 days	Two to three cycles: artery chemoembolization, Gemcitabine (1.2–2.0 g) and cisplatin (60–80 mg) day1, every 21–28 days	95	Range: 1–36*

RFA, radiofrequency ablation; CT, computed tomography.
*Unpublished, retrieved from the survival curve.

10.3389/fimmu.2023.1240149

TABLE 2 Characteristics of patients and outcome summary of studies.

Reference	Type	Phase	Test group						Control group					
			N	Age	Male %	Size cm	Median OS, mo	Overall mortality	N	Age	Male %	Size cm	Median OS, mo	Overall mortality
RFA plus chemotherapy vs. chemotherapy														
Xu et al., 2022 (12)	NSCLC, SCLC, brain metastases	I - IV	128	48.69 ± 6.74	53.90	2.54 ± 0.36	17.5	12 mo: 92.82%*	128	48.69 ± 6.74	52.30	2.54 ± 0.36	13.4	12 mo: 67.13%*
Yu, 2020 (23)	NSCLC	III, IV	40	60.49 ± 4.28	67.50	31.93 ± 4.20[a]	None	12 mo: 92.60%* 24 mo: 92.60%* 36 mo: 87.50%*	40	61.08 ± 5.01	72.50	32.07 ± 3.97[a]	36.0*	12 mo: 85.01%* 24 mo: 65.10%* 36 mo: 50.01%*
Sun et al., 2019 (24)	SCLC, liver metastases	IV	24	60[c]	54.17	≤3.0: 60% <5.0: 40%	10.7	12 mo: 33.27%*	30	64[c]	60.00	≤3.0: 75% <5.0: 25%	6.9	12 mo: 3.45%
Chen et al., 2018 (25)	NSCLC, liver and bone metastases	III, IV	40	60.5 ± 11.9	65.00	4.34 ± 1.35	14.5	12 mo: 74.21%* 24 mo: 10.14%*	40	59.7 ± 11.2	57.50	4.34 ± 1.51	8.4	12 mo: 27.54%* 24 mo: 3.34%*
Du et al., 2017 (34)	NSCLC	III, IV	77	61.8	61.04	4.2	22.1	12 mo: 70.74% 24 mo: 39.31%	56	62.2	71.43	3.7	18.1	12 mo: 54.54% 24 mo: 19.49%
Yang et al., 2016 (26)	NSCLC	III, IV	43	67.2 ± 1.9	67.44	4.8 ± 0.3[b]	21	12 mo: 90.7% 24 mo: 58.1% 36 mo: 20.9%	61	68.2 ± 1.8	65.57	5.1 ± 0.4[b]	14	12 mo: 57.4% 24 mo: 24.6% 36 mo: 11.5%
Zhou et al., 2015 (27)	NSCLC	III, IV	48	60.31 ± 8.56	64.58	4.12 ± 1.47	13.9	12 mo: 61.29%*	74	63.15 ± 9.49	75.68	4.89 ± 1.63	8.12	12 mo: 22.66%*
Zhu et al., 2014 (28)	NSCLC	III, IV	21	70 ± 12	76.19	5.9 ± 2.7	None	12 mo: 90.55%* 24 mo: 85.81%*	34	69 ± 14	67.65	6.0 ± 2.9	None	12 mo: 70.65%* 24 mo: 58.73%*
Pu et al., 2013 (29)	NSCLC	III, IV	16	61 (48-76)[d]	75.00	3.1-10.4	18	12 mo: 81.01%* 24 mo: 5.33%*	16	61 (45-78)[d]	87.50	3.2-9.8	15	12 mo: 56.19%* 24 mo: 1.14%*
Lee et al., 2012 (30)	NSCLC	III, IV	12	69.4 ± 6.4	83.30	4.6 ± 1.6	42	12 mo: 100% 24 mo: 83.3% 36 mo: 0%	18	67.6 ± 5.2	77.80	5.2 ± 0.3	29	12 mo: 77.8% 24 mo: 63.3% 36 mo: 0%
Wang et al., 2005 (31)	NSCLC	III, IV	34	64.4 (45-81)[d]	82.35	5.6-12.4	17.4	12 mo: 76.5% 24 mo: 44.1% 36 mo: 17.6%	30	62.7 (42-70)[d]	83.33	None	9.2	12 mo: 43.3% 24 mo: 13.3% 36 mo: 0%
RFA plus chemotherapy vs. RFA														
Wang et al., 2020 (32)	NSCLC	III, IV	61	59.45 ± 6.23	63.93	4.82 ± 0.44[b]	28	12 mo: 90.16% 24 mo: 57.38% 36 mo: 32.79%	53	60.25 ± 5.88	62.26	4.93 ± 0.56[b]	15.0*	12 mo: 58.49% 24 mo: 32.08% 36 mo: 11.32%

(Continued)

TABLE 2 Continued

Reference	Type	Phase	Test group						Control group					
			N	Age	Male %	Size cm	Median OS, mo	Overall mortality	N	Age	Male %	Size cm	Median OS, mo	Overall mortality
Yang et al., 2016 (26)	NSCLC	III, IV	43	67.2 ± 1.9	67.44	4.8 ± 0.3[b]	21	12 mo: 90.7% 24 mo: 58.1% 36 mo: 20.9%	34	67.7 ± 2.0	61.76	4.6 ± 0.6[b]	15.0	12 mo: 58.8% 24 mo: 32.4% 36 mo: 11.8%
Chua et al., 2010 (11)	Colorectal pulmonary metastases	I-IV	59	65 ± 11[e]	None	≤5.0	None	12 mo: 96.36%* 24 mo: 83.51%* 36 mo: 62.56%*	41	65 ± 11[e]	None	≤5.0	20.8*	12 mo: 74.18%* 24 mo: 43.06%* 36 mo: 25.18%*
Sun et al., 2010 (33)	Unclassified	III, IV	14	54 (40-71)[d]	71.43	None	None	12 mo: 85%	15	54 (41-76)[d]	66.67	None	18.2*	12 mo: 76%
RFA vs. chemotherapy														
Yang et al., 2016 (26)	NSCLC	III, IV	34	67.7 ± 2.0	61.76	4.6 ± 0.6[b]	15	12 mo: 58.8% 24 mo: 32.4% 36 mo: 11.8%	61	68.2 ± 1.8	65.57	5.1 ± 0.4[b]	14	12 mo: 57.4% 24 mo: 24.6% 36 mo: 11.5%

RFA, radiofrequency ablation; OS, overall survival; NSCLC, non-small cell lung cancer; SCLC, small cell lung cancer; N, number; mo, month.
*Estimated as the overall survival curve; [a], area of the tumors, cm^2; [b], the maximum size of tumors; [c], median age; [d], mean age and range; [e], mean age and standard deviation for test and control group.

(n = 1,010) (12, 23–31, 34). Four trials were included in the comparisons of RFA plus chemotherapy vs. RFA alone (n = 320) (11, 26, 32, 33). Only one study compared RFA with chemotherapy (n = 95) (26). One study included those three comparisons with RFA plus chemotherapy (n = 43), chemotherapy (n = 61), and RFA (n = 34) (26). Three studies (11, 31, 33) supplied HR in the articles; others were calculated by OS. Only one trial supplied the PFS curve (12).

Risk of bias assessment

Supplementary Figures S1, S2 provide the Cochrane risk of bias. The NOS results are listed in Supplementary Table S2. The majority of the included studies were felt to have a low risk of bias. The adequacy of follow-up was often not described in the included studies, which raises the question of bias.

Survival analysis of RFA plus chemotherapy vs. chemotherapy

A significant benefit of OS was observed in favor of RFA plus chemotherapy vs. chemotherapy (HR 0.50, 95% CI 0.41–0.61; p < 0.00001) (Figure 2). This benefit corresponded to a 50% reduction in the risk of dying and an absolute benefit of 29.6% (95% CI 23.7–35.5), 19.2% (95% CI 10.1–28.2), and 22.9% (95% CI 12.0–33.7) at 12 months, 24 months, and 36 months, respectively (Figure 3A). Heterogeneity between trials was not significant (χ^2 = 5.13, p = 0.88, I^2 = 0%). We further performed the subgroup analysis, as shown in Table 3, and the primary result was independent of case type, cancer type, chemotherapy drugs, and tumor size. However, no statistically significant correlation was found in the Korean population (p = 0.72), TNM stage IV (p = 0.10), age ≥65 years (p = 0.08), RFA in or after the chemotherapy (p = 0.05), and follow-up periods longer than 36 months (p = 0.07) (Table 3).

Survival analysis of RFA plus chemotherapy vs. RFA

A significant benefit of OS was also observed in favor of RFA plus chemotherapy vs. RFA (HR 0.53, 95% CI 0.41–0.70; p < 0.00001) (Figure 4). This benefit corresponded to a 46% reduction in the risk of dying and an absolute benefit of 27.1% (95% CI 18.3–35.8), 31.0% (95% CI 19.9–41.9), and 24.9% (95% CI 15.0–34.7) at 12 months, 24 months, and 36 months, respectively (Figure 3B). Heterogeneity between trials was not significant (χ^2 = 1.20, p = 0.75, I^2 = 0%). As implied by the subgroup analysis, RFA combined with chemotherapy still significantly improved OS in various subgroups of geographic region and TNM stage (Table 4). No statistically significant correlation was detected in RCTs (p = 0.73), size larger than 5.0 cm (p = 0.73), age ≤60 years (p = 0.73), follow-up ≤24 months (p = 0.73), and RFA in the chemotherapy (p = 0.06) (Table 4).

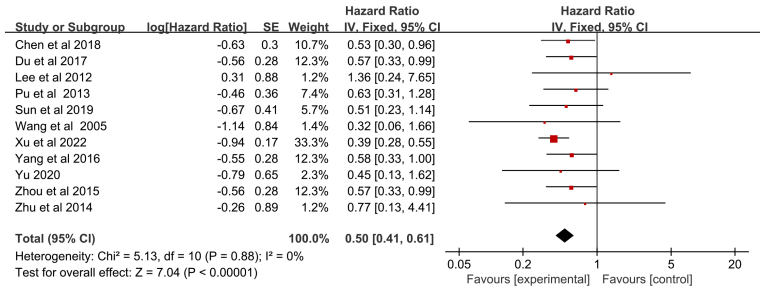


FIGURE 2
Overall survival for radiofrequency ablation plus chemotherapy compared with chemotherapy alone.

Survival analysis of RFA vs. chemotherapy

The pooled analysis showed that, compared with chemotherapy alone, RFA did not significantly increase OS. There is only one trial evaluating RFA vs. chemotherapy. No significant difference in the survival rate was detected in this trial (HR = 0.98, 95% CI 0.60–1.60; p = 0.94) (Figure 5), with an absolute benefit of 1.4% (95% CI -19.2 to 22.1), 7.8% (95% CI -11.3 to 26.8), and 0.3% (95% CI -13.2 to 13.8) at 12 months, 24 months, and 36 months, respectively (Figure 3C). From the indirect comparison, the HR was 0.94 (95% CI 0.67–1.31; p = 0.72). Combining the indirect and direct comparisons yielded an overall HR of 0.95 (95% CI 0.72–1.26; p = 0.74) (Figure 5). The heterogeneity was not significant (χ^2 = 0.02, p = 0.89, I^2 = 0%).

Published bias analysis

Assessment of publication bias was performed using funnel plots (Supplementary Figure S3) and the Egger regression model. The Egger test showed that no publication bias was present for RFA plus chemotherapy vs. chemotherapy (p = 0.0986 > 0.05).

Discussion

This meta-analysis demonstrates a statistical survival advantage for patients treated with RFA plus chemotherapy compared with those treated with chemotherapy alone or RFA alone, while RFA seems not to significantly improve OS compared with chemotherapy. Our findings provide strong evidence that RFA plus chemotherapy can improve survival in the disease.

To our knowledge, this paper represents the most comprehensive and up-to-date review of the treatment comparisons (RFA plus chemotherapy vs. chemotherapy, RFA plus chemotherapy vs. RFA, RFA vs. chemotherapy) for lung cancer and pulmonary metastases. Few previous meta-analyses have used HR to compare the OS of RFA and/or chemotherapy. Liu et al. (15) found that RFA combination with chemotherapy increased survival rate (response rate (RR) = 1.49, 95% CI 1.35–1.65) and reduced postoperative recrudescence (RR = 0.51, 95% CI 0.32–0.82) compared with chemotherapy for advanced NSCLC. In another meta-analysis (14), the authors also found that RFA plus chemotherapy improved the OS rate compared to chemotherapy alone for advanced NSCLC (1 year, RR = 2.01, 95% CI 1.41–2.86; 2 years, RR = 2.48, 95% CI 1.51–4.07; 3 years, RR = 2.29, 95% CI 1.24–4.22). Peter et al. (16) conducted a meta-analysis of the survival outcomes among lung tumors in nonsurgical patients treated with RFA plus post-ablation chemotherapy vs. RFA. They found that RFA plus post-ablation chemotherapy of lung tumors yielded improved outcomes in terms of local tumor progression, OS, and disease-free survival compared with RFA alone (16). A key limitation of those studies was that they used adjusted and unadjusted odds ratios that do not take into account time-to-over outcome measures.

Since most patients with lung cancer have advanced disease (stage III or IV), they miss the optimal therapeutic window for curative resection. For patients with inoperable cancer, chemotherapy is the mainstay of management. It is a systemic treatment because the chemicals or drugs travel throughout the

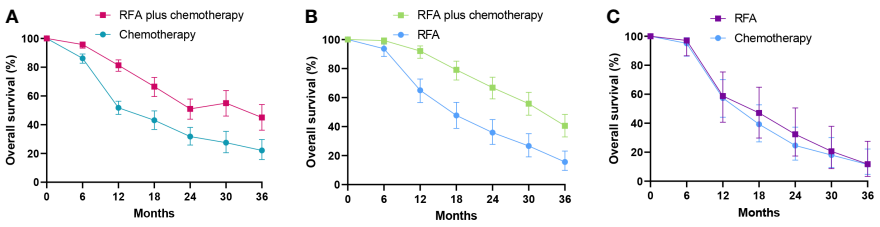


FIGURE 3
Comparison of overall survival curves for radiofrequency ablation and/or chemotherapy. **(A)** Overall survival curves of radiofrequency ablation plus chemotherapy compared with chemotherapy alone. **(B)** Overall survival curves of radiofrequency ablation plus chemotherapy compared with radiofrequency ablation alone. **(C)** Overall survival curves of radiofrequency ablation compared with chemotherapy. RFA, radiofrequency ablation.

10.3389/fimmu.2023.1240149

TABLE 3 Subgroup analysis of RFA plus chemotherapy vs. chemotherapy.

Subgroup factors	No. of studies	No. of patients	Effect model	HR(95% CI)	p	Heterogeneity	
						I^2 (%)	p
Total	11	1,010	Fixed	0.50 (0.41-0.61)	<0.00001	0	0.88
Case type							
RCTs	8	192	fixed	0.56 (0.36-0.85)	0.007	0	0.89
Cohort studies	3	818	fixed	0.49 (0.39-0.61)	<0.00001	0	0.71
Geographic region							
China	10	980	Fixed	0.50 (0.41-0.60)	<0.00001	0	0.57
South Korea	1	30	–	1.36 (0.24-7.65)	0.72	–	–
Cancer type							
NSCLC	8	620	Fixed	0.57 (0.43-0.77)	0.0002	0	0.95
Multiple	3	390	Fixed	0.43 (0.33-0.57)	<0.00001	0	0.6
TNM stage							
I-IV	1	256	–	0.39 (0.28-0.55)	<0.00001	–	–
III IV	9	700	Fixed	0.57 (0.45-0.73)	<0.0001	0	0.99
IV	1	54	–	0.51 (0.23-1.14)	0.1	–	–
Age							
≤60	1	189	–	0.39 (0.28-0.55)	<0.00001	–	–
60-65	7	565	Fixed	0.55 (0.42-0.72)	<0.0001	0	0.99
≥65	3	256	Fixed	0.64 (0.39-1.05)	0.08	0	0.63
Tumor size							
≤3.0 cm	1	256	–	0.39 (0.28-0.55)	<0.00001	–	–
≤5.0 cm	4	389	Fixed	0.55 (0.41-0.75)	0.0001	0	0.99
>5.0 cm	6	365	Fixed	0.61 (0.41-0.91)	0.01	0	0.82
Chemotherapy drugs							
GP	6	415	Fixed	0.56 (0.40-0.77)	0.0004	0	0.98
TP	1	256	–	0.39 (0.28-0.55)	<0.00001	–	–
Other	4	339	Fixed	0.58 (0.41-0.82)	0.002	0	0.79
Time of RFA							
Before chemotherapy	6	517	Fixed	0.46 (0.35-0.60)	<0.00001	0	0.55
In chemotherapy	1	122	–	0.57 (0.33-0.99)	0.05	–	–
After chemotherapy	1	104	–	0.58 (0.33-1.00)	0.05	–	–
Follow-up							
≤24 months	4	397	Fixed	0.44 (0.33-0.58)	<0.00001	0	0.57
24> Time ≤36 months	5	450	Fixed	0.54 (0.40-0.74)	0.0001	0	0.97
>36 months	2	163	Fixed	0.62 (0.37-1.04)	0.07	0	0.35

RFA, radiofrequency ablation; NSCLC, non-small cell lung cancer; GP, gemcitabine and cisplatin; TP, paclitaxel and cisplatin.

body and kill cancer cells. The main international guidelines recommend platinum-based chemotherapy as the standard of care for first-line therapy of advanced lung cancer, while those compounds indiscriminately attack all rapidly dividing cells, leading to severe side effects and inducing drug resistance (35). Furthermore, residual tumor cells remain present within resolving lesions after chemotherapy. The posttreatment prognosis of these patients remains poor. The meta-analysis of SCLC suggests that the

10.3389/fimmu.2023.1240149

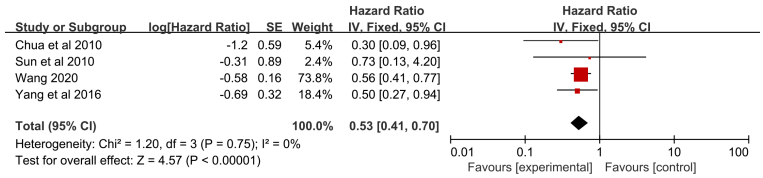


FIGURE 4
Overall survival for radiofrequency ablation plus chemotherapy compared with radiofrequency ablation alone.

TABLE 4 Subgroup analysis of RFA plus chemotherapy vs. RFA.

Subgroup factors	No. of studies	No. of patients	Effect model	HR(95% CI)	p	Heterogeneity	
						I^2 (%)	p
Total	4	320	Fixed	0.53 (0.41-0.70)	<0.00001	0	0.75
Case type							
RCTs	1	29	–	0.73 (0.13-4.20)	0.73	–	–
Cohort studies	3	291	Fixed	0.53 (0.40-0.70)	<0.00001	0	0.59
Geographic region							
China	3	220	fixed	0.50 (0.41-0.60)	<0.00001	0	0.57
Australia	1	100	–	0.30 (0.09-0.96)	0.04	–	–
Cancer type							
NSCLC	2	191	Fixed	0.55 (0.41-0.73)	<0.0001	0	0.76
Pulmonary metastases	1	100	–	0.30 (0.09-0.96)	0.04	–	–
Unclassified	1	29	–	0.73 (0.13-4.20)	0.73	–	–
TNM stage							
I-IV	3	220	Fixed	0.30 (0.09-0.96)	0.04	–	–
III IV	1	100	–	0.55 (0.42-0.73)	<0.0001	0	0.91
Age							
≤60	1	29	–	0.73 (0.13-4.20)	0.73	–	–
60-65	1	114	–	0.56 (0.41-0.77)	0.0003	–	–
≥65	2	177	fixed	0.45 (0.26-0.78)	0.004	0	0.45
Tumor size							
≤5.0 cm	3	291	Fixed	0.53 (0.40-0.70)	<0.00001	0	0.59
>5.0 cm	1	29	–	0.73 (0.13-4.20)	0.73	–	–
Chemotherapy drugs							
GP	2	191	Fixed	0.55 (0.41-0.73)	<0.0001	0	0.76
Other	2	129	Fixed	0.40 (0.15-1.04)	0.06	0	0.4
Time of RFA							
In chemotherapy	2	129	Fixed	0.40 (0.15-1.04)	0.06	0	0.4
After chemotherapy	1	77	–	0.50 (0.27-0.94)	0.03	–	–
Follow-up							
≤24 months	1	29	–	0.73 (0.13-4.20)	0.73	–	–

(Continued)

TABLE 4 Continued

Subgroup factors	No. of studies	No. of patients	Effect model	HR(95% CI)	p	Heterogeneity	
						I^2 (%)	p
24> Time ≤36 months	2	191	Fixed	0.55 (0.41-0.73)	<0.0001	0	0.76
>36 months	1	100	–	0.30 (0.09-0.96)	0.04	–	–

RFA, radiofrequency ablation; NSCLC, non-small cell lung cancer; GP, gemcitabine and cisplatin.

6-month survival rate was 75.3% and 72.7% and the 1-year survival rate was 36.2% and 35.0% for cisplatin and carboplatin, respectively (36). Another meta-analysis of NSCLC, which included 38 randomized trials, showed that the 1-year survival rate for the platinum-containing regimens was 34% (37). Thus, more effective and less invasive strategies for advanced lung cancer remain a widespread necessity. As a precise localized and minimally invasive technique, RFA has good safety and effectiveness that can improve the clinical treatment effect and prolong the survival time of patients. It has been widely used in the clinical treatment of lung cancer (38). RFA is also an alternative to surgery for local treatment to eradicate the tumors and has been officially approved as a treatment for NSCLC. The principle of RFA uses high-frequency electromagnetic waves to make intracellular polar molecules agitate and friction to generate heat, leading to protein degeneration and the killing of tumor cells. RFA has an obvious advantage in lung cancer treatment, for a high amount of air in the lung can speed up the accumulation of heat, which causes a rapid temperature increase.

Only one study that met the inclusion criteria for this meta-analysis has directly compared RFA with chemotherapy for NSCLC (26). It seemed that RFA was not significantly beneficial compared with chemotherapy for OS (HR 0.98). Additionally, the absolute difference between 12 months and 36 months was very small in the trial. To help with future trial design and individual patient treatment decisions, we intended to measure the relative survival benefits when these two therapy modalities were directly compared. Weak evidence (5%) in favor of chemotherapy was found in the overall indirect comparison of RFA and chemotherapy (HR 0.95). Shi and Xu (39) compared the survival time and quality of life in patients with lung metastasis from a malignant tumor of the digestive tract between RFA via fiber-optic bronchoscopy and conservative chemotherapy. They reported that the 3-year survival rate with RFA (53.3%) was significantly higher than that of chemotherapy (31.1%) ($p < 0.05$). Lee et al. (30) reported that the 3-year lung survival rate of NSCLC patients with RFA was 33.3% and chemotherapy alone was 32.4%. The disadvantage may be caused by the fact that RFA effectively kills tumor cells directly. However, this indirect comparison might have been prone to selection bias, and more direct comparisons are needed to test it.

RFA plus chemotherapy provided a better OS. Compared with chemotherapy alone, the HR was 0.50. And compared with RFA alone, the HR was 0.53. We speculate that the improvement in OS of RFA plus chemotherapy compared with RFA alone or chemotherapy alone is due to the following reasons: Firstly, RFA can not only effectively kill tumor cells but also release tumor antigens that can provoke a systemic immune response (40). RFA induces massive necrotic cell death through frictional heating and inflammatory effects. Inflammatory infiltrates that include neutrophils, macrophages, dendritic cells, and natural killer cells are found in the transitional zone. B cells and T cells are specific to the ablated tissue. These immune cell subsets have also been observed in distant untreated tumors and the bloodstream in both patients and animals (41). These results suggest an overall immune activation by RFA. The levels of immunoglobulin A, immunoglobulin G, and immunoglobulin M were increased significantly after RFA (42). The immune response provoked by the localized RFA treatment may have a therapeutic effect on distant primary lesions. This may be the reason why tumor markers decreased after RFA. The combined use of RFA and chemotherapy could decrease further than chemotherapy alone (38). Secondly, chemotherapy resistance limits our ability to effectively treat lung cancer. Some lung tumors are intrinsically resistant to chemotherapy, and in virtually all cases, even the initial responders rapidly develop acquired resistance. RFA induced coagulation necrosis and cell death in the centrally located

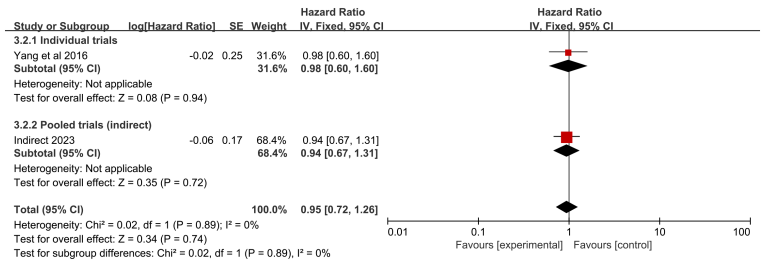


FIGURE 5
Overall survival for radiofrequency ablation compared with chemotherapy.

hypoxic tumor, which is typically less responsive to chemotherapy. RFA, which is a type of hyperthermia, inhibits DNA polymerase-mediated damage repair, increases functional multidrug resistance (MDR) proteins, and abrogates drug resistance (43). In the short-term effect study of middle- and late-period NSCLC, the effective rate of chemotherapy was 27.3%, RFA was 64.3%, and RFA combined with chemotherapy was 80.0%. A previous meta-analysis (15) also indicated that RFA combined with chemotherapy improved short-term effect than chemotherapy (RR = 0.93, 95% CI 0.72–1.20). Thirdly, the goal of combining chemotherapy with thermal ablation is often to enhance tumor cell death in the peripheral or transitional zone, which, at sublethal temperatures, is an area recovering from reversible injury. Apoptosis that is triggered by heat-induced cell injury is increased by the cytotoxic injury of chemotherapies. Chemotherapy is more sensitive to oxygen-enriched cells than to hypoxic cells, while RFA is more sensitive to hypoxic cells. RFA can cause "*in situ* thermal injury" to the large tumor mass, which can lead to a "chemotherapy-sensitizing effect" and make the chemotherapy more effective (44). The synergistic effect of the combination of RFA and chemotherapy has been proven (45). Finally, RFA targets tumors that can be seen in imaging but cannot treat subclinical or small lesions. Moreover, insufficient RFA can lead to the expression of tumor stem markers, promote the generation of tumor stem cells, and further lead to residual cancer recurrence. Chemotherapy is a systemic treatment that has a better effect on subclinical lesions, small lesions, and residual cancer. The benefit of combination survival was also proven in the rabbit VX2 lung tumor model (46). The combination has complementary advantages that increase the disease control rate, objective response rate, and survival (13, 47).

Furthermore, we performed subgroup analyses on case type, therapeutic approaches, and patient characteristics and tried to delve into their applicability. For the Chinese population, a statistically significant correlation was found between the combined application of RFA and chemotherapy vs. sole chemotherapy, whereas this difference was not significant in the Korean population (p = 0.72). Simultaneously, Chinese and Australian patients with lung cancer had comparable outcomes when comparing RFA combined with chemotherapy vs. RFA alone. The literature reports the results of RFA treatment for lung cancer in the United States (48) and Europe (49), but unfortunately, we did not find any trials of relevant comparisons. This may be due to a variety of factors, including the sample size, dissimilarities in populations and biological characteristics of tumors, and disparities in local clinical management (50). It indicated that variances in patient populations across different regions could impact the efficacy of the treatment. The combination of RFA with chemotherapy significantly improved survival compared to chemotherapy alone in different tumor sizes, drugs, and types of lung cancer including NSCLC, SCLC, and pulmonary metastases. Hiraki et al. (51) showed in their meta-analysis that tumor type did not impact local control by RFA in the lungs. Maybe the benefit is derived from the combined synergistic effects of both comprehensive treatment strategies and local therapies.

The subgroup analysis also showed the OS benefit for RFA prior to chemotherapy than for RFA during and after chemotherapy in the comparison of RFA plus chemotherapy and chemotherapy. These findings are comparable to a previously published research by Matsui et al. (52) who retrospectively studied 21 patients who underwent metastasectomy for pulmonary metastases from esophageal cancer. They estimated that 1-year, 3-year, and 5-year survival rates for RFA prior to chemotherapy were 93.3%, 63.8%, and 47.9%, respectively, while those for RFA after chemotherapy were 87.5%, 31.3%, and 31.3% respectively. This difference may be due to the fact that RFA effectively reduces the tumor size, alters the microenvironment of the tumor cells and triggers an immune response, and reduces drug resistance, thus helping to improve the efficacy of subsequent chemotherapy.

When conducting subgroup analyses comparing chemotherapy combined with RFA to RFA, we found tumor size >5.0 cm did differ from the overall analysis. The local efficacy of RFA for the treatment of lung cancer depends on tumor size and the type of electrode used (53). Dupuy et al. (48) reported the results of the American College of Surgeons Oncology Group Z4033 Trial that prospectively evaluated RFA for stage IA NSCLC in medically inoperable patients in 2015. The difference in local control between tumors 3 cm or less in size and tumors larger than 3 cm and therapeutic outcomes are better in smaller cancers. Kodama et al. (54) and Herrera et al. (55) reported a better treatment response in tumors smaller than 5 cm. RFA is strictly dependent on anatomical criteria, such as nodule size and location. Therefore, lesions larger than 5 cm should be excluded from RFA (56).

Our study has certain limitations that should be taken into account. Several studies included in the analysis were not RCTs. Only one retrospective study has been designed to compare chemotherapy directly with RFA for patients with NSCLC (26). Therefore, we conducted a cross-study analysis of data from the comparing of RFA plus chemotherapy with chemotherapy alone and RFA plus chemotherapy with RFA alone. The PFS of those comparisons was also low in the literature. The HR was not directly obtained by the included studies; therefore, it might have led to deviations in the calculated HR. In making treatment decisions, we need to consider toxicity or side effects. However, the adverse events were not analyzed in this paper because the definition, measurement, and reporting of adverse events in the trials were not standard-grade toxicities.

Conclusion

In conclusion, based on the present evidence, RFA plus chemotherapy improves OS compared with RFA alone or chemotherapy alone. Further research is still needed to compare the efficacy and safety of RFA plus chemotherapy and RFA alone or chemotherapy alone.

Data availability statement

The original contributions presented in the study are included in the article/Supplementary Material. Further inquiries can be directed to the corresponding author.

Author contributions

All authors were involved in the design of the trial, organization of the study, manuscript writing, and approval of final version of the manuscript. ZY, XL, HY, LH and RZ developed the protocol. ZY, XL, HY, BW, DX, LH and YH generated the search strategy, performed literature search and select. ZY, XL, HY, LH and RZ extracted and summarized the data. ZY did the data analyses, and XL and YH checked the data analysis and validity. ZY, XL, HY, BW, DX, YH and BD interpreted the data. ZY and XL were chief.

Funding

This work was supported by the Sichuan provincial administration of tradition Chinese medicine (2021MS157).

Conflict of interest

The authors declare that the research was conducted in the absence of any commercial or financial relationships that could be construed as a potential conflict of interest.

Publisher's note

All claims expressed in this article are solely those of the authors and do not necessarily represent those of their affiliated organizations, or those of the publisher, the editors and the reviewers. Any product that may be evaluated in this article, or claim that may be made by its manufacturer, is not guaranteed or endorsed by the publisher.

Supplementary material

The Supplementary Material for this article can be found online at: https://www.frontiersin.org/articles/10.3389/fimmu.2023.1240149/full#supplementary-material

References

1. Ferlay J, Ervik M, Lam F, Colombet M, Mery L, Piñeros M, et al. *Global Cancer Observatory: Cancer Today* (2020). Available at: https://gco.iarc.fr/today/.

2. Sung H, Ferlay J, Siegel RL, Laversanne M, Soerjomataram I, Jemal A, et al. Global cancer statistics 2020: GLOBOCAN estimates of incidence and mortality worldwide for 36 cancers in 185 countries. *CA Cancer J Clin* (2021) 71:209–49. doi: 10.3322/caac.21660

3. Siddiqui F, Vaqar S, Siddiqui AH. *Lung Cancer* (2022). Available at: https://www.ncbi.nlm.nih.gov/books/NBK482357/.

4. Rossi A, Chiodini P, Sun JM, O'Brien ME, von Plessen C, Barata F, et al. Six versus fewer planned cycles of first-line platinum-based chemotherapy for non-small-cell lung cancer: a systematic review and meta-analysis of individual patient data. *Lancet Oncol* (2014) 15:1254–62. doi: 10.1016/S1470-2045(14)70402-4

5. Yuh D, Vricella L, Yang S, Doty J. *Johns Hopkins Textbook of Cardiothoracic Surgery. 2nd ed*. New York: McGraw-Hill Education Medical (2014) p. 119–55.

6. Wood DE, Kazerooni EA, Baum SL, Eapen GA, Ettinger DS, Hou L, et al. Lung cancer screening, version 3.2018, NCCN clinical practice guidelines in oncology. *J Natl Compr Canc Netw* (2018) 16:412–41. doi: 10.6004/jnccn.2018.0020

7. Jamil A, Kasi A. *Lung Metastasis* (2023). Available at: https://www.ncbi.nlm.nih.gov/books/NBK553111/.

8. Raz DJ, Zell JA, Ou SH, Gandara DR, Anton-Culver H, Jablons DM. Natural history of stage I non-small cell lung cancer: implications for early detection. *Chest* (2007) 132:193–9. doi: 10.1378/chest.06-3096

9. Schiller JH, Harrington D, Belani CP, Langer C, Sandler A, Krook J, et al. Comparison of four chemotherapy regimens for advanced non-small-cell lung cancer. *N Engl J Med* (2002) 346:92–8. doi: 10.1056/NEJMoa011954

10. Lencioni R, Crocetti L, Cioni R, Suh R, Glenn D, Regge D, et al. Response to radiofrequency ablation of pulmonary tumours: a prospective, intention-to-treat, multicentre clinical trial (the RAPTURE study). *Lancet Oncol* (2008) 9:621–8. doi: 10.1016/S1470-2045(08)70155-4

11. Chua TC, Thornbury K, Saxena A, Liauw W, Glenn D, Zhao J, et al. Radiofrequency ablation as an adjunct to systemic chemotherapy for colorectal pulmonary metastases. *Cancer* (2010) 116:2106–14. doi: 10.1002/cncr.24952

12. Xu F, Cai Z, Xu B, Song J, Liu H, Li X, et al. Clinical research on the combined use of systemic chemotherapy and CT-guided radiofrequency ablation in treatment of lung cancer. *LASER Med Sci* (2022) 37:233–9. doi: 10.1007/s10103-020-03222-9

13. Yu S, Wu ZZ, Si HT, Yang S, Liu GM, Zhao XD. Short-term effect analysis of radiofrequency ablation combined chemotherapy on middle and late period non-small cell lung cancer. *Oncol Lett* (2016) 12:4399–402. doi: 10.3892/ol.2016.5276

14. Wei Y, Li Z, Mi D, Wen Z, Li Z. A systematic review of radiofrequency ablation combined with radiotherapy or chemother-apy in the treatment of advanced non-small cell lung cancer. *Modern Oncol* (2015) 23:2609–14. doi: 10.3969/j.issn.1672-4992.2015.18.17

15. Liu W, Zeng X, Liu X, Li X, Guo Y. Radiofrequency ablation and chemotherapy combination versus chemotherapy monotherapy in non-small cell lung cancer:A systematic review of meta analysis. *Chin Clin Oncol* (2012) 17:530–8. doi: 10.3969/j.issn.1009-0460.2012.06.012

16. Peter A, Sandra J, Mario V, LYR M, Stephen O. Local tumor control and survival outcomes of percutaneous radiofrequency ablation plus post-ablation chemotherapy for lung tumors in nonsurgical patients: A meta-analysis. *J Clin Oncol* (2013) 31:9550. doi: 10.1200/jco.2013.31.15_suppl.9550

17. Moher D, Liberati A, Tetzlaff J, Altman DG. Preferred reporting items for systematic reviews and meta-analyses: the PRISMA statement. *BMJ* (2009) 339:b2535. doi: 10.3736/jcim20090918

18. Sterne J, Savović J, Page MJ, Elbers RG, Blencowe NS, Boutron I, et al. Rob 2: a revised tool for assessing risk of bias in randomised trials. *BMJ* (2019) 366:l4898. doi: 10.1136/bmj.l4898

19. Higgins JPT, Thomas J, Chandler J, Cumpston M, Li T, Page MJ, Welch VA (editors). Cochrane Handbook for Systematic Reviews of Interventions. *2nd Edition*. Chichester (UK): John Wiley & Sons. (2019).

20. Wells G, Shea B, O'Connell D, Peterson J, Welch V, Losos M, et al. The Newcastle-Ottawa Scale (NOS) for assessing the quality of nonrandomised studies in meta-analyses. (2011). Available at: https://www.ohri.ca/programs/clinic.

21. Tierney JF, Stewart LA, Ghersi D, Burdett S, Sydes MR. Practical methods for incorporating summary time-to-event data into meta-analysis. *TRIALS* (2007) 8:16. doi: 10.1186/1745-6215-8-16

22. Lacas B, Bourhis J, Overgaard J, Zhang Q, Grégoire V, Nankivell M, et al. Role of radiotherapy fractionation in head and neck cancers (MARCH): an updated meta-analysis. *Lancet Oncol* (2017) 18:1221–37. doi: 10.1016/S1470-2045(17)30458-8

23. Yu X. Clinical efficacy of chemotherapy combined with radiofrequency ablation in the treatment of locally advanced non small cell lung cancer. *J Clin Res* (2020) 37:136–8. doi: 10.3969/j.issn.1671-7171.2020.01.044

24. Sun J, Luo J, Xu L, Zhao L, Si T, Chen S, et al. Discussion on the treatment mode of liver metastasis in patients with extensive small cell lung cancer. *J Tianjin Med Univ* (2019) 25:577–80.

25. Chen D, Ye J, Xiong X, Wang J, Shi D, Peng G. Therapeutic efficacy of radiofrequency ablation combined with chemotherapy for advanced non-small cell lung cancer. *Chin J Clin Oncol Rehabil* (2018) 25:1073–6.

26. Yang X, Wu G, Li Z, Wu H, Sun Y, Wen H, et al. Efficacy for artery chemoembolization combined with radiofrequency ablation in the treatment of advanced non-small cell lung cancer. *Natl Med J China* (2016) 96:539–43. doi: 10.3760/cma.j.issn.0376-2491.2016.07.010

27. Zhou J, Li H, Lv W, Wang S, Zheng X, Lin L. Curative effect of radiofrequency ablation combined with chemotherapy on middle-late stage non-small cell lung cancer. *J Pract Med* (2015) 31:1786–9. doi: 10.3969/j.issn.1006-5725.2015.11.019

28. Zhu Y, Zhou C, Lu B, Zhou Y, Zhao W, Wang Y, et al. The short-term efficacy of radiofrequency ablation combined with chemotherapy in the treatment of locally advanced non small cell lung cancer. *Modern Pract Med* (2014) 26:829–30. doi: 10.3969/j.issn.1671-0800.2014.07.024

29. Pu D, Liao J. Radiofrequency ablation combined with GP chemotherapy for stage III and IV peripheral non-small cell lung cancer: a clinical observation. *J Interventional Radiol* (2013) 22:129–32. doi: 10.3969/j.issn.1008-794X.2013.02.010

30. Lee H, Jin GY, Han YM, Chung GH, Lee YC, Kwon KS, et al. Comparison of survival rate in primary non-small-cell lung cancer among elderly patients treated with radiofrequency ablation, surgery, or chemotherapy. *Cardio Vasc Interventional Radiol* (2012) 35:343–50. doi: 10.1007/s00270-011-0194-y

31. Wang S, Chen J, Cao W, Chen Y, Cheng B. The observation of the clinical effect for combination therapy of RFA with GP on advanced stage lung cancer. *Chin J Clin Oncol* (2005) 32:628–30. doi: 10.3969/j.issn.1000-8179.2005.11.009

32. Wang Q, Yu L. Efficacy and prognosis of radiofrequency ablation combined with artery chemoembolization in the treatment of advanced non small cell lung cancer. *J Clin Res* (2020) 37:925–8. doi: 10.3969/j.issn.1671-7171.2020.06.040

33. Sun H, Liu R, Liu Y, Yang Y, Shen H, Wang H, et al. Radiofrequency ablation combined with arterial infusion chemotherapy for locally advanced lung cancer. *J Pract Oncol* (2010) 24:168–71. doi: 10.3969/j.issn.1002-3070.2010.02.018

34. Du S, Qin D, Pang R, Zhao S, Hu M, Zhi X. Long-term efficacy of radiofrequency ablation combined with chemotherapy in the treatment of patients with advanced non-small cell lung cancer-A retrospective study. *Zhongguo Fei Ai Za Zhi* (2017) 20:675–82. doi: 10.3779/j.issn.1009-3419.2017.10.03

35. Rossi A, Di Maio M. Platinum-based chemotherapy in advanced non-small-cell lung cancer: optimal number of treatment cycles. *Expert Rev Anticancer Ther* (2016) 16:653–60. doi: 10.1586/14737140.2016.1170596

36. Rossi A, Di Maio M, Chiodini P, Rudd RM, Okamoto H, Skarlos DV, et al. Carboplatin- or cisplatin-based chemotherapy in first-line treatment of small-cell lung cancer: the cocis meta-analysis of individual patient data. *J Clin Oncol* (2012) 30:1692–8. doi: 10.1200/JCO.2011.40.4905

37. D'Addario G, Pintilie M, Leighl NB, Feld R, Cerny T, Shepherd FA. Platinum-based versus non-platinum-based chemotherapy in advanced non-small-cell lung cancer: a meta-analysis of the published literature. *J Clin Oncol* (2005) 23:2926–36. doi: 10.1200/JCO.2005.03.045

38. Xu F, Song J, Lu Y, Wang J, Wang J, Xiao H, et al. Clinical efficacy of systemic chemotherapy combined with radiofrequency ablation and microwave ablation for lung cancer: a comparative study. *Int J Hyperther* (2021) 38:900–6. doi: 10.1080/02656736.2021.1936214

39. Shi Y, Xu X. Survival time and quality of life follow -up of fiberoptic bronchoscopy ablation and conservative chemotherapy for treating patients with lung metastasis of Malignant tumor of digestive tract. *Modern Digestion Intervention* (2016) 21:383–6. doi: 10.3969/j.issn.1672-2159.2016.03.003

40. Qi X, Yang M, Ma L, Sauer M, Avella D, Kaifi JT, et al. Synergizing sunitinib and radiofrequency ablation to treat hepatocellular cancer by triggering the antitumor immune response. *J Immunother Cancer* (2020) 8:e001038. doi: 10.1136/jitc-2020-001038

41. Chu KF, Dupuy DE. Thermal ablation of tumours: biological mechanisms and advances in therapy. *Nat Rev Cancer* (2014) 14:199–208. doi: 10.1038/nrc3672

42. Cheng R, Li Y, Su L, Wang L, Cao Y. Clinical effect of cold and heat ablation on patients with advanced lung cancer and its influence on immune function. *Am J Transl Res* (2023) 15:2939–48.

43. Stein U, Jürchott K, Walther W, Bergmann S, Schlag PM, Royer HD. Hyperthermia-induced nuclear translocation of transcription factor YB-1 leads to enhanced expression of multidrug resistance-related ABC transporters. *J Biol Chem* (2001) 276:28562–9. doi: 10.1074/jbc.M100311200

44. Li X, Wang J, Li W, Huang Z, Fan W, Chen Y, et al. Percutaneous CT-guided radiofrequency ablation for unresectable hepatocellular carcinoma pulmonary metastases. *Int J Hyperther* (2012) 28:721–8. doi: 10.3109/02656736.2012.736669

45. Exner AA, Weinberg BD, Stowe NT, Gallacher A, Wilson DL, Haaga JR, et al. Quantitative computed tomography analysis of local chemotherapy in liver tissue after radiofrequency ablation. *Acad Radiol* (2004) 11:1326–36. doi: 10.1016/j.acra.2004.09.007

46. Ueki A, Okuma T, Hamamoto S, Miki Y. Therapeutic effects of CT-guided radiofrequency ablation with concurrent platinum-doublet chemotherapy in a rabbit VX2 lung tumor model. *Radiology* (2017) 283:391–8. doi: 10.1148/radiol.2016160414

47. Huang BY, Zhou JJ, Yu ZQ, Song XY, Lin Y, Li XM, et al. Long-term observation of ct-guided radiofrequency ablation of lung neoplasm in 476 consecutive patients by a thoracic surgical service: a single-institutional experience. *Acad Radiol* (2017) 24:1517–25. doi: 10.1016/j.acra.2017.06.018

48. Dupuy DE, Fernando HC, Hillman S, Ng T, Tan AD, Sharma A, et al. Radiofrequency ablation of stage ia non-small cell lung cancer in medically inoperable patients: results from the american college of surgeons oncology group z4033 (alliance) trial. *Cancer-Am Cancer Soc* (2015) 121:3491–8. doi: 10.1002/cncr.29507

49. De Baère T, Aupérin A, Deschamps F, Chevallier P, Gaubert Y, Boige V, et al. Radiofrequency ablation is a valid treatment option for lung metastases: experience in 566 patients with 1037 metastases. *Ann Oncol* (2015) 26:987–91. doi: 10.1093/annonc/mdv037

50. Møller H, Coupland VH, Tataru D, Peake MD, Mellemgaard A, Round T, et al. Geographical variations in the use of cancer treatments are associated with survival of lung cancer patients. *Thorax* (2018) 73:530–7. doi: 10.1136/thoraxjnl-2017-210710

51. Hiraki T, Gobara H, Mimura H, Sano Y, Tsuda T, Iguchi T, et al. Does tumor type affect local control by radiofrequency ablation in the lungs? *Eur J Radiol* (2010) 74:136–41. doi: 10.1016/j.ejrad.2009.01.026

52. Matsui Y, Hiraki T, Gobara H, Fujiwara H, Iguchi T, Shirakawa Y, et al. Percutaneous radiofrequency ablation for pulmonary metastases from esophageal cancer: retrospective evaluation of 21 patients. *J Vasc Interv Radiol* (2014) 25:1566–72. doi: 10.1016/j.jvir.2014.06.030

53. Hiraki T, Gobara H, Mimura H, Toyooka S, Fujiwara H, Yasui K, et al. Radiofrequency ablation of lung cancer at okayama university hospital: a review of 10 years of experience. *Acta Med Okayama* (2011) 65:287–97. doi: 10.18926/AMO/47010

54. Kodama H, Yamakado K, Hasegawa T, Fujimori M, Yamanaka T, Takaki H, et al. Radiofrequency ablation using a multiple-electrode switching system for lung tumors with 2.0-5.0-cm maximum diameter: phase ii clinical study. *Radiology* (2015) 277:895–902. doi: 10.1148/radiol.2015141153

55. Herrera LJ, Fernando HC, Perry Y, Gooding WE, Buenaventura PO, Christie NA, et al. Radiofrequency ablation of pulmonary Malignant tumors in nonsurgical candidates. *J Thorac Cardiovasc Surg* (2003) 125:929–37. doi: 10.1067/mtc.2003.18

56. Beland MD, Wasser EJ, Mayo-Smith WW, Dupuy DE. Primary non-small cell lung cancer: review of frequency, location, and time of recurrence after radiofrequency ablation. *Radiology* (2010) 254:301–7. doi: 10.1148/radiol.00000090174

frontiers | Frontiers in Immunology

TYPE Original Research
PUBLISHED 13 October 2023
DOI 10.3389/fimmu.2023.1243233

Check for updates

OPEN ACCESS

EDITED BY
Qun Xue,
Affiliated Hospital of Nantong University, China

REVIEWED BY
Jessica Dal Col,
University of Salerno, Italy
Isabel Barragan,
University of Malaga, Spain

*CORRESPONDENCE
László G. Puskás
laszlo@avidinbiotech.com
Gábor J. Szebeni
szebeni.gabor@brc.hu

†These authors have contributed equally to this work

RECEIVED 20 June 2023
ACCEPTED 27 September 2023
PUBLISHED 13 October 2023

CITATION
Neuperger P, Szalontai K, Gémes N, Balog JÁ, Tiszlavicz L, Furák J, Lázár G, Puskás LG and Szebeni GJ (2023) Single-cell mass cytometric analysis of peripheral immunity and multiplex plasma marker profiling of non-small cell lung cancer patients receiving PD-1 targeting immune checkpoint inhibitors in comparison with platinum-based chemotherapy. *Front. Immunol.* 14:1243233. doi: 10.3389/fimmu.2023.1243233

COPYRIGHT
© 2023 Neuperger, Szalontai, Gémes, Balog, Tiszlavicz, Furák, Lázár, Puskás and Szebeni. This is an open-access article distributed under the terms of the Creative Commons Attribution License (CC BY). The use, distribution or reproduction in other forums is permitted, provided the original author(s) and the copyright owner(s) are credited and that the original publication in this journal is cited, in accordance with accepted academic practice. No use, distribution or reproduction is permitted which does not comply with these terms.

Single-cell mass cytometric analysis of peripheral immunity and multiplex plasma marker profiling of non-small cell lung cancer patients receiving PD-1 targeting immune checkpoint inhibitors in comparison with platinum-based chemotherapy

Patrícia Neuperger[1,2], Klára Szalontai[3], Nikolett Gémes[1,2], József Á. Balog[1], László Tiszlavicz[4], József Furák[5], György Lázár[5], László G. Puskás[1,6*†] and Gábor J. Szebeni[1,7,8*†]

[1]Laboratory of Functional Genomics, HUN-REN Biological Research Centre, Szeged, Hungary, [2]PhD School in Biology, University of Szeged, Szeged, Hungary, [3]Csongrád County Hospital of Chest Diseases, Deszk, Hungary, [4]Department of Pathology, University of Szeged, Szeged, Hungary, [5]Department of Surgery, University of Szeged, Szeged, Hungary, [6]Avicor Ltd., Szeged, Hungary, [7]Department of Physiology, Anatomy and Neuroscience, Faculty of Science and Informatics, University of Szeged, Szeged, Hungary, [8]CS-Smartlab Devices Ltd., Kozármisleny, Hungary

Introduction: The effect of platinum-based chemotherapy (Chem.) and second- or multiple- line immune checkpoint PD-1 blocking therapy by Nivolumab or Pembrolizumab (ICI) was assayed in the peripheral blood of non-small cell lung cancer (NSCLC) patients.

Methods: Flow cytometry was used to detect NSCLC-related antigen binding IgG antibodies. The Luminex MagPix multiplex bead-based cytokine/chemokine detecting system was used to quantitatively measure 17 soluble markers in the plasma samples. Single-cell mass cytometry was applied for the immunophenotyping of peripheral leukocytes.

Results: The incubation of patient derived plasma with human NSCLC tumor cell lines, such as A549, H1975, and H1650, detected NSCLC-specific antibodies reaching a maximum of up to 32% reactive IgG-positive NSCLC cells. The following markers were detected in significantly higher concentration in the plasma of Chem. group versus healthy non-smoker and smoker controls: BTLA, CD27, CD28, CD40, CD80, CD86, GITRL, ICOS, LAG-3, PD-1, PD-L1, and TLR-2. The following markers were detected in significantly higher concentration in the

plasma of ICI group versus healthy non-smoker and smoker controls: CD27, CD28, CD40, GITRL, LAG-3, PD-1, PD-L1, and TLR-2. We showed the induction of CD69 and IL-2R on CD4+ CD25+ T-cells upon chemotherapy; the exhaustion of one CD8+ T-cell population was detected by the loss of CD127 and a decrease in CD27. CD19+CD20+, CD79B+, or activated B-cell subtypes showed CD69 increase and downregulation of BTLA, CD27, and IL-2R in NSCLC patients following chemotherapy or ICI.

Discussion: Peripheral immunophenotype caused by chemotherapy or PD-1 blocking was shown in the context of advanced NSCLC.

KEYWORDS

non-small cell lung cancer, platinum-based chemotherapy, PD-1 blocking, Nivolumab, Pembrolizumab

1 Introduction

Lung cancer, the most common cancer type causes approximately 13% of all cancer deaths worldwide (1). Lung cancer is a heterogeneous disease classified by histology into two major types: small-cell lung carcinoma (22%) and non-small-cell lung carcinoma (NSCLC), which is further classified into adenocarcinoma (40%), squamous cell carcinoma (30%), and large cell carcinoma (8%) (2). The overall 5-year survival rate is approximately 15% for non-small cell lung cancer and approximately 6% for small-cell lung carcinoma (3, 4). Tobacco smoking has been described to be responsible for 87% of all lung-cancer-related deaths in the USA (5). Although both types are affected differently by tobacco smoking, it has been proven that tobacco smoke is the main preliminary environmental causative factor for lung cancer (2). The main therapeutic options are surgery, radiation therapy, chemotherapy, targeted therapy of the driver mutations of cancer cells, or immunotherapies. A combination of these therapies can be also used following recent guidelines and local recommendations. Platinum-based chemotherapeutics, such as cisplatin, carboplatin, and oxaliplatin, are gold standard chemotherapy treatment options for lung adenocarcinoma without targetable mutation (6, 7). In the advent of immunotherapy, the application of ICIs has dramatically changed patient overall survival (OS) of well-responders; first, PD-1 blocking Nivolumab and Pembrolizumab were applied as second-line treatment options showing superior objective response rate (ORR) and OS compared to docetaxel in NSCLC (8–10). Unfortunately, the tumor progression often outperforms initial response, or resistance to ICI also may develop (11). Several immune mechanisms may counteract with the success of ICI therapy, such as T-cell exhaustion, decreased antigen presentation, altered metabolism, or downregulation of co-stimulatory molecules (12). Although PD-L1 expression is a strong indication, we still lack prognostic markers that could increase patient benefit to PD- 1-targeting ICI therapy (13).

We focus here on the peripheral immune compartment in smoker lung adenocarcinoma patients receiving cisplatin/carboplatin chemotherapy or second- or multiple-line PD-1-targeting immunotherapy. It has been widely known that most of the malignancies bear tumor antigens; carcinogenic compounds of tobacco smoke *per se* generates mutations in the lung, making tissues more immunogenic. However, continuous tobacco smoking triggers a myriad of immune reactions; the activation state and polarization of both myeloid and lymphoid cells are affected in smoker lung cancer patients, making the immune infiltrate irresponsive, the so- called tolerogenic toward arising malignant cells (14). The emergence of myeloid-derived suppressor cells, M2 macrophages, and regulatory T-cells and production of transforming growth factor-β, IL-10, or PD-L1 may sustain the tumor- prone microenvironment (15–17). The deeper insight into the heterogeneity of inflammatory cells in the blood could help to understand the mechanisms responsible for the switch from a tumor suppressor to a tumor promoter immunophenotype. The knowledge of multi-cellular phenotypes and molecular mechanisms responsible behind chronic inflammation and tolerance toward malignancy in lung cancer could reveal novel therapeutic targets. The immune system, due to its high plasticity, can represent different polarization states. Upon activation, innate hematopoietic cells infiltrate the respiratory tract, generating pulmonary inflammation *via* TLR4/MyD88 and IL-1R1/MyD88 signaling- dependent mechanisms (18–20). Among others, we have previously reviewed how tobacco smoking may pave the way for chronic obstructive pulmonary disease (COPD) frequently leading to lung cancer (3, 21). Our interest turned toward the immunophenotyping of peripheral mononuclear cells (PBMCs) comparing smoker NSCLC cases who underwent first- line chemotherapy with cases receiving second/multiple line PD-1-blocking therapy. Our goal was to understand better the obstacles to boost antitumor immunity or overcome tumor- induced tolerance. We aimed to identify leukocyte subsets that are capable of suppressing tumor development; moreover, we aimed to identify

leukocyte subsets that are immunosuppressive and unable to mount an effective anti-tumor immune response in lung cancer patients.

2 Materials and methods

2.1 Cell culturing

Cell culturing was performed as described previously by our group (22). Briefly, the human non-small cell lung cancer (NSCLC) cells, namely, adenocarcinoma cell lines A549, H1975, and H1650, were purchased from the American Type Culture Collection. The H1975 and H1650 cells were maintained in Dulbecco's Modified Eagle Medium (DMEM) or A549 cells in DMEM/F12 (DMEM, PAN-Biotech GMBH, Aidenbach, Germany; DMEM/F12 Nut mix, Gibco, Thermo Fisher Scientific, Waltham, MA, USA) containing 4.5 g/L glucose, 10% fetal bovine serum (FBS) (Gibco), 2 mM GlutaMAX (Gibco, Waltham, MA, USA), 100 U/ml penicillin, and 100 g/ml streptomycin antibiotics (penicillin G sodium salt and streptomycin sulfate salt, Sigma-Aldrich, St. Louis, MO, USA). The cells were cultured in a standard tissue culture Petri dish, 10 mm in diameter (Corning Life Sciences, Corning, NY, USA) at maximum 80% confluence in a standard atmosphere of 95% air and 5% CO_2.

2.2 Study design

Subjects were recruited from the following groups: (1) non-smoker healthy control (without known disease and without regular medication, n=12), (2) smoker lung NSCLC patients receiving first-line chemotherapy (Chem., n=10, only one case was non-smoker), and (3) smoker lung adenocarcinoma receiving second- or multiple- line immunotherapy, where first- line chemotherapy was already terminated before starting the immunotherapy (ICI, n=10). Plasma samples of healthy smoker controls (n=9) were available for multiplex quantitative analysis of soluble markers using the Luminex MagPix system. These healthy smoker controls were recruited with minimum 5 years smoking history with minimum of 10 cigarettes per day without the awareness of chronic illness and without regular medication. The experimental procedures are cross-sectional with the collection and the analysis of 20 ml venous peripheral blood at one time point. However, the follow-up of the patients provided progression- free survival (PFS) and OS data (Table 1). The immunotherapy significantly improved the OS (Supplementary Figure S1). Patients were included with histologically or cytologically confirmed NSCLC (primarily squamous cell or adenocarcinoma) and patients with stage IV or selected stage IIIB disease by the International Staging System (lung cancer). Stage IIIB patients had to have a positive pleural effusion or multiple ipsilateral lung nodules (potentially inoperable disease). Inclusion criteria were bidimensional measurable or assessable disease, PS (performance status) of 0 or 1. Previous surgery and radiotherapy were allowed. One group of patients received first-line platinum-based chemotherapy treatment (Chem.), and the other group received second- or multiple-line immunotherapy after failed chemotherapy (ICI) (in accordance with the Hungarian financing protocol). The samples for the Chem. group were isolated following a minimum of four cycles of platinum-based chemotherapy. The samples for the ICI group were isolated when initial chemotherapy was already terminated, and the following ICI therapy was applied for at least 3 months.

Patient's clinical data are summarized in Supplementary Table S1.

2.3 Ethical statement

The subjects gave their informed consent for inclusion before participating in the study. The study was conducted in accordance with the Declaration of Helsinki, and the protocol ("Immunophenotyping in COPD and lung cancer") was approved by the Ethics Committee of the National Public Health Center,

TABLE 1 Demographic and clinical characteristics of the enrolled patients.

Subjects	Age (years) Median ± SD	Female	Lung cancer histology	Therapy See details in Supplementary Table S1	Progression- free survival to initial therapy (month) Median ± SD	Overall survival (month) Median ± SD
Control	60.5 ± 7.6	50%	none	none	Not relevant	Not relevant
Smoker Control	54 ± 7.3	66%	none	none	Not relevant	Not relevant
Chem.	67.3 ± 5.6	40%	50% adenocarcinoma 50% squamous cell c.	Cisplatin, or Carboplatin, or combined with Pemetrexed, or Gemcitabine	11 ± 13.4	14 ± 20.5 months
ICI	65.1 ± 5.0	50%	60% adenocarcinoma, 30% squamous cell, c. 10% adenocarcinoma + squamous cell c.	Second-line Nivolumab or Pembrolizumab, min. 6 cycles	11 ± 25.9	59.5 ± 45.8 months

Hungary under the 33815-7/2018/EÜIG Project identification code and by the Ethics Committee of the University of Szeged under the 163/2018-SZTE Project identification code.

2.4 PBMC isolation

After the collection of 20 ml of blood into an EDTA vacutainer (Becton Dickinson, Franklin-Lakes, USA), PBMCs were purified by Leucosep tubes (Greiner Bio-One, Kremsmünster, Austria) according to the manufacturer's instructions. Plasma samples were harvested, aliquoted, and stored at −80°C. If the pellet was light red, 2 mL ACK Lysing Buffer (ACK: 0.15 M NH_4Cl, 10 mM $KHCO_3$, 0.1 mM Na_2EDTA, pH 7.3; Merck, Darmstadt, Germany) was applied at room temperature (RT) for 2 min. Samples were washed twice with 10 ml phosphate-buffered saline (PBS) (Merck), and subsequently, cell count and viability check were performed with Trypan Blue (Merck) exclusion. Cryopreservation of PBMCs was carried out in stocks of 4×10^6 cells of 1 ml FBS (Capricorn Scientific, Ebsdorfergrund, Germany) supplemented with 1:10 dimethyl sulfoxide (DMSO) (Merk) [v/v] in cryotubes (Greiner Bio-One) in liquid nitrogen (Messer, Bad Soden, Germany).

2.5 Tumor- cell- specific antibody binding assay

The supernatant of A549, H1975, or H1650 cells grown in 80% confluence in 10 mm diameter Petri dish was removed, and cells were washed with 5 ml PBS and detached by 2 ml Accutase (Thermo Fisher Scientific), centrifuged at 350*g*, 5 min, washed by 5 ml PBS, centrifuged at 350*g*, 5 min, and resuspended in 1ml IFB (Immune Fluorescence Buffer: PBS with 2% FCS). Cells were counted using a Bürker chamber and Trypan Blue, and 2×10^5 viable cells were pipetted into a 1. 5-ml tube (Eppendorf) in 50 µl IFB. Plasma samples were diluted 1:1 in IFB, 25µl + 25 µl, and added to the cells, incubated in 100 µl final volume (4× dilution of the plasma) at 4°C for 60 min. Samples were washed with 1 ml IFB, centrifuged 350*g*, 5 min. Secondary antibody anti-human Alexa488 (Cat. num. 409322, clone HP6017, BioLegend) detecting IgG antibodies (IgA and IgM is not detected) was added in 1:25 dilution in IFB for 30 min at 4°C. Cells were resuspended in 300 µl IFB; 10 µg/ml propidium iodide was added right before the acquisition by FACS Calibur (Becton Dickinson) to gate out dead cells. A schematic cartoon of the assay is illustrated in Supplementary Figure S2. Manual gating was used in CellQuest (Beckton Dickinson) analyzing PI-negative but anti-human-Alexa488- positive cells (Supplementary Figure S3).

2.6 Measurement of plasma proteins

The measurement of plasma proteins was performed as described previously by our group with minor modifications (23, 24). Briefly, after the withdrawal of 20 ml blood into an EDTA vacutainer (Becton Dickinson), human peripheral blood mononuclear cells and plasma samples were purified by Leucosep tubes (Greiner Bio- One). Plasma fractions were stored at −80°C in aliquots before running the assay. Luminex xMAP (MAGPIX®) technology was used to determine the protein concentrations of 17 distinct soluble mediators (BTLA, CD28, CD80, CD27, CD40, CD86, CTLA-4, GITR, GTRL, HVEM, ICOS, LAG-3, PD-1, PD-L1, PD-L2, TIM-3, and TLR-2) performing the Human Immuno-Oncology Checkpoint Protein Panel 1—Immuno-Oncology Multiplex Assay (Cat. num. HCKP1-11, Merck) according to the instructions of the manufacturer. Briefly, all samples were thawed and diluted with sterile PBS to 1:1 and were tested in a blind fashion and in duplicate. A total of 25 µl volume of each sample, standard, and universal assay buffer was added to a 96-well plate (provided with the kit) containing 50 µl of capture antibody-coated, fluorescent-coded beads. Biotinylated detection antibody mixture and streptavidin- PE were added to the plate after the appropriate incubation period. After the last washing step, 120 µl reading buffer was added to the wells, and the plate was incubated for an additional 5 min and read on the Luminex MAGPIX® instrument. Luminex xPonent 4.2 software was used for data acquisition. Five-PL regression curves were generated to plot the standard curves for all analytes by the Analyst 5.1 (Merck) software, calculating with bead median fluorescence intensity values. The scatter plots of the individual values are demonstrated in Supplementary Figure S4. The panel of the investigated 17 plasma proteins and the range of the detection (in pg/ml from the lower limit to the upper limit) are available in Supplementary Table S2. Data were pooled from two independent measurements and plotted in GraphPad Prism v8 (Dotmatics, Boston, USA).

2.7 Cell preparation for CyTOF (cytometry by time-of-flight)

Cells were processed for CyTOF as described previously by our group (25). Briefly, cryotubes were thawed in a 37°C water bath, and cells were transferred into 14 ml of 37°C warm RPMI 10% FBS (Capricorn Scientific) and centrifugated at 350*g* for 6 min at RT. PBMCs were washed again with 10 ml RPMI 10% FBS, and cells were counted and viability determined with Trypan Blue exclusion. PBMCs, 2.5×10^6 cells/sample, were plated on a 96-well repellent plate (Greiner Bio-One) separately in 200 µl RPMI 10% FBS. After 2 h, cells were stimulated with 10 ng/ml phorbol myristate acetate (PMA), 1 µg/ml ionomycin, and 5 µg/ml Brefeldin A for 16 h in an incubator with 5% CO_2 at 37°C. Next, cells were collected and washed twice with Maxpar Cell Staining Buffer (MCSB; Fluidigm, South San Francisco, USA).

2.8 Antibody staining

The antibody staining of cells for CyTOF was performed as described previously by our group with minor modifications (26, 27). Before harvesting, cells were incubated with 100 mM EDTA for 15 min RT. Briefly, viability was determined by cisplatin (5 µM

^{195}Pt, Fluidigm) staining for 3 min on ice in 500 µl PBS. The sample was diluted by 3 ml Maxpar Cell Staining Buffer (MCSB, Fluidigm) and centrifuged at 350 g for 5 min. Cells were resuspended in 50 µl MCSB supplemented with 1:20 v/v TrueStain FcX™ FC receptor blocking solution (Biolegend, San Diego, USA) and incubated at RT for 10 min. Without a washing step, samples were barcoded by adding 50 µl of different metal-tagged (A-^{89}Y, B-^{112}CD, C-^{113}CD, D-^{114}CD, and E-^{116}CD) CD45 antibodies (clone: 30-F11; Fluidigm) at a final concentration of 1:100 v/v per antibody and incubated at 4°C for 30 min. The codes of the barcoding were the following: 1. AB, 2. AC, 3. AD, 4. AE, 5. DC, 6.BD, 7. BE, 8. CD, 9. CE, and 10. DE. Following the barcoding, 10 samples were pooled for the subsequent antibody staining. First, cells were stained with cell surface antibodies from our Immune Checkpoint Panel designed in-house and bought antibodies from Fluidigm and incubated at 4°C for 30 min, washed twice with 2 ml MCSB. The list of the antibodies used for the study is in Table 2. Fixation was performed with 1 ml Maxpar Fix I buffer (5×) diluted in PBS, incubated at RT for 30 min, and washed twice with 2 ml Maxpar PermS Buffer, centrifugated at 800*g*, 5 min. Cells were stained with the intracellular markers (TNF-α, IL-6, IL-2, granzyme B, and perforin) and incubated at RT for 30 min. Cells were washed twice with MCSB and fixed with 1 ml Pierce™ formaldehyde (Thermo Fisher Scientific) solution diluted in PBS to 1.6% and incubated at RT for 10 min. Stained and fixed cells were centrifuged at 800 g at RT for 6 min and resuspended in 800 µl Fix & Perm solution (Fluidigm) supplemented with 1:1,000 v/v ^{191}Ir-^{193}Ir DNA intercalator (Fluidigm) for overnight incubation.

2.9 CyTOF data acquisition and data preprocessing

The acquisition of the samples for CyTOF was executed as described previously by our group with minor modifications (25, 27). Briefly, samples were washed twice with MCSB and once with PBS prior filtered through a 30-µm Celltrics (Sysmex, Bornbarch, Germany) gravity filter, and the cell concentration was adjusted to 7×10^5/ml in Maxpar Cell Acquisition Solution (Fluidigm). Finally, EQ four- element calibration beads (Fluidigm) were added at a 1:10 ratio (v/v) and acquired on a properly tuned Helios mass cytometer (CyTOF, Fluidigm). We collected 1×10^6 events per barcoded sample. The generated flow cytometry standard (FCS) files were randomized and normalized with the default setting of the internal FCS-processing unit of the CyTOF Software (Fluidgm, version:7.0.8493). The analysis was carried out in Cytobank (Beckman Coulter) by manual gating. The gating hierarchy is shown in Supplementary Figure S5. The raw median values were exported from Cytobank and archinh transformed in MS Excel.

2.10 Statistical analysis

Data were analyzed with GraphPad Prism 8.0.1. Normality of distributions was tested with D'Agostino and Pearson test with an 0.05

TABLE 2 The list of the antibodies used for the mass cytometry.

Marker	Clone	Metal tag	Supplier
Gal-1	2C1/6	^{141}Pr	Monostori's lab (28)
CD40	5C3	^{142}Nd	Fluidigm
CD5	SK1	^{143}Nd	Fluidigm
CD69	FN50	^{144}Nd	Fluidigm
CD138	DL-101	^{145}Nd	Fluidigm
CD11c	3.9	^{146}Nd	Fluidigm
CD20	2H7	^{147}Sm	Fluidigm
IgA	Polyclonal	^{148}Nd	Fluidigm
CD86	IT2.2	^{150}Nd	Fluidigm
HLA-DR	G46-6	^{151}Eu	Fluidigm
TNF-α	Mab11	^{152}Sm	Fluidigm
Mac-2/Gal-3	M3/38	^{153}Eu	Fluidigm
CD3	UCHT1	^{154}Sm	Fluidigm
CD279 (PD-1)	EH12.2H7	^{155}Gd	Fluidigm
IL-6	MQ2-13AS	^{156}Gd	Fluidigm
CD134 (OX40)	ACT35	^{158}Gd	Fluidigm
CD274 (PD-L1)	29E.2A3	^{159}Tb	Fluidigm
CD28	CD28.2	^{160}Gd	Fluidigm
CD80 (B7-1)	2D10.4	^{161}DY	Fluidigm
CD79B	CB3-1	^{162}Dy	Fluidigm
CD272 (BTLA)	NIH26	^{163}Dy	Fluidigm
CD19	HIB19	^{165}Ho	Fluidigm
IL-2	MQ1-17H12	^{166}Er	Fluidigm
CD27	L-128	^{167}Er	Fluidigm
CD8a	SK1	^{168}Er	Fluidigm
CD25 (IL-2R)	2A3	^{169}Tm	Fluidigm
CD152 (CTLA-4)	14D3	^{170}Er	Fluidigm
Granzyme B	GB11	^{171}Yb	Fluidigm
IgM	MHM-88	^{172}Yb	Fluidigm
CD4	SK3	^{174}Yb	Fluidigm
Perforin	B-D48	^{175}Lu	Fluidigm
CD127	A019D5	^{176}Yb	Fluidigm
CD16	3G8	^{209}Bi	Fluidigm
CD45	HI30	^{89}Y	Fluidigm
CD45	Hl30	^{112}Cd	Fluidigm
CD45	Hl30	^{113}Cd	Fluidigm
CD45	Hl30	^{114}Cd	Fluidigm
CD45	Hl30	^{116}Cd	Fluidigm

alpha value. We used non-parametric Kruskal–Wallis test for the four group comparisons with non-normal distribution. Dunn's test was used for multiple comparisons. The log-rank test was used for OS data. Differences are considered significant at *p < 0.05, **p < 0.01, and ***p < 0.001.

3 Results

3.1 Platinum-based chemotherapy and second- or multiple-line PD-1 blockade of well-responders increased humoral immunity in NSCLC patients

Among others, we have previously shown the immunomodulatory effects of platinum-based chemotherapeutics, such as cisplatin or carboplatin used in the current study (25, 29, 30). Here, we developed a flow- cytometry-based assay to measure the increase in NSCLC-related cell surface epitope binding IgG antibodies in cancer patients. The incubation of patient-derived plasma with human NSCLC tumor cell lines, such as A549, H1975, and H1650, were used to detect NSCLC -specific antibodies. The percentage of reactive A549 cells in control samples were between min–max of 0.4% –2.2% (mean, 1; SD, 0.4; SEM, 0.1) compared to the chemotherapy- treated group reaching a maximum of 8.9% of cells (min–max, 1.1% –8.9%; mean, 3.1; SD, 2.6; SEM, 0.8; *p<0.05). The ICI treatment led to the production of A549 binding antibodies between min–max of 0.3%–12.8% (mean, 3; SD, 4; SEM, 1.2) (Figure 1A). The percentage of reactive H1975 cells in control samples were between min–max of 0.2%–4% (mean, 1; SD, 1.1; SEM, 0.3) versus chemotherapy- treated group reaching maximum 5.8% (min–max, 0.7%–5.8%; SD, 1.6; SEM, 0.5; *p<0.05). The ICI treatment led to the production of H1975 binding antibodies between min–max of 0%–32.2% (mean, 6.1; SD, 9.7; SEM, 3) (Figure 1B). The percentage of reactive H1650 cells in control samples were between min–max of 0.1%–2.5% (mean, 0.9; SD, 0.7; SEM, 0.2) versus chemotherapy- treated group reaching a maximum of 8.1% (min–max, 2.1%–8.1%; SD, 1.8; SEM, 0.5; *p<0.05). The ICI treatment led to the production of H1650 binding antibodies between min–max of 0.1%–6.2% (mean, 2.7; SD, 2.3; SEM, 0.7) (Figure 1C).

3.2 The pattern of immune-oncology mediators in the plasma of platinum-based chemotherapy and second- or multiple-line PD-1 blockade- treated patients

The multiplex Luminex MagPix technology was used to measure the concentration of 17 soluble immune checkpoint modulators in the plasma samples of platinum-based chemotherapy (cisplatin or carboplatin; Chem.) or second- or multiple-line PD-1 blockade immune checkpoint inhibitor (Nivolumab or Pembrolizumab; ICI)- treated patients versus non-smoker healthy controls (Contols) or versus smoker healthy controls, respectively. The list of the proteins measured in the plasma of the human subjects enrolled in the study including full name, alternative name, gene ID, Uniprot ID, and the range of the detection is summarized in Supplementary Table S2. The individual concentrations of the cytokine/chemokines/immune checkpoint modulators are demonstrated in scatter plots in Supplementary Figure S4. The following markers were detected in significantly higher concentration in the plasma of Chem. group versus healthy non-smoker and smoker controls: BTLA, CD27, CD28, CD40, CD80, CD86, GITRL, ICOS, LAG-3, PD-1, PD-L1, and TLR-2. The following markers were detected in significantly higher concentration in the plasma of ICI group versus healthy non-smoker and smoker controls: CD27, CD28, CD40, GITRL, LAG-3, PD-1, PD-L1, and TLR-2 (Table 3; Supplementary Figure S4). There was no marker showing significantly different concentrations between the non-smoker controls and smoker controls. The CD80 and ICOS were increased in the Chem. group but not in the ICI group in relation with the controls.

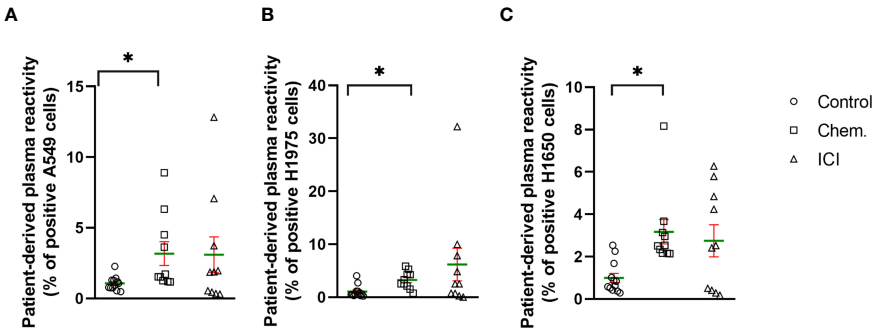


FIGURE 1
Platinum-based chemotherapy and PD-1 blockade increased the production of tumor cell surface-specific IgG antibodies in well-responder NSCLC patients. The scatter plots demonstrate the effect of platinum-based chemotherapy (Chem., n=10) or second- line immunotherapy (ICI, n=10) to the level of IgG antibodies in the plasma of patients with reactivity of **(A)** A549, **(B)** H1975, or **(C)** H1650 NSCLC cell line cell surface epitopes. Age- and gender-matched healthy controls were recruited without known illness (Control, n=12). The experimental details can be found in the *Materials and Methods*. Briefly, flow cytometry was used to detect human NSCLC cell- line-specific cell surface binding IgG antibodies. *p < 0.05.

10.3389/fimmu.2023.1243233

TABLE 3 The summary of the soluble immune checkpoint modulator plasma concentrations in healthy non-smoker controls (Controls, n=10), in healthy smoker controls (n=9), in Chem. (n=10) or in the ICI (n=10) groups (Cont., n=10).

Marker	Cohort	Mean (pg/ml)	SD	SEM	CI (95%)
					0
BTLA	Cont.	2,644	2,773	876.9	660.2 –4628
	Smoker control	2,622	1,384	461.2	1,559 –3,686
	Chem.	7,168	3,467	1,096	4,688 –9,649
	ICI	6,283	1,999	632.2	4,853 –7,713
CD27	Cont.	663.4	417	131.9	365.1 –961.7
	Smoker control	562.8	315.3	105.1	320.5 –805.2
	Chem.	1,416	428.9	135.6	1,109 –1,723
	ICI	1,307	404.5	127.9	1,018 –1,597
CD28	Cont.	6,308	6,304	1,993	1,799 –10,818
	Smoker control	6,224	3,957	1,319	3,182 –9,265
	Chem.	17,623	9,540	3,017	10,798 –24,447
	ICI	17,726	7,738	2,447	12,190 –23,261
CD40	Cont.	322.7	143.2	45.28	220.3 –425.2
	Smoker control	260.1	111.8	37.28	174.2 –346.1
	Chem.	633.3	155.7	49.22	522 –744.6
	ICI	615.6	146.5	46.32	510.8 –720.4
CD80/B7-1	Cont.	456.1	457.3	144.6	129 –783.2
	Smoker control	416.6	228.4	76.12	241 –592.1
	Chem.	1,063	455.8	144.1	737.1 –1,389
	ICI	955.7	286.6	90.63	750.7 –1,161
CD86/B7-2	Cont.	1,440	1,944	614.9	49.44 –2,831
	Smoker control	1,110	695.8	231.9	574.7 –1,644
	Chem.	4,920	3,020	954.9	2,760 –7,080
	ICI	4,412	2,159	682.7	2,868 –5,957
CTLA-4	Cont.	168	206.2	65.22	20.46 –315.5
	Smoker control	167.3	99.0	33.0	91.21 –243.7
	Chem.	469.3	243.9	77.11	294.9 –643.8
	ICI	425.7	163.5	51.69	308.8 –542.6
GITR	Cont.	366.4	508.9	160.9	2.37 –730.4
	Smoker control	405.1	274.3	91.44	194.3 –616.0
	Chem.	1,363	799.4	252.8	791.4 –1,935
	ICI	1,370	712.4	225.3	859.9 –1,879
GITRL	Cont.	1,798	1,439	455	768.9 –2,828
	Smoker control	1,582	807.3	269.1	961.2 –2,202
	Chem.	3,790	1,411	446.2	2,781 –4,800
	ICI	3,859	1,061	335.4	3,100 –4,617

(Continued)

10.3389/fimmu.2023.1243233

TABLE 3 Continued

Marker	Cohort	Mean (pg/ml)	SD	SEM	CI (95%)
HVEM	**Cont.**	538.3	193.7	61.24	399.7 –676.8
	Smoker control	374.7	181.6	60.54	235.1 –514.4
	Chem.	981.4	375.5	118.7	712.8 –1,250
	ICI	923.7	348	110.1	674.7 –1,173
ICOS	**Cont.**	2,911	3,449	1,091	444.3 –5,378
	Smoker control	2,913	1,834	611.4	1,503 –4,323
	Chem.	7,712	3,989	1,262	4,858 –10,566
	ICI	6,564	2,126	672.1	5,043 –8,084
LAG-3	**Cont.**	35,046	36,480	11,536	8,950 –61,142
	Smoker control	30,775	18,096	6,032	16,866 –44,685
	Chem.	84,508	33,650	10,641	60,437 –108,580
	ICI	88,290	21,631	6,840	72,816 –103,763
PD-1	**Cont.**	1,318	1,489	470.9	252.5 –2,383
	Smoker control	1,158	681.9	227.3	633.6 –1,682
	Chem.	3,766	1,906	602.6	2,403 –5,130
	ICI	4,763	1,383	437.4	3,773 –5,752
PD-L1	**Cont.**	322.1	398.8	126.1	36.78 –607.4
	Smoker control	323.9	197	65.65	172.5 –475.3
	Chem.	986.5	481.2	152.2	642.3 –1,331
	ICI	955.3	351	111	704.2 –1,206
PD-L2	**Cont.**	4,934	571.1	180.6	4,525 –5,342
	Smoker control	3,753	672.7	224.2	3,236 –4,270
	Chem.	5,588	867	274.2	4,967 –6,208
	ICI	5,407	896.8	283.6	4,766 –6,049
TIM-3	**Cont.**	974.3	332.4	105.1	736.5 –1,212
	Smoker control	645	183.9	61.31	503.7 –786.4
	Chem.	1,526	454.6	143.7	1,201 –1,852
	ICI	1,512	556	175.8	1,114 –1,910
TLR-2	**Cont.**	2,754	3,170	1,003	486.1 –5,022
	Smoker control	2,407	1,630	543.3	1,154 –3,660
	Chem.	8,641	4,289	1,356	5,573 – 11,710
	ICI	7,750	3,145	994.6	5,500 –10,000

The arithmetic means (Mean), standard deviation (SD), and the standard error of the mean (SEM) of the plasma marker concentrations were calculated. The multiple comparisons of the concentrations of each marker were carried out by the Kruskal–Wallis test. Significant differences are labeled in Supplementary Figure S4. The 95% confidence intervals (CI, 95%) were calculated for each marker in all groups, separately.

10.3389/fimmu.2023.1243233

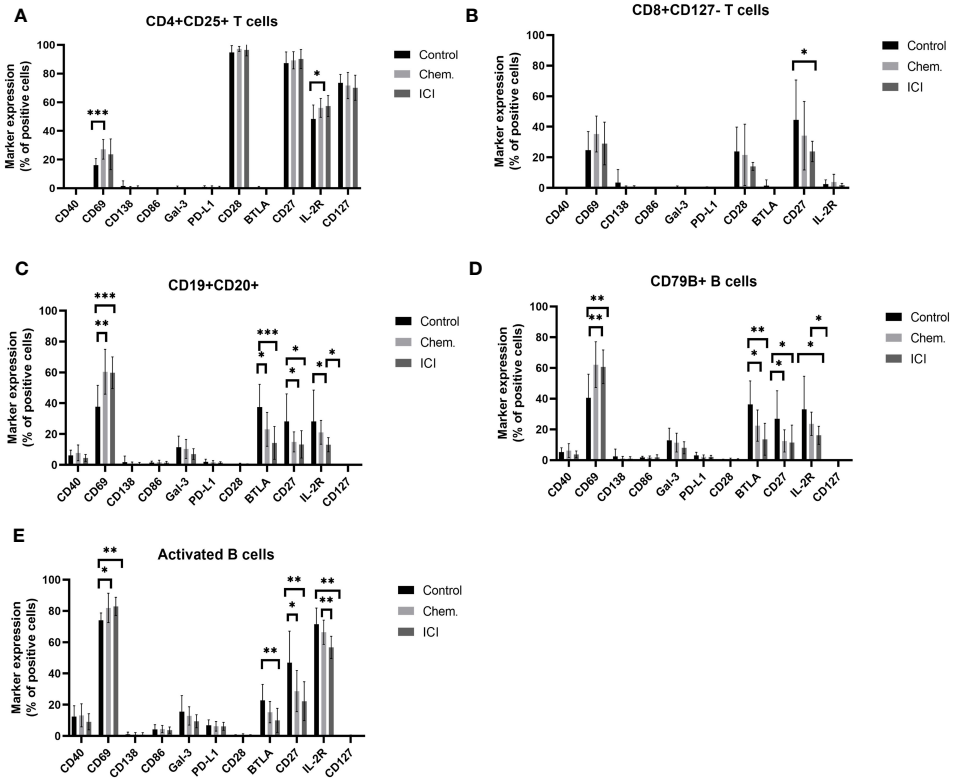


FIGURE 2
Expression profile of immune regulatory molecules on T- or B-cell subsets following platinum-based chemotherapy or PD-1 blockade. The PBMCs were purified from the peripheral blood of platinum-based chemotherapy (Chem.) or second- or multiple-line PD-1 blockade immunotherapy (ICI) patients and assayed for single- cell mass cytometry as described in *Materials and Methods*. The panel of the antibodies used for CyTOF is listed in Table 2. Manual gating was performed in Cytobank, and it is shown in Supplementary Figure S5. The T-cell **(A, B)** or B-cell subsets **(C–E)**, positive for the expression of cell surface immune regulatory molecules CD40, CD69, CD138, CD86, Gal-3, PD-L1, CD28, BTLA, CD27, IL-2R, and CD127, are shown as the percentages of parental population. *p < 0.05, **p < 0.01, ***p < 0.001.

3.3 The effect of first-line platinum-based chemotherapy or multiple-line PD-1 blockade on the peripheral immunophenotype detected by single cell mass cytometry

Single- cell mass cytometry (CyTOF) was used for the immunophenotyping of patient-derived peripheral leukocytes. The expression of CD69 increased upon platinum-based chemotherapy 27.19% ± 6.81% versus 16.24% ± 4.47% (mean ± SD) of CD4+CD25+ T-cells. A slight increase in the percentage of IL-2R positivity was also observed upon chemotherapy (56.09% ± 6.58% vs. 48.42 ± 9.69%) (Figure 2A). Exhaustion of CD8+ T-cells was also measured by the decrease in the expression of costimulatory CD27 on the IL-7Rα chain (CD127 −) negative subpopulation in the average of the ICI patients compared to controls (23.9 ± 6.66 vs. 44.55 ± 26.09) (Figure 2B). Three B-cell populations were gated, the CD19+CD20+ B-cells, CD79B+ B-cells, and activated B-cells (CD19+CD25+/CD69+). The $CD69^{bright}$ and $IL\text{-}2R^{bright}$ positive cells were gated on B-cell variants. The CD69 is a type II C-type lectin involved in the migration of lymphocytes highly expressed upon activation in both T- and B-cells (31, 32). The CD69 bright cells increased in all gated B-cell subtypes upon chemotherapy and ICI compared to that in healthy controls (Figures 2C–E). The BTLA-negative regulator of activation was suppressed upon chemotherapy and ICI in CD19+CD20+ B-cells (Supplementary Figure S6) and CD79B+ B-cells, and only ICI led to the significant decrease in BTLA on activated B-cells (10.06 ± 7.72 vs. 22.72 ± 10.34 in controls) (Figures 2C–E). Representative viSNE plots show the downregulation of cell surface BTLA on Chem.- or ICI- treated samples on CD19+CD20+ B-cells (Supplementary Figure S6). The positive regulators of activation, both CD27 and $IL\text{-}2R^{bright}$ populations, were significantly reduced upon chemotherapy or ICI in the average of the study cohorts on the surface of all investigated B-cell subtypes (Figures 2C–E).

Following the frequencies of T- or B-cell subsets, marker expression intensities (arcsinh-transformed medians) were investigated. The negative regulator of immune activation BTLA was significantly decreased in CD3-CD19+ and CD19+CD20+ conventional B-cells, and in IgM+ B-cells, CD79B+, and in IgA+ B-cells (Figure 3A). In parallel, the CD69 involved in lymphocyte activation and migration was increased in CD3-CD19+ and CD19+CD20+ conventional B-cells, IgM+ B-cells, and in the B-cell receptor component CD79B+ B-cells (Figure 3B). However, for markers important for activation or extravasation, the IL-2R (CD25) was decreased in the cell surface of IgA+ B-cells and activated B-cells (Figure 3C), and similarly, the CD29 (beta 1 integrin) was also decreased in activated B-cells (Figure 3D).

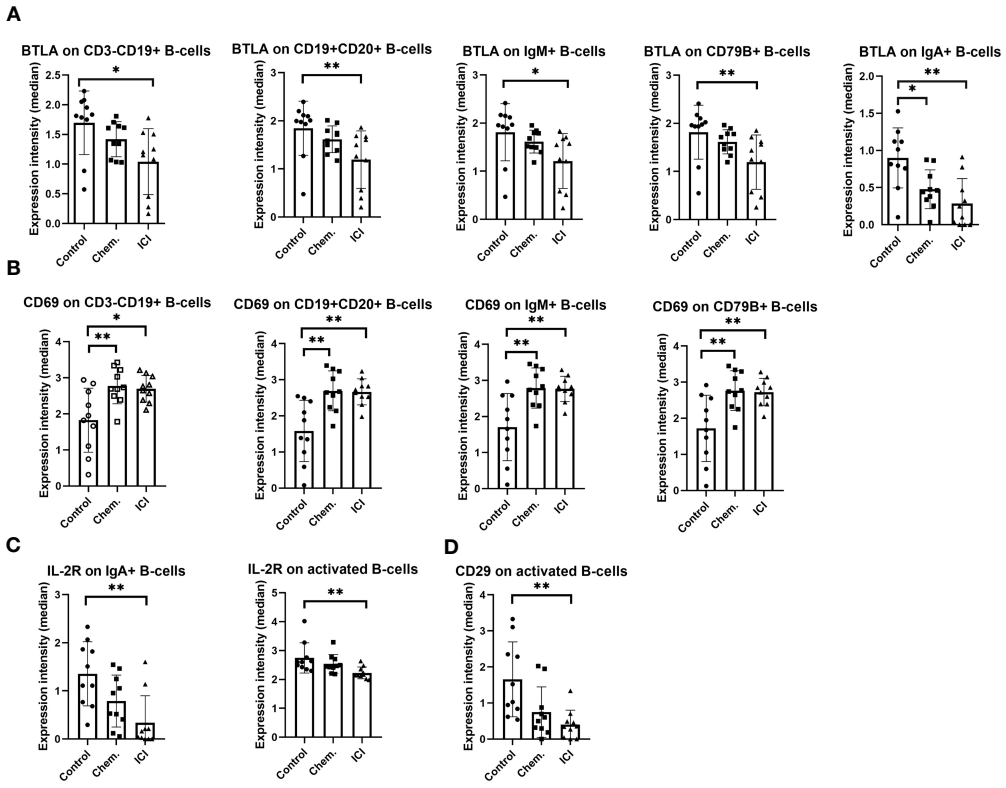


FIGURE 3
The expression intensity of BTLA, CD69, IL-2R, and CD29 on different B-cell subsets. The PBMCs were purified from the peripheral blood of platinum-based chemotherapy (Chem.) or multiple-line PD-1 blockade immunotherapy (ICI) patients and assayed for single- cell mass cytometry as described in *Materials and Methods*. The panel of the antibodies used for CyTOF is listed in Table 2. Manual gating was performed in Cytobank, and it is shown in Supplementary Figure S5. The median metal intensities for **(A)** BTLA, **(B)** CD69, **(C)** IL-2R, and **(D)** CD29 are proportional with marker densities on the surface of the analyzed B-cell subsets **(A–D)**. *p < 0.05, **p < 0.01.

The CD4+ helper T-cells may support both the humoral and cellular arms of the immune defense against the malignant cells. The second- line anti-PD-1 blocking ICI therapy increased the TNF-α in CD4+ T-cells and in costimulatory OX40+/CD4+ or CD25+/CD4+ T-cell populations (Figure 4A). The IL-2R density also increased upon multiple-line ICI treatment on CD4+ T-cells or on CD4+/OX40+ T-cells (Figure 4B). The platinum-based chemotherapy increased CD69 expression on CD4+/CD25+ T-cells (Figure 4C).

4 Discussion

The manifestation of most type of solid tumors occurs following the escape from immunosurveillance (33). A clinical study with 931 patients recruited between 2013 and 2020 identified a significant correlation between smoking shistory and higher tumor mutational burden in non-small cell lung cancer, lung adenocarcinoma (34). Additionally, in the case of lung cancer, the tobacco- smoking-generated airway inflammation further skews the polarization of immune cells to a tumor promoter phenotype (3, 21, 35). Previously, we have shown the immunomodulatory effect of cisplatin in triple negative murine breast cancer model reducing the emergence of splenic CD44+, IL-17A+ myeloid suppressor cells (25). Here, we focused on smoker human NSCLC, adenocarcinoma patients receiving platinum-based chemotherapy, or multiple-line PD-1 blocking immunotherapy. In our cross-sectional study, cisplatin or carboplatin were used as first-line platinum-based chemotherapeutics (Chem. group), or Nivolumab and Pembrolizumab were used for PD-1 blocking second- or multiple-line immunotherapy (ICI group) enrolled between November 2018 and June 2019. The OS of the ICI- treated patients was significantly improved (Supplementary Figure S1). We have developed a flow-cytometry-based assay to measure the humoral immunity against NSCLC-derived antigens. The human NSCLC cell lines (A549, H1975, and H1650) were incubated with NSCLC-patient-derived plasma and assayed for IgG antibodies bound on the surface of the NSCLC cell lines bearing putative NSCLC-related cell surface antigens. It has to be emphasized that using three different human cell lines instead of the corresponding patient- matched self-reactive tumor biopsy specimens to detect tumor reactive IgG level is a limitation of our study, but the access to patient-matched lung cancer fresh biopsy was not available. However, using the A549, H1975, and H1650 recipient cells, we were able to show a significant increase in NSCLC- reactive IgG antibodies in plasma upon chemotherapy and a tendentious increase upon multiple-line ICI therapy reaching up to 32% positivity of H1975 cells in one well-responder case. Further

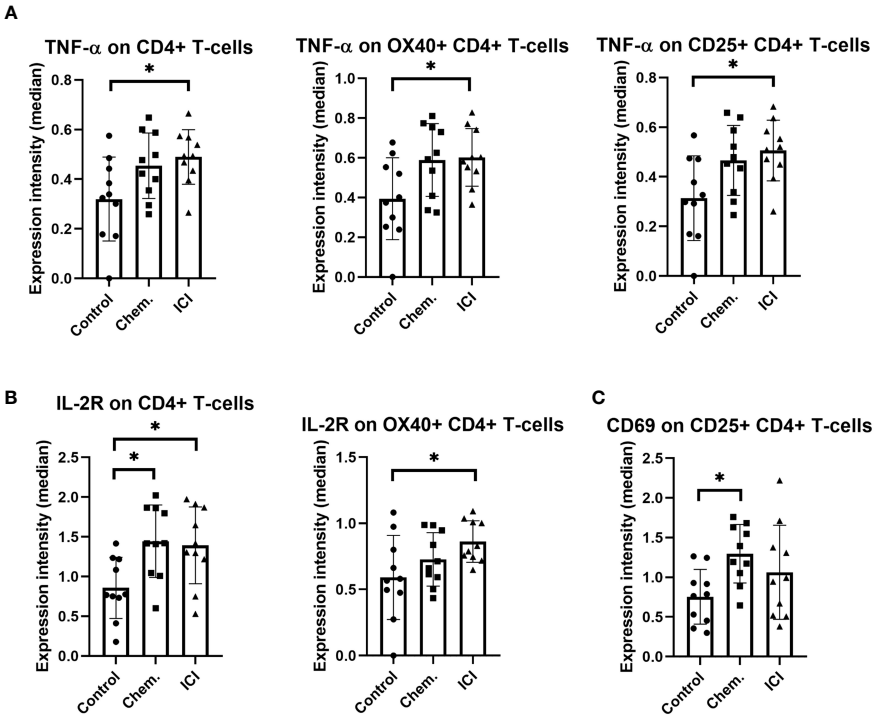


FIGURE 4
The expression intensities of TNF-α, IL-2R, and CD69 on different CD4+ T-cell subsets. The PBMCs were purified from the peripheral blood of platinum-based chemotherapy (Chem.) or multiple-line PD-1 blockade immunotherapy (ICI) patients and assayed for single- cell mass cytometry as described in *Materials and Methods*. The panel of the antibodies used for CyTOF is listed in Table 2. Manual gating was performed in Cytobank, and it is shown in Supplementary Figure S5. The median metal intensities for **(A)** TNF-α, **(B)** IL-2R, and **(C)** CD69 are proportional with marker expression intensities of the analyzed CD4+ T-cell subsets **(A–C)**. *p < 0.05.

analysis of NSCLC tumor cell line reactive plasma samples of well-responder cases may help to identify IgG sequences for the development of therapeutic antibodies, but this work is beyond the capacities of our laboratory. Another important component of patient-derived plasma samples, soluble immune checkpoint mediators were quantitatively measured using the multiplex Luminex MagPix system. The lung cancer patients recruited for our cross-sectional study were in advanced stage receiving chemotherapy or second-line ICI following failed chemotherapy. Authors may suppose that this was the reason why the Chem. and ICI groups were not differentiated in terms of the plasma concentrations of the 17 soluble markers. However, the following markers were detected in significantly higher concentration of the plasma of Chem. group versus healthy non-smoker and smoker controls: BTLA, CD27, CD28, CD40, CD80, CD86, GITRL, ICOS, LAG-3, PD-1, PD-L1, and TLR-2. The following markers were detected in significantly higher concentration in the plasma of ICI group versus healthy non-smoker and smoker controls: CD27, CD28, CD40, GITRL, LAG-3, PD-1, PD-L1, and TLR-2. The increased concentration of CD80 and ICOS was present only in the Chem. group differentiating from the ICI group in relation with the controls. There was no marker showing significantly different concentration between the non-smoker controls and smoker controls. The functional categories of these soluble mediators represent immune checkpoint inhibitors such as BTLA, LAG-3, PD-1. PD-L1, and PD-L2; decoy TLR2 inhibiting innate activation upon danger signals; or costimulatory molecules such as CD27, CD28, CD40, CD80, CD86, GITRL, and ICOS (36–39). This mixed phenotype of the elevated inhibitory and costimulatory molecules may be associated with cancer-driven inflammation and may counteract with the success of ICI therapy. Next, we aimed to deeply analyze the immunophenotype of the peripheral immune system, comparing the PBMCs in Chem. group with multiple-line ICI- treated NSCLC patients using the state-of-the-art single cell mass cytometry (CyTOF). A mixed immunophenotype was detected, both the immunostimulatory effect of platinum-based chemotherapeutics and the exhaustion of CD4+ or CD8+ T-cells were shown. The BTLA was identified as a negative regulator of humoral immune activation inhibiting the IL-6 pathway (40, 41). Our CyTOF experiments showed downregulation of BTLA on conventional, CD19+; CD19+/CD20+ B-cells, IgM+; IgA+, or CD79B+ B-cells following the PD-1 blocking therapy. The increased expression of TNF-α or IL-2R in CD4+; CD4+/OX40+ T-cells showed the immunoactivation. However, one obstacle of cancer immunotherapy is the exhaustion of T-cells, which was shown by the decrease in CD27 and CD127 on CD8+ T-cells upon ICI therapy in our current study. Moreover, the IL-2R and CD29 were decreased on IgA+ or activated B-cells. The role of CD69 is controversial because it is a type II transmembrane glycoprotein with a C-type lectin domain that is a marker of early lymphocyte

activation (42). However, deficiency in CD69 in animal models or targeting CD69 showed an attenuated tumor growth and improved anti-tumor immunity (43, 44). Therefore, CD69 is becoming a factor regulating anti-tumor immunity through T-cell exhaustion (45). In line with this, a study conducted on the Cancer Treatment Response gene signature DataBase revealed CD69 expression as a prognostic factor for responding to PD-1 blocking therapy (46). In our experiments, CD69 was upregulated in the percentages of CD4 +CD25+ helper T-cells, conventional CD19+CD20+ B-cells, and in the frequency of CD79B+ B-cells, or activated B-Cells (CD19+, $CD69^{bright}$ IL-$2R^{bright}$). Analyzing the median expression intensities, the cell surface density of CD69 was also increased on B-cell subsets: on CD3-CD19+ and CD19+CD20+ conventional B-cells, IgM+ B-cells, and on the B-cell receptor component CD79B+ B-cells. B-cell activation may result in the production of tumor-specific antibodies, and B-cells can present antigens to CD4 or CD8 T-cells facilitating cellular immunity also (47). Higher CD69 expression on CD19+ B-cells was reported with longer survival in colorectal cancer (48).Understanding the complexity of the polarization of T- or B-cell subsets, myeloid cell types in response to ICI therapy is the focus of the current research. In agreement with our study, others reported also the "Janus" scenario regarding the anti-tumor immune response following ICI therapy. Sorin et al. published the spatial single- cell immunophenotyping of the tumor microenvironment of 27 NSCLC patients following ICI and found that CXCL13 expression on CD4+ T-cells was associated with good prognosis (49). Rahim et al. showed in head and neck squamous cell carcinoma that exhausted CD8+ T-cells reduced in frequency following ICI but localized nearer to DCs in the lymph nodes (50). Luo et al. identified CD103+ CD39+ T-cells in colorectal cancer patients with an exhausted but cytotoxic phenotype as a good prognosis in response to ICI therapy (51). Lavoie et al. showed that PD1 − CD4+ T cells had higher TNFα and higher CCR4 expression, while their PD1+ CD4+ T cells had higher interferon-γ and lower CCR4 expression in non-responder cases to ICI in urothelial and renal cell carcinoma (52). Xiao et al. analyzed 26 melanoma patients who underwent PD-1 blocking therapy and showed the abundance of CD27+ and TIM-3+ T-cells in the tumor microenvironment of well- responders. Sidiropoulos et al. analyzed the T-cell polarization states in pancreatic ductal adenocarcinoma, melanoma, and hepatocellular carcinoma upon immunotherapies and established single-cell trajectory inference and non-negative matrix factorization methods to CyTOF data to trace the dynamics of T- cell states (53). Their state-of-the art method is demonstrated to monitor patient-specific T-cell states including naive, memory, and effector T- cell phenotypes during immunotherapy.

Taken together, we could show the humoral immune activation in the Chem. group, since the anti-tumor IgG antibodies were significantly increased following chemotherapy (Figure 1). In line with this, CD69 and CD79 were also upregulated after chemotherapy on the cell surface of B-cells (Figure 2). The ICI therapy enhanced the effect of chemotherapy in the increase in IL-2R on CD4+CD25+ T-cells and increased the decline of CD27 on CD8+CD127 − T-cells (Figure 2). The ICI therapy potentiated the effect of chemotherapy in the decline of BTLA on B-cell subsets and in the increase in CD69 on B-cell subsets (Figure 3). Looking at Figure 4, it is also turned out that chemotherapy induced TNF-α in CD4+ T-cells, in CD4+OX40+ T-cells, and in CD4+CD25+ T-cells and that TNF-α induction was further increased by second-line ICI therapy. However, only ICI provided statistically significant TNF-a induction.

Finally, limitations of our study should be mentioned: (1) cell lines were used as a model system expressing putative NSCLC -related antigens, (2) second- or multiple-line application of PD-1 blockade therapy, (3) cross-sectional study without longitudinal follow-up of the soluble mediators or cell surface markers, (4) relatively small number of subjects in the study cohorts, and (5) the complex immunophenotyping of smoker but non-tumorous cases would be relevant, but in those cases, the appearance and disappearance of previous tumors could not be ruled out. Therefore, the authors suggest that the analysis of smoking on the immunophenotype without the manifestation of solid tumors should be a proposed future study. However, we could show the appearance of NSCLC tumor cell line reactive IgG antibodies in the plasma of the patients. The concentration of 17 soluble mediators, immune checkpoint regulators, were measured in advanced NSCLC patients. Moreover, single- cell mass cytometry showed a Janus-faced immunophenotype with the emergence of immune activation in line with T-cell exhaustion. Further research is warranted about the complex immunophenotype on first-line PD-1 blockade with prospective follow-up in comparison with platinum-based chemotherapy.

Data availability statement

The original contributions presented in the study are included in the article/Supplementary Material. Further inquiries can be directed to the corresponding authors.

Ethics statement

The studies involving humans were approved by Ethics Committee of the National Public Health Center, Hungary under the 33815-7/2018/EÜIG Project identification code and by the Ethics Committee of the University of Szeged under the 163/2018-SZTE Project identification code. The studies were conducted in accordance with the local legislation and institutional requirements. The participants provided their written informed consent to participate in this study.

Author contributions

GL, LP, and GS conceived the project. GS and KS was involved in the experimental design. PN, NG, JB, LT, and JF performed the experiments. NG, PN, and GS analyzed the data. GS drafted the manuscript. All authors contributed to the article and approved the submitted version.

Funding

This research was funded by the 2020-1.1.6-JÖVŐ–2021-00003 and 142877 FK22, KFI_16-1-2017-0105 grant from the National Research, Development, and Innovation Office (NKFI), Hungary. This work was supported by the János Bolyai Research Scholarship of the Hungarian Academy of Sciences BO/00582/22/8 (GS) and by the by the ÚNKP-23-5 -SZTE-694 New National Excellence Program of the Ministry for Innovation and Technology (GS). This manuscript was supported by the KDP-2021 Program of the Ministry for Innovation and Technology from the source of the National Research, Development and Innovation Fund for NG (C1764415).

Conflict of interest

LP is the CEO of Avidin Ltd. and GS an employee of CS-Smartlab-Devices Ltd.

The remaining authors declare that the research was conducted in the absence of any commercial or financial relationships that could be construed as a potential conflict of interest.

Publisher's note

All claims expressed in this article are solely those of the authors and do not necessarily represent those of their affiliated organizations, or those of the publisher, the editors and the reviewers. Any product that may be evaluated in this article, or claim that may be made by its manufacturer, is not guaranteed or endorsed by the publisher.

Supplementary material

The Supplementary Material for this article can be found online at: https://www.frontiersin.org/articles/10.3389/fimmu.2023.1243233/full#supplementary-material

References

1. Mouronte-Roibas C, Leiro-Fernandez V, Fernandez-Villar A, Botana-Rial M, Ramos-Hernandez C, Ruano-Ravina A. COPD. emphysema and the onset of lung cancer. A systematic review. *Cancer Lett* (2016) 382(2):240–4. doi: 10.1016/j.canlet.2016.09.002

2. Kenfield SA, Wei EK, Stampfer MJ, Rosner BA, Colditz GA. Comparison of aspects of smoking among the four histological types of lung cancer. *Tob Control* (2008) 17(3):198–204. doi: 10.1136/tc.2007.022582

3. Szalontai K, Gemes N, Furak J, Varga T, Neuperger P, Balog JA, et al. Chronic obstructive pulmonary disease: epidemiology, biomarkers, and paving the way to lung cancer. *J Clin Med* (2021) 10(13):2889. doi: 10.3390/jcm10132889

4. Gomes M, Teixeira AL, Coelho A, Araujo A, Medeiros R. The role of inflammation in lung cancer. *Adv Exp Med Biol* (2014) 816:1–23. doi: 10.1007/978-3-0348-0837-8_1

5. Peters EN, Warren GW, Sloan JA, Marshall JR. Tobacco assessment in completed lung cancer treatment trials. *Cancer* (2016) 122(21):3260–2. doi: 10.1002/cncr.30223

6. Bodor JN, Kasireddy V, Borghaei H. First-line therapies for metastatic lung adenocarcinoma without a driver mutation. *J Oncol Pract* (2018) 14(9):529–35. doi: 10.1200/JOP.18.00250

7. Lee SH. Chemotherapy for lung cancer in the era of personalized medicine. *Tuberc Respir Dis (Seoul)* (2019) 82(3):179–89. doi: 10.4046/trd.2018.0068

8. Borghaei H, Paz-Ares L, Horn L, Spigel DR, Steins M, Ready NE, et al. Nivolumab versus docetaxel in advanced nonsquamous non-small-cell lung cancer. *N Engl J Med* (2015) 373(17):1627–39. doi: 10.1056/NEJMoa1507643

9. Brahmer J, Reckamp KL, Baas P, Crino L, Eberhardt WE, Poddubskaya E, et al. Nivolumab versus docetaxel in advanced squamous-cell non-small-cell lung cancer. *N Engl J Med* (2015) 373(2):123–35. doi: 10.1056/NEJMoa1504627

10. Herbst RS, Baas P, Kim DW, Felip E, Perez-Gracia JL, Han JY, et al. Pembrolizumab versus docetaxel for previously treated, PD-L1-positive, advanced non-small-cell lung cancer (KEYNOTE-010): a randomised controlled trial. *Lancet* (2016) 387(10027):1540–50. doi: 10.1016/S0140-6736(15)01281-7

11. Mamdani H, Matosevic S, Khalid AB, Durm G, Jalal SI. Immunotherapy in lung cancer: current landscape and future directions. *Front Immunol* (2022) 13:823618. doi: 10.3389/fimmu.2022.823618

12. Fares CM, Van Allen EM, Drake CG, Allison JP, Hu-Lieskovan S. Mechanisms of resistance to immune checkpoint blockade: why does checkpoint inhibitor immunotherapy not work for all patients? *Am Soc Clin Oncol Educ Book* (2019) 39:147–64. doi: 10.1200/EDBK_240837

13. Lahiri A, Maji A, Potdar PD, Singh N, Parikh P, Bisht B, et al. Lung cancer immunotherapy: progress, pitfalls, and promises. *Mol Cancer* (2023) 22(1):40. doi: 10.1186/s12943-023-01740-y

14. Domagala-Kulawik J. The role of the immune system in non-small cell lung carcinoma and potential for therapeutic intervention. *Transl Lung Cancer Res* (2015) 4 (2):177–90. doi: 10.3978/j.issn.2218-6751.2015.01.11

15. Strauss L, Sangaletti S, Consonni FM, Szebeni G, Morlacchi S, Totaro MG, et al. RORC1 regulates tumor-promoting "Emergency" Granulo-monocytopoiesis. *Cancer Cell* (2015) 28(2):253–69. doi: 10.1016/j.ccell.2015.07.006

16. Szebeni GJ, Vizler C, Nagy LI, Kitajka K, Puskas LG. Pro-tumoral inflammatory myeloid cells as emerging therapeutic targets. *Int J Mol Sci* (2016) 17(11):1958. doi: 10.3390/ijms17111958

17. Szebeni GJ, Vizler C, Kitajka K, Puskas LG. Inflammation and cancer: extra- and intracellular determinants of tumor-associated macrophages as tumor promoters. *Mediat Inflamm* (2017) 2017:9294018. doi: 10.1155/2017/9294018

18. Doz E, Noulin N, Boichot E, Guenon I, Fick L, Le Bert M, et al. Cigarette smoke-induced pulmonary inflammation is TLR4/MyD88 and IL-1R1/MyD88 signaling dependent. *J Immunol* (2008) 180(2):1169–78. doi: 10.4049/jimmunol.180.2.1169

19. Kearley J, Silver JS, Sanden C, Liu Z, Berlin AA, White N, et al. Cigarette smoke silences innate lymphoid cell function and facilitates an exacerbated type I interleukin-33-dependent response to infection. *Immunity* (2015) 42(3):566–79. doi: 10.1016/j.immuni.2015.02.011

20. Botelho FM, Gaschler GJ, Kianpour S, Zavitz CC, Trimble NJ, Nikota JK, et al. Innate immune processes are sufficient for driving cigarette smoke-induced inflammation in mice. *Am J Respir Cell Mol Biol* (2010) 42(4):394–403. doi: 10.1165/rcmb.2008-0301OC

21. Taucher E, Mykoliuk I, Lindenmann J, Smolle-Juettner FM. Implications of the immune landscape in COPD and lung cancer: smoking versus other causes. *Front Immunol* (2022) 13:846605. doi: 10.3389/fimmu.2022.846605

22. Neuperger P, Balog JA, Tiszlavicz L, Furak J, Gemes N, Kotogany E, et al. Analysis of the single-cell heterogeneity of adenocarcinoma cell lines and the investigation of intratumor heterogeneity reveals the expression of transmembrane protein 45A (TMEM45A) in lung adenocarcinoma cancer patients. *Cancers (Basel)* (2021) 14(1):144. doi: 10.3390/cancers14010144

23. Balog JA, Kemeny A, Puskas LG, Burcsar S, Balog A, Szebeni GJ. Investigation of newly diagnosed drug-naive patients with systemic autoimmune diseases revealed the cleaved peptide tyrosine tyrosine (PYY 3-36) as a specific plasma biomarker of rheumatoid arthritis. *Mediat Inflamm* (2021) 2021:5523582. doi: 10.1155/2021/5523582

24. Toth ME, Dukay B, Peter M, Balogh G, Szucs G, Zvara A, et al. Male and female animals respond differently to high-fat diet and regular exercise training in a mouse model of hyperlipidemia. *Int J Mol Sci* (2021) 22(8):4198. doi: 10.3390/ijms22084198

25. Balog JA, Hackler LJr., Kovacs AK, Neuperger P, Alfoldi R, Nagy LI, et al. Single cell mass cytometry revealed the immunomodulatory effect of cisplatin via downregulation of splenic CD44+, IL-17A+ MDSCs and promotion of circulating IFN-gamma+ Myeloid cells in the 4T1 metastatic breast cancer model. *Int J Mol Sci* (2019) 21(1):170. doi: 10.3390/ijms21010170

26. Alfoldi R, Balog JA, Farago N, Halmai M, Kotogany E, Neuperger P, et al. Single Cell Mass Cytometry of Non-Small Cell Lung Cancer Cells Reveals Complexity of *In vivo* And Three-Dimensional Models over the Petri-dish. *Cells* (2019) 8(9):1093. doi: 10.3390/cells8091093

27. Balog JA, Honti V, Kurucz E, Kari B, Puskas LG, Ando I, et al. Immunoprofiling of drosophila hemocytes by single-cell mass cytometry. *Genomics Proteomics Bioinf* (2021) 19(2):243–52. doi: 10.1016/j.gpb.2020.06.022

28. Kovacs-Solyom F, Blasko A, Fajka-Boja R, Katona RL, Vegh L, Novak J, et al. Mechanism of tumor cell-induced T-cell apoptosis mediated by galectin-1. *Immunol Lett* (2010) 127(2):108–18. doi: 10.1016/j.imlet.2009.10.003

29. Hato SV, Khong A, de Vries IJ, Lesterhuis WJ. Molecular pathways: the immunogenic effects of platinum-based chemotherapeutics. *Clin Cancer Res* (2014) 20(11):2831–7. doi: 10.1158/1078-0432.CCR-13-3141

30. Rebe C, Demontoux L, Pilot T, Ghiringhelli F. Platinum derivatives effects on anticancer immune response. *Biomolecules* (2019) 10(1):13. doi: 10.3390/biom10010013

31. Zimmermann M, Rose N, Lindner JM, Kim H, Goncalves AR, Callegari I, et al. Antigen extraction and B cell activation enable identification of rare membrane antigen specific human B cells. *Front Immunol* (2019) 10:829. doi: 10.3389/fimmu.2019.00829

32. Vazquez BN, Laguna T, Carabana J, Krangel MS, Lauzurica P. CD69 gene is differentially regulated in T and B cells by evolutionarily conserved promoter-distal elements. *J Immunol* (2009) 183(10):6513–21. doi: 10.4049/jimmunol.0900839

33. Starzer AM, Preusser M, Berghoff AS. Immune escape mechanisms and therapeutic approaches in cancer: the cancer-immunity cycle. *Ther Adv Med Oncol* (2022) 14:17588359221096219. doi: 10.1177/17588359221096219

34. Wang X, Ricciuti B, Nguyen T, Li X, Rabin MS, Awad MM, et al. Association between smoking history and tumor mutation burden in advanced non-small cell lung cancer. *Cancer Res* (2021) 81(9):2566–73. doi: 10.1158/0008-5472.CAN-20-3991

35. Liang F, Wang GZ, Wang Y, Yang YN, Wen ZS, Chen DN, et al. Tobacco carcinogen induces tryptophan metabolism and immune suppression via induction of indoleamine 2,3-dioxygenase 1. *Signal Transduct Target Ther* (2022) 7(1):311. doi: 10.1038/s41392-022-01127-3

36. Ning Z, Liu K, Xiong H. Roles of BTLA in immunity and immune disorders. *Front Immunol* (2021) 12:654960. doi: 10.3389/fimmu.2021.654960

37. Nandi D, Pathak S, Verma T, Singh M, Chattopadhyay A, Thakur S, et al. T cell costimulation, checkpoint inhibitors and anti-tumor therapy. *J Biosci* (2020) 45:50. doi: 10.1007/s12038-020-0020-2

38. Nocentini G, Riccardi C. GITR: a modulator of immune response and inflammation. *Adv Exp Med Biol* (2009) 647:156–73. doi: 10.1007/978-0-387-89520-8_11

39. Henrick BM, Yao XD, Taha AY, German JB, Rosenthal KL. Insights into soluble toll-like receptor 2 as a downregulator of virally induced inflammation. *Front Immunol* (2016) 7:291. doi: 10.3389/fimmu.2016.00291

40. Chen YL, Lin HW, Chien CL, Lai YL, Sun WZ, Chen CA, et al. BTLA blockade enhances Cancer therapy by inhibiting IL-6/IL-10-induced CD19(high) B lymphocytes. *J Immunother Cancer* (2019) 7(1):313. doi: 10.1186/s40425-019-0744-4

41. Stienne C, Virgen-Slane R, Elmen L, Veny M, Huang S, Nguyen J, et al. Btla signaling in conventional and regulatory lymphocytes coordinately tempers humoral immunity in the intestinal mucosa. *Cell Rep* (2022) 38(12):110553. doi: 10.1016/j.celrep.2022.110553

42. Kimura MY, Hayashizaki K, Tokoyoda K, Takamura S, Motohashi S, Nakayama T. Crucial role for CD69 in allergic inflammatory responses: CD69-Myl9 system in the pathogenesis of airway inflammation. *Immunol Rev* (2017) 278(1):87–100. doi: 10.1111/imr.12559

43. Esplugues E, Sancho D, Vega-Ramos J, Martinez C, Syrbe U, Hamann A, et al. Enhanced antitumor immunity in mice deficient in CD69. *J Exp Med* (2003) 197 (9):1093–106. doi: 10.1084/jem.20021337

44. Wei SM, Pan HL, Wang L, Yin GL, Zhong K, Zhou Y, et al. Combination therapy with dendritic cell-based vaccine and anti-CD69 antibody enhances antitumor efficacy in renal cell carcinoma-bearing mice. *Turk J Med Sci* (2017) 47(2):658–67. doi: 10.3906/sag-1601-198

45. Mita Y, Kimura MY, Hayashizaki K, Koyama-Nasu R, Ito T, Motohashi S, et al. Crucial role of CD69 in anti-tumor immunity through regulating the exhaustion of tumor-infiltrating T cells. *Int Immunol* (2018) 30(12):559–67. doi: 10.1093/intimm/dxy050

46. Hu ZW, Sun W, Wen YH, Ma RQ, Chen L, Chen WQ, et al. CD69 and SBK1 as potential predictors of responses to PD-1/PD-L1 blockade cancer immunotherapy in lung cancer and melanoma. *Front Immunol* (2022) 13:952059. doi: 10.3389/fimmu.2022.952059

47. Patel AJ, Richter A, Drayson MT, Middleton GW. The role of B lymphocytes in the immuno-biology of non-small-cell lung cancer. *Cancer Immunol Immunother* (2020) 69(3):325–42. doi: 10.1007/s00262-019-02461-2

48. Xu Y, Wei Z, Feng M, Zhu D, Mei S, Wu Z, et al. Tumor-infiltrated activated B cells suppress liver metastasis of colorectal cancers. *Cell Rep* (2022) 40(9):111295. doi: 10.1016/j.celrep.2022.111295

49. Sorin M, Karimi E, Rezanejad M, Yu MW, Desharnais L, McDowell SAC, et al. Single-cell spatial landscape of immunotherapy response reveals mechanisms of CXCL13 enhanced antitumor immunity. *J Immunother Cancer* (2023) 11(2): e005545. doi: 10.1136/jitc-2022-005545

50. Rahim MK, Okholm TLH, Jones KB, McCarthy EE, Liu CC, Yee JL, et al. Dynamic CD8(+) T cell responses to cancer immunotherapy in human regional lymph nodes are disrupted in metastatic lymph nodes. *Cell* (2023) 186(6):1127–43 e18. doi: 10.1016/j.cell.2023.02.021

51. Luo Y, Zong Y, Hua H, Gong M, Peng Q, Li C, et al. Immune-infiltrating signature-based classification reveals CD103(+)CD39(+) T cells associate with colorectal cancer prognosis and response to immunotherapy. *Front Immunol* (2022) 13:1011590. doi: 10.3389/fimmu.2022.1011590

52. Lavoie JM, Baichoo P, Chavez E, Nappi L, Khalaf D, Kollmannsberger CK, et al. Comprehensive immune profiling of patients with advanced urothelial or renal cell carcinoma receiving immune checkpoint blockade. *Front Oncol* (2022) 12:973402. doi: 10.3389/fonc.2022.973402

53. Sidiropoulos DN, Stein-O'Brien GL, Danilova L, Gross NE, Charmsaz S, Xavier S, et al. Integrated T cell cytometry metrics for immune-monitoring applications in immunotherapy clinical trials. *JCI Insight* (2022) 7(19):e160398. doi: 10.1172/jci.insight.160398

frontiers | Frontiers in Immunology

TYPE Review
PUBLISHED 17 October 2023
DOI 10.3389/fimmu.2023.1279495

Check for updates

OPEN ACCESS

EDITED BY
Jie Mei,
Wuxi People's Hospital Affiliated to Nanjing Medical University, China

REVIEWED BY
Diem Tran,
Medical Genetics Institute (Vietnam), Vietnam
Hui Xiao,
Shanghai First People's Hospital, China

*CORRESPONDENCE
Sonia Molina-Pinelo
smolina-ibis@us.es

RECEIVED 18 August 2023
ACCEPTED 06 October 2023
PUBLISHED 17 October 2023

CITATION
Castillo-Peña A and Molina-Pinelo S (2023) Landscape of tumor and immune system cells-derived exosomes in lung cancer: mediators of antitumor immunity regulation. *Front. Immunol.* 14:1279495. doi: 10.3389/fimmu.2023.1279495

COPYRIGHT
© 2023 Castillo-Peña and Molina-Pinelo. This is an open-access article distributed under the terms of the Creative Commons Attribution License (CC BY). The use, distribution or reproduction in other forums is permitted, provided the original author(s) and the copyright owner(s) are credited and that the original publication in this journal is cited, in accordance with accepted academic practice. No use, distribution or reproduction is permitted which does not comply with these terms.

Landscape of tumor and immune system cells-derived exosomes in lung cancer: mediators of antitumor immunity regulation

Alejandro Castillo-Peña [1] and Sonia Molina-Pinelo [1,2]*

[1]Institute of Biomedicine of Seville (IBiS), HUVR, CSIC, University of Seville, Seville, Spain, [2]Spanish Center for Biomedical Research Network in Oncology (CIBERONC), Madrid, Spain

The immune system plays a critical role in cancer, including lung cancer, which is the leading cause of cancer-related deaths worldwide. Immunotherapy, particularly immune checkpoint blockade, has revolutionized the treatment of lung cancer, but a large subset of patients either do not respond or develop resistance. Exosomes, essential mediators of cell-to-cell communication, exert a profound influence on the tumor microenvironment and the interplay between cancer and the immune system. This review focuses on the role of tumor-derived exosomes and immune cells-derived exosomes in the crosstalk between these cell types, influencing the initiation and progression of lung cancer. Depending on their cell of origin and microenvironment, exosomes can contain immunosuppressive or immunostimulatory molecules that can either promote or inhibit tumor growth, thus playing a dual role in the disease. Furthermore, the use of exosomes in lung cancer immunotherapy is discussed. Their potential applications as cell-free vaccines and drug delivery systems make them an attractive option for lung cancer treatment. Additionally, exosomal proteins and RNAs emerge as promising biomarkers that could be employed for the prediction, diagnosis, prognosis and monitoring of the disease. In summary, this review assesses the relationship between exosomes, lung cancer, and the immune system, shedding light on their potential clinical applications and future perspectives.

KEYWORDS

exosome, lung cancer, immune cell, immunotherapy, tumor microenvironment

Introduction

Lung cancer has a significant impact worldwide: it is the leading cause of cancer-related deaths and the second most commonly diagnosed type of cancer (1). Most lung cancers are diagnosed at an advanced stage, which contributes to the poor survival rate of the disease. Environmental factors play an important role, as tobacco smoke is the leading cause of lung cancer, both through primary and second-hand exposure (2). Lung cancer is classified into

two main groups, based on morphology and immunohistochemistry, small-cell carcinoma (SCLC) and non-small-cell carcinoma (NSCLC). SCLC has a worse prognosis, although NSCLC is the predominant type, representing 83% of diagnosed cases, and is subdivided into adenocarcinoma (ADC), squamous cell carcinoma (SqCC) and other minority subgroup, such as large-cell carcinoma (LCLC) (3). ADC is the most common type of NSCLC, accounting for over 40% of all lung cancer cases. It is defined as a malignant epithelial tumor exhibiting glandular differentiation, which can produce mucin. ADC presents, in general, a peripheral location in the lung. In the case of SqCC, it represents about 20% of lung cancer cases and is usually located in a central region. SqCC is defined as a malignant epithelial tumor that shows keratinization and/or intercellular bridges (4). Smoke inhalation has a more significant influence on SqCC, which was the most common subtype of lung cancer before 1998-2002, than on ADC. This shift seems to be related to changes in smoking behavior (5). NSCLC englobes a heterogeneous group of subtypes widely divergent from each other, as can be observed comparing ADC and SqCC (6).

The immune system plays a fundamental role in cancer (7). Lung cancer is no exception, and immunotherapy has revolutionized its treatment in the last decade, despite being considered a non-immunogenic disease in the past (8). In particular, immune checkpoint blockade has transformed the landscape of cancer immunotherapy, demonstrating unprecedented clinical efficacy in more than 15 cancer types, including NSCLC, through the use of programmed death 1 (PD1) and programmed death 1 ligand (PDL1). Moreover, immune checkpoint inhibitors (ICI) have recently been established as a first-line treatment for SCLC in combination with chemotherapy, although with modest clinical impact (9). Tumor cells habitually present immune evasion mechanisms of diverse nature and specifics that suppress the immune response. Comprehending these mechanisms and developing treatments such as the one mentioned above, which make it possible to overcome them with significant efficacy and thus enhance the antitumor immune response, is the backbone of immunotherapy.

Unfortunately, only a subset of patients shows benefits from immunotherapy. The development of innate or acquired resistance, in addition to late diagnosis in lung cancer, highlights the need for new biomarkers that allow identifying tumor characteristics and optimal therapy. Therefore, interest in liquid biopsy has been raised in recent years (10). For clinical diagnosis, liquid biopsy has some advantages over solid biopsy: there are easy access and minimally invasive samples, which show better tumor heterogeneity. Furthermore, liquid biopsy can be used for real-time tumor monitoring (11). Any biological fluid containing tumor material can be used, such as blood, pleural fluid or saliva, among others (12). The main biomarkers characterized in liquid biopsy samples are circulating tumor DNA, circulating tumor cells and exosomes (11, 12) The main topic of this review is the role of exosomes in lung cancer immune response.

General characteristics of exosomes

Exosomes are single-membrane secreted vesicles, between 30 and 200 nanometers in diameter, with the same topology as the cell. Exosomes play a myriad of biological roles, including the remodeling of the extracellular matrix (ECM), and exosome-mediated signaling and molecular transfer between cells (13). All types of cells release exosomes and other extracellular vesicles (EVs) during their physiology and also due to acquired abnormalities. Exosomes have been detected in plasma, serum, urine, synovial fluid, and several other biological fluids. The isolation of exosomes is complex due to their heterogeneity and their physiochemical and biochemical similarities with others EVs. Commonly used strategies for exosome isolation are ultracentrifugation, ultrafiltration, size-exclusion chromatography, polymer centrifugation and microfluidics immunoaffinity capture methodology. All of these methods have their advantages and disadvantages; however, there is currently not a robust, reproducible and standardized method that allows obtaining high purity exosomes (14). Ultracentrifugation-based techniques still remain the gold standard for exosome isolation, despite their limitations (15).

Endosomal budding is the classical procedure proposed for exosome biogenesis, which comprises three main steps: first, an early-sorting endosome (ESE) is formed by endocytosis; second, the endosomal membrane buds inward, generating multiple intraluminal vesicles (ILVs) and, therefore, ESE mature into multivesicular bodies (MVBs). This step is essential in cargo sorting and can occur via two types of pathways: the endosomal-sorting complex required for transport (ESCRT) complex-dependent pathway and the ESCRT complex-independent transport; and third, MVBs fuse with the plasma membrane releasing ILVs, which form exosomes, to the extracellular space (16). Additionally, evidence also supports that exosomes bud from the plasma membrane (13).

In addition to their heterogeneity in size, cellular origin and functional impact, exosomes are widely diverse in content. Exosomes can enclose proteins, RNA, DNA and metabolites, although not all exosomes have a similar abundance of a given cargo. The markers also differ between exosomes, which is based in part on the pathway followed in the biogenesis. The cell of origin and its microenvironment have an impact on the content of the exosomes. However, certain nucleic acids and proteins, compared to the cell of origin, are enriched in exosomes (17).

Exosomal proteins can derive from the membrane, cytosol, nucleus and ECM, and they are distributed both in the membrane and within the lumen of the exosomes. The exosomal proteome helps determine their effects in different types of target. Two sets of exosomes can exert antagonistic effects on their respective receptor cells (13). Regarding the use of proteins as exosomal biomarkers, the levels of tetraspanins CD9, CD63 and CD81, which are used to purify and define exosomes, appear to be heterogeneous, with low expression in exosomes of certain cellular populations. A study suggests that biogenesis-related proteins are ubiquitous in exosomes and that one of them, syntenin-1, could be used for exosome detection due to its high abundance (18). In what concerns exosomal RNA, exosomes are enriched in small noncoding RNAs (ncRNAs), such as microRNAs (miRNAs), small nuclear RNAs and fragmented RNAs, but they also present mRNAs. Exosomal RNA is composed of a skewed subpopulation of cellular RNA and is enriched in determined RNA species related to the cellular RNA

profile. Those RNAs can be transferred to other cells and tissues via exosomes, transforming them (19).

Exosomes and cancer development: a double-edged sword

Exosomes are involved in several diseases, and play an important role in cancer. Exosomes are implicated in tumor initiation, progression, angiogenesis, metastasis, and drug resistance (20). Tumor cells release larger amounts of exosomes than normal cells, with multiple strategies to favoring tumor-promoting exosomes. In fact, certain elements of the exosome biogenesis machinery are oncogenes or tumor suppressors, and aberrant expression of its components can directly modulate the composition, functions and quantity of exosomes (21). Moreover, evidence suggests that exosomes secreted by polarized cells diverge in composition depending on whether they originate from the apical or basolateral side (16).

Tumor progression depends on the cross-talk between cancer cells with each other, with normal cells and immune system. Due to their role in cell-to-cell communication, exosomes have a huge impact on the tumor microenvironment (TME) (20). For example, a study indicates that in NSCLC, tumor-derived exosomes with high expression of one circular RNA (circRNA) called circUSP7 promote $CD8^+$ T cell dysfunction and resistance to anti-PD1 (22). The TME designates to the cellular environment surrounding the tumor, comprising the non-cancerous host cells such as immune cells, endothelial cells and fibroblast; and non-cellular components, which englobe the ECM and soluble products, including molecules released by the tumor (23).

As mentioned above, tumor-derived exosomes can influence recipient cells and reprogram their phenotype, promoting carcinogenesis through a myriad of different processes. For example, A549 lung cancer cells exposed to fine particulate matter secrete exosomes with high levels of Wnt3a, and these exosomes stimulate A549 cell proliferation *in vitro* and *in vivo*, via Wnt3a/β-catenin pathway (24). In another study, human bronchial epithelial cells (HBEC) were transformed to a mesenchymal phenotype common in NSCLC. Exosomes derived from the mesenchymal HBECs containing ZEB1 mRNA, a relevant transcription factor in epithelial-mesenchymal transition (EMT), could induce parental HBECs conversion to a mesenchymal and chemoresistant phenotype (25). In colorectal cancer (CRC), miRNA miR-25-3p is transferred via exosomes from CRC cells to endothelial cells, promoting vascular permeability and angiogenesis, which increased CRC metastasis in liver and lung of mice (26). In summary, proteins, RNAs, DNAs and metabolites associated with exosomes can modify the fate of recipient cells, either the cell itself that releases them by autocrine pathway or other cells via paracrine signaling (27).

On the other hand, exosomes can also have antitumor effects. For example, exosomes derived from antigen-presenting cells, such as dendritic cells (DCs), can activate naïve immune cells, and exosomes of pro-inflammatory M1 macrophages have been reported to propagate and induce an immune stimulating microenvironment (28). Even tumor-derived exosomes can activate immune responses, through antigens and/or MHC-peptide complexes that activate T cells through cross-presenting by DCs or direct presentation (27).

Besides, exosomes have become promising clinical tools due to their properties. The therapeutic use of exosomes as vehicles for the delivery of corrective cargo is being actively investigated. This interest is based on exosome stability, permeability and specific cell recognition, coupled with their ability to pass through the blood-brain barrier and minimal immunogenicity (17, 27). Furthermore, mesenchymal stem cells (MSC)-derived exosomes have some unique characteristics and may be therapeutic by themselves, making them one of the best options to develop drug carriers *in vivo* (29). Another application of exosomes is their potential role as biomarkers. As mentioned above, exosomes can be isolated, characterized and detected from liquid biopsy, opening up doors to the use of exosomal RNAs and proteins in the diagnosis, treatment, monitoring and prediction of prognosis of cancer and other diseases (30). For example, differences in exosomal miRNAs are being investigated to establish a set that could be used to discriminate between conditions, such as NSCLC patients and healthy subjects, patients with NSCLC and with SCLC or for the early detection of NSCLC (31–33). It is relevant to emphasize that the use of exosomes in the diagnosis, prognosis, prediction, and monitoring of the disease extends beyond tumor-derived exosomes: it can also encompass those derived from immune cells. For instance, in cases of head and neck cancers, the ratio of tumour/immune-cell-derived exosomes changed during and after therapy, showing a substantial decrease after surgical procedures. This ratio increased during the follow-up period, registering a higher ratio in non-responders compared to responders (34). Given the predominant focus of studies on tumor-derived exosomes, knowledge regarding the potential applications of immune cell-derived exosomes as biomarkers remains limited. Exploring this specific area of study could yield interesting insights in the future. However, there are a few limitations: the high heterogeneity and small size of exosomes make it difficult for their isolation and detection from human body fluids. Therefore, there is no a standardized method for the exosome isolation and the use of exosomal cargo as biomarkers in cancer precision medicine (30).

Synthetizing, the role of exosomes in cancer is complex and can influence tumor progression in both ways. A relevant part of this setting is the effect of exosomes on the interaction between tumor cells and immune system.

Exosome-mediated communication network between immune and lung cancer cells

Cancer cells develop several mechanisms to escape immune response. Exosomes interact with the immune system components of the TME and exert a direct impact that can suppress or promote immune activity (35). Tumor-derived exosomes can fuse with the

surface membrane of the immune cell through receptor-mediated recognition and uptake, releasing their content into the cytoplasm, or deliver signals through interacting with surface molecules, activating downstream cascades that alter recipient cell expression. This interaction contributes to cancer development by silencing antitumor immune responses (36), while immune cell-derived exosomes can have the opposite effect and suppress tumor progression by stimulating immune process such as inflammation (37).

Tumor derived-exosomes can contain either immunosuppressive signaling molecules, such as checkpoint receptor ligands, death receptor ligands, inhibitory cytokines or ectoenzymes; or immunostimulatory molecules such as costimulatory molecules, MHCI/II or tumor associated antigens. Depending on the molecular profile of the exosomes, their function can be tumor suppressing or tumor promoting (36) (Figure 1).

External factors also participate in the interaction between immune system and carcinogenesis. The lungs are particularly exposed to the environment, including tobacco and pathogenic microorganisms. Smoking and pulmonary infections promote lung cancer complications through chronic inflammation and, therefore, through the infiltration of inflammatory cells that release proinflammatory factors, leading to mutations and the stimulation of tumorigenic process such as metastasis (38). Exosomes play a role in this interaction. For example, macrophages produce IL-6, IL-10 and other proinflammatory cytokines that induce characteristics of stem cells in cancer cells. This communication, which contributes to cell growth, can be established by exosomes in addition to secretory pathways and cell fusion (39). Thus, immune cell-derived exosomes do not invariably suppress tumor progression, resulting in a more complex interaction network. Therefore, there is a wide spectrum of immune cells both innate (macrophages, dendritic cell, neutrophils, among others) and adaptive (B and T cells) that, together with cancer cells, determines whether the immune response is pro- or anti-tumorigenic (40), being a key factor exosomal cargo mediating immune cell-tumor cell communication (Figure 2). Concerning immune cell-derived exosomes, their cargo may contain proteins and miRNAs that exert either immunosuppressive or immunostimulatory effects. Often, these molecules exhibit similarities to those previously described for tumor-derived exosomes, including proinflammatory proteins and checkpoint receptor ligands, such as the proinflammatory proteins S100A8 and S100A9 in myeloid-derived suppressor cell (MDSC)-derived exosomes or PDL1 in T cell-derived exosomes (41, 42). Given the diverse range of immune cells, a myriad of molecules could be involved in these processes.

Innate immune response cells

Innate or nonspecific immunity comprises the cells that respond to multiple antigens with the same mechanism, conforming the first line of defense (43). Some of these cells also fulfill a role in adaptive immunity.

Natural killer cells

NK cells are the main effector component of innate immunity due to their ability to autonomously kill target cells, playing a role in tumor immunosuppression. Cancer cells present several mechanisms to avoid

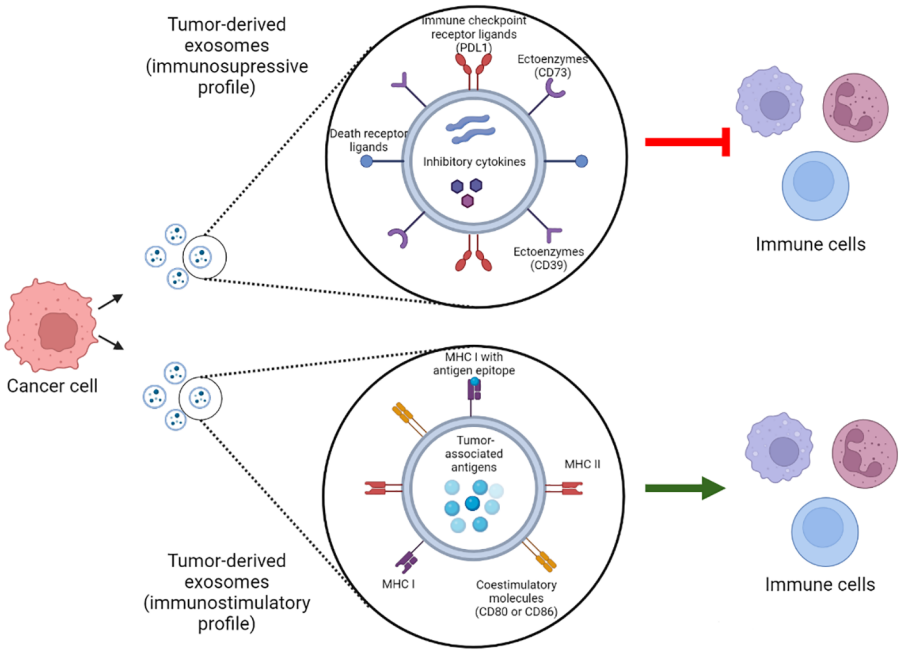


FIGURE 1
Tumor-derived exosomes molecular profiles. Tumor derived exosomes can contain immunosuppressive and immunostimulatory molecules that modulate their function. Which of these molecules compose the exosome molecular profile and their abundance determine whether the exosome play a tumor suppressing or tumor promoting role. PDL1, programmed death 1 ligand; MHC, Major histocompatibility complex. Created with BioRender.com.

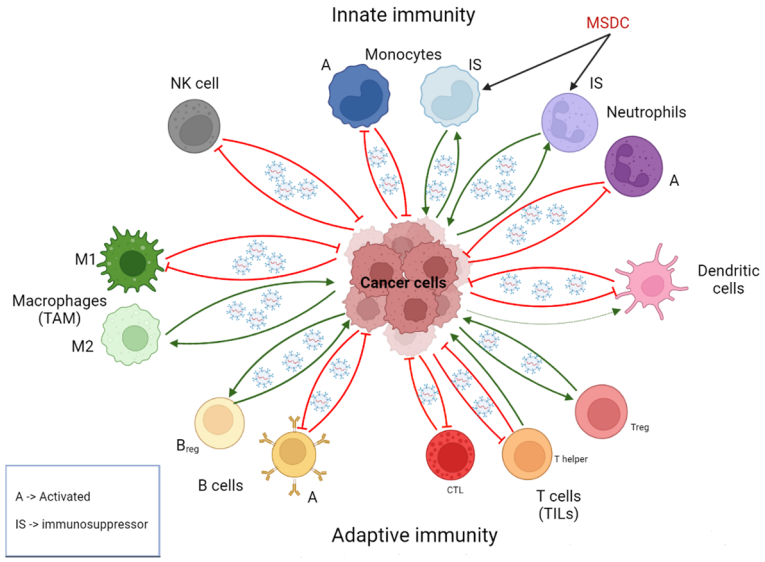


FIGURE 2
Role of exosomes in the intercommunication between immune cells and cancer cells. Immune cell-derived exosomes can promote or suppress tumor initiation and progression depending on the context and the cell of origin. Usually but not in all cases, exosomes derived from immunosuppressive immune cells are pro-tumorigenic, whereas exosomes derived from activated immune cells are anti-tumorigenic. Cancer cell-derived exosomes can reprogram immune cell, stimulating in general tumor-promoting phenotypes. A, activated; Breg, Regulatory B cells; CTL, $CD8^+$ T cells; IS, immunosupressor; MSDC, Myeloid-derived suppressor cell; NK, natural killer; TAM, tumor-associated macrophages; Treg: regulatory T cell; TILs, tumor-infiltrating lymphocytes. Created with BioRender.com.

elimination mediated by NK cells, leading to a procarcinogenic immune response (44). First, the cytotoxic activity of NK cells extends to EV produced by them, such as exosomes. Therefore, NK cells-derived exosomes show antitumor properties (45). In lung cancer patients, NK cell-derived exosomes carrying miR-30c were significantly downregulated compared to NK cell-derived exosomes from healthy individuals. *In vitro* knockdown of miR-30c was shown to decrease the cytotoxic activity of NK cells against lung cancer cells. Polypeptide N-acetylgalactosaminyltransferase 7 was proposed as target gene of miR-30c and involved in the activation of the PI3K/AKT pathway (46). Therefore, the GALTN7-miR30c axis modulates PI3K/AKT activity, considered as a hallmark of cancer. On the other hand, seen from another point of view, tumor-derived exosomes can also help avoid the elimination of cancer cells mediated by NK cells. Lung cancer-derived exosomes have been proposed to promote NK cell apoptosis by binding of pro-nerve growth factor to the p75 neurotrophin receptor-sortilin complex (47). Previous studies show the presence of sortilin in lung cancer exosomes (48), although there are still no experimental data to support this hypothesis. In addition, therapeutic approach as radiotherapy can promote NSCLC-derived exosomes production and are released of a radiation dose rate-dependent manner, leading to NK cell polarization in peripheral blood mononuclear cells (PBMCs) and immune cell redistribution (49). These cell phenotype changes induced by NSCLC-derived exosomes released by radiotherapy could trigger a more or less effective antitumor immune response.

Monocytes

Monocytes are innate immune cells can differentiate into tumor-associated macrophages (TAMs) and DCs. Moreover, they perform other tasks such as phagocytosis, lymphocytes recruitment, promotion of angiogenesis, remodeling of the ECM, and releasing of tumoricidal mediators, thus contributing to pro- and anti-tumoral immunity (50). Tumor derived exosomes have the ability to alter monocytes differentiation, which leads to the formation of immunosuppressive $CD14^+$ $HLA\text{-}DR^{lo/neg}$ monocytes, characterized for the absence of HLA-DR and costimulatory molecules. $CD14^+$ $HLA\text{-}DR^{lo/neg}$ monocytes abundance directly correlates with poor clinical outcomes (51).

There is little information about the relationship among lung cancer, exosomes and monocytes. Exosomes derived from pulmonary epithelial cancer cells metabolize leukotriene C4 to leukotriene D4, a pro-inflammatory factor that promotes bronchoconstriction and other effects, and is related to some chronic inflammatory diseases. Monocytes are a major source of leukotriene C4 in the lung TME, which conversion to leukotriene D4 stimulates proliferation and migration of cancer cells (52). In contrast, the relevance of this subset of cells have been described in others cancer types. For example, Pancreatic cancer-derived exosomes promote an immunosuppressive phenotype increasing STAT3 signaling, fostering an incremented expression of arginase and reactive oxygen species production in monocytes (53). Considering their role in other tumors and that high levels of these monocytes influence negatively to the clinical outcome of NSCLC patients administered with a telomerase peptide vaccine (54), it would be important to deepen in the interrelation between exosomes and monocytes in lung cancer.

Neutrophils

Neutrophils are a central component of innate immune response and the first responders to infection and inflammation,

performing functions such as phagocytosis, degranulation, and release of neutrophil extracellular traps. Within peripheral leukocytes, neutrophils are the most abundant population in humans. Traditionally, depending on their role in cancer, neutrophils have been classified into two types: tumor-restraining N1 population and tumor-promoting N2 population. However, plasticity and heterogeneity of neutrophils may indicate that this binary compartmentalization is obsoleted (55).

Tumor-derived exosomes foster a protumor N2 phenotype in several types of cancer, such as gastric cancer, where exomes carrying HMGB1 induced the N2 phenotype by TLR4/NF-κB signaling (56) or CRC, where CRC stem cell-derived exosomes enhances neutrophils survival through the transfer of triphosphate RNAs that stimulates IL-1β expression (57). Regarding lung cancer, exosomes derived from nicotine-activated N2 neutrophils promote brain metastasis, via a process that implicates exosomal miR-4466: N2 neutrophils with activated STAT3 are recruited into the premetastatic niche and secreted the mentioned miRNA, promoting stemness and a metabolic switching that foster metastasis (58). This shows the relevance of environmental factors, such a smoking, in lung cancer, and how these factors can influence in the content and function of exosomes. Hence, it is essential to consider the smoking habit in studies related to exosomes and the lung.

Myeloid-derived suppressor cells

Monocytes and neutrophils with an immunosuppressive phenotype are named MDSCs. Despite they usually are described in pathological conditions, MDSCs also play a role in physiological processes. Based on their myeloid cell lineage origin, MDSC are classified into granulocytic/polymorphonuclear MDSCs (PMN-MDSCs) and monocytic MDSCs (M-MDSCs). In fact, N2 neutrophils terminology describes PMN-MDSCs (59).

Tumor-derived exosomes from diverse types of cancer potentiates MDSCs induction. Lewis lung carcinoma (LLC) cell line derived exosomes stimulate MDSC expansion in a mouse tumor model and in $CD14^+$ monocytes *in vitro*, through a miR-21a-dependent mechanism. Exosomal miR-21a downregulates programmed cell death protein 4, which inhibits IL6 production in bone marrow cells (60). Tumor derived exosomes can also promote MDSC differentiation into other immunosuppressive immune cells: exosomal circPTK2/circHIPK3, observed to be enriched in the serum of Kras-related NSCLC patients compared to healthy individuals, especially in metastatic stages, stimulate monocytic MDSC recruitment and their differentiation into alternatively activated (M2) macrophages (61), contributing to favoring pro-tumorigenic processes. On the other hand, MDSCs-derived exosomes also contribute to tumor progression. For example, exosomal miRNA-143-3p derived from PMN-MDSCs downregulates integral membrane protein 2B in lung cancer tissues, activating PI3K/AKT signaling pathway and enhancing cell proliferation (62). Finally, again in lung cancer, PMN-MDSCs have been shown to inhibit NK cell activity through cell-to-cell contact, MDSCs-derived exosomes act as inhibitory mediators of NK cells, and exosomal cargo included several immune-modulatory miRNAs, such as miR-146a-5p, miR-150-5p, miR-378a-3p, miR27a-5p, and miR-218-5p (63).

Macrophages

Macrophages are monocyte-derived cells that phagocyte and clear away cells, pathogens and other harmful matter. They also secrete a myriad of immunomodulatory cytokines that can lead to inflammation. Therefore, they participate in innate immunity and adaptive immunity. Macrophages can be polarized into two main phenotypes: classically activated (M1) macrophages, functionally pro-inflammatory; or M2 macrophages, which are anti-inflammatory. Macrophages recruited to the TME become TAMs. M1-like TAMs contribute to restrain the tumor, whereas M2-like TAMs promote cancer development (35).

Lung tumor-derived exosomes can polarize M0 macrophages to an M2 phenotype, altering their transcriptional and bioenergetics signatures. This polarization showed a general increase in oxygen consumption, which is consistent with the bioenergetics state of M2 macrophages (64). Furthermore, hypoxia appears to induce lung cancer to release exosomes enriched in miRNAs like miR-103a, stimulating angiogenesis and blood vessel permeability in the TME. Tumor-exosomal miR-103a reduces PTEN expression, stimulating macrophage polarization to a M2 phenotype by activating PI3K/Akt and STAT3 pathways (65). In another study, the oncogenic lncRNA long intergenic non-coding RNA 00963 promoted exosome-induced M2 macrophage polarization in ADC, by inhibiting the ubiquitination and degradation of Zeb1, a transcriptional factor related to EMT (66).

Furthermore, tumor-exosomal miRNAs, that are transferred to the recipient cell where they bind to their target mRNA, can function also as agonists of TLR receptors in macrophages to stimulate a prometastatic inflammatory response. Using a mice model injected with LLC cells, tumor-exosomal miR-21 and miR-29a interacted with TLR receptors in macrophages, increasing the secretion of IL6 and TNF-α and stimulating the formation of lung multiplicities (67).

On the other hand, exosomes released by macrophages themselves are also relevant, it was found that M2 TAMs secrete exosomes containing miR-155 and miR-196a-5p that can promote EMT, cell migration, cell invasion and cell viability in NSCLC (68). TAM-derived exosomes can also favor EGFR-TKI resistance in NSCLC via activation of AKT, ERK1/2 and STAT3 signaling pathways (69). On the contrary, macrophages themselves and other immune cells, even some diseased cells, can polarize the naïve macrophages via exosomes toward a M1 phenotype (70).

Dendritic cells

DCs are specialized antigen-presenting cells that modulate immune signals through cell-cell contacts and cytokines. DCs play a central role in the initiation of antigen-specific immunity and tolerance, presenting antigens to naïve T cells, promoting their activation and effector differentiation. Therefore, DCs are key elements in the antitumor immune response. However, certain inhibitory signals induce in DCs a tolerogenic phenotype, leading to T cell apoptosis and Treg cells generation. TME contains

immunosuppressive factors that can inhibit DC infiltration and favor the tolerogenic phenotype, generating dysfunctional DCs (71).

Tumor-derived exosomes can contribute to the formation of tolerogenic DCs, which alter the immune response. In a study with the lung cancer cell lines LLC and A549, lung carcinoma cell-derived exosomes suppress DC costimulatory molecule expression, inflammatory response and promote DCs autophagy via MALAT1, a transcript that stimulates the AKT/mTOR pathway (72). In a xenograft mouse model of EGFR-mutant lung cancer, LLC cells transferred EGFR with the deletion mutation E746-A750 to the surface of the DCs via exosomes. This induction of anergic DCs dampened the proliferation of T cells within the lymph nodes and diminished tumor T cell infiltration (73). Tumor-derived exosomes can also block DC maturation: exosomes derived from LLC cells suppress DC maturation and migration, ultimately reducing T helper 1 (T_H1) cell differentiation and increasing regulatory T (T_{reg}) cell levels. PDL1 may be involved in this process (74). Additionally, exosomes secreted by other cellular types influence DCs function: Treg derived exosomes transferred miR-150-5p and miR-142-3p to DCs, promoting a tolerogenic phenotype by upregulating IL10 and downregulating proinflammatory cytokine IL6 production (75).

On the other hand, tumor-derived exosomes also have been shown to promote DCs maturation and enhance antigen presentation, stimulating tumor specific CTLs response with more potential that tumor cell lysates (76). Dendritic cell-derived exosomes, also known as dexosomes, can be loaded with antigens and present them to naïve DCs potentially eliciting a strong antitumor activity. Hence, tumor-derived exosomes could be used to develop DCs vaccines that foster antitumor immune response (76, 77).

Adaptive immune response cells

Adaptive or specific immunity is directed against a determined pathogen that has been previously presented. Their main cellular component are T and B lymphocytes (43).

B lymphocytes

B cells play a crucial role in the humoral response, producing antibodies that may be secreted or incorporated into the plasma membrane of the cell. In addition to producing immunoglobulins, B cells can influence the functions of other immune cells by releasing cytokines, presenting antigens and providing costimulation. B cells comprehend a functionally heterogeneous population: the balance among the different subsets in the TME may determine whether B cells contribute or suppress immune response (78).

Regulatory B cells (B_{reg}) are a subset of B cells that correlate with poor clinical outcome in certain types of cancer. B_{reg} cells produce molecules such as IL10, IL21 or PDL1 and promote T_{reg} cell production, thus inhibiting pro-inflammatory lymphocytes (79). Tumor-derived exosomes enhance B_{reg} proliferation and increase their resistance to apoptosis through mechanism dependent on IL10 and TGF-β, which later inhibit CTLs activities (80). There is a lot of field to be studied, for example, it could be interesting to analyze the effects of B cell populations on the lung TME.

T lymphocytes

There are three main subtypes of T lymphocytes: cytotoxic $CD8^+$ T cells (CTLs), which are able to directly kill the target cell; $CD4^+$ T helper cells, which activate and promote the effector and memory functions of CTLs and modulate the TME; and T_{reg} cells, related to the mechanism of tolerance necessary to avoid autoimmunity. CTLs and T_H1 cells play a major role in anti-tumor immune responses, while T_{reg} cells contributes to their suppression (81). Lymphocytes infiltrated in the TME configure the tumor-infiltrating lymphocytes (TILs) population. The present of TILs, in general, constitutes a favorable prognostic factor in NSCLC, although the composition of the TILs population determines its contribution to the disease. For example, population enriched in $FOXP3^+$ T_{reg} is associated with worse prognosis (82, 83).

CTLs, when activated, can eliminate tumor cells. Hence, their abundance correlates positively with a better clinical response to immunotherapy. However, CTL function can be disrupted by several mechanisms that induce an exhausted phenotype, which cannot respond to the presentation of the antigen. One of them is the aberrant activation of the immune checkpoints: When receptors such as PD1, T cell immunoglobulin and mucin domain-3 protein (Tim-3), T cell immunoglobulin and ITIM domain (TIGIT), lymphocyte-activation gene 3 (Lag-3), or cytotoxic T lymphocyte antigen-4 (CTLA-4), localized on the T cell surface, interact with their ligands, an inhibitory signal is sent to the T cell (84). In lung cancer, exosomes can induce T cell exhaustion, which promotes the expression of PDL1 in cancer cells or PD1 expression in CTLs. This has been observed in lung ADC, where tumor cells upregulate circRNA-002178, which is delivered through exosomes to promote PDL1 and PD1 expression (85). Exosomes can also contain PDL1, allowing them to suppress immune response at distance, not only locally, by systematically inhibiting T cell function in TME (86). Another mechanism consists of inhibiting the secretion of cytokines by CTLs. Exosomal circUSP7 secreted by NSCLC cells inhibits the secretion of IFN-γ, TNF-α, Granzyme-B and Perforin. Moreover, exosomal circUSP7 upregulates Src homology region 2-containing protein tyrosine phosphatase 2, a protein recruited by the PD1/PDL1 interaction that suppress TCR-mediated signaling (22).

The link between T helper cells and lung cancer progression is more complex. The recruitment and expansion of T_H1 cells promote an effective antitumor immune response. The role of T helper 17 (T_H17) cells is ambivalent: they can either enhance the activation of immune cells or stimulate cancer development through angiogenesis and immunosuppression processes (35). There are few studies about the relationship between exosomes and T helper cells in lung cancer. Nevertheless, there is evidence that both are associated with cancer. For example, T helper cell-derived EVs, in addition to IL2, foster CTLs activation in a melanoma mouse model, therefore enhancing antitumor immune response (87). On the other hand, tumor-derived exosomes cause the loss of CD69 on the surface of conventional $CD4^+$ T cells, leading to their functional decline (88).

T_{reg} cells are a subgroup of $CD4^+$ T cells. Their presence in the TME contributes to tumor progression due to their immunosuppressive functions. In a study with *in vitro* and *in vivo* models, the effects of tumor-derived exosomes isolated from LLC cells on lung tumor formation and metastasis were investigated. The lung fibroblast secreted large amounts of CCL1, which activated its specific receptor CCR8 that induced the differentiation of $CD4^+$ $FOXP3^+$ T_{reg} cells. The number of T_{regs} cells in the lungs increased, promoting the establishment of an immunologically tolerant pre-metastatic niche (89). Moreover, another study showed that tumor-derived exosomes induce GPX3 expression in a subpopulation of alveolar type 2 epithelial cells, inducing high production of IL-10 and ultimately improving T_{reg} cells generation and inhibiting the proliferation of T helper cells (90). These data suggest that cancer cells can recruit T_{regs} cells to induce tumor-tolerance via exosomes. Tumor-derived exosomes can also upregulate the biological activities of T_{reg} cells. For example, tumor-derived exosomes foster the expression of CD39 in several types of cancer, an ATP-hydrolase that increases the production of the immunosuppressive factor adenosine (79).

There is a fourth subtype of T lymphocyte of interest that has been associated with lung cancer via exosomes: the $CD3^+CD4^-CD8^-$ double-negative T (DNT) cells. These cells express PD1 and the TNF-related apoptosis-inducing ligand (TRAIL) in high quantities, among others. In a study, DNT cells present in malignant pleural effusions (MPE) derived from lung cancer patients expressed PD1 and TRAIL at higher levels. Whereas DNT cells from healthy donors could kill lung cancer cells, this activity was reduced by MPE: MPE supernatant-derived exosomes, exhibiting immune checkpoint molecules like CEACAM1 and PDL1, have been observed to inhibit the cytotoxicity of DNT cells, at least partially, through CEACAM1/TIM3 and PDL1/PD1 pathways. The blockage of Tim-3 and PD1 rescued the cytotoxic potential in DNT cells (91).

Role of exosomes in lung cancer immunotherapy

Throughout this review, several mechanisms by which exosomes can enhance the immune response have been explained. Therefore, exosomes have the potential to be used as therapeutic tools to induce antitumor immunity (Figure 3) (35). For example, the antitumor properties of NK cells-derived exosomes could be employed as a personalized cancer therapy. They have the shared advantage with NK cells of not requiring antigen presentation for their effector activity, but offer higher stability, modification versatility, and lower immunogenicity compared to their cells of origin (45). It has been observed that EVs derived from NK cells stimulated with cytokines IL-15 and IL-21 exhibit enhanced cytotoxic activity against cancer cells (92). Hence, the use of NK cells-derived exosomes could be an interesting objective to pursue in immunotherapy.

As mentioned above, MSC-derived exosomes also possess intrinsic therapeutic properties. There are several studies that relate the biomedical applications of MSC with their released components, opening up the possibility of cell-free therapies in regenerative medicine that overcome the side effects associated with

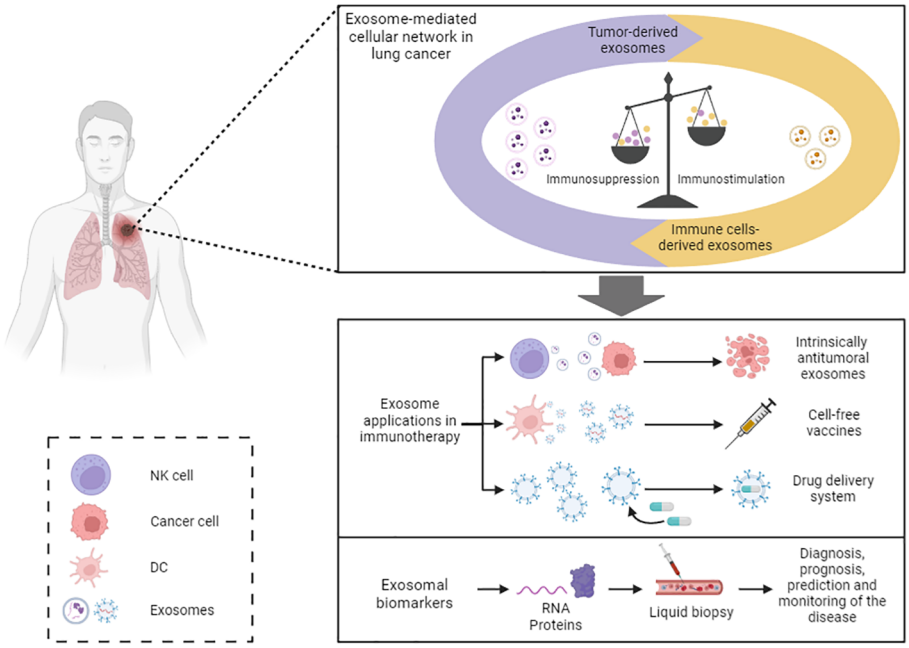


FIGURE 3
Exosome-based immunotherapy. Exosome-based immunotherapy. Exosomes offer diverse therapeutic applications: exosomes derived from specific cell types, like NK cells and MSC, exhibit inherent antitumor properties that could be harnessed; exosomes derived from DCs and tumor cells could be utilized as cell-free vaccines; and exosomes may serve as effective drug delivery systems. Moreover, exosomal cargo can be employed as biomarkers of the disease. NK, natural killer; DC, dendritic cell.

stem cell transplantation (93). For example, MSC-derived EV have been used in diverse *in vivo* models of inflammatory lung diseases, exhibiting therapeutic effects similar to those of their cells of origin (94). The role of MSC-derived exosomes in cancer is more complex, with contradictory functions that can either promote angiogenesis and tumor development or suppress tumor growth and progression (93). Considering the multiple cell types that release exosomes with the potential to stimulate immune response and antitumor immunity, and that these cells often can play opposite roles depending on the TME, we believe that the use of exosomes from immunoresponsive cancer patients to stimulate the immune response in patients with an immunosuppressive TME could be an interesting area of study.

The use of exosomes as delivery systems could be leveraged for immunotherapy. For example, engineered exosomes could enable the reprogramming of TAMs, targeting M2-like TAMs and inducing their polarization to an M1-like phenotype: exosomes with the clustered regularly interspaced short palindromic repeats interference (CRISPRi) internally engineered and a TAM specific peptide expressed onto the membrane were produced. These exosomes silenced PI-3 kinase gamma and promoted TAMs polarization to M1, which reactivated tumor immunity (95). In another study, they used M1 macrophages exosomes transfected with NF-κB p50 siRNA and miR-511-3p to foster M2-like TAM reprogramming into a M1 phenotype, inhibiting tumor growth and stimulating anti-tumor immune response (96). Therefore, the modification of the exosomal content and its targeted delivery may be a good mechanism for cell repolarization.

Another potential application of exosomes in immunotherapy is their use as a cell-free vaccine. Antigen-loaded dexosomes can start an antitumor immune response and can be obtained from monocyte-derived DCs isolated by peripheral blood leukapheresis procedure (97). Dexosomes contain different antigen-presenting molecules, such as MHC I/II proteins and costimulatory factors like CD86, that can trigger CTLs and $CD4^+$ T cells activation and proliferation (98). For example, exosomes derived from DCs primed with A549 cell lysates induced T cell proliferation and allogeneic PBMCs mediated cytotoxicity against A549 lung cancer cells *in vitro* (99). The use of dexosomes as cell-free anticancer vaccines has been studied in several phase I and phase II clinical trials, demonstrating their ability to trigger both innate and adaptive immune responses, through T cells and NK cells, respectively. However, despite their excellent tolerability and safety, dexosomes showed limited therapeutic benefit (100–103). Clinical trials related to exosome-based cell-free vaccines for lung cancer are listed in Table 1. The results obtained with dexosomes vaccines improve in combination with other therapy regimes. For instance, when combined with metronomic oral low-dose cyclophosphamide, CTLs priming against tumor increased in mice, although metronomic oral low-dose cyclophosphamide-dexosome combination chemotherapy in humans, which has been implemented in the phase II trial, appears to require the presence of genuine adjuvants (97).

Tumor cell-derived exosomes can also stimulate antitumor immunity and be used as cell-free vaccines. In a study, a nanovesicle was designed by engineering tumor cell-derived exosomes with the fibroblast activation protein-α (FAP) gene, with the purpose of serve as a tumor vaccine and to overcome the immunosuppressive characteristics of TME. FAP is overexpressed in cancer-associated fibroblasts, which constitute the most abundant stromal cells within the TME. This vaccine induced a strong CTL immune response against tumor cells and FAP^+CAF and remodeled the immunosuppressive TME in lung, colon, breast, and melanoma cancer models (104).

The potential use of exosomes and their cargo as biomarkers is another field that can be exploited in cancer immunotherapy. Several exosomes-dependent mechanisms are related to anti-tumor immunity resistance. The ICIs targeting PD1 and PDL1, despite showing a good clinical response in a variety of cancer types, fail to ameliorate the disease in a significant number of patients. This resistance to therapy could be caused by exosome-mediated systemic immunosuppression. As discussed above, two main mechanisms of exosome-mediated resistance are endogenous tumor exosomal PDL1 and PDL1 expression induced by tumor-derived exosomes (105). Exosomes-based liquid biopsies could be used to predict whether a patient will respond to the treatment and even monitor their response over time. For example, PDL1 overexpression is necessary for pembrolizumab treatment, an anti-PD1 antibody that blocks the immune checkpoint, and mutational burden is linked with a major clinical benefit in pembrolizumab treatment. Exosome-derived biomarkers may contribute to determining these factors before initiating the therapy, without the need to obtain a tissue biopsy, and enable the selection of the most appropriate treatment for each patient (106). Several studies have focused on the search for exosomes-derived biomarkers that can predict and monitor cancer therapy immunoresistance or immunosensitivity (107, 108). In fact, most clinical trials related to exosomes and lung cancer are associated with their use as biomarkers (Table 1).

Future perspective and conclusions

There is a plethora of research that support the relevance of exosomes in cell communication and in the interrelationship between processes such as cancer and immunity. In lung cancer, as in other types of cancer, exosomes can promote or prevent the initiation and development of tumors by regulating the immune response, among other mechanisms. Although the vast majority of the bibliography has been focused on the role of tumor-derived exosomes, exosomes released by immune cells and other cell types composing the TME have an important role in the disease and should be taken into consideration to better understand the origin and evolution of the disease. In the same way, the intercommunication between tumor cells and other cells types has been extensively studied, but it could be interesting to analyze the interaction between the different cell subsets that compose the TME, as it could have indirect effects on the tumor.

Besides, due to lung exposition to the environment, external factors play a fundamental role in the disease. Tobacco consumption and infections are related to pro-carcinogenic immune responses; therefore, it could be relevant to study their

TABLE 1 Clinical trials employing exosomes related to immune response.

ClinicalTrials.gov identifier	Recruitment status	Phase	Cancer type	Exosome clinical use	Intervention/ treatment
NCT01159288	Completed	II	NSCLC	Dexosome Vaccine	Dex2
NCT04427475	Recruiting	NA	NSCLC	Biomarker	Plasma exosomes
NCT02869685	Unknown	NA	NSCLC	Biomarker	Plasma exosomes
NCT02921854	Completed	NA	NSCLC	Biomarker	Serum exosomes

NA, Not applicable; Dex, tumor antigen-loaded dendritic cell-derived exosomes.

effects on immune cells and exosome release, not only their role in cell malignization. In addition to the interaction between external factors and endogenous exosomes, the role of exogenous exosomes, such as dietary exosomes, should be considered. Edible exosomes may be a potential immunotherapeutic tool against cancer (109, 110), although exosomes derived from determined foods have been associated with cancer promotion (109).

As discussed in this review, exosomes have enormous potential as immunotherapy tools due to their characteristics and role in the disease. Exosomes could provide a solution to the challenges in cancer drug delivery, because of their stability in circulation, biocompatibility, and low immunogenicity. Additionally, surface engineering helps to locally concentrate exosomes at the compromised site, reducing possible side effects (111). However, further studies are necessary for the application of these therapies at the clinical level. Meanwhile, exosome-based vaccines have been used in clinical trials and could be a safer alternative to cell vaccines, although the antitumor immune responses achieved have been limited. The use of engineered exosome-like nanovesicles could contribute to improved clinical outcomes. The most extended application of exosomes in clinical trials is their use as biomarkers: liquid biopsies can serve for prediction, diagnosis, prognosis, and real-time tumor monitoring of the disease. The use of exosomes and their cargo as biomarkers would facilitate precision medicine in lung cancer and oncology in general, helping to select the best treatment and reject other alternatives in the early stages of the disease (12). However, to establish this in the clinical routine, several obstacles that must be overcome. Regarding exosome isolation, there is no standardized method for high yield and high-purity separation. Exosome similarities with other EVs, heterogeneity, and low isolation efficiency complicate reliable molecular characterization for clinical practice. The establishment of a standardized high-throughput isolation method, alongside future technologies, such as single exosome detection and analysis technology, could help to overcome these issues (30).

In summary, exosomes play a critical role in lung cancer and immunity, incredibly complex and sometimes ambiguous: a cell can release pro-tumorigenic and anti-tumorigenic exosomes, depending on the cell context and expression patterns. Considering that exosomes are a key component of cell communication, the analysis of the interaction among the different components of the TME is crucial to fully understand their relevance in the disease, although a vast number of studies focus on the effects of individual exosomal molecules. Due to their biological role and characteristics, exosomes are interesting tools and targets for immunotherapy. Despite being in its beginnings, it is an evolving field with great potential.

Author contributions

AC-P: Investigation, Writing – original draft, Writing – review & editing. SM-P: Investigation, Writing – original draft, Writing – review & editing, Conceptualization, Supervision.

Funding

The author(s) declare financial support was received for the research, authorship, and/or publication of this article. The authors acknowledge funding from ISCIII (PI20/01109) and co-funded by FEDER from Regional Development European Funds (European Union), the Ministry of Health and Social Welfare of the Junta de Andalucía (Nicolas Monardes Program RC-0004-2020, and PECART-0091-2020), Andalusian Research, Development and Innovation Plan (PY20_00992), and Andalusia-Roche Network Mixed Alliance in Precision Medical Oncology, resources of which are composed of financial contribution from Andalusian Public Health System though of grant entitled "ALIANZA MIXTA EN RED ANDALUCÍA - ROCHE EN ON ONCOLOGÍA MÉDICA DE PRECISIÓN (INVESTIGACIÓN BÁSICA/ TRASLACIONAL)" financed by Regional Ministry of Health and Families (PIP-0044-2020) through a competitive public call for proposals and by Roche Farma S. A. with private funds. Roche Farma S.A had no role in the study design, data collection and analysis, decision to publish, or preparation of the manuscript.

Conflict of interest

The authors declare that the research was conducted in the absence of any commercial or financial relationships that could be construed as a potential conflict of interest.

Publisher's note

All claims expressed in this article are solely those of the authors and do not necessarily represent those of their affiliated organizations, or those of the publisher, the editors and the reviewers. Any product that may be evaluated in this article, or claim that may be made by its manufacturer, is not guaranteed or endorsed by the publisher.

References

1. Sung H, Ferlay J, Siegel RL, Laversanne M, Soerjomataram I, Jemal A, et al. Global cancer statistics 2020: GLOBOCAN estimates of incidence and mortality worldwide for 36 cancers in 185 countries. *CA Cancer J Clin* (2021) 71:209–49. doi: 10.3322/CAAC.21660

2. Oliver AL. Lung cancer: epidemiology and screening. *Surg Clinics North America* (2022) 102:335–44. doi: 10.1016/J.SUC.2021.12.001

3. Nicholson AG, Tsao MS, Beasley MB, Borczuk AC, Brambilla E, Cooper WA, et al. The 2021 WHO classification of lung tumors: impact of advances since 2015. *J Thorac Oncol* (2022) 17:362–87. doi: 10.1016/J.JTHO.2021.11.003

4. Travis WD, Brambilla E, Nicholson AG, Yatabe Y, Austin JHM, Beasley MB, et al. The 2015 world health organization classification of lung tumors: impact of genetic, clinical and radiologic advances since the 2004 classification. *J Thorac Oncol* (2015) 10:1243–60. doi: 10.1097/JTO.0000000000000630

5. Hutchinson BD, Shroff GS, Truong MT, Ko JP. Spectrum of lung adenocarcinoma. *Semin Ultrasound CT MR* (2019) 40:255–64. doi: 10.1053/J.SULT.2018.11.009

6. Relli V, Trerotola M, Guerra E, Alberti S. Abandoning the notion of non-small cell lung cancer. *Trends Mol Med* (2019) 25:585–94. doi: 10.1016/J.MOLMED.2019.04.012

7. Abbott M, Ustoyev Y. Cancer and the immune system: the history and background of immunotherapy. *Semin Oncol Nurs* (2019) 35:150923. doi: 10.1016/J.SONCN.2019.08.002

8. Raez LE, Cassileth PA, Schlesselman JJ, Sridhar K, Padmanabhan S, Fisher EZ, et al. Allogeneic vaccination with a B7.1 HLA-A gene-modified adenocarcinoma cell line in patients with advanced non-small-cell lung cancer. *J Clin Oncol* (2004) 22:2800–7. doi: 10.1200/JCO.2004.10.197

9. Mamdani H, Matosevic S, Khalid AB, Durm G, Jalal SI. Immunotherapy in lung cancer: current landscape and future directions. *Front Immunol* (2022) 13:823618/BIBTEX. doi: 10.3389/FIMMU.2022.823618/BIBTEX

10. Brozos-Vázquez EM, Díaz-Peña R, García-González J, León-Mateos L, Mondelo-Macía P, Peña-Chilet M, et al. Immunotherapy in nonsmall-cell lung cancer: current status and future prospects for liquid biopsy. *Cancer Immunol Immunother* (2021) 70:1177–88. doi: 10.1007/S00262-020-02752-Z

11. Li W, Bin LJ, LK H, Yu F, Zhang J, Wu W, et al. Liquid biopsy in lung cancer: significance in diagnostics, prediction, and treatment monitoring. *Mol Cancer* (2022) 21. doi: 10.1186/S12943-022-01505-Z

12. Nikanjam M, Kato S, Kurzrock R. Liquid biopsy: current technology and clinical applications. *J Hematol Oncol* (2022) 15:131. doi: 10.1186/S13045-022-01351-Y

13. Pegtel DM, Gould SJ. Annual review of biochemistry exosomes. (2019) 83:487–514. doi: 10.1146/annurev-biochem-013118

14. Patel G, Agnihotri TG, Gitte M, Shinde T, Gomte SS, Goswami R, et al. Exosomes: a potential diagnostic and treatment modality in the quest for counteracting cancer. *Cell Oncol* (2023) 11:1–21. doi: 10.1007/S13402-023-00810-Z

15. Chen J, Li P, Zhang T, Xu Z, Huang X, Wang R, et al. Review on strategies and technologies for exosome isolation and purification. *Front Bioeng Biotechnol* (2022) 9:811971/BIBTEX. doi: 10.3389/FBIOE.2021.811971/BIBTEX

16. Xie S, Zhang Q, Jiang L. Current knowledge on exosome biogenesis, cargo-sorting mechanism and therapeutic implications. *Membranes (Basel)* (2022) 12:498. doi: 10.3390/MEMBRANES12050498

17. Kalluri R, LeBleu VS. The biology, function, and biomedical applications of exosomes. *Science* (2020) 367:eaau6977. doi: 10.1126/SCIENCE.AAU6977

18. Kugeratski FG, Hodge K, Lilla S, McAndrews KM, Zhou X, Hwang RF, et al. Quantitative Proteomics Identifies the Core Proteome of Exosomes with Syntenin-1 as the highest abundant protein and a Putative Universal Biomarker. *Nat Cell Biol* (2021) 23:631. doi: 10.1038/S41556-021-00693-Y

19. Hu W, Liu C, Bi ZY, Zhou Q, Zhang H, Li LL, et al. Comprehensive landscape of extracellular vesicle-derived RNAs in cancer initiation, progression, metastasis and cancer immunology. *Mol Cancer* (2020) 19:102. doi: 10.1186/S12943-020-01199-1

20. Zhou Y, Zhang Y, Gong H, Luo S, Cui Y. The role of exosomes and their applications in cancer. *Int J Mol Sci* (2021) 22:12204. doi: 10.3390/IJMS222212204

21. Han QF, Li WJ, Hu KS, Gao J, Zhai WL, Yang JH, et al. Exosome biogenesis: machinery, regulation, and therapeutic implications in cancer. *Mol Cancer* (2022) 21:1–26. doi: 10.1186/S12943-022-01671-0

22. Chen SW, Zhu SQ, Pei X, Qiu BQ, Xiong D, Long X, et al. Cancer cell-derived exosomal circUSP7 induces CD8+ T cell dysfunction and anti-PD1 resistance by regulating the miR-934/SHP2 axis in NSCLC. *Mol Cancer* (2021) 20:144. doi: 10.1186/S12943-021-01448-X

23. Xiao Y, Yu D. Tumor microenvironment as a therapeutic target in cancer. *Pharmacol Ther* (2021) 221:107753. doi: 10.1016/J.PHARMTHERA.2020.107753

24. Xu H, Jiao X, Wu Y, Li S, Cao L, Dong L. Exosomes derived from PM2.5-treated lung cancer cells promote the growth of lung cancer via the Wnt3a/β-catenin pathway. *Oncol Rep* (2019) 41:1180–8. doi: 10.3892/OR.2018.6862

25. Lobb RJ, van Amerongen R, Wiegmans A, Ham S, Larsen JE, Möller A. Exosomes derived from mesenchymal non-small cell lung cancer cells promote chemoresistance. *Int J Cancer* (2017) 141:614–20. doi: 10.1002/IJC.30752

26. Zeng Z, Li Y, Pan Y, Lan X, Song F, Sun J, et al. Cancer-derived exosomal miR-25-3p promotes pre-metastatic niche formation by inducing vascular permeability and angiogenesis. *Nat Commun* (2018) 9:1–14. doi: 10.1038/s41467-018-07810-w

27. Zhang L, Yu D. Exosomes in cancer development, metastasis, and immunity. *Biochim Biophys Acta Rev Cancer* (2019) 1871:455–68. doi: 10.1016/J.BBCAN.2019.04.004

28. Wang P, Wang H, Huang Q, Peng C, Yao L, Chen H, et al. Exosomes from M1-polarized macrophages enhance paclitaxel antitumor activity by activating macrophages-mediated inflammation. *Theranostics* (2019) 9:1714. doi: 10.7150/THNO.30716

29. Sun Y, Liu G, Zhang K, Cao Q, Liu T, Li J. Mesenchymal stem cells-derived exosomes for drug delivery. *Stem Cell Res Ther* (2021) 12:561. doi: 10.1186/S13287-021-02629-7

30. Yu D, Li Y, Wang M, Gu J, Xu W, Cai H, et al. Exosomes as a new frontier of cancer liquid biopsy. *Mol Cancer* (2022) 21:56. doi: 10.1186/S12943-022-01509-9

31. Poroyko V, Mirzapoiazova T, Nam A, Mambetsariev I, Mambetsariev B, Wu X, et al. Exosomal miRNAs species in the blood of small cell and non-small cell lung cancer patients. *Oncotarget* (2018) 9:19793. doi: 10.18632/ONCOTARGET.24857

32. Rabinowits G, Gerçel-Taylor C, Day JM, Taylor DD, Kloecker GH. Exosomal microRNA: a diagnostic marker for lung cancer. *Clin Lung Cancer* (2009) 10:42–6. doi: 10.3816/CLC.2009.N.006

33. Lai X, Friedman A. Exosomal miRs in lung cancer: A mathematical model. *PloS One* (2016) 11:e0167706. doi: 10.1371/JOURNAL.PONE.0167706

34. Theodoraki MN, Laban S, Jackson EK, Lotfi R, Schuler PJ, Brunner C, et al. Changes in circulating exosome molecular profiles following surgery/(chemo) radiotherapy: early detection of response in head and neck cancer patients. *Br J Cancer* (2021) 125:1677–86. doi: 10.1038/s41416-021-01567-8

35. Kugeratski FG, Kalluri R. Exosomes as mediators of immune regulation and immunotherapy in cancer. *FEBS J* (2021) 288:10–35. doi: 10.1111/FEBS.15558

36. Whiteside TL. Exosomes and tumor-mediated immune suppression. *J Clin Invest* (2016) 126:1216–23. doi: 10.1172/JCI81136

37. Kurywchak P, Tavormina J, Kalluri R. The emerging roles of exosomes in the modulation of immune responses in cancer. *Genome Med* (2018) 10:1–4. doi: 10.1186/S13073-018-0535-4/FIGURES/1

38. Taucher E, Mykoliuk I, Lindenmann J, Smolle-Juettner FM. Implications of the immune landscape in COPD and lung cancer: smoking versus other causes. *Front Immunol* (2022) 13:846605. doi: 10.3389/FIMMU.2022.846605

39. Chen Y, Tan W, Wang C. Tumor-associated macrophage-derived cytokines enhance cancer stem-like characteristics through epithelial-mesenchymal transition. *Onco Targets Ther* (2018) 11:3817–26. doi: 10.2147/OTT.S168317

40. Chen DS, Mellman I. Oncology meets immunology: the cancer-immunity cycle. *Immunity* (2013) 39:1–10. doi: 10.1016/J.IMMUNI.2013.07.012

41. Xie QH, Zheng JQ, Ding JY, Wu YF, Liu L, Yu ZL, et al. Exosome-mediated immunosuppression in tumor microenvironments. *Cells* (2022) 11:1946. doi: 10.3390/CELLS11121946

42. Theodoraki MN, Hoffmann TK, Whiteside TL. Separation of plasma-derived exosomes into CD3(+) and CD3(-) fractions allows for association of immune cell and tumour cell markers with disease activity in HNSCC patients. *Clin Exp Immunol* (2018) 192:271–83. doi: 10.1111/CEI.13113

43. Vella LA, Finn OJ. Innate and adaptive immunity in lung cancer. *Novartis Found Symp* (2006) 279:206–12. doi: 10.1002/9780470035399.ch16

44. Wu SY, Fu T, Jiang YZ, Shao ZM. Natural killer cells in cancer biology and therapy. *Mol Cancer* (2020) 19:120. doi: 10.1186/S12943-020-01238-X

45. Kang YT, Niu Z, Hadlock T, Purcell E, Lo TW, Zeinali M, et al. On-chip biogenesis of circulating NK cell-derived exosomes in non-small cell lung cancer exhibits antitumoral activity. *Advanced Sci* (2021) 8:2003747. doi: 10.1002/ADVS.202003747

46. Gao F, Han J, Jia L, He J, Wang Y, Chen M, et al. MiR-30c facilitates natural killer cell cytotoxicity to lung cancer through targeting GALNT7. *Genes Genomics* (2023) 45:247–60. doi: 10.1007/s13258-022-01306-0

47. Zhu MC, Xiong P, Li GL, Zhu M. Could lung cancer exosomes induce apoptosis of natural killer cells through the p75NTR–proNGF–sortilin axis? *Med Hypotheses* (2017) 108:151–3. doi: 10.1016/J.MEHY.2017.09.003

48. Wilson CM, Naves T, Vincent F, Melloni B, Bonnaud F, Lalloué F, et al. Sortilin mediates the release and transfer of exosomes in concert with two tyrosine kinase receptors. *J Cell Sci* 127:3983–97. doi: 10.1242/jcs.149336

49. Lei QQ, Sui JD, Jin F, Luo HL, Shan JJ, Tang L, et al. Impact of high-dose rate radiotherapy on B and natural killer (NK) cell polarization in peripheral blood mononuclear cells (PBMCs) via inducing non-small cell lung cancer (NSCLC)-derived exosomes. *Transl Cancer Res* (2021) 10:3538–47. doi: 10.21037/TCR-21-536

50. Olingy CE, Dinh HQ, Hedrick CC. Monocyte heterogeneity and functions in cancer. *J Leukoc Biol* (2019) 106:309–22. doi: 10.1002/JLB.4RI0818-311R

51. Hollmén M, Elkord E, Gustafson MP, Mengos AE, Gastineau DA. The CD14 + HLA-DR lo/neg monocyte: an immunosuppressive phenotype that restrains responses

to cancer immunotherapy. *Front Immunol* (2019) 1:1147. doi: 10.3389/fimmu.2019.01147

52. Lukic A, Ji J, Idborg H, Samuelsson B, Palmberg L, Gabrielsson S, et al. Pulmonary epithelial cancer cells and their exosomes metabolize myeloid cell-derived leukotriene C4 to leukotriene D4. *J Lipid Res* (2016) 57:1659–69. doi: 10.1194/JLR.M066910

53. Javeed N, Gustafson MP, Dutta SK, Lin Y, Bamlet WR, Oberg AL, et al. Immunosuppressive CD14+HLA-DRlo/neg monocytes are elevated in pancreatic cancer and "primed" by tumor-derived exosomes. *Journal: Oncoimmunology* (2016) 6:e1252013. doi: 10.1080/2162402X.2016.1252013

54. Lund Hansen G, Gaudernack G, Fredrik Brunsvig P, Cvancarova M, Amund Kyte J. Immunological factors influencing clinical outcome in lung cancer patients after telomerase peptide vaccination. *Cancer Immunol Immunother* (2015) 3:1609–21. doi: 10.1007/s00262-015-1766-5

55. Hedrick CC, Malanchi I. Neutrophils in cancer: heterogeneous and multifaceted. *Nat Rev Immunol* (2021) 22:173–87. doi: 10.1038/s41577-021-00571-6

56. Zhang X, Shi H, Yuan X, Jiang P, Qian H, Xu W. Tumor-derived exosomes induce N2 polarization of neutrophils to promote gastric cancer cell migration. *Mol Cancer* (2018) 17:146. doi: 10.1186/S12943-018-0898-6

57. Hwang WL, Lan HY, Cheng WC, Huang SC, Yang MH. Tumor stem-like cell-derived exosomal RNAs prime neutrophils for facilitating tumorigenesis of colon cancer. *J Hematol Oncol* (2019) 12:10. doi: 10.1186/S13045-019-0699-4

58. Tyagi A, Wu SY, Sharma S, Wu K, Zhao D, Deshpande R, et al. Exosomal miR-4466 from nicotine-activated neutrophils promotes tumor cell stemness and metabolism in lung cancer metastasis. *Oncogene* (2022) 41:3079. doi: 10.1038/S41388-022-02322-W

59. Veglia F, Sanseviero E, Gabrilovich DI. Myeloid-derived suppressor cells in the era of increasing myeloid cell diversity. *Nat Rev Immunol* (2021) 21:485. doi: 10.1038/S41577-020-00490-Y

60. Zhang X, Li F, Tang Y, Ren Q, Xiao B, Wan Y, et al. miR-21a in exosomes from Lewis lung carcinoma cells accelerates tumor growth through targeting PDCD4 to enhance expansion of myeloid-derived suppressor cells. *Oncogene* (2020) 39:6354–69. doi: 10.1038/s41388-020-01406-9

61. Katopodi T, Petanidis S, Domvri K, Zarogoulidis P, Anestakis D, Charalampidis C, et al. Kras-driven intratumoral heterogeneity triggers infiltration of M2 polarized macrophages via the circHIPK3/PTK2 immunosuppressive circuit. *Sci Rep* (2021) 11:15455. doi: 10.1038/s41598-021-94671-x

62. Zhou JH, Yao ZX, Zheng Z, Yang J, Wang R, Fu SJ, et al. G-MDSCs-Derived Exosomal miRNA-143-3p Promotes Proliferation via Targeting of ITM2B in Lung Cancer. *Onco Targets Ther* (2020) 13:9701. doi: 10.2147/OTT.S256378

63. Tumino N, Besi F, Martini S, Laura Di Pace A, Munari E, Quatrini L, et al. Polymorphonuclear myeloid-derived suppressor cells are abundant in peripheral blood of cancer patients and suppress natural killer cell anti-tumor activity. *Article* (2022) 12:803014. doi: 10.3389/fimmu.2021.803014

64. Pritchard A, Tousif S, Wang Y, Hough K, Khan S, Strenkowski J, et al. Lung tumor cell-derived exosomes promote M2 macrophage polarization. *Cells* (2020) 9:1303. doi: 10.3390/CELLS9051303

65. Hsu YL, Hung JY, Chang WA, Jian SF, Lin YS, Pan YC, et al. Hypoxic lung-cancer-derived extracellular vesicle microRNA-103a increases the oncogenic effects of macrophages by targeting PTEN. *Mol Ther* (2018) 26:568–81. doi: 10.1016/J.YMTHE.2017.11.016

66. Hu R, Xu B, Ma J, Li L, Zhang L, Wang L, et al. LINC00963 promotes the Malignancy and metastasis of lung adenocarcinoma by stabilizing Zeb1 and exosomes-induced M2 macrophage polarization. *Mol Med* (2023) 29:1. doi: 10.1186/S10020-022-00598-Y

67. Fabbri M, Paone A, Calore F, Galli R, Gaudio E, Santhanam R, et al. MicroRNAs bind to Toll-like receptors to induce prometastatic inflammatory response. *Proc Natl Acad Sci U.S.A.* (2012) 109:E2110-6. doi: 10.1073/PNAS.1209414109

68. Li X, Chen Z, Ni Y, Bian C, Huang J, Chen L, et al. Tumor-associated macrophages secret exosomal miR-155 and miR-196a-5p to promote metastasis of non-small-cell lung cancer. *Transl Lung Cancer Res* (2021) 10:1338. doi: 10.21037/TLCR-20-1255

69. Yuan S, Chen W, Yang J, Zheng Y, Ye W, Xie H, et al. Tumor-associated macrophage-derived exosomes promote EGFR-TKI resistance in non-small cell lung cancer by regulating the AKT, ERK1/2 and STAT3 signaling pathways. *Oncol Lett* (2022) 24:356. doi: 10.3892/OL.2022.13476

70. Baig MS, Roy A, Rajpoot S, Liu D, Savai R, Banerjee S, et al. Tumor-derived exosomes in the regulation of macrophage polarization. *Inflammation Res* (2020) 69:435–51. doi: 10.1007/S00011-020-01318-0

71. Wculek SK, Cueto FJ, Mujal AM, Melero I, Krummel MF, Sancho D. Dendritic cells in cancer immunology and immunotherapy. *Nat Rev Immunol* (2019) 20:7–24. doi: 10.1038/s41577-019-0210-z

72. Liu Y, Yin Z, Lu P, Ma Y, Luo B, Xiang L, et al. Lung carcinoma cells secrete exosomal MALAT1 to inhibit dendritic cell phagocytosis, inflammatory response, costimulatory molecule expression and promote dendritic cell autophagy via AKT/mTOR pathway. *Onco Targets Ther* (2020) 13:10693–705. doi: 10.2147/OTT.S256669

73. Yu S, Sha H, Qin X, Chen Y, Li X, Shi M, et al. EGFR E746-A750 deletion in lung cancer represses antitumor immunity through the exosome-mediated inhibition of dendritic cells. *Oncogene* (2020) 39:2643–57. doi: 10.1038/s41388-020-1182-y

74. Ning Y, Shen K, Wu Q, Sun X, Bai Y, Xie Y, et al. Tumor exosomes block dendritic cells maturation to decrease the T cell immune response. *Immunol Lett* (2018) 199:36–43. doi: 10.1016/J.IMLET.2018.05.002

75. Tung SL, Boardman DA, Sen M, Letizia M, Peng Q, Cianci N, et al. Regulatory T cell-derived extracellular vesicles modify dendritic cell function. *Sci Rep* (2018) 8:6065. doi: 10.1038/S41598-018-24531-8

76. Wang C, Huang X, Wu Y, Wang J, Li F, Guo G. Tumor cell-associated exosomes robustly elicit anti-tumor immune responses through modulating dendritic cell vaccines in lung tumor. *Int J Biol Sci* (2020) 16:633. doi: 10.7150/IJBS.38414

77. Li J, Li J, Peng Y, Du Y, Yang Z, Qi X. Dendritic cell derived exosomes loaded neoantigens for personalized cancer immunotherapies. *J Control Release* (2023) 353:423–33. doi: 10.1016/J.JCONREL.2022.11.053

78. Tsou P, Katayama H, Ostrin EJ, Hanash SM. The emerging role of b cells in tumor immunity. *Cancer Res* (2016) 76:5591–601. doi: 10.1158/0008-5472.CAN-16-0431/660582/P/THE-EMERGING-ROLE-OF-B-CELLS-IN-TUMOR-IMMUNITYB

79. Alipoor SD, Mortaz E, Varahram M, Movassaghi M, Kraneveld AD, Garssen J, et al. The potential biomarkers and immunological effects of tumor-derived exosomes in lung cancer. *Front Immunol* (2018) 9:819. doi: 10.3389/FIMMU.2018.00819

80. Chen W, Jiang J, Xia W, Huang J. Tumor-related exosomes contribute to tumor-promoting microenvironment: an immunological perspective. *J Immunol Res* (2017) 2017:1073947. doi: 10.1155/2017/1073947

81. Speiser DE, Ho PC, Verdeil G. Regulatory circuits of T cell function in cancer. *Nat Rev Immunol* (2016) 16:599–611. doi: 10.1038/nri.2016.80

82. Gueguen P, Metoikidou C, Dupic T, Lawand M, Goudot C, Baulande S, et al. Contribution of resident and circulating precursors to tumor-infiltrating CD8+ T cell populations in lung cancer. *Sci Immunol* (2021) 6:eabd5778. doi: 10.1126/SCIIMMUNOL.ABD5778/SUPPL_FILE/SCIIMMUNOL.ABD5778_TABLES_S1_TO_S5.ZIP

83. Maibach F, Sadozai H, Seyed Jafari SM, Hunger RE, Schenk M. Tumor-infiltrating lymphocytes and their prognostic value in cutaneous melanoma. *Front Immunol* (2020) 11:2105. doi: 10.3389/FIMMU.2020.02105

84. Thommen DS, Schumacher TN. T cell dysfunction in cancer. *Cancer Cell* (2018) 33:547–62. doi: 10.1016/J.CCELL.2018.03.012

85. Wang JF, Zhao XH, Wang YB, Ren FH, Sun DW, Yan YB, et al. circRNA-002178 act as a ceRNA to promote PDL1/PD1 expression in lung adenocarcinoma. *Cell Death Dis* (2020) 11:32. doi: 10.1038/S41419-020-2230-9

86. Fan Z, Wu C, Chen M, Jiang Y, Wu Y, Mao R, et al. The generation of PD-L1 and PD-L2 in cancer cells: From nuclear chromatin reorganization to extracellular presentation. *Acta Pharm Sin B* (2022) 12:1041–53. doi: 10.1016/J.APSB.2021.09.010

87. Shin S, Jung I, Jung D, Kim CS, Kang SM, Ryu S, et al. Novel antitumor therapeutic strategy using CD4+ T cell-derived extracellular vesicles. *Biomaterials* (2022) 289:121765. doi: 10.1016/J.BIOMATERIALS.2022.121765

88. Muller L, Mitsuhashi M, Simms P, Gooding WE, Whiteside TL. Tumor-derived exosomes regulate expression of immune function-related genes in human T cell subsets. *Sci Rep* (2016) 6:1–13. doi: 10.1038/srep20254

89. Wang M, Qin Z, Wan J, Yan Y, Duan X, Yao X, et al. Tumor-derived exosomes drive pre-metastatic niche formation in lung via modulating CCL1+ fibroblast and CCR8+ Treg cell interactions. *Cancer Immunol Immunother* (2022) 71:2717–30. doi: 10.1007/S00262-022-03196-3/FIGURES/7

90. Wang Z, Zhu J, Liu Y, Wang Z, Cao X, Gu Y. Tumor-polarized GPX3+AT2 lung epithelial cells promote premetastatic niche formation. *Proc Natl Acad Sci U.S.A.* (2022) 119:e2201899119. doi: 10.1073/PNAS.2201899119/-/DCSUPPLEMENTAL

91. Wu J, Zhu R, Wang Z, Chen X, Xu T, Liu Y, et al. Exosomes in Malignant pleural effusion from lung cancer patients impaired the cytotoxicity of double-negative T cells. *Transl Oncol* (2023) 27:101564. doi: 10.1016/J.TRANON.2022.101564

92. Enomoto Y, Li P, Jenkins LM, Anastasakis D, Lyons GC, Hafner M, et al. Cytokine-enhanced cytolytic activity of exosomes from NK Cells. *Cancer Gene Ther* (2021) 29:734–49. doi: 10.1038/s41417-021-00352-2

93. Hassanzadeh A, Rahman HS, Markov A, Endjun JJ, Zekiy AO, Chartrand MS, et al. Mesenchymal stem/stromal cell-derived exosomes in regenerative medicine and cancer; overview of development, challenges, and opportunities. *Stem Cell Res Ther* (2021) 12:1–22. doi: 10.1186/S13287-021-02378-7

94. Fujita Y, Kadota T, Araya J, Ochiya T, Kuwano K. Clinical application of mesenchymal stem cell-derived extracellular vesicle-based therapeutics for inflammatory lung diseases. *J Clin Med* (2018) 7:355. doi: 10.3390/JCM7100355

95. Zhang L, Lin Y, Li S, Guan X, Jiang X. *In situ* reprogramming of tumor-associated macrophages with internally and externally engineered exosomes. *Angewandte Chemie Int Edition* (2023) 62:e202217089. doi: 10.1002/ANIE.202217089

96. Gunassekaran GR, Poongkavithai Vadevoo SM, Baek MC, Lee B. M1 macrophage exosomes engineered to foster M1 polarization and target the IL-4 receptor inhibit tumor growth by reprogramming tumor-associated macrophages into M1-like macrophages. *Biomaterials* (2021) 278:121137. doi: 10.1016/J.BIOMATERIALS.2021.121137

97. Nikfarjam S, Rezaie J, Kashanchi F, Jafari R. Dexosomes as a cell-free vaccine for cancer immunotherapy. *J Exp Clin Cancer Res* (2020) 39:1–20. doi: 10.1186/S13046-020-01781-X

98. Théry C, Boussac M, Véron P, Ricciardi-Castagnoli P, Raposo G, Garin J, et al. Proteomic analysis of dendritic cell-derived exosomes: a secreted subcellular

compartment distinct from apoptotic vesicles. *J Immunol* (2001) 166:7309–18. doi: 10.4049/JIMMUNOL.166.12.7309

99. Than UTT, Le HT, Hoang DH, Nguyen XH, Pham CT, Van BKT, et al. Induction of antitumor immunity by exosomes isolated from cryopreserved cord blood monocyte-derived dendritic cells. *Int J Mol Sci* (2020) 21:1834. doi: 10.3390/IJMS21051834

100. Besse B, Charrier M, Lapierre V, Dansin E, Lantz O, Planchard D, et al. Dendritic cell-derived exosomes as maintenance immunotherapy after first line chemotherapy in NSCLC. *Oncoimmunology* (2015) 5. doi: 10.1080/2162402X.2015.1071008

101. Morse MA, Garst J, Osada T, Khan S, Hobeika A, Clay TM, et al. A phase I study of dexosome immunotherapy in patients with advanced non-small cell lung cancer. *J Transl Med* (2005) 3:9. doi: 10.1186/1479-5876-3-9

102. Dai S, Wei D, Wu Z, Zhou X, Wei X, Huang H, et al. Phase I clinical trial of autologous ascites-derived exosomes combined with GM-CSF for colorectal cancer. *Mol Ther* (2008) 16:782–90. doi: 10.1038/MT.2008.1

103. Escudier B, Dorval T, Chaput N, André F, Caby MP, Novault S, et al. Vaccination of metastatic melanoma patients with autologous dendritic cell (DC) derived-exosomes: results of thefirst phase I clinical trial. *J Transl Med* (2005) 3:10. doi: 10.1186/1479-5876-3-10

104. Hu S, Ma J, Su C, Chen Y, Shu Y, Qi Z, et al. Engineered exosome-like nanovesicles suppress tumor growth by reprogramming tumor microenvironment and promoting tumor ferroptosis. *Acta Biomater* (2021) 135:567–81. doi: 10.1016/J.ACTBIO.2021.09.003

105. Morrissey SM, Yan J. Exosomal PD-L1: Roles in tumor progression and immunotherapy. *Trends Cancer* (2020) 6:550. doi: 10.1016/J.TRECAN.2020.03.002

106. Huang C, Liu S, Tong X, Fan H. Extracellular vesicles and ctDNA in lung cancer: biomarker sources and therapeutic applications. *Cancer Chemother Pharmacol* (2018) 82:171–83. doi: 10.1007/S00280-018-3586-8

107. Indini A, Rijavec E, Grossi F. Circulating biomarkers of response and toxicity of immunotherapy in advanced non-small cell lung cancer (NSCLC): A comprehensive review. *Cancers (Basel)* (2021) 13:1794. doi: 10.3390/CANCERS13081794

108. Li C, Li C, Zhi C, Liang W, Wang X, Chen X, et al. Clinical significance of PD-L1 expression in serum-derived exosomes in NSCLC patients. *J Transl Med* (2019) 17:1–10. doi: 10.1186/S12967-019-2101-2/FIGURES/5

109. Banikazemi Z, Haji HA, Mohammadi M, Taheripak G, Iranifar E, Poursadeghiyan M, et al. Diet and cancer prevention: Dietary compounds, dietary MicroRNAs, and dietary exosomes. *J Cell Biochem* (2018) 119:185–96. doi: 10.1002/JCB.26244

110. Ju S, Mu J, Dokland T, Zhuang X, Wang Q, Jiang H, et al. Grape exosome-like nanoparticles induce intestinal stem cells and protect mice from DSS-induced colitis. *Mol Ther* (2013) 21:1345–57. doi: 10.1038/MT.2013.64

111. Liang Y, Duan L, Lu J, Xia J. Engineering exosomes for targeted drug delivery. *Theranostics* (2021) 11:3183. doi: 10.7150/THNO.52570

Glossary

SCLC	Small-cell carcinoma
NSCLC	Non-small-cell carcinoma
ADC	Adenocarcinoma
SqCC	Squamous cell carcinoma
LCLC	Large-cell carcinoma
PD1	Programmed death 1
PDL1	Programmed death 1 ligand
ICI	Immune checkpoint inhibitors
EV	Extracellular vesicles
ESE	Early-sorting endosome
ILVs	Intraluminal vesicles
MVBs	Multivesicular bodies
ESCRT	Endosomal-sorting complex-independent transport
ncRNAs	Small noncoding RNAs (ncRNAs)
miRNAs	microRNAs
TME	Tumor microenvironment
circRNA	circular RNA
ECM	extracellular matrix
HBEC	Human bronchial epithelial cells
EMT	Epithelial-mesenchymal transition
CRC	colorectal cancer
DCs	dendritic cells
MSC	Mesenchymal stem cells
NK	Natural Killer
PBMCs	Peripheral blood mononuclear cells
TAMs	Tumor-associated macrophages
MDSCs	Myeloid-derived suppressor cells
PMN-MDSCs	Polymorphonuclear MDCs
M-MDSCs	Monocytic MDSCs
LLC	Lewis Lung carcinoma
M2 macrophages	Alternatively activated macrophages
M1 macrophages	Classically activated macrophages
T_H1 cell	T helper 1 cell
T_{reg} cell	Regulatory T cell
B_{reg} cell	Regulatory B cell
CTLs	Cytotoxic $CD8^+$ T cells
TILs	Tumor-infiltrating lymphocytes
Tim-3	mucin domain-3 protein
TIGIT	T cell immunoglobulin and ITIM domain
Lag-3	Lymphocyte-activation gene 3
CTLA4	Cytotoxic T lymphocyte antigen-4
T_H17 cell	T helper 17 cell
DNT cell	Double-negative T cells
TRAIL	TNF-related apoptosis-inducing ligand
MPE	malignant pleural effusions
CRISPRi	clustered regularly interspaced short palindromic repeats interference
FAP	Fibroblast activation protein- α.

frontiers | Frontiers in Oncology

TYPE Original Research
PUBLISHED 17 October 2023
DOI 10.3389/fonc.2023.1181176

Check for updates

OPEN ACCESS

EDITED BY
Qun Xue,
Affiliated Hospital of Nantong University, China

REVIEWED BY
Samit Chatterjee,
University of Rajasthan, India
Feiyue Xing,
Jinan University, China

*CORRESPONDENCE
Zhaoqing Yang
yangzhaoqing1@kmmu.edu.cn
Xiaoping Chen
chen_xiaoping@gibh.ac.cn
Li Qin
qin_li@cas-lamvac.com

†These authors have contributed equally to this work

RECEIVED 07 March 2023
ACCEPTED 18 September 2023
PUBLISHED 17 October 2023

CITATION
Chen X, Tao Z, Liang Y, Ma M, Adah D, Ding W, Chen L, Li X, Dai L, Fanuel S, Zhao S, Hu W, Wu D, Duan Z, Zhou F, Qin L, Chen X and Yang Z (2023) *Plasmodium* immunotherapy combined with gemcitabine has a synergistic inhibitory effect on tumor growth and metastasis in murine Lewis lung cancer models. *Front. Oncol.* 13:1181176. doi: 10.3389/fonc.2023.1181176

COPYRIGHT
© 2023 Chen, Tao, Liang, Ma, Adah, Ding, Chen, Li, Dai, Fanuel, Zhao, Hu, Wu, Duan, Zhou, Qin, Chen and Yang. This is an open-access article distributed under the terms of the Creative Commons Attribution License (CC BY). The use, distribution or reproduction in other forums is permitted, provided the original author(s) and the copyright owner(s) are credited and that the original publication in this journal is cited, in accordance with accepted academic practice. No use, distribution or reproduction is permitted which does not comply with these terms.

Plasmodium immunotherapy combined with gemcitabine has a synergistic inhibitory effect on tumor growth and metastasis in murine Lewis lung cancer models

Xiao Chen[1,2†], Zhu Tao[2,3†], Yun Liang[2,4], Meng Ma[2,5], Dickson Adah[2], Wenting Ding[3], Lili Chen[2], Xiaofen Li[2], Linglin Dai[2], Songwe Fanuel[2,6], Siting Zhao[2,3], Wen Hu[3], Donghai Wu[2], Ziyuan Duan[2], Fang Zhou[3], Li Qin[3*], Xiaoping Chen[2,3*] and Zhaoqing Yang[7*]

[1]Department of Medical Oncology, First Affiliated Hospital of Kunming Medical University, Kunming, Yunnan, China, [2]State Key Laboratory of Respiratory Disease, Center for Infection and Immunity, Guangzhou Institutes of Biomedicine and Health, Chinese Academy of Sciences (CAS), Guangzhou, Guangdong, China, [3]CAS-Lamvac (Guangzhou) Biomedical Technology Co., Ltd., Guangzhou, Guangdong, China, [4]Department of Hepatobiliary Surgery, First Affiliated Hospital of Kunming Medical University, Kunming, Yunnan, China, [5]The Ministry of Education Key Laboratory of Laboratory Medical Diagnostics, College of Laboratory Medicine, Chongqing Medical University, Chongqing, China, [6]Department of Applied Biosciences and Biotechnology, Faculty of Science and Technology, Midlands State University, Gweru, Zimbabwe, [7]Department of Pathogen Biology and Immunology, Kunming Medical University, Kunming, Yunnan, China

Objective: Our previous studies have demonstrated that *Plasmodium* immunotherapy (infection) has antitumor effects in mice. However, as a new form of immunotherapy, this therapy has a weakness: its specific killing effect on tumor cells is relatively weak. Therefore, we tested whether *Plasmodium* immunotherapy combined with gemcitabine (Gem), a representative chemotherapy drug, has synergistic antitumor effects.

Methods: We designed subcutaneously and intravenously implanted murine Lewis lung cancer (LLC) models to test the antitumor effect of *Plasmodium chabaudi* ASS (Pc) infection in combination with Gem treatment and explored its underlying mechanisms.

Results: We found that both Pc infection alone and Gem treatment alone significantly inhibited tumor growth in the subcutaneous model, and combination therapy was more effective than either monotherapy. Monotherapy only tended to prolong the survival of tumor-bearing mice, while the combination therapy significantly extended the survival of mice, indicating a significant synergistic effect of the combination. In the mechanistic experiments, we found that the combination therapy significantly upregulated E-cadherin and downregulated Snail protein expression levels, thus inhibiting epithelial-mesenchymal transition (EMT) of tumor cells, which may be due to the blockade of CXCR2/TGF-β-mediated PI3K/Akt/GSK-3β signaling pathway.

Conclusion: The combination of Pc and Gem plays a synergistic role in inhibiting tumor growth and metastasis, and prolonging mice survival in murine lung cancer models. These effects are partially attributed to the inhibition of EMT of tumor cells, which is potentially due to the blockade of CXCR2/TGF-β-mediated PI3K/Akt/GSK-3β/Snail signaling pathway. The clinical transformation of *Plasmodium* immunotherapy combined with Gem for lung cancer is worthy of expectation.

KEYWORDS

***Plasmodium* immunotherapy, *Plasmodium chabaudi* ASS, gemcitabine, anticancer effect, synergism, mouse lung cancer model**

Introduction

Lung cancer is the most common cancer in the world, with the highest mortality and the second morbidity among all types of malignant tumors (1). Even though the traditional methods of surgery and chemoradiotherapy have improved, more than 40% of patients with non-small cell lung cancer (NSCLC) treated in early stage still have tumor recurrence and metastasis (2). In addition, about 65.33% of patients diagnosed with NSCLC are in the late stage (3), and the effect of conventional chemotherapy or radiotherapy is limited. Although some patients respond to targeted therapy, the development of drug resistance leads to tumor progression in a certain period (4). Since 2013, cancer immunotherapy represented by immune checkpoint inhibitors has been crowned as one of the breakthroughs of science and technology (5). However, some challenges remain to be addressed, including immune-related toxicities (6, 7), and primary/acquired resistance to therapy (8). There are no ideal and effective treatment models with little toxicity and the ability to inhibit tumor metastasis to improve the therapeutic effect of lung cancer patients so far.

Malaria is a disease caused by the infection of *Plasmodium* parasite, which is the most common parasitic infection in humans and animals. Studies have indicated that *Plasmodium* infection activates the immune system (9–11), which may help to repress tumor growth. Our previous studies have demonstrated that *Plasmodium* infection inhibits Lewis lung cancer (LLC) growth and metastasis by activating antitumor immune response (12), inhibiting angiogenesis (13, 14) and counteracting the tumor immunosuppressive microenvironment in mice (15). However, as a new form of immunotherapy, namely, *Plasmodium* immunotherapy, we still need to further enhance the specific killing effect of this therapy to increase its efficacy. In principle, chemotherapeutic drugs just have this effect, and gemcitabine (Gem) as a typical representative of these drugs is an effective and commonly used cytotoxic agent for the treatment of various tumors including NSCLC (16). Therefore, we designed murine NSCLC (LLC) models to examine the effects of *Plasmodium* infection in combination with Gem treatment on the inhibition of tumor growth and metastasis.

Tumor metastasis is a complex process that involves numerous factors and multiple steps, of which the epithelial-mesenchymal transition (EMT) is considered the initial and critical event in many types of carcinoma (17, 18). Chemokines, which are small chemoattractants in regulating cell positioning and cell recruitment into tissues, have been found to play an important role in cancer metastasis and EMT (19). Multiple signaling pathways participate in the progression of EMT, of which the chemokine-mediated PI3K/Akt/GSK−3β/Snail signaling is an essential process (20, 21). Therefore, in our current study, we tested whether *Plasmodium* infection in combination with Gem inhibited tumor metastasis and EMT, and whether these inhibitions were associated with the blocking of the above-mentioned pathways. Our results indicated that the combination of *Plasmodium* infection and Gem treatment significantly suppressed tumor metastasis and EMT, and these suppressions were potentially associated with the blockade of CXCR2/TGF-β-mediated PI3K/Akt/GSK-3β/Snail signaling pathway.

Materials and methods

Ethics statement

Our animal experiment facilities were approved by the Guangdong Provincial Department of Science and Technology. The animal experiments were approved by the Welfare Committee of the Center of Experimental Animals, Guangzhou Institutes of Biomedicine and Health (GIBH), Chinese Academy of Sciences (approval no. N2019014; Guangzhou, China), and strictly followed the standard guidelines for the care of animals. Animal suffering was minimized during the experiments.

Animals, cells, and parasites

Six- to eight-week-old female C57BL/6 mice were purchased from Vital River Experiment Animal Limited Company (Beijing, China) and kept in a specific pathogen-free (SPF) animal facility of the GIBH. *Plasmodium yoelii* 17XNL (MRA-593, Py) and *Plasmodium chabaudi* ASS (MRA-429, Pc) strains were both donated by Malaria Research and Reference Reagent Resource Center (MR4). The murine LLC cells were obtained from ATCC

and cultured with the medium containing Dulbecco's modified Eagle's medium (DMEM, Gibco), penicillin (80 U/ml), streptomycin (100 U/ml) and 10% fetal bovine serum (FBS, Gibco) in a humidified atmosphere of 5% CO_2 at 37°C. Py and Pc were both intraperitoneally injected and propagated in C57BL/6 mice, respectively. Peripheral blood parasitemia was measured in thin blood smear by Giemsa staining (Sigma-Aldrich). Parasitemia (%) was calculated by counting the parasitized erythrocytes in at least 1000 erythrocytes.

Subcutaneous tumor model and treatment

For the subcutaneous tumor model, 5×10^5 LLC cells were subcutaneously (s.c.) inoculated into the right flank of C57BL/6 mice. Mice were randomly divided into four groups of 15 mice each according to body weight stratification: Control group (Con); Pc infection group (Pc); Gem treatment group (Gem); Pc infection combined with Gem treatment group (Pc+Gem). Mice were then intraperitoneally (i.p.) injected with 5×10^5 Pc infected red blood cells on day 7 in the Pc group and Pc+Gem group. Mice were treated with Gem (50 mg/kg; 0.2 mL per time) i.p. for twice on day 6 and day 13 in the Gem group and Pc+Gem group. The tumor volume was recorded every two days after the tumor became palpable. The formula for calculating the volume is $V = (ab^2)/2$, where "a" represents the long diameter, and "b" represents the short diameter of the tumor (12). Five mice randomly selected from each group were sacrificed on day 17 for calculating their body weight and tumor weight, and for analyzing their tumor tissues. The remaining mice were continually observed for their survival.

Intravenous tumor model and treatment

For intravenous tumor model, 5×10^5 LLC cells were intravenously (i.v.) injected into the C57BL/6 mice. Mice were randomly divided into four groups of 15 mice each: Con group, Pc group, Gem group, and Pc+Gem group. Each mouse of the Pc group and Pc+Gem group was i.p. injected with 5×10^5 (Pc) parasitized erythrocytes on day 2. Each mouse in the Gem group and Pc+Gem group was (i.p.) given Gem (50 mg/kg, 0.2 ml per time) for twice on day 12 and 19. Five mice randomly selected from each group were sacrificed for counting individual metastatic nodules on the surface of lung under a microscope on day 32. The remaining mice continued to be observed for their survival.

Protein extraction and Western blotting

Total protein was extracted from the tumor tissue using lysis buffer (RIPA, Beyotime) with protease inhibitor (Biotool) and phosphatase inhibitor cocktail (CST). Protein concentration was determined by BCA method. Total protein (50-100 μg) was separated by 10%-12% SDS-PAGE electrophoresis and then transferred to a PVDF membrane (Millipore). The membrane was blocked with 3% skim milk powder in tris-buffered saline with 0.1% tween 20 (TBST, Thermo Fisher Scientific, Inc) for 90 minutes at room temperature, and then it was incubated overnight with a solution containing the primary antibody. After washing with TBST for three times, the membrane was incubated at room temperature for 1 hour with horseradish peroxidase–conjugated secondary antibody diluted in TBST. Protein bands were observed by enhanced chemiluminescence (Pierce) and detected by BioImaging Systems (BIO-RAD ChemiDoc™ MP Imaging System, USA). GAPDH expression was used as a normalized protein.

Reagents list used in the study

Antibodies: GAPDH (cat. no. ab9385; Abcam), E-cadherin (cat. no. BS1098; Bioworld Technology, Inc.), Snail (cat. no. 3879S; Cell Signaling Technology, Inc.), PI3K (cat. no. ab151549; Abcam), phosphorylated (p)PI3K p85 (Tyr458)/p55 (Tyr199) (cat. no. 4228S; Cell Signaling Technology, Inc.), Akt (cat. no. 9272S; Cell Signaling Technology, Inc.), pAkt (Ser473) (cat. no. 4060S; Cell Signaling Technology, Inc.), GSK 3β (cat. no. 12456S; Cell Signaling Technology, Inc.), pGSK 3β Ser9 (cat. no. 5558S; Cell Signaling Technology, Inc.), CXCR2 (cat. no. ab217314; Abcam) and TGF-β (cat. no. ab25121; Abcam).

Statistical analysis

The survival was analyzed by Kaplan-Meier and compared by the Log-rank test. Data between groups were analyzed by Student's t-test. p values less than 0.05, 0.01, and 0.001 were considered statistically significant and indicated by *, ** and ***, respectively, ns means "no significance" in each. All statistical analysis was performed using GraphPad Prism8.0 (GraphPad Software, Inc. https://www.graphpad.com/scientific-software/prism/).

Results

The combination of Pc with Gem significantly inhibited LLC subcutaneous tumor growth in mice

To investigate the antitumor effect of the combination of Pc and Gem, subcutaneously implanted tumor-bearing mice were treated with Pc in combination with Gem (Figure 1A). The subcutaneous tumors of mice in Pc+Gem group had less blood supply, and looked like benign tumors (Figure 1B). Both Pc infection alone ($p = 0.005$) and Gem treatment alone ($p = 0.002$) significantly inhibited tumor growth in the subcutaneous model. Furthermore, tumor growth was significantly slower in the combination (Pc+Gem) group than in the control group($p < 0.001$), and Pc alone ($p = 0.006$) or Gem alone ($p = 0.03$) group respectively (Figure 1C). The tumor weights and the ratios of tumor weight to the body weight in the combination group were also significantly lower than those in any other group (all $p < 0.05$) (Figures 1D, S1). The median survival time was 27.5 days, 34 days, 35 days and 41 days in the control group, Pc group,

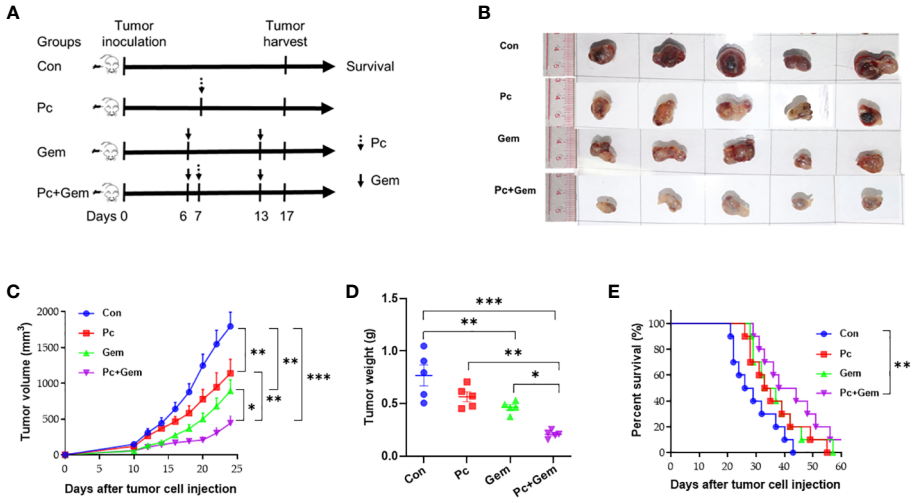


FIGURE 1
Pc+Gem combination treated lung cancer in the s.c. implanted murine LLC model. **(A)** Simplified experimental flow chart of s.c. implanted murine LLC model. **(B)** The image of tumor size on day 17 after tumor cells injection (n=5). **(C)** Tumor growth curves (n = 10 each group). **(D)** Tumor weight on day 17 after tumor cells injection (n = 5). The statistical differences were analyzed with an unpaired two-tailed Student's t-test. **(E)** Kaplan-Meier survival curves (n = 10). Survival curves were analyzed by a log-rank test. *p* values less than 0.05, 0.01, and 0.001 were considered statistically significant and indicated by *, ** and ***, respectively.

Gem group and Pc+Gem group, respectively (Figure 1E). Compared with the control, single treatment (Pc alone or Gem alone) only tended to prolong the life span of tumor-bearing mice without statistically significant differences in survival time between groups. Nevertheless, the life span of the combined treatment group was significantly longer than that of the control group ($p = 0.007$), suggesting a synergistic effect of the combination (Figure 1E).

The combination of Pc with Gem significantly inhibited LLC metastasis in mice

To determine the anti-metastatic effect of Pc+Gem, we established a mouse tumor model with intravenous injection of LLC cells (Figure 2A). The number of lung tumor nodules on day 32 in the Pc alone group or combination group was significantly less than that in the control group ($p = 0.005$ and $p = 0.003$, respectively) and Gem alone group ($p = 0.02$ and $p = 0.02$, respectively) (Figure 2B). These phenomena suggested that the role of Pc on the inhibition of metastasis was greater than that of Gem. In the control group, large transparent gelatinoid metastastic nodules were observed on the lung surface, some of which were accompanied by local bleeding. In the treatment groups, the metastases were smaller, and most of the metastases were only observed under magnifying glass after lung tissue dissection (Figure 2C). The median survival time was 44.5 days, 57 days, 59.5 days and 69.5 days in the control group, Pc group, Gem group and Pc+Gem group, respectively (Figure 2D). Accordingly, we also found that the mice in the Pc group, Gem group and Pc+Gem group survived significantly longer than the mice in the control group ($p = 0.02$, $p = 0.006$ and $p < 0.001$, respectively), the mice in the combination treatment group appeared to live longer than those in any monotherapy group, but the differences between the groups were not statistically significant (Figure 2D).

The combination of Pc and Gem significantly inhibited the EMT of tumor cells

Tumor cells obtain an invasive phenotype for metastatic progression through EMT, which allows them to dissociate from the primary tumor into the blood circulation (22). The loss of E-cadherin expression has been considered a landmark for EMT (23). Our experimental results showed that there were no significant differences in the protein expression level of E-cadherin between each monotherapy group and the control group, but the level of this molecule in the combination treatment group was significantly higher than that in the control group or that in Pc group and Gem group ($p < 0.001$, $p = 0.002$ and $p < 0.001$, respectively) (Figures 3A, B), suggesting a significantly synergistic effect of the combined treatment. The Snail superfamily of Zinc-finger transcription factors is a crucial transcription inhibitor for EMT, which can directly lead to inhibition of E-cadherin (24). Our results indicated that the expression level of Snail protein in the Pc group and Pc+Gem group was significantly lower than that in the control group ($p = 0.02$ and $p = 0.002$, respectively). Although there were no significant differences between the treatment groups, the level of this molecule in Gem group was not statistically significant than that in the control group, which suggested that combination treatment group has a synergistic effect on the inhibition of Snail protein expression and the role of Pc on the inhibition of Snail protein expression was greater than that of Gem (Figures 3A, C).

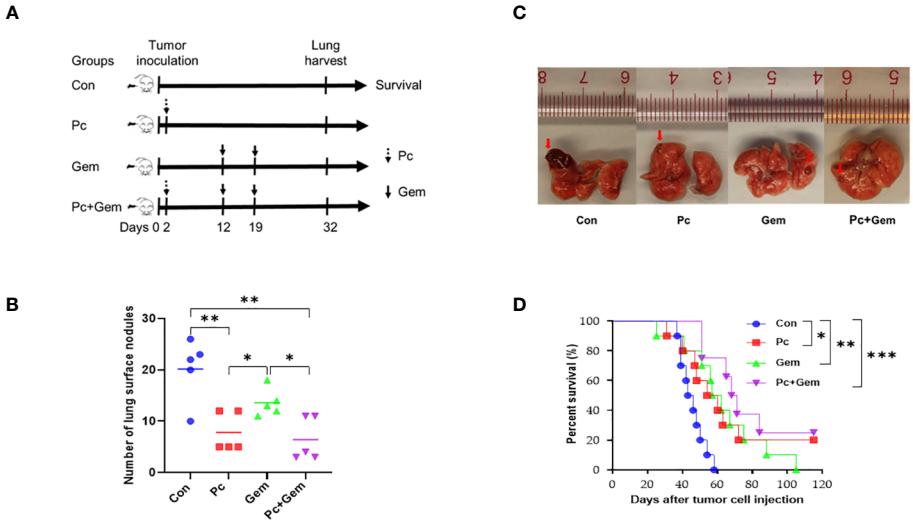


FIGURE 2
Pc+Gem treated lung cancer in the i.v. inoculated murine LLC model. **(A)** Simplified experimental flow chart of i.v. inoculated murine LLC model. **(B)** Number of tumor nodules in the lung tissues on day 32 after intravenous tumor inoculation (n = 5). The statistical differences were analyzed with an unpaired two-tailed Student's t-test. **(C)** The representative image of tumor nodules in the lung tissues on day 32 after intravenous tumor inoculation. **(D)** Kaplan-Meier survival curve (n = 10). Survival curves were analyzed by a log-rank test. *p* values less than 0.05, 0.01, and 0.001 were considered statistically significant and indicated by *, ** and ***, respectively.

The combination of Pc and Gem significantly suppressed the activation of PI3K/Akt/GSK-3β signaling pathway

Some studies have indicated that the PI3K/Akt/GSK-3β signaling pathway plays an important role by affecting the activity of the transcription factor, Snail that is related to EMT in many types of tumors (20, 21). Therefore, we examined PI3K/Akt/GSK-3β protein expression levels in the tumors of these mice. The results of Western blotting analysis indicated that the phosphorylation level of PI3K in any treatment group (Pc, Gem, or Pc+Gem) was lower than that in the control group ($p = 0.007$, $p = 0.04$ and $p = 0.02$, respectively), but there were no significant differences between the treatment groups, suggesting that the combination of the two

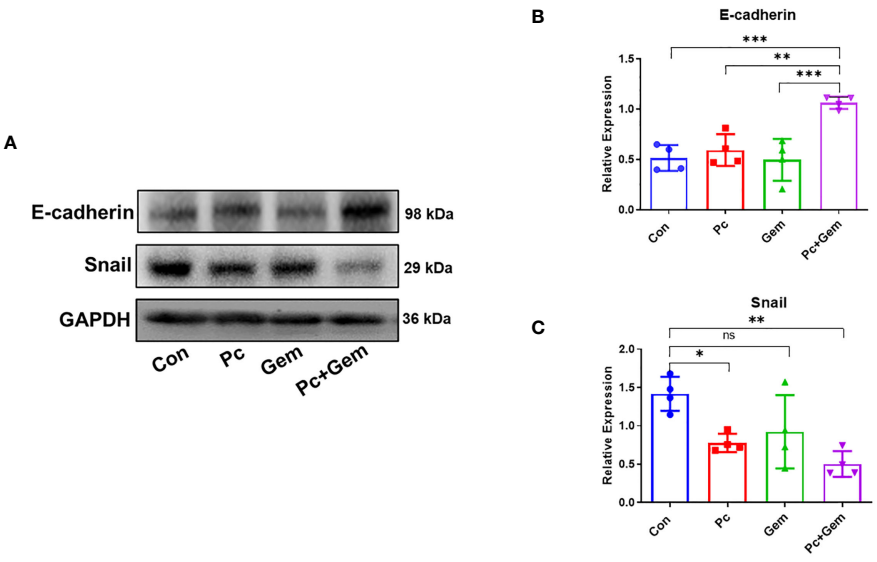


FIGURE 3
Pc+Gem significantly up-regulated E-cadherin and down-regulated Snail protein expression levels. The experimental scheme was shown in Figure 1A. **(A)** The results of Western blotting analysis of E-cadherin and Snail in LLC subcutaneous tumors on day 17 after tumor cells injection. **(B)** The relative expression of E-cadherin/GAPDH (n = 4). **(C)** The relative expression of Snail/GAPDH (n = 4). The statistical differences were analyzed with an unpaired two-tailed Student's t-test. *p* values less than 0.05, 0.01, and 0.001 were considered statistically significant and indicated by *, ** and ***, respectively. *p* values more than 0.05 were considered statistically non-significantly and indicated by ns.

treatments had neither synergistic nor antagonistic effect on this molecule (Figures 4A, B). Similarly, the phosphorylation level of Akt in any treatment group (Pc, Gem, or Pc+Gem) was also lower than that in the control group ($p = 0.02$, $p = 0.03$ and $p < 0.001$, respectively). Furthermore, the phosphorylation level of Akt in Pc +Gem group was significantly lower than the Gem group ($p = 0.02$). At the same time, the expression level of phosphorylated Akt in the Pc+Gem group also appeared to be lower than the Pc group, but the difference between the two groups was not statistically significant. These results suggested that the combination of the two treatments had a synergistic effect on the expression of this molecule (Figures 4A, C). The phosphorylation level of GSK-3β in any of the treatment groups (Pc, Gem, or Pc+Gem) was lower than that in the control group ($p = 0.02$, $p = 0.03$ and $p = 0.005$, respectively), but there were no significant differences between the treatment groups, suggesting that the combination of the two treatments did not have a synergistic effect on the expression of this molecule, neither did it have an antagonistic effect (Figures 4A, D).

The combination of Pc and Gem significantly downregulated the expression of CXCR2/TGF-β

CXC-chemokine receptor 2 (CXCR2) has been demonstrated to have the ability to activate PI3K/Akt/GSK-3β/Snail signaling pathways and promote cell migration (25, 26). Therefore, we examined the expression of these molecules in tumor tissues of mice. The Western blotting results showed that there were no significant differences in CXCR2 protein expression level between any single treatment (Pc or Gem) group and the control group, but the level of this molecule in the Pc+Gem group was significantly lower than that in the control group ($p = 0.03$). In addition, the expression level of this molecule in the Pc+Gem group was also significantly lower than that in the Pc group ($p = 0.02$). These phenomena suggested that the combination of the two treatments had a synergistic effect on this molecule (Figures 5A, B). We further examined the expression level of TGF-β which has also been shown to promote EMT through PI3K/Akt/GSK-3β/Snail signaling (27). Our results indicated that the expression level of TGF-β protein in any treatment (Pc, Gem or Pc+Gem) group was significantly lower than that in the control group ($p < 0.001$, $p = 0.03$ and $p = 0.003$, respectively), but there were no significant differences between the treatment groups, suggesting that the combined treatment had no synergistic effect, neither did it show any antagonistic effect on the expression of this molecule (Figures 5A, C).

Discussion

Our current study indicates that the combination of *Plasmodium* (Pc) infection with Gem treatment has a synergistic effect on the inhibition of tumor growth and prolongation of survival in a subcutaneously inoculated mouse lung cancer model (Figure 1) and a synergistic effect on the inhibition of tumor metastasis and prolongation of survival in an intravenously inoculated mouse tumor model (Figure 2). Pc infection may contribute more than the Gem treatment in the inhibition of tumor metastasis (Figure 2B). These results are consistent with those of our previous studies that *Plasmodium yoelii* 17XNL (Py)

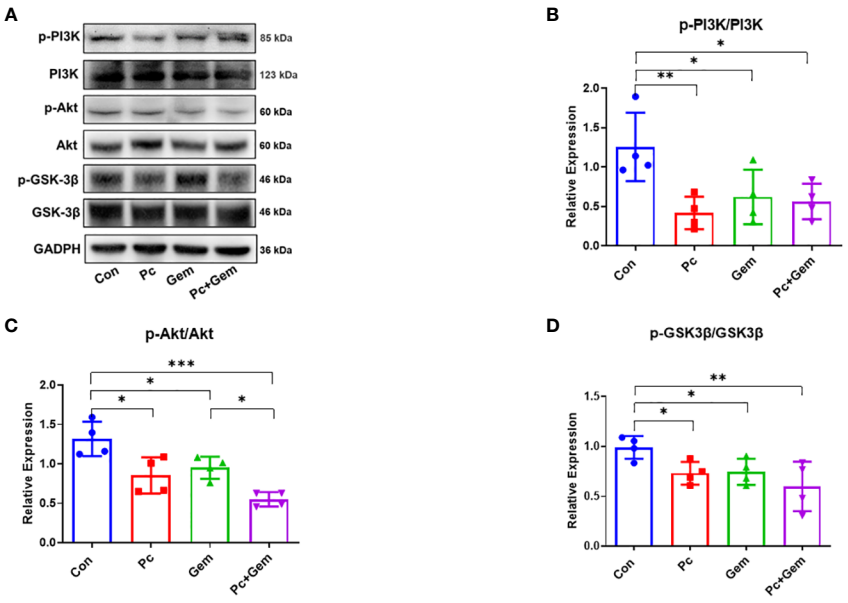


FIGURE 4
Pc+Gem significantly inhibited the activation of the PI3K/Akt/GSK-3β signaling pathway. The experimental scheme was shown in Figure 1A. **(A)** The results of Western blotting analysis of PI3K/Akt/GSK-3β in LLC subcutaneous tumors on day 17 after tumor cells injection. **(B)** The relative expression of p-PI3K/PI3K (n = 4). **(C)** The relative expression of p-Akt/Akt (n = 4). **(D)** The relative expression of p-GSK-3β/GSK-3β (n = 4). The statistical differences were analyzed with an unpaired two-tailed Student's t-test. *p* values less than 0.05, 0.01, and 0.001 were considered statistically significant and indicated by *, ** and ***, respectively.

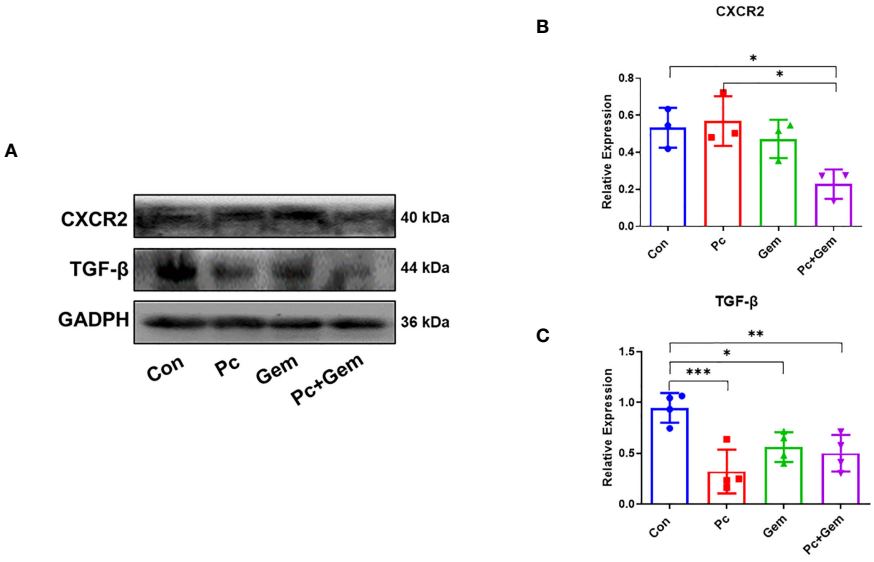


FIGURE 5
Pc+Gem significantly down-regulated the protein expression levels of CXCR2/TGF-β. The experimental scheme was shown in Figure 1A. **(A)** The results of Western blotting analysis of CXCR2/TGF-β in LLC subcutaneous tumors on day 17 after tumor cells injection. **(B)** The relative expression of CXCR2/GAPDH (n = 3). **(C)** The relative expression of TGF-β/GAPDH (n = 4). The statistical differences were analyzed with an unpaired two-tailed Student's t-test. *p* values less than 0.05, 0.01, and 0.001 were considered statistically significant and indicated by *, ** and ***, respectively.

infection significantly reduces tumor metastasis and recurrence after the original tumor is removed through operation in a murine liver cancer model (21), and that the combination of Py infection with DNA cancer vaccine treatment has a synergistic antitumor effect in a murine lung cancer model (12).

Studies have shown that tumor metastasis is highly related to EMT of tumor cells and the apparent characteristics of EMT are a downregulation of E-cadherin and an upregulation of Snail in tumor cells (17–19). Our current results have demonstrated that Pc infection in combination with Gem treatment significantly up-regulates the protein expression level of E-cadherin and down-regulates the protein expression level of Snail in tumor tissues (Figure 3), which indicates a significant inhibition of EMT. Even though Gem alone may induce EMT in patient-derived pancreatic ductal adenocarcinoma xenografts (28), we did not observe a similar effect represented by the expression levels of E-cadherin and Snail in our current murine lung cancer model (Figure 3).

Our previous study has suggested that Py infection inhibits PI3K/Akt/GSK-3β/Snail signaling pathway and therefore inhibits EMT in a murine liver cancer model (21). In our current study, we tested whether the combination of Pc and Gem or Pc infection alone or Gem treatment alone inhibited this pathway in a murine lung cancer model. The results show that the combination or Pc infection alone or Gem treatment alone indeed inhibits this pathway (Figure 4). Then we asked whether CCR10 mediated this pathway as demonstrated in our previous study of a liver cancer model infected with Py (21). The result suggested that the CCR10 protein level in lung cancer tissue was not affected by Pc infection, or Gem treatment or the combination of both (Figure S2). Then we tested the protein expression levels of CXCR2 and TGF-β, because some studies have indicated that CXCR2 can also mediate PI3K/Akt/GSK-3β/Snail signaling pathway (25, 26), and many researches have revealed that CXCR2 is also significant in the recruitment of different cells (tumor-associated macrophages, tumor-associated neutrophils, myeloid-derived suppressor cells, regulatory T cells) which constitute the tumor microenvironment (29–32). These components can cause EMT by regulating TGF-β secretion which can be involved in PI3K/Akt/GSK-3β pathway (27). The results show that the combination of Pc and Gem treatment significantly downregulates the protein level of CXCR2 compared with the control group, but Pc alone or Gem alone does not affect its level (Figures 5A, B). Finally, our current results show that Pc infection alone or Gem treatment alone or the combination of both significantly inhibits the protein expression level of TGF-β (Figures 5A, C). Based on the results mentioned above, we summarize the possible mechanism of action of Pc infection in combination with Gem treatment on EMT of tumor cells in murine lung cancer models as shown in Figure 6.

Studies have suggested that high EMT score of tumor cells promotes immune evasion, while low EMT score promotes antitumor immune response, and vice versa, an effective antitumor immune response can inhibit EMT and kill tumor cells at the same time (33–35). Other studies have pointed out that STAT3 signaling plays an important role in the occurrence and development of EMT, and the interaction between STAT3 and TGF-β not only induces EMT, but also serves as the central regulatory signal molecules for the formation of immunosuppressive network in the tumor microenvironment (36–39). Our previous study in mouse tumor models shows that *Plasmodium* infection significantly downregulates the phosphorylated level of STAT3 (pSTAT3) within MDSCs in tumor tissues and the expression level of TGF-β in tumor tissues, thus releasing the tumor immunosuppressive microenvironment (15). Combined with the findings of current study, namely,

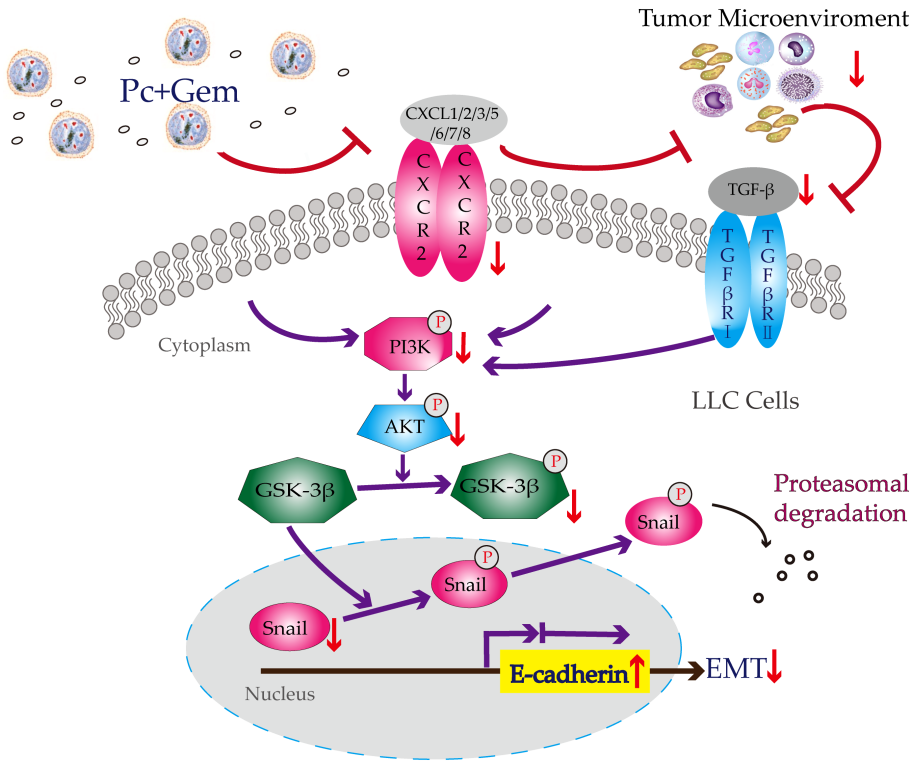


FIGURE 6
Potential mechanism of action of Pc+Gem in the inhibition of tumor cell EMT in murine Lewis lung cancer models. Pc+Gem induces: 1) down-regulation of CXCR2/TGF-β; 2) down-regulation of p-PI3K, but not PI3K, suggesting the inhibition of the phosphorylase of PI3K; 3) downregulation of p-Akt, but not Akt, suggesting the inhibition of the phosphorylase of Akt; 4) down-regulation of p-GSK-3β, but not GSK-3β, suggesting the inhibition of the phosphorylase of GSK-3β; 5) down-regulation of Snail; 6) up-regulation of E-cadherin. The down-regulation of Snail and up-regulation of E-cadherin are the main characteristics of suppression of the EMT in murine LLC models.

Plasmodium infection blocks TGF-β-induced EMT, we believe that the activation of the immune system of the tumor-bearing host, the relief of the immunosuppressive state, and the inhibition of EMT by *Plasmodium* infection, are highly unified because they share certain signaling pathways and key targets. By inhibiting these targets and pathways, *Plasmodium* infection can promote the body's anti-tumor immune response, inhibit tumor growth and metastasis, and thus prolong the life of tumor-bearing hosts.

However, there have been many conflicting results and controversies regarding whether *Plasmodium* infection suppresses or activates the immune system (40–42). Urban BC et al. proposed a hypothesis to reconcile these conflicting results, where they suggested that high density of parasitemia or high concentration of malaria pigment (hemozoin) inhibited dendritic cells (DC) and downstream T and B cells, while low density of parasitemia or low concentration of hemozoin activated DC and its downstream immune cells (43). Nevertheless, what we observed in *Plasmodium*-infected tumor-bearing mice is inconsistent with this hypothesis. First, we compared the parasitemia induced by Py and Pc. In both tumor-free mice and lung cancer-bearing mice, the parasite density (red blood cell infection rate) induced by Py was significantly higher than that induced by Pc, and the duration of high parasitemia was significantly longer in Py than in Pc (Figure S3). Then, we compared the inhibitory effect of Py and Pc on lung cancer in mice and found that the effect of Py was significantly better than that of Pc (Figure S4). Finally, we observed a positive correlation of parasite density with spleen size (represents the degree of immune response to the infection) and a negative correlation of parasite density with tumor size (Figure S5), suggesting that *Plasmodium* infection could induce antitumor immune response in a parasitemia-dependent manner. In fact, one of the best ways to test whether *Plasmodium* infection activates or suppresses the immune system is to observe it in a tumor-bearing host, because the immune system of the tumor-bearing host is inhibited by tumor cells, if it suppresses the immune system, it would promote tumor growth, if it activates the immune system, it would inhibit tumor growth. In brief, what we observed in the tumor-bearing hosts is that *Plasmodium* infection generally activates rather than suppresses the immune system, when the immune system has already been suppressed by the tumor cells. This has also been preliminarily demonstrated in our clinical trial of *Plasmodium* immunotherapy for advanced solid tumors. We used a relatively benign form of human parasite, namely, *Plasmodium vivax* (Pv), in clinical trials, and the parasitemia level of natural Pv infection in humans is fairly low compared to Py or Pc in mice (44). Furthermore, to ensure the safety of clinical trials, we used artesunate to control the parasitemia to very low levels (0.1% or less), and the low parasitemia has been shown to activate the immune system of patients with advanced cancer (45) and therefore has effect on the treatment of clinical tumors

(unpublished data). Our clinical data preliminarily suggest that high parasitemia not only increases toxicity, but is also positively associated with poor prognosis in cancer patients (unpublished data), so we must strictly control the infection rate of the parasite. It is very important that the parasite that we have selected is a strain of *Plasmodium* vivax that is sensitive to all current antimalarial drugs, especially artesunate, and a single low dose of artesunate administered intravenously in a very short period of time can control the parasite density to less than 0.1%, so the side effects of *Plasmodium* immunotherapy are limited and manageable.

It is worthy of note that in our previous study, Py infection inhibits the CCR10-mediated PI3K/Akt/GSK-3β/Snail signaling pathway in a murine liver cancer model, but in our current study, Pc infection inhibits the CXCR2/TGF-β-mediated PI3K/Akt/GSK-3β/Snail signaling pathway in murine lung cancer models. There are two possible reasons for these differences. (1) Different murine cancer models: liver cancer versus lung cancer; (2) different murine *Plasmodium* parasites: Py versus Pc. This merits further study.

A series of previous studies conducted by us have shown that *Plasmodium* infection plays anticancer roles through multiple targets and multiple pathways, for example, it activates the innate and adaptive antitumor immune responses (12, 46); systematically removes the tumor immunosuppressive microenvironment through *Plasmodium*-associated exosomes that inhibit tumor cell secretion of cytokines and chemokines which have the ability to recruit the precursors of immune suppressor cells including myeloid-derived suppressor cells (MDSC) and regulatory T cells (Treg) into tumor tissue, thereby significantly down-regulating the number of these cells and inhibiting their function through undefined mechanisms (15); inhibits tumor angiogenesis through micro-RNA (miRNA) 16/322/497/17 within exosomes and long noncoding RNA (lncRNA F66), both of which target VEGF/VEGFR2 pathway via different mechanisms of action or through changing the functional phenotype of tumor-associated macrophages (TAM) via engulfing hemozoin that blocks IGF-1/MMP9 signal pathways (13, 14, 47), and inhibits EMT of tumor cells (21). By comparing *Plasmodium* immunotherapy with a single-target anticancer immunotherapy known as immune checkpoint blockade, we propose the notion that *Plasmodium* immunotherapy is an ecological therapy that systemically targets cancer as an ecological disease (45). However, *Plasmodium* immunotherapy also has an obvious shortage, that is, the specific killing of tumor cells is relatively weak, therefore, needs to be combined with other therapies to further improve its efficacy. Our current study has preliminarily confirmed that *Plasmodium* (Pc) infection combined with Gem treatment has a synergistic effect on the inhibition of EMT and tumor metastasis, and the prolongation of survival in lung cancer-bearing mice, without significantly enhancing their toxicity (Figure S6). Since Gem treatment induces immunogenic death of cancer cells (48) and inhibits MDSC, Treg, and TGF-β (49), Pc infection in combination with Gem may also have synergistic effects on immune killing of tumor cells. This merits further study. Nevertheless, since both *Plasmodium* infection and Gem treatment exert anticancer effects through multiple targets and multiple pathways, their synergistic effects on the overall anticancer effect, that is, inhibiting tumor growth and metastasis and prolonging the life span of tumor-bearing mice, do not mean that they must have synergistic effects on every signaling pathway and every target. Importantly, antagonism between them was not observed throughout the study.

There are some shortcomings in this study: we were unable to use some specific gene knockout mice for experiments. For example, IFN-γ, an inflammatory cytokine, is important for both anti-tumor immunity (50, 51) and anti-*Plasmodium* immunity, especially for its antagonistic effect on anti-inflammatory cytokine TGF-β (52). However, IFN-γ knockout mice would die when infected with *Plasmodium* parasites (53). Therefore, we are currently designing single-cell transcriptome studies to look for important target genes for *Plasmodium* immunotherapy.

In summary, we report for the first time the antitumor results of Pc alone and the synergistic effects of Pc combined with Gem in murine lung cancer models in our present study. These results indicate that Pc infection in combination with Gem treatment significantly inhibits tumor growth and metastasis, and prolongs the survival of lung cancer-bearing mice partially through inhibiting EMT of tumor cells that is possibly related to the blockade of CXCR2/TGF-β-mediated PI3K/Akt/GSK-3β/Snail signaling pathway. Based on the results of our series of preclinical studies in murine tumor models and our epidemiological data analysis showing a significant negative correlation between global malaria incidence and tumor mortality (54), clinical trials of *Plasmodium* immunotherapy for advanced cancer have been approved and are ongoing in China (NCT02786589, NCT03474822 and NCT04165590). Our current study provides a candidate for future clinical trials of *Plasmodium* immunotherapy in combination with other therapies for the treatment of cancer.

Data availability statement

The original contributions presented in the study are included in the article/Supplementary Material. Further inquiries can be directed to the corresponding authors.

Ethics statement

The animal study was approved by Guangzhou Institutes of Biomedicine and Health. The study was conducted in accordance with the local legislation and institutional requirements.

Author contributions

XC and ZT conceived, planned and carried out this work. YL, MM, DA, LC, WD, XL, LD, SF, and SZ helped in the animal experiments. WH, DW, ZD, and FZ performed consultation and

analyzed the results. LQ, XPC, and ZY supervised the research project. XPC and ZY revised the manuscript. All authors discussed the results and contributed to this work. All authors read and approved the final manuscript.

Funding

This work was supported by grants from the Open Project of the State Key Laboratory Respiratory Disease (grant number: SKLRD-OP-201802), Program Grant of Guangzhou Innovation Leading Team in Sciences and Technologies (grant number: 201909010007) and the Applied Basic Research Projects of Yunnan Province (grant number: 202101AY070001-084).

Conflict of interest

Authors ZT, WD, SZ, WH, FZ, and XPC were employed by CAS-Lamvac Guangzhou Biomedical Technology Co., Ltd.

The remaining authors declare that the research was conducted in the absence of any commercial or financial relationships that could be construed as a potential conflict of interest.

Publisher's note

All claims expressed in this article are solely those of the authors and do not necessarily represent those of their affiliated organizations, or those of the publisher, the editors and the reviewers. Any product that may be evaluated in this article, or claim that may be made by its manufacturer, is not guaranteed or endorsed by the publisher.

Supplementary material

The Supplementary Material for this article can be found online at: https://www.frontiersin.org/articles/10.3389/fonc.2023.1181176/full#supplementary-material

References

1. Sung H, Ferlay J, Siegel RL, Laversanne M, Soerjomataram I, Jemal A, et al. Global cancer statistics 2020: GLOBOCAN estimates of incidence and mortality worldwide for 36 cancers in 185 countries. *CA Cancer J Clin* (2021) 71(3):209–49. doi: 10.3322/caac.21660

2. Zheng YW, Li RM, Zhang XW, Ren XB. Current adoptive immunotherapy in non-small cell lung cancer and potential influence of therapy outcome. *Cancer Invest* (2013) 31(3):197–205. doi: 10.3109/07357907.2013.775294

3. Chen VW, Ruiz BA, Hsieh MC, Wu XC, Ries LA, Lewis DR. Analysis of stage and clinical/prognostic factors for lung cancer from SEER registries: AJCC staging and collaborative stage data collection system. *Cancer* (2014) 120 Suppl 23:3781–92. doi: 10.1002/cncr.29045

4. Lim SM, Syn NL, Cho BC, Soo RA. Acquired resistance to EGFR targeted therapy in non-small cell lung cancer: Mechanisms and therapeutic strategies. *Cancer Treat Rev* (2018) 65:1–10. doi: 10.1016/j.ctrv.2018.02.006

5. Couzin-Frankel J. Breakthrough of the year 2013. Cancer immunotherapy. *Science* (2013) 342(6165):1432–3. doi: 10.1126/science.342.6165.1432

6. Johnson DB, Balko JM, Compton ML, Chalkias S, Gorham J, Xu Y, et al. Fulminant myocarditis with combination immune checkpoint blockade. *N Engl J Med* (2016) 375(18):1749–55. doi: 10.1056/NEJMoa1609214

7. Kanai O, Nakatani K, Fujita K, Okamura M, Mio T. Concurrence of nivolumab-induced interstitial lung disease and cancer invasion. *Respirol Case Rep* (2017) 5(6): e00257. doi: 10.1002/rcr2.257

8. Marin-Acevedo JA, Dholaria B, Soyano AE, Knutson KL, Chumsri S, Lou Y. Next generation of immune checkpoint therapy in cancer: new developments and challenges. *J Hematol Oncol* (2018) 11(1):39. doi: 10.1186/s13045-018-0582-8

9. Stevenson MM, Riley EM. Innate immunity to malaria. *Nat Rev Immunol* (2004) 4 (3):169–80. doi: 10.1038/nri1311

10. Dobbs KR, Crabtree JN, Dent AE. Innate immunity to malaria-The role of monocytes. *Immunol Rev* (2020) 293(1):8–24. doi: 10.1111/imr.12830

11. Kurup SP, Butler NS, Harty JT. T cell-mediated immunity to malaria. *Nat Rev Immunol* (2019) 19(7):457–71. doi: 10.1038/s41577-019-0158-z

12. Chen L, He Z, Qin L, Li Q, Shi X, Zhao S, et al. Antitumor effect of malaria parasite infection in a murine Lewis lung cancer model through induction of innate and adaptive immunity. *PloS One* (2011) 6(9):e24407. doi: 10.1371/journal.pone.0024407

13. Yang Y, Liu Q, Lu J, Adah D, Yu S, Zhao S, et al. Exosomes from Plasmodium-infected hosts inhibit tumor angiogenesis in a murine Lewis lung cancer model. *Oncogenesis* (2017) 6(6):e351. doi: 10.1038/oncsis.2017.52

14. Qin L, Zhong M, Adah D, Qin L, Chen X, Ma C, et al. A novel tumour suppressor lncRNA F630028O10Rik inhibits lung cancer angiogenesis by regulating miR-223-3p. *J Cell Mol Med* (2020) 24(6):3549–59. doi: 10.1111/jcmm.15044

15. Adah D, Yang Y, Liu Q, Gadidasu K, Tao Z, Yu S, et al. Plasmodium infection inhibits the expansion and activation of MDSCs and Tregs in the tumor microenvironment in a murine Lewis lung cancer model. *Cell Commun Signal* (2019) 17(1):32. doi: 10.1186/s12964-019-0342-6

16. Suzuki E, Sun J, Kapoor V, Jassar AS, Albelda SM. Gemcitabine has significant immunomodulatory activity in murine tumor models independent of its cytotoxic effects. *Cancer Biol Ther* (2007) 6(6):880–5. doi: 10.4161/cbt.6.6.4090

17. Brabletz T, Kalluri R, Nieto MA, Weinberg RA. EMT in cancer. *Nat Rev Cancer* (2018) 18(2):128–34. doi: 10.1038/nrc.2017.118

18. Ye X, Tam WL, Shibue T, Kaygusuz Y, Reinhardt F, Ng Eaton E, et al. Distinct EMT programs control normal mammary stem cells and tumour-initiating cells. *Nature* (2015) 525(7568):256–60. doi: 10.1038/nature14897

19. Alizadeh AM, Shiri S, Farsinejad S. Metastasis review: from bench to bedside. *Tumour Biol* (2014) 35(9):8483–523. doi: 10.1007/s13277-014-2421-z

20. Zhang B, Yin C, Li H, Shi L, Liu N, Sun Y, et al. Nir1 promotes invasion of breast cancer cells by binding to chemokine (C-C motif) ligand 18 through the PI3K/Akt/GSK3β/Snail signalling pathway. *Eur J Cancer* (2013) 49(18):3900–13. doi: 10.1016/j.ejca.2013.07.146

21. Liang Y, Chen X, Tao Z, Ma M, Adah D, Li X, et al. Plasmodium infection prevents recurrence and metastasis of hepatocellular carcinoma possibly via inhibition of the epithelial–mesenchymal transition. *Mol Med Rep* (2021) 23(6). doi: 10.3892/mmr.2021.12057

22. Nieto MA, Huang RY, Jackson RA, Thiery JP. EMT: 2016. *Cell* (2016) 166(1):21–45. doi: 10.1016/j.cell.2016.06.028

23. Campbell K, Casanova J. A role for E-cadherin in ensuring cohesive migration of a heterogeneous population of non-epithelial cells. *Nat Commun* (2015) 6:7998. doi: 10.1038/ncomms8998

24. Dong C, Wu Y, Wang Y, Wang C, Kang T, Rychahou PG, et al. Interaction with Suv39H1 is critical for Snail-mediated E-cadherin repression in breast cancer. *Oncogene* (2013) 32(11):1351–62. doi: 10.1038/onc.2012.169

25. Zhou SL, Zhou ZJ, Hu ZQ, Li X, Huang XW, Wang Z, et al. CXCR2/CXCL5 axis contributes to epithelial-mesenchymal transition of HCC cells through activating PI3K/Akt/GSK-3β/Snail signaling. *Cancer Lett* (2015) 358(2):124–35. doi: 10.1016/j.canlet.2014.11.044

26. Zhou Y, Shurin GV, Zhong H, Bunimovich YL, Han B, Shurin MR. Schwann cells augment cell spreading and metastasis of lung cancer. *Cancer Res* (2018) 78 (20):5927–39. doi: 10.1158/0008-5472.CAN-18-1702

27. Gonzalez DM, Medici D. Signaling mechanisms of the epithelial-mesenchymal transition. *Sci Signal* (2014) 7(344):re8. doi: 10.1126/scisignal.2005189

28. Bulle A, Dekervel J, Libbrecht L, Nittner D, Deschuttere L, Lambrecht D, et al. Gemcitabine induces Epithelial-to-Mesenchymal Transition in patient-derived pancreatic ductal adenocarcinoma xenografts. *Am J Transl Res* (2019) 11(2):765–79.

29. Zhang M, Huang L, Ding G, Huang H, Cao G, Sun X, et al. Interferon gamma inhibits CXCL8-CXCR2 axis mediated tumor-associated macrophages tumor

trafficking and enhances anti-PD1 efficacy in pancreatic cancer. *J Immunother Cancer* (2020) 8(1). doi: 10.1136/jitc-2019-000308

30. Chao T, Furth EE, Vonderheide RH. CXCR2-dependent accumulation of tumor-associated neutrophils regulates T-cell immunity in pancreatic ductal adenocarcinoma. *Cancer Immunol Res* (2016) 4(11):968–82. doi: 10.1158/2326-6066.CIR-16-0188

31. Lv M, Xu Y, Tang R, Ren J, Shen S, Chen Y, et al. miR141-CXCL1-CXCR2 signaling-induced Treg recruitment regulates metastases and survival of non-small cell lung cancer. *Mol Cancer Ther* (2014) 13(12):3152–62. doi: 10.1158/1535-7163.MCT-14-0448

32. Li BH, Garstka MA, Li ZF. Chemokines and their receptors promoting the recruitment of myeloid-derived suppressor cells into the tumor. *Mol Immunol* (2020) 117:201–15. doi: 10.1016/j.molimm.2019.11.014

33. Terry S, Savagner P, Ortiz-Cuaran S, Mahjoubi L, Saintigny P, Thiery JP, et al. New insights into the role of EMT in tumor immune escape. *Mol Oncol* (2017) 11 (7):824–46. doi: 10.1002/1878-0261.12093

34. Chockley PJ, Keshamouni VG. Immunological consequences of epithelial-mesenchymal transition in tumor progression. *J Immunol* (2016) 197(3):691–8. doi: 10.4049/jimmunol.1600458

35. Chou MY, Yang MH. Interplay of immunometabolism and epithelial-mesenchymal transition in the tumor microenvironment. *Int J Mol Sci* (2021) 22 (18). doi: 10.3390/ijms22189878

36. Liu RY, Zeng Y, Lei Z, Wang L, Yang H, Liu Z, et al. JAK/STAT3 signaling is required for TGF-β-induced epithelial-mesenchymal transition in lung cancer cells. *Int J Oncol* (2014) 44(5):1643–51. doi: 10.3892/ijo.2014.2310

37. Hu R, Han Q, Zhang J. STAT3: A key signaling molecule for converting cold to hot tumors. *Cancer Lett* (2020) 489:29–40. doi: 10.1016/j.canlet.2020.05.035

38. Sadrkhanloo M, Entezari M, Orouei S, Ghollasi M, Fathi N, Rezaei S, et al. STAT3-EMT axis in tumors: Modulation of cancer metastasis, stemness and therapy response. *Pharmacol Res* (2022) 182:106311. doi: 10.1016/j.phrs.2022.106311

39. Yu H, Pardoll D, Jove R. STATs in cancer inflammation and immunity: a leading role for STAT3. *Nat Rev Cancer* (2009) 9(11):798–809. doi: 10.1038/nrc2734

40. Millington OR, Di Lorenzo C, Phillips RS, Garside P, Brewer JM. Suppression of adaptive immunity to heterologous antigens during Plasmodium infection through hemozoin-induced failure of dendritic cell function. *J Biol* (2006) 5(2):5. doi: 10.1186/jbiol34

41. Amorim KN, Chagas DC, Sulczewski FB, Boscardin SB, et al. Dendritic cells and their multiple roles during malaria infection. *J Immunol Res* (2016) 2016:2926436. doi: 10.1155/2016/2926436

42. Osii RS, Otto TD, Garside P, Ndungu FM, Brewer JM. The impact of malaria parasites on dendritic cell-T cell interaction. *Front Immunol* (2020) 11:1597. doi: 10.3389/fimmu.2020.01597

43. Urban BC, Todryk S. Malaria pigment paralyzes dendritic cells. *J Biol* (2006) 5 (2):4. doi: 10.1186/jbiol37

44. Fink J, Jones PD. High prevalence of low-level parasitemia with plasmodium vivax in makira-ulawa province presents a challenge for the diagnosis and eradication of malaria in Solomon Islands. *Ochsner J* (2021) 21(1):76–80. doi: 10.31486/toj.20.0023

45. Chen X, Qin L, Hu W, Adah D. The mechanisms of action of Plasmodium infection against cancer. *Cell Commun Signal* (2021) 19(1):74. doi: 10.1186/s12964-021-00748-5

46. Pan J, Ma M, Qin L, Kang Z, Adah D, Tao Z, et al. Plasmodium infection inhibits triple negative 4T1 breast cancer potentially through induction of CD8(+) T cell-mediated antitumor responses in mice. *BioMed Pharmacother* (2021) 138:111406. doi: 10.1016/j.biopha.2021.111406

47. Wang B, Li Q, Wang J, Zhao S, Nashun B, Qin L, et al. Plasmodium infection inhibits tumor angiogenesis through effects on tumor-associated macrophages in a murine implanted hepatoma model. *Cell Commun Signal* (2020) 18(1):157. doi: 10.1186/s12964-020-00570-5

48. Zhang X, Wang D, Li Z, Jiao D, Jin L, Cong J, et al. Low-dose gemcitabine treatment enhances immunogenicity and natural killer cell-driven tumor immunity in lung cancer. *Front Immunol* (2020) 11:331. doi: 10.3389/fimmu.2020.00331

49. Eriksson E, Wenthe J, Irenaeus S, Loskog A, Ullenhag G. Gemcitabine reduces MDSCs, tregs and TGFβ-1 while restoring the teff/treg ratio in patients with pancreatic cancer. *J Transl Med* (2016) 14(1):282. doi: 10.1186/s12967-016-1037-z.

50. Kaplan DH, Shankaran V, Dighe AS, Stockert E, Aguet M, Old LJ, et al. Demonstration of an interferon gamma-dependent tumor surveillance system in immunocompetent mice. *Proc Natl Acad Sci U.S.A.* (1998) 95(13):7556–61. doi: 10.1073/pnas.95.13.7556

51. Takeda K, Nakayama M, Hayakawa Y, Kojima Y, Ikeda H, Imai N, et al. IFN-γ is required for cytotoxic T cell-dependent cancer genome immunoediting. *Nat Commun* (2017) 8:14607. doi: 10.1038/ncomms14607

52. Omer FM, de Souza JB, Riley EM. Differential induction of TGF-beta regulates proinflammatory cytokine production and determines the outcome of lethal and nonlethal Plasmodium yoelii infections. *J Immunol* (2003) 171(10):5430–6. doi: 10.4049/jimmunol.171.10.5430

53. Su Z, Stevenson MM. Central role of endogenous gamma interferon in protective immunity against blood-stage Plasmodium chabaudi AS infection. *Infect Immun* (2000) 68(8):4399–406. doi: 10.1128/IAI.68.8.4399-4406.2000

54. Qin L, Chen C, Chen L, Xue R, Ou-Yang M, Zhou C, et al. Worldwide malaria incidence and cancer mortality are inversely associated. *Infect Agent Cancer* (2017) 12:14. doi: 10.1186/s13027-017-0117-x

frontiers | Frontiers in Pharmacology

TYPE Case Report
PUBLISHED 31 October 2023
DOI 10.3389/fphar.2023.1259221

Check for updates

OPEN ACCESS

EDITED BY
Wenjun Mao,
The Affiliated Wuxi People's Hospital of Nanjing Medical University, China

REVIEWED BY
Yu Yao,
The First Affiliated Hospital of Xi'an Jiaotong University, China
Qing Zhou,
Guangdong Provincial People's Hospital Lung Cancer Institute, China

*CORRESPONDENCE
Xiangqi Chen,
drchxqtg@126.com
Sheng Yang,
dryangxh@126.com

†These authors share first authorship

RECEIVED 15 July 2023
ACCEPTED 16 October 2023
PUBLISHED 31 October 2023

CITATION
Zhang S, Guo N, Zhang Q, Wang Y, Yang S and Chen X (2023), Case report: Clinical management of recurrent small cell lung cancer transformation complicated with lung cancer-induced acute pancreatitis after lung adenocarcinoma surgery. *Front. Pharmacol.* 14:1259221. doi: 10.3389/fphar.2023.1259221

COPYRIGHT
© 2023 Zhang, Guo, Zhang, Wang, Yang and Chen. This is an open-access article distributed under the terms of the Creative Commons Attribution License (CC BY). The use, distribution or reproduction in other forums is permitted, provided the original author(s) and the copyright owner(s) are credited and that the original publication in this journal is cited, in accordance with accepted academic practice. No use, distribution or reproduction is permitted which does not comply with these terms.

Case report: Clinical management of recurrent small cell lung cancer transformation complicated with lung cancer-induced acute pancreatitis after lung adenocarcinoma surgery

Suyun Zhang[1], Ningjing Guo[2†], Qianyuan Zhang[3†], Yao Wang[2], Sheng Yang[2*] and Xiangqi Chen[4*]

[1]Departments of Internal Medicine, Fujian Medical University Union Hospital, Fuzhou, Fujian, China, [2]Oncology Medicine, Fujian Medical University Union Hospital, Fuzhou, Fujian, China, [3]General Medicine, Fujian Medical University Union Hospital, Fuzhou, Fujian, China, [4]Respiratory Medicine, Fujian Medical University Union Hospital, Fuzhou, Fujian, China

In the diagnosis and treatment of non-small cell lung cancer (NSCLC), the histological type may change from lung adenocarcinoma to lung squamous cell cancer or small cell lung cancer (SCLC). Pancreatic metastasis is extremely rare in advanced lung cancer, and pancreatitis characterized by lung cancer metastasis-induced acute pancreatitis (MIAP) is more rare. This paper reports in detail the clinical diagnosis and treatment of a female patient with lung adenocarcinoma who relapsed after radical surgery and progressed after multiple treatments. A second pathological biopsy revealed SCLC transformation, and the patient developed pancreatic metastasis and lung cancer MIAP during follow-up treatment. This paper mainly suggests that clinicians should pay attention to the possibility of pathological type transformation in the progression of advanced NSCLC, closely observe the dynamic changes of tumor markers and pay attention to the re-biopsy pathological analysis. In addition, it provides clinical experience and scientific reference for the discovery, diagnosis and treatment of transforming SCLC and lung cancer MIAP.

KEYWORDS

lung adenocarcinoma, small cell lung cancer, acute pancreatitis, pathological type transformation, case report

Brief medical history

A 58-year-old female patient was referred to the Department of Thoracic Surgery of Fujian Medical University Union Hospital due to "a lung nodule found in the left lower lobe" during a physical examination at the local Hospital A in Fujian Province, China on 23 March 2016. After various examinations, a main clinical diagnosis was made that confirmed the presence of a lung nodule in the left lower lobe. However, to determine whether this nodule is a malignant lung tumor, further examinations were required. After active preparation, the patient underwent "thoracoscopic left lower lobectomy + systematic mediastinal lymph node (LN) dissection" under general anesthesia on 30 March 2016. The postoperative pathological

diagnosis was as follows: The size of the lesion in the left lower lobe was 2.5 cm × 2.3 cm × 2.0 cm, including 70% of invasive adenocarcinoma and approximatively 30% of mucinous adenocarcinoma (Figure 1) that did not involve the visceral pleura. No metastases were detected in all groups of LNs. Immunohistochemical results indicated adenocarcinoma that was diffuse positive for NapsinA, TTF-1, CK7, and SP-B, partially positive for CK20, negative for CDX2, and that has an epidermal growth factor receptor (EGFR) exon 19del. The postoperative pathological stage was pT1cN0M0, stage Ia3. After discharge from the hospital, the patient was followed up through regular outpatient reviews. On 6 April 2017, the patient was reexamined at the Outpatient Department of Fujian Medical University Union Hospital. There was no abnormality after physical and imaging examinations, but the level of the blood tumor marker, carcinoma embryonic antigen (CEA) (6.9 ng/L), was slightly higher than the normal value (<5 ng/L). CEA level gradually rose during the close follow-up, and the patient chose to take first-generation TKI gefitinib for prevention and treatment, but CEA still gradually increased, so she switched to third-generation TKI osimertinib. Whole-body positron emission tomography-computed tomography (PET-CT) examination was performed at the Outpatient Department of Fujian Medical University Union Hospital on 13 October 2017, indicating the presence of multiple LN metastases in the mediastinum, bilateral supraclavicular, and infraclavicular regions, and bilateral neck. At the same time, the CEA level was as high as "14.6 ng/L." The patient was admitted to the Department of Thoracic Surgery on 26 October 2017, and then received "EBUS-TBNA" under general anesthesia on 2 November 2017, however, no cancer cells were discovered in the postoperative pathology. Therefore, the patient was referred to the First Affiliated Hospital, Zhejiang University School of Medicine where she underwent "puncture of the right supraclavicular mass" at the Outpatient Department on 26 November 2017. The immunohistochemical results of the punctured tissues showed adenocarcinoma with possible pulmonary origin.

Treatment history

Treatments before SCLC transformation

The patient was readmitted at the Department of Thoracic Surgery of Fujian Medical University Union Hospital on 15 December 2017 due to the presence of multiple LN metastases in the mediastinum, bilateral supraclavicular and infraclavicular regions and bilateral neck after radical surgery for invasive adenocarcinoma in the left lower lobe. As the stage of the punctured tumor tissues was not sufficient to support the detection of related lung cancer (LC) driver genes, a hematological test was performed, and the results were negative. The patient was then treated with a regimen including "pemetrexed, cisplatin and bevacizumab at q21d" for 6 cycles from 2 January 2018 to 7 May 2018, and the comprehensive evaluation of efficacy was "stable disease (SD)" at the periodic reexamination. However, the whole-body CT examination at the Outpatient Department of

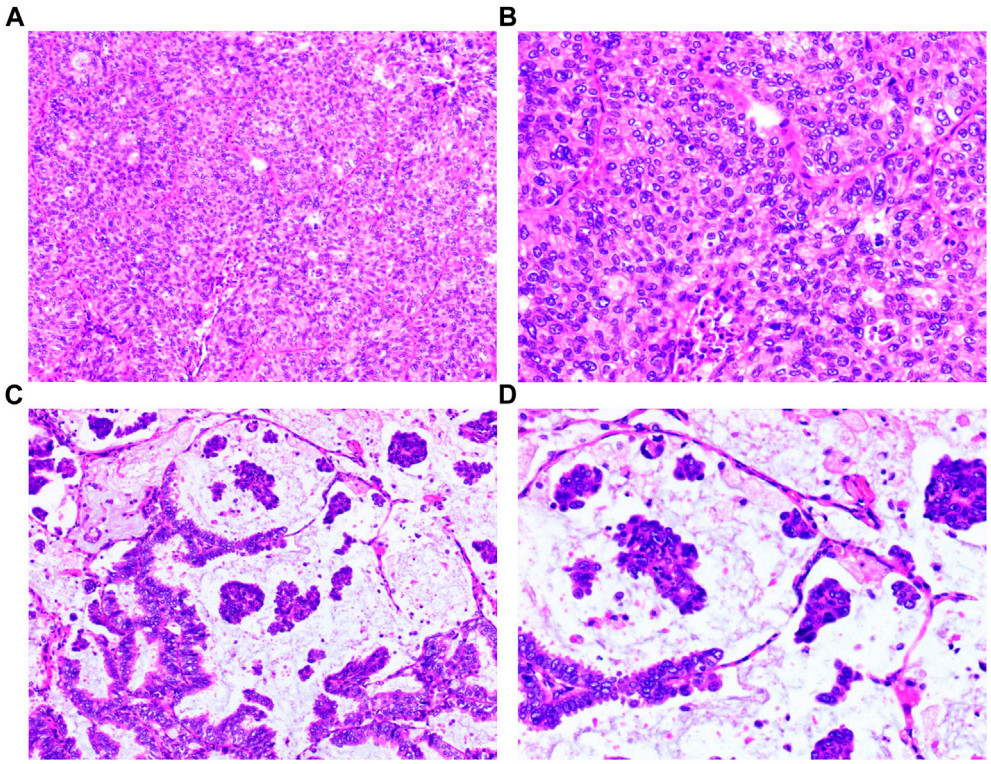


FIGURE 1
Histopathology of the surgical tumor. **(A)** Invasive adenocarcinoma (HE: ×100); **(B)** Invasive adenocarcinoma (HE: ×200); **(C)** Mucinous adenocarcinoma (HE: ×100); **(D)** Mucinous adenocarcinoma (HE: ×200).

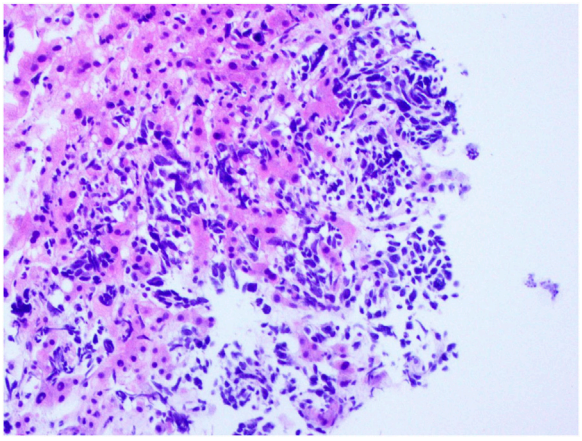


FIGURE 2
Biopsy pathology of liver mass: small cell cancer (HE: ×200).

the hospital on 28 June 2020, indicated that the mediastinal LNs and the right axillary LNs are significantly larger than before, and the comprehensive assessment of the efficacy was "progressive disease (PD)." Through multidisciplinary discussion, the following main opinion was made: The patient's cancer is significantly developed, and there are indications for continuing palliative chemotherapy and local radiotherapy. The patient accepted a 10-cycle treatment regimen of "albumin paclitaxel at q21d," combined with "antiangiogenic bevacizumab/PD-1 inhibitor tislelizumab" at the Department of Thoracic Surgery of Fujian Medical University Union Hospital from 13 June 2020 to 23 March 2021. Moreover, the patient received "Cyberknife" radiotherapy at the Radiotherapy Department from 2 February to 17 February 2021.

The detection of SCLC transformation

On 17 March 2021, the patient underwent a second whole-body CT examination at the Outpatient Department of Fujian Medical University Union Hospital, which indicated the presence of multiple small enlarged LNs in the left neck, mediastinum, right supraclavicular region, and axillary fossa shrank. There were multiple nodes with abnormal signals in the liver and behind the peritoneum, which were metastatic. The comprehensive assessment of efficacy was "progressive disease (PD)" due to "new liver lesions." Additionally, several hematological tumor markers were found changed during this reexamination. Specifically, progastrin-releasing peptide (proGRP) raised to "287 pg/mL (normal value < 69.2 ng/L)" and neuron-specific enolase (NSE) increased to "27.29 ng/mL" while CEA decreased to "9.5 ng/mL." The primary opinion made *via* a multidisciplinary discussion among practitioners at the outpatient departments of thoracic surgery, respiratory medicine, radiotherapy, and medical oncology was as follows: There is a high probability of transformation of lung adenocarcinoma into small cell lung cancer (SCLC), and therefore, a puncture biopsy of the liver metastases is recommended. The patient was admitted to the Department of Medical Oncology of Fujian Medical University Union Hospital and underwent CT-guided puncture of liver metastasis on 25 March 2021. The immunohistochemical results showed small cell cancer (Figure 2). The main clinical diagnosis was multiple metastases in the mediastinum, bilateral supraclavicular and infraclavicular regions, and bilateral cervical LNs, and liver metastases and SCLC transformation after radical treatment of invasive adenocarcinoma in the left lower lobe. From 03 November 2017 to 03 April 2021, this patient, with lung adenocarcinoma who relapsed after radical surgery, survived for 41 months after multiple treatments.

Clinical management after SCLC transformation

She then received 2 cycles of chemotherapy with "etoposide + carboplatin at q21d" for advanced SCLC from 3 April to 25 April 2021. The comprehensive assessment of the efficacy was "SD" on 30 April 2021. On 8 May 2021, her brain magnetic resonance (MR) examination results suggested the existence of multiple intracranial metastases. After multidisciplinary discussions, she was recommended to accept radiotherapy for brain metastases and to change the systemic chemotherapy regimen. But, considering that intracranial metastases were relatively small and did not cause any brain discomfort, she requested to suspend radiotherapy, and to continue the "etoposide + carboplatin at q21d" chemotherapy, as there was a good control of the extracranial lesions by this regimen. After the 4th and 6th cycles, the comprehensive assessment of the efficacy was "SD". However, later, on 20 October 2021, it turned into "PD", as both intrahepatic and intracranial metastases were found to be larger and more numerous than before and higher levels of hematological tumor markers were tested (proGRP 798.20 pg/mL, CEA 126.7 ng/mL, and NSE 38.37 ng/mL). Therefore she started second-line therapy. From 26 October 2021 to 11 January 2022, four cycles of chemotherapy with "irinotecan at q21d" were selected, and whole-brain radiotherapy was performed during the chemotherapy interval. Radiotherapy was performed using IMRT with the whole brain as the clinical target volume (CTV), an external expansion of 0.3 cm as the planning target volume (PTV)-CTV, and a DT 30Gy/10F. On 16 December 2021, the comprehensive assessment of the efficacy was "SD". However, it became "PD" on 10 February 2022 due to new metastases found in the liver, the right acetabulum, the right sacrum, and the left ilium. She was transferred to the third-line therapy, during which oral targeted therapy with "10 mg of Anlotinib Hydrochloride Capsules at $d_{1\text{-}14}$ and q21d" was selected, and diphosphonate was used to resist bone metastasis as specified. Afterward, the disease kept relatively stable.

The occurence of LC-induced MIAP

On 24 May 2022, she was admitted to our hospital due to a feeling of intermittent abdominal oppressive pain and discomfort, with the main clinical diagnosis of abdominal pain of undeterminded reason, SCLC with mutiple metastases (to the brain, liver, bones, and right supraclavicular and right axillary LNs), and recurrence of left lung adenocarcinoma after surgery. Following positive symptomatic treatment, the symptoms were

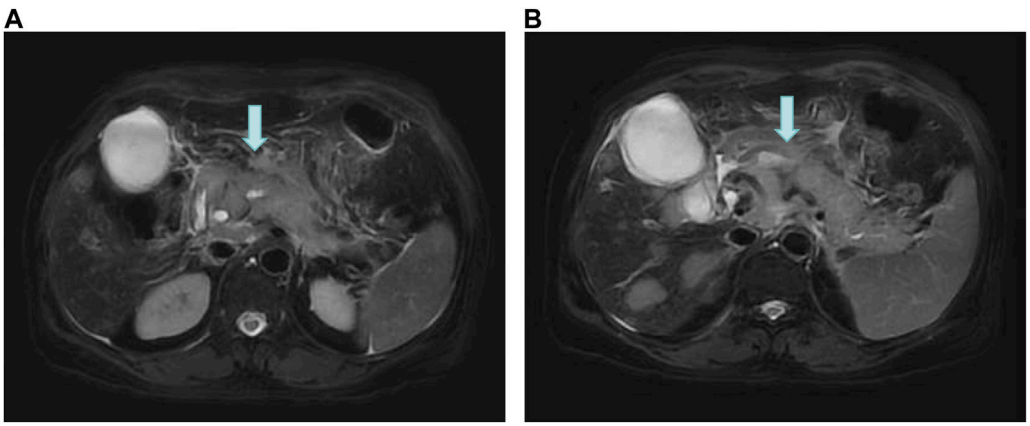


FIGURE 3
MR Examination of the pancreas. **(A)** Pancreatitis with peripheral exudation; **(B)** Multiple malignant tumors (possible metastases) of the pancreas.

slightly improved, and no obvious specific abnormalities were detected in the whole blood routine and biochemical tests. However, the comprehensive assessment of the efficacy was "PD" because of the increased size and number of intrahepatic metastases and higher levels of hematological tumor markers (proGRP 10550 pg/mL, CEA 146.8 ng/mL, and NSE 30.22 ng/mL). Besides, a acute pancreatitis (AP) with undefined cause was also discovered through plain + enhanced MR of the abdomen. On 29 May 2022, the patient's blood amylase was 300 IU/L, the blood lipase was 5,396 U/L, and the urinary amylase was 2,240 IU/L. She was transferred to the Department of Gastroenterology for further diagnosis and treatment.

Treatments mainly for LC-induced MIAP

On 16 June 2022, the blood amylase was 592 IU/L, the blood lipase was 10,809 U/L, the urinary amylase was 10,112 IU/L, and the total bilirubin was 32.5 μmol/L (normal range: 2.0–22.0 μmol/L). Images from plain + enhanced CT of the whole abdomen (Supplementary Figure S1), magnetic resonance cholangiopancreatography (MRCP) and MR examination of pancreas (Figure 3) indicated acute pancreatitis accompanied by possible multiple pancreatic metastases. On 20 June 2022, She was diagnosed with postoperative recurrence of the left lung adenocarcinoma (mutiple metastases in the brain, liver, pancreas, bones, right supraclavicular region LNs, and right axillary fossa LNs), which was subsequently transformed into SCLC complicated with post-treatment LC-induced AP. Based on these observations, it was recommended that a comprehensive antitumor therapy should be carefully selected. On 23 June 2022, her growing blood amylase (874 IU/L), urinary amylase (24,705 IU/L), total bilirubin (150.2 μmol/L), and conjugated bilirubin (108.4 μmol/L, normal range: 0–8.0 μmol/L) indicated the complications of LC-induced MIAP and obstructive jaundice. Considering that inconspicuous intrahepatic bile duct dilatation was not suitable for PTCD surgery at that time, she was recommended to start with palliative radiotherapy for the pancreatic metastasis, followed by an antitumor drug therapy. The patient received five sessions of radiotherapy from 24 June 2022 to 1 July 2022, during which she was regularly treated with oral "imidazolotetrazine alkylating agents, temozolomide and pamiparib." On 26 June 2022, the total blood bilirubin was 129.9 μmol/L, and the conjugated bilirubin was 95.5 μmol/L. On 29 June 2022, the blood amylase was 157 IU/L, and the urinary amylase was 1,322 IU/L. The patient's condition was gradually improving. On 3 July 2022, the blood amylase was 85 IU/L, urinary amylase was 331 IU/L, the blood total bilirubin was 36.5 μmol/L, and the conjugated bilirubin was 24.0 μmol/L. On 4 July 2022, MR Examination of pancreas indicated that pancreatitis accompanied by peripheral exudation, multiple malignant tumors (metastatic tumor possible) of pancreas, smaller than before (Figure 4). On 5 July 2022, she was discharged due to disease improvement. Thereafter, she went to the local hospital for regular hematological examinations, which revealed gradual recovery to normal conditions without significant abnormalities.

On 9 October 2022, the patient was readmitted to our hospital for reexamination and the comprehensive assessment of the efficacy was "PD" due to the enlargement of metastases in liver and LNs and higher hematological tumor markers (proGRP 2165 pg/mL, CEA 926.5 ng/mL, and NSE 118.9 ng/mL). However, there were no specific abnormalities in the blood routine, the liver and kidney functions, and the levels of blood amylase, blood lipase, and urinary amylase. She started to receive the first cycle of chemotherapy with "paclitaxel at q21d" of the fifth-line therapy for SCLC and the first split-course radiotherapy, during which "the right neck + right supraclavicular LNs were selected as the GTV, with an external expansion of 0.5 cm as the PTV-GTV (treated with 5Gy/1F). The whole liver was also set as the GTV, with an external expansion of 0.5 cm as the PTV-CTV (treated with 5Gy/1F)." Besides, the targeted therapy combined with "poly-ADP-ribose-polymerase (PARP) inhibitor, pamiparib" was continued, the patient was discharged due to improvement on 3 November 2022. From 03 April 2021 to 30 November 2022, this patient had been treated for the transformed SCLC for 20 months. Thereafter, she went to the local hospital for further treatments and lost follow-up.

Case discussion

Based on incidence and mortality rates, LC currently ranks top among the malignant tumors worldwide. This cancer seriously

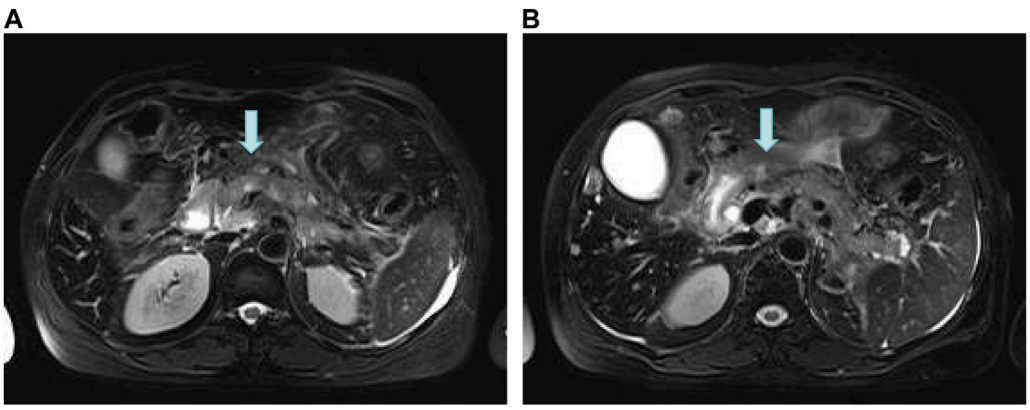


FIGURE 4
MR Examination of the pancreas. **(A)** Pancreatitis accompanied by peripheral exudation; **(B)** Multiple malignant tumors (metastatic tumor possible) of pancreas, smaller than before.

threatens human life and health (Bray et al., 2021). LC can be divided into non-SCLC (NSCLC) and SCLC according to pathological types, of which the former accounts for approximately 85% of diagnosed LCs, which mainly includes adenocarcinoma, squamous cell carcinoma, and large cell cancer. For inoperable driver gene-positive NSCLC, targeted therapy is the preferred strategy, while simple chemotherapy is the cornerstone treatment for NSCLC without driver alterations. Simple chemotherapy can be combined with anti-angiogenic/immunotherapy or radiotherapy (Ettinger et al., 2019). Numerous studies have shown that resistance to first-line antineoplastic drugs for advanced NSCLC mostly occurs at 6–12 months. The resistance to the first use of antineoplastic drugs is known as primary or intrinsic resistance, while resistance that emerges during treatment is known as acquired or secondary resistance (Han et al., 2017). It has been found that the mechanism of chemoresistance is closely related to abnormal activities of multidrug resistance genes and mitochondrial signaling pathways, which involve the effects of multiple factors including chromosome abnormality in tumor cells, reduced intracellular drug accumulation, enhanced DNA damage repair function, strengthened cellular detoxification function, apoptosis inhibition, abnormal vascularization, cytoskeleton abnormality, and abnormal density of extracellular peripheral matrix. However, the specific mechanism of chemoresistance is still unclear and more detailed mechanisms need to be explored. Ferrer et al. (2019) retrospectively analyzed post-treatment clinical data on the transformation of wild-type NSCLC into SCLC in 10 adenocarcinoma patients and 3 squamous carcinoma patients (EGFR) and found that among the SCLCs patients who were treated with second-line therapies on average at the time of pathological transformation, more than 85% received etoposide combined with platinum-based chemotherapy regimens and that the overall survival was approximately 37 months. Previous studies suggested that the treatment pressure of chemotherapy or radiotherapy rarely leads to the transformation of NSCLC to SCLC (Marcoux et al., 2019). In 2006, Zakowski et al. (2006), at the Memorial Sloan-Kettering Cancer Center, first reported a case of a 45-year-old female patient with lung adenocarcinoma who suffered disease progression after EGFR-tyrosine kinase inhibitor (TKI) treatment and chemotherapy, and which biopsy pathology showed synaptophysin-positive SCLC. Since then, SCLC transformation has been gradually recognized, and studies have uncovered that 5%–15% of EGFR-mutated NSCLCs undergo SCLC transformation during the disease evolution. However, studies have also found that SCLC transformation commonly occurs in patients with EGFR-mutated NSCLC progression after TKI treatment, and that SCLC transformation may also occur following antineoplastic drug treatment for fusion mutation of anaplastic lymphoma kinase (ALK), c-ROS proto-oncogene 1 receptor tyrosine kinase (ROS1)-fused adenocarcinoma, EGFR wild-type lung adenocarcinoma, and lung squamous cell carcinoma (Caumont et al., 2016; Sehgal et al., 2020).

In this case, the patient was diagnosed with systemic multiple metastases after lung adenocarcinoma surgery through imaging and pathological puncture biopsy, and received "pemetrexed" and "albumin paclitaxel" chemotherapy as the main second-line therapy. After combination with radiotherapy, the biopsy indicated the occurrence of non-driver gene-positive advanced adenocarcinoma with SCLC transformation, and this was in the absence of targeted therapy using TKI drugs. In the retrospective analysis of Ferrer et al. (2019), SCLC transformation occurred in 13 cases of post-treatment EGFR wild-type NSCLC, which is a more realistic reflection of the clinical diagnosis and treatment, and different molecular features and treatment processes that may lead to a rare transformation, including SCLC. Many studies have argued that the transformation of pathological types may be a true phenotypic transformation, but it may also result from a malignant biological activity of mixed LCs containing both SCLC and adenocarcinoma, during which, the latter transforms into LC, dominated by post-treatment SCLC (Ahmed et al., 2018). Thus, the changing NSCLC types should be alerted during treatment despite the original pathological type, and the objective existence of complexity of LC pathology. Spatial and temporal heterogeneities and clonal subtypes should also be fully considered (Pignataro et al., 2020). Therefore, during clinical management, the dynamic changes of pathological types at the primary lesion, especially at the metastasis, should be considered in the case of rapid progression of advanced NSCLC or failure of multiline therapy during antitumor

drug therapy. Additionally, the time of transformation of blood tumor markers, should also be considered. In this case, the early diagnosis of SCLC transformation was determined relatively early mainly due to the continuous monitoring of NSCLC and SCLC markers' transformations. For example, it was discovered that proGRP is abnormally elevated, which is worth considering for when performing another biopsy in clinical management. To date, most studies have concluded that the treatment of transformed SCLC is similar to that of classic SCLC. In fact, additional in-depth studies and new strategies, should be explored for the diagnosis and treatment of LC transformed pathological types, and stronger clinical trial evidence should be obtained to support relevant clinical decisions (Roca et al., 2017). Meanwhile, it is noteworthy to highlight that TP53 gene mutation, loss of RB gene function, FHIT methylation and other phenotypes, are mostly detectable in SCLC tumor tissue specimens. However, such genetic phenotypes are poor prognostic factors for advanced NSCLC, just like a TP53 non-breaking mutation, and there are no effective targeted therapies (George et al., 2015; Wu et al., 2016; Hayashi et al., 2020). Therefore, more attention should be paid to the potential SCLC transformation in such NSCLC patients. It is also suggested that a timely monitoring of gene mutations for timely adjustment of treatment regimens, should also be an important investigative direction for patients with post-treatment sudden progression.

In this case, the patient was diagnosed with systemic multiple metastases after lung adenocarcinoma surgery through imaging combined with pathological puncture biopsy (October 2017). The patient received "pemetrexed" and "albumin paclitaxel" chemotherapy as the main second-line therapy. After combined radiotherapy, another biopsy was conducted. Approximatively 41 months later, SCLC transformation occurred (March 2021). Thereafter, the patient was diagnosed and treated by reference to the specifications, guidelines, and consensus for the diagnosis and treatment of extensive-disease SCLC for approximatively 21 months. During the process, the patient developed AP in April 2022, which was timely detected with the support of a multidisciplinary team and controlled by scientific diagnosis and treatment strategies. This approach laid a good foundation for further improving the patient's quality of life and prolonging survival. AP is a common disease in gastroenterology, with an incidence of approximatively 13–45/100,000, and that shows a continuously increasing trend. Approximatively 75% of AP cases are caused by cholelithiasis, hyperlipidemia, and alcohol abuse, while other rare causes include surgery, trauma, and drugs with approximatively 10% of idiopathic AP cases (Wu et al., 2017). Metastasis-induced AP (MIAP) is relatively rare and may be the primary or secondary clinical manifestation of a tumor, and therefore, it is often undetected leading to a poor prognosis. AP can be classified as mild AP (MAP), moderately severe AP (MSAP), and severe AP (SAP) according to the 2012 Atlanta criteria (Banks et al., 2013). The incidence rate of pancreatic metastasis in LC patients is low with approximatively 0.12%–7.50%. However, SCLC metastasis to the pancreas in SCLC autopsy reports, is not negligible as it accounts for approximatively 24%–40% (Wood et al., 2018). Studies have found that cases of LC-induced MIAP mostly have atypical symptoms, with mild or no symptoms. A small number of patients with pancreatic metastases manifest abdominal pain, AP, and obstructive jaundice. These patients often miss the timing of anti-lung cancer treatment due to the relative lack of a certain degree of clinical vigilance. The early detection of LC-induced MIAP is more conducive to improving LC prognosis. It has also been shown that patients with LC-induced MIAP are older and more vulnerable to anemia, main pancreatic duct dilatation, and abdominal LN enlargement than those with non-tumor-related AP (Gonlugur et al., 2014; Yamanashi et al., 2015). Xiong et al. (2020) reported that 7 out of 8 patients (87.5%) with LC-induced MIAP have a SCLC pathological type. Tanaka et al. (2009) retrospectively summarized 25 cases of LC-induced MIAP, including 19 (76.0%) cases of SCLC. Maeno et al. (1998) reported that the common pathological type of LC-induced pancreatic metastasis is SCLC, accounting for approximatively 50%, followed by adenocarcinoma (34.6%), squamous cell carcinoma (11.5%), and large cell lung cancer (3.9%). Besides, the proportion of MIAP in SCLC-induced pancreatic metastasis is high, which should be emphasized by clinicians. To date, there are few reports of LC-induced MIAP in both individual and multiple cases. In this case, the patient was diagnosed with the NSCLC transformation into SCLC, namely, SCLC accompanied with MIAP. The diagnosis was mainly confirmed by abdominal CT, MRI and ERCP examinations due to the patient's abdominal pain, and the abnormal increases in blood amylase, blood lipase, and urinary amylase. Moreover, jaundice was gradually worsening, with a maximum level of total bilirubin of 149.2 μmol/L (normal range: 2.0–22.0 μmol/L). The patient's clinical experience of MIAP is consistent with that of the results of related previous studies. It is believed that LC-induced MIAP may have multiple pathogeneses: 1) Mechanical compression of the pancreatic ducts by metastatic tumors or enlarged peripancreatic LNs; 2) Ischemia-induced pancreatic injury due to tumor invasion of blood vessels; and 3) Diffuse tumor infiltration to the pancreas and destruction of the pancreatic lobules. Studies have also observed that patients with LC-induced MIAP are mostly at an advanced stage at the time of detection, generally associated with poor conditions and high risks of surgical resection or puncture biopsy of pancreatic lesions or abdominal occupancies. Besides, such patients are often less willing to have a biopsy, and thus, the metastatic lesions of most these patients are clinically diagnosed by imaging findings (excluding AP induced by other reasons) (Okutur et al., 2015). It was reported that the treatment strategy for LC-induced MIAP mainly favors symptomatic and supporting treatment at the initial stage, and that MAP patients should start chemotherapy and/or radiotherapy as early as possible, to facilitate AP recovery. SAP patients may not be able to tolerate chemotherapy due to their poor physical conditions (Okutur et al., 2015). In this case, the LC patient developed MAP during treatment, which was improved with pharmacological chemotherapy combined with local radiotherapy and without AP recurrence. The patient has a good survival status with an ECOG score of 2 points at the follow-up to date, resulting in a prolonged median survival, compared to the extensive-disease SCLC reported in the National Comprehensive Cancer Network (NCCN) clinical practice guidelines. Of course, after postoperative, the recurrence of the left lung adenocarcinoma that subsequently transformed into SCLC complicated with LC-induced AP, was controlled. Statistics showed that a total of 5 lines of therapy were conducted after SCLC transformation, including chemotherapeutic agents "etoposide, irinotecan, cisplatin, carboplatin, temozolomide, and paclitaxel," targeted agents

"anlotinib (a new small molecule multi-target tyrosine kinase inhibitor), surufatinib (a selective tyrosine kinase inhibitor targeting vascular endothelial receptor (VEGFR) and fibroblast growth factor receptor (FGFR)), and pamiparib (a DNA repair enzyme (PARP) inhibitor)." Furthermore, a split-course radiotherapy, which significantly improved the patients' quality of life and prolonged her survival, was also performed (Nyquist et al., 2020). In conclusion, the clinical symptoms of LC-induced MIAP are not specific, and the clinical types are mainly MAP, with poor prognosis, but an early diagnosis and a timely treatment may greatly improve the prognosis. For elderly patients, emaciation, or manifestation of other affected systems, anemia, main pancreatic duct dilatation, pancreatic occupancy and abdominal LN enlargement, are important clues for the diagnosis of LC-induced MIAP that require in clinical treatment.

The currently available clinical evidence indicates that SCLC has a shorter survival and fewer therapeutic options than NSCLC. As clinical studies have progressed, the transformation of SCLC pathological types is not uncommon under the pressure of therapeutic selection. Such pressure is not only attributed to the application of EGFR-TKI, but also involves that induced by chemotherapy. Moreover, whether the combination of anti-angiogenic, radiotherapy, immunotherapy, and surgery leads to the transformation of SCLC pathological types, needs to be confirmed by more relevant clinical studies. With the improvement of clinical practice skills and the rapid development of tumor molecular biology, the awareness of re-biopsy and dynamic genetic testing should be enhanced in the whole process of NSCLC multidisciplinary management of NSCLC to formulate the best treatment strategy for patients with greater precision (Zhu et al., 2019). Of course, for complications that are still relatively uncommon and rare, it is necessary to pay a high attention to the thought, and a timely and early detection, and a correct and active management. Additionally, attention should be paid to prevention in the clinical practice of overall tumor treatment. In conclusion, there is still a long way to go in investigating the molecular mechanisms of the occurrence and development of rare and uncommon complications during the diagnosis and treatment of the transformation of NSCLC into SCLC that requires more effective treatment strategies.

Data availability statement

The raw data supporting the conclusion of this article will be made available by the authors, without undue reservation.

Ethics statement

The studies involving humans were approved by Medical Ethics Committees of Fujian Medical University Union Hospital. The studies were conducted in accordance with the local legislation and institutional requirements. The participants provided their written informed consent to participate in this study. Written informed consent was obtained from the individual(s) for the publication of any potentially identifiable images or data included in this article.

Author contributions

SZ: Data curation, Writing–original draft. NG: Data curation, Writing–original draft. QZ: Data curation, Writing–original draft. YW: Data curation, Writing review and editing. SY: Funding acquisition, Supervision, Writing review and editing. XC: Funding acquisition, Supervision, Writing review and editing.

Funding

The authors declare financial support was received for the research, authorship, and/or publication of this article. This study was supported by the Fujian Provincial Health Technology Project (2020CXB016); the Joint Funds for the innovation of science and Technology, Fujian province (2020Y9090).

Acknowledgments

The authors would like to express their gratitude to EditSprings (https://www.editsprings.cn) for the expert linguistic services provided.

Conflict of interest

The authors declare that the research was conducted in the absence of any commercial or financial relationships that could be construed as a potential conflict of interest.

Publisher's note

All claims expressed in this article are solely those of the authors and do not necessarily represent those of their affiliated organizations, or those of the publisher, the editors and the reviewers. Any product that may be evaluated in this article, or claim that may be made by its manufacturer, is not guaranteed or endorsed by the publisher.

Supplementary material

The Supplementary Material for this article can be found online at: https://www.frontiersin.org/articles/10.3389/fphar.2023.1259221/full#supplementary-material

References

Ahmed, T., Vial, M. R., Ost, D., Stewart, J., Hasan, M. A., and Grosu, H. B. (2018). Non-small cell lung cancer transdifferentiation into small cell lung cancer: a case series. *Lung Cancer* 122, 220–223. doi:10.1016/j.lungcan.2018.06.024

Banks, P. A., Bollen, T. L., Dervenis, C., Gooszen, H. G., Johnson, C. D., Sarr, M. G., et al. (2013). Classification of acute pancreatitis—2012: revision of the Atlanta classification and definitions by international consensus. *Gut* 62 (1), 102–111. doi:10.1136/gutjnl-2012-302779

Bray, F., Laversanne, M., Weiderpass, E., and Soerjomataram, I. (2021). The ever-increasing importance of cancer as a leading cause of premature death worldwide. *Cancer* 127 (16), 3029–3030. doi:10.1002/cncr.33587

Caumont, C., Veillon, R., Gros, A., Laharanne, E., Bégueret, H., and Merlio, J.-P. (2016). Neuroendocrine phenotype as an acquired resistance mechanism in ALK-rearranged lung adenocarcinoma. *Lung Cancer* 92, 15–18. doi:10.1016/j.lungcan.2015.12.001

Ettinger, D. S., Wood, D. E., Aggarwal, C., Aisner, D. L., Akerley, W., Bauman, J. R., et al. (2019). NCCN guidelines insights: non-small cell lung cancer, version 1.2020. *J. Natl. Compr. Cancer Netw.* 17 (12), 1464–1472. doi:10.6004/jnccn.2019.0059

Ferrer, L., Levra, M. G., Brevet, M., Antoine, M., Mazieres, J., Rossi, G., et al. (2019). A brief report of transformation from NSCLC to SCLC: molecular and therapeutic characteristics. *J. Thorac. Oncol.* 14 (1), 130–134. doi:10.1016/j.jtho.2018.08.2028

George, J., Lim, J. S., Jang, S. J., Cun, Y., Ozretić, L., Kong, G., et al. (2015). Comprehensive genomic profiles of small cell lung cancer. *Nature* 524 (7563), 47–53. doi:10.1038/nature14664

Gonlugur, U., Mirici, A., and Karaayvaz, M. (2014). Pancreatic involvement in small cell lung cancer. *Radiology Oncol.* 48 (1), 11–19. doi:10.2478/raon-2013-0022

Han, B., Jin, B., Chu, T., Niu, Y., Dong, Y., Xu, J., et al. (2017). Combination of chemotherapy and gefitinib as first-line treatment for patients with advanced lung adenocarcinoma and sensitive EGFR mutations: a randomized controlled trial. *Int. J. cancer* 141 (6), 1249–1256. doi:10.1002/ijc.30806

Hayashi, T., Takamochi, K., Kohsaka, S., Kishikawa, S., Suehara, Y., Takahashi, F., et al. (2020). Transformation from EGFR/PTEN co-mutated lung adenocarcinoma to small cell carcinoma in lymph node metastasis. *Pathol. Int.* 70 (5), 295–299. doi:10.1111/pin.12919

Maeno, T., Satoh, H., Ishikawa, H., Yamashita, Y., Naito, T., Fujiwara, M., et al. (1998). Patterns of pancreatic metastasis from lung cancer. *Anticancer Res.* 18 (4B), 2881–2884.

Marcoux, N., Gettinger, S. N., O'Kane, G., Arbour, K. C., Neal, J. W., Husain, H., et al. (2019). EGFR-mutant adenocarcinomas that transform to small-cell lung cancer and other neuroendocrine carcinomas: clinical outcomes. *J. Clin. Oncol.* 37 (4), 278–285. doi:10.1200/JCO.18.01585

Nyquist, M. D., Corella, A., Coleman, I., De Sarkar, N., Kaipainen, A., Ha, G., et al. (2020). Combined TP53 and RB1 loss promotes prostate cancer resistance to a spectrum of therapeutics and confers vulnerability to replication stress. *Cell Rep.* 31 (8), 107669. doi:10.1016/j.celrep.2020.107669

Okutur, K., Bozkurt, M., Korkmaz, T., Karaaslan, E., Guner, L., Goksel, S., et al. (2015). Metastasis-induced acute pancreatitis successfully treated with chemotherapy and radiotherapy in a patient with small cell lung cancer. *Case Rep. Oncol. Med.* 2015, 304279. doi:10.1155/2015/304279

Pignataro, D., Bertaglia, V., Bironzo, P., Olmetto, E., Pisano, C., Napoli, V. M., et al. (2020). Oligoprogressive disease with SCLC transformation in EGFR-mutated NSCLC: how biology knowledge can change the game rules. *J. Thorac. Oncol.* 15 (10), e170–e172. doi:10.1016/j.jtho.2020.06.020

Roca, E., Gurizzan, C., Amoroso, V., Vermi, W., Ferrari, V., and Berruti, A. (2017). Outcome of patients with lung adenocarcinoma with transformation to small-cell lung cancer following tyrosine kinase inhibitors treatment: a systematic review and pooled analysis. *Cancer Treat. Rev.* 59, 117–122. doi:10.1016/j.ctrv.2017.07.007

Sehgal, K., Varkaris, A., Viray, H., VanderLaan, P. A., Rangachari, D., and Costa, D. B. (2020). Small cell transformation of non-small cell lung cancer on immune checkpoint inhibitors: uncommon or under-recognized? *J. Immunother. cancer* 8 (1), e000697. doi:10.1136/jitc-2020-000697

Tanaka, H., Nakazawa, T., Yoshida, M., Miyabe, K., Okumura, F., Naitoh, I., et al. (2009). Metastasis-induced acute pancreatitis in a patient with small cell carcinoma of the lungs. *JOP* 10 (5), 557–561.

Wood, D. E., Kazerooni, E. A., Baum, S. L., Eapen, G. A., Ettinger, D. S., Hou, L., et al. (2018). Lung cancer screening, version 3.2018, NCCN clinical practice guidelines in oncology. *J. Natl. Compr. Cancer Netw.* 16 (4), 412–441. doi:10.6004/jnccn.2018.0020

Wu, D., Tang, M., Zhao, Y., Zhou, S., Xu, X., Wang, F., et al. (2017). Impact of seasons and festivals on the onset of acute pancreatitis in Shanghai, China. *Pancreas* 46 (4), 496–503. doi:10.1097/MPA.0000000000000795

Wu, X., Wu, G., Yao, X., Hou, G., and Jiang, F. (2016). The clinicopathological significance and ethnic difference of FHIT hypermethylation in non-small-cell lung carcinoma: a meta-analysis and literature review. *Drug Des. Dev. Ther.* 10, 699–709. doi:10.2147/DDDT.S85253

Xiong, Y., Xu, Y., Zhao, Y., Sun, H., Bai, X., Wu, D., et al. (2020). Clinical characteristics of metastasis-induced acute pancreatitis in patients with lung cancer. *Zhonghua yi xue za zhi* 100 (6), 442–446. doi:10.3760/cma.j.issn.0376-2491.2020.06.009

Yamanashi, K., Marumo, S., Saitoh, M., and Kato, M. (2015). A case of metastasis-induced acute pancreatitis in a patient with small cell lung cancer. *Clin. Case Rep.* 3 (2), 96–98. doi:10.1002/ccr3.163

Zakowski, M. F., Ladanyi, M., Kris, M. G., and Memorial Sloan-Kettering Cancer Center Lung Cancer OncoGenome Group (2006). EGFR mutations in small-cell lung cancers in patients who have never smoked. *N. Engl. J. Med.* 355 (2), 213–215. doi:10.1056/NEJMc053610

Zhu, K., Li, Q., Zhang, S., Wu, G., Xiang, Q., Fang, Z., et al. (2019). Rebiopsy in patients with or without prior TKIs revealed complicated histology of lung cancer. *Am. Soc. Clin. Oncol.* 37, e20525. doi:10.1200/jco.2019.37.15_suppl.e20525

frontiers | Frontiers in Immunology

TYPE Review
PUBLISHED 15 November 2023
DOI 10.3389/fimmu.2023.1277243

Check for updates

OPEN ACCESS

EDITED BY
Qun Xue,
Affiliated Hospital of Nantong University, China

REVIEWED BY
Chengming Li,
Shandong University, China
Ling Bi,
Shanghai University of Traditional Chinese Medicine, China

*CORRESPONDENCE
Zhengtao Qian
467524118@qq.com
Qinglin Zhang
zhang517068@126.com

†These authors have contributed equally to this work

RECEIVED 14 August 2023
ACCEPTED 30 October 2023
PUBLISHED 15 November 2023

CITATION
Miao K, Liu W, Xu J, Qian Z and Zhang Q (2023) Harnessing the power of traditional Chinese medicine monomers and compound prescriptions to boost cancer immunotherapy.
Front. Immunol. 14:1277243.
doi: 10.3389/fimmu.2023.1277243

COPYRIGHT
© 2023 Miao, Liu, Xu, Qian and Zhang. This is an open-access article distributed under the terms of the Creative Commons Attribution License (CC BY). The use, distribution or reproduction in other forums is permitted, provided the original author(s) and the copyright owner(s) are credited and that the original publication in this journal is cited, in accordance with accepted academic practice. No use, distribution or reproduction is permitted which does not comply with these terms.

Harnessing the power of traditional Chinese medicine monomers and compound prescriptions to boost cancer immunotherapy

Keyan Miao[1†], Weici Liu[2†], Jingtong Xu[3], Zhengtao Qian[4*] and Qinglin Zhang[5*]

[1]Medical College, Soochow University, Suzhou, Jiangsu, China, [2]Department of Thoracic Surgery, The Affiliated Wuxi People's Hospital of Nanjing Medical University, Wuxi People's Hospital, Wuxi Medical Center, Nanjing Medical University, Wuxi, Jiangsu, China, [3]The First School of Clinical Medicine, Nanjing Medical University. Nanjing, Jiangsu, China, [4]Department of Clinical Laboratory, Changshu Medicine Examination Institute, Changshu, Jiangsu, China, [5]Department of Gastroenterology, The Affiliated Wuxi People's Hospital of Nanjing Medical University, Wuxi People's Hospital, Wuxi Medical Center, Nanjing Medical University, Wuxi, Jiangsu, China

At present, cancer is the largest culprit that endangers human health. The current treatment options for cancer mainly include surgical resection, adjuvant radiotherapy and chemotherapy, but their therapeutic effects and long-term prognosis are unsatisfactory. Immunotherapy is an emerging therapy that has completely transformed the therapeutic landscape of advanced cancers, and has tried to occupy a place in the neoadjuvant therapy of resectable tumors. However, not all patients respond to immunotherapy due to the immunological and molecular features of the tumors. Traditional Chinese Medicine (TCM) provides a new perspective for cancer treatment and is considered to have the potential as promising anti-tumor drugs considering its immunoregulatory properties. This review concludes commonly used TCM monomers and compounds from the perspective of immune regulatory pathways, aiming to clearly introduce the basic mechanisms of TCM in boosting cancer immunotherapy and mechanisms of several common TCM. In addition, we also summarized closed and ongoing trials and presented prospects for future development. Due to the significant role of immunotherapy in the treatment of non-small cell lung cancer (NSCLC), TCM combined with immunotherapy should be emphasized in NSCLC.

KEYWORDS

traditional Chinese medicine, natural products, tumor immunity, cancer immunotherapy, immunomodulators, cytokines

Highlights

- TCM is a promising cancer treatment with three primary advantages including fewer side effects, personalized treatment, and potential immune system benefits.
- TCM exerts an effect on tumor immunity through multiple modalities of regulation.
- The pertinent studies and mechanisms of several commonly utilized TCM active ingredients were preliminarily reported and unconcealed.
- Immunotherapy in combination with TCM selectively targets cancer cells for suppression, leaving normal cells unharmed.

1 Introduction

Due to its profound impact on public health, the malignant tumor has emerged as a pressing concern in society, characterized by substantial morbidity and mortality rates (1). Presently, surgery and chemotherapy stand as the primary modalities for cancer treatment (2). Despite decades of dedicated research efforts towards unearthing more efficacious approaches, the global incidence of malignant tumors continues to remain alarmingly high. The intricate and heterogeneous nature of tumors has prompted a paradigm shift in cancer management, transitioning from a singular target approach to a multifaceted strategy that encompasses the tumor microenvironment (TME) (2–4).

Tumor immunotherapy, which refers to a type of cancer therapies that aims to harness the natural ability of the immune system to identify and finally eliminate tumor cells, seems to display a promising future as a potential therapeutic option for various kinds of tumors (5, 6). This approach involves the application of various therapeutic agents and strategies that modulate or enhance immune responses against cancer, including agents that activate immune cells such as T cells, antibodies that target specific cancer cells, and cellular therapies that involve the transfer of genetically engineered T cells or other immune cells into cancer patients (7, 8). Unlike traditional cancer therapies such as chemotherapy and radiation, which target both cancerous and normal cells, tumor immunotherapy has an edge of selectively targeting and eliminating cancer cells and minimizing damage to normal tissues. Current drugs have a therapeutic effect on cancer in the short term, but their major side effects can cause serious physical and mental problems for patients. Therefore, there is an urgent need to explore new therapeutic methods that have definite efficacy and mild adverse effects and can be taken for a long time.

For centuries, TCM has been employed as a therapeutic approach for various ailments, with cancer included, boasting a track record of safety, gentleness, and prolonged efficacy (9, 10). TCM adopts a holistic perspective, considering tumors as systemic diseases where treatment should encompass the entire body rather than solely focusing on localized areas. Approaches limited to local therapies often fail to provide comprehensive clinical benefits to cancer patients, thereby contributing to the underlying factors responsible for tumor recurrence and metastasis even after surgical interventions, chemotherapy, or targeted therapies. The advantages of TCM in the tumor immunotherapy can be summarized into three aspects——fewer side effects, personalized treatment, and potential immune system benefits (11–13). Chinese herbal therapy typically takes advantage of natural substances that are less toxic and have fewer side effects compared to chemoradiotherapy drugs (11). Chemoradiotherapy can cause side effects such as nausea, vomiting, hair loss, and fatigue, whereas Chinese herbal therapy is generally well-tolerated and can improve quality of life (12, 13). Chinese herbal therapy is tailored to the individual patient's needs and can be adjusted based on their response to treatment. Chemoradiotherapy, on the other hand, is a standardized treatment that is prescribed based on the type and stage of cancer, and may not consider the individual differences in patients' overall health or response to treatment. Chinese herbal therapy can enhance the body's natural immune system, which can effectively detect and eliminate cancer cells and prevent recurrence. Chemoradiotherapy can weaken the immune system, making the patient more vulnerable to infections and other complications (14, 15). Overall, while there is still much to learn about the potential of TCM for the treatment of tumor, research to date suggests that it may have a role to play in improving outcomes for cancer patients (12, 15).

Currently, research on immunotherapy methods is underway, however, the investigation of possible targets from the perspective of TCM is still in its infancy. Considering this, it is desperately demanded to explore the potential and development direction of TCM as an immunotherapy approach. We will discuss the specific monomers and compounds found in TCM that have been identified to have potential in boosting cancer immunotherapy, as well as the mechanisms by which they work. We will also explore the results of clinical studies that have investigated the application of TCM in combination with cancer immunotherapy, as well as the obstacles and future directions for research in this field.

2 The regulatory effects of TCM monomers and compounds on TME

Immunomodulation means the ability of a substance to modify and regulate the immune response, either by enhancing or

Abbreviations: TME, tumor microenvironment; TCM, Traditional Chinese Medicine; NF-kB, nuclear factor-kappa B; IL, interleukin; TNF-α, tumor necrosis factor-alpha; MDSC, myeloid-derived suppressor cell; PSP, pupa polysaccharide; LPS, lipopolysaccharide; ConA, concanavalin A; GSBXD, Gansui-Banxia Decoction; TAM, tumor-associated macrophage; XSD, Xiaoshui decoction; DC, endritic cell; SND, Sini decoction; VEGF, vascular endothelial growth factor; MMP, matrix metalloproteinase; TRPM8, transient receptor potential melastatin subtype 8; TRPV1, transient receptor potential vanilloid 1; ECM, extracellular matrix; GQD, Gegen Qinlian decoction; BBR, Berberine; Treg, regulatory T cell; NSCLC, non-small cell lung cancer; NCT, national clinical trial; ERS, reticulum stress; EMT, epithelial-mesenchymal transition; *PNS, Panax notoginseng Saponins;* FAK, focal adhesion kinase; CAR, chimeric antigen receptor.

suppressing it. Chinese herbal medicine has been uncovered to have both immunostimulatory and immunosuppressive effects, depending on the specific herbs and the context in which they are applied (16–18). The immunoregulatory effects of Chinese medicine include the stimulation of immune cell activity, regulation of cytokine production, inhibition of inflammation, antioxidant activity, modulation of immune cell signaling pathways, etc (16, 19–21). TCM monomers such as baicalin, quercetin, and resveratrol have been reported to modulate the production of cytokines by regulating immune cells (22–25). These monomers can either enhance or suppress cytokine production, relying on the specific immune cells and the specific environment in which they are distributed (26). TCM monomers such as curcumin and berberine have been discovered to have anti-inflammatory effects through suppressing the production of pro-inflammatory cytokines and inhibiting the activation of immune cells such as macrophages. TCM monomers can regulate a variety of signaling pathways involved in immune cell activation and function. For instance, curcumin has been revealed to inhibit the nuclear factor-kappa B (NF-kB) signaling pathway, which plays a crucial role in regulating immune cell activity and inflammation (27, 28). Subsequently, this review expounds upon the potentiality of TCM in the realm of tumor immunotherapy, elucidating the prevailing clinical advancements in the manipulation via immune cells, modulation of cytokine signaling, angiogenesis and vascular normalization, extracellular matrix remodeling, inflammatory and immune responses, targeting immune checkpoints, and the modulation of immunosuppression and immune escape, respectively (Figure 1).

2.1 Modulation of immune cells

Tumor biological behaviors as a hot research topic have long been being investigated, including tumor initiation, progression, invasion, intravasation, dissemination, extravasation, dormancy, activation, and colonization. Immune cells matter a lot in affecting a series of tumor biological behaviors. Recently, TCMs have been reported to inhibit tumor biological behaviors via regulating immune cells. Relevant studies are introduced as follows and summarized in Table 1 (29–46), and an elaborated graph is presented in the form of Taiji to demonstrate the interactions and relationships among tumor cells, immune cells and TCMs (Figure 2).

2.1.1 T cells

T cells are a type of leukocytes that play an essential role in the immune system. T cells are responsible for recognizing and attacking foreign pathogens such as viruses, bacteria, and parasites, as well as abnormal or cancerous cells in the body (47). Based on their functions and surface markers, T cells can be categorized into various types, including helper T cells, cytotoxic T cells, regulatory T cells and memory T cells (48). TCM can intervene with T cell activity through various mechanisms. For instance, acidic polysaccharides in ginseng can induce the production of Th1 cells and macrophages, thus synergizing with recombinant interleukin-2 (rIL-2) to generate lymphokine-activated killer cells, potentially contributing to its anti-tumor mechanisms (49). Takei et al. discovered that ginsenosides can promote the transformation of initial T cells into typical Th1 cells, leading to the production of substantial amounts of IFN-γ and IL-4 (50). Additionally, research has indicated that baicalin may achieve the suppression of Th17 cells by reducing RORγt expression, upregulating Foxp3, and decreasing IL-17 expression. Moreover, baicalin can inhibit Th17 cell differentiation through reducing RORγt expression (51). Hence, baicalin holds promise as a therapeutic agent for Th17 cell-mediated diseases. In the tumor microenvironment, immunosuppressive factors secreted by tumor cells lead to increased frequency of CD4+Foxp3+ Tregs and MDSCs, which creates an immunosuppressive environment that reduces CD8 activity. By modulating the immunosuppressive state, Chinese herbal medicine fosters increased CD8+ T cell infiltration while exerting immunomodulatory effects on the tumor microenvironment, ultimately impeding tumor growth (18). For example, ginseng polysaccharide has demonstrated the ability to elevate interleukin-2 (IL-2), interleukin-8 (IL-8), and tumor necrosis factor-alpha (TNF-α) levels, activating Th1 cell-mediated anti-infection immune responses and enhancing immune regulation in the body (29). A meta-analysis has also shown that combining ginsenoside Rg3 with chemotherapy leads to increased peripheral blood T lymphocyte subsets, including CD3, CD4, CD8, and CD4/CD8, in non-small cell lung cancer (NSCLC) patients compared to chemotherapy alone, indicating improved immune system function in these patients (30). Moreover, a study by Liu at al. highlighted the immunomodulatory efficacy of the renowned TCM prescription, Bu-Zhong-Yi-Qi-Tang (BZYQT), which stimulates the production of several cytokines, including IL-2, IL-4, IL-5, and IFN-γ, from T lymphocytes (31). Furthermore, the Quxie capsule has shown its potential to impede intestinal tumorigenesis through the downregulation of pro-inflammatory cytokine expression and the reduction in the proportion of myeloid-derived suppressor cells (MDSCs), while concurrently increasing the fraction of CD8+ T cells within colon tumors (32). Hence, it can be inferred that individual constituents and compounds derived from TCM have the potential to modulate T cell immune function through diverse mechanisms, ultimately manifesting anti-tumor effects.

2.1.2 B cells

B cells, a type of leukocytes, play a crucial role in the immune system by producing antibodies, which are proteins that aid in defending the body against infections. When a foreign pathogen enters the body, B cells recognize the pathogen's unique antigens and produce antibodies that specifically target and neutralize the pathogen. Also, they are involved in the process of immunological memory, thus being essential for long-term immunity against many infectious diseases. Ginseng, a commonly used Chinese medicine, is believed to possess diverse pharmacological activities, including potential anti-tumor effects. Studies have indicated that ginseng can enhance B cell activity, promote antibody production, and enhance

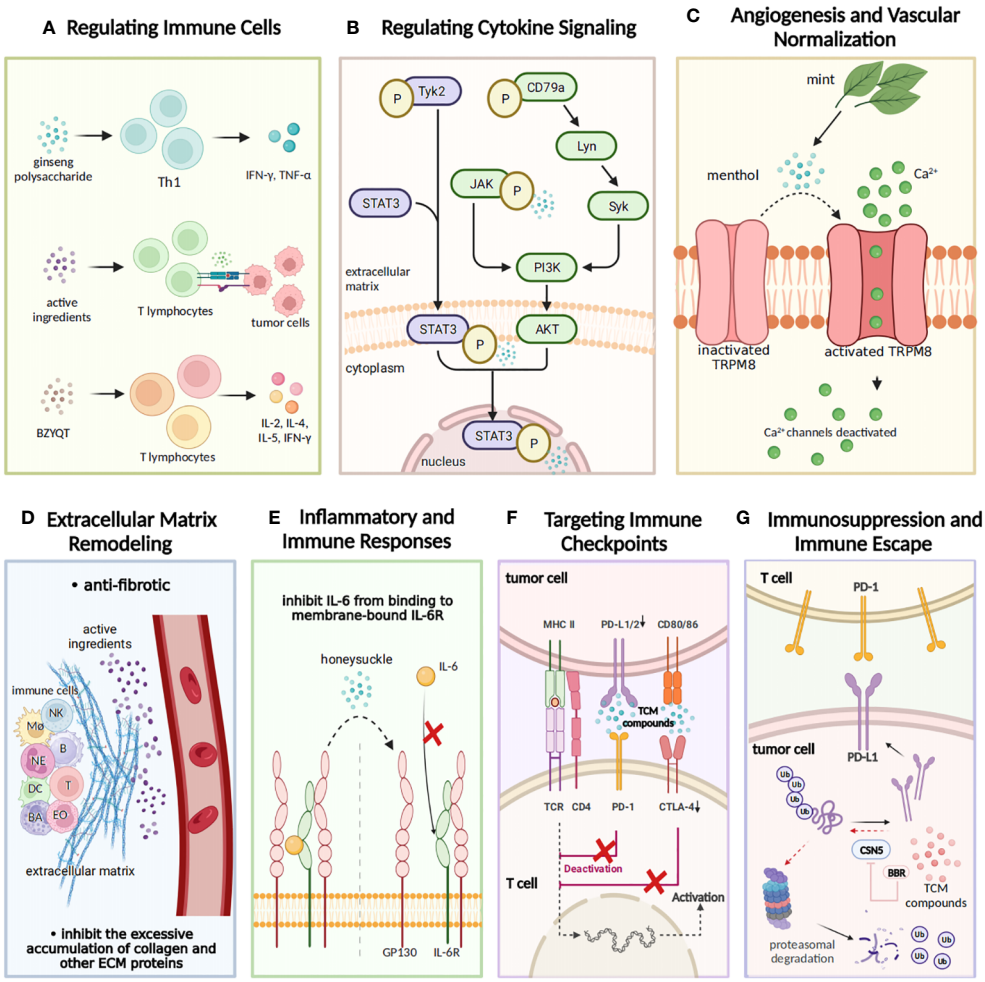


FIGURE 1
The regulatory effects of TCM on tumor immunity. TCM exerts a regulatory influence on tumor immunity from seven aspects. **(A)** Regulating immune cells: TCM exhibits immunomodulatory properties by elevating levels of IL-2, IL-8, and TNF-α and facilitating the recognition and binding of T lymphocytes to tumor cells. The TCM prescription Bu-Zhong-Yi-Qi-Tang (BZYQT) stimulates cytokine production from T lymphocytes including IL-2, IL-4, IL-5, and IFN-γ, thus demonstrating its immunomodulatory efficacy. **(B)** Modulating cytokine signaling: Gansui-Banxia Decoction (GSBXD), a classic TCM formula, exerts anti-tumor immune activity by downregulating AKT/STAT3/ERK signaling pathways and suppressing IL-1β and IFN-γ. **(C)** Angiogenesis and vascular normalization: Menthol activates angiogenesis by promoting the opening of TRPM8 ion channels and facilitating calcium ion flow. **(D)** Remodeling of extracellular matrix: TCM compounds regulate the intricate processes of extracellular matrix (ECM) remodeling, including degradation and deposition of ECM components. Additionally, they effectively inhibit excessive accumulation of collagen and other ECM proteins. **(E)** Inflammatory and immune responses: Honeysuckle inhibits the binding of IL-6 to membrane-bound IL-6R, thereby impeding tumor initiation and progression. **(F)** Targeting immune checkpoints: TCM compounds disrupt the binding of programmed cell death ligand 1 (PD-L1) and programmed cell death protein 1 (PD-1), impacting their inhibitory effect and promoting normal immune function. **(G)** Immunosuppression and immune escape: TCM compounds inhibit the expression of immune checkpoint molecules, such as PD-1 and cytotoxic T-lymphocyte associated protein 4 (CTLA-4), hence restoring immune cell functionality and facilitating robust tumor immune responses.

the function of the immune system (33). Shi et al. unearthed the remarkable potential of gambogic acid, a flavonoid compound extracted from the resin of the *Garcinia hanburyi*, in inducing growth inhibition and apoptosis in activated B-cell-like diffuse large B-cell lymphoma (DLBCL) tumor cells, both *in vitro* and *in vivo* (34). Similarly, Kim et al. unveiled the immune-enhancing capabilities of *Angelica gigas* polysaccharides, which not only boost B-cell immunogenicity but also directly hamper tumor cell adhesion, thereby restraining tumor growth and metastasis (35). Although there are some studies supporting the relevance of TCM to the B cell-related pathway, these studies are still preliminary and more research is demanded to validate and further explore the mechanisms of action of TCM in the anti-tumor field.

2.1.3 Natural killer cells

NK cells are important non-specific immune cells in the body. In the presence of tumor or virus-specific IgG antibodies, NK cells can specifically recognize and eliminate target cells bound to these IgG antibodies. Activated NK cells can also secrete cytokines such as IFN-γ, IL-2 and TNF to play an immunomodulatory role. Wang et al. reported that ginseng polysaccharide can effectively enhance the activation of NK92-MI cells, which then leads to the upregulation of receptors such as NKp30, NKp44, and NKp46, consequently improving the killing ability of NK92-MI cells by increasing the expression of key mediators like perforin and granzyme B (36). Furthermore, *Astragalus membranaceus* exhibits anti-tumor effects by upregulating IL-17D expression and inducing the aggregation of

TABLE 1 mmunological intervention of TCM monomers and compound prescriptions on different cell types.

Cell Type	Medicine	Mechanism	Reference
T cell	Ginseng polysaccharide	Th1 cell-mediated anti-infection immune responses	(29)
	Ginsenoside Rg3	Increasing peripheral blood T lymphocyte subsets	(30)
	Bu-Zhong-Yi-Qi-Tang	Stimulating cytokines	(31)
	Quxie capsule	Increasing the fraction of CD8+ T cells	(32)
B cell	Ginseng	Enhancing B cell activity	(33)
	Gambogic acid	Inducing growth inhibition	(34)
	Angelica gigas polysaccharide	Boosting B cell immunogenicity	(35)
Natural killer cell	Ginseng	Enhancing NK92-MI cells activation	(36)
	Astragalus membranaceus	Upregulating IL-17D expression & inducing the aggregation of NK cells aggregation	(37)
	Sijunzi Tang	Decreasing PD-1/PD-L1 expression	(38)
	Gansui-Banxia Decoction	AKT/STAT3/ERK signaling pathway	(39)
Macrophage	Shuangshen Granule	Decreased TAMs & mTOR signalling inhibition	(40)
	Safflower polysaccharide	Through notch1 signaling pathway	(41, 42)
	Baicalin	Reducing M1-type polarization	(43)
	Angelica root	Inhibiting Stat3 phosphorylation	(44)
	Xiaoshui decoction	Enhancement of autophagy	(45)
Dendritic cell	Plantain	Triggering toll-like receptor 4	(46)

NK cells in the lung, which plays a vital role in the therapeutic approach for lung cancer (37). The efficacy of Sijunzi Tang, a classic TCM prescription, in impeding the proliferation of colon cancer cells has been substantiated through its ability to decrease the expression of PD-1/PD-L1 while augmenting the activity of NK cells (38). As reported by Feng et al., Gansui-Banxia Decoction (GSBXD) was observed to elevate the proportion of CD3- NK1.1+ NK cells, demonstrating its immunomodulatory potential by inhibiting the AKT/STAT3/ERK signaling pathway and suppressing IL-1β and IFN-γ (39). From the researches above, we can infer that TCM active compounds have a relatively close relationship with the activation of NK cells, then stimulating the natural immune system.

2.1.4 Macrophages

Macrophages are multifunctional non-specific immune cells capable of phagocytosis and destruction of foreign bodies and self-dying cells. In the investigation involving K-Ras G12D spontaneous lung cancer model mice and Lewis lung cancer mice, the intervention of Shuangshen Granule (a combination of *Panax quinquefolius L*, *Cordyceps sinensis*, and *Panax notoginseng*) resulted in a notable reduction in subcutaneous tumor volume and a remarkable decrease in the proportion of F4/80+CD206+ tumor-associated macrophages (TAMs) (40). Further analyses on the genetic level also suggested the effects of Shuangshen Granule on immune microenvironment of lung cancer by modulating bone marrow differentiation through mTOR signalling inhibition (40). A study by Zhang et al. uncovered that safflower polysaccharide induced the polarization of macrophages to M1-type by activating the Notch1 signaling pathway to inhibit the invasion and metastasis of melanocytes (41). Similarly, Ando et al. observed that safflower polysaccharide induced the production of molecules associated with M1-type macrophage polarization in peritoneal macrophages of mice (42). Another study confirmed that baicalin could mitigate acute lung injury in mice by reducing M1-type polarization of U937 macrophages through the inhibition of HMGB-1 (23). Additionally, Angelica polysaccharide was found to suppress tumor metastasis by inhibiting Stat3 phosphorylation in macrophages and preventing their polarization toward the M2 phenotype (43). The TCM compound prescription, Xiaoshui decoction (XSD), has been documented to exhibit a notable capacity in stimulating the proliferation of M1 macrophages and diminishing the presence of M2 macrophages through the enhancement of autophagy. These findings signify the potential of XSD as a promising and innovative therapeutic option for integrated approaches targeting malignant pleural effusion (44). Accordingly, TCM can enhance immune activity by enhancing phagocytosis and killing of macrophages, thus playing the anti-tumor role.

2.1.5 Dendritic cells

Dendritic cells (DCs) act as messengers between the innate and adaptive immune systems. They recognize and capture foreign antigens, such as bacteria, viruses, and tumor cells, and then present them to other immune cells, such as T cells and B cells (16, 45). Moreover, they help prevent the immune system from attacking the body's own normal cells by presenting self-antigens to immune cells in a way that they do not stimulate an immune response (52). Studies have found that plantain, a perennial plant, plays a positive role in defending against viruses, inhibiting tumor cell proliferation, and enhancing immune function. In addition to whole Psyllium, the polysaccharide extracted from *Psyllium* is also one of the active components of immune regulation (46). Studies have revealed that the PLP-2 polysaccharide derived from *Plantago asiatica L.* can promote the phenotypic and functional maturation of dendritic cells and PLP-2 may activate the MAPK and NF-κB pathway by triggering toll-like receptor 4 on DCs (53, 54).

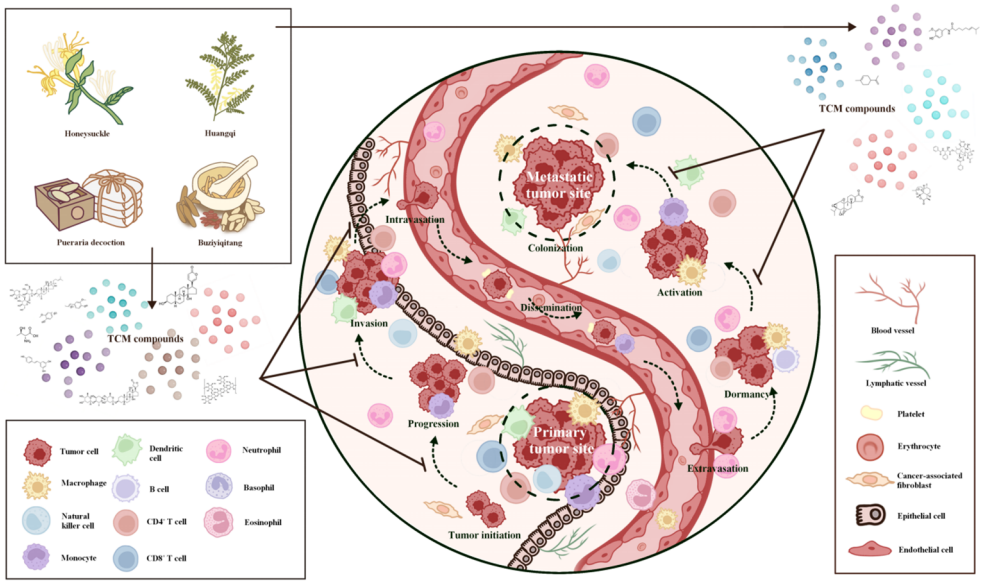


FIGURE 2
Inhibition of primary and metastatic tumor sites by virtue of traditional Chinese medicine-insights into its therapeutic potential. (Presented in the form of Taiji). TCM demonstrates a multifaceted impact on the suppression of primary and metastatic tumor sites. TCM restrains the growth and expansion of primary tumor cells by regulating cellular proliferation and apoptosis, impeding angiogenesis, and inhibiting tumor-promoting factors. Through its intricate network of bioactive compounds, TCM disrupts key signaling pathways implicated in tumor growth, progression, invasion, and metastasis, ultimately inhibiting tumor biological behaviors. TCM attenuates the formation of pre-metastatic niches by impeding the release of pro-metastatic factors, preventing the colonization and establishment of secondary tumor sites. By interfering with the epithelial-mesenchymal transition process, TCM hinders tumour cells from gaining invasive traits and reduces the likelihood of metastasis. By suppressing the invasive and migratory behavior of tumor cells, TCM curbs their ability to initiate metastasis and invade distant tissues. TCM exerts a modulatory effect on the tumor microenvironment, promoting immune surveillance and enhancing anti-tumor immune responses, which eventually hinders tumor development. These collective actions of TCM underscore its potential as an adjunctive therapy for combating primary and metastatic tumors, holding promise for the advancement of novel therapeutic strategies.

2.2 Modulation of cytokine signaling

Cytokines, essential molecular messengers that orchestrate immune responses, are targets of interest for modulating tumor immunity with TCM compounds. For instance, baicalein, an active ingredient extracted from *Scutellaria baicalensis*, was reported to play an anti-tumor role by regulating cytokine signaling pathway. It effectively inhibits tumor cell growth, induces apoptosis, and modulates immune cell activity. Notably, it inhibits IL-6 and STAT3 signaling pathways, thus impeding tumor growth and metastasis (55). Sini decoction (SND) is another widely used TCM known for its ability to suppress colorectal cancer liver metastasis and alleviate liver injury *in vivo* (56). SND achieves this by upregulating IL-2 and IFN-γ and downregulating IL-10 and TGF-β (38). Another traditional prescription, Gansui-Banxia Decoction (GSBXD), created by sage Zhang Zhongjing, is employed to treat stagnation of evil heat and obstruction of qi. Studies by Feng et al. have demonstrated GSBXD's antitumor immune activity by reducing the accumulation of MDSCs *in vivo*, possibly achieved through down-regulation of AKT/STAT3/ERK signaling pathways and suppression of IL-1β and IFN-γ (39). Wenjinghuoluo prescription, a TCM compound treatment of rheumatoid arthritis, was discovered to decrease the expression of pro-inflammatory cytokines (TNF-α, IL-1β, IL-6, and IL-17), thus effectively inhibiting bone erosion and osteophyte formation in joints (57). Considering the crucial role of cytokines in tumor occurrence and development, various Chinese medicines hold significant potential for development in regulating cytokine pathways to exert anti-tumor effects.

2.3 Modulation of angiogenesis and vascular normalization

Angiogenesis, the process of forming new blood vessels, is essential for tumor growth and metastasis. Emerging reports indicate that TCM compounds possess anti-angiogenic properties, inhibiting the abnormal and excessive blood vessel formation within the TME (58). These compounds specifically target key molecular pathways involved in angiogenesis, such as the vascular endothelial growth factor (VEGF) signaling. Additionally, TCM compounds have demonstrated the ability to induce vascular normalization, promoting the restoration of a more normal and functional vasculature within the tumor. This normalization can enhance drug delivery, immune cell infiltration, and overall therapeutic efficacy. Notably, β-Elemene stands out as it regulates the expression of crucial molecules implicated in tumor angiogenesis and metastasis, including VEGF, matrix metalloproteinases (MMPs), E-cadherin, N-cadherin, and vimentin (59). Another promising natural phytochemical is Ginsenoside Rg3, which has been extensively studied for its potential in cancer prevention and treatment. Its mechanisms of action encompass a

wide range of anti-cancer activities, including apoptosis induction, inhibition of proliferation, metastasis, and angiogenesis, as well as boosting the immune response against cancer cells (30). In the quest for effective anti-angiogenic agents, researchers have looked into other natural compounds such as catechin gallate, astragaloside, and curcumin. These compounds have demonstrated their ability to effectively inhibit angiogenesis, thereby impeding the formation of new blood vessels that are crucial for tumor growth and metastasis (60). Curcumol, another natural substance, has shown promise in restraining cell growth and angiogenesis in non-small cell lung cancer (NSCLC). This potential is attributed to its ability to regulate the SP1/miR-125b-5p/VEGFA pathway, thus suppressing the expression of VEGF and limiting tumor blood vessel formation (61). Additionally, the compound menthol has been found to block the trans-activation of the transient receptor potential vanilloid 1 (TRPV1) by activating the transient receptor potential melastatin subtype 8 (TRPM8) ion channel. This activation inhibits VEGF-induced angiogenesis in specific cancer cells, such as uveal melanoma UM92.1 cells and PC-3 cells, providing a novel approach to target angiogenesis in cancer therapy (62–64). In conclusion, TCM compounds have shown anti-angiogenic properties by targeting key molecular pathways involved in angiogenesis, such as VEGF signaling. They can inhibit abnormal blood vessel formation within the TME and promote vascular normalization. This normalization enhances drug delivery, immune cell infiltration, and overall therapeutic efficacy.

2.4 Modulation of extracellular matrix remodeling

The extracellular matrix (ECM) within the TME plays a crucial role in providing structural support to tumor cells and exerting a significant influence on their behavior. Studies have demonstrated that TCM compounds possess the ability to regulate the intricate processes of ECM remodeling, including the degradation and deposition of ECM components. Notably, certain compounds exhibit compelling anti-fibrotic property, effectively inhibiting the excessive accumulation of collagen and other ECM proteins, which can otherwise impede the infiltration of immune cells (65). Furthermore, TCM compounds display the capacity to modulate the activity of MMPs, a group of enzymes involved in ECM degradation, thus exerting a consequential impact on tumor invasion and metastasis (66). For instance, a notable example is the Kushen injection compound, which has been corroborated to uniformly block the migration and invasion through EMC in colon, brain, and breast cancer cell lines (67). These findings underscore the potential of TCM in regulating the dynamic interactions between tumor cells and the ECM, suggesting their therapeutic relevance in impeding tumor progression and metastasis.

2.5 Modulation of inflammatory and immune responses

Inflammation and immune dysregulation within the TME contribute to tumor growth, immune evasion, and therapy resistance. TCM has been corroborated to exert immunomodulatory effects on tumor cells, influencing inflammatory and immune responses in the TME (68). For instance, extracts derived from *Curcuma longa* have demonstrated the capacity to modulate immune-inflammatory responses, offering a potential avenue for regulating the occurrence and progression of glioma (69). Furthermore, the extraordinary attributes of honeysuckle and Huangqi have been recognized in their ability to suppress pro-inflammatory cytokines, including IL-6 and TNF-α. These cytokines play pivotal roles in the initiation and progression of tumors (70). The presence of inflammation and immune dysregulation within the TME significantly contributes to tumor growth, immune evasion, and resistance to therapy.

2.6 Targeting immune checkpoints

Immune checkpoints are essential regulatory molecules that help maintain immune homeostasis. However, cancer cells can exploit these checkpoints to evade detection and destruction by the immune system, allowing tumors to evade immune surveillance (71). TCM compounds have shown promise in their ability to modulate immune checkpoint molecules, including PD-1, CTLA-4, and LAG-3 (72). One such example is the Gegen Qinlian decoction (GQD), a classical TCM formula. When used in combination with anti-mouse PD-1 treatment, GQD has been found to downregulate PD-1 expression and increase the levels of IL-2, effectively restoring T-cell functions by suppressing inhibitory checkpoints (73). Berberine (BBR), a well-known anti-inflammatory drug in TCM, has also been identified as a negative regulator of PD-L1 by researchers like Liu et al. Its administration has been shown to enhance the sensitivity of tumor cells to co-cultured T-cells by reducing PD-L1 levels in cancer cells (74). Additionally, Zhang et al. have reported that a compound known as CFF-1 exhibits tumor growth inhibition and prevents lung metastasis by blocking the PD-1/PD-L1 pathway. This action leads to an improved T lymphocyte immune response via the EGFR/JAK1/STAT3 pathway. As a result, CFF-1 shows promise as a potentially effective treatment to counteract tumor immunosuppression, particularly in prostate cancer patients (41). In short, TCM compounds have shown promise in modulating immune checkpoint molecules, such as PD-1, CTLA-4, and LAG-3, which are essential for maintaining immune homeostasis but can be exploited by tumors to evade immune surveillance.

2.7 Immunosuppression and immune escape

TME frequently demonstrates its immunosuppressive characteristics that enable tumors to evade immune surveillance. Extensive research has focused on exploring the potential of TCM compounds to counteract immunosuppression within the TME. One remarkable aspect of TCM compounds is their ability to modulate the activity of immunosuppressive cells, such as regulatory T cells (Tregs) and myeloid-derived suppressor cells (MDSCs). By targeting these cells, TCM compounds effectively reduce their negative impact on the anti-tumor immune response, creating a more conducive environment for fighting cancer (75).

Moreover, TCM compounds have demonstrated the ability to inhibit the expression of immune checkpoint molecules, such as PD-1 and CTLA-4, thus reinstating immune cell functionality and facilitating robust tumor immune responses (60, 74, 76). In the pursuit of novel approaches, researchers have explored innovative strategies involving TCM compounds. For instance, co-encapsulation of drugs in nanoparticles has demonstrated encouraging chemo-immunotherapeutic effects in mice with hepatocellular carcinoma (HCC). This approach enhances survival rates without causing significant toxicity, pointing towards a potential breakthrough in cancer treatment (77). Furthermore, specific TCM compounds, like Feiji Recipe, have been identified for their ability to restore T cell functionality within the cancer microenvironment. In non-small cell lung cancer (NSCLC), Feiji Recipe interferes with the indoleamine-2,3-dioxygenase pathway, a critical mediator of immune escape, offering a potential therapeutic avenue to counteract immune evasion in this type of cancer (78). By effectively addressing immunosuppression and reinvigorating the anti-tumor immune response, TCM-based treatments offer a potential complement or alternative to conventional therapies.

3 New findings of TCM natural products and derivatives as immunomodulating agents in cancer treatment

Numerous studies have provided evidence supporting the multifaceted potential of TCM. These properties encompass antibacterial, antioxidant, anti-inflammatory, anti-proliferative, anti-cancer, and various other beneficial effects. In this part, pertinent studies on several typical TCM natural products that have potential anti-cancer property are expounded in the following paragraphs and summarized in Table 2 (39, 79, 80, 82–124, 132). Additionally, some closed and ongoing national clinical trials (NCT) on the association between TCMs and multiple cancer types are also displayed in Table 3.

Polyphenols represent a class of naturally occurring compounds abundantly found in multiple plants, encompassing fruits, vegetables, and herbs. These molecules possess distinctive chemical and biological properties owing to their multiple phenol rings. Research has consistently revealed the wide-ranging health benefits of polyphenols, including their remarkable anti-inflammatory, antioxidant, and anti-cancer effects (125, 126). These compounds have been observed to exert modulatory influences on a series of cellular pathways critical to disease development and progression, such as cell cycle regulation, apoptosis, and angiogenesis (125, 127). *Curcumin*, derived from the dried rhizome of turmeric, is rich in phenols, terpenoids, flavonoids, and other constituents. Specifically categorized as a diphenyl heptane within the phenolic group, curcumin treatment has been discovered to effectively impede the proliferation and promote the apoptosis of colon cancer cells (128). Notably, curcumin treatment elevates the expression of miR-206, which subsequently influences the functional behavior of colon cancer cells. Via augmenting colon cancer cell apoptosis and suppressing PD-L1 expression, miR-206 enhances the cytotoxic effects of T cells on tumor cells. This potentiation is achieved through the inhibition of PD-L1 via suppression of the JAK/STAT3 pathway (57). These compounds, with their distinctive phenol rings, have been consistently shedding light on new horizons in cancer immunotherapy.

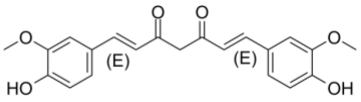
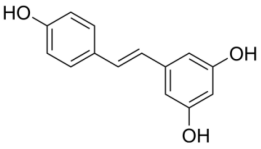
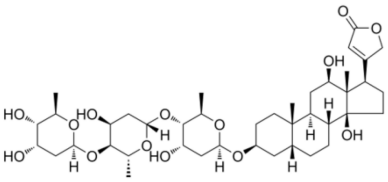
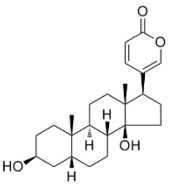
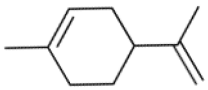
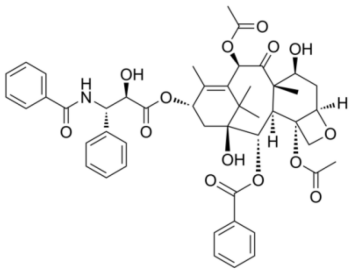
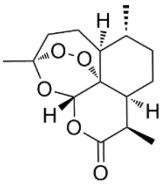
Resveratrol (Rsv), another prominent polyphenol compound, is predominantly sourced from plants such as peanuts, grapes, *Polygonum cuspidatum*, and mulberries (82). Resveratrol exhibits a multitude of pharmacological property, notably its antioxidant, anti-inflammatory, and anti-cancer activities, which render it highly beneficial for the treatment of gastric diseases (83). Resveratrol's mechanisms of action involve modulating the SLC7A11-HMMR interaction, activating ferroptosis, enhancing CD8+ T cell cytotoxicity, and regulating the tumor immune microenvironment (82). In summary, polyphenols offer a promising avenue in the field of health and disease management, with their diverse chemical properties and potential effects on essential cellular pathways. The specific polyphenols curcumin and resveratrol have shown remarkable impacts on cancer cells and the immune microenvironment, holding significant potential for therapeutic applications.

Cardiac glycosides, natural sterols derived from plants and animals, are known for their cardiotonic properties, enhancing cardiac contractions by targeting the cellular sodium-potassium ATPase pump (85). Extensive evidence suggests the remarkable antitumor property of cardiac glycosides, making them highly recommended for the treatment of diverse cancer types (85, 129, 130). Moreover, mutated or dysregulated transcription factors have emerged as promising therapeutic targets amenable to selective intervention. *Neriifolin*, a cardiac glycoside, has demonstrated its potential in suppressing malignant characteristics of prostate cancer cells. It achieves this by activating endoplasmic reticulum stress (ERS), which impacts the induction of antitumor inhibitory receptors, thereby enhancing DNA damage and apoptosis (131). *Digoxin*, a classic cardiac glycoside, exhibits potential in reducing inflammation and fibrosis in a mouse model of pulmonary fibrosis. Its mechanism involves inhibiting the mTORC2/AKT/IRF4 signaling pathway and macrophage M2 polarization (86). *Bufalin*, a major component of the dried secretion of Bufo, represents another cardiac steroid widely employed for therapeutic purposes. *Bufalin* exerts anti-breast cancer effects through multiple pathways and targets. It inhibits the PI3K/AKT pathway, induces apoptosis via the mitochondrial pathway, triggers programmed necrosis through the RIP11/RIP3/PARP-1 signaling pathway, and hinders cell proliferation and invasion by influencing cell cycle progression and inhibiting epithelial-mesenchymal transition (EMT) (89, 90, 132). In summation, cardiac glycosides have etched their mark not only in the realm of cardiotonic therapy but also as a burgeoning frontier in the battle against cancer.

Terpenoids, an expansive and diverse class of organic compounds prevalent in numerous plants, including cannabis, contribute significantly to the distinctive aroma and flavor of various botanical specimens. Additionally, terpenoids are renowned for their remarkable medicinal property, with several of them demonstrating potent anti-cancer effects. One such terpenoid,

10.3389/fimmu.2023.1277243

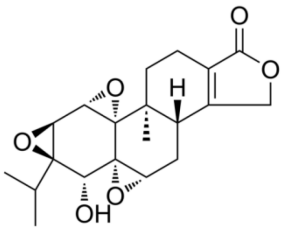
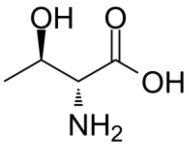
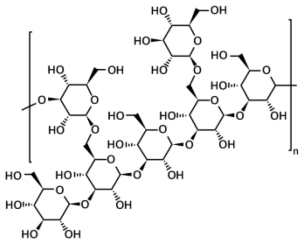
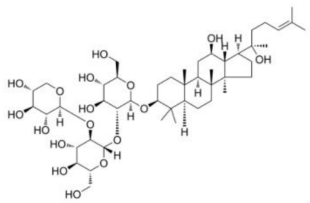
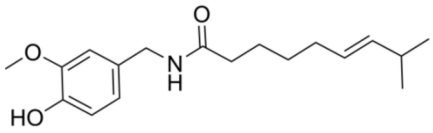
TABLE 2 The summary table of several significant anti-tumor TCMs.

Category	Drug name	Structure	Main function	Target	Pathway	Reference
Polyphenols	*Curcumin* (PubChem CID: 969516)		Antioxidant and anti-inflammatory	NF-κB; COX-2; TNF-α	1)NF-κB pathway; 2)MAPKs pathway; 3)PI3K/Akt pathway; 4)Wnt/β-catenin pathway; 5)Notch pathway	(79–81)
	Resveratrol (Rsv) (PubChem CID: 445154)		Antioxidant and anti-inflammatory	IKKβ; autophagy; mitophagy	1)autophagy pathways; 2)NF-κB pathway	(82–84)
Cardiotonic steroids	*Digoxin* (PubChem CID: 2724385)		Positive inotropic action	Na+/K+ ATPase	Na+/K+ ATPase	(85–88)
	Bufalin (PubChem CID: 9547215)		Cardiotonic, anti-inflammatory, and cancer suppressive	Na+/K+ ATPaseα3	c-Myc/NF-κB pathway	(89–93)
Terpenoids	*Limonene* (PubChem CID: 22311)		Antibacterial, anti-proliferative, antioxidant, and anti-inflammatory	TRP3; TRP4	1)Ras pathway; 2)Akt/mTOR pathway	(94–96)
	Paclitaxel (PubChem CID: 36314)		Stabilizing microtubules, inducing cell cycle arrest and inhibition of cell division	Microtubule protein; tubulin	1)antibody-drug conjugate: ADC cytotoxin; 2) cytoskeleton: microtubules/ tubulin; 3)mitotic checkpoint pathway; 4)apoptotic pathways	(97, 98)
	Artemisinin (PubChem CID: 68827)		Antimalarial activity	Plasmodium falciparum ATPase 6	Heme detoxification pathway	(99–101)
	Triptolide (PubChem CID: 107985)		Immunosuppressive, anti-inflammatory, and anti-proliferative	HSP90; NF-κB; MDM-2/p53	1)NF-κB pathway; 2)JAK-STAT pathway; 3)Wnt/β-	(102–108)

(Continued)

10.3389/fimmu.2023.1277243

TABLE 2 Continued

Category	Drug name	Structure	Main function	Target	Pathway	Reference
					catenin pathway	
	Polysaccharides (PubChem SID: 405235487)		Immunomodulatory, anti-inflammatory, and antioxidant effects	MMP-2; MMP-9; ERK1; ERK2	1)MAPK/ERK pathway; 2)JNK pathway	(109–111)
Polysaccharides	*Lentinan* (PubChem CID: 37723)		Immunomodulatory activity	Dectin-1; TLR2; TLR4	1)NF-κB pathway; 2)MAPK pathway	(112–115)
Saponins	*Panax notoginseng Saponins* (PubChem CID: 297)		Influencing cardiovascular function, inflammation, and oxidative stress	Endothelial nitric oxide synthase (eNOS)	1)PI3K/Akt pathway; 2)ERK pathway	(39, 116–118)
Capsaicin	*Capsaicin* (PubChem CID: 1548943)		Interacting with sensory neurons (TRPV1) ion channel; anti-inflammatory	TRPV1; neutrophils; macrophages	1)MAPK pathway; 2)NF-κB pathway	(119–124)

Thymol, can induce an anticancer effect in acute promyelocytic leukemia cells by arresting the cell cycle at G0/G1 phase and mitochondrial depolarization through reactive oxygen species production followed by mitochondrial membrane deterioration (133). Another noteworthy terpenoid, *limonene*, abundantly found in citrus fruits and specific cannabis strains, has shown anti-cancer effects by inducing apoptosis in breast cancer cells, promoting programmed cell death in the cancerous cells (94). *Paclitaxel*, a chemotherapy drug derived from the *Pacific yew* tree, hinders cancer cell division and growth by effectively inhibiting the breakdown of microtubules, cellular structures vital for maintaining cell shape and facilitating cell division. By binding to microtubules, *paclitaxel* prevents their disassembly, thereby thwarting the ability of cancer cells to divide and proliferate (97). *Artemisinin*, a compound derived from the sweet wormwood plant and long utilized in TCM for malaria treatment, has recently been discovered to possess anti-cancer property by generating free radicals within cancer cells, leading to oxidative stress and subsequent cell death. *Artemisinin* has exhibited notable efficacy against breast cancer cells (99, 100). *Triptolide*, derived from the thunder god vine plant and traditionally employed in Chinese medicine to address many conditions, including inflammation and autoimmune diseases, has also demonstrated potent anti-cancer property inhibiting the NF-kB protein, a crucial regulator of cell survival, and inducing apoptosis in cancer cells (102–104).

Polysaccharides, intricate carbohydrates abundant in plants, fungi, and bacteria, exhibit a diverse array of health benefits, including their remarkable anti-cancer property. Extensive research has demonstrated that polysaccharides possess the ability to impede the growth and proliferation of cancer cells through activating the immune system and promoting the production of cytokines. After the immune system is activated, polysaccharides facilitate the identification and elimination of cancer cells (109). Moreover, polysaccharides showcase direct anti-cancer effects in addition to their immune-boosting attributes. Notably, polysaccharides derived from mushrooms have demonstrated desirable efficacy in inhibiting cancer cell growth by inducing apoptosis or programmed cell death. Furthermore, by inducing

TABLE 3 Closed and ongoing national clinical trials (NCT) on the association between TCMs and multiple cancer types.

Clinical trial. gov identifier	Official title	Model	Conditions	Intervention/ Treatment	Enrollment/ Estimated enrollment	Primary outcome	Completion date/ Estimated completion date
NCT01780181	Randomized Double-blind Controlled Clinical Study of Chemotherapy Combined With or Without Traditional Chinese Medicine on Survival Effect of Elderly Patients With Advanced Non-small-cell Lung Cancer	Case-control	Lung cancer	TCM	82	Progression free survival	2016/09/01
NCT01745302	Study of Chinese Medicine Plus EGFR-TKI Versus EGFR-TKI in Advanced Pulmonary Adenocarcinoma: a Randomized Double-blind Controlled Clinical Trial	Case-control	Pulmonary adenocarcinoma	TCM	470	Progression free survival	2016/12/01
NCT03332368	Clinical Study on Prevention and Treatment of Recurrent and Metastasis of Triple Negative Breast Cancer (TNBC) With Traditional Chinese Medicine(TCM)	Cohort	Pulmonary adenocarcinoma	TCM	620	Progression free survival; overall survival	2019/01/01
NCT03607656	The Effect of Traditional Chinese Treatment Combined Adjuvant Chemotherapy in IIIb and IIIc Gastric Cancer: A Randomized Controlled Trial	Parallel assignment	Gastric cancer	Oxaliplatin	270	3-year disease free survival rate	2023/12/31
NCT02889692	Study of Chinese Medicine Plus Targeted Therapy Maintenance Versus Targeted Therapy Maintenance in Advanced Pulmonary Adenocarcinoma: A Randomized Double-blind Controlled Clinical Trial	Parallel assignment	Pulmonary adenocarcinoma	TCM	23	Overall survival	2017/06/01
NCT04482829	Efficacy and Safety of Jing-yuan-kang Granule in the Treatment of Lung Adenocarcinoma	Parallel assignment	Lung adenocarcinoma	Jing-yan-kang granule	144	1) The quality of life will be evaluated by the European Organization for Research and Treatment of Cancer Quality of life Questionnaire Core-30 (EORTC QLQ-C30) scale; 2) Quality of life will be evaluated by Quality of life Questionnaire Lung Cancer-13 (QLQ-LC13)	2022/06/30

(Continued)

TABLE 3 Continued

Clinical trial. gov identifier	Official title	Model	Conditions	Intervention/ Treatment	Enrollment/ Estimated enrollment	Primary outcome	Completion date/ Estimated completion date
NCT01975454	A Pilot Study of Teng-Long-Bu-Zhong-Tang Based Herbal Therapy in Combination With Chemotherapy in Patients With Metastatic Colorectal Cancer	Parallel assignment	Metastatic colorectal cancer	Herbal therapy	62	Progression free survival	2017/12/01
NCT02929693	Clinical Study of Yiqi-yangyin-jiedu Decoction Combined With Gefitinib in Advanced Pulmonary Adenocarcinoma Patients With Activating EGFR Mutation	Parallel assignment	Pulmonary adenocarcinoma	Yiqi-yangyin-jiedu decoction	198	Progression free survival	2019/06/01
NCT04438564	Immunoassay and Regulation of Traditional Chinese Medicine on Cancer Patients	Single group assignment	breast Cancer	TCM	300	The IL-2, TNF-α and IFN-γ expression by TCM treatment on cancer patients	2023/07/31
NCT05894694	Survival Benefit of Compound Kushen Injection in Treatment of Advanced Colorectal Cancer Based on Real World Registration Platform	Parallel assignment	Colorectal carcinoma	Kushen injection	318	Progression free survival	2024/12/30
NCT00094445	Phase II Trial of Curcumin in Patients With Advanced Pancreatic Cancer	Single group assignment	Pancreatic neoplasms	Curcumin	50	Six-month participant survival	2014/04/01
NCT03980509	A "Window Trial" on Curcumin, the Active Compound in Turmeric, for Invasive Breast Cancer Primary Tumors	Single group assignment	Breast cancer	Curcumin	22	Changes in tumor proliferation rate	2023/08/31
NCT03769766	A Randomized, Double-Blind, Placebo-Controlled Trial of Curcumin to Prevent Progression of Biopsy Proven, Low-risk Localized Prostate Cancer Patients Undergoing Active Surveillance	Parallel assignment	Prostate cancer	Curcumin	291	Rate of disease progression	2026/11/01
NCT01476592	A Biological Study of Resveratrol's Effects on Notch-1 Signaling in Subjects With Low Grade Gastrointestinal Tumors	Single group assignment	Gastrointestinal tumors	Resveratrol	7	Notch1 activation in post-treatment tumor biopsy specimens when compared to pretreatment levels	2018/10/11
NCT00256334	Resveratrol for Patients With Colon Cancer	Single group assignment	Colon cancer	Resveratrol	11	Test the hypothesis that resveratrol modulates Wnt signaling *in vivo* in colon cancer and normal colonic mucosa	2009/04/01

(Continued)

TABLE 3 Continued

Clinical trial. gov identifier	Official title	Model	Conditions	Intervention/ Treatment	Enrollment/ Estimated enrollment	Primary outcome	Completion date/ Estimated completion date
NCT01162135	A Pilot Phase II Study of Digoxin in Patients With Recurrent Prostate Cancer as Evident by a Rising PSA	Single group assignment	Prostate cancer	Digoxin	16	Rate of positive PSADT outcome	2013/05/01
NCT01046929	Clinical Study of Limonene in Women With a Recent Diagnosis of Early Stage Breast Cancer Electing to Undergo Excision Surgery	Single group assignment	Breast cancer	Limonene	59	Breast tissue limonene level	2011/03/01
NCT00002917	A Phase I/II Institutional Study of Intravesical Taxol (Paclitaxel) Instillation for the Treatment of Superficial Bladder Cancer	Not provided	Bladder cancer	Paclitaxel	19	Not provided	2004/05/01
NCT00989131	An Open, Randomized, Multicenter Study in Patients With Recurrent Epithelian Cancer, Primary Peritoneal Cancer or Fallopian Tube Cancer to Compare the Efficacy and Safety of Paclitaxel (Micellar) Nanoparticles and Paclitaxel (Cremophor® EL)	Parallel assignment	Epithelial ovarian cancer	Paclical	789	1) Progression free survival; 2) Changes in area under the curve of CA-125; 3) Incidence and severity of hypersensitivity reactions	2013/10/01
NCT00764036	Prospective Open Uncontrolled Phase I Study of Compatibility, Safety&Pharmacokinetics of Artesunate, a Semisynthetic Derivative of Artemisinin From the Chinese Herb Artemisia Annua in Patients With Metastatic/Locally Advanced Breast Cancer	Sequential assignment	Breast Cancer	Artesunate	23	Dose limiting adverse events with possible, probable or definite relation with the respective dose level of the add-on therapy	2013/11/01

apoptosis and inhibiting the formation of blood vessels crucial for cancer cell proliferation and metastasis, mushroom polysaccharides demonstrate potent anti-cancer efficacy (29, 109, 110). For instance, *lentinan*, a polysaccharide extracted from the shiitake mushroom, has garnered significant attention for its anti-cancer potential. It effectively hinders cancer cell growth and proliferation by activating the immune system and stimulating cytokine production, thus enhancing immune responses against cancer cells (112, 134). Clinical trials evaluating lentinan have shown promising therapeutic capabilities, particularly in gastric cancer and colorectal cancer. Patients treated with lentinan experienced improved survival rates and enhanced quality of life, as the polysaccharide not only combats cancer cells but also alleviates the side effects of chemotherapy and radiation therapy (112). In essence, polysaccharides, with their immune-activating and direct anti-cancer attributes, stand at the forefront of the evolving landscape of cancer therapy.

Saponins, a group of plant glycosides with their distinctive ability to generate abundant foam in aqueous solutions, have garnered attention due to their profound anti-cancer effects (116, 135). These compounds effectively impede cancer cell growth and proliferation by inducing apoptosis. In Chen's clinical trial, a significant discovery was made regarding the therapeutic potential of combining ginsenoside Rg3 with MF chemotherapy. The findings revealed a notable reduction in serum VEGF concentration, resulting in improved survival rates for patients with advanced gastric cancer (136). Another notable saponin, *Saikosaponin D*, demonstrated impressive efficacy in enhancing apoptosis mediated

by TNF-α in HepG2 cells. This effect was attributed to the inhibition of NF-κB activation and downregulation of target genes associated with cancer cell proliferation, angiogenesis, invasion, and survival (137). Notably, ginsenoside Rg-3 has recently gained recognition in China as a promising anti-angiogenic and anti-cancer drug (116). By activating the immune system and stimulating cytokine production, saponins can identify and suppress the activity of cancer cells. *Panax notoginseng Saponins (PNS)* have shown cytotoxicity and enhanced chemosensitivity in pancreatic cancer cells treated with Gemcitabine. This effect was achieved through the inhibition of autophagy and promotion of apoptosis, providing a potential treatment option for pancreatic cancer (116). These compounds, by effectively curbing cancer cell growth and proliferation through apoptosis induction, offer a compelling avenue for exploring innovative cancer therapeutics.

Capsaicin, a vanilloid phytochemical found in chili peppers and pepper extracts, exhibits significant anti-cancer properties against various human cancers, including lung, gastric, colon, and breast cancer. Its anti-cancer effects are attributed to its ability to induce apoptosis and inhibit tumor cell proliferation. Additionally, capsaicin exhibits noteworthy anti-inflammatory property, which contribute to its cancer-preventive potential by mitigating chronic inflammation. In specific cancer types, capsaicin has been observed to induce apoptosis in ORL-48 cells through the intrinsic apoptotic pathway, involving disruption of mitochondrial membrane potential and activation of caspase-3, -7, and -9 (138). In bladder cancer cells, capsaicin downregulates tNOX expression, leading to enhanced apoptosis and reduced cell growth. The inhibition of extracellular regulated protein kinases activation by capsaicin results in decreased phosphorylation of paxillin and focal adhesion kinase (FAK), leading to reduced cell migration (119). Thoennissen et al. found that in breast cancer cells, capsaicin modulates the EGFR/HER-2 pathway, suggesting its potential role in breast cancer treatment and prevention (120). Furthermore, Jin et al. reported capsaicin's profound anti-proliferative effects on colon cancer cells involve cell cycle arrest in the G0/G1 phase and promotion of apoptosis, associated with increased expression of p21, Bax, and cleaved poly ADP-ribose polymerase (PAARP), which play essential roles in regulating cell cycle progression and apoptosis (121). In conclusion, *capsaicin*, whose impact reverberates across various human cancers, from lung and gastric to colon and breast cancer, offers a promising avenue for novel cancer interventions.

4 Future perspectives

Tumor immunotherapy can activate the immune system to identify and eliminate cancer cells. Accordingly, cancer cells produce suppressive proteins to alleviate immune responses and evade immune surveillance. Immunotherapy agents possess the capability to block these proteins, thereby facilitating the immune system's efficient recognition and elimination of cancer cells (5, 129, 139). The paramount significance of tumor immunotherapy stems from its capability to harness the formidable potential of the immune system to destroy cancer cells. Diverging from conventional cancer treatments like chemotherapy and radiation therapy, which indiscriminately harm both normal and cancerous cells, immunotherapy selectively targets cancer cells and spares normal cells from harm. Consequently, this approach holds promise as a more potent and less toxic treatment modality for cancer patients (140). Additionally, immunotherapy has displayed promising outcomes in the treatment of multiple cancer types, including melanoma, lung cancer, and bladder cancer (141, 142). It has also demonstrated desirable efficacy in treating cancers that have developed resistance to conventional therapeutic interventions.

Despite its considerable potential benefits, tumor immunotherapy is accompanied by several limitations that necessitate attention and resolution. One primary limitation is the heterogeneous response observed among patients undergoing immunotherapy (143). While some individuals have exhibited remarkable and favorable responses, others have not experienced any discernible benefits. This heterogeneity may arise from variances in patients' immune system profiles or the distinct characteristics of their specific cancers. Another limitation of immunotherapy pertains to the potential occurrence of side effects (144). Although immunotherapy generally exhibits lower toxicity compared to traditional cancer treatments, it can still induce immune-related side effects such as inflammation, fatigue, and cutaneous manifestations (144, 145). In certain instances, these side effects may severely manifest and urgently demand intervention. The third limitation is its relatively high expenditure. Immunotherapy drugs often incur greater expenses than conventional cancer treatments, thereby posing a financial barrier to access for some cancer patients with low income.

TCM harbors notable potential in the realm of tumor immunity for several compelling reasons. Acknowledging the interconnected nature of the immune system with other bodily systems, TCM endeavors to rectify underlying imbalances, thus enhancing the body's inherent defense mechanisms, including tumor immunity (146). Secondly, TCM compounds have exhibited immunomodulatory property, influencing the function of immune cells, cytokine signaling, and immune responses. These compounds possess the capacity to augment the activity of immune cells crucial for tumor immunity, while concurrently suppressing immunosuppressive cell populations. Through modulating the immune response, TCM compounds are promising in promoting anti-tumor immune responses and bolstering tumor eradication. They can concurrently target multiple immune checkpoints, cytokines, and cellular pathways, culminating in a comprehensive and multi-faceted approach that augments tumor immunity. Such multimodal effects hold the potential to surmount the limitations associated with therapies focusing on a single target and subsequently enhance therapeutic outcomes. Furthermore, TCM places considerable emphasis on personalized medicine, tailoring treatments to address the specific requirements and imbalances exhibited by each individual patient (147). This personalized approach acknowledges the inherent variability of tumor immunity among patients, attributable to factors such as genetic predisposition, immune status, and the distinctive characteristics of the tumor microenvironment. Lastly, TCM boasts a rich historical heritage, spanning centuries of utilization in China and other Asian nations, thereby accumulating extensive clinical experience in managing a diverse range of health conditions. Traditional herbal formulations and treatment methodologies have been refined over time based on empirical

observations and accumulated wisdom. This fusion of historical knowledge with modern scientific investigations presents a distinctive opportunity to harness the potential of TCM in optimizing tumor immunity.

TCM encompasses an extensive repertoire of herbal compounds, possessing infinite potential for immunomodulation. One avenue of progress involves the identification and isolation of specific active compounds present in TCM formulations that exert robust effects on tumor immunity. By isolating these compounds and subjecting them to rigorous scientific scrutiny, their mechanisms of action can be elucidated, enabling a more precise evaluation of their efficacy and safety. Further investigations are warranted to comprehend the underlying mechanisms by which TCM compounds modulate tumor immunity. This necessitates exploring the signaling pathways, cellular interactions, and molecular targets involved in the immunomodulatory effects of TCM compounds. Mechanistic studies offer invaluable insights into the precise actions of TCM compounds on immune cells, cytokine signaling, immune checkpoints, and the tumor microenvironment, thereby guiding the advancement of targeted therapeutic interventions. Given the complexity and heterogeneity of tumor immunity, which varies among individuals and tumor types (148), the development of personalized TCM treatment strategies hinges on the identification of biomarkers capable of predicting treatment responses and patient outcomes. The identification of such biomarkers can facilitate the selection of TCM compounds and formulations tailored to individual patients, optimizing their potential to enhance tumor immunity and improve treatment efficacy (149). By steadfastly pursuing the above exploratory directions, TCM can continuously evolve as a valuable approach for augmenting tumor immunity, ultimately contributing to the advancement of more efficacious and personalized strategies for cancer treatment.

The emergence of precision medicine has fundamentally transformed the landscape of cancer treatment, revolutionizing therapeutic approaches by tailoring interventions to individual patients based on their unique genetic and molecular characteristics (150). In this context, TCM emerges as a highly promising complementary modality, capable of augmenting the efficacy and personalization of cancer immunotherapy. Through the identification of specific TCM compounds and formulations that align with individual tumor and immune profiles, clinicians are more likely to optimize treatment strategies, enhance therapeutic outcomes, and minimize adverse effects. Moreover, the integration of TCM with conventional cancer therapies like chemotherapy and radiation, paves the way for synergistic effects and novel therapeutic avenues. Notably, studies have indicated that TCM compounds can enhance the effectiveness of these treatments by sensitizing tumor cells to cytotoxic agents, modulating the tumor microenvironment, and mitigating treatment-associated side effects (72). Furthermore, the combination of TCM with emerging immunotherapies, such as cancer vaccines and chimeric antigen receptor (CAR) T-cell therapy, embraces a promising future in unleashing robust anti-tumor immune responses and ultimately improving patient outcomes. Finally, the combination of traditional wisdom and modern scientific advancements assumes paramount importance in propelling the progress of TCM within the realm of cancer immunotherapy (151). To this end, rigorous scientific investigations on preclinical and clinical studies are indispensable for elucidating the mechanisms of action, validating efficacy, and ensuring the safety of TCM compounds.

5 Conclusion

The potential of TCM in the realm of anti-cancer immunotherapy is supposed to be cherished, and its immunoregulatory mechanisms should be shed light on. This review summarizes the current state of research, also categorizing and expounding broadly applied TCM approaches that possess anti-cancer property. Additionally, the curative effects and underlying mechanisms of several frequently used Chinese medicines are discussed meticulously. Moreover, the mechanism of several commonly used TCM monomers and compound prescription were explained in detail. Overall, our work presents a comprehensive overview of the progress made in TCM for cancer treatment, providing valuable insights into its advancement in this field.

Author contributions

KM: Resources, Visualization, Writing – original draft. WL: Data curation, Visualization, Writing – original draft. JX: Visualization, Writing – review & editing. ZQ: Conceptualization, Resources, Project administration, Visualization, Writing – review & editing. QZ: Conceptualization, Funding acquisition, Project administration, Visualization, Writing – review & editing.

Funding

The author(s) declare financial support was received for the research, authorship, and/or publication of this article. This work is supported by the Project of Wuxi Health Commission (Q202109) and General Project of Wuxi Medical Center of Nanjing Medical University (WMCG202326).

Conflict of interest

The authors declare that the research was conducted in the absence of any commercial or financial relationships that could be construed as a potential conflict of interest.

Publisher's note

All claims expressed in this article are solely those of the authors and do not necessarily represent those of their affiliated organizations, or those of the publisher, the editors and the reviewers. Any product that may be evaluated in this article, or claim that may be made by its manufacturer, is not guaranteed or endorsed by the publisher.

References

1. Zaimy MA, Saffarzadeh N, Mohammadi A, Pourghadamyari H, Izadi P, Sarli A, et al. New methods in the diagnosis of cancer and gene therapy of cancer based on nanoparticles. *Cancer Gene Ther* (2017) 24:233–43. doi: 10.1038/cgt.2017.16

2. Wang J-J, Lei K-F, Han F. Tumor microenvironment: recent advances in various cancer treatments. *Eur Rev Med Pharmacol Sci* (2018) 22:3855–64. doi: 10.26355/eurrev_201806_15270

3. Bejarano L, Jordão MJC, Joyce JA. Therapeutic targeting of the tumor microenvironment. *Cancer Discovery* (2021) 11:933–59. doi: 10.1158/2159-8290.CD-20-1808

4. Mz J, Wl J. The updated landscape of tumor microenvironment and drug repurposing, Signal Transduct. *Targeting Ther* (2020) 5(1):166. doi: 10.1038/s41392-020-00280-x

5. Zhang Y, Zhang Z. The history and advances in cancer immunotherapy: understanding the characteristics of tumor-infiltrating immune cells and their therapeutic implications. *Cell Mol Immunol* (2020) 17:807–21. doi: 10.1038/s41423-020-0488-6

6. Wang D-R, Wu X-L, Sun Y-L. Therapeutic targets and biomarkers of tumor immunotherapy: response versus non-response. *Signal Transduction Targeting Ther* (2022) 7:331. doi: 10.1038/s41392-022-01136-2

7. Finck AV, Blanchard T, Roselle CP, Golinelli G, June CH. Engineered cellular immunotherapies in cancer and beyond. *Nat Med* (2022) 28:678–89. doi: 10.1038/s41591-022-01765-8

8. Jogalekar MP, Rajendran RL, Khan F, Dmello C, Gangadaran P, Ahn B-C. CAR T-Cell-Based gene therapy for cancers: new perspectives, challenges, and clinical developments. *Front Immunol* (2022) 13:925985. doi: 10.3389/fimmu.2022.925985

9. Huang Y, Ma S, Wang Y, Yan R, Wang S, Liu N, et al. The role of traditional Chinese herbal medicines and bioactive ingredients on ion channels: A brief review and prospect. *CNS Neurol Disord Drug Targets* (2019) 18:257–65. doi: 10.2174/1871527317666181026165400

10. Ma H-D, Deng Y-R, Tian Z, Lian Z-X. Traditional Chinese medicine and immune regulation. *Clin Rev Allergy Immunol* (2013) 44:229–41. doi: 10.1007/s12016-012-8332-0

11. Liu R, Li X, Huang N, Fan M, Sun R. Toxicity of traditional Chinese medicine herbal and mineral products. *Adv Pharmacol San Diego Calif* (2020) 87:301–46. doi: 10.1016/bs.apha.2019.08.001

12. Ruhlmann CH, Herrstedt J. New treatments on the horizon for chemoradiotherapy-induced nausea and vomiting, Expert Opin. *Pharmacother* (2016) 17:1623–9. doi: 10.1080/14656566.2016.1202923

13. Wang Z, Liu W, Zhang J, Chen X, Wang J, Wang K, et al. Antiemetic prophylaxis for chemoradiotherapy-induced nausea and vomiting in locally advanced head and neck squamous cell carcinoma: a prospective phase II trial. *Strahlenther. Onkol* (2022) 198:949–57. doi: 10.1007/s00066-022-01958-7

14. Rückert M, Flohr A-S, Hecht M, Gaipl US. Radiotherapy and the immune system: More than just immune suppression. *Stem Cells Dayt. Ohio* (2021) 39:1155–65. doi: 10.1002/stem.3391

15. Rallis KS, Lai Yau TH, Sideris M. Chemoradiotherapy in cancer treatment: rationale and clinical applications. *Anticancer Res* (2021) 41:1–7. doi: 10.21873/anticanres.14746

16. Li J, Li J, Zhang F. The immunoregulatory effects of Chinese herbal medicine on the maturation and function of dendritic cells. *J Ethnopharmacol* (2015) 171:184–95. doi: 10.1016/j.jep.2015.05.050

17. Shen C, Li J, Lian Y, Lan H, Pu F, Zhang W, et al. Chinese herbal medicine for incomplete immune reconstruction in patients with AIDS undergoing antiretroviral treatment: A systematic review of randomized trials. *J Tradit. Chin Med Sci* (2021) 8:291–301. doi: 10.1016/j.jtcms.2021.10.005

18. Xiang M-F, Jin C-T, Sun L-H, Zhang Z-H, Yao J-J, Li L-C. Efficacy and potential mechanisms of Chinese herbal compounds in coronavirus disease 2019: advances of laboratory and clinical studies. *Chin Med* (2021) 16:130. doi: 10.1186/s13020-021-00542-y

19. Wang S, Long S, Deng Z, Wu W. Positive role of Chinese herbal medicine in cancer immune regulation. *Am J Chin Med* (2020) 48:1577–92. doi: 10.1142/S0192415X20500780

20. Qi Y, Gao F, Hou L, Wan C. Anti-inflammatory and immunostimulatory activities of astragalosides. *Am J Chin Med* (2017) 45:1157–67. doi: 10.1142/S0192415X1750063X

21. Hoffman RD, Li C-Y, He K, Wu X, He B-C, He T-C, et al. Chinese herbal medicine and its regulatory effects on tumor related T cells. *Front Pharmacol* (2020) 11:492. doi: 10.3389/fphar.2020.00492

22. Bai L, Li X, He L, Zheng Y, Lu H, Li J, et al. Antidiabetic potential of flavonoids from traditional Chinese medicine: A review. *Am J Chin Med* (2019) 47:933–57. doi: 10.1142/S0192415X19500496

23. Tao Y, Zhan S, Wang Y, Zhou G, Liang H, Chen X, et al. Baicalin, the major component of traditional Chinese medicine Scutellaria baicalensis induces colon cancer cell apoptosis through inhibition of oncomiRNAs. *Sci Rep* (2018) 8:14477. doi: 10.1038/s41598-018-32734-2

24. Bhatia NK, Modi P, Sharma S, Deep S. Quercetin and baicalein act as potent antiamyloidogenic and fibril destabilizing agents for SOD1 fibrils. *ACS Chem Neurosci* (2020) 11:1129–38. doi: 10.1021/acschemneuro.9b00677

25. Yang D, Wang T, Long M, Li P. Quercetin: its main pharmacological activity and potential application in clinical medicine. *Oxid Med Cell Longev* (2020) 2020:e8825387. doi: 10.1155/2020/8825387

26. Dong C. Cytokine regulation and function in T cells. *Annu Rev Immunol* (2021) 39:51–76. doi: 10.1146/annurev-immunol-061020-053702

27. Reuter S, Charlet J, Juncker T, Teiten M-H, Dicato M, Diederich M. Effect of curcumin on nuclear factor kappaB signaling pathways in human chronic myelogenous K562 leukemia cells. *Ann N Y. Acad Sci* (2009) 1171:436–47. doi: 10.1111/j.1749-6632.2009.04731.x

28. Park J-Y, Sohn H-Y, Koh YH, Jo C. Curcumin activates Nrf2 through PKCδ-mediated p62 phosphorylation at Ser351. *Sci Rep* (2021) 11:8430. doi: 10.1038/s41598-021-87225-8

29. Kim M, Yi Y-S, Kim J, Han SY, Kim SH, Seo DB, et al. Effect of polysaccharides from a Korean ginseng berry on the immunosenescence of aged mice. *J Ginseng Res* (2018) 42:447–54. doi: 10.1016/j.jgr.2017.04.014

30. Sun M, Ye Y, Xiao L, Duan X, Zhang Y, Zhang H. Anticancer effects of ginsenoside Rg3 (Review). *Int J Mol Med* (2017) 39:507–18. doi: 10.3892/ijmm.2017.2857

31. Liu L, Hu L, Yao Z, Qin Z, Idehara M, Dai Y, et al. Mucosal immunomodulatory evaluation and chemical profile elucidation of a classical traditional Chinese formula, Bu-Zhong-Yi-Qi-Tang. *J Ethnopharmacol* (2019) 228:188–99. doi: 10.1016/j.jep.2018.08.003

32. Zhang Z, Chen Y, Zheng Y, Wang L, Shen S, Yang G, et al. Quxie capsule alleviates colitis-associated colorectal cancer through modulating the gut microbiota and suppressing A. fumigatus-induced aerobic glycolysis. *Integr Cancer Ther* (2022) 21:15347354221138534. doi: 10.1177/15347354221138534

33. Kachur K, Suntres ZE. The antimicrobial properties of ginseng and ginseng extracts. *Expert Rev Anti Infect Ther* (2016) 14:81–94. doi: 10.1586/14787210.2016.1118345

34. Shi X, Lan X, Chen X, Zhao C, Li X, Liu S, et al. Gambogic acid induces apoptosis in diffuse large B-cell lymphoma cells *via* inducing proteasome inhibition. *Sci Rep* (2015) 5:9694. doi: 10.1038/srep09694

35. Kim SH, Lee SW, Park HJ, Lee SH, Im WK, Kim YD, et al. Anti-cancer activity of Angelica gigas by increasing immune response and stimulating natural killer and natural killer T cells. *BMC Complement. Altern. Med* (2018) 18:218. doi: 10.1186/s12906-018-2277-7

36. Sun Y, Guo M, Feng Y, Zheng H, Lei P, Ma X, et al. Effect of ginseng polysaccharides on NK cell cytotoxicity in immunosuppressed mice. *Exp Ther Med* (2016) 12:3773–7. doi: 10.3892/etm.2016.3840

37. Sha X, Xu X, Liao S, Chen H, Rui W. Evidence of immunogenic cancer cell death induced by honey-processed Astragalus polysaccharides in *vitro* and in *vivo*. *Exp Cell Res* (2022) 410:112948. doi: 10.1016/j.yexcr.2021.112948

38. Chen J, Zheng X, Xu G, Wang B, Hu L, Mao J, et al. Sini decoction inhibits tumor progression and enhances the anti-tumor immune response in a murine model of colon cancer. *Comb. Chem High Throughput Screen.* (2023) 26(14):2517–26. doi: 10.2174/1386207326666230320103437

39. Feng X-Y, Chen B-C, Li J-C, Li J-M, Li H-M, Chen X-Q, et al. Gansui-Banxia Decoction extraction inhibits MDSCs accumulation *via* AKT /STAT3/ERK signaling pathways to regulate antitumor immunity in C57bl/6 mice. *Phytomedicine Int J Phytother. Phytopharm* (2021) 93:153779. doi: 10.1016/j.phymed.2021.153779

40. Wei H, Guo C, Zhu R, Zhang C, Han N, Liu R, et al. Shuangshen granules attenuate lung metastasis by modulating bone marrow differentiation through mTOR signalling inhibition. *J Ethnopharmacol* (2021) 281:113305. doi: 10.1016/j.jep.2020.113305

41. Zhang Y, Wei Y, Jiang S, Dang Y, Yang Y, Zuo W, et al. Traditional Chinese medicine CFF-1 exerts a potent anti-tumor immunity to hinder tumor growth and metastasis in prostate cancer through EGFR/JAK1/STAT3 pathway to inhibit PD-1/PD-L1 checkpoint signaling. *Phytomedicine Int J Phytother. Phytopharm* (2022) 99:153939. doi: 10.1016/j.phymed.2022.153939

42. de Camargo JBB, Brigatto FA, Zaroni RS, Germano MD, Souza D, Bacurau RF, et al. Does beta-alanine supplementation enhance adaptations to resistance training? A randomized, placebo-controlled, double-blind study. *Biol Sport* (2023) 40:217–24. doi: 10.5114/biolsport.2023.112967

43. Shen J, Zhang M, Zhang K, Qin Y, Liu M, Liang S, et al. Effect of Angelica polysaccharide on mouse myeloid-derived suppressor cells. *Front Immunol* (2022) 13:989230. doi: 10.3389/fimmu.2022.989230

44. Jin Z, Shen C, Zhang H, Qi R, Guo Q, Liu R, et al. Chinese medicine Xiaoshui decoction inhibits Malignant pleural effusion in mice and mediates tumor-associated macrophage polarization by activating autophagy. *J Ethnopharmacol* (2020) 249:112412. doi: 10.1016/j.jep.2019.112412

45. Liu J, Zhang X, Cheng Y, Cao X. Dendritic cell migration in inflammation and immunity. *Cell Mol Immunol* (2021) 18:2461–71. doi: 10.1038/s41423-021-00726-4

46. Gao J, Zhang Y-N, Cui J, Zhang J, Ming Y, Hao Z, et al. A polysaccharide from the whole plant of Plantago asiatica L. Enhances the antitumor activity of dendritic cell-based immunotherapy against breast cancer. *Front Pharmacol* (2021) 12:678865. doi: 10.3389/fphar.2021.678865

47. Shepherd FR, McLaren JE. T cell immunity to bacterial pathogens: mechanisms of immune control and bacterial evasion. *Int J Mol Sci* (2020) 21:6144. doi: 10.3390/ijms21176144

48. Saravia J, Chapman NM, Chi H. Helper T cell differentiation. *Cell Mol Immunol* (2019) 16:634–43. doi: 10.1038/s41423-019-0220-6

49. Kim KH, Lee YS, Jung IS, Park SY, Chung HY, Lee IR, et al. Acidic polysaccharide from Panax ginseng, ginsan, induces Th1 cell and macrophage cytokines and generates LAK cells in synergy with rIL-2. *Planta Med* (1998) 64:110–5. doi: 10.1055/s-2006-957385

50. Takei M, Tachikawa E, Umeyama A. Dendritic cells promoted by ginseng saponins drive a potent Th1 polarization. *biomark Insights* (2008) 3:269–86. doi: 10.4137/bmi.s585

51. Yang J, Yang X, Chu Y, Li M. Identification of baicalin as an immunoregulatory compound by controlling TH17 cell differentiation. *PloS One* (2011) 6:e17164. doi: 10.1371/journal.pone.0017164

52. Wculek SK, Cueto FJ, Mujal AM, Melero I, Krummel MF, Sancho D. Dendritic cells in cancer immunology and immunotherapy. *Nat Rev Immunol* (2020) 20:7–24. doi: 10.1038/s41577-019-0210-z

53. Jiang L, Huang D, Nie S, Xie M. Polysaccharide isolated from seeds of Plantago asiatica L. induces maturation of dendritic cells through MAPK and NF-κB pathway. *Saudi J Biol Sci* (2018) 25:1202–7. doi: 10.1016/j.sjbs.2017.09.011

54. Huang D, Nie S, Jiang L, Xie M. A novel polysaccharide from the seeds of Plantago asiatica L. induces dendritic cells maturation through toll-like receptor 4. *Int Immunopharmacol* (2014) 18:236–43. doi: 10.1016/j.intimp.2013.11.024

55. Pang H, Wu T, Peng Z, Tan Q, Peng X, Zhan Z, et al. Baicalin induces apoptosis and autophagy in human osteosarcoma cells by increasing ROS to inhibit PI3K/Akt/mTOR, ERK1/2 and β-catenin signaling pathways. *J Bone Oncol* (2022) 33:100415. doi: 10.1016/j.jbo.2022.100415

56. Wang Y, Zhang X, Li J, Zhang Y, Guo Y, Chang Q, et al. Sini decoction ameliorates colorectal cancer and modulates the composition of gut microbiota in mice. *Front Pharmacol* (2021) 12:609992. doi: 10.3389/fphar.2021.609992

57. Wu X, Shou Q, Chen C, Cai H, Zhang J, Tang S, et al. An herbal formula attenuates collagen-induced arthritis *via* inhibition of JAK2-STAT3 signaling and regulation of Th17 cells in mice. *Oncotarget* (2017) 8:44242–54. doi: 10.18632/oncotarget.17797

58. Dudley AC, Griffioen AW. Pathological angiogenesis: mechanisms and therapeutic strategies. *Angiogenesis* (2023) 26(3):313–47. doi: 10.1007/s10456-023-09876-7

59. Zhai B, Zhang N, Han X, Li Q, Zhang M, Chen X, et al. Molecular targets of β-elemene, a herbal extract used in traditional Chinese medicine, and its potential role in cancer therapy: A review. *Biomed Pharmacother. Biomedecine Pharmacother* (2019) 114:108812. doi: 10.1016/j.biopha.2019.108812

60. Ai Y, Zhao Z, Wang H, Zhang X, Qin W, Guo Y, et al. Pull the plug: Anti-angiogenesis potential of natural products in gastrointestinal cancer therapy. *Phytother. Res PTR.* (2022) 36:3371–93. doi: 10.1002/ptr.7492

61. Ma C, Tang X, Tang Q, Wang S, Zhang J, Lu Y, et al. Curcumol repressed cell proliferation and angiogenesis *via* SP1/mir-125b-5p/VEGFA axis in non-small cell lung cancer. *Front Pharmacol* (2022) 13:1044115. doi: 10.3389/fphar.2022.1044115

62. Zhao Y, Pan H, Liu W, Liu E, Pang Y, Gao H, et al. Menthol: An underestimated anticancer agent. *Front Pharmacol* (2023) 14:1148790. doi: 10.3389/fphar.2023.1148790

63. Zhu G, Wang X, Yang Z, Cao H, Meng Z, Wang Y, et al. Effects of TRPM8 on the proliferation and angiogenesis of prostate cancer PC-3 cells in *vivo*. *Oncol Lett* (2011) 2:1213–7. doi: 10.3892/ol.2011.410

64. Walcher L, Budde C, Böhm A, Reinach PS, Dhandapani P, Ljubojevic N, et al. TRPM8 activation *via* 3-iodothyronamine blunts VEGF-induced transactivation of TRPV1 in human uveal melanoma cells. *Front Pharmacol* (2018) 9:1234. doi: 10.3389/fphar.2018.01234

65. Li L-C, Kan L-D. Traditional Chinese medicine for pulmonary fibrosis therapy: Progress and future prospects. *J Ethnopharmacol* (2017) 198:45–63. doi: 10.1016/j.jep.2016.12.042

66. Lihua J, Haodan K, Yuan XU. Efficacy of Buzhong Yiqi decoction on benign prostatic hyperplasia and its possible mechanism. *J Tradit. Chin Med Chung Tsa Chih Ying Wen Pan* (2023) 43:533–41. doi: 10.19852/j.cnki.jtcm.2023.03.003

67. Nourmohammadi S, Aung TN, Cui J, Pei JV, De Ieso ML, Harata-Lee Y, et al. Effect of compound kushen injection, a natural compound mixture, and its identified chemical components on migration and invasion of colon, brain, and breast cancer cell lines. *Front Oncol* (2019) 9:314. doi: 10.3389/fonc.2019.00314

68. Zhao H, Wu L, Yan G, Chen Y, Zhou M, Wu Y, et al. Inflammation and tumor progression: signaling pathways and targeted intervention. *Signal Transduction Targeting Ther* (2021) 6(1):263. doi: 10.1038/s41392-021-00658-5

69. Li H, Li Y. Network pharmacology analysis of molecular mechanism of curcuma longa L. Extracts regulating glioma immune inflammatory factors: implications for precise cancer treatment. *Curr Top Med Chem* (2022) 22:259–67. doi: 10.2174/1568026621666210910123749

70. Yeh Y-C, Doan LH, Huang Z-Y, Chu L-W, Shi T-H, Lee Y-R, et al. Honeysuckle (Lonicera japonica) and Huangqi (Astragalus membranaceus) Suppress SARS-CoV-2 Entry and COVID-19 Related Cytokine Storm in Vitro. *Front Pharmacol* (2022) 12:765553. doi: 10.3389/fphar.2021.765553

71. Gaikwad S, Agrawal MY, Kaushik I, Ramachandran S, Srivastava SK. Immune checkpoint proteins: Signaling mechanisms and molecular interactions in cancer immunotherapy. *Semin Cancer Biol* (2022) 86:137–50. doi: 10.1016/j.semcancer.2022.03.014

72. Yu Y-X, Wang S, Liu Z-N, Zhang X, Hu Z-X, Dong H-J, et al. Traditional Chinese medicine in the era of immune checkpoint inhibitor: theory, development, and future directions. *Chin Med* (2023) 18(1):59. doi: 10.1186/s13020-023-00751-7

73. Lv J, Jia Y, Li J, Kuai W, Li Y, Guo F, et al. Gegen Qinlian decoction enhances the effect of PD-1 blockade in colorectal cancer with microsatellite stability by remodelling the gut microbiota and the tumour microenvironment. *Cell Death Dis* (2019) 10:415. doi: 10.1038/s41419-019-1638-6

74. Liu Y, Liu X, Zhang N, Yin M, Dong J, Zeng Q, et al. Berberine diminishes cancer cell PD-L1 expression and facilitates antitumor immunity *via* inhibiting the deubiquitination activity of CSN5. *Acta Pharm Sin B* (2020) 10:2299–312. doi: 10.1016/j.apsb.2020.06.014

75. Su L, Zhang F, Liu M, Li H, Li Q, Zhu Y, et al. The Tian-Men-Dong decoction suppresses the tumour-infiltrating G-MDSCs *via* IL-1β-mediated signalling in lung cancer. *J Ethnopharmacol* (2023) 313:116491. doi: 10.1016/j.jep.2023.116491

76. Pan J, Yang H, Zhu L, Lou Y, Jin B. Qingfei Jiedu decoction inhibits PD-L1 expression in lung adenocarcinoma based on network pharmacology analysis, molecular docking and experimental verification. *Front Pharmacol* (2022) 13:897966. doi: 10.3389/fphar.2022.897966

77. Han S, Bi S, Guo T, Sun D, Zou Y, Wang L, et al. Nano co-delivery of Plumbagin and Dihydrotanshinone I reverses immunosuppressive TME of liver cancer. *J Control. Release Off J Control. Release Soc* (2022) 348:250–63. doi: 10.1016/j.jconrel.2022.05.057

78. Luo B, Que Z-J, Zhou Z-Y, Wang Q, Dong C-S, Jiang Y, et al. Feiji Recipe inhibits the growth of lung cancer by modulating T-cell immunity through indoleamine-2,3-dioxygenase pathway in an orthotopic implantation model. *J Integr Med* (2018) 16:283–9. doi: 10.1016/j.joim.2018.04.008

79. Hsu K-Y, Ho C-T, Pan M-H. The therapeutic potential of curcumin and its related substances in turmeric: From raw material selection to application strategies. *J Food Drug Anal* (2023) 31:194–211. doi: 10.38212/2224-6614.3454

80. Jang SY, Kim J, Hong E, Lee K, Na Y, Yeom CH, et al. Curcumin inhibits human cancer cell growth and migration through downregulation of SVCT2. *Cell Biochem Funct* (2023) 41(6):696–703. doi: 10.1002/cbf.3824

81. Hussain A, Kumar A, Uttam V, Sharma U, Sak K, Saini RV, et al. Application of curcumin nanoformulations to target folic acid receptor in cancer: Recent trends and advances. *Environ Res* (2023), 116476. doi: 10.1016/j.envres.2023.116476

82. Shan G, Minchao K, Jizhao W, Rui Z, Guangjian Z, Jin Z, et al. Resveratrol improves the cytotoxic effect of CD8 +T cells in the tumor microenvironment by regulating HMMR/Ferroptosis in lung squamous cell carcinoma. *J Pharm Biomed Anal* (2023) 229:115346. doi: 10.1016/j.jpba.2023.115346

83. Zhang X, Jiang A, Qi B, Ma Z, Xiong Y, Dou J, et al. Resveratrol Protects against Helicobacter pylori-Associated Gastritis by Combating Oxidative Stress. *Int J Mol Sci* (2015) 16:27757–69. doi: 10.3390/ijms161126061

84. Wu M, Song D, Li H, Ahmad N, Xu H, Yang X, et al. Resveratrol enhances temozolomide efficacy in glioblastoma cells through downregulated MGMT and negative regulators-related STAT3 inactivation. *Int J Mol Sci* (2023) 24(11):9453. doi: 10.3390/ijms24119453

85. Kumavath R, Paul S, Pavithran H, Paul MK, Ghosh P, Barh D, et al. Emergence of cardiac glycosides as potential drugs: current and future scope for cancer therapeutics. *Biomolecules* (2021) 11:1275. doi: 10.3390/biom11091275

86. Jia L, Yang M, Tian X, Zhao P, Mei X, Bai Y. [Digoxin alleviates pulmonary fibrosis by regulating phosphatidylinositol-3-kinase/Akt signaling through inhibiting the activation of fibroblast: an in *vivo* and in *vitro* experiment]. *Zhonghua Wei Zhong Bing Ji Jiu Yi Xue.* (2022) 34:1161–6. doi: 10.3760/cma.j.cn121430-20220628-00508

87. Ashbrook AW, Lentscher AJ, Zamora PF, Silva LA, May NA, Bauer JA, et al. Antagonism of the sodium-potassium ATPase impairs chikungunya virus infection. *mBio* (2016) 7:e00693–16. doi: 10.1128/mBio.00693-16

88. Papale M, Buccarelli M, Mollinari C, Russo MA, Pallini R, Ricci-Vitiani L, et al. Hypoxia, inflammation and necrosis as determinants of glioblastoma cancer stem cells progression. *Int J Mol Sci* (2020) 21:2660. doi: 10.3390/ijms21082660

89. Yu Z, Li Y, Li Y, Zhang J, Li M, Ji L, et al. Bufalin stimulates antitumor immune response by driving tumor-infiltrating macrophage toward M1 phenotype in hepatocellular carcinoma. *J Immunother. Cancer* (2022) 10:e004297. doi: 10.1136/jitc-2021-004297

90. Zhang D, Jia T, Chen X, Jiang H, Guo T, Dong J, et al. Bufalin reverses ABCB1-mediated resistance to docetaxel in breast cancer. *Heliyon* (2023) 9:e13840. doi: 10.1016/j.heliyon.2023.e13840

91. Qian Z, Tian X, Miao Y, Xu X, Cheng X, Wu M, et al. Bufalin inhibits the proliferation of lung cancer cells by suppressing Hippo-YAP pathway. *Cell Signal* (2023) 109:110746. doi: 10.1016/j.cellsig.2023.110746

92. Miao L, Liu Y, Ali NM, Dong Y, Zhang B, Cui X. Bufalin serves as a pharmaceutic that mitigates drug resistance. *Drug Metab Rev* (2023) 55(3):195–204. doi: 10.1080/03602532.2023.2206065

93. Shi S, Zhao S, Tian X, Liu F, Lu X, Zang H, et al. Molecular and metabolic mechanisms of bufalin against lung adenocarcinoma: New and comprehensive evidences from network pharmacology, metabolomics and molecular biology experiment. *Comput Biol Med* (2023) 157:106777. doi: 10.1016/j.compbiomed.2023.106777

94. Thakre A, Zore G, Kodgire S, Kazi R, Mulange S, Patil R, et al. Limonene inhibits Candida albicans growth by inducing apoptosis. *Med Mycol* (2018) 56:565–78. doi: 10.1093/mmy/myx074

95. Araújo-Filho HGD, Dos Santos JF, Carvalho MTB, Picot L, Fruitier-Arnaudin I, Groult H, et al. Anticancer activity of limonene: A systematic review of target signaling pathways. *Phytother. Res* (2021) 35:4957–70. doi: 10.1002/ptr.7125

96. Chebet JJ, Ehiri JE, McClelland DJ, Taren D, Hakim IA. Effect of d-limonene and its derivatives on breast cancer in human trials: a scoping review and narrative synthesis. *BMC Cancer.* (2021) 21:902. doi: 10.1186/s12885-021-08639-1

97. Leung JC, Cassimeris L. Reorganization of paclitaxel-stabilized microtubule arrays at mitotic entry: roles of depolymerizing kinesins and severing proteins. *Cancer Biol Ther* (2019) 20:1337–47. doi: 10.1080/15384047.2019.1638678

98. Su M, Zhao C, Li D, Cao J, Ju Z, Kim EL, et al. Viriditoxin stabilizes microtubule polymers in SK-OV-3 cells and exhibits antimitotic and antimetastatic potential. *Mar Drugs* (2020) 18:445. doi: 10.3390/md18090445

99. Wong YK, Xu C, Kalesh KA, He Y, Lin Q, Wong WSF, et al. Artemisinin as an anticancer drug: Recent advances in target profiling and mechanisms of action. *Med Res Rev* (2017) 37:1492–517. doi: 10.1002/med.21446

100. Tin AS, Sundar SN, Tran KQ, Park AH, Poindexter KM, Firestone GL. Antiproliferative effects of artemisinin on human breast cancer cells requires the downregulated expression of the E2F1 transcription factor and loss of E2F1-target cell cycle genes. *Anticancer. Drugs* (2012) 23:370–9. doi: 10.1097/CAD.0b013e32834f6ea8

101. Xu G, Huang Y-L, Li P, Guo H-M, Han X-P. Neuroprotective effects of artemisinin against isoflurane-induced cognitive impairments and neuronal cell death involve JNK/ERK1/2 signalling and improved hippocampal histone acetylation in neonatal rats. *J Pharm Pharmacol* (2017) 69:684–97. doi: 10.1111/jphp.12704

102. He J, Yu S, Zhu H, Wu J, Qin Z. Triptolide inhibits NF-kappaB activation and reduces injury of donor lung induced by ischemia/reperfusion, Acta Pharmacol. *Sin* (2007) 28:1919–23. doi: 10.1111/j.1745-7254.2007.00701.x

103. Jiang S, Wan F, Lian H, Lu Z, Li X, Cao D, et al. Friend or foe? The dual role of triptolide in the liver, kidney, and heart. *Biomed Pharmacother. Biomedecine Pharmacother* (2023) 161:114470. doi: 10.1016/j.biopha.2023.114470

104. Liu W, Yang Y, Wang J, Wu S, Chen Z. Triptolide-mediated downregulation of FLIPS in hepatoma cells occurs at the post-transcriptional level independently of proteasome-mediated pathways. *Med Oncol Northwood Lond Engl* (2022) 40:7. doi: 10.1007/s12032-022-01857-y

105. Ganguly S, Home T, Yacoub A, Kambhampati S, Shi H, Dandawate P, et al. Targeting HSF1 disrupts HSP90 chaperone function in chronic lymphocytic leukemia. *Oncotarget* (2015) 6:31767–79. doi: 10.18632/oncotarget.5167

106. El-Baba C, Baassiri A, Kiriako G, Dia B, Fadlallah S, Moodad S, et al. Terpenoids' anti-cancer effects: focus on autophagy. *Apoptosis Int J Program. Cell Death* (2021) 26:491–511. doi: 10.1007/s10495-021-01684-y

107. Wang G, Guo H, Ren Y, Chen W, Wang Y, Li J, et al. Triptolide enhances carboplatin-induced apoptosis by inhibiting nucleotide excision repair (NER) activity in melanoma. *Front Pharmacol* (2023) 14:1157433. doi: 10.3389/fphar.2023.1157433

108. Cai J, Zhong M, Xu J, Cheng H, Xu S. Codelivery of triptolide and IFN-γ to boost antitumor immunity for triple-negative breast cancer. *Int Immunopharmacol* (2023) 120:110346. doi: 10.1016/j.intimp.2023.110346

109. Khan T, Date A, Chawda H, Patel K. Polysaccharides as potential anticancer agents-A review of their progress. *Carbohydr. Polym* (2019) 210:412–28. doi: 10.1016/j.carbpol.2019.01.064

110. Zhou M, Yue Y, Wang Y, Yan S. Polysaccharides from Chinese herbs as natural weapons against colorectal cancer. *Biosci Rep* (2023) 43:BSR20230041. doi: 10.1042/BSR20230041

111. Li M, Li H, Fang F, Deng X, Ma S. Astragaloside IV attenuates cognitive impairments induced by transient cerebral ischemia and reperfusion in mice *via* anti-inflammatory mechanisms. *Neurosci Lett* (2017) 639:114–9. doi: 10.1016/j.neulet.2016.12.046

112. Ji X, Su L, Zhang P, Yue Q, Zhao C, Sun X, et al. Lentinan improves intestinal inflammation and gut dysbiosis in antibiotics-induced mice. *Sci Rep* (2022) 12:19609. doi: 10.1038/s41598-022-23469-2

113. You J, Wu Q, Li Y, Li X, Lin Z, Huang J, et al. Lentinan induces apoptosis of mouse hepatocellular carcinoma cells through the EGR1/PTEN/AKT signaling axis. *Oncol Rep* (2023) 50:142. doi: 10.3892/or.2023.8579

114. Xu H, Qi Z, Zhao Q, Xue J, Zhu J, He Y, et al. Lentinan enhances the antitumor effects of Delta-like 1 *via* neutrophils. *BMC Cancer.* (2022) 22:918. doi: 10.1186/s12885-022-10011-w

115. Li M, Du X, Yuan Z, Cheng M, Dong P, Bai Y. Lentinan triggers oxidative stress-mediated anti-inflammatory responses in lung cancer cells. *Mol Cell Biochem* (2022) 477:469–77. doi: 10.1007/s11010-021-04293-0

116. Yao L-C, Wu L, Wang W, Zhai L-L, Ye L, Xiang F, et al. Panax notoginseng Saponins Promote Cell Death and Chemosensitivity in Pancreatic Cancer through the Apoptosis and Autophagy Pathways. *Anticancer Agents Med Chem* (2021) 21:1680–8. doi: 10.2174/1871520620999201110191459

117. Xia L, Liu X, Mao W, Guo Y, Huang J, Hu Y, et al. Panax notoginseng saponins normalises tumour blood vessels by inhibiting EphA2 gene expression to modulate the tumour microenvironment of breast cancer. *Phytomedicine Int J Phytother. Phytopharm* (2023) 114:154787. doi: 10.1016/j.phymed.2023.154787

118. Li S, Pi G, Zeng Y, Ruan C, He X, Xiong X, et al. Notoginsenoside R1 induces oxidative stress and modulates LPS induced immune microenvironment of nasopharyngeal carcinoma. *Int Immunopharmacol* (2022) 113:109323. doi: 10.1016/j.intimp.2022.109323

119. Lin M-H, Lee Y-H, Cheng H-L, Chen H-Y, Jhuang F-H, Chueh PJ. Capsaicin inhibits multiple bladder cancer cell phenotypes by inhibiting tumor-associated NADH oxidase (tNOX) and sirtuin1 (SIRT1). *Mol Basel Switz* (2016) 21:849. doi: 10.3390/molecules21070849

120. Thoennissen NH, O'Kelly J, Lu D, Iwanski GB, La DT, Abbassi S, et al. Capsaicin causes cell-cycle arrest and apoptosis in ER-positive and -negative breast cancer cells by modulating the EGFR/HER-2 pathway. *Oncogene* (2010) 29:285–96. doi: 10.1038/onc.2009.335

121. Jin J, Lin G, Huang H, Xu D, Yu H, Ma X, et al. Capsaicin mediates cell cycle arrest and apoptosis in human colon cancer cells *via* stabilizing and activating p53. *Int J Biol Sci* (2014) 10:285–95. doi: 10.7150/ijbs.7730

122. Chen Z-Y, Huang H-H, Li Q-C, Zhan F-B, Wang L-B, Yang C-H, et al. Capsaicin reduces cancer stemness and inhibits metastasis by downregulating SOX2 and EZH2 in osteosarcoma. *Am J Chin Med* (2023) 51:1–26. doi: 10.1142/S0192415X23500489

123. Wang J, Tian W, Wang S, Wei W, Wu D, Wang H, et al. Anti-inflammatory and retinal protective effects of capsaicin on ischaemia-induced injuries through the release of endogenous somatostatin. *Clin Exp Pharmacol Physiol* (2017) 44:803–14. doi: 10.1111/1440-1681.12769

124. Que T, Ren B, Fan Y, Liu T, Hou T, Dan W, et al. Capsaicin inhibits the migration, invasion and EMT of renal cancer cells by inducing AMPK/mTOR-mediated autophagy. *Chem Biol Interact* (2022) 366:110043. doi: 10.1016/j.cbi.2022.110043

125. Yahfoufi N, Alsadi N, Jambi M, Matar C. The immunomodulatory and anti-inflammatory role of polyphenols. *Nutrients* (2018) 10:1618. doi: 10.3390/nu10111618

126. Rana A, Samtiya M, Dhewa T, Mishra V, Aluko RE. Health benefits of polyphenols: A concise review. *J Food Biochem* (2022) 46(10):e14264. doi: 10.1111/jfbc.14264

127. Maleki Dana P, Sadoughi F, Asemi Z, Yousefi B. The role of polyphenols in overcoming cancer drug resistance: a comprehensive review. *Cell Mol Biol Lett* (2022) 27:1. doi: 10.1186/s11658-021-00301-9

128. Tong Q, Wu Z. Curcumin inhibits colon cancer Malignant progression and promotes T cell killing by regulating miR-206 expression. *Clin Anat. N Y. N* (2023). doi: 10.1002/ca.24057

129. Gao L, Zhao M, Mao Y, Zhang L, Wang X, Li S, et al. Localized microsphere/hydrogel for tumor immunotherapy of cardiac glycoside with minimal toxicity. *ACS Appl Mater Interfaces* (2023) 15:578–90. doi: 10.1021/acsami.2c18693

130. Bejček J, Jurášek M, Spiwok V, Rimpelová S. Quo vadis cardiac glycoside research? *Toxins* (2021) 13:344. doi: 10.3390/toxins13050344

131. Zhao W, Li G, Zhang Q, Chen M, He L, Wu Z, et al. Cardiac glycoside neriifolin exerts anti-cancer activity in prostate cancer cells by attenuating DNA damage repair through endoplasmic reticulum stress. *Biochem Pharmacol* (2023) 209:115453. doi: 10.1016/j.bcp.2023.115453

132. Soumoy L, Ghanem GE, Saussez S, Journe F. Bufalin for an innovative therapeutic approach against cancer. *Pharmacol Res* (2022) 184:106442. doi: 10.1016/j.phrs.2022.106442

133. Kamran S, Sinniah A, Abdulghani MAM, Alshawsh MA. Therapeutic potential of certain terpenoids as anticancer agents: A scoping review. *Cancers* (2022) 14:1100. doi: 10.3390/cancers14051100

134. Zhao D, Chen X, Wang L, Zhang J, Lv R, Tan L, et al. Improvement influenza vaccine immune responses with traditional Chinese medicine and its active ingredients. *Front Microbiol* (2023) 14:1111886. doi: 10.3389/fmicb.2023.1111886

135. Man S, Gao W, Zhang Y, Huang L, Liu C. Chemical study and medical application of saponins as anti-cancer agents. *Fitoterapia* (2010) 81:703–14. doi: 10.1016/j.fitote.2010.06.004

136. Chen Z-J, Cheng J, Huang Y-P, Han S-L, Liu N-X, Zhu G-B, et al. [Effect of adjuvant chemotherapy of ginsenoside Rg3 combined with mitomycin C and tegafur in advanced gastric cancer]. *Zhonghua Wei Chang Wai Ke Za Zhi Chin J Gastrointest. Surg* (2007) 10:64–6.

137. Zhou P, Shi W, He X-Y, Du Q-Y, Wang F, Guo J. Saikosaponin D: review on the antitumour effects, toxicity and pharmacokinetics. *Pharm Biol* (2021) 59:1478–87. doi: 10.1080/13880209.2021.1992448

138. Kamaruddin MF, Hossain MZ, Mohamed Alabsi A, Mohd Bakri M. The antiproliferative and apoptotic effects of capsaicin on an oral squamous cancer cell line of Asian origin, ORL-48. *Med Kaunas Lith* (2019) 55:322. doi: 10.3390/medicina55070322

139. Baxevanis CN, Perez SA, Papamichail M. Cancer immunotherapy. *Crit Rev Clin Lab Sci* (2009) 46:167–89. doi: 10.1080/10408360902937809

140. O'Donnell JS, Teng MWL, Smyth MJ. Cancer immunoediting and resistance to T cell-based immunotherapy. *Nat Rev Clin Oncol* (2019) 16(3):151–67. doi: 10.1038/s41571-018-0142-8

141. Magré L, Verstegen MMA, Buschow S, van der Laan LJW, Peppelenbosch M, Desai J. Emerging organoid-immune co-culture models for cancer research: from oncoimmunology to personalized immunotherapies. *J Immunother. Cancer* (2023) 11: e006290. doi: 10.1136/jitc-2022-006290

142. Saúde-Conde R, Nguyen D, Hendlisz A. Immunotherapies in non-metastatic gastrointestinal cancers. *Curr Opin Oncol* (2023) 35(4):334–46. doi: 10.1097/CCO.0000000000000956

143. Budhu A, Pehrsson EC, He A, Goyal L, Kelley RK, Dang H, et al. Tumor biology and immune infiltration define primary liver cancer subsets linked to overall survival after immunotherapy. *Cell Rep Med* (2023) 4(6):101052. doi: 10.1016/j.xcrm.2023.101052

144. Hu H, Wang K, Jia R, Zeng Z-X, Zhu M, Deng Y-L, et al. Current status in rechallenge of immunotherapy. *Int J Biol Sci* (2023) 19:2428–42. doi: 10.7150/ijbs.82776

145. Lin M, Sun X, Lv L. New insights and options into the mechanisms and effects of combined targeted therapy and immunotherapy in prostate cancer. *Mol Ther Oncolytics* (2023) 29:91–106. doi: 10.1016/j.omto.2023.04.007

146. Liu S, Zhu J-J, Li J-C. The interpretation of human body in traditional Chinese medicine and its influence on the characteristics of TCM theory. *Anat. Rec. Hoboken NJ* (2021) 2007. 304:2559–65. doi: 10.1002/ar.24643

147. Zhang A, Sun H, Wang P, Han Y, Wang X. Future perspectives of personalized medicine in traditional Chinese medicine: a systems biology approach. *Complement. Ther Med* (2012) 20:93–9. doi: 10.1016/j.ctim.2011.10.007

148. Galon J, Bruni D. Tumor immunology and tumor evolution: intertwined histories. *Immunity* (2020) 52:55–81. doi: 10.1016/j.immuni.2019.12.018

149. Nicolaides NC, O'Shannessy DJ, Albone E, Grasso L. Co-development of diagnostic vectors to support targeted therapies and theranostics: essential tools in personalized cancer therapy. *Front Oncol* (2014) 4:141. doi: 10.3389/fonc.2014.00141

150. Tilak T.V.S.V.G.K., Patel A, Kapoor A. Molecular basis and clinical application of targeted therapy in oncology. *Med J Armed Forces India.* (2023) 79:128–35. doi: 10.1016/j.mjafi.2023.02.001

151. Wang Z-D, Wang Y-M, Li K, Shi J, Wang F-Y. The comparison of the wisdom view in Chinese and Western cultures. *Curr Psychol* (2022) 41:8032–43. doi: 10.1007/s12144-020-01226-w

frontiers | Frontiers in Immunology

TYPE Original Research
PUBLISHED 24 November 2023
DOI 10.3389/fimmu.2023.1281888

Check for updates

OPEN ACCESS

EDITED BY
Jie Mei,
Wuxi People's Hospital Affiliated to Nanjing Medical University, China

REVIEWED BY
Jianzhong Cao,
Shanxi Provincial Cancer Hospital, China
Bing Xia,
Hangzhou Cancer Hospital, China

*CORRESPONDENCE
Nan Bi
binan_email@163.com
Ye-Xiong Li
yexiong12@163.com

†These authors have contributed equally to this work

RECEIVED 23 August 2023
ACCEPTED 13 November 2023
PUBLISHED 24 November 2023

CITATION
Yang Y, Wang J, Zhang T, Zhou Z, Wang Y, Jiang Y, Liu W, Xiao Z, Deng L, Feng Q, Wang X, Lv J, Wang W, Xue Q, Wang J, Li Y-X and Bi N (2023) Efficacy and safety of definitive chemoradiotherapy with or without induction immune checkpoint inhibitors in patients with stage III non-small cell lung cancer.
Front. Immunol. 14:1281888.
doi: 10.3389/fimmu.2023.1281888

COPYRIGHT
© 2023 Yang, Wang, Zhang, Zhou, Wang, Jiang, Liu, Xiao, Deng, Feng, Wang, Lv, Wang, Xue, Wang, Li and Bi. This is an open-access article distributed under the terms of the Creative Commons Attribution License (CC BY). The use, distribution or reproduction in other forums is permitted, provided the original author(s) and the copyright owner(s) are credited and that the original publication in this journal is cited, in accordance with accepted academic practice. No use, distribution or reproduction is permitted which does not comply with these terms.

Efficacy and safety of definitive chemoradiotherapy with or without induction immune checkpoint inhibitors in patients with stage III non-small cell lung cancer

Yin Yang[1†], Jianyang Wang[1†], Tao Zhang[1], Zongmei Zhou[1], Yu Wang[1], Ying Jiang[1], Wenyang Liu[1], Zefen Xiao[1], Lei Deng[1], Qinfu Feng[1], Xin Wang[1], Jima Lv[1], Wenqing Wang[1], Qi Xue[2], Jie Wang[3], Ye-Xiong Li[4*] and Nan Bi[4*]

[1]Department of Radiation Oncology, National Cancer Center/National Clinical Research Center for Cancer/Cancer Hospital, Chinese Academy of Medical Sciences and Peking Union Medical College, Beijing, China, [2]Department of Thoracic Surgery, National Cancer Center/National Clinical Research Center for Cancer/Cancer Hospital, Chinese Academy of Medical Sciences and Peking Union Medical College, Beijing, China, [3]State Key Laboratory of Molecular Oncology, Department of Medical Oncology, National Cancer Center/National Clinical Research Center for Cancer/Cancer Hospital, Chinese Academy of Medical Sciences and Peking Union Medical College, Beijing, China, [4]State Key Laboratory of Molecular Oncology, Department of Radiation Oncology, National Cancer Center/National Clinical Research Center for Cancer/Cancer Hospital, Chinese Academy of Medical Sciences and Peking Union Medical College, Beijing, China

Background: In the era of immunotherapy, the optimal combination of immune checkpoint inhibitors (ICIs) and chemoradiotherapy (CRT) for stage III non-small cell lung cancer (NSCLC) is not defined. The current study investigated the efficacy and safety of definitive CRT(dCRT) plus consolidation ICIs with or without induction ICIs in stage III NSCLC.

Methods: 123 consecutive patients treated with dCRT followed by consolidation ICIs at our institution from 2018 to 2022 were retrospectively reviewed. Failure patterns, survival outcomes, and toxicity profiles were analyzed.

Results: The 1- and 2- year PFS rates were 75.3% and 56.9%, respectively, and median PFS was 30.83 months from the start of treatment. In-field failure (18.7%) was the most common failure pattern. The most common adverse event (AE) was pneumonitis caused by ICIs or RT. The incidence of Grade 3-4 and Grade 5 pneumonitis was 5.7% and 1.6%, respectively. Further analysis showed that the induction plus consolidation ICIs group has significantly lower cumulative incidence of distant metastasis rates (HR: 0.30, 95%CI: 0.09-1.00, p=0.043) and higher incidence of pneumonitis (p=0.039) compared with patients in the consolidation ICIs group.

Conclusions: Combined CRT and consolidation ICIs achieved encouraging efficacy and manageable toxicity in patients with stage III NSCLC in China. Induction plus consolidation ICIs might reduce distant metastasis and deserve further investigation.

KEYWORDS

stage III non-small cell lung cancer, chemoradiotherapy, immune checkpoint inhibitors, efficacy, safety

Introduction

Approximately one third of patients with non–small-cell lung cancer (NSCLC) are initially diagnosed at stage III, locally advanced disease (1, 2). The results of the PACIFIC trial demonstrated significantly improved survival benefit by adding immune checkpoint inhibitors (ICIs) to definitive chemoradiotherapy (dCRT) (3). However, the updated survival analyses showed that the 5-year progression-free survival (PFS) rate was 33.1% with consolidation durvalumab, which indicated that nearly 70% of stage III NSCLC is not controlled (4). Thus, more effective treatment is urgently needed and being explored (5–8).

Novel treatment strategies used in a variety of ongoing trials are under evaluation to improve outcomes in this setting, including different anti-programmed cell death protein 1/programmed death-ligand 1(anti-PD-1/anti-PD-L1) antibodies after CRT, induction ICIs with or without chemotherapy before CRT, etc (9). The main reason for upfront ICIs before CRT is to engage immunotherapy on the basis of a healthy immune system, not impaired by chemoradiotherapy (10). Both preclinical (11) and clinical (12) studies have demonstrated that induction ICIs play a key role in activating immune surveillance against micrometastatic disease and deducing distant metastasis. Our retrospective study of induction ICIs plus chemotherapy followed by dCRT for bulky locally advanced NSCLC has shown the similar PFS and overall survival (OS) compared with those reported in the PACIFIC trial (13). Two prospective studies investigating induction ICIs followed by CRT and consolidation ICIs in stage III NSCLC, also showed the comparable PFS with PACIFIC trial (7) (14). However, cross-trial comparison is particularly challenging in these settings due to the different time of ICIs delivery and different trial inclusion and exclusion criteria.

Therefore, we assessed the benefit of the adding induction ICIs plus chemotherapy before dCRT in stage III NSCLC and exploring the optimal combination of ICIs and CRT.

Methods

Patient population

This study was approved by our institutional review board of Cancer Hospital, Chinese Academy of Medical Sciences. Consecutive patients treated with dCRT followed by consolidation ICIs with or without induction ICIs plus chemotherapy at our institution from September 2018 to June 2022 now were retrospectively reviewed. The inclusion criteria for the study were patients who had a pathologically confirmed unresectable stage III NSCLC according to the 8th AJCC staging system, undergone dCRT and consolidation anti-PD-1/anti-PD-L1 ICIs, ≥18 years of age, >6 months follow-up. The exclusion criteria were patients who received surgery, or palliative treatment, non-completion of radiotherapy, with incomplete clinical information and so on.

Treatment strategy

All patients received intensity modulated radiation therapy or volumetric modulated arc radiation therapy with the prescribed dose of 60 Gy, concurrently or sequentially combined with platinum-based doublet chemotherapy. Radiation therapy simulation was performed using 4-dimensional computed tomography (4D-CT) scans for all patients. The gross target volume (GTV) of the primary tumor (GTVp) was defined as the primary tumor delineated on simulation CT images, and the GTV of the lymph nodes (GTVn) was defined as any regionally involved lymph nodes with short axis >1 cm on pretreatment CT or high fluorodeoxyglucose uptake on positron emission tomography scans. For patients received induction chemotherapy with or without immunotherapy, GTVp and GTVn included the post-induction volume on the 4D-CT. The clinical target volume (CTV) comprised a margin of 0.5 cm beyond the GTV (GTVp plus GTVn) and the pre-treatment involved hilar and mediastinal nodal regions, even when the enlarged lymph nodes disappeared after induction therapy. The PTV included a margin of 0.5 cm beyond the CTV. Details of simulation, target volume definition, prescription, planning were published previously (13, 15). Patients without severe adverse events (AEs) during induction treatment and CRT could further be treated with consolidation immunotherapy for up to 1 year.

Data collection

Baseline demographic and therapeutic data, including age, ECOG status, sex, smoking history, NSCLC pathology, cancer staging, epidermal growth factor receptor (EGFR) and PD-L1 expression, radiotherapy dose and technology, ICIs cycle and

sequence, and so on, were extracted from electronic medical records. The toxicities were graded according to the Common Terminology Criteria for Adverse Events, version 5.0. During the follow-up, radiographic imaging was performed every 12 weeks for 2 years, every 6 months to 5 years, and then every year until tumor progression. The tumor response evaluation was according to Response Evaluation Criteria in Solid Tumors version 1.1. Locoregional failure (LR) was defined as clinical and/or biopsy-proven recurrence in the primary tumor or the ipsilateral hilum, mediastinum, or supraclavicular, irrespective of distant metastasis. Distant metastasis (DM) was defined as any evidence of metastatic disease beyond locoregional regions previously mentioned. Locoregional failure was further classified as in-field failure or out-field failure based on the component of disease progression occurring within or without the 95% isodose line, respectively.

Statistical analysis

All data are expressed as median (interquartile, IQR) for continuous variables and as numbers (percentages) for categorical variables. Intergroup comparisons were performed using Mann-Whitney U test for continuous variables and the chi-square test or Fisher's exact test when appropriate for categorical variables. One to one propensity score matching (PSM) was conducted to adjust for prespecified baseline characteristics that were potentially confounding variables. PFS was defined as the time from first treatment to the first documented event of tumor progression or death in the absence of disease progression. OS was defined as the time from first treatment to death from any cause. In the exploratory analysis for subgroup patients received consolidation ICIs, OS and PFS was further calculated from 6 weeks after RT, to better compare with the PACIFIC trial. Kaplan-Meier survival analysis was used to evaluate the PFS and OS. To properly evaluate the patterns of failure, the first site of recurrence (locoregional or distant) was analyzed by considering death as a competing risk, respectively. Univariate Cox regression model was used to calculate hazard ratio (HR) and 95% confidence interval (CI). All tests were two sided, and statistical significance was set at a p-value <0.05. Statistical analysis was performed with SPSS (version 26.0), data visualization was performed using R software (version 4.1.1).

Result

Patient characteristics

A total of 123 patients were identified. The baseline demographic and therapeutic characteristics of patients are presented in Table 1. The median age was 65 years (IQR, 57-67 years). There were 106 males (86.2%), 93 smokers (75.6%), 73 patients (59.3%) with squamous cell carcinoma, 63 patients (51.2%) presented with stage IIIB and 19 (15.4%) with stage IIIC, 79 (64.2%) patients received concurrent CRT. The median number of ICIs cycles was 12 (IQR, 6-22). 71 patients (57.7%) received the first dose of ICIs within 42 days after RT, and 67 patients (54.5%) received anti-PD-L1 ICIs which included durvalumab and sugemalimab, and other consolidation ICI drugs included pembrolizumab, camrelizumab, tislelizumab, toripalimab, sintilimab, nivolumab, atezolizumab and penpulimab. 41 patients received induction ICIs plus chemotherapy before CRT (induction plus consolidation ICIs group), all of the induction ICIs were anti-PD-1 drugs and the median number of induction ICIs cycles was 3 (IQR, 2-4). 82 patients received the first dose of ICIs followed CRT (consolidation ICIs group). Baseline characteristics were well balanced between the two groups, except a high proportion of patients in consolidated ICIs group received concurrent CRT, anti-PD-L1 ICIs, had stage N3 disease and were younger compared with induction plus consolidation ICIs group.

Survival outcome

With a median follow-up of 25.57 months (IQR 18.8-32.4), 52 patients (42.3%) had experienced disease progression and 23 patients (18.7%) had died. The 1-, 2- and 3- year OS rates were 94.2%, 82.5% and 77.9%, respectively, and median OS was not reached (Figure 1A). The 1-, 2- and 3- year PFS rates were 75.3%, 56.9% and 47.4%, respectively, and median PFS was 30.83 months for the entire cohort (Figure 1B). There was no significant difference in OS rate (HR: 0.81, 95%CI: 0.32-2.05, p=0.650) and PFS rate (HR: 1.07, 95%CI: 0.62-1.87, p=0.801) between the induction plus consolidation ICIs group and consolidation ICIs group (Figures 1C, D). However, a trend for PFS benefit with induction ICIs plus chemotherapy was observed in some subgroups, including patients with age younger than 65 years, stage N3 disease, concurrent CRT, and the number of induction ICIs cycles less than or equal to 3 (Supplementary Figure 1).

82 patients received the first dose of anti-PD-1/PD-L1 ICIs followed CRT, and the number of patients received durvalumab is 53, which represent the real-world data of Pacific regimen in China. The survival analysis for the 82 patients showed that the 1-, 2- and 3-year OS rates calculated from 6 weeks after RT were 90.1%, 78.9% and 76.8%, respectively, and median OS was not reached (Supplementary Figure 2A). The 1-, 2- and 3-year PFS rates calculated from 6 weeks after RT were 63.0%, 52.9% and 46.6%, respectively, and median PFS was 33.23 months (Supplementary Figure 2B).

Duration of consolidation ICIs discontinuation

By the time of the analysis, 51(42.3%) patients have completed 12 months or more consolidation ICIs, 5 patients were continuing the consolidation ICIs, and 67 patients had discontinued consolidation ICIs due to various reasons. The most frequent cause leading to discontinuation of consolidation ICIs was pneumonitis caused by ICIs or RT, which accounted for 22.8% of the total cases, the other reasons included disease progression (19.5%), other ICIs related AEs (2.4%), pneumonia (2.4%) and patient decision (6.5%) (Supplementary Table 1).

10.3389/fimmu.2023.1281888

TABLE 1 Baseline characteristics (N=123).

	Total (n=123)	Induction plus consolidation ICIs (n=41)	Consolidation ICIs (n=82)	p
Age, median (IQR), y	63 (57-67)	66 (58.0-69.0)	62 (55.75-67.0)	0.020*
ECOG				0.564
0	24 (19.5)	10 (24.4)	14 (17.1)	
1	97 (78.9)	30 (73.2)	67 (81.7)	
2	2 (1.6)	1 (2.4)	1 (1.2)	
Sex				0.854
Male	106 (86.2)	35 (85.4)	71 (86.6)	
Female	17 (13.8)	6 14.6)	11 (13.4)	
Smoking history				0.373
Yes	93 (75.6)	29 (70.7)	64 (78.0)	
No	30 (24.4)	12 (29.3)	18 (22.0)	
Pathology, n(%)				0.069
Squamous cell carcinoma	73 (59.3)	29 (70.7)	44 (53.7)	
Non-squamous carcinoma	50 (40.7)	12 (29.3)	38 (46.3)	
T stage, n(%)				0.204
T1	15 (12.2)	2 (4.9)	13 (15.9)	
T2	39 (31.7)	14 (34.1)	25 (30.5)	
T3	32 (26)	14 (34.1)	18 (22)	
T4	37 (30.1)	11 (26.8)	26 (31.7)	
N stage, n(%)				0.016*
N0	4 (3.3)	1 (2.4)	3 (3.7)	
N1	11 (8.9)	5 (12.2)	6 (7.3)	
N2	68 (55.3)	29 (70.7)	39 (47.6)	
N3	40 (32.5)	6 (14.6)	34 (41.5)	
TNM stage, n(%)				0.211
IIIA	41 (33.3)	15 (36.6)	26 (31.7)	
IIIB	63 (51.2)	23 (56.1)	40 (48.8)	
IIIC	19 (15.4)	3 (7.3)	16 (19.5)	
PD-L1 status, n(%)				0.554
<1%	17 (13.8)	6 (14.6)	11 (13.4)	
≥1%	35 (28.5)	14 (34.1)	21 (25.6)	
NA	71 (57.7)	21 (51.2)	50 (61.0)	
EGFR status, n(%)				0.392
Mutated	4 (3.3)	1 (2.4)	3 (3.7)	
Wild type	26 (21.1)	6 (14.6)	20 (24.4)	
NA	93 (75.6)	34 (82.9)	59 (72.0)	
Concurrent CRT, n(%)				0.011*
Yes	79 (64.2)	20 (48.8)	59 (69.5)	

(Continued)

TABLE 1 Continued

	Total (n=123)	Induction plus consolidation ICIs (n=41)	Consolidation ICIs (n=82)	p
No	44 (35.8)	21 (51.2)	23 (30.5)	
ICIs cycle, median (IQR)	12 (6-22)	12 (7-21.5)	12 (5-22)	0.473
Time of ICIs post RT, n(%)				0.302
≤42	71 (57.7)	21 (51.2)	50 (61.0)	
>42	52 (42.3)	20 (48.8)	32 (39.0)	
Consolidation ICIs regimen, n(%)				<0.001*
Anti-PD-L1	67 (54.5)	13 (31.7)	54 (65.9)	
Anti-PD-1	56 (45.5)	28 (68.3)	28 (34.1)	

*p < 0.05.
IQR, interquartile range; ECOG, Eastern Cooperative Oncology Group; PD-L1, programmed death ligand-1; EGFR, epidermal growth factor receptor; CRT, chemoradiotherapy; ICIs, immune checkpoint inhibitors; RT, radiotherapy; PD-1, programmed cell death-1.

Pattern of progression

31 patients (25.2%) experienced locoregional progression as the site of first failure, and 21 patients (17.1%) experienced distant metastasis as the site of first failure in the entire cohort (Figure 2). The 1-, 2- and 3-year cumulative incidence of locoregional progression rates were 9.9%, 24.5% and 30.6%, respectively (Figure 3A). The 1-, 2- and 3- year cumulative incidence of distant metastasis rates were 10.9%, 15.6% and 22.2%, respectively (Figure 3B).

The patterns of first failure were different between these two groups. Specifically, locoregional progression and distant metastasis were observed in 12 (29.3%) and 2 (4.9%) patients, respectively in the induction plus consolidation ICIs group and 19 (23.2%) and 19 (23.2%) patients, respectively in the consolidation ICIs group. And the rate of distant metastasis was significantly lower in the induction plus consolidation ICIs group than consolidation ICIs group (p=0.011) (Supplementary Table 2). Further analysis for the 31 patients who had locoregional progression as the site of first failure showed that in-field failure and out-field failure developed in 9 (22.0%) and 3 (7.3%) patients, respectively in the induction plus consolidation ICIs group and 14 (17.1%) and 5 (6.1%) patients, respectively in the consolidation ICIs group (Figure 2). There was no significant difference in cumulative incidence of locoregional progression rate (HR: 1.39, 95%CI: 0.67-2.87, p=0.323) between the

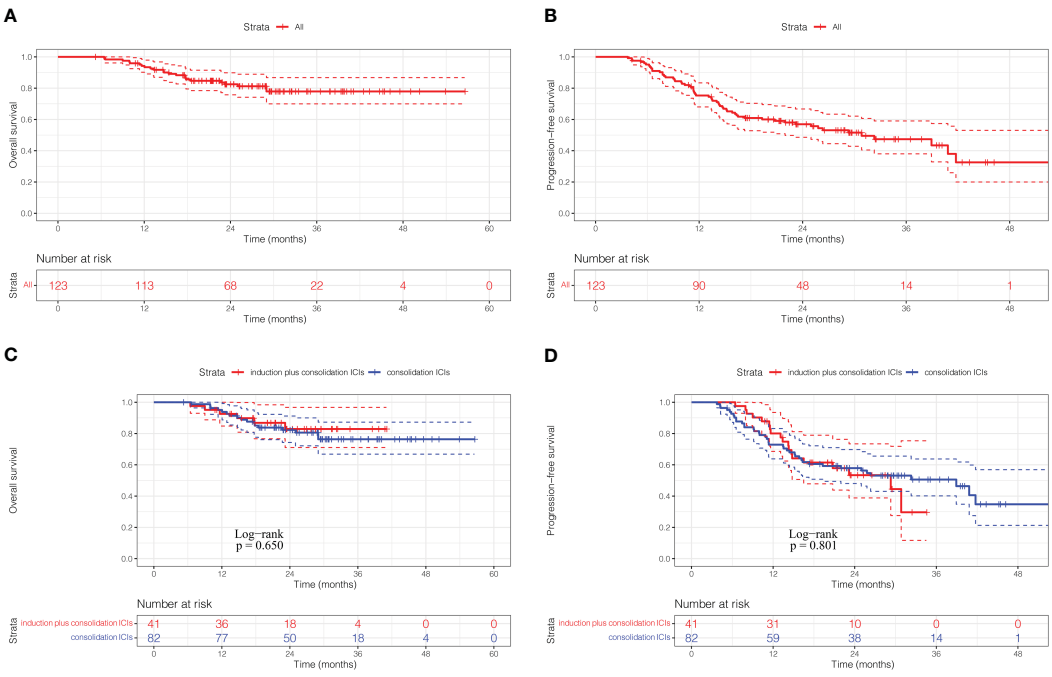


FIGURE 1
Kaplan-Meier curves of overall survival **(A)** and progression-free survival **(B)** for the full analysis set. Kaplan-Meier curves of overall survival **(C)** and progression-free survival **(D)** according to ICIs sequence. ICIs, immune checkpoint inhibitors.

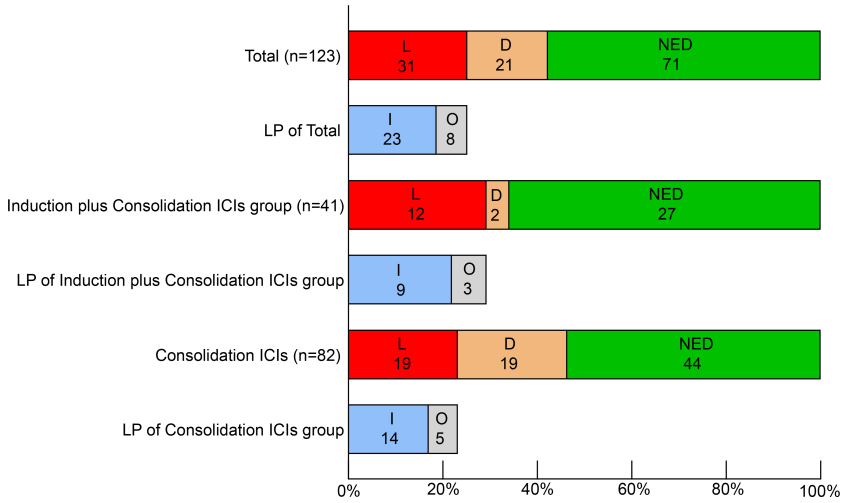


FIGURE 2
Patterns of first failure. L, locoregional progression. D, distant metastasis, NED, no evidence of disease. I, in-field failure. O, out-field failure. ICIs, immune checkpoint inhibitors.

induction plus consolidation ICIs group and consolidation ICIs group (Figure 3C). However, induction plus consolidation ICIs reduced cumulative incidence of distant metastasis rates significantly (HR: 0.23, 95%CI: 0.05-0.94, p=0.030). Specifically, the 1- and 2 - year cumulative incidence of distant metastasis rates were 4.9% and 4.9%, respectively in the induction plus consolidation ICIs group and 14.0% and 20.5%, respectively in the consolidation ICIs group (Figure 3D).

The incidence of new lesions is listed in Supplementary Table 3, the common sites were lung, lymph node, and bone, which accounts for 12.2%, 5.7% and 4.9% of the total cases, respectively. Moreover, the incidence of brain metastasis was 2.4% in this study.

Safety profile

All adverse events in these patients are summarized in Table 2. In total, the incidence of Grade 1-2, Grade 3-4 and Grade 5 AEs was 96.7%, 21.1% and 1.6%, respectively. These AEs rates were similar between induction plus consolidation ICIs group and consolidation

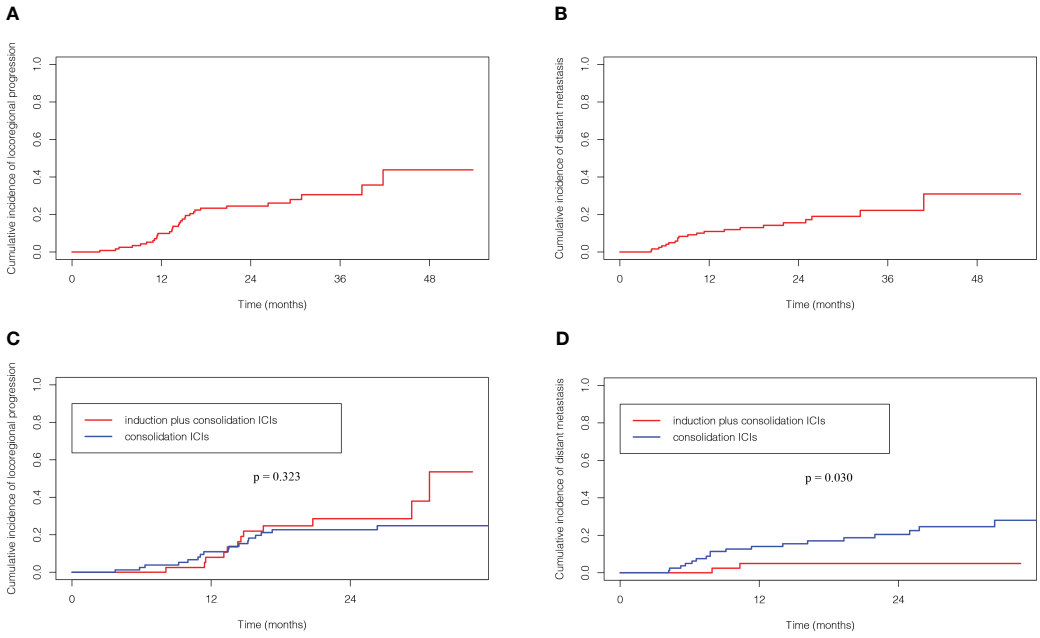


FIGURE 3
Competing risk analysis of cumulative incidence of locoregional progression **(A)** and distant metastasis **(B)** for the full analysis set. Cumulative incidence of locoregional progression **(C)** and distant metastasis **(D)** according to ICIs sequence. ICIs, immune checkpoint inhibitors.

ICIs group, except significantly higher incidence of ≥Grade 3 pneumonitis was observed in induction plus consolidation ICIs group than consolidation ICIs group. Specifically, the incidence of Grade 3-4 and Grade 5 pneumonitis was 9.8% and 4.9%, respectively in the induction plus consolidation ICIs group and 3.7% and 0, respectively in the consolidation ICIs group (Table 2).

PSM analysis for induction plus consolidation group versus consolidation group

After adjusting for confounding variables via PSM, all clinical features were balanced between the induction plus consolidation ICIs group and consolidation ICIs group (Supplementary Table 4). The OS rate (HR: 0.77, 95%CI: 0.27-2.17, p=0.619), PFS rate (HR: 0.99, 95%CI: 0.53-1.84, p=0.963) and cumulative incidence of locoregional progression rate (HR: 0.97, 95%CI: 0.44-2.16, p=0.979) were similar between the induction plus consolidation ICIs group and consolidation ICIs group (Supplementary Figures 3A–C). However, patients in the induction plus consolidation ICIs group had significantly lower cumulative incidence of distant metastasis rates compared with patients in the consolidation ICIs group (HR: 0.21, 95%CI: 0.05-0.92, p=0.032). Specifically, the 1- and 2- year cumulative incidence of distant metastasis rates were 4.9% and 4.9%, respectively in the induction plus consolidation ICIs group, and 16.1% and 19.8%, respectively in the consolidation ICIs group (Supplementary Figure 3D). As for the toxicity, except significantly higher incidence of ≥Grade 3 pneumonitis was observed in induction plus consolidation ICIs group than consolidation ICIs group

TABLE 2 Treatment-related adverse events.

	Total (n=123)			Induction plus consolidation ICIs (n=41)			Consolidation ICIs (n=82)			p
	Grade 1-2	Grade 3-4	Grade 5	Grade 1-2	Grade 3-4	Grade 5	Grade 1-2	Grade 3-4	Grade 5	
Any event	119 (96.7)	26 (21.1)	2 (1.6)	39 (95.1)	9 (22.0)	2 (4.9)	80 (97.6)	17 (20.7)	0	0.153
Pneumonitis[†]	81 (65.9)[#]	7 (5.7)	2 (1.6)	28 (68.3)	4 (9.8)	2 (4.9)	53 (64.6)	3 (3.7)	0	0.039*
Leukopenia	36 (29.3)	14 (11.4)	0	10 (24.4)	4 (9.8)	0	26 (31.7)	10 (12.2)	0	0.582
Anemia	38 (30.9)	3 (2.4)	0	14 (34.1)	0	0	24 (29.3)	3 (3.7)	0	0.266
Thrombocytopenia	21 (17.1)	6 (4.9)	0	6 (14.6)	1 (2.4)	0	15 (18.3)	5 (6.1)	0	0.535
Esophagitis	62 (50.4)	1 (0.8)	0	16 (39)	0	0	46 (56.1)	1 (1.2)	0	0.118
Radiation dermatitis	22 (17.9)	0	0	5 (12.2)	0	0	17 (20.7)	0	0	0.244
Elevated blood glucose	16 (13)	0	0	5 (12.2)	0	0	11 (13.4)	0	0	0.850
Hypothyroidism	14 (11.4)	0	0	4 (9.8)	0	0	10 (12.2)	0	0	0.526
Rash	13 (10.6)	0	0	5 (12.2)	0	0	8 (9.8)	0	0	0.681
Pruritus	13 (10.6)	0	0	3 (7.3)	0	0	10 (12.2)	0	0	0.394
Renal toxicity	13 (10.6)	0	0	3 (7.3)	0	0	10 (12.2)	0	0	0.394
Hyperthyroidism	12 (9.8)	0	0	5 (12.2)	0	0	7 (8.5)	0	0	0.685
Fatigue	6 (4.9)	0	0	2 (4.9)	0	0	4 (4.9)	0	0	1.000
Pancreatitis	6 (4.9)	3 (2.4)	0	3 (7.3)	2 (4.9)	0	3 (3.7)	1 (1.2)	0	0.324
Musculoskeletal pain	5 (4.1)	0	0	0 (0)	0	0	5 (6.1)	0	0	0.168
Myocarditis	3 (2.4)	0	0	1 (2.4)	0	0	2 (2.4)	0	0	1.000
Vascular hyperplasia	2 (1.6)	0	0	2 (4.9)	0	0	0 (0)	0	0	0.109
Cough	2 (1.6)	0	0	0 (0)	0	0	2 (2.4)	0	0	0.552
Peripheral neuropathy	1 (0.8)	0	0	0 (0)	0	0	1 (1.2)	0	0	1.000

*$p < 0.05$.
[†]including radiation pneumonitis and immune-related pneumonitis.
[#]With Grade 1 being 26.0% and Grade 2 being 39.8%.
ICIs, immune checkpoint inhibitors.

(p=0.049), these rates of other AEs were similar for patients in both groups (Supplementary Table 5).

Discussion

This is the first study to compare the dCRT followed by consolidation ICIs with or without induction ICIs plus chemotherapy in one cohort of unresectable, stage III NSCLC patients. This study identified encouraging efficacy and manageable toxicity of the combined ICIs and CRT for patients with stage III NSCLC, and demonstrated that induction and consolidation ICIs might reduce distant metastasis, while achieve similar survival benefit compared with consolidation ICIs.

Since the publication of the PACIFIC trial (3) in 2017 which demonstrated significantly improved survival benefit under the addition of consolidation ICIs followed by CRT in unresectable, stage III NSCLC patients, other novel treatment strategies including induction ICIs before CRT given to engage with a healthy immune system have been used in a variety of ongoing trials (7, 14). In this retrospective study, all the patients received CRT and consolidation ICIs, the current standard of care, among whom some patients received induction ICIs plus chemotherapy because of patient's willingness to undergo surgery or challenging to initial definitive CRT. The survival analysis showed similar OS, PFS and cumulative incidence of locoregional progression between the two treatment groups. Notably, the induction plus consolidation ICIs group achieved significantly lower distant metastasis rate compare with consolidation ICIs group, which is reasonable as both preclinical (11) and clinical (12) studies have demonstrated that induction ICIs play a key role in activating immune surveillance against micrometastatic disease and reducing distant metastasis. However, the reduced distant metastasis was not translated into a PFS or OS benefit in the induction ICIs group. Although the exact reasons are not known, we think it could be explained by the following aspects. First, given that the rate of distant metastasis has already been significantly reduced for patients with stage III NSCLC under the treatment of consolidation ICIs (4), the further reduced distant metastasis by the adding induction ICIs plus chemotherapy exerted limited effects on improving PFS or OS, especially in this cohort whose dominant pattern of failure was locoregional progression. Second, a significantly higher incidence of ≥Grade 3 pneumonitis in the induction plus consolidation ICIs group was observed in this cohort, which exerted negative impact on PFS and OS (16). Based on these results, we get the preliminary conclusion that different ICIs strategies were needed based on the tumor characteristic and the potential failure pattern. In our retrospective study for bulky tumor, which was defined as primary tumor ≥5 cm in greatest dimension or regionally involved lymph nodes ≥2 cm in shortest diameter, has shown that induction ICIs plus chemotherapy played a key role in shrinking tumor volume and achieved the similar prognosis compared with PACIFIC trial (13). However, excessive induction ICIs plus chemotherapy may result in early pneumonitis or tumor progression, which delaying or discontinuing the following definitive CRT and consolidation ICIs (13). Last, the finding should be interpreted with caution given the retrospective nature, moderate sample size, and heterogeneous ICI agents of our study. Nevertheless, this study provides preliminary evidence, and well-designed randomized studies with large sample sizes are warranted to validate these conclusions. Moreover, individualized therapy according to other tumor characteristic and biomarker is lacking and deserve further investigation.

By the time of the analysis, about half of these patients (42.3%) completed 12 months or more consolidation ICIs in our cohort, which is close to those reported in Pacific-R trial (47.1%) and Pacific trial (48.7%) (17). The incidence of new lesions was 23.6%, and the most frequent sites were lung and lymph node in this study, which was consistent with those reported in PACIFIC trial (4). In addition, locoregional progression was the dominant pattern of first failure in our cohort. Analysis for the patients who had locoregional progression showed that in-field failure(18.7%) was more common compared with out-field failure(6.5%). Noriko et al. (18) also reported that in-field recurrence was the most common locoregional progression pattern in patients with stage III NSCLC received CRT followed ICIs, which is consistent with our study. Further improvement of the in-field control is still a major problem even in the ICIs era.

The survival rates in this study were numerically superior to those in the PACIFIC trial (4) and Pacific-R trial (19). In the PACIFIC trial (4), the 1-, 2- and 3-year OS rates were 83.1%, 66.3% and 56.7%, respectively. The 1-, 2- and 3-year PFS rates were 55.7%, 45.0% and 39.7%, respectively, and the median PFS was 16.9 months. And in Pacific-R trial (19), the 2-year OS and PFS rates were 71.2% and 48.2%, respectively. Two possible reasons exist for the superior treatment effect of our results with previous reports. First, Asian patients with NSCLC under the treatment of ICIs gain better prognosis compared with non-Asian patients. As the multivariable cox regression analysis in the PACIFIC trial showed that Asian, accounted for 26.9% of the total cases, is independent protective factor of OS (4). In addition, the real-world data for Korean from PACIFIC-KR trial also showed superior PFS and OS than those reported in PACIFIC trial (4) and Pacific-R trial (19). Second, assessments after treatment could sometimes be delayed in retrospective study, which led to overestimated prognosis.

In terms of toxicity, the most common AEs was pneumonitis caused by ICIs or RT. In some cases, the differentiation between radiation pneumonitis and immune-relate pneumonitis was difficult. The overall pneumonitis incidence was markedly higher (65.9%) than it reported in the PACIFIC trial (33.9%) (3). Two possible reasons exist for the discrepancy of our results with previous reports in the incidence of pneumonitis. First, the incidence of pneumonitis varies by race/ethnicity. A meta-analysis of real-world studies has been demonstrated that the incidence of pneumonitis was about three times higher to Asian populations than non-Asian populations (20). Given that Asian population accounted for only 9% of the total cases in PACIFIC trial but 100% of our study, it is understandable that the incidence of pneumonitis is markedly higher than it reported in the PACIFIC trial. Second, the incidence of pneumonitis varies by anti-PD-1/PD-

L1 ICIs. A meta-analysis had indicated that the incidence of pneumonitis with use of anti-PD-1 ICIs was about three times higher than anti-PD-L1 ICIs (21). A valid hypothesis explaining the discrepancy is that anti-PD-1 blockade may shift the balance in PD-L2 interaction with its other binding partners and lead to pneumonitis (22, 23). Considering that 56.1% of patients received anti-PD-1 ICIs in this study, it is reasonable that the incidence of pneumonitis is markedly higher. However, the treatment was overall well-tolerated and most of the pneumonitis was Grade 1-2 (with Grade 1 being 26.0% and Grade 2 being 39.8%) and clinically manageable. The incidence of Grade 3-4 and Grade 5 pneumonitis was 5.7% and 1.6%, respectively, which is similar to the patients with induction and consolidation ICIs in the KEYNOTE-799 trial (5% and 5%, respectively) (8).

There are several limitations in this study. Firstly, this is a single institution retrospective analysis. Secondly, not long follow-up time and significantly improved treatment effect in this study gave rise to limited events of tumor progression and death, a longer follow-up may be more informative. However, under the circumstance that there is no study to investigate the optimal combination of ICIs and CRT for LA-NSCLC, our analysis can provide a rationale for the design RCTs, as well as clinical practice. Future RCTs are expected to validate and update these results.

Conclusion

This is the first study to evaluate the dCRT followed by consolidation ICIs with or without induction ICIs plus chemotherapy in one cohort of stage III NSCLC patients. This study identified encouraging efficacy and manageable toxicity of the combined ICIs and CRT for patients with stage III NSCLC in China, and demonstrated that induction plus consolidation ICIs could reduce distant metastasis and gain similar survival benefit compared with consolidation ICIs.

Data availability statement

The raw data supporting the conclusions of this article will be made available by the authors, without undue reservation.

Ethics statement

The studies involving humans were approved by National Cancer Center/National Clinical Research Center for Cancer/Cancer Hospital, Chinese Academy of Medical Sciences and Peking Union Medical College. The studies were conducted in accordance with the local legislation and institutional requirements. The ethics committee/institutional review board waived the requirement of written informed consent for participation from the participants or the participants' legal guardians/next of kin because of the retrospective nature of this research.

Author contributions

YY: Data curation, Formal analysis, Methodology, Writing – original draft. JYW: Investigation, Methodology, Resources, Writing – original draft. TZ: Data curation, Resources, Writing – review & editing. ZZ: Data curation, Resources, Writing – review & editing. YW: Data curation, Methodology, Writing – review & editing. YJ: Data curation, Methodology, Writing – review & editing. WL: Investigation, Resources, Writing – review & editing. ZX: Investigation, Resources, Writing – review & editing. LD: Investigation, Resources, Writing – review & editing. QF: Investigation, Resources, Writing – review & editing. XW: Investigation, Resources, Writing – review & editing. JL: Investigation, Resources, Writing – review & editing. WW: Investigation, Resources, Writing – review & editing. QX: Conceptualization, Resources, Writing – review & editing. JW: Conceptualization, Resources, Writing – review & editing. Y-XL: Conceptualization, Project administration, Supervision, Writing – review & editing. NB: Conceptualization, Funding acquisition, Supervision, Writing – review & editing.

Funding

The author(s) declare financial support was received for the research, authorship, and/or publication of this article. This study is supported by the National Natural Science Foundation Key Program (82173348) and the Beijing Municipal Science & Technology Commission (Z211100002921058).

Conflict of interest

The authors declare that the research was conducted in the absence of any commercial or financial relationships that could be construed as a potential conflict of interest.

Publisher's note

All claims expressed in this article are solely those of the authors and do not necessarily represent those of their affiliated organizations, or those of the publisher, the editors and the reviewers. Any product that may be evaluated in this article, or claim that may be made by its manufacturer, is not guaranteed or endorsed by the publisher.

Supplementary material

The Supplementary Material for this article can be found online at: https://www.frontiersin.org/articles/10.3389/fimmu.2023.1281888/full#supplementary-material

References

1. Siegel RL, Miller KD, Fuchs HE, Jemal A. Cancer statistics, 2022. *CA Cancer J Clin* (2022) 72(1):7–33. doi: 10.3322/caac.21708

2. Zhang S, Sun K, Zheng R, Zeng H, He J. Cancer incidence and mortality in China, 2015. *J Natl Cancer Cent* (2020) 1(1):2–11. doi: 10.1016/j.jncc.2020.12.001

3. Antonia SJ, Villegas A, Daniel D, Vicente D, Murakami S, Hui R, et al. Durvalumab after chemoradiotherapy in stage III non-small-cell lung cancer. *N Engl J Med* (2017) 377(20):1919–29. doi: 10.1056/NEJMoa1709937

4. Spigel DR, Faivre-Finn C, Gray JE, Vicente D, Planchard D, Paz-Ares L, et al. Five-year survival outcomes from the PACIFIC trial: durvalumab after chemoradiotherapy in stage III non-small-cell lung cancer. *J Clin Oncol* (2022) 40 (12):1301–11. doi: 10.1200/jco.21.01308

5. Zhou Q, Chen M, Jiang O, Pan Y, Hu D, Lin Q, et al. Sugemalimab versus placebo after concurrent or sequential chemoradiotherapy in patients with locally advanced, unresectable, stage III non-small-cell lung cancer in China (GEMSTONE-301): interim results of a randomised, double-blind, multicentre, phase 3 trial. *Lancet Oncol* (2022) 23 (2):209–19. doi: 10.1016/s1470-2045(21)00630-6

6. Ohri N, Jolly S, Cooper BT, Kabarriti R, Bodner WR, Klein J, et al. The selective personalized radio-immunotherapy for locally advanced NSCLC trial (SPRINT): initial results. *J Clin Oncol* (2022) 40(16):Supplement 1. doi: 10.1200/JCO.2022.40.16_suppl.8510

7. Ross HJ, Kozono DE, Urbanic JJ, Williams TM, DuFrane C, Bara I, et al. AFT-16: Phase II trial of neoadjuvant and adjuvant atezolizumab and chemoradiation (CRT) for stage III non-small cell lung cancer (NSCLC). *J Clin Oncol* (2021) 39(15 SUPPL). doi: 10.1200/JCO.2021.39.15-suppl.8513

8. Jabbour SK, Berman AT, Decker RH, Lin Y, Feigenberg SJ, Gettinger SN, et al. Phase 1 trial of pembrolizumab administered concurrently with chemoradiotherapy for locally advanced non-small cell lung cancer: A nonrandomized controlled trial. *JAMA Oncol* (2020) 6(6):848–55. doi: 10.1001/jamaoncol.2019.6731

9. Cortiula F, Reymen B, Peters S, Van Mol P, Wauters E, Vansteenkiste J, et al. Immunotherapy in unresectable stage III non-small-cell lung cancer: state of the art and novel therapeutic approaches. *Ann Oncol* (2022) 33(9):893–908. doi: 10.1016/j.annonc.2022.06.013

10. Wang F, Yang M, Luo W, Zhou Q. Characteristics of tumor microenvironment and novel immunotherapeutic strategies for non-small cell lung cancer. *J Natl Cancer Cent* (2022) 2(4):243–62. doi: 10.1016/j.jncc.2022.10.002

11. Liu J, Blake SJ, Yong MC, Harjunpää H, Ngiow SF, Takeda K, et al. Improved efficacy of neoadjuvant compared to adjuvant immunotherapy to eradicate metastatic disease. *Cancer Discovery* (2016) 6(12):1382–99. doi: 10.1158/2159-8290.Cd-16-0577

12. Wang C, Chen KN, Chen Q, Wu L, Wang Q, Li X, et al. Neoadjuvant nivolumab (NIVO) + chemotherapy (chemo) vs chemo in Chinese patients (pts) with resectable NSCLC in CheckMate 816. *Cancer Res* (2023) 83(8). doi: 10.1158/1538-7445.AM2023-CT081

13. Wang Y, Zhang T, Wang J, Zhou Z, Liu W, Xiao Z, et al. Induction immune checkpoint inhibitors and chemotherapy before definitive chemoradiation therapy for patients with bulky unresectable stage III non-small cell lung cancer. *Int J Radiat Oncol Biol Phys* (2023) 116(3):590–600. doi: 10.1016/j.ijrobp.2022.12.042

14. Jabbour SK, Lee KH, Frost N, Breder V, Kowalski DM, Pollock T, et al. Pembrolizumab plus concurrent chemoradiation therapy in patients with unresectable, locally advanced, stage III non-small cell lung cancer: the phase 2 KEYNOTE-799 nonrandomized trial. *JAMA Oncol* (2021) 7(9):1–9. doi: 10.1001/jamaoncol.2021.2301

15. Zhang T, Xu K, Bi N, Zhang L, Jiang W, Liang J, et al. Efficacy and safety of immune checkpoint inhibitor consolidation after chemoradiation in patients of Asian ethnicity with unresectable stage III non-small cell lung cancer: Chinese multicenter report and literature review. *Thorac Cancer* (2020) 11(10):2916–23. doi: 10.1111/1759-7714.13631

16. Edwards DM, Sankar K, Alseri A, Jiang R, Schipper M, Miller S, et al. Pneumonitis after chemoradiation and adjuvant durvalumab in stage III non-small-cell lung cancer. *Int J Radiat Oncol Biol Phys* (2023). doi: 10.1016/j.ijrobp.2023.09.050

17. Antonia SJ, Villegas A, Daniel D, Vicente D, Murakami S, Hui R, et al. Overall survival with durvalumab after chemoradiotherapy in stage III NSCLC. *N Engl J Med* (2018) 379(24):2342–50. doi: 10.1056/NEJMoa1809697

18. Kishi N, Matsuo Y, Shintani T, Ogura M, Mitsuyoshi T, Araki N, et al. Recurrence patterns and progression-free survival after chemoradiotherapy with or without consolidation durvalumab for stage III non-small cell lung cancer. *J Radiat Res* (2023) 64(1):142–53. doi: 10.1093/jrr/rrac057

19. Girard N, Bar J, Garrido P, Garassino MC, McDonald F, Mornex F, et al. Treatment characteristics and real-world progression-free survival in patients with unresectable stage III NSCLC who received durvalumab after chemoradiotherapy: findings from the PACIFIC-R study. *J Thorac Oncol* (2023) 18(2):181–93. doi: 10.1016/j.jtho.2022.10.003

20. Wang Y, Zhang T, Huang Y, Li W, Zhao J, Yang Y, et al. Real-world safety and efficacy of consolidation durvalumab after chemoradiation therapy for stage III non-small cell lung cancer: A systematic review and meta-analysis. *Int J Radiat Oncol Biol Phys* (2022) 112(5):1154–64. doi: 10.1016/j.ijrobp.2021.12.150

21. Khunger M, Rakshit S, Pasupuleti V, Hernandez AV, Mazzone P, Stevenson J, et al. Incidence of pneumonitis with use of programmed death 1 and programmed death-ligand 1 inhibitors in non-small cell lung cancer: A systematic review and meta-analysis of trials. *Chest* (2017) 152(2):271–81. doi: 10.1016/j.chest.2017.04.177

22. Xiao Y, Yu S, Zhu B, Bedoret D, Bu X, Francisco LM, et al. RGMb is a novel binding partner for PD-L2 and its engagement with PD-L2 promotes respiratory tolerance. *J Exp Med* (2014) 211(5):943–59. doi: 10.1084/jem.20130790

23. Chen DS, Irving BA, Hodi FS. Molecular pathways: next-generation immunotherapy–inhibiting programmed death-ligand 1 and programmed death-1. *Clin Cancer Res* (2012) 18(24):6580–7. doi: 10.1158/1078-0432.Ccr-12-1362

frontiers | Frontiers in Immunology

TYPE Original Research
PUBLISHED 27 November 2023
DOI 10.3389/fimmu.2023.1289207

Check for updates

OPEN ACCESS

EDITED BY
Qun Xue,
Affiliated Hospital of Nantong University, China

REVIEWED BY
Ruiguang Zhang,
Huazhong University of Science and Technology, China
Haihua Yang,
Wenzhou Medical University, China

*CORRESPONDENCE
Lujun Zhao
zhaolujun@tjmuch.com

†These authors have contributed equally to this work and share first authorship

RECEIVED 05 September 2023
ACCEPTED 13 November 2023
PUBLISHED 27 November 2023

CITATION
Guan S, Zhang S, Ren K, Li X, Li X and Zhao L (2023) Induction chemoimmunotherapy may improve outcomes of chemoradiotherapy in patients with unresectable stage III NSCLC. *Front. Immunol.* 14:1289207. doi: 10.3389/fimmu.2023.1289207

COPYRIGHT
© 2023 Guan, Zhang, Ren, Li, Li and Zhao. This is an open-access article distributed under the terms of the Creative Commons Attribution License (CC BY). The use, distribution or reproduction in other forums is permitted, provided the original author(s) and the copyright owner(s) are credited and that the original publication in this journal is cited, in accordance with accepted academic practice. No use, distribution or reproduction is permitted which does not comply with these terms.

Induction chemoimmunotherapy may improve outcomes of chemoradiotherapy in patients with unresectable stage III NSCLC

Song Guan[1,2,3,4†], Shufeng Zhang[1,2,3,4†], Kai Ren[1,2,3,4], Xingyue Li[1,2,3,4], Xue Li[1,2,3,4] and Lujun Zhao[1,2,3,4*]

[1]Department of Radiation Oncology, Tianjin Medical University Cancer Institute and Hospital, Tianjin, China, [2]National Clinical Research Center for Cancer, Tianjin Medical University Cancer Institute and Hospital, Tianjin, China, [3]Key Laboratory of Cancer Prevention and Therapy, Tianjin, China, [4]Tianjin's Clinical Research Center for Cancer, Tianjin, China

Background: Currently, the value of induction chemoimmunotherapy before chemoradiotherapy (CRT) in unresectable stage III non-small cell lung cancer (NSCLC) has not been explored. This study was designed to explore the efficacy and safety of induction chemoimmunotherapy in patients with unresectable stage III NSCLC.

Methods: Unresectable stage III NSCLC patients who received CRT with or without induction chemoimmunotherapy between August 2014 and December 2021 were retrospectively enrolled. Progression-free survival (PFS) and overall survival (OS) were assessed from the initiation of treatment and estimated by the Kaplan-Meier method. The potential factors affecting PFS and OS were analyzed by univariate and multivariate Cox regression models. One-to-one propensity score matching (PSM) was used to further minimize confounding.

Results: A total of 279 consecutive patients were enrolled, with 53 (19.0%) receiving induction chemoimmunotherapy followed by CRT (I-CRT group), and the remaining 226 (81.0%) receiving CRT alone (CRT group). After PSM, the median PFS was 24.8 months in the I-CRT group vs. 13.3 months in the CRT group (P=0.035). The median OS was not reached (NR) vs. 36.6 months ((P=0.142). The incidence of treatment-related adverse events (TRAEs) was similar in both groups, except that the incidence of hematological toxicity was higher in the I-CRT group (77.1% vs. 58.3%, P=0.049). Compared to induction chemotherapy, induction chemoimmunotherapy demonstrated a superior objective response rate (60.4% vs. 22.2%, P<0.001) and further prolonged PFS (median NR vs. 13.2 months, P=0.009) and OS (median NR vs. 25.9 months, P=0.106) without increasing the incidence of TRAEs in patients receiving concurrent chemoradiotherapy.

Conclusion: Induction chemoimmunotherapy is safe and may improve outcomes of CRT in patients with unresectable stage III NSCLC. Moreover, induction chemoimmunotherapy may further improve treatment response and survival outcomes compared to induction chemotherapy before cCRT.

KEYWORDS

chemoradiotherapy, induction chemotherapy, induction chemoimmunotherapy, non-small cell lung cancer, prognosis

1 Introduction

Based on the practice-changing result of the PACIFIC trial, concurrent chemoradiotherapy (cCRT) followed by consolidation immunotherapy has become the standard of care for patients with unresectable stage III non-small cell lung cancer (NSCLC) (1). However, the optimal sequence of immunotherapy remains unclear. In the surgical setting, immunotherapy can benefit patients whether used preoperatively or postoperatively (2–4), raising the question of whether upfront chemoimmunotherapy before chemoradiotherapy (CRT) could benefit patients with unresectable stage III NSCLC. However, there is a paucity of data on induction chemoimmunotherapy followed by CRT. Although a recent retrospective study demonstrated the feasibility of induction chemoimmunotherapy with target volume reduction, it was a single-arm study (5). Furthermore, given that induction chemotherapy in the pre-immunotherapy era did not further improve survival in stage III NSCLC patients receiving cCRT (6, 7), it remains unclear whether adding immunotherapy to induction chemotherapy could further improve survival. Herein, to investigate the value of induction chemoimmunotherapy before CRT and to determine whether the addition of immunotherapy to induction treatment could improve treatment efficacy, we performed this retrospective study.

2 Materials and methods

2.1 Patient selection

Patients with unresectable stage III NSCLC who received CRT with or without induction chemoimmunotherapy at Tianjin Cancer Hospital between August 2014 and December 2021 were enrolled. The inclusion criteria were as follows: 1) age ≥ 18; 2) histologically or cytologically proven stage III NSCLC; and 3) receiving CRT with or without induction PD-1/PD-L1 inhibitor plus chemotherapy. The exclusion criteria were as follows: 1) history of any cancer-specific treatment; 2) treatment with targeted therapy; 3) receipt of induction immunotherapy alone; and 4) immunotherapy concurrent with and/or after radiotherapy.

Patients were categorized into two treatment groups based on whether they received induction chemoimmunotherapy before CRT: the induction chemoimmunotherapy followed by CRT (I-CRT) group and the CRT alone (CRT) group. In the exploratory analysis, patients who received cCRT were classified into two groups according to the induction treatment: the induction chemotherapy followed by cCRT (C-cCRT) group and the induction chemoimmunotherapy followed by cCRT (I-cCRT) group. Patients' baseline characteristics were extracted from their medical records. Individual NSCLC cases' histological type and stage were determined according to the WHO criteria (8) and the International Association for the Study of Lung Cancer classification (8th edition) (9), respectively.

2.2 Drug treatment

Immune checkpoint inhibitors (ICIs) used in patients receiving immunotherapy included camrelizumab, nivolumab, pembrolizumab, sintilimab and tislelizumab. These five kinds of ICI agents have been approved for the treatment of NSCLC based on promising outcomes in NSCLC patients (10). Each patient's chemotherapy regimen was determined by the histological type of the tumor, the clinical condition of the patient, etc.

2.3 Study outcomes

The primary endpoints in this study were progression-free survival (PFS) and overall survival (OS). Following induction treatment, objective response rates (ORRs) and disease control rates (DCRs) were assessed. PFS was estimated from the start of treatment to the date of the first documented event of disease progression, death without progression, or last follow-up. OS was calculated from the initiation of treatment until death or last follow-up. According to RECIST v1.1, ORR was defined as partial response (PR) plus complete response (CR), while DCR was defined as PR and CR plus stable disease (SD). Individual patients' treatment-related adverse events (TRAEs) were evaluated according to CTCAE version 5.0. Patients underwent follow-up visits every 3 months for 2 years and every 6 months thereafter, including clinical evaluation, CT or PET, and additional investigations when clinically indicated.

2.4 Statistical analysis

One-to-one propensity score matching (PSM) with baseline characteristics was used to minimize confounding. Patient characteristics between treatment groups were analyzed using the Chi-square test or Fisher's exact test for categorical variables. Survival outcomes were estimated by Kaplan-Meier analysis and evaluated by the log-rank test. The hazard ratios (HRs) and the corresponding 95% confidence intervals (CIs) were calculated with the Cox proportional hazards model. When the univariate Cox analysis yielded a P value of ≤ 0.15, the variable was incorporated into the multivariate Cox regression analysis. Subgroup analyses (age [< 65 years or ≥ 65 years], sex [male or female], WHO histology type [squamous, non-squamous, or not otherwise specified], cancer stage [IIIA, IIIB, or IIIC], chemoradiotherapy modality [sequential or concurrent], radiotherapy dose [< 54 Gy or ≥ 54 Gy], smoking history [never, former or current], ECOG performance status [0, 1 or 2]) for PFS and OS were performed to assess the consistency of treatment effects in patient subgroups. Subgroup analyses used an unstratified Cox proportional hazards model with treatment as a covariate. A P value inferior to 0.05 was considered statistically significant. All statistical analyses were performed using SPSS version 25.0 (IBM, Armonk, NY, USA).

3 Results

3.1 Baseline characteristics

A total of 279 consecutive patients were enrolled in this study (Figure 1). Among them, 53 (19.0%) patients received induction chemoimmunotherapy followed by CRT, and the remaining 226 (81.0%) received CRT alone. None of these patients received consolidation immunotherapy. Patients had a median age of 61 years and were predominantly male with an ECOG PS score of 1. Only two patients with adenocarcinoma who received induction chemoimmunotherapy had unknown driver-gene status, while the rest had wild-type driver-genes. After 1:1 PSM, the patients' characteristics were well balanced (Table 1).

3.2 Treatment

All patients in the I-CRT group received induction chemoimmunotherapy, with a median of 4 cycles of induction immunotherapy (range 1-9) and chemotherapy (range 2-8). The ICI agents used included camrelizumab (15.1%, n=8), nivolumab (5.7%, n=3), pembrolizumab (20.8%, n=11), sintilimab (47.2%,

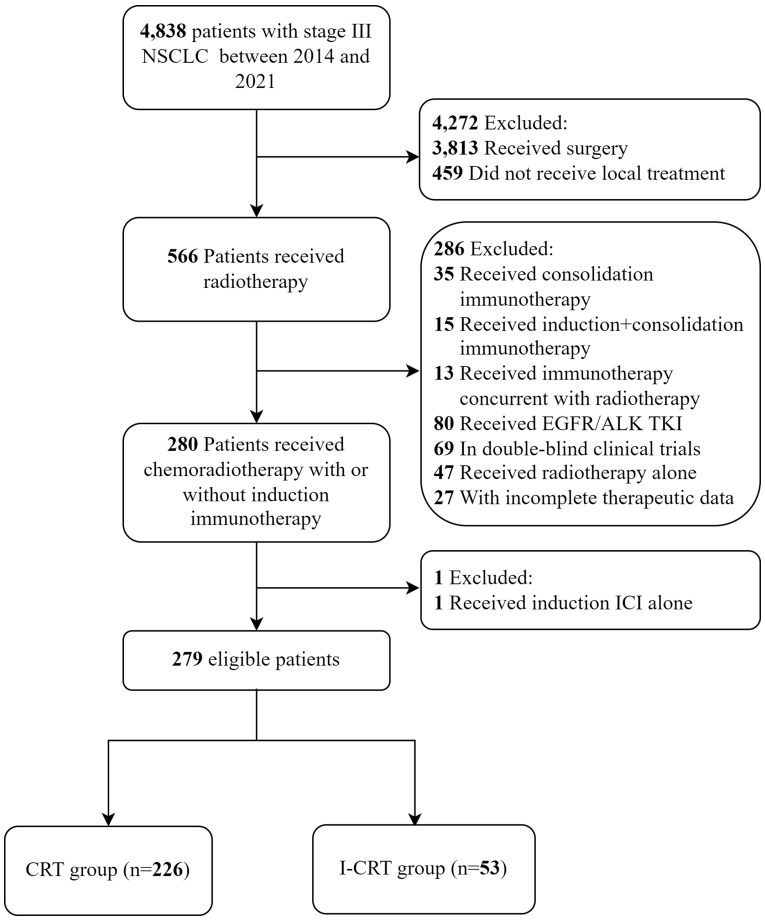


FIGURE 1
Patient inclusion flow chart.

TABLE 1 Baseline demographic and clinical characteristics of the patients.

Characteristics	Before PSM		P	After PSM		P
	CRT (*n*=226)	I-CRT (*n*=53)		CRT (*n*=48)	I-CRT (*n*=48)	
	No. (%)	No. (%)		No. (%)	No. (%)	
Age						
<65	155(68.6)	32(60.4)	0.253	29(60.4)	28(58.3)	0.835
≥65	71(31.4)	21(39.6)		19(39.6)	20(41.7)	
Sex						
Male	185(81.9)	45(84.9)	0.600	36(75.0)	40(83.3)	0.315
Female	41(18.1)	8(15.1)		12(25.0)	8(16.7)	
WHO histology						
Squamous	150(66.4)	38(71.7)	0.261	34(70.8)	35(72.9)	0.191
Non-squamous	70(31.0)	12(22.6)		14(29.2)	10(20.8)	
NOS	6(2.7)	3(5.7)		0(0.0)	3(6.3)	
Stage						
IIIA	96(42.5)	24(45.3)	0.924	26(54.2)	22(45.8)	0.733
IIIB	109(48.2)	24(45.3)		19(39.6)	22(45.8)	
IIIC	21(9.3)	5(9.4)		3(6.3)	4(8.3)	
CRT modality						
Sequential	139(61.5)	36(67.9)	0.384	30(62.5)	31(64.6)	0.832
Concurrent	87(38.5)	17(32.1)		18(37.5)	17(35.4)	
Dose						
<54 Gy	3(1.3)	3(5.7)	0.152	1(2.1)	1(2.1)	1.000
≥54 Gy	223(98.7)	50(94.3)		47(97.9)	47(97.9)	
Smoking						
Never	38(16.8)	12(22.6)	0.319	12(25.0)	10(20.8)	0.627
Former/Current	188(83.2)	41(77.4)		36(75.0)	38(79.2)	
ECOG						
0	21(9.3)	4(7.5)	0.575	4(8.3)	4(8.3)	0.763
1	198(87.6)	46(86.8)		40(83.3)	42(87.5)	
2	7(3.1)	3(5.7)		4(8.3)	2(4.2)	

n=25), and tislelizumab (11.3%, n=6). Twenty-three patients in the CRT group received CRT alone without induction chemotherapy, while the remaining 203 patients received a median of 4 cycles of induction chemotherapy (range 1-7).

3.3 Efficacy

In the whole population, the median follow-up from the initiation of treatment was 24.9 months (range 4.3-86.5). The median PFS and OS were 13.4 and 34.3 months, respectively. During the investigation, 213 patients developed progressive disease (PD), including 21 (39.6%) in the I-CRT group and 192 (85.0%) in the CRT group. A total of 149 patients had died when analyzed, including 8 (15.1%) and 141 (62.4%) cases in the two groups, respectively.

The median follow-up for the I-CRT and CRT groups was 16.1 (range 5.3-41.8) months and 26.7 (range 4.3-86.5), respectively. The median PFS was 24.8 months in the I-CRT group vs. 12.7 months in the CRT group, with a 1-year PFS rate of 69.5% vs. 54.6% and a 2-year PFS rate of 54.8% vs. 26.6% (P=0.008, Figure 2A). The median OS was not reached (NR) vs. 30.9 months, with a 1-year OS rate of

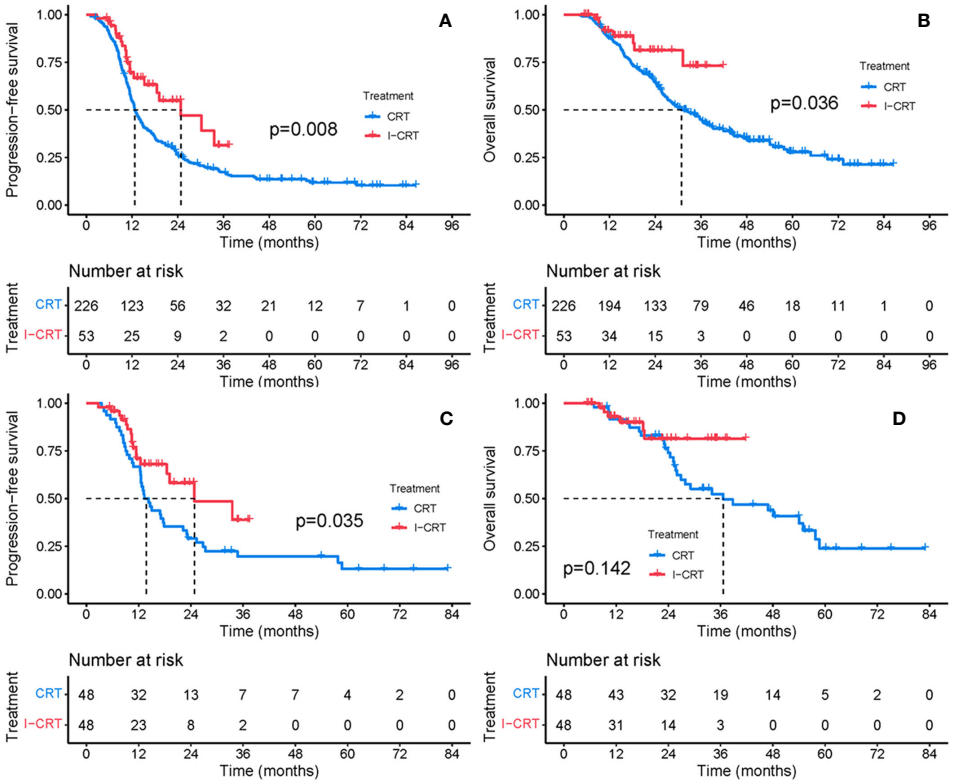


FIGURE 2
PFS and OS between the CRT group and the I-CRT group before and after PSM. **(A)** PFS from the initiation of treatment before PSM. **(B)** OS from the initiation of treatment before PSM. **(C)** PFS from the initiation of treatment after PSM. **(D)** OS from the initiation of treatment after PSM.

91.4% vs. 88.0% and a 2-year OS rate of 81.3% vs. 64.5% (P=0.036, Figure 2B). The univariate and multivariate analyses further confirmed the positive effect of induction chemoimmunotherapy on improving PFS (HR=0.562, P=0.013, Supplementary Table 1 in the Supplementary Material) and OS (HR=0.517, P=0.074, Supplementary Table 2 in the Supplementary Material). PFS and OS benefits with induction chemoimmunotherapy were observed across most prespecified subgroups (Figures 3, 4).

After 1:1 PSM, patients receiving induction chemoimmunotherapy demonstrated a consistent improvement in PFS and OS. The median PFS was 24.8 months in the I-CRT group vs. 13.3 months in the CRT group, with a 1-year PFS rate of 70.9% vs. 66.7% and a 2-year PFS rate of 58.1% vs. 29.2% (P=0.035, Figure 2C). The median OS was NR vs. 36.6 months, with a 1-year OS rate of 93.0% vs. 91.5% and a 2-year OS rate of 81.4% vs. 74.0% (P=0.142, Figure 2D).

3.4 Treatment-related adverse events

Table 2 demonstrates that in the matched population, the incidence of treatment-related adverse events (TRAEs) was similar between the two groups, except that the incidence of hematological toxicity was higher in the I-CRT group (77.1% vs. 58.3%, P=0.049). In addition, one patient developed grade 1 capillary hyperplasia and 2 patients each developed dermatitis and peripheral neurotoxicity in the I-CRT group.

3.5 Induction chemoimmunotherapy vs. induction chemotherapy

In all patients who received induction treatment before CRT, the ORR after induction treatment was significantly higher in the I-CRT group than in the CRT group (60.4% vs. 22.2%, P<0.001), while the DCR after induction treatment was only numerically higher in the I-CRT group than in the CRT group (98.1% vs. 93.1%, P=0.292).

When patients were restricted to receiving induction treatment before cCRT, i.e. induction chemoimmunotherapy followed by cCRT (I-cCRT) vs. induction chemotherapy followed by cCRT (C-cCRT), the results did not appreciably change. Baseline demographic and clinical characteristics between the two treatment groups were basically balanced (Table 3). The median follow-up for the I-cCRT and C-cCRT groups was 11.5 (range 5.3-37.1) and 23.1 (range 6.9-77.1) months, respectively. As shown in Figure 5, PFS was significantly superior in the I-cCRT group compare to the C-cCRT group (median NR vs. 13.2 months, P=0.009). One- and 2-year PFS rates were 83.7% vs. 56.1% and 83.7% vs. 29.7%, respectively. OS was numerically prolonged in the I-cCRT group than in the C-cCRT group (median NR vs. 25.9 months, P=0.106). One- and 2-year OS rates were 91.7% vs. 85.7% and 91.7% vs. 55.9%, respectively. The incidence of TRAEs was similar in both groups, except that the incidence of grade 3/4 hematological toxicity appeared to be higher in the I-cCRT group than in the C-cCRT group (41.2% vs. 23.4%, P=0.248, Table 4).

10.3389/fimmu.2023.1289207

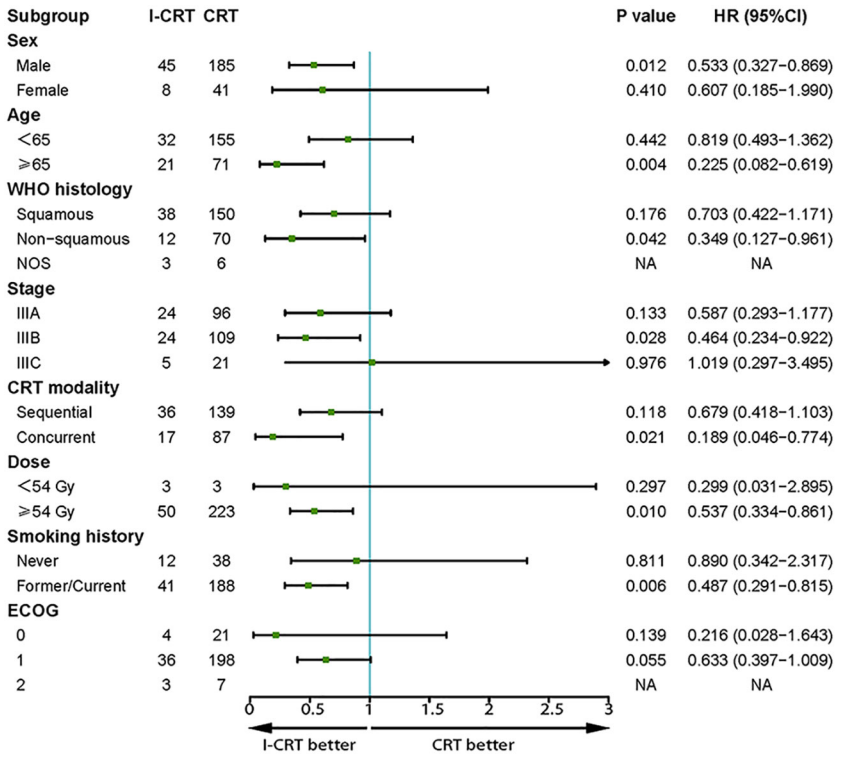


FIGURE 3
Subgroup analysis of prognostic factors for PFS in the whole population.

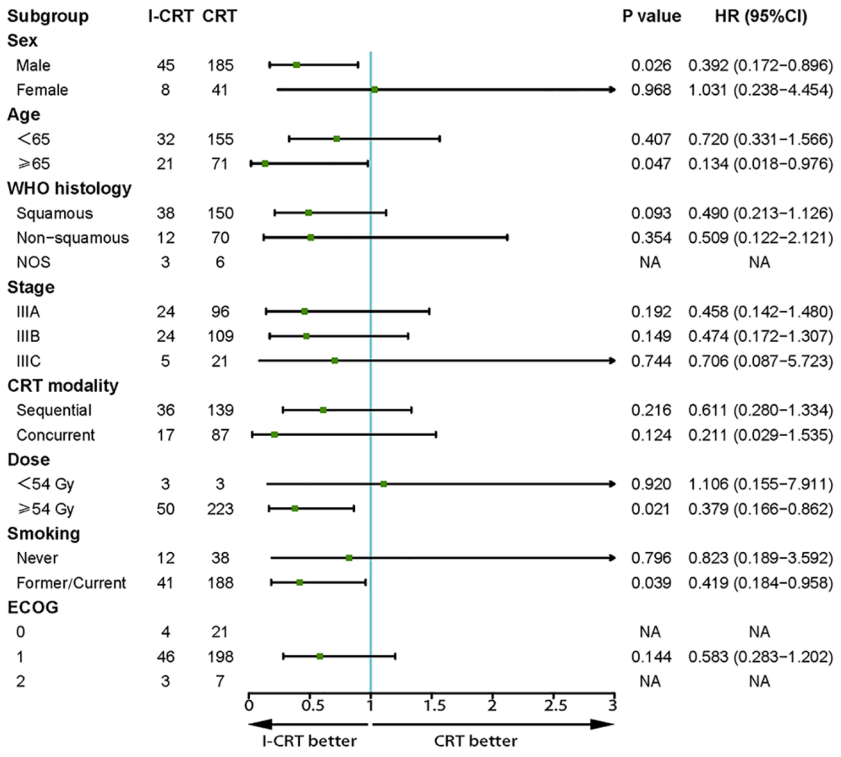


FIGURE 4
Subgroup analysis of prognostic factors for OS in the whole population.

TABLE 2 TRAEs between the CRT and I-CRT groups.

TRAE	CRT		I-CRT		P
	No.	%	No.	%	
Whole population					
Pneumonitis	133	58.8	34	64.2	0.479
G3/4 pneumonitis	22	9.7	2	3.8	0.262
Esophagitis	42	18.6	7	13.2	0.355
G3/4 esophagitis	0	0.0	0	0.0	not applicable
Hematologic toxicity	156	69.0	40	75.5	0.356
G3/4 hematologic toxicity	55	24.3	12	22.6	0.795
Matched population					
Pneumonitis	25	52.1	31	64.6	0.214
G3/4 pneumonitis	4	8.3	1	2.1	0.358
Esophagitis	10	20.8	6	12.5	0.273
G3/4 esophagitis	0	0.0	0	0.0	not applicable
Hematologic toxicity	28	58.3	37	77.1	**0.049**
G3/4 hematologic toxicity	5	10.4	11	22.9	0.100

Statistically significant P value was written in bold font.

4 Discussion

Although consolidation immunotherapy after cCRT is the current standard of care for patients with unresectable stage III NSCLC, a considerable number of patients are unsuitable for or refuse to consolidation immunotherapy, resulting in the majority of patients still receiving CRT alone. In addition, not only is the proportion of patients receiving consolidation immunotherapy poor, but the proportion of patients receiving cCRT is also poor due to excessive target volumes or poor tolerability (11, 12). Despite the benefit of consolidation immunotherapy after sequential CRT, it is less than after cCRT (13, 14). Therefore, it is important to optimize the combination of CRT and immunotherapy to benefit more patients. In the surgical setting, both preoperative and postoperative application of immunotherapy can benefit patients with resectable NSCLC, raising the question of whether upfront immunotherapy before CRT could benefit patients with unresectable NSCLC. To our knowledge, this is the first real-world study to evaluate the efficacy and safety of induction chemoimmunotherapy and to demonstrate a survival benefit in patients with unresectable stage III NSCLC.

Considering that a significant proportion of patients in the real world are unsuitable for cCRT due to the high tumor burden or higher risk of pulmonary toxicity and the poor proportion of patients receiving subsequent consolidation immunotherapy, upfront immunotherapy before CRT is increasingly recommended. Compared to consolidation immunotherapy, induction immunotherapy has the advantage of shrinking the target volume to meet normal tissue constraints that allow subsequent cCRT, early treatment of distant micrometastatic disease and screening of immunotherapy-sensitive populations (15, 16). Moreover, administering a limited number of cycles of immunotherapy before CRT could greatly improve patient compliance compared to 1 or even 2 years of consolidation immunotherapy. At our center, induction chemoimmunotherapy is being attempted in a proportion of patients with a high tumor burden or a strong desire for surgery when the lesion is unresectable, providing a unique opportunity to investigate the role of induction chemoimmunotherapy. Although every eligible patient was advised to receive consolidation immunotherapy, a considerable number of patients refused because of the financial burden, fear of adverse events or the prospect of noncompliance due to 1 or even 2 years of treatment. Given the small number of patients receiving consolidation immunotherapy, and to minimize confounding by consolidation immunotherapy, we therefore excluded patients receiving consolidation immunotherapy to evaluate the efficacy and safety of the novel treatment modality of induction chemoimmunotherapy alone. Nevertheless, induction chemoimmunotherapy alone still showed promising outcomes. The addition of only a median of 4 cycles of induction chemoimmunotherapy doubled the median PFS and 2-year PFS rates in unresectable stage III NSCLC patients receiving CRT and provided a significant improvement in OS as well. Moreover, survival benefits or trends toward prolonged survival were consistently observed across most subgroups; a larger sample size could possibly have turned the trend observed in our analysis into statistical significance.

Further analysis demonstrated the superiority of induction chemoimmunotherapy over induction chemotherapy. The ORR of 60.4% for induction chemoimmunotherapy in the present study, which was similar to the 76.1% reported by Wang et al. (5), was significantly higher than the ORR of 22.2% for induction

10.3389/fimmu.2023.1289207

TABLE 3 Baseline characteristics between the I-cCRT and C-cCRT groups.

Characteristic	C-cCRT (*n*=64)		I-cCRT (*n*=17)		P
	No.	%	No.	%	
Age					
<65	51	79.7	12	70.6	0.636
≥65	13	20.3	5	29.4	
Sex					
Male	55	85.9	14	82.4	1.000
Female	9	14.1	3	17.6	
WHO histology					
Squamous	39	60.9	11	64.7	0.208
Non-squamous	23	35.9	4	23.5	
NOS	2	3.1	2	11.8	
Stage					
IIIA	25	39.1	10	58.8	0.226
IIIB	33	51.6	5	29.4	
IIIC	6	9.4	2	11.8	
Dose					
<54 Gy	0	0.0	0	0.0	not applicable
≥54 Gy	64	100.0	17	0.0	
Smoking					
Never	13	20.3	5	29.4	0.636
Former/Current	51	79.7	12	70.6	
ECOG					
0	8	12.5	1	5.9	0.389
1	55	85.9	15	88.2	
2	1	1.6	1	5.9	

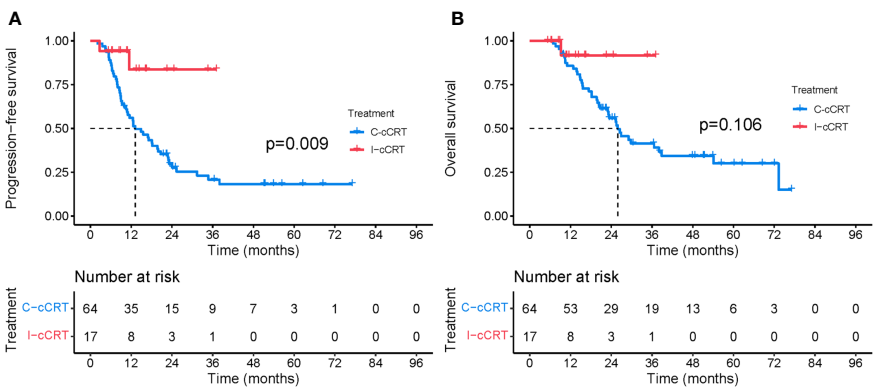


FIGURE 5
PFS and OS between the C-cCRT group and the I-cCRT group. **(A)** PFS from the initiation of treatment. **(B)** OS from the initiation of treatment.

TABLE 4 TRAEs between the C-cCRT and I-cCRT groups.

TRAE	C-cCRT		I-cCRT		P
	No.	%	No.	%	
Pneumonitis	38	59.4	10	58.8	0.967
G3/4 pneumonitis	7	10.9	0	0.0	0.347
Esophagitis	15	23.4	2	11.8	0.474
G3/4 esophagitis	0	0.0	0	0.0	not applicable
Hematologic toxicity	46	71.9	14	82.4	0.572
G3/4 hematologic toxicity	15	23.4	7	41.2	0.248

chemotherapy in the present study and the ORR of approximately 30% for induction chemotherapy in previous studies (6, 7). However, whether the short-term efficacy benefit of induction chemoimmunotherapy translates into a survival benefit in patients with stage III NSCLC receiving cCRT has not yet been confirmed. Before the era of immunotherapy, induction chemotherapy was confirmed to have no additional survival benefit in patients receiving cCRT (6, 7). The advantage of the downstaging effect of induction chemotherapy does not translate into a significant PFS or OS benefit. In this study, adding immunotherapy to induction chemotherapy significantly prolonged survival in patients receiving cCRT. Moreover, although calculated from the start of treatment, the 83.7% 2-year PFS rate and 91.7% 2-year OS rate in the present study were non-inferior to the 45.0% 2-year PFS rate and 66.3% 2-year OS rate in the PACIFIC trial, suggesting that induction chemoimmunotherapy before cCRT may achieve similar outcomes to consolidation immunotherapy with fewer cycles of immunotherapy. However, the small sample size limits the ability to draw a definitive conclusion. Prospective randomized controlled trials focusing on the comparison between these two treatment modalities are needed in the future.

The risk of treatment-related adverse events is another primary concern. Previous data have indicated that combining immunotherapy with CRT could increase the incidence of pneumonitis (17–19). In this study, there was no significant difference in the incidence of pneumonitis regardless of whether patients received induction chemoimmunotherapy before CRT. The incidence of grade 3/4 pneumonitis in patients receiving induction chemoimmunotherapy was approximately 3%, which was slightly lower than the findings of Wang et al. (9.3%) and the incidence of pneumonitis in the real-world PACIFIC regimen (4.4%-6.0%) (5, 20, 21). Only one-third of patients receiving induction chemoimmunotherapy in the present study received cCRT, which may have contributed to this result. The incidence of the remaining common TRAEs was similar between the two groups, except for a higher but still acceptable incidence of hematological toxicity in patients receiving induction chemoimmunotherapy. When cases were further restricted to those receiving induction treatment plus cCRT, the addition of immunotherapy did not significantly increase the incidence of grade 3/4 TRAEs, suggesting that the toxicity of induction chemoimmunotherapy plus CRT or even cCRT is tolerable.

This study represents a retrospective analysis of data and thus has some evident limitations. First, this is a retrospective single-institution study, which may limit the generalizability of the results. Second, this study spanned a relatively long period, and the improved treatment may lead to an over-interpretation of the results. Third, data regarding PD-L1 expression are sparse because it is not routinely tested in stage III NSCLC at our center. In addition, the heterogeneous treatment approach, including different ICI agents, may also bias the results. Although a previous study demonstrated no statistically significant differences in the safety and efficacy between various ICIs (22), future studies should use identical ICI agents and stratify by PD-L1 expression to minimize confounding. Furthermore, as previously mentioned, the moderate sample size of patients treated with induction chemoimmunotherapy and the subsequent analysis in the cCRT setting further reduced the sample size, which may also influence the results. Finally, this novel treatment modality was not compared with the PACIFIC regimen due to the low proportion of patients receiving consolidation immunotherapy, and future large-scale clinical trials are warranted to confirm whether it can achieve comparable outcomes to consolidation immunotherapy and whether the combination of induction and consolidation immunotherapy can provide further survival benefits. Despite these limitations, our analysis demonstrates the safety and efficacy of induction chemoimmunotherapy before CRT with relatively few cycles of immunotherapy and, more importantly, may provide a new option for patients who cannot or refuse to receive 1 or even 2 years of consolidation immunotherapy due to the high economic burden and so on. To the best of our knowledge, this is the first study to evaluate the prognostic role of induction chemoimmunotherapy in unresectable stage III NSCLC patients. We believe this study could provide a new direction for research or a treatment option for patients who cannot or refuse to receive consolidation immunotherapy.

5 Conclusions

In conclusion, induction chemoimmunotherapy is safe and may improve outcomes of CRT in patients with unresectable stage III NSCLC. Moreover, induction chemoimmunotherapy may further improve treatment response and survival outcomes compared to induction chemotherapy before cCRT.

Data availability statement

The raw data supporting the conclusions of this article will be made available by the authors, without undue reservation.

Ethics statement

The studies involving humans were approved by Institutional Review Board of Cancer Institute and Hospital of Tianjin Medical University. The studies were conducted in accordance with the local legislation and institutional requirements. The need for informed consent was waived owing to the retrospective nature of the study.

Author contributions

SG: Conceptualization, Data curation, Formal analysis, Writing – original draft. SZ: Data curation, Formal analysis, Writing – original draft. KR: Data curation, Formal analysis, Writing – review & editing. XYL: Data curation, Formal analysis, Writing – review & editing. XL: Formal analysis, Funding acquisition, Investigation, Writing – review & editing. LZ: Conceptualization, Funding acquisition, Supervision, Writing – review & editing.

Funding

The author(s) declare financial support was received for the research, authorship, and/or publication of this article. This research was funded by the Tianjin Key Medical Discipline (Specialty) Construction Project (TJYXZDXK-009A) and the National Natural Science Foundation of China (No. 81903121).

Conflict of interest

The authors declare that the research was conducted in the absence of any commercial or financial relationships that could be construed as a potential conflict of interest.

Publisher's note

All claims expressed in this article are solely those of the authors and do not necessarily represent those of their affiliated organizations, or those of the publisher, the editors and the reviewers. Any product that may be evaluated in this article, or claim that may be made by its manufacturer, is not guaranteed or endorsed by the publisher.

Supplementary material

The Supplementary Material for this article can be found online at: https://www.frontiersin.org/articles/10.3389/fimmu.2023.1289207/full#supplementary-material

References

1. Spigel DR, Faivre-Finn C, Gray JE, Vicente D, Planchard D, Paz-Ares L, et al. Five-year survival outcomes from the PACIFIC trial: durvalumab after chemoradiotherapy in stage III non-small-cell lung cancer. *J Clin Onol* (2022) 40 (12):1301–11. doi: 10.1200/JCO.21.01308

2. Forde PM, Spicer J, Lu S, Provencio M, Mitsudomi T, Awad MM, et al. Neoadjuvant nivolumab plus chemotherapy in resectable lung cancer. *New Engl J Med* (2022) 386(21):1973–85. doi: 10.1056/NEJMoa2202170

3. Felip E, Altorki N, Zhou C, Csőszi T, Vynnychenko I, Goloborodko O, et al. Adjuvant atezolizumab after adjuvant chemotherapy in resected stage IB-IIIA non-smallcell lung cancer (IMpower010): a randomised, multicentre, open-label, phase 3 trial. *Lancet* (2021) 398(10308):1344–57. doi: 10.1016/S0140-6736(21)02098-5

4. O'Brien M, Paz-Ares L, Marreaud S, Dafni U, Oselin K, Havel L, et al. Pembrolizumab versus placebo as adjuvant therapy for completely resected stage IB-IIIA non-small-cell lung cancer (PEARLS/KEYNOTE-091): an interim analysis of a randomised, triple-blind, phase 3 trial. *Lancet Oncol* (2022) 23(10):1274–86. doi: 10.1016/S1470-2045(22)00518-6

5. Wang Y, Zhang T, Wang J, Zhou Z, Liu W, Xiao Z, et al. Induction immune checkpoint inhibitors and chemotherapy before definitive chemoradiation therapy for patients with bulky unresectable stage III non-small-cell lung cancer. *Int J Radiat Oncol* (2023) 116(3):590–600. doi: 10.1016/j.ijrobp.2022.12.042

6. Kim S, Kim M, Choi E, Sohn H, Lee D, Lee CS, et al. Induction chemotherapy followed by concurrent chemoradiotherapy (CCRT) versus CCRT alone for unresectable stage III non-small cell lung cancer (NSCLC): randomized phase III trial. *J Clin Oncol* (2007) 25(18_Suppl):7528. doi: 10.1200/jco.2007.25.18_suppl.7528

7. Vokes EE, Herndon JE, Kelley MJ, Cicchetti MG, Ramnath N, Neill H, et al. Induction chemotherapy followed by chemoradiotherapy compared with chemoradiotherapy alone for regionally advanced unresectable stage III nonsmall-cell lung cancer: Cancer and Leukemia Group B. *J Clin Oncol* (2007) 25(13):1698–704. doi: 10.1200/JCO.2006.07.3569

8. Travis WD, Brambilla E, Nicholson AG, Yatabe Y, Austin JHM, Beasley MB, et al. The 2015 World Health Organization Classification of Lung Tumors: impact of genetic, clinical and radiologic advances since the 2004 classification. *J Thorac Oncol* (2015) 10 (9):1243–60. doi: 10.1097/JTO.0000000000000630

9. Detterbeck FC, Boffa DJ, Kim AW, Tanoue LT. The eighth edition lung cancer stage classification. *Chest* (2017) 151(1):193–203. doi: 10.1016/j.chest.2016.10.010

10. Gan J, Huang Y, Fang W, Zhang L. Research progress in immune checkpoint inhibitors for lung cancer in China. *Ther Adv Med Oncol* (2021) 13:17588359211029826. doi: 10.1177/17588359211029826

11. Cotarla I, Boron ML, Cullen SL, Spinner DS, Faulkner EC, Carroll MC, et al. Treatment decision drivers in stage III non–small-cell lung cancer: outcomes of a web-based survey of oncologists in the United States. *JCO Oncol Pract* (2020) 16(10):e1232–42. doi: 10.1200/JOP.19.00781

12. Xing L, Yu J, Zhao R, Yang W, Guo Y, Li J, et al. 125P Real-world treatment patterns in stage III NSCLC patients: Interim results of a prospective, multicenter, noninterventional study (MOOREA). *J Thorac Oncol* (2023) 18(4_Suppl):S111–2. doi: 10.1016/S1556-0864(23)00380-5

13. Zhou Q, Chen M, Jiang O, Pan Y, Hu D, Lin Q, et al. Sugemalimab versus placebo after concurrent or sequential chemoradiotherapy in patients with locally advanced, unresectable, stage III non-small-cell lung cancer in China (GEMSTONE-301): interim results of a randomised, double-blind, multicentre, phase 3 trial. *Lancet Oncol* (2022) 23(2):209–19. doi: 10.1016/S1470-2045(21)00630-6

14. Bruni A, Scotti V, Borghetti P, Vagge S, Cozzi S, D'Angelo E, et al. A real-world, multicenter, observational retrospective study of durvalumab after concomitant or sequential chemoradiation for unresectable stage III non-small cell lung cancer. *Front Oncol* (2021) 11:744956. doi: 10.3389/fonc.2021.744956

15. Chang JY. When constrained by constraints: thinking outside of the box in both technology and biology. *Int J Radiat Oncol* (2021) 110(2):266–7. doi: 10.1016/j.ijrobp.2020.10.014

16. Lang P, Palma D. Too big to fail: miracle drugs or false hope? *Int J Radiat Oncol* (2021) 110(2):264. doi: 10.1016/j.ijrobp.2020.10.013

17. Shaverdian N, Beattie J, Thor M, Offin M, Shepherd AF, Gelblum DY, et al. Safety of thoracic radiotherapy in patients with prior immune-related adverse events from immune checkpoint inhibitors. *Ann Oncol* (2020) 31(12):1719–24. doi: 10.1016/j.annonc.2020.09.016

18. Aiad M, Fresco K, Prenatt Z, Tahir A, Ramos-Feliciano K, Stoltzfus J, et al. Comparison of pneumonitis rates and severity in patients with lung cancer treated by immunotherapy, radiotherapy, and immunoradiotherapy. *Cureus* (2022) 14(6):e25665. doi: 10.7759/cureus.25665

19. Cousin F, Desir C, Ben Mustapha S, Mievis C, Coucke P, Hustinx R, et al. Incidence, risk factors, and CT characteristics of radiation recall pneumonitis induced by immune checkpoint inhibitor in lung cancer. *Radiother Oncol* (2021) 157:47–55. doi: 10.1016/j.radonc.2021.01.001

20. Antonia SJ, Villegas A, Daniel D, Vicente D, Murakami S, Hui R, et al. Durvalumab after chemoradiotherapy in stage III non-small-cell lung cancer. *New Engl J Med* (2017) 377(20):1919–29. doi: 10.1056/NEJMoa1709937

21. Wang Y, Zhang T, Huang Y, Li W, Zhao J, Yang Y, et al. Real-world safety and efficacy of consolidation durvalumab after chemoradiation therapy for stage III non-small cell lung cancer: A systematic review and meta-analysis. *Int J Radiat Oncol* (2022) 112(5):1154–64. doi: 10.1016/j.ijrobp.2021.12.150

22. Miao K, Zhang X, Wang H, Si X, Ni J, Zhong W, et al. Real-world data of different immune checkpoint inhibitors for non-small cell lung cancer in China. *Front Oncol* (2022) 12:859938. doi: 10.3389/fonc.2022.859938

frontiers | Frontiers in Immunology

TYPE Review
PUBLISHED 29 November 2023
DOI 10.3389/fimmu.2023.1279735

Check for updates

OPEN ACCESS

EDITED BY
Zichao Luo,
National University of Singapore, Singapore

REVIEWED BY
Zhen Dong,
Southwest University, China
Qi Wu,
Shanghai Children's Hospital, China
Matias I Hepp,
Universidad Católica de la Santísima Concepción, Chile

*CORRESPONDENCE
Shali Yu
7693539@ntu.edu.cn
Xinyuan Zhao
zhaoxinyuan@ntu.edu.cn
Lin Chen
xiaobei227@sina.com

†These authors have contributed equally to this work

RECEIVED 18 August 2023
ACCEPTED 13 November 2023
PUBLISHED 29 November 2023

CITATION
Yu M, Ji W, Yang X, Tian K, Ma X, Yu S, Chen L and Zhao X (2023) The role of m6A demethylases in lung cancer: diagnostic and therapeutic implications.
Front. Immunol. 14:1279735.
doi: 10.3389/fimmu.2023.1279735

COPYRIGHT
© 2023 Yu, Ji, Yang, Tian, Ma, Yu, Chen and Zhao. This is an open-access article distributed under the terms of the Creative Commons Attribution License (CC BY). The use, distribution or reproduction in other forums is permitted, provided the original author(s) and the copyright owner(s) are credited and that the original publication in this journal is cited, in accordance with accepted academic practice. No use, distribution or reproduction is permitted which does not comply with these terms.

The role of m6A demethylases in lung cancer: diagnostic and therapeutic implications

Mengjiao Yu[1†], Wenqian Ji[2†], Xu Yang[1†], Kai Tian[1], Xinyi Ma[1], Shali Yu[1*], Lin Chen[3*] and Xinyuan Zhao[1*]

[1]Department of Occupational Medicine and Environmental Toxicology, Nantong Key Laboratory of Environmental Toxicology, School of Public Health, Nantong University, Nantong, China, [2]College of International Studies, Southwest University, Chongqing, China, [3]Nantong Institute of Liver Diseases, Nantong Third People's Hospital Affiliated Nantong Hospital of Nantong University, Nantong, China

m6A is the most prevalent internal modification of eukaryotic mRNA, and plays a crucial role in tumorigenesis and various other biological processes. Lung cancer is a common primary malignant tumor of the lungs, which involves multiple factors in its occurrence and progression. Currently, only the demethylases FTO and ALKBH5 have been identified as associated with m6A modification. These demethylases play a crucial role in regulating the growth and invasion of lung cancer cells by removing methyl groups, thereby influencing stability and translation efficiency of mRNA. Furthermore, they participate in essential biological signaling pathways, making them potential targets for intervention in lung cancer treatment. Here we provides an overview of the involvement of m6A demethylase in lung cancer, as well as their potential application in the diagnosis, prognosis and treatment of the disease.

KEYWORDS

lung cancer, m6A demethylase, FTO, ALKBH5, immunotherapy

1 Introduction

Lung cancer is a highly prevalent and devastating form of primary lung malignancy, contributing to a significant portion of cancer-related deaths worldwide. It accounts for approximately 18% of all cancer fatalities. Unfortunately, the survival rates for lung cancer remain alarmingly low, with five-year relative survival rates of 23% (1). Understanding the diverse histopathological classifications is crucial for comprehending the complexity of this disease. In terms of histopathologically, lung cancer can be categorized into non-small cell lung cancer (NSCLC) and small cell lung cancer (SCLC). NSCLC is the most common type, and it accounts for approximately 85% of all cases, while SCLC represents about 15%. Within the subtypes of NSCLC, lung adenocarcinoma is the most prevalent histological variant, making up around 40% of NSCLC cases. Lung squamous cell carcinoma closely follows, comprising approximately 35% of NSCLC cases (2).

Epigenetic modifications play a crucial role in the initiation and progression of various tumours. These modifications mainly involve regulation of gene function and expression

through processes such as DNA methylation, regulation of non-coding RNA, histone modification, and chromatin remodelling. By modifying these epigenetic marks, tumor cells can manipulate gene activity and disrupt normal cellular processes, thereby contributing to the development and advancement of cancer (3). Among the various epigenetic modifications, one of the most extensively studied is N6-adenylate methylation (m6A), which is a common internal modification in eukaryotic mRNA molecules. It represents around 60% of all known RNA modifications identified in mammals (4, 5). m6A takes place when methylation occurs at the sixth position of adenylate (A) nucleotides within the RNA molecule (6). The discovery of m6A modification provides new insights into the intricate regulation of gene expression in cancer cells. This modification serves as a dynamic and reversible mark that can impact multiple aspects of mRNA metabolism, such as splicing, stability, localization, and translation efficiency. Through m6A modification, tumor cells possess the ability to precisely regulate the expression of crucial genes that are involved in pathways essential for cell survival, proliferation, invasion, and metastasis (7). In addition, there is evidence indicating that dysregulation of m6A modification machinery and aberrant m6A patterns are commonly observed in various cancer types, can affect the occurrence and development of breast cancer, ovarian cancer, gastric cancer, lung cancer, colon cancer and other cancers (8–12). These changes can affect the behaviour of tumour cells, leading to disease advancement and resistance to treatment. Consequently, some researchers have concentrated their efforts on uncovering the specific mechanisms involved in m6A modification and its functional implications in the development of tumors (13, 14).

The occurrence of m6A modification involves the participation of multiple enzymes, including Writers, Readers and Erasers. During the transcription of DNA into RNA, the sixth N of adenosine is methylated and modified by methyltransferases such as METTL3, METTL14 and WTAP (15–17). These enzyme are referred to as Writers, specifically methylases. RNA base sites often require specific enzymes to recognize them after methylation. These enzymes, known as Readers, primarily include YTH domain proteins, nuclear heterogeneous riboproteins (hnRNPs) and eukaryotic initiation factors (eIFs) (18–20). Readers can recognize the bases where m6A methylation occurs and have the functions that include participating in mRNA degradation, downstream translation, and accelerating the rate of mRNA nuclear export. m6A demethylases are called Erasers, mainly including Fat mass and obesity-associated protein (FTO) and human AlkB homolog 5 (ALKBH5). FTO, a member of the Alkb protein family, is the first m6A demethylase that acts on mRNA in an iron-dependent manner (21). It primarily localizes in the nucleus and exhibits a punctate pattern in the nucleoplasm, partially co-localizing with splicing or splicing-related spot factor SART1 (22). Under physiological conditions, FTO demonstrates the highest affinity for m6A as a substrate. Changes or dysfunction in FTO expression may contribute to the occurrence and development of various tumors, where it can act as either a tumour suppressor gene or oncogene. FTO has been found to play a critical role in tumor cell proliferation, metastasis and apoptosis. ALKBH5, another important m6A demethylase, is capable of demethylating mRNA in the nucleus. It possesses an alanine-rich region at the N-terminus and a unique coiled-coil structure (23). Current studies have revealed dysregulation of ALKBH5 expression in various cancers, including lung, breast, and gastric cancer. ALKBH5 can exert both carcinogenic and tumor-suppressive effects, depending on the specific cancer type. Its involvement in cancer is closely related to death, migration, invasion, and metastasis (12, 24, 25).

In general, m6A demethylases catalyze the removal of methylation at the N6 position of adenylate in mRNA, thereby modulating the epigenetic information of mRNA. Upregulation of their expression decreases m6A modification, impacting the stability and translation efficiency of mRNA. m6A modification has been implicated in the promotion of lung cancer growth and progression, affecting the proliferation, invasion, and metastasis of lung cancer cells. Aberrant m6A modification may result from abnormal expression of writers and erasers. When exposed to external factors such as environmental pollutants, m6A modification abnormalities may occur, influencing the onset and progression of lung cancer and other cancers. Additionally, other proteins and signaling pathways involved in m6A modification may also play a role in lung cancer. m6A modification can influence the characteristics and maintenance of lung cancer stem cells, thereby facilitating tumor initiation (26, 27). It can also impact the transcription and translation processes in lung cancer cells, thereby regulating key signaling pathways and promoting tumor progression and metastasis. Moreover, m6A modification can modulate the expression of genes associated with lung cancer by altering mRNA stability, thereby affecting crucial processes such as cell cycle control and apoptosis (10, 28). Notably, lung cancer is a multifaceted disease influenced by various contributors, including genetic mutations, epigenetic alterations, and environmental factors. Thus, further investigations are needed to comprehensively elucidate the precise mechanisms underlying m6A modification in lung cancer.

Understanding the significance of m6A modification in cancer is crucial for the advancement of targeted treatment strategies and the discovery of potential biomarkers. By unraveling the intricate interplay between m6A writers, erasers, and readers, researchers can gain insights into the molecular mechanisms driving tumor progression. Recent studies have highlighted the importance of FTO and ALKBH5, as erasers involved in m6A RNA demethylation, in the development of lung cancer. These demethylases have been found to be closely associated with occurrence and development of the cancer. Furthermore, we will discuss future directions of research in this field and explore the potential clinical applications of targeting of FTO and ALKBH5 in the treatment of lung cancer. The relationship between erasers and lung cancer is shown in Figures 1, 2.

2 The impact of m6A demethylases on lung cancer progression

m6A, as the most prevalent mRNA modification, has methyltransferases like METTL3 being responsible for adding methyl groups to specific mRNA sites, while m6A demethylases FTO and ALKBH5 are responsible for removing methyl groups from m6A. The interaction between methyltransferases and demethylases helps maintain a balanced level of m6A. When

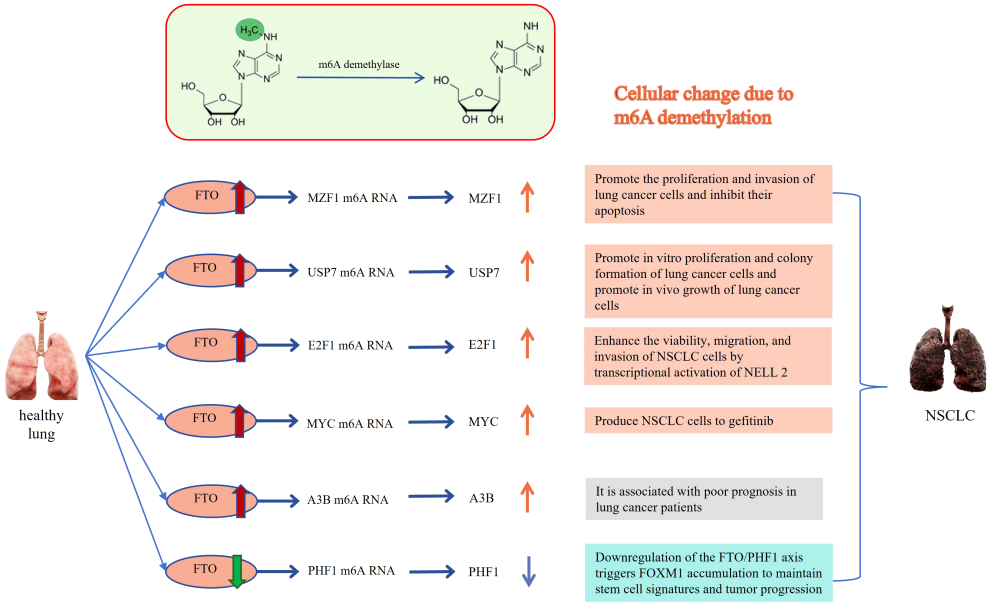


FIGURE 1
Relationship between FTO and lung cancer: The m6A methylated RNA can be demethylated by FTO, resulting in the occurrence of cytological behaviors that contribute to the development of NSCLC. MZF1, Myeloid Zinc Finger Protein 1; USP7, ubiquitin-specific protease-7; E2F1, E2F transcription factor-1; MYC, v-myc avian myelocytomatosis viral oncogene homolog; A3B, APOBEC3B; PHF1, Human Plant Homeodomain (PHD) finger protein 1. The Red and orange arrows represent increased m6A demethylase levels or m6A modification levels of RNA; The green and blue arrows represent decreased m6A demethylase levels or m6A modification levels of RNA.

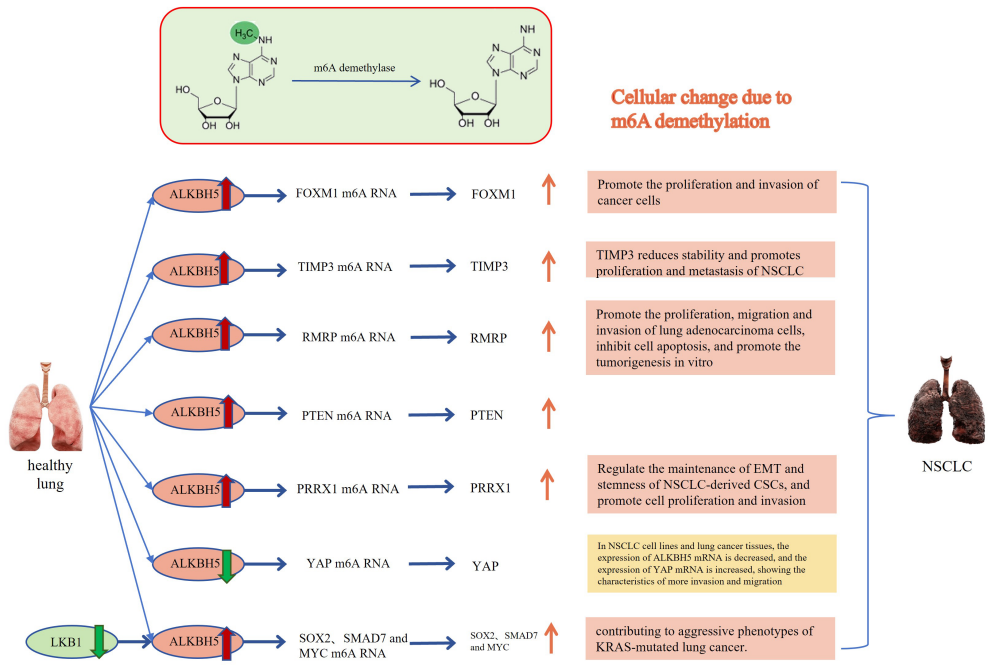


FIGURE 2
Relationship between ALKBH5 and lung cancer: The m6A methylated RNA undergoes demethylation through the action of ALKBH5, leading to the occurrence of cytological behaviors that promote the development of NSCLC. FOXM1, Forkhead box M1; TIMP3, TIMP metallopeptidase inhibitor 3; RMRP, RNA Component of Mitochondrial RNA Processing Endoribonuclease; PTEN, Phosphatase and tensin homolog deleted on chromosome 10; PRRX1, Paired related homeobox 1; YAP, Yes-associated protein; SOX2, SRY-box transcription factor 2; SMAD7, SMAD family member 7. The Red and orange arrows represent increased m6A demethylase levels or m6A modification levels of RNA; The green and blue arrows represent decreased m6A demethylase levels or m6A modification levels of RNA.

m6A levels are stable, mRNA transcripts with appropriate m6A levels can undergo proper splicing, transport, translation, or degradation. Imbalanced m6A regulation can lead to RNA metabolism defects (29, 30). FTO and ALKBH5 are known to be upregulated in lung cancer tissues. They have been found to play a crucial in tumor cell proliferation, apoptosis, invasion, and migration, and their functions are dependent on the presence of m6A modifications (31, 32). These demethylases also contribute to the regulation of tumor progression in lung cancer (33). The possible mechanisms by which m6A demethylation affects the development and progression of lung cancer are listed in Table 1.

2.1 The role of demethylase overexpression in cell proliferation and apoptosis

The research on the relationship between demethylase and lung cancer, as well as its mechanism is still in the early stages. However, increasing evidence suggests that m6A demethylases FTO and ALKBH5 are frequently overexpressed in lung cancer and significantly associated with the tumor's prognosis. As research progresses, the involvement of m6A modification in lung cancer is gradually being confirmed. Numerous studies have demonstrated that the demethylation process in lung cancer cells plays a crucial role in regulating the expression of key genes involved in essential cellular processes such as cell proliferation and apoptosis. Disturbances in DNA methylation patterns can disrupt the normal regulation of these genes, leading to increased proliferation of lung cancer cells and decreased apoptosis. These alterations contribute to progression and aggressiveness of tumors (46, 47). In lung cancer, abnormal DNA demethylation can occur at specific genomic regions, resulting in the activation of oncogenes or the silencing of tumor suppressor genes (48). Through the removal of the methyl groups from the DNA molecule, demethylation can lead to the overexpression of genes that promote cell proliferation, giving cancer cells a growth advantage (10). Moreover, the suppression of genes responsible for apoptosis can enable cancer cells to evade programmed cell death, aiding in their survival and expansion (28).

TABLE 1 Biological function of M6A demethylase in lung cancer.

Function	m6A demethylases	Targeted genes	Ref.
Involved in regulating the proliferation and invasion of lung cancer cells.	FTO, ALKBH5	USP7, E2F1	(34–36)
Regulate angiogenesis in the lungs.	ALKBH5	PVT1	(37)
Regulate transcriptional and post-transcriptional modification levels in lung cancer cells.	FTO, ALKBH5	MZF1	(38, 39)
Affect drug tolerance of lung cancer cells.	FTO, ALKBH5	ABCC10, cMyc, WIF1	(40–42)
Regulate the properties and self-renewal ability of lung cancer stem cells.	FTO, ALKBH5	KRT7	(26, 27)
Participate in the metastasis and invasion process of lung cancer.	FTO, ALKBH5	UBE2C, IGF2BP	(27, 28)
Affect the mechanism of apoptosis and apoptosis evasion in lung cancer cells.	FTO, ALKBH5	UBE2C, TIMP3, IGF2BP	(10, 28, 43)
Interact with other signaling pathways to affect the survival and proliferation of lung cancer cells	FTO, ALKBH5	FOXM1, miR-607, A3B	(24, 44, 45)

Li et al. conducted a study that revealed a significant association between high expression of m6A demethylase FTO and cancer development. The overexpression of FTO could promote cell proliferation and colony formation (34, 49, 50). Both mRNA and protein levels of FTO were observed to be overexpressed in human NSCLC tissues and cell lines. Conversely, the loss of FTO function resulted in a reduced proliferation rate of cancer cells. Mechanistically, FTO can decrease m6A levels through its demethylase activity, enhance the stability of ubiquitin-specific protease (USP7) mRNA, and promote the growth of lung cancer cells (49, 50). Another study demonstrated that FTO can promote the proliferation and invasion of LUSC by reducing the m6A level in myeloid zinc finger 1 (zinc finger 1, MZF1) mRNA transcription and maintaining the mRNA stability (38). Additionally, some studies have shown that circular RNAs can act as miRNA sponges, promoting cancer cell proliferation and participating in the process of NSCLC. For instance, Hsa_circ_0072309 can sponge miR-607, leading to the upregulation of its target gene FTO and promoting the occurrence of NSCLC (44). Another m6A demethylase also ALKBH5 also plays a key role in promoting or inhibiting cell proliferation and apoptosis. FOXM1 is involved in important cellular processes such as cell proliferation, cell differentiation, cell cycle regulation, angiogenesis and metastasis. It is often upregulated in human malignant tumors, indicating a poor prognosis (51, 52). Studies have shown that upregulation of ALKBH5 in cancer cells can enhance the translation efficiency of FOXM1 mRNA, leading to increased FOXM1 protein expression and promoting the proliferation and invasion of cancer cells (24). Similarly, Zhu et al. demonstrated in their studies that ALKBH 5 promotes the proliferation of NSCLC cells and reduces apoptosis *in vitro*. Knockdown of ALKBH5 *in vivo* inhibited tumor growth primarily by destabilizing TIMP 3 mRNA. ALKBH5 interacts with the methylation site of TIMP3 in the 3'UTR to facilitate protein production (10). Additionally, studies have shown that knockout ALKBH5 can induce G1 phase arrest, inhibit the cancer cell proliferation, and increase the number of apoptotic cells (43). ALKBH5 also can indirectly regulating autophagy. For instance, UBE2C, a ubiquitin-conjugating enzyme, selectively inhibits autophagy in NSCLC. Destroying UBE2C-mediated autophagy inhibition weakens the proliferation and clonogenicity of NSCLC. ALKBH5 stabilizes UBE2C transcription by reducing the m6A methylation level in its mRNA (28). Indeed, m6A demethylation

plays a significant role in lung cancer cell proliferation, providing important insights into the understanding and treatment of lung cancer. The biological function and specific mechanism leading to cancer development and progression of m6A demethylation are not fully understood, and further research is required for validation.

2.2 m6A demethylases-mediated regulation of invasion and migration in lung cancer cells

Demethylation is closely related to the invasion and migration of lung cancer cells as well. Studies have shown that demethylation can affect the metastatic ability of lung cancer cells, thus facilitating the metastasis and invasion of these cells. Demethylation plays a role in gene expression regulation, particularly in relation to cell metastasis by transcription factors and signaling molecules. One example is the activation of cell migration by FTO through mRNA demethylation. This activation can contribute to the progression of lung cancer and affect the prognosis of patients (35). Liu et al.'s study demonstrated that the higher levels of FTO are associated with worse prognosis in LUSC patients. FTO acts as an m6A mRNA demethylase, promoting cell migration and invasion (38). Another study found that FTO can inhibit the M6A modification of E2F1 *in vivo*, leading to increased expression of E2F1. E2F1, in turn, enhances the survival, migration, and invasion of NSCLC cells by activating NELL2 transcriptionally. Furthermore, FTO can promote the formation and metastasis of NSCLC through the FTO/E2F1/NELL2 axis *in vitro* (36). As for ALKBH5, some studies have found that ALKBH5 can promote cell migration and invasion. In lung cancer patients, the levels of ALKBH5 protein expression have been observed to be positively associated with tumor size, TNM staging, and clinical staging. Research by Yu et al. indicated that patients with higher ALKBH5 gene expression had a poorer prognosis (53). ALKBH5 upregulates the expression of RMRP through demethylation, and the upregulation of RMRP promotes the proliferation and invasion of lung adenocarcinoma cells while inhibiting cell apoptosis. However, other researchers have discovered that overexpression of ALKBH5 effectively reverses the proliferation, colony formation and migration of kras mutant lung cancer cells that are regulated by LKB1 (47).

The impact of demethylation on the phenotypic transition of cells, such as the transition from epithelial cells to mesenchymal cells, and its effect on the invasion and migration of lung cancer cells have yielded different conclusions, including both promotion and inhibition of lung cancer cell migration by ALKBH. Experiments conducted by Guo et al. demonstrated that downregulation of ALKBH5 using miR-381 and siRNA specifically impedes the EMT of NSCLC cells, thereby inhibiting their migration and invasive growth (28). Liu et al. also found that ALKBH 5 is highly expressed in NSCLC-derived CSCs (cancer stem cells), and downregulation of ALKBH5 significantly reduces Sox2 expression, leading to increased levels of E-cadherin protein, inhibition of EMT, and suppression of tumor invasive development and metastasis (54). However, some researchers have come to the opposite conclusion. Studies have shown that TGF-β induces EMT in NSCLC and regulate cell migration and invasion. Interestingly, overexpression of ALKBH 5 can inhibit the metastasis of NSCLC cells stimulated by TGF-β *in vivo* (45). Jin et al. also believe that ALKBH5 acts as an inhibitor of NSCLC cell migration and invasion, ALKBH5 regulates the miR-107/LATS2 axis in a HURP-dependent manner, thereby reducing the expression and activity of YAP, thereby inhibiting tumor growth and metastasis (48). The possible explanation for this phenomenon is that when the gene interacts with a tumor suppressor gene it promotes cancer cell growth and metastasis while when it interacts with an oncogene it inhibits cancer cell growth. In addition, lung cancer is a highly heterogeneous disease, and biological diversity and subtype differences in lung cancer need to be considered. The specific reasons for the differences still need to be explored. Notably, patients with Trp53 gene mutations tend to have a poorer prognosis when FTO is expressed at high levels, while patients with the wild-type gene don't exhibit the same trend (39). This suggests that the observed phenomenon may be associated with specific genotype mutations, highlighting the need for further research. Overall, demethylation is a critical factor in the invasion and migration of lung cancer cells, playing a role in their metastatic potential. By influencing gene expression, the phenotypic transition of cells and other processes, demethylation can promote the acquisition of invasive and migratory characteristics in lung cancer cells. Further research focusing on the identification of specific genes and molecular pathways affected by demethylation in the context of lung cancer metastasis could offer valuable insights for targeted therapies to address metastatic disease.

3 Potential applications of m6A demethylase in the diagnosis, prognosis assessment and treatment of lung cancer

3.1 Application of m6A demethylase in the lung cancer diagnosis

Recent studies have shown that significant application value of m6A demethylase in diagnosing lung cancer. Specifically, by comparing the expression levels of m6A demethylase in lung cancer tissue and normal lung tissue, researchers have observed significant alterations in its expression, either upregulation or downregulation, indicating its potential as a diagnostic marker for lung cancer. These findings have garnered considerable attention in the field of lung cancer diagnosis. Among the m6A demethylases, FTO and ALKBH5 may be associated with lung cancer, and their relationship has been gradually studied. These enzymes have demonstrated potential in developing risk assessment models that enhance the accuracy of diagnosing lung adenocarcinoma (LUAD), a prevalent histological subtype of lung cancer. By incorporating methylation-related enzymes, such as FTO and ALKBH5, into these risk assessment models, researchers have achieved improved prediction accuracy for LUAD diagnosis (55). Moreover, evaluating the expression levels of m6A demethylases in blood or

tissue samples from lung cancer patients holds the potential for early diagnosis, pathological classification, and staging of lung cancer staging (47). The application of m6A demethylases in lung cancer diagnosis is an exciting area of research with significant clinical implications. By incorporating these enzymes into diagnostic algorithms and utilizing their association with tumorigenesis, healthcare professionals may enhance the accuracy and efficiency of lung cancer diagnosis (56). Additionally, the ability to detect m6A demethylase expression in various sample types, including blood and tissue, may offer a non-invasive and easily accessible approach for the early detection and monitoring of lung cancer (57, 58). Indeed, additional research is required to validate and enhance the diagnostic potential of m6A demethylases in lung cancer. Large-scale clinical studies involving diverse patient populations are necessary to establish robust diagnostic models and determine the specific thresholds for demethylase expression levels in different stages and subtypes of lung cancer (59, 60). These investigations will aid in developing standardized diagnostic protocols and facilitate the integration of m6A demethylases into routine clinical practice for accurate lung cancer diagnosis. In summary, recent studies have demonstrated the potential value of m6A demethylases in diagnosing lung cancer. The differential expression of these enzymes in lung cancer tissue and their potential integration into risk assessment models underscore their diagnostic potential (61). Moreover, assessing m6A demethylase expression levels in blood or tissue samples shows promise for early diagnosis, pathological typing, and lung cancer staging (62). Further research and validation are needed to fully realize the diagnostic capabilities of m6A demethylases, leading to improved lung cancer diagnosis and patient care.

3.2 Application of m6A demethylase in the lung cancer prognosis assessment

m6A demethylases have shown significant potential in the prognostic assessment of lung cancer. The expression levels of these enzymes in lung cancer tissues have been strongly correlated with patient survival rates and overall prognosis (63). Abnormally expression of demethylases, either too high or too low, may serve as indicators of poor clinical outcomes. Studies have indeed reported that high expression of ALKBH5 and FTO is associated with a favourable prognosis in lung cancer patients (64). Elevated levels of these demethylases may indicate better outcomes for patient (65). Furthermore, the expression levels of m6A demethylases can be used to develop prognostic models to assess the risk of poor prognosis in patients. Recent research has focused on the construction of such models using factors including FTO and other genes. For instance, Zhang et al. developed a model, and found that a two-gene model combining FTO and METTL3 was more effective in guiding prognostic assessment of lung cancer (66). Additionally, researchers have utilized methylation-related enzymes such as FTO and ALKBH5 to develop risk assessment models for LUAD patients. These models divide LUAD patients into high-risk and low-risk categories based on the constructed models, and correlations have been observed with various clinical factors including TNM staging, lymph node staging, gender, and tumour stage (55). This suggests that the risk assessment model based on m6A demethylases can provide valuable insights into the prognosis and clinical characteristics of LUAD patients. These findings highlight the potential of m6A demethylases as prognostic markers in lung cancer. Incorporating m6A demethylase expression levels into prognostic models or risk assessment models can improve the accuracy of prognostic evaluation and assist in clinical decision-making. By considering the expression levels of these demethylases along with other relevant clinical factors, healthcare professionals can better predict patient outcomes and tailor treatment strategies accordingly. It is important to note that further research and validation are necessary to establish standardized prognostic models incorporating m6A demethylases in lung cancer (67, 68). Large-scale studies involving diverse patient populations must be conducted to confirm the associations between demethylase expression, prognostic risk, and clinical characteristics (69). These efforts will contribute to developing reliable prognostic tools that can guide patient management and improve prognostic assessments in lung cancer. m6A demethylase, along with other m6A regulatory factors, collaborates to regulate methylation in the body. Relying solely on ALKBH5 and FTO is not reliable for diagnosing and predicting prognosis in lung cancer patients. Therefore, it is more meaningful to collectively detect various regulatory factors than focusing on individual ones, as it can better reflect the actual conditions of lung cancer patients (70, 71). In clinical practice, monitoring the expression level of m6A demethylase in lung cancer patients is expected to offer personalized treatment recommendations and an accurate assessment of efficacy and prognosis. Numerous studies have indicated that m6A demethylase has the potential as a diagnostic and prognostic marker for lung cancer.

3.3 Application of m6A demethylation drugs in lung cancer treatment

Lung cancer, particularly NSCLC, continues to be the primary cause of cancer-associated mortality globally, constituting 85% of newly diagnosed cases (72). With the in-depth study of m6A demethylase mechanism in lung cancer, the potential application of m6A demethylation drugs in treating lung cancer is becoming increasingly evident. Significant progress has been made in the laboratory and clinical trials small molecule inhibitors and activators targeting demethylases such as FTO and ALKBH5 have made certain research progress. At present, the most commonly used m6A demethylase drugs are mainly focused on m6A demethylase inhibitors, which can regulate the activity of m6A demethylase by binding to its active site. FTO inhibitors included FB23 and FB23-2, rhein, Meclofenamic acid, fluorescein, R-2-hydroxyglutarate (R-2HG), et al. (73–77). In recent years, 44/ZLD115, Xanthine derivatives and other FTO inhibitors have been developed. Among them, 44/ZLD115 shows good anti-leukemia activity in xenograft mice and is a very promising FTO inhibitor (78, 79). With the continuous progress of scientific research, the development of

ALKBH inhibitors is also ongoing. For example,2- [(1-hydroxy-2-oxo-2-phenylethyl) sulfanyl] acetic acid (3) and 4-[(furan-2-yl) methyl] amino-1,2-diazinane-3,6-dione (6). These two novel ALKBH5 inhibitors could selectively inhibit the growth of leukemia cell lines (80). These drugs have shown promise in affecting tumor cell growth, invasion and metastasis by regulating the activity of m6A demethylase. However, the current development of m6A demethylase inhibitors is mainly focused on various types of leukemia, breast cancer, bowel cancer and other cancers, but they have shown promising characteristics, while m6A demethylase inhibitors for lung cancer still need to be developed by researchers.

A research team reported that the synthesis of an FTO inhibitor, which demonstrated its ability to inhibit cancer progression via the inhibition of cell invasion, migration, and EMT (epithelial-mesenchymal transition). Additionally, the inhibitor showed potential in inhibiting angiogenesis, a critical process for tumor growth and metastasis (27). Therapeutic resistance to multiple small molecules, including chemotherapeutics and targeted agents, is a significant factor contributing to poor prognosis in NSCLC (71, 81). Gefitinib, an essential drugs for treating lung cancer, has been found to be associated with demethylase-related resistance in NSCLC. Specifically, studies have reported that there is an association between the methylation level of WIF1 in cfDNA (Cell-free DNA) and the insensitivity of gefitinib in the treatment of lung cancer. In patients with more advanced disease, the DNA methylation levels of the WIF1 promoter are significantly elevated (41). Co-administration of GE (gefitinib) with MA (meclofenamic acid) has been demonstrated to enhance the sensitivity of drug-resistant NSCLC cells to treatment (42). This effect is attributed to the inhibition of BCRP and MRP7 expression levels through the FTO/m6A/MYC axis. These findings suggest that combining drugs can potentially overcome treatment resistance in NSCLC. Moreover, exosomes derived from gefitinib-resistant (GR) cells can play a role in intercellular transmission of gefitinib resistant through the FTO/YTHDF2/ABCC10 axis. These findings confirm the Feasibility of targeting FTO-m6A axis to prevent or delay the acquisition of gefitinib resistance in NSCLC (40).

In the future, m6A demethylation drugs have the potential to become a vital component of the comprehensive treatment strategy for lung cancer. By combining these drugs with traditional treatments such as surgery, radiotherapy, and chemotherapy, it is expected that the survival rate and quality of life for lung cancer patients can be improved. It is important to highlight that the research and development of drugs targeting m6A demethylation still encounter certain challenges. Firstly, there is a need to enhance the effectiveness of these drugs and minimize the occurrence of side effects by further refining their the selectivity and specificity (82). In addition, owing to the considerable heterogeneity of lung cancer, variations in the response of different patients to m6A demethylating drugs may exist (83). Hence, it is imperative to study biomarkers that can predict patient response to drugs and prognosis in order to achieve precision medicine (84). Overall, m6A demethylases hold significant potential for applications in lung cancer diagnosis, prognosis assessment, and therapy. Future research should focus on gaining a deeper understanding of the mechanism of action of m6A demethylase, expediting the development of drugs, and providing more effective and personalized treatment options for lung cancer patients (85). Additionally, interdisciplinary cooperation and clinical trials will play an essential role in advancing the application of M6A demethylase in lung cancer.

4 Environment specific factor for abnormal m6A modification in lung cancer

Research has indicated that prolonged exposure to environments with heavy metals increases the risk of lung cancer in humans. For instance, exposure to beryllium (Be) and arsenic (As) compounds, both *in vivo* and *in vitro* is strongly associated with the occurrence and development of lung cancer (86). m6A demethylase also plays a role in the interaction between heavy metals and lung cancer. For example, FTO protein is highly expressed in tumor samples of NSCLC patients and it can mediate the reduction of m6A modification induced by arsenic in A3B, resulting in increased expression of A3B (87). Similarly, ALKBH5 can regulate the m6A methylation level of PTEN mRNA and reduce the stability of PTEN mRNA and promoting the cadmium-induced malignant transformation of human bronchial epithelial cells, as well as enhancing proliferation, migration and invasion of cancer cells (88). Furthermore, ALKBH5 may be involved in silica-induced pulmonary fibrosis, which may be through the miR-320a-3p/FOXM1 axis or by directly targeting FOXM1 (89). However, there is limited knowledge regarding how m6A demethylases contribute to the pathogenesis of lung cancer and their relationship with heavy metal exposure. Studying and understanding these mechanisms is of great significance as it can provide new ideas and methods for the treatment and prevention lung cancer.

5 Discussion

In recent years, m6A demethylase, a novel RNA-modifying enzyme, has emerged as a prominent molecular mechanisms in lung cancer research. Studies have demonstrated that m6A demethylase affects the stability, transcription, and translation of target genes, subsequently impacting the proliferation, migration, invasion and other processes of lung cancer cells. It also interacts with other molecules such as MZF1, USP7, FOXM1, forming a complex molecular regulatory network. Additionally, m6A demethylase can regulate certain MicroRNAs, including miR-107, miR-607 (44, 48), thereby affecting various physiological functions in the body. Furthermore, researchers have discovered that m6A demethylase may also have an impact on cancer metastasis. For example, m6A modification can regulate the malignancy of breast cancer lung metastasis cells, and overexpression of FTO can significantly inhibit

the lung colonization of BT-549LMF3 cells (26). All these findings highlight the close association between m6A demethylase and the malignant progression of lung cancer. Increasing evidence suggests that m6A demethylase holds significant potential in the diagnosis, prognosis evaluation, and treatment of lung cancer. However, the current research is unable to fully elucidate the complete functionality of m6A demethylase. m6A methylation can be likened to a double-edged sword since its overexpression may contribute to certain tumor types, while the absence of m6A modification may drive the progression of other tumors. The inconsistent results observed among researchers can be attributed to various factors. Therefore, conducting more multicenter, large-scale studies is imperative in order to delve deeper into this topic and establish a solid foundation for the effective treatment of human tumors. Advancing the field of m6A demethylases requires a thorough investigation into their underlying mechanisms. By unravelling the complex molecular pathways and regulatory networks involved in the malignant transformation of lung cancer cells, researchers can lay the foundation for development of more precise and targeted treatments (90). Gaining a comprehensive understanding of the specific role of m6A demethylases within these networks will provide valuable theoretical insights and offer practical support for the design and implementation of effective therapeutic strategies. Additionally, investigating molecular network regulation models involving m6A demethylases in lung cancer holds great potential. By unraveling the intricate interactions between m6A demethylases and other critical genes implicated in the progression of lung cancer, researchers can identify novel targets and pathways that can be targeted for therapeutic purposes (91, 92). This approach has the potential to revolutionize the treatment landscape by enabling the development of innovative combination therapies or the identification of specific molecular signatures that can guide personalized treatment approaches for individuals with lung cancer.

Although it will be some time before m6A demethylase can be applied to clinical practice, the current study has shown its translational value. This requires large-scale clinical samples and cell model studies to obtain sufficient data support. In addition, accurate and meticulous analysis of the large amount of RNA modification data is also a difficult point that needs to be broken through. The development of targeted drugs for different stages of lung cancer may be challenging and promising.

6 Conclusion

Overall, m6A modification is one of the most common RNA modifications. It not only plays an important role in various cell biological processes, but also participates in the occurrence and development of cancers, such as lung cancer, acute myeloid leukemia and breast cancer, etc. Therefore, m6A-modified related molecules are considered as potential tumor diagnostic markers and therapeutic targets. Conducting in-depth research on the mechanisms of m6A demethylase function and its intricate network interactions in lung cancer will greatly enhance our understanding of the disease and o provide opportunities for targeted treatments. Through rigorous scientific inquiry, researchers can establish the groundwork for the development of more effective therapies to fight against lung cancer and well-being of patients affected by this condition.

Author contributions

MY: Methodology, Conceptualization, Data curation, Formal Analysis, Investigation, Writing – original draft. WJ: Methodology, Supervision, Writing – review & editing. XY: Data curation, Formal Analysis, Writing – review & editing. KT: Writing – review & editing, Formal Analysis, Visualization. XM: Formal Analysis, Visualization, Writing – review & editing. SY: Writing – review & editing, Conceptualization, Supervision. LC: Conceptualization, Supervision, Writing – review & editing. XZ: Supervision, Writing – review & editing, Funding acquisition, Methodology, Project administration.

Funding

The author(s) declare financial support was received for the research, authorship, and/or publication of this article. This work was supported by the National Natural Science Foundation of China (82173554); the Natural Science Foundation of Jiangsu Province (BK20201444); Qing Lan Project for Excellent Young Key Teachers of Colleges and Universities of Jiangsu Province (2020).

Conflict of interest

The authors declare that the research was conducted in the absence of any commercial or financial relationships that could be construed as a potential conflict of interest.

The reviewer ZD declared a shared affiliation with the author WJ to the handling editor at the time of review.

Publisher's note

All claims expressed in this article are solely those of the authors and do not necessarily represent those of their affiliated organizations, or those of the publisher, the editors and the reviewers. Any product that may be evaluated in this article, or claim that may be made by its manufacturer, is not guaranteed or endorsed by the publisher.

References

1. Siegel RL, Miller KD, Wagle NS, Jemal A. Cancer statistics, 2023. *CA Cancer J Clin* (2023) 73(1):17–48. doi: 10.3322/caac.21763

2. Leon G, MacDonagh L, Finn SP, Cuffe S, Barr MP. Cancer stem cells in drug resistant lung cancer: Targeting cell surface markers and signaling pathways. *Pharmacol Ther* (2016) 158:71–90. doi: 10.1016/j.pharmthera.2015.12.001

3. Sun L, Zhang H, Gao P. Metabolic reprogramming and epigenetic modifications on the path to cancer. *Protein Cell* (2022) 13(12):877–919. doi: 10.1007/s13238-021-00846-7

4. Xu J, Liu Y, Liu J, Xu T, Cheng G, Shou Y, et al. The identification of critical m(6) A RNA methylation regulators as Malignant prognosis factors in prostate adenocarcinoma. *Front Genet* (2020) 11:602485. doi: 10.3389/fgene.2020.602485

5. Chen Y, Zhou W, Gong Y, Ou X. N6-methyladenosine-related long noncoding RNA is a potential biomarker for predicting pancreatic cancer prognosis. *Tumor Discovery* (2022) 1(2):165. doi: 10.36922/td.v1i2.165

6. Roundtree IA, Evans ME, Pan T, He C. Dynamic RNA modifications in gene expression regulation. *Cell* (2017) 169(7):1187–200. doi: 10.1016/j.cell.2017.05.045

7. Sun T, Wu R, Ming L. The role of m6A RNA methylation in cancer. *BioMed Pharmacother* (2019) 112:108613. doi: 10.1016/j.biopha.2019.108613

8. Chang G, Shi L, Ye Y, Shi H, Zeng L, Tiwary S, et al. YTHDF3 induces the translation of m(6)A-enriched gene transcripts to promote breast cancer brain metastasis. *Cancer Cell* (2020) 38(6):857–71 e7. doi: 10.1016/j.ccell.2020.10.004

9. Liu T, Wei Q, Jin J, Luo Q, Liu Y, Yang Y, et al. The m6A reader YTHDF1 promotes ovarian cancer progression via augmenting EIF3C translation. *Nucleic Acids Res* (2020) 48(7):3816–31. doi: 10.1093/nar/gkaa048

10. Zhu Z, Qian Q, Zhao X, Ma L, Chen P. N(6)-methyladenosine ALKBH5 promotes non-small cell lung cancer progress by regulating TIMP3 stability. *Gene* (2020) 731:144348. doi: 10.1016/j.gene.2020.144348

11. Yang P, Wang Q, Liu A, Zhu J, Feng J. ALKBH5 holds prognostic values and inhibits the metastasis of colon cancer. *Pathol Oncol Res* (2020) 26(3):1615–23. doi: 10.1007/s12253-019-00737-7

12. Zhang J, Guo S, Piao HY, Wang Y, Wu Y, Meng XY, et al. ALKBH5 promotes invasion and metastasis of gastric cancer by decreasing methylation of the lncRNA NEAT1. *J Physiol Biochem* (2019) 75(3):379–89. doi: 10.1007/s13105-019-00690-8

13. Muller S, Glass M, Singh AK, Haase J, Bley N, Fuchs T, et al. IGF2BP1 promotes SRF-dependent transcription in cancer in a m6A- and miRNA-dependent manner. *Nucleic Acids Res* (2019) 47(1):375–90. doi: 10.1093/nar/gky1012

14. Yang X, Zhang S, He C, Xue P, Zhang L, He Z, et al. METTL14 suppresses proliferation and metastasis of colorectal cancer by down-regulating oncogenic long non-coding RNA XIST. *Mol Cancer* (2020) 19(1):46. doi: 10.1186/s12943-020-1146-4

15. Chen X, Xu M, Xu X, Zeng K, Liu X, Pan B, et al. METTL14-mediated N6-methyladenosine modification of SOX4 mRNA inhibits tumor metastasis in colorectal cancer. *Mol Cancer* (2020) 19(1):106. doi: 10.1186/s12943-020-01220-7

16. Lin S, Choe J, Du P, Triboulet R, Gregory RI. The m(6)A methyltransferase METTL3 promotes translation in human cancer cells. *Mol Cell* (2016) 62(3):335–45. doi: 10.1016/j.molcel.2016.03.021

17. Wei W, Sun J, Zhang H, Xiao X, Huang C, Wang L, et al. Circ0008399 interaction with WTAP promotes assembly and activity of the m(6)A methyltransferase complex and promotes cisplatin resistance in bladder cancer. *Cancer Res* (2021) 81(24):6142–56. doi: 10.1158/0008-5472.CAN-21-1518

18. Cho S, Lee G, Pickering BF, Jang C, Park JH, He L, et al. mTORC1 promotes cell growth via m(6)A-dependent mRNA degradation. *Mol Cell* (2021) 81(10):2064–75. e8. doi: 10.1016/j.molcel.2021.03.010

19. Li S, Qi Y, Yu J, Hao Y, He B, Zhang M, et al. Nuclear Aurora kinase A switches m(6)A reader YTHDC1 to enhance an oncogenic RNA splicing of tumor suppressor RBM4. *Signal Transduct Target Ther* (2022) 7(1):97. doi: 10.1038/s41392-022-00905-3

20. Wang X, Lu Z, Gomez A, Hon GC, Yue Y, Han D, et al. N6-methyladenosine-dependent regulation of messenger RNA stability. *Nature* (2014) 505(7481):117–20. doi: 10.1038/nature12730

21. Ning J, Wang F, Bu J, Zhu K, Liu W. Down-regulated m6A reader FTO destabilizes PHF1 that triggers enhanced stemness capacity and tumor progression in lung adenocarcinoma. *Cell Death Discovery* (2022) 8(1):354. doi: 10.1038/s41420-022-01125-y

22. Jia G, Fu Y, Zhao X, Dai Q, Zheng G, Yang Y, et al. N6-methyladenosine in nuclear RNA is a major substrate of the obesity-associated FTO. *Nat Chem Biol* (2011) 7(12):885–7. doi: 10.1038/nchembio.687

23. Purslow JA, Nguyen TT, Egner TK, Dotas RR, Khatiwada B, Venditti V. Active site breathing of human alkbh5 revealed by solution NMR and accelerated molecular dynamics. *Biophys J* (2018) 115(10):1895–905. doi: 10.1016/j.bpj.2018.10.004

24. Chao Y, Shang J, Ji W. ALKBH5-m(6)A-FOXM1 signaling axis promotes proliferation and invasion of lung adenocarcinoma cells under intermittent hypoxia. *Biochem Biophys Res Commun* (2020) 521(2):499–506. doi: 10.1016/j.bbrc.2019.10.145

25. Zhang C, Zhi WI, Lu H, Samanta D, Chen I, Gabrielson E, et al. Hypoxia-inducible factors regulate pluripotency factor expression by ZNF217- and ALKBH5-mediated modulation of RNA methylation in breast cancer cells. *Oncotarget* (2016) 7 (40):64527–42. doi: 10.18632/oncotarget.11743

26. Chen F, Chen Z, Guan T, Zhou Y, Ge L, Zhang H, et al. N(6) -methyladenosine regulates mRNA stability and translation efficiency of KRT7 to promote breast cancer lung metastasis. *Cancer Res* (2021) 81(11):2847–60. doi: 10.1158/0008-5472.CAN-20-3779

27. Xie G, Wu XN, Ling Y, Rui Y, Wu D, Zhou J, et al. A novel inhibitor of N (6)-methyladenosine demethylase FTO induces mRNA methylation and shows anti-cancer activities. *Acta Pharm Sin B* (2022) 12(2):853–66. doi: 10.1016/j.apsb.2021.08.028

28. Guo J, Wu Y, Du J, Yang L, Chen W, Gong K, et al. Deregulation of UBE2C-mediated autophagy repression aggravates NSCLC progression. *Oncogenesis* (2018) 7 (6):49. doi: 10.1038/s41389-018-0054-6

29. Zhang H, Shi X, Huang T, Zhao X, Chen W, Gu N, et al. Dynamic landscape and evolution of m6A methylation in human. *Nucleic Acids Res* (2020) 48(11):6251–64. doi: 10.1093/nar/gkaa347

30. Wang J, Wang K, Liu W, Cai Y, Jin H. m6A mRNA methylation regulates the development of gestational diabetes mellitus in Han Chinese women. *Genomics* (2021) 113(3):1048–56. doi: 10.1016/j.ygeno.2021.02.016

31. Zhao T, Wang J, Wu Y, Han L, Chen J, Wei Y, et al. Increased m6A modification of RNA methylation related to the inhibition of demethylase FTO contributes to MEHP-induced Leydig cell injury(☆). *Environ Pollut* (2021) 268(Pt A):115627. doi: 10.1016/j.envpol.2020.115627

32. Hu Y, Gong C, Li Z, Liu J, Chen Y, Huang Y, et al. Demethylase ALKBH5 suppresses invasion of gastric cancer via PKMYT1 m6A modification. *Mol Cancer* (2022) 21(1):34. doi: 10.1186/s12943-022-01522-y

33. Feng M, Xie X, Han G, Zhang T, Li Y, Li Y, et al. YBX1 is required for maintaining myeloid leukemia cell survival by regulating BCL2 stability in an m6A-dependent manner. *Blood* (2021) 138(1):71–85. doi: 10.1182/blood.2020009676

34. Li J, Han Y, Zhang H, Qian Z, Jia W, Gao Y, et al. The m6A demethylase FTO promotes the growth of lung cancer cells by regulating the m6A level of USP7 mRNA. *Biochem Biophys Res Commun* (2019) 512(3):479–85. doi: 10.1016/j.bbrc.2019.03.093

35. Ding Y, Qi N, Wang K, Huang Y, Liao J, Wang H, et al. FTO facilitates lung adenocarcinoma cell progression by activating cell migration through mRNA demethylation. *Onco Targets Ther* (2020) 13:1461–70. doi: 10.2147/OTT.S231914

36. Wang Y, Li M, Zhang L, Chen Y, Zhang S. m6A demethylase FTO induces NELL2 expression by inhibiting E2F1 m6A modification leading to metastasis of non-small cell lung cancer. *Mol Ther Oncolytics* (2021) 21:367–76. doi: 10.1016/j.omto.2021.04.011

37. Shen W, Pu J, Zuo Z, Gu S, Sun J, Tan B, et al. The RNA demethylase ALKBH5 promotes the progression and angiogenesis of lung cancer by regulating the stability of the LncRNA PVT1. *Cancer Cell Int* (2022) 22(1):353. doi: 10.1186/s12935-022-02770-0

38. Liu J, Ren D, Du Z, Wang H, Zhang H, Jin Y. m(6)A demethylase FTO facilitates tumor progression in lung squamous cell carcinoma by regulating MZF1 expression. *Biochem Biophys Res Commun* (2018) 502(4):456–64. doi: 10.1016/j.bbrc.2018.05.175

39. Zhao Z, Wan J, Guo M, Wang Y, Yang Z, Zhou F, et al. Expression and prognostic significance of m6A-related genes in TP53-mutant non-small-cell lung cancer. *J Clin Lab Anal* (2022) 36(1):e24118. doi: 10.1002/jcla.24118

40. Xiao P, Liu YK, Han W, Hu Y, Zhang BY, Liu WL. Exosomal Delivery of FTO Confers Gefitinib Resistance to Recipient Cells through ABCC10 Regulation in an m6A-dependent Manner. *Mol Cancer Res* (2021) 19(4):726–38. doi: 10.1158/1541-7786.MCR-20-0541

41. Shen Z, Chen C, Sun J, Huang J, Liu S. The status of WIF1 methylation in cell-free DNA is associated with the insusceptibility for gefitinib in the treatment of lung cancer. *J Cancer Res Clin Oncol* (2021) 147(8):2239–48. doi: 10.1007/s00432-021-03640-4

42. Chen H, Jia B, Zhang Q, Zhang Y. Meclofenamic acid restores gefinitib sensitivity by downregulating breast cancer resistance protein and multidrug resistance protein 7 via FTO/m6A-demethylation/c-myc in non-small cell lung cancer. *Front Oncol* (2022) 12:870636. doi: 10.3389/fonc.2022.870636

43. Tsuchiya K, Yoshimura K, Iwashita Y, Inoue Y, Ohta T, Watanabe H, et al. m(6) A demethylase ALKBH5 promotes tumor cell proliferation by destabilizing IGF2BPs target genes and worsens the prognosis of patients with non-small-cell lung cancer. *Cancer Gene Ther* (2022) 29(10):1355–72. doi: 10.1038/s41417-022-00451-8

44. Mo WL, Deng LJ, Cheng Y, Yu WJ, Yang YH, Gu WD. Circular RNA hsa_circ_0072309 promotes tumorigenesis and invasion by regulating the miR-607/FTO axis in non-small cell lung carcinoma. *Aging (Albany NY)* (2021) 13(8):11629–45. doi: 10.18632/aging.202856

45. Sun Z, Su Z, Zhou Z, Wang S, Wang Z, Tong X, et al. RNA demethylase ALKBH5 inhibits TGF-beta-induced EMT by regulating TGF-beta/SMAD signaling in non-small cell lung cancer. *FASEB J* (2022) 36(5):e22283. doi: 10.1096/fj.202200005RR

46. Li H, Zhang Y, Guo Y, Liu R, Yu Q, Gong L, et al. ALKBH1 promotes lung cancer by regulating m6A RNA demethylation. *Biochem Pharmacol* (2021) 189:114284. doi: 10.1016/j.bcp.2020.114284

47. Zhang D, Ning J, Okon I, Zheng X, Satyanarayana G, Song P, et al. Suppression of m6A mRNA modification by DNA hypermethylated ALKBH5 aggravates the

oncological behavior of KRAS mutation/LKB1 loss lung cancer. *Cell Death Dis* (2021) 12(6):518. doi: 10.1038/s41420-021-00435-x

48. Jin D, Guo J, Wu Y, Yang L, Wang X, Du J, et al. m(6)A demethylase ALKBH5 inhibits tumor growth and metastasis by reducing YTHDFs-mediated YAP expression and inhibiting miR-107/LATS2-mediated YAP activity in NSCLC. *Mol Cancer* (2020) 19(1):40. doi: 10.1186/s12943-020-01161-1

49. Sun Y, Cao L, Sheng X, Chen J, Zhou Y, Yang C, et al. WDR79 promotes the proliferation of non-small cell lung cancer cells via USP7-mediated regulation of the Mdm2-p53 pathway. *Cell Death Dis* (2017) 8(4):e2743. doi: 10.1038/cddis.2017.162

50. Wang Y, Wen L, Zhao SH, Ai ZH, Guo JZ, Liu WC. FoxM1 expression is significantly associated with cisplatin-based chemotherapy resistance and poor prognosis in advanced non-small cell lung cancer patients. *Lung Cancer* (2013) 79 (2):173–9. doi: 10.1016/j.lungcan.2012.10.019

51. Liao GB, Li XZ, Zeng S, Liu C, Yang SM, Yang L, et al. Regulation of the master regulator FOXM1 in cancer. *Cell Commun Signal* (2018) 16(1):57. doi: 10.1186/s12964-018-0266-6

52. Malapelle U, Morra F, Ilardi G, Visconti R, Merolla F, Cerrato A, et al. USP7 inhibitors, downregulating CCDC6, sensitize lung neuroendocrine cancer cells to PARP-inhibitor drugs. *Lung Cancer* (2017) 107:41–9. doi: 10.1016/j.lungcan.2016.06.015

53. Yu H, Zhang Z. ALKBH5-mediated m6A demethylation of lncRNA RMRP plays an oncogenic role in lung adenocarcinoma. *Mamm Genome* (2021) 32(3):195–203. doi: 10.1007/s00335-021-09872-6

54. Liu X, Wang Z, Yang Q, Hu X, Fu Q, Zhang X, et al. RNA Demethylase ALKBH5 Prevents Lung Cancer Progression by Regulating EMT and Stemness via Regulating p53. *Front Oncol* (2022) 12:858694. doi: 10.3389/fonc.2022.858694

55. Zhuang Z, Chen L, Mao Y, Zheng Q, Li H, Huang Y, et al. Diagnostic, progressive and prognostic performance of m(6)A methylation RNA regulators in lung adenocarcinoma. *Int J Biol Sci* (2020) 16(11):1785–97. doi: 10.7150/ijbs.39046

56. Li N, Zhan X. Identification of pathology-specific regulators of m(6)A RNA modification to optimize lung cancer management in the context of predictive, preventive, and personalized medicine. *EPMA J* (2020) 11(3):485–504. doi: 10.1007/s13167-020-00220-3

57. Liu WR, Zhang B, Chen C, Li Y, Ye X, Tang DJ, et al. Detection of circulating genetically abnormal cells in peripheral blood for early diagnosis of non-small cell lung cancer. *Thorac Cancer* (2020) 11(11):3234–42. doi: 10.1111/1759-7714.13654

58. Yang Q, Chen M, Gu J, Niu K, Zhao X, Zheng L, et al. Novel biomarkers of dynamic blood PD-L1 expression for immune checkpoint inhibitors in advanced non-small-cell lung cancer patients. *Front Immunol* (2021) 12:665133. doi: 10.3389/fimmu.2021.665133

59. Li TT, Gao X, Gao L, Gan BL, Xie ZC, Zeng JJ, et al. Role of upregulated miR-136-5p in lung adenocarcinoma: A study of 1242 samples utilizing bioinformatics analysis. *Pathol Res Pract* (2018) 214(5):750–66. doi: 10.1016/j.prp.2018.02.017

60. Ye Z, Zhang X, Luo Y, Li S, Huang L, Li Z, et al. Prognostic values of vimentin expression and its clinicopathological significance in non-small cell lung cancer: A meta-analysis of observational studies with 4118 cases. *PloS One* (2016) 11(9): e0163162. doi: 10.1371/journal.pone.0163162

61. Li Y, Qi D, Zhu B, Ye X. Analysis of m6A RNA methylation-related genes in liver hepatocellular carcinoma and their correlation with survival. *Int J Mol Sci* (2021) 22 (3):1474. doi: 10.3390/ijms22031474

62. Zhang M, Yang C, Ruan X, Liu X, Wang D, Liu L, et al. CPEB2 m6A methylation regulates blood-tumor barrier permeability by regulating splicing factor SRSF5 stability. *Commun Biol* (2022) 5(1):908. doi: 10.1038/s42003-022-03878-9

63. Monzon AZ, Franco-Lopez Á, Culebras JM. Benefits and harms of screening: Overdiagnosis and anticipatory medicine – A secondary publication. *Tumor Discovery* (2022) 1(2):228. doi: 10.36922/td.v1i2.228

64. Zhu J, Wang M, Hu D. Deciphering N(6)-methyladenosine-related genes signature to predict survival in lung adenocarcinoma. *BioMed Res Int* (2020) 2020:2514230. doi: 10.1155/2020/2514230

65. Wang L, Feng X, Jiao Z, Gan J, Meng Q. Characterization of the prognostic and diagnostic values of ALKBH family members in non-small cell lung cancer. *Pathol Res Pract* (2022) 231:153809. doi: 10.1016/j.prp.2022.153809

66. Zhang K, Han Z, Zhao H, Liu S, Zeng F. An integrated model of FTO and METTL3 expression that predicts prognosis in lung squamous cell carcinoma patients. *Ann Transl Med* (2021) 9(20):1523. doi: 10.21037/atm-21-4470

67. Robles AI, Arai E, Mathe EA, Okayama H, Schetter AJ, Brown D, et al. An Integrated Prognostic Classifier for Stage I Lung Adenocarcinoma Based on mRNA, microRNA, and DNA Methylation Biomarkers. *J Thorac Oncol* (2015) 10(7):1037–48. doi: 10.1097/JTO.0000000000000560

68. Xie Y, Xiao G, Coombes KR, Behrens C, Solis LM, Raso G, et al. Robust gene expression signature from formalin-fixed paraffin-embedded samples predicts prognosis of non-small-cell lung cancer patients. *Clin Cancer Res* (2011) 17 (17):5705–14. doi: 10.1158/1078-0432.CCR-11-0196

69. Liu J, Mei J, Li S, Wu Z, Zhang Y. Establishment of a novel cell cycle-related prognostic signature predicting prognosis in patients with endometrial cancer. *Cancer Cell Int* (2020) 20:329. doi: 10.1186/s12935-020-01428-z

70. Shao L, Hong W, Zheng L, He C, Zhang B, Xie F, et al. Joint serum tumor markers serve as survival predictive model of erlotinib in the treatment of recurrent non-small cell lung cancer. *Zhongguo Fei Ai Za Zhi* (2014) 17(5):391–400. doi: 10.3779/j.issn.1009-3419.2014.05.05

71. Zhou S, Huang R, Cao Y. Detection of epidermal growth factor receptor mutations in peripheral blood circulating tumor DNA in patients with advanced non-small cell lung cancer: A PRISMA-compliant meta-analysis and systematic review. *Med (Baltimore)* (2020) 99(40):e21965. doi: 10.1097/MD.0000000000021965

72. Vansteenkiste J, Wauters E, Reymen B, Ackermann CJ, Peters S, De Ruysscher D. Current status of immune checkpoint inhibition in early-stage NSCLC. *Ann Oncol* (2019) 30(8):1244–53. doi: 10.1093/annonc/mdz175

73. Huang Y, Su R, Sheng Y, Dong L, Dong Z, Xu H, et al. Small-molecule targeting of oncogenic FTO demethylase in acute myeloid leukemia. *Cancer Cell* (2019) 35 (4):677–91 e10. doi: 10.1016/j.ccell.2019.03.006

74. Su R, Dong L, Li C, Nachtergaele S, Wunderlich M, Qing Y, et al. R-2HG exhibits anti-tumor activity by targeting FTO/m(6)A/MYC/CEBPA signaling. *Cell* (2018) 172 (1-2):90–105 e23. doi: 10.1016/j.cell.2017.11.031

75. Wang T, Hong T, Huang Y, Su H, Wu F, Chen Y, et al. Fluorescein derivatives as bifunctional molecules for the simultaneous inhibiting and labeling of FTO protein. *J Am Chem Soc* (2015) 137(43):13736–9. doi: 10.1021/jacs.5b06690

76. Huang Y, Yan J, Li Q, Li J, Gong S, Zhou H, et al. Meclofenamic acid selectively inhibits FTO demethylation of m6A over ALKBH5. *Nucleic Acids Res* (2015) 43 (1):373–84. doi: 10.1093/nar/gku1276

77. Chen B, Ye F, Yu L, Jia G, Huang X, Zhang X, et al. Development of cell-active N6-methyladenosine RNA demethylase FTO inhibitor. *J Am Chem Soc* (2012) 134 (43):17963–71. doi: 10.1021/ja3064149

78. Tanaka K, Suda A, Uesugi M, Futaki S, Imanishi M. Xanthine derivatives inhibit FTO in an L-ascorbic acid-dependent manner. *Chem Commun (Camb)* (2023) 59 (72):10809–12. doi: 10.1039/D3CC02484A

79. Xiao P, Duan Z, Liu Z, Chen L, Zhang D, Liu L, et al. Rational design of RNA demethylase FTO inhibitors with enhanced antileukemia drug-like properties. *J Med Chem* (2023) 66(14):9731–52. doi: 10.1021/acs.jmedchem.3c00543

80. Selberg S, Seli N, Kankuri E, Karelson M. Rational design of novel anticancer small-molecule RNA m6A demethylase ALKBH5 inhibitors. *ACS Omega* (2021) 6 (20):13310–20. doi: 10.1021/acsomega.1c01289

81. Lim ZF, Ma PC. Emerging insights of tumor heterogeneity and drug resistance mechanisms in lung cancer targeted therapy. *J Hematol Oncol* (2019) 12(1):134. doi: 10.1186/s13045-019-0818-2

82. Mao W, Cai Y, Chen D, Jiang G, Xu Y, Chen R, et al. Statin shapes inflamed tumor microenvironment and enhances immune checkpoint blockade in non-small cell lung cancer. *JCI Insight* (2022) 7(18):e161940. doi: 10.1172/jci.insight.161940

83. Peterson BS. Editorial: Biomarkers in precision medicine for mental illnesses. *J Child Psychol Psychiatry* (2020) 61(12):1279–81. doi: 10.1111/jcpp.13357

84. Milne S, Sin DD. Biomarkers in chronic obstructive pulmonary disease: the gateway to precision medicine. *Clin Chest Med* (2020) 41(3):383–94. doi: 10.1016/j.ccm.2020.06.001

85. Laranjeira ABA, Hollingshead MG, Nguyen D, Kinders RJ, Doroshow JH, Yang SX. DNA damage, demethylation and anticancer activity of DNA methyltransferase (DNMT) inhibitors. *Sci Rep* (2023) 13(1):5964. doi: 10.1038/s41598-023-32509-4

86. Boffetta P, Fryzek JP, Mandel JS. Occupational exposure to beryllium and cancer risk: a review of the epidemiologic evidence. *Crit Rev Toxicol* (2012) 42(2):107–18. doi: 10.3109/10408444.2011.631898

87. Gao M, Qi Z, Feng W, Huang H, Xu Z, Dong Z, et al. m6A demethylation of cytidine deaminase APOBEC3B mRNA orchestrates arsenic-induced mutagenesis. *J Biol Chem* (2022) 298(2):101563. doi: 10.1016/j.jbc.2022.101563

88. Li L, Zhou M, Chen B, Wang Q, Pan S, Hou Y, et al. ALKBH5 promotes cadmium-induced transformation of human bronchial epithelial cells by regulating PTEN expression in an m6A-dependent manner. *Ecotoxicol Environ Saf* (2021) 224:112686. doi: 10.1016/j.ecoenv.2021.112686

89. Sun W, Li Y, Ma D, Liu Y, Xu Q, Cheng D, et al. ALKBH5 promotes lung fibroblast activation and silica-induced pulmonary fibrosis through miR-320a-3p and FOXM1. *Cell Mol Biol Lett* (2022) 27(1):26. doi: 10.1186/s11658-022-00329-5

90. Shen S, Zhang R, Jiang Y, Li Y, Lin L, Liu Z, et al. Comprehensive analyses of m6A regulators and interactive coding and non-coding RNAs across 32 cancer types. *Mol Cancer* (2021) 20(1):67. doi: 10.1186/s12943-021-01362-2

91. Xie Q, Li Z, Luo X, Wang D, Zhou Y, Zhao J, et al. piRNA-14633 promotes cervical cancer cell Malignancy in a METTL14-dependent m6A RNA methylation manner. *J Transl Med* (2022) 20(1):51. doi: 10.1186/s12967-022-03257-2

92. Lan T, Li H, Zhang D, Xu L, Liu H, Hao X, et al. KIAA1429 contributes to liver cancer progression through N6-methyladenosine-dependent post-transcriptional modification of GATA3. *Mol Cancer* (2019) 18(1):186. doi: 10.1186/s12943-019-1106-z

frontiers | Frontiers in Immunology

TYPE Original Research
PUBLISHED 06 December 2023
DOI 10.3389/fimmu.2023.1276107

Check for updates

OPEN ACCESS

EDITED BY
Qun Xue,
Affiliated Hospital of Nantong University, China

REVIEWED BY
Kewei Wang,
Affiliated Hospital of Jiangnan University, China
Danay Saavedra,
Center of Molecular Immunology, Cuba

*CORRESPONDENCE
Peihua Lu
lphty1_1@163.com

RECEIVED 11 August 2023
ACCEPTED 20 November 2023
PUBLISHED 06 December 2023

CITATION
Wang Y, Lu J, Wu C, Fei F, Chu Z and Lu P (2023) Clinical markers predict the efficacy of several immune checkpoint inhibitors in patients with non-small cell lung cancer in China.
Front. Immunol. 14:1276107.
doi: 10.3389/fimmu.2023.1276107

COPYRIGHT
© 2023 Wang, Lu, Wu, Fei, Chu and Lu. This is an open-access article distributed under the terms of the Creative Commons Attribution License (CC BY). The use, distribution or reproduction in other forums is permitted, provided the original author(s) and the copyright owner(s) are credited and that the original publication in this journal is cited, in accordance with accepted academic practice. No use, distribution or reproduction is permitted which does not comply with these terms.

Clinical markers predict the efficacy of several immune checkpoint inhibitors in patients with non-small cell lung cancer in China

Yuxin Wang[1,2], Jiahui Lu[1,3], Chenxi Wu[1,3], Fei Fei[1,3], Zhuze Chu[1,3] and Peihua Lu[1,3]*

[1]The Affiliated Wuxi People's Hospital of Nanjing Medical University, Wuxi People's Hospital, Wuxi Medical Center, Nanjing Medical University, Wuxi, China, [2]Department of Breast Surgery, The First Affiliated Hospital of Nanjing Medical University, Nanjing, China, [3]Department of Oncology, Wuxi People's Hospital Affiliated to Nanjing Medical University, Wuxi, China

Objectives: Immune checkpoint inhibitors (ICIs) are one of the most significant oncological treatment modalities as a result of the rapid advancement of immunotherapy. Programmed Cell Death-Ligand 1 (PD-L1) and tumor mutational burden (TMB) have emerged as key markers for predicting the efficacy and prognosis of ICIs in non-small cell lung cancer (NSCLC), and the predictive role of tumor-infiltrating lymphocytes (TILs) has also received significant attention. However, the prognosis of some individuals cannot be determined by these indicators; for instance, some patients with low PD-L1 expression also benefit from longer survival. Therefore, the purpose of this research was to investigate the connection between new haematological and pathological markers and clinical outcomes in NSCLC patients receiving ICIs.

Methods: Seventy-six patients with stage III-IV NSCLC treated with ICIs were included in this study. We used the Mann-Whitney test, COX regression and Kaplan-Meier analysis to retrospectively analyze peripheral blood indicators and survival prognostic data of 76 patients in order to investigate the relationship between baseline neutrophil-to-lymphocyte ratio (NLR) and the efficacy of ICIs. To investigate the correlation between CXCL13, CXCR5, CD8 and the efficacy of ICIs, we assessed the expression levels of aforementioned indicators in biopsied tissues of 10 non-small cell lung tumors by immunohistochemistry (IHC) and immunofluorescence (IF) and performed statistical analysis.

Results: Disease control rate (DCR) was higher in patients with baseline NLR <3.4 (p=0.016) and neutrophil percentage <71% (P=0.015). Baseline NLR (HR=2.364, P=0.003) and neutrophil percentage (HR=2.824, P=0.013) had the greatest influence on patients' survival prognosis, with baseline NLR exhibiting a stronger predictive value (AUC=0.717), according to univariate and multifactorial COX regression analyses of progression-free survival (PFS) and overall survival (OS). In NSCLC tissues, higher expression of CXCL13 was associated with better clinical outcomes (P=0.032) and higher expression of CD8 was associated with prolonged survival (P=0.022).

Conclusion: Low baseline NLR in peripheral blood and high expression of CD8 in tissues are associated with longer PFS and may have a potential predictive value for patients with stage III-IV NSCLC using ICIs.

KEYWORDS

non-small cell lung cancer, immune checkpoint inhibitors, neutrophil-to-lymphocyte ratio, CXCL13, CD8, biomarker, prognostic value

Introduction

Lung cancer is currently the malignant tumor with the highest mortality rate worldwide, and non-small cell lung cancer (NSCLC) is the most common tissue type among lung cancers (1). Many patients with NSCLC are already in advanced stages when they are discovered because of the insidious nature of tumors and the fact that early screening is not widely practiced (2). The current treatment for NSCLC mainly includes targeted therapies against oncogenic drivers and immunotherapy such as Immune checkpoint inhibitor (ICI) therapy and Chimeric Antigen Receptor (CAR) T-cell Therapy (CAR-T) (3). ICI therapy has been extensively studied as one of the major classes of immunotherapy and the predictive markers for their efficacy and prognosis are in full swing. The expression levels of Programmed Cell Death-Ligand 1 (PD-L1), tumor mutational burden (TMB), tumor-infiltrating lymphocytes (TILs) and gene expression profiles (GEP) are all recognized for their predictive role in the treatment of NSCLC with ICI, but all have its limitations (4, 5). Many patients with PD-L1 <1% have a substantial clinical benefit to ICI therapy (6), and TILs in the immune microenvironment require simultaneous observation by at least two pathologists and exists heterogeneity of observers (7). Therefore, it is important to explore more new predictive biomarkers.

Neutrophil-to-lymphocyte ratio (NLR) refers to the ratio between absolute peripheral blood neutrophil count and absolute lymphocyte count, which is a biomarker representing the balance between inflammation and anti-tumor immune response in the body (8). It can be easily obtained from routine blood tests and is highly clinically accessible. Baseline NLR refers to the NLR status within 2 weeks prior to the first ICI treatment and reflects the basal status *in vivo* prior to immunotherapy. The prognostic value of NLR for Nivolumab and Pembrolizumab in the treatment of NSCLC, gastric cancer, colorectal cancer, and melanoma has been studied, and higher NLR levels often represent a worse survival prognosis (9–12). However, compared with the early marketed ICIs such as Pembrolizumab and Nivolumab, the Chinese-developed ICIs such as Camrelizumab, Tislelizumab and Sintilimab have only been marketed and included in health insurance in the last five years, benefiting the majority of Chinese people, yet there are fewer studies on the efficacy of NLR to predict the above ICIs in NSCLC, so it is necessary to figure out a set of prognostic markers suitable for Chinese people. Camrelizumab, Tislelizumab and Sintilimab are all PD-1 inhibitors, of which Sindilizumab is the first PD-1 monoclonal antibody to enter China's medical insurance catalog and also has the most first-line indications, including NSCLC. Camrelizumab has received a significant price cut after health insurance negotiations, and its emergence has pushed the price advantage of PD-1 inhibitors to new heights. Tislelizumab is also a PD-1 inhibitor independently developed by China. Studies have shown that the dissociation rate of Tislelizumab is 30 times slower than that of Nivolumab and 50 times slower than that of Pembrolizumab, which makes the affinity of Tislelizumab 30-50 times higher than that of the other two antibodies (13). Therefore, we performed this retrospective study to explore the prognostic value of NLR on NSCLC treated with the above-mentioned ICIs.

The CXCL13-CXCR5 axis is a chemokine ligand that regulates its activity by interacting with seven transmembrane G protein-coupled receptors (GPCRs), resulting in a chemokine ligand/receptor pair axis that has both pro-tumor and anti-tumor effects (14). It has been shown that patients with NSCLC have higher levels of CXCL13 and CXCR5 than the normal people (15, 16). CXCL13 $CD8^+$ T cells were confirmed as poor prognostic factors for immunotherapy due to the presence of immune checkpoints such as Programmed cell death protein 1 (PD-1), but Mark Sorin et al. demonstrated by single cell spatial landscape that CXCL13 enhances the sensitivity of tumors to ICIs and has a positive prognostic effect (17). In addition, it was shown that five-year disease-free survival (DFS) was significantly lower in CXCR5-positive group of NSCLC patients, but after it was found that CXCL13 was able to recruit circulating CXCR5+ B cells and CXCR5+ CD4+ Follicular helper T (TFH) cell population to the intratumoral tertiary lymphoid structure (TLS), CXCR5+ CD8+ T cells showed greater proliferative capacity, more granzyme B production, tumor necrosis factor-α (TNF-α) and interferon-γ (IFN-γ) expression in different types of tumor tissues, thus specifically lysing tumor cells (18). Finally, $CD8^+$T cell is a major

Abbreviations: ICIs, Immune checkpoint inhibitors; PD-L1, Programmed Cell Death-Ligand 1; NSCLC, Non-small cell lung cancer; TILs, Tumor-infiltrating lymphocytes; NLR, Neutrophil-to-lymphocyte ratio; IHC, Immunohistochemistry; IF, Immunofluorescence; DCR, Disease control rate; PFS, Progression-free survival; OS, Overall survival; CAR-T, Chimeric Antigen Receptor (CAR) T-cell Therapy; TMB, Tumor mutational burden; GPCRs, G protein-coupled receptors; PD-1, Programmed cell death protein 1; DFS, Disease-free survival; TFH, Follicular helper T cell; TLS, Tertiary lymphoid structure; TNF-α, Tumor necrosis factor-α; IFN-γ, Interferon-γ; WBC, White blood cell; PD, Disease progression; ROC, Receiver operating characteristic; AUC, Area under the curve; PR, Partial response; SD, Stable disease; MSI, Microsatellite instability; MMP9, Matrix metalloproteinase 9.

component of TILs, which is also a good predictor of the prognosis of ICIs (19). Therefore, we evaluated the expression levels of CXCL13, CXCR5 and CD8 in tissues by Immunohistochemistry (IHC) and Immunofluorescence (IF) to explore the prognostic value of the above pathological markers for NSCLC treated with ICIs.

Methods

Patients and specimens

This retrospective study included 76 patients with stage III-IV NSCLC treated with ICIs at Wuxi People's Hospital affiliated to Nanjing Medical University from November 2019 to July 2022. Basic clinical information and baseline hematological data were collected, and all patients were followed up until February 2023 with the aim of exploring the relationship between patients' basic information and baseline hematological data and the relationship between the efficacy of ICIs. Ten of the 76 patients were randomly selected, and paraffin samples from their pre-treatment lung cancer tissue biopsies were requested for IHC and IF, with the aim of exploring the relationship between the expression levels of CXCL13, CXCR5, CD8 and the efficacy of ICIs in NSCLC tissues. This study was conducted with the consent of the Institutional Review Board of Wuxi People's Hospital affiliated to Nanjing Medical University.

Inclusion and exclusion criteria

Inclusion criteria: (i) all patients were over 18 years of age; (ii) diagnosis of NSCLC was confirmed by pathology; (iii) clinical stage was III/IV; (iv) baseline hematological data were obtained within 2 weeks before the first ICIs treatment. Exclusion criteria: (i) Patients were treated with ICIs for less than 3 courses; (ii) have undergone surgical treatment for NSCLC; (iii) severe side effects such as bone marrow suppression and impaired liver and kidney function have occurred during treatment.

Clinical variables

Basic information of patients included gender, age, type of pathology, clinical stage, the expression level of PD-L1, kinds of ICIs, times of ICIs, treatment line, whether combined with chemotherapy, hypertension status and diabetes status. Baseline hematology data included white blood cell (WBC) count, lymphocyte count, monocyte count, neutrophil count, lymphocyte percentage, monocyte percentage, neutrophil percentage, baseline NLR (within 2 weeks prior to the first ICI treatment), later NLR (after the first course of treatment) and (WBC count-neutrophil count)/lymphocyte count (dNLR).

Efficacy and survival assessment

Efficacy assessment can be categorized as complete remission, partial remission, stable disease, and disease progression, and the best outcome during the treatment of patients with ICIs was used as the final outcome assessment in this study. PFS is the time between the start of treatment and the detection of clinical/imaging progression or death from any cause. OS is the time between the start of treatment and death from any cause.

Immunohistochemistry

Paraffin specimens from the pre-treatment biopsies of 10 patients were provided by the Department of Pathology, Wuxi People's Hospital. We prepared four serial paraffin sections for each paraffin specimen using a sectioning machine, and the first one was stained with hematoxylin-eosin. We performed IHC for CXCL13 (dilution 1:500; Abcam). To analyze the immunohistochemical staining of CXCL13, the staining was independently evaluated by two investigators, based on a cell staining intensity score of 0-3, with 0 for no positive staining (negative), 1 for pale yellow (weakly positive), 2 for yellow (positive), and 3 for brown (strongly positive); the percentage of positive cells (0-100%) was calculated using ImageJ. The final score of CXCL13 immunohistochemistry was staining intensity × percentage of positive cells/3 random of high-power fields (HPFs) (400× magnification).

Immunofluorescence

We performed Immunofluorescence double staining for CXCR5 (dilution 1:200; Abcam) and CD8 (dilution 1:200; Servicebio). We used orthomorphic fluorescence microscope (Nikon Eclipse C1) for observation under HPFs (200× magnification) and 3DHISTECH for shooting. The mean number of CXCR5+T and CD8+T cells/HPF was from 3 random fields and recorded by two investigators independently.

Statistical analyses

IBM SPSS statistics version 24.0 was used for data analysis and GraphPad Prism 8.0.2 was used for graphic plotting. Clinical characteristics of patients were expressed as counts and percentages, and hematological data were expressed as medians and interval ranges. All independent clinical variables were included in the univariate COX regression, and those with $P<0.2$ were continued in the multivariate COX regression. The cutoff values of NLR and neutrophil percentage were confirmed using X-tile and were divided into high and low groups. Patients with disease progression (PD) were included in the no-benefit group and the remaining patients were included in the benefit group. The Mann-Whitney test was used to analyze the clinical and histological variables in the benefit and no-benefit groups. The chi-square test was used to analyze the relationship between the independent variables of clinical differences and efficacy. The receiver operating characteristic (ROC) curve was created to predict efficacy, and the Kaplan-Meier survival curves were used to analyze the differences in survival benefit. The chi-square test was

used to perform basic information matching analysis. $P < 0.05$ was considered a statistically significant difference.

Results

Characteristics of patients

A total of 76 patients with advanced NSCLC treated with ICIs were enrolled in this study, with specific information in the Table 1. Among them, 68 were male, 8 were female, and 26 (34.2%) were younger than 65 years. Among the pathological types, adenocarcinoma accounted for the majority (44.8%), squamous carcinoma for 36.8% and the rest for 18.4%. 24 (31.6%) patients had stage III NSCLC and 52 (68.4%) had stage IV. In the case of ICI use, 32 patients (42.1%) used Camrelizumab, 22 (28.9%) used Tislelizumab, 17 (22.4%) used Sintilimab, 3 (3.9%) used Durvalumab, and 1 (1.3%) used Atezolizumab. The majority of patients who underwent 5-10 courses of ICI treatment were 39 (51.3%). The majority of patients (36, 47.4%) were treated with 1st-line ICI. Of the total number of patients, 71 (93.4%) had concurrent chemotherapy, 26 (34.2%) had hypertension, and 7 (9.2%) had diabetes. The median baseline NLR was 2.99 with a range of 0.48-8.65. The median Later NLR was 2.21 with a range of 0.95-6.98. The median dNLR was 1.59 with a range of 1.09-3.11. The median WBC count was 6.23×10^6 with a range of $(2.78\text{-}13.86)\times10^6$. The median lymphocyte count was 1.37×10^6 with a range of (0.44-2.75)×106. The median Monocyte count was 0.66×10^6 with a range of $(0.18\text{-}1.66)\times10^6$. The median neutrophil count was 4.03×10^6 with a range of $(1.11\text{-}10.16)\times10^6$. The median Lymphocyte percentage was 21.4% with a range of 9.6-60.1%. The median Monocyte percentage was 9.7% with a range of 1.8-20.1%. The median neutrophil percentage was 65.5% with a range of 29.1-83.4%. The median CD4/CD8 was 1.49 with a range of 0.49-3.81. The median score of CXCL13 was 26.25 with a range of 13.7-65.6. The median CXCR5 (cells/HPFs) was 6.17 with a range of 3.33-13. The median CD8 (cells/HPFs) was 13.84 with a range of 3-36.33.

Prognostic impact of clinical variables

Basic patient information and hematological data were included in a univariate COX regression (Table 2). For PFS, clinical stage (HR=1.642, P=0.123), times of ICIs (HR=0.425, P=0.041), treatment line (HR=0.428, P=0.117), baseline NLR (HR=1.225, P=0.029), later NLR (HR=1.253, P=0.022), neutrophil count (HR=1.110, P=0.149), lymphocyte percentage (HR=0.976, P=0.195) contributed to the prognosis (threshold: P<0.2). For OS, clinical stage (HR=2.511, P=0.062), times of ICIs (HR=0.142, P=0.003), baseline NLR (HR=1.179, P=0.146), later NLR (HR=1.282, P=0.045), neutrophil count (HR=1.143, P=0.142), lymphocyte percentage (HR=0.968, P=0.195), neutrophil percentage (HR=1.039, P=0.079) contributed to the prognosis (threshold: P<0.2). The X-tile software was used to determine the cutoff values of 3.4 for baseline NLR, 2.2 for later NLR, 3.5×10^6 for neutrophil count, 18 for Lymphocyte percentage and 71 for

TABLE 1 Basic information.

Basic information	Number
Patients	76
Sex	
Male	68 (89.5%)
Female	8 (10.5%)
Age	
<65	26 (34.2%)
≥65	50 (65.8%)
Histology	
Adenocarcinoma	34 (44.8%)
Squamous carcinoma	28 (36.8%)
others	14 (18.4%)
Clinical Stage	
III	24 (31.6%)
IV	52 (68.4%)
PD-L1 status	26
<1%	12 (46.1%)
≥1%	14 (53.9%)
Kinds of ICI	
Camrelizumab	32 (42.1%)
Tislelizumab	22 (28.9%)
Sintilimab	17 (22.4%)
Atezolizumab	1 (1.3%)
Durvalumab	3 (3.9%)
Times of ICI	
<5	22 (28.9%)
5-10	39 (51.3%)
≥10	15 (19.8%)
Treatment line	
1	36 (47.4%)
2	32 (42.1%)
≥3	8 (10.5%)
Combined chemotherapy	
No	5 (6.6%)
Yes	71 (93.4%)
Blood pressure status	
No	50 (65.8%)
Yes	26 (34.2%)
Diabetes status	

(Continued)

10.3389/fimmu.2023.1276107

TABLE 1 Continued

Basic information	Number
No	69 (90.8%)
Yes	7 (9.2%)
Baseline NLR×10^6	2.99 (0.48-8.65)
Later NLR×10^6	2.21 (0.95-6.98)
dNLR	1.59 (1.09-3.11)
WBC count×10^6	6.23 (2.78-13.86)
Lymphocyte count×10^6	1.37 (0.44-2.75)
Monocyte count×10^6	0.66 (0.18-1.66)
Neutrophil count×10^6	4.03 (1.11-10.16)
Lymphocyte percentage×100%	21.4 (9.6-60.1)
Monocyte percentage×100%	9.7 (1.8-20.1)
Neutrophil percentage×100%	65.5 (29.1-83.4)
CD4/CD8	1.49 (0.49-3.81)
CXCL13 (score)	26.25 (13.7-65.6)
CXCR5 (cells/HPFs)	6.17 (3.33-13)
CD8 (cells/HPFs)	13.84 (3-36.33)

neutrophil percentage. Multifactorial COX regression analysis showed that times of ICIs (HR=0.336, P=0.011) and baseline NLR (HR=2.364, P=0.003) were the two largest independent influencing factors for PFS (Table 3); clinical stage (HR=3.822, P=0.010), times of ICIs (HR=0.077. P=0.000), neutrophil count (HR=4.225, P=0.009) and neutrophil percentage (HR=2.824, P=0.013) were the four largest independent influencing factors for OS (Table 4).

Next, the differences in these factors above between the benefit and no-benefit groups were analyzed by the Mann-Whitney test, the baseline NLR was significantly lower in the benefit group than in the no-benefit group (P=0.006) (Figure 1A), and the neutrophil percentage was also lower in the benefit group than in the no-benefit group (P=0.03) (Figure 1D). However, the differences in the times of ICIs used and clinical stage between the benefit and no-benefit groups that were statistically significant in the multifactorial COX regression were not statistically significant. The receiver operating characteristic (ROC) curve for baseline NLR predicting PFS showed that an area under the curve (AUC) was 0.717 (Figure 1B), and the Kaplan-Meier survival curve showed that the low baseline NLR group had a better PFS benefit than the high baseline NLR group (p=0.012) (Figure 1C). The ROC curve for neutrophil percentage predicting OS showed that the AUC was 0.680 and the Kaplan-Meier survival curve showed that the low neutrophil percentage group had a better OS benefit than the high

TABLE 2 Univariate Cox regression of PFS and OS.

Variable	Category	PFS			OS		
		HR	95%CI	P-value	HR	95%CI	P-value
Sex	Male	Reference	–	–	Reference	–	–
	Female	0.644	0.256-1.623	0.351	1.141	0.395-3.294	0.807
Age	<60	Reference	–	–	Reference	–	–
	≥65	0.932	0.530-1.640	0.808	1.634	0.697-3.831	0.259
Histology	Adenocarcinoma	Reference	–	0.907	Reference	–	0.935
	Squamous carcinoma	0.906	0.488-1.682	0.754	1.167	0.511-2.666	0.714
	others	1.065	0.517-2.192	0.865	1.066	0.405-2.811	0.897
Clinical Stage	III	Reference	–	–	Reference	–	–
	IV	1.642	0.874-3.084	0.123	2.511	0.954-6.611	0.062
PD-L1 status	<1%	Reference	–	–	Reference	–	–
	≥1%	0.726	0.319-1.652	0.445	0.500	0.155-1.611	0.245
Kinds of ICI	Camrelizumab	Reference	–	0.779	Reference	–	0.602
	Tislelizumab	0.806	0.408-1.592	0.535	1.127	0.423-3.003	0.812
	Sintilimab	1.032	0.504-2.113	0.931	1.427	0.573-3.551	0.445
	Atezolizumab	1.194	0.160-8.911	0.863	5.049	0.631-40.393	0.127
	Durvalumab	1.846	0.551-6.184	0.320	0.867	0.114-6.615	0.890
Times of ICI	<5	Reference	–	0.080	Reference	–	0.003
	5-10	0.566	0.304-1.054	0.073	0.359	0.164-0.782	0.010

(Continued)

TABLE 2 Continued

Variable	Category	PFS			OS		
		HR	95%CI	P-value	HR	95%CI	P-value
	≥10	0.425	0.187-0.966	0.041	0.142	0.039-0.511	0.003
Treatment line	1	Reference	–	0.292	Reference	–	0.680
	2	0.863	0.486-1.532	0.615	1.388	0.635-3.034	0.411
	≥3	0.428	0.148-1.237	0.117	0.998	0.278-3.588	0.997
Combined chemotherapy	No	Reference	–	–	Reference	–	–
	Yes	1.088	0.263-4.497	0.907	0.948	0.224-4.009	0.943
Blood pressure status	No	Reference	–	–	Reference	–	–
	Yes	0.902	0.504-1.612	0.727	1.098	0.516-2.339	0.808
Diabetes status	No	Reference	–	–	Reference	–	–
	Yes	0.933	0.370-2.353	0.884	.651	0.154-2.748	0.559
Baseline NLR	/	1.225	1.021-1.469	0.029	1.179	0.944-1.473	0.146
Later NLR	/	1.253	1.034-1.518	0.022	1.282	1.006-1.635	0.045
dNLR	/	0.961	0.432-2.141	0.923	0.539	0.153-1.897	0.336
WBC count	$\times10^6$	1.060	0.952-1.181	0.290	1.068	0.930-1.227	0.348
Lymphocyte count	$\times10^6$	0.983	0.552-1.752	0.954	0.978	0.470-2.032	0.952
Monocyte count	$\times10^6$	1.427	0.540-3.771	0.473	1.310	0.386-4.441	0.665
Neutrophil count	$\times10^6$	1.110	0.963-1.280	0.149	1.143	0.956-1.366	0.142
Lymphocyte percentage	×100%	0.976	0.940-1.013	0.195	0.968	0.922-1.017	0.195
Monocyte percentage	×100%	0.984	0.912-1.062	0.681	0.970	0.872-1.080	0.581
Neutrophil percentage	×100%	1.012	0.984-1.040	0.404	1.039	0.9961.084	0.079
CD4/CD8	/	0.768	0.481-1.226	0.268	0.801	0.430-1.491	0.484

neutrophil percentage group (P=0.004) (Figures 1E, F). It is worth noting that disease control rates (DCR) were also better in patients with baseline NLR <3.4 and in patients with neutrophil percentage <71% (Table 5, Figure 2). Moreover, to investigate the effect of differential independent variables on efficacy in different ICI subgroups, a Mann-Whitney test was performed and found that baseline NLR levels were significantly lower in the benefit group than in the no-benefit group in both the Tislelizumab subgroup (P=0.004) and the Sintilimab subgroup (P=0.001) (Figures 3D, G). Unfortunately, other analyses in the ICI subgroup were not statistically significant (Figures 3A–C, E, F).

Finally, basic information matching analysis by chi-square test revealed that baseline NLR matched all basic information, while neutrophil percentage was strongly correlated with the pathological type of NSCLC (P=0.001) (Table 6). The difference in neutrophil percentage between the benefit and no-benefit groups was not significant in both adenocarcinoma (P=0.067) and squamous carcinoma (P=0.069) (Figures 4A, D), the ROC curves showed AUC of 0.709 and 0.746 (Figures 4B, E), and Kaplan-Meier survival curves also showed that there was no significant prognostic difference between high level neutrophil percentage and low level neutrophil percentage in adenocarcinoma (P=0.292) and squamous

TABLE 3 Multivariate Cox regression of PFS.

		HR	95%CI	P-value
Times of ICI	<5	Reference	–	0.024
	5-10	0.462	0.243-0.878	0.018
	≥10	0.336	0.145-0.780	0.011
Baseline NLR	Low (<3.4)	Reference	–	–
	High (≥3.4)	2.364	1.335-4.184	0.003

TABLE 4 Multivariate Cox regression of OS.

		HR	95%CI	P-value
Clinical Stage	III	Reference	–	–
	IV	3.822	1.382-10.570	0.010
Times of ICI	<5	Reference	–	0.000
	5-10	0.143	0.055-0.371	0.000
	≥10	0.077	0.019-0.306	0.000
Neutrophil count	Low (<3.5×10^6)	Reference	–	–
	High (≥3.5×10^6)	4.225	1.431-12.479	0.009
Neutrophil percentage	Low (<71%)	Reference	–	–
	High (≥71%)	2.824	1.194-6.679	0.013

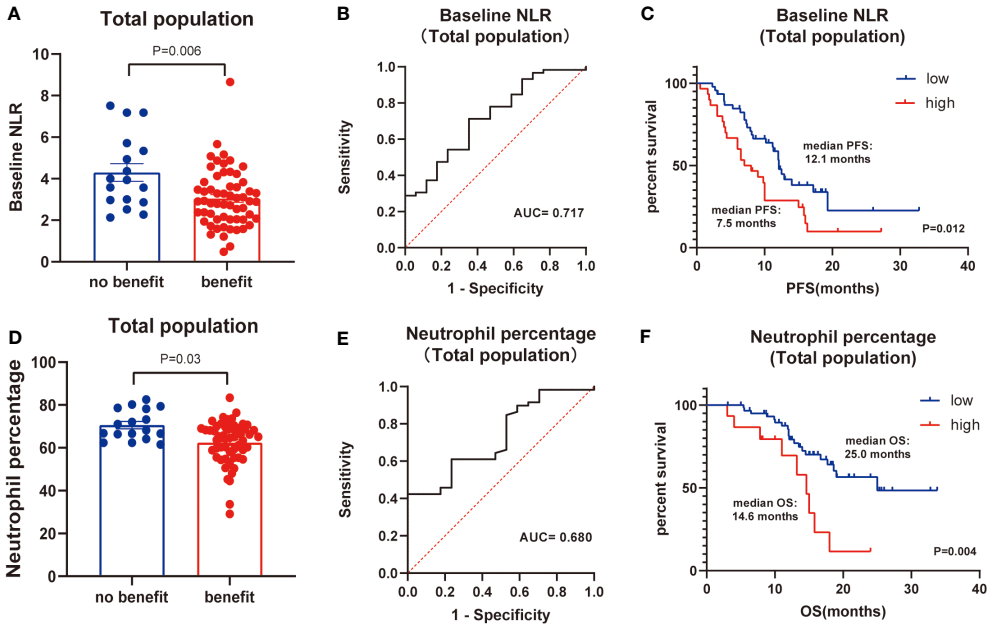


FIGURE 1
Total population analysis. **(A)** Differences of baseline NLR between benefit group and no-benefit group. **(B)** ROC curve of baseline NLR. **(C)** Kaplan-Meier survival curve of different levels of baseline NLR. **(D)** Differences of neutrophil percentage between benefit group and no-benefit group. **(E)** ROC curve of neutrophil percentage. **(F)** Kaplan-Meier survival curve of different levels of neutrophil percentage.

TABLE 5 Comparing treatment efficacy between two groups.

	Baseline NLR<3.4	Baseline NLR≥3.4	P-value	Neutrophil percentage<71%	Neutrophil percentage≥71%	P-value
CR	0 (0%)	0 (0%)	–	0 (0%)	0 (0%)	–
PR	12 (26.1%)	8 (26.6%)	–	16 (27.1%)	4 (23.5%)	–
SD	28 (60.9%)	11 (36.7%)	–	34 (57.6%)	5 (29.4%)	–
PD	6 (13.0%)	11 (36.7%)	–	9 (15.3%)	8 (47.1%)	–
DCR	40 (87.0%)	19 (63.3%)	0.016	50 (84.7%)	9 (52.9%)	0.015

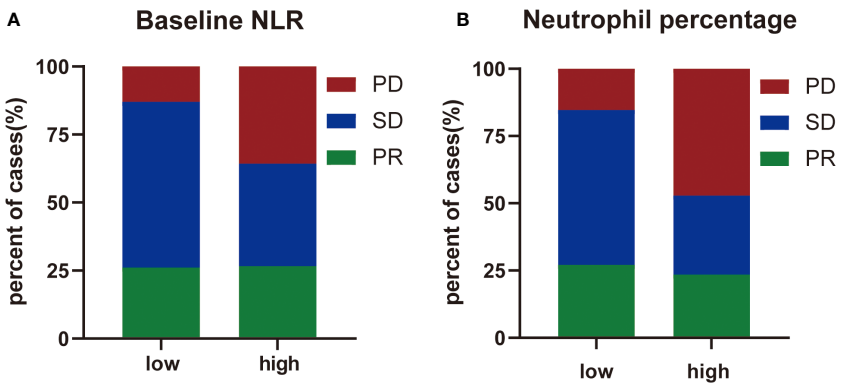


FIGURE 2
The distribution of treatment efficacy. **(A)** The distribution of treatment efficacy between high level group and low level group of baseline NLR. **(B)** The distribution of treatment efficacy between high level group and low level group of neutrophil percentage.

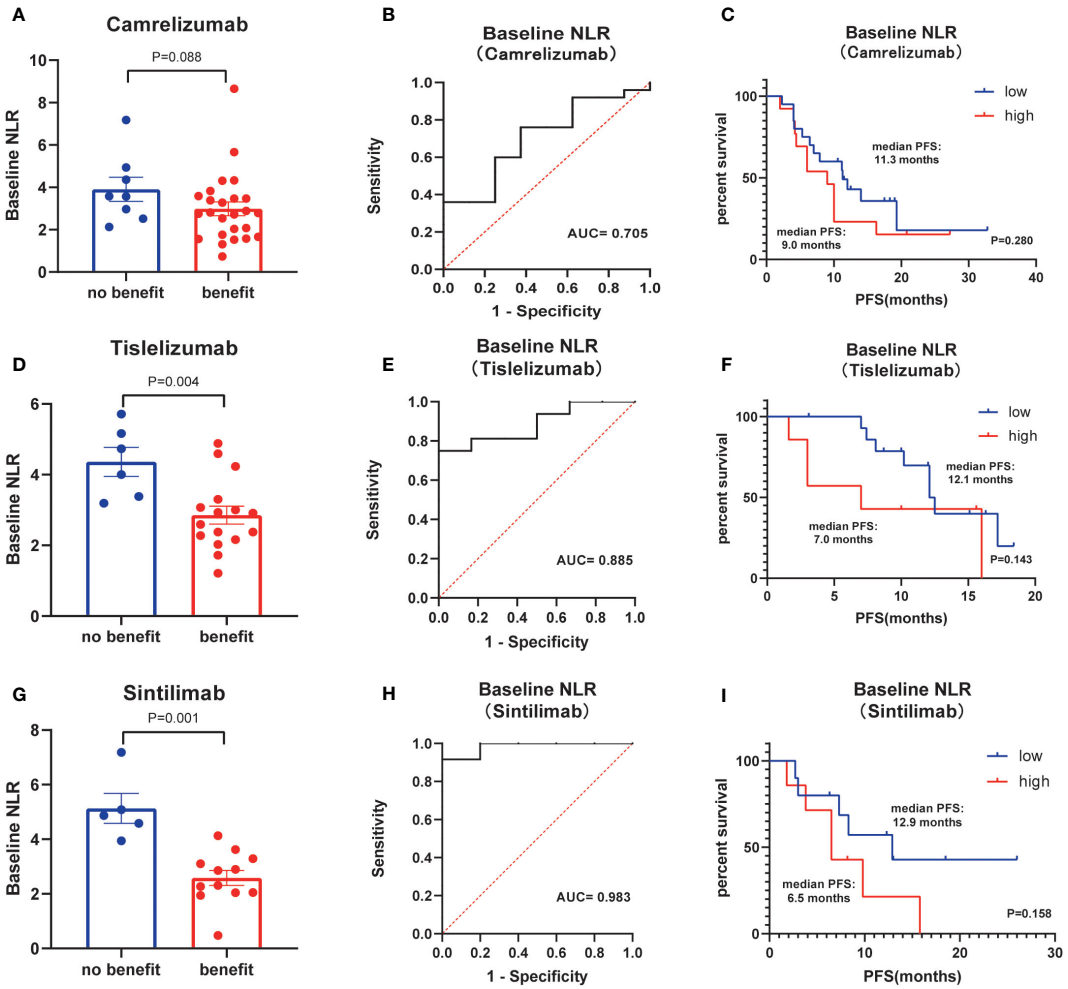


FIGURE 3
Subgroup analysis of kinds of ICIs. **(A)** Differences of baseline NLR between benefit group and no-benefit group among the ICI of Camrelizumab. **(B)** ROC curve of baseline NLR among the ICI of Camrelizumab. **(C)** Kaplan-Meier survival curve of different levels of baseline NLR among the ICI of Camrelizumab. **(D)** Differences of baseline NLR between benefit group and no-benefit group among the ICI of Tislelizumab. **(E)** ROC curve of baseline NLR among the ICI of Tislelizumab. **(F)** Kaplan-Meier survival curve of different levels of baseline NLR among the ICI of Tislelizumab. **(G)** Differences of baseline NLR between benefit group and no-benefit group among the ICI of Sintilimab. **(H)** ROC curve of baseline NLR among the ICI of Sintilimab. **(I)** Kaplan-Meier survival curve of different levels of baseline NLR among the ICI of Sintilimab.

10.3389/fimmu.2023.1276107

TABLE 6 Basic information matching analysis.

	Baseline NLR		P-value	Neutrophil percentage		P-value
	Low	High		Low	High	
Patients	46	30		60	16	
Sex			0.794			1.000
Male	42(91.3%)	26(86.7%)		53(89.8%)	15(88.2%)	
Female	4(8.7%)	4(13.3%)		6(10.2%)	2(11.8%)	
Age			0.532			0.636
<65	17(37.0%)	9(30%)		21(35.6%)	5(29.4%)	
≥65	29(63.0%)	21(70%)		38(64.4%)	12(70.6%)	
Histology			0.091			0.001
Adenocarcinoma	25(54.3%)	9(30.0%)		30(50.8%)	4(14.8%)	
Squamous carcinoma	15(32.6%)	13(43.3%)		19(32.2%)	9(33.3%)	
others	6(13.1%)	8(26.7%)		10(17.0%)	14(51.9%)	
Clinical Stage			0.790			0.119
III	14(30.4%)	10(33.3%)		16(27.1%)	8(47.1%)	
IV	32(69.6%)	20(66.7%)		43(72.9%)	9(52.9%)	
Kinds of ICI			0.214			0.167
Camrelizumab	20(43.5)	13(43.4%)		29(49.2%)	4(23.5%)	
Tislelizumab	15(32.6%)	7(23.3%)		16(27.1%)	6(35.3%)	
Sintilimab	10(21.7%)	7(23.3%)		12(20.3%)	5(29.4%)	
Atezolizumab	1(2.2%)	0(0.0%)		1(1.7%)	0(0.0%)	
Curvalumab	0(0.0%)	3(10.0%)		1(1.7%)	2(11.8%)	
Times of ICI			0.981			0.600
<5	13(28.3%)	9(30%)		16(27.1%)	6(35.3%)	
5-10	24(52.2%)	15(50%)		30(50.8%)	9(52.9%)	
≥10	9(19.5%)	6(20%)		13(22.1%)	2(11.8%)	
Treatment line			0.204			0.276
1	22(47.8%)	14(46.7%)		27(45.8%)	9(52.9%)	
2	17(37.0%)	15(50%)		24(40.7%)	8(47.1%)	
≥3	7(15.2%)	1(3.3%)		8(13.5%)	0(0.0%)	
Combined chemotherapy			1.000			1.000
No	3(6.5%)	2(6.7%)		4(6.8%)	1(5.9%)	
Yes	43(93.5%)	28(93.3%)		55(93.2%)	16(94.1%)	
Blood pressure status			0.532			0.292
No	29(63.0%)	21(70.0%)		37(62.7%)	13(76.5%)	
Yes	17(37.0%)	9(30.0%)		22(37.3%)	4(23.5%)	
Diabetes status			1.000			0.950
No	42(91.3%)	27(90.0%)		53(89.8%)	16(94.1%)	
Yes	4(8.7%)	3(10.0%)		6(10.2%)	1(5.9%)	

10.3389/fimmu.2023.1276107

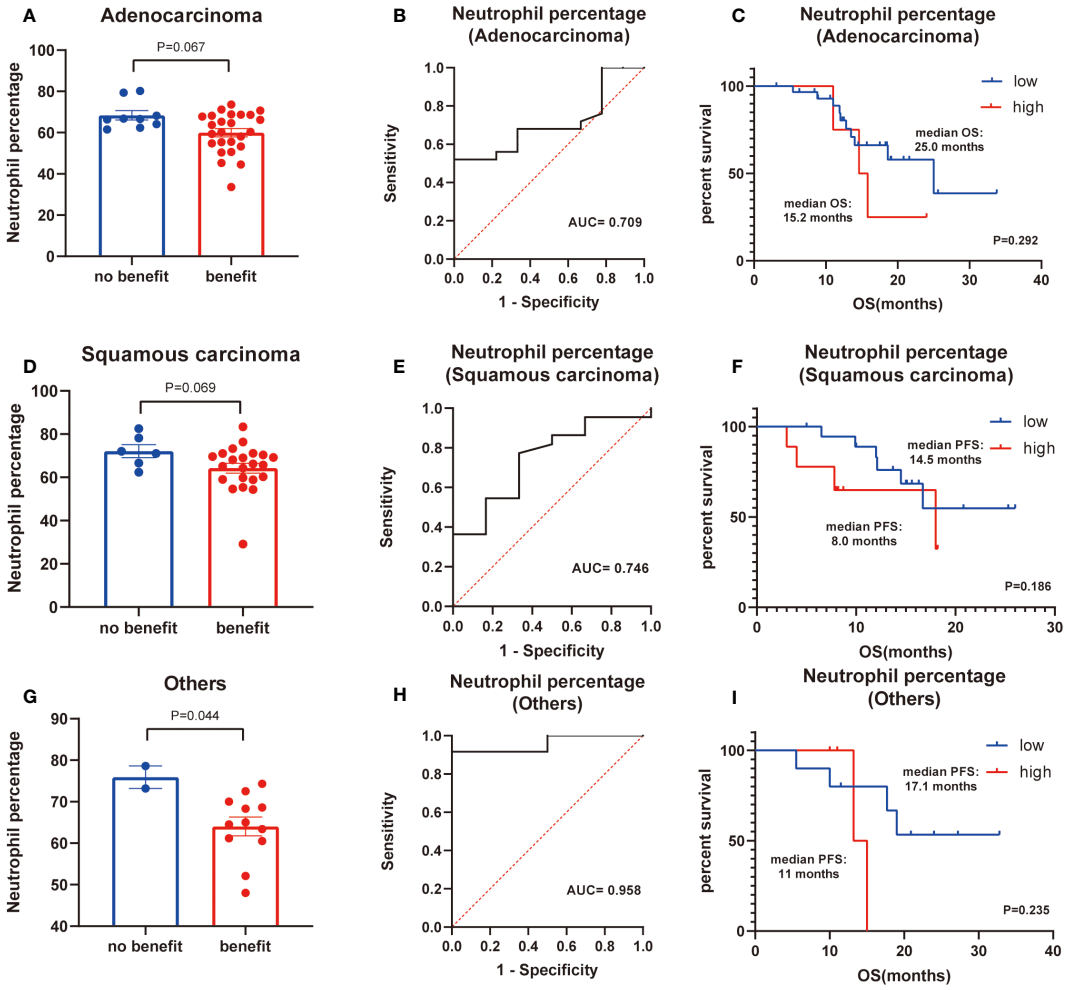


FIGURE 4
Subgroup analysis of histology of NSCLC. **(A)** Differences of neutrophil percentage between benefit group and no-benefit group among the adenocarcinoma. **(B)** ROC curve of neutrophil percentage among the adenocarcinoma. **(C)** Kaplan-Meier survival curve of different levels of neutrophil percentage among the adenocarcinoma. **(D)** Differences of neutrophil percentage between benefit group and no-benefit group among the squamous carcinoma. **(E)** ROC curve of neutrophil percentage among the squamous carcinoma. **(F)** Kaplan-Meier survival curve of different levels of neutrophil percentage among the squamous carcinoma. **(G)** Differences of neutrophil percentage between benefit group and no-benefit group among the other types of NSCLC. **(H)** ROC curve of neutrophil percentage among the other types of NSCLC. **(I)** Kaplan-Meier survival curve of different levels of neutrophil percentage among the other types of NSCLC.

carcinoma (P=0.186) (Figures 4C, F). In other types of NSCLC, the difference in neutrophil percentage between the benefit and no-benefit groups was statistically different (P=0.044) (Figure 4G), and the ROC curve showed an AUC of 0.958 (Figure 4H), but the Kaplan-Meier survival curve showed that high level neutrophil percentage and low level neutrophil percentage did not have a significant prognostic difference in other types of NSCLC (P=0.235) (Figure 4I).

Prognostic impact of pathological markers

To identify the presence of CXCR5, CD8, and CXCR5 in NSCLC, we performed immunohistochemistry and double immunofluorescence staining (Figure 5). CXCR5 expression was found to be lower in the adenocarcinoma group than in the other cancer groups by the Mann-Whitney test (P=0.043) (Figure 5B), CXCL13 was higher in the benefit group than in the no-benefit group (P=0.032) (Figure 5C), and a better PFS benefit was found in the high CD8 group than in the low CD8 group by the Kaplan-Meier survival curve (P=0.022) (Figure 5D). The heat map shows the levels of expression of different pathological markers in the 10 samples (Figure 5E). The expression levels of CD8, CXCR5 and CXCL13 were generally higher in the partial response (PR) and stable disease (SD) groups than in the PD group, and there was some consistency in the expression levels of the three pathological markers.

Discussion

Lung cancer remains the number one cancer with the highest mortality rate worldwide, and NSCLC is the most dominant type of lung cancer, the importance and severity of which cannot be

10.3389/fimmu.2023.1276107

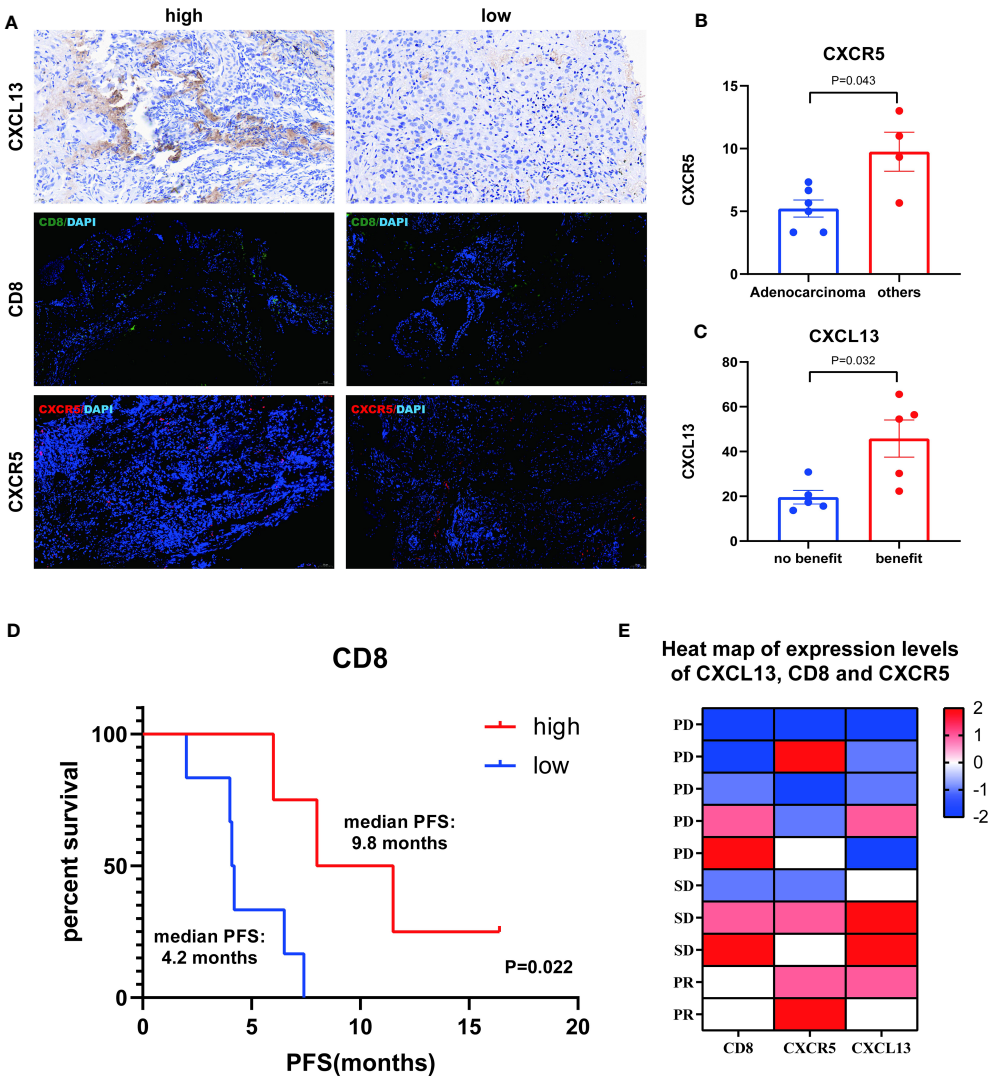


FIGURE 5
Analysis of CXCL13, CD8 and CXCR5. **(A)** Representative IHC and IF images of high and low expression of CXCL13, CD8 and CXCR5. **(B)** Differences of CXCR5+ cells between adenocarcinoma group and other cancer group. **(C)** Differences of CXCL13+ cells between benefit group and no-benefit group. **(D)** Kaplan-Meier survival curve of different levels of CD8+ cells. **(E)** Heat map of expression levels of CXCL13, CD8 and CXCR5.

overstated (20). With the advent of immunotherapy, the treatment of NSCLC is becoming more and more diversified and targeted, and ICIs are developing more and more rapidly among them (21). Pembrolizumab and Nivolumab were approved for marketing as early as 2014, and studies on the efficacy and prognosis of these two ICIs have been very comprehensive (22), while Camrelizumab, Tislelizumab, and Sintilimab developed and launched by China were approved for marketing only in the last five years, and studies on their efficacy and prognosis still need to be conducted.

While many patients benefit from ICI therapy such as Camrelizumab, there are some patients who do not respond to ICI therapy or whose disease progresses quickly after treatment, so it is important to tap into clear predictive markers. The main biomarkers for predicting ICI efficacy are PD-L1, TMB, and microsatellite instability (MSI), of which only PD-L1 is approved for clinical prediction (23). However, approximately 15% of PD-L1-negative patients have clinical benefit and 40% of PD-L1-positive patients have no clinical benefit (24). Therefore, it is necessary to explore more potential biomarkers.

NLR is an important blood inflammatory marker that has been shown to be associated with the prognosis of a variety of tumors, asthma, and chronic obstructive pulmonary disease (COPD) (25, 26), but the prognosis of Camrelizumab, Tislelizumab, and Tislelizumab for NSCLC has been less well studied. In addition, the role of neutrophils on tumors has been extensively studied, and it has a dual role in cancer (27). On the one hand, N1-type neutrophils have high immune activity and promote the activation of $CD8^+$ T cells to induce tumor cell killing; on the other hand, N2-type neutrophils can release matrix metalloproteinase 9 (MMP 9) to promote angiogenesis and spread of tumor cells (28). Therefore, studying neutrophil counts and percentages alone is also very important for the prognosis of NSCLC treated with ICIs. Our study found a statistically significant effect of baseline NLR and neutrophil percentage on the prognosis

of NSCLC. First, we listed the basic information of 76 clinical patients, and then screened independent influences on prognosis by univariate and multifactorial COX regression. In addition, the Mann-Whitney test analyzed the differences between the benefit and no-benefit groups for indicators that were statistically different in the multifactor COX regression. Unfortunately, only baseline NLR and neutrophil percentage were statistically significant, so we focused on the prognostic significance of baseline NLR and neutrophil percentage for survival. Kaplan-Meier curves showed a median PFS of 12.1 months in the low baseline NLR level group and 7.5 months in the high baseline NLR level group, with a statistically significant difference between the two (P=0.012); median OS of 25.0 months in the low neutrophil percentage level group and 14.6 months in the high neutrophil percentage level group, with a statistically significant difference between the two (P=0.004). This also suggested that low baseline NLR level and low neutrophil percentage level are independent influences on the positive prognosis of NSCLC treated with ICIs. All these statistically significant results provided a good basis for follow-up studies.

The pro-cancer and anti-cancer effects of CXCL13-CXCR5 axis on NSCLC still remain to be studied (29), and some scholars have pointed out that it is a poor prognostic factor for immunotherapy because of the presence of PD-1 on the surface of $CXCL13^+$ T cells and $CXCR5^+$ T cells (30). However, from the analysis of the principle of ICI therapy, the PD-L1 inhibitor in ICIs binds to the immune checkpoint PD-L1, thus reducing the binding of PD-L1 to PD-1, which may offset the adverse effect of increased PD-1 expression (31), and CXCL13 can also enhance the sensitivity of tumors to ICIs (17), so the prognostic role of CXCL13 and CXCR5 deserves to be further investigated. In addition, CD8+ T cells are one of the most important immune cells of the organism and its expression level in tissues deserves to be explored (32). Kaplan-Meier curves showed a median PFS of 9.8 months in the high CD8 level group and 4.2 months in the low CD8 level group, with a statistically significant difference between the two (P=0.022). We also found significant differences in CXCL13 between the clinical benefit and no-benefit groups. These statistically significant results also provided a good basis for follow-up large-sample studies.

Many studies have confirmed that the combined predictive effect is more accurate than single prediction. Although only 10 pathological samples of enrolled patients were included in this study so far, the preliminary analysis of CXCL13, CXCR5, and CD8 has been statistically significant, and we will further expand the sample size in the future to further investigate the accuracy and validity of the combined prediction of peripheral blood markers NLR and pathological markers.

The study also had a few drawbacks. First of all, it was a retrospective study, and even if the principle of randomization was used, bias was unavoidable. Some patients did not reach the endpoint and still required additional follow-up, necessitating the need for more prospective studies in the future to fill these gaps. In addition, the total sample size included in this study was small due to the limited number of patients treated with more than 2 ICI sessions in a given time period at one hospital, and future multi-center studies and additional validation cohorts could be conducted. It is worth noting that the number of pathology samples included in this study was small due to sample accessibility and other issues, which may lack a certain degree of representativeness, and this deficiency can be addressed in subsequent prospective studies.

Conclusion

Our findings suggest that in hematological data, baseline NLR and neutrophil ratio are strong predictors of outcome and prognosis in NSCLC patients treated with ICIs. This result is very indicative of the importance of studying the efficacy of NLR for predicting ICIs in NSCLC locally in China. In histological samples, CXCL13 expression was higher in the clinical benefit group than in the no-benefit group, and CD8 expression levels were strongly predictive of NSCLC patients treated with ICIs. Therefore, in the future, we have to further develop the joint prediction of NLR and CXCL13, CD8 and other indicators, establish a joint prediction model, and figure out a prognostic prediction model suitable for Chinese people. Several of these indicators have the potential to be effective biomarkers, and we need further prospective studies to demonstrate them.

Data availability statement

The raw data supporting the conclusions of this article will be made available by the authors, without undue reservation.

Ethics statement

The studies involving humans were approved by the Institutional Review Board of Wuxi People's Hospital Affiliated to Nanjing Medical University. The studies were conducted in accordance with the local legislation and institutional requirements. The participants provided their written informed consent to participate in this study.

Author contributions

YW: Writing – original draft. JL: Writing – original draft. CW: Writing – original draft. FF: Writing – original draft. ZC: Writing – original draft. PL: Writing – review & editing.

Funding

The author(s) declare financial support was received for the research, authorship, and/or publication of this article. This work was supported by the "333" Engineering Project Jiangsu Province ([2022]21-003). Wuxi Health Commission General Program (M202205). Wuxi Science and

Technology Development Fund (Y20212002-1). Wuxi Health Commission "Double Hundred" Top Talent (BJRC-13).

Conflict of interest

The authors declare that the research was conducted in the absence of any commercial or financial relationships that could be construed as a potential conflict of interest.

Publisher's note

All claims expressed in this article are solely those of the authors and do not necessarily represent those of their affiliated organizations, or those of the publisher, the editors and the reviewers. Any product that may be evaluated in this article, or claim that may be made by its manufacturer, is not guaranteed or endorsed by the publisher.

References

1. Wang M, Herbst RS, Boshoff C. Toward personalized treatment approaches for non-small-cell lung cancer. *Nat Med* (2021) 27:1345–56. doi: 10.1038/s41591-021-01450-2

2. Chen P, Liu Y, Wen Y, Zhou C. Non-small cell lung cancer in China. *Cancer Commun (Lond)* (2022) 42:937–70. doi: 10.1002/cac2.12359

3. Liu SM, Zheng M, Pan Y, Liu S, Li Y, Wu Y. Emerging evidence and treatment paradigm of non-small cell lung cancer. *J Hematol Oncol* (2023) 16:40. doi: 10.1186/s13045-023-01436-2

4. Lu S, Stein JE, Rimm DL, Wang DW, Bell JM, Johnson DB, et al. Comparison of biomarker modalities for predicting response to PD-1/PD-L1 checkpoint blockade: A systematic review and meta-analysis. *JAMA Oncol* (2019) 5:1195–204. doi: 10.1001/jamaoncol.2019.1549

5. Mino-Kenudson M, Schalper K, Cooper W, Dacic S, Hirsch FR, Jain D, et al. Predictive biomarkers for immunotherapy in lung cancer: perspective from the international association for the study of lung cancer pathology committee. *J Thorac Oncol* (2022) 17:1335–54. doi: 10.1016/j.jtho.2022.09.109

6. Tjokrowidjaja A, Lord SJ, John T, Lewis CR, Kok PS, Marschner IC, et al. Pre- and on-treatment lactate dehydrogenase as a prognostic and predictive biomarker in advanced non–small cell lung cancer. *Cancer* (2022) 128:1574–83. doi: 10.1002/cncr.34113

7. Park S, Ock C, Kim H, Pereira S, Park S, Ma M, et al. Artificial intelligence–powered spatial analysis of tumor-infiltrating lymphocytes as complementary biomarker for immune checkpoint inhibition in non–small-cell lung cancer. *J Clin Oncol* (2022) 40:1916–28. doi: 10.1200/JCO.21.02010

8. Diem S, Schmid S, Krapf M, Flatz L, Born D, Jochum W, et al. Neutrophil-to-Lymphocyte ratio (NLR) and Platelet-to-Lymphocyte ratio (PLR) as prognostic markers in patients with non-small cell lung cancer (NSCLC) treated with nivolumab. *Lung Cancer* (2017) 111:176–81. doi: 10.1016/j.lungcan.2017.07.024

9. Gou M, Qu T, Wang Z, Yan H, Si Y, Zhang Y, et al. Neutrophil-to-lymphocyte ratio (NLR) predicts PD-1 inhibitor survival in patients with metastatic gastric cancer. *J Immunol Res* (2021) 2021:1–09. doi: 10.1155/2021/2549295

10. Fan X, Wang D, Zhang W, Liu J, Liu C, Li Q, et al. Inflammatory markers predict survival in patients with advanced gastric and colorectal cancers receiving anti-PD-1 therapy. *Front Cell Dev Biol* (2021) 9:638312. doi: 10.3389/fcell.2021.638312

11. Peng L, Wang Y, Liu F, Qiu X, Zhang X, Fang C, et al. Peripheral blood markers predictive of outcome and immune-related adverse events in advanced non-small cell lung cancer treated with PD-1 inhibitors. *Cancer Immunol Immunother* (2020) 69:1813–22. doi: 10.1007/s00262-020-02585-w

12. Bartlett EK, Flynn JR, Panageas KS, Ferraro RA, Sta. Cruz JM, Postow MA, et al. High neutrophil-to-lymphocyte ratio (NLR) is associated with treatment failure and death in patients who have melanoma treated with PD-1 inhibitor monotherapy. *Cancer* (2019) 126:76–85. doi: 10.1002/cncr.32506

13. Hong Y, Feng Y, Sun H, Zhang B, Wu H, Zhu Q, et al. Tislelizumab uniquely binds to the CC′ loop of PD-1 with slow-dissociated rate and complete PD-L1 blockage. *FEBS Open Bio* (2021) 11:782–92. doi: 10.1002/2211-5463.13102

14. Wang B, Wang M, Ao D, Wei X. CXCL13-CXCR5 axis: Regulation in inflammatory diseases and cancer. *Biochim Biophys Acta (BBA) - Rev Cancer* (2022) 1877:188799. doi: 10.1016/j.bbcan.2022.188799

15. Yue Z, Ningning D, Lin Y, Jianming Y, Hongtu Z, Ligong Y, et al. Correlation between CXCR4, CXCR5 and CCR7 expression and survival outcomes in patients with clinical T1N0M0 non-small cell lung cancer. *Thorac Cancer* (2020) 11:2955–65. doi: 10.1111/1759-7714.13645

16. Singh R, Gupta P, Kloecker GH, Singh S, Lillard JJ. Expression and clinical significance of CXCR5/CXCL13 in human non–small cell lung carcinoma. *Int J Oncol* (2014) 45:2232–40. doi: 10.3892/ijo.2014.2688

17. Sorin M, Karimi E, Rezanejad M, Yu MW, Desharnais L, McDowell S, et al. Single-cell spatial landscape of immunotherapy response reveals mechanisms of CXCL13 enhanced antitumor immunity. *J Immunother Cancer* (2023) 11:e005545. doi: 10.1136/jitc-2022-005545

18. Hussain M, Adah D, Tariq M, Lu Y, Zhang J, Liu J. CXCL13/CXCR5 signaling axis in cancer. *Life Sci* (2019) 227:175–86. doi: 10.1016/j.lfs.2019.04.053

19. Simoni Y, Becht E, Fehlings M, Loh CY, Koo S, Teng KWW, et al. Bystander CD8+ T cells are abundant and phenotypically distinct in human tumour infiltrates. *Nature* (2018) 557:575–79. doi: 10.1038/s41586-018-0130-2

20. Sung H, Ferlay J, Siegel RL, Laversanne M, Soerjomataram I, Jemal A, et al. Global cancer statistics 2020: GLOBOCAN estimates of incidence and mortality worldwide for 36 cancers in 185 countries. *CA: A Cancer J Clin* (2021) 71:209–49. doi: 10.3322/caac.21660

21. Archilla-Ortega A, Domuro C, Martin-Liberal J, Muñoz P. Blockade of novel immune checkpoints and new therapeutic combinations to boost antitumor immunity. *J Exp Clin Cancer Res* (2022) 41:68–85. doi: 10.1186/s13046-022-02264-x

22. Bagley SJ, Kothari S, Aggarwal C, Bauml JM, Alley EW, Evans TL, et al. Pretreatment neutrophil-to-lymphocyte ratio as a marker of outcomes in nivolumab-treated patients with advanced non-small-cell lung cancer. *Lung Cancer* (2017) 106:1–07. doi: 10.1016/j.lungcan.2017.01.013

23. Honrubia-Peris B, Garde-Noguera J, García-Sánchez J, Piera-Molons N, Llombart-Cussac A, Fernández-Murga ML. Soluble biomarkers with prognostic and predictive value in advanced non-small cell lung cancer treated with immunotherapy. *Cancers (Basel)* (2021) 13:4280. doi: 10.3390/cancers13174280

24. Reck M, Rodríguez-Abreu D, Robinson AG, Hui R, Csőszi T, Fülöp A, et al. Pembrolizumab versus chemotherapy for PD-L1–positive non–small-cell lung cancer. *N Engl J Med* (2016) 375:1823–33. doi: 10.1056/NEJMoa1606774

25. Paliogiannis P, Fois AG, Sotgia S, Mangoni AA, Zinellu E, Pirina P, et al. Neutrophil to lymphocyte ratio and clinical outcomes in COPD: recent evidence and future perspectives. *Eur Respir Rev* (2018) 27:170113. doi: 10.1183/16000617.0113-2017

26. Ma H, Yang L, Liu L, Zhou Y, Guo X, Wu S, et al. Using inflammatory index to distinguish asthma, asthma-COPD overlap and COPD: A retrospective observational study. *Front Med (Lausanne)* (2022) 9:1045503. doi: 10.3389/fmed.2022.1045503

27. Papayannopoulos V. Neutrophil extracellular traps in immunity and disease. *Nat Rev Immunol* (2018) 18:134–47. doi: 10.1038/nri.2017.105

28. Gungabeesoon J, Gort-Freitas NA, Kiss M, Bolli E, Messemaker M, Siwicki M, et al. A neutrophil response linked to tumor control in immunotherapy. *Cell* (2023) 186:1448–64. doi: 10.1016/j.cell.2023.02.032

29. Hsieh C, Jian C, Lin L, Low G, Ou P, Hsu C, et al. Potential role of CXCL13/CXCR5 signaling in immune checkpoint inhibitor treatment in cancer. *Cancers (Basel)* (2022) 14:294. doi: 10.3390/cancers14020294

30. Dai S, Zeng H, Liu Z, Jin K, Jiang W, Wang Z, et al. Intratumoral CXCL13+ CD8 + T cell infiltration determines poor clinical outcomes and immunoevasive contexture in patients with clear cell renal cell carcinoma. *J Immunother Cancer* (2021) 9:e1823. doi: 10.1136/jitc-2020-001823

31. Pardoll DM. Inducing autoimmune disease to treat cancer. *Proc Natl Acad Sci* (1999) 96:5340–42. doi: 10.1073/pnas.96.10.5340

32. Park J, Hsueh P, Li Z, Ho P. Microenvironment-driven metabolic adaptations guiding CD8+ T cell anti-tumor immunity. *Immunity* (2023) 56:32–42. doi: 10.1016/j.immuni.2022.12.008

frontiers | Frontiers in Oncology

TYPE Original Research
PUBLISHED 22 December 2023
DOI 10.3389/fonc.2023.1239451

Check for updates

OPEN ACCESS

EDITED BY
Sharon R. Pine,
University of Colorado Anschutz Medical Campus, United States

REVIEWED BY
Ritesh Rathore,
Boston University, United States
Shi Yan,
Beijing Cancer Hospital, China

*CORRESPONDENCE
Yi Shen
dryishen@nju.edu.cn

†These authors share first authorship

RECEIVED 13 June 2023
ACCEPTED 15 November 2023
PUBLISHED 22 December 2023

CITATION
Wang Q, Qi C, Luo J, Xu N, Xu M-t, Qiang Y, Zhang C and Shen Y (2023) Evaluation of the efficacy and surgical-related safety of neoadjuvant immunochemotherapy in advanced resectable none small cell lung cancer (NSCLC). *Front. Oncol.* 13:1239451. doi: 10.3389/fonc.2023.1239451

COPYRIGHT
© 2023 Wang, Qi, Luo, Xu, Xu, Qiang, Zhang and Shen. This is an open-access article distributed under the terms of the Creative Commons Attribution License (CC BY). The use, distribution or reproduction in other forums is permitted, provided the original author(s) and the copyright owner(s) are credited and that the original publication in this journal is cited, in accordance with accepted academic practice. No use, distribution or reproduction is permitted which does not comply with these terms.

Evaluation of the efficacy and surgical-related safety of neoadjuvant immunochemotherapy in advanced resectable none small cell lung cancer (NSCLC)

Qin Wang[1†], Chen Qi[1†], Jing Luo[1†], Nan Xu[2], Mao-tian Xu[3], Yong Qiang[4], Chi Zhang[1] and Yi Shen[1*]

[1]Department of Cardiothoracic Surgery, Jinling Hospital, Medical School of Nanjing University, Nanjing, China, [2]Department of Ultrasound, Jinling Hospital, Medical School of Nanjing University, Nanjing, China, [3]Department of Cardiothoracic Surgery, Jinling Hospital, School of Clinical Medicine, Nanjing Medical University, Nanjing, China, [4]Department of Cardiothoracic Surgery, Jinling Hospital, School of Medicine, Southeast University, Nanjing, China

Background: The emergence of immune checkpoint inhibitors (ICIs) has brought about a paradigm shift in the treatment landscape of non-small cell lung cancer (NSCLC). Despite the promising long-term survival outcomes and optimization of pathological complete response (cPR) demonstrated by various studies such as Impower010 and Checkmate-816, the effectiveness of neoadjuvant immunotherapy in advanced resectable NSCLC remains a subject of debate. Although previous research has explored the connection between the efficacy of neoadjuvant therapy and surgical-related safety, limited studies have specifically investigated the surgical-related safety of neoadjuvant immunotherapy. Therefore, our study aims to assess the efficacy and surgical-related safety of neoadjuvant immunotherapy in advanced resectable non-small cell lung cancer.

Method: We conducted a retrospective study on a cohort of 93 patients with stage IIIA-IIIC NSCLC who underwent neoadjuvant therapy and surgical resection. Among them, 53 patients received neoadjuvant immunotherapy, 18 patients underwent neoadjuvant chemotherapy while the remaining 22 underwent neoadjuvant targeted therapy. The patients were separated into further groups according to their pathological type. Data analyses were performed using Mann-Whitney U test, chi-square test.

Results: All patients were categorized into six distinct groups. Notably, the neoadjuvant immunotherapy squamous carcinoma group exhibited a favorable edge over the neoadjuvant targeted squamous carcinoma group concerning the duration of drainage tube indwelling and the extent of lymph node dissection. Furthermore, the neoadjuvant immunotherapy adenocarcinoma group outperformed neoadjuvant targeted therapy adenocarcinoma counterpart in terms of achieving complete pathological response (cPR). Simultaneously, the neoadjuvant immunotherapy adenocarcinoma group surpassed the neoadjuvant

chemotherapy adenocarcinoma group in the incidence of hydrothorax. Nevertheless, no statistically significant disparities were noted between the neoadjuvant immunotherapy squamous carcinoma group and the neoadjuvant chemotherapy carcinoma group.

Conclusion: Regarding surgical outcomes, neoadjuvant immunotherapy conferred notable advantages compared to conventional neoadjuvant chemotherapy and neoadjuvant targeted therapy for patients diagnosed with adenocarcinoma. In the case of squamous carcinoma, neoadjuvant immunotherapy exhibited superiority over neoadjuvant targeted therapy, although additional evidence is required to conclusively establish its precedence over neoadjuvant chemotherapy.

KEYWORDS

non-small cell lung cancer, neoadjuvant therapy, neoadjuvant immunotherapy, neoadjuvant immunochemotherapy, surgical-related safety

Introduction

Lung cancer (LC) poses a significant global health challenge, with non-small cell lung cancer (NSCLC) accounting for approximately 80% to 85% of newly diagnosed cases. According to the cancer statistics worldwide, LC accounts for up to 2 million diagnosed cases and contributes to more than 1.5 million deaths annually. Despite of the persistent decline in the LC incidence and mortality among American and European countries, the number of newly diagnosed LC in China is still on the rise and the LC-related deaths rank first in the cancer-specific mortality (1–5). Surgical resection with curative intent continuous served as the principal treatment for resectable NSCLC and offed the best chance of cure (6). However, its five-year survival rate ranging from 36% to 60% for stage IIIA disease to stage IIA disease respectively remained dissatisfactory (7). Randomized trials had elucidated the latent advantage of adjuvant therapy versus surgery alone, albeit with only a modest 5% benefit was identified in the five-year overall survival (OS) (6, 8). Taken together, an urgent need for the advent of novel treatment was put forward (9).

Neoadjuvant therapy has emerged as a groundbreaking approach in the management of resectable NSCLC, offering significant advantages such as improved long-term survival and an increased likelihood of cPR (7). Theoretically, neoadjuvant therapy has the potential to enhance the resection rate and enable the timely elimination of subclinical micro-metastatic disease. Additionally, compared to traditional adjuvant therapy, neoadjuvant therapy demonstrates superior compliance due to the pathetic surgery recovery (10). A systematic review and meta-analysis conducted by the NSCLC Meta-analysis Collaborative Group delineated a potential 5% benefit in the 5-year survival rate when neoadjuvant chemotherapy was compared to surgery alone (11). In contrast, another systematic review showed no significant difference in the 5-year survival between the adjuvant and neoadjuvant therapy (12). Collectively, the advancement of neoadjuvant therapy holds promise in converting unresectable NSCLC into resectable cases through tumor shrinkage and early intervention in patients at high risk of developing tumor metastasis. Therefore, the safety of the surgical procedure is closely linked to the efficacy of neoadjuvant therapy, as improved tumor shrinkage results in a safer surgical approach and a reduced incidence of postoperative complications.

Despite the treatment landscape of NSCLC such as screening, minimally invasive techniques and radiotherapy had evolved mildly, the development of neoadjuvant therapy remained nascent during the past decades (13, 14). Immunotherapy with the detection of immune checkpoint inhibitors (ICIs) such as programmed cell death protein 1(PD-1), programmed cell death receptor-legend 1(PD-L1) and cytotoxic T-lymphocyte-associated protein 4(CTLA-4) stirred up ripples in the in the field of neoadjuvant therapy for NSCLC (15–17). Mechanistically, ICIs function by facilitating the recognition of tumor cells by host T-cells, leading to the activation of T-cells, the release of cytokines, and subsequent tumor cell elimination following blockade of inhibitory interactions by ICI antibodies. Tumors with larger sizes, which carry a higher antigen burden, are more likely to elicit a robust anti-tumor T-cell response and therefore stand to benefit more from immunotherapy (18–20). Various studies such as Impower010, Checkmate-816 and NEOSTAR had identified the significant advantage of neoadjuvant immunotherapy to date (21–23).

However, the current clinical landscape of first-line neoadjuvant immunotherapy for NSCLC is characterized by rapid variations both domestically and internationally, with no established guidelines for the selection of ICIs at present (24, 25). The ICIs approved by the U.S. Food and Drug Administration include pembrolizumab, atezolizumab, nivolumab, ipilimumab, and durvalumab. However, in China, there is a rapid differentiation in the ICIs utilized as first-line treatment for NSCLC, such as tislelizumab, sintilimab, and toripalimab (26–29). Moreover,

previous studies on the efficacy of neoadjuvant immunotherapy have produced inconsistent results, which can be attributed to the limited sample sizes and the inclusion of NSCLC patients at different clinical stages, further intensifying the controversy surrounding these outcomes (30–33). Given the inconsistent findings from prior research and the absence of standardized guidelines for neoadjuvant treatment in advanced NSCLC, it becomes imperative to conduct additional studies to evaluate the efficacy of neoadjuvant immunotherapy in patients with advanced clinical stage NSCLC. Moreover, despite the strong association between the efficacy of neoadjuvant therapy and surgical-related safety, few studies have focused on the surgical-related safety following neoadjuvant immunotherapy. Therefore, our study aims to assess the efficacy and surgical-related safety of neoadjuvant immunotherapy in advanced NSCLC by comparing the outcomes of neoadjuvant therapy with immunotherapy to that of neoadjuvant therapy without immunotherapy in patients diagnosed with clinical stages IIIA-IVA NSCLC.

Method

Patient characteristics

A cohort of 104 NSCLC patients (≥18 years) diagnosed with a clinical stage ranging from IIIA to IVA were included. These patients underwent neoadjuvant therapy followed by surgical resection at the Department of Oncology and Cardiothoracic Surgery of Jinling Hospital between January 2016 and April 2023. Two patients were excluded from the study due to the use of neoadjuvant radiotherapy, which slightly increased the surgical risk due to the potential development of severe pleural adhesion (34). Nine patients were excluded with the clinical stage of IVA. This study was conducted in accordance with the Helsinki Declaration of 1964 and the latest version and met the ethical standards of the responsible committee on human experimentation of Jinling Hospital. Since this study was retrospective in nature, obtaining informed consent was not deemed necessary.

Data collection

Patients' data including age, gender, smoking history, clinical stage (cTNM), histological type of NSCLC and comorbid disease (cardiovascular disease, hypertension, diabetes mellitus) were extracted and analyzed. The surgery-related data included intraoperative blood loss, time of operation, indwelling time of drainage tube, total drainage volume, postoperative hospital stay, R0 resection, complete pathological response(cPR), the number of lymph node dissection fields, infection, sever pain, pneumothorax and hydrothorax. In consideration of the cPR, we collected the postoperative pathological report of all patients participated and cPR was referred to as no specific tumor remains among the widely drawing materials (35). The cTNM were according to the 8th American Joint Commission on Cancer (AJCC) Cancer Staging Manual (36). No immune-related adverse events(irAEs) of grade 3 or 4 was recorded in our study (37).

Treatment strategy

A total of 93 patients was divided into 6 groups according to their treatment strategy and pathological type. 53 patients received 2-4 cycles of neoadjuvant immunotherapy combined with neoadjuvant chemotherapy, 38 of them came up with the pathological type of squamous carcinoma while the rest 15 were adenocarcinoma. 22 patients achieved 2-4 cycles of neoadjuvant targeted therapy, among them 6 were squamous carcinoma and 16 were adenocarcinoma. Among the 22 patients, 8 applied Gefitinib, 5 used Afatinib, 4 employed Almonertinib, 4 applied Osimertinib, 1 used Crizotinib. 18 received 2-4 cycles of neoadjuvant chemotherapy with 10 squamous carcinomas and 8 adenocarcinomas. All of the patients received an interval no less than four weeks between the neoadjuvant therapy and surgery (38). Due to the lack of guidelines regarding the selection of neoadjuvant immunotherapy, the diverse treatment approaches made it impractical to subgroup patients within the neoadjuvant immunochemotherapy group based on their distinct strategies. The neoadjuvant chemotherapy or neoadjuvant targeted therapy followed the National Comprehensive Cancer Network (NCCN)version 2.2023 guidelines NSCLC (39). Thoracoscopic minimally invasive surgery was performed on all 93 patients in a standardized manner, with lymph node dissection carried out according to established protocols. The postoperative pathological reports were reviewed and verified by pathologists with over 10 years of experience.

Statistical analyses

Statistical analysis was performed using SPSS 26.0. The comparison of continuous variables was conducted using the Mann-Whitney U test, and the results were presented as the median (M) and interquartile range (IQR, P25-P50). For categorical variables, the chi-square test was utilized, and the findings were reported as the number (n) with the corresponding percentage (%). A p-value < 0.05 was considered statistically significant.

Results

Neoadjuvant immunotherapy squamous carcinoma group(n=38) neoadjuvant targeted therapy squamous carcinoma group (n=6)

In terms of demographics and baseline characteristics, no significant difference was observed within two groups. Through univariate analyses, neoadjuvant immunotherapy squamous carcinoma group exhibited advantages in terms of the indwelling time of drainage tube(P=0.023) and the number of lymph node dissection fields (P<0.001) (Figure 1).

10.3389/fonc.2023.1239451

A Baseline characteristics

		Neoadjuvant immunotherapy squamous carcinoma group (n=38)	Neoadjuvant targeted therapy squamous carcinoma group (n=6)	Z/c^2	P
Age		65 (59, 70)	70 (58, 73)	-0.754	0.451
Weight		62 (56, 70)	68 (63, 71)	-0.737	0.644
Gender	M	37 (97.4%)	6 (100.0%)	-	0.864
	F	1 (2.6%)	0 (0.0%)		
Smoking history	No	5 (13.2%)	1 (16.7%)	-	0.609
	Yes	33 (86.8%)	5 (83.3%)		
Hypertension	No	25 (65.8%)	5 (83.3%)	-	0.367
	Yes	13 (34.2%)	1 (16.7%)		
Diabetes	No	34 (89.5%)	6 (100.0%)	-	0.544
	Yes	4 (10.5%)	0 (0.0%)		
Coronary heart disease	No	37 (97.4%)	6 (100.0%)	-	0.864
	Yes	1 (2.6%)	0 (0.0%)		
Clinical stage (cTNM)	IIIA	23 (60.6%)	4 (66.7%)	-	0.902
	IIIB	14 (36.8%)	2 (33.3%)		
	IIIC	1 (2.6%)	0 (0.0%)		

B Surgical related outcomes

		Neoadjuvant immunotherapy squamous carcinoma group (n=38)	Neoadjuvant targeted therapy squamous carcinoma group (n=6)	Z/c^2	P
Transit opening	No	36 (94.7%)	6 (100.0%)	-	1.000
	Yes	2 (5.3%)	0 (0.0%)		
Ro resection	No	1 (2.6%)	0 (0.0%)	-	1.000
	Yes	37 (97.4%)	6 (100.0%)		
Intraoperative blood loss		300 (200, 400)	225 (88, 300)	-1.508	0.114
Time of operation		170 (129, 230)	148 (117, 233)	-0.411	0.681
Indwelling time of drainage tube		3 (2, 4)	5 (6, 7)	-2.282	0.023
Total drainage volume		785 (474, 1133)	740 (618, 978)	-0.086	0.923
Number of lymph node dissection fields		4 (4, 4)	3 (3, 3）	-3.528	＜0.001
Postoperative hospital stays		5 (4, 6)	8 (6, 9)	-2.316	0.021
Infection	No	19 (50.0%)	1 (16.7%)	-	0.198
	Yes	19 (50.0%)	5 (83.3%)		
Post operation pain	No	23 (62.7%)	2 (33.3%)	-	0.378
	Yes	15 (37.3%)	4 (66.7%)		
Pneumothorax	No	31 (81.7%)	5 (83.3%)	-	1.000
	Yes	7 (18.3%)	1 (16.7%)		
Hydrothorax	No	28 (73.7%)	5 (83.3%)	-	1.000
	Yes	10 (26.3%)	1 (16.7%)		
Complete pathological response	No	23 (60.5%)	4 (66.7%)	6.42	1.000
	Yes	15 (39.5%)	2 (33.3%)		

FIGURE 1
Neoadjuvant immunotherapy squamous carcinoma group and neoadjuvant targeted therapy squamous carcinoma group. **(A)** Baseline characteristics; **(B)** Surgical related outcomes.

Neoadjuvant immunotherapy squamous carcinoma group (n=38) neoadjuvant chemotherapy squamous carcinoma group (n=10)

No significant difference was found between the two groups with regards to both baseline characteristics and surgical related outcomes. The cPR rate was 39.5% in the neoadjuvant immunotherapy squamous carcinoma group and 20.0% in the neoadjuvant chemotherapy group, however without heterogeneity (P=0.459) (Figure 2).

Neoadjuvant immunotherapy adenocarcinoma group (n=15) and neoadjuvant targeted therapy adenocarcinoma group (n=16)

As to baseline characteristics, the neoadjuvant immunotherapy adenocarcinoma group had a higher possibility of younger patients compared to the neoadjuvant targeted therapy adenocarcinoma group. (P=0.043) The cPR rate was 40% and 6.2% in the neoadjuvant immunotherapy adenocarcinoma group and

A Baseline characteristics

		Neoadjuvant immunotherapy squamous carcinoma group (n=38)	Neoadjuvant chemotherapy squamous carcinoma group (n=10)	Z/c²	P
Age		65 (59, 70)	70 (62, 74)	-1.260	0.208
Weight		62 (56, 70)	70 (55, 74)	-0.687	0.492
Gender	M	37 (97.4%)	10 (100.0%)	-	1.000
	F	1 (2.6%)	0 (0.0%)		
Smoking history	No	5 (13.2%)	2 (20.0%)	-	0.625
	Yes	33 (86.8%)	8 (80.0%)		
Hypertension	No	25 (65.8%)	5 (50.0%)	-	0.468
	Yes	13 (34.2%)	5 (50.0%)		
Diabetes	No	34 (89.5%)	7 (70.0%)	-	0.147
	Yes	4 (10.5%)	3 (30.0%)		
Coronary heart disease	No	37 (97.4%)	9 (90.0%)	-	1.000
	Yes	1 (2.6%)	1 (10.0%)		
Clinical stage (cTNM)	IIIA	23 (60.6%)	6 (60.0%)	-	0.902
	IIIB	14 (36.8%)	4 (33.3%)		
	IIIC	1 (2.6%)	0 (0.0%)		

B Surgical related outcomes

		Neoadjuvant immunotherapy squamous carcinoma group (n=38)	Neoadjuvant chemotherapy squamous carcinoma (n=10)	Z/c²	P
Transit opening	No	36 (94.7%)	10 (100.0%)	-	1.000
	Yes	2 (5.3%)	0 (0.0%)		
Ro resection	No	1 (2.6%)	0 (0.0%)	-	1.000
	Yes	37 (97.4%)	10 (100.0%)		
Intraoperative blood loss		300 (200, 400)	300 (300, 325)	-0.73	0.466
Time of operation		170 (129, 230)	208 (163, 238)	-1.385	0.116
Indwelling time of drainage tube		3 (2, 4)	4 (3, 9)	-1.698	0.090
Total drainage volume		785 (474, 1133)	935 (539, 1938)	-0.901	0.367
Number of lymph node dissection fields		4 (4, 4)	4 (4, 4)	-0.465	0.642
Postoperative hospital stays		5 (4, 6)	6 (5, 12)	-1.945	0.048
Infection	No	19 (50.0%)	3 (30.0%)	-	0.307
	Yes	19 (50.0%)	7 (70.0%)		
Post operation pain	No	23 (62.7%)	4 (40.0%)	-	0.297
	Yes	15 (37.3%)	6 (60.0%)		
Pneumothorax	No	31 (81.7%)	8 (80.0%)	-	1.000
	Yes	7 (18.3%)	2 (20.0%)		
Hydrothorax	No	28 (73.7%)	5 (50.0%)	-	0.249
	Yes	10 (26.3%)	5 (50.0%)		
Complete pathological response	No	23 (60.5%)	8 (80.0%)	-	0.459
	Yes	15 (39.5%)	2 (20.0%)		

FIGURE 2
Neoadjuvant immunotherapy squamous carcinoma group and neoadjuvant chemotherapy squamous carcinoma group. **(A)** Baseline characteristics; **(B)** Surgical related outcomes.

neoadjuvant targeted therapy adenocarcinoma group separately, with great heterogeneity (P=0.037). No other significant disparity was observed in the surgical-related outcomes (Figure 3).

Neoadjuvant immunotherapy adenocarcinoma group (n=15) and neoadjuvant chemotherapy adenocarcinoma group (n=10)

In terms of baseline characteristics, no significant disparity was exhibited between the two groups. As to surgical related outcomes, neoadjuvant immunotherapy adenocarcinoma group demonstrated priority with regard to the rate of hydrothorax (6.7%VS 50%, P=0.033). No other difference with statistical significance was observed between the two groups (Figure 4).

To conclude, among the six groups, neoadjuvant immunotherapy squamous carcinoma group exhibited advantage over neoadjuvant targeted squamous carcinoma group in terms of the indwelling time of drainage tube and the number of lymph node dissection fields. Neoadjuvant immunotherapy adenocarcinoma group was superior to the neoadjuvant targeted therapy adenocarcinoma group with regard to the cPR. Meanwhile, neoadjuvant immunotherapy adenocarcinoma group overperformed neoadjuvant chemotherapy

A Baseline characteristics

		Neoadjuvant immunotherapy adenocarcinoma group (n=15)	Neoadjuvant targeted therapy adenocarcinoma group(n=16)	Z/c^2	P
Age		57 (54, 65)	63 (59, 68)	-2.019	0.043
Weight		69 (66, 74)	69 (61, 75)	-0.554	0.579
Gender	M	13 (86.7%)	11 (68.8%)	-	0.394
	F	2 (13.3%)	5 (31.2%)		
Smoking history	No	3 (20.0%)	7 (43.8%)	-	0.252
	Yes	12 (80.0%)	9 (56.2%)		
Hypertension	No	8 (53.3%)	13 (81.3%)	-	0.135
	Yes	7 (46.7%)	3 (18.7%)		
Diabetes	No	13 (86.7%)	13 (81.3%)	-	1.000
	Yes	2 (13.3%)	3 (18.7%)		
Coronary heart disease	No	13 (86.7%)	14 (87.5%)	-	1.000
	Yes	2 (13.3%)	2 (12.5%)		
Clinical stage (cTNM)	IIIA	10 (66.7%)	13 (81.3%)	-	0.833
	IIIB	3 (20.0%)	2 (12.5%)		
	IIIC	2 (13.3%)	1 (6.2%)		

B Surgical related outcomes

		Neoadjuvant immunotherapy adenocarcinoma group (n=15)	Neoadjuvant targeted therapy adenocarcinoma group (n=16)	Z/c^2	P
Transit opening	No	14 (93.3%)	10 (100.0%)	-	0.484
	Yes	1 (6.7%)	0 (0.0%)		
Ro resection	No	0 (0.0%)	0 (0.0%)	-	1.000
	Yes	15 (100.0%)	16 (100.0%)		
Intraoperative blood loss		200 (80, 400)	200 (150, 288)	-0.500	0.617
Time of operation		210 (160, 240)	166 (113, 187)	-1.700	0.089
Indwelling time of drainage tube		3 (2, 4)	4 (3, 5)	-1.686	0.092
Total drainage volume		530 (400, 760)	780 (416, 1042)	-0.693	0.488
Number of lymph node dissection fields		4 (3, 6)	4 (3, 4）	-1.422	0.155
Postoperative hospital stays		4 (3, 7)	6 (4, 7)	-1.146	0.252
Infection	No	7 (46.7%)	9 (56.3%)	-	0.724
	Yes	8 (53.3%)	7 (43.8%)		
Post operation pain	No	9 (60.0%)	10 (62.5%)	-	1.000
	Yes	6 (40.0%)	6 (37.5%)		
Pneumothorax	No	14 (93.3%)	13 (81.3%)	-	0.600
	Yes	1 (6.7%)	3 (18.7%)		
Hydrothorax	No	14 (93.3%)	12 (75.0%)	-	0.333
	Yes	1 (6.7%)	4 (25.0%)		
Complete pathological response	No	9 (60.0%)	15 (93.8%)	-	0.037
	Yes	6 (40.0%)	1 (6.2%)		

FIGURE 3
Neoadjuvant immunotherapy adenocarcinoma group and neoadjuvant targeted therapy adenocarcinoma group. **(A)** Baseline characteristics; **(B)** Surgical related outcomes.

adenocarcinoma group in the rate of hydrothorax. However, no significant difference was observed between the neoadjuvant immunotherapy squamous carcinoma group and the neoadjuvant chemotherapy carcinoma group.

Discussion

To the best of our knowledge, there have been limited investigations conducted to elucidate the surgical-related safety and effectiveness of neoadjuvant immunochemotherapy in patients with stage IIIA-IIIC NSCLC who have undergone surgical resection. In our study, we validated the potential advantages of neoadjuvant immunotherapy in terms surgical-related outcomes for advanced stage IIIA-IIIC NSCLC patients.

It is imperative to underscore that, having been categorized into six distinct subgroups, the sample size within each group was relatively modest. Regrettably, this limitation hindered our ability to obtain more profound and satisfying results. For instance, the complete pathological response (cPR) rate was 39.6% in the immunotherapy squamous carcinoma group and 20% in the neoadjuvant chemotherapy squamous carcinoma group, with no

10.3389/fonc.2023.1239451

A Baseline characteristics

		Neoadjuvant immunotherapy adenocarcinoma group (n=15)	Neoadjuvant chemotherapy adenocarcinoma group (n=8)	Z/c²	P
Age		57 (54, 65)	65 (58, 72)	-0.323	0.746
Weight		69 (66, 74)	65 (57, 70)	-1.812	0.070
Gender	M	13 (86.7%)	3 (37.5%)	-	0.026
	F	2 (13.3%)	5 (62.5%)		
Smoking history	No	3 (20.0%)	7 (87.5%)	-	0.006
	Yes	12 (80.0%)	1 (12.5%)		
Hypertension	No	8 (53.3%)	5 (62.5%)	-	1.000
	Yes	7 (46.7%)	3 (37.5%)		
Diabetes	No	13 (86.7%)	7 (87.5%)	-	1.000
	Yes	2 (13.3%)	1 (12.5%)		
Coronary heart disease	No	13 (86.7%)	8 (100.0%)	-	0.526
	Yes	2 (13.3%)	0 (0.0%)		
Clinical stage (cTNM)	IIIA	10 (66.7%)	4 (50.0%)	-	0.653
	IIIB	3 (20.0%)	3 (37.5%)		
	IIIC	2 (13.3%)	1 (12.5%)		

B Surgical related outcomes

		Neoadjuvant immunotherapy adenocarcinoma group (n=15)	Neoadjuvant chemotherapy adenocarcinoma group (n=8)	Z/c²	P
Transit opening	No	14 (93.3%)	8 (100.0%)	-	1.000
	Yes	1 (6.7%)	0 (0.0%)		
Ro resection	No	0 (0.0%)	0 (0.0%)	-	1.000
	Yes	15 (100.0%)	8 (100.0%)		
Intraoperative blood loss		200 (80, 400)	250 (125, 375)	-0.249	0.769
Time of operation		210 (160, 240)	180 (127, 227)	-0.517	0.609
Indwelling time of drainage tube		3 (2, 4)	3 (3, 4)	-0.204	0.838
Total drainage volume		530 (400, 760)	610 (284, 923)	-0.484	0.638
Number of lymph node dissection fields		4 (3, 6)	4 (3, 4）	-1.450	0.147
Postoperative hospital stays		4 (3, 7)	4 (4, 5)	-0.729	0.488
Infection	No	7 (46.7%)	2 (25.0%)	-	0.400
	Yes	8 (53.3%)	6 (75.0%)		
Post operation pain	No	9 (60.0%)	4 (50.0%)	-	0.685
	Yes	6 (40.0%)	4 (50.0%)		
Pneumothorax	No	14 (93.3%)	7 (87.5%)	-	1.000
	Yes	1 (6.7%)	1 (12.5%)		
Hydrothorax	No	14 (93.3%)	4 (50.0%)	-	0.033
	Yes	1 (6.7%)	4 (50.0%)		
Complete pathological response	No	9 (60.0%)	6 (75.0%)	-	0.369
	Yes	6 (40.0%)	2 (25.0%)		

FIGURE 4
Neoadjuvant immunotherapy adenocarcinoma group and neoadjuvant chemotherapy adenocarcinoma group. **(A)** Baseline characteristics; **(B)** Surgical related outcomes.

detectable heterogeneity. Notably, our neoadjuvant immunotherapy group achieved a cPR rate of 39.6%, significantly higher than the rates of 24.0% in Checkmate-816 (23), 28.6% in NEOSTAR (2021) (22) and 33.3% in Shu et al. (2020) (40). These studies reported respective operation rates of 83.2%, 84.1%, and 96.7%, while our study boasted a flawless 100.0% operation rate. This data strongly reinforces the concept that a higher operation rate correlates positively with a heightened cPR rate following neoadjuvant immunochemotherapy. This suggests that the potential benefits of neoadjuvant immunotherapy may include rendering unresectable NSCLC cases amenable to surgery through tumor shrinkage and preemptive treatment in patients at elevated risk of developing metastatic tumors. Notably, our neoadjuvant targeted squamous carcinoma group achieved a cPR rate of 33%, a figure significantly surpassing the outcomes observed in previous studies (13). This outcome can potentially be attributed in part to preoperative imaging screenings that identified tumor shrinkage.

Of great significance, both cases displaying a complete pathological response were classified as clinical stage IIIA and did not exhibit lymphatic metastasis. Despite the absence of exon 19 deletions or Leu858Arg substitutions in squamous carcinoma, there is a plausible speculation that targeted therapy might hold

promise for those patients who are free from lymphatic metastasis (41).

Despite the significant advancements achieved through the use of various drugs as first-line clinical treatments, the diversity in treatment strategies poses significant challenges in comprehending the true extent of the therapeutic benefits of neoadjuvant immunotherapy for NSCLC. Inconsistent outcomes arise from variations in trial endpoints, such as OS, relapse-free survival (RFS), cPR, and major pathological response (mPR), as well as the inclusion of patients with different stages of NSCLC. Moreover, it is essential to acknowledge the significance of Grade 3 or higher irAEs, despite their absence in our study. The mechanism underlying irAEs remains unknown, and the occurrence rates differ considerably across different ICIs (37, 42, 43). The absence of irAEs in our study may illustrate that irAEs generally took place before surgery and impact the suitability of patients for surgical resection. To conclude, conducting further studies on different ICIs is imperative to demonstrate the mechanisms of immunotherapy, understand the relationship between neoadjuvant immunotherapy and irAEs, and establish standardized ICI protocols for different types of NSCLC.

Our study was subject to several inherent limitations. Firstly, being a single-center retrospective study, the sample size was relatively small in our six subgroups which may have introduced sampling errors. Moreover, the diverse range of first-line clinical immunotherapy approaches and the empirical application of neoadjuvant immunotherapy posed significant challenges in standardizing treatment strategies. As a result, the EGFR data and PD-L1 data was not available for all of the patients. Additionally, the follow-up period for prognosis was relatively short for patients who underwent neoadjuvant immunochemotherapy, preventing us from conducting comprehensive survival analyses. In light of these limitations, there is an urgent need for further prospective multicenter clinical studies to provide a more comprehensive understanding of the efficacy and surgical-related safety of neoadjuvant immunotherapy in advanced NSCLC patients.

Conclusion

In terms of surgical related outcomes, neoadjuvant immunotherapy offered advantages over traditional neoadjuvant chemotherapy and neoadjuvant targeted therapy for patients with the pathological type of adenocarcinoma. With regard to squamous carcinoma, neoadjuvant immunotherapy was superior to neoadjuvant targeted therapy. while more evidence was necessary in order to prove its' priority over neoadjuvant chemotherapy. Further studies are crucial to address the limitations of our study and contribute to the ongoing debate on this topic.

Data availability statement

The raw data supporting the conclusions of this article will be made available by the authors, without undue reservation.

Ethics statement

The studies involving humans were approved by ethics committee of Jinling Hospital. The studies were conducted in accordance with the local legislation and institutional requirements. The participants provided their written informed consent to participate in this study. Written informed consent was obtained from the individual(s) for the publication of any potentially identifiable images or data included in this article.

Author contributions

QW and YS conceived of the idea and were major contributors in writing the manuscript. M-TX and CQ collected the data. NX, YQ, and CZ performed the statistical analysis. LJ made great comtributions in the statistical analysis in the revision of this manuscript and provided construction ideals. QY performed statistical analysis of this manuscript and made contribution in the revision of this manuscript. All authors contributed to the interpretation of the results and critically reviewed the first draft. All authors contributed to the article and approved the submitted version.

Funding

The author(s) declare financial support was received for the research, authorship, and/or publication of this article. This work was sustained by the National Natural Science Foundation of China [81702444] and the Natural Science Foundation of Jiangsu Province [BK20181239].

Acknowledgments

Authors would like to acknowledge the support of all colleagues in department of Cardiothoracic Surgery in Jingling Hospital.

Conflict of interest

The authors declare that the research was conducted in the absence of any commercial or financial relationships that could be construed as a potential conflict of interest.

Publisher's note

All claims expressed in this article are solely those of the authors and do not necessarily represent those of their affiliated organizations, or those of the publisher, the editors and the reviewers. Any product that may be evaluated in this article, or claim that may be made by its manufacturer, is not guaranteed or endorsed by the publisher.

References

1. Siegel RL, Miller KD, Wagle NS, Jemal A. Cancer statistics, 2023. *CA Cancer J Clin* (2023) 73(1):17–48. doi: 10.3322/caac.21763

2. Sung H, Ferlay J, Siegel RL, Laversanne M, Soerjomataram I, Jemal A, et al. Global cancer statistics 2020: globocan estimates of incidence and mortality worldwide for 36 cancers in 185 countries. *CA Cancer J Clin* (2021) 71(3):209–49. doi: 10.3322/caac.21660

3. Luo YH, Chiu CH, Scott Kuo CH, Chou TY, Yeh YC, Hsu HS, et al. Lung cancer in Republic of China. *J Thorac Oncol* (2021) 16(4):519–27. doi: 10.1016/j.jtho.2020.10.155

4. Chen P, Liu Y, Wen Y, Zhou C. Non-small cell lung cancer in China. *Cancer Commun (Lond)* (2022) 42(10):937–70. doi: 10.1002/cac2.12359

5. Miller KD, Nogueira L, Devasia T, Mariotto AB, Yabroff KR, Jemal A, et al. Cancer treatment and survivorship statistics, 2022. *CA Cancer J Clin* (2022) 72(5):409–36. doi: 10.3322/caac.21731

6. Chaft JE, Shyr Y, Sepesi B, Forde PM. Preoperative and postoperative systemic therapy for operable non-small-cell lung cancer. *J Clin Oncol* (2022) 40(6):546–55. doi: 10.1200/jco.21.01589

7. Kang J, Zhang C, Zhong WZ. Neoadjuvant immunotherapy for non-small cell lung cancer: state of the art. *Cancer Commun (Lond)* (2021) 41(4):287–302. doi: 10.1002/cac2.12153

8. Stupp R, Mayer M, Kann R, Weder W, Zouhair A, Betticher DC, et al. Neoadjuvant chemotherapy and radiotherapy followed by surgery in selected patients with stage Iiib non-small-cell lung cancer: A multicentre phase Ii trial. *Lancet Oncol* (2009) 10(8):785–93. doi: 10.1016/s1470-2045(09)70172-x

9. Uprety D, Mandrekar SJ, Wigle D, Roden AC, Adjei AA. Neoadjuvant immunotherapy for nsclc: current concepts and future approaches. *J Thorac Oncol* (2020) 15(8):1281–97. doi: 10.1016/j.jtho.2020.05.020

10. Shen J, Sun N, Zens P, Kunzke T, Buck A, Prade VM, et al. Spatial metabolomics for evaluating response to neoadjuvant therapy in non-small cell lung cancer patients. *Cancer Commun (Lond)* (2022) 42(6):517–35. doi: 10.1002/cac2.12310

11. Preoperative chemotherapy for non-small-cell lung cancer: A systematic review and meta-analysis of individual participant data. *Lancet* (2014) 383(9928):1561–71. doi: 10.1016/s0140-6736(13)62159-5

12. Lim E, Harris G, Patel A, Adachi I, Edmonds L, Song F. Preoperative versus postoperative chemotherapy in patients with resectable non-small cell lung cancer: systematic review and indirect comparison meta-analysis of randomized trials. *J Thorac Oncol* (2009) 4(11):1380–8. doi: 10.1097/JTO.0b013e3181b9ecca

13. Saw SPL, Ong BH, Chua KLM, Takano A, Tan DSW. Revisiting neoadjuvant therapy in non-small-cell lung cancer. *Lancet Oncol* (2021) 22(11):e501–e16. doi: 10.1016/s1470-2045(21)00383-1

14. Ettinger DS, Wood DE, Aisner DL, Akerley W, Bauman JR, Bharat A, et al. Non-small cell lung cancer, version 3.2022, Nccn clinical practice guidelines in oncology. *J Natl Compr Canc Netw* (2022) 20(5):497–530. doi: 10.6004/jnccn.2022.0025

15. Yi JS, Ready N, Healy P, Dumbauld C, Osborne R, Berry M, et al. Immune activation in early-stage non-small cell lung cancer patients receiving neoadjuvant chemotherapy plus ipilimumab. *Clin Cancer Res* (2017) 23(24):7474–82. doi: 10.1158/1078-0432.Ccr-17-2005

16. Kimura H, Araya T, Yoneda T, Shirasaki H, Kurokawa K, Sakai T, et al. Long-lasting responses after discontinuation of nivolumab treatment for reasons other than tumor progression in patients with previously treated, advanced non-small cell lung cancer. *Cancer Commun (Lond)* (2019) 39(1):78. doi: 10.1186/s40880-019-0423-3

17. Patil NS, Nabet BY, Müller S, Koeppen H, Zou W, Giltnane J, et al. Intratumoral plasma cells predict outcomes to Pd-L1 blockade in non-small cell lung cancer. *Cancer Cell* (2022) 40(3):289–300.e4. doi: 10.1016/j.ccell.2022.02.002

18. Liu J, Blake SJ, Yong MC, Harjunpää H, Ngiow SF, Takeda K, et al. Improved efficacy of neoadjuvant compared to adjuvant immunotherapy to eradicate metastatic disease. *Cancer Discovery* (2016) 6(12):1382–99. doi: 10.1158/2159-8290.Cd-16-0577

19. Keir ME, Butte MJ, Freeman GJ, Sharpe AH. Pd-1 and its ligands in tolerance and immunity. *Annu Rev Immunol* (2008) 26:677–704. doi: 10.1146/annurev.immunol.26.021607.090331

20. Litchfield K, Reading JL, Puttick C, Thakkar K, Abbosh C, Bentham R, et al. Meta-analysis of tumor- and T cell-intrinsic mechanisms of sensitization to checkpoint inhibition. *Cell* (2021) 184(3):596–614.e14. doi: 10.1016/j.cell.2021.01.002

21. Felip E, Altorki N, Zhou C, Csőszi T, Vynnychenko I, Goloborodko O, et al. Adjuvant atezolizumab after adjuvant chemotherapy in resected stage Ib-Iiia non-small-cell lung cancer (Impower010): A randomised, multicentre, open-label, phase 3 trial. *Lancet* (2021) 398(10308):1344–57. doi: 10.1016/s0140-6736(21)02098-5

22. Cascone T, William WN Jr., Weissferdt A, Leung CH, Lin HY, Pataer A, et al. Neoadjuvant nivolumab or nivolumab plus ipilimumab in operable non-small cell lung cancer: the phase 2 randomized neostar trial. *Nat Med* (2021) 27(3):504–14. doi: 10.1038/s41591-020-01224-2

23. Forde PM, Spicer J, Lu S, Provencio M, Mitsudomi T, Awad MM, et al. Neoadjuvant nivolumab plus chemotherapy in resectable lung cancer. *N Engl J Med* (2022) 386(21):1973–85. doi: 10.1056/NEJMoa2202170

24. Daly ME, Singh N, Ismaila N, Antonoff MB, Arenberg DA, Bradley J, et al. Management of stage Iii non-small-cell lung cancer: Asco guideline. *J Clin Oncol* (2022) 40(12):1356–84. doi: 10.1200/jco.21.02528

25. Singh N, Temin S, Baker S Jr., Blanchard E, Brahmer JR, Celano P, et al. Therapy for stage iv non-small-cell lung cancer with driver alterations: Asco living guideline. *J Clin Oncol* (2022) 40(28):3310–22. doi: 10.1200/jco.22.00824

26. Vaddepally RK, Kharel P, Pandey R, Garje R, Chandra AB. Review of indications of Fda-approved immune checkpoint inhibitors per Nccn guidelines with the level of evidence. *Cancers (Basel)* (2020) 12(3):738. doi: 10.3390/cancers12030738

27. Ren Z, Xu J, Bai Y, Xu A, Cang S, Du C, et al. Sintilimab plus a bevacizumab biosimilar (Ibi305) versus sorafenib in unresectable hepatocellular carcinoma (Orient-32): A randomised, open-label, phase 2-3 study. *Lancet Oncol* (2021) 22(7):977–90. doi: 10.1016/s1470-2045(21)00252-7

28. Wang J, Lu S, Yu X, Hu Y, Sun Y, Wang Z, et al. Tislelizumab plus chemotherapy vs chemotherapy alone as first-line treatment for advanced squamous non-small-cell lung cancer: A phase 3 randomized clinical trial. *JAMA Oncol* (2021) 7(5):709–17. doi: 10.1001/jamaoncol.2021.0366

29. Zhu X, Sun L, Song N, He W, Xie B, Hu J, et al. Safety and effectiveness of neoadjuvant Pd-1 inhibitor (Toripalimab) plus chemotherapy in stage Ii-Iii Nsclc (Lungmate 002): an open-label, single-arm, phase 2 trial. *BMC Med* (2022) 20(1):493. doi: 10.1186/s12916-022-02696-4

30. Wang Z, Wu L, Li B, Cheng Y, Li X, Wang X, et al. Toripalimab plus chemotherapy for patients with treatment-naive advanced non-small-cell lung cancer: A multicenter randomized phase Iii trial (Choice-01). *J Clin Oncol* (2023) 41(3):651–63. doi: 10.1200/jco.22.00727

31. Yang X, Yin R, Xu L. Neoadjuvant Pd-1 blockade in resectable lung cancer. *N Engl J Med* (2018) 379(9):e14. doi: 10.1056/NEJMc1808251

32. O'Brien M, Paz-Ares L, Marreaud S, Dafni U, Oselin K, Havel L, et al. Pembrolizumab versus placebo as adjuvant therapy for completely resected stage Ib-Iiia non-small-cell lung cancer (Pearls/keynote-091): an interim analysis of a randomised, triple-blind, phase 3 trial. *Lancet Oncol* (2022) 23(10):1274–86. doi: 10.1016/s1470-2045(22)00518-6

33. Chaft JE, Oezkan F, Kris MG, Bunn PA, Wistuba II, Kwiatkowski DJ, et al. Neoadjuvant atezolizumab for resectable non-small cell lung cancer: an open-label, single-arm phase Ii trial. *Nat Med* (2022) 28(10):2155–61. doi: 10.1038/s41591-022-01962-5

34. Neri S, Takahashi Y, Terashi T, Hamakawa H, Tomii K, Katakami N, et al. Surgical treatment of local recurrence after stereotactic body radiotherapy for primary and metastatic lung cancers. *J Thorac Oncol* (2010) 5(12):2003–7. doi: 10.1097/JTO.0b013e3181f8a785

35. Hellmann MD, Chaft JE, William WN Jr., Rusch V, Pisters KM, Kalhor N, et al. Pathological response after neoadjuvant chemotherapy in resectable non-small-cell lung cancers: proposal for the use of major pathological response as a surrogate endpoint. *Lancet Oncol* (2014) 15(1):e42–50. doi: 10.1016/s1470-2045(13)70334-6

36. Rice TW, Patil DT, Blackstone EH. 8th edition Ajcc/Uicc staging of cancers of the esophagus and esophagogastric junction: application to clinical practice. *Ann Cardiothorac Surg* (2017) 6(2):119–30. doi: 10.21037/acs.2017.03.14

37. Schoenfeld AJ, Arbour KC, Rizvi H, Iqbal AN, Gadgeel SM, Girshman J, et al. Severe immune-related adverse events are common with sequential Pd-(L)1 blockade and osimertinib. *Ann Oncol* (2019) 30(5):839–44. doi: 10.1093/annonc/mdz077

38. Zhou C, Chen G, Huang Y, Zhou J, Lin L, Feng J, et al. Camrelizumab plus carboplatin and pemetrexed versus chemotherapy alone in chemotherapy-naive patients with advanced non-squamous non-small-cell lung cancer (Camel): A randomised, open-label, multicentre, phase 3 trial. *Lancet Respir Med* (2021) 9(3):305–14. doi: 10.1016/s2213-2600(20)30365-9

39. Ettinger DS, Wood DE, Aisner DL, Akerley W, Bauman JR, Bharat A, et al. Nccn guidelines® Insights: non-small cell lung cancer, version 2.2023. *J Natl Compr Canc Netw* (2023) 21(4):340–50. doi: 10.6004/jnccn.2023.0020

40. Shu CA, Gainor JF, Awad MM, Chiuzan C, Grigg CM, Pabani A, et al. Neoadjuvant atezolizumab and chemotherapy in patients with resectable non-small-cell lung cancer: an open-label, multicentre, single-arm, phase 2 trial. *Lancet Oncol* (2020) 21(6):786–95. doi: 10.1016/s1470-2045(20)30140-6

41. Niu Z, Jin R, Zhang Y, Li H. Signaling pathways and targeted therapies in lung squamous cell carcinoma: mechanisms and clinical trials. *Signal Transduct Target Ther* (2022) 7(1):353. doi: 10.1038/s41392-022-01200-x

42. Shankar B, Zhang J, Naqash AR, Forde PM, Feliciano JL, Marrone KA, et al. Multisystem immune-related adverse events associated with immune checkpoint inhibitors for treatment of non-small cell lung cancer. *JAMA Oncol* (2020) 6(12):1952–6. doi: 10.1001/jamaoncol.2020.5012

43. Kennedy LB, Salama AKS. A review of cancer immunotherapy toxicity. *CA Cancer J Clin* (2020) 70(2):86–104. doi: 10.3322/caac.21596

frontiers | Frontiers in Immunology

TYPE Case Report
PUBLISHED 18 January 2024
DOI 10.3389/fimmu.2023.1272450

Check for updates

OPEN ACCESS

EDITED BY
Jie Mei,
Wuxi People's Hospital Affiliated to Nanjing Medical University, China

REVIEWED BY
Chel Hun Choi,
Samsung, Republic of Korea
Zhiwen Luo,
Fudan University, China

*CORRESPONDENCE
Qinghua Zhou
prof_qh_zhou@126.com

†These authors have contributed equally to this work

RECEIVED 04 August 2023
ACCEPTED 29 December 2023
PUBLISHED 18 January 2024

CITATION
Mei T, Wang T, Lei C, Jiang D and Zhou Q (2024) Pathological complete response to neoadjuvant therapy with serplulimab and chemotherapy in stage IIIB small cell lung cancer: a case report and literature review. *Front. Immunol.* 14:1272450. doi: 10.3389/fimmu.2023.1272450

COPYRIGHT
© 2024 Mei, Wang, Lei, Jiang and Zhou. This is an open-access article distributed under the terms of the Creative Commons Attribution License (CC BY). The use, distribution or reproduction in other forums is permitted, provided the original author(s) and the copyright owner(s) are credited and that the original publication in this journal is cited, in accordance with accepted academic practice. No use, distribution or reproduction is permitted which does not comply with these terms.

Pathological complete response to neoadjuvant therapy with serplulimab and chemotherapy in stage IIIB small cell lung cancer: a case report and literature review

Ting Mei[1,2†], Ting Wang[1,2†], Chuanfen Lei[3], Dan Jiang[3] and Qinghua Zhou[1,2*]

[1]Department of Medical Oncology, Cancer Center, West China Hospital, Sichuan University, Chengdu, Sichuan, China, [2]Lung Cancer Center, West China Hospital, Sichuan University, Chengdu, Sichuan, China, [3]Department of Pathology, West China Hospital, Sichuan University, Chengdu, Sichuan, China

Chemotherapy combined with immunotherapy has significantly improved survival in patients with extensive-stage small cell lung cancer (ES-SCLC), and neoadjuvant immunotherapy combined with chemotherapy has emerged as the standard treatment for those with resectable non-small cell lung cancer (NSCLC). However, the potential benefits of surgery following neoadjuvant immunotherapy combined with chemotherapy in locally advanced SCLC remain unclear. Herein, we report a patient diagnosed with stage IIIB SCLC, who was administered five cycles of neoadjuvant serplulimab combined with chemotherapy followed by surgery, and subsequently achieved a pathologic complete response (pCR). Within a follow-up duration of six months, the patient displayed neither recurrence nor metastasis and experienced no treatment-related adverse reactions of any grade. Based on this case, for locally advanced SCLC, neoadjuvant serplulimab combined with chemotherapy followed by surgery may present an effective, safe, and potentially curative treatment strategy. Nonetheless, further prospective studies are needed to verify our findings.

KEYWORDS

small cell lung cancer, immunotherapy, neoadjuvant therapy, pathological complete response, serplulimab, case report

Introduction

Small cell lung cancer (SCLC) accounts for approximately 13-15% of all lung cancer cases (1). Characterized by its rapid progression, aggressive behavior, and propensity for distant metastasis, SCLC is often associated with a poor prognosis (2). Approximately 1/3 of SCLC patients are in the limited stage (LS-SCLC) at the time of initial diagnosis (3). Although LS-SCLC is highly sensitive to chemotherapy and radiotherapy, the median survival is limited to 16-24 months, emphasizing the urgent need to improve efficacy and expand the scope of current treatment strategies (4).

Surgery, an integral facet of multimodal cancer management, is currently only recommended for patients with T1-2N0M0 SCLC (5). And a study has shown that stage IIIA SCLC patients who receive neoadjuvant chemotherapy have a disappointingly low postoperative pCR rate of only 5% (6). Given these considerations, the role of surgery in managing stage III SCLC remains contentious, and their standard treatment regimen is concurrent chemoradiotherapy.

Results from the Checkmate 816 study demonstrated that neoadjuvant immunotherapy combined with chemotherapy extended event-free survival (EFS) and elevated rates of pCR compared with chemotherapy alone in patients with resectable NSCLC (7). A previous case report by Zhang et al. also showed that neoadjuvant tislelizumab combined with chemotherapy brought LS-SCLC patients an event-free survival of up to 23 months (8). Moreover, previous IMpower133 and CASPIAN studies have established that incorporating PD-L1 inhibitors into chemotherapy can significantly improve the overall survival (OS) of patients with ES-SCLC (9, 10). Serplulimab, a PD-1 inhibitor characterized by its strong affinity and low immunogenicity, has been substantiated in the ASTRUM-005 study to effectively improve the prognosis of ES-SCLC patients when combined with chemotherapy, yielding a median progression-free survival (PFS) and OS of 5.7 and 15.4 months, respectively (11). Based on these observations, we hypothesized that after LS-SCLC received neoadjuvant immunotherapy combined with chemotherapy, the tumor might undergo further shrinkage and down-staging, thus allowing for more comprehensive resection and potentially resulting in enhanced survival. However, there are very few data on stage III SCLC patients who received neoadjuvant chemotherapy combined with immunotherapy followed by surgery.

Here we report a case of stage IIIB SCLC patient who underwent five cycles of neoadjuvant serplulimab combined with chemotherapy and achieved pCR after surgery.

Case report

General conditions

In July 2022, a 51-year-old female presented to the West China Hospital of Sichuan University with complaints of persistent cough and sputum production. She reported no history of smoking or any notable medical conditions. On physical examination, no palpable lymphadenopathy was detected throughout her body and her cardiopulmonary examination was unremarkable. Blood tests revealed elevated levels of enolase (76.6ng/ml). The contrast-enhanced chest computed tomography (CT) demonstrated a mass measuring approximately 9 cm x 6.9 cm in the lower lobe of the left lung, encasing a part of the left lower lobe bronchi and resulting in occlusion of the corresponding bronchial lumen (Figures 1A, B). Additionally, enlargement of mediastinal and left hilar lymph nodes was observed, with a maximum size of 3.4 cm x 3.2 cm (Figure 1C). Contrast-enhanced abdominal CT, brain magnetic resonance imaging (MRI), and bone scan all returned normal findings. A bronchoscopic biopsy conducted via a fiberoptic bronchoscope from the basal segment of the left lower lobe confirmed the diagnosis of SCLC. Immunohistochemical profile was as follows: CK7(−), TTF-1(+), NapsinA(−), CK5/6(−), P63(−), Syn(+), CK (Pan)(+), CD56(+), CgA(+), Ki-67(MIB-1,+, 90%), P53(+), RB(−, expression loss). EBER (*in situ* hybridization, −).

Diagnosis and treatment process

The patient was diagnosed with SCLC of the left lower lobe with metastasis to the left hilar and mediastinal lymph nodes, classified as cT4N2M0 stage IIIB. Despite concurrent chemoradiotherapy being the standard treatment recommended by the guidelines for such cases, the patient expressed a strong preference for surgery. Upon consultation with a multidisciplinary team, it was considered that the patient's tumor was potentially resectable. Based on the Checkmate 816 study, we posited that a preoperative regimen of neoadjuvant immunotherapy and chemotherapy followed by surgery might be an optimal strategy. Moreover, Zhang et al. also previously reported that stage IIIB SCLC patients obtained pCR after receiving neoadjuvant tislelizumab combined with chemotherapy, and the recurrence-free survival time was as long as 23 months. In addition, the results of the ASTRUM-005 study showed that serplulimab combined with chemotherapy significantly improved the OS of patients with ES-SCLC. The patient ultimately opted for a neoadjuvant regimen consisting of etoposide (100 mg/m^2, days 1-3), cisplatin (75 mg/m^2, days 1-3), and serplulimab (300 mg, day 1). She received five cycles of this combined EP with a serplulimab regimen, specifically: etoposide 150mg on days 1-3, cisplatin 40mg on days 1-2 and 30mg on day 3, and serplulimab 300mg on day 1, administered intravenously every three weeks.

Results

Following two cycles of neoadjuvant therapy, the patient's left lower lobe lesion diminished to 3.5 cm, and the size of the largest mediastinal lymph node reduced to 2.5 cm x 2.0 cm (Figures 1D–F), demonstrating a partial response (PR) to the treatment. After completing four cycles of neoadjuvant therapy, the left lower lobe lesion in the patient had further reduced to 1.5 cm, and the largest mediastinal lymph node had shrunken to 1.8 cm x 1.0 cm (Figures 1G–I), signifying a sustained PR to the treatment. After 5 cycles of treatment, the tumor did not shrink further, nor did the NSE level decrease further. The changes in NSE values during the course of the disease are shown in Figure 1J. And the patient

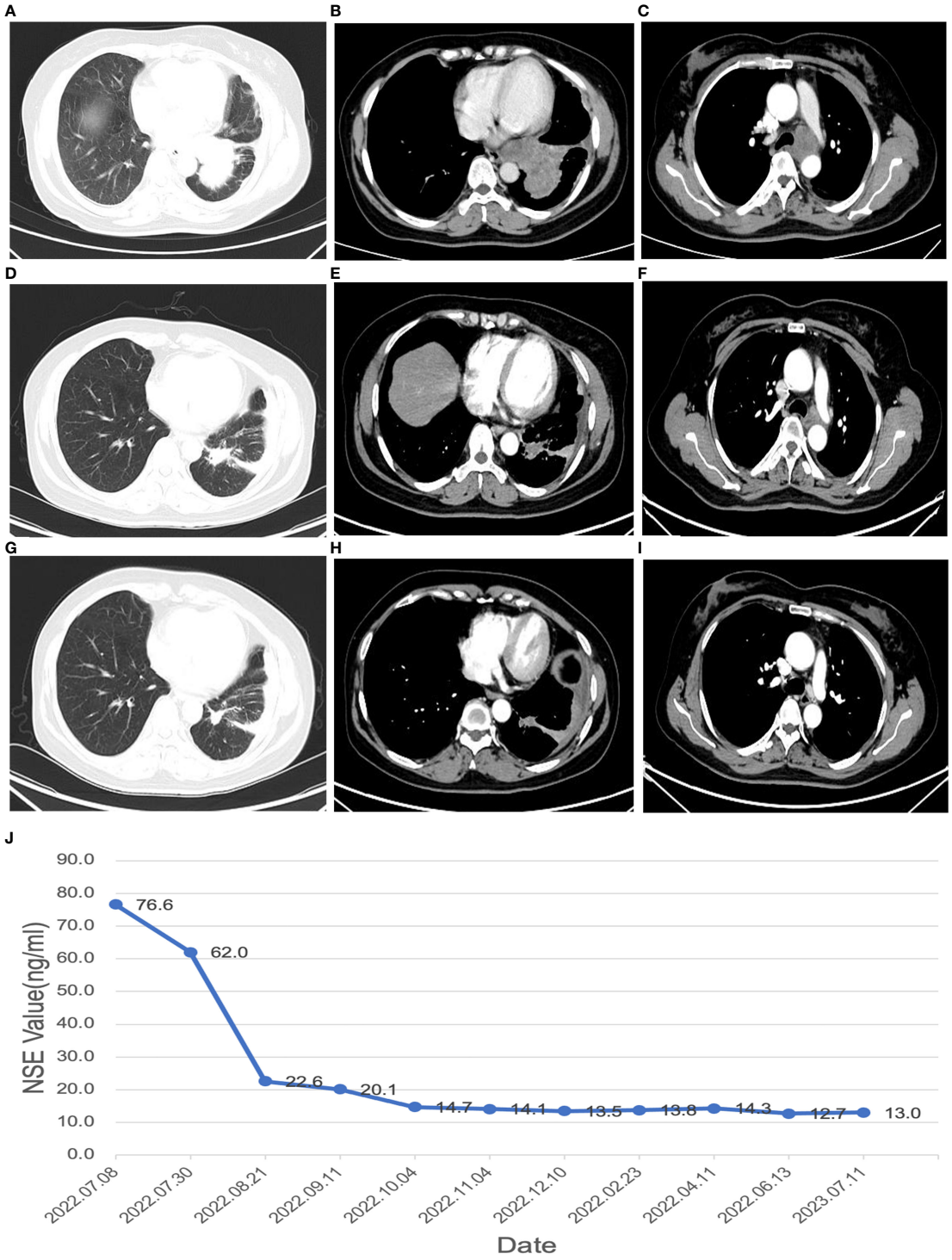


FIGURE 1
Changes in maximum tumor volume by chest CT scans and changes in NSE value during the disease **(A–C)**, CT images at the time of initial diagnosis; **(D–F)**, CT images after receiving 2 cycles of neoadjuvant therapy; **(G–I)**, CT images after 4 cycles of neoadjuvant therapy; **(J)**, changes in NSE value during the disease.

underwent a left lower lobectomy coupled with lymph node dissection 47 days after the completion of the neoadjuvant therapy. Postoperatively, the treatment efficacy was evaluated as a pCR (Figure 2). Post-surgery, the patient was administered one cycle of adjuvant therapy combining EP regimen with serplulimab, and then did not receive serplulimab maintenance therapy. Routine imaging evaluations were conducted bimonthly during the follow-up period. From the time of receiving neoadjuvant serplulimab combined with chemotherapy to the cut-off time of follow-up, which lasted up to 12 months, no tumor recurrence or metastasis was found (Figure 3). No adverse effects were noted during treatment.

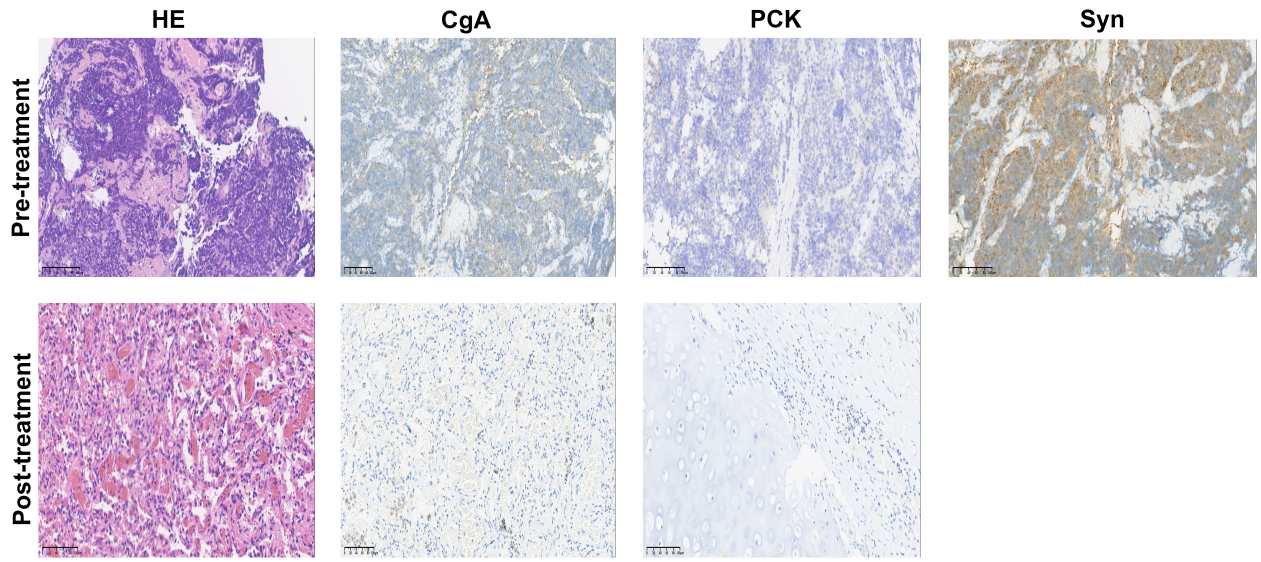


FIGURE 2
Hematoxylin-eosin (HE) and immunohistochemistry staining in the tumor bed. Staining of the post-treatment lung mass showed no viable tumor cells; pan-cytokeratin (PCK) and chromogranin A (CgA) were negative; Syn staining was omitted due to the absence of remaining tumor cells after treatment. Scale bar, 100 μm.

Discussion

The current NCCN guidelines only recommend radical surgery for LS-SCLC patients with T1-2N0M0 staging (5). However, less than 5% of initially diagnosed SCLC patients meet this standard (12). For the majority of LS-SCLC patients, concurrent chemoradiotherapy is the standard treatment modality, despite the high response rate of up to 80% for first-line treatment, and most patients experience relapse within six months of completing their initial treatment (13). Therefore, the pursuit of more effective therapeutic strategies remains an ongoing focus of our research endeavors.

Historically, surgery has not been recommended treatment for SCLC, a position informed by the findings of two large-scale, randomized prospective trials. The MRC study, executed by the UK Medical Research Council in the 1960s, demonstrated a superiority of definitive radiotherapy over surgery in patients with LS-SCLC, evidenced by a notably longer OS (14, 15). Adding to this, another multicenter randomized phase III study by the Lung Cancer Study Group (LCSG) further supported the non-recommendation of surgery (16). In that study, 146 LS-SCLC patients with regional lymph nodes involvement (T3N1-2M0) received five cycles of neoadjuvant chemotherapy (comprising cyclophosphamide,

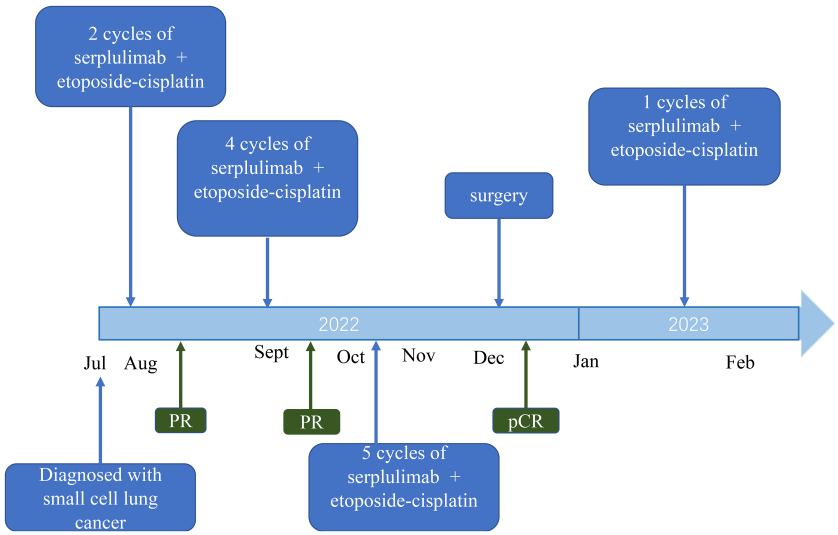


FIGURE 3
Timeline from July 2022 to July 2023.

doxorubicin, and vincristine), following which they were randomized to surgical or non-surgical groups. The study found no disparity in OS between the two groups, with both displaying a 2-year survival rate of 20%. The limitations of these earlier studies include the lack of chemotherapy in the MRC study and the absence of platinum-based chemotherapy in the neoadjuvant phase in the LCSG study. In recent years, however, advancements in diagnostic and surgical technologies, along with the emergence of novel therapeutic modalities like immunotherapy, have necessitated a reevaluation of the role of surgery in SCLC management. This has prompted extensive reconsideration in a series of large-scale retrospective observational studies conducted recently (17, 18).

In NSCLC patients, the results of the Checkmate 816 study showed a significant enhancement in the pCR rate with neoadjuvant nivolumab combined with chemotherapy as compared to neoadjuvant chemotherapy alone (24% vs. 2.2%, p< 0.0001), it also demonstrated a noticeably extended EFS (31.6 months vs. 20.8 months, p=0.0052), and the safety profiles of both treatment groups were analogous, exhibiting similar incidences of grade 3-4 treatment-related adverse events (TRAE) at 34% and 37%, respectively (7). Moreover, the study emphasized that neoadjuvant immunotherapy combined with chemotherapy, when compared to chemotherapy alone, does not impact the surgery rate, timing and completeness of resection, nor does it escalate the operational complexity or the risk of surgical complications. And for SCLC, several previous studies have corroborated that the combination of chemotherapy combined with immunotherapy significantly improves the overall response rate (ORR), PFS and OS of ES-SCLC compared to chemotherapy alone (9–11). Previous case reports and retrospective studies have also reported the role of neoadjuvant immunotherapy combined with chemotherapy in LS-SCLC. Liu et al. conducted a retrospective study and the results showed that neoadjuvant immunotherapy combined with chemotherapy followed by surgical resection is safe and effective in patients with stage I-IIIA SCLC (19). Next, Zhang et al. reported a case of more than 23 months of event-free survival after receiving neoadjuvant tislelizumab combined with chemotherapy (8). Later, a multicenter single-arm study demonstrated that neoadjuvant atezolizumab combined with chemotherapy significantly improved the pCR of resectable SCLC, and AEs were controllable (20). In addition, a network meta-analysis conducted by Wu et al. on the efficacy of first-line immune checkpoint inhibitors (ICIs) combined with chemotherapy revealed that, in comparison to other ICIs, the combination of serplulimab and chemotherapy was most likely to yield superior PFS and OS in patients with ES-SCLC (21). Our study suggests that the treatment strategy of neoadjuvant chemotherapy combined with serplulimab is also applicable to potentially resectable SCLC cases, with the ability to achieve postoperative pCR and ultimately provide patients with an extended EFS.

To explore the changes in the tumor immune microenvironment before and after neoadjuvant immunochemotherapy, we performed multiplex immunofluorescence staining on T cells, macrophages, monocytes, and myeloid-derived suppressor cells (MDSC) in the patient's preoperative and postoperative specimens (Figure 4). We found that the infiltration of T cells and monocytes in patients' postoperative specimens increased significantly, while MDSC and macrophages decreased significantly. In recent years, different immune cell subpopulations have been divided into "positive" immune cell subpopulations and "negative" immune cell subpopulations. "Positive" immune cell subpopulations include CD4+T cells, NK cells CD8+T cells, etc. (22–24), while "negative" immune cell subpopulations include Tregs, tumor-associated macrophages, myeloid-derived suppressor cells (MDSCs), etc (25–27). Therefore, after treatment, the abundance of "positive" immune cell subpopulations increases and the abundance of "negative" immune cell subpopulations decreases, which may indicate that the patient will benefit from immunotherapy. As shown in the case we report.

However, it is important to highlight a discrepancy in the number of preoperative neoadjuvant therapy cycles between the Checkmate 816 study and our case. In the former, patients underwent three cycles of therapy, while in our case, the patient received five cycles of neoadjuvant serplulimab combined with chemotherapy before surgery, aligning with the cycle of neoadjuvant therapy implemented in the LCSG study. As far as we know, most phase II/III clinical trials involving neoadjuvant immunotherapy, either as monotherapy or in

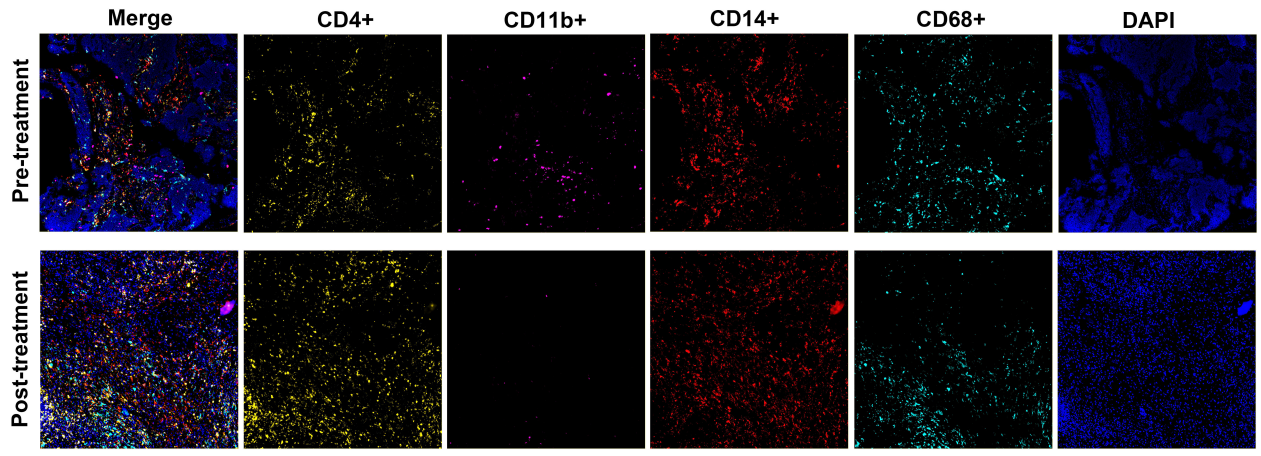


FIGURE 4
Tumor immune microenvironment before and after treatment.

combination with chemotherapy, employ 2-4 cycles (7, 28–31). Nonetheless, due to the absence of direct comparisons among different cycle groups, a definitive conclusion regarding the optimal number of treatment cycles for neoadjuvant immunotherapy combined with chemotherapy remains elusive. To address this issue, He et al. conducted a retrospective study, which found that the major pathologic response (MPR) rates of NSCLC patients who received 2, 3, 4, and ≥ 4 cycles of neoadjuvant immunotherapy combined with chemotherapy were 44.8%, 61.4%, 66.7%, and 40.0%, respectively (32). To adjust for the potential of subjectively reducing treatment cycles due to significant tumor downstaging, they performed a subgroup analysis on patients who achieved complete or partial response (CR/PR) and found that MPR rates of 2, 3, 4, and ≥ 4 cycles are 43.8%, 71.0%, 71.4%, and 33.3%, respectively. In summary, extending NSCLC neoadjuvant immunotherapy combined with chemotherapy to 3-4 cycles has shown a higher MPR rate than 2 cycles, and this extension to 3-4 cycles remains beneficial even if imaging reveals CR/PR. In our study, the rationale behind administering five cycles of preoperative neoadjuvant therapy hinged on several factors. First, the high risk of distant metastasis in SCLC suggests that additional treatment cycles could potentially eradicate micrometastases. Second, the size of the primary tumor and lymph node size continued to shrink before the fifth cycle of treatment. After the fifth cycle, the tumor size stabilized, meeting the conditions for surgical R0 resection. And before the fifth cycle, NSE continued to decline, and after the fifth cycle, the NSE was in a stable period. Moreover, we observed no TRAE of any grade, attesting to the safety and feasibility of this treatment strategy.

Limitations and challenges: First, although the probability of tumor progression in SCLC during the neoadjuvant treatment phase is low, if disease progression occurs, patients may lose the opportunity for local treatment; Second, clinicians generally use imaging to evaluate the response of solid tumors to systemic therapy, but the Response Evaluation Criteria in Solid Tumors (RECIST) cannot accurately evaluate ICI neoadjuvant therapy; Third, the patient's postoperative pathology achieved pCR, suggesting that the patient has the potential to be cured. The relationship between pCR after neoadjuvant therapy and the prognosis of NSCLC has been confirmed by many studies, but whether pCR after neoadjuvant therapy for SCLC is related to prognosis (DFS/OS) has a close correlation, which has yet to be proven by research, and we still need to remain cautiously optimistic; Fourth, it is still questionable whether sequential surgery after neoadjuvant treatment can challenge the existing standard treatment of concurrent chemoradiotherapy, which is also the basis for our plan for subsequent clinical trials; Fifth, after neoadjuvant treatment followed by surgery, there is still a lack of standard reference for implementation decisions of adjuvant chemotherapy, adjuvant radiotherapy, adjuvant immunotherapy and even prophylactic cranial radiotherapy. These may affect prognosis and should be designed and explored as scientifically as possible in future studies.

Conclusions

Our case illustrates that neoadjuvant serplulimab combined with chemotherapy followed by surgery could potentially serve as an effective therapeutic strategy for the curative treatment of locally advanced SCLC. Future prospective randomized controlled studies are needed to further validate our findings.

Data availability statement

The raw data supporting the conclusions of this article will be made available by the authors, without undue reservation.

Ethics statement

The studies involving humans were approved by the ethics review committee of West China Hospital Sichuan University. The studies were conducted in accordance with the local legislation and institutional requirements. Written informed consent for participation was not required from the participants or the participants' legal guardians/next of kin in accordance with the national legislation and institutional requirements. Written informed consent was obtained from the individual(s) for the publication of any potentially identifiable images or data included in this article.

Author contributions

TM: Conceptualization, Formal analysis, Methodology, Writing – original draft, Writing – review & editing. TW: Funding acquisition, Supervision, Writing – review & editing. CFL: Data curation, Writing – review & editing. DJ: Data curation, Writing – review & editing. QHZ: Conceptualization, Supervision, Writing – review & editing.

Funding

The author(s) declare financial support was received for the research, authorship, and/or publication of this article. This project was supported by a grant from Regional Innovation Cooperation Project of Sichuan Science and Technology Program (2021YFQ0029).

Conflict of interest

The authors declare that the research was conducted in the absence of any commercial or financial relationships that could be construed as a potential conflict of interest.

Publisher's note

All claims expressed in this article are solely those of the authors and do not necessarily represent those of their affiliated organizations, or those of the publisher, the editors and the reviewers. Any product that may be evaluated in this article, or claim that may be made by its manufacturer, is not guaranteed or endorsed by the publisher.

References

1. Saltos A, Shafique M, Chiappori A. Update on the biology, management, and treatment of small cell lung cancer (SCLC). *Front Oncol* (2020) 10:1074. doi: 10.3389/fonc.2020.01074

2. Raso MG, Bota-Rabassedas N, Wistuba II. Pathology and classification of SCLC. *Cancers* (2021) 13(4):820. doi: 10.3390/cancers13040820

3. Wang S, Zimmermann S, Parikh K, Mansfield AS, Adjei AA. Current diagnosis and management of small-cell lung cancer. *Mayo Clin Proc* (2019) 94(8):1599–622. doi: 10.1016/j.mayocp.2019.01.034

4. Faivre-Finn C, Snee M, Ashcroft L, Appel W, Barlesi F, Bhatnagar A, et al. Concurrent once-daily versus twice-daily chemoradiotherapy in patients with limited-stage small-cell lung cancer (CONVERT): an open-label, phase 3, randomised, superiority trial. *Lancet Oncol* (2017) 18(8):1116–25. doi: 10.1016/S1470-2045(17)30318-2

5. National Comprehensive Cancer Network (NCCN). *Clinical practice guidelines in oncology: small cell lung cancer (version 1.2023)*. Washington: NCCN (2023).

6. Li S, Jin K, Pan Y, Wu C, Ren S, Jiang G, et al. Role of surgery in a case-control study of patients with clinical stage IIIA small cell lung cancer. *J Thorac Dis* (2021) 13(5):2738. doi: 10.21037/jtd-20-3047

7. Forde PM, Spicer J, Lu S, Provencio M, Mitsudomi T, Awad MM, et al. Neoadjuvant nivolumab plus chemotherapy in resectable lung cancer. *New Engl J Med* (2022) 386(21):1973–85. doi: 10.1056/NEJMoa2202170

8. Zhou N, Chen Y, Huang Q, Jiang L, Liao H, Gou H, et al. Pathological complete response to neoadjuvant tislelizumab plus chemotherapy in stage IIIB small cell lung cancer: A case report and literature review. *Front Immunol* (2023) 14:1111325. doi: 10.3389/fimmu.2023.1111325

9. Horn L, Mansfield AS, Szczęsna A, Havel L, Krzakowski M, Hochmair MJ, et al. First-line atezolizumab plus chemotherapy in extensive-stage small-cell lung cancer. *N Engl J Med* (2018) 379(23):2220–9. doi: 10.1056/NEJMoa1809064

10. Paz-Ares L, Dvorkin M, Chen Y, Reinmuth N, Hotta K, Trukhin D, et al. Durvalumab plus platinum-etoposide versus platinum-etoposide in first-line treatment of extensive-stage small-cell lung cancer (CASPIAN): a randomised, controlled, open-label, phase 3 trial. *Lancet* (2019) 394(10212):1929–39. doi: 10.1016/S0140-6736(19)32222-6

11. Cheng Y, Han L, Wu L, Chen J, Sun H, Wen G, et al. Effect of first-line serplulimab vs placebo added to chemotherapy on survival in patients with extensive-stage small cell lung cancer: the ASTRUM-005 randomized clinical trial. *Jama* (2022) 328(12):1223–32. doi: 10.1001/jama.2022.16464

12. Takei H, Kondo H, Miyaoka E, Asamura H, Yoshino I, Date H, et al. Surgery for small cell lung cancer: a retrospective analysis of 243 patients from Japanese Lung Cancer Registry in 2004. *J Thorac Oncol* (2014) 9(8):1140–5. doi: 10.1097/JTO.0000000000000226

13. Zarogoulidis K, Ziogas E, Papagiannis A, Charitopoulos K, Dimitriadis K, Economides D, et al. Interferon alpha-2a and combined chemotherapy as first line treatment in SCLC patients: a randomised trial. *Lung Cancer* (1996) 15(2):197–205. doi: 10.1016/0169-5002(95)00583-8

14. Miller AB, Fox W, Tall R. Five-year follow-up of the medical research council comparative trial of surgery and radiotherapy for the primary treatment of small-celled or oat-celled carcinoma of the bronchus: A report to the medical research council working party on the evaluation of different methods of therapy in carcinoma of the bronchus. *Lancet* (1969) 294(7619):501–5. doi: 10.1016/S0140-6736(69)90212-8

15. Fox W, Scadding JG. Medical research council comparative trial of surgery and radiotherapy for primary treatment of small-celled or oat-celled carcinoma of bronchus: Ten-year Follow-up. *Lancet* (1973) 302(7820):63–5. doi: 10.1016/S0140-6736(73)93260-1

16. Lad T, Piantadosi S, Thomas P, Payne D, Ruckdeschel J, Giaccone G. A prospective randomized trial to determine the benefit of surgical resection of residual disease following response of small cell lung cancer to combination chemotherapy. *CHEST* (1994) 106(6):320S–3S. doi: 10.1378/chest.106.6.320S

17. Hoda MA, Klikovits T, Klepetko W. Controversies in oncology: surgery for small cell lung cancer? It's time to rethink the case. *ESMO Open* (2018) 3(3). doi: 10.1136/esmoopen-2018-000366

18. Liu T, Chen Z, Dang J, Li G. The role of surgery in stage I to III small cell lung cancer: A systematic review and meta-analysis. *PloS One* (2018) 13(12):e0210001. doi: 10.1371/journal.pone.0210001

19. Liu J, Wang L, Shu W, Zhang L, Wang Y, Lv W, et al. Safety and effectiveness of neoadjuvant immunotherapy combined with chemotherapy followed by surgical resection in patients with stage I-IIIA small-cell lung cancer: a retrospective single-arm clinical trial. *J Thorac Dis* (2022) 14(11):4405–15. doi: 10.21037/jtd-22-1287

20. Duan H, Shi L, Shao C, Wang Y, Wang Z, Ni Y, et al. A multicenter, single-arm, open study of neoadjuvant or conversion atezolizumab in combination with chemotherapy in resectable small cell lung cancer (Cohort Study). *Int J Surg* (2023) 109(9):2641–9. doi: 10.1097/JS9.0000000000000501

21. Wang S, Li Y, Liu Z, Tian W, Zeng Y, Liu J, et al. Efficacy and safety of first-line immune checkpoint inhibitors combined with chemotherapy for extensive-stage small cell lung cancer: A network meta-analysis. *Lung Cancer* (2023) 178:47–56. doi: 10.1016/j.lungcan.2023.02.003

22. Pasero C, Gravis G, Granjeaud S, Guerin M, Thomassin-Piana J, Rocchi P, et al. Highly effective NK cells are associated with good prognosis in patients with metastatic prostate cancer. *Oncotarget* (2015) 6(16):14360. doi: 10.18632/oncotarget.3965

23. Fridman WH, Pagès F, Sautès-Fridman C, Galon J. The immune contexture in human tumours: impact on clinical outcome. *Nat Rev Cancer* (2012) 12(4):298–306. doi: 10.1038/nrc3245

24. Peranzoni E, Lemoine J, Vimeux L, Feuillet V, Barrin S, Kantari-Mimoun C, et al. Macrophages impede CD8 T cells from reaching tumor cells and limit the efficacy of anti–PD-1 treatment. *Proc Natl Acad Sci* (2018) 115(17):E4041–E50. doi: 10.1073/pnas.1720948115

25. Umansky V, Blattner C, Gebhardt C, Utikal J. The role of myeloid-derived suppressor cells (MDSC) in cancer progression. *Vaccines* (2016) 4(4):36. doi: 10.3390/vaccines4040036

26. Tanaka A, Sakaguchi S. Regulatory T cells in cancer immunotherapy. *Cell Res* (2017) 27(1):109–18. doi: 10.1038/cr.2016.151

27. Yang L, Zhang Y. Tumor-associated macrophages: from basic research to clinical application. *J Hematol Oncol* (2017) 10(1):1–12. doi: 10.1186/s13045-017-0430-2

28. Lee J, Chaft J, Nicholas A, Patterson A, Waqar S, Toloza E, et al. PS01. 05 surgical and clinical outcomes with neoadjuvant atezolizumab in resectable stage IB–IIIB NSCLC: LCMC3 trial primary analysis. *J Thorac Oncol* (2021) 16(3):S59–61. doi: 10.1016/j.jtho.2021.01.320

29. Rothschild SI, Zippelius A, Eboulet EI, Savic Prince S, Betticher D, Bettini A, et al. SAKK 16/14: durvalumab in addition to neoadjuvant chemotherapy in patients with stage IIIA (N2) non–small-cell lung cancer—a multicenter single-arm phase II trial. *J Clin Oncol* (2021) 39(26):2872–80. doi: 10.1200/JCO.21.00276

30. Forde PM, Chaft JE, Smith KN, Anagnostou V, Cottrell TR, Hellmann MD, et al. Neoadjuvant PD-1 blockade in resectable lung cancer. *New Engl J Med* (2018) 378(21):1976–86. doi: 10.1056/NEJMoa1716078

31. Wakelee H, Liberman M, Kato T, Tsuboi M, Lee SH, Gao S, et al. Perioperative pembrolizumab for early-stage non-small-cell lung cancer. *N Engl J Med* (2023) 389(6):491–503. doi: 10.1056/NEJMoa2302983

32. Deng H, Liang H, Chen J, Wang W, Li J, Xiong S, et al. Preoperative immunochemotherapy for locally advanced non-small cell lung cancer: an analysis of the clinical outcomes, optimal number of cycles, and peripheral immune markers. *Transl Lung Cancer Res* (2022) 11(12):2364–81. doi: 10.21037/tlcr-22-439

Frontiers in Immunology

Explores novel approaches and diagnoses to treat immune disorders.
The official journal of the International Union of Immunological Societies (IUIS) and the most cited in its field, leading the way for research across basic, translational and clinical immunology.

Discover the latest Research Topics

See more →



Frontiers

Avenue du Tribunal-Fédéral 34
1005 Lausanne, Switzerland
frontiersin.org

Contact us

+41 (0)21 510 17 00
frontiersin.org/about/contact